LIBRARY
FISH & WILDLIFE SERVICE
PACIFIC OCEANIC FISHERY
INVESTIGATIONS

WOODS HOLE OCEANOGRAPHIC INSTITUTION

COLLECTED REPRINTS

1951

JULY, 1952

WOODS HOLE OCEANOGRAPHIC INSTITUTION

COLLECTED REPRINTS

1951

1710

JULY, 1952

This volume contains contributions from the
WOODS HOLE OCEANOGRAPHIC INSTITUTION
which appeared in 1951 in publications other than
Papers in Physical Oceanography and Meteorology;
also the Annual Report of the Director
for the year 1951

TABLE OF CONTENTS

Contribution No.

ARNOLD B. ARONS and STOMMEL, HENRY
A Mixing-length Theory of Tidal Flushing 544

BIGELOW, HENRY B. and WILLIAM C. SCHROEDER
A New Genus and Species of Anacanthobatid Skate from the Gulf of Mexico . 554
Three New Skates and a New Chimaerid Fish from the Gulf of Mexico . . . 555

CASTLE, EDWARD S.
Electrical Control of Marine Fouling 539

ERICSON, D. B., MAURICE EWING and BRUCE C. HEEZEN
Deep-sea Sands and Submarine Canyons 575

FUGLISTER, F. C.
Annual Variations in Current Speeds in the Gulf Stream System 557
Multiple Currents in the Gulf Stream System 584

FUGLISTER, F. C. and L. V. WORTHINGTON
Some Results of a Multiple Ship Survey of the Gulf Stream 548

KETCHUM, BOSTWICK H.
Plankton Algae and their Biological Significance 366
The Exchanges of Fresh and Salt Waters in Tidal Estuaries 516
The Flushing of Tidal Estuaries 536

ARTHUR A. KLEBBA and STOMMEL, HENRY
A Simple Demonstration of Coriolis Force 545

LANGWELL, PATRICIA A.
Forced Convection Cell Circulation in Clear Air 527
The Onset of Rain from Cumuli 568

MALKUS, JOANNE STARR, ANDREW F. BUNKER and KENNETH McCASLAND
A Formation of Pileus-like Veil Clouds over Cape Cod, Massachusetts . . . 534

MENARD, HENRY W. and A. J. BOUCOT
Experiments on the Movement of Shells by Water 546

MOORE, HILARY B.
The Seasonal Distribution of Oceanic Birds in the Western North Atlantic . . 560

NORTHROP, JOHN
Ocean-bottom Photographs of the Neritic and Bathyal Environment South of Cape Cod, Massachusetts 573

NORTHROP, JOHN and BRUCE C. HEEZEN
An Outcrop of Eocene Sediment on the Continental Slope 523

Contribution No.

POLLAK, MARTIN J.
The Sources of the Deep Water of the Eastern Mediterranean Sea 556

REDFIELD, ALFRED C. and LIONEL A. WALFORD
A Study of the Disposal of Chemical Waste at Sea 586

RILEY, GORDON A.
Parameters of Turbulence in the Sea 577

SAID, RUSHDI
Foraminifera of Narragansett Bay 491
Organic Origin of some Calcareous Sediments from the Red Sea 540
Preliminary Note on the Spectroscopic Distribution of Elements in the Shells of some Recent Calcareous Foraminifera 541

SEIWELL, H. R.
Experimental Correlogram Analyses of Artificial Time Series (with special Reference to Analyses of Oceanographic Data) 531

SOULE, FLOYD M.
Physical Oceanography of the Grand Banks Region, the Labrador Sea and Davis Strait in 1949 550
Physical Oceanography of the Grand Banks Region and the Labrador Sea in 1950 551

STOMMEL, HENRY
An Elementary Explanation of Why Ocean Currents are Strongest in the West . 532
Entrainment of Air into a Cumulus Cloud II 533
Streaks on Natural Water Surfaces 538
Determination of the Lateral Eddy Diffusivity in the Climatological Mean Gulf Stream 552

STOMMEL, HENRY and ALFRED H. WOODCOCK
Diurnal Heating of the Surface of the Gulf of Mexico in the Spring of 1942 . 553

TOLSTOY, IVAN
Submarine Topography in the North Atlantic 559

TURNER, HARRY J., JR., DAVID B. SAWYER, CARL N. SHUSTER, JR. and JULIUS A. POSGAY
Third Report on Investigations of Methods of Improving the Shellfish Resources of Massachusetts 564

von ARX, WILLIAM S.
Dead Reckoning by Surface Current Observation 526

WOODCOCK, ALFRED H. and A. F. McBRIDE
Wave-riding Dolphins 522

THE WOODS HOLE OCEANOGRAPHIC INSTITUTION
Report for the year 1951

LIST OF CONTRIBUTIONS

Contribution
No.

The following contributions, published in 1951, are not included in this volume.

KETCHUM, BOSTWICK H., ALFRED C. REDFIELD and JOHN C. AYERS
The Oceanography of the New York Bight 549

PHLEGER, FRED B.
Ecology of Foraminifera, Northwest Gulf of Mexico. Part I. Foraminifera Distribution 565

PHLEGER, FRED B. and FRANCES L. PARKER
Ecology of Foraminifera, Northwest Gulf of Mexico. Part II. Foraminifera Species 566

RILEY, GORDON A.
Oxygen, Phosphate and Nitrate in the Atlantic Ocean 542

Contribution No. 366

Chapter 17

PLANKTON ALGAE AND THEIR BIOLOGICAL SIGNIFICANCE

by

BOSTWICK H. KETCHUM

Reprinted, for private circulation, without change of pagination, from **'Manual of Phycology — an Introduction to the Algae and their Biology'**, *edited by* GILBERT M. SMITH ("A New Series of Plant Science Books", Vol. 27), WALTHAM, MASS., U. S. A., THE CHRONICA BOTANICA CO., 1951.

Chapter 17

PLANKTON ALGAE AND THEIR BIOLOGICAL SIGNIFICANCE[1]

by

BOSTWICK H. KETCHUM

THE vast areas of the seas, which cover about 71 per cent of the surface of the earth, depend upon the photosynthetic activity of microscopic algae for the support of all organic life. These algae, the phytoplankton, though individually small in size, contribute an enormous quantity of the organic matter of the world. It is obvious, a priori, that all of the animals in the sea must derive their food from the plant syntheses, and these algae thus support the fisheries upon which man relies for food.

This chapter will discuss the factors which determine the growth and photosynthesis of the phytoplankton under natural conditions. More extensive discussions will be found in "The Oceans" by SVERDRUP, JOHNSON, & FLEMING (1942), "Biological Chemistry and Physics of Sea Water" and "Recent Advances in the Chemistry and Biology of Sea Water" by HARVEY (1928, 1945), and in "Marine Microbiology" by ZoBELL (1946). Descriptions of the geographical distribution of various members of the planktonic community will be found in expedition reports, such as those of the *Challenger, Meteor* and *Discovery* (CASTRACANE, 1884, HENTSCHEL, 1932, 1936, HART, 1934, 1942) and in various briefer discussions which will be referred to in the text.

Collection and Measurement of Phytoplankton:— The phytoplankton are those plants which float freely in the water. They may be collected in fine silk nets of about No. 20 bolting cloth. The volume of water strained should be directly measured as is done in the CLARKE & BUMPUS (1940) plankton sampler. Because of the failure of the nets to retain the smaller cells, and the reduction in straining efficiency as the nets become clogged only part of the phytoplankton are obtained this way. BIGELOW *et al.* (1940) found that the nets collected only one to ten per cent of the phytoplankton in water samples. The cells may be quantitatively removed from water samples by settling, by centrifuging or by filtration through membrane or parchment filters. After collection the cells may be identified and counted under a compound microscope. The results are then recorded as cells per unit volume of water.

This method of evaluation has obvious advantages in studying the distribution and seasonal variations of the species involved. It has, however, the serious disadvantage that the results of observations are not quantitatively comparable as to the mass of plant material or the potential photosynthetic activity. This is essential if the production of organic matter in the sea is to be studied. An approximation of the mass of plant material can be made if the results are converted to "cells of average content" (HARVEY *et al.* 1935) but direct chemical determination of some constituent of the cells is generally preferable for this purpose. The measurement of plant pigments by the method of KREPS and VERJBINSKAYA (1930) as modified by HARVEY (1934) or of chlorophyll, as done by RILEY (1938), KREY (1939) and GRAHAM (1943) probably gives the most useful indication of the potential photosynthetic activity. Analyses of the phosphorus, nitrogen, or carbon content of the cells will also give an accurate indication of the mass of organic material.

---

[1] Contribution No. 366, from the Woods Hole Oceanographic Institution, Woods Hole, Mass.

Composition of the Phytoplankton:— The most important planktonic algae of the sea are the diatoms and the dinoflagellates. Groups of less general distribution and importance in the economy of the sea include the Myxophyceae, which are common in fresh and brackish waters, the Chlorophyceae, the Phaeophyceae, and the Rhodophyceae. Most of these latter groups are large, well developed plants which are common along shore, but which are of little importance in the plankton. The area of the sea suitable for attached plants is only about 2 per cent of the entire sea surface, and their contribution to the organic matter of the sea as a whole is correspondingly small in spite of their conspicuous nature.

The diatoms form an important part of every collection of planktonic algae. GRAN (1905), HUSTEDT (1930), and CUPP (1943) describe the species of diatoms important in the plankton populations. These keys will permit recognition of most forms wherever they may be collected. The diatoms are true plant cells, assimilating the inorganic nutrients from sea water and synthesizing organic matter from them in the presence of light.

The dinoflagellates are a diverse group of organisms some of which are photosynthetic, some are animal-like, ingesting particulate food, and some are saprophytic, living upon dead organic matter. Because of their size, which permits their collection in the nets used for the phytoplankton, and because some members are known to contribute importantly to photosynthesis in the sea, they are included with studies of the planktonic algae. Important genera of dinoflagellates in the sea are *Ceratium, Peridinium, Dinophysis* and *Gonyaulax*. KOFOID & SWEZY (1921), KOFOID & SKOGSBERG (1928), and FRITSCH (1935) give detailed descriptions of this group.

Nannoplankton is a collective term applied to those organisms which are too small to be retained by the nets ordinarily used to collect phytoplankton. Included are the smaller diatoms and dinoflagellates, the microflagellates, coccolithophores, protozoa, and bacteria. Many are chlorophyll containing forms which generally disintegrate rapidly in preserved samples unless special precautions are taken. ATKINS (1945) gives evidence that their importance in the economy of the sea has been greatly underestimated.

Chemical Composition of the Phytoplankton:— REDFIELD (1934) showed that the concentrations of carbonate, nitrate, and phosphate in samples of sea water of widely different origin vary in a correlated way as a result of biological activity. The composition of the plankton, as deduced from the changes which occur in sea water, indicate that the proportions carbon : nitrogen : phosphorus equal 100 : 16.7 : 2.5 grams. The phosphate analyses have been corrected for the salt effect as determined by COOPER (1938). Similar average proportions were found in various samples of plankton, though marked deviations from the ratios were found for individual types of organisms. FLEMING (1940) has collected analyses of plankton, and gives a table of "plankton equivalents" which interrelate various physical and chemical properties of the phytoplankton community.

Studies of pure cultures of algae have shown that the cellular content of these elements can be varied widely. The assimilation of phosphate in the light by the marine diatom *Nitzschia Closterium* was found by KETCHUM (1939) to depend upon the concentration of both phosphate and nitrate in the culture medium; while the assimilation of nitrate was dependent only on the concentration of nitrate. Cells grown in media deficient in these substances continued to divide, and cells were produced which contained as little as a third of the normal phosphorus and a fifth of the normal nitrogen content (Ketchum, 1939A). Such cells can assimilate phosphate or nitrate in the dark to satisfy these deficiencies. This mechanism allows the continuous utilization of nutrients, though photosynthesis takes place only during daylight, and, as Harvey (1945) points out, may permit growth at greater dilutions than would otherwise be possible.

Factors Controlling Phytoplankton Populations:— The population of phytoplankton at any particular place and time depends upon the rate of reproduction of the individuals in the population and upon the rate of removal of these individuals by death; by consumption by herbivores, or by passive transport in the water currents. The rate of growth, in turn, depends upon the type and size of the parent stock, upon the light intensity falling on the surface and the transparency of the water, and upon the concentration and availability of the elements essential for photosynthesis and plant growth. The net result of the interaction of these various factors is to determine the standing crop at any particular time, and the total quantity of organic matter produced by the area over a period of time.

Light:— The effective production of organic matter in the sea by photosynthesis is dependent upon the intensity of incident light at the sea surface, and upon the depth to which adequate light can penetrate. Both the intensity and spectral composition of the light change with depth (Clarke, 1933, 1936). The "compensation point" is reached when the daily assimilation of carbon dioxide in photosynthesis is equal to the daily release of carbon dioxide in the respiration of the plant cell. Though photosynthesis proceeds at greater depths it is not sufficient to meet the needs of the plants, and no surplus organic matter is provided for animal consumption. The depth at which this compensation point is found varies widely, depending upon the incident solar radiation, which fluctuates seasonally and geographically, and upon the turbidity of the water, which varies with distance from shore and bottom, and with the plankton which the water contains. The compensation depth may also vary because of the difference in the effect of temperature on respiration and on photosynthesis (Spoehr, 1926) or because of differences in the species of algae present. Schreiber (1927), for example, found that the optimum light intensity for the diatom, *Biddulphia mobiliensis,* was only half of that for the green flagellated alga *Carteria.* Variations in the depth of the compensation point from 4.5—100 meters at different localities and times of year are indicated in Table I.

Table I.— *Depths at which the Photosynthetic and Respiratory Rates are Equal (compensation point) at Various Locations:—*

Location	Date	Compensation Depth, Meters	Reference
Sargasso Sea	August	> 100[a]	Clarke, 1936
Georges Bank	June maximum	59[c]	Clarke, 1946
English Channel	July	45[b]	Jenkin, 1937
Gulf of Maine	June	24-30[a]	Clarke & Oster, 1934
Loch Striven	Summer	20-30[b]	Marshall & Orr, 1928
Passamaquoddy Bay	Summer	17[a]	Gran & Braarud, 1935
Puget Sound	Summer	10-18[a]	Gran & Thompson, 1930
Oslo Fjord	March	10[a]	Gaarder & Gran, 1927
Georges Bank	April minimum	9[c]	Clarke, 1946
Woods Hole Harbor	August	7[a]	Clarke & Oster, 1934
Loch Striven	March	5[b]	Marshall & Orr, 1928
Helsingør Sound	Annual range	4.5-7[b]	Steemann Nielsen, 1937

[a] Exposed for short periods during daylight only.
[b] Exposed for 24 hour period.
[c] Calculated from incident light and transparency.

Chemical Nutrients:— Most of the elements essential for plant growth are present in great excess in the sea. Others, however, are reduced to negligible quantities in the surface waters during periods of intensive flowerings, and may limit plant production. HARVEY (1926) and REDFIELD (1934) have shown that the stores of both nitrate and phosphate are exhausted at about the same time as a result of plant growth. Plant growth, however, never completely ceases even when the nutrient concentration is low. It is the rate of supply of these compounds to the surface waters which determines the fertility of the region. They are supplied by the processes of decomposition of organic matter and regeneration of the nutrients, and by vertical mixing of the water which makes some of the stores of nutrients in the deeper water available at the surface. These processes go on throughout the year but the latter is most rapid during the winter when the cooling of the surface waters permits rapid vertical mixing, so that the nutrients again become uniformly distributed from top to bottom of the water column. In spring, therefore, the plants have a large supply of nutrients available.

The assimilation of nutrients in plant growth reduces their concentration in the water, and this, in turn, limits the rate of reproduction. HARVEY (1933, 1940) found a marked reduction in the rate of photosynthesis of cultures of *Nitzschia Closterium* when the phosphate concentration fell below 10 μg P per liter. KETCHUM (1939) found that the rate of cell division of the same diatom was decreased when the phosphate concentration fell below about 17 μg P per liter. The rate of division was independent of nitrate above concentrations of 47 μg N per liter, the lowest concentration tested. CHU (1942, 1943) has shown that there may be an optimum concentration of nutrients, above and below which the growth is less rapid. RILEY, STOMMEL and BUMPUS (1949) has shown that the rate of photosynthesis of natural phytoplankton populations is limited by the phosphate concentration if it is present in a quantity less than that needed for five days' growth of the population. For the areas studied nitrogen compounds were not found to limit the growth of the population.

Other elements may also be important in limiting the growth of phytoplankton. ATKINS (1923A, 1926), COOPER (1933), HART (1934, 1942) and CLOWES (1938) find that much of the silicate of sea water is removed during diatom growth. The relation between growth of diatoms and silicate content of the water is not known, though thin walled diatoms may be produced in waters low in silicate.

GRAN (1931, 1933) found the growth of the various species of marine diatoms could be stimulated by the addition of soil extract when adequate amounts of phosphate and nitrate were present in the water. Addition of iron (ferro ligno protein) and manganese solutions gave increases equal to those of soil extract. COOPER (1937) concluded that little iron could exist in sea water in ionic equilibrium with ferric hydroxide, but it may be present in colloidal suspension (HARVEY, 1937). COOPER (1935) has shown that plankton organisms contain relatively large amounts of iron and THOMPSON & BREMMER (1935) and HARVEY (1937) have demonstrated a reduction in the quantity of iron in sea water during phytoplankton blooms.

THOMPSON & WILSON (1935) find a variable, small quantity of manganese in Pacific waters. HARVEY (1939) finds that the addition of small amounts of manganese improved the growth of the diatom, *Ditylum Brightwelli,* in some samples of water. In other samples some compound containing divalent sulphur was required. It is possible that these materials, and others as yet unsuspected, may limit the production of phytoplankton under some circumstances.

Decomposition of Organic Matter and Regeneration of Nutrients:— The evidence of some studies of the productivity of the sea suggest that each unit of phosphorus and of nitrogen must be reassimilated several times each year to permit the synthesis of the amount of organic material produced. Estimates of the rate of supply of the inorganic nutrients to the water by regeneration are not yet satisfactory. REDFIELD, SMITH & KETCHUM (1937) found that about 93 per cent of the phosphorus in the upper meter of water in the Gulf of Maine in August was in organic combination. In November, 27.2 per cent of the total phosphorus of the water column (250 meters deep) was combined in organic compounds. This had fallen to 11.1 per cent by February. During this period about 1.7 grams of phosphate phosphorus per square meter of sea surface had been regenerated. KREPS & VERJBINSKAYA (1932) found only about one-quarter of this rate of regeneration (0.45 grams P/square meter) in the Barents Sea. Although direct measures of regeneration during periods of active phytoplankton growth are not possible, since the material regenerated is directly reassimilated by the plants, the process must proceed at all times. The rates given above are minimum estimates of this important process.

It was once thought that the decomposition of proteins, with the liberation of the inorganic forms of nitrogen necessary for plant growth, occurred mainly in bottom deposits. COOPER (1933) and REDFIELD & KEYS (1938) have shown that the distribution of ammonia in the water can be explained if decomposition occurs throughout the water column. ATKINS (1930) and RAKESTRAW (1936) have shown that nitrite may be present in considerable amounts in water at mid-depths in the sea. RAKESTRAW rarely detected its presence near the bottom at 250 meters. In shoaler waters, less than 100 meters, much of the nitrite was found near the bottom. REDFIELD & KEYS (1938) show that distribution of ammonia and nitrite in the water is similar, as would be expected if the nitrite is derived from ammonia. They conclude that nitrite is a shorter-lived link in the chain of nitrogen transformations than is ammonia. These results may all be interpreted on the basis that oxidation of organic matter occurs at all depths. Attempts to isolate the nitrifying bacteria from the surface waters have not, however, been successful (WAKSMAN *et al.*, 1933, 1933A, CAREY & WAKSMAN, 1934). Both ammonia and nitrite may be absent or low in concentration in the surface waters since they can be directly assimilated by the plants (SCHREIBER, 1927, BRAARUD & FØYN, 1930, HARVEY, 1933, ZOBELL, 1935). The complete nitrogen cycle has been duplicated in the laboratory by VON BRAND, RAKESTRAW and their collaborators in a series of experiments which have included studies of such variables as time, temperature, source of water, organic matter and the effects of various enzyme poisons (1937-1947). COOPER (1937A) and GILSON (1937) have reviewed and evaluated the importance of the various steps of the nitrogen cycle in the sea.

Circulation of the Water:— Since the plankton include, by definition, the organisms which are passively transported by the water, its circulation is of primary importance in plankton studies. The horizontal circulation sweeps different populations past any given point; the vertical transport may bring essential nutrient elements to the photosynthetic zone, and may carry the cells below the compensation depth where they can no longer synthesize enough organic matter for their own respiratory needs.

Increased vertical transport of nutrient-rich, deep ocean water occurs at the boundaries of oceanic currents because of increased turbulence. Along the western coasts of Africa and America the prevailing winds result in a net offshore surface current, and in upwelling of the deeper water. SVERDRUP & ALLEN (1939) found the largest populations of diatoms in the "new water," *i.e.* that which had recently been brought to the sea surface, while the water which had been at the surface for a longer time was relatively poor in phytoplankton. The richness of the flora and fauna in areas of upwelling has long been recognized

(Moberg, 1928, Bigelow & Leslie, 1930, Hentschel & Wattenberg, 1930, Gunther, 1936).

Even in relatively stable bodies of water, where upwelling does not contribute to the circulation, the vertical circulation may play an important role in supplying nutrients to the surface waters. The data of Redfield, Smith & Ketchum (1937) show that about 73 per cent of the phosphorus utilized by the phytoplankton in the Gulf of Maine during six summer months was provided by vertical transport (Ketchum, 1947).

That the vertical transport may also carry the plants below the depth at which effective photosynthesis may occur has been shown by Atkins (1928), and Braarud & Klem (1931). Gran & Braarud (1935) conclude that turbulence is responsible for the small phytoplankton production in the Bay of Fundy. Hart (1934) and Riley (1942) have described other cases where turbulence plays a part in limiting phytoplankton populations in the temperate seas.

Interrelations between Phyto- and Zoo-plankton:— It has been observed that large concentrations of phyto- and zoo-plankton are rarely found at the same time (Harvey *et al.,* 1935, Wimpenny, 1936, Steemann Nielsen, 1937A, Mare, 1940, and Hart, 1941). Two hypotheses have been advanced to explain this. The simplest one is that the zooplankton graze down the phytoplankton population (Harvey, 1934A). Hardy & Gunther (1935) and Hardy (1936) postulate that the zooplankton avoid areas rich in phytoplankton—that they are excluded from the area. They found large zooplankton concentrations in the Antarctic in areas of low phytoplankton. The phosphate content of the water was high, indicating that phytoplankton growth had been low for some time.

Steemann Nielsen (1937A) points out that the phytoplankton crop can develop within a few days under favorable conditions, but a much longer period is required for the development of the zooplankton. Consequently the peaks of the two populations will not fall at the same time. Harvey (1945) calculates the effect of grazing as follows: if one plant in every ten is eaten a population of 100 plants will produce 3400 in six divisions, compared to the 6400 which would be produced if there were no grazing. Only 413 plants are consumed to produce this result. Similar effects of grazing have been calculated by Fleming (1939).

Productivity of the Sea:— The productivity of an aquatic environment is determined by the interaction of the various factors which have been discussed above. The term "productivity" has been given many meanings in the literature. These include the *gross production,* which is the total amount of organic matter synthesized by the plant cells, and the *plant* or *phytoplankton production* which is the gross production corrected for respiration of the plant cells. In addition to these terms, which are concerned with the synthesis of new organic material, the production of any other step in the food chain in the sea may be described. Thus one may speak of zooplankton production, fish production, etc. The production is best expressed in terms of the total energy or carbon fixation by the population. The volume, weight, glucose equivalent or nutrient salt content of the population have also been used. Within limits, these can all be converted to the units desired using the plankton equivalents of Fleming (1940).

The methods used to estimate the magnitude of plant production in the sea have been reviewed by Sargent (1940). The three methods described are the census of the standing crop, the determination of changes in the amounts of an ingredient of the water which is correlated with the activities of the phytoplankton, and the direct experimental measurement of the rate of photosynthesis of the natural population. Considerable progress has been made in recent years in obtaining these estimates, but so few thorough studies have been made that it is still impossible to compare the fertility of different regions of the sea or to delimit the variations from year to year with any certainty. The values available do give an appreciation of the order of magnitude of organic production in the sea.

The Standing Crop:— The population of organisms in the water at any time is a momentary balance between the growth of the individuals, and their death or removal from the area. The magnitude of the standing crop is not a direct indication of the productivity of the waters (CLARKE, 1946). A small population may be synthesizing organic matter rapidly under favorable conditions, but it may show no apparent increase in numbers because of active consumption by herbivores. A large population may, on the other hand, fail to synthesize organic matter if a lack of nutrients or adequate light is limiting its growth. An estimate of production can be calculated from successive observations of the size of the standing crop, if the rates of growth, of consumption and of sinking and transport are taken into account.

RILEY (1946) has found that the rate of change of the standing crop of phytoplankton, $\frac{dP}{dt}$, in Atlantic coastal waters may be described by the equation:

$$\frac{dP}{dt} = P\ (P_h - R - G)$$

where P is the quantity of phytoplankton measured in any convenient units, P_h is the photosynthetic rate, R is the rate of respiration of the phytoplankton and G is the rate of removal of phytoplankton by the grazing of herbivores.

The total population at the end of any given time, t, is:

$$P_t = P_o\ e^{(P_h - R - G)t}$$

where P_o is the original population and P_t the population at the end of time t. Further analysis shows that the rate of photosynthesis can be computed from the chlorophyll content of the plankton, the incident light intensity, the transparency of the water, the depth of the mixed layer and the quantity of phosphate if it is present in limiting quantities. These equations may not describe production in other areas adequately, but it is significant that the factors controlling production are sufficiently understood to permit their expression in physical and chemical units.

Nutrient Utilization:— If the quantity of phosphorus or nitrogen removed from the water is known, a calculation of the quantity of organic matter synthesized can be made using the normal proportions of these materials in the organisms. In northern waters, where the concentrations of these elements is reduced drastically during periods of active plant growth, these estimates are possible. RILEY (1938A, 1939, 1941) has calculated carbon production from measurements of phosphorus and nitrogen consumption in experimental observations. ATKINS (1923), COOPER (1938A), KREPS & VERJBINSKAYA (1930, 1932) computed production from observations on the natural environment. As discussed above an estimate based upon the utilization of nutrient salts will be minimal unless the effects of vertical transport and regeneration are evaluated.

Photosynthesis Estimates:— Direct measurements of photosynthesis of natural populations may be made experimentally. Samples of the natural water, with measured oxygen content, are placed in two bottles. One is kept in the light to measure the net effect of photosynthesis and respiration; the other in the dark to measure respiration. The difference in the oxygen content of the two bottles at the end of the experiment is a direct measure of the gross production of the population. The experiment should be carried out for 24, or some multiple of 24, hours to include both day and night conditions. If the experiment is conducted at various depths the complete estimate of the production of the entire water column may be made. Accurate values would be obtained only if the water samples were exposed at the same depth they were collected, or if corrections are made for the variation of the population with depth. If measurements are made only at the surface, the total production must be calculated using values for the total incident solar energy and its diminution with depth computed from the transparency of the water. This method has been used extensively in both marine and fresh water studies (Gran, 1927, Marshall & Orr, 1928, Jenkin, 1937, Steemann Nielsen, 1937, Riley, 1938A, 1939, 1940, 1941, 1941A, 1943, Manning, Juday & Wolf, 1938).

During periods of active phytoplankton growth the water in the euphotic layer may become supersaturated with oxygen and this change in the oxygen content has been used to estimate photosynthesis (Cooper, 1933). Such estimates, and similar ones based on the change of carbon dioxide (Atkins, 1922, Cooper, 1933) are minimal, since the changes resulting from photosynthesis are decreased by respiration and exchanges with the atmosphere.

Carbon Production:— Some values for the carbon production of natural phytoplankton populations have been summarized by Riley (1941) and by Harvey (1945). The variations they observed are shown in Table II. The total range of the measurements lies between 44 and 1000 grams of carbon per square meter of sea surface per year. The lower values generally characterize shallow bodies of water where the depth of the photosynthetic zone is not great. The higher values are for areas where the depth of the photosynthetic zone is great, or where considerable water mixing increases the supply of nutrients at the surface. Considering the wide variations in conditions studied the total range of values obtained is surprisingly small.

Table II.— *Total Organic Production from Various Estimates:—*

Location	Production	Reference
English Channel	39- 101 gC/m²/6 mos.	Harvey, 1945
Long Island Sound	95-1000 gC/m²/year	Riley, 1941
Western Atlantic, 28°-38° N.	530 gC/m²/year	Riley, 1941
38°-41° N.	320 gC/m²/year	Riley, 1941
28°-41° N.	140- 530 gC/m²/year	Riley, 1941
3°-13° N.	278 gC/m²/year	Seiwell, 1935
Pacific, off S. Cal.	215- 430 gC/m²/year	Sverdrup & Fleming, 1941
Gulf of Maine	120 gC/m²/year	Redfield *et alii* (1937)*
Barents Sea	170- 330 gC/m²/year	Kreps & Verjbinskaya, 1932
Helsingør Sound	44 gC/m²/year	Steemann Nielsen (1937)

* Calculated for this table using the C: P ratio of 100:2.5.

It has long been thought that the tropical seas are areas of low production, but the data in Table II do not substantiate this view. Riley (1939) concluded that there is little or no difference between the production in low and high latitudes. It is true that the concentration, or standing crop, of plankton in the surface waters in low latitudes was not as great as the summer crop in higher latitudes, but the depth of the photosynthetic zone was greater and the total crop in the entire vertical water column was somewhat greater in the southern waters.

From these measurements Riley (1944) has estimated that the photosynthetic activity of the oceans of the world provides between 44×10^9 and 208×10^9 tons of organic carbon per year. Adding the terrestrial contribution gives a total annual carbon production which lies between 59×10^9 and 233×10^9 tons. With our present knowledge these estimates cannot be made more accurately but it will be noted that they attribute a large proportion of the total annual production of carbon to the seas of the world.

Efficiency of Aquatic Production:— The efficiency of production is the ratio of the energy fixed in chemical compounds to the incident light energy. Part of the incident light is reflected, part absorbed by the water and by particles other than the plant cells. The overall efficiency is, therefore, always less than the photosynthetic efficiency. RILEY (1940, 1941, 1941A) has computed efficiencies of plant production of 0.31 per cent for Long Island Sound, 0.3 per cent for Georges Bank and about 0.056 per cent for Linsley Pond, Connecticut. CLARKE (1946) gives a range of 0.043—0.38 per cent efficiency for a series of Wisconsin lakes. For comparison he quotes an efficiency of 1.2 per cent for corn, grown for 100 days under the best conditions in Ohio (TRANSEAU, 1926), and an annual efficiency of about 0.25 per cent for the best forests (KROGH, 1934). A further decrease in efficiency is observed if the production of animal material is considered. CLARKE (1946) estimates that the zooplankton (herbivores) utilize about 0.015 per cent of the incident light energy and that the efficiency of fish production (estimated from the amount of commercial fish landed from 1923-1945) is only 0.00005 to 0.00025 per cent. At best, therefore, less than one-thousandth of the total plant production in the sea is converted into commercial fish harvest.

The Fertilization of Aquatic Areas:— In recent years many attempts have been made to increase the production of aquatic areas by fertilization. The yield of fish may be increased by adding organic food directly (SNIESZKO, 1941), or by adding chemical fertilizers to increase the phytoplankton production, and thus to increase the food supply for the fish. Fertilization has increased fish production in fresh water ponds several fold (SWINGLE & SMITH, 1941). JUDAY & SCHLOEMER (1938) and JUDAY (1943) have fertilized Wisconsin lakes, and JUDAY found that the standing crop of phytoplankton was increased more by the use of soy and cottonseed meal than by chemical fertilizers.

The fertilization of sea water to increase its production has been mainly studied in Europe (GAARDER, 1932, GAARDER & ALVSAKER, 1941, GROSS, 1942, GROSS, RAYMONT, MARSHALL & ORR, 1944). The experiments of GROSS and co-workers on fertilization of Scottish sea lochs have shown that the added chemical nutrients disappear from the water rapidly, and this is followed by great increases in the phytoplankton. The greatest increase occurred in the small flagellates; smaller increases of diatoms and dinoflagellates were observed. The bottom fauna of fertilized areas increased by as much as 300 per cent, and the rate of growth of fish in these areas was greatly accelerated (RAYMONT, 1947).

These observations confirm the belief that the chemical nutrients essential for plant growth are the factors which limit production in the sea.

Comparison of Production in the Sea and on Land:— The estimates in Table II for the production of organic carbon in the sea are converted to values of 0.52 to 10.35 tons dry plankton per acre per year, using the equivalence factor suggested by FLEMING (1940). RILEY (1944) considers a value of about 3.2 tons dry plankton per acre per year (340 tons carbon per square kilometer) as the best average value. Most land crops do not exceed these values. TRANSEAU (1926) gives a value of 6.6 tons per acre as the fresh weight of an entire corn crop grown under the best conditions. The grain yield alone was 2.36 tons. Similar values for other crops range from about half a ton for oats to about thirteen tons fresh weight per acre per year for sugar beets. These estimates are not strictly comparable since the agricultural results, with the exception of TRANSEAU'S, do not include the foliage necessary to produce the crop. They are, however, fresh weight figures, and would be reduced if the moisture content were known. The production in the sea is gross production, *i.e.,* it is not corrected for the respiration of the plants, and would be reduced to 75-90 per cent of the values given if this correction were applied. In terms of value to man the estimates given are even more distorted. As shown above only 0.1 per cent of the production over an intensively fished bank is available as food for man, and the production of vast areas of the sea is not utilized at all.

Bibliography:—

Atkins, W. R. G. 1922. Hydrogen ion concentration in sea water in its biological relations. Jour. Marine Biol. Assn., U. K. 12: 717-771. 1 chart.

Atkins, W. R. G. 1923. The phosphate content of fresh and salt waters in its relationship to the growth of algal plankton. *Ibid.* 13: 119-150. 8 figs.

Atkins, W. R. G. 1923A. The silica content of some natural waters and of culture media. *Ibid.* 13: 151-159.

Atkins, W. R. G. 1926. Seasonal changes in silica content of natural waters in relation to the phytoplankton. *Ibid.* 14: 89-99. 3 figs.

Atkins, W. R. G. 1928. Seasonal variations in phosphate and silicate content of sea water during 1926 and 1927 in relation to the phytoplankton crop. *Ibid.* 15: 191-205.

Atkins, W. R. G. 1930. Seasonal changes in the nitrite content of sea water. *Ibid.* 16: 515-518.

Atkins, W. R. G. 1945. Autotrophic flagellates as the major constituent of the oceanic phytoplankton. Nature. 156: 446-447.

Bigelow, H. B. & M. Leslie. 1930. Reconnaissance of the waters and plankton of Monterey Bay, July 1928. Bull. Mus. Comp. Zool., Harvard Coll. 70: 429-581. 43 figs.

Bigelow, H. B., L. Lillick & M. Sears. 1940. Phytoplankton and planktonic protozoa of the offshore waters of the Gulf of Maine. Trans. Amer. Phil. Soc. 31: 149-191. 10 figs.

Braarud, T. & B. Føyn. 1930. Beiträge zur Kenntnis des Stoffwechsels im Meere. Avhandl., Norske Vidensk. Akad. I Oslo. I. Matem-Naturvid. Klasse. Nr. 14: 24 pp.

Braarud, T. & A. Klem. 1931. Hydrographical and chemical investigations in the coastal waters off Møre and in the Romsdalsfjord. Norske Vidensk. Akad. I Oslo. Hvalrådets Skrifter. Nr. 1: 88 pp. 21 figs.

von Brand, T. & N. W. Rakestraw. 1940. Decomposition and regeneration of nitrogenous organic matter in sea water. III. Influence of temperature and source and condition of water. Biol. Bull. 79: 231-236. 2 figs.

von Brand, T. & N. W. Rakestraw. 1941. Decomposition and regeneration of nitrogenous organic matter in sea water. IV. Interrelationship of various stages; influence of concentration and nature of particulate matter. *Ibid.* 81: 63-69. 4 figs.

von Brand, T., N. W. Rakestraw, & C. E. Renn. 1937. The experimental decomposition and regeneration of nitrogenous organic matter in sea water. *Ibid.* 72: 165-175. 2 figs.

von Brand, T., N. W. Rakestraw, & C. E. Renn. 1939. Further experiments on the decomposition and regeneration of nitrogenous organic matter in sea water. *Ibid.* 77: 285-296. 2 figs.

von Brand, T., N. W. Rakestraw & J. W. Zabor. 1942. Decomposition and regeneration of nitrogenous organic matter in sea water. V. Factors influencing the length of the cycle; observations upon the gaseous and dissolved organic nitrogen. *Ibid.* 83: 273-282. 5 figs.

Carey, C. L. & S. A. Waksman. 1934. The presence of nitrifying bacteria in deep seas. Science. 79: 349-350.

Castracane, F. 1884. Report on the Diatomaceae collected by HMS Challenger during the years 1873-1876. Report of the scientific results of the voyage of HMS Challenger. Botany, vol. II: 1-178. 30 plates.

Chu, S. P. 1942. The influence of the mineral composition of the medium on the growth of planktonic algae. Part I. Methods and culture media. Jour. Ecol. 30: 284-325. 8 figs.

Chu, S. P. 1943. The influence of the mineral composition of the medium on the growth of planktonic algae. Part II. The influence of the concentration of inorganic nitrogen and phosphate phosphorus. *Ibid.* 31: 109-148. 23 figs.

Clarke, G. L. 1933. Observations on the penetration of daylight into mid-Atlantic and coastal waters. Biol. Bull. 65: 317-337. 5 figs.

Clarke, G. L. 1936. Light penetration in the western North Atlantic and its application to biological problems. Cons. Perm. Int. p. l'Explor. de la Mer, Rapp. et Proc.-Verb. 101: pt. 2, no. 3. 14 pp. 6 figs.

Clarke, G. L. 1946. Dynamics of production in a marine area. Ecol. Monogr. 16: 321-337. 9 figs.

Clarke, G. L. & D. F. Bumpus. 1940. The plankton sampler—an instrument for quantitative plankton investigations. Limnolog. Soc. Amer., Spec. Publ. 5: 1-8. 5 figs. Ann Arbor.

Clarke, G. L. & R. H. Oster. 1934. The penetration of the blue and red components of daylight into Atlantic coastal waters and its relation to phytoplankton metabolism. Biol. Bull. 67: 59-75. 6 figs.

Clowes, A. J. 1938. Phosphate and silicate in the southern ocean. *Discovery* Reports 19: 1-120. 29 figs. 25 plates.

Cooper, L. H. N. 1933. Chemical constituents of biological importance in the English Channel, November 1930-January 1932, parts I and II. Jour. Marine Biol. Assn., U. K. 18: 677-753. 15 figs.

Cooper, L. H. N. 1935. Iron in the sea and in marine plankton. Proc. Roy. Soc. of London, Ser. B. 118: 419-438. 2 figs.

Cooper, L. H. N. 1937. Some conditions governing the solubility of iron. *Ibid.* 124: 299-307.

Cooper, L. H. N. 1937A. The nitrogen cycle in the sea. Jour. Marine Biol. Assn., U. K. 22: 183-204. 2 figs.

Cooper, L. H. N. 1938. Salt error in determinations of phosphate in sea water. *Ibid.* 23: 171-179.

Cooper, L. H. N. 1938A. Phosphate in the English Channel 1933-38 with a comparison with earlier years, 1916 and 1923-32. *Ibid.* 23: 181-195. 1 fig.

Cupp, E. E. 1943. Marine plankton diatoms of the west coast of North America. Bull. Scripps Inst. Oceanog. v. 5 no. 1: 237 pp. 5 plates. 160 text figs. Univ. Cal. Press, Berkeley and Los Angeles.

Fleming, R. H. 1939. The control of diatom populations by grazing. Cons. Perm. Int. p. l'Explor. de la Mer., J. du Cons. 14: 210-227. 5 figs.

Fleming, R. H. 1940. The composition of plankton and units for reporting populations and production. Sixth Pacific Science Congress, Cal. 1939. Proc. 3: 535-540.

Fritsch, F. E. 1935. The structure and reproduction of the algae, vol. I. London. xvii + 791 pp. 245 figs.

Gaarder, T. 1932. Untersuchungen über Produktions- und Lebensbedingungen in norwegischen Austern-Pollen. Bergens Museums Arbok, Naturvidenskapelig rekke, Nr. 3, 64 pp. 11 figs.

Gaarder, T. & E. Alvsaker. 1941. Biologie und Chemie der Auster in den norwegischen Pollen. *Ibid.* Nr. 6, 236 pp. 69 figs.

Gaarder, T. & H. H. Gran. 1927. Investigation of the production of plankton in the Oslo Fjord. Cons. Perm. Int. p. l'Explor. de la Mer., Rapp. et Proc.-Verb. 42: 1-48. 2 figs.

Gilson, H. C. 1937. The nitrogen cycle. Scientific reports of the John Murray Expedition, 1933-34. 2: 21-81. 16 figs.

Graham, H. W. 1943. Chlorophyll-content of marine plankton. Jour. Marine Res. 5: 153-160. 1 fig.

Gran, H. H. 1905. Diatomeen. *In* Brandt and Apstein, Nordisches Plankton, Botanischer Teil. 19: 1-146. 178 figs. Kiel und Leipzig.

Gran, H. H. 1927. The production of plankton in the coastal waters off Bergen. March to April 1922. Report on Norwegian Fish. and Mar. Invest. 3: no. 8. 74 pp. 8 figs. Bergen.

Gran, H. H. 1931. On the conditions for the production of plankton in the sea. Cons. Perm. Int. p. l'Explor. de la Mer, Rapp. et Proc.-Verb. 75: 37-46.

Gran, H. H. 1933. Studies on the biology and chemistry of the Gulf of Maine. II. Distribution of phytoplankton in August, 1932. Biol. Bull. 64: 159-182.

Gran, H. H. & T. Braarud. 1935. A quantitative study of the phytoplankton in the Bay of Fundy and the Gulf of Maine (including observations on hydrography, chemistry and turbidity). Jour. Biol. Board of Canada. 1: 279-467. 69 figs.

Gran, H. H. & T. G. Thompson. 1930. The diatoms and the physical and chemical conditions of the sea water of the San Juan Archipelago. Publ. Puget Sound Biol. Sta. 7: 169-204. 9 figs.

Gross, F. 1942. The harvest of the sea. Proc. Roy. Phil. Soc. Glasgow. 66: 79-90.

Gross, F., J. E. G. Raymont, S. M. Marshall & A. P. Orr. 1944. A fish farming experiment in a sea loch. Nature. 153: 483-489.

Gunther, E. R. 1936. A report on oceanographical investigations in the Peru coastal current. *Discovery* Reports. 13: 107-276. 71 figs. 3 plates.

Hardy, A. C. 1936. Plankton ecology and the hypothesis of animal exclusion. Proc. Linn. Soc. London, 148th session 64-70.

Hardy, A. C. & E. R. Gunther. 1935. The plankton of the South Georgia whaling grounds and adjacent waters. 1926-1927. *Discovery* Reports. 11: 1-456. 193 figs.

Hart, T. J. 1934. On the phytoplankton of the south-west Atlantic and the Bellingshausen Sea. *Ibid.* 8: 3-268. 84 figs.

Hart, T. J. 1942. Phytoplankton periodicity in Antarctic surface waters. *Ibid.* 21: 261-356. 19 figs.

Harvey, H. W. 1926. Nitrate in the sea. Jour. Marine Biol. Assn., U. K. 14: 71-88. 3 figs.

Harvey, H. W. 1928. Biological chemistry and physics of sea water. x + 194 pp. 65 figs. Cambridge.

Harvey, H. W. 1933. On the rate of diatom growth. Jour. Marine Biol. Assn., U. K. 19: 253-276. 3 figs.

Harvey, H. W. 1934. Measurement of phytoplankton. *Ibid.* 19: 761-773. 9 figs.

Harvey, H. W. 1934A. Annual variation of planktonic vegetation, 1933. *Ibid.* 19: 775-792. 5 figs.

Harvey, H. W. 1937. The supply of iron to diatoms. *Ibid.* 22: 205-219. 2 figs.

Harvey, H. W. 1939. Substances controlling the growth of a diatom. *Ibid.* 23: 499-520.

Harvey, H. W. 1940. Nitrogen and phosphorus required for the growth of phytoplankton. *Ibid.* 24: 115-123. 2 figs.

Harvey, H. W. 1945. Recent advances in the chemistry and biology of sea water. vii + 164 pp. 29 figs. 16 tables. Cambridge.

Harvey, H. W., L. H. N. Cooper, M. V. Lebour, & F. S. Russell. 1935. Plankton production and its control. Jour. Marine Biol. Assn., U. K. 20: 407-441. 16 figs.

Hentschel, E. 1932. Die biologischen Methoden und das biologische Beobachtungsmaterial der *Meteor* Expedition. Wiss. Erg. Deutsche Atlantische Expedition *Meteor.* 10: vi + 274 pp. 7 figs. 1 chart.

Hentschel, E. 1936. Allgemeine Biologie des Südatlantischen Ozeans. *Ibid.* 11: xii + 343 pp. 123 figs. 42 charts.

Hentschel, E. & H. Wattenberg. 1930. Plankton und Phosphat in der Oberflachenschicht des Südatlantischen Ozeans. Ann. der Hydrogr. und maritimem Meteorol., Berlin, 58: 273-277.

Hustedt, F. 1930. Die Kieselalgen Deutschlands Österreichs und der Schweiz. Rabenhorst's Kryptogamen-Flora. Band VII. Leipzig, xii + 920 pp. 542 figs.

Jenkin, P. M. 1937. Oxygen production by the diatom *Coscinodiscus excentricus* in relation to submarine illumination in the English Channel. Jour. Marine Biol. Assn., U. K. 22: 301-342. 9 figs.

Juday, C. 1943. The utilization of aquatic food resources. Science. 97: 456-458.

Juday, C. & C. L. Schloemer. 1938. Effect of fertilizers on plankton production and on fish growth in a Wisconsin lake. Prog. Fish Culturist. 40: 24-27.

Ketchum, B. H. 1939. The absorption of phosphate and nitrate by illuminated cultures of *Nitzschia Closterium.* Amer. Jour. Bot. 26: 399-407. 4 figs.

Ketchum, B. H. 1939A. The development and restoration of deficiencies in the phosphorus and nitrogen composition of unicellular plants. Jour. Cell. and Comp. Physiol. 13: 373-381.

Ketchum, B. H. (1947). Biochemical relations between marine organisms and their environment. Ecol. Monogr. 17: 309-315. 5 figs.

Kofoid, C. A. & T. Skogsberg. 1928. The Dinoflagellata: The Dinophysoidae. (Report *Albatross* Exped. 1904-1905). Mem. Mus. Comp. Zool., Harvard Coll. 51: 766 pp. 103 figs. 31 plates.

Kofoid, C. A. & O. Swezy. 1921. The free-living unarmored Dinoflagellata. Mem. of the Univ. Cal. 5: 562 pp. 388 figs. 12 plates.

Kreps, E. & N. Verjbinskaya. 1930. Seasonal changes in the phosphate and nitrate content and in hydrogen ion concentration in the Barents Sea. Cons. Perm. Int. p. l'Explor. de la Mer, J. du Cons. 5: 329-346. 8 figs.

Kreps, E. & N. Verjbinskaya. 1932. The consumption of nutrient salts in the Barents Sea. *Ibid.* 7: 25-45. 8 figs.

Krey, J. 1939. Die Bestimmung des Chlorophylls in Meerwasser-Schöpfproben. *Ibid.* 14: 201-209. 4 figs.

Krogh, A. 1934. Conditions of life in the ocean. Ecol. Monogr. 4: 421-429.

Manning, W. M., C. Juday & M. Wolf. 1938. Photosynthesis of aquatic plants at different depths in Trout Lake, Wisconsin. Trans. Wis. Acad. Sci. Arts & Letters. 31: 377-410. 13 figs.

Mare, M. F. 1940. Plankton production off Plymouth and the mouth of the English Channel in 1939. Jour. Marine Biol. Assn., U. K. 24: 461-482. 10 figs.

Marshall, S. M. & A. P. Orr. 1928. The photosynthesis of diatom cultures in the sea. *Ibid.* 15: 321-360. 24 figs.

Moberg, E. G. 1928. The interrelation between diatoms, their chemical environment and upwelling water in the sea, off the coast of Southern California. Proc. Nat. Acad. Sci. 14: 511-518.

Nielsen, E. Steemann (*see* Steeman Nielsen, E.).

Rakestraw, N. W. 1936. The occurrence and significance of nitrite in the sea. Biol. Bull. 71: 133-167. 12 figs.

Rakestraw, N. W. & T. von Brand. 1947. Decomposition and regeneration of nitrogenous organic matter in sea water. VI. The effect of enzyme poisons. *Ibid.* 92: 110-114. 1 fig.

Raymont, J. E. G. 1947. A fish farming experiment in Scottish sea lochs. Sears Foundation: Jour. Marine Res. 6: 219-227.

Redfield, A. C. 1934. On the proportions of organic derivatives in sea water and their relation to the composition of plankton. James Johnstone Memorial Volume, Univ. of Liverpool, 176-192. 5 figs.

Redfield, A. C. & A. B. Keys. 1938. The distribution of ammonia in the waters of the Gulf of Maine. Biol. Bull. 74: 83-92. 6 figs.

Redfield, A. C., H. P. Smith & B. H. Ketchum. 1937. The cycle of organic phosphorus in the Gulf of Maine. *Ibid.* 73: 421-443. 4 figs.

Riley, G. A. 1938. The measurement of phytoplankton. Internat. Rev. der ges. Hydrobiol. und Hydrogr. 36: 371-373.

Riley, G. A. 1938A. Plankton studies. I. A preliminary investigation of the plankton of the Tortugas region. Sears Foundation: Jour. Marine Res. 1: 335-352. 4 figs.

Riley, G. A. 1939. Plankton studies. II. The Western North Atlantic, May-June, 1939. *Ibid.* 2: 145-162. 3 figs.

Riley, G. A. 1940. Limnological studies in Connecticut. Part III. The plankton of Linsley Pond. Ecol. Monogr. 10: 279-306. 8 figs.

Riley, G. A. 1941. Plankton studies. III. Long Island Sound. Bingham Oceanog. Coll. Bull. 7: art. 3, 1-93. 14 figs.

Riley, G. A. 1941A. Plankton studies. IV. Georges Bank. *Ibid.* 7: art. 4, 1-73. 4 figs.

Riley, G. A. 1942. The relationship of vertical turbulence and spring diatom flowerings. Sears Foundation: Jour. Marine Res. 5: 67-87. 6 figs.

Riley, G. A. 1943. Physiological aspects of spring diatom flowerings. Bingham Oceanog. Coll. Bull. 8: art. 4, 1-53. 15 figs.

Riley, G. A. 1944. The carbon metabolism and photosynthetic efficiency of the earth as a whole. American Scientist. 32: 129-134.

Riley, G. A. 1946. Factors controlling phytoplankton populations on Georges Bank. Sears Foundation: Jour. Marine Res. 6: 54-73. 8 figs.

Riley, G. A., H. Stommel & D. F. Bumpus. 1949. Quantitative ecology of the plankton of the western North Atlantic. Bingham Oceanog. Coll. Bull. 12, art. 3. 1-169. 39 figs.

Sargent, M. C. 1940. A theoretical definition of production. Sixth Pacific Science Congress, Cal., 1939. Proc. 3: 513-516.

Schreiber, E. 1927. Die Reinkultur von marinem Phytoplankton und deren Bedeutung für die Erforschung der Productionsfähigkeit des Meerwassers. Komm. z. wissensch. Untersuch. der deutschen Meere in Kiel und d. biologischen Anstalt auf Helgoland, Wissensch. Meeresuntersuch., N. F. Abt. Helgoland 16, H. 2, Nr. 10: 1-34. 11 figs. 1 plate.

Seiwell, H. R. 1935. The annual organic production and nutrient phosphorus requirement in the tropical Western North Atlantic. Cons. Perm. Int. p. l'Explor. de la Mer, J. du Cons. 10: 20-32. 1 fig.

Snieszko, S. F. 1941. Pond fish farming in Poland. *In* "A Symposium on Hydrobiology." 227-240. 5 figs. Madison, Wisconsin.

Spoehr, H. A. 1926. Photosynthesis. New York. 393 pp. 16 figs.

Steemann Nielsen, E. 1937. The annual amount of organic matter produced by the phytoplankton in the Sound off Helsingør. Medd. fra Kommissionen f. Danmarks Fiskeri-og Havundersøgelser. Serie: Plankton. Band III, Nr. 3. 38 pp. 6 figs.

Steemann Nielsen, E. 1937A. On the relation between the quantities of phytoplankton and zooplankton in the sea. Cons. Perm. Int. p. l'Explor. de la Mer, J. du Cons. 12: 147-154. 1 fig.

Sverdrup, H. W. & W. E. Allen. 1939. Distribution of diatoms in relation to the character of water masses and currents off Southern California in 1938. Sears Foundation: Jour. Marine Res. 2: 131-144. 12 figs.

Sverdrup, H. W. & R. H. Fleming. 1941. The waters off the coast of Southern California. March to July, 1937. Scripps Inst. Oceanog. Bull. 4: 261-378. 66 figs.

Sverdrup, H. W., M. W. Johnson, & R. H. Fleming. 1942. The Oceans. Their physics, chemistry and general biology. x + 1087 pp. 265 figs. 7 charts. New York.

Swingle, H. S. & E. V. Smith. 1941. The management of ponds for the production of game and pan fish. *In* "A Symposium on Hydrobiology." 218-226. 5 figs. Madison, Wisconsin.

Thompson, T. G. & R. Bremmer. 1935. The occurrence of iron in the waters of the North East Pacific Ocean. Cons. Perm. Int. p. l'Explor. de la Mer, J. du Cons. 10: 39-47. 5 figs.

Thompson, T. G. & T. Wilson. 1935. The occurrence and determination of manganese in sea water. Jour. Amer. Chem. Soc. 57: 233-236.

Transeau, E. N. 1926. The accumulation of energy by plants. Ohio Jour. Sci. 26: 1-10.

von Brand, T. (*see* Brand, von, T.).

Waksman, S. A., M. Hotchkiss, & C. L. Carey. 1933. Marine bacteria and their rôle in the cycle of life in the sea. II. Bacteria concerned in the cycle of nitrogen in the sea. Biol. Bull. 65: 137-167. 8 figs.

Waksman, S. A., H. W. Reuszer, C. L. Carey, M. Hotchkiss, & C. E. Renn. 1933A. Studies on the biology and chemistry of the Gulf of Maine. III. Bacteriological investigations of the sea water and marine bottoms. *Ibid.* 64: 183-205.

Wimpenny, R. S. 1936. The distribution, breeding and feeding of some important plankton organisms of the South-West North Sea in 1934. Fish. Invest. Gt. Britain. Ser. II, 15: no. 3, 53 pp. 24 figs.

ZoBell, C. E. 1935. The assimilation of ammonium nitrogen by *Nitzschia Closterium* and other marine phytoplankton. Proc. Nat. Acad. Sci. 21: 517-522. 1 fig.

ZoBell, C. E. 1946. Marine Microbiology. xv + 240 pp. 12 figs. Waltham, Mass.

Contents of Manual of Phycology

("A NEW SERIES OF PLANT SCIENCE BOOKS", Vol. 27)

1) **History of Phycology,** *by* G. W. PRESCOTT, Michigan State College, East Lansing, Michigan 1

2) **The Classification of Algae,** *by* G. M. SMITH, Stanford University, Stanford, California 13

3) **Chlorophyta,** *by* M. O. P. IYENGAR, University of Madras, Madras, India 21

4) **Euglenophyta,** *by* T. L. JAHN, University of California, Los Angeles, California 69

5) **Chrysophyta,** *by* F. E. FRITSCH, Queen Mary College, University of London, London, England 83

6) **Pyrrophyta,** *by* H. W. GRAHAM, United States Fish and Wildlife Service, Oakland, California 105

7) **Phaeophyta,** *by* G. F. PAPENFUSS, University of California, Berkeley, California 119

8) **Cyanophyta,** *by* F. DROUET, Natural History Museum, Chicago, Illinois .. 159

9) **Rhodophyta,** *by* K. M. DREW, University of Manchester, Manchester, England 167

10) **Fossil Algae,** *by* J. H. JOHNSON, Colorado School of Mines, Golden, Colorado 193

11) **Cytology of Algae,** *by* H. C. BOLD, Vanderbilt University, Nashville, Tennessee 203

12) **Sexuality of Algae,** *by* G. M. SMITH, Stanford University, Stanford, California 229

13) **The Pigments of Algae,** *by* H. H. STRAIN, Division of Plant Biology, Carnegie Institution of Washington, Stanford, California 243

14) **Physiology and Biochemistry of Algae,** *by* L. R. BLINKS, Hopkins Marine Station, Stanford University, Stanford, California 263

15) **Ecology of Fresh Water Algae,** *by* L. H. TIFFANY, Northwestern University, Evanston, Illinois 293

16) **Ecology of Marine Algae,** *by* J. FELDMANN, Faculté des Sciences de Paris, Paris, France 313

17) **Plankton Algae and their Biological Significance,** *by* B. H. KETCHUM, Woods Hole Oceanographic Institution, Woods Hole, Massachusetts .. 335

Appendix A) **Methods for the Cultivation of Algae,** *by* E. G. PRINGSHEIM, University of Cambridge, Cambridge, England 347

Appendix B) **Microtechnique,** *by* D. A. JOHANSEN, California Botanical Materials Company, Pomona, California 359

Contribution No. 491

Reprinted from CONTRIBUTIONS FROM THE CUSHMAN FOUNDATION FOR FORAMINIFERAL RESEARCH
Volume II, Part 3, October, 1951
Printed by Dorr's Print Shop, Bridgewater, Massachusetts, U. S. A.

30. FORAMINIFERA OF NARRAGANSETT BAY[1]

RUSHDI SAID
Mount Holyoke College, South Hadley, Massachusetts

ABSTRACT—Results are given of a quantitative study of the Foraminifera of Narragansett Bay in an attempt to decipher the ecologic conditions which determine the appearance of the species in the area. Two foraminiferal populations are noticed: the first is characteristic of the southern and more saline waters and the second thrives in the northern brackish areas. The topography of the bottom and the type of sediment exert control on the appearance of the species, while salinity is a dominant factor in their distribution. Foraminiferal numbers in the Bay are lower than those in the continental shelf and larger numbers are observed in the interior brackish areas of the Bay.

INTRODUCTION

Narragansett Bay includes the intercommunicating system of water ways that discharge into the Atlantic Ocean through the navigable entrances between Point Judith and Sakonnet Point in the state of Rhode Island. Conanicut Island and Rhode Island separate the southern portion of this water area into three passages known as Western Passage, Eastern Passage and Sakonnet River. A number of smaller islands are distributed over the Bay, and many small bays and river entrances indent its shores. Of the tributary streams the two most important are Providence River and Taunton River which flow into the northern and eastern parts of the Bay respectively. The various passages serve as highways for water-borne traffic to and from the numerous towns situated on the Bay. Of major importance are the ports of Newport, about three miles inside the entrance to Eastern Passage; Providence, at the head of Providence River about twenty-seven miles from the ocean; and Fall River, at the mouth of Taunton River about eighteen miles from Newport.

In spite of the fact that Narragansett Bay is one of the important fishing centers of the East Coast of the United States, very little work has been done on its hydrography. As far as the author is aware, Haight's work (1938) is the only study on the hydrography of the area. This work is particularly concerned with the tidal currents which regularly sweep into the Bay. The results of Haight's calculations are reproduced in condensed chart form by the U. S. Coast and Geodetic Survey (1945). Narragansett Bay is subjected to tidal currents which move freely in and out of the Bay and make possible the mixing of all water bodies.

The salinity and temperature distribution of the Bay has not been observed in detail, although the general pattern is known (Riley 1948; Sumner, Osborn and Cole 1913). The salinity distribution in the numerous bays that indent the East Coast of America is subjected to great variations and the pattern is complex and varied. Fresh water enters Narragansett Bay through the two main rivers and runoff and the surface water is likely to have very low salinities. In general salinities between 25 and 28 o/oo may be expected at the bottom waters even near the rivers. Although no complete data is available, it is almost certain that these salinities do increase gradually by approaching the open ocean. Saline waters are known to penetrate the rivers as far as the tidal currents are effective.

The bottom configuration of Narragansett Bay is very irregular. Apparently little change in bottom topography occurred after the inundation of the area in post-glacial time. The Eastern Passage is a deep irregular basin of some 150 feet in maximum depth and with an average depth of 80 feet. The Western Passage is a shallow flat with a maximum depth of some 50 feet and an average depth of 25 feet. The Sakonnet River is a shallow and slightly irregular waterway with a maximum depth of 50 feet and an average of 25 feet in depth. The northern areas of both the Eastern and Western Passages around Prudence Island are shallower flats with some irregularity and an average depth of 30 feet.

Sediments vary from gravels, which are common in the Eastern Passage, to sand and silt. The sediments on the whole are not well sorted, although they become better sorted near the river mouths. The results of mechanical analyses of some samples are given in table I in terms of median diameter and sorting coefficient. Mechanical analyses were carried out by sieving and pipette methods (Krumbein and Pettijohn 1938). Wentworth size classification is used in designating the names of the sediments except for the coarse sediments where gravel was preferred to pebble as the former name appears in the charts of the U. S. Coast and Geodetic Survey. The "muds" which the charts of the Survey show are probably silts (in the Wentworth sense).

No data are available on the nitrogen percentage of the sediments of Narragansett Bay, but the analyses of four samples show that the sediments of the Bay possess high organic content. The result of these analyses is given in table I. The determination of nitrogen was made by the Kjeldahl method and the procedure of analysis followed was that described by Trask and Patnode (1942, pp. 36-38).

Acknowledgments: The writer is much indebted to Dr. Charles J. Fish, Director of Narragansett Marine

---

[1] Contribution No. 491 from the Woods Hole Oceanographic Institution.

TABLE I

Sample No.	Depth (in ft.)	Location		Md (in mm)	So	N %	Remarks
		Lat.	Long.				
1	70	41°25′40″	71°25′10″	.04	1.72		Core
2	76	41 25 40	71 22 40				Grab
3	89	41 25 30	71 19 40				Core
4	76	41 26 20	71 17 00				Grab
5	42	41 29 20	71 13 30	.38	1.12		Grab
6	33	41 34 10	71 13 00				Core
7	38	41 37 00	71 13 40	.02	1.81		Core
8	20	41 39 30	71 14 50	.02	1.95		Core
9	27	41 36 25	71 23 00				Grab
10	16	41 38 30	71 22 00	.51	1.71	.16	Grab
11	21	41 38 30	71 23 40				Core
12	14	41 40 40	71 25 00			.18	Core
13	4	41 40 50	71 25 00	.14	1.08		Grab
14	20	41 41 00	71 18 00	.07	1.31		Core
15	16	41 41 20	71 21 20	.18	1.11		Grab
16	10	41 42 40	71 20 00	.20	1.12		Grab
17	22	41 38 30	71 19 40				Core
18	25	41 38 30	71 17 00				Core
19	75	41 36 00	71 17 30	.19	1.09		Grab
20	95	41 34 30	71 18 00				Core
21	90	41 31 40	71 20 00				Core
22	78	41 31 40	71 21 30				Core
23	55	41 31 40	71 23 40	.17	1.07		Grab
24	24	41 31 40	71 24 00	.17	1.13	.22	Grab
25	26	41 30 20	71 23 30	.18	1.10		Grab
26	30	41 27 30	71 25 10	.31	1.40		Grab
27	47	41 27 50	71 24 20				Core
28	100	41 27 30	71 22 30	.17	1.13		Grab
29	128	41 20 30	71 20 30	1.62	1.88		Grab
30	131	41 30 40	71 20 40	2.20	1.97		Grab
31	43	41 33 30	71 20 40	.07	1.62		Core
32	32	41 34 30	71 21 30				Core
33	26	41 34 30	71 23 00				Core
34	20	41 34 30	71 24 40	.04	1.59	.21	Core

Biological Laboratory for allowing the full use of one of the ships of his laboratory for the collection of samples. He is also indebted to Professor Henry C. Stetson for his keen interest in the problem and for the help he has so generously given during the progress of this work. Sincere thanks are offered to Dr. Alfred R. Loeblich, Jr., and to Miss Ruth Todd for checking some of the foraminiferal identifications.

Collection of samples: Thirty-four samples (eighteen cores and sixteen grabs) were collected from Narragansett Bay during the summer of 1950. Core samples were collected by a Hough coring tube and the grab samples were obtained by an "orange peel" (for the description of these devices, see Hough, 1939). Only the top parts of cores were examined. Table I gives the locations, the median grain size diameter, the sorting coefficient and the nitrogen percentage of the different samples. Figure 1 shows the areal distribution of the samples collected.

SYSTEMATIC WORK

Fifty-five species of Foraminifera observed in Narragansett Bay are arranged systematically below according to Cushman's classification.

ASTRORHIZIDAE

Rhabdammina cf. **R. linearis** H. B. Brady

SACCAMMINIDAE

Psammosphaera fusca F. E. Schultze
Proteonina atlantica Cushman
Armorella sphaerica Heron-Allen and Earland
Tholosina bulla (H. B. Brady)
Thurammina papillata H. B. Brady

HYPERAMMINIDAE

Saccorhiza ramosa (H. B. Brady)

REOPHACIDAE

Reophax dentaliniformis H. B. Brady
R. nana Rhumbler

LITUOLIDAE

Haplophragmoides columbiense Cushman

TEXTULARIIDAE

Textularia cf. **T. tenuissima** Earland

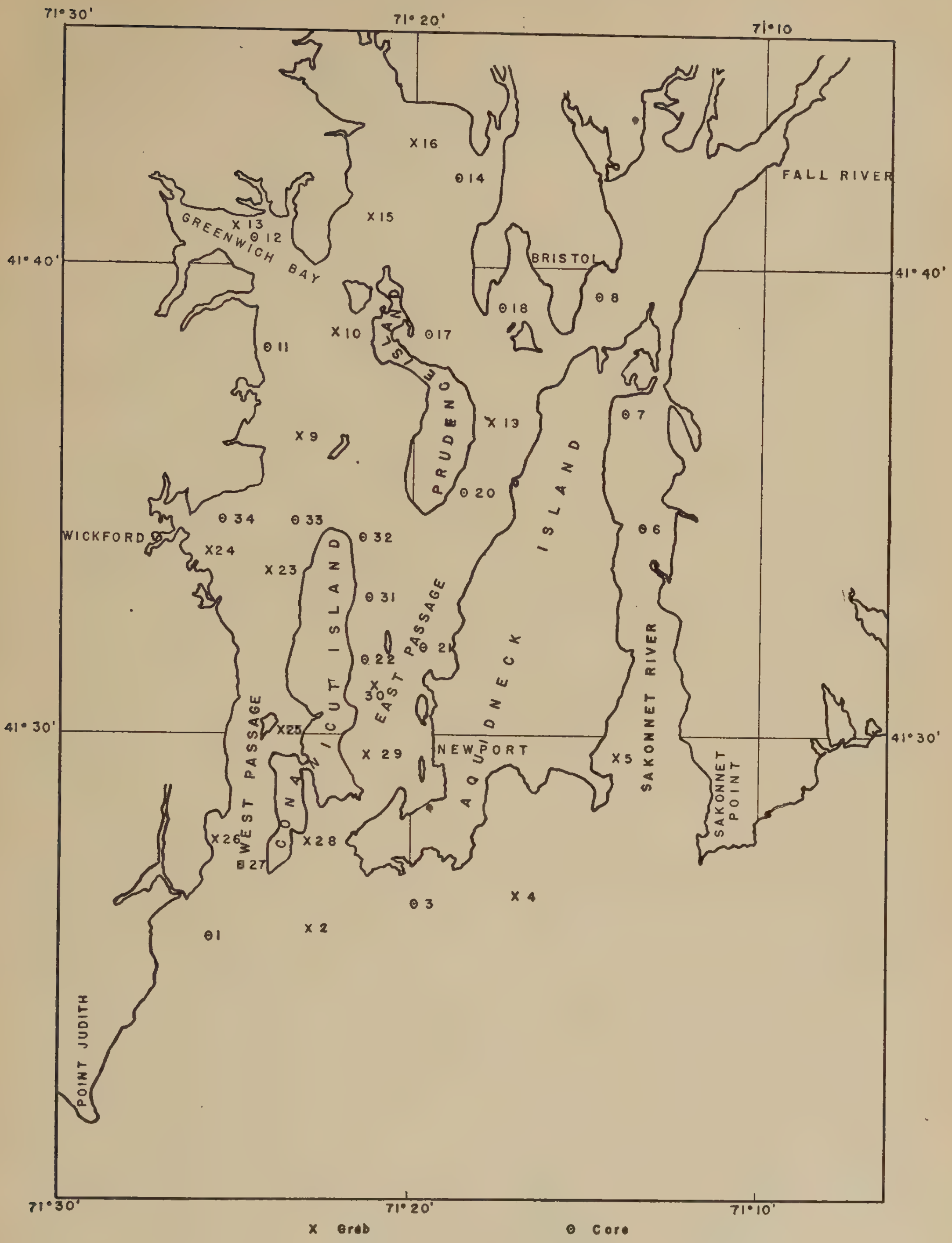
71° 30'
71° 20'
71° 10
41° 40'
41° 40'
41° 30'
41° 30'
71° 30'
71° 20'
71° 10'
FALL RIVER
X 16
⊖ 14
X 15
GREENWICH BAY
X 13
⊖ 12
BRISTOL
⊖ 8
⊖ 18
X 10
⊖ 17
⊖ 11
PRUDENCE ISLAND
X 13
⊖ 7
X 9
⊖ 20
⊖ 6
⊖ 34
⊖ 33
⊖ 32
WICKFORD
X 24
X 23
⊖ 31
EAST PASSAGE
⊖ 22
⊖ 21
X 30
AQUIDNECK ISLAND
SAKONNET RIVER
WEST PASSAGE
CONANICUT ISLAND
X 25
X 29
NEWPORT
X 5
SAKONNET POINT
X 26
X 28
⊖ 27
⊖ 3
X 4
⊖ 1
X 2
POINT JUDITH
X Grab
⊖ Core

Figure 1: Map of Narragansett Bay showing Sample Locations

VALVULINIDAE

Eggerella advena (Cushman)

MILIOLIDAE

Quinqueloculina seminula (Linné)
Q. seminula (Linné) var. **jugosa** Cushman
Q. disciformis (Macgillivray)
Q. vulgaris d'Orbigny
Miliolinella sp.
Triloculina tricarinata d'Orbigny
Pyrgo subsphaerica (d'Orbigny)

SILICINIDAE

Miliammina fusca (H. B. Brady)

OPHTHALMIDIDAE

Cornuspira planorbis Schultze

TROCHAMMINIDAE

Trochammina lobata Cushman
T. inflata (Montagu)
T. squamata Parker and Jones

LAGENIDAE

Lagena gracillima (Seguenza) var. **mollis** Cushman

POLYMORPHINIDAE

Guttulina lactea (Walker and Jacob)
Globulina glacialis Cushman and Ozawa
Pseudopolymorphina novangliae (Cushman)

NONIONIDAE

Nonion pauciloculum Cushman
N. tisburyensis Butcher
Nonionella atlantica Cushman
Elphidium advenum (Cushman)
E. advenum (Cushman) var. **margaritaceum** Cushman
E. discoidale (d'Orbigny)
E. excavatum (Terquem)
E. frigidum Cushman
E. incertum (Williamson)
E. incertum (Williamson) var. **clavatum** Cushman
E. subarcticum Cushman

BULIMINIDAE

Buliminella elegantissima (d'Orbigny)
Bulimina elegans d'Orbigny
B. marginata d'Orbigny
Fissurina laevigata Reuss
F. globosa (Montagu)
Virgulina fusiformis (Williamson)
Bolivina pseudoplicata Heron-Allen and Earland
Hopkinsina pacifica Cushman var. **atlantica** Cushman

ROTALIIDAE

Discorbis bertheloti (d'Orbigny) var. **floridensis** Cushman
D. subaraucana Cushman
Eponides frigidus (Cushman) var. **calidus** Cushman and Cole
Poroeponides lateralis (Terquem)
Rotalia beccarii (Linne)
R. beccarii (Linne) var. **tepida** Cushman

ANOMALINIDAE

Cibicides lobatulus (Walker and Jacob)
C. concentricus (Cushman)

All species recorded in the area have been described and figured by Cushman (1944) with the exception of the following: *Rhabdammina* cf. *R. linearis*, *Thurammina papillata*, *Textularia tenuissima*, *Miliolinella* sp., *Nonion tisburyensis*, *Nonionella atlantica*, *Elphidium frigidum*, *Bulimina elegans*, *Virgulina fusiformis*, and *Rotalia beccarii tepida*.

It is possible that *Nonion orbiculare* (H. B. Brady) of Cushman (1944, p. 24, pl. 3, fig. 24) is conspecific with *Elphidium frigidum* of this paper. Cushman (1944, p. 24) notes that some of the specimens tend "to develop what seem like very primitive retral processes and possibly this could be placed in *Elphidium*." *E. frigidum* is an obiquitous species in Narragansett Bay, occurring in both the northern and southern areas of the Bay in more or less equal abundance. The species is characterized by poorly developed retral processes. The two genera *Elphidium* and *Nonion* grade into one another in the Narragansett material and the problem is further complicated because some species of *Elphidium* (e. g. *E. incertum clavatum*) pass through an early *Nonion*-like stage without retral processes in their ontogeny. A preliminary investigation of the structure of the wall of *Elphidium* and *Nonion* has confirmed Wood's findings (1949) of the sharp difference in the character of their walls. A more detailed study of this problem is now under way and will be the subject of a future publication.

Cushman's *Reophax* sp. (1944, p. 10, pl. 1, fig. 20) is placed in the synonymy of *R. nana*. *Trochammina propria* Cushman (1944, p. 19, pl. 2, fig. 11) is suppressed and placed in the synonymy of *T. squamata*.

Narragansett Bay's *Reophax dentaliniformis* is without the characteristic neck. *Miliolinella* sp. of the above list resembles *Quinqueloculina vulgaris* in every detail except for the typical triangular large and flat tooth which closes the aperture.

THE DISTRIBUTION OF FORAMINIFERA

Method of study: Fifty grams of the dried grab samples and ten grams of the dried core samples were wet-sieved and fractions finer than 0.07 mm (200 mesh) were discarded. Coarser fractions were then treated by carbon tetrachloride for the separation of Foraminifera from the sediment. Foraminifera of each sample were then counted using the method described previously by the author (1950). Table II presents the results of this quantitative work in terms of numbers of specimens per gram of sediment. This method of presentation is believed to have the advantage of eliminating the discrepancies of the percentage method of presentation. For a complete discussion of the problems of the quantitative study of Foraminifera reference is given to a previous publication by the author (1950). Of the fifty-five species recorded in the area, only twenty-five occur abundantly enough to be counted separately and are therefore the only species to appear in table II. The remainder of the species occur in small numbers and in no case did they exceed 6% of the total number of Foraminifera.

Total numbers of Foraminifera: All Foraminifera observed in Narragansett Bay are benthonic. Coastal bays and protected lagoons are apparently unfavorable for the flourishing of pelagic species. The foraminiferal numbers of the Bay are small when compared with

TABLE II

	Proteonina atlantica	Armorella sphaerica	Reophax nana	Eggerella advena	Quinqueloculina seminula	Pyrgo subsphaerica	Trochammina lobata	Lagena gracillima mollis	Pseudopolymorphia novangliae	Nonion pauciloculum	N. tisburyensis	Nonionella atlantica	Elphidium advenum	E. frigidum	E. incertum	E. incertum clavatum	Bulimina elegans	Bolivina pseudoplicata	Hopkinsina pacifica atlantica	Discorbis bertheloti	Eponides frigidus calidus	Poroeponides lateralis	Rotalia beccarii	Cibicides lobatulus	Foraminiferal Number
1	☒			☒									▨	▨	⧓	▨				▨	▨		☒		21
2	☒			☒		▨	▨						▨		☒	▨	▨				▨		☒		12
3	☒			▨			▨					▨			▨	▨	▨						▨		4
4	▨			▨	▨	▨	▨	▨					▨	▨									▨		1
5				▨	☒	▨	▨		▨				▨	▨	▨	▨		▨		▨	▨	▨	☒		7
6											▨				☒	⧓					☒				18
7							▨			▨	▨		▨	▨	☒	▨					▨		▨		5
8							▨			▨	☒		▨	▨	⧗	☒					☒		▨		40
9		☒	▨							◢	☒		▨	☒	⧗	☒					◢		☒		80
10		▨	▨		▨				▨	☒			☒	◢	☒	⧗					◢				52
11		▨												☒	⧓	■					▨		☒		100
12															◢	⧓					▨		☒		25
13					▨										▨	▨									2
14														☒	⧓	⧗					☒				50
15										◢			☒	⧓	⧓	■					⧓		☒		150
16										☒			☒	☒	☒	⧗					◢		▨		38
17														☒	■	⧓					☒				100
18					▨				▨					☒	⧓	⧗					☒				60
19				▨										☒	◢	☒					☒		▨		15
20														▨	◢	▨					☒				10
21	▨	☒					▨		▨					▨	◢	☒					▨		▨		13
22				▨				▨						☒	◢								☒		14
23				☒	▨					☒	▨		☒	☒	☒	◢					☒	▨	☒		25
24					▨					☒	☒		☒	◢	☒	⧓					☒	▨	☒		36
25			▨		▨					☒	◢		▨	◢	☒	⧓					⧓		☒		58
26			▨		◢	☒	☒			◢	■	☒	⧓	☒	☒	⧓				⧓	⧓		⧓	◢	160
27				☒	▨					▨	⧓			◢	⧓	⧗				☒	☒		⧓		90
28		▨												▨	☒						☒		▨		2
29		☒	▨	▨	▨	▨	▨			☒	☒		☒	☒	▨	☒	▨	▨	☒	◢		☒	☒	☒	36
30	☒	☒	▨	☒			▨			☒				▨	◢	☒		▨	☒			▨	☒	▨	26
31	▨	▨		◢											☒	☒							☒		4
32	▨														☒	☒							▨		7
33											☒			☒	■	⧓					☒		☒		90
34														☒	■	☒					☒		☒		60

specimens in one gram of sediment

□ none ▨ less than one ☒ 1 5 ◢ 5-10 ⧓ 10-20 ⧗ 20-40 ■ more than 40 the West Atlantic Shelf (Parker 1948) or the Red Sea (Said 1950). The average foraminiferal number of all samples studied is 41 specimens per gram of sediment, a figure which is much lower than the average of 200-300 specimens per gram found in the open-ocean areas. It must be emphasized that the count per gram is affected by the terrigenous material received in the basin of deposition. Detrital material tends to decrease foraminiferal numbers per unit weight of sediment and it is probable that lower foraminiferal numbers in Narragansett Bay are partly due to more rapid deposition of sediment than for example in the Red Sea, which is situated in an arid region. For this reason, it may prove of more correlative value to record the number of Foraminifera per unit area. The calculation of such numbers was possible in the case of Narragansett Bay by counting the number of Foraminifera in the top layer of a core (surface area of the core used is 57 cm^2). The average number of Foraminifera in the core area is about 400, which would give roughly about 7 specimens per cm^2. It might be of interest to mention that the number of Foraminifera recorded in Narragansett Bay could be roughly estimated as 2.5×10^{13}, an impressive number for such a small area which is also less densely populated than many of the normal marine areas.

The small foraminiferal numbers could be attributed to lower salinities of the Bay, since the "overwhelming majority of Foraminifera are adapted to normal salinity" (Glaessner 1945). However, some species seem to flourish under conditions of lower salinity and one would expect these species to fill in the niche left by the elimination of other stenohaline species. In other words salinity should be expected to affect the kind of species living in the area rather than the total numbers. However, as will be seen in the following discussion, there is a distribution pattern of the species which can only be regarded as indicative of salinity control. It is probable that diurnal and seasonal temperature fluctuations coupled with salinity could bring an explanation of the small number of Foraminifera recorded in the Bay.

Figure 2 shows the concentration of Foraminifera in the different areas of the Bay. It is interesting to note that in general, foraminiferal numbers increase progressively away from the open ocean. This is contrary to the findings of Morishima (1948) in the Ago Bay, Kii Peninsula, Japan. It is possible that Morishima's results would be substantially altered if *Globigerina* and other pelagic species abundant at the entrance of the Ago Bay were not counted. Larger numbers of Foraminifera per gram of sediment are noticed near the approaches of the Providence River, around Prudence Island and along the Western Passage particularly near Wickford. This area is characterized by lower salinities and sandy bottoms and flat topography. Greenwich Bay, a small bay in the north west corner of the area, is characterized by very low numbers of Foraminifera, particularly in the near shore sample No. 13. This sample is procured from the tidal flat and is subject to drought during at least part of the low tide.

The foraminiferal numbers of the Eastern and Western Passages around Conanicut Island are sharply contrasted, the former having low numbers (average foraminiferal number is 12) and the latter having higher numbers (average foraminiferal number is 65). It seems that flat shallow sandy bottoms of the Western Passage are more favorable for the Foraminifera, than the gravelly, irregular and deep bottom of the Eastern Passage. Sakonnet River area is shallow and silty and the foraminiferal numbers are very low, in fact the lowest recorded in the area (average foraminiferal number is 6).

Optimum depth conditions for the development of Foraminifera in Narragansett Bay is between 15 and 30 feet (average foraminiferal number of samples collected between these depths is 71). Samples procured from deeper water are impoverished in Foraminifera (average foraminiferal numbers of samples collected from areas deeper than thirty feet is 18).

An interesting feature in Narragansett Bay is the presence in some impoverished samples of a large number of faecal pellets. The pellets are rod-like structures, circular in section and homogeneous in consistency, built of very fine sand bound by mucous material and are apparently of the simple "rod-type" described by Moore (1939, p. 517). It is likely that the small number of Foraminifera in these samples is due to a sand-eating invertebrate of probable molluscan affinities. Foraminifera in Narragansett Bay are therefore subject to drastic reduction in numbers because of the predatory habits of some molluscs which tend to clear the area of Foraminifera. Samples No. 7 and 8 are composed of the same species of Foraminifera present in the same percentages, although sample No. 7 has a low foraminiferal number and a great quantity of these faecal pellets.

It is interesting to note that Arrhenius (1950) has recently emphasized the effect of mud-eating organisms on the breakage of accumulated dead pelagic Foraminifera in the deep sea. In spite of the fact that Narragansett Bay is infested by predators as can be attested by the abundance of faecal pellets, no broken foraminiferal shells have been observed. Myers (1942, p. 34) has noted that foraminiferal shells attacked by mud eaters "could pass through the digestive tract of most invertebrates many times before they could show . . . . resolution." It seems therefore that predators influence benthonic foraminiferal populations by attacking and completely eliminating a large number of the young and early naked stages of benthonic Forami-

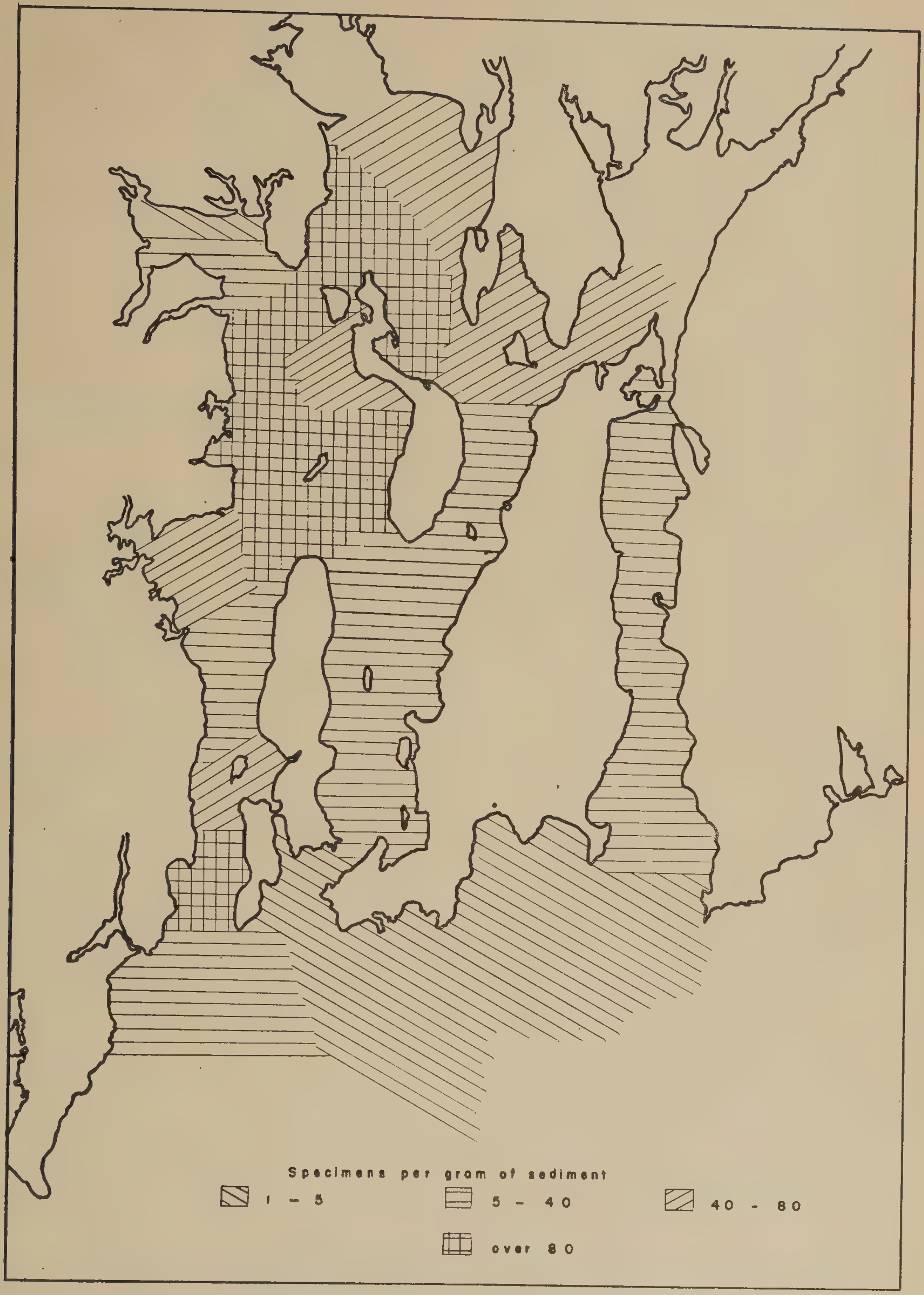
Specimens per gram of sediment
1 - 5
5 - 40
40 - 80
over 80

Figure 2 : The Distribution of Foraminifera in Narragansett Bay

nifera hindering the full development of the population. In the case of deep sea basins receiving largely dead shells of adult pelagic species, however, it is likely that the effect of predators would be the breakage of shells. Pelagic forms are more spherical and fragile than benthonic Foraminifera making them susceptible to crushing. It is therefore concluded that predators reduce total benthonic foraminiferal numbers without breaking the shells, while in a thanatocoenose of pelagic Foraminifera, the effect will be the destruction of shells without influencing directly total pelagic foraminiferal numbers.

Distribution of species: The number of foraminiferal species recorded in Narragansett Bay is limited, only fifty-five species having been observed. *Elphidium incertum* and *E. incertum clavatum* are by far the most abundant species in the area except in a few of the deeper water samples in the approaches of the Western Passage. These two species seem to have their maximum development in the less saline areas around Prudence Island. In fact, the number of specimens of these two species increases progressively away from the open ocean. Figure 3 shows the distribution of *E. incertum* in the Bay. Large numbers of this species are found in the Wickford area and along the eastern edge of Prudence Island, the approaches of Providence River and Taunton River. Greenwich Bay also has high numbers. The greatest concentration of *E. incertum clavatum* (as shown in figure 4) is along the western side of Prudence Island, although areas around Bristol also seem to favor the development of this species. The Western Passage has greater numbers of *E. incertum clavatum* than the Eastern Passage. An interesting observation is that the number of specimens of these two species increases away from the point of their origin, obviously the continental shelf of the Atlantic. This inference is of significance in view of the fact that some authors tend to consider the point of maximum number of a given species as the point of origin of that species. Biotic pressure is always in operation, but the success of the species is dependent not on its distance from the point of its origin, but on the suitability of the new environment. Although *E. incertum* and *E. incertum clavatum* occur together in most samples, one or the other is dominant in numbers: *E. incertum* is more common in silt samples, while *E. incertum clavatum* flourishes in sand samples.

The number of species in the northern samples is much less than those found in the southern approaches of the Bay. This is in harmony with Morishima's findings (1948). *Discorbis bertheloti, Proteonina atlantica, Eggerella advena, Bulimina elegans* and *Nonionella atlantica* are typical for the more saline southern waters. They either disappear completely in the northern areas or are represented only by a few specimens. It must be emphasized that although the southern part of the Bay contains a more diversified foraminiferal fauna, the foraminiferal numbers are lower.

Rotalia beccarii seems to flourish in the southern parts of the Bay. The number of specimens of this species is small and the species seems to occur uniformly along the southern approaches of the Bay in the Eastern and Western Passages as well as Sakonnet River, although there is evidence that it increases in numbers in sand samples. This is in harmony with Pratje's findings in the North Sea (1930). The restriction of this species to the southern parts of the Bay is in contrast with its widespread distribution in the Jade Bay (Bartenstein 1938).

Attached and arenaceous forms are few, but they seem to occur abundantly in the gravelly and deeper waters of the Eastern Passage.

Between the northern and southern foraminiferal assemblages, there is a zone of intermediate composition, particularly in the southern approaches of the Eastern Passage.

The distribution of *Nonion tisburyensis* is unique. This species occurs in large numbers in the approaches of the Western Passage, and less abundantly in Sakonnet River. It is not recorded in the normally saline waters off the Bay. *Elphidium* and *Nonion* assemblages found in the brackish upper Miocene deposits of the North Caucasus were interpreted as the result of grain size control (Glaessner 1945, p. 192). This is not apparent in Narragansett Bay, where *Nonion* specimens seem to be abundant in few samples irrespective of the mechanical composition of the sample.

Quinqueloculina seminula is the commonest representative of the family Miliolidae. This euryhaline species seems to develop abundantly in the more saline waters of the southern parts of the Bay. The distribution pattern of this species in Narragansett Bay coincides with its distribution in the Jade Bay (Bartenstein 1938, table 1b, p. 399).

SUMMARY AND CONCLUSIONS

The quantitative study of the Foraminifera occurring in thiry-four samples from Narragansett Bay is presented. The Bay is a coastal area characterized by an irregular bottom and shallow depth. The salinity is lower than normal and bottom temperatures vary greatly diurnally and seasonally. The sediments are either gravelly, sandy or silty. High nitrogen percentages are characteristic.

The total number of Foraminifera in the Bay is low, probably due to adverse conditions, particularly with regard to salinity. Zonation of the Bay into two facies is possible. There is a northern inner Bay facies characterized by an abundance of *Elphidium incertum* and *E. incertum clavatum* together with such euryhaline species as *E. frigidum* and *Eponides frigidus calidus*, and a southern outer bay facies characterized by the presence of *Proteonina atlantica, Discorbis bertheloti,*

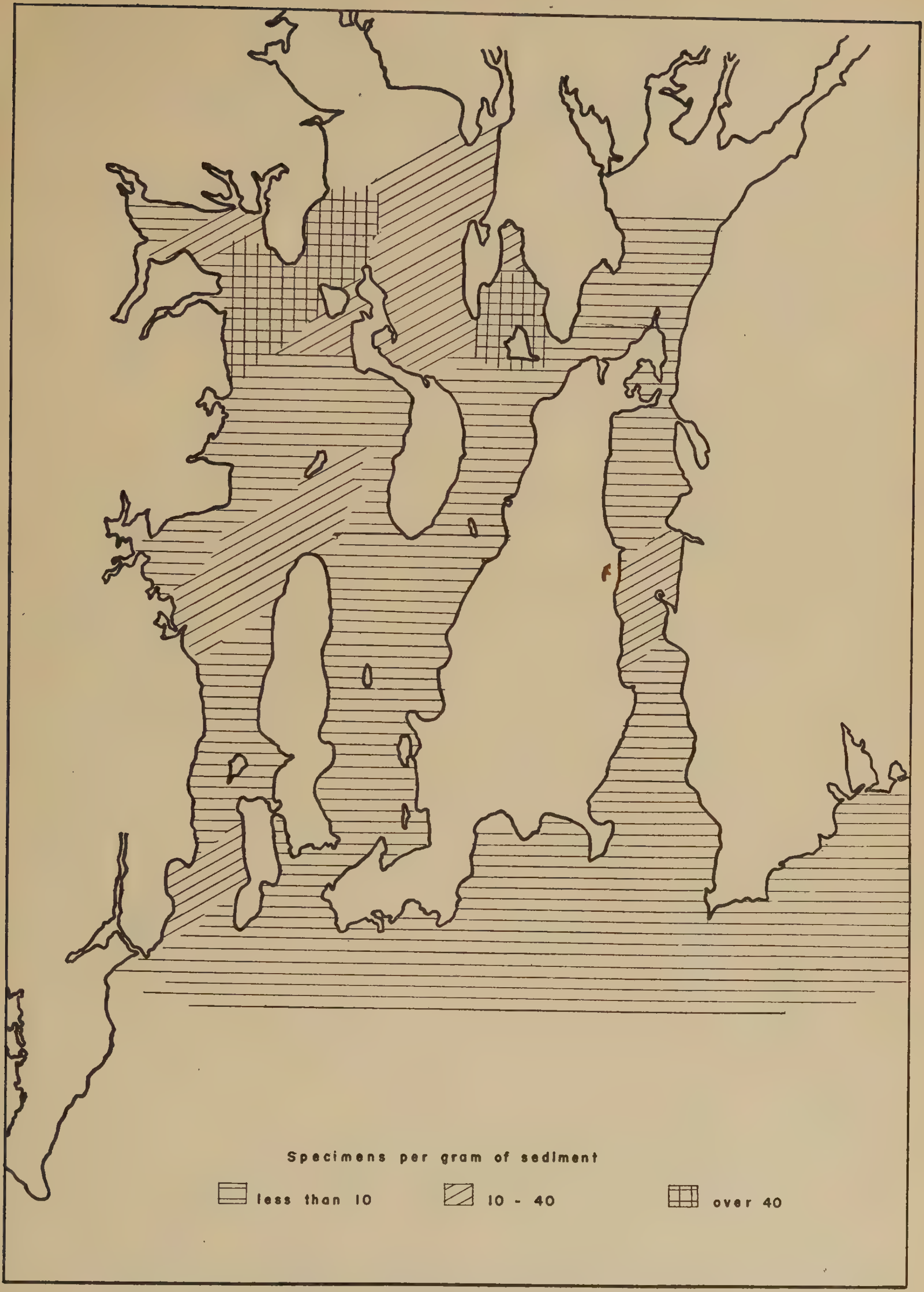
Specimens per gram of sediment
less than 10
10 - 40
over 40

Figure 3 : The Distribution of *Elphidium incertum* in Narragansett Bay

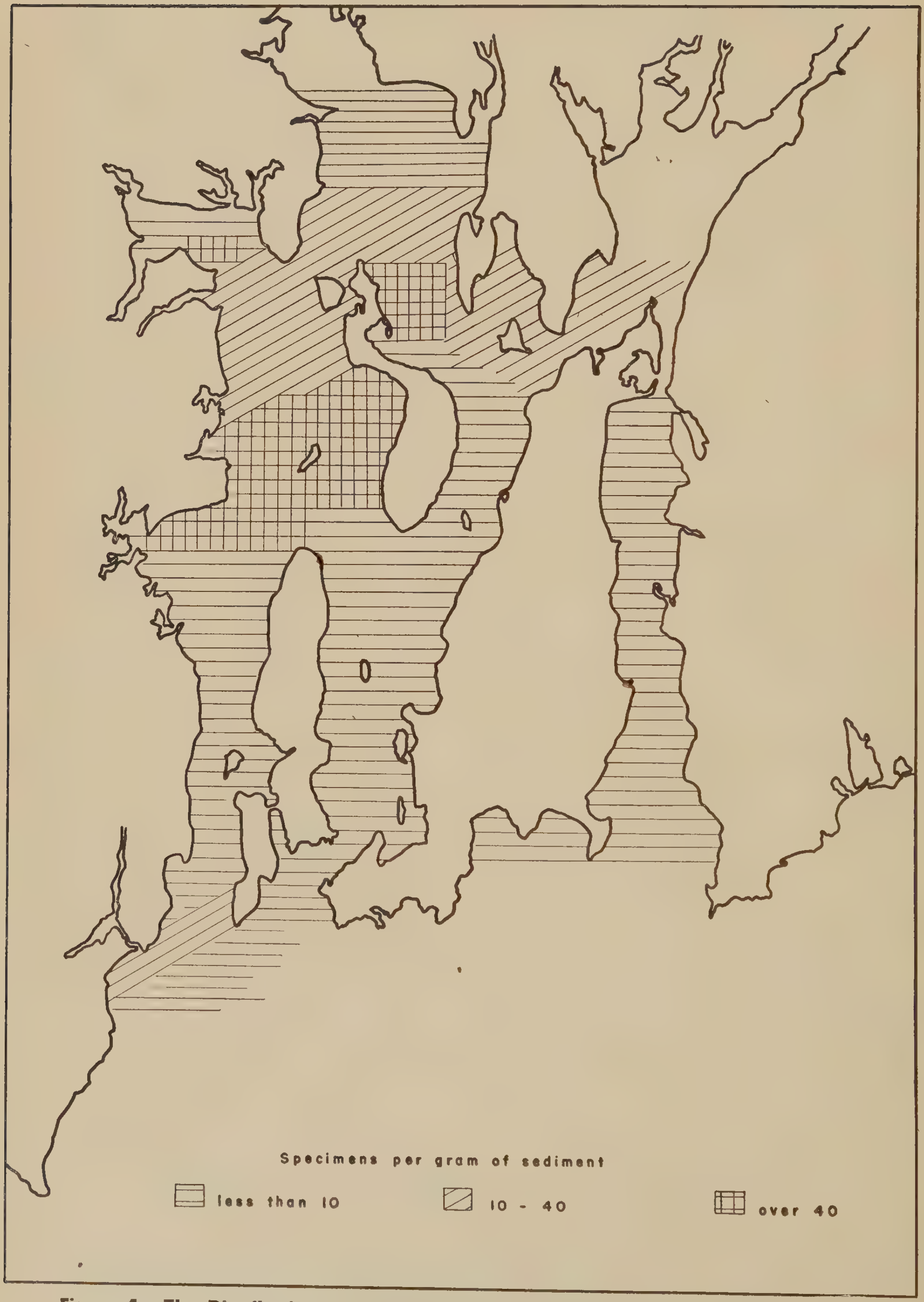
Specimens per gram of sediment
less than 10
10 - 40
over 40

Figure 4 : The Distribution of Elphidium incertum clavatum in Narragansett Bay

Eggerella advena, Nonionella atlantica, Cibicides lobatulus and *C. concentricus.* An intermediate zone between these two facies is noticed with *Nonion tisburyensis, N. pauciloculum, Rotalia beccarii* and *Quinqueloculina seminula.* This zonation is probably due to salinity control.

Hiltermann (1949) has recently summarized and supplemented Remane's work on the North Sea postulating the presence of five brackish water biotopes defined by the salinity of the water. It is possible that the two facies recognized in Narragansett Bay correspond to Hiltermann's brachyhaline (16½-30 o/oo salinity) and pliohaline (9-16 o/oo) brackish-marine water facies. The general characteristics of analogous areas in Narragansett Bay coincides well with Hiltermann's observations.

The bottom topography and type of sediment exert some influence on the appearance of species: gravelly bottoms are more favorable for the development of attached arenaceous Foraminifera, sandy bottoms seem to influence the numbers of *E. incertum clavatum* favorably, while finer silty bottoms are essential for the development of *E. incertum.* The fact that the Eastern and Western Passages differ in their bottom topography and type of sediment is reflected in the different foraminiferal populations of the two areas.

Predators play an important role in determining the number of Foraminifera present in the sediment. Evidence of the drastic effect of a sand-eating mollusc on the numbers of Foraminifera is particularly noticeable in Sakonnet River and the northern reaches of the Eastern Passage.

Foraminiferal numbers increase northward away from the open ocean although the number of species recorded decreases in the same direction. This may be attributed to flourishing under less competitive environment. Temperature does not seem to be of importance in Narragansett Bay in the local distribution of Foraminifera, inasmuch as the entire Bay is subject to more or less the same temperature conditions. However, the bottom of Narragansett Bay is exposed to drastic diurnal and seasonal temperature fluctuations and this might render the area unfavorable for the development of larger populations.

With few exceptions all foraminiferal species recorded in the area belong to the typical fauna characteristic of the areas south of Cape Cod. Cushman (1944) has already extended to the Foraminifera the well-known observation of the effect of the Cape Cod area as a barrier separating the northern and southern faunas of the Atlantic Coast. Six foraminiferal species previously recorded only from north of Cape Cod are now seen in very small numbers south of the Cape for the first time: *Tholosina bulla, Saccorhiza ramosa, Haplophragmoides columbiense, Triloculina tricarinata, Lagena gracillima mollis* and *Fissurina globosa.*

REFERENCES

Arrhenius, G., 1950, Foraminifera and Deep Sea Stratigraphy: Science, vol. 111, p. 288.

Bartenstein, H., 1938, Foraminiferen der meerischen und brackischen Bezirke des Jade-Gebietes: Senckenbergiana, vol. 20, pp. 386-412.

Cushman, J. A., 1944, Foraminifera from the shallow water of the New England Coast: Cushman Lab. Foram. Research, Special Publ. 12.

Glaessner, M. F., 1945, Principles of Micropalaeontology: Melbourne University Press, Melbourne.

Haight, F. J., 1938, Currents in Narragansett Bay, Buzzards Bay and Nantucket and Vineyard Sound: U. S. Coast and Geodetic Survey, Washington, D. C.

Hiltermann, H., 1949, Klassifikation der natürlischen Brackwässer: Erdöl und Kohle, vol. 2, pp. 4-8.

Hough, J. L., 1939, Bottom-sampling Apparatus: Recent Marine Sediments, P. D. Trask ed., Amer. Assoc. Petr. Geologists, Tulsa, Okla.

Krumbein, W. C. and Pettijohn, F. J., 1938, Manual of Sedimentary Petrography: Appleton Century, New York.

Moore, H. B., 1939, Faecal Pellets in Relation to Marine Sediments: Recent Marine Sediments, P. D. Trask, ed., Amer. Assoc. Petr. Geologists, Tulsa, Okla.

Morishima, M., 1948, Foraminiferal thanatocoenoses of Ago Bay, Kii Peninsula, Japan: Rep. Comm. Marine Ecol. and Paleoecol., No. 8, Nat. Res. Council, pp. 111-117.

Myers, E. H., 1942, Ecologic Relationships of some Recent and Fossil Foraminifera: *ibid,* No. 2, pp. 31-36.

Parker, F. L., 1948, Foraminifera of the Continental Shelf from the Gulf of Maine to Maryland: Bull. Mus. Comp. Zoology, Harvard, vol. 100, No. 2, pp. 213-241.

Pratje, O., 1930, Die Beziehungen der Foraminiferen der Deutschen Bucht (Nordsee) zu ihrer Umgebung: Paläont. Zeitschr., vol. 12, pp. 209-213.

Riley, G. A., 1948, Technical Report No. 11 on the Hydrography of the Western Atlantic; the Long Island and Block Island Sounds: Woods Hole Oceanogr. Inst., pp. 1-30.

Said, R., 1950, The Distribution of Foraminifera in the northern Red Sea: Contrib. Cushman Found. Foram. Research, vol. 1, pp. 9-29.

Sumner, F. B., Osborn, R. C. and Cole, L. J., 1913, A Biological Survey of the Water of Woods Hole and Vicinity, sec. 1 Physical and Zoological: Bull. U. S. Bur. Fisheries, vol. 31, pt. 1, pp. 11-441.

Trask, P. D. and Patnode, H. W., 1942, Source Beds of Petroleum: Amer. Assoc. Petr. Geologists, Tulsa, Okla.

U. S. Coast and Geodetic Survey, 1945, Tidal Current charts Narragansett Bay to Nantucket Sound: Washington, D. C.

Wood, A., 1949, The Structure of the Wall of the Test of Foraminifera; its Value in Classification: Quart. Journ. Geol. Soc. London, vol. 104, pp. 229-255.

Manuscript received February 6, 1951

Contribution No. 516

THE EXCHANGES OF FRESH AND SALT WATERS IN TIDAL ESTUARIES[1]

BY

BOSTWICK H. KETCHUM

Woods Hole Oceanographic Institution
Woods Hole, Massachusetts

ABSTRACT

An empirical theory is presented which describes the exchanges between various parts of an estuary as a result of tidal oscillations, and which permits the calculation of the average distribution of fresh and salt water within the estuary. The characteristics of the estuary used in the calculations are the mean range of tides, the river flow, and the topography, all readily available for most estuaries.

The calculations are shown to produce results which are similar to distributions observed in three very different estuaries. The theory will permit calculation of the changes in distribution of salinity and fresh water in any given estuary to be expected as a result of variation of river flow.

INTRODUCTION

In studies of the ecology of tidal estuaries the exchanges of fresh and salt water are of primary importance in determining the character of the environment. Thus, for example, the distribution of salinity and the extreme conditions to which sedentary organisms will be exposed are determined by these exchanges. The distribution of planktonic populations, of eggs spawned within the estuary, of pollutants introduced by cities or industries, in short, the distribution of any material dissolved or suspended in the water, is determined by the circulation of fresh and salt water and by the exchanges between various parts of the estuary. These exchanges, and the resulting distributions, are related in a regular way over short periods of time to the tidal oscillations and over longer periods of time to fluctuations of river flow. They are likewise related in more erratic ways to the effects of winds.

Although numerous estuarine studies have been made, the theoretical basis of the circulation is only slightly understood. Interpretation of survey data is improved by using the river water as a tracer to determine exchange ratios, flushing times and nontidal drifts (Tully, 1949; Ketchum, 1950; Ketchum, Redfield and Ayers, 1951).

In this paper an empirical theory is presented which describes the exchanges across various cross sections and which permits the calcu-

---

[1] Contribution No. 516 from the Woods Hole Oceanographic Institution. This investigation was supported in part by research grants from the National Institutes of Health, Public Health Service.

Reprint from SEARS FOUND. JOURN. MAR. RES.

lation of the resulting average distribution of fresh and salt water in an estuary. The exchanges of any other property of the water can be derived in a similar way. The data used in the calculations are tidal heights, river flow and the topography of the basin, all readily available on most important estuaries. The calculation is applied to three estuaries, and the hydrographic conditions which influence the results of the calculation are discussed.

SIMPLIFYING CONCEPTS

An estuary is defined as a region where river water mixes with, and measurably dilutes, sea water. The theory attempts to predict average conditions in successive volume segments of an estuary for a constant rate of river flow and the mean tidal range. Variations in the horizontal distribution of fresh water within a cross section, such as are commonly found as a result of Coriolis' forces, are neglected. The effects of vertical stratification will be discussed below.

The following simplifying concepts are involved:

1. *Steady State Distribution.* It is assumed that there is a steady state distribution of fresh and salt water within the estuary. This is obviously true for long periods of time, since estuaries are not becoming either fresher or more saline. At times of changing runoff of the rivers, however, the average distribution within the estuary changes, and the steady state distribution cannot be assumed.

In order to maintain a steady state the following conditions must be met at every complete cross section of the estuary:

a.) *Salt:* There must be no net exchange of salt during a tidal cycle across the section. This, of course, does not mean that the circulation of salt water is zero but that there is a balance between the inflow and outflow of sea water.

b.) *Fresh water:* During a tidal cycle there must move seaward a volume of fresh water equal to the volume introduced by the river in the same period of time.

2. *Inner End of Estuary.* The inner end of the estuary is defined as the section above which the volume required to raise the level of the water from low to high water mark is equal to the volume contributed by the river during a tidal cycle. There will be no net exchange of water through this section during a flood tide, since the entire rise of tide above the section is contributed by river flow. During the ebb tide there will be a loss through this section of one river flow per tide. Since there is no exchange on the flood tide the water above this section should be completely fresh. It will be noted that this is a

dynamic, not a geographic definition, since the boundary will move corresponding to changes in river flow.

3. *Segmentation of the Estuary.* The above paragraph defines a section which is the seaward boundary of the innermost volume segment of the tidal portion of the river. This is called Segment 0. Consecutive volume segments are defined so that the distance between their inner and outer boundaries is equal to the average excursion of a particle of water on the flooding tide. The average excursion is derived from the volume entering each part of the estuary on the flooding tide as well as the topography of the estuary. If the volume entering on the flooding tide were to act like a piston, displacing and pushing upstream its own volume of water from the next landward segment, the distance moved would be the average excursion of a particle of water on the flood tide in that part of the estuary. The segment so defined would contain, at high tide, a volume equal to that contained in the adjacent seaward segment at low tide. Consequently, along the length of the estuary each segment is so defined that the high tide volume in the landward one is equal to the low tide volume in the adjacent seaward one. Beginning with Segment 0, defined above, the entire estuary can thus be subdivided into a series of volume segments.

With R as the volume of river water introduced during a tidal cycle, P the local intertidal volume[2] and V the low tide volume of each segment, the following equations summarize these fundamental definitions:

1. The inner end of the estuary is defined as the section above which $P_0 = R$.
2. The limits of each successive volume segment are placed so that

$$\begin{aligned} V_1 &= V_0 + P_0, \\ V_2 &= V_1 + P_1 = V_0 + P_0 + P_1, \\ V_3 &= V_2 + P_2 = V_0 + P_0 + P_1 + P_2 \text{ etc.} \end{aligned}$$

It will be noted that the low tide volume in each segment equals the total tidal prism within the inner boundary of the segment, plus the low tide volume in Segment 0; that is,

$$V_n = V_0 + \Sigma_0^{n-1} P,$$

or, since $P_0 = R$: $$V_n = V_0 + R + \Sigma_1^{n-1} P.$$

---

[2] The tidal prism is defined as the volume of water required to produce the observed rise in water level in the estuary on the flooding tide. The part of the total tidal prism in each segment at high tide is called the local intertidal volume.

THE EXCHANGE RATIO

The estuary is divided into volume segments defined as above, so that the limits of each segment show the average excursion of a particle of water on the flood tide. If it is assumed that the water within such a volume segment is completely mixed at high tide, the proportion of water removed on the ebb tide will be given by the ratio between the local intertidal volume and the high tide volume of the segment. This same proportion of river water and of anything dissolved or suspended in the water will be removed by the ebb tide. Thus, an exchange ratio (r) can be defined for each segment (n):

$$r_n = \frac{P_n}{P_n + V_n} .$$

The effect of incomplete mixing on the exchanges will be discussed below.

The river water present in each segment is a mixture of river water accumulated during many tidal cycles. Each segment receives on each tidal cycle a volume of river water (R) equal to the volume introduced by the river in the same period of time. If we take R_1 as the volume of river water arriving during the current tidal cycle, then the amount removed on the ebb tide will be rR_1, and the amount remaining behind will be $(1 - r)R_1$. This same proportion of river water (R_2) arriving on the previous tidal cycle was left behind by the previous ebb tide, and the amount of this river water (of age two tidal cycles) removed will be $r\,(1 - r)R_2$ and the amount of this water remaining, after being depleted by two successive ebb tides, will be $(1 - r)^2\,R_2$. The proportion of water of various tidal ages removed, and remaining behind, as a result of the exchanges on any given ebb tide may be summarized as follows:

Age in Tidal Cycles	*River Water Removed*	*River Water Remaining*
1	rR_1	$(1 - r)\,R_1$
2	$r\,(1 - r)\,R_2$	$(1 - r)^2\,R_2$
3	$r\,(1 - r)^2\,R_3$	$(1 - r)^3\,R_3$
m	$r\,(1 - r)^{m-1}\,R_m$	$(1 - r)^m\,R_m$;

here 1, 2, 3 . . . m represent the number of tides each portion of the river water has been within the segment considered.

If the river flow is constant, all values of R are equal and the steady state condition can be assumed to exist. The total volume (Q_n) of river water accumulated within any volume segment (n) of the estuary at high tide is then the sum of the remaining volumes given in the final column above. Since the equation is written for the high tide condition, one volume of the river flow which has not yet been depleted is also present; that is,

$$Q_n = R\{1 + (1 - r_n) + (1 - r_n)^2 + (1 - r_n)^3 + \ldots + (1 - r_n)^m\} .$$

As m becomes large, this series will approach the limit

$$Q_n = R \frac{1 - (1 - r_n)^m}{r_n} .$$

Since $(1 - r)$ is always less than unity, $(1 - r)^m$ approaches zero after an infinite number of tidal cycles, and the sum can be reduced to

$$Q_n = \frac{R}{r_n} .$$

It will be remembered that one qualification of the steady state distribution was that the river water passing seaward through each cross section on each tidal cycle must equal the volume of river water (R) introduced during the same period of time. The above relationship states that the volume of river water moving seaward is the product of the exchange ratio and the accumulated volume of river water (rQ). It is readily seen that this product equals R, so that this criterion of steady state distribution is satisfied.

The exchange ratio is defined on the assumption of complete mixing of the volume of water in each segment at high tide. The average excursion of water during the flooding tide is presumed to set the upper limit of the length of the estuary over which complete mixing can be logically assumed. It is for this reason that the subdivision of the estuary is essential in the application of the theory.

Incomplete vertical mixing can be detected readily if salinity observations are available, since the water diluted by river effluent will be limited to the upper layers of the water column. Only the mixed volume of water should be considered in such a case, and the exchange ratio applicable would be

$$r'_n = \frac{P_n}{P_n + V_n} \times \frac{D}{H} ,$$

in which D is the average depth of the Segment n and H is the depth of the mixed layer. The exchange ratio so calculated will be greater, and the resulting accumulation of river water (Q) will be smaller than would be obtained if the entire depth were used. In such a case the segmentation of the estuary is also made using volumes computed to the mixed depth. The entire treatment is developed, therefore, as though the water below the mixed zone had no part in the tidal mixing process and could be replaced, without changing the distribution, by a false bottom.

Incomplete horizontal mixing will also modify the distributions to be expected. The effects are not incorporated into the theory since there are no independent criteria to evaluate their magnitude. The effects of incomplete horizontal mixing will be discussed qualitatively below.

EXCHANGES IN A MODEL ESTUARY

The exchanges in a theoretical estuary, rectangular in cross section, in which the depth at low tide is half of the high tide depth (i. e. $P = V$), will be calculated in order to indicate how the theory is applied. The results are presented in Table I. For every volume segment the exchange ratio is 0.5, and the accumulation of river water is $2R$. Taking R as unity, the volume enclosed in Segment 0 at high tide is 2, which is all river water—100% fresh. In Segment I, having a relative high tide volume of 4, half of the water is river water. On the ebb tide Segment I receives one volume (all of it fresh water) from the river (Segment 0) and loses 3 volumes ($P_0 + P_1$) at a concentration of 50% fresh water (1.5 volumes of river water) to Segment II. At low tide, therefore, Segment I contains 2 volumes, three-quarters of which is river water. On the flooding tide Segment I loses no water landward, since, above its inner limit, river flow is sufficient to provide the observed rise in water level. It receives from the adjacent seaward segment two volumes which contain 25% river water. The high tide content is thus returned to the original condition. The net result of the tidal oscillation has been to add to Segment I a volume of river water from the river, and to move an equal volume of river water from Segment I to Segment II. Similar treatments, shown for the river boundary and for the first four segments, can be expanded to the nth segment with the same net seaward transport of river water through every cross section. The fact that each segment returns to its original high tide content shows that the net exchange of salt during a tidal cycle is zero, and thus the steady state requirements are satisfied.

A basic assumption of the theory is that the mixing is complete within volume segments defined by the average excursion of a particle of water on the flooding tide. For each segment in Table I, complete mixing of the volumes of water added during the tidal cycle will produce mixed water of the same characteristics as the water present at high tide. In Segment I, for example, one volume of water is added on the ebb tide and two volumes on the flood tide. These three volumes contain a total of 1.5 volumes of river water. If they were mixed together the composition would be 50% fresh water—the same composition as the high tide content of the segment. However the mixing may be accomplished, the net effect of the mixing processes must be equivalent to the mixing of the volumes of water added to each segment during a tidal cycle if the theory is reliable.

APPLICATION TO NATURAL ESTUARIES

The total accumulation of river water has been calculated by the above method for Raritan River and Bay, New Jersey, for Alberni Inlet, B. C., and for Great Pond, near Falmouth, Massachusetts. These three estuaries are different in almost all characteristics. In all three, survey data are available which permit calculation of the fresh water content from the salinity distribution, so that the results of the survey and of the calculation can be compared. The method used, and described here for Raritan Bay, is similar for the other two locations.

Raritan River and Bay, New Jersey. A survey of Raritan River and Bay was made in December 1948, which permits comparison of the computed distribution of fresh and salt water with the observed distribution over a length of about 20 miles of the estuary. Raritan River and Bay have sandy or marshy shores, a maximum depth of 40 feet in dredged channels, and they vary in width from 0.1 to 7.0 miles. The surface area of the surveyed portion of the estuary was 1,670 million square feet, or about 45 square nautical miles. Since the mean range of tides is 5.5 feet, the total volume of the tidal prism is 9,200 million cubic feet. This is almost 300 times greater than the volume introduced by the river during a tidal cycle at the time of our survey.

In the Bay the average salinity for each of five cross sections was determined from the results obtained at 4 to 7 stations. These stations were occupied once each hour throughout the complete tidal cycle. The high tide data are used for comparison with the theory. In the river the results of a single station, occupied at high tide, was used to determine the average salinity across each section. The method used for calculating the distribution of fresh water from the salinity observations has been described by Ketchum, 1950.

The first step in the application of the theory is to determine the total low tide volume of the estuary enclosed by various cross sections. This is done by drawing numerous cross sections with the aid of a navigation chart and determining their cross-sectional area with a planimeter. The volume is computed by multiplying the distance

TABLE I. NET EXCHANGES IN A MODEL ESTUARY AS A RESULT OF TIDAL OSCILLATIONS AND RIVER FLOW (all volumes expressed as multiples of river flow).

Segment	*0*		*1*		*2*		*3*		*4*	
Intertidal volume (P_n)	1		2		4		8		16	
High tide volume ($P_n + V_n$)	2		4		8		16		32	
Exchange ratio (r_n)	0.5		0.5		0.5		0.5		0.5	
River water content (Q_n)	2.0		2.0		2.0		2.0		2.0	
% Fresh	100		50		25		12.5		6.25	
EBB TIDE EXCHANGES	Vol.	Fresh	Vol.	Fresh	Vol.	Fresh	Vol.	Fresh	Vol.	Fresh
Landward	0	0	+1.0	+1.0	+3.0	+1.5	+ 7.0	+1.75	+15.0	+1.875
Seaward	−1.0	−1.0	−3.0	−1.5	−7.0	−1.75	−15.0	−1.875	−31.0	−1.9375
Net change	−1.0	−1.0	−2.0	−0.5	−4.0	−0.25	− 8.0	−0.125	−16.0	−0.0625
FLOOD TIDE EXCHANGES										
Landward	+1.0	+1.0	−0	−0	−2.0	−0.5	− 6.0	−0.75	−14.0	−0.875
Seaward	0	0	+2.0	+0.5	+6.0	+0.75	+14.0	+0.875	+30.0	+0.9375
Net change	+1.0	+1.0	+2.0	+0.5	+4.0	+0.25	+ 8.0	+0.125	+16.0	+0.0625

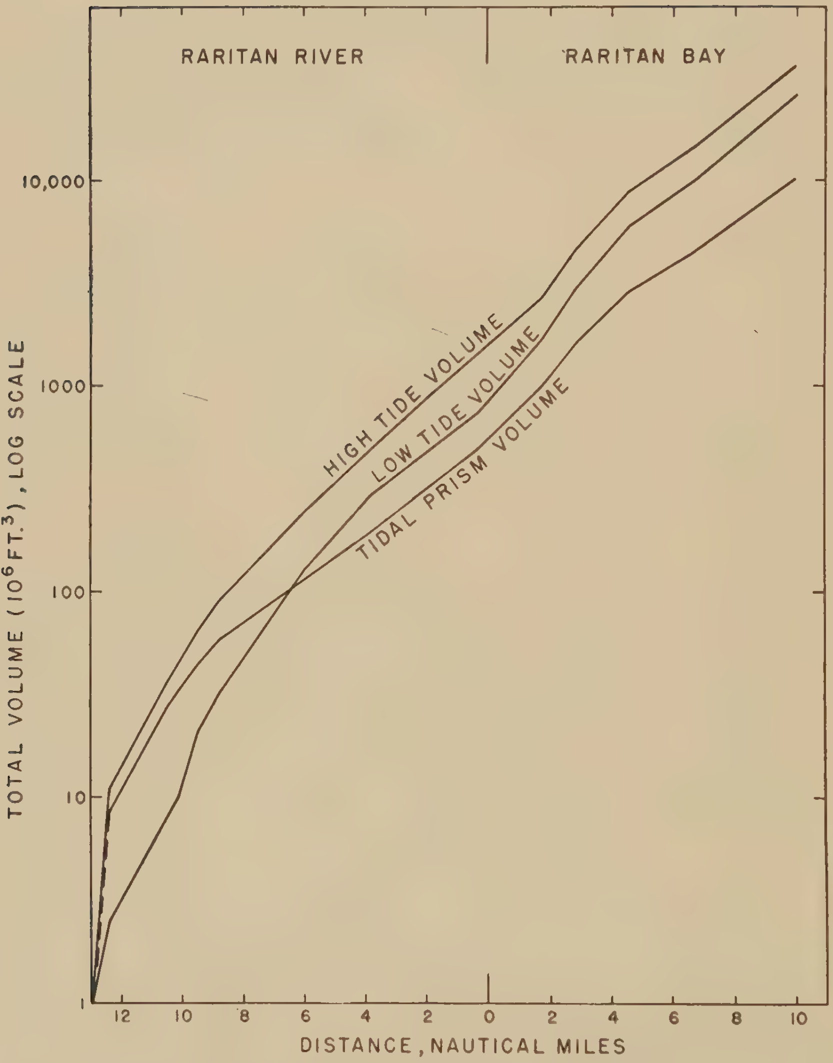

Figure 1. The cumulative volumes of water at low tide, high tide, and in the tidal prism enclosed by various cross sections in Raritan River and Bay. The river end of the estuary is at the left. (The semi-log scale is used for convenience only.)

between sections by the average of their cross-sectional areas. The cross sections drawn should be selected so that the change in width and depth of the estuary between sections is as uniform and gradual as possible. The sum of the volumes enclosed at low tide by each section is determined and plotted against the length of the estuary, as in Fig. 1.

The volume of the tidal prism is computed from the chart and from the tide tables using the mean range of tides. This volume is also plotted against the length of the estuary. The sum of these low tide and tidal prism volumes gives the high tide volume enclosed by each section, which is calculated and also plotted.

Determination of the segmentation of the estuary is illustrated in Table II for the average river flow that obtained during the survey conducted in December 1948 (33 x 10^6 ft.^{3}/tidal cycle). The distance at which the volume of tidal prism is equivalent to the river flow per tide (P_0) is read from the graph, and for the same distance the low tide (V_0) and high tide volumes ($P_0 + V_0$) are recorded. This defines Section 0 through which there is no net exchange on the flooding tide. The next section is located at the point where the enclosed low tide volume ($V_0 + V_1$) has increased by a volume equal to the high tide volume ($V_0 + P_0$) of the previous segment. The low tide, high tide and tidal prism volumes at this point, read from the various curves, are recorded. This process is repeated, placing each successive boundary where the increase in the low tide volume equals the high tide volume within the adjacent landward segment. The lengths of the segments enclosed by successive boundaries give the average excursion of a particle of water on the flooding tide.

TABLE II. SEGMENTATION OF RARITAN RIVER AND BAY, USING A RIVER FLOW OF 33 x 10^6 FT.^{3}/TIDAL CYCLE (740 FT.^{3}/SEC.)

	Segment	*Distance from River Mouth*	*Length of Segment*	*Cumulative Volumes* (10^6 *ft.*^{3})		
				Low Tide	*Tidal Prism*	*High Tide*
	(n)	*miles*	*miles*	$\Sigma_0^n V$	$\Sigma_0^n P$	$\Sigma_0^n (P + V)$
RARITAN RIVER	0	10.1	2.90	10	33	43
	I	7.8	2.30	53	75	128
	II	5.8	2.00	138	116	254
	III	4.1	1.70	264	180	444
	IV	2.2	1.90	454	305	759
	V	0.2	2.00	770	500	1,270
RARITAN BAY	VI	1.1	1.30	1,280	800	2,080
	VII	2.2	1.10	2,090	1,190	3,280
	VIII	3.1	0.90	3,290	1,710	5,000
	IX	4.2	1.10	5,010	2,500	7,510
	X	5.5	1.30	7,520	3,500	11,020
	XI	7.1	1.60	11,030	4,960	15,990
	XII	8.3	1.20	16,000	6,600	22,600
	XIII	9.6	1.30	22,610	9,200	31,810

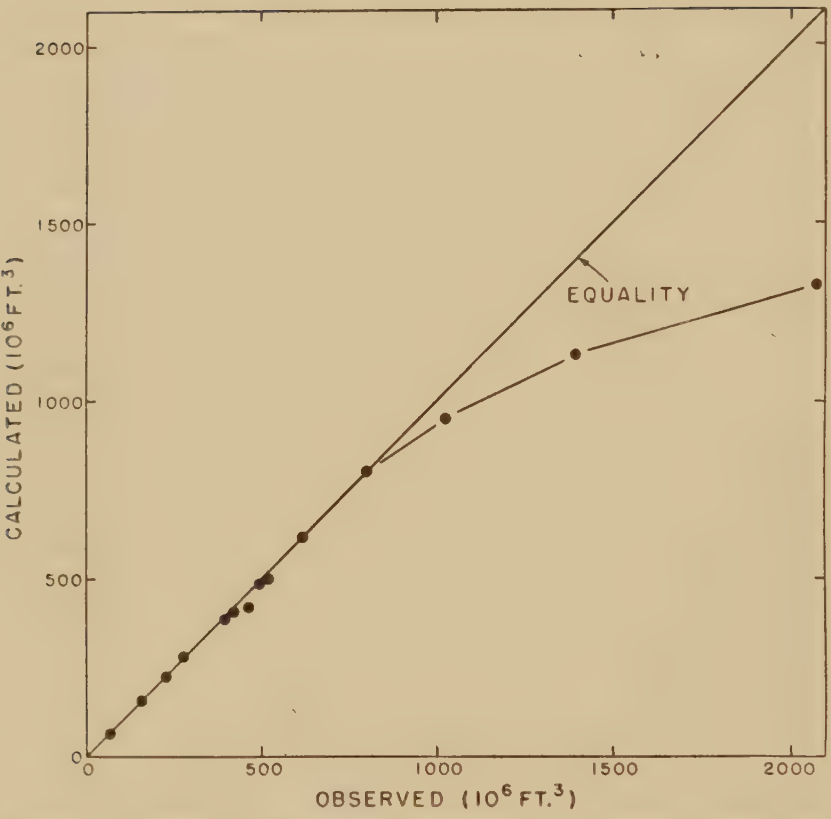

Figure 2. Comparison of the calculated accumulation of river water in Raritan River and Bay with the accumulation observed during a survey conducted in December 1948. The river flow was 33 x 10^6 ft.^{3}/tidal cycle (740 ft.^{3}/sec.).

The volumes within each segment, the tidal exchange ratios, and the calculated accumulation of river water are listed in Table III. The total volume of river water accumulated within the area has also been calculated from the salinity distribution observed during the hydrographic survey made in December 1948 (Ayers, Ketchum and Redfield, 1949). In Fig. 2 the accumulation of river water calculated by the theory described in this paper is compared to the accumulation observed during the survey. Excellent agreement between calculated and observed values was obtained within the eleven miles of the River and the first four miles of the Bay, where the total accumulated volume of river water was almost 800 million cubic feet. This volume of river water corresponds to 24 times the volume contributed by the river

TABLE III. CALCULATION OF THE ACCUMULATION OF RIVER WATER IN RARITAN RIVER AND BAY, USING A RIVER FLOW OF 33 x 10^6 FT.^{3}/TIDAL CYCLE (740 FT.^{3}/SEC.)

Segment	*Length of Segment*	*Local Volumes* Intertidal	High Tide	*Exchange Ratio*	*Accumulation*	
		P_n	$P_n + V_n$		Q_n	$\Sigma_0^n Q$
(*n*)	*miles*	10^6 *ft.*^{3}	10^6 *ft.*^{3}	*r*	10^6 *ft.*^{3}	10^6 *ft.*^{3}
0	2.90	33	43	0.767	43	43
I	2.30	42	85	0.494	67	110
II	2.00	41	126	0.325	102	212
III	1.70	64	190	0.337	98	310
IV	1.90	125	315	0.397	83	393
V	2.00	195	510	0.382	86	479
VI	1.30	300	810	0.370	89	568
VII	1.10	390	1200	0.325	102	670
VIII	0.90	520	1720	0.302	109	779
IX	1.10	790	2510	0.315	105	884
X	1.30	1000	3510	0.285	116	1000
XI	1.60	1460	4970	0.294	112	1112
XII	1.20	1640	6610	0.248	133	1245
XIII	1.30	2600	9210	0.282	117	1362

during a tidal cycle, i. e., to about the first 12 days of transport. Beyond this, the accumulation of river water calculated from the theory is less than the observed volumes of river water.

From the calculated accumulation of river water in each volume segment of the estuary, the percentage of fresh water and the salinity this would produce have been calculated. In Fig. 3 these are compared with the observed distribution of salinity and fresh water.[3] It will be seen that the difference between the calculated values and the observed values of accumulated river water in the outer part of the Bay correspond to small salinity differences. Since the plot in Fig. 2 is a cumulative one, and since the volumes in the Bay are great, this small difference in the salinity value results in a comparatively large discrepancy in the calculated total volumes. It is possible that the discrepancy is the result of incomplete horizontal mixing, the effects of which will be discussed below. The seepage of ground water into the Bay may contribute to the discrepancy.

It has been stated above that the subdivision of the estuary defines

---

[3] The source "sea water" which mixes with the Raritan River water is actually a mixture of Hudson River water and sea water which has a salinity of 27°/₀₀ (cf. Ayers, Ketchum and Redfield, 1949). This is the reason the salinity approaches 27°/₀₀ rather than a higher salinity as the percentage of Raritan River water approaches zero.

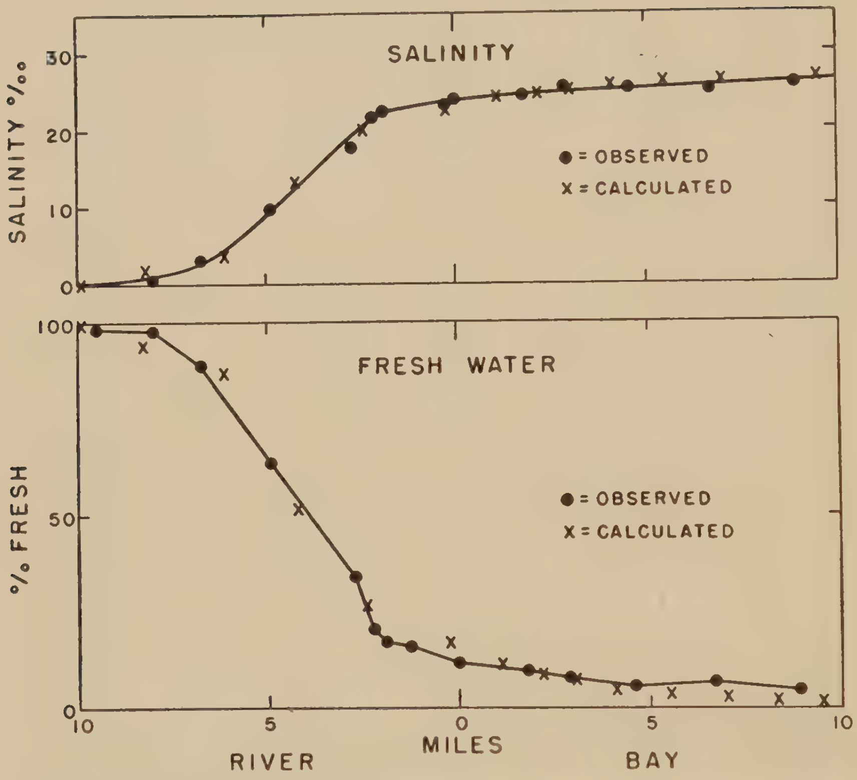

Figure 3. The observed and calculated distributions of salinity and fresh water in Raritan River and Bay in December 1948.

the average excursion of a particle of water on the flooding tide. A comparison of the distances between the boundaries in Table II with tidal currents measured by the Coast and Geodetic Survey (Marmer, 1935) is informative. Within the segments numbered X and XI, for example, the observed tidal currents at four stations at the center of the Bay produced transports which averaged 2.35 miles on the flooding tide.[4] The average velocity across the section would be approximately 0.7 of the velocity measured near the axis of the current. The average transport at this point would thus be about 1.65 miles per tide. The length of Segment X is 1.3 miles, of XI 1.6 miles. Measured currents at other locations within the Bay also gave trans-

---

[4] These transports are computed on the assumption that the tidal current curve approximates a cosin curve and that the average current velocity is $2/\pi$ multiplied by the maximum velocity.

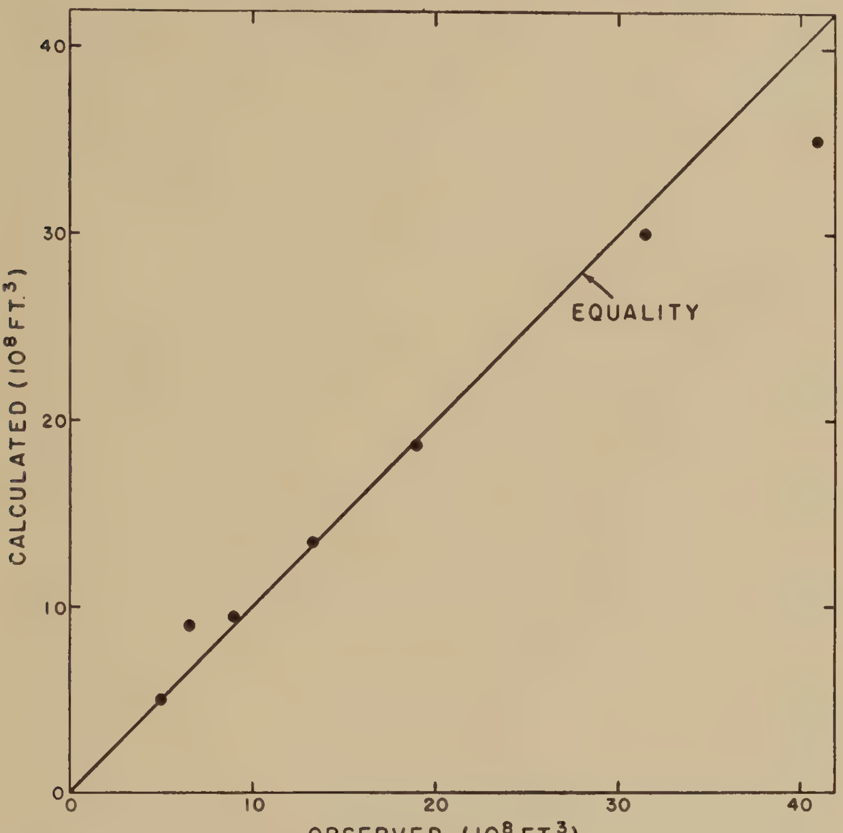

Figure 4. Comparison of the calculated accumulation of river water in Alberni Inlet with the accumulation observed by Tully (1949) on June 4, 1941 when the river flow was 1.2 x 10^8 ft.^{3}/tidal cycle (2,740 ft.^{3}/sec.).

ports which are approximately the same as the distances between boundaries calculated from the tidal displacement.

It may be concluded that the calculated distribution of fresh and salt water in Raritan River and Bay closely approximates the observed distribution for a length of about 15 miles of the estuary. The volume of river water within this part of the estuary corresponds to the volume introduced by the river during 24 tidal cycles.

Alberni Inlet, Vancouver Island, B. C. Tully (1949) has made extensive studies of the distribution of salinity and river water in Alberni Inlet. The Inlet is a typical fjord, having precipitous rocky sides with depths within the inlet as great as 1000 feet. This deep water is separated from water at comparable depths in the Pacific Ocean by an outer sill at a depth of 120 feet. A length of more than 21 miles was surveyed, and the average width of the inlet over this distance was 1.2 miles. The total tidal prism for the surveyed area is about 40 x 10^8 cubic feet, which is approximately 30 times as great as the volume contributed by river flow during a tidal cycle at the time selected for comparison of results. In almost all respects, therefore, it is different from Raritan River and Bay.

Tully found that the river water was always limited in distribution to the upper 10 meters of water. The Inlet has therefore been subdivided into volume segments which consider only the upper 30 feet, and the exchange ratios have been computed accordingly. This treatment produces an average transport through the outermost section during the flood tide of 2.5 miles. The transport computed for the entire depth of water was only 0.15 miles. Although direct current measurements appear not to be available for comparison, Tully records float observations for the upper end of the estuary which indicate that the larger transport is more likely to be correct.

Tully, in his Table XIV, presents data showing the total accumulated river water at various times. On June 4, 1941, the data given for the two innermost stations were collected at high water, the next two stations were occupied on the ebbing tide, the outermost station on the flooding tide. These data are not strictly comparable, therefore, to the calculation of high tide distribution, but the inner end of the estuary, where variations with the stage of the tide would be greatest, was surveyed at the appropriate time.

Fig. 4 compares the accumulation of river water calculated from the tidal exchange theory with Tully's values for the accumulation. Except at the outer end of the estuary, where the calculated accumulation is too small, the agreement is reasonably good. The maximum accumulation corresponds to nearly 34 times the contribution from the river during a tidal cycle.

Great Pond, Falmouth, Mass. Great Pond is a narrow, sandy embayment on the south shore of Cape Cod which receives the outflow of the Coonamessett River. The Pond is about a mile and a half in length, averages less than a quarter of a mile in width, and has a maximum depth of 9 feet at high tide. The mean range of tide is about 1.5 feet. The tidal prism volume for the surveyed part of the pond is 7.6 x 10^6 cubic feet, which is about 15 times as great as the volume introduced by the river during a tidal cycle at the time of the survey.

A survey of this pond was made in June 1950 when the river flow was half a million cubic feet per tide (10.7 $\text{ft.}^3/\text{sec.}$). The

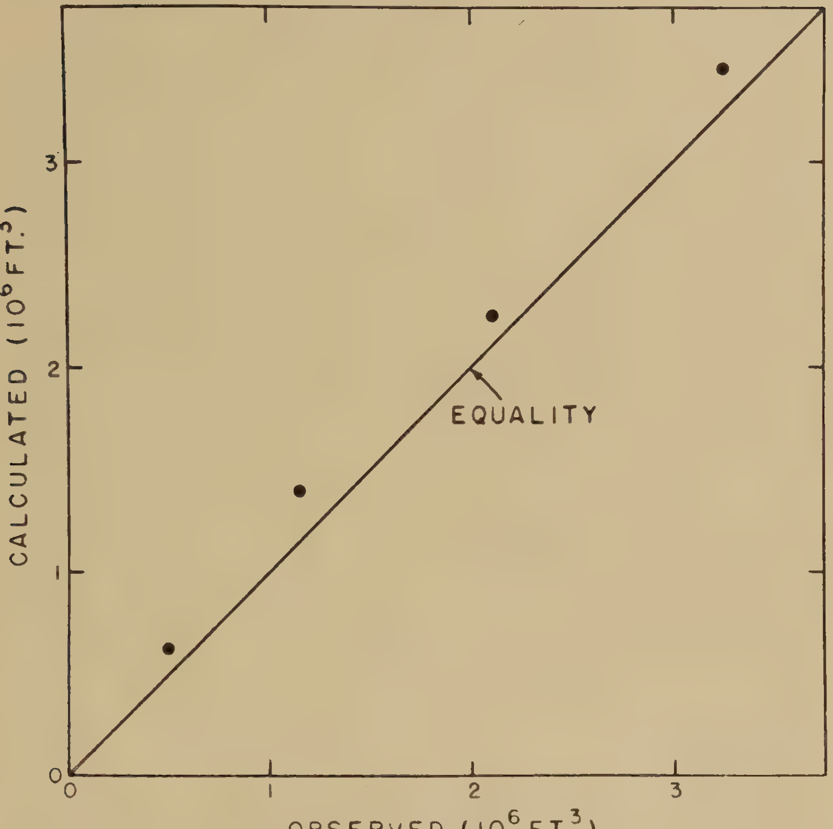

Figure 5. Comparison of the calculated accumulation of river water in Great Pond with the accumulation observed during a survey conducted on June 26, 1950 when the river flow was 0.5 x 10^6 ft.^{3}/tidal cycle (10.7 ft.^{3}/sec.).

salinity indicated that the river water was mainly restricted in depth to the upper half of the pond at high water. Consequently, in this pond, as in Alberni Inlet, the calculation must be made to the depth of the mixed layer in order to correct for incomplete vertical mixing.

The calculated volume of river water accumulated in the pond is compared to the volume deduced from the salinity distribution in Fig. 5. The agreement is good for the first mile of the estuary, which was as far as the calculation could be carried, since the next cross section would have been located beyond the limits covered by the survey. The total volume of accumulated river water was seven times as great as the volume contributed by the river during a tidal cycle.

DISCUSSION

It is somewhat surprising that a theory as simplified as this can be applied to such dissimilar estuaries as Raritan River and Bay, Alberni Inlet, and Great Pond. In order to illustrate the range of differences, some characteristics of the three estuaries are listed in Table IV. Perhaps one of the most interesting comparisons is between the volumes of the tidal prism and river flow, since these are the characteristics used in the calculations. There is more than a thousandfold range in the volume of the tidal prism and a range of 240 in the volume of river flow. The ratios between the tidal prism volume and river flow are also given in Table IV; they show that the tidal prism volumes vary from 15 to 279 times as great as the volume of river water contributed during a tidal cycle, an almost twentyfold range.

TABLE IV. Some Characteristics of the Three Estuaries Discussed

Characteristic	*Raritan River and Bay*	*Alberni Inlet*	*Great Pond*
Surveyed Length—Nautical miles	20	21	1.5
Surface Area—Sq. nautical miles	45	16	0.375
Maximum High Tide Depth—Feet	40	1000	9.0
Depth of Mixed Layer—Feet	Total*	30	3.5 – 5
Mean Range of Tides—Feet	5.5	6.4	1.5
Tidal Prism Volume (10^6 ft.^{3})	9200	4000	7.6
River Flow Per Tidal Cycle (10^6 ft.^{3})	33	120	0.5
Ratio $\frac{\text{Prism Volume}}{\text{River Flow}}$	279	33	15

* At each station the salinity was practically homogeneous from top to bottom. This survey was made in winter, and other observations show that stratification exists in summer.

The theory is based upon an assumption of complete mixing of water within various defined volume segments of the estuary at high tide. It will be useful to discuss, in a qualitative way, how incomplete mixing will influence the results of the calculation.

1. *Vertical Mixing.* The effects of incomplete vertical mixing have been discussed above but will be reviewed here. If the distribution of river water is restricted vertically to a surface layer, the actual tidal exchange will be greater than the exchange ratio calculated for the entire depth. A simple example will make this clear. If the mixed layer is half of the total depth at high tide, then the actual exchange will be $\frac{P}{0.5\,(P+V)}$. The exchange ratio (r) for half the depth would thus be twice as great as one calculated for the entire depth. The actual volume of river water accumulated within each segment (Q)

would be half of the volume which would be computed if the limitation of mixing to the upper half of the water column were ignored. This discrepancy can be corrected if salinity observations are available, and the correction has been used in both Alberni Inlet and in Great Pond.

2. *Transverse Horizontal Mixing.* It is frequently observed that the salinity contours in an estuary will indicate that, facing upstream, the salt water penetrates further on the right whereas the less saline water extends further seaward on the left of the estuary.[5] This is the result of the rotation of the earth. In such a distribution the mixing is obviously not complete in a transverse section across the estuary. A simple example will show the effect of this. If one postulates a distribution so that the estuary is divided into half longitudinally by the isohaline characteristic of pure sea water, one can assume that there is no seaward transport of river water through the right-hand half (facing upstream). Therefore all of the river water is escaping through the other half. The exchange ratio in this case would be $\frac{0.5\,P}{0.5\,(P + V)}$. The exchange ratio is thus the same as it would be for the entire segment and one would expect the same quantity of river water to accumulate. Since the river water would be contained in half of the total volume, however, it would obviously be present at twice the concentration.

3. *Longitudinal Horizontal Mixing.* If the mixing is not complete lengthwise between the sections defining the limits of a volume segment, the calculated exchange ratio will be too large and consequently the accumulation will be too small. If, for example, the mixing were complete over half, instead of over the total distance traversed by a particle of water during a flood tide, one should apply the same exchange ratio to two adjacent segments instead of to the single segment in order to compute the actual accumulation. The volume segment would thus contain double the accumulation calculated by the unmodified theory. It is possibly this error which results in the low calculated values at the outer ends of both Raritan Bay and Alberni Inlet. Unfortunately, there is no independent criterion which can be used to correct the exchange ratio for this condition. It can be recognized only by comparison of calculated with observed distributions.

The subdivision of the estuary is an integral and essential part of the theory. Sanitary engineers have considered the entire tidal prism at any cross section as though it were available for the dilution of introduced pollution. This inherently assumes that the mixing is complete longitudinally throughout the length of the estuary. Such a use of the tidal prism is an extreme example of incomplete longitudinal mixing. The above discussion shows that such an assumption will give too small an accumulation of river water, since a single exchange ratio is applied to the estuary as a unit. This leads to an exaggerated estimate of the rate of flushing. The application of the theory described in this paper to sanitary engineering problems is discussed by Ketchum (1951).

---

[5] This description applies to the northern hemisphere and would be reversed in the southern hemisphere.

Two criteria are available to determine whether the tidal exchange theory will give valid estimates of the distribution of fresh and salt water within the estuary. Where current data are available, comparison of the average excursion per tide with measured tidal currents provides a valuable check on the definition of the volume segments. It should be remembered, however, that sufficient current data are rarely available to obtain an accurate average flow across the complete cross section. Approximations must be used, such as those described by Keulegan and Hall (1950), as was done in this paper for Raritan Bay. Absolute agreement cannot be expected.

The salinity data can be used to determine whether mixing is vertically complete or not, and if it is not complete the correction for vertical mixing can be applied. The comparison of average salinity at any cross section in the estuary with a plot of the calculated longitudinal distribution of salinity, such as that shown in Fig. 3, gives a check on the horizontal mixing anomaly for the part of the estuary where salinity data are available.

The value of the theory lies in the fact that it describes the exchanges throughout the estuary which are necessary to maintain the steady state distribution. This implies that the physical processes controlling the distribution are incorporated in the theory, though the individual effect of each process cannot yet be evaluated. The major practical advantage of the theory is that it permits calculation of the distribution of fresh water and salinity to be expected in any given estuary with a variety of river flows. The calculations can be made without undertaking field work, since existing data found in tide tables, water supply journals, and navigation charts are used. The validity of the calculated distribution can be checked by comparison with salinities at high tide at various points within the estuary.

The theory has been developed with river water as an indicator substance. It should be pointed out that the same exchange ratio will apply to anything suspended or dissolved in the water. Thus, for example, if one were interested in the distribution of plankton, fish eggs, or pollution, the exchange ratio multiplied by the observed concentration would give a measure of the movements of the material to be expected during a tidal cycle. If, however, there is not a continuous and constant rate of supply of the material, the steady state conditions would not apply. If the rate of supply is known, however, the exchanges can be calculated and the distribution deduced as the tidal exchange distributes the material throughout the estuary.

SUMMARY

1. An empirical theory is presented which describes the exchanges between various parts of an estuary as a result of tidal oscillations and which permits the calculation of the average distribution of fresh and salt water within the estuary.

2. The characteristics of the estuary used in the calculation are the mean range of tides, the river flow, and the topography, all readily available for most estuaries.

3. The fundamental assumptions are: a) That a steady state distribution of fresh and salt water will exist throughout the estuary if the river flow is constant; b) that complete mixing will occur within volume segments defined horizontally by the width of the estuary and by the average excursion of a particle of water on the flood tide and vertically by the depth of the mixed layer. Discrepancies produced by incomplete mixing are discussed.

4. The calculated distributions of river water are compared with observed distributions for three very different estuaries, Raritan River and Bay, Alberni Inlet, and Great Pond. The tidal prism for these three estuaries includes more than a thousandfold range of volume, and the river flow varies by a factor of 240. The theory produces results which correspond closely with observed distributions of salinity and fresh water in all three estuaries.

REFERENCES

Ayers, J. C., B. H. Ketchum and A. C. Redfield
1949. Hydrographic considerations relative to the location of sewer outfalls in Raritan Bay. Woods Hole oceanogr. Inst., Rep. 49–13: 41 pp.; 16 figs.
Ketchum, B. H.
1950. Hydrographic factors involved in the dispersion of pollutants introduced into tidal waters. J. Boston Soc. civ. Engrs., *37:* 296–314.
1951. The flushing of tidal estuaries. Sewage and industrial wastes (in press).
Ketchum, B. H., A. C. Redfield and J. C. Ayers
1951. Hydrography of the New York Bight. Pap. phys. Oceanogr., *12* (1).
Keulegan, G. H. and J. V. Hall
1950. A formula for the calculation of the tidal discharge through an inlet. Bull. Beach Erosion Bd., *4:* 15–29.

Marmer, H. A.
1935. Tides and currents in New York Harbor. Spec. Publ. U. S. Cst. geod. Surv., No. 111: VII + 198 pp.

Tully, J. P.
1949. Oceanography and prediction of pulp mill pollution in Alberni Inlet. Bull. Fish. Res. Bd. Canada, *83:* 169 pp.

United States
Tide tables (Revised annually), U. S. Cst. geod. Surv., U. S. Gov't. Printing Office, Washington, D. C.
Surface water supply of the United States (Issued periodically), U. S. geol. Surv., U. S. Gov't. Printing Office, Washington, D. C.

Contribution No. 522

REPRINTED FROM THE JOURNAL OF EXPERIMENTAL BIOLOGY,
VOL. 28, NO. 2, pp. 215–217, JUNE 1951
[*All rights reserved*] PRINTED IN GREAT BRITAIN

WAVE-RIDING DOLPHINS*

BY A. H. WOODCOCK AND A. F. McBRIDE†

(*Received* 18 *May* 1950)

In an effort to explain the apparent ability of dolphins to ride the bow wave of a ship at a speed of 10 knots (Woodcock, 1948) it seemed necessary to show that the animals had weight while immersed. Measurements of the weight of an immersed *Stenella plagiodon* have been made.‡ First results indicate that a dead animal, which weighs 200 lb. in air, and is 6·5 ft. long, weighs 9·2 lb. when immersed in sea water. This animal, which was in good physical condition, was killed by injection just before the weighings were made.

Irving, Scholander & Grimel (1941, p. 152) have indicated that the lungs of dead *Tursiops truncatus* are collapsed. It is assumed therefore that the lungs of the dead *Stenella* were also collapsed at the time of weighing and that 9·2 lb. is near the maximum weight in sea water.

Irving *et al.* (1941) indicate that the volume of tidal air per 100 lb. of body weight for *Tursiops* is 2·7 l. Assuming the same proportions for *Stenella*, the tidal air volume for a 200 lb. animal is 5·4 l. At atmospheric pressure 5·4 l. of air will displace 5·54 kg. of sea water or 12·4 lb. Hence the *Stenella*, with tidal air expelled and weighing 9·2 lb., will weigh 9·2–12·4 lb., or −3·2 lb. in sea water with tidal air in its lungs. Thus these rough figures indicate that by breathing, dolphins can become lighter or heavier than the water which they displace. This indication is amply supported by the behaviour of *Stenella* in the tank at Marineland.

Stenella in the Marineland tank are observed to expel air from their lungs and to rest on the bottom for 4–6 min.§ Irving has said (personal communication) that dolphins can store oxygen in body fluids to such an extent that it is reasonable to suppose that they can stop breathing for several minutes with lungs empty of tidal air. It is therefore assumed that wave-riding dolphins remain 'heavy' in water by expelling tidal air.

Can a dolphin, which weighs 9·2 lb. in sea water fall down a wave front (either wind or bow wave) at a speed of 10 knots without swimming effort and at the same time gain sufficient dynamic lift to maintain position against gravity?

In order to remain at constant depth and position within the advancing face of a moving wave it seems clear that the dolphin must receive a lift of 9·2 lb. from the water and that his drag at wave speed must not exceed the component of gravity acting at the angle of inclination of the water layers. That is, D must not exceed

---

* Contribution No. 522 from the Woods Hole Oceanographic Institution.

† Former curator of Marine Studios, Marineland, Florida; died December 1949.

‡ These measurements were made by Dr Henry Kritzler, associate curator of Marine Studios, Marineland, Florida.

§ These observations were made by Dr H. Kritzler (l.c.) and W. E. Schevill of the Woods Hole Oceanographic Institution, Woods Hole, Mass.

$W-F_b$; where D is the total drag and $W-F_b$ is weight minus the buoyant force of the sea water. If an inclination of the wave of 15° is assumed,[*] the component of the gravitational force acting will be $W \sin 15°$ (i.e. $9{\cdot}2 \times 0{\cdot}259$, or about 2·4 lb.). A force of 3·1 lb. results when an angle of 20° is assumed.

A restatement of the above question now takes the following form: does the drag of a 6·5 ft. dolphin exceed 2·4 lb. when its speed is 10 knots and its lift is 9·2 lb.? Gray (1936) has given figures for computing the drag of a rigid body of the same size and shape as a dolphin, presumably a body having zero lift. Following Gray, and assuming a negligible increase in resistance due to a lift of 9 lb.,[†] the drag is derived as follows:

$$D=\frac{d\rho AV^2}{g}, \tag{1}$$

where d = drag coefficient, ρ = density (64 lb. ft.^{-3}), A = surface area (15 ft.^2), V = speed (16·8 ft. sec.^{-1}), g = gravity (32 ft. sec.^{-2}), D = drag (lb.).

From the above equation and using Gray's tabulation of drag coefficients (see Table 1), it is found that the drag on a rigid body having the general size and shape of the *Stenella* would be 11·16 lb. when turbulent flow is assumed and 1·72 lb. when laminar flow is assumed (in sea water at a temperature of 70° F.).

Table 1. (*See Gray*, 1936.)

Reynolds' no.	Drag coefficient	
	Laminar flow	Turbulent flow
10^5	$2{\cdot}1 \times 10^{-3}$	—
2×10^5	$1{\cdot}5 \times 10^{-3}$	—
3×10^5	$1{\cdot}2 \times 10^{-3}$	—
4×10^5	$1{\cdot}0 \times 10^{-3}$	—
5×10^5	$0{\cdot}9 \times 10^{-3}$	$1{\cdot}0 \times 10^{-3}$
10^6	$0{\cdot}7 \times 10^{-3}$	$1{\cdot}5 \times 10^{-3}$
2×10^6	$0{\cdot}5 \times 10^{-3}$	$1{\cdot}6 \times 10^{-3}$
4×10^6	$0{\cdot}3 \times 10^{-3}$	$1{\cdot}56 \times 10^{-3}$
8×10^6	$0{\cdot}2 \times 10^{-3}$	$1{\cdot}4 \times 10^{-3}$
10^7	$0{\cdot}2 \times 10^{-3}$	$1{\cdot}3 \times 10^{-3}$
2×10^7	$0{\cdot}15 \times 10^{-3}$	$1{\cdot}25 \times 10^{-3}$

Reynolds' no. = Vl/ν, where V = velocity, l = length and ν = kinematic viscosity of sea water.

Gray has indicated that the force required per lb. of muscle was excessive, if the resistance of an actively swimming dolphin is equal to that of a rigid model towed at the same speed. With the assumption of laminar flow, Gray found that the power developed per lb. of muscle agreed closely with that developed by other types of mammalian muscle.

If a reasonable balance of forces is to occur, it also seems necessary to assume laminar flow about the relatively motionless dolphin which is riding a bow wave. The total weight of the *Stenella* in sea water (9·2 lb.) is inadequate to balance a drag of 11·16 lb. This drag is about 4·6 times the resultant force of gravity acting at an inclination of 15°.($W - F_b$ sin 15°) and about 3·6 times this resultant at an angle of 20°. When the drag coefficient for laminar flow is used (see Table 1) the computed drag of 1·72 lb. is less than the available weight of 2·4 lb. Thus force exceeds drag when the speed is 10 knots and when the angle is 15°. For a 20° wave slope, force (3·1 lb.) equals drag at about 14·2 knots.

---

[*] W. H. Munk of Scripps Institution of Oceanography has said, in a personal communication, that 15° is a reasonable angle to assume for the inclination of the water surface on the advancing face of the larger wind waves. It would be interesting to know the slopes of bow waves of large sea-going vessels.

[†] Durand (1943, p. 132) indicates little change in drag of similar streamline bodies resulting from a small lifting force at low positive angles of attack.

The above preliminary attempt to explain wave-riding of dolphins on the basis of the excess of total weight over buoyancy seems to give further support to the idea that the flow about their bodies is laminar.

Gray has suggested that, in contrast to rigid forms, dolphins may be able to prevent the onset of turbulence through effects arising from their swimming motions. Since wave-riding dolphins appear to be relatively motionless, the apparent necessity of assuming laminar flow about their bodies at 10 knots* implies that smooth flow may also occur with little or no swimming motion.

A further point, which arises from this study, concerns the significance of observations of the speed of dolphins about the bows of vessels or among wind waves on the open sea. If these animals can utilize gravitational force as a propelling aid on the inclined surfaces of bow or wind waves, then it seems clear that this force should be considered in any estimate of the dolphins' capacity for sustained work which is based upon observed speeds at sea. It is reasonable to suppose that dolphins may, by a burst of effort, place themselves in the bow wave of a passing vessel and then, with the aid of gravity, maintain this high speed with a swimming effort which is reduced in proportion to the force derived from the wave. Presumably the animals could equally well utilize, in a similar way, the energy of wind waves. For the wave-riding dolphin which is making no swimming effort the force of gravity is assumed to be equal and opposite to the drag force, thus making propulsive effort unnecessary.

REFERENCES

Durand, W. F. (1943). *Aerodynamic Theory*, 4, 434 pp. California: California Institute of Technology.
Gray, James (1936). Studies in animal locomotion. VI. The propulsive powers of the dolphin. *J. Exp. Biol.* **13**, 192.
Hill, A. V. (1950). The dimensions of animals and their muscular dynamics. *Sci. Prog. Twent. Cent.* **38**, 150, 209.
Irving, L., Scholander, P. F. & Grimel, S. W. (1941). The respiration of the porpoise, *Tursiops truncatus*. *J. cell. comp. Physiol.* **17**, 145.
Woodcock, A. H. (1948). The swimming of dolphins. *Nature, Lond.*, **161**, 602.

---

* This assumption is based upon Gray's table which shows turbulent flow beginning at a Reynolds' number of 5×10^5. More recent experimental work with carefully streamlined bodies has indicated, however, that in some rare cases laminar flow obtains at Reynolds' numbers as high as $1·5 \times 10^7$ (see Hill, 1950, p. 216).

Contribution No. 523

Reprinted for private circulation from
THE JOURNAL OF GEOLOGY
Vol. 59, No. 4, July 1951
PRINTED IN U.S.A.

AN OUTCROP OF EOCENE SEDIMENT ON THE CONTINENTAL SLOPE[1]

JOHN NORTHROP AND BRUCE C. HEEZEN
Lamont Geological Observatory (Columbia University)

During August, 1947, the authors carried out submarine geological work on the continental shelf and slope south of Cape Cod, Massachusetts. Exploration was done[2] with the Ewing underwater camera (Ewing, Vine, and Worzel, 1946*a*) modified to obtain a short core simultaneously with the bottom photograph. Five separate profiles crossing the continental shelf and part of the continental slope were completed. The first of these profiles (fig. 1) extended 100 miles offshore due south of Vineyard Lightship and consisted of fifty-three bottom photograph stations spaced about 2 miles apart. At thirty-six of these stations, cores averaging 23 cm. long were obtained from the seaward portion of the profile, where bottom deposits were "soft" enough for the coring tube to penetrate. The cores, except the one obtained at the farthest seaward station, D-20 of the first profile, contained reworked Pleistocene and Recent material.

This paper concerns station D-20 located on the continental slope at 39°50′ N. lat., 70°50′ W. long., at which place the coring tube brought up Eocene Globigerina ooze from a depth of 500 fathoms (1,000 meters wire sounding). The ocean-bottom photograph taken simultaneously shows the Eocene outcrop to be a part of a submarine slope. Similar Eocene material has been reported by Stetson (1949) on the continental slope beneath 10 cm. of Recent "slumped" material in one place and 122 cm. in another. Another occurrence, under 8 cm. of Recent material, is also reported from the margin of the Blake Plateau.[3]

---

[1] Lamont Geological Observatory Contr. 20; Woods Hole Oceanographic Institution Contr. 523. Manuscript received June 10, 1950.

[2] Work done on the research vessel "Balanus" of the Woods Hole Oceanographic Institution and supported by the U.S. Navy Bureau of Ships under contract No. NObsr-39092.

The Ewing underwater camera was attached to a 12-foot wooden pole weighted at the base with 10 pounds of lead and fitted with a $1\frac{1}{2}$-inch I.D. steel coring tube, 23 cm. long. This assembly was lowered to the sea floor on $\frac{3}{16}$-inch wire rope paid out from a winch. The apparatus was designed so that, as the coring tube penetrated bottom deposits, a magnet was moved past a magnetic switch, which closed the circuit from the battery to the flash bulb and camera shutter; the core and photograph were thus taken simultaneously. The coring tube usually came up filled with sediment, but at station D-20 it was only three-quarters full, showing that the material was more consolidated than usual and that the Eocene sediment was exposed on the sea floor, as no covering material could have been pushed out of the top of the tube.

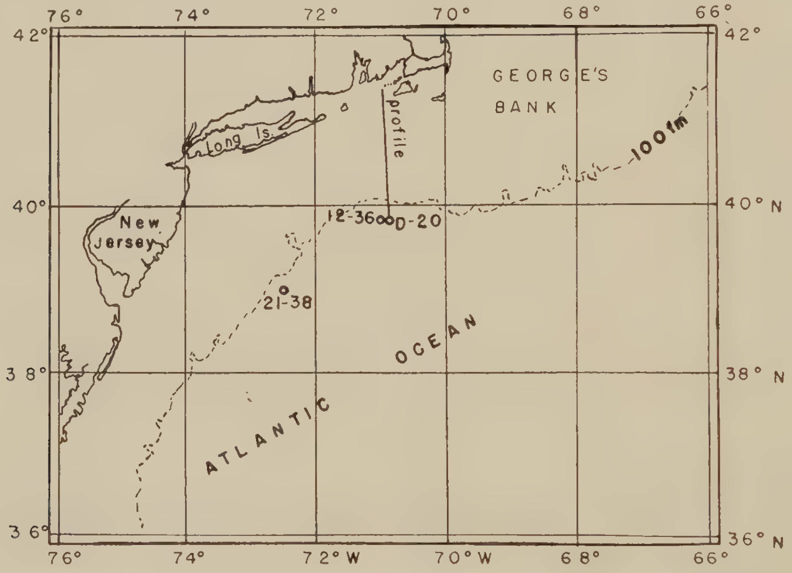

FIG. 1.—Location of profile across the continental shelf and out to the camera station D-20. Stations 12–36 and 21–38 are where Stetson has cored similar material.

The sediment was cream-yellow when wet, but hardened and became chalk-white after drying. Samples from the top, middle, and bottom of the core, respectively, were washed through a 0.061-mm. sieve to catch the microfossils. The coarse fraction contained abundant Foraminifera, the majority of which were *Globigerina*. Samples were submitted to Dr. S. K. Fox, of Princeton University, who states in a personal communication that

> the faunal assemblage is distinctly Tertiary in aspect, probably upper Eocene, closest to the Jackson fauna and maybe dips down a little bit to the Lower Eocene. Some Wilcox and Claiborne elements are present and the material is slightly older than that described by Cushman from Stetson's cores. Some of the forms appear to be more damaged than others and it may represent a slightly reworked deposit. Glauconite is present as casts of some Eocene species.

Dr. Fox has identified the following forms:

A. Those similar to the Upper Eocene fauna of the Jackson formation:
   Dentalina jacksonensis (Cushman and Applin)
   Robulus alato-limbatus (Gumbel)

---

[3] Unpublished data of D. B. Ericson describing material in a piston core obtained by the research vessel "Atlantis" in May, 1949.

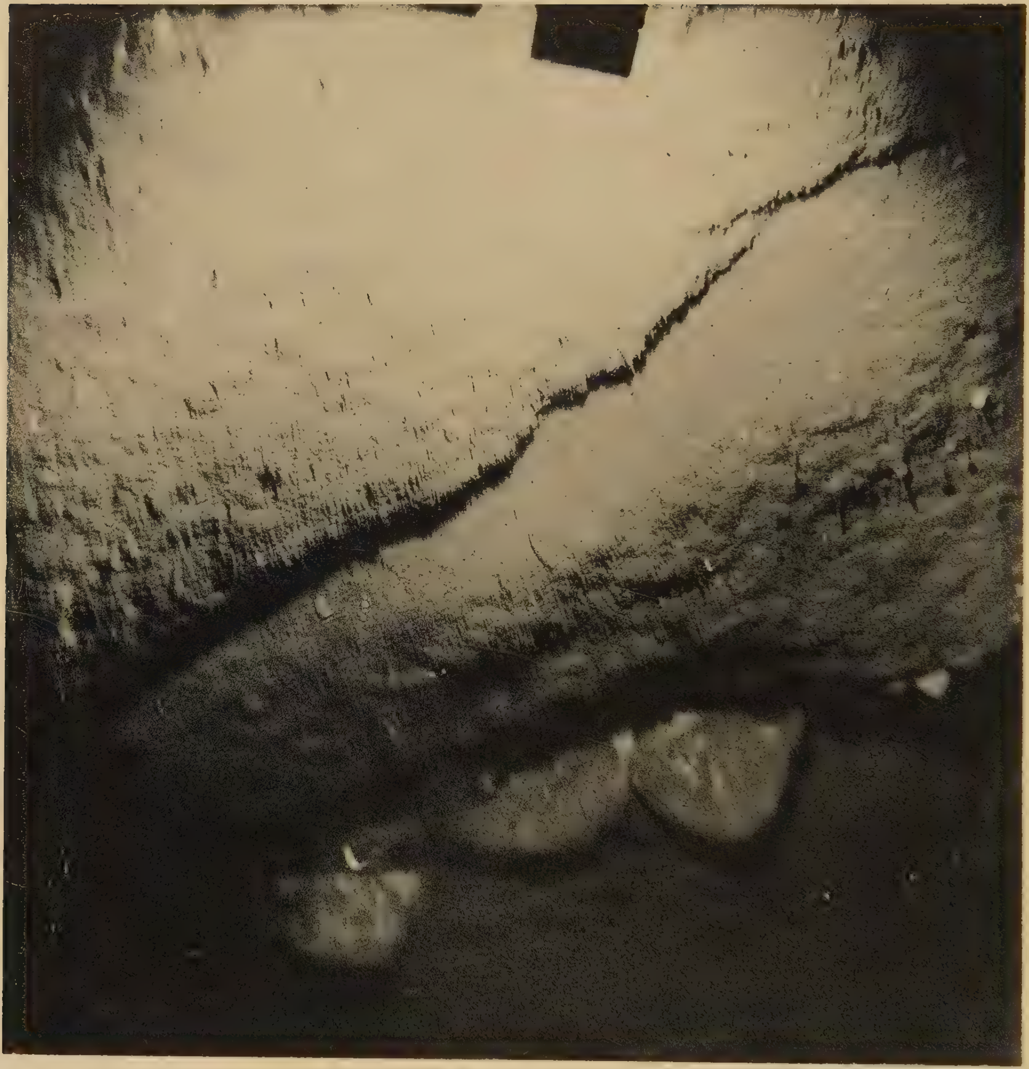

Eocene sediment outcropping on the continental slope

- *Eponides cocoaensis* Cushman
- *Anomalina bilateralis* Cushman
- *Anomalina jacksonensis* (Cushman and Applin)
- *Vulvulina advena* Cushman
- *Bulimina elongata* d'Orbigny
- *Nonion micrum* Cole

B. Those similar to the Upper Wilcox and Claiborne groups of the Middle Eocene:

- *Globigerina triloculinoides* Plummer
- *Bulimina ovata* d'Orbigny
- *Parrella expansa* Toulmin
- *Globerotalia membranacea* (Ehrenberg)
- *Globorotalia wilcoxensis* Cushman and Ponton, Var. *acuta* Toulmin, 1941
- *Gumbelina* sp., very close to *venezuelana* Nuttal *Cibicides* sp., similar to *Cibicides praecursorius* (Schwager) from the Middle and Upper Eocene of Alabama, but without the lip and slightly larger

C. Those similar to those described by Cushman (1939) from Stetson's Eocene cores:

- *Karrariella arenasensis* Cushman and Bermudez
- *Pleurostomella cubensis* Cushman and Bermudez

D. B. Ericson, of the Lamont Geological Observatory (Columbia University), has also looked at the fauna and states that "the assemblage is not as rich as that in Stetson's cores and is slightly older."

Foraminifera tests in the ooze give it a high carbonate content; random samples of the material analyzed before sieving contain 74 per cent carbonate by weight. Thermal analysis was made of the fraction finer than 0.061 mm. in two samples. Dr. J. L. Kulp (of Lamont Geological Observatory [Columbia University]) says, "comparing the thermal curve with those for carbonates of known chemical composition, the sample contains 40% ± 10% of very finely divided calcium carbonate and 10% ± 5% of dolomite. There is no quartz reaction, but silica may be present in other forms along with some clay minerals." The sediment was therefore deposited in a marine environment that was receiving little terrigenous detritus and yet shallow enough so that the carbonate shells were not dissolved.

The photograph (pl. 1) shows the Eocene sediment as it cropped out on the ocean floor. The core was obtained from a point directly below the black rectangular shadow (top-center of the print) at the same moment that the photograph was made. The camera, axis nearly vertical, was 7 feet above the shadow. About 35 square feet of surface would have shown in the photograph if the sea floor had been horizontal. However, the distinct shadows, which run diagonally across the photograph, show the rock farthest from the camera pole to be lower than that cored directly below the camera. The outcrop is thus in the form of an escarpment in which there are benches of more resistant strata that make the shadows appearing in the photograph. The most resistant layer appears as a series of angular protrusions that crop out in a line from the central left-hand margin of the photograph to the upper right corner.

The authors were unable to map the topography in detail at station D-20 because the "Balanus' " fathometer was inoperative at that depth. However, a chart published by Veatch and Smith (1939, pl. 1) shows a small submarine canyon to be present at camera station D-20. Stetson's cores 12–36 and 21–38 were also taken from canyons. The few centimeters of Recent green silt covering the Eocene in Stetson's cores show that the later continental-shelf sediment has been eroded locally. The outcrop photographed shows that this erosion is occurring today.

ACKNOWLEDGMENT.—Acknowledgment is made to Maurice Ewing, who supervised the research; to S. K. Fox and D. B. Ericson, who identified the Foraminifera; to J. I. Ewing and J. L. Worzel, who aided and technically advised the authors; and to H. C. Stetson and G. P. Woollard and the Woods Hole Oceanographic Institution.

PLATE 1

Ocean-bottom photograph of Eocene sediment outcropping on the continental slope. Station 20-D: depth, 1,000 meters; latitude, 39°50′ N.; longitude, 70°50′ W.; flash bulb No. 5; distance from camera to light, 43 inches; camera to bottom, 77 inches; focus, 4.5 feet; stop, *f*/9; shutter speed, $\frac{1}{25}$ second.

REFERENCES CITED

CUSHMAN, J. A. (1939) Eocene Foraminifera from submarine cores off the eastern coast of North America: Contr. to Foraminiferal Research, vol. 15, pt. 3, no. 210, pp. 49–76.

EWING, M.; VINE, A.; and WORZEL, J. L. (1946*a*) Photography of the ocean botton: Jour. of the Optical Soc. America, vol. 36, no. 6, pp. 307–321.

——— ——— — ——— (1946*b*) Recent results in submarine geophysics; Geol. Soc. America Bull. 57, pp. 902–934.

STETSON, H. C. (1949) Sediments and stratigraphy of the east coast continental margin; Georges Bank to Norfolk Canyon; Papers in Physical Oceanography and Meteorology, vol. 11, no. 2.

VEATCH, A. C., and SMITH, P. A. (1939) Atlantic submarine valleys of the United States and the Congo submarine valley: Geol. Soc. America Special Papers no. 7.

Contribution No. 526

Reprinted from the Journal of the Institute of Navigation (London) Volume IV, No. 2, April 1951

Dead Reckoning by Surface Current Observation

William S. von Arx
(*Woods Hole Oceanographic Institution*)

1. INTRODUCTION. Recently an electromagnetic method for measuring the velocities of ocean currents for oceanographic purposes has been shown to be reliable enough for the observed velocity of the surface current to be taken into account in dead reckoning navigation in the open ocean. A preliminary test of the electromagnetic method as a navigational aid was made in 1949 on one cruise covering a distance of 1000 miles across the Gulf Stream and back. A total of 52 miles of lateral drift was corrected to produce a straight line of travel through the observed currents, and this correction enabled the ship to return to within 2 miles of the starting point. Seven less formal experiments performed in 1950 indicate that ordinarily, on straight-away courses, the lateral drift component caused by currents can be measured and corrected with the expectation that the undetected drift will be less than 1 per cent of the distance travelled.

2. THE INSTRUMENTS AND METHOD. The oceanographic research equipment in present use for electromagnetic measurements of ocean current velocities, named the Geomagnetic Electrokinetograph or G.E.K., consists of a pair of electrodes mounted in tandem on each of two conductors in a cable streamed astern, a potentiometer recorder on board, and the ship's compass. Observations of the direction and potential difference between the electrodes are made under way. The magnitude of the potential difference is proportional to the rate of lateral drift through the frame of reference provided by the Earth's magnetic field and the potential difference changes sign when currents set the ship to port or to starboard. Measurements of the potential differences on two courses provide the drift or component velocities at 90° to the directions of these two courses. The components of drift are then composed to find the resultant rate and direction of the drift due to the local ocean current.

For the first dead reckoning navigation experiment a triangle bounded by the ocean current velocity vector and the ship's velocity vector was closed every hour to indicate the next course to be steered to maintain the intended line of progress, and the expected rate of progress along that line. Since the intended line lay across the Gulf Stream, where currents of more than four knots were encountered, the bow was occasionally turned as much as 54° upstream to counteract the drift. In order to avoid too frequent course changes with each observed fluctuation of

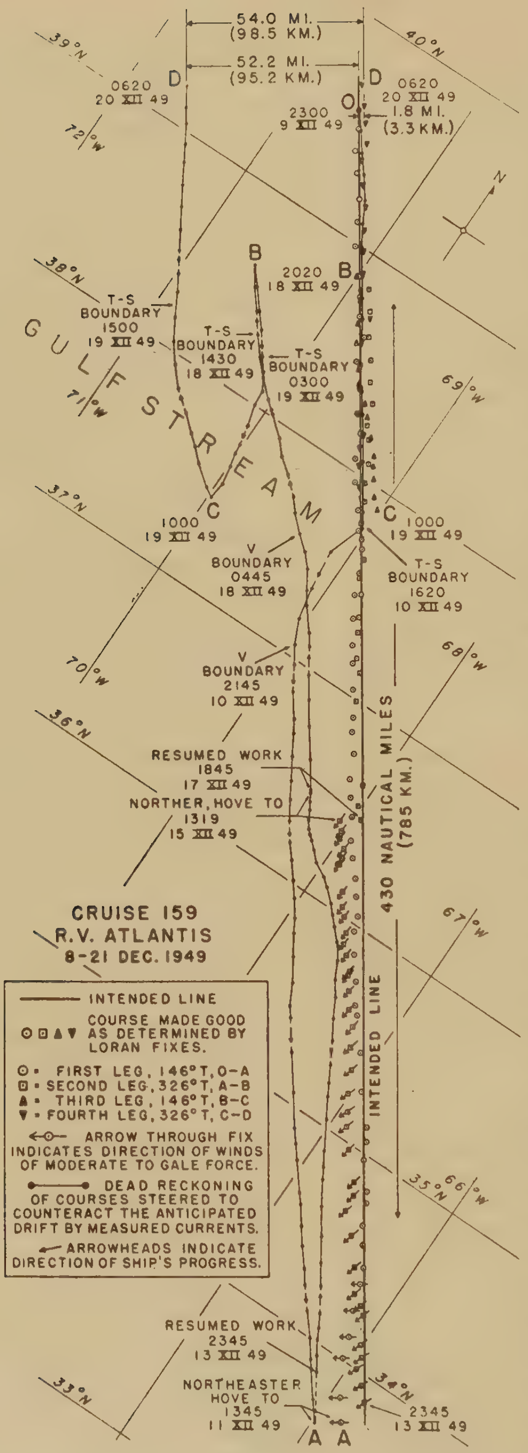
54.0 MI.
(98.5 KM.)
52.2 MI.
(95.2 KM.)
39°N
40°N
72°W
D
0620
20 XII 49
D
0620
20 XII 49
O
2300
9 XII 49
1.8 MI.
(3.3 KM.)
N
B
B
2020
18 XII 49
38°N
T-S
BOUNDARY
1500
19 XII 49
T-S
BOUNDARY
1430
18 XII 49
T-S
BOUNDARY
0300
19 XII 49
GULF STREAM
71°W
69°W
37°N
C
1000
19 XII 49
C
1000
19 XII 49
V
BOUNDARY
0445
18 XII 49
T-S
BOUNDARY
1620
10 XII 49
V
BOUNDARY
2145
10 XII 49
70°W
68°W
36°N
430 NAUTICAL MILES
(785 KM.)
RESUMED WORK
1845
17 XII 49
NORTHER, HOVE TO
1319
15 XII 49
67°W
CRUISE 159
R.V. ATLANTIS
8-21 DEC. 1949
INTENDED LINE
INTENDED LINE
COURSE MADE GOOD
○ ◻ ▲ ▼ AS DETERMINED BY
LORAN FIXES.
○ • FIRST LEG, 146°T, O-A
◻ • SECOND LEG, 326°T, A-B
▲ • THIRD LEG, 146°T, B-C
▼ • FOURTH LEG, 326°T, C-D
←○— ARROW THROUGH FIX
INDICATES DIRECTION OF WINDS
OF MODERATE TO GALE FORCE.
●———● DEAD RECKONING
OF COURSES STEERED TO
COUNTERACT THE ANTICIPATED
DRIFT BY MEASURED CURRENTS.
←— ARROWHEADS INDICATE
DIRECTION OF SHIP'S PROGRESS.
35°N
66°W
RESUMED WORK
2345
13 XII 49
NORTHEASTER
HOVE TO
1345
11 XII 49
34°N
2345
13 XII 49
33°N
A
A

Fig. 1.

current, the headings correct at the beginning of each hour were maintained throughout the hour. Thus, in increasing currents the ship was drifted downstream by an amount proportional to the increase and in decreasing currents the ship worked upstream by an amount proportional to the decrease. Since approximately the same current systems were traversed in opposite directions, this rule of action is presumed to have introduced no important systematic errors in the results for the whole cruise, or for corresponding legs in opposite directions. The cruise is plotted in detail in Fig. 1.

3. EXPERIMENTAL RESULTS. In Fig. 1, the light solid line to the left of the intended line is the ordinary D.R. of the track that the ship steered with respect to the water. The points clustered near the intended line are Loran fixes made at the points actually reached by the ship. Had the ship been steered steadily on the heading of the intended line, the track over the bottom would have been the reflection of the D.R. track across the intended line. Throughout this experiment the ratio of the true current strength to the observed current strength

was assumed to be unity. The ratio of the error of closure to the accumulated normal component of drift indicates that a more suitable over-all value of the ratio for this cruise would have been 1·04 ± 0·03.

It is to be expected from theory that the current magnitude readings given by the electromagnetic method will be too small by about the ratio of the effective thickness of the moving surface layer to the total depth of water. In the first D.R. experiment, the ship traversed currents having effective thicknesses which are perhaps as great as one-third of the total depth. These currents, associated with the Gulf Stream system, are so narrow compared with the total distance traversed that the larger signal deficiency in this band is lost in combination with the proportionately higher signal strengths obtained in the waters on either side. Subsequent experiments confined to the vicinity of the Gulf Stream reveal the signal strength deficiency more clearly, but the data require more study before general results can be announced. It is clear that quantitative prediction of the signal strength deficiency requires rather more oceanographic knowledge than is available at present.

It will be noted in Fig. 1 that the Loran fixes toward the Bermuda end of the intended line joining Montauk Point, Long Island and Bermuda, are struck through with arrows to indicate the direction of winds of gale force, and that these fixes depart most from the intended line. It has been the practice in oceanographic work to take the direction of the keel of the ship as that of the line joining the electrodes. In strong beam winds the interelectrode line makes a small angle with the keel, consequently ocean currents are reliably indicated, but from a navigational point of view the measured drift of the ship is in error by the amount of the ship's windage. Were the electrodes somehow mounted rigidly in line with the keel, the windage component would be included in the measured drift.

4. Historical background. The fundamental principles of the electromagnetic method were described by Faraday [1] in the Bakerian lecture of 1832. Faraday proposed that, theoretically, the motion of sea water through the Earth's magnetic field would cause potential differences to exist in the water, and that electric currents would necessarily flow in the moving water and in the sea bed. Following the middle of the nineteenth century the effect was observed. Early in the twentieth century the effect was clearly confirmed and its navigational possibilities pointed out by Young, Gerrard and Jevons.[2] More recently the problem of electric and magnetic effects of tidal flow in channels has been studied theoretically and experimentally by Barber and Longuet-Higgins.[3, 4, 5] At about the same time the oceanographic uses of the effect in the deep sea were studied by Stommel [6] and von Arx.[7]

5. Physical explanation. Just as in the armature coils of an electric generator, electric potentials are produced as ocean currents move through the Earth's magnetic field. Similarly, electric potentials are developed in suitable measuring apparatus being moved by these ocean currents. When the measuring apparatus is connected to the sea surface

at two points, the apparatus will indicate the difference between the motional electromotive force generated in the line between the points of contact and the potential difference between the same two points in the sea. The potentials in the sea and in moving measuring apparatus would be equal, and could not be recorded, were it not that the potential differences induced in the parts of the sea in motion are short-circuited through the sea bottom and through relatively motionless masses of water at great depths.

In that the oceans of the world are roughly one thousand times wider than they are deep, and their circulations are mainly wind-driven, their principal motions are horizontal and usually most rapid at the surface. Everywhere below the greatest horizontal surface velocities there are smaller parallel components of velocity that become very small at great depths. This deep mass of water, possessing small or negligible intrinsic motional electric potentials, produces a very effective short-circuit of the motional potential differences generated near the surface. The water-saturated bottom sediments must also contribute to this short-circuiting effect. Thus in the surface of the open ocean, where it is generally found that more than 80 per cent of the local motional electromotive force is short-circuited at depth, surface observation of the motional potential difference generated in drifting apparatus yields about that same proportion of the true motional electromotive force. Theoretically, there is reason to believe that similarly favourable results might be obtained in approximately the first thousand metres of depth below the surface.

While a qualitative understanding of the factors permitting measurements of velocity can be reasoned fairly easily, it is practically difficult to compute the observable fraction of the total motional electromotive force without a complete knowledge of the velocity field and some good estimate of the resistivity of the sea bottom. The scatter of experimental points shown in Fig. 2 suggests how each of these two factors influences the result in nature. The ordinate is given in terms of *k*, a dimensionless factor by which the current measured electromagnetically must be increased to yield the true current determined by other experimental means. The marked variability of results, particularly in shoal water, is partly due to error in the non-electromagnetic means of current measurement, but it is believed that the general distribution of the points is significant. The scatter begins to be small at about the 100-metre isobath where, on the coast of New England, the rotary tides of the continental shelf give way to the circulation of the Slope Water. The tidal currents on the continental shelf are almost uniform in velocity from top to bottom, hence the principal short-circuiting path is through the higher resistance of the sedimentary deposits composing the upper parts of the continental shelf. The circulation in the Slope Water is oceanic in character in that it decreases in intensity with increasing depth. Electromagnetic measurements of surface velocity improve rapidly in this area and remain uniformly good, certainly as far north as Davis Straits, south to the West Indies, and east as far as the Spanish coast, the limits of observations to date. Because the electromagnetic method depends on the vertical component of geomagnetic flux it ceases to be effective at the magnetic equator and perhaps for a little distance either side.

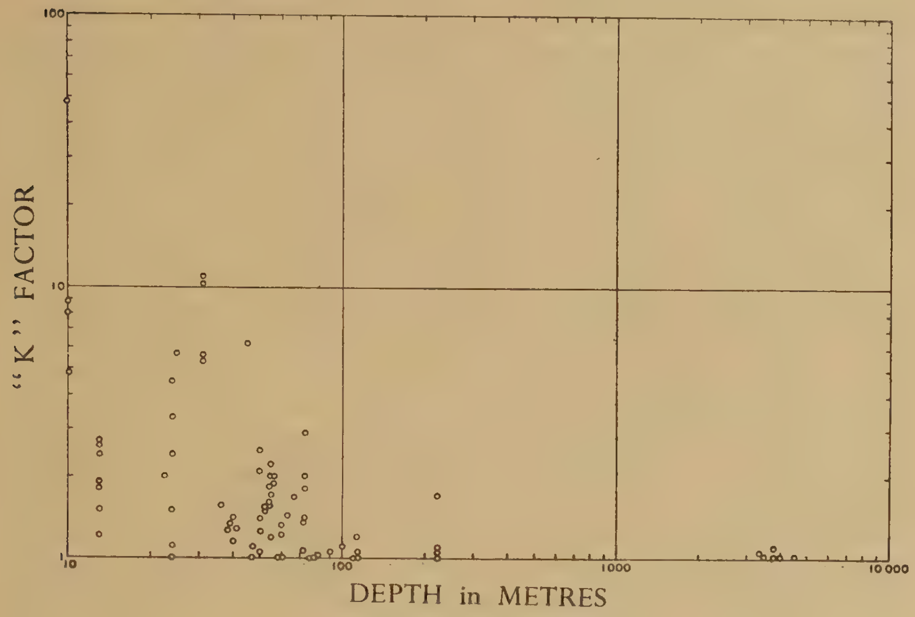

Fig. 2. The scatter of experimental points.

6. Quantitative relationships. The magnitude of the horizontal component of motional electromotive force that is fundamentally present in both the sea and the measuring instruments is determined from the product of the intensity of the local vertical component of the Earth's magnetic field, the horizontal distance between the points of contact with the sea, and the horizontal velocity of the sea water and apparatus. (The signal strength ordinarily lies in the orders 0·1 to 10 millivolts per 100 metres.) The relationship between the direction of the electric, velocity and magnetic vectors is given by the vector cross product, $E = v \times H$. That is the electric vector, E, is perpendicular to the plane common to the velocity vector, v, and the magnetic vector, H, and is directed in the sense of progress of a right-hand screw turned from v towards H through the smaller of the angles between them. Since the principal interest for navigational purposes lies in knowing the horizontal component of motion, measurements of the effects of the electric field in the horizontal plane ($E = -\text{grad } V$), together with a knowledge of the magnetic field intensity, lead to a knowledge of the horizontal component of motion. In the northern magnetic hemisphere the vertical magnetic component is directed downward, hence the set of an ocean current lies

90° to the right of the direction of the corresponding electric vector. When measurements of motional potential differences are made between two electrodes in contact with the sea and towed astern in tandem, the distant electrode will be positive with respect to the nearer one when the ship and measuring apparatus are set to starboard. The convention has been adopted that the more distant electrode should be connected to the terminal of the potentiometer which when made positive gives the potentiometer index a right-hand deflection. Thus when an observer sits facing forward before the instrument, the direction of deflection of the index is the same as the set produced by the current acting on the ship. The amount of the deflection is proportional to the rate of lateral drift and is independent of the forward speed of the ship.

In order to measure the forward component of velocity it is necessary to observe the potential difference between two electrodes on a line athwartships. It is of interest to note that the signal from an athwartships pair is proportional to the rate of the ship's progress over the sea bottom, for the signal includes the effects of both winds and ocean currents in addition to that of inboard propulsion.

7. DIFFICULTIES. Were it possible to mount both a fore-and-aft and an athwartships pair of electrodes on the hull, the ground velocity of a ship might be known continuously. Unfortunately the hull is a source of physical disturbance which requires the points of contact with the sea to be remote. During oceanographic observations of surface current velocity, very little use has been made of the athwartships array of electrodes to measure the forward velocity component partly because of its minor significance to the ship's work and mainly because of the difficulty of maintaining the electrode spacing. However, the forward component of water velocity has been measured regularly by simply turning the ship and longitudinal electrode string 90° to the base course. This manœuvre provides a current fix. If the 90° course change is retraced before resuming the base course, the zero point of the electrodes is determined as well. A zero point determination is required because at present even the best electrode pair (silver silver-chloride) is never precisely balanced for all conditions of temperature and salinity in the ocean. The small difference in potential of the electrodes has the effect of a weak battery in series with the potentiometer. But if the potential difference of this battery effect is measured at regular intervals and used as the origin of electrical measurements, the motional potentials due to drift by ocean currents are obtained without further difficulty.

8. FUTURE POSSIBILITIES. The necessary calibration of unsymmetrical potential changes in electrodes makes present research methods of electromagnetic current velocity measurement too clumsy for direct commercial application. The sailing plan used hourly for zero point determination and current fixing delays the ship about 17 per cent. Still, there may be advantages for some ships to fix the current with existing equipment at intervals of a watch in order to avoid stemming strong

currents, and incidentally to steer a geographically straighter course in between. During oceanographic surveys in the vicinity of the Gulf Stream, occasional coastwise and trans-oceanic vessels have been sighted steaming south-westward into currents as swift as 5 knots when as little as 20 miles to the south-east or north-west they would have found currents either much weaker or even favourable. Current fixing at intervals of a watch would slow these ships about 5 per cent, but improve their progress through this limited area by possibly as much as 50 per cent. On the return trip they might seek the swiftest currents and use them to advantage. Recent studies of the Gulf Stream system show that the maximum surface current is considerably more confined and more vigorous than has been generally thought and it may be supposed that corresponding currents in other oceans have similar surface velocity characteristics. It is also found that transient surface current velocities in excess of 1 knot exist in areas where systematic drifts are not usually present.

As soon as electrodes can be perfected to the point that their individual differences are made stable and smaller by at least one order of magnitude, it should be possible to make usefully exact two-component measurements of a ship's velocity and of the local ocean current. By the same development it would also be possible and simpler to measure only the ship's velocity component athwartships without change of course. This means might be used, either regularly or on occasions when celestial fixing is impossible and the ship is beyond the range of hyperbolic radio fixing methods, to effect a fair landfall from starting points as remote as mid-ocean. While such a development would only provide information on lateral drift, this would be at least as reliable as present information on forward speed and permit the navigator to reason with nearly equal certainty of his lateral and longitudinal velocity.

With either one or two measured velocity components it should also be possible to devise and place before the helmsman an automatic potentiometer-computer system which would indicate the sense and approximate magnitude of lateral set, perhaps by shifting an auxiliary index to the right or left of the standard lubber line. Automatic or manual steering by the index would necessarily counteract most of the effects of lateral drift and would require helmsmen to learn very little in the way of new skills. The computer might also provide velocity data to an instrument akin to existing dead reckoning plotting equipment.

Since the electromagnetic method is capable of indicating current direction it is potentially useful in locating objects that have drifted with the current. Objects of relatively small draft and low freeboard should be drifted mainly in the direction of the surface currents ordinarily detected by means of surface towed electrode strings. Icebergs[8] and other deep draft objects may drift in response to deeper currents which can be detected by means of submerged electrode strings. Recently it has been possible to make simultaneous observations at the surface and at a depth of 100 metres without alteration of either the speed of the ship or the manœuvring plan. It is hoped that with existing cable and depressor combinations, present efforts will soon succeed in extending measurements to depths in the vicinity of 500 metres.

In any electromagnetic system based on present views, two adjustments of sensitivity would be needed to correct the indications for changes in the local magnetic latitude and the ship's forward speed. The magnetic latitude adjustments, required once every watch or two, might have to be made manually by the officer of the watch, but the ship's forward speed could be monitored continuously. In a two-component system the athwartships electrode pair would provide a forward ground speed component. But in a one-component system the forward speed with respect to the water could be provided either by electromagnetic means [9, 10] or by suitable connection with the shaft-tachometer or taffrail log. In the latter instance it might be possible to arrange the towed cable and electrodes to rotate and actuate the taffrail log. It should be emphasized that the success of the suggested commercial developments of the electromagnetic method for navigation depends on the prior development of very much better electrodes to avoid the course changes required at present for zero point determinations.

9. Conclusion. The navigational possibilities of the electromagnetic method were suggested at the beginning by Faraday and were clearly defined by Young, Gerrard and Jevons in connection with their experiments. It is encouraging to find that the results are at their best in the open ocean, where ships are most often forced to depend on their own observational resources.

Acknowledgements. The work described was supported by the United States Office of Naval Research under Contract N6onr–277–1 with the Woods Hole Oceanographic Institution. This paper is Contribution No. 526 from the Woods Hole Oceanographic Institution; permission to publish it is gratefully acknowledged.

REFERENCES

[1] Faraday, M. (1832). Art. VI (The Bakerian Lecture), Experimental Researches in Electricity, Second Series, Sec. 5, Terrestrial Magneto-electric Induction. *Phil. Trans. Roy. Soc. London*, 1832, Part I, pp. 163–177, vid. 176, par. 190.

[2] Young, F. B., H. Gerrard and W. Jevons (1920). On Electrical Disturbances Due to Tides and Waves. *Phil. Mag.* Ser. 6, 40, pp. 149–159.

[3] Barber, N. F. (1948). The Magnetic Field Produced by Earth Currents Flowing in an Estuary or Sea Channel. *Mon. Not. Roy. Astr. Soc.*, Geophys. Suppl., 5 (7), pp. 258–269.

[4] Barber, N. F. and M. S. Longuet-Higgins (1948). Water Movements and Earth Currents: Electrical and Magnetic Effects. *Nature*, Vol. 161, pp. 192–193.

[5] Longuet-Higgins, M. S. (1949). The Electrical and Magnetic Effects of Tidal Streams. *Mon. Not. Roy. Astr. Soc.*, Geophys. Suppl., 5 (8), pp. 295–307.

[6] Stommel, H. (1948). The Theory of the Electric Field Induced in Deep Ocean Currents. *J. Mar. Res.*, Vol. 7, No. 3, pp. 386–392.

[7] von Arx, W. S. (1950). An Electromagnetic Method for Measuring the Velocities of Ocean Currents from a Ship Under Way. *Papers in Phys. Oceanog. and Met.*, M.I.T.–W.H.O.I., Vol. XI, No. 3.

[8] Soule, F. M., H. H. Carter and L. A. Cheney (1950 in press). International Ice Observation and Ice Patrol Service in the North Atlantic Ocean—Season 1948, *U.S. Coast Guard Bull.* 34, p. 96.

[9] Guelcke, R. W., and C. A. Schoute-Vanneck (1947). The Measurement of Sea Water Velocities by Electromagnetic Induction. *Jour. Inst. Elec. Eng.*, 94, Part II (37), pp. 71–74.

[10] Denman, H. H. (1950). An Analysis of an Electromagnetic Method of Measuring Velocities of Moving Conducting Media.—Masters Thesis (mimeographed) Univ. of Cincinnati, Cincinnati, Ohio.

MADE AND PRINTED IN GREAT BRITAIN BY
WILLIAM CLOWES AND SONS, LIMITED
LONDON AND BECCLES

Contribution No. 527

Transactions, American Geophysical Union Volume 32, Number 1 February 1951

FORCED CONVECTION CELL CIRCULATION IN CLEAR AIR

Patricia A. Langwell

(Contribution No. 527 of the Woods Hole Oceanographic Institution)

Abstract--The characteristics of a two-dimensional convection cell with an applied heat force are derived from the equations of motion, continuity, and the first law of thermodynamics. The solutions are compared with observations made over the water north of Puerto Rico. It is found theoretically that large, slow-moving cells can always exist, and will persist for one to two hours.

Introduction--Observations have shown that the lower atmosphere in the West Indies trade-wind region, near Puerto Rico, may be divided into several layers: the homogeneous layer, the cloud layer, and the air above the trade inversion [BUNKER and Others, 1949]. Within the cloud layer, clear areas with a diameter greater than 20 mi exist between patches of cumulus clouds. This paper is concerned with the characteristics of these clear areas.

Within the clear areas, horizontal traverses show oscillations of temperature and moisture which are 180° out of phase. Owing to the long over-water trajectory and the relatively isothermal sea surface, advective and diurnal changes may be disregarded. Moreover, this air is essentially non-turbulent. It was stated that the origin of these fluctuations is probably the residue of dissipated clouds [LANGWELL, 1948]. In this paper an attempt is made to approximate, in easily manipulated forms, the solution of the equations which describe the motion of air in a convection cell, when a heat source is added. The study was initiated in order to discover whether cool moist pockets under an inversion, in a conditionally stable atmosphere, could initiate cellular circulation. Because the temperature fluctuations are not assumed to be reinforced, denser air, moving downward to a lower inversion is replaced by warmer and drier air, which causes the cold source to become weaker. This effect is treated in the equations as a dissipative force.

Convective circulation may be initiated by heating at the base of the layer, or by cooling at the top. Because the amount of heat necessary to initiate the circulation at the base of the layer is no less than the degree of coolness necessary at the top, a heat source rather than a cold source may be included in the equations. For mathematical convenience, the former has been used. The scale of the model (no larger than ten to 20 km) justifies the assumption of a flat, non-rotating Earth, but the inclusion of the heat source suggests the less usual assumption of a compressible atmosphere in which a heat source can produce density changes. Ideally, the temperature would appear as an arbitrary function of height. Because this paper attempts to give only approximate solutions, this degree of refinement is not used, and the temperature is assumed to be constant, or to vary as a linear function of elevation. In the latter case, only a first approximation to the solution is given. Since this paper is concerned with slow-moving cells in clear air, the equations include none of the effects of condensation.

Historical background--STOMMEL [1947] has usefully discussed the literature dealing with convective phenomena. His paper is one of an extensive collection of reports on this subject, which also contains a paper by MUNK [1947] stating that the Coriolis force may be ignored in the analysis of convection cells of the size studied below.

It would be impractical to list all the works within this large field. The papers described below represent those which most nearly approximate the type of problem and approach to be discussed here.

The first of these studies is that of LOVE [1891] who studied the effect on an incompressible fluid of a stream function which is assumed to be periodic in horizontal distance and time. If the percentual decrease of density with height is constant, the variation of the streamline with height is the product of an exponential and a periodic function. The next treatment of interest is that of BJERKNES and Others [1934, pp. 361 and 396]. Because they used Lagrange's equations, it is difficult to compare their results with those of the present paper. DOPORTO [1945], in his study of the isopycnic layer, translated their equations into the Eulerian form. His values of the free oscillations can be shown, by a change in notation, to be the same as those calculated below for an isothermal atmosphere. More recently STARR [1949] has included a heat source in a treatment of the problem of convection, using a method is some respects similar to Love's. The present paper differs from its predecessors in the attempt to include the concept of a heat source while using the method of Bjerknes and Doporto.

Method--A coordinate system is chosen with the origin at the base of the layer, moving with the speed of the undisturbed wind, and the x-axis is oriented in that direction. If the wind shear is is neglected, the undisturbed velocities vanish throughout the layer. The basic equations of the problem are the equations of motion, and that of continuity. Within this moving coordinate system, the problem is treated in two dimensions, and the cells are assumed to be of infinite extent in the third dimension.

The equations of motion are written as

$$Du/Dt = -(1/M)\,\partial P/\partial x \tag{1}$$

and

$$Dw/Dt = -g - (1/M)\,\partial P/\partial z \tag{2}$$

where u and w are the horizontal and vertical perturbation velocities, M is the total density, P is the total pressure, and g is the gravitational force. The equation of continuity is

$$(1/M)\,DM/Dt + (\partial u/\partial x + \partial w/\partial z) = 0 \tag{3}$$

As the fourth equation, the first law of thermodynamics, as applied to a unit mass of an ideal gas, is used in the form

$$(1/M)\,DM/Dt = (1/\lambda P)\cdot DP/Dt - (R/c_p)(M/P)\,Q(x, z, t) \tag{4}$$

where R and c_p have their usual meanings, $\lambda = c_p/c_v$, and Q(x, z, t) is the rate at which heat is added to the system.

The atmosphere is assumed to be in hydrostatic equilibrium before the disturbance. If the undisturbed conditions are denoted by a zero subscript, this may be represented schematically as

$$\partial p_0/\partial z = -\rho_0 g$$

and

$$\partial p_0/\partial x = 0$$

The usual assumptions involved in the use of the perturbation method [HAURWITZ, 1941] are made, only the first order terms being retained. This permits reduction to the following simplified forms

$$\partial u/\partial t = -(1/\rho_0)\partial p/\partial x \tag{5}$$

$$\partial w/\partial t = -(1/\rho_0)(\partial p/\partial z + g\rho) \tag{6}$$

$$\partial \rho/\partial t + w\,\partial \rho_0/\partial z + \rho_0(\partial u/\partial x + \partial w/\partial z) = 0 \tag{7}$$

$$\partial \rho/\partial t + w\,\partial \rho_0/\partial z = (1/\lambda R T_0)(\partial p/\partial t + w\partial p_0/\partial z) - (R\rho_0^{\,2})Q(x, z, t)/c_p p_0 \tag{8}$$

where ρ and p are perturbation density and pressure, respectively.

Since these four equations involve six unknowns, further information is necessary, in order to integrate the equations. If the temperature and heat source are known as functions of height, it is possible to find u, w, p, and ρ. The isothermal case and that of the constant lapse-rate will be considered below. The rate of heat added to the system, Q, is always assumed to be a first order perturbation term of the form

$$Q(x, z, t) = Q(x, t)\, e^{-\phi z}$$

The basic assumption concerning the form of the solutions is that

$$u, w, p, \rho, Q \propto A, B, C, D, E \exp(i\mu x - \gamma t) \quad \ldots\ldots (9)$$

where the amplitudes of the perturbation quantities are functions of height alone. The horizontal dimension of the cell is π/μ, and γ is the damping factor which describes the dissipation effect on the heat source due to the circulation itself. It may also be considered that γ includes a measure of the effect of friction.

Isothermal atmosphere--If the assumption is made that $dT_0/dz = 0$, then from the hydrostatic equation and the equation of state one obtains

$$\partial\rho_0/\partial z = -\rho_0 g/RT_0$$

Substitution of this value and the set of assumptions (9) into the equations makes it possible to express the equations in terms of height alone. It may then be seen that

$$-\gamma A = -i\mu C/\rho_0 \quad \ldots\ldots (10)$$

$$-\gamma B = -(1/\rho_0)(dC/dz + gD) \quad \ldots\ldots (11)$$

$$-\gamma D - \rho_0 gB/RT_0 + \rho_0(i\mu A + dB/dz) = 0 \quad \ldots\ldots (12)$$

$$-\gamma D - \rho_0 gB/RT_0 = -\gamma C/\lambda RT_0 - \rho_0 gB/\lambda RT_0 - R\rho_0{}^2E/c_p p_0 \quad \ldots\ldots (13)$$

Since A may be eliminated by using (10), the subtraction of (13) from (12) gives the result that

$$\rho_0 dB/dz - \rho_0 gB/\lambda RT_0 - (\mu^2/\gamma + \gamma/\lambda RT_0)C = R\rho_0{}^2E/c_p p_0 \quad \ldots\ldots (14)$$

The coefficient of density D may be eliminated between (11) and (12), so that

$$gdB/dz - (\gamma^2 + g^2/RT_0)B + (\gamma/\rho_0)\, dC/dz - \mu^2 gC/\rho_0\gamma = 0 \quad \ldots\ldots (15)$$

From (14), it can be seen that

$$dC/dz = [\rho_0\gamma/(\mu^2\lambda RT_0 + \gamma^2)]\, [-(R/c_v)\, dE/dz + \lambda RT_0\, d^2B/dz^2$$
$$- gdb/dz - (g/RT_0)(- RE/c_v + \lambda RT_0 dB/dz - gB)] \quad \ldots\ldots (16)$$

If the expressions for C and dC/dz are substituted into (15), the resultant equation is

$$d^2B/dz^2 - (g/RT_0)\, dB/dz - (\mu^2 + \gamma^2/\lambda RT_0 + \mu^2 g\Gamma/\gamma^2 T_0)B$$
$$- (g/\lambda R^2 T_0{}^2 + \mu^2 g/\gamma^2\lambda RT_0)RE/c_v \quad \ldots\ldots (17)$$

where Γ is the dry adiabatic lapse rate. It will be assumed that $E = E'e^{-\phi z}$, where ϕ is a positive constant and E' is the value of the heat source at $z = 0$. With this assumption, together with the fact that (17) has constant coefficients, the equation may be easily solved. The general solution is

$$B_h = B_1 e^{r_1 z} + B_2 e^{r_2 z}$$

where

$$r = g/2RT_0 \pm \sqrt{g^2/4R^2T_0{}^2 + \mu^2 + \gamma^2/\lambda RT_0 + \mu^2 g\Gamma/\gamma^2 T_0}$$

where the plus sign is used for r_1 and the minus for r_2. The total solution is

$$B = B_1 e^{r_1 z} + B_2 e^{r_2 z} + B_3 e^{-\phi z} \quad \ldots\ldots (18)$$

where

$$B_3 = [-\phi/c_pT_o - (g/\lambda R^2T_o{}^2 + \mu^2 g/\gamma^2\lambda RT_o)R/c_v]E'/$$
$$[\phi^2 + g\phi/RT_o - (\mu^2 + \gamma^2/\lambda RT_o + \mu^2 g\Gamma/\gamma^2T_o)]$$

If B_3 were to become infinite, the solutions would not satisfy the conditions of the perturbation method. Since $\phi > 0$, the denominator of B_3 vanishes only if

$$\phi = -g/2RT_o + \sqrt{g^2/4R^2T_o{}^2 + \mu^2 + \gamma^2/\lambda RT_o + \mu^2 g\Gamma/\gamma^2T_o}$$

The quantities in this equation are presented in a following section on evaluation of the roots. They give an approximate value for ϕ of 0.6×10^{-3}/cm. Since the value of ϕ used in the problem is 10^{-5}/cm, B_3 needs no modification to allow for a singularity. Later changes in the problem, due to the introduction of a lapse-rate, will not change the value of B_3 sufficiently to introduce this difficulty.

Since the solution above is exact, the approximations below must approach it as the lapse rate approaches zero. The solutions below, however, represent a more realistic atmosphere.

Constant lapse-rate--If it is assumed that $dT_o/dz = -\delta$, where δ is a constant, it is found that

$$\partial\rho_o/\partial z = -\rho_o(g - R\delta)/RT_o$$

This value must be substituted in (7) and (8). The set of assumptions (9) is applied, with the result that the form of (14) and (15) is unchanged. Since the temperature is now a function of height

$$dC/dz = \rho_o\gamma\Big\{-(R/c_v)\,dE/dz + \lambda RT_o\,d^2B/dz^2 - (g + \lambda R\delta)dB/dz$$
$$+ (-RE/c_v + \lambda RT_o\,dB/dz - gB)[-(g - R\delta)/RT_o + \mu^2\lambda R\delta/(\mu^2\lambda RT_o + \gamma^2)]\Big\}/$$
$$(\mu^2\lambda RT_o + \gamma^2) \quad \ldots\ldots\ldots\ldots\ldots\ldots\ldots\ldots\ldots \quad (19)$$

When (14), (15), and (19) are combined

$$d^2B/dz^2 - [g/RT_o - \mu^2\lambda R\delta/(\mu^2\lambda RT_o + \gamma^2)]\,dB/dz - [\mu^2 + \gamma^2/\lambda RT_o$$
$$+ \mu^2 g(\Gamma - \delta)/\gamma^2T_o + \mu^2 g\delta/(\mu^2\lambda RT_o{}^2 + \gamma^2T_o)]B = (1/c_pT_o)\,dE/dz$$
$$- [(g - R\delta)/RT_o - \mu^2\delta/(\mu^2\lambda RT_o{}^2 + \gamma^2T_o) + \mu^2 g/\gamma^2\lambda RT_o]RE/c_v \quad \ldots\ldots\ldots\ldots \quad (20)$$

In order that the equation be integrable in simple functions, it is necessary to replace $T_o(z)$ by T, the average temperature through the height interval. The substitution of T for T_o results in an error no greater than two per cent. With this limitation, the general solution of the homogeneous equation is

$$B_h = B_1e^{r_1z} + B_2e^{r_2z}$$

where

$$r = g/2RT - \mu^2\lambda R\delta/2(\mu^2\lambda RT + \gamma^2)$$
$$\pm\sqrt{[g/2RT - \mu^2\lambda R\delta/2(\mu^2\lambda RT + \gamma^2)]^2 + \mu^2 + \gamma^2/\lambda RT + \mu^2 g(\Gamma - \delta)/\gamma^2T + \mu^2 g\delta/(\mu^2\lambda RT^2 + \gamma^2T)}$$

The particular solution is $B_3e^{-\phi z}$, and B_3 may easily be calculated from the differential equation by substituting this expression in the equation.

In order to simplify the equations, the numerical values of the physical model will be substituted into these results, before the boundary conditions are applied. It must be noted, therefore, that while the preceding equations are reasonably general, the work which follows applies only to the specific problem described below.

Evaluation of the roots--In a previous paper [LANGWELL, 1948], the author described observations made over the water north of Puerto Rico. (For further data on this region, see also BUNKER and Others [1949].) Within the "cloud" layer, which is a conditionally stable region about two kilometers thick bounded above and below by inversions, a horizontal period of about

12 mi is observed in the temperature and moisture measurements taken through the extensive clear areas. These periods are 180° out of phase. The amplitude of the variations increases with height. This results in cold moist sacs being found below the upper limit of the cloud layer. It was suggested that these sacs, probably the residue of dissipated clouds, would initiate cellular motion within the layer. The horizontal extent of a cell is assumed to be half the period of the temperature variations. The heat source is assumed to decrease with height at the same rate as the cold pockets decrease from the upper inversion downward. The range of temperature for a horizontal traverse was measured at two heights, and an exponential decrease assumed between them. The following values have been substituted in the evaluation of the roots.

$R = 2.87 \times 10^{6}\ \mathrm{cm^2/sec^2\ deg}$
$\Gamma = 10^{-4}\ \mathrm{deg/cm}$
$T = 285°\ \mathrm{K}$
$\lambda = 1.4$

$\mu = 3 \times 10^{-6}/\mathrm{cm}$, $\mu^2 = 9 \times 10^{-12}/\mathrm{cm}^2$
$g = 980\ \mathrm{cm/sec^2}$
$\delta = 0.6 \times 10^{-4}\ \mathrm{deg/cm}$
$\phi = 10^{-5}/\mathrm{cm}$

Further, the value $\gamma = 10^{-4}/\mathrm{sec}$ was chosen as appropriate to the data. If $\gamma = 10^{-3}$, the disturbance is reduced by e^{-1} in about 15 min, and would be difficult to observe. On the other hand, if $\gamma = 10^{-5}$, a reduction by e^{-1} would take over a day.

It is then found that, to a high degree of approximation,

$$g/2RT - \mu^2\lambda R\delta/2(\mu^2\lambda RT + \gamma^2) = 5 \times 10^{-7} = (g/2RT - \delta/2T)/\mathrm{cm}$$

$$\sqrt{[g/2RT - \mu^2\lambda R\delta/2(\mu^2\lambda RT + \gamma^2)]^2 + \mu^2 + \gamma^2/\lambda RT + \mu^2 g(\Gamma - \delta)/\gamma^2 T + \mu^2 g\,\delta/(\mu^2\lambda RT + \gamma^2)}$$
$$= 3 \times 10^{-4} = \mu\sqrt{g(\Gamma - \delta)/T}/\gamma/\mathrm{cm}$$

and

$$B_3 = E'/c_p(\Gamma - \delta)\ \mathrm{cm/sec}$$

It can be seen from the above that it is reasonable to state that

$$B = B_1 e^{\mu/\gamma\sqrt{g/T(\Gamma - \delta)}z} + B_2 e^{-\mu/\gamma\sqrt{g/T(\Gamma - \delta)}z} + E'e^{-\phi z}/c_p(\Gamma - \delta) \quad \ldots\ldots\ldots\ldots (21)$$

Boundary condition--In order that cellular motion exist, it is necessary that w and hence B, vanish at the base and at some other height, h. If these conditions are imposed on B, the relationship between B_1 and B_2 may be expressed as

$$B_1 + B_2 = -E'/c_p(\Gamma - \delta)$$

and

$$B_1 e^{\mu/\gamma\sqrt{g/T(\Gamma - \delta)}h} + B_2 e^{-\mu/\gamma\sqrt{g/T(\Gamma - \delta)}h}$$
$$+ E'e^{-\phi h}/c_p(\Gamma - \delta) = 0$$

To the degree of approximation that

$$e^{-\mu/\gamma\sqrt{g/T(\Gamma - \delta)}h} = e^{-60} = 0$$

$$B = E'[-e^{-\phi h}\, e^{-\mu/\gamma\sqrt{g/T(\Gamma - \delta)}(h - z)} - e^{-\mu/\gamma\sqrt{g/T(\Gamma - \delta)}z} + e^{-\phi z}]/c_p(\Gamma - \delta) \quad \ldots\ldots\ldots (22)$$

The vertical component of the velocity may now be written as

$$w = E'e^{i\mu x - \gamma t}\,[-e^{-\phi h}\, e^{-\mu/\gamma\sqrt{g/T(\Gamma - \delta)}(h - z)} - e^{-\mu/\gamma\sqrt{g/T(\Gamma - \delta)}z} + e^{-\phi z}]/c_p(\Gamma - \delta)$$

or, taking the real part,

$$w = E'e^{-\gamma t} \cos\mu x[-e^{-\phi h}\, e^{-\mu/\gamma\sqrt{g/T(\Gamma - \delta)}(h - z)} - e^{-\mu/\gamma\sqrt{g/T(\Gamma - \delta)}z} + e^{-\phi z}]/c_p(\Gamma - \delta) \;.\; (23)$$

After the value for B is inserted in (14), the real part of the perturbation pressure is

$$\begin{aligned} p = {} & \rho_0 E' e^{-\gamma t} \cos\mu x \, [e^{-\phi z} (\gamma(\Gamma-\delta)/\mu^2 T - \gamma g/\mu^2 \lambda RT - \gamma\phi/\mu^2) \\ & + e^{-\phi h} e^{-\mu/\gamma\sqrt{g/T(\Gamma-\delta)}(h-z)} (\gamma g/\mu^2\lambda RT - \sqrt{g(\Gamma-\delta)/T}/\mu) \\ & + e^{-\mu/\gamma\sqrt{g/T(\Gamma-\delta)}z} (\gamma g/\mu^2\lambda RT + \sqrt{g(\Gamma-\delta)/T}/\mu)]/c_p(\Gamma-\delta) \quad \ldots\ldots\ldots\ldots (24) \end{aligned}$$

SSimilarly, it may be seen from (10) that

$$\begin{aligned} u = {} & E' e^{-\gamma t} \sin\mu x \, [e^{-\phi z} (-(\Gamma-\delta)/\mu T - g/\mu\lambda RT - \phi/\mu) \\ & + e^{-\phi h} e^{-\mu/\gamma\sqrt{g/T(\Gamma-\delta)}(h-z)} (g/\mu\lambda RT - \sqrt{g(\Gamma-\delta)/T}/\gamma) \\ & + e^{-\mu/\gamma\sqrt{g/T(\Gamma-\delta)}z} (g/\mu\lambda RT + \sqrt{g(\Gamma-\delta)/T}/\gamma)]/c_p(\Gamma-\delta) \quad \ldots\ldots\ldots\ldots (25) \end{aligned}$$

The last three equations are the perturbation quantities which describe the cellular motion. Each is a separable function of x, z, and t. In order to make these results as clear as possible, the velocities are discussed as a function of each variable. It can be seen from (23) and (25) that, at a given point in space

$$u = U_1 e^{-\gamma t}$$

and

$$w = W_1 e^{-\gamma t}$$

where U_1 and W_1 are constants determined by the x and z. The circulation, therefore, dies out exponentially with time. At a given height and time

$$u = U_2 \sin\mu x$$

and

$$w = W_2 \cos\mu x$$

where U_2 and W_2 are constant at any z and t, and x varies from 0 to π/μ. The horizontal velocity vanishes at the edges of the cell, and reaches a maximum at $x = \pi/2\mu$, while the vertical velocity is a maximum at one edge, decreasing monotonically to a minimum at the other. For a given time and location (in x)

$$\begin{aligned} u = U_3 \Big\{ & e^{-\phi z} [-(\Gamma-\delta)/\mu T - g/\mu\lambda RT - \phi/\mu] \\ & + e^{-\phi h} e^{-\mu/\gamma\sqrt{g/T(\Gamma-\delta)}(h-z)} (g/\mu\lambda RT - \sqrt{g(\Gamma-\delta)/T}/\gamma) \\ & + e^{-\mu/\gamma\sqrt{g/T(\Gamma-\delta)}z} (g/\mu\lambda RT + \sqrt{g(\Gamma-\delta)/T}/\gamma) \Big\} \end{aligned}$$

and

$$w = W_3 [- e^{-\phi h} e^{-\mu/\gamma\sqrt{g/T(\Gamma-\delta)}(h-z)} - e^{-\mu/\gamma\sqrt{g/T(\Gamma-\delta)}z} + e^{-\phi z}]$$

where U_3 and W_3 are constant, and z varies from zero to two kilometers. In Table 1, the values are presented in the reverse of the usual order, as an aid to visualization.

Table 1--The change of the perturbation velocities with height

z	u/U_3	w/W_3
cm		
2×10^5	- 15.4	0
1.8×10^5	- 0.68	0.16
1.5×10^5	- 0.74	0.22
10^5	- 1.2	0.37
10^4	+ 0.52	0.88
10^3	+ 79.1	0.29
10^2	+110	0.04
10	+114	0.01
0	+114	0

The large values of u/U_3 through the uppermost and lowest meter of the cell are due to the dominance of the terms involving γ^{-1} through these height intervals. Complete symmetry of the terms from the free oscillations is prevented by the rapid damping of the heat source with height. The oscillation of u/U_3 is caused by the relative importance of the first term through the center of the layer. It will be noted that the horizontal velocity changes sign well below the midpoint of the interval, at about the same height as w/W_3 reaches a maximum. The circulation is deformed by the decrease of the heat source with height, in such a way that the mass transport through the lowest 100 m is counterbalanced by motion through the remaining 1900 m.

Discussion of results--In the previous section, it was shown that the two equations determining B_1 and B_2 are inhomogeneous. Solution of these equations is possible for all non-trivial values of E' and h. Cellular motion can always exist through any height interval of an atmosphere disturbed from hydrostatic equilibrium by a heat source. Because the perturbation velocities and pressure are proportional to $E'/(\Gamma - \delta)$, the amplitude of the disturbance is directly proportional to the magnitude of the heat source and inversely proportional to the stability. For a given source, the magnitude of the disturbance decreases with increasing thickness of the layer. The characteristics of the solutions given above are in agreement with what might be qualitatively expected. Since the purpose of this paper is to determine whether the circulation started by the sinking of the denser air is sufficient to initiate cellular motion of any duration, it is necessary to know the value of E' (the rate at which heat must be added to the system to maintain motions of the required scale). If w is never greater than 5 cm/sec at any height

$$5 = E'/c_p(\Gamma - \delta)$$

and

$$E' = 4.8 \times 10^{-5} \text{ cal/gm sec}$$

In order to evaluate the effectiveness of the temperature difference available, the first law of thermodynamics is used. As a first approximation, it is assumed that $dp = 0$. It may then be stated that

$$- E'\Delta t = - c_p \Delta T$$

Since a temperature difference from the surrounding air as great as 1.2° K is generally observed at 6000 ft or higher

$$\Delta t \approx 6000 \text{ sec}$$

It is thus reasonable to estimate that the sacs of cold air initiate cellular motion which persists for one to two hours.

The factors omitted from this problem are the curvature of the Earth, its rotation, and the wind shear. Those included are the compressibility of the atmosphere, a localized heat source, a self-dissipative term, and a qualitative measure of a constant lapse-rate. Within this framework, it has been shown that the cellular motion set up by the cold sacs would be maintained for one to two hours.

Since the temperature fluctuations are largest in the non-turbulent air, and the temperature and moisture vary oppositely, making the virtual temperature less variable than the dry-bulb temperature, the assumption that these fluctuations are initially caused by dissipated clouds seems proprobable [LANGWELL, 1948]. It is therefore reasonable to expect that they would be regenerated several times a day. The combination of these two factors is sufficient to make such cells a semipermanent feature of this weather situation.

Possible extensions--The equations used in this paper may be modified in several ways, to extend the solution to other problems. If the coordinate system is presumed to be fixed, a constant wind is added, and $-\gamma$ is replaced by $-\gamma + i\mu u_0$ in Eq. (10) to (13). A velocity of the circulation relative to the undisturbed wind may also be included by assuming that the perturbations are of the form $\exp [i\mu(x - ct) - \gamma t]$. The term $-\gamma + i \; (u_0 - c)$ will replace $-\gamma$ in the perturbation equations. The problem may still be solved by the same techniques, but both terms of the exponential are complex, and some manipulation is required to reduce the solutions to a usable form. Similarly, the inclusion of the third dimension and a constant Coriolis force will add to the length of the equations, but not to the mathematical difficulty of the problem. However, it is beyond the scope of this type of solution to deal any more exactly with wind shear or a variable Coriolis parameter than has been possible with the temperature lapse-rate.

Acknowledgments--The author desires to thank the members of the Woods Hole Oceanographic Institution for their assistance, and especially B. Haurwitz for his continued help and encouragement. The work was initiated under contract with the Bureau of Ships, and continued under the sponsorship of the Office of Naval Research.

This paper was presented in partial fulfillment of the requirements for the degree of doctor of philosophy in meteorology at New York University.

References

BJERKNES, V., J. BJERKNES, H. SOLBERG, and T. BERGERON, Hydrodynamique Physique, Presses Univ. France, 3 v., 1934.
BUNKER, A. F., B. HAURWITZ, J. S. MALKUS, and H. STOMMEL, Vertical distribution of temperature and humidity over the Caribbean Sea, Pap. Phys. Oceanogr. and Met., Mass. Inst. Tech. and Woods Hole Oceanogr. Inst., v. 11, no. 1, 1949.
DOPORTO, MARIANO, Cell motion in the atmosphere, Dept. Ind. Comm., Met. Sec., Dublin, Tech. Note no. 6, 1945 (unpublished).
HAURWITZ, B., Dynamic meteorology, McGraw-Hill, 1941.
LAMB, H., Hydrodynamics, Dover Pub., 1945.
LANGWELL, PATRICIA A., Inhomogeneities of turbulence, temperature and moisture in the West Indies trade-wind region, J. Met., v. 5, pp. 243-246, 1948.
LOVE, A. E. H., Wave motions in a heterogeneous heavy liquid, Proc. London Math. Soc., v. 22, p. 307, 1891.
MUNK, WALTER H., Effect of Earth's rotation upon convection cells, Ann. N. Y. Acad. Sci., v. 48, Art. 8, pp. 815-820, 1947.
STARR, V., A mathematical theory of convection, J. Met., v. 6, pp. 188-192, 1949.
STOMMEL, HENRY, A summary of the theory of convection cells, Ann. N. Y. Acad. Sci., v. 48, Art. 8, pp. 715-726, 1947.

Department of Meteorology,
College of Engineering,
New York University,
New York 53, New York

(Manuscript received April 14, 1950; presented before the American Meteorological Society at the time of the Thirty-First Annual Meeting, Washington, D. C., May 2, 1950; open for formal discussion until July 1, 1951.)

Contribution No. 531

EXPERIMENTAL CORRELOGRAM ANALYSES OF ARTIFICIAL TIME SERIES (WITH SPECIAL REFERENCE TO ANALYSES OF OCEANOGRAPHIC DATA)

H. R. SEIWELL
WOODS HOLE OCEANOGRAPHIC INSTITUTION

CONTENTS

PAGE
1. Introduction . . . 639
2. Computational procedure . . . 640
3. Experimental model I . . . 640
4. Experimental model II . . . 648
5. Experimental model III . . . 652
6. Experimental model IV . . . 662

1. Introduction

When dealing with data as they come from nature, the applied statistician is frequently faced with the prospect of selecting and modifying theoretical mathematical methods to fit the special conditions imposed by the data themselves. Since theoretical mathematical tools are developed for specific situations they may become unsafe for applications outside the framework for which they were originally intended. Observations on natural phenomena cannot usually be controlled in the sense of a controlled laboratory experiment, and for obvious reasons, they are finite in scope. Hence, some form of experimental modification of theoretical formulae is usually essential if the maximum correct information is to be obtained from the data.

Data dealing with time variations of natural phenomena usually leave much to be desired in that the lengths of observed series may be woefully short, they are masked by various degrees of error and are sometimes sporadic and disconnected. Furthermore, the dynamics of the generating mechanisms are frequently not known, so that *a priori* considerations are purely speculative. A further complication concerns the length of the time series to be utilized for computation. The individual members of the series being dependent, one on the other, so that regardless how many are chosen, within practical limits, the number becomes small in light of the requirements imposed by random sampling. A further point of

---

This paper is contribution No. 531 from the Woods Hole Oceanographic Institution and U.S. Navy Office of Naval Research Contract No. N6onr 277 Task Orders 1 and 8. At the time of his death on March 7, 1951, the author was a John Simon Guggenheim Memorial Fellow, 1950–1951.

Reprinted from
Proceedings of the Second Berkeley Symposium on Mathematical Statistics and Probability

significance is that the observed sequence of events may be stationary only for brief intervals and, hence, imposes a limit to the length of series entering into the analysis.

Experience has indicated the superiority of the correlogram method in certain analyses of geophysical time series. However, it is new and practical experimentation is required to interpret the results revealed by its application to natural data. Hence, at a risk of being considered not too fashionable, an experimental study of correlogram analyses of several artificially generated series has been undertaken. The following is a descriptive account of the first results of these researches on four mathematical models. The information obtained has been very useful in the interpretation of correlogram analyses of natural data with which we are concerned. Although experience with many analyses has revealed the power of the correlogram method, general conclusions have at this time been avoided. It is to be hoped that the following results will stimulate additional research.

2. Computational procedure

Both hand and machine procedures for computation of autocorrelation coefficients, as undertaken in this laboratory, have been previously described [7].

The large amount of computation required for the investigation was under the supervision of Mr. Thomas C. Duke and Mrs. Mary M. Hunt.

3. Experimental model I

3.1. *Pattern of analyses*. Model I is an analysis of the function

$$y = \sin \frac{2\pi x}{10} + \epsilon \tag{1}$$

where ϵ is an assumed rectangularly distributed random variable.

The object of the study was to obtain general information on the correlogram of the function and to observe the effect of a changing stochastic variable on statistical properties of both the basic data and the correlogram. Variations in the function studied were:

$$\text{Series A} = \epsilon$$

$$\text{Series B} = 5\epsilon$$

$$\text{Series C} = 8\epsilon$$

$$\text{Series D} = 10\epsilon\,.$$

Each series, composed of a sine wave plus added random numbers, may be likened to a message containing a basic signal masked by a degree of noise. A fundamental problem is to isolate the signal from the message and to discover as much as possible about its physical properties. Although the models have no particular physical significance, they may approximate a type of function underlying natural time series. In the special case of Oceanography, it appears reasonable that at times the sea surface roughness pattern may be represented by a single cyclical component (sea swell) plus random disturbances (local sea) [5]. However, regardless of the exact nature of the phenomenon, it is significant in the beginning to demonstrate that for series of the type represented by model I, conclusions regarding the physical properties of the phenomena require special transformations of the basic data.

3.2. *Properties of the basic data.* Statistical properties of the basic data (figure 1) tabulated in table I are based on a minimum of twenty-five complete cycles (200 units). The computed means and variances for the series do not differ significantly from theoretical values and the samples closely approximate properties of the parent.

The presence of the random disturbances masks the underlying rhythmic cycle and it will not be recognized by the distances between successive peaks or successive upcrosses. Thus, for series A, where the cosine variance is 86 percent of the total variance, the mean distance between peaks is not 10, but 4.86 units. This distance between peaks becomes less as the magnitude of randomness is increased, and at the five fold mark, its mean value is but little more than the theoretical value of 3 units, characteristic of a random sequence.

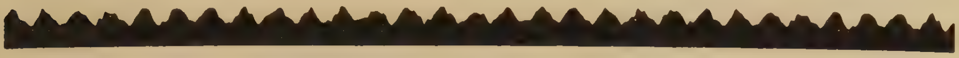

Series A

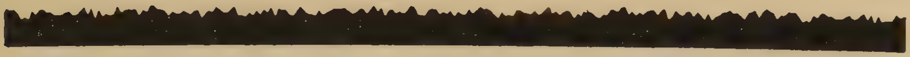

Series B

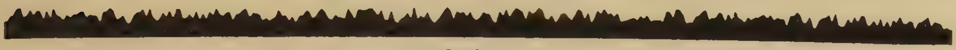

Series C

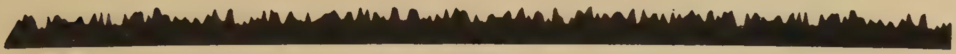

Series D

FIGURE 1

Graphs of model I data

Distances between upcrosses indicate essentially the same situation; for series A, the mean distance of 8.76 units rapidly diminishes with increased randomness to the theoretical value of 4 units, characteristic of a random series.

Hence, it is apparent that when the underlying rhythmic component of a simple time series is disturbed by a random influence (noise), the properties of the component (or even its presence) are not revealed by the method of measuring distances between peaks or upcrosses in the basic data. This information is not new. It has been discussed by other investigators, and in particular, M. G. Kendall [2] has shown its unreliability for several well known economic series. The argument that selective methods may be used for identifying peaks appears equally unsound unless the effect of the randomness can be first eliminated.

TABLE I

SELECTED STATISTICAL PROPERTIES OF MODEL I

PROPERTY	SYMBOL	COMPUTED VALUES				THEORETICAL VALUES			
		Series A	Series B	Series C	Series D	Series A	Series B	Series C	Series D
Distribution of ϵ		R(0, 1)	R(0, 5)	R(0, 8)	R(0, 10)	......	......	......	......
Function mean	M	0.516	2.539	4.001	5.068	0.500	2.500	4.000	5.000
Average deviation	AD	0.667	1.330	2.120	2.542	......	......	......	......
Standard deviation	σ	0.773	1.579	2.523	2.914	0.764	1.607	2.415	2.972
Deviation ratio	AD/σ	0.863	0.842	0.840	0.872	......	......	......	......
Mean dist. peaks		4.86	3.03	3.01	2.94	9.13	6.14	4.80	3.56
Mean dist. upcrosses		8.76	3.90	4.08	4.06	9.99	9.65	8.62	5.24
Total variance	σ_y^2	0.598	2.492	6.366	8.727	0.583	2.582	5.831	8.833
Cosine variance	$\sigma_{\cos}^2$	......	....	......	......	0.500	0.500	0.500	0.500
ϵ variance	σ_ϵ^2	0.092	2.1212	5.856	8.485	0.083	2.082	5.331	8.333
Period cosine	T	10.0	10.0	10.0	......	10.0	10.0	10.0	10.0
Amplitude cosine	C	0.991	0.854	1.128	0.778	1.00	1.00	1.00	1.00
Terminal amplitude	r_T	0.89	0.19	0.12	0.0	0.857	0.194	0.086	0.057

To carry the above a little further, theoretical distances between peaks and upcrosses of the four series were computed by the method of M. G. Kendall, which is applicable to a simple linear autoregressive series of the type

$$u_{t+2} + au_{t+1} + bu_t = \epsilon_{t+2} \tag{2}$$

where ϵ is a random variable, and u_t normally distributed. This method and procedure is discussed in detail in the section on autoregression, to which it is applicable. The results obtained from its application to model I are tabulated in table I. They do not, as expected, throw any particular light on the subject and are presented only for future reference. However, it is to be noted that for series A, the computation, based on the first two autocorrelations, gives correct period for distance between upcrosses.

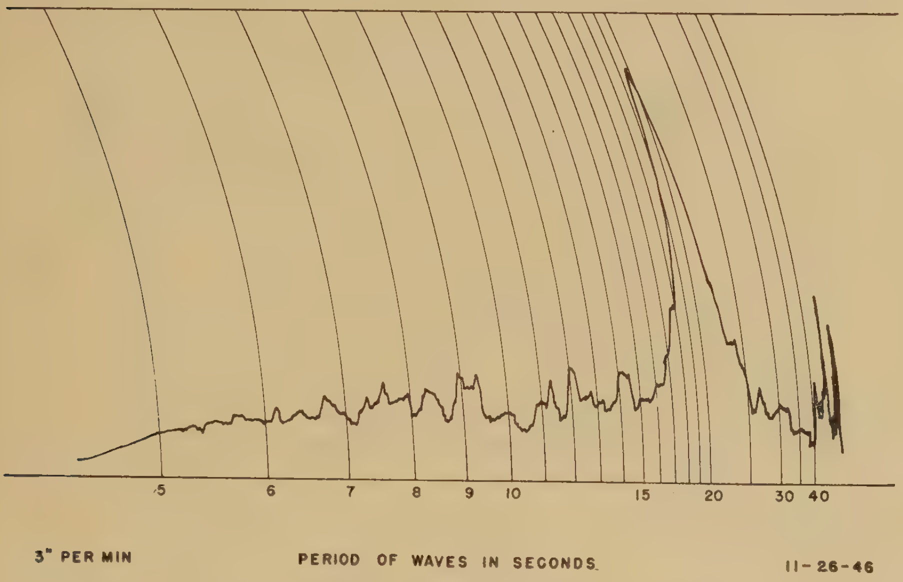

FIGURE 2

Periodogram model I, series A; period scale 2 × units

The masking effect of the random component on amplitudes of the trigonometric is also revealed by data in table I, where the sine amplitude C computed by least squares for a ten unit period in the basic data, attained 99 percent of its value for series A, and diminished to 78 percent for series D.

Other statistics of the basic data are tabulated in table I for reference purposes. The ratio of the average deviation to the standard deviation is significant in that it lies between 0.84 and 0.87, a value fairly close to the theoretical AD/σ ratio for cosines. This property is discussed in a later section.

3.3. *Periodogram analyses.* Classical periodogram analysis of natural time series, for which there is no *a priori* knowledge of periodicity, has fallen into more or less disrepute. The results of periodogram analyses performed on each of the four series (figures 2 to 5) by means of a mechanical periodogram analyzer [4], are

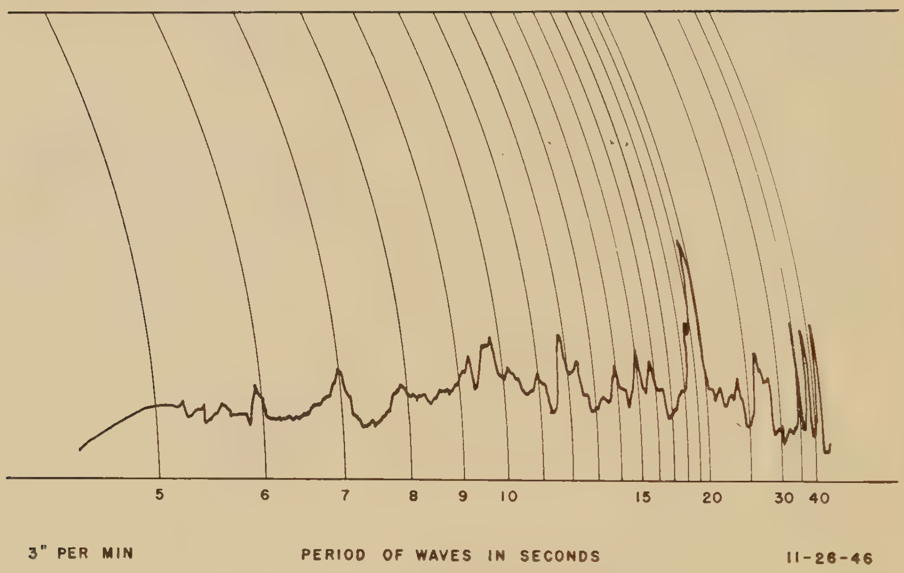

Figure 3

Periodogram model I, series B; period scale 2 × units

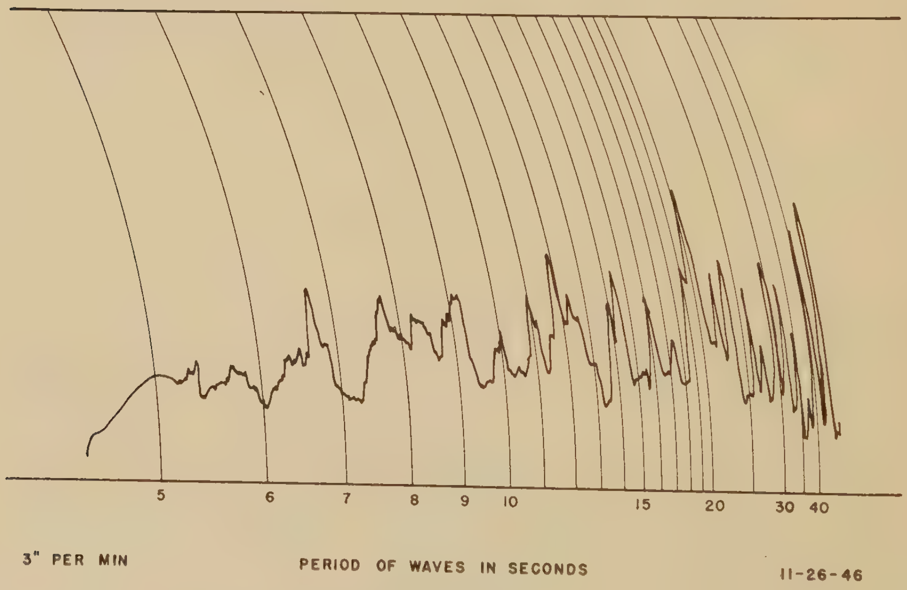

Figure 4

Periodogram model I, series C; period scale 2 × units presented to illustrate the danger of misinterpreting fundamental properties of natural time series.

In the case of series A (variance of random component 14 percent of the total variance) the ten unit peak is clearly defined in its periodogram and provided minor peaks are ignored, the analysis could be correctly interpreted. However, as the magnitude of the random component increases, as in series B (variance of random component 81 percent of total or about five times the cosine variance) the relative magnitudes of the spurious peaks increase, and although the ten unit peak is still superior, there is danger of interpreting the periodogram as representing an interference pattern comprised of other frequencies, particularly those between 5 and 30 units.

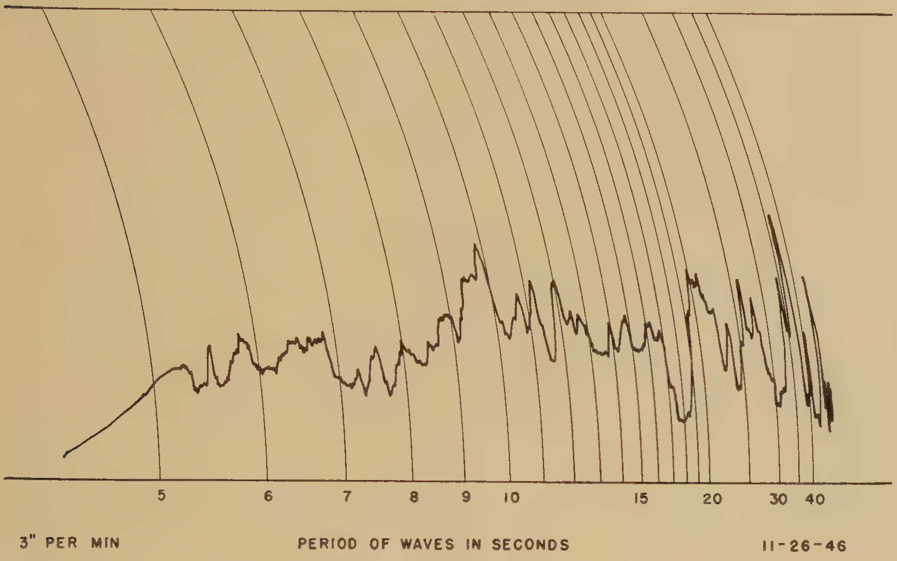

FIGURE 5

Periodogram model I, series D; period scale 2 × units

As the magnitude of the random component increased still further, the periodogram became more complex, and for series C (variance of random component approximately 12 times the cosine variance) the dozen or more principal peaks could be interpreted as indicating an equal number of harmonic components in the basic data.

In the final case of series D (variance of random component approximately 17 times the cosine variance), the ten unit peak is completely masked and unrecognizable in its periodogram.

Periodograms similar to these frequently result from the analyses of natural data for which there is no *a priori* knowledge of periodicity and have been interpreted as providing clues to physical properties of the data [1]. The subject is not new and various investigators have discussed the fallacy of conclusions from periodogram analyses of economic and natural time series [2], [8]. Our experiments indicate that periodogram analyses of finite data may possibly be interpreted with a degree of reliability only when the random component is absent or of very low magnitude, and only then by the point location of the most prominent peak on the frequency scale. Its breadth is not sufficient evidence of a train of waves in the basic data.

The above analyses were undertaken on finite series comprised of 215 units. Although some deleterious effects of periodogram analyses are eliminated by using larger and larger amounts of data, a situation is rapidly approached where the computational labor becomes prohibitive.

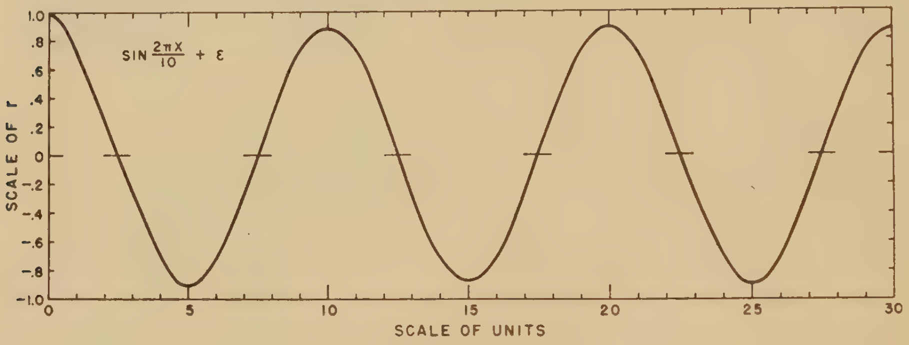

FIGURE 6

Correlogram model I, series A

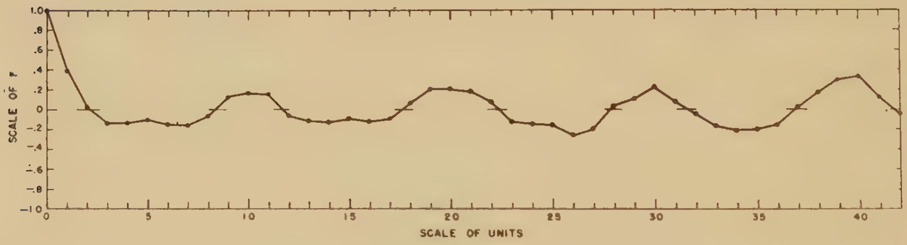

FIGURE 7

Correlogram model I, series B

3.4. *Correlogram analyses.* (a) *Basic data.* In these analyses we follow a pattern developed for ocean wave observations. After preliminary study, the basic data are subjected to autocorrelation analyses, the correlogram is drawn and then evaluated. The particular procedure applied to model I is applicable to natural data only in the special case where its correlogram clearly reveals a single rhythmic component and when it damps to a terminal amplitude. When this is the case, the amplitude, associated with the frequency determined by autocorrelation, is computed and the residue, remaining after its subtraction from the basic data, is again subjected to autocorrelation analyses.

The correlograms of the four series (figures 6 to 9) when viewed together clearly demonstrate the power of autocorrelation analysis as a means of revealing the period of the rhythmic component in the basic data, provided it is not completely masked by the random component. Thus, for series A and B, the ten unit period is clearly defined by the correlogram; in series C, it may be estimated with reasonable accuracy; but, in series D, the random variable is too large to permit period identification. When natural data are being investigated, periods revealed in this fashion are utilized for determining the amplitude of the rhythmic component.

The correlograms of series A, B and C, are characteristic of those for a single trigonometric with added random noise. They damp to terminal amplitudes and remain constant. This, together with the uniform correlogram period of ten units, provides information on physical properties of unknown series and is similar to a type of correlogram which has been obtained for sea surface wave heights [5], [6]. The terminal amplitudes observed for the correlograms agree well with their theoretical values (table I) and demonstrate the reliability of the autocorrelation computation on finite amounts of data for this type of function when not completely masked by random noise.

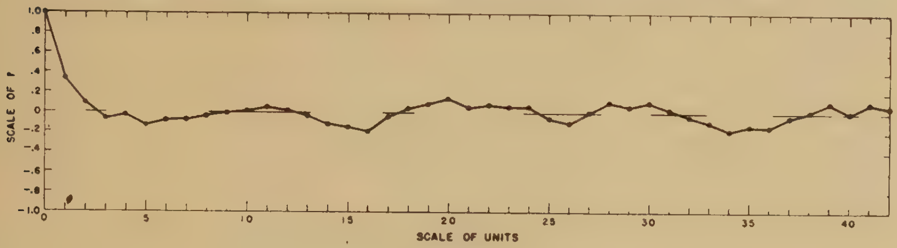

FIGURE 8

Correlogram model I, series C

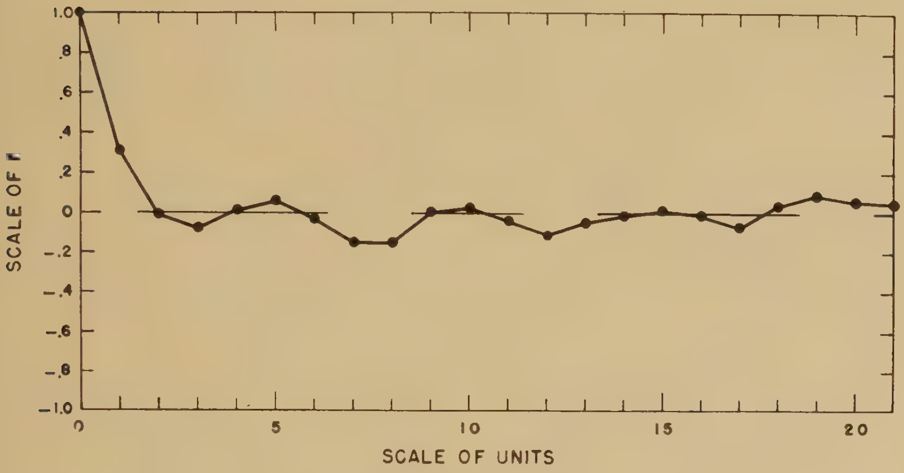

FIGURE 9

Correlogram model I, series D

The theoretical terminal amplitude r_T of a sine with added random component is

$$r_T = \frac{\text{variance cosine}}{\text{total variance}}. \tag{3}$$

It expresses the percent reduction due to the cyclical component and is an important property of the data.

(b) *Residual data.* The correlogram for the residuals of series A (figure 10) is similar to that for a series of random (or nearly so) numbers. It demonstrates that practically complete removal of the cosine from the basic data is possible under the circumstances outlined.

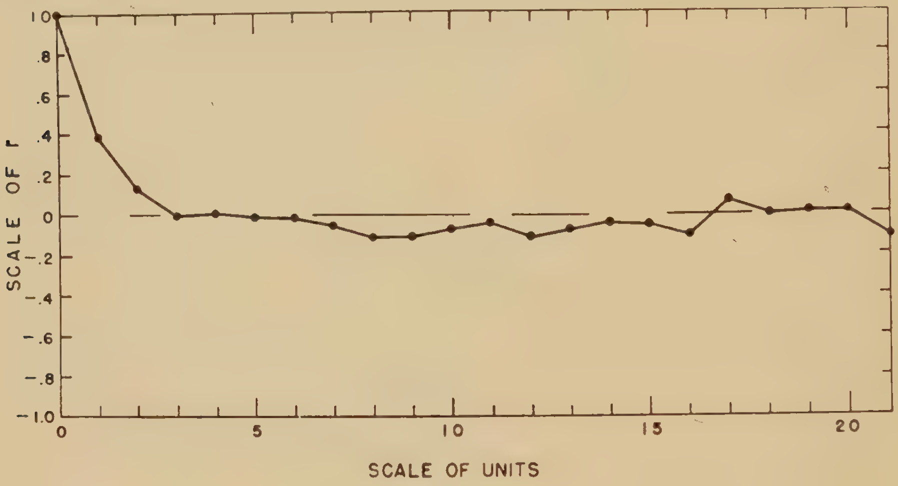

FIGURE 10

Correlogram of residuals model I, series A

4. Experimental model II

4.1. *Pattern of analyses.* Model II is concerned with analyses of combinations of a sum of sines:

$$y = a_1 \sin \frac{2\pi}{T_1} k + a_2 \sin \frac{2\pi}{T_2} k + a_3 \sin \frac{2\pi}{T_3} k . \tag{4}$$

It is known that the correlogram of a series of several harmonic terms will have a sinusoidal form which does not damp to zero. However, the form of the correlogram varies according to the combination of cyclical components making up the original series. It is important that the properties of correlograms of such combinations be examined for distinguishing characteristics to provide a general guide in correlogram analyses of natural series.

In this section we are concerned only with the forms of the correlograms drawn in each case from sixty theoretical autocorrelation coefficients r_k in one unit steps, and computed according to the general equation:

$$r_k = \frac{a_1^2 \cos \frac{2\pi}{T_1} k + a_2^2 \cos \frac{2\pi}{T_2} k + a_3^2 \cos \frac{2\pi}{T_3} k}{a_1^2 + a_2^2 + a_3^2} . \tag{5}$$

The various combinations of harmonic terms considered in this section are as follows. Key characteristics of their correlograms (illustrated in figure 11) are tabulated in tables II and III.

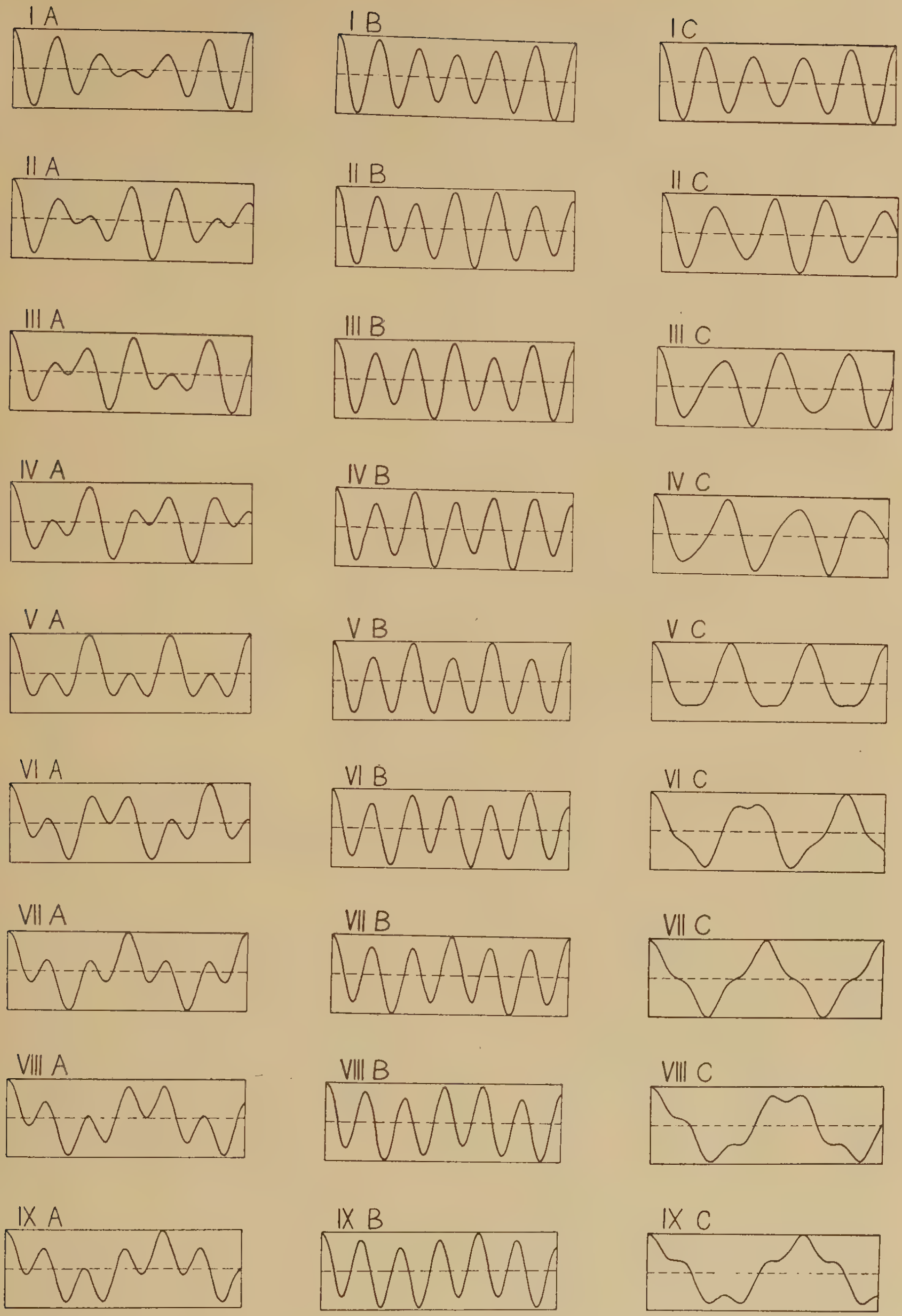

FIGURE 11

Correlograms of combinations of sums of two sines of model II. See table II for period and amplitude combinations. In each correlogram, abscissa is scale of units from 0 to 60 and ordinate is scale of r from -1.0 to $+1.0$. Left column—series I–A to IX–A; middle column—series I–B to IX–B; right column—series I–C to IX–C.

Series A. Nine combinations of two sines

$$a_1 = a_2 \,,$$

$$T_1 = 10 \,, \qquad T_2 = 12 \text{ to } 40 \,.$$

Series B. Nine combinations of two sines

$$a_1 = 1 \,, \qquad a_2 = 0.5 \,,$$

$$T_1 = 10 \,, \qquad T_2 = 12 \text{ to } 40 \,.$$

Series C. Nine combinations of two sines

$$a_1 = 1 \,, \qquad a_2 = 2 \,,$$

$$T_1 = 10 \,, \qquad T_2 = 12 \text{ to } 40 \,.$$

Series D. Seven combinations of three sines

$$a_1,\ a_2,\ a_3 = \text{combinations of } 1 \text{ and } 2 \,,$$

$$T_1 = 10 \,, \qquad T_2 = 12 \,, \qquad T_3 = 14 \,.$$

Series E. Seven combinations of three sines

$$a_1,\ a_2,\ a_3 = \text{combinations of } 1 \text{ and } 2 \,,$$

$$T_1 = 10, \qquad T_2 = 12 \,, \qquad T_3 = 40 \,.$$

Series F. Three combinations of three sines

$$a_1,\ a_2,\ a_3 = \text{combinations of } 1 \text{ and } 2 \,,$$

$$T_1 = 10 \,, \qquad T_2 = 20 \,, \qquad T_3 = 30 \,.$$

4.2. *Summary of correlogram characteristics for series composed of more than one cyclical component.* The correlograms of series consisting of two sines with various amplitude and period combinations have unequal distances between cycles, they do not damp to zero, but show alternating damping and growth. Series of this type generally are recognizable within the first few correlogram cycles, as distinguished from correlograms of series having a single cyclical component. Unequal distances between correlogram peaks always occurred within the first four cycles, the usual difference of 1 to 3 units occasionally attained 23 units. As the periods of the two sine combinations diverge, distances between successive peaks of the correlogram tend to become more uniform but the alternate damping and growing increases. In the case where the longer period wave has the larger amplitude, the correlogram is less symmetrical, and damping is consistent through 1 to 3 cycles only. It is the irregular nature of the damping and growth and the unequal distances between peaks, usually occurring within the first 3 to 4 cycles, and the occurrence of ripples, which permit identification of the correlogram as representing a basic series containing more than one trigonometric.

Correlograms of series composed of three sines appear to be, in general, more symmetrical than the above; although rippling increases and asymmetry increases when the longer period sine has the larger amplitude. Damping is consistent only through the first 1 to 4 cycles and distances between individual cycles range up to 16 units within the first 2 to 5 cycles. Differences in distances within the first 2 cycles are generally of the order of 0.5 to 3.5 units. In these cases, as in the above, the nature of the damping and of the differences in distances between peaks and the occurrence of ripples permit some discrimination of the correlogram within the first 3 or 4 cycles.

In practice correlograms of natural time series which indicate the presence of more than one cyclical component are subjected to a Fourier transform of their autocorrelation coefficients. In this manner it is frequently possible to identify the frequencies of the components and evaluate their other properties.

TABLE II

PROPERTIES OF CORRELOGRAMS OF TWO SINES: $a_1 \sin \frac{2\pi}{T_1} k + a_2 \sin \frac{2\pi}{T_2} k$

Series A: $a_1 = a_2$; Series B: $a_1 = 1$, $a_2 = 0.5$; Series C: $a_1 = 1$, $a_2 = 2$

Curve Designation	Column: 1		2	3	4	5	6	7	8	9	10	11
	Unit Periods		Unit Distances between Peaks for Cycles:						Max. Difference	Min. No. Cycles	First Two Cycle Difference	Consistent Damping to Cycle
	T_1	T_2	1	2	3	4	5	6				
I A	10	12	11	10.5	8.5	8.5	10.5	11	2.5	3	0.5	3
II A	10	14	11	8	10.5	11	10.5	8	3	2	3	2
III A	10	16	11	8	11.5	9.5	9.5	....	3.5	3	3	1
IV A	10	18	10.5	9.0	11.5	8	12	8	3.5	4	1.5	1
V A	10	20	10	10	10	10	10	10	0	...	0	1
VI A	10	25	9.5	11	9	11	9.5	9.5	2	3	1.5	1
VII A	10	30	9.5	11	9.5	9.5	11	9.5	1.5	2	1.5	1
VIII A	10	35	9.5	11	10	9	10	10.5	1.5	2	1.5	1
IX A	10	40	9.5	10.5	10.5	9.5	9.5	10.5	1	2	1	1
I B	10	12	10.5	10	9.5	9.5	10	10.5	1	3	0.5	3
II B	10	14	10.5	9.5	9.5	10.5	10	9.5	1	2	2	2
III B	10	16	10.5	9.5	10.5	10	10	10	1.5	2	1.5	1
IV B	10	18	10	9.5	10.5	9.5	10.5	9	1	3	0.5	1
V B	10	20	10	10	10	10	10	10	0	...	0	1
VI B	10	25	10	10	10	10	10	10	0	...	0	1
VII B	10	30	10	10	10	10	10	10	0	...	0	1
VIII B	10	35	10	10	10	10	10	10	0	...	0	1
IX B	10	40	10	10	10	10	10	10	0	...	0	1
I C	10	12	11.5	12	12.5	12	11.5	....	1	3	0.5	3
II C	10	14	13.5	15	13	15	....	....	2	3	1.5	1
III C	10	16	17	14	17.5	....	....	....	3.5	3	3	1
IV C	10	18	19	19	14	....	....	....	5	3	0	1
V C	10	20	20	20	20	....	....	....	0	...	0	0
VI C	10	25	22	6	22	....	....	....	16	2	16	1
VII C	10	30	30	30	....	....	....	....	0	...	0	0
VIII C	10	35	31	8	....	....	....	....	23	2	23	1
IX C	10	40	20	20	....	....	....	....	0	...	0	1

Tables II and III list the data discussed above. The first column tabulates the periods of the two sine combinations (table II) and amplitudes (table III) of the three sine combinations. Columns 2 to 7 tabulate the unit distances between successive correlogram peaks for six cycles and column 8 gives the maximum difference in unit distance between correlogram peaks. Then column 9 lists the minimum number of correlogram cycles in which the column 8 range occurred and in column 10 appears the differences in the first two correlogram peak distances. Finally, the last column tabulates the number of peaks (cycles) over which the correlogram consistently damped before growth.

TABLE III

PROPERTIES OF CORRELOGRAMS OF THREE SINES: $a_1 \sin \frac{2\pi}{T_1} k + a_2 \sin \frac{2\pi}{T_2} k + a_3 \sin \frac{2\pi}{T_3} k$

Top group: $T_1 = 10$, $T_2 = 12$, $T_3 = 14$; *Center group:* $T_1 = 10$, $T_2 = 12$, $T_3 = 40$
Bottom group: $T_1 = 10$, $T_2 = 20$, $T_3 = 30$

Column: 1			2	3	4	5	6	7	8	9	10	11
Amplitudes			Unit Distances between Peaks for Cycle:						Max. Difference	Min. No. Cycles	First Two Cycle Difference	Consistent Damping to Cycle
a_1	a_2	a_3	1	2	3	4	5	6				
1	1	1	11.5	10.5	6.5	11.0	9.5	10.0	5	3	1	2
1	1	2	13	15	13	16.5	....	....	3.5	5	2	2
1	2	2	12.5	13.5	13	9	10.5	....	4.5	4	1	4
1	2	1	11.5	12.5	13	11.5	11	....	2	5	1	3
2	1	1	10.5	9 5	9.5	10.5	9.5	9.0	1	2	1	2
2	1	2	11.5	8	10	11	10	8.5	3.5	2	3.5	2
2	2	1	11	10.5	8.0	9.0	10.5	10.5	3	3	0.5	3
1	1	2	10	13	16	9	12	....	7	4	3	1
1	1	1	10.5	11	10.5	6.5	10.5	11	4.5	4	0.5	1
2	1	1	10.5	10	9.5	9.5	10	10.5	1	3	0.5	1
1	2	2	11	13	13	11	12	....	2	2	2	1
1	2	1	11.5	12	13	12	11.5	....	1.5	3	0.5	1
2	1	2	10	10.5	10	9	10	10.5	1.5	4	0.5	1
2	2	1	10.5	11	9	8	10.5	11	3	4	0.5	3
1	1	1	9.5	12	8.5	9.5	11	9.5	3.5	3	2.5	0
1	1	2	23	7	7.5	22.5	....	....	16	2	16	1
2	1	2	9.5	11	9.5	9.5	11	9.5	1.5	2	1.5	1

5. Experimental model III

5.1. *The autoregressive scheme.* Knowledge of the autoregressive scheme is due primarily to the work of Maurice Kendall [2], [3]. We consider a series defined by the difference equation:

$$u_{t+2} = -a\, u_{t+1} - b\, u_t + \epsilon_{t+2}\,, \tag{6}$$

which may be regarded as expressing the regression of u_{t+2} on u_{t+1} and u_t. The term ϵ_{t+2} being a residual error.

The theoretical correlogram for a series generated by this difference equation will be damped and is given by

$$r_k = \frac{p^k \sin(k\theta + \psi)}{\sin \psi} \tag{7}$$

where the damping factor

$$p = \sqrt{b} \tag{8}$$

and

$$\cos \theta = -\frac{a}{2\sqrt{b}}, \tag{9}$$

$$\tan \psi = \frac{1+b}{1-b} \tan \theta\,. \tag{10}$$

The autoregressive period is:

$$\frac{2\pi}{\theta}. \tag{11}$$

Kendall points out that typical series of this kind have no "periods" in the strict sense. The lengths from peak to peak or from upcross to upcross vary and experiments indicate that the distributions are unimodal having central values somewhere near the mean distances. Hence, this central value of the distribution is considered the "period" of an autoregressive series.

The first two theoretical autocorrelations $r_0 = 1$ in terms of the coefficients are:

$$r_1 = \frac{-a}{1+b}, \tag{12}$$

$$r = \frac{a^2 - b(1+b)}{1+b}. \tag{13}$$

Also,

$$a = -\frac{r_1(1-r_2)}{1-r_1^2}, \tag{14}$$

$$b = -1 + \frac{1-r_2}{1-r_1}. \tag{15}$$

The estimate of the coefficients is quite sensitive to superimposed errors and it is unsafe to estimate the autoregressive period without reference to the correlogram. In our practical wave record analyses we base estimates of the autoregressive periods on values of the autocorrelations as well as on locations of the first valley and first peak of the correlogram.

The theoretical total variance of the autoregressive series is:

$$\sigma_y^2 = \frac{\sigma_\epsilon^2}{1 + a r_1 + b r_2} \tag{16}$$

where σ_ϵ^2 is the random variance.

In the practical applications of the autoregressive scheme to natural time series, certain properties of the basic data, as the mean distances between peaks and upcrosses, are important to identify properties of the series. For the normal series, the theoretical mean distance between peaks is given by:

$$\text{M.D. peaks} = \frac{2\pi}{\text{arc cos } \tau} \tag{17}$$

where

$$\tau = \frac{-1 + 2r_1 - r_2}{2(1-r_1)} \tag{18}$$

or

$$\tau = \frac{b^2 - (1+a)^2}{2(1+a+b)} = \frac{b-a-1}{2}. \tag{19}$$

The theoretical mean distance between upcrosses is

$$\text{M.D. upcrosses} = \frac{2}{\text{arc cos } r_1}. \tag{20}$$

Thus, for a random series the theoretical mean distance between peaks is 3 and that between upcrosses is 4.

5.2. *Pattern of analyses.* This section is concerned with an experimental correlogram analysis of eight autoregressive series of the type

$$x_{n+2} = -a x_{n+1} - b x_n + \epsilon_{n+2} . \tag{21}$$

Computations of autocorrelations of each series were based on a minimum of 180 to 500 terms. Duplicate computations were carried out on one series (G) using 180 and 500 terms, respectively. Two of the series (I and J) were identical with the exception of the stochastic variable being rectangularly distributed between -1 and 1 in one case and normally distributed between 0 and 1 in the other. Principal variations within the model, each indicated by a series letter, were produced by changing the damping coefficient (b) and holding the autoregressive period constant at 10 units. In table IV are tabulated the coefficients and the data pertinent to describe the various series. Properties of the series are tabulated in table V.

TABLE IV

Series	Constants		Period	Dist.	No. Terms
	a	b		ϵ	
B	−1.62	1.00	10	$R(-2, 2)$	215
F	−1.54	0.90	10	$R(-3, 3)$	215
G	−1.45	0.80	10	$R(-1, 1)$	180
G-1	−1.45	0.80	10	$R(-1, 1)$	500
I	−1.14	0.50	10	$R(-1, 1)$	180
J	−1.14	0.50	10	$N(\ 0, 1)$	180
K	−0.89	0.30	10	$N(\ 0, 1)$	180
L	−1.35	0.70	10	$N(\ 0, 1)$	500
M	−1.25	0.60	10	$N(\ 0, 1)$	400

5.3. *The mean distance between peaks and upcrosses.* From equations of the autoregressive period (11), the mean distances between peaks (17) and between upcrosses (20) in the basic data, we have as the ratio of mean distance between peaks T_p and autoregressive period T

$$\frac{T_p}{T} = \frac{1}{T} \operatorname{arc\,cos} \tfrac{1}{2} \left(b + 2 \sqrt{b} \cos \frac{2\pi}{T} - 1 \right) \tag{22}$$

and as the ratio of mean distance between upcrosses T_u and autoregressive period T

$$\frac{T_u}{T} = \frac{2\pi}{T \operatorname{arc\,cos} \left[\dfrac{2\sqrt{b}}{1+b} \cos \dfrac{2\pi}{T} \right]} . \tag{23}$$

The theoretical T_p/T and T_u/T ratios for all possible values of the coefficient, b, and the frequency range encountered in our research are illustrated by figures 12 and 13.

It is apparent that only in certain cases will either T_p or T_u alone, provide a reasonable estimate of the autoregressive period. On the other hand, the T_p/T and T_u/T ratios may assist in discovering facts about unknown natural series,

TABLE V

PROPERTIES OF ARTIFICIALLY GENERATED AUTOREGRESSIVE SERIES (SEE TEXT)

Series	B	F	G	G–1	I	J	K	L	M
Function mean M	−0.079	0.046	−0.077	−0.003	−0.068	0.035	0.12	0.100	0.015
Average deviation AD	7.794	6.316	1.120	1.196	0.717	1.314	1.116	1.836	1.660
Standard deviation σ	9.300	7.747	1.374	1.503	0.882	1.685	1.377	2.264	2.063
Deviation ratio AD/σ	0.84	0.81	0.81	0.80	0.81	0.78	0.81	0.81	0.81
Mean dist. peaks (computed)	10.02	8.29	6.56	6.68	4.54	4.85	3.93	6.12	5.33
Mean dist. peaks (theoretical)	10.03	8.19	7.02	7.02	5.05	5.05	4.26	6.17	5.55
Mean dist. upcrosses (computed)	9.99	9.90	9.42	9.56	8.07	7.20	7.28	9.20	9.82
Mean dist. upcrosses (theoretical)	10.03	10.04	9.91	9.91	8.88	8.88	7.69	9.62	9.32
Total variance (computed) σ_y^2	86.49	60.01	1.89	2.26	0.78	2.84	1.90	5.12	4.26
ϵ variance (computed) σ_ϵ^2	1.35	2.79	0.31	0.32	0.31	1.03	0.97	1.01	1.03
r_1 (computed)	0.77	0.80	0.79	0.71	0.73	0.74	0.73	0.76	0.69
r_1 (theoretical)	0.809	0.808	0.804	0.804	0.763	0.763	0.682	0.796	0.783
r_2 (computed)	0.28	0.30	0.30	0.30	0.26	0.36	0.29	0.20	0.22
r_2 (theoretical)	0.309	0.340	0.363	0.363	0.373	0.373	0.305	0.377	0.382
Total variance (theoretical)	....	48.619	2.675	2.675	1.0524	3.158	2.064	5.376	4.000
ϵ variance (theoretical)	1.333	3.000	0.3333	0.3333	0.3333	1.000	1.000	1.000	1.000

particularly when they are used in conjunction with another statistical property.

The mean distances between successive peaks and successive upcrosses scaled from curves of the basic data, and those computed from equations 17 and 20 (theoretical) for the nine artificial autoregressive series are tabulated in table V. The autoregressive period $2\pi/\theta$ was identical for all series, and the results together with figures 12 and 13 permit the following conclusions.

1. The mean distances between upcrosses are greater than those between peaks

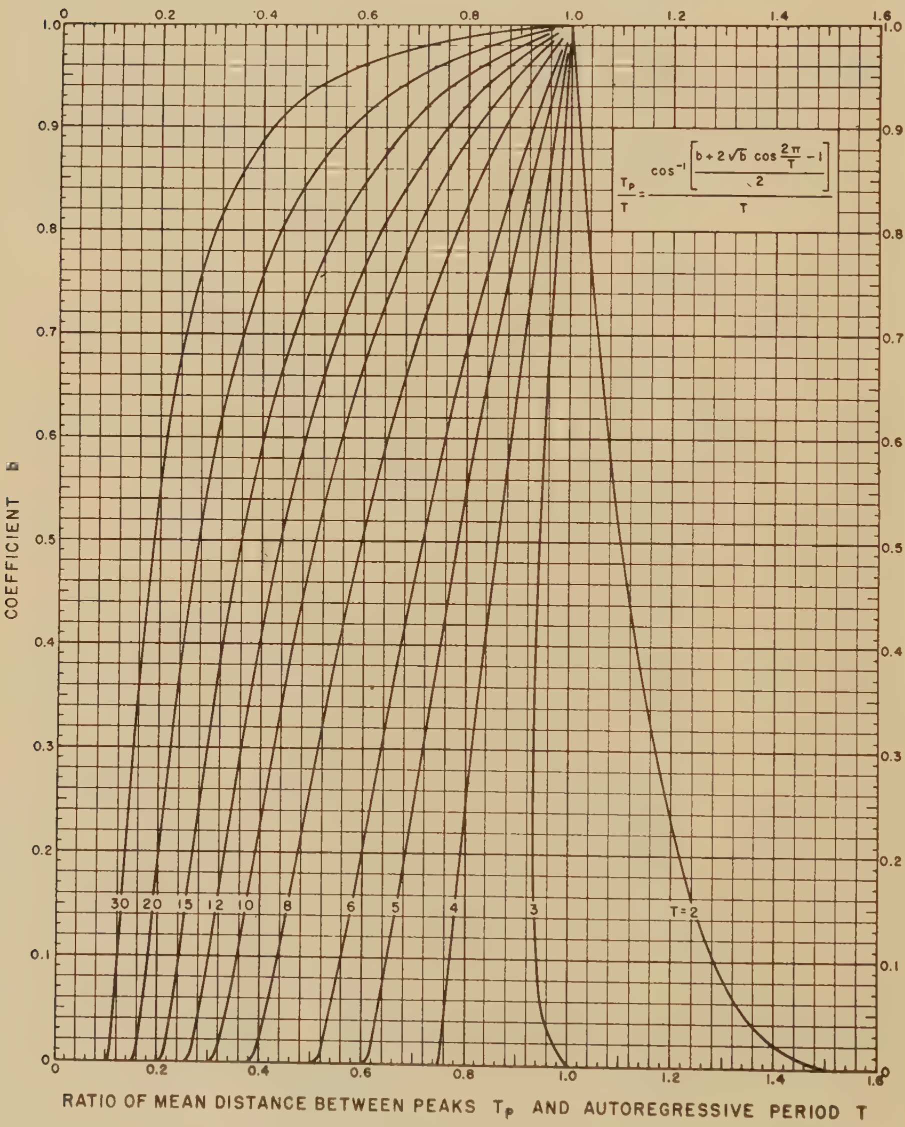

FIGURE 12

Ratio of mean distance between peaks T_p and autoregressive period T

and provide considerably better estimates of the autoregressive period for larger values of the coefficient b.

2. The computed and the observed mean distances between upcrosses were very close to the autoregressive period for values of the coefficient $b = 0.8$ and above. Departures will become greater for increased values of T and for diminishing values of b (figure 13).

3. The agreement between observed and theoretical values is, in general, good; the latter being usually the larger.

The above findings are similar to those from Kendall's [2] experimental study of

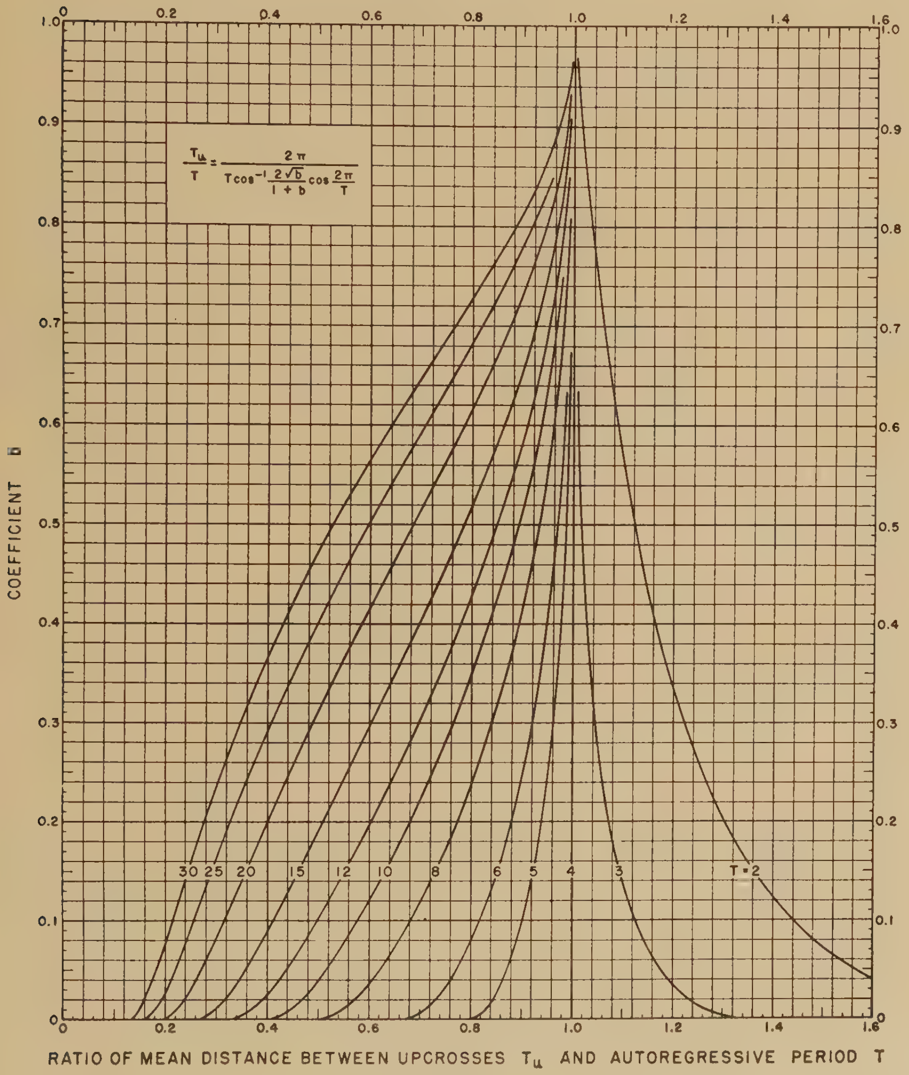

FIGURE 13

Ratio of mean distance between upcrosses T_u and autoregressive period T

four autoregressive series. For completeness, we tabulate certain of his results in table VI showing the ratios of computed peak and upcross distances to the autoregressive periods. With the exception of series 2, there is good agreement with theoretical expectancy (figures 12, 13).

5.4. *Correlogram analyses.* Each of the series was subjected to analysis and the autocorrelation coefficients r_k plotted against the interval, k, form the correlograms

TABLE VI

RATIOS OF COMPUTED PEAK AND UPCROSS DISTANCES TO AUTOREGRESSIVE PERIODS*

Series	Coefficients a	Coefficients b	Auto Period T	M.D. (Peaks) T_p	M.D. (Peaks) T_p/T	M.D. (Upcrosses) T_u	M.D. (Upcrosses) T_u/T
1	−1.2	0.4	9.25	4.96	0.536	8.40	0.908
2	−1.5	0.8	19.53	4.96	0.254	11.61	0.594
3	−1.0	0.6	6.92	5.69	0.822	6.87	0.993
4	−0.8	0.8	3.00	2.60	0.866	2.73	0.910

* Data from Kendall's four experimental autoregressive series.

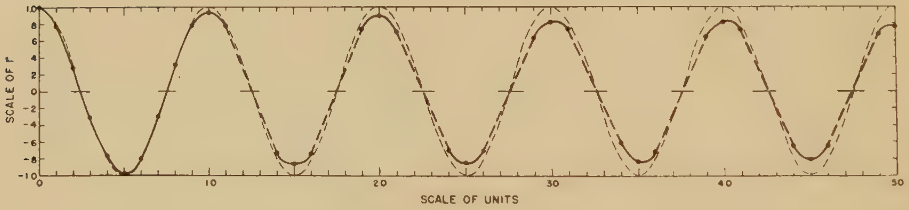

FIGURE 14

Correlogram model III, series B with superimposed theoretical values

of figures 14 to 22. They are referred to as computed correlograms. The theoretical correlograms superimposed on the computed correlograms were obtained from theoretical autocorrelation coefficients computed as follows:

$$r_k = \frac{p^k}{(1+p^2)\sin\theta}\{\sin(k+1)\,\theta - p^2\sin(k-1)\,\theta\}\,. \tag{24}$$

In considering the general properties of the correlograms, figures 14 to 22 reveal that significant differences may exist between the theoretical and those computed from finite amounts of data. However, similarities in key properties of both need be studied for the purpose of inferring, in so far as possible, the physical properties of correlograms of natural time series. In particular, the nature of the damping and the symmetry of the computed correlograms permit certain inferences to be made concerning properties of the basic series.

The theoretical correlogram of an autoregressive series (equation 24) will damp very close to zero within a very few cycles; the rate of damping depending on the magnitude of the coefficient b. In our experiments, theoretical correlograms damped to less than $r = 0.05$ by the end of the fifth cycle for a value of the

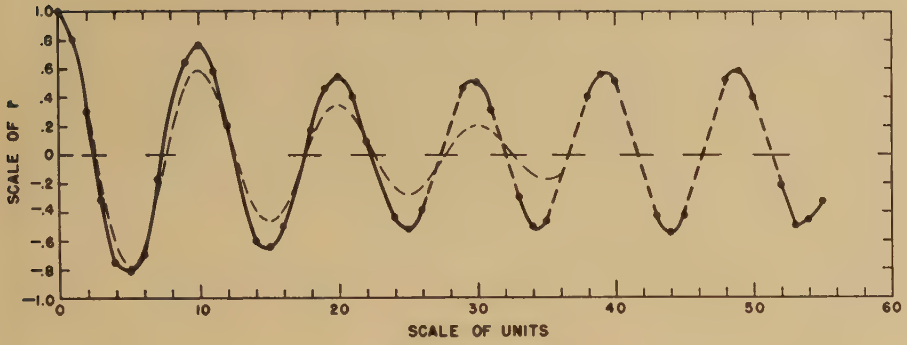

Figure 15

Correlogram model III, series F with superimposed theoretical values

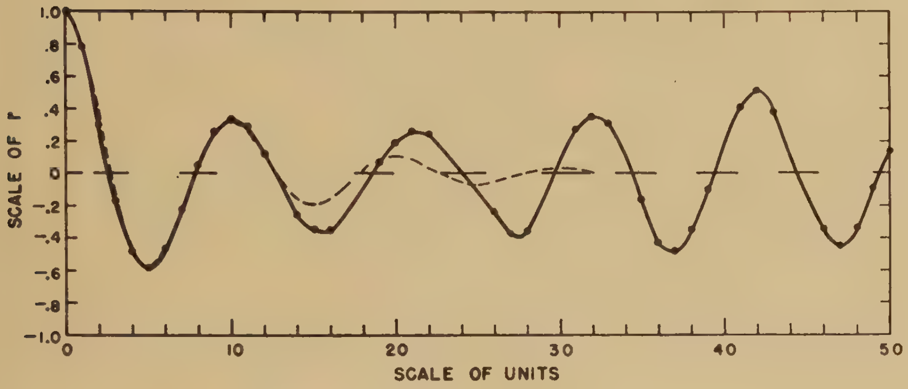

Figure 16

Correlogram model III, series G with superimposed theoretical values

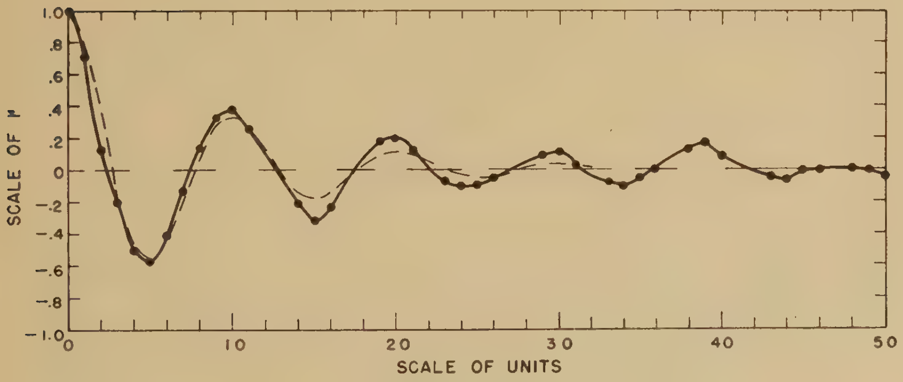

Figure 17

Correlogram model III, series G–1 with superimposed theoretical values coefficient $b = 0.9$ (series F) and by the end of the first cycle when the coefficient b was 0.5 or less.

On the other hand, the computed correlograms of autoregressive series of finite length, may be less strongly damped than expected from theory. This, in general, will depend on the length of the series analyzed and on its damping factor. Our experiments show that when the coefficient b is large, longer series of observations are required to approach theoretical damping than when b is small. This is demonstrated (figures 16 and 17) by the series G ($b = 0.80$) correlograms based on 180 and 500 terms, respectively. The correlogram computed from 180 terms damped only to the second cycle and then grew, whereas that of the 500 unit series damped very nearly in accordance with theoretical expectations; at the third cycle, the computed r_k was 0.1 as compared with a theoretical r_k of 0.04. The computed correlogram was completely damped at the end of the fifth cycle.

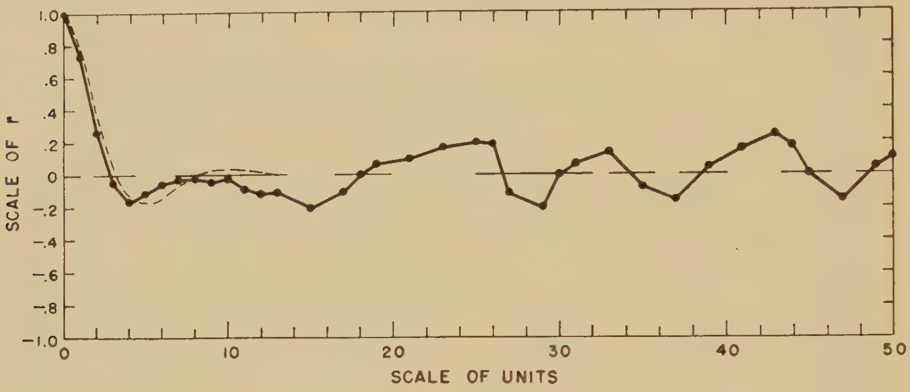

FIGURE 18

Correlogram model III, series I with superimposed theoretical values

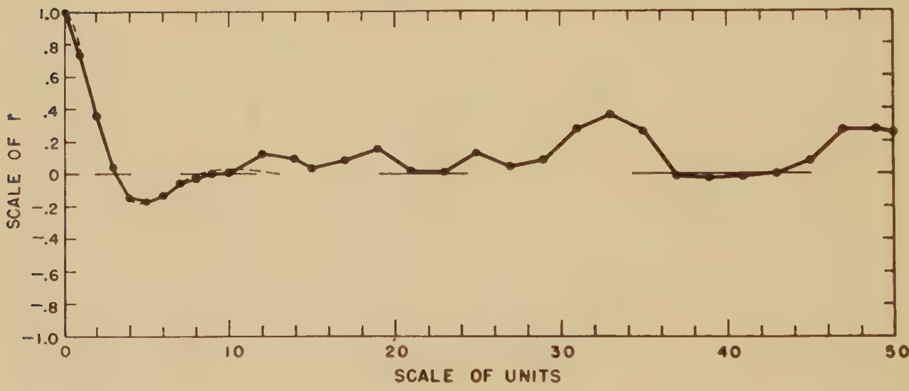

FIGURE 19

Correlogram model III, series J with superimposed theoretical values

In the case of the autoregressive series with coefficient $b = 0.5$, or less, correlograms damped to near zero by the end of the first cycle and then grew with irregular oscillatory features. In this, they tend to resemble the theoretical correlograms of mixed sine waves, although the phenomenon results from finiteness of the data.

In series with coefficient $b = 0.6$ and $b = 0.7$, the correlograms based on 400 and 500 units, respectively, damped very nearly in accordance with theoretical expectations (figures 21 and 22).

It appears reasonable that good approximations to theory are obtained by using

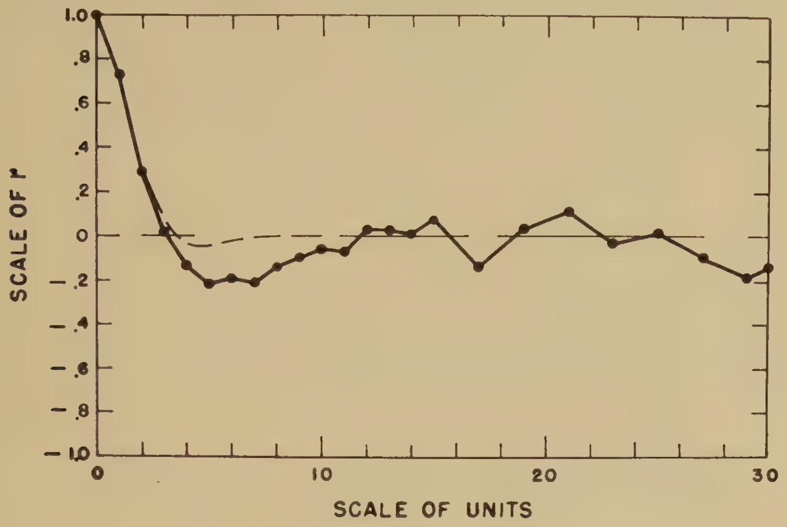

FIGURE 20

Correlogram model III, series K with superimposed theoretical values

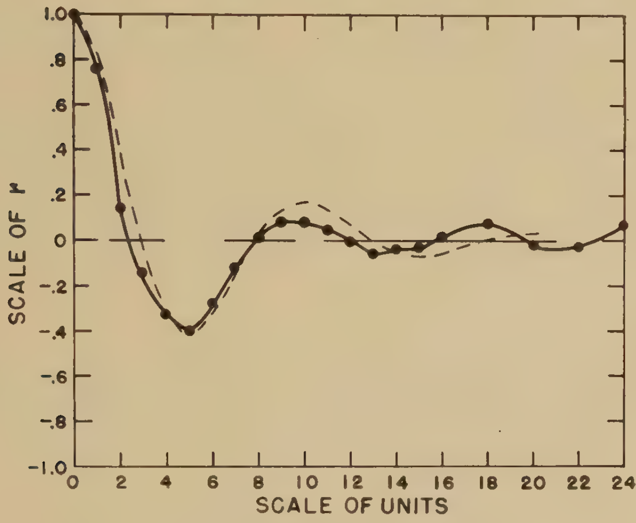

FIGURE 21

Correlogram model III, series L with superimposed theoretical values

400 to 500 (40 to 50 cycles) terms in an autoregressive series. However, when data are not available, failure of the computed correlogram to damp according to theory is not grounds for rejection of the theory of autoregression. This confirms the evidence of Kendall, and it is apparent that the correlogram itself must serve as the final guide for estimating properties of unknown natural time series.

Earlier it was shown that the correlogram for series consisting of a single cyclical component and not completely masked by a random component, symmetrically defines the period, and its terminal amplitude damps close to that required by theory. On the other hand, the correlogram of series composed of several cyclical components is not necessarily symmetrical, it frequently shows minor humps or ripples in the first cycle, but the period is not revealed and a Fourier transform of the autocorrelation is required for additional information. The correlogram of the autoregressive series is somewhat similar to that of the first case and the autoregressive period usually indicated by the location of the first valley and frequently, also, by its first peak when not too strongly damped.

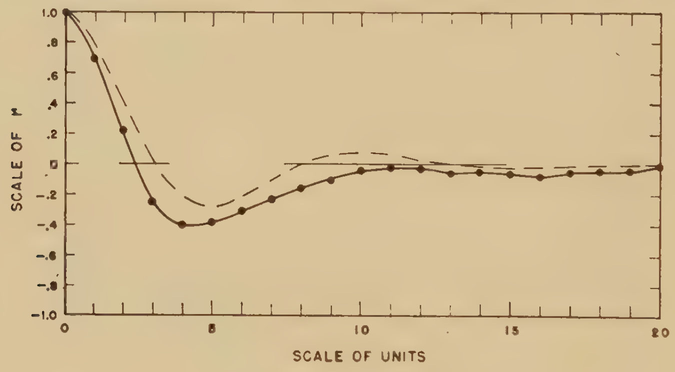

FIGURE 22

Correlogram model III, series M with superimposed theoretical values

Estimation of the autoregressive period from the first two computed autocorrelations (equation 11) is so sensitive to departures from theory that in event of significant difference with the period indicated by the first correlogram cycle it should be viewed with suspicion. Tabulation of computed autocorrelation coefficients (table V) shows that at times agreement may be poor, as for instance, for series L and M.

6. Experimental model IV

6.1. *Pattern of analyses.* This section is concerned with an experimental correlogram analysis of five series, each consisting of an autoregressive function to which are added cosine waves of different amplitudes and periods. The autoregressive function (series G of model III) was identical for the first four series (A to D); namely,

$$x_{n+2} = 1.45x_{n+1} - 0.80x_n + \epsilon_{n+2} \tag{25}$$

with ϵ rectangularly distributed between -1 and $+1$. The autoregressive function of series E was strongly damped (series J of model III). Namely,

$$x'_{n+2} = 1.14x'_{n+1} - 0.50x'_n + \epsilon_{n+2} \tag{26}$$

with ϵ normally distributed between 0 and 1.

The five artificial series analyzed in this section were formed as follows:

Series A: $y = x_{n+2} + \cos \frac{2\pi x}{10}$, 180 units;

Series B: $y = x_{n+2} + 4 \cos \frac{2\pi x}{10}$, 180 units;

Series C: $y = x_{n+2} + 4 \cos \frac{2\pi x}{5}$, 180 units;

Series D: $y = x_{n+2} + 4 \cos \frac{2\pi x}{20}$, 180 units;

Series E: $y = x'_{n+2} + 4 \cos \frac{2\pi x}{10}$, 360 units.

In three of the above cases the period of the cosine was identical with the autoregressive period (10 units). Statistical properties of the series are tabulated in table VII.

TABLE VII

PROPERTIES OF ARTIFICIALLY GENERATED MODEL IV SERIES

Property	Series A	Series B	Series C	Series D	Series E
Mean	−0.01	−0.08	−0.08	−0.08	−0.19
Average deviation	1.24	2.65	2.70	2.73	2.57
Standard deviation	1.53	3.12	3.13	3.19	3.08
Deviation ratio	0.81	0.85	0.86	0.86	0.84
Mean dist. peaks	7.23	9.41	5.00	9.81	7.64
Mean dist. upcrosses	9.93	9.97	5.10	16.03	9.77
Total variance					
computed	2.35	9.73	9.81	10.15	9.50
theoretical	3.19	10.69	10.69	10.69	11.15
Cosine variance					
computed	0.50	8.01	8.01	8.00	8.04
theoretical	0.500	8.00	8.000	8.000	8.00
Autoregressive variance					
computed	1.89	1.89	1.89	1.89	2.84
theoretical	2.68	2.68	2.68	2.68	3.16
r_1	0.79	0.79	0.27	0.85	0.71
r_2	0.35	0.27	−0.54	0.68	0.19

6.2. *Properties of the basic data.* The mean distances between peaks and upcrosses for the autoregressive series G and J of model III are:

		Computed	Theoretical
Series G	M.D. peaks	6.56	7.02
	M.D. upcrosses	9.42	9.91
Series J	M.D. peaks	4.85	5.05
	M.D. upcrosses	7.20	8.88

The computed and theoretical values agreed within one half unit, except for the M.D. upcrosses of the strongly damped series J. The addition of a cosine to the autoregressive changes the mean distances between peaks and upcrosses (table VII) in a fashion that they approach the value of the cosine period. This is particularly noticeable for the series having a cosine period of 5 (series C) and of 20 (series D) units which masks the ten unit autoregressive period.

A property of pure autoregressive series is that the ratio of average deviation to standard deviation lay between 0.78 and 0.81 or very close to $\sqrt{2/\pi}$, a ratio usually characterizing unimodal curves approaching symmetry. The addition of a cosine to the autoregressive increased this ratio, 0.81 to 0.86, to approximate the AD/σ ratio of $2\sqrt{2}/\pi$ for cosines.

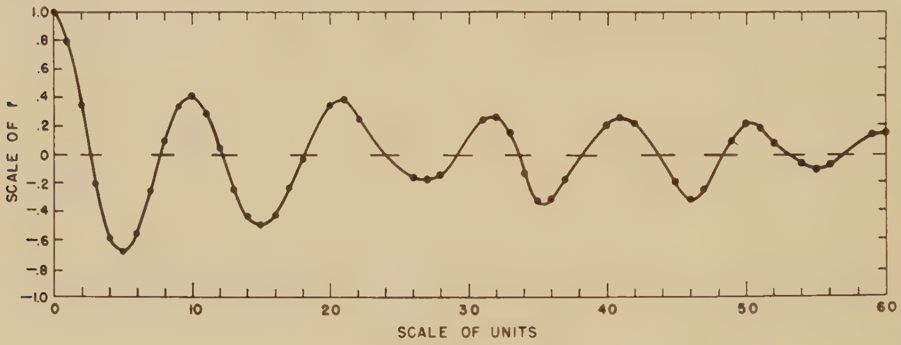

FIGURE 23

Correlogram model IV, series A

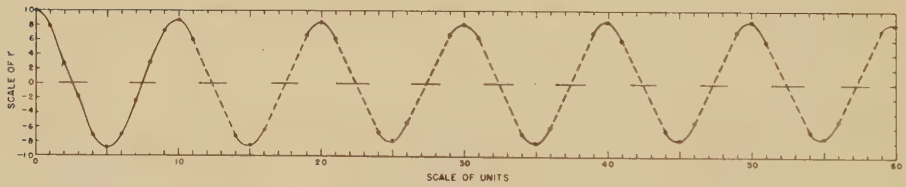

FIGURE 24

Correlogram model IV, series B

6.3. *Correlogram analyses.* Each of the five series was subjected to analysis as in previous models and the autocorrelation coefficients r_k plotted against the interval k to form the correlograms of figures 23 to 27. We briefly consider their properties and variations from those of pure autoregressive series.

A prominent correlogram feature is the regulation of its period by the cosine. Thus, while the correlogram for the pure autoregressive series G (figure 16) indicated a period of 10 units only for the first cycle (after which, distances from peak to peak and valley to valley became irregular) the addition of a 10 unit cosine strengthened its symmetry. Again, the series E correlogram had uniformly spaced (10 units) peaks and valleys, though more than six cycles, while the series C

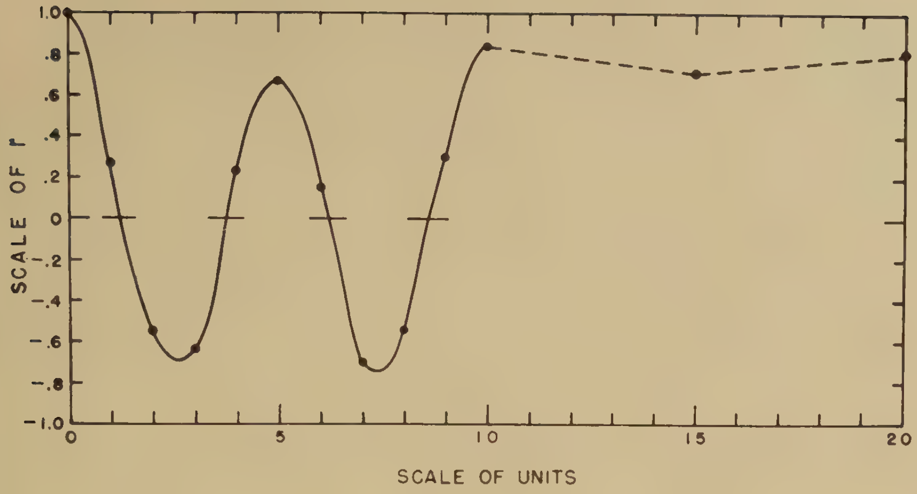

FIGURE 25

Correlogram model IV, series C

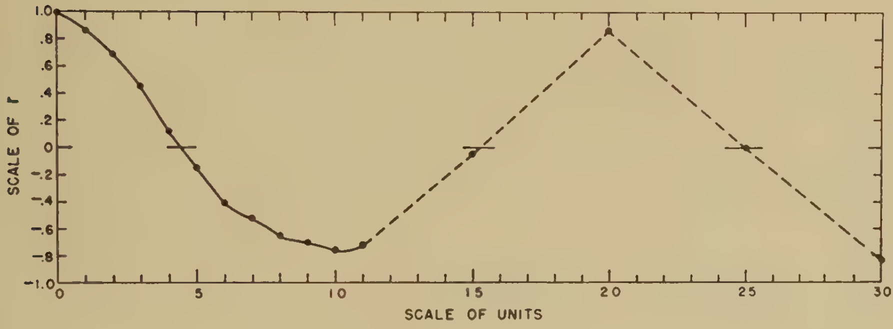

FIGURE 26

Correlogram model IV, series D

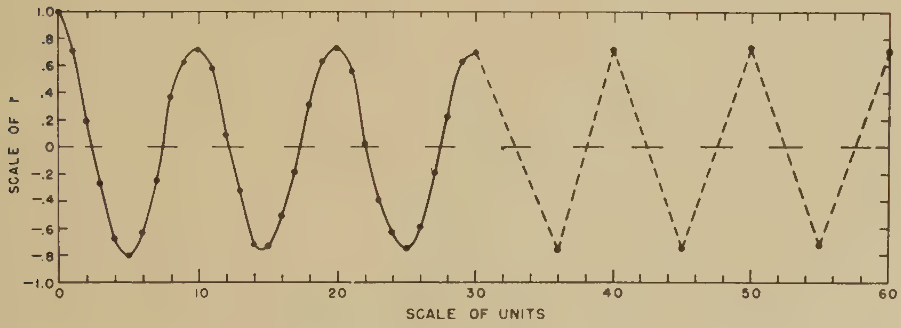

FIGURE 27

Correlogram model IV, series E

correlogram is striking with equally spaced five unit peaks and valleys. Series D revealed its twenty unit cosine period in the first correlogram cycle.

The correlograms of this model will not damp to zero except in the case where a trigonometric should be completely masked by the autoregressive. In this respect, they are similar to those for a sum of sines (model A) and the autoregressive appears to exert the influence of a single trigonometric of like period. The magnitude of the influence is related to its coefficient b and its autoregressive period in relation to the period and amplitude of the trigonometric.

The effect of the added cosine on damping of the correlogram is illustrated from autocorrelation values at the first valley (half cycle, $r_{k/2}$) and the first peak (first cycle, r_k) tabulated in table VIII. Both series B and E correlograms are similar to those for the combination of a single trigonometric and a random component and damp to terminal amplitudes at the first cycle; series B to about 0.85 and series E to 0.7. On the other hand, series A (smaller amplitude) correlogram damps continuously to the sixth peak when it attains a terminal amplitude of about 0.15. The series C (cosine one half the period of the autoregressive) correlogram shows alternate damping and growth, similar to a combination of two cosines. A similar situation is indicated for the series D correlogram (cosine period twice that of the autoregressive).

TABLE VIII

Model	r_T (th)	r_T (comp)	r_T (obs)	$r_{k/2}$	r_k
III-G	....	....	......	−0.58	0.33
IV-A	0.16	0.20	(0.15)	−0.67	0.41
B	0.75	0.81	(0.8)	−0.88	0.87
C	0.75	0.81	......	−0.70	0.66
D	0.75	0.82	......	−0.76	0 87
III-J	....	....	......	−0.17	0.13
IV-E	0.72	0.72	(0.7)	−0.80	0.72

REFERENCES

[1] G. E. R. Deacon, "Waves and swell," *Quarterly Jour. Roy. Meteorological Soc.*, Vol. 75, No. 325 (1949), pp. 227–238.

[2] M. G. Kendall, "Contributions to the study of oscillatory time series," *Occasional Papers IX, National Institute of Economic and Social Research*, Cambridge University Press, Cambridge, 1946.

[3] M. G. Kendall, *The Advanced Theory of Statistics*, Vol. 2, Griffin, London, 1948.

[4] A. A. Klebba, "Details of shore-based wave recorder and ocean wave analyzer," *Annals New York Acad. Sci.*, Vol. 51 (1949), pp. 533–544.

[5] H. R. Seiwell and G. P. Wadsworth, "A new development in ocean wave research," *Science*, Vol. 109 (1949), pp. 271–274.

[6] H. R. Seiwell, "The principles of time series analyses applied to ocean wave data," *Proc. Nat. Acad. Sci.*, Vol. 35, No. 9 (1949), pp. 518–528.

[7] ———, "A new mechanical autocorrelator," *Review of Scientific Instruments*, Vol. 21, No. 5 (1950), pp. 481–484.

[8] E. B. Wilson, "The periodogram of American business activity," *Quarterly Jour. of Economics* (1934), pp. 375–417.

PRINTED IN U·S·A

Contribution No. 532

"Reprint from Bulletin American Meteorological Soc.,Vol.32,No.1,Jan.1951,pp.21-23"

An Elementary Explanation of Why Ocean Currents are Strongest in the West *

HENRY STOMMEL

Woods Hole Oceanographic Institution, Woods Hole, Mass.

DURING the last three years a series of papers has been published on the detailed nature of the ocean currents set up by broad steady wind currents. These have culminated in the research of Munk [1950] who has succeeded in showing that the major features of the observed surface ocean currents may be quantitatively attributed to the mean wind stress. The history of the speculations leading to this new ocean current theory has been summarized by the author in another place [Stommel 1950]. Because the details of the theory are necessarily mathematical its basic physical plausibility may escape the general reader. It is the purpose of this article to explain the physical reason for the westward intensification of ocean currents in ordinary words. In so doing we are only doing qualitatively what has already been done quantitatively [Stommel 1948, Munk 1950].

That there really is an observed intensification of most ocean currents toward the west, regardless of hemisphere, seems to be an established fact. In the North Atlantic Ocean the Gulf Stream is an outstanding example, the Kuroshio is the counterpart in the North Pacific. In the Indian Ocean the Agulhas Current hugs the coast of Africa. In the South Atlantic there is the Brazil Current. The coastlines and areas of these oceans are quite different, so we are tempted to think that local bathygraphic peculiarities are not an essential influence in the western intensification of ocean currents; thus the existence of the Straits of Florida is not essential to the formation of the Gulf Stream. If the Antilles were excavated the Gulf Stream would still exist. However, the South Pacific Ocean offers a somewhat embarrassing exception. There does not appear to be any current of great intensity off Australia; in fact the Humboldt Current off Peru is the strongest South Pacific Current, and it lies in the eastern portion of the South Pacific. With this important exception the following rule does seem to hold: on the western edge of most of the world's oceans there is a system of strong currents. Now we may ask ourselves, why is this so? If the wind system, a broad wide-spread phenomenon, drives the ocean currents, how is it that the resulting ocean current system should be so asymmetrical; in particular, why should the strongest currents be squeezed into a narrow belt on the western edge of the oceans? It is this question to which the present theory purports to supply the answer.

The physical picture is as follows: Suppose we consider a large ocean basin such as shown in FIGURE 1 with an anticyclonic wind circulating over it. Our intuition tells us that this wind will produce an ocean surface current in an anticyclonic sense. From what little we know about the distribution of properties in the deeper portions of the ocean it seems reasonable to suppose that the current which the wind induces does not extend to the bottom. Our intuition also tells us that if the ocean current system has arrived at a state of steady motion under the stress of the wind, the free surface and isopleths of density in the ocean will have adjusted themselves so as to produce the horizontal pressure gradients necessary to balance the Coriolis forces acting upon the moving water; also, that frictional dissipation of the energy added to the sea by the wind is necessary. But that is about as far as our intuition takes us, and it gives no hint of the necessary asymmetry in the current system. To progress further it is necessary to consider the processes tending to increase or decrease the vorticity of the ocean water.

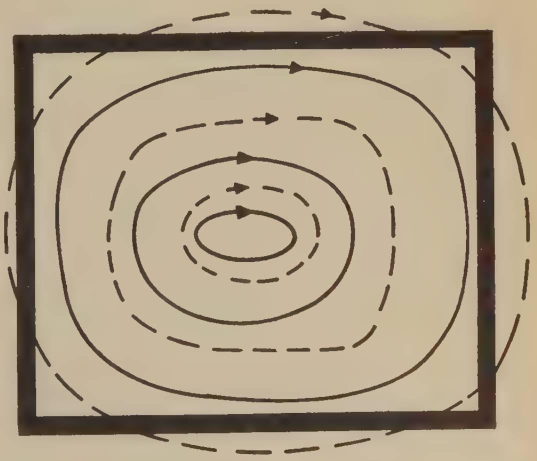

FIG. 1. Symmetric circulation of water (solid lines) under an anticyclonic wind (dashed lines). The coastline is drawn schematically as rectangular.

---

* Contribution No. 532 from the Woods Hole Oceanographic Inst.

The vorticity of a vertical column of water † is taken as positive if counterclockwise, and negative if clockwise. If the spin is measured relative to the earth, we speak of relative vorticity; by adding the Coriolis parameter to the relative vorticity we obtain the absolute vorticity of the column. Unlike the velocity distribution, the vorticity distribution in the ocean may be discussed without reference to the pressure field (formally the vorticity equation is obtained by elimination of the pressure from the equations of motion by cross-differentiation), a fact which greatly simplifies qualitative discussions. The wind system of FIGURE 1 is chosen so that it tends to decrease (make negative) the relative vorticity of all the water columns in the ocean. In the steady state of motion which must exist under a prolonged exposure of the ocean to this wind system, the relative vorticity has a fixed value at each point of the ocean independent of time. This means that other influences must act to counteract the negative vorticity tendency due to the wind alone. Horizontal convergence and divergence are ruled out on account of the steady state condition; advection of vorticity from one region to another seems to be, for the most part, negligible. This leaves two processes by which the negative vorticity tendency due to the wind may be counteracted.

The first of these is friction, but since, as we have already seen, the ocean surface circulation does not seem to be frictionally bound to the bottom, it must be frictionally bound to the ocean shores by horizontal eddies. Moreover, this horizontal viscosity would provide a positive vorticity tendency over the ocean of FIGURE 1. A numerical check, using values of lateral eddy viscosity inferred from the distribution of conservative properties and a horizontal oceanic circulation which looks like the wind system, without any evidence of asymmetry, requires a circulation many times faster than the real ocean circulation to produce enough positive vorticity tendency to balance the wind stress vorticity tendency.

The second process is the planetary vorticity tendency. Columns of water moving northward without convergence or divergence have a negative vorticity tendency, and those moving southward a positive vorticity tendency regardless of hemisphere. This follows from the conservation of angular momentum or, putting it in other words, the variation of the Coriolis parameter with latitude. Since the net meridional transport of water across a parallel of latitude is zero (as much water moves north as south), the planetary vorticity tendency is positive for water in the eastern part of the ocean of FIGURE 1, and negative in the western part. Therefore the planetary vorticity tendency alone is incapable of balancing the wind stress vorticity tendency. In the steady state we must have a zero over-all vorticity tendency, by definition. That is, at every point in the ocean the wind-stress-, frictional-, and planetary-vorticity tendencies must add up to zero.

TABLE 1. VORTICITY TENDENCIES IN A SYMMETRIC CIRCULATION

	North flowing currents in the western ocean	South flowing currents in the eastern ocean
Wind stress	−1	−1
Frictional	+0.1	+0.1
Planetary	−1.0	+1.0
Total	−1.9	+0.1

The distribution of the wind stress vorticity tendency may be regarded as fixed, let us say of an order of magnitude − 1. If there were only a broad current system without the asymmetry that is actually observed, but with a transport of water similar to the observed transport, the frictional vorticity tendency would be an order of magnitude too small, say + 0.1, and the planetary vorticity tendency would be of the order − 1 in the western and + 1 in the eastern part of the ocean of FIGURE 1. Thus there would be an approximate balance of tendencies in the eastern portion of the ocean, but the western part would not be equilibrium, so

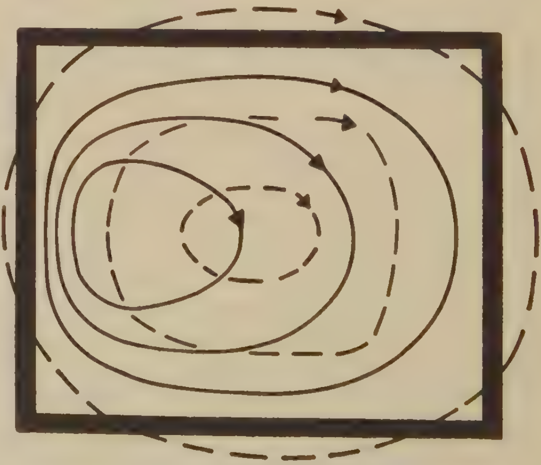

FIG. 2. Asymmetric circulation.

---

† The vorticity of an element of fluid is twice its angular velocity. An element of fluid in a shearing motion is subjected to an instantaneous spin. In this article the qualitative reasoning is done entirely in terms of the vorticity of a vertical water column, that is, the sum of the vertical components of vorticity of all the elements of a vertical water column.

that a symmetrical current system is not physically possible in the steady state. The state of affairs is summarized in Table 1.

However, if we let the current system be strongly asymmetrical, as shown in Figure 2, we do not affect seriously the balance between the wind stress and planetary vorticity tendencies in the eastern portion of the ocean where frictional vorticity tendency is very small. However, on the western side where the velocity and shear are great because of the narrowness of the western meridional current, the frictional and planetary vorticity tendencies are greatly enhanced, to orders of magnitude greater than the wind stress, say + 10 and − 10, respectively. In this way we may achieve a balance between the tendencies in the western side of the ocean as well, and so obtain a steady state. Table 2 shows the balance of terms in an asymmetric circulation.

Table 2. Vorticity Tendencies in an Asymmetric Circulation

	Strong north currents in the western edge	South flowing current over rest of ocean
Wind stress	− 1.0	−1.0
Frictional	+10.0	+0.1
Planetary	− 9.0	+0.9
Total	0.0	0.0

If one analyzes ocean currents in this qualitative manner for anticyclonic and cyclonic wind systems in both hemispheres he will find that the necessary intensification of the ocean circulation is always on the western side of the ocean.

Among the interesting consequences of this theory are: (*1*) the fact that although energy is added to the oceans by the work of the wind over the entire surface, it is dissipated chiefly in the strong western currents; (*2*) that a good representation of the circulation outside of the western currents can be obtained from a knowledge of the field of the wind stress alone, independent of friction, as was shown by Sverdrup [1947].

In view of the fact that the theory gives an adequate schematic picture of the oceanic surface circulation, one is tempted to suppose that it is physically sound. The transports computed by Munk are about one-half the observed values. This discrepancy may arise simply from the very crude estimates of the wind stress that were available, or it may be due to some physical factor which has not yet been considered.

References

Munk, W. H., 1950: On the Wind-Driven Ocean Circulation, *Jour. of Meteorology, 7*: 79–93.

Stommel, Henry, 1948: The Westward Intensification of Wind-Driven Ocean Currents, *Trans. Amer. Geophys. Union, 29*: 202–206.

Stommel, Henry, 1950: The Gulf Stream, a Brief History of the Ideas Concerning its Cause, *The Scientific Monthly,* 70: 242–253.

Sverdrup, H. U., 1947: Wind-Driven Currents in a Baroclinic Ocean; with Application to the Equatorial Currents of the Eastern Pacific, *Proc. Nat. Acad. Sci., 33*: 318–326.

Contribution No. 533

"Reprinted from Journal of Meteorology, Vol. 8, April 1951, pp. 127-129"

ENTRAINMENT OF AIR INTO A CUMULUS CLOUD II

By Henry Stommel

Woods Hole Oceanographic Institution[1]

(Manuscript received 9 September 1950)

Introduction.—Several years ago the writer (Stommel, 1947) attempted to show that the lapse rate inside some trade cumuli observed by Wyman and Woodcock (see Bunker *et al.*, 1949) could be explained on the hypothesis that the clouds entrained air from their environment. The theory proceeded on the crude assumptions of complete horizontal mixing within the cloud, and of a steady state. A graphical method was presented for determining the rate of entrainment from the wet- and dry-bulb temperature soundings.

A further result, the liquid-water content, was obtained on the assumption of no precipitation. Malkus (1949) explored the effect of a vertical wind-shear on the development of the cloud. Entrainment in clouds other than trade cumuli has been confirmed (Byers and Braham, 1949).

The need for further soundings in trade cumuli was emphasized, but, so far as the writer is aware, none have been made. There is, therefore, no further observational evidence to offer. However, the theory of entrainment does lead to a few results in addition to those originally published. It is the purpose of this note to record them. In short, from the computed entrainment, it should be possible to deduce the vertical-velocity distribution in the cloud and derive a convective-stability criterion involving the entrainment.

Vertical-velocity distribution.—At some level z, the horizontal cross-sectional area of a cloud is S, the density ρ, the vertical velocity w, and the total vertical mass-flux M. The density of air outside the cloud is taken as ρ'.

Now consider the momentum flow through a lamina between the levels z and $z + \delta z$. The total vertical flux of momentum into the lamina through the level z is Mw. The total flow out through the level $z + \delta z$ is

$$[M + (dM/dz)\,\delta z][w + (dw/dz)\,\delta z].$$

The excess of outflow over inflow is therefore given by

$$(w\,dM/dz + M\,dw/dz)\,\delta z.$$

In the steady state, if the entrained air has no vertical motion, this must be balanced by the production of vertical momentum by the buoyant force acting upon the cloud mass in the lamina. The buoyant acceleration per unit mass is denoted by $\gamma = g\rho'^{-1}(\rho' - \rho)$ (the buoyance is reduced by the falling liquid water, but this is an effect of secondary importance in these soundings); the mass of the lamina is $S\rho\,\delta z \equiv Mw^{-1}\,\delta z$. Therefore, the vertical equation of motion is satisfied by the equation

$$(w\,dM/dz + M\,dw/dz)\,\delta z = \gamma M w^{-1}\,\delta z.$$

This reduces to the simple form

$$d(M^2w^2)/dz = 2\gamma M^2.$$

---

[1] This work was performed during a short visit to the University of Chicago for the Office of Naval Research. Contribution No. 533 from the Woods Hole Oceanographic Institution.

TABLE 1. Sample computations of vertical-velocity distributions. For details regarding soundings, see Bunker *et al.* (1949), tables 27 and 21.

Alt. ft	$\frac{\rho' - \rho}{\rho'}$	M	M^2	$M^2 \frac{\rho' - \rho}{\rho'}$	Σ	$2\int_r^z \gamma M^2\,dz$ ft² sec⁻²	w^2 ft² sec⁻²	w ft sec⁻¹
2000	0.0000	1.0	1.0	0.0000	0.0000	0	0	0.0
2500	0.0000	1.4	2.6	0.0000	0.0000	0	0	0.0
3000	0.0030	1.4	2.0	0.0060	0.0060	192	96	9.8
3500	0.0050	1.4	2.0	0.0100	0.0160	510	255	15.9
4000	0.0070	1.5	2.3	0.0210	0.0370	1180	510	22.5
4500	0.0060	1.5	2.3	0.0138	0.0508	1620	700	26.4
5000	0.0040	1.6	2.6	0.0104	0.0612	1950	750	27.4
5500	0.0020	1.7	2.9	0.0058	0.0670	2140	730	27.0
6000	−0.0050	2.0	4.0	−0.0200	0.0470	1500	375	19.4
6500	−0.0050	2.3	5.3	−0.0265	0.0205	640	120	11.0
2000	0.0000	1.0	1.0	0.0000	0.0000	0	0	0.0
2500	0.0020	1.2	1.4	0.0028	0.0028	90	64	8.0
3000	0.0030	1.7	1.9	0.0057	0.0085	272	143	11.9
3500	0.0010	2.1	4.4	0.0044	0.0129	410	93	9.7
4000	−0.0020	3.2	11.2	−0.0244	−0.0095	−302	−30	
4500	−0.0060	4.3*	18.5*					
5000	−0.0060							

* Extrapolated.

If $M = M_0$ and $w = w_0$ at $z = 0$,

$$M^2w^2 = M_0^2w_0^2 + 2\int_0^z \gamma M^2\,dz.$$

Since both M and γ can be computed from soundings, this provides a method for computation of the vertical velocity within the cloud.

Examples of computation of vertical velocity.—Two examples of the vertical-velocity distribution were computed on the basis of the above treatment, using the soundings from Bunker *et al.* (1949) and the computed entrainments from Stommel (1947).

The results are tabulated in table 1, and plotted in figs. 1 and 2.

The stability criterion.—It is evident that if a layer of the atmosphere has a lapse rate between the moist- and dry-adiabatic rates, its stability will depend upon the rate of entrainment of outside air (Austin and Fleischer, 1948). The process can best be described on a thermodynamic diagram. For convenience, the tephigram is chosen.

The abscissa is temperature; the ordinate is potential temperature. Two points of the sounding in a clear area are shown plotted on their pressure levels p and $p - \delta p$. If the air at A (fig. 3) is displaced as a parcel upward to $p - \delta p$, it follows the wet adiabat to point C and, hence, in this case the air is unstable. If the air is not saturated, it moves along the dry adiabat until

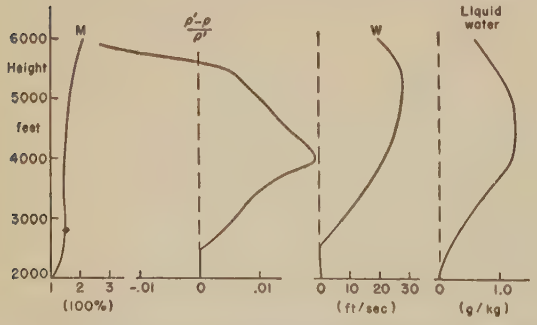

FIG. 1. Total vertical mass-flux, buoyant acceleration, liquid-water content, and vertical velocity of first cloud considered in table 1.

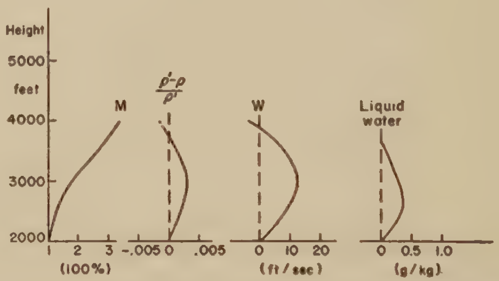

FIG. 2. Total vertical mass-flux, buoyant acceleration, liquid-water content, and vertical velocity of second cloud considered in table 1.

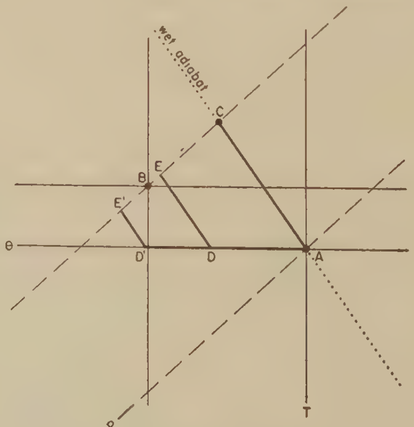

FIG. 3. Illustrative tephigram.

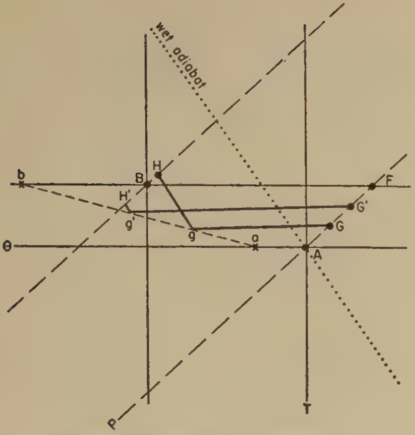

FIG. 4. Illustrative tephigram.

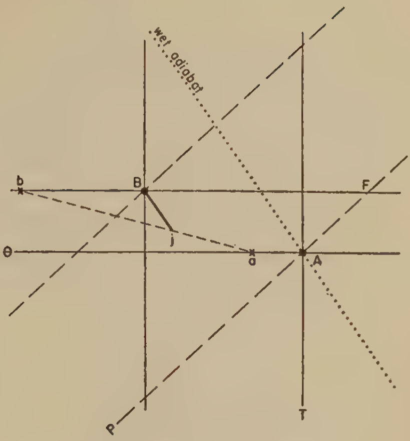

FIG. 5. Illustrative tephigram.

it intersects its saturation mixing-ratio (D or D′), and then ascends the wet adiabat to $p - \delta p$ (E or E′). Thus, it may be either stable or unstable.

To study the effect of entrainment, the mixing ratios corresponding to the soundings A and B may be plotted at a and b on the potential-temperature lines (fig. 4). The point F represents the state of a parcel of air at B brought down to pressure p. If a mixing of x parts of upper air is made with $1 - x$ parts of lower air at p, the resultant temperature is given by the point G, which is located according to the rule

$$\overline{AG}(\overline{FG})^{-1} = x(1 - x)^{-1} = M^{-1}(dM/dp)\,\delta p.$$

The resultant mixing-ratio is located at g on the same potential-temperature line as G. If, after mixing, the parcel is raised from G, it follows the dry adiabat to g and the wet adiabat to H. In the case portrayed, the convection is unstable. Had the entrainment been greater, the convection would have been stable; for example, the process G′, g′, H′.

To determine the critical entrainment for a particular sounding, a wet adiabat is drawn through B (fig. 5). Its intersection with the line between the mixing ratios is at j, and

$$(M^{-1}\,dM/dp)_{\text{critical}} = \overline{aj}(\overline{bj}\,\delta p)^{-1}.$$

Concluding remarks.—The result of this *tour de force* of the steady-state model of a cloud must be accepted only with grave reservations. For example, one is inclined to doubt the high vertical velocities obtained by the computation, although it is impossible to be certain as vertical velocities have not been observed in trade cumuli.

No theory will be wholly acceptable until it explains the dynamics of the entrainment process itself, and incorporates the idea of a life cycle of a cloud.

REFERENCES

Austin, J., and A. Fleischer, 1948: A thermodynamic analysis of cumulus convection, *J. Meteor.*, **5**, 240–243.

Bunker, A., B. Haurwitz, J. S. Malkus, and H. Stommel, 1949: The vertical distribution of temperature and humidity over the Caribbean Sea. *Pap. phys. Ocean. Meteor., Mass. Inst. Tech. and Woods Hole Ocean. Instn.*, **11**, No. 1.

Byers, H. R., and R. R. Braham, 1949: *The thunderstorm.* Washington, U. S. Government Printing Office, 287 pp.

Malkus, J. S., 1949: Effects of wind shear on some aspects of convection. *Trans. Amer. geophys. Union*, **30**, 19–25.

Stommel, H., 1947: Entrainment of air into a cumulus cloud. *J. Meteor.*, **4**, 91–94.

Contribution No. 534

[Reprinted from BULLETIN OF THE AMERICAN METEOROLOGICAL SOCIETY, Vol. 32, No. 2, February, 1951, pp. 61–66]
Printed in U. S. A.

A Formation of Pileus-like Veil Clouds Over Cape Cod, Massachusetts [1, 2]

JOANNE STARR MALKUS
Woods Hole Oceanographic Institution and Illinois Institute of Technology

ANDREW F. BUNKER
Woods Hole Oceanographic Institution

AND

KENNETH MCCASLAND
Woods Hole Oceanographic Institution

ABSTRACT

A case of low-altitude veil clouds from which cumulus later grew is studied by means of airplane, photographic, and synoptic data. Convergence due to the land-sea temperature contrast is indicated as the critical factor in this unusual cloud formation. This conclusion is further supported by an airplane study of the cumulus structure.

IN the course of an observational program to study convection and cumulus clouds in the region of Cape Cod and the adjacent islands, a particularly interesting case was encountered on July 24, 1950. Although superficially typical in many ways of the average manner of cumulus formation over the Cape, an unusual and striking feature of this case was the formation at altitudes of 3000 ft or lower of large numbers of dark, tenuous, pileus-like veils. These first appeared entirely alone so that they resembled many "eyebrows" in the sky (see FIG. 1) and fifteen to twenty minutes later small cumuli began to sprout, the veils remaining visible at their bases. This situation should be contrasted with the more usual examples of pileus formation at the tops of vigorous cumuli, which occur frequently when convective clouds push upwards against an inversion. By means of airplane traverses and soundings in the cloud area in conjunction with local synoptic data, the present formation can be understood as a somewhat specialized outgrowth of convergence caused by land-sea temperature contrast.

Previous observational work by the writers [1] has demonstrated that the cumulus streets formed by Cape Cod and adjacent islands are intimately related to the heating of the land surfaces relative to the surrounding waters. In the cases previously studied, the cloud streets have been observed to form and decay at times coincident with the rise and decline of solar heating. That the sea-breeze circulation is also a consequence of differential heating is well known and the present case provides evidence that some, at least, of the weaker cloud streets may owe their existence to the superposition of such convergence upon the more direct consequences of heating and mixing the air, similar to the "Lanai-type" Hawaiian cloud streets discussed by Leopold [2].

In the case of July 24, the cloud streets which formed out of the pileus-shaped veils were oriented along the northern shore of Cape Cod as illustrated in FIGURE 2. The whole area was in a moderately strong high-pressure cell with the polar front quite far to the south, and a weak gradient flow from a southeasterly direction prevailed until the onset of the sea-breeze effect. The water temperature was almost identical with that of the lower air as it started inland and began its rapid heating by the sandy soil of the Cape. A description of the initial character of this air is given by the 11 a.m. E.D.T. Nantucket sounding (FIG. 3), the striking features of which are weak conditional instability and a rapid decrease of the dewpoint temperature with height. The convection condensation level (as defined by Spilhaus and Miller [3]) for the lowest 3000-ft layer is, however, higher than 10,000 ft, and only with the addition of sufficient moisture to extend the surface value of the mixing ratio up to 3000 ft is it lowered to the observed cloud base. An airplane sounding made over Falmouth Airport at 3:15 p.m. E.D.T., however, showed a well-mixed layer with mixing

---

[1] Contribution No. 534 from the Woods Hole Oceanographic Institution.

[2] The observational work discussed in this paper was carried on under Contract No. N6-onr 277, Task Order No. II, NR-082-021 by the Office of Naval Research and the Woods Hole Oceanographic Institution, and analysis of the results was completed under Contract No. Nonr-174(00) with the Office of Naval Research and the Illinois Institute of Technology.

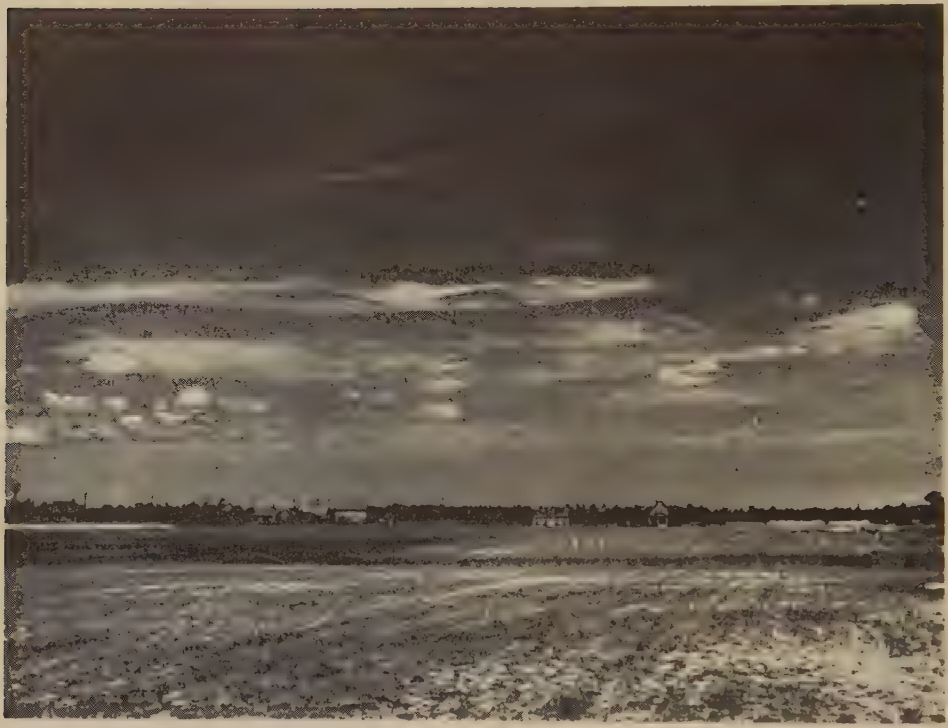

a

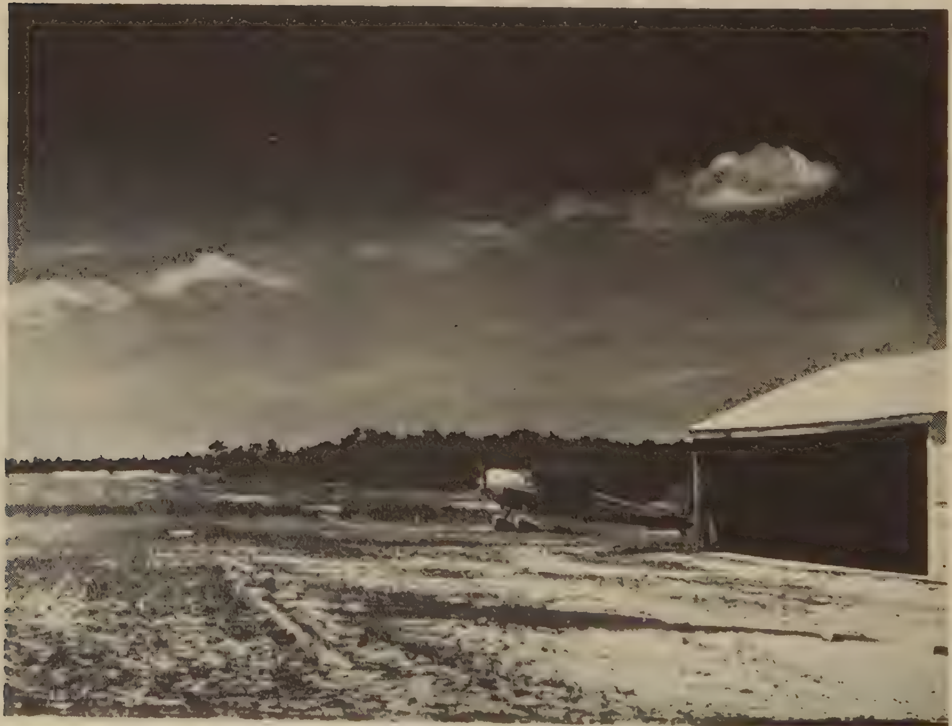

b

FIG. 1 (a and b). Photographs looking northward from Falmouth Airport at about 2 p.m. E.D.T. showing how small cumuli were already beginning to sprout from the veil clouds. Plane flight into the cloud area revealed that the veils were all at altitudes close to 3000 ft. 1b is a section of a photograph taken at nearly the same time as 1a, enlarged to show some of the veil clouds which had not yet sprouted cumuli.

ratio constant only up to 1000 ft, gradually decreasing from there to the level of cloud base (see Fig. 3).

On the other hand, the rapid drying out with height shown by the Nantucket sounding is unusually pronounced for the area and time of year and probably accounts for the form and sequence of condensation phenomena observed. It is hypothesized that when the air flowing from the southeast over the Cape encountered the inward-moving sea breeze on the northern shore, it underwent convergence and bodily lifting. Due to the strong moisture gradient, its lower layers approached saturation first and became visible as the dark, eyebrow-shaped veils. Once such a layer became saturated, large buoyancy forces were available to it, so that the cumuli built up from the veils as bases. That the cumuli were penetrating extremely dry air is revealed by the time-lapse motion pictures which showed their average lifetime was only 5–7 minutes *in toto*, and by their notable lack of development into swelling cumulus despite the slight stability aloft.

Without further observational evidence, however, it might still be suggested that the "eyebrows" need not have been integrally related to the air structure and cloud-formation process but were due perhaps to some accidental concentration of highly hygroscopic nuclei on that particular day. Fortunately, the pileus-shaped veils recurred fleetingly in the same spot on October 17, 1950. The similarity in lapse rates on the two days, including the marked drying out with height, was too great to be coincidental and supports the contention that the veils were the first step in a somewhat unusual method of cumulus formation. It should be pointed out that the more common summer cumulus in this area is associated with pronounced conditional instability, and is not preceded by veil formation.

Considerable observational evidence also exists to show that on July 24th convergence of the re-

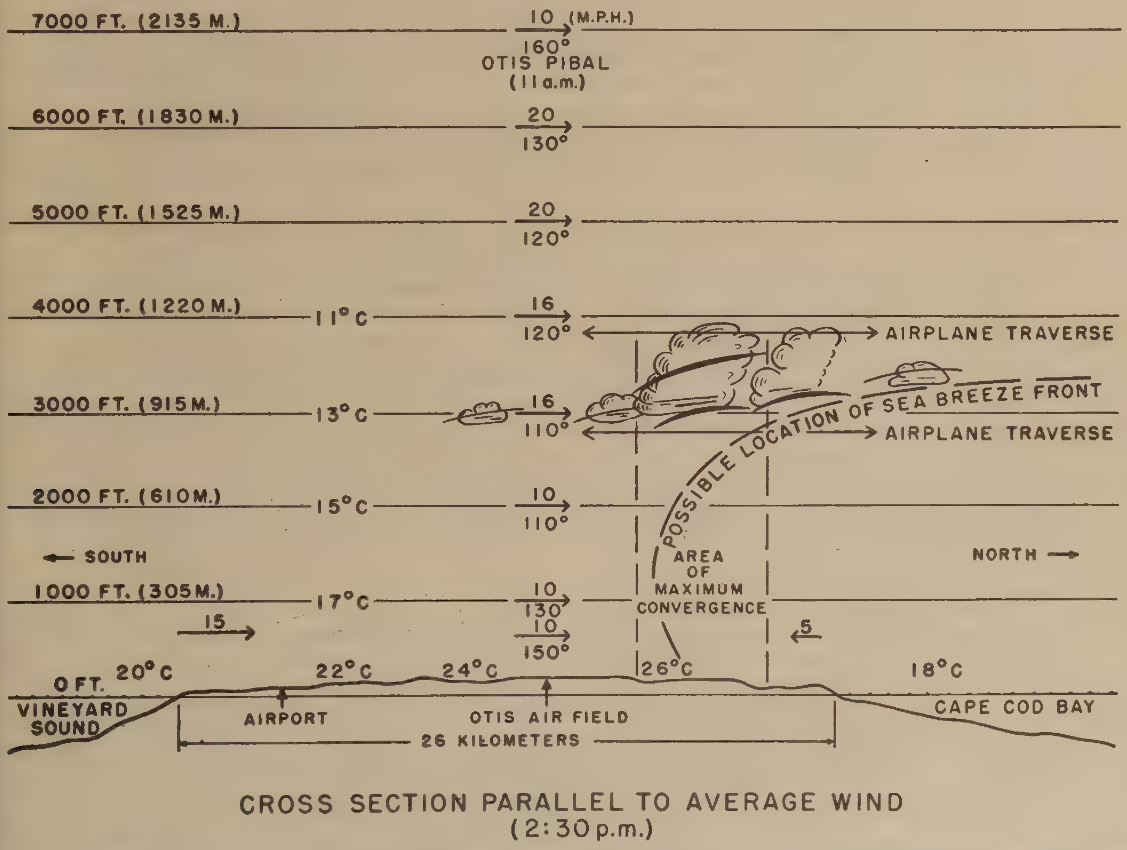
7000 FT. (2135 M.)
10 (M.P.H.)
160°
OTIS PIBAL
(11 a.m.)
6000 FT. (1830 M.)
20
130°
5000 FT. (1525 M.)
20
120°
4000 FT. (1220 M.)
11°C
16
120°
AIRPLANE TRAVERSE
SEA BREEZE FRONT
3000 FT. (915 M.)
13°C
16
110°
POSSIBLE LOCATION OF SEA BREEZE FRONT
AIRPLANE TRAVERSE
2000 FT. (610 M.)
15°C
10
110°
SOUTH
AREA OF MAXIMUM CONVERGENCE
NORTH
1000 FT. (305 M.)
17°C
10
130°
15
10
150°
5
0 FT.
20°C
22°C
24°C
26°C
18°C
VINEYARD SOUND
AIRPORT
OTIS AIR FIELD
26 KILOMETERS
CAPE COD BAY
CROSS SECTION PARALLEL TO AVERAGE WIND
(2:30 p.m.)

Fig. 2. North-south cross-section of Cape Cod from Sandwich to Falmouth, showing the major features of the case studied. The Otis Field pilot balloon observation, however, was made at 11 a.m. E.D.T. and by the time of flight at 2:30 p.m. (time for which the section is drawn) a southwesterly wind extended down to about 3000 ft.

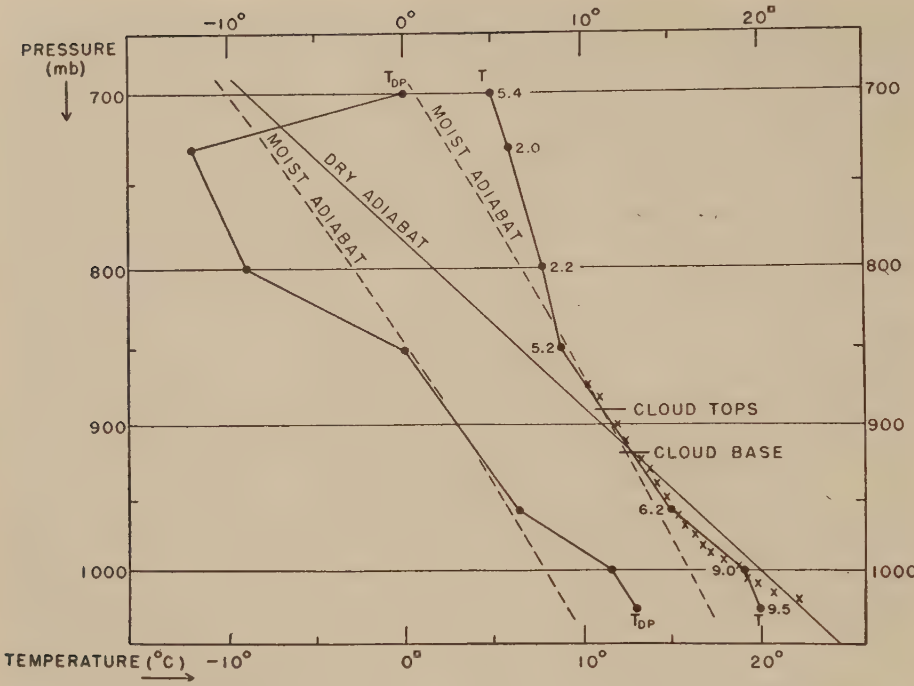

FIG. 3. The Nantucket sounding for 11 a.m. E.D.T. on July 24 is given by the heavy lines, T and T_{dp}, the temperature and dewpoint curves, respectively. The mixing ratio in gm/kg is given beside each point on the temperature curve. Nantucket is about 25 miles upwind (over water) from the Falmouth shore of the Cape. The airplane temperature sounding made over Falmouth Airport at 3:15 p.m. E.D.T. is shown by the crosses.

quired magnitude actually did take place. The appearance of the veils at 1:45 p.m. E.D.T. in a rather sudden burst is consistent with the accepted picture [4, 5] of the abrupt arrival of a "sea-breeze front" when the sea breeze is opposed by the gradient flow. That such convergence has a sharp maximum along a rather narrow line, often marked by rows of cumuli, has been found in several studies [2, 6]. A marked decrease in surface wind between Falmouth and Otis Field (see FIG. 2) is customary on such days, and in this case corresponded to a convergence of 1 per hour,[3] comparable to the magnitude of the cumulus-stage convergence found on the Florida peninsula by the Thunderstorm Project [7]. An average convergence of this magnitude maintained in a one-kilometer-thick airmass for one hour gives an average lifting of the airmass of roughly 500 m. Since the convergence at the sea-breeze front on July 24th probably far exceeded this figure, the 1 km lifting required to saturate the lowest points on the Nantucket sounding could easily have occurred along this boundary.

Unfortunately, no wind measurements were made on this particular day at the northern shore of the Cape. However, following Wexler [4], the assumption that the sea-breeze front cannot penetrate farther inland than the point at which the marine air becomes heated to the temperature of the inland air gives results consistent with an average inflow of 5–7 mph from the northern beach to the inshore limit of the cumulus formation, about 6–7 miles inland (illustrated in FIG. 2). Synoptic surface observations showed that upon arrival at Falmouth Airport, the lowest air had warmed 2.2C° above the Vineyard Sound water temperature of 20°C. Since the distance, parallel to the wind direction, from shore to airport is 2.2 miles and the wind speed was 15 mph, this represents a heating rate of 15C° per hour. Using the temperature at Otis Field at 3:25 p.m. E.D.T. (FIG. 2), and a mean wind speed of 12 mph between shore and Otis Field, the average rate of heating between the Sound and Otis Field (6 miles) is about 8C° per hour, both these figures being in excellent agreement with similar measurements made in sea-breeze air near Danzig. This means that the rate of heating between the airport and Otis Field had dropped to about 4C° per hour. Extrapolating the latter warming rate (and the Otis Field wind speed of 10 mph) 6 miles further along the surface wind to the cloud boundary gives a temperature of about 26°C at the sea-breeze front. Since the water temperature just north of the Cape

---

[3] Results of detailed surface wind observations in many places on Cape Cod on a day similar to the one studied here showed that the components of surface wind normal to the section shown in FIGURE 2 would, if anything, add to the convergence calculated.

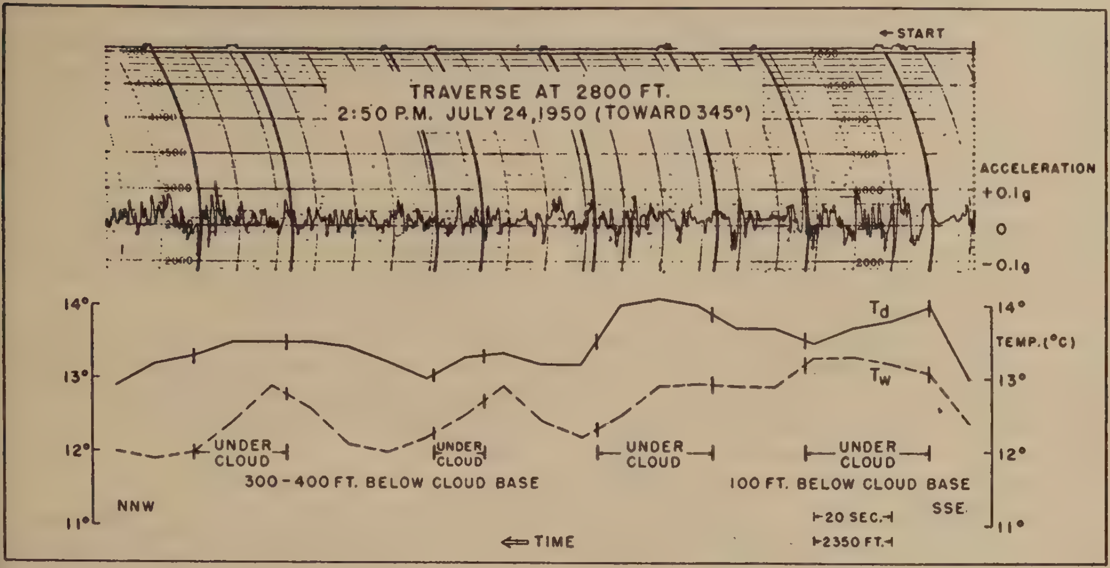

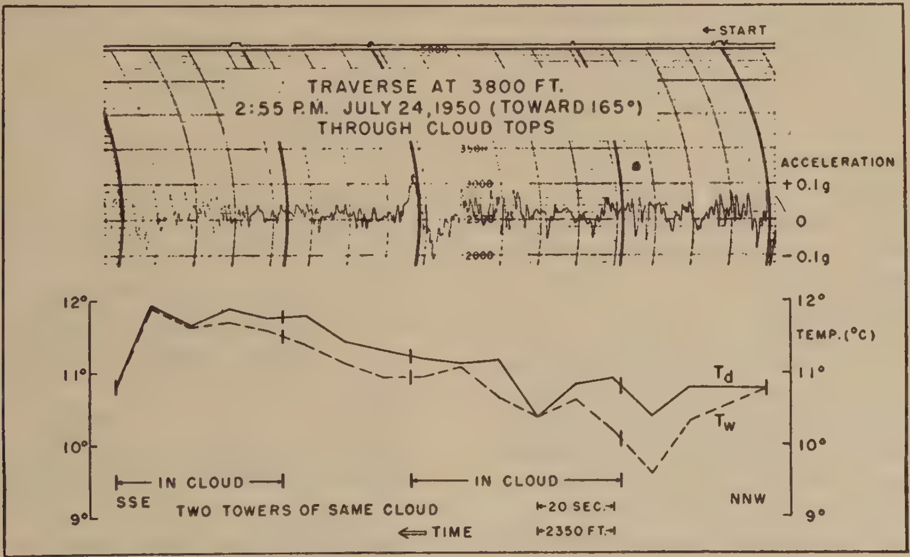

Fig. 4. Data obtained from horizontal airplane traverses in the cloud area. The dry-bulb temperature trace is indicated by T_d and the wet-bulb trace by T_w. The amplitude of the accelerations indicates the development of small scale turbulence but gives no direct information about the presence of drafts, which show up better in the temperatures. In the 2800 ft traverse, the displacement between the observer's recording of "under cloud" and the temperature peaks is almost certainly due to the slope of the updrafts with height toward the northeast along the wind shear vector (verified by the time-lapse pictures) rather than due to the asymmetries between draft and liquid cloud discussed by Malkus [10] which must be very small near cloud base, although located similarly with respect to the shear vector. These asymmetries, in both turbulence and temperature (slight), appear in the same location with respect to the shear vector on the 3800 ft traverse, despite reversal in direction of flight.

(Cape Cod Bay) is commonly nearly 2C° colder than that in Vineyard Sound to its south, this means that the fresher marine air flowing in from the north (sea-breeze front) must be warmed about 8C° in the 5–7 miles. Since the average heating rate over this land mileage might again be expected to be about 8C° per hour, the inflow speed of 5–7 mph observed there on similar sunny days is consistent with all phases of the observations in the present case.

A detailed airplane microstudy [4] of the cumulus clouds themselves corroborates the above theory concerning their origin. Horizontal traverses with accelerometer and recording dry- and wet-bulb thermometer were made below and through the clouds. An interesting fact revealed by the traverse at the constant altitude of 2800 ft toward 345° was the increase in height of the cloud base from less than 100 ft above the plane at the start of the traverse to 300–400 ft above it at the end, 4 miles later. If the cloud base can be identified with the top of the newest marine air, this gives a slope of the sea-breeze front a little steeper than 1/100 along the cross-section perpendicular to the shore (Fig. 2), in excellent agreement with the Danzig observations [4].

The accelerometer and temperature records made on this same 2800 ft traverse are reproduced in Figure 4. While the cloud "roots" are quite apparent in the turbulence and dry- and wet-bulb traces 100 ft below the cloud base, they can be discerned only weakly at a distance of 300–400 ft under the clouds. Further evidence that little of the cloud air was being carried up from the lower levels is given by the cloud direction, which was noted by both plane and ground observers to be from the southwest, the same as the wind direction at cloud level. Since the wind underwent a marked turning from northerly at the ground up to southwesterly at about 2800 ft, if any appreciable amounts of air from lower levels were entering the clouds, they would show some component of horizontal momentum in a direction different from that of the ambient wind. This effect is discussed quantitatively by the writers elsewhere [1].

The fact that the updrafts associated with the cumulus (to be distinguished from the gradual, more uniform lifting of the entire airmass, which would consist of vertical motions too slow to show up directly on the aircraft records) were thus confined largely to the cloud layer, and that warm, moist bubbles or columns of rising air could not be traced far below the level of the visible cloud seems consistent with the importance of the sea-breeze convergence and lifting on this occasion. In ordinary fine-weather cumulus formation over heated land, glider pilots have frequently been able to follow the rising columns from a few hundred feet altitude right on up into the individual clouds. Further observational evidence under many conditions of the air beneath cumulus is greatly needed, however, to confirm this point.

The writers would like to thank Captain John Glascow, U.S.A.F., of the Otis Air Force Base Weather Station for kindly making available much of the synoptic data used in this study.

---

[4] The aircraft, how it was flown, and the details of the instrumentation are described in other reports of the Woods Hole Oceanographic Institution [1, 8, 9].

References

[1] Malkus, J. S., Bunker, A. F., and McCasland, K., 1949: *Observational Studies of Convection.* Tech. Rep. No. 3, submitted to the Office of Naval Research under Contract No. N6onr-277, Task Order No. II, NR-082-021. Reference No. 49–51 of the Woods Hole Oceanographic Institution.

[2] Leopold, L. B., 1949: The Interaction of Trade Wind and Sea-Breeze, Hawaii, *Jour. Meteor.*, Vol. 6, No. 5, pp. 312–320.

[3] Spilhaus, A. F. and Miller, J. E., 1942: *Workbook in Meteorology.* McGraw-Hill Book Company, Inc., New York, New York, pp. 133–134.

[4] Wexler, R., 1946: Theory and Observation of Land and Sea Breezes. *Bulletin of the AMS,* Vol. 27, No. 6, pp. 272–287.

[5] Koschmeider, H. and Hornickel, K., 1936, 1941, 1942: Danziger Seewind Studien I–III. *Danziger Meteorol. Observ., Forschungsarbeiten,* Hefte 8, 10, and 11.

[6] Braak, C., 1928: Beobachtungen über den Seewind, *Ann. d. Hydr.,* Jg. 56, pp. 190–192.

[7] Byers, H. R. and Braham, R. R., Jr., 1949: *The Thunderstorm.* Report of the Thunderstorm Project. United States Government Printing Office, Washington, D. C., p. 21.

[8] Vine, A. C., 1945: *Accelerometer for Air Turbulence Measurements.* Memorandum on file at the Woods Hole Oceanographic Institution.

[9] Wyman, J. and Collaborators, 1946: *Vertical Motion and Exchange of Heat and Water Between the Air and the Sea in the Region of the Trades.* Report of the Woods Hole Oceanographic Institution (unpublished).

[10] Malkus, J. S., 1949: Effects of Wind Shear on Some Aspects of Convection. *Trans. Amer. Geophys. Un.,* Vol. 30, No. 1, pp. 19–25.

Contribution No. 536

Reprinted from SEWAGE AND INDUSTRIAL WASTES, Vol. 23, No. 2, February, 1951
Printed in U. S. A.

THE FLUSHING OF TIDAL ESTUARIES *

By BOSTWICK H. KETCHUM
Woods Hole Oceanographic Institution, Woods Hole, Mass.

Methods developed at the Woods Hole Oceanographic Institution to determine the accumulation of river water within an estuary and the rate of its transport through the estuary have been described elsewhere (1)(2)(3). The survey data showed that estuaries do not flush as rapidly as the tidal prism calculation would indicate, but the reasons for the discrepancy were unknown. This paper attempts to explain the discrepancy by presenting a modification of the tidal prism concept which produces results agreeing closely with observed conditions in a variety of estuaries.

The tidal prism concept has been used to evaluate the ability of an estuary to disperse introduced pollution. The tidal prism is equal to the difference between the volumes of water in the estuary at high and low tides. Part of this volume is contributed by river flow, part by water which must enter through the seaward boundary of the estuary on the flooding tide. As one moves seaward from the river, the proportion contributed by the ocean becomes much greater than the river flow. The volume of water entering the estuary from the ocean is presumed, in the classical application of the tidal prism concept, to be the volume available for the dilution and removal of the pollution added during each tidal period. This presumption involves the following tacit assumptions:

1. The entering water mixes completely and uniformly with the water present in the estuary at low tide.
2. The volume of water moving seaward on the ebb tide escapes and is not returned to the area on the next flood tide.

Under actual conditions neither of these assumptions is correct. A horizontal gradient of salinity is always observed, ranging from negligible values in the river to maximum values at the seaward end. This shows that horizontal mixing is not complete. Because tidal currents are oscillatory, some of the water removed on one ebb tide is always returned on the next flood tide. The practical problem is to define the volume of water which escapes, on the ebb tide, through any cross section of the estuary, and does not return on the succeeding flood tides.

The proposed modifications of the tidal prism concept permit the calculations of tidal exchanges between various parts of the estuary, the total accumulation of river water, or its contained pollution, within the estuary, and the average length of time the river water has been in the estuary. The total volume which escapes on the ebb tide through various cross sections, and does not return on succeeding flood tides, is also calculated. It is this escaping volume, rather than the total volume of the tidal prism, which is available for the dilution of introduced pollution.

---

* Presented at 23rd Annual Meeting, Federation of Sewage and Industrial Wastes Associations; Washington, D. C.; October 9–12, 1950.

Theoretical Considerations

An estuary may be defined as a body of water in which the river water mixes with and measurably dilutes sea water. The inner end of the estuary can be precisely defined as the cross section above which the volume of water involved in raising the height from the low tide level to the high tide level is all contributed by river flow. On the flooding tide there will be no net exchange of water through this cross section, as the river flow contributes all of the water necessary to fill the intertidal volume. Thus, the water above this cross section should be completely fresh. On the ebb tide there is a net loss through this cross section of a volume of fresh water equal to the volume introduced by the river during a tidal cycle. It will be noted that this is a dynamic, and not a geographic boundary, and implies that the inner end of the estuary moves upstream and downstream with changes in the volume of river flow. No attempt is made to define the seaward end of the estuary, as the salinity of the water approaches the salinity of pure sea water gradually. The seaward boundary can be drawn at any convenient location and the area enclosed is considered as the estuary.

It is assumed that there will be a steady state distribution of fresh and salt water throughout the estuary if the river flow remains constant. During each tidal cycle the salinity at any location varies with the stage of the tide, but on successively similar tidal stages the salinity returns to substantially the same value. Figure 1 shows an example of the variation of salinity with tidal time for three locations in Raritan (N. J.) Bay. The lower curve was obtained nearest the river mouth, where the lowest salinities and the maximum variation during the tidal cycle were observed. The other two curves show conditions at

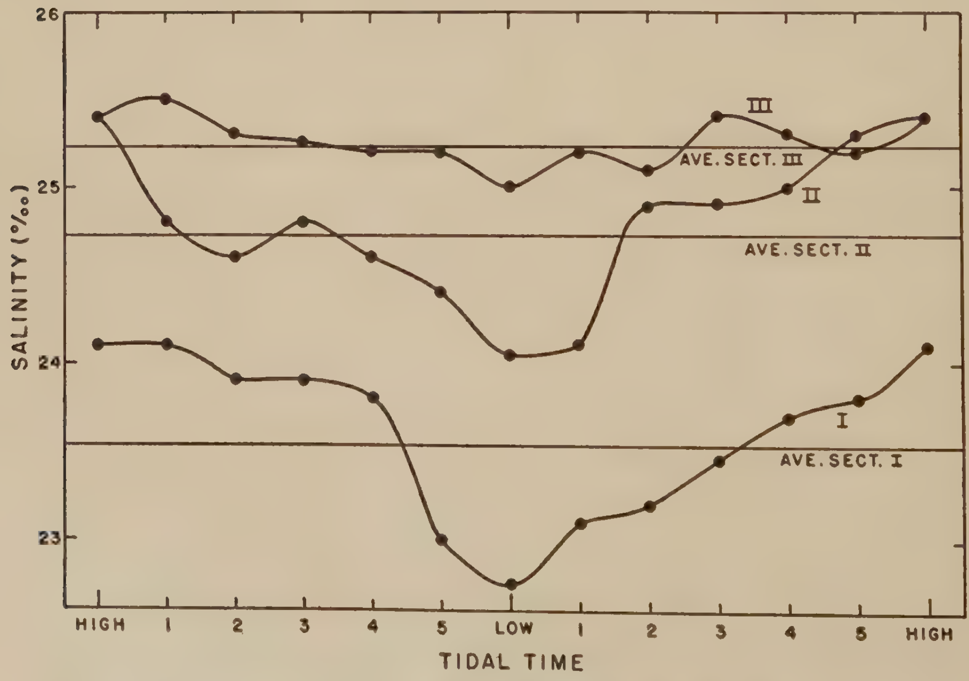

FIGURE 1.—Average salinity variations during a tidal cycle for three cross sections in Raritan Bay. Section I was 1.8 mi., Section II 2.9 mi., and Section III 4.6 mi. from the mouth of the Raritan River.

greater distances from the river mouth, where the salinities were higher and the variations were smaller. In each case the salinity at successive high tides returned to approximately the value previously observed.

In order to maintain a steady state distribution of this sort, two conditions must be met at every complete cross section of the estuary:

1. There must be a net seaward transport, during any tidal cycle, of a volume of fresh water equal to the volume introduced by the river in the same period of time.
2. There must be no net exchange of salt through the cross section during the tidal cycle.

It will be recognized that these conditions do not define the total circulation, but do define the net exchange which is the result of the circulation. The circulation of salt water, for example, may be considerable, but the quantity of salt introduced by the more saline water entering on the flood tide must be exactly balanced by a loss of an equal quantity of salt in the mixed water escaping on the ebb tide.

The tidal prism concept tacitly assumes complete mixing of the water entering on the flood tide with all of the water present in the estuary at low tide. The velocities of tidal currents, however, are generally not great enough to transport the water more than a fraction of the length of the estuary. It seems logical to assume that the maximum length of the estuary over which complete mixing is possible will be determined by the average excursion of a particle of water on the flooding tide. In the proposed modification of the tidal prism concept, subdivision of the estuary into segments defined by the average excursion on the flood tide is an essential and integral part of the treatment.

A chart of Raritan River and Bay, illustrating the volume segments limited horizontally by the width of the estuary and by the average excursion on the flood tide, is shown in Figure 2. In this estuary, 15 volume segments are so defined. The tidal flushing theory assumes complete mixing of the water in each of these segments at high tide. On the ebb tide, the water making up the local intertidal volume of each segment permanently escapes into the adjacent seaward segment. The flushing is thus accomplished by a series of tidal exchanges, with part of the river water, and its contained pollution, moving one segment seaward each tidal cycle.

It should be pointed out that it is unnecessary to have direct current measurements in order to determine the length of the segments in an estuary. The average excursion can be obtained directly from the volumes of water in the estuary at low and high tides. Each segment is defined so that the volume it contains at high tide is equal to the volume of tidal prism water which must enter through the seaward boundary on the flooding tide. If this entering water were to act as a piston, displacing and pushing upstream the low tide water previously present, the distance traveled would be equal to the average excursion on the flood tide. The low tide water displaced equals the volume of the total tidal prism for the remainder of the estuary, and fills the adjacent landward segment at high tide. Thus, the low tide volume of each segment equals the high tide volume of the adjacent landward segment. A definition of the inner end of the estuary has been given above. The segmentation may be started at this boundary, the location of which is determined by the river flow. Near this boundary the size of the segments varies with different river flows. As the tidal prism volume increases for successive seaward boundaries, however, the effect of differences in river flow becomes negligible. This method of segmentation of estuaries is described in more detail elsewhere (4).

If it is assumed that the water present in each of the volume segments is completely mixed at high tide, the proportion of water removed by the ebbing tide is given by the ratio between the local intertidal volume (that part of the tidal prism within each volume segment) and the local high tide volume. This is defined as an exchange ratio, r, having the value

$$r_n = \frac{P_n}{P_n + V_n}$$

in which P_n is the intertidal volume and V_n is the low tide volume of the nth segment.

The river water present in each segment is made up of varying proportions of water that arrived at the location under consideration during a series of tidal cycles. Using the tidal exchange ratio, the proportion of river water of various tidal ages removed during each cycle, and the proportion

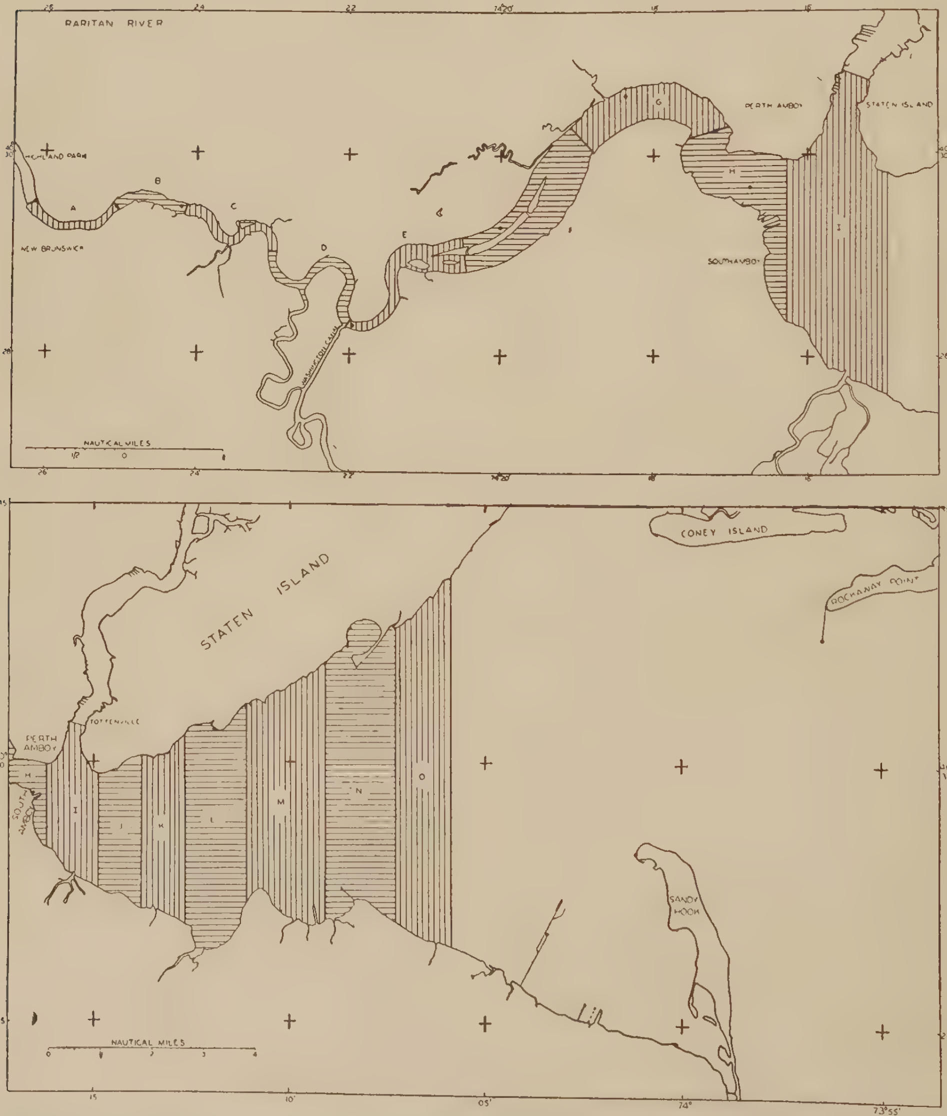
RARITAN RIVER
HIGHLAND PARK
NEW BRUNSWICK
A
B
C
D
E
G
H
I
PERTH AMBOY
STATEN ISLAND
SOUTH AMBOY
WASHINGTON CANAL
NAUTICAL MILES
1/2
0
1
CONEY ISLAND
ROCKAWAY POINT
STATEN ISLAND
TOTTENVILLE
PERTH AMBOY
SOUTH AMBOY
J
K
L
M
N
O
SANDY HOOK
NAUTICAL MILES
0
1
2
3
4
15
10'
05'
74°
73°55'
40°30'
25

FIGURE 2.—Subdivision of Raritan River and Bay into volume segments defined horizontally by the estuary width and the average excursion of a water particle on the flood tide. (River chart scale about twice that of bay chart; volume segment I identical in each.)

left behind, may be summarized as follows:

Age (tidal cycles)	River Water Removed	River Water Remaining
1	$r R_1$	$(1 - r)R_1$
2	$r(1 - r)R_2$	$(1 - r)^2 R_2$
3	$r(1 - r)^2 R_3$	$(1 - r)^3 R_3$
k	$r(1 - r)^{k-1} R_k$	$(1 - r)^k R_k$

in which R_1, R_2, R_3, . . . , R_k are the volumes of river water which arrived 1, 2, 3, . . . , k tidal cycles prior to the time considered.

If the river flow is constant, all values of R are equal and steady state conditions may be presumed to exist. The total volume, Q_n, of river water accumulated within any volume segment, n, of the estuary at high tide is then the sum of the remaining volumes given in the final column above. Because the equation is written for the high tide condition, there is also present one volume of river flow which has not yet been depleted. That is,

$$Q_n = R[1 + (1 - r) + (1 - r)^2 + (1 - r)^3 + \cdots + (1 - r)^k]$$

This series will approach, as k becomes large, the limit:

$$Q_n = R\,\frac{1 - (1 - r)^k}{r}$$

Because $(1 - r)$ is always less than unity, $(1 - r)^k$ approaches 0 after an infinite number of tidal cycles, and the sum can be reduced to:

$$Q_n = \frac{R}{r_n}$$

It will be remembered that one qualification of the steady state distribution was that the river water passing seaward through every cross-section on each tidal cycle must equal the volume of fresh water introduced by the river during the same period of time. The above relationship states that the volume of river water moving seaward is the product of the exchange ratio and the accumulated volume of river water; that is, $r\,Q$. It is readily seen that this product equals R so that this criterion of steady state distribution is satisfied.

This theory has been applied to three very different estuaries; namely, Raritan River and Bay, N. J., Alberni Inlet, B. C., and Great Pond, near Falmouth, Mass. These calculations and the comparison of the results with actual conditions observed during hydrographic surveys are given by Ketchum (4). The effect of incomplete mixing on the exchanges and accumulation are also discussed.

Age of the River Water

The river water present at any time in each segment of the estuary is a mixture of water which has accumulated during an infinite number of tidal cycles. The length of time various proportions of the water have been present is directly represented by the individual remaining volumes listed above. It is thus possible to determine the average age, in tidal cycles, of the river water in each segment. The importance of assessing the age of the river water is obvious in evaluating the distribution of oxygen, coliform bacteria, or any other substance subject to change with time.

The proportion of the river water left behind after being depleted by a series of tidal exchanges is shown in Figure 3 for segments characterized by different exchange ratios. The half-life of the water is the time when half of the river water introduced on one tide has been removed, and is indicated in Figure 3 by the horizontal dashed line. The half-life, for the exchange ratios selected, ranges from 0.4 tides for $r = 0.8$, to 6.5 tides for $r = 0.1$.

The mean age of the water is the average length of time required for the river water, and its contained pollution, to move through the segment. This has also been defined (3) as the flushing time, which is calculated, from the data of hydrographic surveys, by dividing the total volume of river water within the area by the volume of river water introduced each tidal

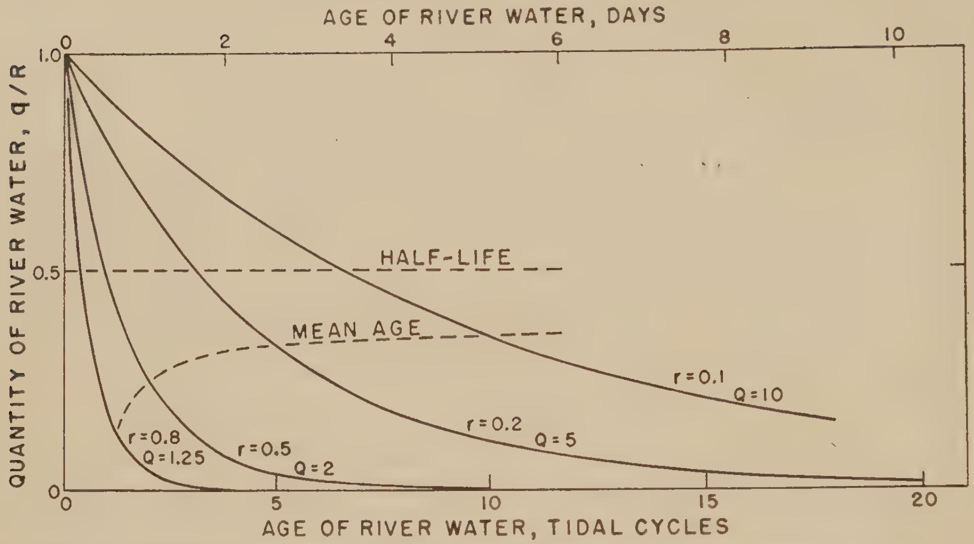

FIGURE 3.—Age composition of river water in estuarine segments characterized by various exchange ratios.

cycle. This ratio is numerically equal, in each volume segment, to the reciprocal of the exchange ratio previously defined. The mean age, or flushing time, illustrated in Figure 3 varies from 1.25 tides (for $r = 0.8$) to 10 tides (for $r = 0.1$).

The above discussion, and the data in Figure 3, are directly applicable only to the first segment of the estuary. The river water entering this segment each tidal cycle has not aged within the estuary, and can be considered new water. For each successive segment down the estuary the water entering on each tidal cycle has already been in the estuary for some time. The water entering the second segment, for example, has been within the first segment for an average length of time equal to its mean age. Similarly, the water entering each successive segment has been within the estuary for progressively longer periods of time. In order to determine the average total length of time the river water in any given segment has been within the estuary, the sum of the average times occupied in passing through all of the enclosed segments must be added to the mean age within the segment considered.

Procedure of Evaluation

The evaluation of an estuary for the disposal of pollution will be illustrated using data for Raritan River and Bay. This location was selected because survey data are available for comparison (1). It must be emphasized, however, that this paper is not primarily a description of a particular estuary, but of methods of evaluation applicable to any tidal estuary.

The first step in evaluation is to compute the distribution of fresh water for various volumes of river flow. In Raritan Bay this has been done for the maximum and minimum mean monthly flow during 1948. An additional calculation was made for the average flow for December, 1948, in order to permit comparison between the calculated and survey results. The cumulative volume of river water is plotted against the length of the estuary in Figure 4. The points, representing the accumulation calculated from survey data, agree closely with the calculated distribution for about 15 mi. of the estuary. The fact that the calculated accumulation of river water near the outer end of the estuary is less than the accumulation observed

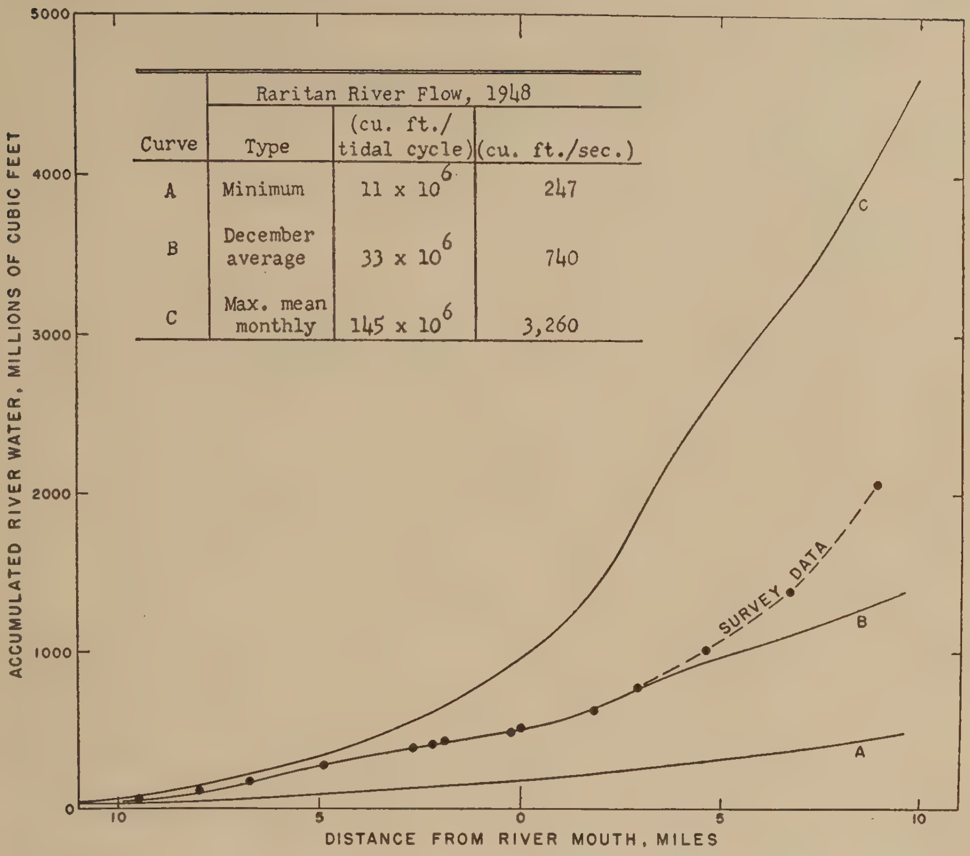

Curve	Raritan River Flow, 1948		
	Type	(cu. ft./ tidal cycle)	(cu. ft./sec.)
A	Minimum	11×10^6	247
B	December average	33×10^6	740
C	Max. mean monthly	145×10^6	3,260

FIGURE 4.—Calculated accumulation of Raritan River water in estuary. Survey data from a hydrographic survey in December, 1948.

on the survey is probably an indication that mixing is horizontally incomplete in this part of the estuary (4). This low calculated accumulation will also be apparent in subsequent values, which are based upon these data. The total flushing times calculated from the data in Figure 4 range from 32 tides

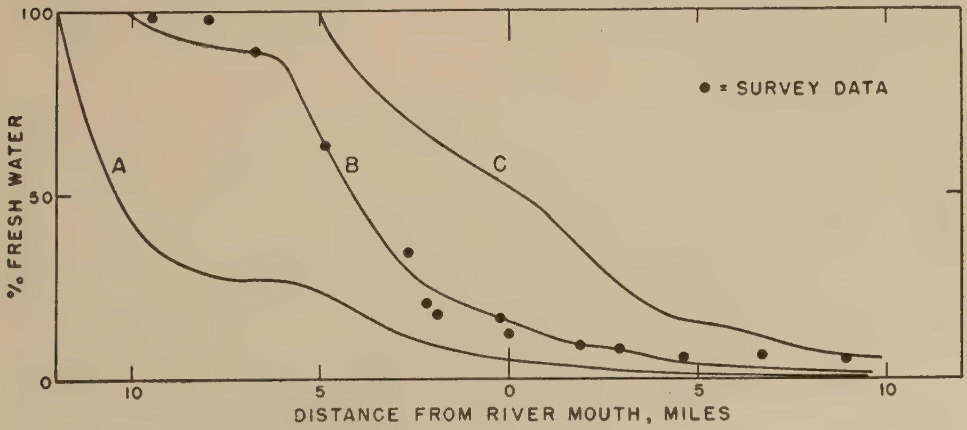

FIGURE 5.—Average percentage of river water in various parts of Raritan River and Bay for three rates of river flow listed in Figure 4.

(for maximum river flow) to 42 tides (for minimum river flow). The survey data indicate a flushing time for the entire estuary of 60 tides. It is of interest that 15 to 30 days are required, on the average, to flush the river water through this area.

The average proportions of river water at various points within the estuary also have been calculated (Figure 5) for the same three rates of river flow. The average proportion is determined by dividing the total quantity of accumulated river water in each segment by the high tide volume of the segment. The results of the survey made in December, 1948, are again used for comparison. All of the water is river water above the boundary defining the inner end of the estuary. This boundary moves a distance of almost 7 mi. downstream as the river flow changes from minimum to maximum values. Seaward from this boundary the proportion of river water decreases, reaching values ranging from less than 1 to almost 6 per cent of the total volume at the outer end. The higher proportion of river water is, of course, associated with the greater river flow.

As mentioned previously, the practical problem which must be solved in order to provide useful data for the sanitary engineer is to define the volume of water which escapes through each cross section and does not return on the succeeding flood tides. The tidal prism concept assumes that the entire volume of tidal prism escapes; it gives exaggerated estimates of the rate of flushing. The modified tidal prism calculation described in this paper assumes that the local intertidal volume in each segment escapes through the seaward boundary and does not return. This produces an escaping volume much smaller than the total tidal prism volume. The escaping volume can also be calculated from the salinity data of a hydrographic survey. At any location within the estuary the water present is a mixture of fresh and salt water. Enough of this mixture must escape on each tidal cycle to remove the volume of fresh water

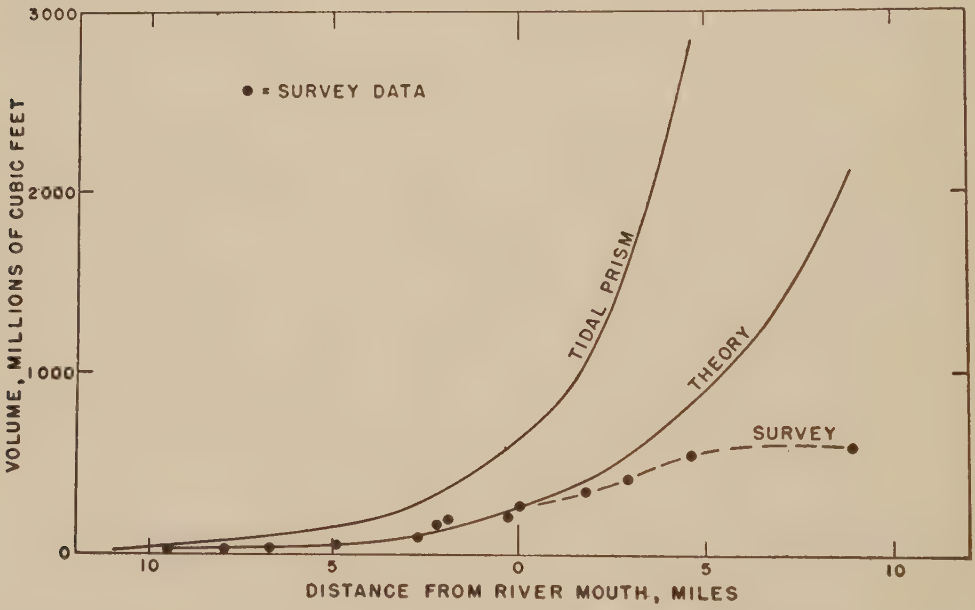

FIGURE 6.—Volume of the tidal prism, and escaping volumes computed from the theory and from survey data. (Tidal prism volume at 9 mi. is 9,200,000,000 cu. ft.)

contributed by the river in the same period of time. The total escaping volume can be obtained by dividing the river flow per tide, R, by the fraction of fresh water in the mixture, F; that is,

$$\frac{R}{F} = \text{Escaping Volume}$$

Thus, if the mixture contains 10 per cent fresh water ($F = 0.1$), 10 volumes of mixed water must escape in order to carry away one volume of fresh water.

These three methods of computing the escaping volume may be compared for the outer boundary of the first segment in Raritan Bay (Segment I, Figure 2). The total tidal prism volume at this location is almost 1,200,000,000 cu. ft. The local intertidal volume, which the tidal flushing theory assumes to be the escaping volume, is 390,000,000 cu. ft., or about one-third the volume of the total tidal prism. The survey data gave an average fraction of fresh water of 0.093, which, with a river flow of 33,000,000 cu. ft. per tidal cycle, produces an escaping volume of 355,000,000 cu. ft. It appears that the proposed theory gives an evaluation of the flushing of the estuary which closely approximates the actual conditions, whereas, in this location, the classical tidal prism method is in error by a factor of 3.

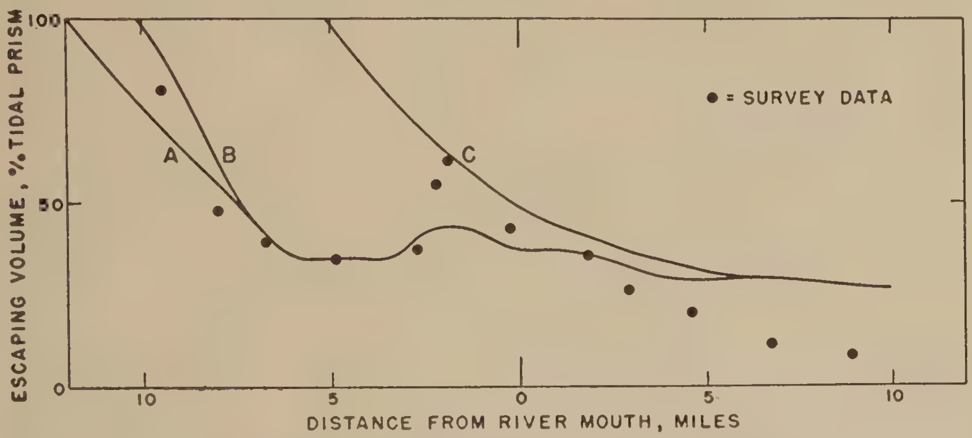

FIGURE 7.—Escaping volumes in Raritan River and Bay for three rates of river flow (see Figure 4) as percentage of tidal prism volumes.

The total tidal prism volumes and the calculated escaping volumes for various locations in Raritan River and Bay are shown in Figure 6. The average December, 1948, river flow has been used to permit direct comparison with the survey data. Throughout the length of the river and the first 3 mi. of the bay, the calculated escaping volume corresponds closely with the escaping volume deduced from survey data. For the outer end of the bay the calculation produces an escaping volume almost six times as great as the escaping volume computed from survey data. The total tidal prism volume at this boundary, however, is almost 30 times as great as the escaping volume computed from the survey data.

The escaping volume can also be expressed as a percentage of the tidal prism volume. This presentation of the data is shown in Figure 7 for the three rates of river flow. The point where the escaping volume is equal to the tidal prism volume shows the location of the dynamic inner boundary of the estuary. The flushing of the inner end of the estuary varies greatly with variations of river flow. Near the outer end, however, the theory predicts that the flushing rate is independent of river flow. Presumably, flushing of this part of the estuary is determined primarily by tidal action. The calculated escaping volume varies from 100 per cent of the tidal prism volume at the inner end of the estuary, to about 26 per cent of this volume at the outer boundary. The escaping volume calculated from the survey data shows reasonably good agreement throughout most of the estuary, but falls to a value only 8 per cent of the tidal prism volume at the outer boundary. This indicates that the tidal flushing theory predicts exaggerated rates of flushing only at the seaward end of the estuary. In contrast, the classical tidal prism concept produced accurate predictions only where the water was completely fresh, and exaggerated the rate of flushing throughout the entire length of the estuary.

The comparison between the volumes available for dilution of pollution in the river and in the estuary should not be neglected in discussing these results. For the first segment in the bay in December, 1948, for example, the volume available on each tidal cycle for the dilution of pollution introduced into the estuary was more than 10 times as great as the volume of river flow per tidal cycle. At the outer boundary, the available diluting volume on each tidal cycle is 20 times greater than the river flow. It is obvious that the universal belief that estuaries are more effective in diluting and removing pollution than the tributary river was well founded, even though the tidal prism concept produced an overly optimistic evaluation.

Discussion

The empirical theory, upon which the calculations in this paper are based, has been described in more detail in a separate paper (4). The theory is not foolproof, and the original paper gives both details of the method of application and ways to check the accuracy of the results. The effects of incomplete vertical and horizontal mixing, which can greatly modify the distribution of river water, are also discussed. The calculations have been applied to only three estuaries. In two of the three, corrections for incomplete vertical mixing were necessary to produce a good correlation. Although the modified theory gives more realistic results than the classical tidal prism concept in the cases tested, much more experience is necessary in order to determine its general usefulness.

The basic data required for the application of the theory are the mean range of tides, the river flow, and the topography of the estuary. All of these are readily available for most estuaries. The theory permits the calculation of the following estuary circulation characteristics, which should be of value to sanitary engineers:

1. The concentration and quantity of river water in various parts of the estuary for various volumes of river flow. The dilution of any pollutant carried by the river water can be directly derived from these data.
2. The mean life of the river water in any segment of the estuary, and the average time required for the river water to reach any part of the estuary. Time-dependent processes, such as oxygen consumption or mortality of bacteria, can be studied using this information.
3. The total volume of water which escapes seaward, and does not return on succeeding flood tides, through various cross sections. This volume is the volume of water available for the dilution of pollution introduced directly into the estuary by sewer outfalls.

River water has been used as a tracer in describing the exchanges within the estuary. It is apparent that any water-borne pollutant will respond in a similar way to the forces and processes controlling the distribution of river water. From the distribution of river water, the distribution of any pollutant within the estuary can be derived.

Acknowledgments

This paper is contribution No. 536 of the Woods Hole Oceanographic Institution, Woods Hole, Mass. The investigation reported herein was supported, in part, by research grants from the National Institutes of Health, U. S. Public Health Service.

References

1. Ayers, J. C., Ketchum, B. H., and Redfield, A. C., "Hydrographic Considerations Relative to the Location of Sewer Outfalls in Raritan Bay." Report 49-13, Woods Hole Oceanographic Institution (1949).
2. Ketchum, B. H., Redfield, A. C., and Ayers, J. C., "Hydrography of the New York Bight." *Papers in Phys. Ocean. and Meteor.*, **12**, No. 1 (1951).
3. Ketchum, B. H., "Hydrographic Factors Involved in the Dispersion of Pollutants Introduced into Tidal Waters." *Jour.*, Boston Soc. Civil Eng., **37**, 3, 296 (July, 1950).
4. Ketchum, B. H., "The Exchanges of Fresh and Salt Waters in Tidal Estuaries." *Jour. Marine Res.* Sears Foundation. (In press.)

DISCUSSION

By A. M. Rawn

Chief Engineer and General Manager, Los Angeles County Sanitary Districts, Los Angeles, Calif.

The author is to be congratulated for presenting a logical method of calculating the effective dilution of fresh water flowing into an estuary and also a means for determining the ratio of fresh to salt water at any location in the estuary if the physical characteristics of the latter, the rate of river flow, and the position of the tide are known. The fallacy of the tidal prism theory becomes immediately apparent upon examination of Mr. Ketchum's scholarly analysis.

Two factors not discussed at length by the author may, at times, set at variance the results predicted by his theory with what will actually be measured at a known location. One of these (1) is the tendency for fresh water, because of its lesser density, to stratify and flow over the top of the salt water, and the other is the tendency for the colder, heavier, sea water on the incoming tide to move shoreward under the overlying warmer waters and crowd them seaward.

As an example of the first of these two factors, the writer's staff analyzed a proposal to discharge primary effluent from a sewage treatment plant into the Long Beach, Calif., intermediate harbor. The proposal had been made following a study based on the tidal prism theory and the conclusions drawn indicated that the dilution would be so great as to render the effluent inoffensive in the harbor waters. When analyzed by a process which involved, in part, that described by the author and, in part, the stratification idea, the conclusions proved to be wholly fallacious. The "steady state" was of necessity disregarded and the tidal range influence computed.

The tidal prism theory led to the assumption that the entire increase in sea water from low tide to high tide was available for dilution in each tidal cycle. By contrast, as a result of the writer's analysis it was determined that new incoming sea water reached the area over the submerged sewer outlet only on 10 days in any 30-day period, and that mixed sewage and sea water reached the outlet from the intermediate harbor into the outer harbor in appreciable quantities only 12 days out of 30.

The stratification theory indicated that practically all of the sewage proposed to be discharged in the intermediate harbor would find its way quite promptly, mixed with the sea water, into the upper 5 ft. of the 40-ft. depth of harbor water, and that for this reason some seven-eighths of the incoming tidal flow would be too far below the surface to contribute much to dilution. Also, only about 3 per cent of the incoming salt water, actually would reach the site of the outfall in an unpolluted condition, and, on the average, sewage or mixed sewage and sea water would be retained in the intermediate harbor an average of three days before escaping into the outer harbor.

Stratification of fresh water on salt water is aptly demonstrated where the Fraser River discharges into the Straits of Georgia. On one occasion during an inspection trip of these waters, the writer noted that the small boats' wakes were quite blue; whereas the surrounding waters had been turned completely brown by the muddy waters of the Fraser. The depth of stratification in this instance would be the upper zone marked in depth by the disturbance created by the small boats' propellors.

Another clear picture of the persistence of the stratification of fresh on salt water is obtained by an analysis of the salt waters in the vicinity of the mouth of the Fraser. The oscillatory motion imparted to the river by the extremes in tidal range permits the formation of fresh water islands overlying salt water in the straits and these fresh water islands preserve their identity for a number of days before becoming completely diffused in the upper strata of the underlying salt water. Their separation from one another is easily detected by salinity analyses.

The second of the factors which may affect the author's conclusions—namely, that of the flowing of denser waters underneath the lighter surface waters and displacing them from the bottom up, is believed by the writer to account for the clean-up of dead-end salt-water inlets into which crude sewage is constantly discharged. The writer is aware of one dead-end tidal inlet on the Pacific Coast extensively used for docking and shipping and into which, at the extreme inland end, is emptied a large quantity of untreated sewage and industrial waste. This harbor has a narrow mouth and expands then into a basin of considerable area. It has no stream of non-saline water (excepting sewage) tributary to it. Nevertheless, the extreme inland waters, into which millions of gallons per day of crude sewage are emptied, are in pretty fair condition and putrefying sludge banks are not at all extensive. In this instance, it would seem that the only explanation for the extensive amount of diluting water which reaches the sewage is that the heavier, colder water travels upstream under the lighter, overlying strata, and that perhaps the combination of stratification and vertical displacement accounts for the presence of the cleaner sea water.

Evaluating the effect of stratification and bottom density currents is a difficult task, but that they are factors in the tidal flushing action can scarcely be questioned.

Again the writer wishes to congratulate Mr. Ketchum upon his excellent presentation of this sometimes confused—and, at times, confusing—phenomenon, and to express the hope that the tidal prism theory, with all of its fallacies, will no longer be substituted for the better and more accurate analysis which the author presents.

Reference

1. **Rawn, A. M., and Palmer, H. K.**, "Pre-Determining the Extent of a Sewage Field in Sea Water." *Trans.*, A.S.C.E., **94**, 1036 (1930).

Contribution No. 538

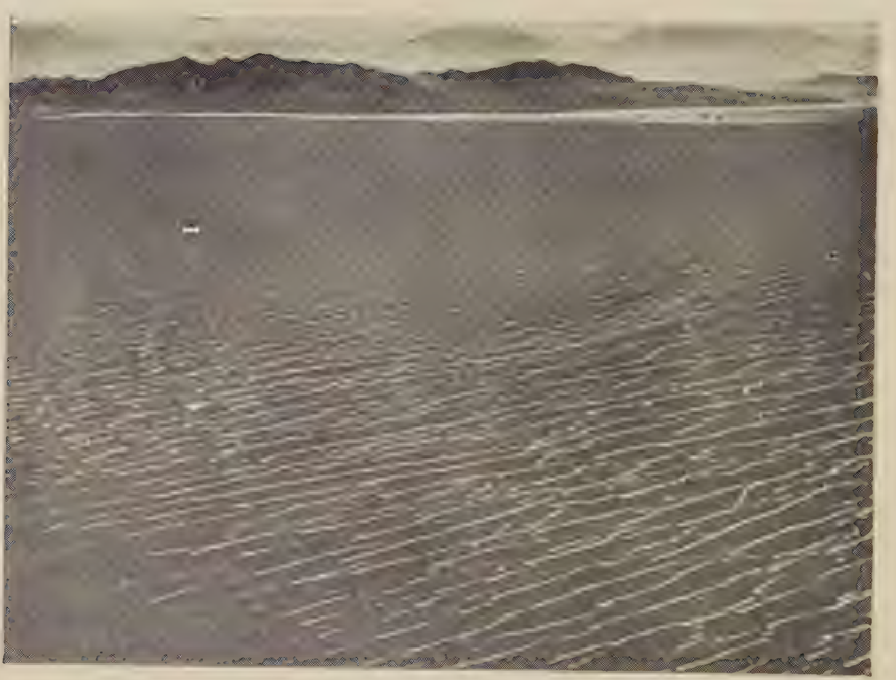

'Venous streaks' on the Great Salt Lakes of Utah

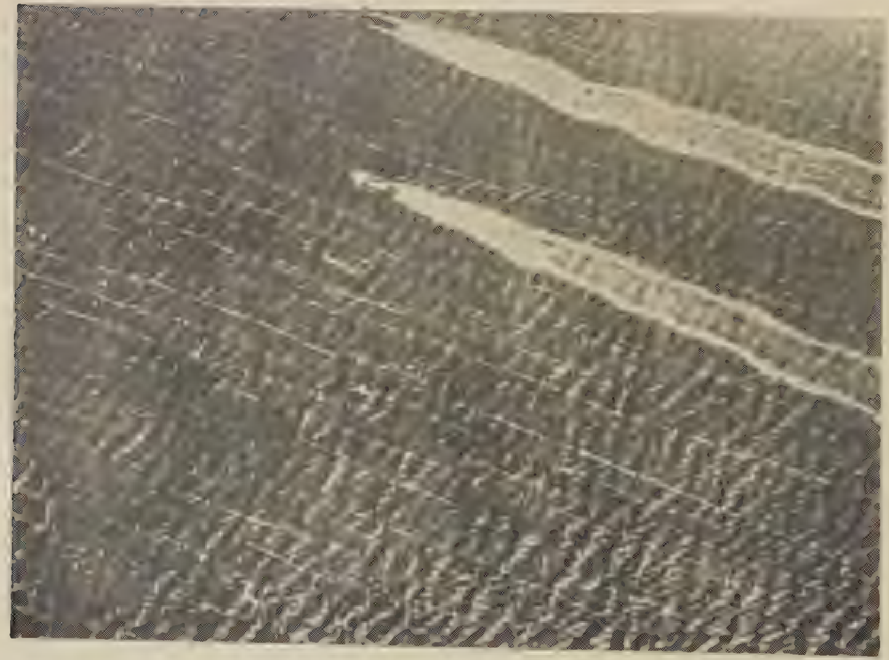

'Parallel streaks' on the Banana River

PLATE 9

Reprinted from 'WEATHER', *March 1951*

STREAKS ON NATURAL WATER SURFACES

Contribution No. 538 from the Woods Hole Oceanographic Institution

By H. STOMMEL

I was very much interested to see Mr. A. K. Totton's photographs of markings on the water (in the August 1950 issue of *Weather*, Pl. IV) because recently I have been trying to collect as much information about such phenomena as possible. I enclose two photographs which may interest the readers of *Weather*; one, showing 'venous streaks' on the surface of the Great Salt Lake of Utah, was kindly given to me by Prof. A. J. Eardley of the University of Utah (Plate 9); the other, a picture of the Banana River in Florida, shows a remarkable development of 'parallel streaks', which was taken by Mr. Alfred Woodcock, of Woods Hole (Plate 9, lower).

Most natural bodies of water have a streaky appearance which results from a natural process, although artificial streaks (due to the passage of a ship, for example) are also frequently observed. There has been quite a difference of opinion in the literature as to the nature of the process which produces streaks. I am personally inclined to admit that under certain circumstances any one of the processes suggested may account for them; to attribute all streaks to the same mechanism would be a great mistake. I should like, therefore, to review briefly what little material there is in the literature about these streaks on the surface of natural bodies of water.

The streaks themselves may consist of accumulations of floating objects, such as Gulf-weed (Woodcock 1950), pine needles or bubbles of foam, all of which are visible because of their colour. Others are local concentrations of an oil film (presumably of planktonic origin) which damp the tiny wind-raised capillary waves. These are visible because of the marked difference in reflectivity of sky light between ruffled and slick areas.

SINGLE STREAKS

Single long streaks are often observed in harbours. They may stream out from a single continuous source of contamination, and run downwind with the surface water, or follow tidal or other currents. For convenience they may be called 'trail-streaks'. Single long streaks may also develop from an initially localized concentration of surface contamination in regions of strong horizontal shear by a simple stretching of elements of water in the shear zone. These 'shear-streaks' occur on the edges of strong tidal currents and in rivers. A third kind of commonly observed single streak is seen to remain parallel to a coast-line a hundred feet or so offshore, most frequently with an onshore wind. The cause of these 'shore-streaks' is not known, but I venture to suggest that they are due to the horizontal convergence and sinking of surface water which is driven toward the shore by the wind, sinking somewhere off-shore, where the water is reasonably deep, rather than at the vanishingly small depths at the very water's edge.

MULTIPLE STREAKS

The kinds of single streaks mentioned above are described in order to avoid confusion with other kinds which are really more interesting. I am referring to the large numbers of streaks often arranged in geometric patterns over large areas of a lake or ocean. Although it may be dangerous to draw a sharp distinction, these multiple streaks usually appear either in long parallel lines or with a vein-like pattern. I find it convenient to call them ' parallel ' and ' venous ' streaks respectively.

Parallel and venous streaks are plentiful in nature. Windrows of Gulf-weed in the deep ocean (Woodcock 1944, 1950) are conspicuous examples of parallel streaks. Unfortunately there are no good photographs of these lines of weed. I have tried to photograph them on several occasions, as have others at this institution, and so far we have had no success. Similar streaks are observed on lakes, and have been carefully studied (Langmuir 1938).

AIR- AND WATER-CELL THEORIES

A large proportion of the parallel and venous streaks are aligned up- and down-wind. Two possible mechanisms have been suggested. One is the air-cell theory, which maintains that there is a cellular structure of the wind, which sweeps the surface water into lines. Langmuir (1938) on the other hand has reported that cellular motions exist in the water and that the streaks are located along lines of surface convergence and sinking water, a mechanism which may be called the water-cell theory. He has suggested that the cellular motion extends down to the thermocline, and indeed that it plays an important rôle in the formation of the thermocline. If this idea be true it certainly deserves further investigation, because the lack of an adequate theory of the thermocline is one of the most glaring lacunæ in oceanography and limnology. Langmuir believes the water-cells are mechanically driven by the wind, although in just what manner is obscure. Woodcock (1944) indicated the presence of films of colder water on the surfaces of lakes and ocean waters and suggested that the water-cells are thermally driven convection-cells similar to those observed in the laboratory (Stommel, 1946). I do not think the results of these laboratory studies are directly applicable to lake and ocean processes without further investigation.

Ewing (1950) has observed other parallel streaks whose orientation bears no obvious relation to the direction of the wind. He attributes them to alternate contractions and dilatations of the surface film due to progressive internal waves travelling along at some distance beneath the surface.

CINEMATOGRAPHIC STUDIES

During June and July of last year I made a number of cinematographic studies of streaks on small ponds on Cape Cod, Massachusetts. They were of the venous and parallel types, and consisted of oil-slicks and lines of foam. The steadier the wind direction, the more nearly parallel they seemed. Upon showing the pictures at some 80 times their normal speed interesting features, which otherwise escaped the eye, were visible : the structure of the wind was so gusty and turbulent that it was obvious that no permanent structure in the air maintained the streaks ; these were so quickly re-oriented after a shift of wind (only 1 or 2 minutes was necessary) that deep motions such as those reported by Langmuir did not seem likely. Thermal convection seemed also unlikely because the streaks occurred at times of intense heating of the ponds and with a very stable *epilimnion* ($0{\cdot}1\ ^{\circ}\mathrm{C.\,m}^{-1}$). Although surface convergence into the lines was confirmed, using Woodcock's ballasted-bottle technique, cellular motions were not observed at depths of one foot or deeper. The indications were that these streaks were due to a process confined to the top few inches at most, and did not play a rôle in the formation of the deep thermocline, which in this instance was at a depth of about thirty feet. It seems, therefore, that they were due to yet another process, perhaps associated with differences of wind-stress in and out of streaks, but which I must admit I do not understand. It would be misleading to conclude that this classification of various types of surface marking is complete. For example, Woodcock and Wyman (1946) have published photographs of mysterious bands on the surface of the ocean which may be due to some still undiscovered process.

If any of your readers have in their possession further data and pictures on these things, I should be most grateful to hear from them.

REFERENCES

DIETZ, R. S. and E. L. LAFOND 1950 Natural slicks on the ocean. *J. Mar. Res.*, Vol. 9, pp. 69–76.

EWING, C. C. 1950 Relation between band slicks at the surface and interna waves in the sea. *Science*, vol. 111 (2874), pp. 91–95.

FORBES, ALEXANDER 1945 Photogrammetry applied to aerology. *Photogrammetric Eng.* (1945), pp. 181–192

LANGMUIR, I. 1938 Surface motion of water induced by wind. *Science*, Vol. 87 (2550), pp. 119–123

SCHMIDT, WILHELM 1936 Cause of ' oil patches ' on water surfaces. *Nature*, London, Vol. 137, p. 777

SHULEIKIN, V. V. 1941 Fizika moria. *Izdat akad nauk SSSR*, Moscow, p. 833.

STOMMEL, HENRY 1946 A summary of the theory of convection cells. *Ann. N.Y. Acad. Sci.*, Vol. 48 (Art. 8), pp. 715–726

THOMPSON, JAMES 1862 On the calm lines often seen on a rippled sea. *Phil. mag.* (4) (1862), pp. 247–248

WOODCOCK, A. H. 1941 Surface cooling and steaming in shallow fresh and salt waters. *J. Mar. Res.*, Vol. 4 (2), pp. 153–161

——————— 1944 A theory of surface water motion deduced from the wind-induced motion of the *Physalia*. *J. Mar. Res.*, Vol. 5 (3), pp. 196–205

——————— 1950 Sub-surface pelagic *Sargassum*. *J. Mar. Res.*, Vol. 9, pp. 77–92.

——————— & JEFFRIES WYMAN 1946 Convective motion in air over the sea. *Ann. N.Y. Acad. Sci.*, Vol. 48 (Art. 8), pp. 749–776

Contribution No. 539

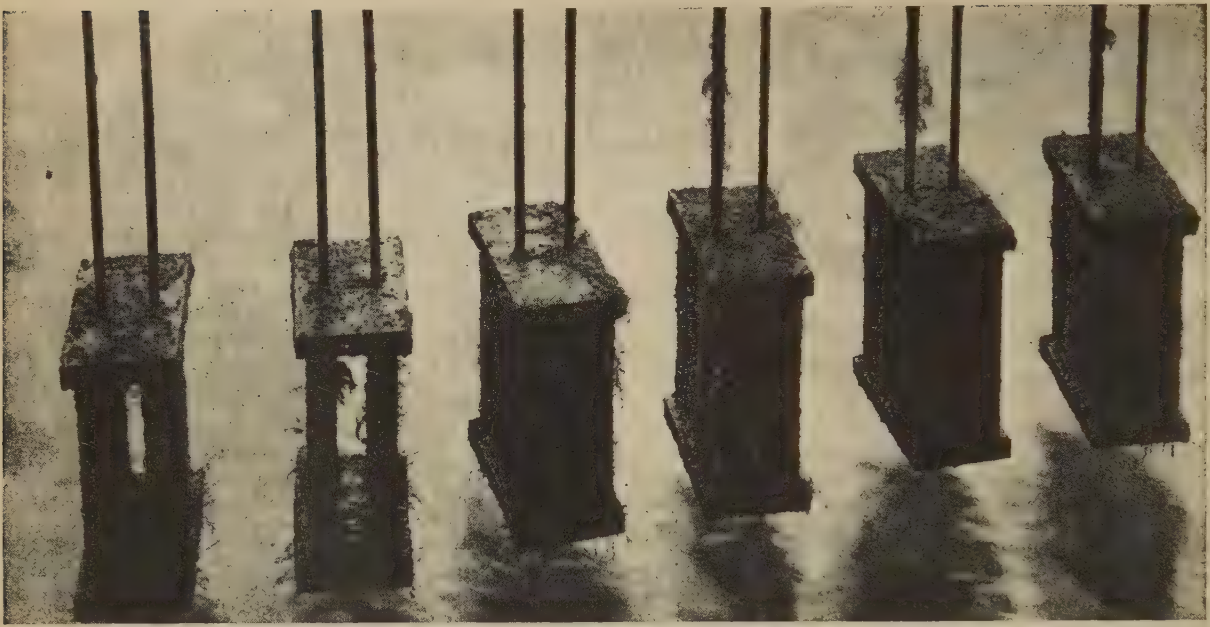

Figure 1. Installation in First Series of Tests, with Electrode Boxes Raised from Water for Inspection of Abundant Fouling (Mainly Barnacles) on the Exterior

Table I summarizes the outcome of the test. Figure 2 is a photograph of the six cathodes removed from their boxes at the end of the test and grouped. The tests show that, over a range of continuous current densities from 10 to 100 ma. per square foot, fouling occurs on steel cathodes in sea water practically as readily as on electrically untreated control surfaces. At a current density of 300 ma. per square foot, the accumulation of fouling organisms on the cathode is definitely less than on control surfaces. A cathode receiving continuous current of density 1000 ma. per square foot can remain free of barnacles for 40 days, although it remains possible that certain hydroids can tolerate these conditions. A continuous current density of 3000 ma. per square foot gives complete protection from fouling to a cathode immersed in the sea for 40 days.

There is clearly an inverse relation between the rate of exfoliation of the cathodic layers and the extent of fouling. Exfoliation becomes prominent at current densities above 300 ma. per square foot, as stated in the Cox patent (*1*), and in the present test was greatest at the highest current density used. Rapid sloughing off of the cathodic coatings appears to be an important factor contributing to the absence of fouling on cathodes exposed to current densities greater than 1000 ma. per square foot.

The decrease in fouling on the cathode with increase in current density cannot be due to the spread of chlorine liberated at the anode. Anode and cathode were separated in this test by a distance of only 2 inches, yet barnacles were in all cases able to grow on the 2-inch strip of wood separating the electrodes at the top and bottom of the boxes. These barnacles were much less than 2 inches from the anode. As they were not chlorinated, it is unlikely that the growth of fouling organisms on the more distant cathodic coatings could be inhibited by products of electrolysis diffusing from the anode.

Table I. Summary of Test with Continuous Current of Varied Density

Electrode Pair No.	Current Density, Ma./Sq. Foot	Results at End of Test (40 Days)
1	10	Cathode heavily fouled with barnacles, hydroids, and tunicates; slight rusting
2	30	Cathode heavily fouled; slight rusting
3	100	Slightly less fouling of cathode; no rusting
4	300	Much less fouling; barnacles reduced in number to about $^1/_5$; exfoliation has ceased
5	1000	Practically no fouling; no barnacles, few hydroids; coatings hard, exfoliation rapid
6	3000	No fouling; a few dead hydroids on thick, soft, rapidly exfoliating coating

All the anodes in this test rusted heavily. At current densities of 10, 30, and 100 ma. per square foot they were fouled; at higher current densities rusting was very rapid and no fouling organisms were able to grow on the anodes.

EXPOSURE TO INTERMITTENT ELECTRIC CURRENTS

The purpose of the tests was to study the effect of rapidly intermittent direct current on the attachment and growth of fouling organisms. It is well known from physiological experiments that stimulation of excitable tissues occurs when the rate of change of the stimulating current is sufficiently great, and that steady current flow is less effective than intermittent current. By making and breaking the circuit at intervals it was hoped to discourage the attachment of larval barnacles or to interfere with their feeding mechanisms if they had become established. A second object of the tests was to see if the physical characteristics of the cathodic coatings formed with rapidly intermittent current would be more favorable for exfoliation than coatings formed with continuous current.

Direct current from a storage battery was interrupted by an automatic timing device which permitted periodic flow of current for a definite number of seconds. In all cases this was approximately one fifth of the time, although the frequency of interruption was varied. The electrodes were metal plates with a surface area of 0.1 square foot, separated in the sea by a distance of 4 inches. Table II summarizes the results of the tests. Additional notes on the individual tests follow:

Test L-1. Inconel electrodes and control; current flowed for 2.5 out of every 14 seconds. Barnacles attached and grew on

Table II. Summary of Results of Tests with Intermittent Current

Test No.	Type of Electrodes	Duration of Test, Days	Current Flow, Ma./Sq. Foot	Results at End of Test
L-1	Inconel	14	400, intermittent	Barnacles on cathode and anode much smaller than on Inconel control panel
L-2	Steel	19	1000, intermittent	Barnacles on cathode smaller and fewer than on wood control panel
L-3	Inconel	21	1000, intermittent	Extensive fouling on cathode which has ceased exfoliation; anode fouling slowly
L-4	Stainless steel	21	1000, continuous	Thick cathodic crust, fouling only where a few old areas persist in spite of rapid exfoliation
			1000, intermittent	Fouled, little exfoliation
			100, continuous	Heavily fouled
			Control (no current)	Heavily fouled

all three plates, but were largest on the control. There was only slight exfoliation of the cathodic deposit.

Test L-2. Mild steel electrodes and a control panel of wood; current flowed for 2.5 out of every 14 seconds. Barnacles on control panel were larger and five times as numerous as on the cathode. Anode rusted rapidly and was unfouled.

Test L-3. Current flowed for 0.9 out of every 4.5 seconds. Cathodic coatings were heavily fouled; anode, slightly fouled.

Test L-4. This test gives a comparison of the fouling and the physical characteristics of the cathodic coatings on plates exposed to intermittent and to continuous current of the same density. One cathode was exposed continuously to 1000 ma. per square foot, another to the same current flowing for one fifth of the time (0.9 out of every 4.5 seconds). A third cathode was exposed to 100 ma. per square foot continuously; it fouled as heavily as the control. At the higher current density, exfoliation was more rapid and fouling less on the cathode receiving uninterrupted current.

The tests with intermittent current show that, relative to control panels, fouling is delayed on cathodes exposed to sufficiently high current densities. The retardation does not seem to be due specifically to the making and breaking of the circuit, but to the same factors that operate in tests with continuous current—exfoliation of cathodic layers and probably the action of cathodic products of electrolysis. The delay in fouling of Inconel anodes, where no cathodic coatings are formed, shows that some factor is concerned other than the physical process of exfoliation.

Fouling develops much more rapidly on cathodes exposed for one fifth of the time to current densities of 1000 ma. per square foot than on cathodes exposed continuously to that same current density. Both the extent of fouling and the visible physical characteristics of the cathodic coatings of the cathode receiving current for one fifth of the time resemble the condition of a cathode continuously exposed to current of one fifth that density. Under the conditions of these tests it therefore appears that the condition of a cathode with respect to both fouling and exfoliation is determined more by the total quantity of electricity transferred than by the maximum current density used.

LARGE ELECTRIC CURRENTS OF BRIEF DURATION

Any attempt to control fouling directly by means of electricity presupposes some internal change in the fouling organisms induced by current flow. Such physiological changes can be produced, as shown by laboratory experiments in which feeding barnacles attached to electrodes immersed in a beaker of sea water were exposed to the make and break of direct current densities of the order of 1000 to 5000 ma. per square foot. The barnacles responded by momentary retraction of their rakers and closure of the shell. Those attached to the cathode responded best to the make, those on the anode to the break, of the circuit. They continued their active feeding motions during continuous current flow, in spite of extensive cathodic liberation of hydrogen and other attendant reactions at the electrodes. Moreover, the barnacles adapted rapidly to the flow of current and after responding once to a make or break of the circuit would give no further response for many seconds. It was not found possible, therefore, to interfere seriously with the feeding of barnacles by rapidly repetitive electrical stimuli.

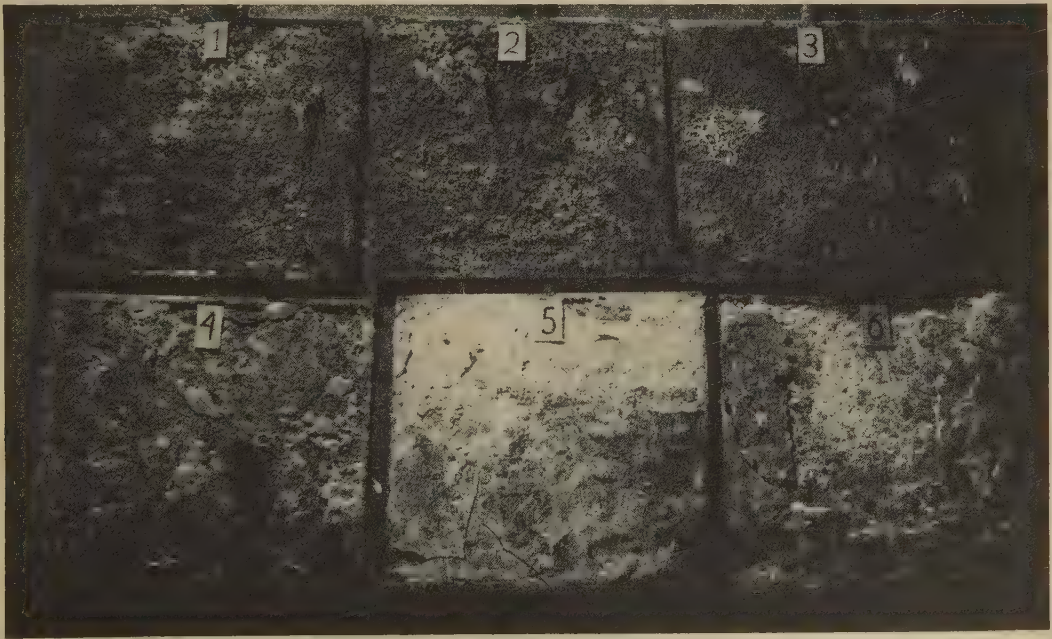

Figure 2. Cathodes in the First Series of Tests Removed from Electrode Boxes and Photographed at End of Test (40 Days)

It was also desired to know whether fouling organisms could be killed by application of periodic electric shocks of large magnitude. The problem is essentially the electrocution of organisms in sea water. The most pertinent previous investigations appear to be the use of electric fish screens (*7*), the collection of fresh water fish by electricity (*2, 3*), and a study of the lower limits of electric current to which marine fish show responses (*8*). Regnart (*8*) found that 10-inch codlings in sea water were capable of showing physiological responses to electric currents of densities as low as a few milliamperes per square foot. McMillan (*7*) was able to stun or paralyze 3-inch salmon in sea water with 5-minute exposure to alternating current densities of about 4300 ma. per square foot. Longer exposures were lethal, and the resistance of the fish to the effects of electric current was found to be inversely proportional to the size of the fish. This last fact suggests that very much larger current densities would be needed to electrocute minute fouling organisms than to kill sizable fish.

A variety of experiments were conducted in the attempt to electrocute barnacles and other fouling organisms which had become attached to metal plates. Inconel strips were hung in the sea to permit attachment of barnacles directly to the metal. These strips were then brought into the laboratory and immersed in a beaker of sea water, and large electric currents passed between them. After they were returned to the sea or to fresh sea water, the barnacles were examined with a microscope to see if they were alive. Direct currents of the greatest density obtainable from storage batteries, current from the secondary of an induction coil (the so-called Harvard inductorium), and 60-cycle 115-volt alternating current were all ineffective in killing barnacles when applied for periods up to 15 minutes. For example, they survived successfully this duration of exposure to 60-cycle alternating current densities estimated to be as high as 1,000,000 ma. per square foot.

Similar drastic electrical treatment has been applied to newly attached cyprid larvae, prior to their metamorphosis into adult barnacles and before they have developed a calcareous shell. No interference with the life or normal development of such larvae has been produced by the use of electricity.

The resistance of fouling organisms to electrocution in sea water appears to be not so much a consequence of their inherent toughness as of the high electrical conductivity of the sea water which surrounds them, combined with the fact that fouling organisms are of small dimensions. When current flows, the sea water must act as a shunt to the circuit through the organisms, the protoplasmic surfaces of which are generally regarded as having very high resistance. It can be understood, therefore, why much less current is required to kill fish in fresh water than in salt water. The factor of size is also important, since the data cited on fish show that they are susceptible to electric currents even in salt water. McMillan (*7*) found that the voltage drop across the fish must be sufficiently great in order to stun or kill. In a given galvanic field, the voltage drop across a fish is very much larger than across a fouling organism 1 mm. or less in size. As the energy liberated in any portion of a circuit is given by the product of time, voltage drop, and current, it is clear that the smaller the voltage drop the less energy is available for lethal or for any other kind of action.

DISCUSSION

As stated earlier, varied views have been held as to how electricity might act as an antifouling agent. The possibility that free-swimming larvae of fouling organisms might be kept away from ships by making the hull cathodic in a galvanic circuit appears altogether unlikely as a result of the present studies. Where fouling was prevented, as by continuous current densities in excess of 1000 ma. per square foot, it appears that physical and chemical factors at the cathode were the casual agents rather than any direct repellent action of the galvanic field on barnacle larvae. With rapidly intermittent current, which might be expected to be more effective in stimulating larvae than continuous current, attachment of barnacles occurred readily on both cathodes and anodes exposed to current densities of 1000 ma. per square foot. It is evident that barnacle larvae cannot be kept away from metallic surfaces in sea water by the presence of galvanic fields of any reasonable magnitude.

The hope that occasional or periodic application of very large currents might serve to kill fouling organisms attached to the underwater metallic parts of ships does not appear justified in view of the enormous currents which barnacles and other fouling organisms are able to tolerate in laboratory experiments. These tests strongly support the idea that, where fouling is prevented by large current densities, the current does not act directly on the organisms but indirectly and principally through flaking off of the cathodic layers.

SUMMARY

Tests on the fouling of metal plates in sea water exposed to a wide range of direct current densities and to varied conditions of current flow were made at Miami Beach, Fla., where the growth of marine fouling organisms, especially barnacles, is abundant. No tests lasted more than 6 weeks.

Fouling develops rapidly on the cathodic coatings electrolytically formed on cathodes by current densities of 10 to 300 ma. per square foot. Fouling is delayed relative to control panels on coatings formed by current densities above 300 ma. per square foot. Fouling is prevented by current densities in excess of 1000 ma. per square foot.

The delay or prevention of fouling by high current densities is due largely to the rapid flaking or sloughing off of the cathodic layers. In addition, cathodic products of electrolysis in solution within short distances of the electrode appear to be unfavorable for the growth of fouling organisms.

The existence of a continuous galvanic field does not keep the free-swimming larvae of fouling organisms away from electrodes immersed in the sea. There is no evidence that electric currents can act directly on larvae to prevent their settling on or attaching to either anodes or cathodes. Current which is rapidly intermittent at intervals of a few seconds is no more effective in controlling fouling than the same quantity of electricity delivered without interruption.

Fouling organisms easily tolerate exposure for 15 minutes to alternating current densities of 1,000,000 ma. per square foot. No feasible method of electrocuting fouling organisms attached to metal surfaces in sea water has been found or is likely.

ACKNOWLEDGMENT

This investigation was carried out by the Woods Hole Oceanographic Institution under contract with the Bureau of Ships, Navy Department, which has given permission to publish the results. The opinions contained herein are those of the author and do not necessarily reflect the official opinion of the Navy Department or of the naval service at large. Particular thanks are due Alfred C. Redfield, for initiating and for aid in planning the work. The help of the following is also gratefully acknowledged: Charles M. Weiss, Woods Hole Oceanographic Institution; F. G. Walton Smith, University of Miami; Scott P. Ewing, Bureau of Ships; F. L. LaQue, International Nickel Co.

LITERATURE CITED

(1) Cox, G. C., U. S. Patent 2,200,469 (1940).
(2) Haskell, D. C., *Trans. Am. Fisheries Soc.*, **69**, 210–15 (1939).
(3) Haskell, D. C., and Zilliox, R. G., *Ibid.*, **70**, 404–9 (1940).
(4) Kühl, H., *Schiffbau*, **37**, 224–6 (1936).
(5) LaQue, F. L., "Electrolytic Protection of Steel in Sea Water by Method of Col. G. C. Cox," Report on Corrosion Tests, International Nickel Co., 1942.
(6) Loeb, J., "Forced Movements, Tropisms, and Animal Conduct," Philadelphia, J. B. Lippincott Co., 1918.
(7) McMillan, F. O., *Bull. Bur. Fisheries*, **44**, 97–128 (1928).
(8) Regnart, H. C., *J. Marine Biol. Assoc. United Kingdom*, **17**, 415–20 (1931).
(9) Visscher, J. P., "Fouling of Ships' Bottoms," Report to U. S. Bur. Ships, **R-15** (1937).

RECEIVED May 15, 1950. Contribution 539 from the Woods Hole Oceanographic Institution.

Contribution No. 540

Reprinted from SCIENCE, May 4, 1951, Vol. 113, No. 2940, pages 517–518.

Organic Origin of Some Calcareous Sediments from the Red Sea[1, 2]

Rushdi Said

Department of Geology,
Mount Holyoke College, South Hadley, Massachusetts

This note describes a preliminary attempt to decipher the origin of the calcareous part of the finer fractions of some samples collected from the northern part of the Red Sea during a voyage of the R.R.S. *Mabaheth* in 1934–35.

Shukri and Higazy (*1, 2*) have discussed the distribution, general character, and mineralogy of the samples collected by the expedition, and certain of their special features have been studied by Mohamed (*3, 4*) and Said (*5, 6*). The submarine topography of the Red Sea basin has been considered in detail by Crossland and Badr (*7*).

The Recent Red Sea sediments are whitish "coral muds" of high $CaCO_3$ content. The coarse fractions of these samples ($> 20\ \mu$) consist largely of fragmentary organic remains (as determined volumetrically under the binocular microscope: 80% corals, 5% foraminifera, 15% echinodermata, mollusca, calcareous algae, etc.). In this investigation only fractions finer than 20 μ were separated by ordinary settling methods for study. The carbonate content of these finer fractions was determined by acid leaching. It was found that the carbonate proportions in them were the same as in the bulk samples. The finer fractions were then separated in bromoform. The lighter portion, composed mainly of calcareous material, together with small amounts of clay, quartz, and feldspar, were dried and weighed. The latter accessory components in no case exceeded 3% by weight.

Spectrochemical analyses of the light part of the finer fraction of sample No. 17, and of a fragment of coral picked from the bulk sample, were made by H. C. Harrison, of the Rhode Island State College, to whom grateful acknowledgment is given. Tables 1 and 2 present the results of these determinations.

The analyses show that the calcareous part of the

TABLE 1

DISTRIBUTION OF ELEMENTS IN SAMPLES

	1*	2*		1*	2*		1*	2*
Si	B^-	B	Au	X	X	B	E	E^-
Al	C^-	C	Ba	E	E	Ce	X	X
Fe	D^-	C^-	Li	X	X	Y	X	X
Mg	B^-	B	Sr	B^+	B	Nd	X	X
Ca	A	A	Rb	Not determined		La	X	X
Na	B	B^-				Gd	X	X
K	Both less than 0.1%		Cs	Not determined		Pr	X	X
						Sc	X	X
Mn	E	D^-	Hg	X	X	Ho	X	X
Re	X	X	Zn	X	X	Dy	X	X
Ti	E	E^+	Cd	X	X	Yb	X	X
Zr	X	X	Ga	X	X	Er	X	X
Hf	X	X	In	X	X	Eu	X	X
Th	X	X	Ti	X	X	Tb	X	X
Pb	F^+	F^+	Co	X	X	Lu	X	X
Sn	X	X	Ni	X	X	Tm	X	X
Ge	X	X	Pt	X	X	Sm	X	X
Cr	E	E^-	Ir	X	X	S	Not determined	
Mo	X	X	Os	X	X			
W	X	X	Pd	X	X	P	Both less than 0.01%	
U	X	X	Rh	X	X			
V	E^-	E^-	Ru	X	X	F	Not determined	
Cb	X	X	Be	X	X			
Ta	X	X	As	X	X			
Cu	E^-	E^-	Sb	X	X	Te	Not determined	
Ag	F^-	F^-	Bi	X	X			

1* Coral fragment.
2* Calcareous part of the finer fraction of sample 17, *Mabaheth* expedition.
$^+$ Higher end of concentration range.
$^-$ Lower end of concentration range.
X Sought but not found.

TABLE 2

SUMMARY OF DISTRIBUTION OF ELEMENTS IN SAMPLES

	A (over 10%)	B (10–1%)	C (1–0.1%)	D (0.1–0.01%)	E (0.01–0.001%)	F (< 0.001%)
1*	Ca	Si, Mg, Na, Sr	Al	Fe	Mn, Ti, Cr, V, Cu, Ba, B	Pb, Ag
2*	Ca	Si, Mg, Na, Sr	Al, Fe	Mn	Ti, Cr, V, Cu, Ba, B	Pb, Ag

---

[1] This work was done during the summer of 1950 while the author was working under a fellowship awarded him by the Woods Hole Oceanographic Institution.

[2] Contribution No. 540, from the Woods Hole Oceanographic Institution.

finer fraction of the sample is almost identical in composition to that of the coral. The sample, however, contains higher percentages of Si, Al, and Fe, which is quite expectable since it was impossible to remove all the clay and other light minerals. The fact that V, B, Ag, Pb, and other trace elements exist in the calcareous part of the finer fraction, as well as in the coral, strongly suggests that the sediment owes its origin for the most part to the accumulation of abraded organic remains. The fact that corals comprise 80% of the bulk sample, and that the spectrochemical analysis of the individual coral sample closely resembles the finer fraction, seems to indicate that such organisms have contributed the largest amount of the calcareous part of the finer fraction. Some other organisms, however, may also have contributed, since additional spectrochemical analyses made for comparison did not differ greatly from that of the finer fraction (*cf.* [*8*]). The data did not completely preclude the possible existence of chemically precipitated carbonate in the sediment, however.

The conclusion that the sediments are largely organic in origin seems most significant in view of the fact that Red Sea oceanographic conditions should be, according to many proponents of the chemical deposition of $CaCO_3$ (*9–11*), ideal for such a mode of accumulation. First, the temperature of the entire water column is high throughout the year and seldom falls below 22° C even at depth during the winter. Second, the salinity ranges from $40^0/_{00}$ to $41^0/_{00}$, which is exceptionally high and is, in fact, among the highest recorded in any existing open sheet of water. Third, the diversified topography of the bottom varies from large shallow flats to deep and highly irregular basins. Fourth, the coast is reef-bound, and a tremendous supply of $CaCO_3$ nuclei should be present as the result of normal marine erosion and attrition. Fifth, although the phytoplankton is not too abundant, it is by no means inconsiderable. Sixth, some areas are continuously agitated; others essentially undisturbed. From the evidence here cited that these Red Sea sediments do not possess significant quantities of chemically precipitated $CaCO_3$, it seems valid to conclude that chemical deposition of $CaCO_3$ is negligible, at least in the present-day seas.

The optimum conditions for formation of calcareous deposits in the Recent seas are: (1) an environment conducive to proliferation of $CaCO_3$ shell-building organisms, (2) conditions under which large quantities of contaminating terrigenous materials are prevented from reaching basins of deposition, thereby masking the calcareous organic debris. For example, basins with reef-bound coasts and virtually no runoff because of aridity are probably the most favorable environments for accumulation of carbonate deposits. In the Red Sea itself, the carbonate percentage increases progressively offshore, irrespective of depth. It seems, therefore, that influx of terrigenous material, normally maximum near shore, reduces the total relative carbonate percentage.

It may also be worth while to note that the mineralogy of the finer calcareous fractions of the samples studied, as determined by x-ray diffraction measurements, indicate they are mainly calcite, with very little aragonite. This observation is of interest, as the coarser calcareous fractions from which the fine fractions are derived consist largely of aragonite (*2*). It seems, therefore, at least in the Red Sea, that inversion of aragonite to calcite requires not too much time during abrasion and transport. The stability of aragonite has long been a controversial subject, but these observations of the Red Sea sediments add evidence of the facility with which aragonite inverts to calcite under the described conditions.

References

1. SHUKRI, N. M., and HIGAZY, R. A. *J. Sediment. Petrology*, **14**, 43 (1944).
2. *Ibid.*, 70.
3. MOHAMED, A. F. *Proc. Roy. Soc.* (*London*), **B**, **128**, 306 (1940).
4. ———. *Am. J. Sci.*, **247**, 116 (1949).
5. SAID, R. *Spec. Pubs. 26*, Cushman Lab. Foram. Research (1949).
6. ———. *Contribs. Cushman Found. Foram. Research*, **1**, 9 (1950).
7. CROSSLAND, C., and BADR, A. *Publs. Marine Biol. Station*, Ghardaqa (Red Sea), **1** (1939).
8. SAID, R. (In press.)
9. CLOUD, P. E., and BARNES, V. E. *Univ. Texas Pub. 4621*, 79 (1946).
10. SVERDRUP, H. U., *et al. The Oceans*. New York: Prentice-Hall (1946).
11. WATTENBERG, H., and TIMMERMANN, E. *Ann. Hydrogr. u. Marine Meteorol.*, **64**, 23 (1936).

Contribution No. 541

21. PRELIMINARY NOTE ON THE SPECTROSCOPIC DISTRIBUTION OF ELEMENTS IN THE SHELLS OF SOME RECENT CALCAREOUS FORAMINIFERA*

Rushdi Said
Mount Holyoke College, South Hadley, Massachusetts

ABSTRACT—Results are given of the spectrochemical analyses of the shells of some Recent calcareous Foraminifera. Seventeen elements are recorded of which silicon, strontium and sodium are present in unusually high quantities. The structure of the shell does not seem to be a constant character determined solely by genetic factors, but rather one which is controlled by the environment and the physiological activity of the organism.

Very little work has been done on the detailed structure of the foraminiferal shell. Clarke and Wheeler in their pioneer work (1922) published the results of their micro-chemical analyses of the tests of seven species of calcareous Foraminifera. They found that these tests accumulate silica in quantities ranging from 0.022 to 15.33%, alumina from 0.022 to 3.98%, $MgCO_3$ from 1.79 to 11.08% and $Ca_3P_2O_8$ was recorded as a trace in two species and questionably present in the remaining five species. These two authors noted that the environment plays an important role in the amount of magnesium concentrated by the shell, there being more in warmer waters than in colder waters.

More recently Wood (1949) studied the structure of the foraminiferal test as observed in polarized light. This author attempted to find a cause for the brown color shown by Recent porcellaneous Foraminifera when observed in transmitted light. He made spectroscopic analyses of some Recent and fossil forms and concluded that the brown color of the Recent forms is probably due to the presence of traces of lead, some of the compounds of which are deeply colored. He recorded the presence in the shells of Foraminifera of calcium, magnesium, iron and lead, as well as other elements not listed.

The following work is an attempt to determine the detailed structure of the shells of some Recent calcareous Foraminifera. The material that forms the basis for this study is from the Red Sea (sample No. 22 of the Mabaheth Expedition, 1934-35)[1], and the Bikini Lagoon. From the Bikini sample were picked approximately one hundred specimens each of *Amphistegina radiata* d'Orbigny and *Calcarina defrancii* d'Orbigny. About one hundred specimens of both *Amphistegina radiata* and *Amphisorus hemprichii* Ehrenberg were obtained from the Red Sea sample. The four lots of specimens were washed with boiling water, ground into fine powder and mixed with equal weights of pure graphite.

The spectrochemical analyses of these four lots were made by Dr. H. C. Harrison of the Rhode Island State College, for whose generous help the author is grateful. Spectrograms of each sample were taken, covering the spectrum range from approximately 2300 A to 4800 A. Since the sensitive spectral lines of such elements as potassium, rubidium and cesium, as well as bands of fluorine compounds, occur in the range above 4800A, these elements were not sought, or were reported with regard to the upper limit of concentration that could be present in the sample.

The results of these analyses as submitted by Dr. Harrison are given in the table on page 12.

Only seventeen elements are recorded. The alkaline earth metals, calcium, strontium and barium constitute a large percentage, of which calcium is by far the most dominant element, while strontium occurs in sizable quantities (1 - 5%). With the exception of the Radiolaria which build their skeleton entirely of strontium sulfate, these values are the highest yet recorded in marine invertebrates. Barium occurs in small quantities ranging from 0.003 to 0.007%. This percentage is higher than Engelhardt's figure (1936) for barium in *Globigerina* ooze which he recorded as 0.0002%. This could be attributed to the fact that my material is a concentrated shell matter rather than an ooze, or to the fact that barium is accumulated in larger quantities in benthonic species.

Of the alkali metals, lithium, sodium, potassium, rubidium and cesium, it is noted that potassium occurs in unusually small quantities (potassium was not recorded quantitatively, but its values were less than 0.01% in all samples). Lithium is completely absent, although this element has been reported to be present as a variable micro-constituent in some organisms (Rankama and Sahama, 1950) and in spite of the fact that Foraminifera assimilate an unusually large number of elements in their shells. Sodium is recorded in rather high quantities (0.5 - 7%). It is seen to be appreciably lower in the Pacific material than in the Red Sea. This observation could be attributed to higher salinities in the latter area.

Silicon is observed in quantities ranging from 1 to 5%. The foraminiferal test seems to accumulate more silicon than any other calcareous invertebrate test, with the exception of certain corals and echinoderms (compare for example Clarke and Wheeler's data [1922]). Magnesium is recorded in rather large quantities. Although no attempt was made to test Clarke

---

* Contribution No. 541 from the Woods Hole Oceanographic Institution.

[1] For further information regarding this sample, see Said (1950).

Reprinted from Contributions from the Cushman Foundation for Foraminiferal Research
Volume II, Part 1, March, 1951

	Amphistegina radiata (Red Sea)	Amphistegina radiata (Bikini)	Calcarina defrancii	Amphisorus hemprichii		Amphistegina radiata (Red Sea)	Amphistegina radiata (Bikini)	Calcarina defrancii	Amphisorus hemprichii		Amphistegina radiata (Red Sea)	Amphistegina radiata (Bikini)	Calcarina defrancii	Amphisorus hemprichii
Si	B—	C+	C+	B—	Cu	E—	E—	E—	E—	As	×	×	×	×
Al	C—	D	D—	D—	Ag	E	F	F+	F	Sb	×	×	×	×
Fe	D+	D—	E+	E+	Au	×	×	×	×	Bi	×	×	×	×
Mg	B—	B—	B+	B+	Ba	E	E	E	E	B	E—	E—	E	E—
Ca	A	A	A	A	Be	×	×	×	×	Ce	×	×	×	×
Na	B—	C+	B—	B+	Li	×	×	×	×	Y	×	×	×	×
K	All less than 0.1%				Sr	B—	B—	B—	B—	Nd	×	×	×	×
Mn	D—	E	E	E+	Rb	Not Determined				La	×	×	×	×
Re	×	×	×	×	Cs	Not Determined				Gd	×	×	×	×
Ti	E	E	E	E	Hg	×	×	×	×	Pr	×	×	×	×
Zr	×	×	×	×	Zn	×	×	×	×	Sc	×	×	×	×
Hf	×	×	×	×	Cd	×	×	×	×	Ho	×	×	×	×
Th	×	×	×	×	Ga	×	×	×	×	Dy	×	×	×	×
Pb	E+	F+	F+	F+	In	×	×	×	×	Yb	×	×	×	×
Sn	E	×	×	×	Tl	×	×	×	×	Er	×	×	×	×
Ge	×	×	×	×	Co	×	×	×	×	Eu	×	×	×	×
Cr	E—	E—	F+	E—	Ni	×	×	×	×	Tb	×	×	×	×
Mo	×	×	×	×	Pt	×	×	×	×	Lu	×	×	×	×
W	×	×	×	×	Ir	×	×	×	×	Tm	×	×	×	×
U	×	×	×	×	Os	×	×	×	×	Sm	×	×	×	×
V	E—	E—	E—	E—	Pd	×	×	×	×	S	Not Determined			
Cb	×	×	×	×	Rh	×	×	×	×	P	All less than 0.01%			
Ta	×	×	×	×	Ru	×	×	×	×	F	Not Determined			
										Te	Not Determined			

	A (over 10%)	B (10 - 1%)	C (1 - 0.1%)	D (0.1 - 0.01%)	E (0.01-0.001%)	F (under 0.001%)
1	Ca	Si, Mg, Na, Sr	Al	Mn, Fe	Ti, Pb, Sn Cr, V, Cu, Ag Ba, B	
2	Ca	Mg, Sr	Si, Na	Al, Fe	Mn, Ti, Cr V, Cu, Ba, B	Pb, Ag
3	Ca	Mg, Na, Sr	Si	Al	Mn, Ti, V, Cu Ba, Fe, B	Pb, Ag, Cr
4	Ca	Si, Mg, Sr, Na		Al	Mn, Ti, Cr, V Cu, Fe, Ba, B	Pg, Ag

(+) means higher end of concentration range
(—) means lower end of concentration range
(×) means sought but not found

(1) Amphistegina radiata (Red Sea)
(2) Amphistegina radiata (Bikini)
(3) Calcarina defrancii (Bikini)
(4) Amphisorus hemprichii (Red Sea)

and Wheeler's theory that magnesium increases with temperature, it was noted that the amount of magnesium varies considerably with little range in temperature.

Boron is recorded in the foraminiferal shell for the first time. It occurs in minor quantities (0.001 - 0.003%). These quantities, however, are higher than the amount of boron recorded by Goldschmidt and Peters (1932) in some corals.

Aluminum, iron, vanadium, lead and silver are common micro-constituents of foraminiferal shells and are invariably recorded with little changes irrespective of locality.

Cobalt, zinc and molybdenum are absent, although it is unusual for calcareous tests not to accumulate these elements.

Summary and conclusions—The detailed spectrochemical analyses of four samples of foraminiferal shells gave the following interesting results:

1. Only seventeen elements were found to be present in the foraminiferal shell. Sixteen of these are common, and tin is erratically recorded in one sample.
2. Foraminifera have a great affinity for strontium, sodium and silicon which occur in their shells in greater quantities than in most other calcareous marine invertebrate shells.
3. One species was found to have a different shell composition in two separate localities, both in regard to the chemical elements present and the quantities of these. It was found that the specimens of *Amphistegina radiata* collected from the Red Sea possess higher percentages of practically all the rarer elements recorded than those collected from the Pacific. This could be attributed to higher salinities of the Red Sea. It is also noted that the Red Sea specimens of *Amphistegina radiata* have incorporated tin, while those from the Pacific have not. It is therefore concluded that the selection of elements for shell building and the amounts of these elements used are not controlled solely by genetic factors, but are probably due to environmental conditions.

It must be remembered, however, that the shells of two species collected from the same area did not have the same composition. It is likely that although certain genetic limitations control the selection of elements somewhat and the environment plays an important role, probably the physiological conditions and the metabolic activity of the organism are also of importance.

4. The chemical composition of the test cannot be used in classifying Foraminifera or in tracing their evolutionary lines. It is interesting to note that Wood (1949) has attempted to use the optical properties of the calcite crystals of the wall of Foraminifera as a basis for classification with some degree of success.
5. Wood's theory (1949) that the presence of minor quantities of lead might cause the brown color of some Recent porcellaneous Foraminifera when seen in transmitted light, cannot be substantiated. Lead in minor quantities occurs in both porcellaneous and hyaline forms.

Due to the small number of analyses made, some of the conclusions presented in this preliminary note are tentative and remain subject to revision when more data become available. It must be emphasized, however, that the field of spectrochemical investigation of the foraminiferal shell is enormous, and that the intention of this preliminary note is to provoke research along this hitherto neglected line.

This work was undertaken at the Woods Hole Oceanographic Institution during the summer of 1950.

REFERENCES

Clarke, F. W. and Wheeler, W. C., 1922, The inorganic constituents of marine invertebrates: U. S. Geol. Survey Prof. Paper 124.

Engelhardt, Wolf v., 1936, Die Geochemie des Barium: Chem. Erde, 10, p. 187.

Rankama, K. and Sahama, T. G., 1950, Geochemistry: University of Chicago.

Said, R., 1950, The distribution of Foraminifera in the northern Red Sea: Contr. Cushman Found. Foram. Research, vol. 1, pp. 9-29.

Wood, A., 1949, The structure of the wall of the test in Foraminifera; its value in classification: Quart. Journ. Geol. Soc., London, 104, pp. 229-255.

Manuscript received September 26, 1950

Contribution No. 544

Transactions, American Geophysical Union Volume 32, Number 3 June 1951

A MIXING-LENGTH THEORY OF TIDAL FLUSHING

Arnold B. Arons and Henry Stommel

(Contribution No. 544 of the Woods Hole Oceanographic Institution
under contract with the Office of Naval Research)

Abstract--The salinity distribution in an idealized estuary where mixing is predominantly due to the tides is computed, using an eddy diffusivity based on the distribution of tidal currents and excursions. Comparison is made to the salinity distribution in real estuaries.

Introduction--The method of computing the steady-state salinity distribution in an estuary due to KETCHUM [in press] is essentially a refinement of the older tidal prism concept used by engineers for many years. The estuary is subdivided along its axis into a number of volumes, each of which is as long as the average excursion of the tide. Complete mixing takes place within each volume. Ketchum has obtained remarkably good agreement between observed salinity distributions along the axis of the Raritan estuary. This success prompted us to attempt a translation of Ketchum's fundamental idea - that the element of mixing volume is bounded by the length of the tidal excursion - into the language of physics of continua.

Kinematics of the model--Consider an estuary of uniform width w, depth H, length L. The origin is placed at the river inflow where the salinity is maintained at s = 0. The x-axis is directed positively downstream. At the seaward end of the estuary, x = L, the salinity is maintained at that of the open ocean s = σ.

The river discharge is D (cu ft/min). The mean velocity of water in the channel due to the river is therefore a = D/wH.

If the length of the channel is small compared to a quarter tidal wave length, the tide will be simultaneous and uniform over the entire channel, and we may express the height of the tide as $\xi = \xi_0 \cos \omega t$, where ω is the angular frequency of the tide.

The tidal current U is obtained from the equation of continuity.

$$\partial\xi/\partial t = - H \, \partial u/\partial x \quad \text{.......................} \quad (1)$$

$$U = U_0 \sin \omega t \quad \text{.......................} \quad (2)$$

where

$$U_0 = \xi_0 \, \omega x/H \quad \text{.......................} \quad (3)$$

The average tidal displacement, ξ, is obtained by integration of the tidal velocity

$$\xi = \xi_0 \cos \omega t \quad \text{.......................} \quad (4)$$

where

$$\xi_0 = - \xi_0 \, x/H \quad \text{.......................} \quad (5)$$

The salt-transfer equation--We will consider the equation describing the mean salinity distribution

$$\partial s/\partial t + u \, \partial s/\partial x = \partial (A \, \partial s/\partial x)/\partial x \quad \text{..................} \quad (6)$$

In this equation s is the time mean salinity at any point x, u is the time mean velocity at x, which we may take as that portion of the flow due to the river (that is, u = a), and A is eddy diffusivity along the x-axis. We express A in terms of a dimensionless number B, a characteristic velocity which we take as the tidal amplitude U_0, and a characteristic length which we take as $2\xi_0$, the total excursion of a particle due to the tides.

$$A = 2B\,\xi_0\,U_0 \quad \text{. . . . .} \quad (7)$$

This form of diffusion equation regards the tides as a turbulent motion superposed upon the steady river flow through the estuary. The simple assumed form of the eddy-diffusivity coefficient is the equivalent of Ketchum's assumption of the dimensions of the mixing volume. It should be clear to the reader that the simplicity of both of these formulations results from a certain vagueness about the physical process involved; the effects of stratification, stability, vertical mixing, bottom roughness, and other influences are not investigated.

In the steady state the time derivative vanishes, and (6) is integrable

$$a\,s = A\,ds/dx + C \quad \text{. . . . .} \quad (8)$$

where C is a constant of integration. At x = 0, both s = 0 and A ds/dx = 0, because there can be no transfer of salt up the river by eddy diffusion; thus the constant of integration C = 0.

The form of the coefficient of eddy diffusion--From (3), (5), and (7) we see that A may be expressed as a function of x

$$A = 2B\,\xi_0^2\,\omega x^2/H^2 \quad \text{. . . . .} \quad (9)$$

Integration of the salt transfer equation--It is convenient to introduce a dimensionless parameter

$$\lambda = x/L \quad \text{. . . . .} \quad (10)$$

to express the distance along the channel in fractions of the total length, and a dimensionless parameter

$$F = a\,H^2/2B\,\xi_0^2\,\omega L \quad \text{. . . . .} \quad (11)$$

which we may call the "flushing number."

Making these various substitutions in (8) the following equation is obtained

$$Fs = \lambda^2\,ds/d\lambda$$

Integration by separation of variable yields the following expression

$$\log_e s = F/\lambda + C'$$

At $\lambda = 1$, $s = \sigma$, so that the constant of integration C is given by

$$C' = F + \log_e \sigma$$

Therefore, it is possible to write the ratio of mean salinity to the ocean salinity in exponential form

$$s/\sigma = e^{F(1-1/\lambda)}$$

The salinity distribution function s/σ --The family of curves on the relation of λ to s/σ is shown in Figure 1 for various values of the flushing number F.

Empirical data for both Alberni Inlet, Vancouver Island, and the Raritan River, New Jersey, are plotted on this figure.

The family of curves is interesting for several reasons: (1) There is a toe to the curves near $\lambda = 0$. (2) The curves are very sensitive to F in region $0.1 < F < 10$. (3) There is a point of inflection at $\lambda = F/2$.

Convenient alternative forms of the flushing number are

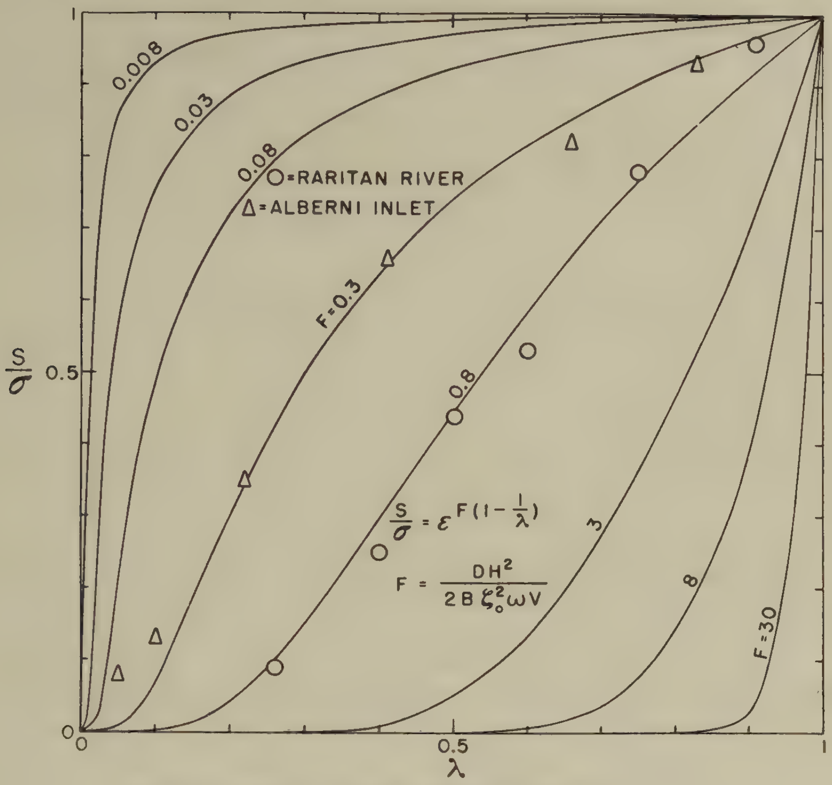

Fig. 1--Family of curves showing relation of λ to s/σ

$$F = D\,H^2/2B\,\xi_0^2\,\omega V = D\,H^2\,T/4\pi B\,\xi_0^2 V = R\,H^2/4\pi B\,\xi_0^2$$

where D is the river discharge, T is the tidal period, V is the mean total estuary volume, and R is the river discharge per tidal cycle.

Interpretation--The curves presented here were developed for a very much idealized situation. For that reason it is somewhat surprising and encouraging to find that empirical data from actual surveys can be plotted on the family with such good agreement.

An attempt to calculate the proportionality factor B from the data was unsuccessful, the values being of an order of magnitude different for the two cases. Therefore, it appears that although the shape of the theoretical curves is in good agreement with the observations at hand, an *a priori* calculation of the flushing number is not yet feasible. Nevertheless, the flushing number may be a convenient concept to characterize estuaries, just as the family of curves themselves is a convenient semi-empirical expression of the mean salinity distribution.

References

KETCHUM, B. H., The exchanges of fresh and salt waters in tidal estuaries, J. Mar. Res., in press.

TULLY, JOHN P., Oceanography and prediction of pulp mill pollution in Alberni Inlet, Fish. Res. Bd., Canada, Bull. 83, 169 pp., 1949.

Woods Hole Oceanographic Institution,
Woods Hole, Massachusetts

(Communicated manuscript received November 24, 1950;
open for formal discussion until November 1, 1951.)

Contribution No. 545

Reprinted from American Journal of Physics, Vol. 19, No. 4, 247, April, 1951
Printed in U. S. A.

A Simple Demonstration of Coriolis Force*

Arthur A. Klebba and Henry Stommel
Woods Hole Oceanographic Institution, Woods Hole, Massachusetts

SEVERAL years ago, in trying to build a simple teaching aid for demonstrating Coriolis forces, we devised the following apparatus. A twelve-inch diameter pan was fastened to a phonograph turntable, and filled, while rotating, with molten paraffin, which formed a paraboloid of revolution upon cooling. The surface of the paraboloid was rather rough at first but was easily made true by repeated melting and solidification of the top surface by means of a heat lamp. A Dove prism was mounted inside a ball-bearing race and rotated by a small variable speed motor at exactly one-half the angular velocity of the turntable. Under these conditions, when the prism assembly was placed above the turntable so that the two axes of revolution coincided, the turntable as viewed through the prism (Fig. 1) appeared to stand still.

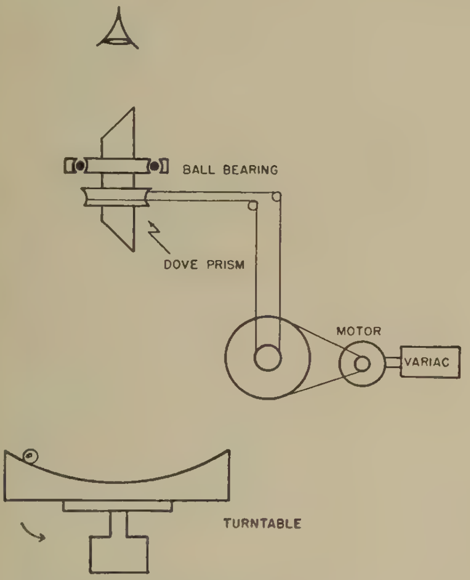

Fig. 1. Apparatus for viewing motion of objects on rotating surface.

The paraboloid is a surface normal to the resultant of the centrifugal and gravity forces, so that a small marble remains at rest at any point on the surface. If displaced by an impulse the marble executes inertial motions[1] which can be clearly seen through the prism. For example, it is easily seen that the marble always moves in a circle relative to the paraboloid with twice the angular velocity of the pan.

The apparatus should be particularly helpful in teaching physical meteorology and oceanography, because it is frequently difficult to impress students with the reality of Coriolis forces. Various modifications of this apparatus to demonstrate other elementary phenomena on a rotating coordinate system will be obvious to the teacher.

---

* Contribution No. 545 from the Woods Hole Oceanographic Institution.

[1] Brunt, D. *Physical and Dynamical Meteorology* (Cambridge University Press, London, 1941), p. 167.

Contribution No. 546

[AMERICAN JOURNAL OF SCIENCE, VOL. 249, FEBRUARY, 1951, PP. 131-151]

EXPERIMENTS ON THE MOVEMENT OF SHELLS BY WATER[1]

HENRY W. MENARD AND A. J. BOUCOT

ABSTRACT. Experiments in a laboratory flume indicate that the current velocity necessary to move terebratuloid brachiopod shells is only about one tenth of the velocity required to move pebbles of the same size. Movement of shells is controlled primarily by the relative ease of movement of the subjacent bed material; a shell may move over a bed of gravel but sink into a bed of sand because of the rapid removal of adjacent sand grains by scouring.

Shape, size, effective density, and ornamentation influence the competent velocity of a shell. Competent velocity increases with sphericity.

INTRODUCTION

PALEOECOLOGISTS are aware that a fossil assemblage of shells does not necessarily represent a community assemblage preserved in place. Instead, the fossil assemblage may constitute a diverse assortment of shells brought together by physical agencies, ordinarily after death, and then buried. Moving water is one of the most important agents affecting the transportation and sorting of unattached dead shells or those otherwise incapable of independent movement. The writers know of no experimental observations on the current velocities required to initiate the movement of shells, nor of the effect of transportation on an assemblage. For these reasons it seemed desirable to make such observations when a hydraulic flume temporarily became available at the Woods Hole Oceanographic Institution in the fall of 1948.

During the experiments, the relations between the variables affecting the movement of the shells seemed to be simple; so no exhaustive study was attempted. Subsequent analysis of the observations revealed that the relations were unexpectedly complex. It is apparent now that many more experiments will be required before the initial movement of shells can be explained completely or predicted. Consequently, the present conclusions cannot be offered as more than first approximations. They are submitted at this time because neither of the writers is likely to have access to a hydraulic flume in the near future.

This paper presents some results of the tests, as well as a brief consideration of their significance with regard to paleoecology. The writers wish to express their appreciation to

---

[1] Contribution No. 546 from the Woods Hole Oceanographic Institution.

P. E. Cloud, W. C. Krumbein, Henry C. Stetson, Fred B. Phleger and J. Wyatt Durham for reading the manuscript and offering suggestions for its improvement. Dr. Cloud initiated the statistical analysis of the data. In this analysis he was advised by F. M. Wadley; W. Peddie made most of these computations. The writers are also indebted to the Woods Hole Oceanographic Institution for the use of laboratory facilities, particularly the flume.

The experiments were done in a wooden flume one foot wide and 6 feet long, with a glass observation panel in one side. In 26 tests, a recess in the central 3 feet of the flume was filled with medium-fine sand (diameter 0.36 mm.) to the level of the flume bottom; in one test, the recess was filled with a gravel composed of grains 2-5 mm. in diameter. The bottom of the flume had a fixed slope of 0.002 during all these tests. In a typical run, a tailgate was fixed in place in order to produce the desired depth of flow in the flume; several shells were placed on the smoothed sand bottom; and the flume was filled with fresh water at a rate slow enough so that neither the shells nor the sand were disturbed; then the flow of water in the flume gradually was increased until one of the shells or the sand moved. The depth of water in the flume and the discharge of the water were measured when movement occurred. The mean current velocity was then calculated by dividing the discharge by the cross-sectional area of the flow within the flume.

Some 27 runs were executed, and 39 individual dry shells, representing 9 species of terebratuloid brachiopods, were tested. Observations were made on the current velocity competent to move the shells, the nature of the movement, scour of sand around the shells, and the orientation of the shells during and after movement. The length, width, thickness, weight, nominal diameter, and sphericity of the shells used in these runs, and the results of the tests are shown in tables 1 and 2.

The velocity required to move a brachiopod shell lying free on a substratum of sand depends on the shell properties of size, effective density, shape, and ornamentation, and on whether the valves are hinged together or separated. All these variables except ornamentation are considered in the present tests. The most important variable governing the initial movement of shells, however, appears to be the relative ease of movement of the shell and the underlying sand grains. Thus, a certain current may roll a shell over a gravel bottom with ease, but be incapable of moving it over sand because the sand moves more readily than the shell. If the sand moves first, a scour is formed around the shell, which may be dropped into it and buried by moving sand. Because of the importance of the relative ease of motion of sand and shells, the detailed discussion of the tests is divided into two sections, one concerned with shells which move more easily than sand, and the other concerned with shells which move less easily than sand.

WHOLE SHELLS WHICH ARE EASIER TO MOVE THAN THE UNDERLYING SAND

Unattached shells are clastic particles in the same sense as grains of sand or gravel, and hence the factors governing their movement are the same. As the movement of sand and gravel has been studied in great detail whereas the movement of shells has not, it seems profitable to consider sediment movement before turning to shell movement.

The characteristics of a grain which influence its initial movement on the bed of a watercourse are the size, density, and shape. Hydraulic engineers generally agree that the current velocity competent to move coarse sand and pebbles is proportional to the square root of the diameter of the grains (Hjulstrom, 1935) ; the same proportionality probably holds for all larger sizes of gravel (Menard, 1949). The competent velocity commonly is thought to be proportional to the square root of the effective density (weight per unit volume if the grains are immersed in water). As to the shape, Krumbein (1942) finds that the more spherical a grain of gravel, the slower the current required to put it in motion.

The present tests show that the initial movement of terebratuloid brachiopods depends primarily on the effective density because that variable appears to govern whether a shell moves more easily than the sand on which it rests. Secondarily, the velocity required to initiate motion appears to depend on the shape and size of the shell. Although the movement of shells and of gravel and sand is necessarily controlled by the same physical characteristics, it is apparent that the relative importance of these characteristics varies.

EFFECTIVE DENSITY

All the whole *Terebratulina* shells tested were moved by currents which were incapable of moving the bed of sand, although the shells weighed as much as 0.605 gram and the sand grains weighed only a few thousandths of a gram. This seeming paradox is due to the very small density of the shell and its contained water as compared to the solid quartz grains. If shell number 4, for example, is filled with water, the shell-water combination has a density in air of 1.28 gms./cc.; however, if the combination is under water, the buoyancy of the displaced water reduces the effective density to 0.28 gm./cc. A water-filled shell moved by a slow current is analogous to an inflated balloon moved by the faintest breeze although the rubber in the balloon weighs several grams.

Species and individuals differ in effective density, and, therefore, in competent velocity. Hence moving water may tend to sort a mixture of individuals of two species into groups according to species—rather than size or shape—if the effective densities of the two species are very different and the range in size and shape is small. Some effective density determinations for terebratuloid brachiopods appear in table 1.[1] The values show that the effective density of *Terebratulina septentrionalis* ranges from 0.28 to 0.43 gm./cc., and that it decreases as the size increases. The effective density of *Terebratalia transversa* ranges from 0.35 to 0.42 but does not vary systematically with size.

Studies of sediment movement indicate that competent velocity is proportional to the square root of effective density. Applying this proportion to brachiopod shells suggests that the competent velocity of a one-centimeter *T. transversa* shell is only slightly larger than that of a *T. septentrionalis* shell of about the same size and shape.

SIZE

The size of irregularly shaped shells may be expressed in terms of a nominal diameter equal to that of a sphere of the same volume. For the present purposes, a nominal diameter has been determined by taking the cube root of the product of the length, width, and thickness of each shell. Thirty-one shells (including single pedicle and brachial valves as well as whole shells) with nominal diameters ranging from 0.41 to 5.50 millimeters were moved while resting on a substratum of either medium-fine sand or gravel. The current velocity required to initiate the motion of each of the shells is shown in graphic form in figure 1, in which the competent velocity in centimeters per second is plotted against the nominal diameter in centimeters. The graph paper is logarithmic because experiments with sediments have shown that functions of these two variables yield a straight line on logarithmic paper. This relation provides an easy means of establishing whether or not the initial movement of shells is controlled by the size of the shells in the same way that the initial movement of sediment is controlled by the size of the grains.

---

[1] A dry shell was weighed in air, and the approximate volume was determined by dividing the weight by the density of calcite (2.72 gms./cc.). The shell was then filled with water and weighed. The weight of the dry shell was substracted from the weight of the water-filled shell in order to obtain the weight of the water, and thereby its volume. The density of the water-filled shell was calculated by dividing the sum of the volume of the shell and of the contained water by the total weight.

The points relating competent velocity and nominal diameter in figure 1 are scattered, but the area in which the points lie has a trend which suggests that the velocity is proportional to the square root of the diameter, as it is for sand and gravel. The coefficient of correlation for a least squares regression line based on all the data in which the bed was sand gives a low positive correlation of 0.585.[2] If the data for a gravel bed are included, a high positive correlation of 0.820[2] is indicated. However, combining data from different experimental conditions introduces some bias into the calculations. The scattering of points indicates that the nominal diameter of a shell is not the only variable affecting its competent velocity. This indication agrees with the general body of hydrodynamical theory and observation. Rouse (1938, p. 216) says that if the wake behind an object is completely turbulent, the drag exerted upon the object by a moving fluid is almost completely independent of the Reynolds number (a criterion of turbulence). The Reynolds number in the present experiments is the product of the current velocity and the nominal diameter divided by the kinematic viscosity; the value of the Reynolds number is great enough to establish that the wake was always turbulent. With regard to shells (nominal diameter larger than about one centimeter), therefore, Rouse's statement indicates that

---

[2] Computed by W. Peddle.

TABLE 1
Physical Characteristics and Flume Behavior of Terebratuloid Brachiopod Shells Resting on a Bed of Sand or Gravel

No.	Species	Type of Shell	Length (cm.)	Width (cm.)	Thickness (cm.)	Weight (gms.)	Sphericity	Nominal Diameter (cm.)	Effective Density (gm./cc.)	Medium Sand Bed: Competent Velocity (cm./sec.)	Medium Sand Bed: Current Velocity At Which Specimens First Turned Over (cm./sec.): Single Valve Concave Upward or Whole Shell	Medium Sand Bed: Current Velocity At Which Specimens First Turned Over (cm./sec.): Single Valve Convex Upward	Gravel Bed: Competent Velocity (cm./sec.)
1	*Terebratulina septentrionalis*	Whole	2.41	1.99	1.21	0.790	0.745	1.80					
2		Whole	2.09	1.74	1.20	0.605							
3		Whole	1.82	1.40	0.81	0.365	.700	1.27		13.8	13.8		
4		Whole	1.70	1.36	0.82	0.325	.728	1.24	0.28	13.3	13.3		
5		Whole	1.63	1.17	0.74	0.230	.688	1.12	(0.30)	13.8	13.8		
6		Whole	1.32	1.10	0.65	0.165	.744	.98	0.32	15.1	15.1		
7		Whole	1.21	0.83	0.57	0.135	.687	.83	(0.36)	11.7	11.7		
8		Whole	0.98	0.75	0.44	0.085	.701	.69	0.43	15.1	15.1		
9		Whole	0.76	0.57	0.36	0.050	.708	.54		11.7	11.7		
10		Whole	0.62	0.46	0.38	0.035	.769	.48		11.7	11.7		
11		Whole	0.62	0.44	0.26	0.020	.667	.41		12.1	12.1		
12		Pedicle valve	2.29	1.60	0.69	0.407	.595	1.36		11.1	12.0	14.9	
13		Pedicle valve	1.92	1.49	0.51	0.307	.591	1.13		11.1			
14		Pedicle valve	1.81	1.34	0.48	0.225	.582	1.05		10.1	10.1	14.7	
15		Pedicle valve	1.61	1.11	0.43	0.115	.569	.92		10.1	10.1	14.9	
16		Pedicle valve	1.19	0.85	0.28	0.055	.551	.66		10.1	11.1 10.6	14.9	
17		Brachial valve	1.65	1.47	0.40	0.217	.600	.99		9.4		SMF*	
18		Brachial valve	1.57	1.31	0.51	0.257	.647	1.02		11.6	11.6	SMF*	
19		Brachial valve	1.50	1.35	0.34	0.135	.589	.88		9.4	10.6	SMF*	
20		Brachial valve	1.35	1.02	0.37	0.112	.592	.80		10.6	10.6	14.4	

TABLE 1 (*Continued*)

										Medium Sand Bed			Gravel Bed
											Current Velocity At Which Specimens First Turned Over (cm./sec.)		
No.	Species	Type of Shell	Length (cm.)	Width (cm.)	Thickness (cm.)	Weight (gms.)	Sphericity	Nominal Diameter (cm.)	Effective Density (gm./cc.)	Competent Velocity (cm./sec.)	Single Valve Concave Upward or Whole Shell	Single Valve Convex Upward	Competent Velocity (cm./sec.)
21	*Terebratulina septentrionalis*	Brachial valves	1.45	1.13	0.38	0.102	.590	.85		9.4	10.6	SMF*	
22			1.04	0.85	0.18	0.042	.522	.54		8.6	9.4	SMF*	
23	*Terebratalia transversa* (Sowerby)	Whole	1.41	1.61	0.68	0.255	.718	1.15	0.35	15.0	15.0	SMF*	
24		Whole	2.19	2.63	1.19	1.763	.721	1.90	0.42	SMF*			
25		Whole	2.74	3.22	1.46	3.036	.728	2.34	0.39	SMF*			SMF*
26		Whole	3.07	3.89	1.83	5.337	.719	2.80	0.41	SMF*			
27		Whole	4.00	4.28	2.53	10.384	.820	3.52	0.37	SMF*			
28		Whole	3.55	4.53	2.30	9.400	.745	3.38		SMF*			SMF*
29	*Magellania flavescens*	Whole	2.95	2.35	1.63	2.496	.761	2.24		17.6	17.6		
30	*Terebratalia rubescens*	Whole	1.94	2.72	1.15	1.467	.639	1.82		SMF*			
31	*Neothyris venosa* (Solander)	Whole	6.95	6.33	3.78	18.677	.791	5.50		SMF*			26.8
32	*Laqueus californicus*	Pedicle valve	3.55	3.90	1.15	5.445	.694	2.52		SMF*			
33		Brachial valve	3.60	4.22	1.15	2.65	.679	2.60		17.6	17.6		
34	*Terebratulina caput-serpentis* (Linné)	Whole	1.96	1.65	0.86	0.410	.718	1.41		17.6			
35	*Waldheimia florida* (Portales)	Pedicle valve	2.05	2.23	0.94	0.295	.650	1.63		12.6			
36		Brachial valve	1.75	2.23	0.59	0.214	.528	1.32		14.8	14.8	16.7	
37		Whole	2.17	2.28	1.50	0.703	.770	1.95		12.6	12.6		
38	*Laqueus californicus*	Whole	2.79	2.44	1.45	0.675	.770	2.14		12.6	12.6		
39	*Terebratella dorsata* (Gmelin)	Whole	3.48	3.63	2.08	4.751	.859	2.98		SMF*			26.8

* Sand Moved First.

( ) Parentheses indicate interpolated values.

of a rectangle and of an airfoil of about the same dimensions, although the form drag of the airfoil is much less than that of the rectangle, and the lift resulting from the shape of the airfoil might have a pronounced effect on its movement. A section of a pecten perpendicular to the hinge line resembles an airfoil, so it is doubtful if any type of sphericity would provide a significant index of its shape in relation to hydraulic behavior.

Figure 2 shows the sphericity of the various shells graphed against the current velocity required to put them in motion. For purposes of comparison, the figure also shows the effect of particle sphericity on the settling velocity and competent velocity of synthetic pebbles with a nominal diameter of about 14.5 mm. (Krumbein, 1942), and also on the settling velocity of molded lead particles (Wadell, 1934). The points relating sphericity and competent velocity of shells are scattered, and the trend of the relation is subject to several interpretations. The four most reasonable interpretations are shown in figure 3. In the first and second interpretations, the data for single valves and whole shells are combined; therefore the relation between sphericity and competent velocity is assumed to be continuous as shown by Wadell (1934). In the third and fourth interpretations, the data for single valves and whole shells are separated; therefore it is assumed that the relation is discontinuous (but continuous for various classes of shapes, such as rollers, disks, or spheriods) as shown by Krumbein (1942). In the first and third interpretations, the data for movement on a sand bed are combined with the data for movement on a gravel bed; in the second and fourth interpretations, these data are not combined. Statistically there is reason to separate the data concerning movement on two sizes of bed material because the experimental conditions were different; combining the data may bias any interpretation. Hydraulically the bias does not appear to be important. The change in bed type probably altered the boundary conditions of the flow in the flume; this probably altered the distribution of velocity in the main body of the flow but the average alteration probably was minor. The shells were all large compared to the thickness of any laminar boundary layer, and therefore most of the surface of shells on either the sand or gravel bed was exposed to the relatively undisturbed turbulent flow outside the boundary layer. The data are subject to too many interpretations to justify any more extensive discussion of this bias.

Despite their diversity, the interpretations indicate that there is some correlation between the sphericity of a shell and the current velocity required to move it. Some measure of the correlation can be determined by drawing a least square regression line for each interpretation, and calculating a coefficient of correlation for the deviation of the points from that line. Interpretation one (figure 3) gives a positive correlation of 0.699[3] for the straight line; no coefficient of correlation can be calculated for a curved line. "Positive" applied to a correlation

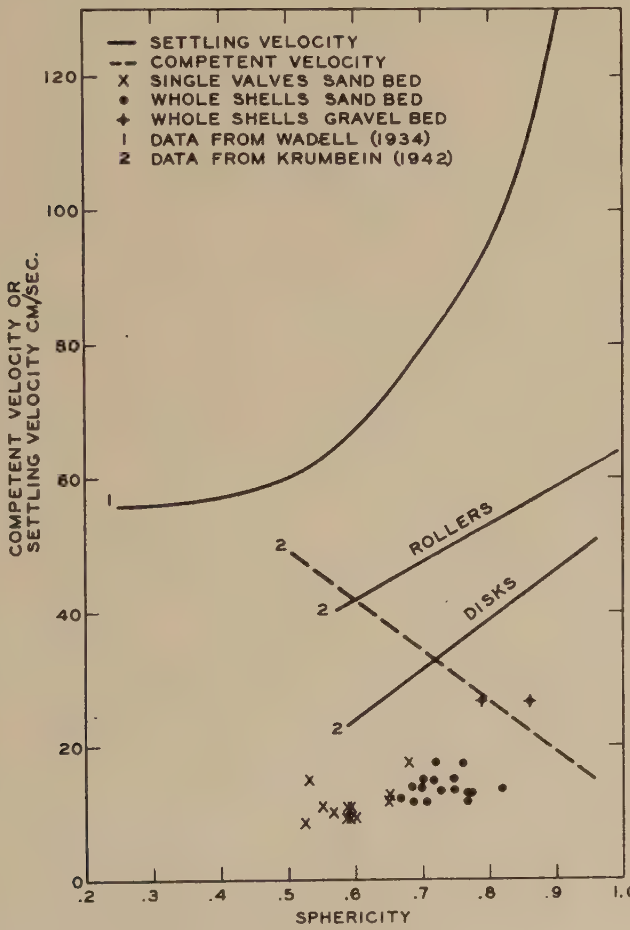

Fig. 2. Effect of sphericity upon the competent velocity and settling velocity of various kinds of particles.

---

[3] Computed by W. Peddle.

coefficient refers only to its algebraic sign. It is not an indication of certainty. Interpretation two gives a low positive correlation of 0.603 for whole shells.[4] Interpretation three gives a low positive correlation of 0.588. Interpretation four gives a positive correlation coefficient of 0.069 for whole shells, indicating no correlation; for all single valves together it gives a low positive correlation of 0.495; for single valves of one species, *Terebratulina septentrionalis*, it gives a positive correlation of 0.659. Thus almost all of the interpretations suggest that the competent velocity of a terebratuloid brachiopod shell depends on the sphericity of the shell; but part of the fourth interpretation indicates no such dependence for the limited number (16) of observations of the movement of whole shells included in the interpretation.

Sphericity is related to shape insofar as the hydraulic behavior of these shells is concerned, but the relation is only approximate. Hence two shells with the same weight, size and sphericity may have different competent velocities because of the shape effect which is not included in the sphericity. This unmeasured shape effect may account for some of the scattering of points in the graphs relating sphericity and competent velocity. Scattering may also be due to the action of turbulent eddies which cause the instantaneous velocity around a shell to vary from the mean velocity.

The present tests with terebratuloid brachiopod shells resting on a substratum of sand indicate that the more spherical shells require a faster current to put them in motion. This qualitative relation between sphericity and competent velocity is diametrically opposed to a relation observed by Krumbein (1942). Krumbein molded a number of artificial pebbles which had about the same weight and nominal diameter but different sphericities. He placed these pebbles in a flume and then observed the velocity required to initiate motion as well as the relative velocity of the current and the pebbles once they began to move. The competent velocities were not published; however, in a letter to Menard in 1949, Dr. Krumbein was kind enough to state that the competent velocity for spheres averaged 14.5 cm./sec., and that for pebbles with a sphericity of about 0.5 the competent velocity averaged 42.2 cm./sec. Thus the velocity required to initiate motion appeared to vary inversely

[4] Computed by W. Peddle.

with the sphericity. Computations by the present writers using Krumbein's published data on critical Froude numbers yield the competence-sphericity relation shown in figure 2.

On the other hand, Krumbein (1942) also measured the settling velocity of the artificial pebbles, and his figure 4 (p. 627) shows that the settling velocity varies directly with the sphericity. Wadell (1934) had noted a similar relation between settling velocity and sphericity. Both Krumbein's and Wadell's data are plotted in figure 2. The settling velocity of particles larger than a few millimeters in diameter is directly proportional to the competent velocity (Hjulstrom, 1935; Menard, 1949). Consequently, with regard to the relation between competent velocity and sphericity, Krumbein's tests with settling velocities agree with the flume tests of the present writers.

The contradictions in observations of the competence-sphericity relation of particles in flumes may be more apparent than real. A particle is put in motion in a flume if the propelling

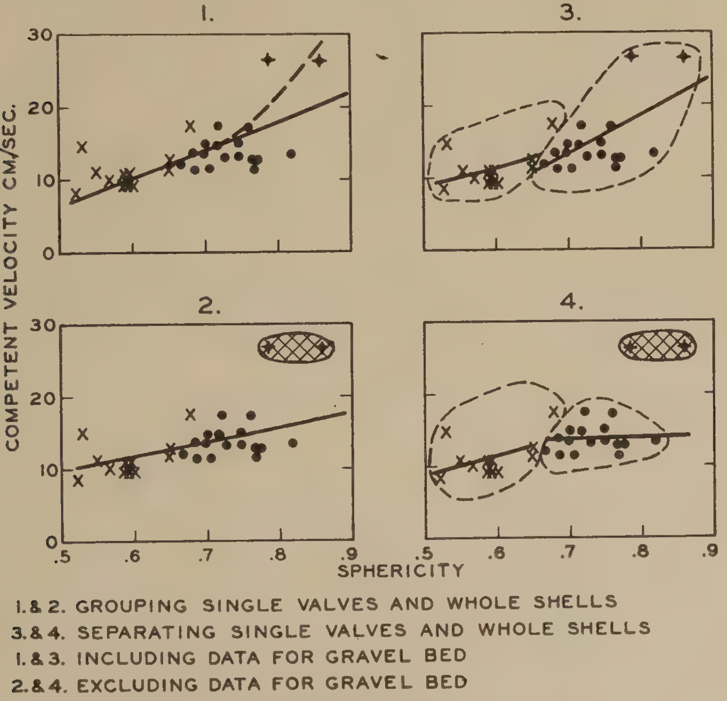

Fig. 3. Possible interpretations of the effect of sphericity upon the competent velocity of terebratuloid brachiopod shells.

force due to moving water exceeds the retarding force due to friction between the particle and the adjacent particles of the bed. Particle shape may have some influence on the effectiveness of both the propelling and the retarding forces. Tentatively, the present writers believe that the differences in the observed influence of sphericity on competence may be ascribed to the differences in the effective density of the particles in the two experiments. The effective density of the shells is less than one-fifth of the effective density of Krumbein's synthetic pebbles. The shape of the shells may have more influence on the effectiveness of the drag due to the moving water than on the effectiveness of the friction between the shells and the sand bed. As a result the relation between sphericity and competence of shells in a flume corresponds to the relation between sphericity and settling velocity (in which there is no friction with adjacent particles). With denser particles, however, the proportion of the grain surface exposed to moving water is much smaller compared to the surface in contact with other particles. Therefore, the influence of particle shape on the effectiveness of the retarding force due to friction between grains may be more pronounced than the influence on the effectiveness of the propelling force due to moving water. If so, the relation between sphericity and competence of solid particles in flumes would depend on the relation between sphericity and friction between grains, and could be just the opposite of the relation between sphericity and the settling velocity of the particles. Granting the validity of both sets of apparently contradictory observations, the fluid velocity required to move shells probably varies directly with the sphericity, but the fluid velocity required to move most solid detritus (density about 2.7 grams per cc.) probably varies inversely with the sphericity.

Although the conclusion is speculative, some field observations also suggest that the velocity required to move shells varies directly with the sphericity. DuBois (1916) found that individuals of *Terebratalia obsoleta* (Sowerby) taken from Puget Sound varied in shape according to the degree of movement of the waters in which they lived. The more spherical shells were developed in the fastest currents. As the variation in shape represents an adaptation to differences in current velocity, the more spherical forms must be those which are best adapted to live where the currents are faster. The shape may be related to some secondary characteristic of fast currents—such as an increased oxygen or food supply—but if the adaptation of shape is necessary in order to counterbalance the velocity of the water, a more spherical shape must be the one which is least affected by moving water. Therefore, the velocity necessary to initiate motion appears to vary directly with the sphericity.

ORNAMENTATION

The effect of variations in ornamentation upon the movement of shells can not be evaluated from the present tests because all the shells are relatively smooth. Variations in ornamentation, however, are variations in shape, so it is apparent that they influence the relative ease with which a shell may be put in motion.

HYDRAULIC FACTORS

The initial movement of a shell on the sandy bed of a watercourse is influenced not only by the characteristics of the sand and shell but also by the flow characteristics of the running water. Friction retards the layer of water next to the bottom and sides of the channel so that the velocity of the water on a sand bed may be only a fraction of the mean velocity of the current. However, the retarded or "boundary" layer rarely is more than a millimeter thick; all but the smallest shells protrude through it and are exposed to the force of the current. Medium and fine sand grains, however, usually lie within the boundary layer and thus may remain undisturbed on a stream bed although shells which are larger and heavier are in motion.

The measured effective densities of terebratuloid brachiopods are so small that the initial motion of any particular shell probably is influenced by the degree of turbulence of the moving water. Hjulstrom (1935) has shown that all natural watercourses are characterized by turbulent, eddying motion. The eddies may move in any direction relative to the general motion of the water, with the result that at any instant some parcels of water move faster than the average and some move slower. Due to the entirely random motion in a turbulent fluid, a comparatively rapidly moving eddy may strike a large shell and put it in motion although a smaller shell only a few centimeters away remains fixed in position because the force of the water in that place is much smaller. The analogous effect of turbulence in air may be observed when a gust of wind swirls a patch of dust upward while the surrounding dust remains in place, or when a "cats-paw" ripples a water surface in some spots but leaves the remainder smooth. These commonplace phenomena indicate how turbulence may cause the larger of two shells of the same species to be moved instead of the smaller.

The quantitative importance of the turbulent eddies with regard to initiating motion in whole shells depends on the comparative velocity of the eddies and the current as a whole. This relation has been the subject of a great deal of study by hydraulic engineers, and it is known that the importance of the eddies increases with the cross-sectional area of the current if all other things are equal. In a small stream, for example, the eddy velocity might be only a fraction of the current velocity, but in a large slow current on a continental shelf the eddies might flow several times as fast as the average current velocity.

Perhaps the most significant conclusion to be derived from this analysis is that some terebratuloid brachiopod shells may be moved so readily that they are capable of being transported by the low current velocities now found on the continental shelves and slopes. All sizes of *Terebratulina septentrionalis* tested were moved by currents with velocities of 11.7 to 15.1 cm./sec.; Shepard (1948) has recorded bottom velocities of 36.7 cm./sec. in 160 fathoms on the California continental borderland, and 14.6 cm./sec. in 1050 fathoms in the Santa Cruz basin. These velocities were measured in the open ocean where tidal effects were negligible. However, in bays and estuaries where the tidal range is large, current velocities commonly are several times as great.

WHOLE SHELLS WHICH ARE MORE DIFFICULT TO MOVE THAN THE UNDERLYING SAND

Flume tests with individuals of *Terebratalia transversa* show that the transportation of shells may depend on a critical relation between the competent velocity of the shells and of the sand in the bed. The smallest of five individuals resting on a bed of monodisperse sand grains with a median diameter of 0.36 mm., was moved by a velocity of 15.0 cm./sec. At the same time the sand was scoured from around the remaining four larger shells. A faster current caused the whole surface of the bed to move although the shells remained fixed. They then began to settle into holes in the sand which were produced by the scour around them. This sequence of events is depicted in figure 4. Similar scour around pebbles was noted in earlier experiments in the flume, and fossil scour marks have been observed by Peabody (1947) in the Moencopi formation of the Grand Canyon area. If a current moves the subjacent sand instead of a shell the shell may become buried. However, this burial may depend on whether the sand is being eroded or

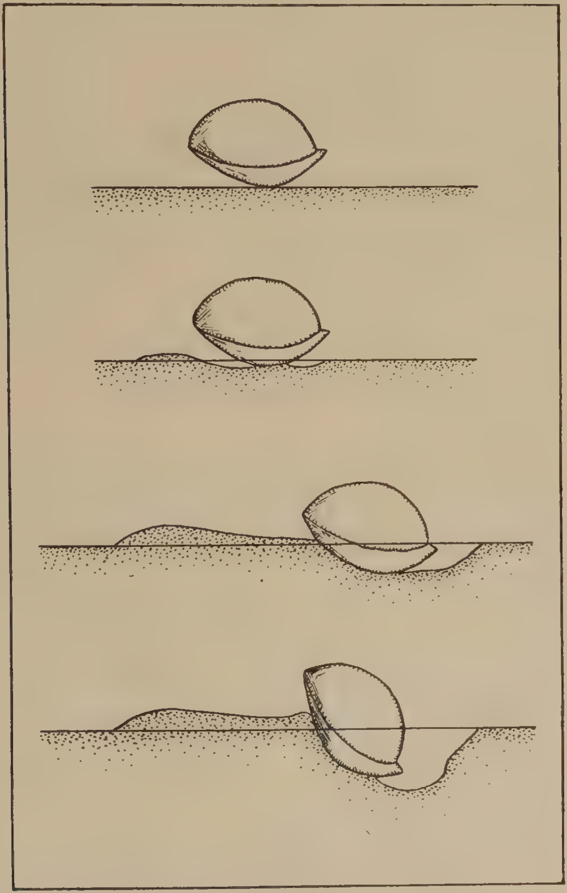

Fig. 4. A terebratuloid brachiopod (*Terebratulina septentrionalis*) being buried in sand because of scour by moving water. Four stages in the burial, of which the first is uppermost, are depicted in cross sections parallel to the direction of flow. In all the stages the water is moving from right to left, and at a constant velocity.

deposited; if erosion prevails, the shell remains exposed, whereas if deposition prevails, it is covered.

It follows that the size of the grains in the bed may determine whether a shell is moved by water with a given current velocity. A current which could move a shell on a bed of coarse sand might cause it to be buried in a finer sand, because the latter would be scoured from around the shell.

The effect of the size of particles in a substratum is shown by the tests with shells number 31 and 39. If these shells were resting on medium sand, they began to be buried when the current velocity was less than 20 cm./sec. and they did not move even when the velocity was increased to the maximum that the flume could produce—about 35 cm./sec. On the other hand, both shells were put in motion by a current with a velocity of 26.8 cm./sec. if they were resting on a substratum of gravel.

In order to establish whether an assemblage of fossil shells can have been transported over a bed of the sand in which it is enclosed, it is necessary to know the competent velocity required to move both the sand and the shells. The competent velocity for any size of sand is known within certain limits (Hjulstrom, 1935), but the velocity required to move any particular shell can be found only by the type of experiment reported in this paper.

SINGLE VALVES

Five pedicle valves of *Terebratulina septentrionalis*, weighing 0.055 to 0.407 gm. and oriented concave upward, were tested simultaneously. All were moved small distances by a current with a velocity of only 11.1 cm./sec. In other tests these shells were oriented convex upward, in which position one valve weighing 0.115 gm. was moved by a current of 11.1 cm./sec., and the other valves were moved small distances by a current with a velocity of 14.9 cm./sec.

Another series of tests featured the six brachial valves of the same species. These valves weighed 0.042 to 0.257 gms. Their behavior at several current velocities is shown in table 2. If the current velocity was increased to more than 14.4 cm./sec. the sand bed began to move and ripples were formed. The valves (convex upward) continued to be fixed in position until a sand ripple moved past. Each then was turned over and moved into the trough behind the ripple; it remained in the trough as the ripple slowly moved downstream.

MOVEMENT OF SHELLS

Most of the whole hinged shells moved over the sand bed by rolling with their longest dimension perpendicular to the current; however, others slid or rolled end over end. At higher current velocities almost all of these latter shells would probably roll with their longest dimension perpendicular to the current, because this position affords the least resistance to movement. Most of the sliding shells maintained a constant orientation relative to the current, but the individuals usually had different orientations. Both sliding and rolling were episodic; a shell slid a few centimeters in a few seconds, then remained fixed for several minutes, and slid or rolled again. The episodic nature of the movement may have been due to the intermittent action of eddies which locally increased the mean velocity enough to initiate movement, but soon dissipated and no longer moved the shell.

The *Terebratulina* shells moving over an immobile sand bed came to rest at random orientations relative to the direction in which the current was moving. In a fossil state these shells would give no clue to the direction of the water movement at

TABLE 2

Movement of Brachial Valves of *Terebratulina septentrionalis*
(Initial Orientation Concave Upward)

No.	Weight (gms.)	Behavior At Current Velocity (cm./sec.)				
		8.6	9.4	10.6	11.6	14.4
18	0.257				Turned over	
17	0.217		Slid 2 cm.	Turned over		
19	0.135		Slid 10 cm.	Turned over		
20	0.112			Turned over		Rolled and slid 2 cm.
21	0.102	Twisted 5°	Slid 20 cm.	Rolled 20 cm. end over end, concave upward	Moved out of flume	Moved out of flume
22	0.042	Slid several cm.	Slid 10 cm. and turned over	Slid 30 cm.	Moved out of flume	Moved out of flume

the time they were deposited. What is more significant to paleoecology is that a small number of shells may have a chance parallel orientation, but that there may be any relation between the shell orientation and the current direction.

Single brachiopod valves moved both by sliding and by turning over so that they were alternately convex upward and downward. It was noticed that the single valves which became buried always did so in a convex-upward attitude, this position seemingly being most stable in the flume. According to the evidence of these tests, however, there is no reason to believe that orientation in sedimentary rocks can be demonstrated by the direction of convexity of a small number of valves, because a sudden stilling of the flow in the flume would have found some valves convex upward and others downward. The sequence of sedimentary rocks may be strongly suggested by consistent orientation of the direction of convexity of a considerable group of brachiopod valves (Shrock, 1948), but the possibility of error increases as the number of valves diminishes.

SUMMARY

1. Some terebratuloid brachiopods are moved by currents in a flume which are moving no faster than natural currents found at a depth of more than 1000 fathoms in the Pacific Ocean.
2. The very low effective density of a shell and its enclosed water permit it to be moved by running water even though it weighs hundreds of times as much as any one of the motionless grains of sand over which it is rolled.
3. The velocity required to initiate the motion of a shell depends on the sphericity (shape) of the shell as well as on the size and weight. The smaller the effective density, the more important the shape.
4. Shells which are more difficult to move than the subjacent sand settle into scours which are formed in the sand around them.
5. The movement of a shell is a function of both current velocity and size of the subjacent sand grains. The same current moves a shell on one stream bed but not on another, depending upon the sand size.
6. The orientation of a small number of movable shells is essentially random in relation to current direction.

REFERENCES

DuBois, H. M., 1916. Variation induced in brachiopods by environmental conditions: Puget Sound Marine Sta. Pub., vol. 1, pp. 177-183.

Hjulstrom, F., 1935. Studies of the morphological activity of rivers as illustrated by the River Fyris: Upsala Univ., Geol. Inst., Bull., vol. 25, pp. 221-525.

Krumbein, W. C., 1941. Measurements and geological significance of shape and roundness of sedimentary particles: Jour. Sedimentary Petrology, vol. 11, pp. 64-72.

————, 1942. Settling-velocity and flume-behavior of non-spherical particles: Am. Geophys. Union Trans., pp. 621-632.

Peabody, F. E., 1947. Current crescents in the Triassic Moencopi formation; Jour. Sed. Pet., vol. 17, pp. 73-76.

Menard, H. W., 1949. Transportation of bed-load by running water, (Unpublished Ph.D. thesis, copy on file Div. Geol. Sci., Harvard Univ., 82 pp.).

Rouse, H., 1938. Fluid mechanics for hydraulic engineers, McGraw-Hill Book Company, New York.

Shepard, F. P., 1948. Submarine geology, Harper and Bros., New York.

Shrock, R. R., 1948. Sequence in layered rocks, McGraw-Hill Book Company, New York.

Wadell, H., 1932. Volume, shape, and roundness of rock particles: Jour. Geology, vol. 40, pp. 443-451.

————, 1934. The coefficient of resistance as a function of Reynolds number for solids of various shapes: Jour. Franklin Inst., vol. 217, pp. 459-490.

U. S. NAVY ELECTRONICS LABORATORY
SAN DIEGO, CALIFORNIA

HARVARD UNIVERSITY
CAMBRIDGE, MASSACHUSETTS

Contribution No. 548

Särtryck ur Tellus, vol. 3, nr 1, 1951

Some Results of a Multiple Ship Survey of the Gulf Stream*

By F. C. FUGLISTER and L. V. WORTHINGTON,
Woods Hole Oceanographic Institution

(Manuscript received 18 December, 1950)

Introduction

The first multiple ship survey of the Gulf Stream Area between Cape Hatteras and the Grand Banks of Newfoundland took place during the period from the 6th to the 23rd of June 1950. The survey was given the code name "Operation Cabot" by the U. S. Navy Hydrographic Office which acted as headquarters during the planning and operational phases of the survey. The civilian scientist in charge of the technical phases of the program was Dr Richard H. Fleming, Director, Division of Oceanography, U. S. Navy Hydrographic Office.

The purpose of Operation Cabot were:

(a) To obtain a synoptic plot of the Gulf Stream's path between Cape Hatteras and the Grand Banks;
(b) to determine the rate of change in the position of the Gulf Stream;
(c) to measure the surface velocities of the Gulf Stream;
(d) to observe what effect the Gulf Stream has on the conditions in the lower atmosphere;
(e) to observe the formation and some of the history of the eddies presumably formed when a larger "meander" or "wave" in the Gulf Stream is cut off;
(f) to obtain observations of the Gulf Stream from a plane and from ships simultaneously.

The following groups took part in the survey.

U. S. Navy Hydrographic Office, Washington, D. C.
U. S. S. SAN PABLO (AGS-30); Captain, A. J. Peterson Comdr. USN.; Scientist in Charge, Dr R. H. Fleming. This vessel acted as flagship for the fleet and Dr Fleming was task unit chief scientist.
U. S. S. REHOBOTH (AGS-50); Captain, R. V. R. Basset, Jr, Comdr. USN; Scientist in Charge, Robert Abel. Two PB4Y-2 Aircraft; Pilots Ensign F. M. Glazier, USNR and Lt J. G. Stewart, USNR; Scientific Observer, W. V. Kielhorn.

Naval Research Establishment, Halifax, Nova Scotia.
H.M.C.S. NEW LISKEARD; Captain, Lt W. W. Maccoll, R.C.N.; Scientist in Charge, Dr William L. Ford.

U. S. Fish and Wildlife Service, Washington, D. C.
ALBATROSS III; Captain, John Collins; Scientist in Charge, V. B. Colton.

Woods Hole Oceanographic Institution, Woods Hole, Mass.
R/V ATLANTIS; Captain, Adrian Lane; Scientist in Charge, Martin Pollak.
R/V CARYN; Captain, John Pike; Scientist in Charge, Dr B. H. Ketchum.

---

* Contribution No 548 from the Woods Hole Oceanographic Institution.

This research was sponsored by the Office of Naval Research under contract N6 onr—277, T. o. 1.

Atlantic Oceanographic Group, St. Andrews, New Brunswick.

The original plans called for the participation of the CNAV WHITETHROAT. Because of last minute difficulties the WHITETHROAT was unable to join in the survey. Dr H. B. HACHEY and Dr L. M. LAUZIER of the organization helped to plan the operation and Dr LAUZIER was on the scientific staff aboard the NEW LISKEARD.

Scripps Institution of Oceanography, La Jolla, Calif.

Dr WALTER MUNK of this organization helped plan the operation and was on the Scientific Staff of the flagship.

U. S. Navy Office of Naval Research, Washington, D. C.

Lt Comdr. R. L. DAHLOFF and J. K. KNAUSS of this organization helped plan the operation. Lt Comdr. DAHLOFF was chief meteorologist of the task unit.

Although not an integral part of Operation Cabot the work done by the U. S. Coast Guard Research Vessel EVERGREEN, while on routine Ice Patrol for the International Ice Patrol, contributed valuable data. Dr FLOYD SOULE was Scientist in Charge on the EVERGREEN.

Operation Cabot was a splendid example of cooperative effort and credit for the success of the survey must be distributed among all the many scientists and seamen who took part.

Operational plans

The planners of Operation Cabot were faced with a new type of oceanographic investigation. Not only were six ships and a plane involved but new instruments for obtaining data with ships underway were to be used. A very large amount of data was to be collected and, although much of it would be collected automatically by seamen technicians, the scientific staffs would be kept busy supervising and evaluating the results.

Oceanographic surveys have traditionally been made according to a pre-arranged plan, and in an area such as the one under consideration, the measurements have been planned along "sections" or at points on a "grid". Recent surveys of the Gulf Stream (ISELIN and FUGLISTER, 1948) have indicated that such a method is inherently wasteful of time and effort where answers to specific questions are sought, because many stations do not provide pertinent information. Nevertheless, detailed plans and instructions were formulated for Operation Cabot. This was done primarily because it was felt that without such prearranged plans the success of the survey would be entirely dependent on successful communications. Considering the variety of ships and equipment involved dependable communications were by no means certain. Also the planners realized that if communications were successful the flagship could alter the plans during the operation as might be desirable.

Briefly the plans for the survey were as follows. The first phase was to be a general reconnoitering of the Gulf Stream from Cape Hatteras to the Grand Banks. The ships would be deployed approximately 150 miles apart along the Gulf Stream, zig-zagging into and out of the current and underway continuously. Bathythermograph, Loran, and weather data were to be obtained at half-hour intervals. Surface current measurements were to be made every hour with the Geomagnetic Electrokinetograph (VON ARX 1950), hereafter referred to as the GEK. Positions of the Stream were to be transmitted every six hours to the flagship.

The second phase was to consist of simultaneous "sections" of hydrographic stations along prearranged meridians of longitude. Bathythermograph, Loran, and weather observations were also to be made along the "sections".

Phase three was to be a detailed study of a restricted area determined by the results of the first two phases.

Throughout the operation continuous sonic depth records were to be made, and a track chart maintained with the depth records referenced to the track chart by hourly markings.

Fortunately communications were very nearly perfect during the entire operation. The first phase of the operation went off as scheduled and the scientific staff aboard the flagship was able to plot the position of the Gulf Stream from off Cape Hatteras to 50° west longitude. For the remainder of the Operation the flagship directed the movements of all vessels and the pre-arranged plans were in a large part discarded.

An enormous amount of data were collected during the 17 days of the survey and the present paper will cover only a portion of the results.

Definition of terms

Early in the planning and operational stages of Operation Cabot it became evident that precise definitions were needed for the various terms used in association with the Gulf Stream. The frequent references to the "cold wall", "edge of the Stream", "warm core" and "front" led to a certain amount of confusion and misunderstanding. The term "inner edge" was most frequently used and most variously interpreted. This confusion is caused primarily because, although the words "Gulf Stream" denote a current, they also imply a distinct water mass and secondarily because water masses that may be motionless are included as part of the Stream because they lie below a surface current.

Since the Gulf Stream is a boundary or front in the western North Atlantic between the slope water and the Sargasso Sea we may define it as follows; it is a *continuous* band stretching from the continental shelf off Cape Hatteras to the 50th meridian of longitude, south of the Grand Banks of Newfoundland. This band consists of a pronounced pressure gradient between the warm highly saline water to the south and the colder fresher water to the north. Using this definition then, the inner and outer limits or edges of the Gulf Stream can be defined as the points where this pressure gradient becomes zero. These points can be located only if deep, closely spaced temperature and salinity data are obtained and the cross current pressure gradients calculated. Also, because of the large eddies found both north and south of the Stream, any section made across the area must be long enough to ascertain whether or not more than one pronounced pressure gradient exists. If only one is found it defines the Gulf Stream, but if more than one are located then the position of the Stream cannot be determined by that single section.

Not to be confused with the inner or left hand edge of the Stream is the temperature-salinity boundary at the surface. This generally abrupt change that occurs to the left of the "warm core" may or may not coincide with the left hand edge of the Gulf Stream as defined above. This applies also to the color boundary and the long thick lines of Sargassum frequently seen on the surface; all of these surface phenomena are apparently associated with shear zones to the left of the "warm core" but they are not necessarily coincident with the left hand or inner edge of the Gulf Stream.

The "warm core" is defined here as that part of the Gulf Stream containing water warmer than the water at the same depth to the right, facing down stream, of the current. This "warm core" is generally 300 to 400 meters deep with the maximum temperature anomalies at a depth of about 100 meters.

The word "front" is considered synonymous with the pronounced pressure gradient and therefore with the Gulf Stream itself.

The term "cold wall" dates back to 1845 and is still frequently used to denote the "inner edge of the Stream" or, according to CHURCH (1937), "the temperature gradient between the slope water and the Gulf Stream". According to these definitions it could equally well be called the "warm wall" though in neither case do we have anything resembling a wall. This temperature gradient exists at different depths across the entire width of the Gulf Stream and therefore cannot be considered as something separate or adjoining the Stream. Because of the misleading connotations of the term "cold wall" it will not be used in this paper.

Synoptic charts

On this survey no attempt was made to locate, precisely, the inner and outer edges of the Gulf Stream. The area covered is shown in fig. 1. It is obvious that to obtain closely spaced, deep hydrographic stations over this large area, in the limited time available, was impossible even with six ships. However a study of recent surveys show that the limits of the Stream can be determined with a fair degree of accuracy from the temperature structure in the upper 200 meter layer. A temperature-depth profile across the Stream shows the following characteristics; facing down stream the left hand edge of the Stream coincides with the point where the temperature at 200 meters reaches a minimum or levels off.

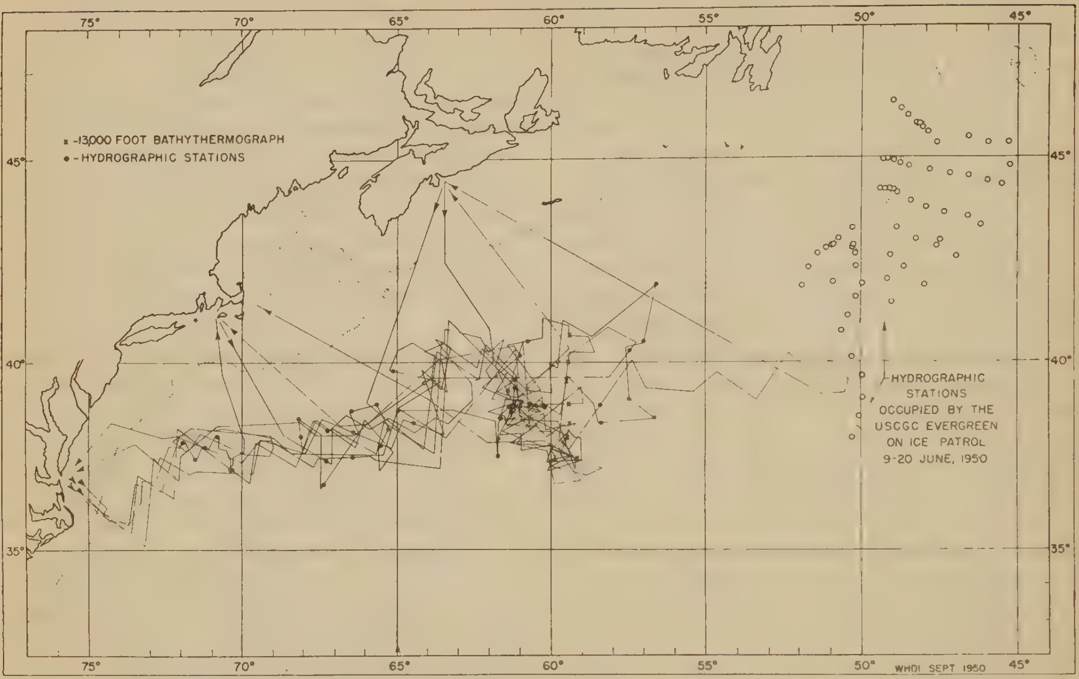
75°
70°
65°
60°
55°
50°
45°
x -13,000 FOOT BATHYTHERMOGRAPH
● -HYDROGRAPHIC STATIONS
45°
40°
35°
HYDROGRAPHIC STATIONS OCCUPIED BY THE USCGC EVERGREEN ON ICE PATROL 9-20 JUNE, 1950
WHOI SEPT 1950

Fig. 1. All ships' tracks on Operation Cabot, 6th to 23rd of June 1950.

The abrupt temperature boundary at the surface may or may not be directly over this point. To the right the isotherms slope downward until the "axis of the warm core" is reached. This is the point where the mean temperature of the upper 200 meter layer is a maximum. Actually the "warm core" reaches to depths of 300 to 400 meters, but since the maximum anomalies are found at about 100 meters, it has proven convenient to use the mean of the upper 200 meter layer to show the position of this core. To the right of the "warm core" the isotherms in the surface layer rise until the temperature at a depth of 200 meters is again a minimum or levels off. This point is taken as the right hand or outer edge of the Stream. The horizontal temperature and salinity gradients at all levels are quite gradual on this side of the Stream so that this "edge" is not nearly so well defined as the "inner edge".

In order to obtain synoptic charts of the Gulf Stream the first step was to calculate, for each bathythermogram, the mean temperature of the upper 200 meter layer. 3,521 bathythermograph observations were obtained during this survey and temperatures were read at eight points on 3,000 of these. Since the bathythermograph grids were in the Fahrenheit scale the labor involved in converting to the Centigrade scale was prohibitive. This explains the various scales used in this paper.

The positions and mean temperature (degrees Fahrenheit) of all bathythermograph observations were plotted geographically on daily charts and the results contoured. The mean temperature isotherms for the 8th of June, over the western portion of the Gulf Stream are shown in fig. 2. The solid lines in this figure show the ships' tracks and give an idea of the amount of interpolation that was generally necessary in drawing the curves. In relatively few of the 165 "sections" made was the entire width of the Gulf Stream covered, but in all cases the abrupt gradient to the left of the "warm core" was crossed. The sections that did cross the "warm core" indicate that it did not vary markedly in width throughout its entire length from Cape Hatteras to the 50th meridian. Fig. 3 shows the positions of the "warm core" during the first and last periods of the survey. The most

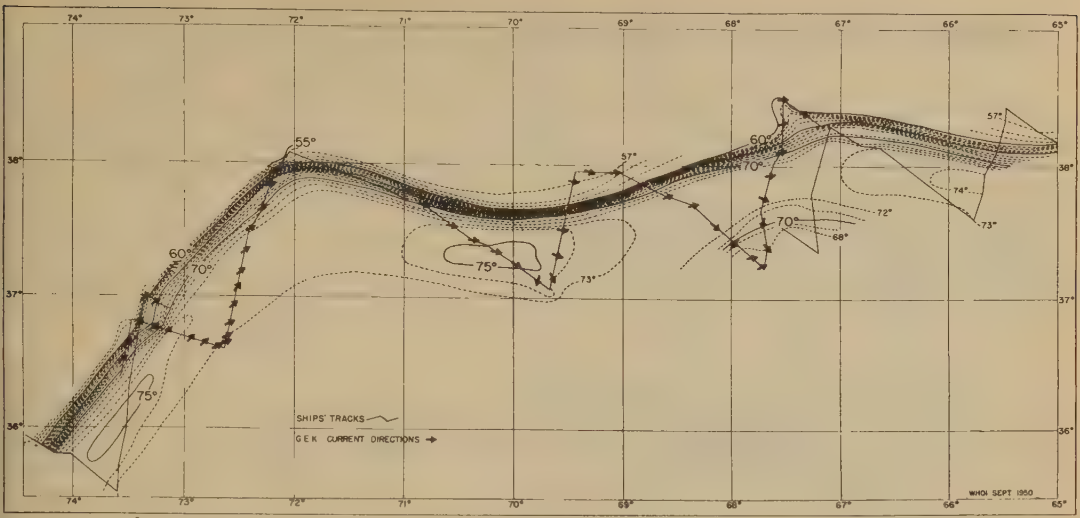

Fig. 2. Mean temperature, °F., in the upper 200 meter layer of the Gulf Stream, on the 8th of June 1950.

striking feature of this chart is, of course, the two large waves and the deep trough separating them in the center of the area. After the 12th of June the chief emphasis of Operation Cabot was to observe the changing conditions in and around this trough. As shown in the figure, the trough eventually "broke off" from the Stream forming, as it did so, an elongated cyclonic eddy to the south.

Although Operation Cabot was the first survey to cover the entire distance from off Cape Hatteras to 50° west longitude, other shorter surveys, show that large waves in the Gulf Stream may occur over a wide range of longitude and that conditions, such as those found on "Cabot" are not exceptional. Fig. 4 is a composite picture, showing the positions of the maximum horizontal temperature gradient at a depth of 100 meters, as obtained on all Gulf Stream surveys made since 1946. Besides the numerous large waves, this diagram shows another elongated, cyclonic eddy centering at 66° west similar to the one found on Operation Cabot.

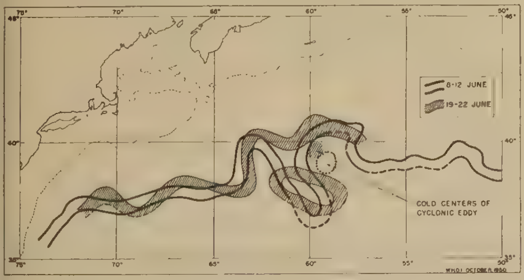

Fig. 3. Positions of the "warm core" of the Gulf Stream during the first and last periods of Operation Cabot.

The variable positions of the major waves in the Stream is stressed here because, during Operation Cabot, there was a strong feeling aboard the flagship that the bottom topography, near 39° north, 61° west, was the primary cause of the deep trough that existed in this area. Further investigation may show that the series of ridges and seamounts in this locality always affect the course of the Gulf Stream, but the occurrence of large waves and eddies in regions where the bottom is relatively flat indicates that bottom topography must be of secondary importance in the formation of such phenomena.

Temperatures of the warm core

Throughout the entire length of the Gulf Stream the mean temperature of the upper 200 meter layer in the warm core was greater than 68° F. An unpublished technical report by FUGLISTER on the monthly average temperatures in the region south of the Stream and north of Bermuda shows the mean temperature for this layer in June to be 67.8° F. Since the Stream moves in an easterly direction for a

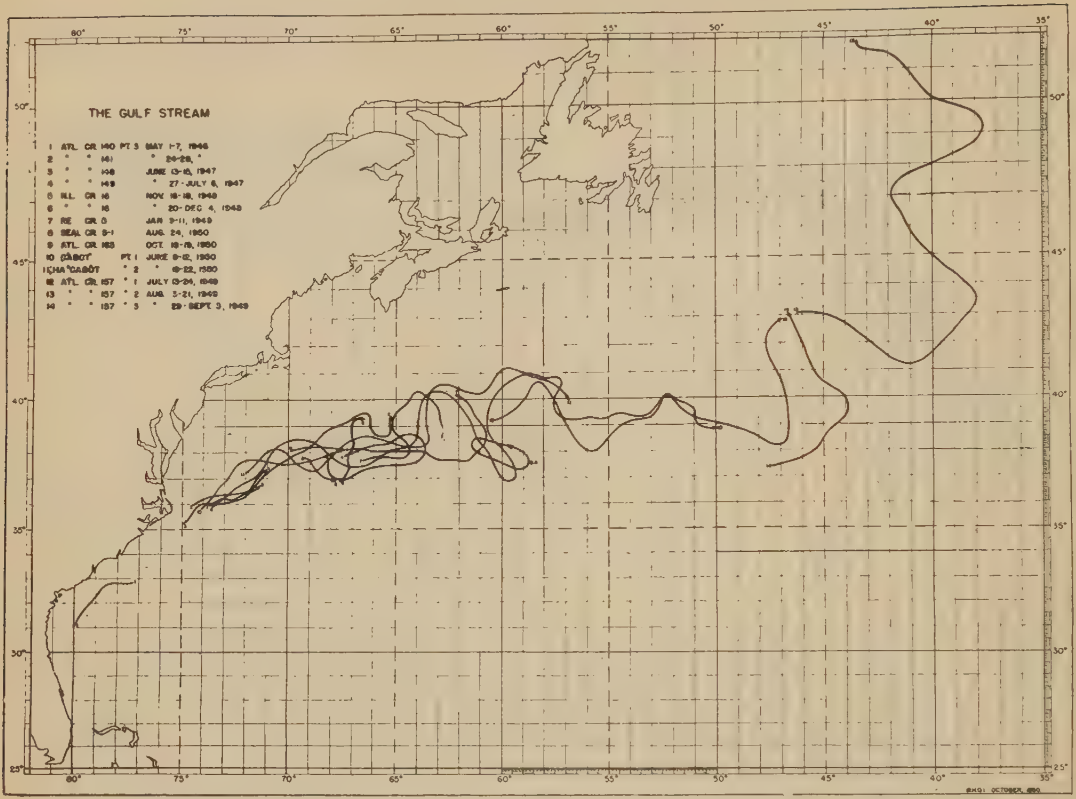
THE GULF STREAM
1 ATL. CR. 140 PT 3 MAY 1-7, 1946
2 " " 141 " 24-28, "
3 " " 148 JUNE 13-16, 1947
4 " " 149 " 27-JULY 6, 1947
5 ALL. CR. 16 NOV. 16-18, 1948
6 " " 16 " 20-DEC. 4, 1948
7 RE CR. 6 JAN. 9-11, 1949
8 SEAL CR. 8-1 AUG. 24, 1950
9 ATL. CR. 163 OCT. 16-19, 1950
10 CABOT PT 1 JUNE 8-12, 1950
11 CHA CABOT " 2 " 18-22, 1950
12 ATL. CR. 157 " 1 JULY 13-24, 1949
13 " " 157 " 2 AUG. 3-21, 1949
14 " " 157 " 3 " 29-SEPT. 3, 1949
80°
75°
70°
65°
60°
55°
50°
45°
40°
35°
50°
45°
40°
35°
30°
25°

Fig. 4. Positions of the maximum cross-current temperature gradients at a depth of 100 meters, from all surveys, 1946 to 1950.

distance of about 1,200 miles it is evident that it must transport over this entire distance water from more southerly latitudes.

The mean temperature at the axis of the "warm core" ranged from 68.3° F. to 75.5° F. As can be seen in fig. 2 these temperatures did not decrease uniformly down stream but what might be called "gobs" of warmer water showed up at intervals along the Stream. These "gobs" were observed as far east as the 57th meridian. The more consistent temperatures on either side of the "warm core" indicate that these "gobs" are not caused by internal wave action. If this is true then these masses of warmer water, appearing at intervals in the Stream, may be evidence of a pulsing action in the current which in turn may have a bearing on the formation of waves and eddies. The pulsing could conceivably be caused by short period variations in the strength of the Trades or in variations in the barometric pressure over the Gulf of Mexico. If a series of temperature sections, say two a day for a period of a month, could be run across the Straits of Florida some of these speculations could be checked. An examination of existing bathythermograph sections in the Florida current between Key West and Cape Canaveral has not revealed any "gobs" but it is not possible, in view of the inadequacy of the data, to conclude that they do not occur there.

Rate of change in the position of the Stream

In the first period of the survey four ships entered the Gulf Stream off Cape Hatteras at 24 hour intervals. During this interval the Stream shifted, at this point, at a rate of 4.5 miles a day toward the southeast. Numerous

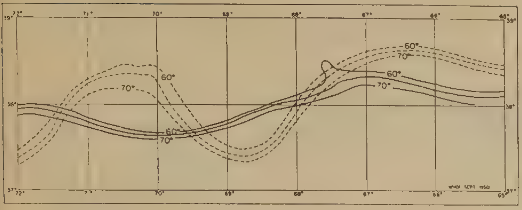

Fig. 5. Positions of the Gulf Stream in the western portion of the survey at the beginning and end of the operation. Mean temperature, °F., of the upper 200 meter layer, for the 8th of June solid lines; for the 21st and 22nd of June dashed lines.

sections made near 72° west showed that the crest of the first wave in the path of the Stream moved toward the east at a rate of approximately 11 miles per day. The overall change in positions of the western portion of the Stream, from the 8th to the 22nd of June, is shown in fig. 5. The daily synoptic charts, of the mean temperature in the upper 200 meter layer, show that all the changing positions of the Stream can be accounted for by lateral movements of not over 11 miles per day. The synoptic charts for the 18th and 19th of June, for the region around the trough (see fig. 6 b), may at first glance indicate a lateral movement more rapid than 11 miles per day if the motion is considered as a north—south one. Actually the water on either side of the trough converged at a rate less than 11 miles per day in cutting off the cyclonic eddy to the south.

Various changes in the Gulf Stream position, are shown in fig. 5, 6 a, and 6 b. Considering the huge volume of the Stream, this shifting of its position by as much as 11 miles per day must produce large vertical motions in the water masses adjacent to the Stream. Although the evidence for these shifts in the Stream is based on observations of the upper 200 meter layer, a sufficient number of deep stations were made during Cabot and other recent Gulf Stream surveys to show that the water at least down to 2,000 meters is affected.

Because of the above measurements it is now possible to evaluate, with more confidence, the results of earlier Gulf Stream surveys made with single ships. The changes in positions of the Stream as found by the Canadian Research Vessel NEW LISKEARD

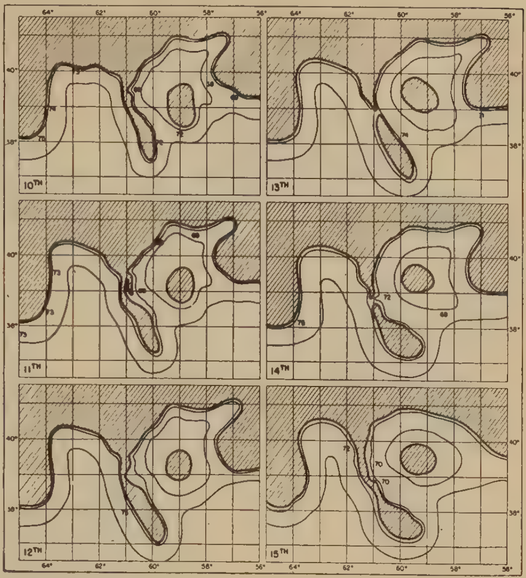

Fig. 6 a. Positions of the Gulf Stream, 10th to 15th June. Shaded areas denote a mean temperature in the upper 200 meter layer of less than 65° F. Thin line is 68° F. isotherm. Small numbers indicate the maximum observed values of the warm core.

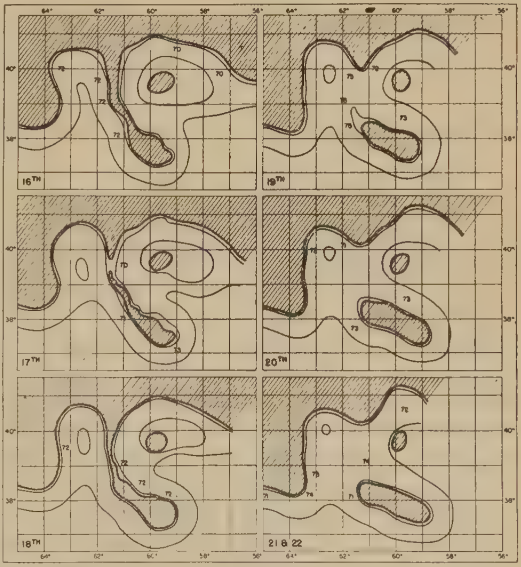

Fig. 6 b. Positions of the Gulf Stream, 16th to 20th June. Shaded areas denote a mean temperature in the upper 200 meter layer of less than 65° F. Thin line is 68° F. isotherm. Small numbers indicate the maximum observed values of the warm core.

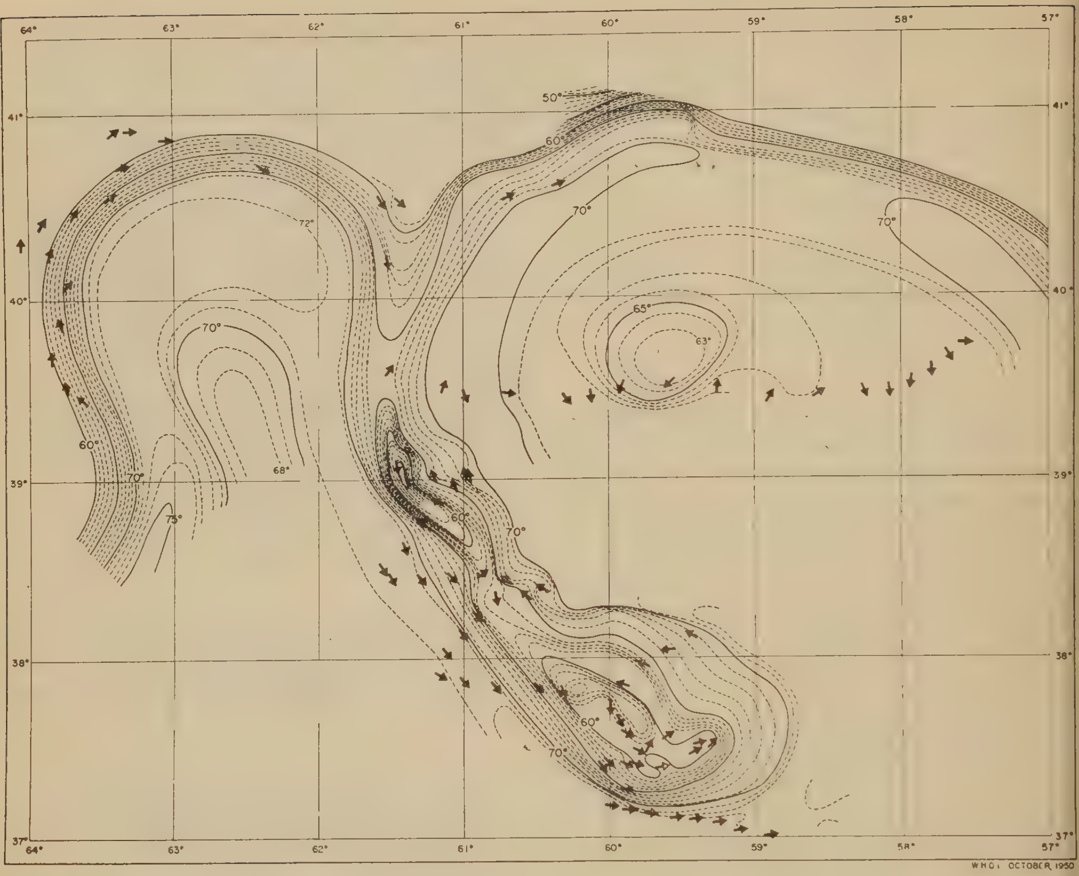

Fig. 7. Mean temperature, °F., in the upper 200 meter layer on the 17th of June. Current directions from the GEK.

in November 1948 and the large eddy, near 66° west longitude, surveyed by the ATLANTIS in June 1947 can be accounted for in detail by lateral shifts of the Stream of the order of 11 miles per day. It is obvious that several ships are required to obtain a synoptic picture of any very extensive portion of the Gulf Stream but, if it does not shift its position at a rate considerably greater than 11 miles per day, a single vessel can still be used to advantage in studying a limited area. In either case, however, the system of using a prearranged "grid" of hydrographic stations must be avoided. To obtain one section of closely spaced, deep stations across the Stream requires about 3 days time; a ship moving at 10 knots could make from 10 to 14 bathythermograph and GEK sections in this time.

Surface currents

Up to this point the positions of the Gulf Stream have been deduced from temperature observations and it has been assumed, first, that the pressure gradients coincide with the temperature gradients, and secondly, that the currents flow along the isobars. One of the most interesting results of Operation Cabot is the evidence that the surface current vectors and the isotherms (showing the mean temperature of the upper 200 meter layer) are parallel where the cross current temperature gradient is sharpest.

As mentioned previously, the mean temperature of the upper 200 meter layer was plotted for each day. This was done without any reference being made to the observed current directions or speeds. At the completion of this work the current vectors, as computed by Mr VON ARX from the GEK data, were superimposed on the isotherms. Examples of the results are shown in figures 2, 7, and 8. To the left of the warm core where the isotherms are most closely spaced it appeared, in nearly all cases, as though the isotherms had been drawn along the current vectors. Current vectors were obtained for 136 out of the 165 sections crossing this temperature gradient and the isotherms and vectors were parallel in 95 % of the cases.

To the right of the warm core the direction of the current as obtained from the GEK data was extremely variable, on many occasions a narrow counter current being indicated. In one region, within the wave east of the deep trough, all sections that crossed the warm core showed a counter current. Actually this current proved to be part of a cyclonic eddy with a cold core similar to, but not as cold as, that found in the larger eddy formed by the deep trough. It has not been determined whether this smaller cyclonic eddy originated as a broken off segment of the Gulf Stream or was simply a counter current that became enclosed or cut off within the large wave to the east of the deep trough.

The current speeds obtained with the GEK are being subjected to a close analysis by Mr VON ARX. He reports that a correction must be applied, in the vicinity of the warm core, where the depth of the current affects the values obtained by his instrument. This correction factor has not been determined. The ship's drift data calculated from Loran observations, in the western half of the area, showed the band of maximum current speed to average between 4 and 5 knots. East of 60° the Loran data were not sufficiently accurate, to justify current calculations by this method. The uncorrected GEK readings showed a falling off of velocities toward the east, the maximum south of the Grand Banks being 85 % of the maximum found near Cape Hatteras. In general the maximum, uncorrected, velocities were found to the left of the axis of the warm core. The maximum shear was also observed to the left of the warm core. The uncorrected readings gave an average shear of $2.5\ 10^{-4}\text{sec}^{-1}$ in the steepest part of the velocity profile.

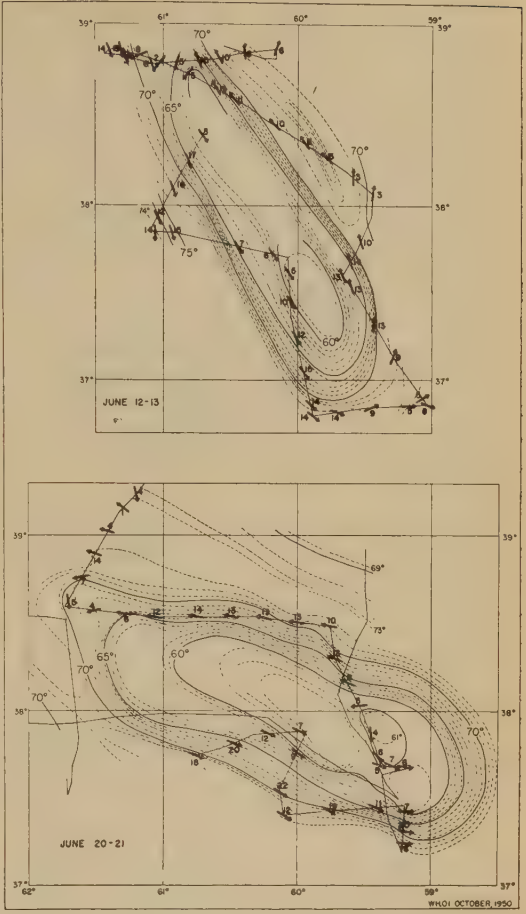

Fig. 8. Temperature and current pattern of "Edgar" during the first and last periods of its observed development. Mean temperature, °F., of the upper 200 meter layer. Current directions from the GEK. Speeds in decimeters per second.

Eddies

For a number of years it has been noted that large cyclonic eddies are frequently encountered south of the Gulf Stream (ISELIN, 1940, ISELIN and FUGLISTER, 1948). In June 1947 the ATLANTIS circumnavigated one of these eddies. Centering at 66° west longitude it extended 200 miles east and west and 60 miles north and south. It was believed that these eddies were formed when a large loop or trough in the Gulf Stream became cut off and separated from the Stream. That this was indeed the case is shown by the observations made on Operation Cabot.

The day by day changes in the Gulf Stream's course in and around the trough at 61° west longitude are shown in fig. 6 a and 6 b. In these figures the water with a mean temperature, in the upper 200 meter layer, of less than 65° F. is indicated by shading. The heavy line is the 65° F. isotherm, the light line the 68° F. isotherm. The light lines are the approximate boundaries of the warm core. The maximum surface currents were observed where these two isotherms (the 65° and 68°) are shown close together, in other words the maximum speeds appeared to the left of the warm core. Details of the temperature and current pattern are shown in fig. 7 and 8.

For how long a period the trough existed before the 10th of June is not known but it is surprising that, considering the narrowness of the "neck", it took nine days for it to break off. During this period the long narrow "neck" was meandering on a relatively small scale and the temperature characteristics in the cold central portion were continuously changing. Since there is comparatively little horizontal flow associated with the cold core these temperature changes must indicate vertical motion. On three occasions temperature profiles across the "neck" indicated that it was about to break off but each time subsequent observations showed the recurrence of colder water in the upper 200 meter layer. The final occlusion in this shallow layer occurred on the 19th of June and on the 20th a deep hydrographic station showed that the break had occurred at all levels.

Even before it broke off, the eddy, which was christened "Edgar" during the cruise, started to turn so that at the end of the survey its major axis was oriented east and west.

The smaller cyclonic eddy northeast of "Edgar" was crossed six times. Details of its size and shape are lacking but there is enough evidence to show that during the period it shrunk in size and moved steadily toward the northwest.

The following questions concerning these eddies were left unanswered by Operation Cabot. Do the eddies once they have broken away from the Stream move, and if so in what direction? How long do they last? Are elongated eddies typical? Do elongated eddies eventually break up into smaller, more nearly circular masses? Is there any preferred point of origin? If it is assumed that the region where "Edgar" was formed is such a "preferred point of origin", because of the ridges and seamounts, then the detached eddies must frequently move in an upstream direction, since they have been found as far west as 73° west longitude. If on the other hand we assume that the detached eddies remain motionless or move down stream then it is even more difficult to explain how an eddy such as "Edgar" could be formed in the relatively confined area near Cape Hatteras or south of it. All the available data show that the Gulf Stream does not start to meander until after it leaves the continental shelf at Hatteras.

An envelope drawn about the curves shown in fig. 4 indicates that it is not until the Stream reaches at least as far east as the 70th meridian that waves large enough to form an eddy could develop. Indeed, such an envelope would make it appear that, if waves of the size of those found on Operation Cabot are necessary to form an eddy, then they do not develop until the Stream reaches close to the longitude where "Edgar" was formed.

These considerations combined with what is known of the bottom topography indicate that the eddies formed by the Gulf Stream originate to the east of 63° west longitude and after being detached move in an upstream direction.

Possible branching of the Gulf Stream

Only two ships operated in the region east of 57° west longitude during this survey. The USCGC EVERGREEN made a bathythermograph and GEK section along the 50th meridian from the Grand Banks south to 38° 30′ north latitude then, returning northward she made a series of hydrographic stations as well as bathythermograph and GEK observations. The HMCS NEW LISKEARD obtained bathythermograph and GEK sections into and out of the Gulf Stream to 50° 20′ west longitude. Both of these tracks are clearly seen in fig. 1.

The current map as calculated aboard the EVERGREEN from the data collected from the 9th to the 20th of June is shown in fig. 9. At about 42° north the EVERGREEN crossed a warm current flowing toward the east. This current was, in every respect, similar to the current that the Ice Patrol finds near this latitude each year. This current is referred to as the North Atlantic current (Soule, 1938). Continuing south the EVERGREEN crossed a minor counter current near 40° north and then at 39° it entered another easterly stream. Three days later the NEW LISKEARD showed that the southernmost current was the Gulf Stream which she had followed continuously from the west.

In August and again in September 1949 the Gulf Stream was located by the ATLANTIS at the 39th parallel south of the Grand Banks. An unpublished chart of the average depth of the 10° C. isotherm in the North Atlantic indicates that the Gulf Stream is south of 40° at this longitude. On the basis of these data and the records of the Ice Patrol it seems evident that at 50° west longitude there are always two easterly currents of major magnitude, one generally located near 41° north the other at about 39° north. According to the definition given for the Gulf Stream it is quite evident that the southernmost current is the Stream. The data from Operation Cabot shows clearly that it forms part of a continuous current reaching from Cape Hatteras to 50° west longitude. What then is the origin of the current to the north and in what way are these two current related? Is the one to the north a band or a branch of the Gulf Stream or is it entirely independent of the Stream?

The temperature-depth profile calculated from the bathythermograph and hydrographic station data collected by the EVERGREEN is shown in fig. 10. The current vectors as obtained by the GEK are plotted across the top of the profile. The deep observations were spaced approximately 30 miles apart while the temperatures down to 250 meters were obtained at 5 mile intervals. The right hand or southern end of the section is a typical temperature profile across the Gulf Stream. The position of the warm core is evident. The narrow weak counter current on the right hand side of the warm core is indicated by the vectors.. The uncorrected current speeds (cm/sec) are shown above the vectors, the maximum speed of 167 cm/sec being to the left of the warm core.

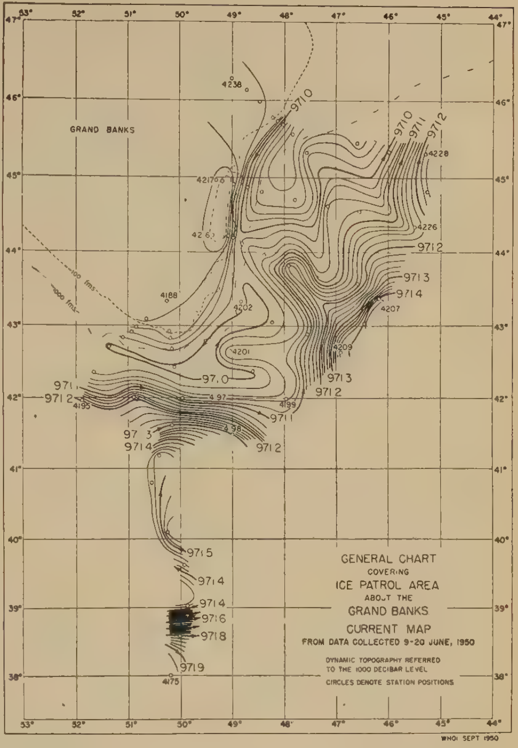
53°
52°
51°
50°
49°
48°
47°
46°
45°
44°
47°
46°
45°
44°
43°
42°
41°
40°
39°
38°
GRAND BANKS
9710
9711
9712
9713
9714
9715
9716
9718
9719
97.0
4238
4228
4226
4207
4209
4201
4202
4188
4195
4175
GENERAL CHART
COVERING
ICE PATROL AREA
ABOUT THE
GRAND BANKS
CURRENT MAP
FROM DATA COLLECTED 9-20 JUNE, 1950
DYNAMIC TOPOGRAPHY REFERRED TO THE 1000 DECIBAR LEVEL
CIRCLES DENOTE STATION POSITIONS
WHOI SEPT 1950

Fig. 9. Current chart obtained from the International Ice Patrol.

The northern end of the profile shows the cold waters of the Labrador current. Between the Gulf Stream and the Labrador current this profile could be interpreted as showing a large anticyclonic eddy that may have been formed originally by a wave in the Gulf Stream breaking off on its northern side. However the Ice Patrol current maps, over a period of years, have indicated that this current near 41° north latitude is of a permanent character and flows generally from the northwest and therefore it cannot be part of an eddy detached from the Gulf Stream.

The other possibility is that the northernmost current is a band or branch of the stream. The authors' interpretation of the data obtained on this survey does not show any such branching of the Gulf Stream although, because of the relative scarcity of observations east of the 58th meridian, it does not preclude the possibility. The most simple interpretation is

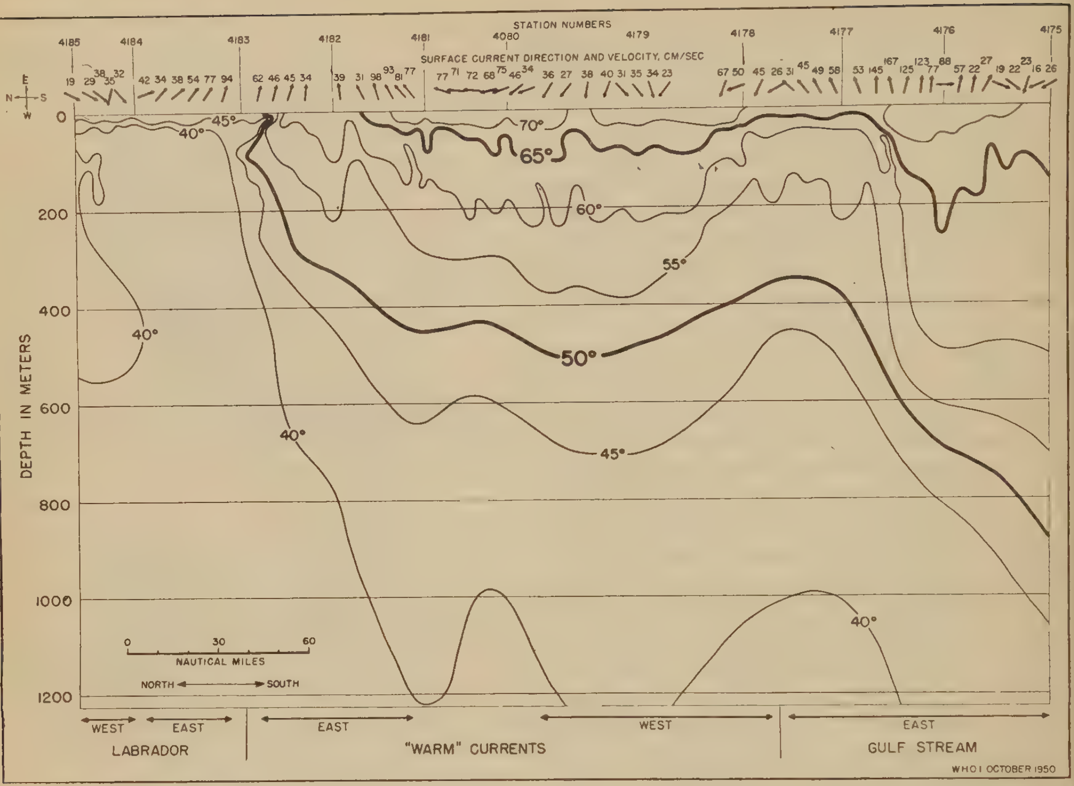

Fig. 10. Temperature, °F., profile from the Grand Banks south on the 50th meridian. Based on combined bathythermograph and hydrographic data. Current directions from GEK and velocities in centimeters per second. See fig. 9 for station positions.

that the northernmost current coincides with the pressure gradient between the slope water and Labrador current water and the two easterly currents at 50° west are independent of each other.

Other observations

The continuous sonic depth records obtained during the survey have been turned over to the U. S. Navy Hydrographic Office to be incorporated in their bottom topography charts. During the cruise the U.S.S. SAN PABLO surveyed two seamounts not shown on the Hydrographic Office charts. The first located at approximately 38° 54′ north and 60° 28′ west had a least depth of 725 fathoms. This was tentatively named San Pablo Seamount. The second at approximately 37° 29′ north and 59° 52′ west was flat-topped with an elongated zone some 8 miles long and 3 miles wide, and less than 700 fathoms. The minimum recorded depth was 675 fathoms. This was tentatively named Cabot Seamount. Both seamounts were explored by running at least three sections across them on different headings. The seamount shown on the charts at approximately 39° 00′ north and 61° 00′ west was found to have depths somewhat less than indicated and that it too was flat-topped at a depth of about 500 fathoms.

Some excellent colored photographs showing shear zones, long thick lines of Sargassum, abrupt changes in wave types, clouds and color changes associated with the Gulf Stream were obtained from the aircraft. The reports of the Stream's positions, based on such visual evidence, were generally in close agreement with shipboard observations. The abrupt changes in the appearance of the sea rface did not however always coincide with e inner edge of the Gulf Stream as defined this paper. Although dye marker experients carried out by the plane showed clearly at the visual boundary was both a velocity iscontinuity and a line of convergence, e ships' observations showed that there ay be more than one such surface boundary, one of which necessarily coincide with the ner edge of the Stream.

Near 41° 00′ north 63° 00′ west, while ollowing a long dense line of Sargassum, the lane encountered the U.S.S. SAN PABLO s it was crossing from south to north through e line of weed. The temperature-depth rofile as obtained by the ship on this section shown in fig. 11. The line of Sargassum dicated convergence at the sea surface. isual observations of the ship's wake and EK data showed that there was an abrupt hange in velocity at this line but both the mperature profile and the GEK showed at the ship was still in the current after it ad passed to the north side of the weed. Fig. 11 ows that the line of Sargassum was about miles from the abrupt temperature change t the surface and about 20 miles from the inner edge" of the Gulf Stream as defined y the pressure gradient.

Color differences associated with the Gulf tream were apparent to the plane only in the esternmost area, west of 71° west longitude. ast of this point lines of weed, differences in ave type, and formations of "typical" Gulf tream cumulus clouds had to be depended pon to locate the Stream. Neither the cumulus louds nor the weed were always present and e wave patterns, of course, depended on the ind velocities and were most pronounced ith moderate winds blowing against the urrent. In general, visual observations failed identify the Stream east of the 65th me- idian.

The authors hope that Mr Kielhorn, the bserver on the plane, or the Hydrographic ffice will publish a complete report on the ircraft participation in Operation Cabot eproducing some of the excellent photographs btained.

The large amount of weather data collected y the planes and ships during the survey have ot as yet been studied. These data, the sea rface temperature data and more details of the surface current data will form the basis of future reports.

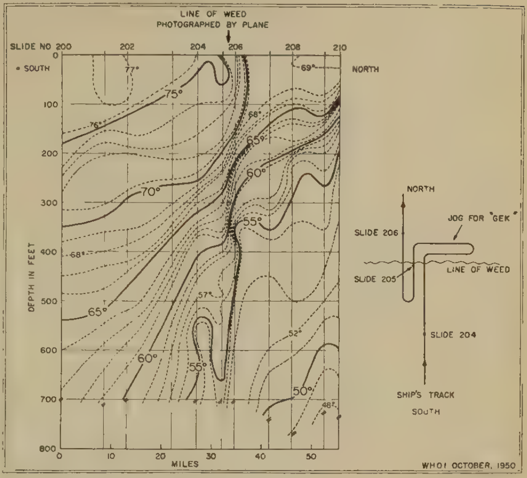

Fig. 11. Temperature profile across the Gulf Stream, 10th of June 1950.

Summary

Operation Cabot, the first oceanographic survey of its kind to date was successful mainly because:

(a) Communications were maintained between all ships and the flagship throughout the survey, enabling the staff aboard the flagship to direct and coordinate the movements of the various vessels as the synoptic picture of the Gulf Stream developed.

(b) Instruments for taking numerous and rapid measurements were available; Loran for navigation, the bathythermograph for water temperatures, the geomagnetic electrokinetograph for current velocities, and the planes for visual observations of the Gulf Stream's positions.

(c) Highly qualified scientific personnel were available to man the six ships and the plane.

In this paper the Gulf Stream has been defined as the continuous band, reaching from the continental shelf off Cape Hatteras to the 50th meridian, where a pronounced pressure gradient exists between the warm, highly saline water to the south and the colder, fresher water to the north. The inner and outer edges of the Stream are the points where this pressure gradient becomes zero. Abrupt changes in temperature and current velocities that occur at the surface do not necessarily coincide with these boundaries.

Daily synoptic plots of the Gulf Stream show that the current may shift its position at a rate of 11 miles per day. Two synoptic plots of the Stream are shown, one for the first and one for the last periods of the survey. The outstanding feature of the first plot is the two large waves separated by a deep trough near 61° west. The second plot shows that the trough became cut off and formed a cyclonic eddy south of the Gulf Stream. The breaking off of the trough was observed in detail and confirmed the theory that the large cyclonic eddies frequently found south of the Gulf Stream are formed in this manner.

A smaller, weaker cyclonic eddy was observed to the East of the deep trough. Although it is assumed that this eddy was formed in the same manner as the larger one, it is pointed out that it may be a portion of the counter current found on the outer side of the Stream, that became enclosed and cut off within the large wave east of the deep trough.

Eddies are probably always formed when the waves in the Gulf Stream reach a certain optimum size. It is estimated that the waves cannot become large enough to form eddies west of longitude 70° and probably not west of longitude 63°. There is the further possibility that the waves only reach this critical size in regions where ridges in the bottom topography affect the course of the Stream.

There is evidence that the cyclonic eddies broken off to the south of the Stream move in a westerly or upstream direction.

The surface currents are shown to flow parallel to the isotherms where these isotherms are closely spaced in the region to the left of the warm core of the Gulf Stream. In the right hand portion of this core the current directions are variable, frequently showing a narrow weak counter current.

Temperatures of the warm core indicate that the Gulf Stream transports water from south of Cape Hatteras to the longitude of the Grand Banks, the mean temperature of the upper 200 meter layer decreasing approximately 6° F. over this 1,200 mile distance. "Gobs" of warmer water, possibly indicating a pulsing action in the Stream, were found at intervals in the warm core from Cape Hatteras to 57° west longitude.

To the south of the Grand Banks two easterly currents are found and the southern one is shown to be the Gulf Stream. No evidence was obtained on this survey to show that the northerly current was in any way connected with the Gulf Stream.

Acknowledgements

Obviously this, or any other paper to be published dealing with Operation Cabot owes its existence to the efforts of the scientists and seamen who took part in the survey. The authors wish to thank these men, and also Dr Rossby of the University of Chicago. Dr Iselin and Mr Stommel of the Woods Hole Oceanographic Institution for their many helpful suggestions. Thanks are also due to Miss Evangeline Tollios and Mr Columbus Iselin Jr who did such a fine job of plotting and calculating.

REFERENCES

Von Arx, William S., 1950: An Electromagnetic Method for Measuring the Velocities of Ocean Currents from a Ship Under Way. *Papers in Physical Oceanography and Meteorology.* Vol. XI, **3**, pp. 1—62.

Church, Phil. E., 1937: Temperatures of the Western North Atlantic from Thermograph Records. *Publ. Scientifique*, **4**, pp. 1—32.

Iselin, C. O'D., 1940: Preliminary Report on Long-Period Variations in the Transport of the Gulf Stream System. *Papers in Physical Oceanography and Meteorology*, **8**, 1, pp. 1—40.

Iselin, C. O'D, and Fuglister, Frederick C., 1948: Some Recent Developments in the Study of the Gulf Stream. *Sears Found., Jour. Mar. Res.*, **7**, 3, pp. 317—329.

Soule, Floyd M., 1938: Oceanography Excerpt from International Ice Observation and Ice Patrol Service in the North Atlantic Ocean, Season of 1937. *U. S. Coast Guard Bull.*, **27**, pp. 71—126.

Esselte, Sthlm 51

Contribution No. 550

PHYSICAL OCEANOGRAPHY OF THE GRAND BANKS REGION, THE LABRADOR SEA AND DAVIS STRAIT IN 1949

BY FLOYD M. SOULE[1]

During 1949 the 180-foot tender-class cutter *Evergreen* was again used as the oceanographic vessel of the ice patrol. The problems of operation from this vessel remained essentially the same as those described in Bulletin No. 34 of this series. Hull vibration continued to be an important factor through its effect on the accuracy of temperature measurements and the deterioration of reversing thermometers, although trouble of the latter category was somewhat re-

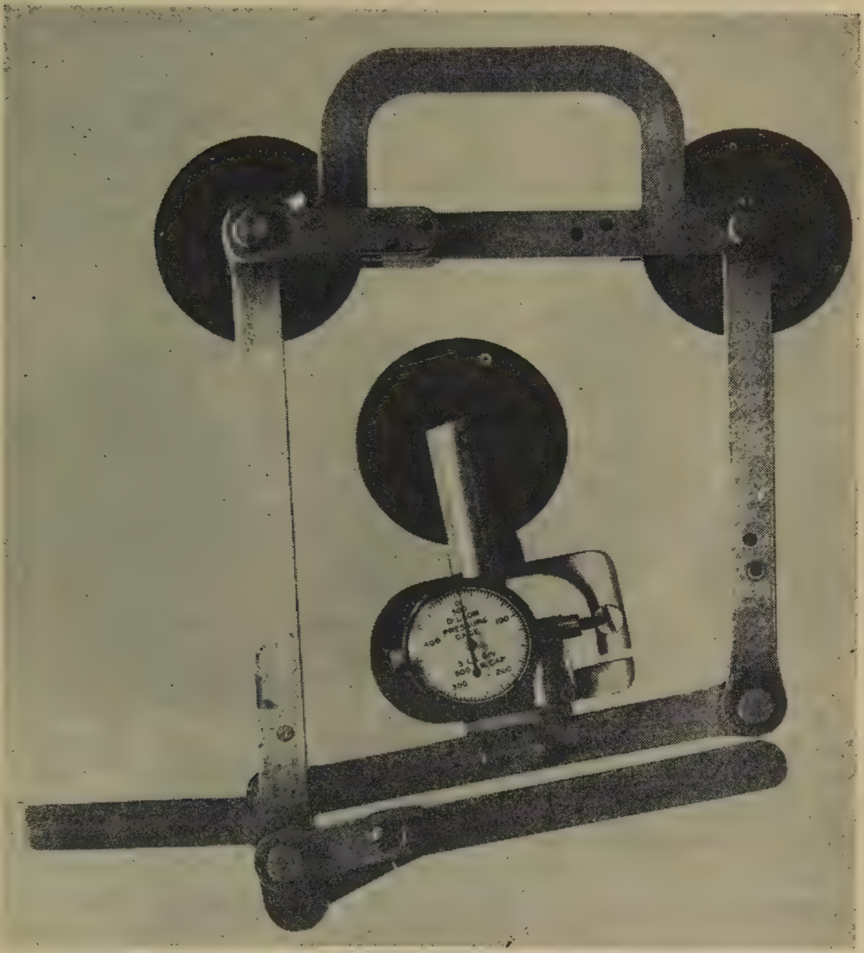

FIGURE 12.—Hand dynamometer designed to measure tension up to 2,500 pounds in wire rope of 5/32 inch diameter.

---

[1] Contribution No. 550 of the Woods Hole Oceanographic Institution.

duced through foam-rubber cushioning of the thermometers during periods of storage. The unfavorable laboratory conditions of vibration, noise, and excessive temperature were basically the same, although salinity measurements were improved by the countermeasures of building a filtered audio amplifier for the salinity bridge detector circuit and introducing an additional ventilator duct near the salinity bridge. New oceanographic winches employing electric drive and hydraulic transmission were installed just prior to the beginning of the season and eliminated many of the electrical and mechanical troubles experienced previously and permitted more rapid occupation of stations.

As very little information is available in the literature regarding the relationship between wire tension with the wire at rest and with the gear being hauled in, some measurements were made to determine what standard operating procedures to follow. A hand dynamometer was built so that it could be applied to the wire to measure the wire tension whether the wire was at rest or in motion. It was designed for 5/32-inch diameter wire rope with full scale deflection at a wire tension of 2,500 pounds, which is the breaking strength of the wire when new. The dynamometer is shown in figure 12. From measurements with the wire at rest and being hauled in at different speeds and with different lengths of wire out it was concluded that for practical purposes the relationship between tension at rest and tension hauling in is linear under the conditions existing on the *Evergreen* and over the range of wire speeds measured (from 74 to 193 meters/minute) and may be expressed as

$$T = [1.55 + 0.0042(S-100)]\ t$$

where T is the tension with a wire speed of S meters per minute and t is the tension with the wire at rest. Considering the protection of the wire against excessive tension, protecting the winch against excessive loads and protection against two-blocking gear from inability to stop in time after the incoming gear is sighted, recommended standard operating procedure with limiting wire speeds is shown in figure 13. This does not represent the operating procedure followed in 1949, since its compilation depended upon measurements made with at least 3,000 meters of wire out and opportunity for these measurements did not arise until the postseason cruise.

At 0600 on 4 April, the *Evergreen* departed Argentia to make a current survey of the area over and immediately seaward of the southwestern, southern, and eastern slopes of the Grand Banks. It had been planned to begin the survey on the southwestern slope and work around the Tail of the Banks and northward along the eastern slope to about latitude 46° N., including in the area as great a length along the margin of the Grand Banks as time permitted. While such

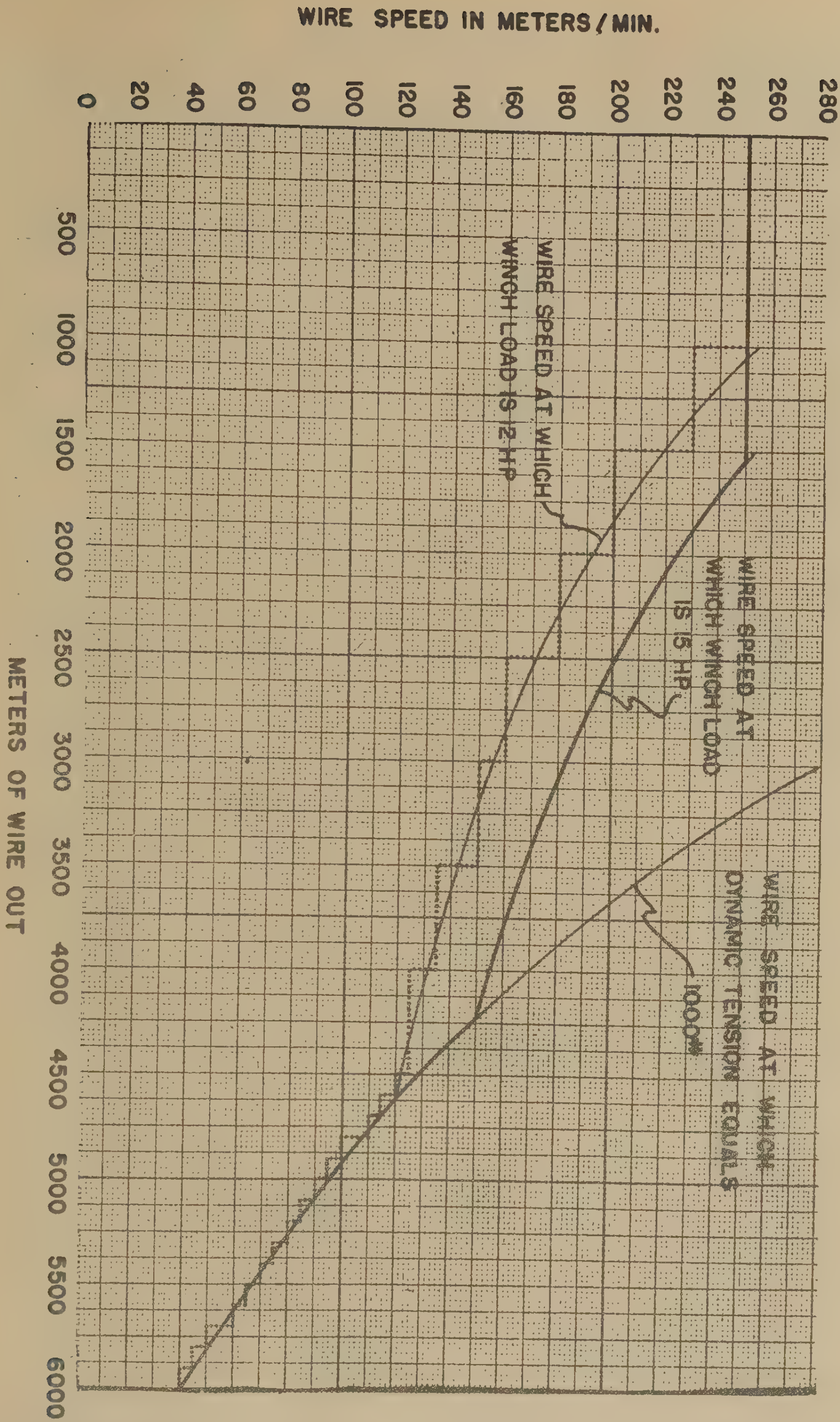

Figure 13.—Winch load and wire tension related to wire speed and length of wire out. Dotted line represents recommended wire speeds at different lengths of wire out.

an area might not extend far enough seaward to include all areas of mixed-water eddies, it would define the western limits to which bergs might be expected to drift, and locate the major eddies and areas where ice might be expected to threaten traffic on the North Atlantic Track Agreement tracks, and indicate areas for more extensive subsequent surveys. The work of collection of data began at station 3747 located at 43°34′ N., 51°30′ W., at 1745 on 5 April. At 0355 on 6 April, it was necessary to heave-to to await better weather. At 2257 on 6 April, station work was resumed at station 3751. However, a fathometer failure which had occurred during the heavy weather was found to be beyond possible repair at sea, and upon completion of station 3753 at 1300 on 7 April, the *Evergreen* laid a course for Argentia to accomplish the necessary repairs, arriving there at 1336 on 8 April.

Advantage was taken of this inport time to replenish exhausted supplies of high-pressure nitrogen for the winches, to stop major leaks in the gas and hydraulic systems of the winches and to clean and adjust their valves to prevent their unloading at wire tensions below about 1,000 pounds. With this done, departure was taken from Argentia at 1130 on 12 April to continue the current survey interrupted by the fathometer failure on the first cruise. Work of collection of data began on 13 April at station 3754, located at 42°02.5′ N., 52°04′ W., and progressed northward without major interruptions, speeding up as inexperienced personnel gained facility in the performance of their various tasks. Gear was shifted to the port side and that winch used during the occupation of stations 3766 to 3773, while a rough valve (replenishing and servo-pump relief valve) in the starboard winch was polished. It was learned from experience that because of the rolling of the ship, hydraulic oil sump levels had to be maintained at higher than indicated normal levels to prevent air getting into the hydraulic system. One 900-foot bathythermograph and one 450-foot bathythermograph were lost through breaking of the wire under circumstances which indicate the wire had been defective. Two reversing thermometers were broken and two messengers were lost overboard during heavy weather. Several miscellaneous Nansen water bottle parts failed. However, few if any essential data were lost and the survey, comprising 57 stations, was completed at station 3810 located at 46°17.5′ N., 49°00′ W., on the afternoon of 23 April and a course laid for Argentia, with arrival there at 1740 on 24 April.

A third cruise was undertaken with departure from Argentia at 0611 on 6 May. Previous cruises had indicated little need for extending subsequent surveys westward of the Tail of the Grand Banks. This survey was therefore intended to cover the area from Flemish Cap to the Tail of the Banks and the work of collection of data began at station 3811 located at 46°47.5′ N., 44°40′ W., at 2040 on 7 May. Work progressed from north toward south without serious interruption and the 62-station survey was completed at station 3872, located at 42°41′ N., 49°10′ W., at 1630 on 17 May. The *Evergreen* then laid a course for Argentia, with arrival there at 1201 on 19 May. During this cruise the deepest bottle at station 3819 dragged on bottom, where the thermometer frame and the two attached reversing thermometers were lost. A third thermometer was put out of action through the breakage of its glass-protecting sheath during attempts to restore the mercury to its proper position when gas in the thermometer separated the mercury column.

To begin a fourth cruise, the *Evergreen* departed Argentia at 0948 on 2 June. This cruise was intended to develop information regarding current conditions in the area immediately northward of the Grand Banks where the Labrador Current divides into the two branches which follow the Avalon Peninsula and the eastern slope of the Grand Banks. Stations were occupied along three sections disposed in the shape of a triangle defined by the corners at approximately 47°24′ N., 50°00′ W., 50°00′ N., 49°00′ W., and 48°44′ N., 52°58′ W. (off Cape Bonavista). The work of collection of data began at station 3873, located at 47°24′ N., 50°00′ W., on the morning of 3 June and progressed without major incident to its completion on the evening of 6 June at station 3902, located near the point of beginning. In accordance with dispatch instructions from Commander, International Ice Patrol, upon completion of the oceanographic survey the *Evergreen* proceeded to relocate and drift with a berg sighted by plane on 2 June at 49°24′ N., 51°48′ W., and on 5 June at 48°55′ N., 51°25′ W. The berg was reached on the afternoon of 7 June and departure was taken from the berg on the afternoon of 8 June for Argentia, with arrival there at 2042 on 9 June.

As the ice-patrol season was terminated on 15 June, the next cruise of the *Evergreen* was considered to be the postseason cruise, part one. The *Evergreen* departed Argentia at 1028 on 16 June to repeat the triangular survey of the fourth cruise to learn something of the stability of the circulation pattern in the vicinity of the branch point of the Labrador Current included in the triangle. The work of collection of data began on the morning of 17 June at station 3903 at the southern corner of the triangle and progressed without major incident around the triangle in a counterclockwise direction, the final station, number 3932, being completed on the afternoon of 20 June near the point of beginning. The *Evergreen* then laid a course for Argentia, with arrival there at 1658 on 21 June.

At 2102 on 2 July, the *Evergreen* departed Argentia on the second and final part of the postseason cruise. It had been planned to occupy a section across the Labrador Sea from South Wolf Island, Labrador, to Cape Farewell, Greenland; a second longitudinal section from the deep water of the Labrador Sea across the ridge at Davis Strait to the deep water of Baffin Bay; a third section across the Labrador Current from the deep water of the Labrador Sea to Loks Land; a fourth section across the West Greenland Current from the deep water of the Labrador Sea across Fyllas Bank to the vicinity of Godthaab, Greenland; a fifth section across the Baffin Land Current from the deep water of Baffin Bay to Cape Kater, Baffin Island; and a sixth section across the West Greenland Current from the deep water of Baffin Bay to the Nugssuak Peninsula just north of the northern end of the Vaigat.

The work of collection of data began off South Wolf Island at station 3933 on the morning of 5 July and progressed toward Cape Farewell until the afternoon of 9 July, when storis blocked further progress and station 3954 was occupied at the edge of the ice 15½ miles off the beach. From this station the *Evergreen* proceeded to 62°14′ N., 56°06′ W., where station 3955 was occupied on the morning of 11 July to begin the Loks Land section. This section was completed at station 3965 on the evening of 12 July, 15½ miles off the beach at the outer edge of the West Ice. The *Evergreen* then returned to the longitudinal section where, on the evening of the 13th, at 62°30′ N., 56°14′ W., station 3966 was occupied to begin the Fyllas Bank section. This section was completed with station 3974, located at 63°59′ N., 52°42′ W., on the morning of 15 July, after which a return to the longitudinal section was made again and work on it resumed on the evening of the 15th at station 3975, located at 63°00′ N., 56°32′ W. From here, work on the longitudinal section progressed northward according to plan until the afternoon of 17 July, when the edge of the West Ice was encountered at station 3984, located at 66°48.5′ N., 58°40′ W. From here northward it was necessary to deviate eastward from the planned course of the longitudinal section as the outer edge of the West Ice was followed. The ice covered the deeper parts of the southern end of Baffin Bay and extended eastward almost to the edge of Great Hellefiske Bank. Near the northern end of this bank it again was possible to work somewhat to the westward, but at only one station, number 3990, was it sufficiently westerly to attain a depth of 1,500 meters. This station was located at 69°06.5′ N., 59°56′ W. From here the edge of the ice again trended east of north and at station 3992, located at 69°51.5′ N., 59°01′ W., the longitudinal section was terminated on the evening of 19 July and the Nugssuak Peninsula section begun since the West Ice precluded any work on the Cape Kater section. The Nugssuak Peninsula section was completed at station 3999, located at 70°38.5′ N., 55°01′ W., in the early afternoon of 20 July, and a course laid for Argentia, with arrival at that port at 1828 on 26 July. After replenishing, departure was taken on the 27th for Woods Hole, with arrival there on the evening of 30 July to discharge oceanographic equipment.

At the 186 stations occupied during the surveys in the Grand Banks area and the triangles just north of the Grand Banks, the observations extended to a depth of about 1,500 meters where the depth of water permitted and the dynamic topography was referred to the 1,000-decibar surface. At the remaining 67 stations occupied during part two of the postseason cruise, the observations extended from the surface to as near bottom as was practicable and the dynamic topography was referred to the 1,500-decibar surface. The intended depths of observation, in meters, were 0, 25, 50, 75, 100, 150, 200, 300, 400, 600, 800, 1,000, and thence by 500-meter intervals. Protected deep-sea reversing thermometers, most of them manufactured by Richter & Wiese, and a few by Negretti & Zambra, and by the G & M Manufacturing Co., were used to measure the temperatures. Depths of observation were based on measurements made with Richter & Wiese unprotected deep-sea reversing thermometers. Intercomparisons were made amongst the thermometers by making periodic shifts in thermometer pairs. Thus most of the thermometers used were each compared with several other thermometers. These intercomparisons helped identify unreliable thermometers. A total of 1,661 individual intercomparisons were made, giving a probable difference between corrected readings of a pair of thermometers of ±0.010° C. As most of the observed temperatures are the means of the corrected readings of a pair of thermometers, it is considered that they are accurate to about ±0.01°.

As in previous years, water samples were collected with Nansen-type reversing water bottles, transferred to rubber-gasketed citrate of magnesia bottles, and salinities determined within 24 hours of collection by means of a Wenner salinity bridge. As the bridge was calibrated by using samples whose salinities were determined by silver-nitrate titration, the accuracy of the salinity measurements is limited to that of the silver-nitrate titration method or about ±0.02 °/oo in salinity. However, the precision of the salinities is better than that and of the order of about ±0.005 °/oo. For the most part they have been tabulated to the nearest 0.01 °/oo. During routine salinity runs, the bridge was standardized each tenth to thirteenth sample in each of the cells with substandard sea water from an oil-sealed carboy. At least once during each run and usually oftener, Copenhagen standard sea water was measured as an unknown to permit final adjustments of salinities for each survey. These salinity adjustments were as follows:

First and second cruises	+0.01 °/oo
Third cruise	No correction
Fourth cruise	+0.01 °/oo
Post season cruise, parts 1 and 2	No correction

The tables show the corrected values of salinity, but since the dynamic heights had already been computed and the topography delineated, the tabulated values of σ_t have not been recomputed but are the originally computed values to which a flat correction of 0.01 has been applied where a correction of 0.01 °/oo salinity was necessary. Similarly, the tabulated dynamic heights in these instances have been adjusted by a constant correction of 8 mm. The dynamic topographic charts showing the results of the first and second cruises and the first triangle have not been corrected and show topography which is about 8 mm too high.

The oceanographic work was under the supervision of Oceanographer Floyd M. Soule, who was assisted by LT. Harry H. Carter. Other assistants in the observational work were William B. Arndt, aerographer's mate third class; Raymond W. Wood, boatswain's mate second class; Francis N. Brown, yeoman third class, and Lydle L. Rickard, boatswain's mate third class.

The seven oceanographic stations occupied during the first cruise are shown in figure 14. Inasmuch as they are disposed in the form of a single section, current patterns cannot be derived from them with accuracy, but the dynamic heights considered with respect to other indicators permit an inference as to the general features of circulation within a limited area bordering the section as shown in figure 14. A von Arx geomagnetic electrokinetograph was in operation along the section and its indications have been taken into account in the preparation of the figure. No negative temperatures were observed, even near the edge of the Grand Banks, the lowest temperature recorded being 1.50° C at a depth of 129 meters at station 3749. The effects of the Gulf Stream system were in evidence at station 3753, where water of more than 11° C and correspondingly high salinity was present just below the surface. The currents in this area were weak and indicated little opportunity for bergs to drift as far west as this section. It was concluded, therefore, that subsequent surveys of the 1949 season need not extend as far westward as this.

The dynamic topography found during the second cruise is shown in figure 15. As in the first cruise, the indications of the von Arx current meter have been considered in drawing the dynamic isobaths. The figure shows the Labrador Current flowing southward along the eastern slope of the Grand Banks. Southward of the Tail of the Banks the western limit of about 50°25′ W. was attained at about 42°30′ N. Although the velocity of the Labrador Current was not great, the offshore limit of the southward moving water was well outside the 1,000-fathom curve and the southern limit of the cold mixed water was south of the area surveyed. Thus any bergs entering the northern part of the area in the Labrador Current and not

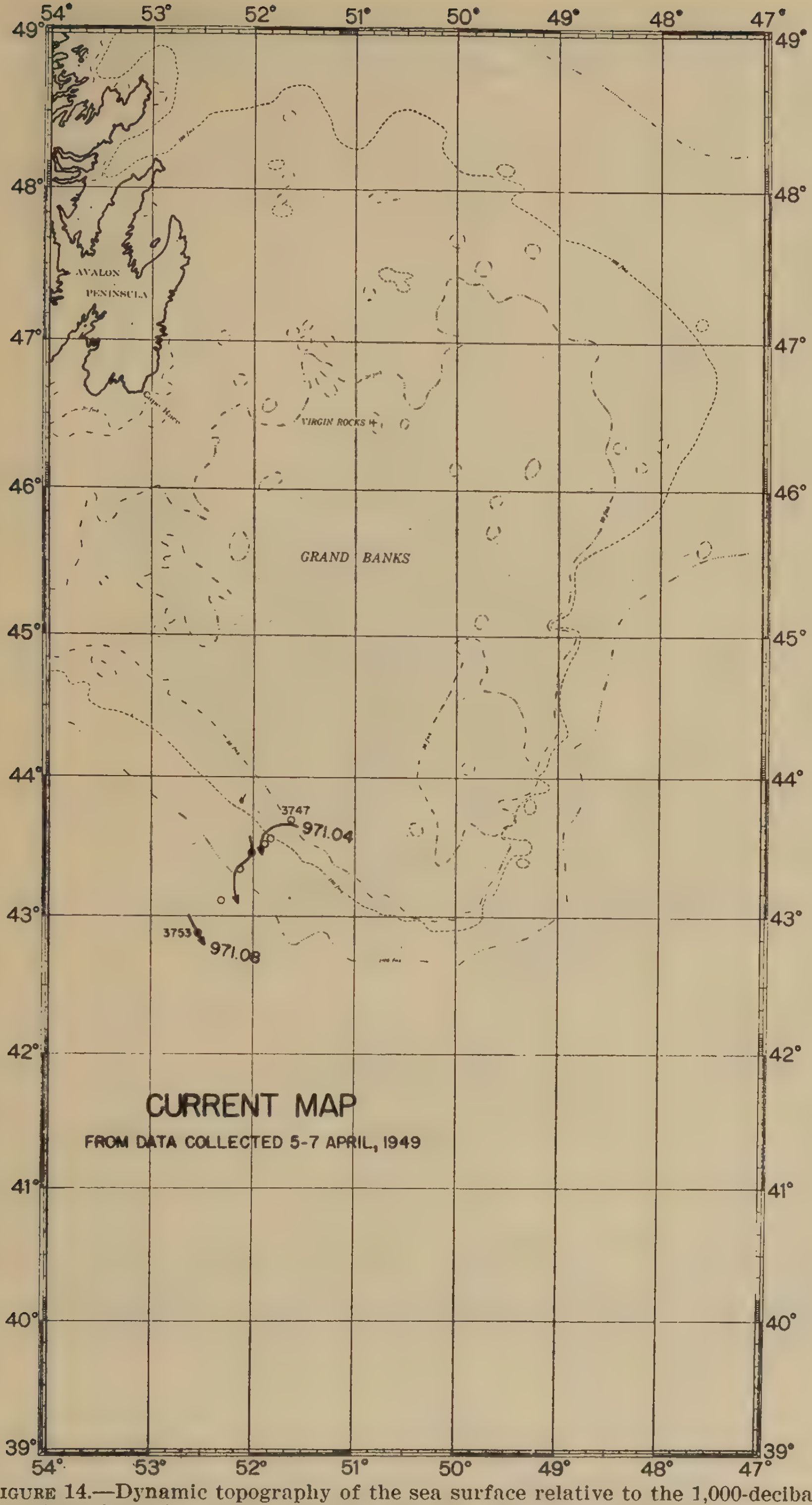
54°
53°
52°
51°
50°
49°
48°
47°
42°
43°
44°
45°
46°
39°
40°
41°
AVALON
PENINSULA
Cape Race
VIRGIN ROCKS
GRAND BANKS
3747
971.04
3753
971.08
CURRENT MAP
FROM DATA COLLECTED 5-7 APRIL, 1949

FIGURE 14.—Dynamic topography of the sea surface relative to the 1,000-decibar surface, from data collected 5–7 April, 1949. Oceanographic station positions are indicated and the station numbers given at turning points.

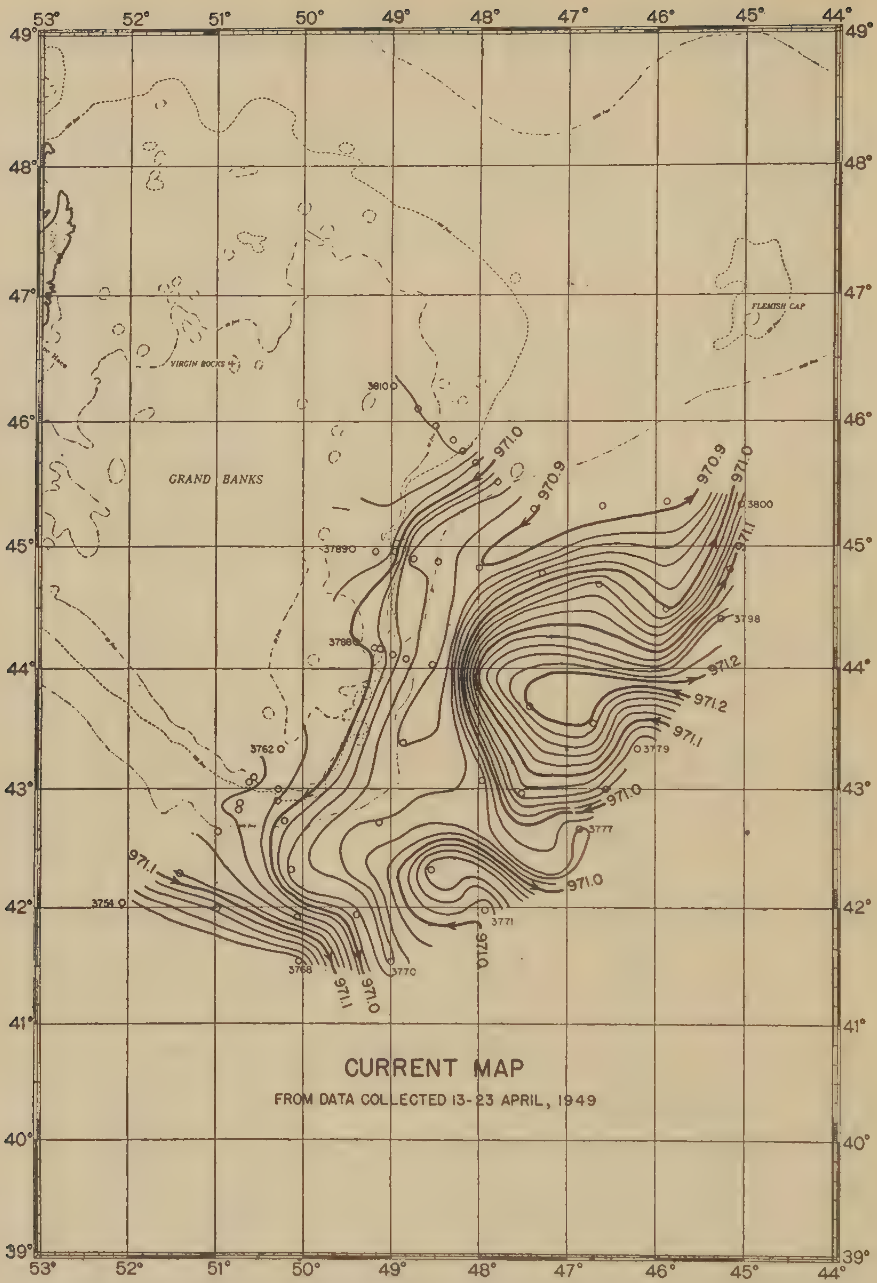
53°
52°
51°
50°
49°
48°
47°
46°
45°
44°
41°
40°
39°
GRAND BANKS
VIRGIN ROCKS
FLEMISH CAP
3810
3800
3798
3789
3788
3762
3779
3777
3754
3771
3768
3770
971.0
970.9
971.1
971.2
CURRENT MAP
FROM DATA COLLECTED 13-23 APRIL, 1949

FIGURE 15.—Dynamic topography of the sea surface relative to the 1,000-decibar surface, from data collected 13–23 April, 1949. Oceanographic station positions are indicated and the station numbers given at turning points.

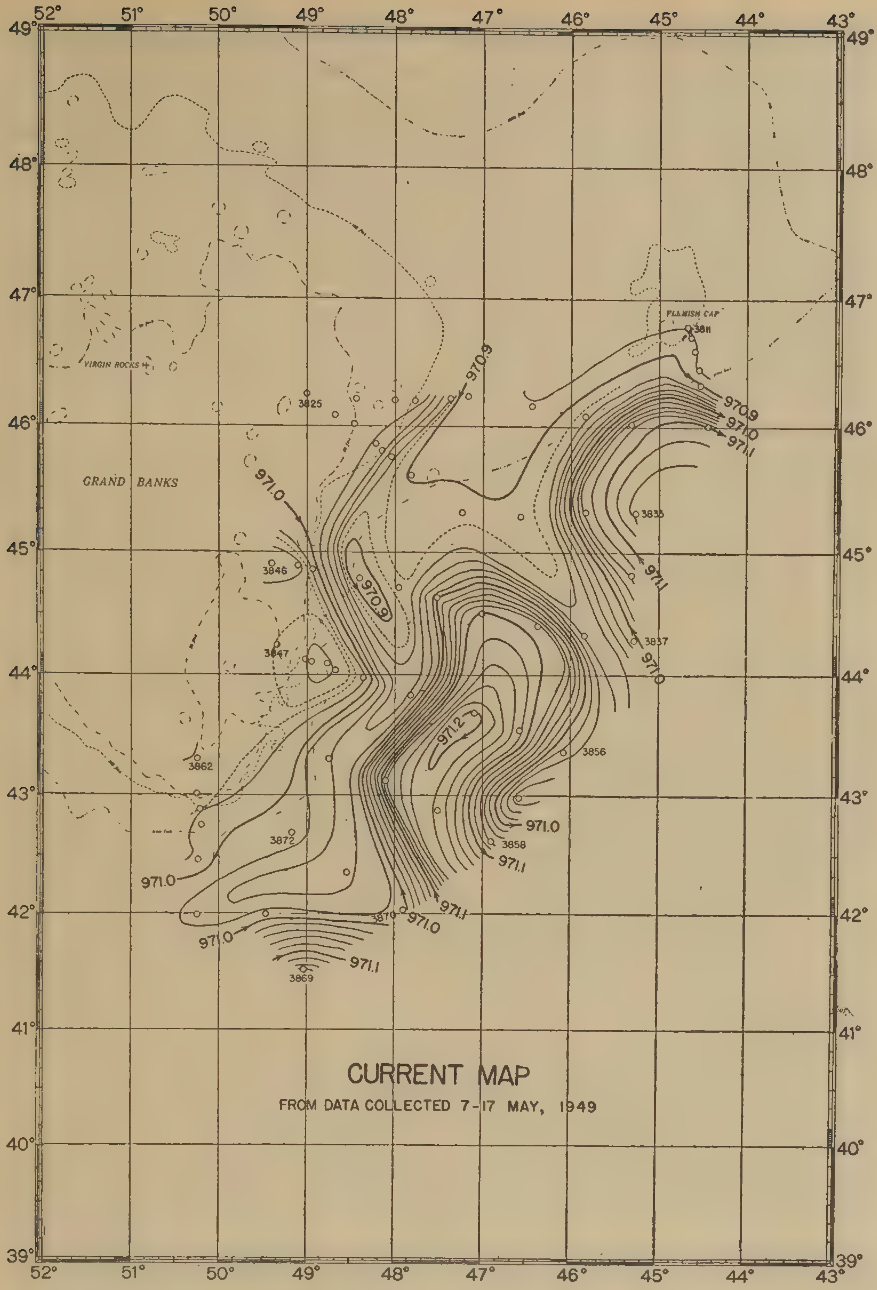
52°
51°
50°
49°
48°
47°
46°
45°
44°
43°
42°
41°
40°
39°
VIRGIN ROCKS
GRAND BANKS
FLEMISH CAP
3811
3825
3835
3837
3846
3847
3856
3858
3862
3869
3870
3872
970.9
971.0
971.1
971.2
CURRENT MAP
FROM DATA COLLECTED 7-17 MAY, 1949

Figure 16.—Dynamic topography of the sea surface relative to the 1,000-decibar surface, from data collected 7–17 May, 1949. Oceanographic station positions are indicated and the station numbers given at turning points.

swept westward to ground on the Grand Banks northward of about 44° N. could have been expected to reach track C at about 49° W. Another area indicated by figure 15 as one of potential ice hazard to traffic following U. S.-European tracks was that southeastward of 42°30′ N., 47°00′ W. In the southwestern part of the area surveyed, the margins of the Gulf Stream system were present with dynamic heights greater than 971.1 dynamic meters. This dynamic isobath also approximated the boundary of the Atlantic Current water in the strong salient extending westward toward the banks between latitudes 43° N. and 45° N. With the current pattern found in this survey, the possibility of a break-through of Labrador Current water and bergs immediately southward of Flemish Cap was limited to latitudes north of 45°30′ N.

Figure 16 shows the dynamic topography found during the third cruise. A striking feature of this survey is the complicated current pattern in the area between about 44° N. and 45° N. and 48° W., and 50° W. A slow counterclockwise eddy has been shown centered near 44° N., 49° W., for simplicity, although the actual dynamic topography may have been better represented by a valley associated with the Labrador Current and extending southwesterly toward 44° N., 49° W., and bordered on its southern side by a promontory associated with the Grand Banks eddy and jutting easterly beyond the 1,000-fathom curve. Such an interpretation would be in accord with the clockwise circulation of the Grand Banks eddy, which is often intensified seasonally and centered around the shoalest part of the Grand Banks. In either case the axis of the Labrador Current is displaced seaward from its usual position and is well outside the 1,000-fathom curve at the 44th parallel. Northward of this latitude the Labrador Current maintained its previous strength and continued to supply the area of cold mixed water southeastward of the Tail of the Banks.

Large diameter clockwise eddies or salients which characterize the outer margins of the Atlantic Current in this region have been observed to progress along the boundaries of that current in the direction of its flow. With the time interval between surveys of the order of magnitude of 1 month and with the diameters of the eddies ranging between about 50 and 150 miles, the only cases in which successive surveys have permitted the identification of such progressing eddies or salients have been those in which the rate of progress has been slow. A comparison of figures 15 and 16 shows the possibility of interpreting the current patterns found during the second and third cruises as a case in which salients have progressed northeastward, with the salient which was centered at about the 44th parallel in figure 15 having moved to the vicinity of 45°30′ N., 45°00′ W., in figure 16, and the tongue shown in figure 15 near 42° N., 48° W., developing into the salient the axis of which is near the 47th meridian in figure 16. As the two surveys were made about 24 days apart and as the salients as thus identified differ in position by about 150 miles, their rate of progress would have averaged about 6 miles a day.

If bergs had been present the region of potential ice hazard would have moved from that southeastward of 42°30′ N., 47°00′ W., to that southward of 44°00′ N., 45°30′ W. These conditions, shown in figure 16, are such as accompany the "break-through" of bergs southeasterly from the area between the Grand Banks and Flemish Cap directly toward the U. S.-European steamer lanes. This break-through of bergs has occurred with sufficient frequency to be considered a seasonal characteristic of early May.

It has been assumed that the formation of the eddies or salients mentioned above is conditioned by factors peculiar to this region, such as bottom topography and the junction of the Labrador and Atlantic Currents.[2] It has been assumed further, that the position of the boundary between the Atlantic Current and the mixed water along its outer edge is controlled by the volumes of flow of the Labrador Current and the Atlantic Current, and that fluctuations in the size, shape, and degree of incursion of the salients are associated with fluctuations in the volume of flow of these two currents. An interesting corollary of such an hypothesis in the light of the apparently seasonal break-through is that there are seasonal fluctuations in the volume of flow of the Labrador Current or the Atlantic Current or both. Aside from its fundamental importance, it is important that the interrelationship of the elements stated above be determined, since it is regarded as a prerequisite to the practical forecasting of the geographical extent of the ice hazard from week to week.

While demonstration of the validity of the assumptions is not adequate, some supporting evidence has accumulated. In an earlier Bulletin of this series,[3] the location of the outer boundary of Atlantic Current water found during the ice seasons of 1934–41 was presented and discussed with relation to observed fluctuations in volume of flow of the Labrador Current and volume of flow of the Atlantic Current inferred from differences in sea level across the Charleston-Bermuda section. The criterion used for the boundary of Atlantic

---

[2] See B. Haurwitz and H. A. Panofski, "Stability and Meandering of the Gulf Stream." Trans. Am. Geophys. Union. Vol. 31, No. 5, pp. 723–731 (Oct. 1950), Washington. In this paper its authors conclude that unstable waves may develop in the Gulf Stream after it leaves the continental shelf and that these unstable waves form the eddies or meanders along the outer edge of the Gulf Stream. The conditions are similar to those existing in that part of the Atlantic Current in the vicinity of the Grand Banks where the observed speed of progress of Atlantic Current salients is of the same order of magnitude as the speed of propagation of unstable waves computed from "realistic values" by Haurwitz and Panofski.

[3] Soule, Floyd M., and C. A. Barnes, "International Ice Observation and Ice Patrol Service in the North Atlantic Ocean—Season of 1941." U. S. Coast Guard Bull. No. 31, pp. 15–24 (1950), Washington.

Current water was the T–S relationship of 6° C corresponding to 34.95 $^{\circ}/_{\circ\circ}$. The area considered was that between the boundary so defined and the fixed limits formed by the 45th parallel, the 49th meridian, and a rhumb line extended from 43° N., 49° W., through 42° N., 47° W. This area was adjusted by the subtraction of 10,000 square kilometers for each million cubic meters per second volume of flow of the Labrador Current entering the area at the northwestern corner (section U). A remarkably good correspondence was found to exist between the difference in sea level Charleston-Bermuda and the adjusted area 13½ months later for each of the 28 surveys made during the ice seasons of 1934–41.

Since the postwar resumption of ice-patrol oceanography, one survey was carried out in 1948 and two in 1949. As the station networks of these surveys do not extend seaward far enough to include all parts of the Atlantic Current water boundary in the sector under discussion, the boundary cannot be delineated with accuracy. In each case an estimate has been made of the course of the boundary and the resulting area has been adjusted for the volume of flow past section U. Whether from errors in estimating the course of the Atlantic Current water boundary, or from more basic causes, these three surveys do not show the same good correspondence found for the earlier 8-year series of measurements. Expressed in units of 10,000 square kilometers, the adjusted areas differed from the values expected from the changes in sea level, Charleston-Bermuda, by the following amounts: June 1948, 5.1 too large; April 1949, 1.4 too small; May 1949, 5.0 too large. Thus, some of the evidence does not clearly support the assumption that the position of the boundary is controlled by the volumes of flow of the Labrador Current and the Atlantic Current.

In 1948 the T–S characteristics of the different water masses in the Grand Banks region could not be established except in general terms, partly because of the small number of stations available for examination and partly because the mixed water did not have the uniformity which usually has characterized it as a virtual water mass. The surveys of April and May, 1949, provided enough observations to determine the approximate course of the T–S curves representing the Labrador Current water, the Atlantic Current water, and the mixed water and these are shown in figure 17 as solid lines. The broken lines represent the T–S relationship found during the 8-year period 1934–41. Except for the upper layers, but two stations from the April survey (3767 and 3779) could not be properly classified, while three stations (3852, 3858 and 3869) from the May survey were atypical. In discarding observations from the upper layers at any station, we are in reality recognizing that at those stations the mixing of water from the parent water masses has not been carried far enough to attain

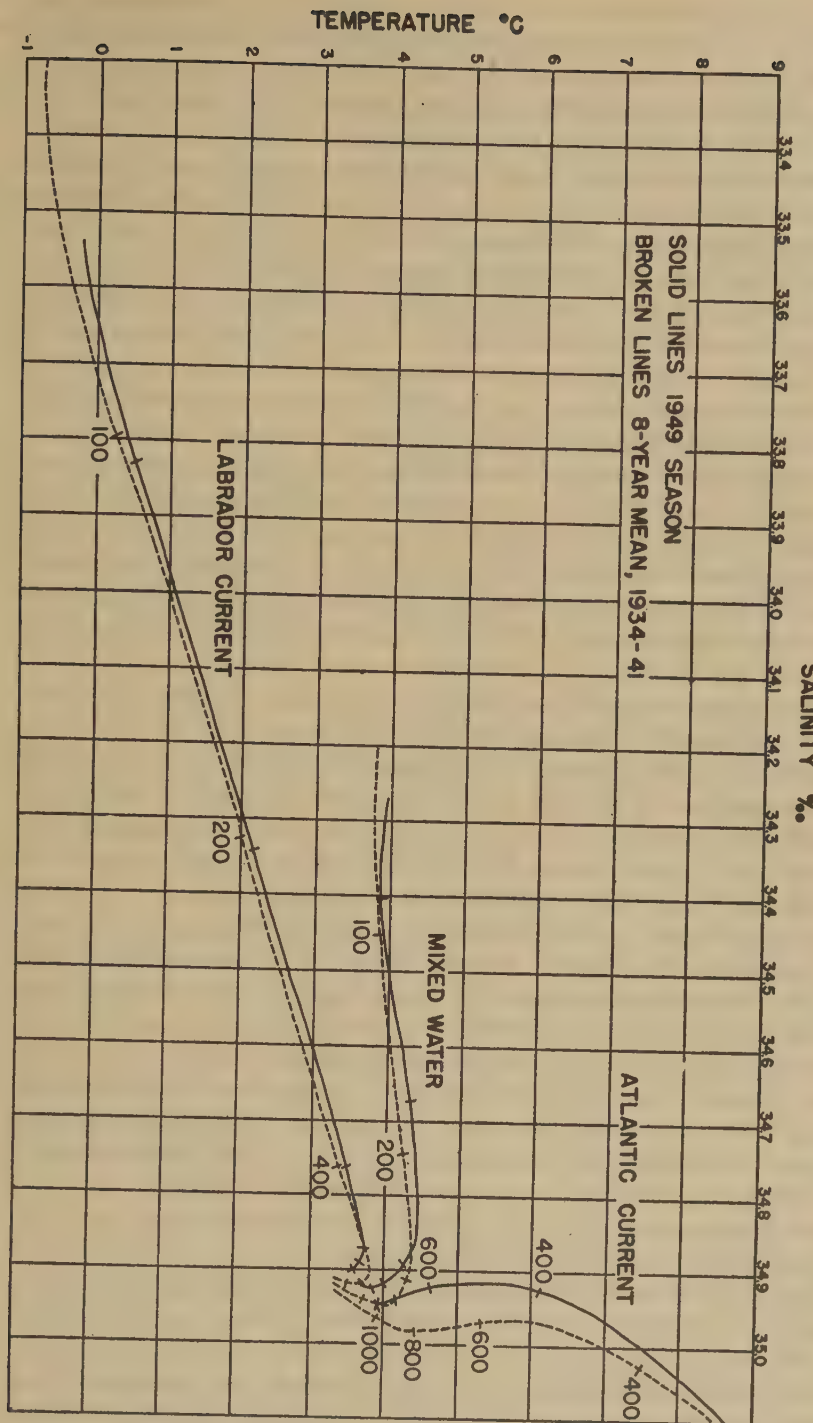

FIGURE 17.—Temperature-salinity correlation for Labrador Current water, Atlantic Current water, and mixed water found in the Grand Banks region. Solid lines show conditions during the 1949 season and broken lines represent the 8-year mean for the period 1934–41. An approximate depth scale in meters is given.

the uniformity found below those layers. Thus water of varying proportions of the parent water masses was found at some stations down to depths of as much as 200 meters, although at most stations the water approached the characteristics of one of the three T–S relationships at depths greater than 70 meters.

From figure 17 it will be seen that down to depths of about 400 meters the Labrador Current water and the mixed water followed much the same characteristic curve as was found for the earlier 8-year mean. These two water masses at the deeper depths, and the Atlantic Current water at all depths, were colder and fresher than the 8-year mean. However, since the differences from the mean temperatures and salinities for the 8-year period oppose each other in affecting the density, changes in σ_t were small and, for the levels of 600, 800, and 1,000 meters were respectively +0.01, −0.02 and −0.02.

To facilitate comparisons of conditions found during different surveys and during different years, certain sections designated T, U, and W have been repeated whenever a survey could be accommodated to permit their occupation. They are located as follows: T running southeasterly from about 46°20′ N., 49°00′ W.; U extending east and west at about the 45th parallel; and W running southerly off the Grand Banks at about the 50th meridian.

The earlier observations (dating from 1934) probably have not been well enough distributed in point of time so that their average values may be taken as normals, but until other data are available these averages are the best basis for comparison that we have and are made use of here. In the following it will be understood that volumes of flow are given in units of 1 million cubic meters per second and temperatures expressed in ° C. With respect to normals and time of year, the April survey showed the Labrador Current passing section T to have a volume of 3.40 (0.53 below normal) and a mean temperature of 1.55 (0.59 below normal). At section U, the volume of flow was 2.87 (2.97 below normal), and the mean temperature was 2.85 (0.81 above normal). At section W, the volume was 2.83 (1.04 below normal), and the mean temperature was 2.43 (0.03 below normal). During the May survey, the volumes of flow past sections T, U, and W were respectively 1.67 (1.88 below normal), 3.51 (1.95 below normal), and 2.19 (1.42 below normal), with corresponding mean temperatures of 1.76 (0.44 below normal), 1.75 (0.39 below normal), and 4.58 (1.96 above normal).

Thus the volume of flow was below normal at each section at each survey and except for section U during the April survey and section W during the May survey, the mean temperature was also below normal. As the Labrador Current is formed by the junction of the Baffin Land Current and that part of the relatively warm West Greenland Current, which branches westward south of Davis Strait, it would seem that the explanation of the deficiency in volume of flow of the Labrador Current in the Grand Banks region accompanied by a subnormal mean temperature is to be sought in a possibly decreased contribution from the West Greenland Current.

In 1948 a beginning was made in the study of the area just northward of the Grand Banks where the Labrador Current divides into a western branch which flows southward along the Avalon Peninsula of Newfoundland, and an eastern branch which follows the eastern edge of the Grand Banks. Three sections, disposed in the form of a triangle which included the branch point, were occupied. In 1949 this triangle was occupied twice; once during the period 3–6 June, and again about two weeks later on 17–20 June.

Figures 18 and 19 show the dynamic topography at the sea surface and at the 100-decibar surface respectively, derived from the first occupation of the triangle; and figures 20 and 21 show the topography at similar surfaces from the second occupation of the triangle. From figure 18 it is concluded that bergs crossing the 49th parallel eastward of about 51°45′ W. would probably follow the eastern branch of the current; that bergs crossing the 49th parallel westward of about 52°00′ W. would probably follow the western branch along the Avalon Peninsula; and that bergs crossing this parallel at intermediate longitudes would probably strand on the northern slope of the Grand Banks. Figure 20 indicates that these critical longitudes were much the same (51°50′ W., and 52°00′ W., respectively) during the second occupation of the triangle.

One of the questions of primary importance to the practical application of studies of the oceanography of this region is whether the current pattern at the sea surface is sufficiently representative of the circulation in the upper 150 or 200 meters to permit the movement of deep-draft bergs to be deduced from the dynamic topography of the sea surface. Comparison of figures 19 and 21 with figures 18 and 20 respectively shows a very encouraging similarity of current pattern at the sea surface and at the 100-decibar surface for each of the two occupations of the triangle.

In considering figures 18 through 21, it should be borne in mind that the occupations of the triangle differ from the usual survey in that the measurements have been confined to the periphery of the area involved and that consequently the deduced current pattern within the triangle is subject to errors which increase with the distance from the sides of the triangle. Thus, while the points of entry or emergence of the dynamic isobaths are well defined, their courses within the triangle can be shown with much less certainty.

The drift of an iceberg which entered the area at about the time of the first occupation of the triangle added information on the question of whether or not the dynamic topography of the sea surface

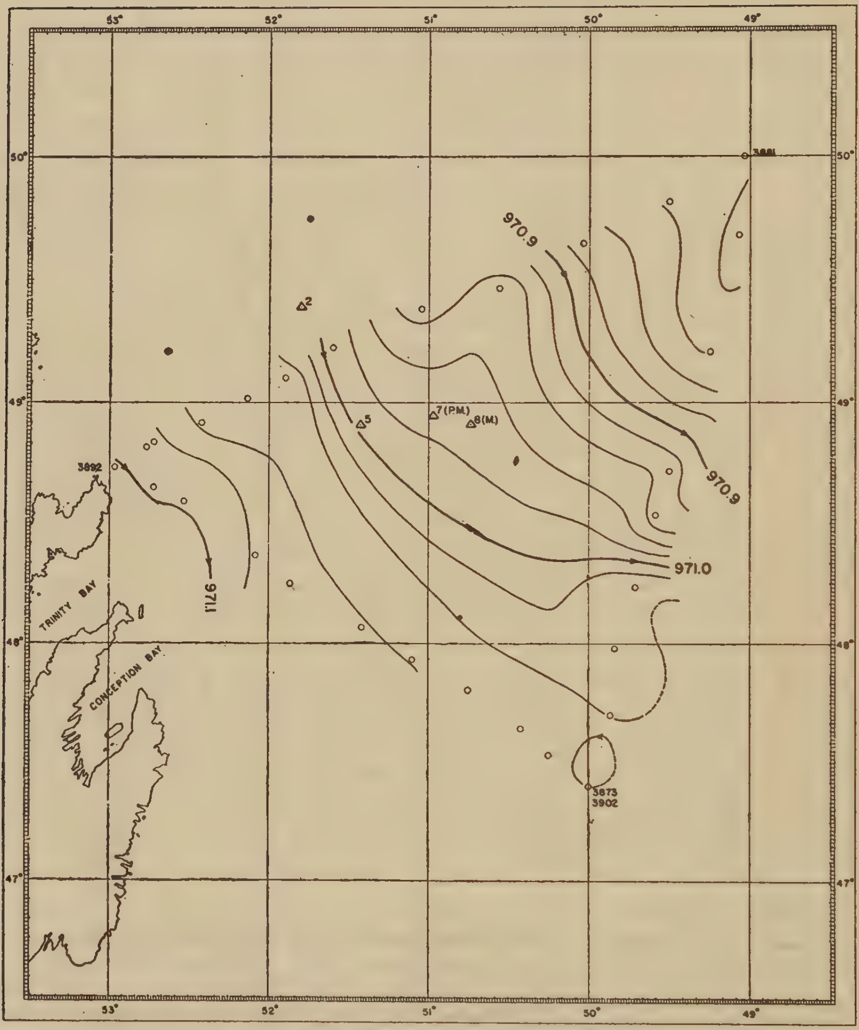
53°
52°
51°
50°
49°
50°
49°
48°
47°
3881
970.9
2
7(P.M.)
8(M.)
5
3892
971.1
TRINITY BAY
CONCEPTION BAY
971.0
3873
3902

FIGURE 18.—Dynamic topography of the sea surface relative to the 1,000-decibar surface, from data collected 3–6 June, 1949. Oceanographic station positions are indicated and the station numbers given at turning points.

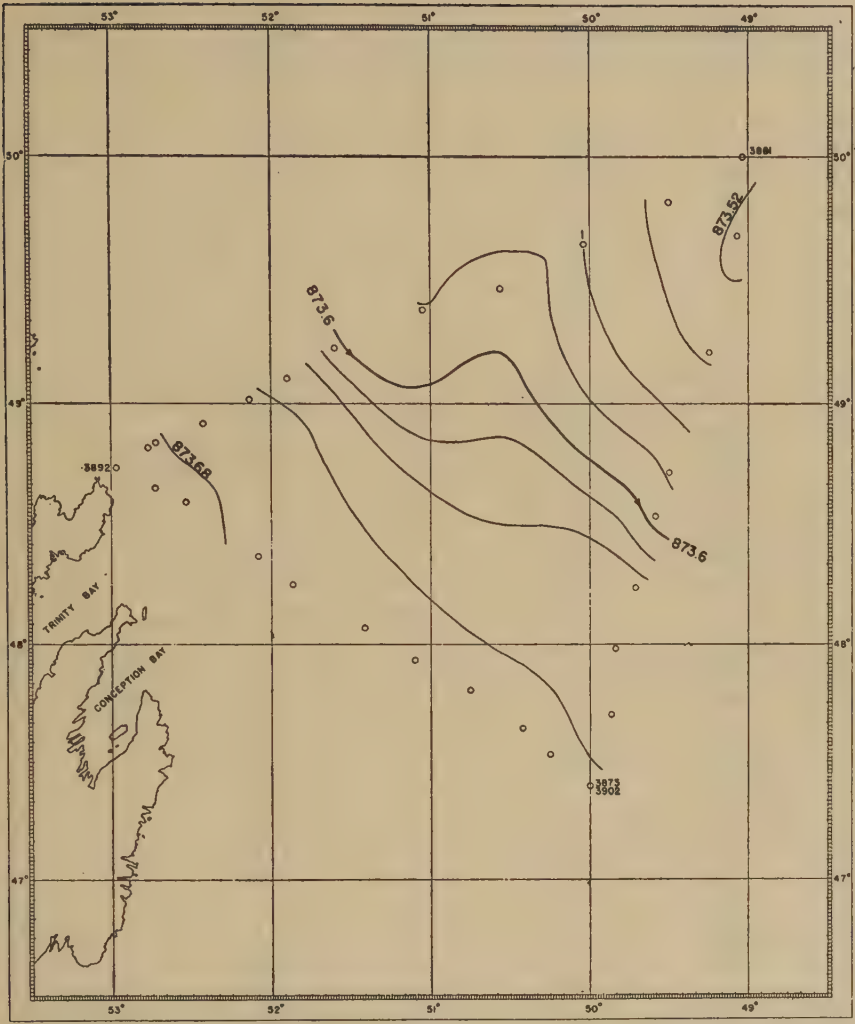
53°
52°
51°
50°
49°
50°
49°
48°
47°
3881
873.52
873.6
873.68
3892
TRINITY BAY
CONCEPTION BAY
873.6
3873
3902

FIGURE 19.—Dynamic topography of the 100-decibar surface relative to the 1000-decibar surface, from data collected 3–6 June, 1949. Oceanographic station positions are indicated and the station numbers given at turning points.

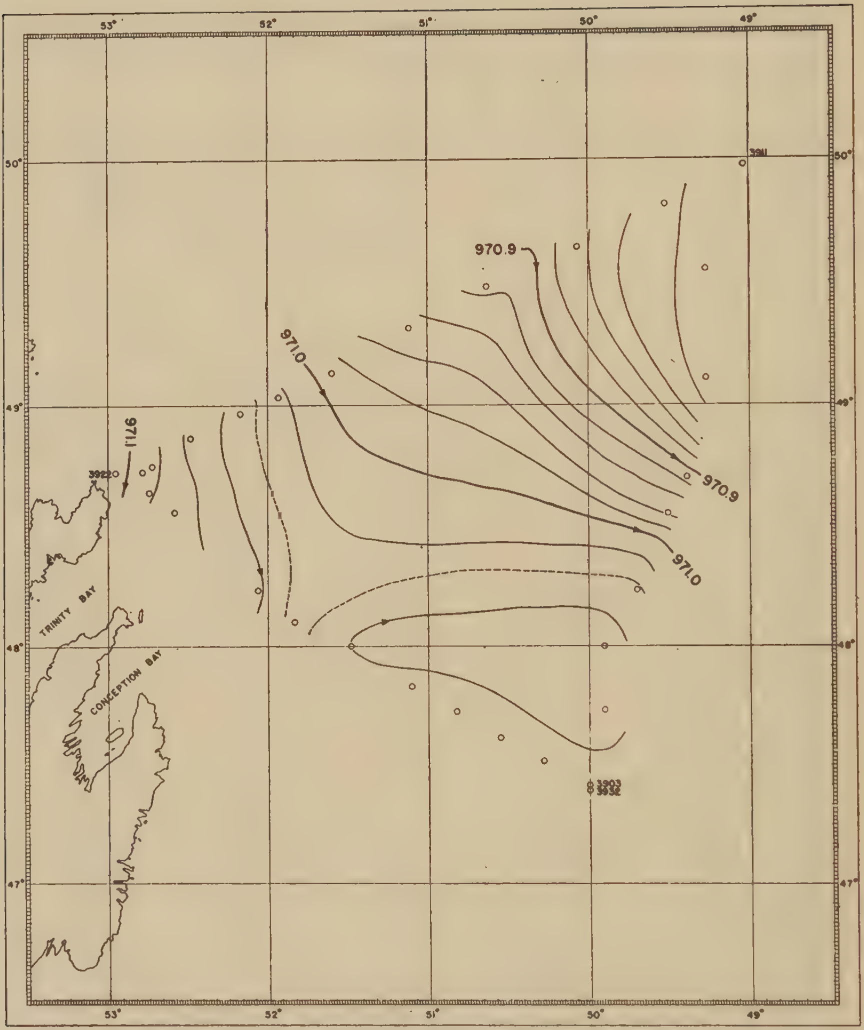
53°
52°
51°
50°
49°
50°
49°
48°
47°
3911
970.9
971.0
971.1
3922
970.9
971.0
TRINITY BAY
CONCEPTION BAY
3903
3932

FIGURE 20.—Dynamic topography of the sea surface relative to the 1,000-decibar surface, from data collected 17–20 June, 1949. Oceanographic station positions are indicated and the station numbers given at turning points.

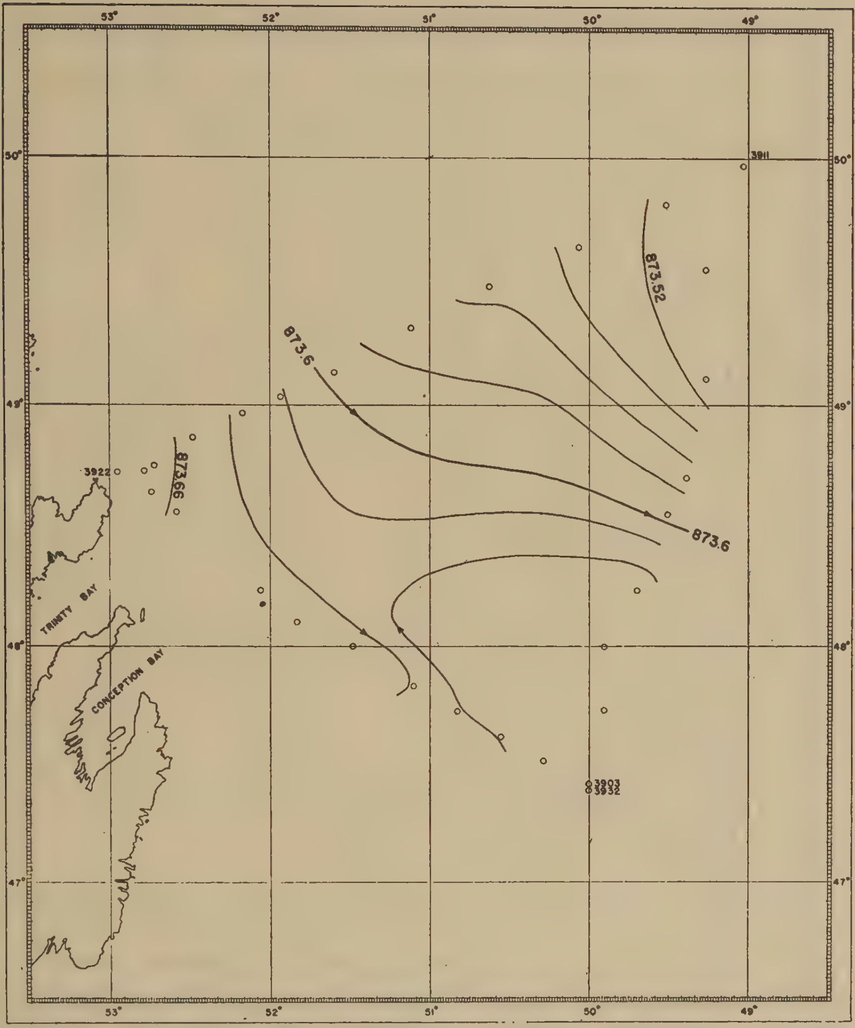
53°
52°
51°
50°
49°
50°
49°
48°
47°
3911
3922
873.52
873.6
873.6
873.66
TRINITY BAY
CONCEPTION BAY
3903
3932

FIGURE 21.—Dynamic topography of the 100-decibar surface relative to the 1,000-decibar surface, from data collected 17–20 June 1949. Oceanographic station positions are indicated and the station numbers given at turning points.

may be of use in determining the effects of water movements on bergs in the area. The berg's position on the 2d and 5th of June, from air sightings, are shown in figure 18. Upon completion of the occupation of the triangle, the *Evergreen* located the berg in the position indicated on the afternoon of the 7th and drifted with the berg until the afternoon of the 8th. The berg's position at noon of that day is also shown in figure 18. During the interval that the *Evergreen* was in the vicinity of the berg, seven current determinations were made with a von Arx current meter. The vector sum of the currents so determined agreed with the observed set of the berg as to direction but was smaller in magnitude than the observed drift and, if the surface current be assumed to equal the berg's drift, would have required a value of the factor K equal to about 1.15. This is quite reasonable in view of the comparatively shallow water and relatively large proportion of the water column presumed to be in motion. Quiet weather prevailed during the period the berg was under observation by the *Evergreen.* The berg's path between the sightings on the 2d and the 5th is in accord with the dynamic isobaths shown in figure 18, and is in that part of the area where the topography is best known. The easterly movement of the berg between the 5th and the 7th, across the isobaths as drawn, may be an exaggeration of the error in drawing the isobaths when it is considered that the berg was small (and consequently more affected by surface conditions) and that from the time of its sighting on the 5th until the evening of the 6th the winds were from the westerly quadrants and briefly reached force 7 from the southwest on the evening of the 5th.

Not much is known regarding the stability of the circulation pattern in the vicinity of this branch point of the Labrador Current. The repetition of the occupation of the triangle 2 weeks after the first occupation was made in the hope of getting some information on how rapidly the circulation pattern changes in this region. Comparison of figure 18 with figure 20 shows very little change in the general pattern during the 2-week interval.

The proportion in which the Labrador Current divides into its eastern and western branches is probably best based on the proportion of the volume of flow in the two branches. Expressed in millions of cubic meters per second the volume of flow past the northern section was computed to be 4.13 during the first occupation and 4.44 during the second occupation. For the southwestern section the first and second occupations showed 0.72 and 0.84 respectively; and for the southeastern section the volume of flow was computed to be 3.45 and 3.63. Thus, during the first occupation about 83 percent of the volume of flow followed the eastern branch and about 81 percent followed the eastern branch during the second occupation. This is to be compared to about 78 percent found during July 1948.

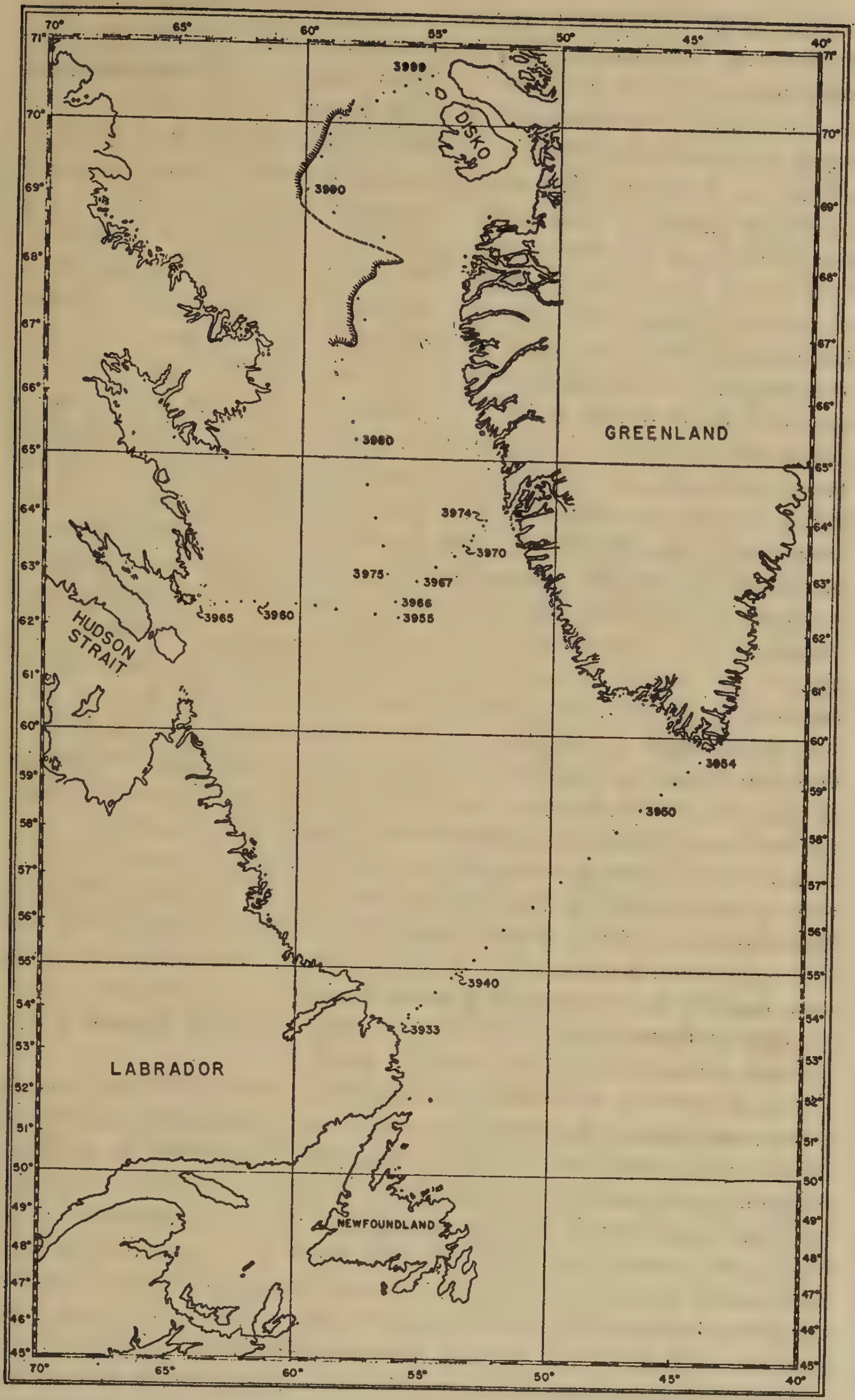

3999
3990
DISKO
3980
GREENLAND
3974
3970
3975
3967
3966
3955
3965
3960
HUDSON STRAIT
3954
3950
3940
3933
LABRADOR
NEWFOUNDLAND
70°
65°
60°
55°
50°
45°
40°
71°
70°
69°
68°
67°
66°
65°
64°
63°
62°
61°
60°
59°
58°
57°
56°
55°
54°
53°
52°
51°
50°
49°
48°
47°
46°
45°

FIGURE 22.—Location of oceanographic stations occupied in the Labrador Sea, Davis Strait and Baffin Bay during the 1949 postseason cruise.

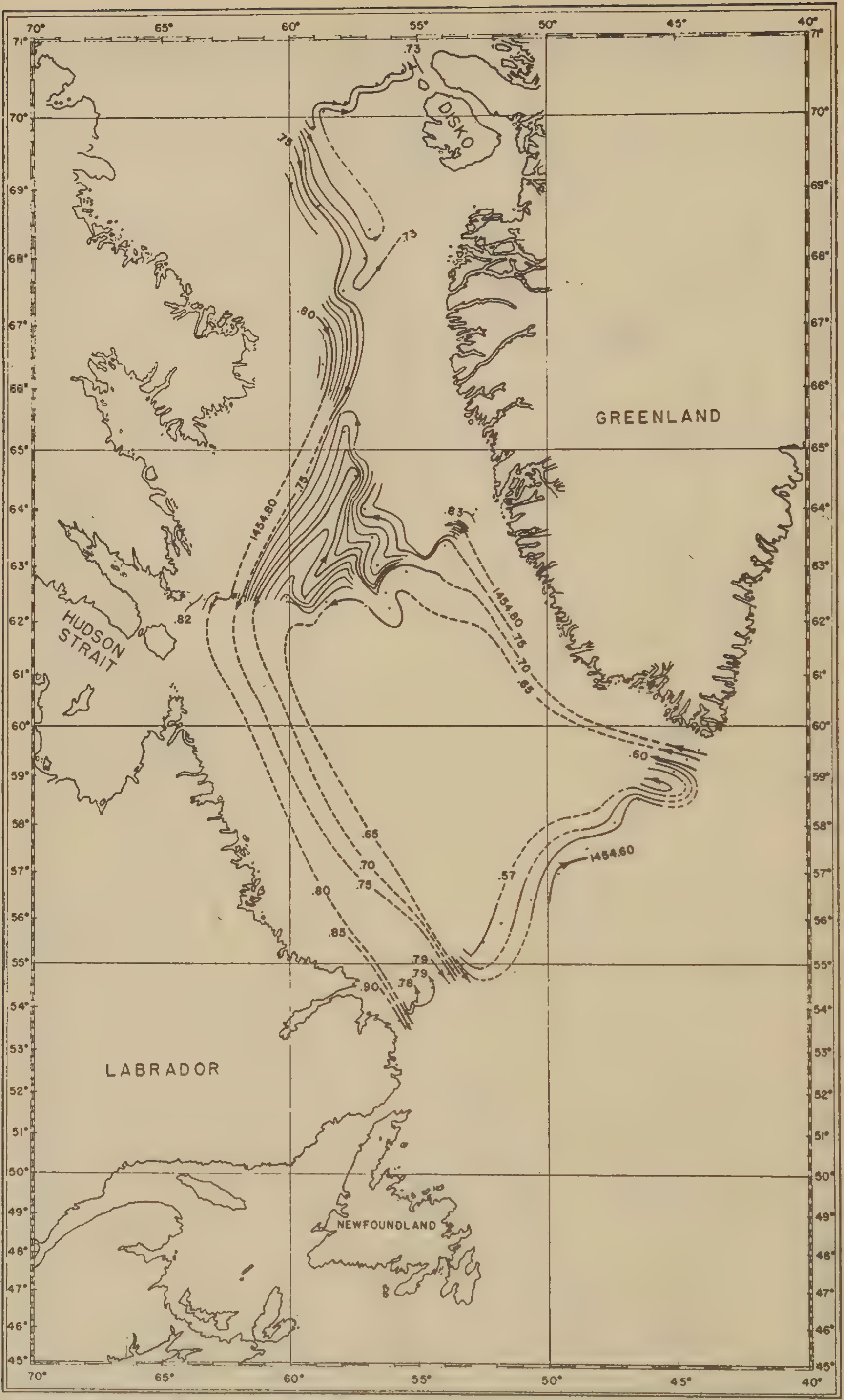
GREENLAND
DISKO
HUDSON STRAIT
LABRADOR
NEWFOUNDLAND
1454.80
1454.60
.73
.75
.80
.83
.82
.60
.65
.70
.57
.79
.78
.85
.90
70°
65°
60°
55°
50°
45°
40°
71°
69°
68°
67°
66°
64°
63°
62°
61°
59°
58°
57°
56°
54°
53°
52°
51°
49°
48°
47°
46°
45°

Figure 23.—Dynamic topography of the sea surface relative to the 1,500-decibar surface, from data collected 5–20 July 1949.

Figure 22 shows the location of the oceanographic stations occupied in the Labrador Sea, Davis Strait, and Baffin Bay on the postseason cruise. Figure 23 shows the dynamic topography of the sea surface relative to the 1,500-decibar surface based on these stations. Only the major features of the current pattern are shown since the distances between the different sections are too great to develop the details. The shoal on the Labrador shelf off Hamilton Inlet is probably responsible for the irregular course of the dynamic isobaths of 1454.78 and 1454.79. The total Labrador Current passing the South Wolf Island section from the beach out to station 3943 was computed at 5.16 million cubic meters per second with a mean temperature of about 2.3° C. Of this amount 1.45 million cubic meters per second are to be seen recurving northeastward between stations 3943 and 3947. By difference, this leaves 3.7 continuing southward. This figure is about 0.7 less than the volume of flow found at the northern section of the second occupation of the triangle about 2 weeks earlier, so it is presumed that about half of the 1.45 moving northeastward between stations 3943 and 3947 came from the vicinity of Flemish Cap and some of this probably represents a contribution from the outer margins of the North Atlantic eddy.

Station 3951 seems to be the center of a closed eddy. The volume of flow between stations 3947 and 3951 is computed as 2.63, which is 1.18 million cubic meters per second greater than the 1.45 found between stations 3943 and 3947, whence 1.18 has been deducted from the 3.70 found to be flowing northwestward between station 3951 and the beach at Cape Farewell to give 2.52 million cubic meters per second as the volume of flow of the West Greenland Current continuing northwestward along the Greenland coast. Of this 2.52 about 1.45 has been contributed from the southwestward, some of it from the closed circulation in the Labrador Sea and some of it as a direct contribution from the outer margins of the Atlantic Current, leaving only about 1.07 as the contribution to the West Greenland Current from the east of Cape Farewell. The mean temperature of this contribution from east of Cape Farewell was computed to be 3.22° C. and that of the West Greenland Current 3.62° C.

Farther north along the west coast of Greenland the section running from the deep water of the Labrador Sea to Fyllas Bank was occupied again. This section has again presented difficulties in the reconciliation of the results obtained there with other observations. This time the volume of flow computed between station 3966 and the beach, 3.95 million cubic meters per second, is about 1.5 larger than would have been expected from the results obtained off Cape Farewell, and is about 1.0 larger than the volume of flow southward past the Loks Land section between station 3956 and the beach. The most reasonable picture consistent with the other observations would require the southward return, between stations 3956 and 3966, of the western part of a closed counterclockwise eddy having a volume of flow of about 1.5 million cubic meters per second. This would stipulate the existence of a ridge in the dynamic topography between stations 3955 and 3966 on the east and 3956 on the west. In the exchange of water through Davis Strait, it would also mean a net contribution from Baffin Bay to the Labrador Sea of about 0.5 million cubic meters per second.

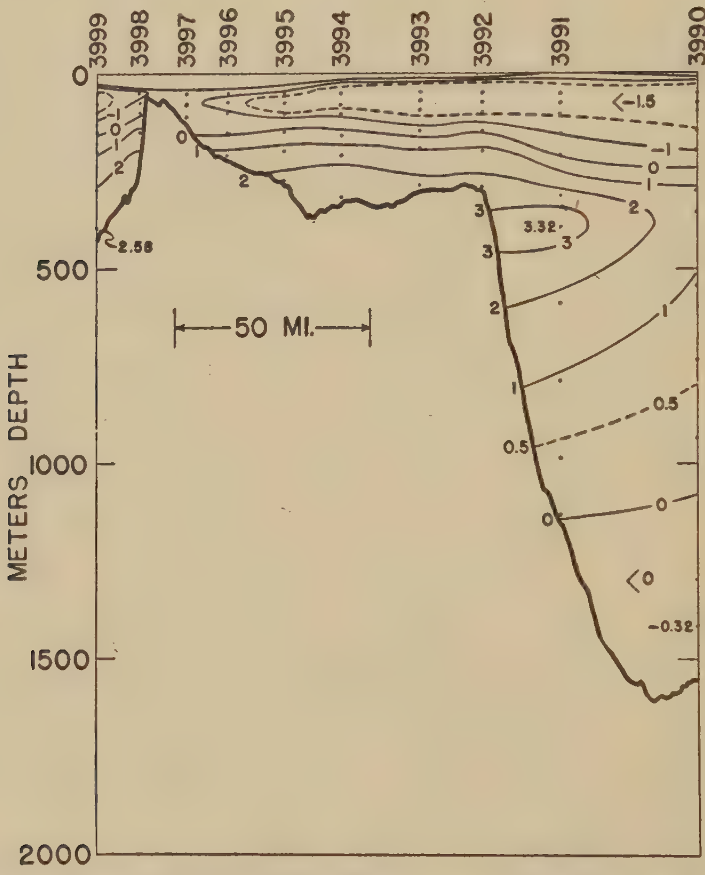

FIGURE 24.—Temperature distribution along a section extending from the deep water of southern Baffin Bay to the vicinity of the Nugssuak Peninsula, Greenland, 19–20 July 1949.

The Labrador Current passing the Loks Land section between station 3956 and the beach was computed to be 2.92 million cubic meters per second. This is made up of that part of the Baffin Land Current which flows southward across Davis Strait ridge and that part of the West Greenland Current which crosses to the American side south of this ridge. The latter, between stations 3956 and 3980, is computed at 0.40, while that part of the former between station 3980 and 3984 is computed as 1.70. This would leave, by difference, about 0.8 million cubic meters per second of the Baffin Land Current between stations 3984 and the beach.

If it is assumed that there was no significant net contribution to the Labrador Sea through Hudson Strait, the difference in volumes of flow past the Loks Land and South Wolf Island sections indicates about 2.2 million cubic meters per second of the circulation of the Labrador Sea passing the latter section was located toward the center of the Labrador Sea from station 3956.

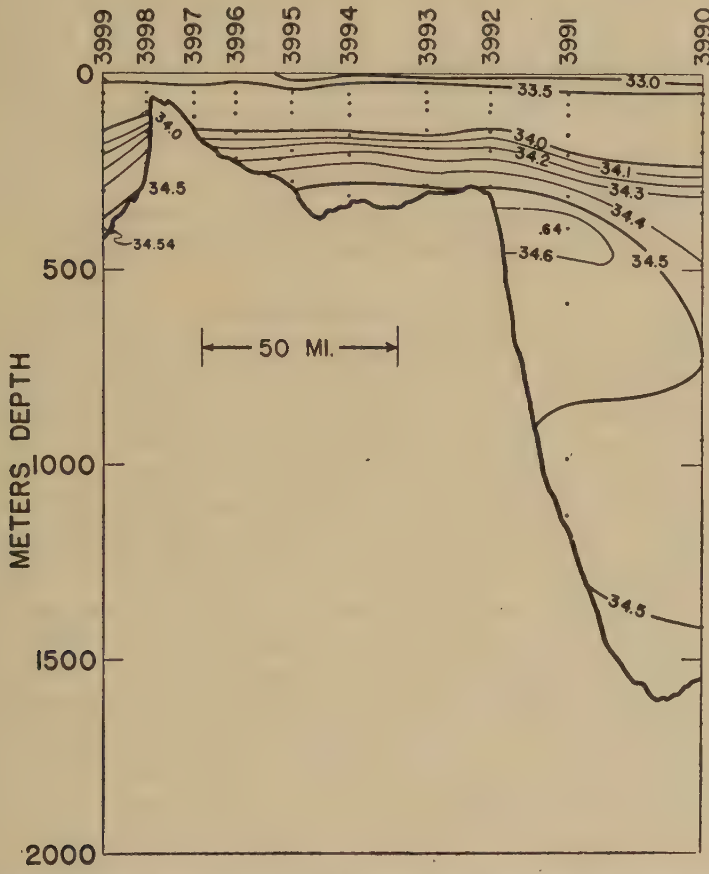

FIGURE 25.—Salinity distribution along a section extending from the deep water of southern Baffin Bay to the vicinity of the Nugssuak Peninsula, Greenland, 19–20 July 1949.

The observations taken along the section ending off the Nugssuak Peninsula at the northern end of the Vaigat are contradictory. The deepest station taken north of Davis Strait ridge and the only one in Baffin Bay extending to a depth of 1,500 meters was station 3990.

This station therefore served as a key station in referring the dynamic heights of the shallower stations to the 1,500-decibar surface. The dynamic topography at all levels above the 1,000-decibar surface was similar to that shown in figure 23 for the sea surface. Between about 1,000 and 1,500 meters at stations 3990 and 3991 a weak northerly flow was indicated by the dynamic heights with a southerly flow above about 1,000 meters. Figures 24 and 25 show the distribution of temperature and salinity respectively along this section and show maxima of each at about 400 meters at station 3991. The temperature of more than 3° C. and the salinity of more than 34.60 °/₀₀ indicate the West Greenland Current as the source of this water and consequently indicate a northward movement here, although at this level the dynamic topography shows a southward movement of about a half a centimeter per second. The results, therefore, of the computations of volume of flow past this section are to be regarded with suspicion and the northward flow, inshore of station 3992, of 0.38 million cubic meters per second is considered to be too small, whereas the southward flow, in the upper levels between stations 3990 and 3992, of 1.05 million cubic meters per second, is considered to be too large.

Figure 26 shows the temperature distribution along the vertical section from South Wolf Island to Cape Farewell found in 1949. On the Labrador shelf, the characteristic temperature minimum of the Labrador Current is present. The tongue of warmer water extending to bottom beneath the Labrador Current at the edge of the shelf is not as warm as usual and only slightly exceeds 3.4° C. This is in agreement with the deficiency of the warmer offshore part of the Labrador Current anticipated from the subnormal volumes of flow and mean temperatures found in the Grand Banks region earlier in the year. On the Greenland side the temperature maximum associated with the Irminger Current component of the West Greenland Current is decidedly colder than usual and less than 5° C. The temperature minimum of the intermediate water of the Labrador Sea is slightly less than 3.3° C. This is somewhat colder than in 1948, but still warmer than the approximately 3.17° found consistently during the summers of 1934 through 1939. The displacement of this temperature minimum toward the Labrador side is considered the result of water from the vicinity of Flemish Cap and the outer margins of the Atlantic Current entering the circulation of the Labrador Sea on the Greenland side.

The marked deficiency in the Irminger Current component of the West Greenland Current, noted in the discussion of the volume of flow at the Cape Farewell section and above in connection with the lower than usual temperature maximum of the West Greenland Current, can best be shown by consideration of the salinity. Figures

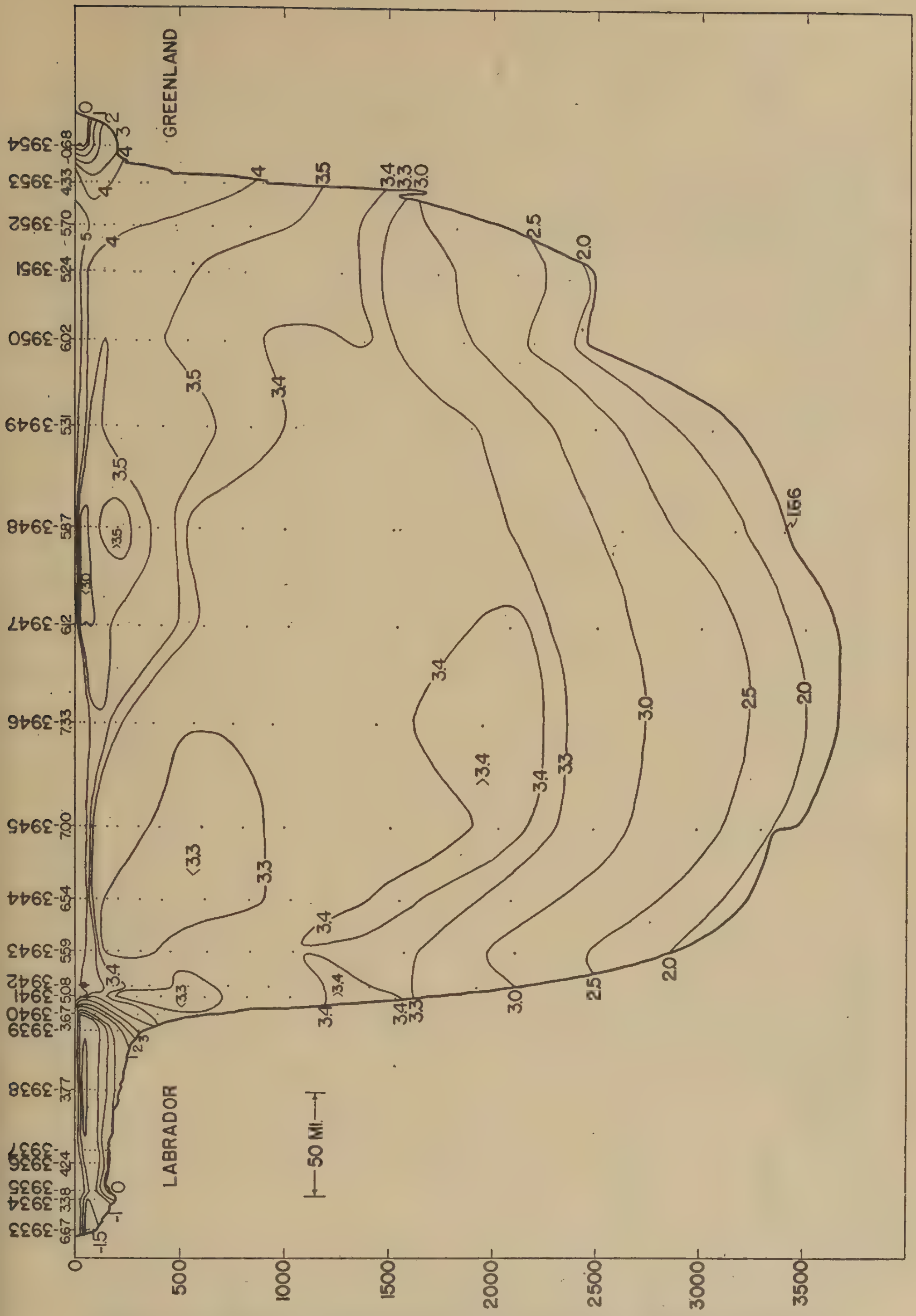

FIGURE 26.—Temperature distribution between South Wolf Island, Labrador, and Cape Farewell, Greenland, 5–9 July 1949.

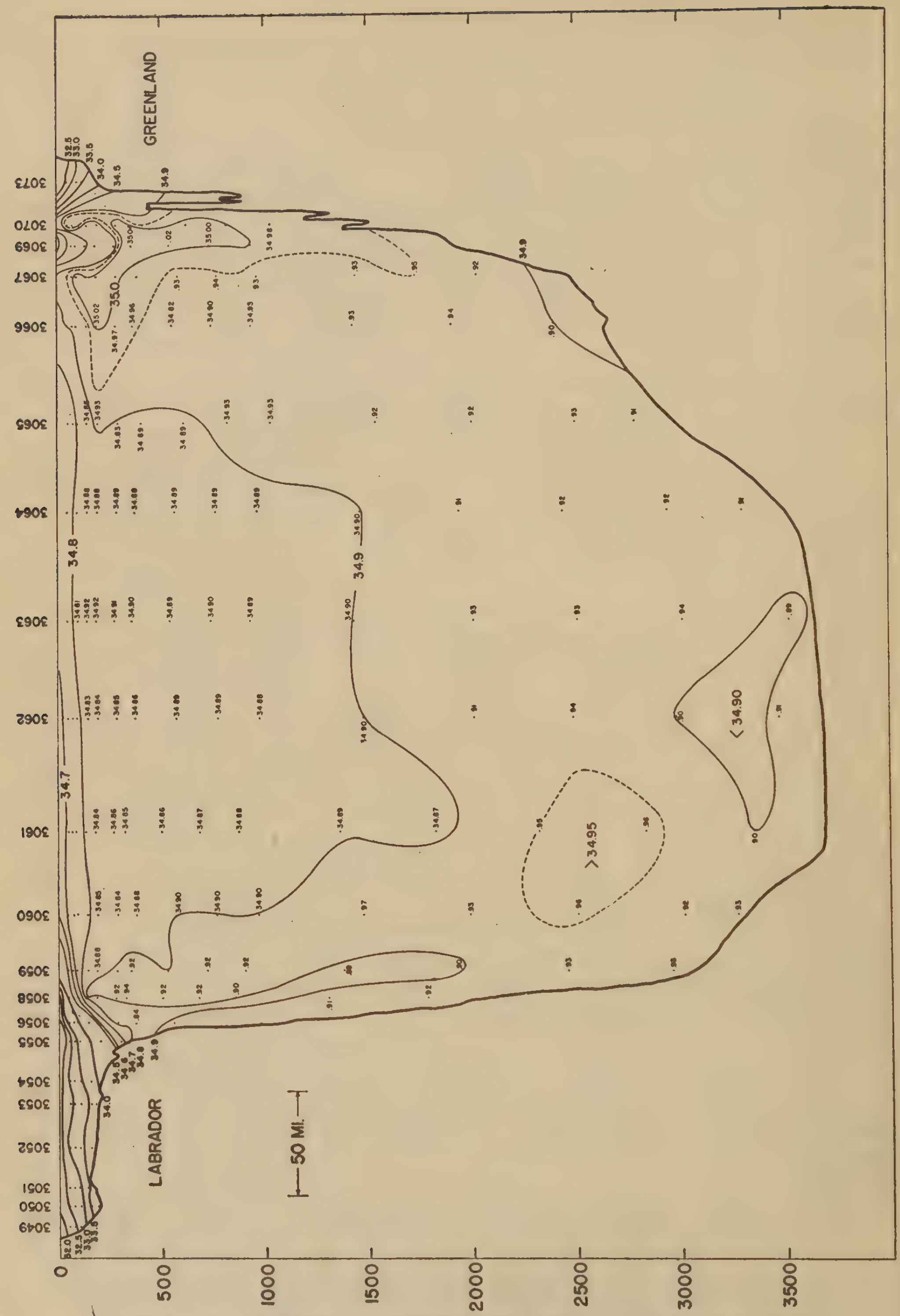

FIGURE 27.—Salinity distribution between South Wolf Island, Labrador, and Cape Farewell, Greenland, 10–15 July 1939.

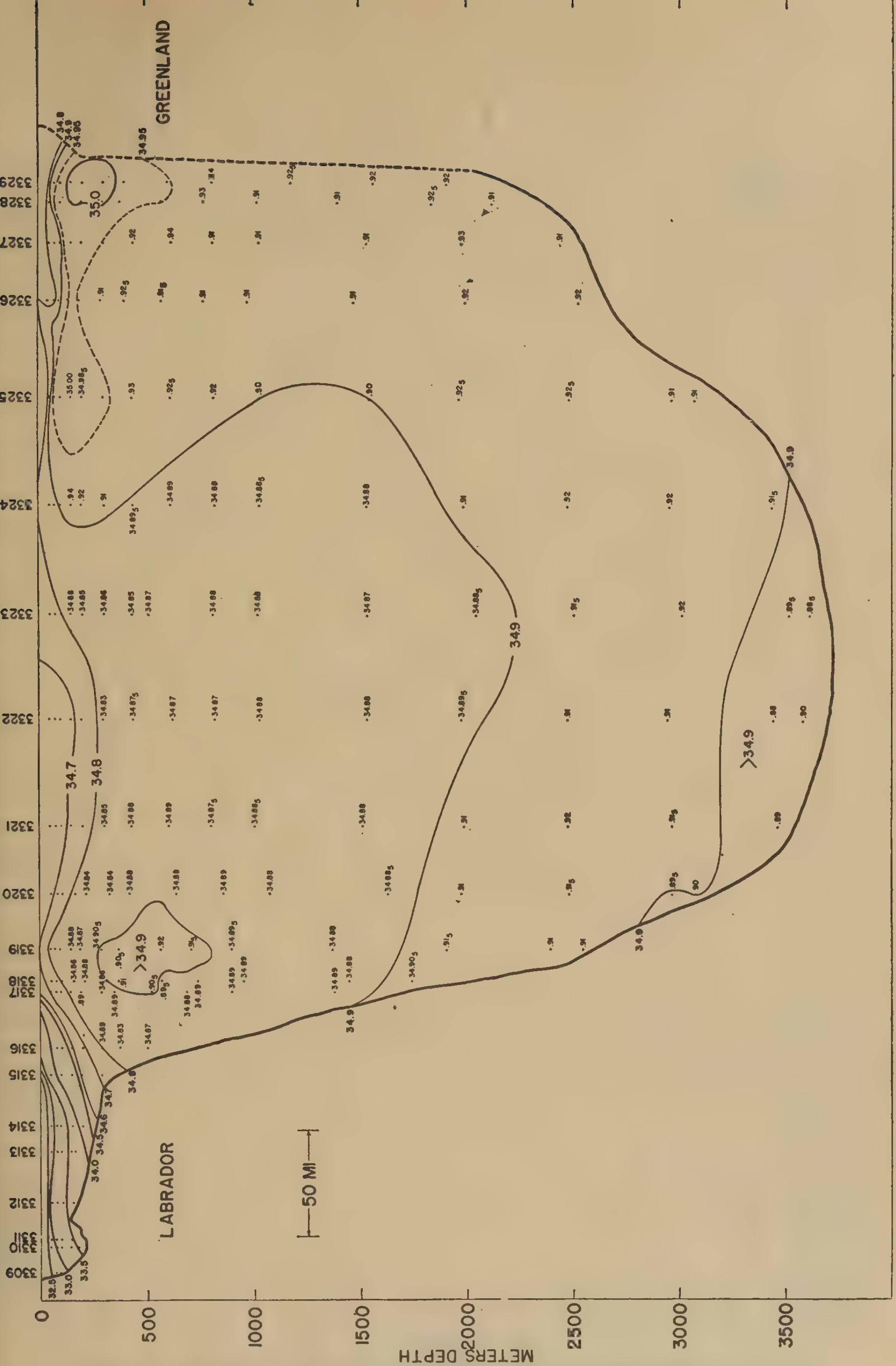

FIGURE 28.—Salinity distribution between South Wolf Island, Labrador, and Cape Farewell, Greenland, 25–29 June 1940.

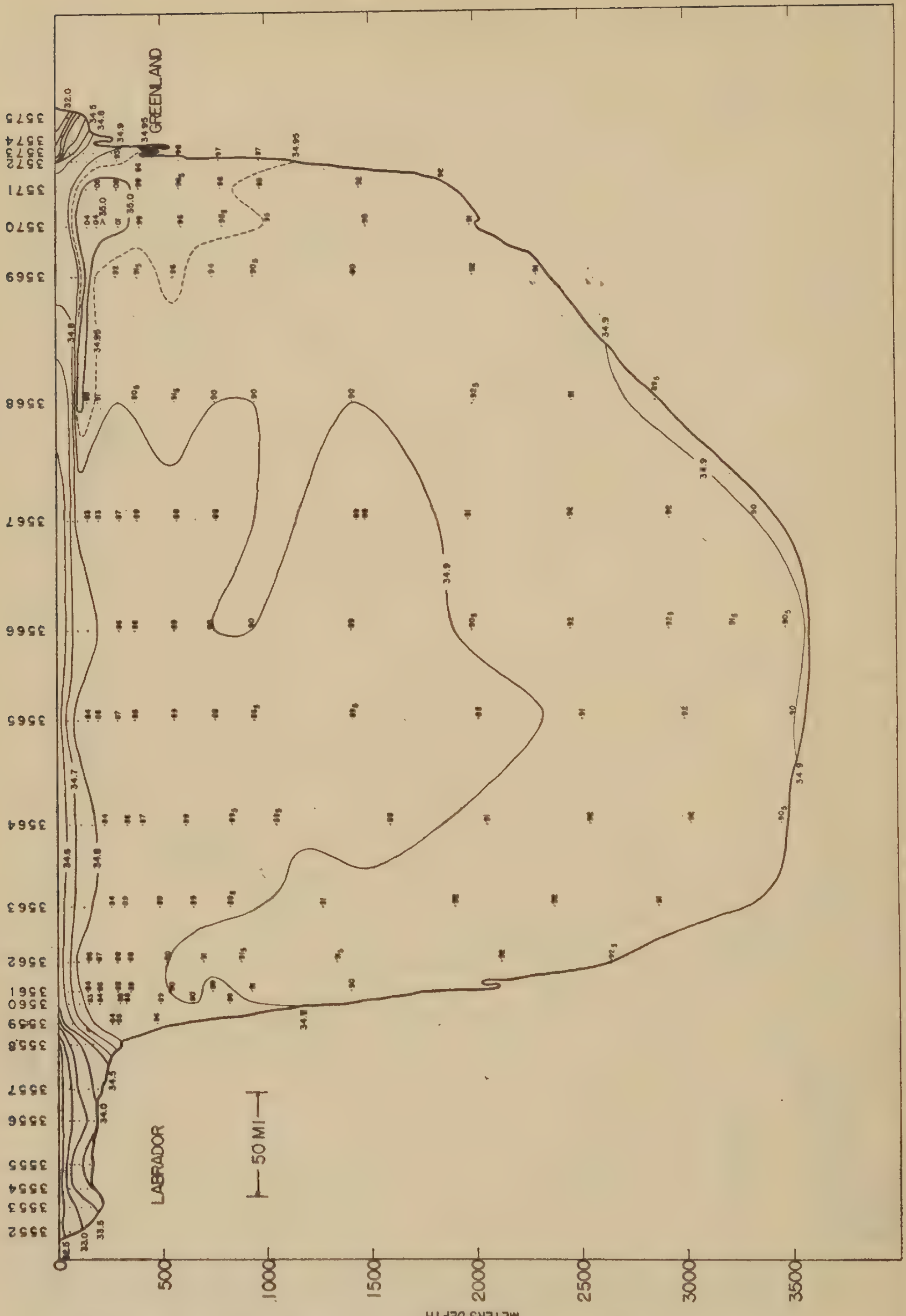

FIGURE 29.—Salinity distribution between South Wolf Island, Labrador, and Cape Farewell, Greenland, 24–29 July 1941.

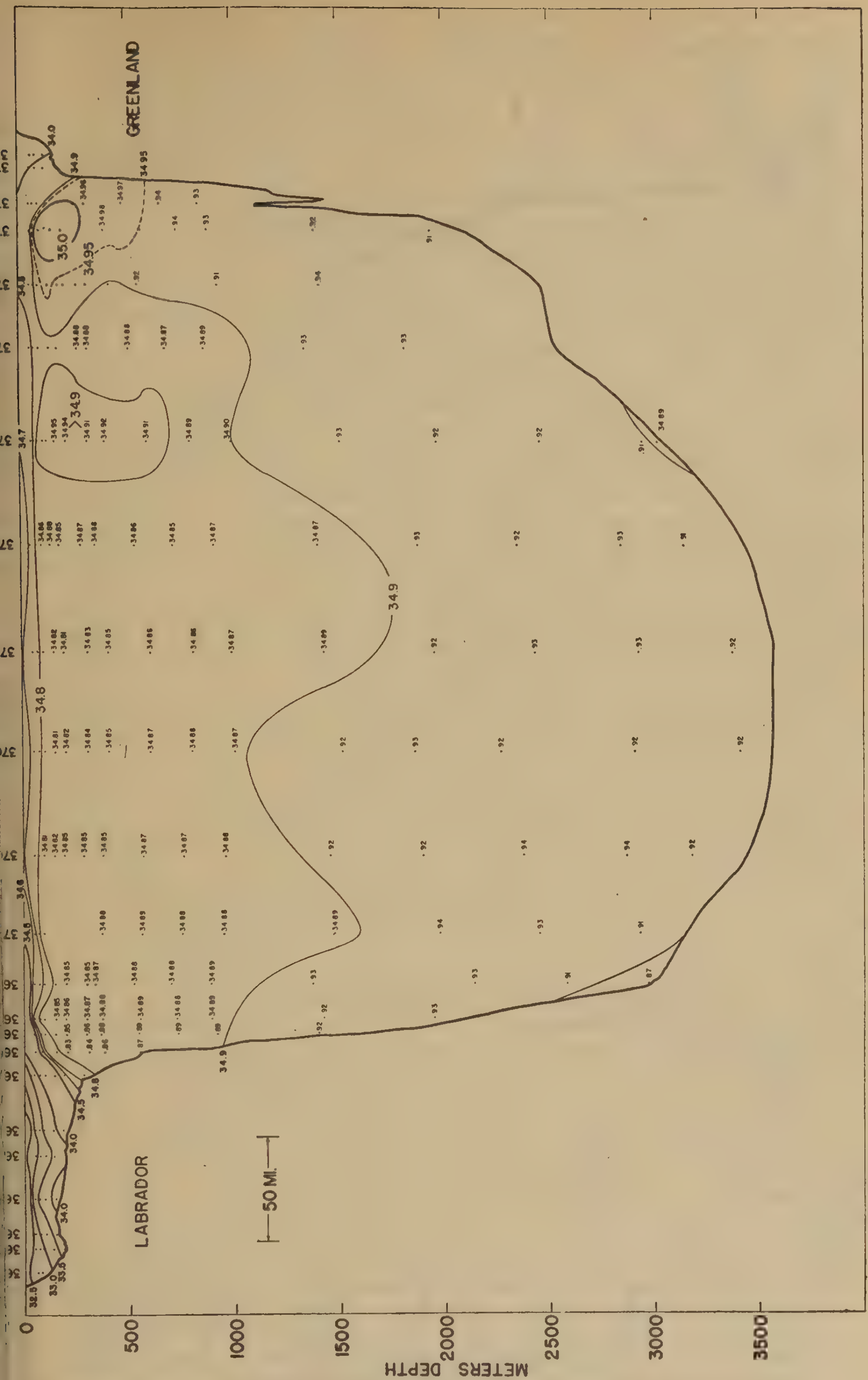

FIGURE 30.—Salinity distribution between South Wolf Island, Labrador, and Cape Farewell, Greenland, 11–17 July 1948.

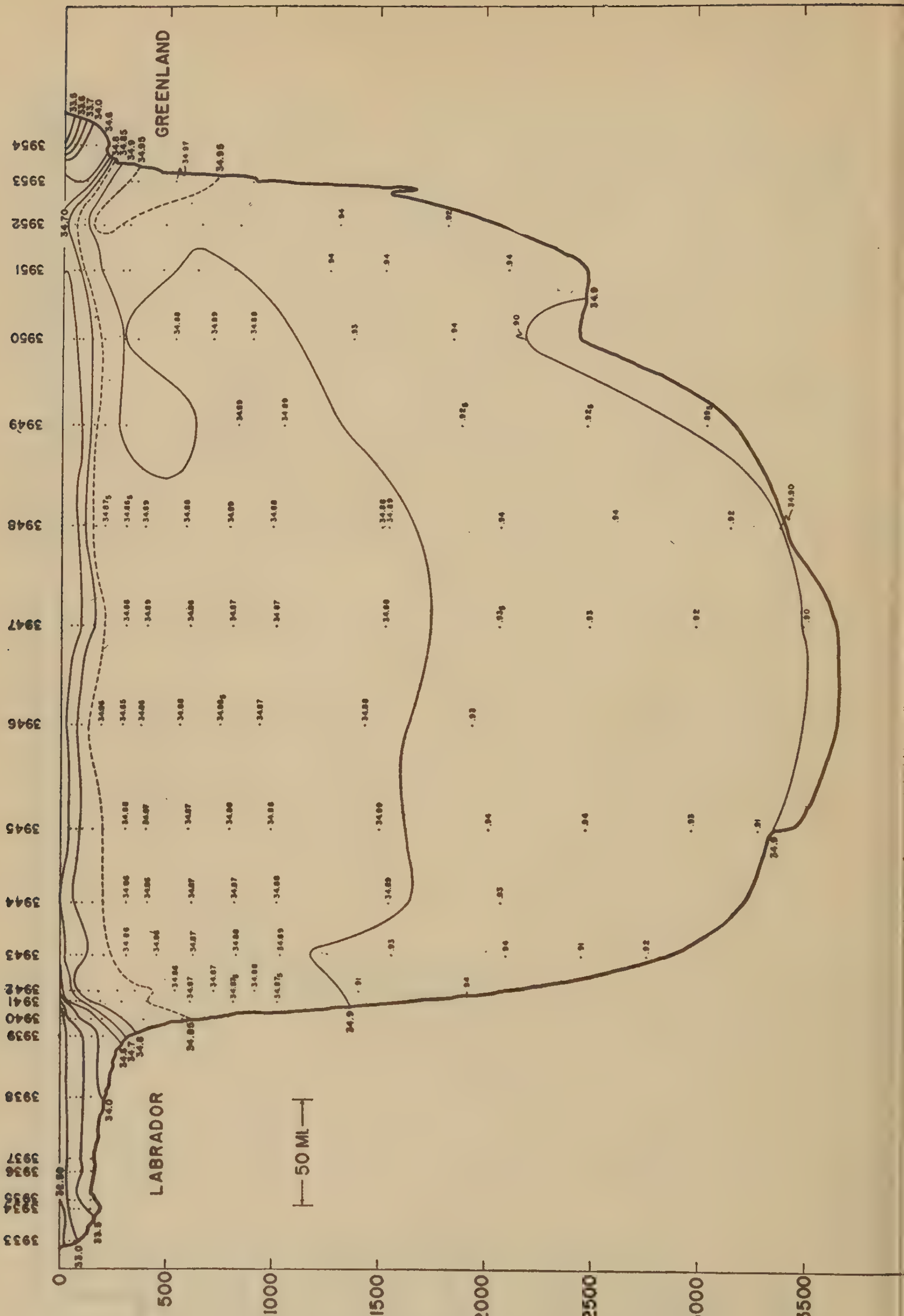

FIGURE 31.—Salinity distribution between South Wolf Island, Labrador, and Cape Farewell, Greenland, 5–9 July 1949.

27 through 31 show the salinity distribution in this section found during the postseason cruises of 1939, 1940, 1941, 1948, and 1949 respectively. The maximum salinity in the core of the Irminger Current component of the West Greenland Current at this section observed during these cruises was 35.04, 35.03, 35.05, 35.04, and 34.97 °/$_{\circ\circ}$ respectively. The remarkable uniformity of the maximum salinity of this water has come to be regarded as a characteristic of this part of the West Greenland Current and the extent of the cross sectional area has been sufficient that the spacing of the stations designed to permit the construction of a good vertical section of anomaly of specific volume has given short enough station intervals to reveal the shape of this warm and salty core.

The temperature is a more effective variable than the salinity of the Irminger Current water. It is therefore that the drop in the salinity shown in figure 31 compared with figures 27 through 30 is such a striking demonstration of the almost total absence of Irminger Current water off Cape Farewell in 1949. Physically and climatologically it is the variation in temperature, rather than salinity, of this warm water core that is of importance. The drop in temperature of the core accompanying the drop in salinity was sufficient to increase its density by about 0.10 in σ_t above the usual values. As it is the Irminger Current component that makes the West Greenland Current a warm current, and as the West Greenland Current supplies most of the water-borne heat to Baffin Bay and forms the relatively warm offshore part of the Labrador Current, any prolonged deficiency in Irminger Current water reaching Cape Farewell can be expected to have serious repercussions in its effect on the extent and duration of the ice cover in Baffin Bay and the mortality rate of bergs in the journey from their parent glaciers in Greenland to the position of their ultimate disintegration near the steamer lanes in the vicinity of the Grand Banks.

In earlier bulletins of this series it has been noted that while the year to year fluctuations in the volume of flow of the West Greenland Current off Cape Farewell are so large as to mask any regular seasonal fluctuation, the mean temperature of this current seemed to have a marked seasonal increase during the summer months. Because of the rapid increase, in spite of the fact that a relatively small part of the volume of water involved is exposed to the surface, it would seem more reasonable to expect the fluctuation to be the result of a changing proportion of the parent currents which join northeastward of Cape Farewell to make up the West Greenland Current. A seasonal fluctuation in the mean temperature of the West Greenland Current can result from seasonal fluctuations in the relatively cold East Greenland Current or the relatively warm Irminger Current, or both.

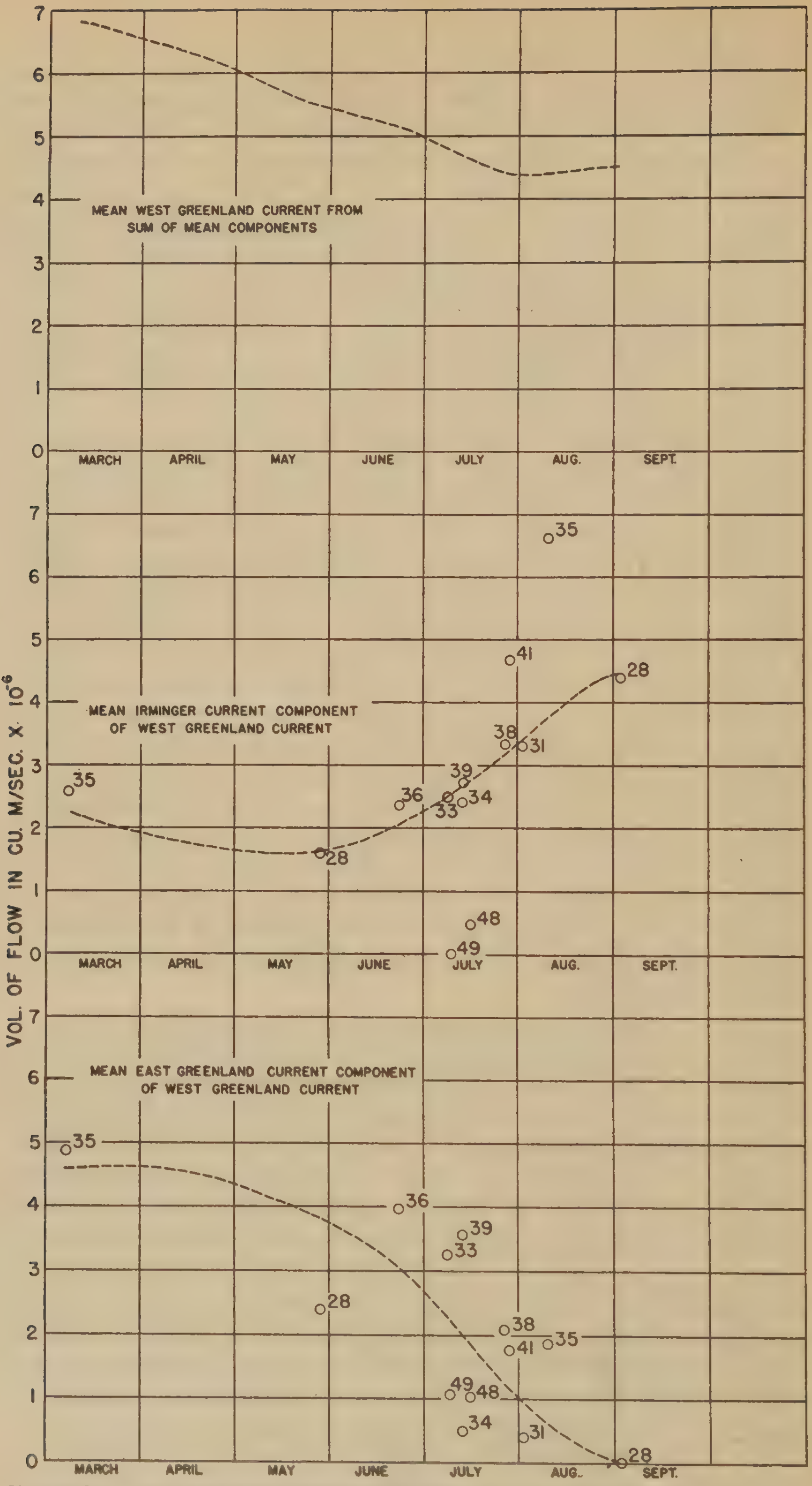

Figure 32.—Computed East Greenland Current and Irminger Current components of the West Greenland Current off Cape Farewell plotted against season. Numerals indicate last two digits of year of observation. Mean curves of seasonal variation of the two components are drawn through the plotted points. The mean curve of seasonal variation of the West Greenland Current is the sum of the

As a first approximation it was assumed that the mean temperature of the East Greenland Current was constant at 3.2° C., the value of the mean temperature of the water contributed to the West Greenland Current from the eastward in 1949 when the Irminger Current was almost completely absent; and that the mean temperature of the Irminger Current was constant at 5.5° C., the highest recorded value of the mean temperature of the West Greenland Current (September 1928). From the total volume of flow of the West Greenland Current and the total heat transport of that current the volume of flow of each of the components was then computed for the 13 occupations of the section which are available over the years from 1928 through 1949. The 13 values for each component were then plotted against time of year with the results shown in figure 32.

There appears to be a seasonal summertime increase in the volume of flow of the Irminger Current and a seasonal summertime decrease in the volume of flow of the East Greenland Current as they contribute to the West Greenland Current at Cape Farewell. The two curves representing these fluctuations and the curve, derived from their sum, representing the seasonal fluctuation in the West Greenland Current are approximations both because the mean temperatures of the two parent currents probably are not constant, as assumed; and because of the small number of points on which they are based. A southward shift of the northern boundary of the North Atlantic eddy, whether arising from a shift of the entire eddy or from a contraction of the eddy, would have the effect of reducing the Irminger Current. Such a reduction conceivably could take place with little or no noticeable change in the northward transport of salt or water-borne heat in the area east of Iceland. In such a circumstance as occurred in the summer of 1949, however, when practically no Irminger Current water reached Cape Farewell, a much greater reduction in the supply of water-borne heat to the Arctic could result.

A seasonal latitudinal shift of the northern boundary of Atlantic Current water in the Grand Banks sector of the North Atlantic eddy has been found and reported in Bulletin No. 31 of this series,[3] and has been correlated with the volume of flow of the Labrador Current and with the seasonal fluctuation in the different in sea level across the Gulf Stream at the Charleston-Bermuda section 13½ months earlier. If a time lag is involved between the Grand Banks sector and the Irminger Current, it might be expected to be of the same order of magnitude. Thus, if the surveys made in the Grand Banks region during a particular ice season show the boundary of Atlantic

---

[3] Soule, Floyd M., and C. A. Barnes, "International Ice Observation and Ice Patrol Service in the North Atlantic Ocean—Season of 1941." U. S. Coast Guard Bull. No. 31, pp. 15-24 (1950), Washington.

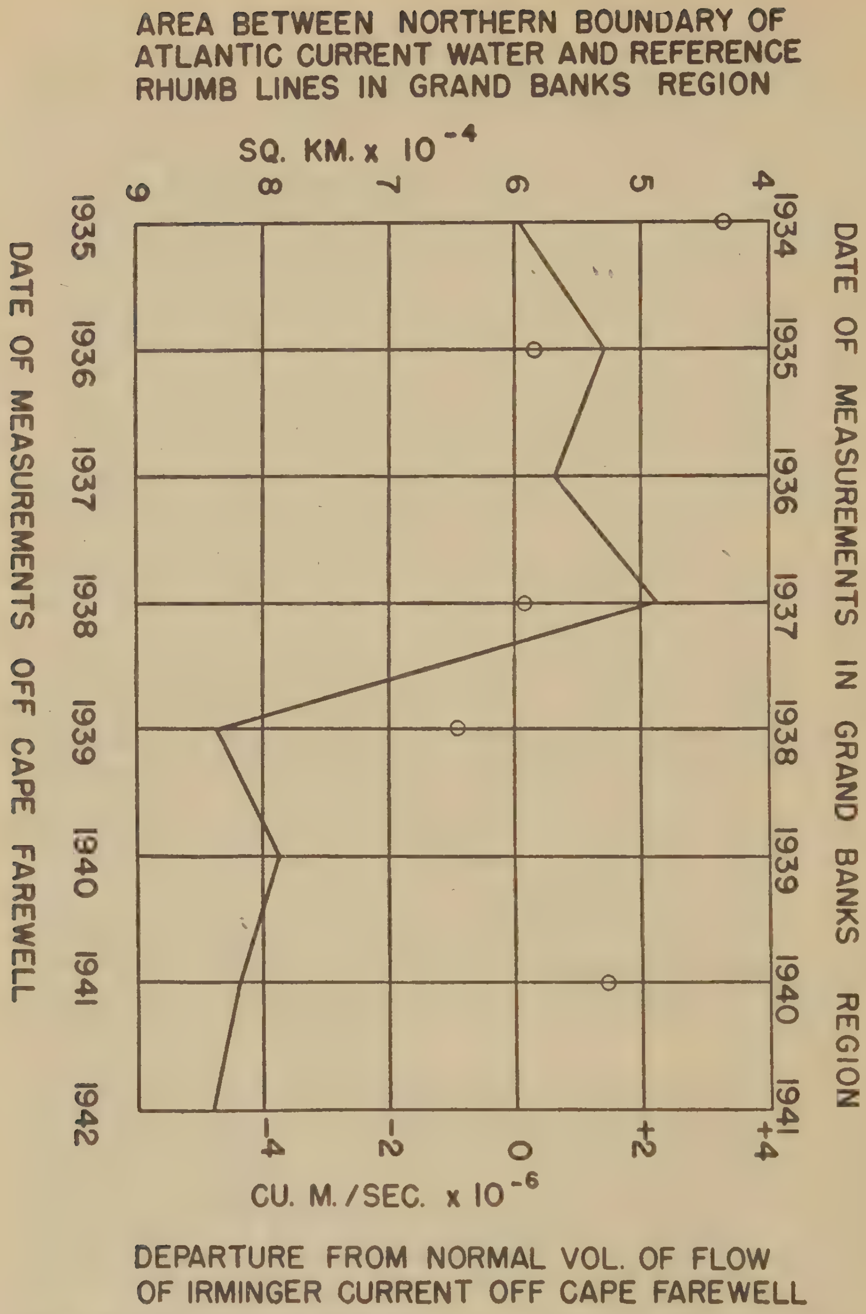

FIGURE 33.—Comparison of the latitudinal position of the northern boundary of Atlantic Current water in the Grand Banks region and the departure from normal volume of flow of the Irminger Current component of the West Greenland Current off Cape Farewell the following year.

Current water to be farther south than usual, one might expect that the Irminger Current contribution to the West Greenland Current at Cape Farewell would be smaller than usual the following summer. The few available data do not show such a simple relationship.

If the area between the boundary of Atlantic Current water and fixed reference rhumb lines in the Grand Banks region be taken as a measure of the southward retreat of the northern margin of the North Atlantic eddy, and if the curve for the Irminger Current water component of the West Greenland Current shown in figure 32 be taken as a normal curve, the southward retreat of the northern boundary of the North Atlantic eddy for the period 1934 to 1941 is represented by the solid curve in figure 33 and the departure from normal of the computed Irminger Current contribution to the West Greenland Current the following summer is represented by the five points plotted in figure 33. Only one other point is available and has been omitted from figure 33 because of the considerable interval of time. The single survey of 1948 gave an area of 7.80 and in 1949 the Irminger Current component of the West Greenland Current was computed to be 2.53 below normal. The units of area are 10,000 square kilometers and the Irminger Current units are 1 million cubic meters per second volume of flow. It would seem from the foregoing that other important modifying factors are interposed between the Grand Banks and the Irminger Current at Cape Farewell.

SUMMARY

1. Three dynamic topographic charts of the ice-patrol area in the Grand Banks region resulting from as many surveys form the basis of a discussion of the circulation in that area during the 1949 ice season.
2. The location of the northern boundary of Atlantic Current water found during one survey made in 1948 and two surveys in 1949 has been discussed with respect to fluctuation in the difference in sea level across the Gulf Stream at the Charleston-Bermuda section and the strength of the Labrador Current in the Grand Banks region.
3. The temperature-salinity relationships of the different water masses found in the Grand Banks region in 1949 have been discussed and compared with conditions found in previous years.
4. The subnormal volume of flow of the Labrador Current in the Grand Banks region, found consistently during the 1949 season, has been related to a deficiency in the contribution of the West Greenland Current to the Labrador Current.
5. The division of the Labrador Current, just north of the Grand Banks, into the branches which flow along the Avalon Peninsula

and along the eastern edge of the Grand Banks, has been discussed on the basis of two triangular surveys made 2 weeks apart.

6. The thermal conditions in the intermediate water of the Labrador Sea found in 1949 have been noted and compared to those found in earlier years.

7. The circulation in the Labrador Sea, Davis Strait, and southern Baffin Bay has been discussed on the basis of six sections across the major currents in these regions.

8. The almost total absence of the Irminger Current component of the West Greenland Current at Cape Farewell in 1949 has been discussed, and mean curves representing the approximate seasonal variation in the volume of flow of the East Greenland Current component and the Irminger Current component of the West Greenland Current deduced from earlier occupations of the Cape Farewell section.

Following are tabulated the data collected during the 1949 season and postseason cruises. The individual station headings give the station number, date, geographic position, depth of water, and the dynamic height of the sea surface used in the construction of the dynamic topographic charts shown in figures 14, 15, 16, 18, and 20 for which the dynamic heights have been referred to the 1,000-decibar surface, and for figure 23 for which the dynamic topography has been referred to the 1,500-decibar surface. The depths of water are uncorrected sonic soundings based on a sounding velocity of 800 fathoms per second. Where the depths of the scaled values are enclosed in parentheses, the data are based on extrapolated vertical distribution curves of temperature or salinity or both. Asterisks appearing before observed temperatures indicate that these temperatures were determined from the depth of reversal and the corrected reading of an unprotected thermometer. The symbol σ_t signifies 1,000(density—1) at atmospheric pressure and temperature t.

TABLES OF OCEANOGRAPHIC DATA

STATIONS OCCUPIED IN 1949

Station 3747; 5 Apr.; latitude 43°41.5′ N., longitude 51°38′ W.; depth 89 meters; dynamic height 971.034

Observed values			Scaled values			
Depth, meters	Temperature, °C.	Salinity, ‰	Depth, meters	Temperature, °C.	Salinity, ‰	σ_t
0	2.76	33.11	0	2.76	33.11	26.42
24	2.79	33.17	25	2.80	33.17	26.47
48	2.89	33.19	50	2.95	33.25	26.52
72	3.74	33.83	(75)	3.80	33.89	26.94

Station 3748; 5 Apr.; latitude 43°34′ N., longitude 51°50′ W., depth 176 meters; dynamic height 971.022

Observed values			Scaled values			
Depth, meters	Temperature, °C.	Salinity, ‰	Depth, meters	Temperature, °C.	Salinity, ‰	σ_t
0	3.84	33.41	0	3.84	33.41	26.56
25	3.90	33.45	25	3.90	33.45	26.59
50	3.96	33.53	50	3.96	33.53	26.65
75	3.59	33.87	75	3.59	33.87	26.95
100	3.61	34.05	100	3.61	34.05	27.09
150	2.38	34.16	150	2.38	34.16	27.29

Station 3749; 5 Apr.; latitude 43°31′ N., longitude 51°54′ W.; depth 348 meters; dynamic height 971.029

Observed values			Scaled values			
Depth, meters	Temperature, °C.	Salinity, ‰	Depth, meters	Temperature, °C.	Salinity, ‰	σ_t
0	3.68	33.37	0	3.68	33.37	26.54
22	3.80	33.45	25	3.80	33.46	26.61
43	4.29	33.61	50	4.60	33.71	26.72
65	5.59	33.93	75	5.20	34.03	26.91
86	4.71	34.11	100	3.70	34.06	27.09
129	1.50	33.95	150	1.55	34.00	27.22
173	1.78	34.08	200	2.55	34.25	27.35
259	4.91	34.60	(300)	5.25	34.76	27.48

Station 3750; 5-6 Apr.; latitude 43°28′ N., longitude 52°01′ W.; depth 842 meters; dynamic height 971.059

Observed values			Scaled values			
Depth, meters	Temperature, °C.	Salinity, ‰	Depth, meters	Temperature, °C.	Salinity, ‰	σ_t
0	5.06	33.71	0	5.06	33.71	26.67
23	5.10	33.71	25	5.10	33.71	26.67
46	5.07	33.70	50	5.10	33.71	26.67
69	5.31	33.83	75	5.30	33.79	26.70
92	5.32	34.57	100	5.45	33.94	26.81
137	7.22	33.75	150	7.00	34.58	27.11
183	6.45	34.67	200	6.25	34.70	27.30
275	5.24	34.65	300	5.00	34.68	27.45
228	6.00	34.76	400	4.45	34.84	27.63
408	4.43	34.84	600	4.20	34.88	27.70
632	4.16	34.89	(800)	4.00	34.90	27.73

Station 3751; 6 Apr.; latitude 43°21′ N., longitude 52°08′ W.; depth 1829 meters; dynamic height 971.058

Observed values			Scaled values			
Depth, meters	Temperature, °C.	Salinity, ‰	Depth, meters	Temperature, °C.	Salinity, ‰	σ_t
0	6.28	33.97	0	6.28	33.97	26.72
24	6.31	33.93	25	6.30	33.97	26.72
48	6.34	33.97	50	6.35	33.97	26.72
71	6.41	33.99	75	6.40	33.99	26.72
95	6.24	33.98	100	6.20	33.98	26.74
143	6.12	34.53	150	6.15	34.58	27.22
191	6.51	34.72	200	6.45	34.73	27.30
286	5.64	34.77	300	5.50	34.78	27.46
392	4.73	34.81	400	4.70	34.81	27.58
589	4.50	34.91	600	4.50	34.92	27.69
789	4.33	34.98	800	4.30	34.98	27.75
987	3.95	34.92	1,000	3.95	34.92	27.75
1,482	3.73	34.97	-------	-------	-------	-------

Station 3752; 7 Apr.; latitude 43°07′ N., longitude 52°19′ W.; depth 2926 meters; dynamic height 971.066

Observed values			Scaled values			
Depth, meters	Temperature, °C.	Salinity, ‰	Depth, meters	Temperature, °C.	Salinity, ‰	σ_t
0	5.40	33.80	0	5.40	33.80	26.70
27	5.48	33.81	25	5.45	33.81	26.71
53	5.85	33.90	50	5.80	33.89	26.72
79	6.19	33.96	75	6.10	33.95	26.74
105	7.05	34.44	100	6.85	34.36	26.96
159	6.97	34.68	150	7.05	34.66	27.17
211	4.60	34.41	200	4.95	34.47	27.29
316	5.43	34.75	300	5.35	34.71	27.43
400	4.82	34.75	400	4.82	34.75	27.52
600	4.00	34.85	600	4.00	34.85	27.69
801	4.07	34.91	800	4.05	34.91	27.73
1,007	3.99	34.92	1,000	4.00	34.92	27.75
1,531	3.77	34.97	-------	-------	-------	-------

Station 3753; 7 Apr.; latitude 42°53′ N., longitude 52°33′ W.; depth 3292 meters; dynamic height 971.080

Observed values			Scaled values			
Depth, meters	Temperature, °C.	Salinity, ‰	Depth, meters	Temperature, °C.	Salinity, ‰	σ_t
0	9.92	34.83	0	9.95	34.83	26.85
24	9.99	34.89	25	10.00	34.89	26.88
49	10.14	34.91	50	10.15	34.91	26.88
73	10.28	34.85	75	10.30	34.96	26.89
98	10.84	35.10	100	10.90	35.12	26.91
147	11.69	35.45	150	11.50	35.45	27.05
195	7.39	34.73	200	7.20	34.73	27.19
293	5.89	34.71	300	5.85	34.71	27.36
364	5.36	34.74	400	5.30	34.77	27.48
550	5.12	34.92	600	4.75	34.91	27.65
740	3.87	34.87	800	3.90	34.93	27.76
877	3.92	35.01	1,000	3.90	35.00	27.82
1,590	3.80	34.96	-------	-------	-------	-------

Station 3754; 13 Apr.; latitude 42°02.5′ N., longitude 52°04′ W.; depth 4024 meters; dynamic height 971.182

Observed values			Scaled values			
Depth, meters	Temperature, °C.	Salinity, ‰	Depth, meters	Temperature, °C.	Salinity, ‰	σ_t
0	13.57	35.69	0	13.57	35.69	26.83
23	13.57	35.69	25	13.55	35.69	26.83
46	13.58	35.70	50	13.60	35.70	26.83
69	13.59	35.70	75	13.60	35.70	26.83
92	13.59	35.70	100	13.60	35.70	26.83
138	13.59	35.69	150	13.45	35.66	26.83
184	12.44	35.51	200	12.00	35.49	26.99
276	-------	-------	300	9.50	35.22	27.23
285	10.00	35.26	400	7.00	35.00	27.44
430	6.54	34.97	600	5.20	34.98	27.66
576	5.35	34.98	800	4.55	34.97	27.73
737	4.67	34.98	1,000	4.15	34.96	27.76
1,165	3.83	34.94	-------	-------	-------	-------

Station 3755; 14 Apr.; latitude 41°59.5′ N., longitude 50°59′ W.; depth 3365 meters; dynamic height 971.126

Observed values			Scaled values			
Depth, meters	Temperature, °C.	Salinity, ‰	Depth, meters	Temperature, °C.	Salinity, ‰	σ_t
0	12.63	35.46	0	12.63	35.46	26.85
27	12.59	35.46	25	12.60	35.45	26.84
53	12.55	35.44	50	12.55	35.44	26.84
80	12.55	35.44	75	12.55	35.44	26.84
105	12.61	35.45	100	12.60	35.45	26.84
159	12.54	35.50	150	12.60	35.50	26.88
212	11.20	35.35	200	11.50	35.38	27.00
317	8.56	35.13	300	9.00	35.16	27.27
360	7.51	35.06	400	6.60	34.99	27.48
562	3.39	34.66	600	3.40	34.70	27.63
780	3.44	34.87	800	3.60	34.87	27.75
998	3.87	34.90	1,000	3.85	34.91	27.75
1,423	3.77	34.94	-------	-------	-------	-------

STATIONS OCCUPIED IN 1949—Continued

Observed values			Scaled values			
Depth, meters	Temperature, °C.	Salinity, ‰	Depth, meters	Temperature, °C.	Salinity, ‰	σ_t
Station 3756; 14 Apr.; latitude 42°21′ N., longitude 51°30′ W.; depth 2743 meters; dynamic height 971.069						
0	5.24	33.61	0	5.24	33.61	26.57
29	5.33	33.66	25	5.30	33.65	26.59
58	7.35	34.21	50	6.70	34.05	26.73
87	10.29	34.79	75	9.40	34.57	26.74
115	7.08	34.43	100	8.50	34.64	26.93
173	6.40	34.65	150	6.60	34.56	27.15
230	6.08	34.71	200	6.25	34.68	27.29
345	5.40	34.81	300	5.65	34.78	27.45
406	4.51	34.75	400	4.55	34.75	27.55
603	4.29	34.89	600	4.30	34.89	27.69
795	4.18	34.92	800	4.15	34.92	27.73
1,013	3.86	34.91	1,000	3.85	34.91	27.75
1,592	3.62	34.94				
Station 3757; 14 Apr.; latitude 42°39′ N., longitude 50° 59′ W., depth 1664 meters; dynamic height 971.042						
0	4.77	33.56	0	4.77	33.56	26.59
22	4.83	33.58	25	4.85	33.58	26.60
44	4.91	33.64	50	4.50	33.63	26.67
66	2.83	33.57	75	2.65	33.61	26.83
88	2.58	33.73	100	3.15	33.92	27.03
132	5.04	34.39	150	5.20	34.47	27.26
176	5.39	34.53	200	5.35	34.58	27.33
264	5.16	34.70	300	4.55	34.68	27.50
293	4.63	34.69	400	3.65	34.65	27.56
455	3.47	34.65	600	3.70	34.83	27.71
629	3.74	34.85	800	4.00	34.89	27.72
789	3.99	34.89	1,000	3.90	34.91	27.75
1,197	3.79	34.93				
Station 3758; 14 Apr.; latitude 42°50′ N., longitude 50°45′ W.; depth 910 meters; dynamic height 971.288						
0	3.31	33.41	0	3.31	33.41	26.61
23	2.98	33.48	25	2.95	33.48	26.70
45	2.88	33.55	50	2.50	33.57	26.81
68	2.44	33.64	75	2.50	33.69	26.90
90	2.83	33.78	100	3.30	33.91	27.01
135	4.81	34.31	150	4.25	34.26	27.19
180	2.58	34.14	200	2.65	34.21	27.31
270	3.33	34.45	300	3.65	34.56	27.49
325	3.96	34.64	400	4.05	34.75	27.60
509	4.06	34.82	600	4.00	34.86	27.70
708	3.88	34.88	800	3.85	34.88	27.73
909	3.81	34.875	(1,000)	3.80	34.87	27.73
Station 3759; 14 Apr.; latitude 42°53′ N., longitude 50°44′ W.; depth 443 meters; dynamic height 971.030						
0	1.82	33.38	0	1.82	33.38	26.71
21	1.55	33.44	25	1.50	33.45	26.79
43	1.15	33.48	50	1.05	33.50	26.86
64	0.87	33.55	75	0.70	33.57	26.94
86	0.63	33.59	100	0.75	33.68	27.03
129	1.11	33.86	150	0.85	33.90	27.19
172	0.57	33.93	200	0.85	34.01	27.28
257	1.44	34.16	300	1.85	34.27	27.42
310	1.98	34.30	400	3.00	34.57	27.57
427	3.36	34.65				

Observed values			Scaled values			
Depth, meters	Temperature, °C.	Salinity, ‰	Depth, meters	Temperature, °C.	Salinity, ‰	σ_t
Station 3760; 14 Apr.; latitude 43°03.5′ N., longitude 50°38′ W.; depth 152 meters; dynamic height 971.034						
0	1.03	33.31	0	1.03	33.32	26.72
21	0.99	33.33	25	0.95	33.34	26.73
42	0.57	33.41	50	0.55	33.47	26.87
64	0.59	33.60	75	0.65	33.67	27.02
85	0.72	33.71	100	0.85	33.75	27.07
127	1.13	33.80	(150)	1.35	33.82	27.10
Station 3761; 14 Apr.; latitude 43°06.5′ N. longitude 50°34′ W.; depth 89 meters; dynamic height 971.034						
0	3.00	33.37	0	3.00	33.37	26.61
23	2.90	33.44	25	2.85	33.45	26.68
46	2.02	33.58	50	1.90	33.61	26.90
69	1.35	33.69	(75)	1.15	33.72	27.03
Station 3762; 15 Apr.; latitude 43°20′ N., longitude 50°15′ W.; depth 69 meters; dynamic height 971.029						
0	2.94	33.30	0	2.94	33.30	26.55
24	2.73	33.39	25	2.70	33.39	26.65
49	2.58	33.41	50	2.55	33.41	26.68
Station 3763; 15 Apr.; latitude 43°00′ N., longitude 50°17′ W.; depth 92 meters; dynamic height 971.029						
0	2.63	33.40	0	2.63	33.40	26.66
24	1.93	33.47	25	1.90	33.47	26.79
49	1.19	33.56	50	1.15	33.56	26.90
73	1.07	33.60	75	1.05	33.60	26.94
Station 3764; 15 Apr.; latitude 42°54′ N., longitude 50°17′ W.; depth 361 meters; dynamic height 971.009						
0	1.99	33.43	0	1.99	33.43	26.75
24	1.61	33.46	25	1.60	33.46	26.79
47	0.75	33.61	50	0.70	33.63	26.99
71	0.63	33.72	75	0.60	33.73	27.07
94	0.61	33.77	100	0.65	33.79	27.11
141	1.02	33.94	150	1.02	33.97	27.24
188	1.27	34.07	200	1.35	34.11	27.33
282	1.98	34.29	300	2.05	34.33	27.46
380	2.48	34.47	(400)	2.55	34.51	27.56
Station 3765; 15 Apr.; latitude, 42°44′ N., longitude 50°14′ W.; depth 1207 meters; dynamic height 970.979						
0	0.75	33.36	0	0.75	33.36	26.76
27	0.62	33.43	25	0.65	33.43	26.83
53	0.48	33.48	50	0.45	33.54	26.92
80	0.80	33.79	75	0.75	33.72	27.06
105	0.93	33.96	100	0.90	33.94	27.22
159	1.45	--------	150	1.35	34.11	27.33
212	2.29	34.33	200	2.10	34.27	27.40
317	2.80	34.73	300	2.75	34.61	27.62
350	2.90	34.61	400	3.05	34.73	27.69
537	3.71	34.95	600	3.75	34.82	27.69
734	3.82	34.835	800	3.80	34.85	27.71
936	3.70	34.875	1,000	3.70	34.88	27.73
1,145	3.62	34.90				

Table of Oceanographic Data—Continued

STATIONS OCCUPIED IN 1949—Continued

Station 3766; 15 Apr.; latitude 42°19′ N., longitude 50°08′ W.; depth 2963 meters; dynamic height 970.947

Observed values			Scaled values			
Depth, meters	Temperature, °C.	Salinity, °/₀₀	Depth, meters	Temperature, °C.	Salinity, °/₀₀	σ_t
0	1.76	33.32	0	1.76	33.32	26.67
22	7.44	34.52	25	7.65	34.53	26.98
43	7.97	34.59	50	7.90	34.59	26.99
66	7.52	34.57	75	5.60	34.42	27.17
87	3.71	34.23	100	3.70	34.30	27.28
131	3.79	34.52	150	3.75	34.53	27.46
217	-------	34.57	200	3.60	34.55	27.49
261	4.79	34.75	300	4.15	34.75	27.59
352	3.52	34.76	400	3.60	34.79	27.68
530	3.80	34.88	600	3.75	34.88	27.74
714	3.66	34.88	800	3.65	34.89	27.75
912	3.65	34.90	1,000	3.65	34.90	27.76
1,119	3.63	-------	-------	-------	-------	-------

Station 3767; 15 Apr.; latitude 41°55′ N., longitude 50°04′ W. depth 3448 meters; dynamic height 971.042

Observed values			Scaled values			
Depth, meters	Temperature, °C.	Salinity, °/₀₀	Depth, meters	Temperature, °C.	Salinity, °/₀₀	σ_t
0	3.76	33.50	0	3.77	33.50	26.64
27	-------	-------	25	6.50	33.88	26.63
52	9.65	-------	50	9.55	34.49	26.65
79	10.30	34.80	75	10.25	34.75	26.73
105	10.08	34.99	100	10.15	34.96	26.91
158	8.96	35.03	150	9.10	35.03	27.15
210	8.06	34.99	200	8.20	35.00	27.26
289	5.85	34.89	300	5.40	34.87	27.55
441	2.94	34.62	400	3.35	34.68	27.62
600	4.06	34.87	600	4.05	34.87	27.70
775	4.15	34.95	800	4.15	34.96	27.76
960	4.18	34.93	(1,000)	4.15	34.98	27.78

Station 3768; 16 Apr.; latitude 41°33.5′ N., longitude 50°03′ W. depth 3841 meters; dynamic height 971.176

Observed values			Scaled values			
Depth, meters	Temperature, °C.	Salinity, °/₀₀	Depth, meters	Temperature, °C.	Salinity, °/₀₀	σ_t
0	13.77	35.59	0	13.77	35.59	26.71
23	13.75	35.60	25	13.75	35.60	26.72
46	13.71	35.60	50	13.70	35.60	26.73
69	13.66	35.59	75	13.70	35.60	26.73
92	13.79	35.63	100	13.80	35.64	26.74
139	13.80	35.66	150	13.55	35.64	26.79
184	12.62	35.54	200	12.25	35.49	26.94
276	10.64	35.28	300	10.22	35.26	27.14
300	10.22	35.28	400	8.35	35.13	27.34
455	7.37	35.07	600	5.35	34.97	27.63
619	5.21	34.97	800	5.05	35.01	27.70
789	5.07	35.01	1,000	4.05	35.07	27.86
973	4.18	35.06	-------	-------	-------	-------

Station 3769; 16 Apr.; latitude 41°56.5′ N., longitude 49°24′ W., depth 3017 meters; dynamic height 970.956

Observed values			Scaled values			
Depth, meters	Temperature, °C.	Salinity, °/₀₀	Depth, meters	Temperature, °C.	Salinity, °/₀₀	σ_t
0	4.47	33.67	0	4.47	33.67	26.71
28	4.45	33.69	25	4.45	33.68	26.72
55	4.94	34.12	50	4.85	34.04	26.95
83	5.71	34.43	75	5.50	34.38	27.15
110	4.39	34.38	100	4.90	34.40	27.23
166	3.61	34.45	150	3.70	34.42	27.38
221	5.00	34.75	200	4.45	34.66	27.49
331	4.83	34.86	300	4.85	34.86	27.60
332	4.78	34.92	400	4.65	34.94	27.69
510	4.40	34.96	600	4.20	34.95	27.75
699	4.06	34.94	800	3.95	34.94	27.76
903	3.85	34.94	1,000	3.80	34.94	27.78
1,117	3.73	34.94	-------	-------	-------	-------

Station 3770; 16 Apr.; latitude 41°32′ N., longitude 48°00′ W., depth 3329 meters; dynamic height 970.931

Observed values			Scaled values			
Depth, meters	Temperature, °C.	Salinity, °/₀₀	Depth, meters	Temperature, °C.	Salinity, °/₀₀	σ_t
0	3.23	33.46	0	3.23	33.46	26.66
24	2.89	33.72	25	2.90	33.73	26.91
47	2.60	33.89	50	2.60	33.91	27.07
71	2.41	34.03	75	2.35	34.05	27.20
94	1.87	34.11	100	2.05	34.17	27.33
141	5.78	34.84	150	5.75	34.85	27.49
188	5.28	34.87	200	5.15	34.87	27.58
282	4.39	34.84	300	4.35	34.85	27.65
426	4.52	34.93	400	4.50	34.92	27.69
639	4.10	34.92	600	4.20	34.92	27.73
854	3.65	34.91	800	3.75	34.91	27.76
1,101	3.58	34.91	1,000	3.60	34.91	27.78
1,293	3.49	34.91	-------	-------	-------	-------

Station 3771; 16 Apr.; latitude 41°58.5′ N., longitude 47°57′ W., depth 3768 meters; dynamic height 970.007

Observed values			Scaled values			
Depth, meters	Temperature, °C.	Salinity, °/₀₀	Depth, meters	Temperature, °C.	Salinity, °/₀₀	σ_t
0	9.11	34.77	0	9.11	34.77	26.94
28	9.21	34.78	25	9.20	34.78	26.94
55	9.09	34.78	50	9.10	34.78	26.95
82	9.12	34.91	75	9.10	34.89	27.03
109	8.50	34.89	100	8.70	34.90	27.11
165	6.97	34.74	150	7.45	34.77	27.20
219	7.29	34.93	200	7.20	34.87	27.31
328	5.61	34.91	300	6.00	34.92	27.51
442	4.93	34.96	400	5.10	34.94	27.63
654	4.63	35.01	600	4.65	35.00	27.74
862	4.21	34.96	800	4.40	34.93	27.75
1,102	3.82	34.93	1,000	3.95	34.94	27.76
1,307	3.72	34.96	-------	-------	-------	-------

Station 3772; 17 Apr.; latitude 42°19′ N., longitude 48°33′ W.; depth 3310 meters; dynamic height 971.055

Observed values			Scaled values			
Depth, meters	Temperature, °C.	Salinity, °/₀₀	Depth, meters	Temperature, °C.	Salinity, °/₀₀	σ_t
0	11.38	35.47	0	11.38	35.47	27.10
18	11.36	35.47	25	11.35	35.46	27.09
35	11.37	35.455	50	11.35	35.46	27.09
52	11.37	35.46	75	11.35	35.46	27.09
69	11.37	35.46	100	11.35	35.46	27.09
105	11.32	35.465	150	11.05	35.43	27.12
139	11.33	35.475	200	9.50	35.21	27.22
209	8.69	35.07	300	6.95	34.93	27.40
264	8.66	35.04	400	5.50	34.80	27.48
402	5.48	34.80	600	4.60	34.90	27.66
546	5.62	34.87	800	4.25	34.95	27.75
693	4.40	34.95	(1,000)	4.05	34.96	27.77
846	4.19	34.955	-------	-------	-------	-------

Station 3773; 17 Apr.; latitude 42°43′ N., longitude 49°08′ W.; depth 2469 meters; dynamic height 970.935

Observed values			Scaled values			
Depth, meters	Temperature, °C.	Salinity, °/₀₀	Depth, meters	Temperature, °C.	Salinity, °/₀₀	σ_t
0	4.79	33.91	0	4.79	33.91	26.86
23	4.92	34.03	25	4.95	34.06	26.96
46	6.11	34.36	50	6.20	34.41	27.08
69	6.46	34.55	75	6.35	34.56	27.18
92	5.96	34.58	100	5.85	34.58	27.27
139	5.40	34.61	150	5.35	34.63	27.37
185	5.29	34.77	200	5.25	34.81	27.52
277	4.92	34.91	300	4.85	34.93	27.66
402	4.68	34.97	400	4.65	34.97	27.72
609	3.87	34.91	600	3.90	34.91	27.75
817	4.05	34.95	800	4.05	34.95	27.76
1,078	3.80	34.94	1,000	3.90	34.94	27.77
1,277	3.71	34.95	-------	-------	-------	-------

Table of Oceanographic Data—Continued

STATIONS OCCUPIED IN 1949—Continued

Station 3774; 17 Apr.; latitude 43°23′ N., longitude 48°52′ W.; depth 1737 meters; dynamic height 970.905

Observed values			Scaled values			
Depth, meters	Temperature, °C.	Salinity, ‰	Depth, meters	Temperature, °C.	Salinity, ‰	σ_t
0	4.88	33.96	0	4.88	33.96	26.89
22	4.77	33.97	25	4.80	33.97	26.91
43	4.88	34.00	50	4.55	34.02	26.97
65	3.81	34.10	75	3.95	34.23	27.21
85	4.05	34.35	100	4.00	34.42	27.35
129	3.90	34.53	150	3.70	34.60	27.52
172	2.54	34.66	200	3.65	34.72	27.62
257	3.96	34.80	300	4.00	34.84	27.68
353	4.05	34.87	400	4.00	34.89	27.72
534	3.76	34.91	600	3.70	34.91	27.77
718	3.62	34.90	800	3.60	34.90	27.77
940	3.55	34.91	1,000	3.55	34.91	27.78
1,414	3.57	34.95				

Station 3775; 17–18 Apr.; latitude 43°04′ N., longitude 47°58′ W.; depth 3383 meters; dynamic height 970.939

Observed values			Scaled values			
Depth, meters	Temperature, °C.	Salinity, ‰	Depth, meters	Temperature, °C.	Salinity, ‰	σ_t
0	4.68	33.93	0	4.68	33.93	26.89
31	5.33	34.10	25	5.20	34.06	26.93
61	6.53	34.50	50	6.10	34.38	27.08
92	4.26	34.31	75	5.50	34.41	27.17
122	4.22	34.42	100	4.20	34.34	27.26
183	3.30	34.49	150	3.80	34.45	27.39
244	3.28	34.62	200	3.30	34.52	27.50
366	4.34	34.89	300	3.70	34.75	27.64
429	4.18	34.88	400	4.25	34.89	27.69
635	4.06	34.94	600	4.05	34.93	27.75
834	4.13	34.93	800	3.95	34.93	27.76
1,062	3.71	34.93	1,000	3.85	34.93	27.77
1,670	3.46	34.93				

Station 3776; 18 Apr.; latitude 42°58′ N., longitude 47°31′ W.; depth 3493 meters; dynamic height 971.061

Observed values			Scaled values			
Depth, meters	Temperature, °C.	Salinity, ‰	Depth, meters	Temperature, °C.	Salinity, ‰	σ_t
0	13.54	35.76	0	13.54	35.76	26.89
28	13.50	35.76	25	13.55	35.76	26.89
54	13.53	35.765	50	13.50	35.76	26.90
82	13.50		75	13.50	35.76	26.90
108	13.01	35.69	100	13.20	35.71	26.92
164	11.33	35.45	150	11.85	35.52	27.04
218	9.36	35.16	200	9.95	35.26	27.19
326	6.47	34.98	300	6.95	35.01	27.46
407	5.79	34.92	400	5.85	34.92	27.53
611	4.47	34,88	600	4.55	34.88	27.66
817	3.59	34.89	800	3.60	34.89	27.76
1,023	3.57	34.97	1,000	3.55	34.96	27.82
1,544	3.55	34.98				

Station 3777; 18 Apr.; latitude 42°39.5′ N., longitude 46°52′ W.; depth 4024 meters; dynamic height 970.953

Observed values			Scaled values			
Depth, meters	Temperature, °C.	Salinity, ‰	Depth, meters	Temperature, °C.	Salinity, ‰	σ_t
0	6.71	33.94	0	6.71	33.94	26.64
27	6.10	33.98	25	6.20	33.98	26.75
53	4.02	34.03	50	4.25	34.02	27.01
80	3.56	34.24	75	3.60	34.20	27.21
106	3.41	34.33	100	3.40	34.31	27.32
160	5.84	34.83	150	5.55	34.74	27.42
213	5.55	34.88	200	5.60	34.87	27.52
319	5.36	34.96	300	5.40	34.95	27.61
398	5.12	34.99	400	5.10	34.99	27.67
598	4.53	34.98	600	4.55	34.98	27.74
799	3.97	34.96	800	3.95	34.95	27.77
1,002	3.91	34.93	1,000	3.90	34.93	27.77
1,513	3.54	34.93				

Station 3778; 18 Apr.; latitude 43°00′ N., longitude 46°34′ W.; depth 4152 meters; dynamic height 971.038

Observed values			Scaled values			
Depth, meters	Temperature, °C.	Salinity, ‰	Depth, meters	Temperature, °C.	Salinity, ‰	σ_t
0	9.90	34.71	0	9.90	34.71	26.76
25	11.39	35.13	25	11.39	35.13	26.83
50	11.35	35.14	50	11.35	35.14	26.84
75	12.17	35.39	75	12.17	35.39	26.88
100	8.27	34.65	100	8.27	34.65	26.98
150	3.53	34.07	150	3.53	34.07	27.12
200	3.61	34.22	200	3.61	34.22	27.23
299	5.64	34.84	300	5.65	34.84	27.49
410	4.66	34.83	400	4.70	34.83	27.60
616	4.76	35.00	600	4.75	34.99	27.71
826	4.17	34.96	800	4.25	34.97	27.76
1,039	3.85	34.935	1,000	3.90	34.94	27.77
1,573	3.58	34.945				

Station 3779; 18–19 Apr.; latitude 43°20′ N., longitude 46°12′ W.; depth 4572 meters; dynamic height 971.046

Observed values			Scaled values			
Depth, meters	Temperature, °C.	Salinity, ‰	Depth, meters	Temperature, °C.	Salinity, ‰	σ_t
0	7.69	34.14	0	7.69	34.14	26.66
27	5.00	33.84	25	5.05	33.85	26.78
53	5.20	33.98	50	5.15	33.94	26.84
80	10.22	35.08	75	10.00	33.93	26.92
106	7.60	34.65	100	8.00	34.73	27.09
159	9.09	35.11	150	9.00	35.05	27.18
212	3.73	34.27	200	4.80	34.42	27.26
318	7.43	35.11	300	6.90	35.02	27.47
425	4.63	34.80	400	5.20	34.86	27.56
633	4.63	34.965	600	4.60	34.95	27.70
842	4.24	34.965	800	4.35	34.97	27.75
1,054	3.98	34.935	1,000	4.05	34.94	27.75
1,590	3.62	34.94				

Station 3780; 19 Apr.; latitude 43°32.5′ N., longitude 46°43′ W.; depth 4280 meters; dynamic height 971.184

Observed values			Scaled values			
Depth, meters	Temperature, °C.	Salinity, ‰	Depth, meters	Temperature, °C.	Salinity, ‰	σ_t
0	12.84	35.62	0	12.84	35.62	26.93
25	12.42	35.64	25	12.82	35.64	26.96
48	12.76	35.35	50	12.75	35.64	26.96
73	12.83	35.65	75	12.80	35.65	26.96
96	12.84	35.66	100	12.85	35.66	26.96
145	12.86	35.67	150	12.90	35.67	26.95
194	12.87	35.67	200	12.85	35.66	26.96
290	10.94	35.37	300	10.65	35.32	27.11
366	8.59	34.01	400	7.40	34.90	27.30
549	4.27	34.63	600	4.40	34.74	27.55
688	4.65	34.93	800	4.40	34.95	27.72
869	4.26	34.95	1,000	4.15	34.95	27.75
1,341	3.82	34.95				

Station 3781; 19 Apr.; latitude 43°41′ N., longitude 47°26′ W.; depth 4024 meters; dynamic height 971.193

Observed values			Scaled values			
Depth, meters	Temperature, °C.	Salinity, ‰	Depth, meters	Temperature, °C.	Salinity, ‰	σ_t
0	12.75	35.59	0	12.75	35.59	26.92
27	12.71	35.59	25	12.70	35.59	26.93
53	12.62	35.59	50	12.65	35.59	26.94
80	12.91	35.65	75	12.85	35.64	26.94
106	13.10	35.72	100	13.05	35.70	26.94
160	13.07	35.71	150	13.10	35.71	26.94
213	12.99	35.69	200	13.00	35.70	26.95
319	9.86	35.13	300	10.30	35.22	27.09
380	8.78	35.07	400	8.35	35.05	27.28
573	5.35	34.86	600	5.20	34.87	27.57
769	4.70	34.96	800	4.60	34.96	27.71
968	4.04	34.93	1,000	3.95	34.93	27.76
1,490	3.61	34.91				

Table of Oceanographic Data—Continued

STATIONS OCCUPIED IN 1949—Continued

Station 3782; 19 Apr.; latitude 43°51′ N., longitude 48°01′ W.; depth 3695 meters; dynamic height 971.091

Observed values			Scaled values			
Depth, meters	Temperature, °C.	Salinity, ‰	Depth, meters	Temperature, °C.	Salinity, ‰	σ_t
0	13.51	35.75	0	13.51	35.75	26.89
24	13.54	35.75	25	13.50	35.75	26.89
48	13.51	35.76	50	13.50	35.76	26.90
72	13.54	35.76	75	13.50	35.76	26.90
96	13.50	35.75	100	13.45	35.75	26.90
144	12.72	35.66	150	12.65	35.65	26.98
193	11.78	35.51	200	11.55	35.48	27.07
289	8.16	35.02	300	7.65	34.99	27.34
385	5.74	34.88	400	5.60	34.88	27.53
571	4.83	34.96	600	4.75	34.96	27.69
753	4.32	34.96	800	4.25	34.96	27.75
949	4.01	34.95	1,000	4.00	34.95	27.77
1,443	3.86	34.94	-------	-------	-------	-------

Station 3783; 19 Apr.; latitude 44°02.5′ N., longitude 48°32′ W.; depth 3054 meters; dynamic height 970.916

Observed values			Scaled values			
Depth, meters	Temperature, °C.	Salinity, ‰	Depth, meters	Temperature, °C.	Salinity, ‰	σ_t
0	4.09	33.75	0	4.09	33.75	26.81
26	4.70	34.05	25	4.70	34.05	26.98
52	4.32	34.13	50	4.35	34.12	27.07
78	4.00	34.30	75	4.00	34.29	27.24
104	4.00	34.41	100	4.00	34.39	27.32
156	4.04	34.61	150	4.05	34.59	27.47
208	4.33	34.79	200	4.25	34.77	27.60
312	4.57	34.93	300	4.55	34.92	27.69
386	4.39	34.93	400	4.35	34.93	27.72
585	-------	34.93	600	4.00	34.93	27.76
792	3.77	34.91	800	3.80	34.91	27.76
998	3.62	34.89	1,000	3.60	34.89	27.76
1,532	3.45	34.93	-------	-------	-------	-------

Station 3784; 19 Apr.; latitude 44°05′ N., longitude 48°50′ W., depth 1444 meters; dynamic height 970.938

Observed values			Scaled values			
Depth, meters	Temperature, °C.	Salinity, ‰	Depth, meters	Temperature, °C.	Salinity, ‰	σ_t
0	0.41	33.19	0	0.41	33.19	26.65
27	0.13	33.21	25	0.15	33.21	26.68
52	0.32	33.64	50	0.30	33.58	26.97
79	3.54	34.10	75	3.30	34.09	27.15
104	1.10	34.05	100	1.35	34.06	27.29
157	2.00	34.33	150	1.90	34.29	27.43
210	4.43	34.75	200	4.15	34.68	27.54
314	3.37	34.73	300	3.50	34.73	27.65
399	4.46	34.94	400	4.45	34.94	27.71
606	3.82	34.905	600	3.85	34.91	27.75
822	3.64	34.95	800	3.65	34.90	27.76
1,030	3.59	34.98	1,000	3.60	34.90	27.77
1,376	3.45	34.90	-------	-------	-------	-------

Station 3785; 20 Apr.; latitude 44°07′ N., longitude 48°59′ W., depth 443 meters; dynamic height 970.962

Observed values			Scaled values			
Depth, meters	Temperature, °C.	Salinity, ‰	Depth, meters	Temperature, °C.	Salinity, ‰	σ_t
0	0.18	33.12	0	0.18	33.12	26.60
25	−0.45	33.17	25	−0.45	33.17	26.67
49	−0.91	33.48	50	−0.90	33.49	26.95
74	−0.12	33.66	75	−0.10	33.66	27.05
98	0.76	33.86	100	0.80	33.87	27.17
148	1.70	34.19	150	1.70	34.20	27.37
197	1.99	34.35	200	2.00	34.36	27.48
295	2.85	34.61	300	3.05	34.62	27.60
263	2.67	34.55	(400)	3.55	34.79	27.68
391	4.46	34.78	-------	-------	-------	-------

Station 3786; 20 Apr.; latitude 44°10′ N., longitude 49°08′ W. depth 150 meters; dynamic height 970.991

Observed values			Scaled values			
Depth, meters	Temperature, °C.	Salinity, ‰	Depth, meters	Temperature, °C.	Salinity, ‰	σ_t
0	0.08	33.15	0	0.08	33.15	26.63
25	0.06	33.27	25	0.06	33.27	26.72
50	−0.49	33.43	50	−0.49	33.42	26.88
75	−0.35	33.55	75	−0.35	33.55	26.96
100	−0.18	33.63	100	−0.18	33.63	27.03
(130)	0.02	33.68	(150)	0.05	33.70	27.07

Station 3787; 20 Apr.; latitude 44°11′ N., longitude 49°12′ W., depth 87 meters; dynamic height 970.985

Observed values			Scaled values			
Depth, meters	Temperature, °C.	Salinity, ‰	Depth, meters	Temperature, °C.	Salinity, ‰	σ_t
0	0.36	33.25	0	0.36	33.25	26.69
20	−0.15	33.27	25	−0.25	33.32	26.77
41	−0.51	33.45	50	−0.30	33.52	26.94
61	−0.01	33.61	(75)	0.30	33.69	27.04

Station 3788; 20 Apr.; latitude 44°13.5′ N., longitude 49°24′ W., depth 46 meters; dynamic height 970.993

Observed values			Scaled values			
Depth, meters	Temperature, °C.	Salinity, ‰	Depth, meters	Temperature, °C.	Salinity, ‰	σ_t
0	2.13	33.35	0	2.13	33.35	26.66
25	2.09	33.37	25	2.09	33.37	26.67
35	1.66	33.39	-------	-------	-------	-------

Station 3789; 20 Apr.; latitude 44°59′ N., longitude 49°27′ W., depth 62 meters; dynamic height 971.023

Observed values			Scaled values			
Depth, meters	Temperature, °C.	Salinity, ‰	Depth, meters	Temperature, °C.	Salinity, ‰	σ_t
0	1.16	33.30	0	1.16	33.30	26.68
25	0.61	33.31	25	0.61	33.31	26.72
48	0.56	33.30	(50)	0.55	33.31	26.72

Station 3790; 20 Apr.; latitude 44°58′ N., longitude 49°10′ W., depth 96 meters; dynamic height 971.023

Observed values			Scaled values			
Depth, meters	Temperature, °C.	Salinity, ‰	Depth, meters	Temperature, °C.	Salinity, ‰	σ_t
0	0.75	33.11	0	0.75	33.11	26.55
24	0.04	33.15	25	0.05	33.16	26.64
49	−0.69	33.42	50	−0.70	33.42	26.88
73	−0.61	33.45	(75)	−0.60	33.45	26.90

Station 3791; 20 Apr.; latitude 44°58′ N., longitude 48°58′ W., depth 572 meters; dynamic height 971.003

Observed values			Scaled values			
Depth, meters	Temperature, °C.	Salinity, ‰	Depth, meters	Temperature, °C.	Salinity, ‰	σ_t
0	0.66	33.04	0	0.66	33.04	26.50
25	−0.38	33.08	25	−0.38	33.08	26.59
49	−1.31	33.33	50	−1.30	33.35	26.84
74	−0.54	33.54	75	−0.55	33.54	26.96
98	−0.27	33.63	100	−0.22	33.64	27.03
147	0.87	33.88	150	0.90	33.89	27.17
197	1.84	34.18	200	1.90	34.20	27.35
295	2.51	34.51	300	2.55	34.52	27.56
367	3.16	34.71	400	3.30	34.68	27.62
571	3.63	34.83	600	3.65	34.84	27.70

Table of Oceanographic Data—Continued

STATIONS OCCUPIED IN 1949—Continued

Station 3792; 20 Apr.; latitude 44°54.5′ N., longitude 48°45′ W., depth 1646 meters; dynamic height 970.926

Observed values			Scaled values			
Depth, meters	Temperature, °C.	Salinity, °/oo	Depth, meters	Temperature, °C.	Salinity, °/oo	σ_t
0	1.98	33.51	0	1.98	33.51	26.81
23	1.11	33.52	25	1.20	33.56	26.90
47	3.74	34.01	50	4.00	34.07	27.07
70	5.22	34.34	75	5.20	34.38	27.19
93	4.93	34.49	100	4.45	34.47	27.34
140	1.83	34.27	150	1.90	34.31	27.45
186	2.52	34.50	200	2.85	34.57	27.58
279	4.67	34.87	300	4.65	34.92	27.68
364	4.47	34.91	400	4.35	34.92	27.71
546	4.08	34.93	600	4.00	34.88	27.72
728	3.85	34.91	800	3.80	34.91	27.76
910	3.73	34.925	1,000	3.70	34.92	27.78
1,364	3.55	34.91	--------	--------	--------	--------

Station 3793; 20 Apr.; latitude 44°53′ N., longitude 48°28′ W., depth 1939 meters; dynamic height 970.928

Observed values			Scaled values			
Depth, meters	Temperature, °C.	Salinity, °/oo	Depth, meters	Temperature, °C.	Salinity, °/oo	σ_t
0	6.57	34.43	0	6.57	34.43	27.06
24	7.01	34.57	25	7.00	34.57	27.10
47	6.99	34.57	50	7.00	34.57	27.10
71	6.74	34.565	75	6.75	34.57	27.14
94	6.80	34.59	100	6.70	34.59	27.16
141	5.36	34.63	150	5.40	34.66	27.38
188	5.69	34.81	200	5.55	34.83	27.50
282	4.65	34.90	300	4.50	34.90	27.67
351	4.24	34.90	400	4.10	34.90	27.72
516	3.90	34.91	600	3.80	34.90	27.75
677	3.71	34.89	800	3.65	34.90	27.76
879	3.63	34.91	1,000	3.60	34.91	27.78
1,441	3.54	34.92	--------	--------	--------	--------

Station 3794; 21 Apr.; latitude 44°50′ N., longitude 48°00′ W., depth 3136 meters; dynamic height 970.894

Observed values			Scaled values			
Depth, meters	Temperature, °C.	Salinity, °/oo	Depth, meters	Temperature, °C.	Salinity, °/oo	σ_t
0	5.48	34.18	0	5.48	34.18	27.00
25	5.63	34.25	25	5.60	34.25	27.03
51	4.87	34.33	50	4.90	34.32	27.17
77	4.32	34.45	75	4.35	34.43	27.32
102	4.43	34.56	100	4.40	34.55	27.41
154	3.91	34.63	150	3.95	34.62	27.51
205	4.20	34.80	200	4.15	34.78	27.62
307	4.44	34.91	300	4.40	34.91	27.69
355	4.15	34.91	400	4.15	34.92	27.73
542	4.15	34.95	600	4.10	34.95	27.76
736	3.93	34.95	800	3.85	34.94	27.77
931	3.76	34.93	1,000	3.70	34.93	27.79
1,440	3.51	34.91	--------	--------	--------	--------

Station 3795; 21 Apr.; latitude 44°47′ N., longitude 47°17′ W., depth 3731 meters; dynamic height 970.962

Observed values			Scaled values			
Depth, meters	Temperature, °C.	Salinity, °/oo	Depth, meters	Temperature, °C.	Salinity, °/oo	σ_t
0	5.93	34.02	0	5.93	34.02	26.82
23	5.76	34.01	25	5.80	34.01	26.82
44	6.73	34.29	50	6.95	34.35	26.93
67	7.40	34.47	75	7.20	34.50	27.02
88	6.85	34.53	100	6.50	34.54	27.14
133	5.65	34.54	150	4.90	34.53	27.34
178	3.70	34.43	200	3.85	34.57	27.48
266	4.57	34.83	300	4.60	34.89	27.65
179	3.68	34.56	400	4.35	34.91	27.70
281	4.65	34.87	600	4.10	34.91	27.73
392	4.38	34.91	800	3.95	34.92	27.75
549	4.17	--------	1,000	3.75	34.92	27.77
1,046	3.70	34.92	--------	--------	--------	--------

Station 3796; 21 Apr.; latitude 44°42′ N., longitude 46°38′ W., depth 3658 meters; dynamic height 971.040

Observed values			Scaled values			
Depth, meters	Temperature, °C.	Salinity, °/oo	Depth, meters	Temperature, °C.	Salinity, °/oo	σ_t
0	12.01	35.39	0	12.01	35.39	26.91
25	11.98	35.37	25	11.98	35.37	26.90
50	10.96	35.13	50	10.96	35.13	26.91
75	10.05	35.01	75	10.05	35.01	26.97
100	9.73	34.94	100	9.73	34.94	26.97
150	10.58	35.34	150	10.58	35.34	27.13
200	8.45	35.01	200	8.45	35.01	27.23
300	6.59	34.93	300	6.59	34.93	27.44
282	6.99	34.97	400	5.30	34.90	27.58
404	5.27	34.90	600	4.55	34.96	27.72
516	4.73	34.95	800	4.15	34.95	27.75
664	4.44	34.96	1,000	3.75	34.93	27.78
1,069	3.69	34.92	--------	--------	--------	--------

Station 3797; 21 Apr.; latitude 44°29.5′ N., longitude 45°53′ W., depth 3914 meters; dynamic height 970.990

Observed values			Scaled values			
Depth, meters	Temperature, °C.	Salinity, °/oo	Depth, meters	Temperature, °C.	Salinity, °/oo	σ_t
0	8.59	34.46	0	8.59	34.46	26.78
21	8.41	34.45	25	8.30	34.44	26.81
41	7.63	34.34	50	7.95	34.43	26.86
62	8.46	34.61	75	5.90	34.27	27.01
82	4.57	34.13	100	4.70	34.20	27.10
123	5.05	34.40	150	6.65	34.79	27.32
164	7.43	34.95	200	7.20	34.98	27.40
246	6.75	34.99	300	6.00	34.96	27.54
317	5.79	34.95	400	4.90	34.92	27.65
473	4.46	34.92	600	4.20	34.93	27.74
628	4.15	34.93	800	4.00	34.94	27.76
810	4.00	34.94	1,000	3.85	34.94	27.77
1,308	3.66	34.93	--------	--------	--------	--------

Station 3798; 21 Apr.; latitude 44°25′ N., longitude 45°16′ W., depth 3992 meters; dynamic height 971.152

Observed values			Scaled values			
Depth, meters	Temperature, °C.	Salinity, °/oo	Depth, meters	Temperature, °C.	Salinity, °/oo	σ_t
0	7.14	33.86	0	7.14	33.86	26.53
27	13.71	35.57	25	13.65	35.43	26.62
53	13.67	35.60	50	13.70	35.60	26.73
80	13.69	35.61	75	13.70	35.61	26.74
106	--------	35.43	100	13.20	35.47	26.74
160	11.95	35.39	150	12.20	35.40	26.88
212	11.51	35.44	200	11.60	35.43	27.02
318	8.73	35.12	300	8.95	35.13	27.25
319	8.09	35.01	400	6.05	34.83	27.44
461	4.43	34.69	600	5.20	34.99	27.66
597	5.20	34.99	800	4.45	34.98	27.75
770	4.55	34.985	1,000	4.10	34.97	27.78
1,246	3.86	34.95	--------	--------	--------	--------

Station 3799; 22 Apr.; latitude 44°49′ N., longitude 45°10′ W.; depth 3659 meters; dynamic height 971.093

Observed values			Scaled values			
Depth, meters	Temperature, °C.	Salinity, °/oo	Depth, meters	Temperature, °C.	Salinity, °/oo	σ_t
0	9.97	34.72	0	9.97	34.72	26.77
27	10.56	34.87	25	10.50	34.85	26.77
53	13.25	35.58	50	13.10	35.54	26.81
80	12.25	35.39	75	12.45	35.42	26.85
106	11.22	35.21	100	11.45	35.25	26.91
160	8.33	34.69	150	8.80	34.75	26.97
213	10.21	35.23	200	9.75	35.11	27.10
319	7.86	35.05	300	8.25	35.08	27.32
372	6.70	34.95	400	6.20	34.93	27.50
551	4.26	34.88	600	4.05	34.88	27.71
728	3.83	34.89	800	3.90	34.91	27.75
910	4.01	34.955	(1,000)	3.90	34.96	27.79

Table of Oceanographic Data—Continued

STATIONS OCCUPIED IN 1949—Continued

Station 3800; 22 Apr.; latitude 45°20.5′ N., longitude 45°02′ W.; depth 3841 meters; dynamic height 971.031

Observed values			Scaled values			
Depth, meters	Temperature, °C.	Salinity, °/₀₀	Depth, meters	Temperature, °C.	Salinity, °/₀₀	σ_t
0	10.13	34.81	0	10.13	34.81	26.81
25	10.85	35.06	25	10.85	35.06	26.87
48	10.67	35.03	50	10.70	35.06	26.90
73	12.13	35.32	75	11.70	35.34	26.93
96	12.15	35.49	100	12.05	35.47	26.97
145	10.37	35.18	150	10.15	35.15	27.06
194	8.01	34.90	200	7.85	34.89	27.23
290	6.31	34.89	300	5.65	34.82	27.48
256	6.24	34.77	400	4.60	34.83	27.61
378	4.59	34.81	600	4.30	34.94	27.72
495	4.62	34.96	800	3.90	34.93	27.77
614	4.27	34.94	(1,000)	3.75	34.93	27.78
900	3.80	34.93				

Station 3801; 22 Apr.; latitude 45°22′ N., longitude 45°58′ W.; depth 3475 meters; dynamic height 970.881

Observed values			Scaled values			
Depth, meters	Temperature, °C.	Salinity, °/₀₀	Depth, meters	Temperature, °C.	Salinity, °/₀₀	σ_t
0	6.19	34.42	0	6.19	34.42	27.09
26	5.96	34.45	25	5.95	34.45	27.15
52	4.51	34.54	50	4.65	34.53	27.37
78	4.34	34.61	75	4.35	34.60	27.45
103	4.13	34.62	100	4.15	34.62	27.49
156	3.97	34.71	150	4.00	34.70	27.57
208	3.85	34.78	200	3.85	34.77	27.64
311	3.84	34.85	300	3.85	34.84	27.69
385	3.95	34.88	400	3.95	34.88	27.72
577	3.90	34.91	600	3.90	34.91	27.75
770	3.63	34.875	800	3.65	34.88	27.75
972	3.59	34.91	1,000	3.55	34.91	27.78
1,495	3.43	34.93				

Station 3802; 22 Apr.; latitude 45°19.5′ N., longitude 46°37′ W.; depth 3292 meters; dynamic height 970.884

Observed values			Scaled values			
Depth, meters	Temperature, °C.	Salinity, °/₀₀	Depth, meters	Temperature, °C.	Salinity, °/₀₀	σ_t
0	4.44	34.07	0	4.44	34.07	27.02
27	5.11	34.24	25	5.05	34.23	27.09
52	4.52	34.47	50	4.60	34.45	27.30
79	4.11	34.53	75	4.15	34.53	27.42
105	3.99	34.59	100	4.00	34.58	27.48
158	4.03	34.69	150	4.00	34.68	27.56
211	4.03	34.75	200	4.05	34.74	27.59
316	3.93	34.84	300	3.95	34.83	27.68
408	3.89	34.88	400	3.85	34.88	27.73
609	3.64	34.89	600	3.65	34.89	27.75
808	3.60	34.90	800	3.60	34.90	27.77
1,014	3.52	34.90	1,000	3.50	34.90	27.78
1,539	3.41	34.925				

Station 3803; 22 Apr.; latitude 45°18.5′ N., longitude 47°24′ W.; depth 2999 meters; dynamic height 970.893

Observed values			Scaled values			
Depth, meters	Temperature, °C.	Salinity, °/₀₀	Depth, meters	Temperature, °C.	Salinity, °/₀₀	σ_t
0	1.80	34.43	0	1.80	34.43	26.76
25	5.48	34.32	25	5.48	34.32	27.10
50	5.69	34.51	50	5.69	34.51	27.23
74	6.19	34.67	75	6.20	34.67	27.29
99	5.29	34.66	100	5.20	34.66	27.41
149	4.48	34.71	150	4.50	34.71	27.52
198	4.96	34.87	200	4.95	34.88	27.61
297	4.70	34.95	300	4.65	34.95	27.70
372	4.34	34.93	400	4.25	34.93	27.73
559	4.03	34.94	600	3.95	34.94	27.76
749	3.63	34.90	800	3.60	34.90	27.77
945	3.55	34.91	1,000	3.50	34.91	27.79
1,460	3.48	34.945				

Station 3804; 23 Apr.; latitude 45°31.5′ N., longitude 47°48′ W.; depth 1463 meters; dynamic height 970.946

Observed values			Scaled values			
Depth, meters	Temperature, °C.	Salinity, °/₀₀	Depth, meters	Temperature, °C.	Salinity, °/₀₀	σ_t
0	0.02	33.03	0	0.02	33.03	26.54
24	0.01	33.03	25	0.00	33.03	26.54
49	0.01	33.49	50	0.00	33.51	26.93
73	0.15	33.69	75	0.15	33.70	27.07
97	0.52	33.89	100	0.65	33.91	27.21
146	2.09	34.25	150	2.10	34.27	27.40
194	2.39	34.47	200	2.40	34.49	26.55
291	3.17	34.69	300	3.20	34.70	27.65
358	3.38	34.78	400	3.50	34.82	27.72
536	3.78	34.88	600	3.75	34.89	27.74
713	3.65	34.89	800	3.60	34.89	27.76
900	3.57	34.90	1,000	3.55	34.90	27.77
1,286	3.62	34.91				

Station 3805; 23 Apr.; latitude 45°41′ N., longitude 48°02′ W.; depth 622 meters; dynamic height 971.018

Observed values			Scaled values			
Depth, meters	Temperature, °C.	Salinity, °/₀₀	Depth, meters	Temperature, °C.	Salinity, °/₀₀	σ_t
0	0.27	33.08	0	0.27	33.08	26.57
25	0.26	33.08	25	0.26	33.08	26.57
50	−1.01	33.17	50	−1.01	33.17	26.69
75	−1.16	33.39	75	−1.16	33.39	26.88
100	−0.33	33.63	100	−0.33	33.63	27.04
150	0.29	33.85	150	0.29	33.85	27.18
201	1.03	34.01	200	1.00	34.01	27.27
301	2.18	34.39	300	2.15	34.38	27.49
389	3.36	34.72	400	3.40	34.74	27.66
583	3.74	34.86	600	3.75	34.87	27.73

Station 3806; 23 Apr.; latitude 45°46.5′ N., longitude 48°12′ W.; depth 169 meters; dynamic height 971.053

Observed values			Scaled values			
Depth, meters	Temperature, °C.	Salinity, °/₀₀	Depth, meters	Temperature, °C.	Salinity, °/₀₀	σ_t
0	0.70	33.11	0	0.70	33.11	26.56
25	0.65	33.11	25	0.65	33.11	26.57
50	−1.04	33.21	50	−1.04	33.21	26.73
75	−1.01	33.39	75	−1.01	33.35	26.87
100	−0.56	33.55	100	−0.56	33.55	26.98
150	−0.38	33.60	150	−0.38	33.60	27.02

Station 3807; 23 Apr.; latitude 45°50.5′ N., longitude 48°18′ W.; depth 115 meters; dynamic height 971.061

Observed values			Scaled values			
Depth, meters	Temperature, °C.	Salinity, °/₀₀	Depth, meters	Temperature, °C.	Salinity, °/₀₀	σ_t
0	0.74	33.11	0	0.74	33.11	26.56
25	0.54	33.10	25	0.54	33.10	26.56
50	−0.35	33.09	50	−0.35	33.09	26.60
76	−1.11	33.26	75	−1.10	33.26	26.77
101	−0.80	33.48	100	−0.80	33.47	26.93

Station 3808; 23 Apr.; latitude 45°58.5′ N., longitude 48°29′ W.; Depth 89 meters; dynamic height 971.054

Observed values			Scaled values			
Depth, meters	Temperature, °C.	Salinity, °/₀₀	Depth, meters	Temperature, °C.	Salinity, °/₀₀	σ_t
0	1.09	33.17	0	1.09	33.17	26.59
26	0.73	33.17	25	0.75	33.17	26.61
52	−0.22	33.19	50	−0.20	33.18	26.67
78	−0.17	33.51	75	−0.20	33.49	26.92

STATIONS OCCUPIED IN 1949—Continued

Station 3809; 23 Apr.; latitude 46°06.5′ N., longitude 48°42′ W.; depth 78 meters; dynamic height 971.052

Observed values			Scaled values			
Depth, meters	Temperature, °C.	Salinity, °/oo	Depth, meters	Temperature, °C.	Salinity, °/oo	σ_t
0	1.73	33.27	0	1.73	33.27	26.63
25	1.18	33.28	25	1.18	33.28	26.68
50	0.87	33.36	50	0.87	33.36	26.76
66	0.83	33.38	(75)	0.80	33.39	26.78

Station 3810; 23 Apr.; latitude 46°17.5′ N., longitude 49°00′ W.; depth 62 meters; dynamic height 971.046

Observed values			Scaled values			
Depth, meters	Temperature, °C.	Salinity, °/oo	Depth, meters	Temperature, °C.	Salinity, °/oo	σ_t
0	2.52	33.38	0	2.52	33.38	26.66
25	1.75	33.41	25	1.75	33.41	26.75
50	1.49	33.44	50	1.49	33.44	26.78

Station 3811; 7 May; latitude 46°47.5′ N., longitude 44°40′ W.; depth 132 meters; dynamic height 970.878

Observed values			Scaled values			
Depth, meters	Temperature, °C.	Salinity, °/oo	Depth, meters	Temperature, °C.	Salinity, °/oo	σ_t
0	5.38	34.26	0	5.38	34.265	27.06
24	5.14	34.28	25	5.15	34.28	27.10
49	4.68	34.26	50	4.65	34.26	27.15
73	3.96	34.32	75	3.95	34.33	27.28
97	3.53	34.44	(100)	3.50	34.46	27.43

Station 3812; 7 May; latitude 46°43′ N., longitude 44°37′ W.; depth 178 meters; dynamic height 970.885

Observed values			Scaled values			
Depth, meters	Temperature, °C.	Salinity, °/oo	Depth, meters	Temperature, °C.	Salinity, °/oo	σ_t
0	5.35	34.27	0	5.35	34.27	27.08
24	5.35	34.26	25	5.35	34.26	27.07
48	4.67	34.28	50	4.65	34.28	27.16
73	4.23	34.31	75	4.20	34.31	27.24
97	3.95	34.35	100	3.95	34.36	27.31
145	3.53	34.50	(150)	3.45	34.52	27.48

Station 3813; 7 May; latitude 46°36.5′ N., longitude 44°35′ W.; depth 220 meters; dynamic height 970.883

Observed values			Scaled values			
Depth, meters	Temperature, °C.	Salinity, °/oo	Depth, meters	Temperature, °C.	Salinity, °/oo	σ_t
0	4.74	34.16	0	4.74	34.16	27.06
24	4.75	34.16	25	4.75	34.16	27.06
72	3.66	34.21	50	4.15	34.17	27.14
120	3.50	34.48	75	3.65	34.22	27.23
215	3.78	34.77	100	3.55	34.38	27.35
			150	3.55	34.58	27.51
			200	3.70	34.73	27.62

Station 3814; 7–8 May; latitude 46°28′ N., longitude 44°32′ W.; depth 778 meters; dynamic height 970.876

Observed values			Scaled values			
Depth, meters	Temperature, °C.	Salinity, °/oo	Depth, meters	Temperature, °C.	Salinity, °/oo	σ_t
0	4.96	34.18	0	4.96	34.18	27.05
22	5.04	34.20	25	5.00	34.20	27.06
44	4.50	34.18	50	4.40	34.19	27.12
66	4.00	34.22	75	3.75	34.29	27.27
88	3.48	34.41	100	3.50	34.48	27.44
132	3.61	34.60	150	3.65	34.65	27.56
177	3.69	34.72	200	3.70	34.76	27.65
265	3.75	34.85	300	3.75	34.86	27.72
310	3.73	34.86	400	3.70	34.87	27.74
397	3.69	34.87	(600)	3.60	34.89	27.76
580	3.59	34.89				

Station 3815; 8 May; latitude 46°21′ N., longitude 44°31′ W., depth 1554 meters; dynamic height 970.900

Observed values			Scaled values			
Depth, meters	Temperature, °C.	Salinity, °/oo	Depth, meters	Temperature, °C.	Salinity, °/oo	σ_t
0	5.01	34.19	0	5.01	34.19	27.05
26	4.86	34.18	25	4.85	34.18	27.06
51	4.30	34.18	50	4.30	34.18	27.12
78	3.65	34.32	75	3.70	34.30	27.28
103	3.50	34.40	100	3.50	34.39	27.37
155	3.36	34.56	150	3.35	34.54	27.50
206	3.55	34.69	200	3.50	34.68	27.60
309	3.69	34.83	300	3.80	34.84	27.70
278	3.88	34.84	400	3.70	34.87	27.74
429	3.66	34.87	600	3.65	34.88	27.74
588	3.66	34.88	800	3.65	34.89	27.75
757	3.66	34.89	1,000	3.60	34.90	27.77
1,202	3.54	34.905				

Station 3816; 8 May; latitude 46°01′ N., longitude 44°26′ W., depth 3932 meters; dynamic height 971.099

Observed values			Scaled values			
Depth, meters	Temperature, °C.	Salinity, °/oo	Depth, meters	Temperature, °C.	Salinity, °/oo	σ_t
0	8.89	34.26	0	8.87	34.26	26.58
26	10.72	34.75	25	10.70	34.74	26.64
52	13.25	35.44	50	13.25	35.38	26.65
78	13.00	35.54	75	12.75	35.54	26.88
103	12.67	35.53	100	12.70	35.53	26.88
156	9.80	35.04	150	10.10	35.08	27.01
208	8.47	34.92	200	8.60	34.93	27.14
311	6.47	34.81	300	6.60	34.84	27.37
292	6.73	34.86	400	6.10	34.95	27.52
429	5.98	34.97	600	3.85	34.83	27.68
562	3.82	34.82	800	3.80	34.88	27.73
720	3.84	34.87	1,000	3.70	34.89	27.75
1,145	3.63	34.90				

Station 3817; 8 May; latitude 46°02′ N., longitude 45°18′ W., depth 3292 meters; dynamic height 971.071

Observed values			Scaled values			
Depth, meters	Temperature, °C.	Salinity, °/oo	Depth, meters	Temperature, °C.	Salinity, °/oo	σ_t
0	11.30	34.92	0	11.30	34.915	26.68
24	11.83	35.08	25	11.85	35.08	26.70
48	12.02	35.31	50	12.00	35.31	26.85
72	11.54	35.24	75	11.45	35.22	26.89
96	10.70	35.10	100	10.55	35.09	26.94
144	9.64	35.05	150	9.60	35.05	27.08
192	9.19	35.10	200	9.05	35.10	27.21
288	7.49	35.02	300	7.15	34.99	27.41
359	5.82	34.87	400	5.65	34.89	27.53
541	5.02	34.98	600	4.75	34.97	27.70
726	4.24	34.94	800	4.00	34.92	27.75
921	3.70	34.89	1,000	3.65	34.89	27.75
1,430	3.53	34.92				

Station 3818; 8 May; latitude 46°05.5′ N., longitude 45°50′ W., depth 2140 meters; dynamic height 970.914

Observed values			Scaled values			
Depth, meters	Temperature, °C.	Salinity, °/oo	Depth, meters	Temperature, °C.	Salinity, °/oo	σ_t
0	6.40	34.18	0	6.40	34.18	26.87
25	6.51	34.26	25	6.51	34.26	26.92
50	5.28	34.21	50	5.28	34.21	27.04
75	4.91	34.44	75	4.91	34.435	27.26
99	4.53	34.50	100	4.50	34.50	27.36
150	4.15	34.66	150	4.17	34.66	27.52
199	3.84	34.68	200	3.80	34.68	27.57
298	3.79	34.76	300	3.80	34.77	27.65
349	3.82	34.79	400	3.80	34.82	27.69
529	3.83	34.89	600	3.75	34.90	27.75
714	3.65	34.91	800	3.60	34.91	27.78
942	3.55	34.90	1,000	3.55	34.91	27.78
1,117	3.52	34.92				

Table of Oceanographic Data—Continued

STATIONS OCCUPIED IN 1949—Continued

Station 3819; 8-9 May; latitude 46°11′ N., longitude 46°26′ W., depth 640 meters; dynamic height 970.881

Observed values			Scaled values			
Depth, meters	Temperature, °C.	Salinity, ‰	Depth, meters	Temperature, °C.	Salinity, ‰	σ_t
0	4.14	33.73	0	4.14	33.73	26.79
20	4.33	33.82	25	4.60	33.87	26.85
40	5.30	-------	50	4.30	34.24	27.17
60	3.05	34.32	75	2.75	34.39	27.44
80	2.77	34.415	100	3.40	34.55	27.51
120	4.12	34.69	150	4.05	34.75	27.60
160	4.03	34.76	200	4.10	34.82	27.66
240	4.15	34.88	300	4.05	34.90	27.72
309	4.03	34.90	400	3.75	34.90	27.75
425	3.71	34.90	(600)	3.60	34.88	27.75
533	3.61	34.885	-------	-------	-------	-------

Station 3820; 9 May; latitude 46°15′ N., longitude 47°10′ W., depth 1065 meters; dynamic height 970.884

Observed values			Scaled values			
Depth, meters	Temperature, °C.	Salinity, ‰	Depth, meters	Temperature, °C.	Salinity, ‰	σ_t
0	2.34	33.62	0	2.34	33.625	26.87
25	2.50	33.66	25	2.50	33.665	26.88
50	4.48	34.29	50	4.48	34.29	27.19
75	2.77	34.41	75	2.77	34.41	27.46
100	2.94	34.53	100	2.94	34.53	27.53
150	3.02	34.62	150	3.02	34.625	27.61
200	3.25	34.73	200	3.25	34.73	27.66
300	3.72	34.85	300	3.72	34.85	27.72
328	3.88	34.87	400	3.80	34.88	27.73
505	3.76	34.89	600	3.70	34.87	27.74
691	3.66	34.85	800	3.60	34.88	27.75
881	3.60	34.90	(1,000)	3.55	34.91	27.78

Station 3821; 9 May; latitude 46°14′ N., longitude 47°22′ W., depth 586 meters; dynamic height 970.923

Observed values			Scaled values			
Depth, meters	Temperature, °C.	Salinity, ‰	Depth, meters	Temperature, °C.	Salinity, ‰	σ_t
0	1.76	33.38	0	1.76	33.38	26.72
26	1.57	33.42	25	1.60	33.42	26.76
52	0.55	33.72	50	0.60	33.69	27.03
78	1.21	34.015	75	1.15	33.98	27.23
104	1.86	34.22	100	1.75	34.19	27.36
154	2.25	34.43	150	2.20	34.41	27.51
206	2.87	34.61	200	2.80	34.59	27.59
310	3.28	34.74	300	3.20	34.73	27.67
342	3.29	34.78	400	3.45	34.80	27.70
549	3.63	34.86	(600)	3.65	34.86	27.73

Station 3822; 9 May; latitude 46°13′ N., longitude 47°46′ W., depth 169 meters; dynamic height 970.991

Observed values			Scaled values			
Depth, meters	Temperature, °C.	Salinity, ‰	Depth, meters	Temperature, °C.	Salinity, ‰	σ_t
0	0.58	32.98	0	0.58	32.985	26.48
25	−0.03	33.22	25	−0.03	33.22	26.99
50	−1.46	33.29	50	−1.46	33.29	26.79
75	−1.16	33.42	75	−1.16	33.42	26.91
99	−0.20	33.62	100	−0.15	33.62	27.02
149	0.60	33.83	150	0.60	33.83	27.14

Station 3823; 9 May; latitude 46°13′ N., longitude 48°00′ W., depth 115 meters; dynamic height 970.992

Observed values			Scaled values			
Depth, meters	Temperature, °C.	Salinity, ‰	Depth, meters	Temperature, °C.	Salinity, ‰	σ_t
0	0.95	33.02	0	0.95	33.02	26.48
25	0.63	33.02	25	0.63	33.02	26.50
49	−1.67	33.25	50	−1.65	33.26	26.78
74	−1.22	33.44	75	−1.10	33.46	26.93
98	0.03	33.71	100	0.10	33.72	27.09

Station 3824; 9 May; latitude 46°14′ N., longitude 48°26′ W., depth 89 meters; dynamic height 970.991

Observed values			Scaled values			
Depth, meters	Temperature, °C.	Salinity, ‰	Depth, meters	Temperature, °C.	Salinity, ‰	σ_t
0	2.42	33.21	0	2.42	33.21	26.54
25	2.23	33.20	25	2.23	33.205	26.54
50	0.80	33.30	50	0.80	33.305	26.71
75	−0.02	33.57	75	−0.02	33.57	26.98

Station 3825; 9 May; latitude 46°16′ N., longitude 49°00′ W., depth 64 meters; dynamic height 970.985

Observed values			Scaled values			
Depth, meters	Temperature, °C.	Salinity, ‰	Depth, meters	Temperature, °C.	Salinity, ‰	σ_t
0	2.73	33.35	0	2.73	33.35	26.61
25	2.68	33.36	25	2.68	33.36	26.62
50	1.74	33.38	50	1.74	33.37	26.71

Station 3826; 9 May; latitude 46°06′ N., longitude 48°40′ W., depth 80 meters; dynamic height 970.988

Observed values			Scaled values			
Depth, meters	Temperature, °C.	Salinity, ‰	Depth, meters	Temperature, °C.	Salinity, ‰	σ_t
0	2.30	33.20	0	2.30	33.20	26.54
25	2.23	33.22	25	2.23	33.22	26.55
50	1.52	33.30	50	1.52	33.30	26.66
65	0.39	33.42	(75)	−0.10	33.50	26.92

Station 3827; 9 May; latitude 46°01.5′ N., longitude 48°27′ W., depth 89 meters; dynamic height 970.987

Observed values			Scaled values			
Depth, meters	Temperature, °C.	Salinity, ‰	Depth, meters	Temperature, °C.	Salinity, ‰	σ_t
0	2.40	33.22	0	2.40	33.215	26.54
25	2.38	33.22	25	2.38	33.22	26.54
49	0.69	33.30	50	0.55	33.31	26.73
74	−0.03	33.54	(75)	−0.05	33.46	26.89

Station 3828; 10 May; latitude 45°52′ N., longitude 48°13′ W., depth 115 meters; dynamic height 970.979

Observed values			Scaled values			
Depth, meters	Temperature, °C.	Salinity, ‰	Depth, meters	Temperature, °C.	Salinity, ‰	σ_t
0	1.31	33.05	0	1.31	33.05	26.49
25	0.04	33.10	25	0.04	33.10	26.59
49	−1.24	33.45	50	−1.25	33.46	26.94
74	−0.76	33.50	75	−0.75	33.50	26.95
98	−0.28	33.64	(100)	−0.20	33.65	27.05

Station 3829; 10 May; latitude 45°49′ N., longitude 48°09′ W., depth 178 meters; dynamic height 970.971

Observed values			Scaled values			
Depth, meters	Temperature, °C.	Salinity, ‰	Depth, meters	Temperature, °C.	Salinity, ‰	σ_t
0	0.43	33.04	0	0.43	33.04	26.53
25	0.24	33.14	25	0.24	33.145	26.62
50	0.37	33.57	50	0.37	33.57	26.96
75	0.23	33.76	75	0.23	33.765	27.12
100	0.33	33.80	100	0.33	33.795	27.14
164	0.55	33.84	150	0.50	33.83	27.15

Table of Oceanographic Data—Continued

STATIONS OCCUPIED IN 1949—Continued

Station 3830; 10 May; latitude 45°46′ N., longitude 48°02′ W., depth 635 meters; dynamic height 970.929

Observed values			Scaled values			
Depth, meters	Temperature, °C.	Salinity, °/oo	Depth, meters	Temperature, °C.	Salinity, °/oo	σ_t
0	1.22	33.35	0	1.22	33.35	26.73
25	1.01	33.39	25	1.01	33.39	26.77
49	0.14	33.66	50	0.15	33.68	27.05
74	0.08	33.82	75	0.10	33.90	27.23
98	1.07	34.06	100	1.15	34.07	27.31
147	2.00	-------	150	2.00	34.34	27.46
196	2.34	34.49	200	2.35	34.50	27.56
294	3.02	34.66	300	3.05	34.67	27.64
395	3.42	34.78	400	3.40	34.79	27.70
591	3.67	34.87	600	3.65	34.87	27.74

Station 3831; 10 May; latitude 45°37′ N., longitude 47°49′ W.; depth 1424 meters; dynamic height 970.898

Observed values			Scaled values			
Depth, meters	Temperature, °C.	Salinity, °/oo	Depth, meters	Temperature, °C.	Salinity, °/oo	σ_t
0	2.39	33.46	0	2.39	33.46	26.73
24	2.36	33.55	25	2.35	33.56	26.82
47	2.40	34.00	50	2.40	34.03	27.18
71	2.08	34.20	75	2.10	34.24	27.37
94	2.40	34.42	100	2.45	34.45	27.51
141	2.83	34.58	150	2.90	34.60	27.60
188	3.11	34.69	200	3.15	34.71	27.66
282	3.35	34.76	300	3.40	34.77	27.69
294	3.40	34.78	400	3.65	34.81	27.69
453	3.73	34.82	600	3.65	34.86	27.73
620	3.67	34.86	800	3.70	34.90	27.76
795	3.68	34.90	1,000	3.60	34.90	27.77
1,170	3.52	34.90	-------	-------	-------	-------

Station 3832; 10 May; latitude 45°20′ N., longitude 47°14′ W.; depth 2743 meters; dynamic height 970.908

Observed values			Scaled values			
Depth, meters	Temperature, °C.	Salinity, °/oo	Depth, meters	Temperature, °C.	Salinity, °/oo	σ_t
0	6.40	34.12	0	6.40	34.12	26.83
25	6.28	34.16	25	6.28	34.16	26.87
48	6.12	34.36	50	6.10	34.38	27.07
73	5.27	34.52	75	5.20	34.52	27.30
97	4.59	34.53	100	4.55	34.53	27.37
146	4.22	34.64	150	4.25	34.65	27.50
194	4.52	34.78	200	4.50	34.79	27.58
291	4.38	34.89	300	4.35	34.89	27.68
358	4.00	34.875	400	3.90	34.88	27.72
549	3.76	34.90	600	3.70	34.90	27.76
749	3.64	34.90	800	3.60	34.90	27.77
953	3.57	34.89	1,000	3.55	34.895	27.77
1,489	3.49	34.94	-------	-------	-------	-------

Station 3833; 10 May; latitude 45°18′ N., longitude 46°34′ W.; depth 3292 meters; dynamic height 970.906

Observed values			Scaled values			
Depth, meters	Temperature, °C.	Salinity, °/oo	Depth, meters	Temperature, °C.	Salinity, °/oo	σ_t
0	6.29	33.91	0	6.29	33.91	26.69
27	5.89	34.07	25	5.90	34.06	26.85
53	5.22	34.24	50	5.25	34.22	27.05
80	5.01	34.56	75	5.05	34.54	27.32
106	4.45	34.59	100	4.55	34.58	27.41
160	4.53	34.75	150	4.50	34.73	27.53
214	3.92	34.76	200	4.00	34.76	27.62
320	3.96	34.86	300	3.95	34.84	27.68
423	3.95	34.89	400	3.95	34.89	27.72
632	3.72	34.905	600	3.75	34.90	27.75
841	3.71	34.915	800	3.70	34.91	27.77
1,058	3.54	34.91	1,000	3.60	34.91	27.78
1,611	3.39	34.93	-------	-------	-------	-------

Station 3834; 10 May; latitude 45°20′ N., longitude 45°50′ W.; depth 3539 meters; dynamic height 971.065

Observed values			Scaled values			
Depth, meters	Temperature, °C.	Salinity, °/oo	Depth, meters	Temperature, °C.	Salinity, °/oo	σ_t
0	13.21	35.05	0	13.21	35.05	26.41
26	12.32	34.97	25	12.35	34.98	26.53
54	10.98	34.925	50	11.20	34.93	26.70
81	9.78	34.86	75	10.00	34.87	26.87
108	10.80	35.20	100	10.55	35.09	26.94
162	9.78	35.07	150	10.05	35.10	27.04
216	8.49	-------	200	8.90	34.98	27.13
324	5.54	34.80	300	6.20	34.82	27.41
404	5.31	34.96	400	5.35	34.96	27.62
605	4.47	34.96	600	4.45	34.9	27.73
804	4.11	34.955	800	4.10	34.96	27.77
1,005	3.97	34.96	1,000	4.00	34.96	27.78
1,516	3.61	34.94	-------	-------	-------	-------

Station 3835; 10–11 May; latitude 45°20′ N., longitude 45°15′ W.; depth 3731 meters; dynamic height 971.153

Observed values			Scaled values			
Depth, meters	Temperature, °C.	Salinity, °/oo	Depth, meters	Temperature, °C.	Salinity, °/oo	σ_t
0	14.49	35.65	0	14.49	35.65	26.61
25	14.45	35.64	25	14.45	35.64	26.60
51	14.08	35.63	50	14.10	35.63	26.67
76	13.31	35.53	75	13.30	35.53	26.76
102	13.09	35.54	100	13.10	35.54	26.81
152	12.84	35.61	150	12.90	35.61	26.91
203	10.56	35.205	200	10.70	35.23	27.02
305	8.27	34.99	300	8.40	35.00	27.23
401	6.15	34.89	400	6.20	34.89	27.56
600	5.12	34.97	600	5.12	34.97	27.66
798	4.56	34.98	800	4.55	34.98	27.73
998	4.30	34.98	1,000	4.30	34.98	27.75
1,509	3.56	34.915	-------	-------	-------	-------

Station 3836; 11 May; latitude 44°50′ N., longitude 45°18′ W.; depth 4061 meters; dynamic height 971.062

Observed values			Scaled values			
Depth, meters	Temperature, °C.	Salinity, °/oo	Depth, meters	Temperature, °C.	Salinity, °/oo	σ_t
0	12.58	35.00	0	12.58	35.00	26.50
22	12.79	35.07	25	12.75	35.07	26.52
45	11.81	35.07	50	11.60	35.07	26.74
67	11.07	35.06	75	11.05	35.08	26.85
90	11.03	35.12	100	10.50	35.03	26.90
134	7.43	34.63	150	7.50	34.73	27.15
179	6.35	34.54	200	6.65	34.68	27.23
269	6.13	34.78	300	6.10	34.83	27.42
199	7.00	34.72	400	4.70	34.83	27.59
298	6.51	34.865	600	4.50	34.94	27.70
398	4.70	34.825	800	4.30	34.97	27.75
512	4.58	34.93	(1,000)	4.00	34.99	27.80
819	4.27	34.97	-------	-------	-------	-------

Station 3837; 11 May; latitude 44°18′ N., longitude 45°16′ W.; depth 4322 meters; dynamic height 970.991

Observed values			Scaled values			
Depth, meters	Temperature, °C.	Salinity, °/oo	Depth, meters	Temperature, °C.	Salinity, °/oo	σ_t
0	8.55	33.86	0	8.55	33.86	26.32
27	9.82	34.48	25	9.80	34.46	26.58
53	6.68	34.285	50	7.05	34.31	26.89
80	4.90	34.23	75	5.15	34.24	27.07
106	6.60	34.62	100	6.25	34.55	27.19
160	5.15	34.54	150	5.35	34.55	27.30
213	4.89	34.64	200	4.95	34.62	27.40
320	4.19	34.74	300	4.30	34.72	27.56
417	4.58	34.905	400	4.55	34.88	27.65
630	4.08	34.93	600	4.10	34.93	27.74
836	3.94	34.93	800	3.95	34.93	27.75
1,050	3.66	34.92	1,000	3.70	34.92	27.78
1,590	3.59	34.94	-------	-------	-------	-------

Table of Oceanographic Data—Continued

STATIONS OCCUPIED IN 1949—Continued

Station 3838; 11 May; latitude 44°20.5′ N., longitude 45°50′ W.; depth 3878 meters; dynamic height 970.933

Observed values			Scaled values			
Depth, meters	Temperature, °C.	Salinity, °/oo	Depth, meters	Temperature, °C.	Salinity, °/oo	σ_t
0	4.23	33.24	0	4.23	33.24	26.39
26	4.15	33.53	25	4.15	33.52	26.62
52	2.94	33.95	50	2.95	33.92	27.05
78	3.34	34.22	75	3.30	34.20	27.24
103	4.40	34.50	100	4.30	34.46	27.35
154	4.22	34.59	150	4.25	34.58	27.44
206	3.55	34.64	200	3.60	34.64	27.56
309	4.52	34.90	300	4.45	34.88	27.66
381	4.87	34.985	400	4.85	34.99	27.70
573	4.15	34.95	600	4.05	34.95	27.76
764	3.82	34.92	800	3.80	34.92	27.77
960	3.73	34.93	1,000	3.70	34.93	27.78
1,459	3.55	34.92	-------	-------	-------	-------

Station 3839; 11 May; latitude 44°25′ N., longitude 46°22′ W.; depth 3731 meters; dynamic height 971.084

Observed values			Scaled values			
Depth, meters	Temperature, °C.	Salinity, °/oo	Depth, meters	Temperature, °C.	Salinity, °/oo	σ_t
0	15.04	35.88	0	15.04	35.88	26.58
24	15.06	35.88	25	15.05	35.88	26.58
48	14.95	35.875	50	14.95	35.88	26.67
73	14.96	35.87	75	14.80	35.86	26.69
96	13.36	35.59	100	13.20	35.57	26.81
145	12.15	35.43	150	12.05	35.42	26.93
193	10.64	35.32	200	10.40	35.30	27.13
289	6.19	34.76	300	6.35	34.85	27.41
334	5.98	34.88	400	5.10	34.89	27.59
500	4.57	34.92	600	4.35	34.94	27.72
669	4.25	34.95	800	3.95	34.94	27.76
850	3.89	34.94	1,000	3.75	34.94	27.78
1;327	3.58	34.925	-------	-------	-------	-------

Station 3840; 12 May; latitude 44°31′ N., longitude 47°00′ W.; depth 3658 meters; dynamic height 971.105

Observed values			Scaled values			
Depth, meters	Temperature, °C.	Salinity, °/oo	Depth, meters	Temperature, °C.	Salinity, °/oo	σ_t
0	14.95	35.87	0	14.95	35.87	26.67
28	14.94	35.87	25	14.95	35.87	26.67
56	12.60	35.48	50	13.00	35.57	26.85
84	13.04	35.66	75	12.90	35.61	26.91
111	12.98	35.65	100	13.00	35.66	26.92
167	12.29	35.53	150	12.60	35.57	26.93
224	10.16	35.28	200	11.30	35.41	27.06
335	5.52	34.71	300	6.65	34.86	27.38
342	5.42	34.70	400	5.25	34.76	27.48
503	4.99	34.87	600	4.70	34.93	27.67
657	4.54	34.97	800	4.00	34.92	27.75
839	3.92	34.91	1,000	3.90	34.93	27.76
1,322	3.80	34.96	-------	-------	-------	-------

Station 3841; 12 May; latitude 44°39′ N., longitude 47°31′ W.; depth 3731 meters; dynamic height 970.991

Observed values			Scaled values			
Depth, meters	Temperature, °C.	Salinity, °/oo	Depth, meters	Temperature, °C.	Salinity, °/oo	σ_t
0	1.99	33.04	0	1.99	33.04	26.43
27	8.94	34.45	25	8.80	34.34	26.65
53	9.43	34.65	50	9.40	34.62	26.78
80	9.19	34.86	75	9.25	34.83	26.96
106	8.13	34.72	100	8.40	34.76	27.04
160	4.27	34.34	150	5.00	34.41	27.23
212	2.27	34.32	200	2.55	34.31	27.40
318	2.97	34.64	300	2.85	34.59	27.59
425	3.60	34.80	400	3.45	34.77	27.68
635	3.82	34.89	600	3.80	34.88	27.73
846	3.67	34.90	800	3.70	34.90	27.76
1,057	3.58	34.91	1,000	3.55	34.91	27.78
1,582	3.52	34.93	-------	-------	-------	-------

Station 3842; 12 May; latitude 44°44′ N., longitude 47°58′ W.; depth 3274 meters; dynamic height 970.915

Observed values			Scaled values			
Depth, meters	Temperature, °C.	Salinity, °/oo	Depth, meters	Temperature, °C.	Salinity, °/oo	σ_t
0	1.73	33.15	0	1.73	33.15	26.54
26	0.79	33.30	25	0.80	33.30	26.71
52	0.55	33.67	50	0.55	33.64	27.00
78	1.00	33.98	75	0.95	33.95	27.22
104	1.89	34.26	100	1.75	34.21	27.38
155	2.69	34.52	150	2.65	34.50	27.54
208	3.17	34.66	200	3.10	34.64	27.61
312	3.52	34.80	300	3.50	34.79	27.69
412	3.81	34.88	400	3.80	34.87	27.73
615	3.69	34.89	600	3.70	34.89	27.75
817	3.58	34.885	800	3.55	34.88	27.75
1,022	3.65	34.91	1,000	3.65	34.91	27.77
1,532	3.53	34.935	-------	-------	-------	-------

Station 3843; 12 May; latitude 44°48′ N., longitude 48°24′ W.; depth 2415 meters; dynamic height 970.884

Observed values			Scaled values			
Depth, meters	Temperature, °C.	Salinity, °/oo	Depth, meters	Temperature, °C.	Salinity, °/oo	σ_t
0	2.48	33.36	0	2.48	33.36	26.64
26	2.32	33.45	25	2.30	33.47	26.75
52	2.03	34.21	50	2.05	34.16	27.32
77	2.41	34.39	75	2.40	34.37	27.46
103	2.52	34.47	100	2.50	34.46	27.52
154	2.99	34.63	150	2.95	34.62	27.61
205	3.38	34.74	200	3.35	34.73	27.65
308	3.71	34.84	300	3.70	34.83	27.70
405	3.82	34.88	400	3.80	34.88	27.73
609	3.90	34.925	600	3.90	34.92	27.76
807	3.82	34.935	800	3.80	34.93	27.77
1,010	3.55	34.90	1,000	3.55	34.90	27.77
1,524	3:61	34.95	-------	-------	-------	-------

Station 3844; 12 May; latitude 44°52′ N., longitude 48°56′ W., depth 856 meters; dynamic height 971.013

Observed values			Scaled values			
Depth, meters	Temperature, °C.	Salinity, °/oo	Depth, meters	Temperature, °C.	Salinity, °/oo	σ_t
0	0.92	33.05	0	0.92	33.05	26.51
24	0.61	33.14	25	0.60	33.15	26.61
48	−0.68	33.38	50	−0.70	33.38	26.85
72	−0.71	33.42	75	−0.70	33.43	26.89
96	−0.53	33.50	100	−0.50	33.52	26.96
144	0.16	33.76	150	0.30	33.80	27.14
192	1.22	34.05	200	1.35	34.09	27.31
287	2.56	34.49	300	2.65	34.53	27.56
362	3.04	34.65	400	3.20	34.70	27.65
554	3.63	34.84	600	3.65	34.86	27.73
757	3.71	34.87	800	3.70	34.87	27.74

Station 3845; 12 May; latitude 44°54′ N., longitude 49°06′ W.; depth 96 meters; dynamic height 971.045

Observed values			Scaled values			
Depth, meters	Temperature, °C.	Salinity, °/oo	Depth, meters	Temperature, °C.	Salinity, °/oo	σ_t
0	3.97	33.06	0	3.97	33.06	26.26
25	1.87	33.08	25	1.87	33.08	26.47
49	0.14	33.22	50	0.15	33.23	26.69
74	−0.06	33.30	(75)	−0.10	33.34	26.79

Station 3846; 12 May; latitude 44°55′ N., longitude 49°24′ W.; depth 75 meters; dynamic height 971.045

Observed values			Scaled values			
Depth, meters	Temperature, °C.	Salinity, °/oo	Depth, meters	Temperature, °C.	Salinity, °/oo	σ_t
0	2.52	33.07	0	2.52	33.07	26.41
23	2.47	33.09	25	2.30	33.10	26.45
54	0.34	33.27	50	0.60	33.24	26.68
-------	-------	-------	(75)	0.05	33.32	26.77

STATIONS OCCUPIED IN 1949—Continued

Station 3847; 13 May; latitude 44°15′ N., longitude 49°22′ W.; depth 47 meters; dynamic height 971.029

Observed values			Scaled values			
Depth, meters	Temperature, °C.	Salinity, ‰	Depth, meters	Temperature, °C.	Salinity, ‰	σ_t
0	3.53	33.32	0	3.53	33.32	26.52
15	3.46	33.30	25	3.35	33.31	26.52
30	3.28	33.31	-------	-------	-------	-------

Station 3848; 13 May; latitude 44°08′ N., longitude 49°01′ W.; depth 93 meters; dynamic height 971.026

Observed values			Scaled values			
Depth, meters	Temperature, °C.	Salinity, ‰	Depth, meters	Temperature, °C.	Salinity, ‰	σ_t
0	1.85	33.03	0	1.85	33.03	26.43
24	1.45	33.12	25	1.45	33.12	26.53
49	-------	33.26	50	0.50	33.26	26.69
73	−0.39	33.26	75	−0.40	33.26	26.74

Station 3849; 13 May; latitude 44°07′ N., longitude 48°57′ W.; depth 174 meters; dynamic height 971.008

Observed values			Scaled values			
Depth, meters	Temperature, °C.	Salinity, ‰	Depth, meters	Temperature, °C.	Salinity, ‰	σ_t
0	2.01	33.02	0	2.01	33.02	26.41
25	−0.32	33.29	25	−0.32	33.29	26.75
50	−0.70	33.36	50	−0.70	33.36	26.83
75	−0.59	33.52	75	−0.59	33.52	26.96
100	−0.13	33.65	100	−0.13	33.65	27.05
150	0.61	33.85	150	0.61	33.85	27.16

Station 3850; 13 May; latitude 44°06′ N., longitude 48°46′ W.; depth 657 meters; dynamic height 971.026

Observed values			Scaled values			
Depth, meters	Temperature, °C.	Salinity, ‰	Depth, meters	Temperature, °C.	Salinity, ‰	σ_t
0	2.40	33.05	0	2.40	33.05	26.40
25	0.75	33.14	25	0.75	33.14	26.59
50	−0.26	33.29	50	−0.26	33.29	26.75
75	−0.50	33.40	75	−0.50	33.40	26.86
100	−0.64	33.48	100	−0.64	33.48	26.93
150	0.03	33.72	150	0.03	33.72	27.10
199	0.98	33.99	200	1.00	34.00	27.26
299	2.52	34.50	300	2.55	34.50	27.55
399	3.20	34.70	400	3.20	34.70	27.65
595	3.66	34.85	600	3.65	34.85	27.72

Station 3851; 13 May; latitude 44°03′ N., longitude 48°40′ W.; depth 1646 meters; dynamic height 971.032

Observed values			Scaled values			
Depth, meters	Temperature, °C.	Salinity, ‰	Depth, meters	Temperature, °C.	Salinity, ‰	σ_t
0	2.67	33.04	0	2.67	33.04	26.38
25	2.07	33.06	25	2.07	33.06	26.44
50	−0.10	33.20	50	−0.10	33.20	26.68
75	−0.82	33.36	75	−0.82	33.36	26.83
100	−0.76	33.52	100	−0.76	33.52	26.95
150	0.08	33.73	150	0.08	33.73	27.09
201	1.33	34.10	200	1.30	34.09	27.31
301	2.25	34.40	300	2.25	34.39	27.48
384	3.24	34.70	400	3.35	34.73	27.65
582	3.74	34.87	600	3.75	34.87	27.73
783	3.70	34.89	800	3.70	34.89	27.75
860	-------	-------	(1,000)	3.65	34.90	27.76

Station 3852; 13 May; latitude 43°59′ N., longitude 48°21′ W.; depth 2999 meters: dynamic height 971.024

Observed values			Scaled values			
Depth, meters	Temperature, °C.	Salinity, ‰	Depth, meters	Temperature, °C.	Salinity, ‰	σ_t
0	11.08	34.82	0	11.08	34.82	26.65
24	10.90	34.86	25	10.90	34.87	26.71
48	12.50	35.52	50	12.45	35.52	26.92
72	11.98	35.44	75	11.90	35.43	26.96
96	11.23	35.33	100	11.10	35.31	27.02
143	9.75	35.15	150	9.45	35.10	27.14
190	6.22	34.68	200	6.15	34.69	27.31
286	5.87	34.85	300	5.75	34.87	27.51
398	5.11	34.94	400	5.10	34.94	27.63
561	4.64	34.96	600	4.50	34.95	27.71
700	4.16	34.94	800	3.95	34.94	27.76
888	3.91	34.94	1,000	3.85	34.94	27.77
1,380	3.66	34.935	-------	-------	-------	-------

Station 3853; 13 May; latitude 43°50.5′ N., longitude 47°49′ W.; depth 3768 meters; dynamic height 970.943

Observed values			Scaled values			
Depth, meters	Temperature, °C.	Salinity, ‰	Depth, meters	Temperature, °C.	Salinity, ‰	σ_t
0	7.62	33.72	0	7.62	33.72	26.35
26	5.89	33.72	25	5.90	33.72	26.58
51	4.21	33.82	50	4.30	33.81	26.83
77	3.39	34.02	75	3.45	34.00	27.07
102	3.32	34.31	100	3.30	34.28	27.30
153	3.97	34.63	150	3.95	34.61	27.50
204	4.17	34.74	200	4.15	34.73	27.57
306	4.26	34.85	300	4.25	34.85	27.66
408	4.38	34.92	400	4.35	34.92	27.71
615	4.08	34.935	600	4.10	34.93	27.74
825	3.75	34.92	800	3.80	34.92	27.77
1,070	3.66	34.92	1,000	3.65	34.92	27.78
1,567	3.61	34.95	-------	-------	-------	-------

Station 3854; 13-14 May; latitude 43°41.5′ N., longitude 47°05′ W.; depth 4029 meters; dynamic height 971.206

Observed values			Scaled values			
Depth, meters	Temperature, °C.	Salinity, ‰	Depth, meters	Temperature, °C.	Salinity, ‰	σ_t
0	13.66	35.62	0	13.66	35.62	26.76
28	13.02	35.61	25	13.05	35.61	26.87
57	12.94	35.66	50	12.95	35.65	26.92
85	12.90	35.66	75	12.90	35.66	26.94
112	12.94	35.66	100	12.90	35.66	26.94
169	12.92	35.67	150	12.95	35.67	26.94
226	12.78	35.64	200	12.90	35.66	26.94
338	10.71	35.34	300	11.45	35.47	27.08
411	8.43	35.04	400	8.80	35.09	27.24
615	5.48	34.94	600	5.60	34.94	27.57
820	4.31	34.92	800	4.35	34.92	27.71
1,035	4.09	34.95	1,000	4.10	34.95	27.76
1,586	3.58	34.92	-------	-------	-------	-------

Station 3855; 14 May; latitude 43°33′N., longitude 46°34′ W.; depth 4500 meters; dynamic height 971.129

Observed values			Scaled values			
Depth, meters	Temperature, °C.	Salinity, ‰	Depth, meters	Temperature, °C.	Salinity, ‰	σ_t
0	14.96	35.85	0	14.96	35.85	26.65
27	14.98	35.85	25	14.95	35.85	26.65
54	14.65	35.82	50	14.70	35.83	26.69
82	14.03	35.70	75	14.20	35.75	26.74
108	12.53	35.40	100	12.95	35.48	26.79
162	12.54	35.54	150	12.55	35.51	26.90
216	11.09	35.27	200	11.50	35.36	26.98
324	6.62	34.80	300	7.70	34.88	27.24
419	5.31	34.86	400	5.50	34.85	27.52
635	4.39	34.93	600	4.45	34.93	27.70
856	3.97	34.93	800	4.05	34.93	27.74
1,079	3.90	34.94	1,000	3.90	34.94	27.77
1,636	3.59	34.94	-------	-------	-------	-------

Table of Oceanographic Data—Continued

STATIONS OCCUPIED IN 1949—Continued

Station 3856; 14 May; latitude 43°22′ N., longitude 46°04′ W.; depth 4470 meters; dynamic height 970.975

Observed values			Scaled values			
Depth, meters	Temperature, °C.	Salinity, °/oo	Depth, meters	Temperature, °C.	Salinity, °/oo	σ_t
0	8.33	33.61	0	8.33	33.61	26.16
25	7.55	34.05	25	7.55	34.05	26.61
50	6.47	34.39	50	6.47	34.39	27.03
75	5.04	34.36	75	5.04	34.36	27.19
100	7.43	34.80	100	7.43	34.80	27.22
150	5.79	34.65	150	5.79	34.65	27.32
200	4.58	34.62	200	4.58	34.62	27.45
300	4.69	34.84	300	4.69	34.84	27.60
363	4.94	34.93	400	4.90	34.96	27.68
548	4.70	35.00	600	4.65	35.00	27.74
734	4.48	35.00	800	4.30	34.99	27.76
921	4.02	34.96	1,000	3.95	34.96	27.78
1,418	3.72	34.95	-------	-------	-------	-------

Station 3857; 14 May; latitude 42°59′ N., longitude 46°34′ W.; depth 4372 meters; dynamic height 970.929

Observed values			Scaled values			
Depth, meters	Temperature, °C.	Salinity, °/oo	Depth, meters	Temperature, °C.	Salinity, °/oo	σ_t
0	8.96	33.80	0	8.96	33.80	26.21
20	6.46	33.96	25	6.35	34.02	26.76
40	6.11	34.20	50	5.45	34.24	27.04
60	4.94	34.28	75	4.40	34.35	27.25
80	4.33	34.37	100	4.35	34.48	27.35
121	-------	-------	150	4.65	34.71	27.51
161	4.73	34.76	200	4.80	34.83	27.58
241	4.82	34.88	300	4.65	34.90	27.66
362	4.52	34.91	400	4.45	34.92	27.70
547	4.27	34.96	600	4.20	34.96	27.76
736	3.95	34.94	800	3.80	34.93	27.77
933	3.68	34.91	1,000	3.65	34.91	27.77
1,446	3.57	34.94	-------	-------	-------	-------

Station 3858; 14 May; latitude 42°37.5′ N., longitude 46°54′ W.; depth 4244 meters; dynamic height 971.055

Observed values			Scaled values			
Depth, meters	Temperature, °C.	Salinity, °/oo	Depth, meters	Temperature, °C.	Salinity, °/oo	σ_t
0	13.53	35.18	0	13.53	35.18	26.45
26	7.67	34.12	25	7.70	34.14	26.66
52	7.32	34.17	50	7.35	34.16	26.73
78	7.29	34.24	75	7.30	34.24	26.80
103	5.10	34.07	100	5.25	34.09	26.94
156	6.35	34.51	150	6.25	34.46	27.12
207	6.81	34.74	200	6.80	34.72	27.25
310	5.35	34.82	300	5.50	34.81	27.49
348	5.21	34.84	400	4.95	34.87	27.60
528	4.61	34.94	600	4.50	34.94	27.70
711	-------	34.93	800	4.10	34.92	27.74
929	-------	34.92	1,000	3.90	34.92	27.76
1,389	3.72	34.95	-------	-------	-------	-------

Station 3859; 14 May; latitude 42°53′ N., longitude 47°30′ W.; depth 3663 meters; dynamic height 971.174

Observed values			Scaled values			
Depth, meters	Temperature, °C.	Salinity, °/oo	Depth, meters	Temperature, °C.	Salinity, °/oo	σ_t
0	13.89	35.56	0	13.89	35.56	26.67
25	13.63	35.66	25	13.63	35.66	26.80
49	-------	-------	50	13.30	35.69	26.88
74	13.05	35.70	75	13.05	35.70	26.94
98	13.04	35.70	100	13.05	35.70	26.94
148	13.04	35.70	150	13.05	35.70	26.94
197	12.99	35.69	200	12.95	35.69	26.95
295	10.58	35.31	300	10.50	35.30	27.12
395	8.12	35.04	400	8.00	35.03	27.31
586	5.04	34.95	600	4.95	34.95	27.66
774	4.44	-------	800	4.35	34.94	27.72
899	-------	-------	(1,000)	3.95	34.93	27.75
1,091	-------	-------	-------	-------	-------	-------

Station 3860; 15 May; latitude 43°08′ N., longitude 48°06′ W.; depth 3402 meters; dynamic height 971.143

Observed values			Scaled values			
Depth, meters	Temperature, °C.	Salinity, °/oo	Depth, meters	Temperature, °C.	Salinity, °/oo	σ_t
0	14.25	35.33	0	14.25	35.33	26.41
25	15.21	35.93	25	15.21	35.93	26.67
50	14.95	35.88	50	14.95	35.88	26.67
75	14.61	35.83	75	14.61	35.83	26.71
100	13.51	35.64	100	13.51	35.64	26.80
150	12.02	35.41	150	12.02	35.41	26.92
200	11.51	35.41	200	11.51	35.41	27.02
300	8.03	34.99	300	8.03	34.99	27.28
225	10.96	35.34	400	6.45	34.96	27.48
338	7.18	34.94	600	5.35	35.02	27.67
450	6.04	34.98	800	4.35	34.96	27.74
567	5.52	35.02	(1,000)	3.95	34.94	27.76
870	4.13	34.95	-------	-------	-------	-------

Station 3861; 15 May; latitude 43°18.5′ N., longitude 48°45′ W.; depth 2652 meters; dynamic height 970.961

Observed values			Scaled values			
Depth, meters	Temperature, °C.	Salinity, °/oo	Depth, meters	Temperature, °C.	Salinity, °/oo	σ_t
0	6.50	33.50	0	6.50	33.50	26.33
25	9.10	34.40	25	9.10	34.40	26.65
50	4.68	33.91	50	4.68	33.91	26.87
75	3.69	34.09	75	3.69	34.09	27.11
99	3.74	34.27	100	3.75	34.28	27.26
150	3.67	34.47	150	3.67	34.47	27.42
200	4.19	34.65	200	4.19	34.65	27.51
299	4.19	34.81	300	4.20	34.81	27.64
373	4.34	34.90	400	4.35	34.90	27.69
564	4.13	34.90	600	4.10	34.90	27.72
759	3.90	34.935	800	3.85	34.93	27.76
962	3.77	34.92	1,000	3.75	34.92	27.77
1,485	3.54	34.93	-------	-------	-------	-------

Station 3862; 15 May; latitude 43°18.5′ N., longitude 50°15′ W.; depth 62 meters; dynamic height 971.038

Observed values			Scaled values			
Depth, meters	Temperature, °C.	Salinity, °/oo	Depth, meters	Temperature, °C.	Salinity, °/oo	σ_t
0	6.63	33.13	0	6.63	33.13	26.00
25	4.21	33.30	25	4.21	33.30	26.43
50	2.07	33.42	50	2.07	33.42	26.74

Station 3863; 15 May; latitude 43°01′ N., longitude 50°15′ W.; depth 100 meters; dynamic height 971.036

Observed values			Scaled values			
Depth, meters	Temperature, °C.	Salinity, °/oo	Depth, meters	Temperature, °C.	Salinity, °/oo	σ_t
0	4.98	32.92	0	4.98	32.92	26.05
25	1.17	33.06	25	1.17	33.06	26.50
50	−0.26	33.26	50	−0.26	33.26	26.73
80	−0.58	33.35	75	−0.55	33.34	26.81

Station 3864; 15 May; latitude 42°53′ N., longitude 50°13′ W.; depth 356 meters; dynamic height 971.034

Observed values			Scaled values			
Depth, meters	Temperature, °C.	Salinity, °/oo	Depth, meters	Temperature, °C.	Salinity, °/oo	σ_t
0	3.77	32.80	0	3.77	32.80	26.09
25	2.94	33.16	25	2.94	33.16	26.44
50	0.82	33.19	50	0.82	33.19	26.63
75	−0.47	33.39	75	−0.47	33.39	26.85
100	−0.64	33.47	100	−0.64	33.47	26.93
150	−0.24	33.62	150	−0.24	33.62	27.03
200	0.99	33.95	200	0.99	33.95	27.22
300	3.24	34.64	300	3.24	34.64	27.59

STATIONS OCCUPIED IN 1949—Continued

Station 3865; 16 May; latitude 42°45′ N., longitude 50°12′ W.; depth 1463 meters; dynamic height 971.006

Observed values			Scaled values			
Depth, meters	Temperature, °C.	Salinity, °/oo	Depth, meters	Temperature, °C.	Salinity, °/oo	σ_t
0	3.63	33.00	0	3.63	33.00	26.25
25	3.32	33.11	25	3.32	33.11	26.37
49	7.64	34.26	50	7.60	34.28	26.78
74	6.68	34.42	75	6.55	34.42	27.05
99	4.97	34.22	100	5.00	34.22	27.08
148	6.25	34.52	150	6.20	34.52	27.17
198	4.17	34.46	200	4.10	34.46	27.37
297	3.35	34.65	300	3.35	34.66	27.60
376	3.96	34.81	400	3.95	34.82	27.67
570	3.77	34.88	600	3.80	34.89	27.74
768	3.91	34.91	800	3.85	34.91	27.75
961	3.74	34.90	1,000	3.75	34.90	27.75
1,348	3.71	34.92	-------	-------	-------	-------

Station 3866; 16 May; latitude 42°27′ N., longitude 50°14′ W.; depth 2798 meters; dynamic height 971.016

Observed values			Scaled values			
Depth, meters	Temperature, °C.	Salinity, °/oo	Depth, meters	Temperature, °C.	Salinity, °/oo	σ_t
0	8.13	33.26	0	8.13	33.26	25.91
24	4.10	33.37	25	4.10	33.44	26.56
48	9.94	34.88	50	9.95	34.91	26.91
72	9.71	34.99	75	9.65	34.99	27.02
96	9.01	34.94	100	8.75	34.93	27.12
143	6.86	34.72	150	6.80	34.73	27.25
191	6.50	34.78	200	6.40	34.80	27.36
287	5.89	34.92	300	5.70	34.91	27.54
280	5.75	34.88	400	5.20	34.95	27.63
426	5.09	34.95	600	4.55	34.97	27.73
575	4.55	34.96	800	4.75	35.06	27.77
740	4.96	35.07	1,000	4.15	34.99	27.78
1,189	3.94	34.965	-------	-------	-------	-------

Station 3867; 16 May; latitude 41°59.5′ N., longitude 50°15′ W.; depth 3658 meters; dynamic height 970.974

Observed values			Scaled values			
Depth, meters	Temperature, °C.	Salinity, °/oo	Depth, meters	Temperature, °C.	Salinity, °/oo	σ_t
0	7.63	33.38	0	7.63	33.38	26.08
27	5.13	33.58	25	5.30	33.57	26.53
53	4.28	33.88	50	4.40	33.84	26.84
80	3.48	33.92	75	3.60	33.91	26.98
106	3.27	34.03	100	3.30	34.00	27.08
160	3.64	34.32	150	3.55	34.26	27.26
213	4.15	34.58	200	4.05	34.52	27.42
319	3.89	34.79	300	3.95	34.76	27.62
437	3.69	34.87	400	3.70	34.85	27.72
654	3.59	34.89	600	3.60	34.89	27.76
871	3.54	34.90	800	3.55	34.90	27.77
1,089	3.61	34.92	1,000	3.60	34.91	27.78
1,634	3.38	34.93	-------	-------	-------	-------

Station 3868; 16 May; latitude 42°00′ N., longitude 49°28′ W.; depth 3292 meters; dynamic height 970.987

Observed values			Scaled values			
Depth, meters	Temperature, °C.	Salinity, °/oo	Depth, meters	Temperature, °C.	Salinity, °/oo	σ_t
0	7.20	33.07	0	7.20	33.07	25.89
26	3.82	33.34	25	3.85	33.33	26.49
51	3.10	33.88	50	3.10	33.85	26.98
77	4.48	34.26	75	4.45	34.25	27.16
103	3.88	34.31	100	3.95	34.30	27.26
153	5.30	34.60	150	5.30	34.59	27.33
204	3.44	34.44	200	3.50	34.45	27.42
307	4.81	34.82	300	4.75	34.81	27.58
396	4.25	34.84	400	4.20	34.84	27.66
593	3.94	34.90	600	3.95	34.90	27.73
791	3.81	34.90	800	3.75	34.90	27.75
995	3.62	34.89	1,000	3.60	34.89	27.76
1,515	3.64	34.925	-------	-------	-------	-------

Station 3869; 16 May; latitude 41°31′ N., longitude 49°02′ W.; depth 3036 meters; dynamic height 971.166

Observed values			Scaled values			
Depth, meters	Temperature, °C.	Salinity, °/oo	Depth, meters	Temperature, °C.	Salinity, °/oo	σ_t
0	12.47	34.02	0	12.47	34.02	25.76
27	4.59	33.40	25	4.75	33.42	26.48
53	10.03	34.71	50	9.20	34.53	26.73
79	12.39	35.34	75	12.35	35.30	26.77
105	12.29	35.29	100	12.35	35.30	26.77
159	9.84	34.93	150	10.25	35.00	26.93
211	7.34	34.67	200	7.90	34.71	27.08
316	6.64	34.77	300	6.80	34.76	27.28
443	3.70	34.52	400	4.60	34.59	27.41
665	4.72	34.935	600	4.40	34.84	27.63
1,109	3.82	34.92	800	4.40	34.93	27.70
1,665	3.60	34.93	1,000	3.95	34.92	27.75

Station 3870; 17 May; latitude 42°02′ N., longitude 47°54′ W.; depth 3713 meters; dynamic height 970.988

Observed values			Scaled values			
Depth, meters	Temperature, °C.	Salinity, °/oo	Depth, meters	Temperature, °C.	Salinity, °/oo	σ_t
0	9.55	33.72	0	9.55	33.72	26.05
23	9.56	34.42	25	9.50	34.44	26.62
46	8.27	34.60	50	8.20	34.62	26.97
69	7.95	34.68	75	7.70	34.66	27.07
93	6.92	34.59	100	6.75	34.60	27.16
138	6.06	34.63	150	5.80	34.63	27.30
184	5.12	34.62	200	5.15	34.66	27.41
277	5.62	34.94	300	5.55	34.96	27.60
385	5.14	34.98	400	5.10	34.98	27.66
579	4.55	34.98	600	4.50	34.98	27.73
774	4.13	34.96	800	4.05	34.96	27.77
973	3.89	34.96	1,000	3.85	34.96	27.79
1,478	3.63	34.95	-------	-------	-------	-------

Station 3871; 17 May; latitude 42°21′ N., longitude 48°32′ W.; depth 3329 meters; dynamic height 970.958

Observed values			Scaled values			
Depth, meters	Temperature, °C.	Salinity, °/oo	Depth, meters	Temperature, °C.	Salinity, °/oo	σ_t
0	6.43	32.69	0	6.43	32.69	25.70
28	5.31	33.80	25	5.40	33.67	26.60
55	4.82	34.23	50	4.95	34.21	27.08
83	3.61	34.24	75	3.90	34.24	27.21
110	4.85	34.45	100	4.35	34.37	27.27
166	5.50	34.74	150	5.40	34.68	27.39
221	5.40	34.86	200	5.45	34.83	27.50
331	4.94	34.94	300	5.05	34.92	27.63
431	4.71	34.98	400	4.80	34.97	27.70
586	4.20	34.95	600	4.15	34.95	27.75
702	3.88	34.94	800	3.75	34.93	27.77
851	3.78	34.93	1,000	3.75	34.93	27.77
1,176	3.70	34.935	-------	-------	-------	-------

Station 3872; 17 May; latitude 42°41′ N., longitude 49°10′ W.; depth 2232 meters; dynamic height 970.991

Observed values			Scaled values			
Depth, meters	Temperature, °C.	Salinity, °/oo	Depth, meters	Temperature, °C.	Salinity, °/oo	σ_t
0	10.76	33.95	0	10.76	33.95	26.02
28	11.69	35.26	25	11.60	35.11	26.77
55	12.38	35.53	50	12.30	35.51	26.95
83	11.20	35.30	75	11.55	35.36	26.97
109	10.69	35.26	100	10.85	35.28	27.04
165	4.25	34.34	150	6.00	34.57	27.24
220	5.65	34.81	200	5.15	34.65	27.40
329	5.25	34.92	300	5.40	34.91	27.58
418	4.52	34.91	400	4.65	34.91	27.67
629	3.82	34.90	600	3.85	34.90	27.74
842	3.80	34.92	800	3.80	34.92	27.77
1,055	3.58	34.91	1,000	3.60	34.91	27.78
1,591	3.58	34.945	-------	-------	-------	-------

STATIONS OCCUPIED IN 1949—Continued

Station 3873; 3 June; latitude 47°24′ N., longitude 50°00′ W.; depth 92 meters; dynamic height 971.032

Observed values			Scaled values			
Depth, meters	Temperature, °C.	Salinity, °/oo	Depth, meters	Temperature, °C.	Salinity, °/oo	σ_t
0	3.42	33.05	0	3.42	33.05	26.32
25	3.25	33.03	25	3.25	33.03	26.31
49	2.05	33.19	50	1.95	33.19	26.55
74	0.32	33.41	75	0.25	33.41	26.84

Station 3874; 3 June; latitude 47°42′ N., longitude 49°52′ W.; depth 117 meters; dynamic height 971.032

Observed values			Scaled values			
Depth, meters	Temperature, °C.	Salinity, °/oo	Depth, meters	Temperature, °C.	Salinity, °/oo	σ_t
0	2.72	32.79	0	2.72	32.79	26.11
25	1.56	32.98	25	1.56	32.98	26.41
50	1.64	33.13	50	1.64	33.13	26.52
75	0.17	33.43	75	0.17	33.43	26.86
100	0.08	33.46	100	0.08	33.46	26.89

Station 3875; 3 June; latitude 47°59′ N., longitude 49°50′ W.; depth 172 meters; dynamic height 971.027

Observed values			Scaled values			
Depth, meters	Temperature, °C.	Salinity, °/oo	Depth, meters	Temperature, °C.	Salinity, °/oo	σ_t
0	2.64	32.89	0	2.64	32.89	26.26
25	0.85	33.01	25	0.85	33.01	26.49
51	0.38	33.18	50	0.40	33.18	26.64
76	−1.48	33.29	75	−1.45	33.29	26.80
101	−1.06	33.44	100	−1.10	33.43	26.91
152	0.14	33.70	150	0.10	33.69	27.06

Station 3876; 3 June; latitude 48°14′ N., longitude 49°43′ W.; depth 225 meters; dynamic height 971.029

Observed values			Scaled values			
Depth, meters	Temperature, °C.	Salinity, °/oo	Depth, meters	Temperature, °C.	Salinity, °/oo	σ_t
0	2.19	32.94	0	2.19	32.94	26.33
25	1.41	33.33	25	1.41	33.00	26.44
50	−0.90	33.16	50	−0.90	33.16	26.69
75	−1.62	33.29	75	−1.62	33.29	26.80
100	−1.63	33.34	100	−1.63	33.34	26.85
150	−0.70	33.59	150	−0.70	33.59	27.02
200	0.85	33.94	200	0.85	33.94	27.22

Station 3877; 3 June; latitude 48°32′ N., longitude 49°35′ W.; depth 703 meters; dynamic height 970.922

Observed values			Scaled values			
Depth, meters	Temperature, °C.	Salinity, °/oo	Depth, meters	Temperature, °C.	Salinity, °/oo	σ_t
0	1.58	33.12	0	1.58	33.12	26.52
25	−0.02	33.76	25	−0.02	33.76	27.13
50	0.95	33.95	50	0.95	33.95	27.22
75	1.53	34.11	75	1.53	34.11	27.31
100	1.81	34.21	100	1.81	34.21	27.38
150	1.81	34.29	150	1.81	34.29	27.44
200	2.11	34.42	200	2.11	34.42	27.52
300	2.58	34.56	300	2.58	34.55	27.59
398	3.23	34.75	400	3.25	34.75	27.68
596	3.38	34.84	600	3.40	34.84	27.74

Station 3878; 4 June; latitude 48°43′ N., longitude 49°30′ W.; depth 1161 meters; dynamic height 970.924

Observed values			Scaled values			
Depth, meters	Temperature, °C.	Salinity, °/oo	Depth, meters	Temperature, °C.	Salinity, °/oo	σ_t
0	1.17	33.37	0	1.17	33.37	26.75
25	1.01	33.36	25	1.01	33.36	26.75
50	0.09	33.48	50	0.09	33.48	26.90
75	0.24	33.81	75	0.24	33.81	27.16
100	0.61	33.99	100	0.61	33.99	27.27
150	1.33	34.25	150	1.33	34.25	27.44
200	2.15	34.47	200	2.15	34.47	27.56
300	2.93	34.69	300	2.93	34.69	27.67
383	3.46	34.80	400	3.50	34.81	27.71
576	3.51	34.86	600	3.50	34.87	27.76
770	3.50	34.89	800	3.50	34.89	27.77
1,068	3.47	34.91	1,000	3.45	34.91	27.79

Station 3879; 4 June; latitude 49°12.5′ N., longitude 49°15′ W.; depth 1639 meters; dynamic height 970.831

Observed values			Scaled values			
Depth, meters	Temperature, °C.	Salinity, °/oo	Depth, meters	Temperature, °C.	Salinity, °/oo	σ_t
0	3.70	34.46	0	3.70	34.46	27.41
24	3.55	34.46	25	3.50	34.46	27.43
47	3.14	34.51	50	3.10	34.51	27.51
71	3.06	34.55	75	3.00	34.56	27.57
94	2.68	34.61	100	2.70	34.63	27.64
141	3.30	34.76	150	3.30	34.77	27.70
188	3.35	34.80	200	3.35	34.81	27.72
282	3.34	34.81	300	3.35	34.84	27.74
316	3.31	34.85	400	3.35	34.85	27.75
485	3.32	34.85	600	3.35	34.85	27.75
662	3.35	34.85	800	3.40	34.87	27.77
842	3.43	34.87	1,000	3.45	34.89	27.77
1,316	3.47	34.93	-------	-------	-------	-------

Station 3880; 4 June; latitude 49°41′ N., longitude 49°04′ W.; depth 1785 meters; dynamic height 970.801

Observed values			Scaled values			
Depth, meters	Temperature, °C.	Salinity, °/oo	Depth, meters	Temperature, °C.	Salinity, °/oo	σ_t
0	3.93	34.64	0	3.93	34.64	27.52
24	3.91	34.67	25	3.90	34.67	27.56
48	2.99	34.62	50	3.00	34.62	27.61
72	3.27	34.70	75	3.25	34.70	27.64
95	3.03	34.71	100	3.00	34.71	27.68
144	3.02	34.77	150	3.05	34.78	27.73
192	3.23	34.83	200	3.25	34.84	27.75
287	3.26	34.85	300	3.30	34.85	27.76
301	3.28	34.85	400	3.30	34.86	27.77
468	3.30	34.86	600	3.30	34.87	27.78
647	3.30	34.88	800	3.30	34.89	27.79
830	3.34	34.89	1,000	3.35	34.90	27.79
1,324	3.44	34.93	-------	-------	-------	-------

Station 3881; 4 June; latitude 50°00′ N., longitude 49°02′ W.; depth1866 meters; dynamic height 970.816

Observed values			Scaled values			
Depth, meters	Temperature, °C.	Salinity, °/oo	Depth, meters	Temperature, °C.	Salinity, °/oo	σ_t
0	4.50	34.62	0	4.50	34.62	27.45
25	4.49	34.61	25	4.49	34.61	27.44
50	3.86	34.63	50	3.86	34.63	27.53
75	3.32	34.67	75	3.32	34.67	27.62
100	3.01	34.68	100	3.01	34.68	27.66
150	3.33	34.80	150	3.33	34.80	27.71
200	3.57	34.87	200	3.57	34.87	27.75
299	3.51	34.87	300	3.55	34.87	27.75
301	3.54	34.875	400	3.45	34.87	27.76
470	3.37	34.875	600	3.35	34.88	27.77
648	3.37	34.875	800	3.40	34.89	27.78
835	3.44	34.895	1,000	3.40	34.90	27.79
1,343	3.42	34.925	-------	-------	-------	-------

Table of Oceanographic Data—Continued

STATIONS OCCUPIED IN 1949—Continued

Station 3882; 4 June; latitude 49°49′ N., longitude 49°30′ W.; depth 1320 meters; dynamic height 970.830

Observed values			Scaled values			
Depth, meters	Temperature, °C.	Salinity, °/₀₀	Depth, meters	Temperature, °C.	Salinity, °/₀₀	σ_t
0	2.36	33.93	0	2.36	33.93	27.11
26	3.28	34.37	25	3.25	34.36	27.37
52	1.89	34.41	50	1.90	34.40	27.52
78	2.64	34.58	75	2.55	34.57	27.61
104	2.85	34.64	100	2.85	34.63	27.63
156	2.99	34.69	150	2.95	34.69	27.66
208	3.16	34.78	200	3.15	34.77	27.71
312	3.33	34.83	300	3.35	34.83	27.74
375	3.48	34.86	400	3.40	34.86	27.76
575	3.38	34.87	600	3.40	34.87	27.77
781	3.35	34.87	800	3.35	34.87	27.77
980	3.37	34.87	1,000	3.35	34.87	27.77
1,320	3.42	34.91	--------	--------	--------	--------

Station 3883; 4 June; latitude 49°39′ N., longitude 50°02′ W.; depth 653 meters; dynamic height 970.861

Observed values			Scaled values			
Depth, meters	Temperature, °C.	Salinity, °/₀₀	Depth, meters	Temperature, °C.	Salinity, °/₀₀	σ_t
0	2.05	33.98	0	2.05	33.98	27.18
25	1.63	34.13	25	1.63	34.13	27.33
50	1.65	34.33	50	1.65	34.33	27.49
75	1.83	34.38	75	1.83	34.38	27.51
100	2.08	34.47	100	2.08	34.47	27.56
149	2.64	34.62	150	2.65	34.62	27.64
199	2.94	34.69	200	2.95	34.69	27.66
299	3.11	34.76	300	3.10	34.76	27.71
393	3.19	34.77	400	3.20	34.77	27.71
592	3.34	34.84	(600)	3.35	34.84	27.74

Station 3884; 5 June; latitude 49°28′ N., longitude 50°34′ W.; depth 324 meters; dynamic height 970.948

Observed values			Scaled values			
Depth, meters	Temperature, °C.	Salinity, °/₀₀	Depth, meters	Temperature, °C.	Salinity, °/₀₀	σ_t
0	1.70	33.19	0	1.70	33.19	26.57
24	1.34	33.33	25	1.35	33.33	26.70
47	−1.06	33.31	50	−1.10	33.35	26.84
71	−0.88	33.59	75	−0.70	33.62	27.05
94	0.26	33.81	100	0.50	33.88	27.20
142	2.24	34.24	150	2.20	34.27	27.40
189	1.90	34.35	200	2.00	34.38	27.50
283	2.89	34.66	(300)	3.05	34.72	27.68

Station 3885; 5 June; latitude 49°23′ N., longitude 51°03′ W.; depth 346 meters; dynamic height 970.923

Observed values			Scaled values			
Depth, meters	Temperature, °C.	Salinity, °/₀₀	Depth, meters	Temperature, °C.	Salinity, °/₀₀	σ_t
0	1.98	33.37	0	1.98	33.37	26.69
24	1.89	33.37	25	1.85	33.38	26.71
49	0.11	33.62	50	0.10	33.63	27.02
73	0.26	33.92	75	0.30	33.94	27.25
97	1.17	34.15	100	1.30	34.17	27.38
146	2.25	34.35	150	2.30	34.36	27.46
195	2.47	34.49	200	2.50	34.51	27.56
292	3.19	34.75	(300)	3.25	34.77	27.70

Station 3386; 5 June; latitude 49°13.5 N., longitude 51°36′ W. Depth 315; dynamic height 970.981.

Observed values			Scaled values			
Depth, meters	Temperature, °C.	Salinity, °/₀₀	Depth, meters	Temperature, °C.	Salinity, °/₀₀	σ_t
0	1.78	32.61	0	1.78	32.68	26.16
23	1.31	32.97	25	1.25	32.99	25.44
47	0.85	33.24	50	0.80	33.28	26.70
70	0.47	33.51	75	0.45	33.57	26.95
93	0.53	33.67	100	0.50	33.71	27.06
140	0.25	33.98	150	0.45	34.03	27.32
186	1.29	34.19	200	1.55	34.26	27.43
279	2.72	34.55	(300)	3.00	34.63	27.62

Station 3887; 5 June; latitude 49°06′ N., longitude 51°54′ W.; depth 287 meters, dynamic height 971.041

Observed values			Scaled values			
Depth, meters	Temperature, °C.	Salinity, °/₀₀	Depth, meters	Temperature, °C.	Salinity, °/₀₀	σ_t
0	2.13	32.32	0	2.13	32.32	25.84
25	−0.85	32.78	25	−0.85	32.78	26.37
50	−1.55	33.16	50	−1.55	33.16	26.70
75	−1.69	33.25	75	−1.69	33.25	26.78
100	−1.73	33.32	100	−1.73	33.32	26.83
150	−1.35	33.43	150	−1.35	33.43	26.92
199	−0.71	33.67	200	−0.65	33.68	27.10
279	2.01	34.31	--------	--------	--------	--------

Station 3888; 5 June; latitude 49°01′ N., longitude 52°08′ W.; depth 269 meters, dynamic height 971.043

Observed values			Scaled values			
Depth, meters	Temperature, °C.	Salinity, °/₀₀	Depth, meters	Temperature, °C.	Salinity, °/₀₀	σ_t
0	2.62	32.22	0	2.62	32.22	25.73
23	0.18	32.92	25	0.10	32.95	26.48
46	−1.53	33.20	50	−1.60	33.22	26.75
69	−1.64	33.27	75	−1.65	33.29	26.80
92	--------	--------	100	−1.55	33.34	26.85
138	−1.34	33.41	150	−1.30	33.47	26.95
183	−0.97	33.59	200	−0.45	33.68	27.09
275	1.62	34.17	--------	--------	--------	--------

Station 3889; 5 June; latitude 48°55′ N., longitude 52°25′ W.; depth 369 meters, dynamic height 971.050

Observed values			Scaled values			
Depth, meters	Temperature, °C.	Salinity, °/₀₀	Depth, meters	Temperature, °C.	Salinity, °/₀₀	σ_t
0	2.72	32.58	0	2.72	32.58	26.00
24	1.51	32.83	25	1.45	32.84	26.31
47	−1.12	33.12	50	−1.25	33.14	26.67
71	−1.59	33.22	75	−1.60	33.23	26.76
95	−1.64	33.29	100	−1.65	33.30	26.81
142	−1.48	33.39	150	−1.40	33.41	26.90
189	−0.86	33.57	200	−0.65	33.63	27.06
284	1.31	34.12	(300)	1.65	34.21	27.39

Station 3890; 5 June; latitude 48°50′ N., longitude 52°43′ W.; depth 230 meters; dynamic height 971.080

Observed values			Scaled values			
Depth, meters	Temperature, °C.	Salinity, °/₀₀	Depth, meters	Temperature, °C.	Salinity, °/₀₀	σ_t
0	4.09	32.25	0	4.09	32.25	25.61
24	1.50	32.45	25	1.40	32.51	26.04
47	−1.42	33.07	50	−1.45	33.10	26.64
71	−1.58	33.21	75	−1.60	33.22	26.75
95	−1.63	33.27	100	−1.65	33.28	26.80
142	−1.59	33.33	150	−1.55	33.34	26.85
189	−1.30	33.43	(200)	−1.20	33.46	26.94

Station 3891; 5 June; latitude 48°49′ N., longitude 52°46′ W.; depth 199 meters; dynamic height 971.078

Observed values			Scaled values			
Depth, meters	Temperature, °C.	Salinity, °/₀₀	Depth, meters	Temperature, °C.	Salinity, °/₀₀	σ_t
0	4.34	32.15	0	4.34	32.15	25.51
23	0.51	32.57	25	0.40	32.62	26.20
45	−0.46	33.05	50	−0.70	33.11	26.63
68	−1.54	33.19	75	−1.55	33.21	26.74
91	−1.60	33.24	100	−1.60	33.25	26.77
136	−1.67	33.32	(150)	−1.70	33.35	26.85
--------	--------	--------	(200)	−1.25	33.46	26.94

STATIONS OCCUPIED IN 1949—Continued

Station 3892; 5 June; latitude 48°44′ N., longitude 52°58′ W.; depth 112 meters; dynamic height 971.099

Observed values			Scaled values			
Depth, meters	Temperature, °C.	Salinity, °/₀₀	Depth, meters	Temperature, °C.	Salinity, °/₀₀	σ_t
0	4.75	32.03	0	4.75	32.03	25.38
27	0.97	32.46	25	1.20	32.43	26.00
52	−0.31	32.73	50	−0.20	32.70	26.28
79	−1.34	33.04	75	−1.20	33.01	26.57
-------	-------	-------	(100)	−1.60	33.21	26.74

Station 3893; 5 June; latitude 48°39′ N., longitude 52°43′ W.; depth 256 meters; dynamic height 971.086

Observed values			Scaled values			
Depth, meters	Temperature, °C.	Salinity, °/₀₀	Depth, meters	Temperature, °C.	Salinity, °/₀₀	σ_t
0	3.90	32.10	0	3.90	32.10	25.51
25	1.55	32.68	25	1.55	32.68	26.17
50	−0.50	32.89	50	−0.50	32.89	26.45
75	−1.18	33.12	75	−1.18	33.12	26.66
100	−1.61	33.23	100	−1.61	33.23	26.76
150	−1.56	33.29	150	−1.56	33.29	26.80
200	−1.24	33.49	200	−1.24	33.49	26.96

Station 3894; 5 June; latitude 48°35.5′ N., longitude 52°32′ W.; depth 222 meters; dynamic height 971.089

Observed values			Scaled values			
Depth, meters	Temperature, °C.	Salinity, °/₀₀	Depth, meters	Temperature, °C.	Salinity, °/₀₀	σ_t
0	2.93	32.45	0	2.93	32.45	25.88
22	2.53	32.51	25	2.40	32.54	26.00
43	1.27	32.87	50	0.80	32.92	26.41
65	−0.27	33.03	75	−0.90	33.10	26.63
86	−1.33	33.16	100	−1.50	33.20	26.73
129	−1.59	33.27	1500	−1.55	33.32	26.83
172	−1.46	33.37	(200)	−1.35	33.43	26.92

Station 3895; 6 June; latitude 48°22′ N., longitude 52°05′ W.; depth 177 meters; dynamic height 971.070

Observed values			Scaled values			
Depth, meters	Temperature, °C.	Salinity, °/₀₀	Depth, meters	Temperature, °C.	Salinity, °/₀₀	σ_t
0	3.27	32.71	0	3.27	32.71	26.06
28	2.80	32.75	25	2.85	32.74	26.12
55	−0.36	32.97	50	0.80	32.94	26.43
83	−1.38	33.24	75	−1.20	33.16	26.69
110	−1.55	33.32	100	−1.50	33.29	26.80
166	−0.18	33.63	150	−0.65	33.53	26.98

Station 3896; 6 June; latitude 48°15′ N., longitude 51°52′ W.; depth 187 meters; dynamic height 971.061

Observed values			Scaled values			
Depth, meters	Temperature, °C.	Salinity, °/₀₀	Depth, meters	Temperature, °C.	Salinity, °/₀₀	σ_t
0	3.10	32.74	0	3.10	32.74	26.10
28	1.50	32.79	25	1.75	32.78	26.24
57	−1.24	33.07	50	−0.75	33.01	26.56
85	−1.45	33.29	75	−1.40	33.24	26.76
113	−1.46	33.38	100	−1.45	33.31	26.81
170	−0.09	33.64	150	−0.65	33.52	26.97

Station 3897; 6 June; latitude 48°04′ N., longitude 51°25′ W.; depth 170 meters; dynamic height 971.053

Observed values			Scaled values			
Depth, meters	Temperature, °C.	Salinity, °/₀₀	Depth, meters	Temperature, °C.	Salinity, °/₀₀	σ_t
0	2.96	32.74	0	2.96	32.74	26.11
25	2.22	32.81	25	2.22	32.81	26.23
49	0.33	32.93	50	0.30	32.94	26.46
74	−0.95	33.22	75	−0.95	33.23	26.74
99	−0.67	33.46	100	−0.65	33.48	26.94
143	0.14	33.69	(150)	0.30	33.72	27.08

Station 3896; 6 June; latitude 47°56′ N., longitude 51°06′ W.; depth 144 meters; dynamic height 971.052

Observed values			Scaled values			
Depth, meters	Temperature, °C.	Salinity, °/₀₀	Depth, meters	Temperature, °C.	Salinity, °/₀₀	σ_t
0	3.05	32.81	0	3.05	32.81	26.17
25	2.36	32.89	25	2.36	32.89	26.28
50	0.11	32.98	50	0.11	32.98	26.50
74	−1.25	33.24	75	−1.25	33.25	26.76
104	−0.45	33.47	100	−0.60	33.44	26.89

Station 3899; 6 June; latitude 47°48′ N., longitude 50°45′ W.; depth 115 meters; dynamic height 971.039

Observed values			Scaled values			
Depth, meters	Temperature, °C.	Salinity, °/₀₀	Depth, meters	Temperature, °C.	Salinity, °/₀₀	σ_t
0	2.86	32.85	0	2.86	32.85	26.21
25	2.48	32.86	25	2.48	32.86	26.25
50	−1.06	33.28	50	−1.06	33.28	26.78
74	−1.45	33.37	75	−1.45	33.37	26.86
99	−0.64	33.52	100	−0.55	33.53	26.97

Station 3900; 6 June; latitude 47°38.5′ N., longitude 50°25′ W.; depth 121 meters; dynamic height 971.045

Observed values			Scaled values			
Depth, meters	Temperature, °C.	Salinity, °/₀₀	Depth, meters	Temperature, °C.	Salinity, °/₀₀	σ_t
0	3.17	32.89	0	3.17	32.89	26.22
25	2.41	32.91	25	2.41	32.91	26.29
50	0.82	33.08	50	0.82	33.08	26.54
75	−0.11	33.40	75	−0.11	33.40	26.84
100	−0.10	33.50	100	−0.10	33.50	26.92

Station 3901; 6 June; latitude 47°32′ N., longitude 50°15′ W.; depth 102 meters; dynamic height 971.042

Observed values			Scaled values			
Depth, meters	Temperature, °C.	Salinity, °/₀₀	Depth, meters	Temperature, °C.	Salinity, °/₀₀	σ_t
0	3.33	32.97	0	3.33	32.97	26.26
25	2.86	32.99	25	2.86	32.99	26.32
51	1.00	33.21	50	1.05	33.20	26.63
76	0.07	33.46	75	0.10	33.45	26.88
86	0.07	33.44	-------	-------	-------	-------

Station 3902; 6 June; latitude 47°24′ N., longitude 50°00′ W.; depth 95 meters; dynamic height 971.041

Observed values			Scaled values			
Depth, meters	Temperature, °C.	Salinity, °/₀₀	Depth, meters	Temperature, °C.	Salinity, °/₀₀	σ_t
0	3.59	33.02	0	3.59	33.02	26.28
25	3.30	33.04	25	3.30	33.04	26.32
50	1.56	33.25	50	1.56	33.25	26.63
75	−0.08	33.51	75	−0.08	33.50	26.92
85	−0.06	33.50	-------	-------	-------	-------

Station 3903; 17 June; latitude 47°25′ N., longitude 50°00′ W.; depth 97 meters; dynamic height 971.037

Observed values			Scaled values			
Depth, meters	Temperature, °C.	Salinity, °/₀₀	Depth, meters	Temperature, °C.	Salinity, °/₀₀	σ_t
0	3.95	32.98	0	3.95	32.98	26.20
24	3.81	32.975	25	3.80	32.98	26.22
48	1.32	33.26	50	1.25	33.28	26.67
72	0.40	33.40	75	0.35	33.41	26.83

Station 3904; 17 June; latitude 47°44′ N., longitude 49°54′ W.; depth 114 meters; dynamic height 971.049

Observed values			Scaled values			
Depth, meters	Temperature, °C.	Salinity, °/₀₀	Depth, meters	Temperature, °C.	Salinity, °/₀₀	σ_t
0	3.66	32.865	0	3.66	32.865	26.15
25	3.32	32.87	25	3.32	32.87	26.18
50	2.52	32.94	50	2.52	32.94	26.31
75	0.28	33.36	75	0.28	33.36	26.79
100	0.03	33.47	100	0.03	33.47	26.90

Table of Oceanographic Data—Continued

STATIONS OCCUPIED IN 1949—Continued

Station 3905; 17 June; latitude 48°00′ N., longitude 49°54′ W.; depth 170 meters; dynamic height 971.041

Observed values			Scaled values			
Depth, meters	Temperature, °C.	Salinity, °/₀₀	Depth, meters	Temperature, °C.	Salinity, °/₀₀	σ_t
0	3.32	32.94	0	3.32	32.94	26.24
23	2.62	32.96	25	2.55	32.96	26.32
46	0.66	33.03	50	0.30	33.08	26.57
69	−1.30	33.28	75	−1.40	33.30	26.80
92	−1.60	33.36	100	−1.55	33.39	26.89
138	−0.42	33.57	(150)	0.00	33.62	27.02

Station 3906; 17 June; latitude 48°14′ N., longitude 49°42′ W.; depth 221 meters; dynamic height 971.034

Observed values			Scaled values			
Depth, meters	Temperature, °C.	Salinity, °/₀₀	Depth, meters	Temperature, °C.	Salinity, °/₀₀	σ_t
0	2.45	33.12	0	2.45	33.12	26.45
25	1.67	33.18	25	1.67	33.18	26.56
49	0.56	33.18	50	0.40	33.18	26.64
74	−1.44	33.28	75	−1.45	33.28	26.79
99	−1.61	33.35	100	−1.60	33.36	26.86
149	−0.96	33.52	150	−0.95	33.52	26.98
198	−0.40	33.68	(200)	−0.40	33.69	27.09

Station 3907; 17 June; latitude 48°33′ N., longitude 49°30′ W.; depth 622 meters; dynamic height 970.959

Observed values			Scaled values			
Depth, meters	Temperature, °C.	Salinity, °/₀₀	Depth, meters	Temperature, °C.	Salinity, °/₀₀	σ_t
0	2.76	33.26	0	2.76	33.26	26.54
25	1.27	33.28	25	1.27	33.28	26.67
49	0.32	33.42	50	0.25	33.42	26.85
75	−0.95	33.55	75	−0.95	33.55	27.00
99	−0.69	33.70	100	−0.65	33.71	27.12
149	1.30	34.08	150	1.40	34.08	27.30
199	1.85	34.33	200	1.85	34.34	27.47
297	2.63	34.62	200	2.65	34.63	27.64
360	3.07	34.735	400	3.20	34.76	27.70
561	3.37	34.845	(600)	3.40	34.86	27.76

Station 3908; 18 June; latitude 48°42′ N., longitude 49°23′ W.; depth 1134 meters; dynamic height 970.910

Observed values			Scaled values			
Depth, meters	Temperature, °C.	Salinity, °/₀₀	Depth, meters	Temperature, °C.	Salinity, °/₀₀	σ_t
0	2.54	33.40	0	2.54	33.40	26.67
22	1.74	33.56	25	1.55	33.59	26.90
43	−0.19	33.80	50	0.00	33.84	27.19
65	0.41	33.91	75	0.50	33.97	27.27
86	0.55	34.015	100	0.65	34.06	27.33
129	0.89	34.15	150	1.20	34.24	27.44
172	1.59	34.34	200	2.05	34.47	27.57
258	3.01	34.73	300	3.15	34.76	27.70
311	3.14	34.76	400	3.20	34.78	27.71
481	3.27	34.80	600	3.30	34.82	27.74
665	3.32	34.84	800	3.40	34.87	27.77
858	3.48	34.88	(1,000)	3.60	34.90	27.77

Station 3909; 18 June; latitude 49°06.5′ N.; longitude 49°16′ W.; depth 1641 meters; dynamic height 970.813

Observed values			Scaled values			
Depth, meters	Temperature, °C.	Salinity, °/₀₀	Depth, meters	Temperature, °C.	Salinity, °/₀₀	σ_t
0	4.90	34.62	0	4.90	34.62	27.41
24	4.37	34.62	25	4.35	34.62	27.47
48	4.33	34.61	50	4.30	34.61	27.47
72	3.55	34.64	75	3.50	34.65	27.58
96	3.35	34.72	100	3.30	34.73	27.66
144	3.00	34.74	150	3.00	34.75	27.71
192	3.21	34.815	200	3.20	34.82	27.75
288	3.30	34.86	300	3.30	34.85	27.76
359	3.31	34.85	400	3.35	34.86	27.76
549	3.32	34.865	600	3.30	34.87	27.78
746	3.32	34.88	800	3.30	34.88	27.78
947	3.34	34.88	1,000	3.35	34.885	27.78
1,470	3.47	34.925	-------	-------	-------	-------

Station 3910; 18 June; latitude 49°33′ N., longitude 49°16′ W.; depth 1609 meters; dynamic height 970.814

Observed values			Scaled values			
Depth, meters	Temperature, °C.	Salinity, °/₀₀	Depth, meters	Temperature, °C.	Salinity, °/₀₀	σ_t
0	5.64	34.66	0	5.64	34.66	27.35
22	4.56	34.64	25	4.55	34.64	27.47
42	4.57	34.65	50	4.50	34.65	27.47
64	4.33	34.65	75	3.80	34.65	27.55
85	3.27	34.65	100	3.15	34.67	27.63
128	3.08	34.71	150	3.10	34.75	27.70
170	3.11	34.78	200	3.20	34.81	27.74
255	3.31	34.85	300	3.30	34.86	27.77
366	3.32	34.87	400	3.35	34.87	27.77
587	3.32	34.88	600	3.30	34.88	27.78
834	3.33	34.88	800	3.30	34.88	27.78
1,047	3.35	34.88	1,000	3.35	34.88	27.78
1,575	3.35	34.935	-------	-------	-------	-------

Station 3911; 18 June; latitude 49°58.5′ N., longitude 49°02′ W.; depth 1796 meters; dynamic height 970.809

Observed values			Scaled values			
Depth, meters	Temperature, °C.	Salinity, °/₀₀	Depth, meters	Temperature, °C.	Salinity, °/₀₀	σ_t
0	4.74	34.61	0	4.74	34.61	27.42
26	3.94	34.62	25	3.95	34.62	27.51
51	3.92	34.61	50	3.90	34.61	27.51
77	3.01	34.68	75	3.10	34.68	27.64
103	2.98	34.69	100	3.00	34.69	27.66
154	3.05	34.77	150	3.05	34.76	27.71
206	3.17	34.82	200	3.15	34.81	27.74
309	3.27	34.85	300	3.25	34.85	27.76
450	3.31	34.87	400	3.30	34.86	27.77
656	3.32	34.87	600	3.30	34.87	27.78
862	3.32	34.88	800	3.30	34.88	27.78
1,065	3.34	34.89	1,000	3.35	34.89	27.78
1,572	3.34	34.93	-------	-------	-------	-------

Station 3912; 18 June; latitude 49°49′ N.; longitude 49°31′ W.; depth 1333 meters; dynamic height 970.825

Observed values			Scaled values			
Depth, meters	Temperature, °C.	Salinity, °/₀₀	Depth, meters	Temperature, °C.	Salinity, °/₀₀	σ_t
0	4.86	34.32	0	4.86	34.32	27.18
25	4.82	34.33	25	4.82	34.33	27.18
49	3.45	34.52	50	3.45	34.52	27.48
74	3.25	34.68	75	3.25	34.68	27.62
99	3.13	34.70	100	3.15	34.70	27.65
148	3.25	34.78	150	3.25	34.78	27.70
197	3.18	34.82	200	3.20	34.82	27.75
296	3.32	34.84	300	3.30	34.84	27.75
391	3.33	34.84	400	3.30	34.84	27.75
589	3.31	34.87	600	3.30	34.87	27.78
788	3.32	34.875	800	3.30	34.88	27.78
985	3.34	34.88	1,000	3.35	34.88	27.78
1,281	3.45	34.915	-------	-------	-------	-------

Station 3913; 18–19 June; latitude 49°38.5′ N., longitude 50°04′ W.; depth 625 meters; dynamic height 970.865

Observed values			Scaled values			
Depth, meters	Temperature, °C.	Salinity, °/₀₀	Depth, meters	Temperature, °C.	Salinity, °/₀₀	σ_t
0	2.55	33.57	0	2.55	33.57	26.81
25	2.11	33.68	25	2.11	33.68	26.93
50	0.69	34.07	50	0.69	34.07	27.34
75	1.13	34.22	75	1.13	34.22	27.43
100	1.62	34.37	100	1.62	34.37	27.52
150	2.46	34.54	150	2.46	34.54	27.58
200	2.88	34.68	200	2.88	34.68	27.66
300	3.19	34.79	300	3.19	34.79	27.72
396	3.29	34.82	400	3.30	34.82	27.74
598	3.43	34.89	(600)	3.45	34.89	27.77

Table of Oceanographic Data—Continued

STATIONS OCCUPIED IN 1949—Continued

Station 3914; 19 June; latitude 49°29′ N.; longitude 50°38′ W.; depth 333 meters; dynamic height 970.913

Observed values			Scaled values			
Depth, meters	Temperature, °C.	Salinity, ‰	Depth, meters	Temperature, °C.	Salinity, ‰	σ_t
0	3.19	33.25	0	3.19	33.25	26.50
25	2.08	33.26	25	2.08	33.26	26.59
49	−0.32	33.64	50	−0.30	33.64	27.05
74	−0.07	33.81	75	0.00	33.81	27.17
98	0.79	34.00	100	0.80	34.01	27.28
147	1.39	34.24	150	1.40	34.24	27.43
196	2.06	34.46	200	2.10	34.48	27.56
294	3.12	34.76	(300)	3.20	34.77	27.71

Station 3915; 19 June; latitude 49°19′ N.; longitude 51°07′ W.; depth 334 meters; dynamic height 970.947

Observed values			Scaled values			
Depth, meters	Temperature, °C.	Salinity, ‰	Depth, meters	Temperature, °C.	Salinity, ‰	σ_t
0	3.55	32.78	0	3.55	32.78	26.09
25	1.15	32.91	25	1.15	32.91	26.38
50	0.79	33.28	50	0.79	33.28	26.70
75	−0.15	33.53	75	−0.15	33.53	26.95
100	0.16	33.82	100	0.16	33.82	27.17
150	1.02	34.18	150	1.02	34.18	27.40
200	1.49	34.32	200	1.49	34.32	27.49
			(300)	2.80	34.72	27.70

Station 3916; 19 June; latitude 49°08′ N., longitude 51°36′ W.; depth 305 meters; dynamic height 970.990

Observed values			Scaled values			
Depth, meters	Temperature, °C.	Salinity, ‰	Depth, meters	Temperature, °C.	Salinity, ‰	σ_t
0	3.80	32.50	0	3.80	32.50	25.84
24	1.56	32.56	25	1.50	32.56	26.08
48	−0.80	33.24	50	−0.85	33.25	26.74
73	−0.85	33.32	75	−0.90	33.33	26.82
97	−1.37	33.44	100	−1.35	33.45	26.93
145	−0.60	33.71	150	−0.45	33.75	27.14
194	1.65	34.22	200	1.75	34.25	27.41
281	2.75	34.56	(300)	2.90	34.63	27.62

Station 3917; 19 June; latitude 49°02′ N., longitude 51°56′ W.; depth 308 meters; dynamic height 971.022

Observed values			Scaled values			
Depth, meters	Temperature, °C.	Salinity, ‰	Depth, meters	Temperature, °C.	Salinity, ‰	σ_t
0	3.50	32.50	0	3.50	32.50	25.86
24	2.20	32.56	25	2.15	32.57	26.04
49	−1.38	33.10	50	−1.40	33.11	26.65
74	−1.39	33.23	75	−1.40	33.23	26.75
98	−1.62	33.30	100	−1.60	33.30	26.81
147	−1.18	33.56	150	−1.10	33.48	26.94
196	0.07	33.89	200	0.15	33.93	27.25
284	2.54	34.46	(300)	2.90	34.54	27.55

Station 3918; 19 June; latitude 48°58′ N., longitude 52°10′ W.; depth 302 meters; dynamic height 971.031

Observed values			Scaled values			
Depth, meters	Temperature, °C.	Salinity, ‰	Depth, meters	Temperature, °C.	Salinity, ‰	σ_t
0	5.04	32.19	0	5.04	32.19	25.46
25	0.31	32.80	25	0.31	32.80	26.34
49	−1.15	33.16	50	−1.15	33.17	26.70
74	−1.58	33.24	75	−1.60	33.24	26.76
99	−1.62	33.29	100	−1.60	33.29	26.80
148	−1.50	33.39	150	−1.45	33.40	26.89
198	−0.95	32.65	200	−0.90	33.67	27.10
287	2.35	34.42	(300)	2.90	34.52	27.54

Station 3919; 19 June; latitude 48°52′ N., longitude 52°29′ W.; depth 353 meters; dynamic height 971.055

Observed values			Scaled values			
Depth, meters	Temperature, °C.	Salinity, ‰	Depth, meters	Temperature, °C.	Salinity, ‰	σ_t
0	5.04	32.08	0	5:04	32.08	25.38
25	−0.53	32.77	25	−0.53	32.77	26.35
50	−1.45	33.15	50	−1.45	33.15	26.68
74	−1.60	33.25	75	−1.60	33.25	26.77
99	−1.61	33.28	100	−1.60	33.28	26.79
149	−1.54	33.34	150	−1.55	33.35	26.86
199	−1.18	33.46	200	−1.15	33.47	26.95
298	1.43	34.18	(300)	1.50	34.20	27.39

Station 3920; 19 June; latitude 48°45′ N., longitude 52°43′ W.; depth 214 meters; dynamic height 971.088

Observed values			Scaled values			
Depth, meters	Temperature, °C.	Salinity, ‰	Depth, meters	Temperature, °C.	Salinity, ‰	σ_t
0	6.16	31.99	0	6.16	31.99	25.18
25	2.51	32.29	25	2.51	32.29	25.78
49	−1.14	33.00	50	−1.15	33.01	26.57
74	−1.49	33.18	75	−1.50	33.18	26.71
99	−1.58	33.21	100	−1.60	33.21	26.74
148	−1.62	33.26	150	−1.60	33.26	26.78
197	−1.53	33.35	(200)	−1.50	33.36	26.86

Station 3921; 19 June; latitude 48°43.5′ N., longitude 52°47′ W.; depth 139 meters; dynamic height 971.089

Observed values			Scaled values			
Depth, meters	Temperature, °C.	Salinity, ‰	Depth, meters	Temperature, °C.	Salinity, ‰	σ_t
0	6.57	31.81	0	6.57	31.81	24.98
23	1.12	32.45	25	0.80	32.49	26.06
45	−0.83	32.85	50	−1.00	32.90	26.47
68	−1.35	33.04	75	−1.45	33.08	26.63
91	−1.56	33.15	100	−1.60	33.16	26.70
118	−1.61	33.19				

Station 3922; 19 June; latitude 48°43.5′ N., longitude 52°57′ W.; depth 101 meters; dynamic height 971.111

Observed values			Scaled values			
Depth, meters	Temperature, °C.	Salinity, ‰	Depth, meters	Temperature, °C.	Salinity, ‰	σ_t
0	6.76	31.86	0	6.76	31.86	25.01
23	4.40	32.10	25	4.00	32.13	25.53
46	0.50	32.55	50	0.00	32.64	26.23
68	−1.05	32.94	75	−1.20	32.99	26.55
91	−1.35	33.07				

Station 3923; 19 June; latitude 48°38.5′ N., longitude 52°44′ W.; depth 174 meters; dynamic height 971.082

Observed values			Scaled values			
Depth, meters	Temperature, °C.	Salinity, ‰	Depth, meters	Temperature, °C.	Salinity, ‰	σ_t
0	6.33	31.78	0	6.33	31.78	24.99
25	0.02	32.63	25	0.02	32.63	26.22
49	−1.32	33.03	50	−1.35	33.03	26.59
74	−1.50	33.10	75	−1.50	33.10	26.64
98	−1.56	33.16	100	−1.55	33.16	26.70
148	−1.62	33.24	(150)	−1.60	33.24	26.76

Station 3924; 19–20 June; latitude 48°33.5′ N., longitude 52°35′ W.; depth 252 meters; dynamic height 971.068

Observed values			Scaled values			
Depth, meters	Temperature, °C.	Salinity, ‰	Depth, meters	Temperature, °C.	Salinity, ‰	σ_t
0	4.85	32.26	0	4.85	32.26	25.55
30	1.90	32.56	25	2.55	32.50	25.95
59	0.07	33.17	50	0.40	33.00	26.50
88	−0.60	33.24	75	−0.35	33.22	26.70
118	−1.58	33.27	100	−0.95	33.25	26.76
176	−1.28	33.42	150	−1.45	33.33	26.83
234	0.40	33.83	200	−0.65	33.57	27.01

STATIONS OCCUPIED IN 1949—Continued

Station 3925; 20 June; latitude 48°14′ N., longitude 52°04′ W.; depth 173 meters; dynamic height 971.043

Observed values			Scaled values			
Depth, meters	Temperature, °C.	Salinity, ‰	Depth, meters	Temperature, °C.	Salinity, ‰	σ_t
0	4.53	32.45	0	4.53	32.45	25.72
24	0.19	32.79	25	0.20	32.80	26.35
47	−0.82	33.10	50	−0.95	33.12	26.65
71	−1.55	33.24	75	−1.55	33.25	26.77
95	−1.55	33.30	100	−1.55	33.31	26.82
142	−1.38	33.42	(150)	−1.35	33.45	26.93

Station 3926; 20 June; latitude 48°06′ N., longitude 51°50′ W.; depth 158 meters; dynamic height 971.028

Observed values			Scaled values			
Depth, meters	Temperature, °C.	Salinity, ‰	Depth, meters	Temperature, °C.	Salinity, ‰	σ_t
0	4.26	32.78	0	4.26	32.78	26.02
24	0.65	32.96	25	0.60	32.97	26.46
49	−1.35	33.18	50	−1.35	33.19	26.72
73	−1.31	33.32	75	−1.30	33.33	26.83
97	−1.37	33.38	100	−1.35	33.39	26.88
146	−0.31	33.59	150	−0.20	33.61	27.02

Station 3927; 20 June; latitude 48°00′ N., longitude 51°29′ W.; depth 182 meters; dynamic height 971.040

Observed values			Scaled values			
Depth, meters	Temperature, °C.	Salinity, ‰	Depth, meters	Temperature, °C.	Salinity, ‰	σ_t
0	4.17	32.73	0	4.17	32.73	25.99
29	2.85	32.84	25	3.20	32.82	26.15
56	−0.94	33.15	50	−0.30	33.09	26.59
85	−1.59	33.34	75	−1.35	33.29	26.79
113	−1.13	33.44	100	−1.40	33.39	26.88
169	0.12	33.68	150	−0.30	33.59	27.00

Station 3928; 20 June; latitude 47°50′ N., longitude 51°06′ W.; depth 148 meters; dynamic height 971.035

Observed values			Scaled values			
Depth, meters	Temperature, °C.	Salinity, ‰	Depth, meters	Temperature, °C.	Salinity, ‰	σ_t
0	4.20	32.81	0	4.20	32.81	26.06
27	3.14	32.82	25	3.30	32.82	26.14
53	−0.18	33.10	50	0.30	33.07	26.56
79	−1.11	33.38	75	−1.05	33.35	26.84
105	−0.33	33.53	100	−0.50	33.51	26.95
141	0.04	33.64				

Station 3929; 20 June; latitude 47°43.5′ N., longitude 50°49′ W.; depth 140 meters; dynamic height 971.035

Observed values			Scaled values			
Depth, meters	Temperature, °C.	Salinity, ‰	Depth, meters	Temperature, °C.	Salinity, ‰	σ_t
0	4.19	32.87	0	4.19	32.87	26.10
25	3.22	32.87	25	3.22	32.87	26.19
49	0.96	33.04	50	0.95	33.05	26.50
74	−0.44	33.34	75	−0.45	33.35	26.82
98	−0.59	33.51	100	−0.60	33.51	26.95
128	−0.52	33.52				

Station 3930; 20 June; latitude 47°37′ N., longitude 50°33′ W.; depth 119 meters; dynamic height 971.037

Observed values			Scaled values			
Depth, meters	Temperature, °C.	Salinity, ‰	Depth, meters	Temperature, °C.	Salinity, ‰	σ_t
0	4.40	32.88	0	4.40	32.88	26.09
25	3.17	32.89	25	3.17	32.89	26.21
50	1.52	32.99	50	1.52	32.99	26.42
76	−0.39	33.36	75	−0.35	33.35	26.80
101	−0.30	33.52	100	−0.30	33.51	26.94

Station 3931; 20 June; latitude 47°31′ N., longitude 50°17′ W.; depth 113 meters; dynamic height 971.034

Observed values			Scaled values			
Depth, meters	Temperature, °C.	Salinity, ‰	Depth, meters	Temperature, °C.	Salinity, ‰	σ_t
0	4.67	32.92	0	4.67	32.92	26.09
25	3.71	32.92	25	3.71	32.92	26.19
50	0.49	33.14	50	0.49	33.14	26.60
76	−0.05	33.45	75	−0.05	33.45	26.88
101	−0.11	33.47	100	−0.10	33.47	26.90

Station 3932; 20 June; latitude 47°23.5′ N., longitude 50°00′ W.; depth 97 meters; dynamic height 971.037

Observed values			Scaled values			
Depth, meters	Temperature, °C.	Salinity, ‰	Depth, meters	Temperature, °C.	Salinity, ‰	σ_t
0	5.11	32.98	0	5.11	32.98	26.09
25	4.10	32.99	25	4.10	32.99	26.20
50	2.13	33.14	50	2.13	33.14	26.50
75	0.21	33.41	75	0.21	33.41	26.84
90	−0.10	33.51				

Station 3933; 5 July; latitude 53°42.5′ N., longitude 55°48′ W.; depth 104 meters; dynamic height 1454.923

Observed values			Scaled values			
Depth, meters	Temperature, °C.	Salinity, ‰	Depth, meters	Temperature, °C.	Salinity, ‰	σ_t
0	6.67	24.845	0	6.67	24.845	19.51
24	0.01	32.52	25	−0.10	32.53	26.14
49	−1.55	32.95	50	−1.55	32.95	26.53
73	−1.70	32.98	75	−1.70	32.98	26.55
97	−1.66	33.03	100	−1.65	33.03	26.59

Station 3934; 5 July; latitude 53°52′ N., longitude 55°30′ W.; depth 200 meters; dynamic height 1454.822

Observed values			Scaled values			
Depth, meters	Temperature, °C.	Salinity, ‰	Depth, meters	Temperature, °C.	Salinity, ‰	σ_t
0	3.38	32.14	0	3.38	32.14	25.60
24	0.38	32.64	25	0.25	32.66	26.23
49	−1.44	33.04	50	−1.45	33.05	26.61
73	−1.53	33.12	75	−1.50	33.12	26.66
97	−1.41	33.25	100	−1.40	33.26	26.77
146	−1.05	33.54	150	−1.05	33.56	27.01
194	−0.80	33.72	200	−0.80	33.73	27.13

Station 3935; 5 July; latitude 53°55′ N., longitude 55°26′ W.; depth 169 meters; dynamic height 1454.785

Observed values			Scaled values			
Depth, meters	Temperature, °C.	Salinity, ‰	Depth, meters	Temperature, °C.	Salinity, ‰	σ_t
0	3.85	32.48	0	3.85	32.48	25.82
25	3.18	32.90	25	3.18	32.90	26.21
50	0.55	33.09	50	0.55	33.09	26.55
75	−1.20	33.46	75	−1.20	33.46	26.94
100	−1.02	33.62	100	−1.02	33.62	27.06
150	0.09	33.97	150	0.09	33.97	27.29

Station 3936; 5 July; latitude 54°05′ N., longitude 55°08′ W.; depth 161 meters; dynamic height 1454.789

Observed values			Scaled values			
Depth, meters	Temperature, °C.	Salinity, ‰	Depth, meters	Temperature, °C.	Salinity, ‰	σ_t
0	4.24	32.50	0	4.24	32.50	25.79
25	0.65	32.76	25	0.65	32.76	26.29
50	−1.05	33.13	50	−1.05	33.13	26.66
75	−1.26	33.33	75	−1.26	33.33	26.83
99	−1.27	33.46	100	−1.25	33.47	26.95
149	−0.35	33.85	150	−0.35	33.86	27.22

Table of Oceanographic Data—Continued

STATIONS OCCUPIED IN 1949—Continued

Observed values			Scaled values			
Depth, meters	Temperature, °C.	Salinity, °/oo	Depth, meters	Temperature, °C.	Salinity, °/oo	σ_t
Station 3937; 5 July; latitude 54°08′ N., longitude 55°02′ W.; depth 163 meters; dynamic height 1454.781						
0	3.96	32.40	0	3.96	32.40	25.75
25	−0.35	32.92	25	−0.35	32.92	26.45
50	−1.45	33.18	50	−1.45	33.18	26.71
75	−1.34	-------	75	−1.34	33.35	26.85
100	−1.31	33.50	100	−1.31	33.50	26.97
150	−0.13	33.93	150	−0.13	33.93	27.27
Station 3938; 5 July; latitude 54°28.5′ N., longitude 54°25′ W.; depth 219 meters; dynamic height 1454.789						
0	3.77	32.22	0	3.77	32.22	25.62
25	−1.37	32.96	25	−1.37	32.96	26.53
50	−1.55	33.10	50	−1.55	33.10	26.65
75	−1.34	33.28	75	−1.34	33.28	26.79
100	−1.15	33.48	100	−1.15	33.48	26.95
150	−0.55	33.80	150	−0.55	33.80	27.18
200	0.12	34.01	200	0.12	34.01	27.32
Station 3939; 5 July; latitude 54°47′ N., longitude 53°49′ W.; depth 331 meters; dynamic height 1454.789						
0	3.29	32.06	0	3.29	32.06	25.54
26	−1.13	32.94	25	−1.00	32.93	26.49
52	−1.46	33.12	50	−1.45	33.11	26.65
77	−1.20	33.32	75	−1.20	33.30	26.80
103	−1.15	33.48	100	−1.15	33.46	26.94
154	−0.47	33.83	150	−0.55	33.80	27.18
206	0.62	34.15	200	0.50	34.12	27.31
309	3.29	34.73	300	3.10	34.68	27.64
Station 3940; 6 July; latitude 54°53′ N., longitude 53°36′ W.; depth 645 meters; dynamic height 1454.693						
0	3.67	32.49	0	3.67	32.49	25.84
25	−1.02	33.36	25	−1.02	33.36	26.84
50	−0.55	33.74	50	−0.55	33.74	27.13
75	−0.15	33.96	75	−0.15	33.96	27.30
100	0.33	34.07	100	0.33	34.07	27.36
150	1.84	34.39	150	1.84	34.39	27.47
200	3.16	34.68	200	3.16	34.68	27.63
300	3.49	34.80	300	3.49	34.80	27.70
397	3.33	34.83	400	3.30	34.83	27.74
586	3.31	34.84	600	3.35	34.84	27.74
Station 3941; 6 July; latitude 54°57′ N., longitude 53°24′ W.; depth 1652 meters; dynamic height 1454.600						
0	5.08	33.59	0	5.08	33.59	26.57
25	4.95	34.52	25	4.95	34.52	27.32
49	4.50	34.68	50	4.45	34.68	27.50
74	3.26	34.68	75	3.25	34.68	27.62
98	3.40	34.76	100	3.40	34.77	27.69
149	3.40	34.80	150	3.40	34.80	27.71
198	3.32	34.81	200	3.30	34.81	27.73
296	3.22	34.83	300	3.20	34.83	27.75
414	3.27	34.85	400	3.25	34.85	27.76
620	3.28	34.87	600	3.30	34.87	27.775
825	3.35	34.875	800	3.30	34.87	27.775
1,030	3.36	34.875	1,000	3.35	34.88	27.775
1,532	3.45	-------	1,500	3.45	34.90	27.78

Observed values			Scaled values			
Depth, meters	Temperature, °C.	Salinity, °/oo	Depth, meters	Temperature, °C.	Salinity, °/oo	σ_t
Station 3942; 6 July; latitude 55°00′ N., longitude 53°17′ W.; depth 2085 meters; dynamic height 1454.586						
0	5.13	34.36	0	5.13	34.36	27.18
23	4.13	34.56	25	4.05	34.57	27.46
46	3.07	34.66	50	3.15	34.69	27.64
69	3.70	34.82	75	3.70	34.82	27.70
91	3.65	34.82	100	3.60	34.82	27.71
137	3.51	34.83	150	3.50	34.83	27.72
183	3.46	34.83	200	3.45	34.83	27.72
274	3.38	34.84	300	3.35	34.84	27.74
358	3.36	34.84	400	3.35	34.84	27.74
543	3.28	34.86	600	3.30	34.86	27.77
731	3.34	34.87	800	3.35	34.87	27.77
923	3.35	34.88	1,000	3.40	34.88	27.77
1,413	3.44	34.91	1,500	3.35	34.91	26.80
1,925	3.13	34.94	2,000	3.10	34.94	27.85
Station 3943; 6 July; latitude 55°12′ N., longitude 52°56′ W.; depth 2898 meters; dynamic height 1454.570						
0	5.59	34.68	0	5.59	34.68	27.37
27	5.00	34.70	25	5.05	34.70	27.45
52	4.08	34.75	50	4.15	34.75	27.59
79	3.79	34.77	75	3.80	34.77	27.65
104	3.48	34.79	100	3.50	34.79	27.69
157	3.28	34.84	150	3.30	34.83	27.74
210	3.29	34.84	200	3.25	34.84	27.75
314	3.29	34.86	300	3.30	34.86	27.77
455	3.31	34.86	400	3.30	34.86	27.77
632	3.33	34.87	600	3.30	34.87	27.775
838	3.38	34.88	800	3.35	34.88	27.775
1,044	3.39	34.89	1,000	3.40	34.89	27.78
1,572	3.38	34.93	1,500	3.35	34.93	27.81
2,107	2.88	34.94	2,000	2.95	34.94	27.86
2,464	2.50	34.91	2,500	2.45	34.91	27.88
2,773	2.15	34.92	-------	-------	-------	-------
Station 3944; 6 July; latitude 55°29.5′ N., longitude 52°25′ W.; depth 3219 meters; dynamic height 1454.571						
0	6.54	34.70	0	6.54	34.70	27.26
26	5.18	34.72	25	5.20	34.72	27.45
52	4.21	34.74	50	4.30	34.74	27.57
78	3.37	34.82	75	3.45	34.82	27.72
103	3.32	34.82	100	3.30	34.82	27.74
156	3.24	34.84	150	3.25	34.84	27.75
207	3.28	34.85	200	3.25	34.85	27.76
310	3.24	34.86	300	3.25	34.86	27.77
417	3.27	34.86	400	3.25	34.86	27.77
622	3.25	34.87	600	3.25	34.87	27.78
829	3.29	34.87	800	3.30	34.875	27.78
1,032	3.32	34.88	1,000	3.35	34.885	27.78
1,556	3.44	34.89	1,500	3.40	34.89	27.78
2,086	3.26	34.93	2,000	3.30	34.93	27.82
-------	3.32	34.88	-------	-------	-------	-------
-------	2.94	34.94	-------	-------	-------	-------
-------	3.25	34.85	-------	-------	-------	-------

Table of Oceanographic Data—Continued

STATIONS OCCUPIED IN 1949—Continued

Station 3945; 6–7 July; latitude 55°54′ N., longitude 51°43′ W.; depth 3429 meters; dynamic height 1454.575

Observed values			Scaled values			
Depth, meters	Temperature, °C.	Salinity, ‰	Depth, meters	Temperature, °C.	Salinity, ‰	σ_t
0	7.00	34.64	0	7.00	34.64	27.15
25	5.67	34.68	25	5.67	34.68	27.36
51	4.04	34.75	50	4.10	34.75	27.60
76	3.60	34.78	75	3.60	34.78	27.67
102	3.33	34.82	100	3.35	34.82	27.73
152	3.34	34.85	150	3.35	34.85	27.75
203	3.36	34.85	200	3.35	34.85	27.75
305	3.33	34.88	300	3.35	34.88	27.77
402	3.31	34.87	400	3.30	34.87	27.78
603	3.28	34.87	600	3.30	34.87	27.78
802	3.25	34.88	800	3.25	34.88	27.78
1,000	3.32	34.88	1,000	3.32	34.88	27.78
1,510	3.35	34.89	1,500	3.35	34.89	27.78
2,026	3.44	34.94	2,000	3.45	34.94	27.81
2,486	3.13	34.94	2,500	3.10	34.94	27.85
2,986	2.67	34.93	3,000	2.65	34.93	27.88
3,296	2.08	34.91				

Station 3946; 7 July; latitude 56°27′ N., lontigude 50°34′ W.; depth 3667 meters; dynamic height 1454.584

Observed values			Scaled values			
Depth, meters	Temperature, °C.	Salinity, ‰	Depth, meters	Temperature, °C.	Salinity, ‰	σ_t
0	7.33	34.66	0	7.33	34.66	27.13
24	6.11	34.70	25	6.05	34.70	27.33
49	4.26	34.76	50	4.20	34.76	27.60
73	3.93	34.80	75	3.90	34.80	27.66
98	3.53	34.82	100	3.55	34.82	27.71
145	3.52	34.86	150	3.50	34.86	27.75
194	3.48	34.86	200	3.45	34.86	27.75
292	3.33	34.85	300	3.35	34.85	27.75
378	3.34	34.86	400	3.30	34.86	27.77
568	3.31	34.88	600	3.30	34.88	27.78
757	3.34	34.885	800	3.35	34.88	27.78
947	3.32	34.87	1,000	3.35	34.87	27.77
1,443	3.35	34.88	1,500	3.35	34.88	27.78
1,953	3.50	34.93	2,000	3.50	34.93	27.80

Station 3947; 7 July; latitude 56°58.5′ N., longitude 49°31′ W.; depth 3662 meters; dynamic height 1454.605

Observed values			Scaled values			
Depth, meters	Temperature, °C.	Salinity, ‰	Depth, meters	Temperature, °C.	Salinity, ‰	σ_t
0	6.12	33.98	0	6.12	33.98	26.76
26	2.19	34.24	25	2.20	34.24	27.37
52	3.45	34.57	50	3.35	34.53	27.49
77	2.98	34.64	75	3.00	34.64	27.62
103	3.23	34.72	100	3.20	34.71	27.66
154	3.39	34.80	150	3.40	34.80	27.71
206	3.66	34.85	200	3.65	34.85	27.72
309	3.67	34.88	300	3.65	34.88	27.74
413	3.61	34.89	400	3.60	34.89	27.76
616	3.36	34.86	500	3.40	34.86	27.76
820	3.37	34.87	600	3.35	34.87	27.77
1,021	3.32	34.87	800	3.35	34.87	27.77
1,543	3.37	34.88	1,000	3.35	34.88	27.78
2,080	3.42	34.935	1,500	3.40	34.93	27.81
2,504	3.10	34.93	2,000	3.10	34.93	27.84
3,006	2.79	34.92	2,500	2.80	34.92	27.86
3,507	1.85	34.90	3,000	1.85	34.90	27.92
			3,500			

Station 3948; 8 July; latitude 57°30′ N., longitude 48°26′ W.; depth 3420 meters; dynamic height 1454.594

Observed values			Scaled values			
Depth, meters	Temperature, °C.	Salinity, ‰	Depth, meters	Temperature, °C.	Salinity, ‰	σ_t
0	5.87	34.10	0	5.87	34.10	26.88
26	2.97	34.31	25	3.00	34.31	27.36
52	2.86	34.57	50	2.85	34.55	27.56
78	3.16	34.70	75	3.10	34.69	27.65
104	3.39	34.78	100	3.35	34.77	27.69
155	3.63	34.86	150	3.60	34.85	27.73
206	3.64	34.875	200	3.60	34.87	27.75
310	3.44	34.865	300	3.45	34.87	27.76
398	3.57	34.89	400	3.55	34.89	27.76
598	3.34	34.88	600	3.35	34.88	27.77
801	3.35	34.89	800	3.35	34.88	27.77
1,006	3.33	34.88	1,000	3.35	34.88	27.77
1,521	3.37	34.88	1,500	3.35	34.89	27.78
1,554	3.36	34.89	2,000	3.30	34.93	27.82
2,084	3.30	34.94	2,500	3,00	34.94	27.86
2,621	2.88	34.94	3,000	2.35	34.93	27.90
3,164	2.10	34.92				
3,406	1.66	34.90				

Station 3949; 8 July; latitude 58°03′ N., longitude 47°18′ W.; depth 3182 meters; dynamic height 1454.588

Observed values			Scaled values			
Depth, meters	Temperature, °C.	Salinity, ‰	Depth, meters	Temperature, °C.	Salinity, ‰	σ_t
0	5.31	34.38	0	5.31	34.38	27.17
25	4.85	34.44	25	4.85	34.44	27.27
50	4.18	34.71	50	4.18	34.71	27.56
75	3.24	34.68	75	3.24	34.68	27.62
101	3.29	34.72	100	3.30	34.72	27.66
151	3.59	34.84	150	3.60	34.83	27.71
201	3.71	34.87	200	3.70	34.87	27.74
302	3.91	34.92	300	3.90	34.92	27.76
421	3.75	34.905	400	3.75	34.91	27.76
631	3.52	34.90	600	3.55	34.90	27.77
842	3.41	34.89	800	3.40	34.89	27.78
1,054	3.38	34.89	1,000	3.40	34.89	27.78
1,899	3.29	34.925	1,500	3.35	34.91	27.80
2,491	2.71	34.925	2,000	3.25	34.92	27.82
3,051	1.72	34.895	2,500	2.70	34.92	27.87
			3,000	1.85	34.90	27.92

Station 3950; 8 July; latitude 58°31′ N., longitude 46°21′ W.; depth 2451 meters; dynamic height 1454.591

Observed values			Scaled values			
Depth, meters	Temperature, °C.	Salinity, ‰	Depth, meters	Temperature, °C.	Salinity, ‰	σ_t
0	6.02	34.58	0	6.02	34.58	27.24
25	5.27	34.59	25	5.27	34.59	27.34
49	4.31	34.67	50	4.30	34.67	27.52
74	3.89	34.74	75	3.90	34.74	27.61
98	3.64	34.74	100	3.65	34.74	27.63
147	3.50	34.81	150	3.50	34.81	27.71
196	3.67	34.86	200	3.70	34.87	27.74
294	3.74	34.90	300	3.70	34.90	27.76
359	3.53	34.87	400	3.50	34.87	27.76
539	3.47	34.88	600	3.45	34.88	27.76
717	3.43	34.89	800	3.40	34.88	27.77
904	3.39	34.88	1,000	3.40	34.88	27.77
1,383	3.41	34.93	1,500	3.35	34.93	27.81
1,858	3.06	34.94	2,000	2.85	34.93	27.86
2,193	2.43	34.90				

Table of Oceanographic Data—Continued

STATIONS OCCUPIED IN 1949—Continued

Station 3951; 9 July; latitude 58°52′ N., longitude 45°34′ W.; depth 2488 meters; dynamic height 1454.554

Observed values			Scaled values			
Depth, meters	Temperature, °C.	Salinity, ‰	Depth, meters	Temperature, °C.	Salinity, ‰	σ_t
0	5.24	34.71	0	5.24	34.71	27.44
24	5.04	34.70	25	5.00	34.70	27.46
48	4.33	34.78	50	4.25	34.78	27.60
72	3.63	34.80	75	3.60	34.80	27.69
96	3.63	34.84	100	3.65	34.84	27.71
143	3.76	34.87	150	3.75	34.88	27.73
190	3.87	34.92	200	3.85	34.92	27.76
286	3.82	34.93	300	3.80	34.93	27.77
316	3.75	34.92	400	3.65	34.92	27.78
478	3.59	34.91	600	3.50	34.90	27.78
642	3.46	34.89	800	3.45	34.90	27.78
816	3.46	34.90	1,000	3.45	34.92	27.80
1,272	3.47	34.94	1,500	3.25	34.94	27.83
1,734	3.08	34.94	2,000	2.85	34.94	27.87
2,117	2.77	34.94				

Station 3952; 9 July; latitude 59°07′ N., longitude 45°03′ W.; depth 2067 meters; dynamic height 1454.572

Observed values			Scaled values			
Depth, meters	Temperature, °C.	Salinity, ‰	Depth, meters	Temperature, °C.	Salinity, ‰	σ_t
0	5.72	34.79	0	5.72	34.79	27.44
24	5.71	34.80	25	5.70	34.80	27.45
47	5.58	34.81	50	5.50	34.82	27.50
71	4.94	34.86	75	4.85	34.87	27.61
94	4.45	34.89	100	4.45	34.90	27.68
142	4.41	34.95	150	4.40	34.95	27.72
189	4.32	34.96	200	4.30	34.96	27.74
283	4.09	34.95	300	4.05	34.95	27.76
317	4.05	34.94	400	3.90	34.93	27.76
484	3.78	34.92	600	3.70	34.91	27.77
659	3.64	34.905	800	3.55	34.91	28.78
840	3.55	34.91	1,000	3.50	34.92	27.80
1,315	3.43	34.94	1,500	3.30	34.93	27.82
1,826	2.75	34.92	(2,000)	2.40	34.91	28.89

Station 3953; 9 July; latitude 59°20.5′ N., longitude 44°32′ W.; depth 1044 meters; dynamic height 1454.620

Observed values			Scaled values			
Depth, meters	Temperature, °C.	Salinity, ‰	Depth, meters	Temperature, °C.	Salinity, ‰	σ_t
0	4.33	34.67	0	4.33	34.67	27.51
27	4.24	34.66	25	4.25	34.66	27.51
53	3.63	34.62	50	3.65	34.62	27.54
80	3.54	34.60	75	3.55	34.60	27.54
106	3.48	34.60	100	3.50	34.60	27.58
161	3.83	34.74	150	3.75	34.70	27.59
214	4.51	34.90	200	4.40	34.86	27.65
320	4.55	34.95	300	4.55	34.95	27.71
350	4.48	34.96	400	4.40	34.97	27.73
530	4.37	34.97	600	4.30	34.96	27.74
713	4.16	34.95	800	4.00	34.94	27.76
900	3.80	34.92	(1,000)	3.65	34.93	27.78

Station 3954; 9 July; latitude 59°31′ N., longitude 44°06′ W.; depth 200 meters; dynamic height 1454.712

Observed values			Scaled values			
Depth, meters	Temperature, °C.	Salinity, ‰	Depth, meters	Temperature, °C.	Salinity, ‰	σ_t
0	−0.68	32.51	0	−0.68	32.51	26.15
24	−0.37	32.82	25	−0.35	32.85	26.41
48	−0.61	33.68	50	−0.60	33.70	27.10
72	0.36	33.92	75	0.40	33.94	27.25
97	1.22	34.10	100	1.35	34.12	27.34
145	2.54	34.45	150	2.55	34.46	27.52
169	2.63	34.46				

Station 3955; 11 July; latitude 62°14′ N., longitude 56°06′ W.; depth 2616 meters; dynamic height 1454.685

Observed values			Scaled values			
Depth, meters	Temperature, °C.	Salinity, ‰	Depth, meters	Temperature, °C.	Salinity, ‰	σ_t
0	3.80	33.74	0	3.80	33.74	26.83
25	3.77	33.74	25	3.77	33.74	26.83
49	0.22	33.92	50	0.20	33.93	27.25
74	0.59	34.08	75	0.60	34.09	27.35
99	0.91	34.22	100	0.95	34.23	27.44
149	2.40	34.50	150	2.45	34.51	27.56
198	3.85	34.76	200	3.85	34.67	27.56
297	4.19	34.87	300	4.15	34.86	27.68
287	4.13	34.85	400	3.90	34.86	27.71
439	3.83	34.86	600	3.75	34.88	27.73
595	3.77	34.88	800	3.75	34.90	27.75
755	3.75	34.90	1,000	3.65	34.90	27.76
1,174	3.61	34.90	1,500	3.55	34.93	27.79
1,610	3.53	34.94	2,000	3.25	34.94	27.83
2,257	2.85	34.94	(2,500)	2.45	34.94	27.90

Station 3956; 11 July; latitude 62°17′ N., longitude 57°01′ W.; depth 2474 meters; dynamic height 1454.643

Observed values			Scaled values			
Depth, meters	Temperature, °C.	Salinity, ‰	Depth, meters	Temperature, °C.	Salinity, ‰	σ_t
0	4.24	33.72	0	4.24	33.72	26.76
25	2.41	33.88	25	2.41	33.88	27.06
51	1.92	34.24	50	1.90	34.23	27.38
76	2.09	34.38	75	2.10	34.38	27.48
102	2.44	34.51	100	2.40	34.50	27.56
153	3.54	34.73	150	3.50	34.72	27.64
204	3.89	34.82	200	3.85	34.81	27.67
306	3.92	34.86	300	3.95	34.86	27.70
288	3.96	34.85	400	3.90	34.87	27.72
452	3.87	34.88	600	3.70	34.87	27.74
630	3.66	34.87	800	3.70	34.90	27.76
821	3.68	34.90	1,000	3.65	34.91	27.77
1,266	3.58	34.93	1,500	3.40	34.93	27.81
1,733	3.27	34.93	2,000	2.90	34.93	27.86
2,234	2.56	34.925				

Station 3957; 11 July; latitude 62°21.5′ N., longitude 58°31′ W.; depth 2076 meters; dynamic height 1454.654

Observed values			Scaled values			
Depth, meters	Temperature, °C.	Salinity, ‰	Depth, meters	Temperature, °C.	Salinity, ‰	σ_t
0	4.64	33.86	0	4.64	33.86	26.83
26	4.10	33.86	25	4.10	33.86	26.89
52	2.36	34.08	50	2.55	34.06	27.20
78	1.51	34.32	75	1.55	34.30	27.46
104	2.36	34.54	100	2.15	34.51	27.59
154	3.90	34.80	150	3.80	34.79	27.66
206	3.62	34.80	200	3.60	34.80	27.69
310	3.77	34.84	300	3.75	34.84	27.70
414	3.72	34.83	400	3.70	34.83	27.70
619	3.61	34.86	600	3.60	34.86	27.74
824	3.48	34.86	800	3.50	34.86	27.75
1,028	3.59	34.89	1,000	3.60	34.89	27.76
1,545	3.47	34.94	1,500	3.50	34.94	27.81
2,062	2.74	34.93	2,000	2.85	34.93	27.86

Table of Oceanographic Data—Continued

STATIONS OCCUPIED IN 1949—Continued

Station 3958; 11 July; latitude 62°24.5′ N., longitude 59°22′ W.; depth 1485 meters; dynamic height 1454.689

Observed values			Scaled values			
Depth, meters	Temperature, °C.	Salinity, °/oo	Depth, meters	Temperature, °C.	Salinity, °/oo	σ_t
0	4.03	33.79	0	4.03	33.79	26.83
25	3.67	33.80	25	3.67	33.80	26.88
49	−0.05	34.11	50	−0.05	34.12	27.42
74	0.81	34.24	75	0.85	34.24	27.46
98	1.66	34.36	100	1.75	34.38	27.51
147	3.76	34.69	150	3.80	34.70	27.59
196	4.16	34.78	200	4.20	34.79	27.62
294	4.51	34.89	300	4.40	34.87	27.66
360	4.35	34.88	400	4.35	34.88	27.67
542	4.04	34.87	600	3.90	34.86	27.71
725	3.66	34.86	800	3.65	34.86	27.73
909	3.65	34.87	1,000	3.60	34.88	27.75
1,371	3.57	34.93	(1,500)	3.55	34.93	27.79

Station 3959; 12 July; latitude 62°27′ N., longitude 60°07′ W.; depth 1306 meters; dynamic height 1454.689

Observed values			Scaled values			
Depth, meters	Temperature, °C.	Salinity, °/oo	Depth, meters	Temperature, °C.	Salinity, °/oo	σ_t
0	4.12	33.77	0	4.12	33.77	26.82
25	3.52	33.78	25	3.52	33.78	26.88
49	0.60	33.98	50	0.60	33.99	27.27
74	0.73	34.22	75	0.80	34.23	27.45
99	1.32	34.34	100	1.40	34.35	27.52
148	2.96	34.61	150	3.00	34.62	27.61
197	4.08	34.80	200	4.10	34.81	27.65
296	4.32	34.88	300	4.35	34.88	27.67
385	4.29	34.90	400	4.25	34.90	27.70
576	3.86	34.88	600	3.85	34.88	27.72
768	3.84	34.91	800	3.85	34.91	27.75
960	3.72	34.92	1,000	3.70	34.92	27.78
1,248	3.47	34.96				

Station 3960; 12 July; latitude 62°27.5′ N., longitude 61°15′ W.; depth 624 meters; dynamic height 1454.703

Observed values			Scaled values			
Depth, meters	Temperature, °C.	Salinity, °/oo	Depth, meters	Temperature, °C.	Salinity, °/oo	σ_t
0	3.72	33.62	0	3.72	33.62	26.75
26	3.53	33.75	25	3.55	33.75	26.86
52	−1.08	33.83	50	−1.00	33.82	27.22
78	−0.50	34.03	75	−0.55	34.02	27.36
104	−0.44	34.14	100	−0.45	34.12	27.44
154	1.42	34.34	150	1.25	34.32	27.51
206	3.67	34.66	200	3.50	34.63	27.56
310	3.68	34.74	300	3.70	34.73	27.62
386	4.10	34.82	400	4.05	34.82	27.66
582	3.78	34.82	600	3.70	34.82	27.70

Station 3961; 12 July; latitude 62°28′ N., longitude 61°46′ W.; depth 391 meters; dynamic height 1454.743

Observed values			Scaled values			
Depth, meters	Temperature, °C.	Salinity, °/oo	Depth, meters	Temperature, °C.	Salinity, °/oo	σ_t
0	2.59	32.87	0	2.59	32.87	26.24
24	0.48	33.19	25	0.45	33.20	26.66
47	−1.52	33.58	50	−1.55	33.59	27.05
71	−1.50	33.69	75	−1.45	33.70	27.14
94	−1.05	33.82	100	−0.90	33.85	27.24
141	0.08	34.07	150	0.25	34.11	27.40
189	1.11	34.27	200	1.40	34.32	27.50
283	3.30	34.64	300	3.30	34.65	27.60
366	3.24	34.67				

Station 3962; 12 July; latitude 62°28′ N., longitude 62°14′ W.; depth 306 meters; dynamic height 1454.800

Observed values			Scaled values			
Depth, meters	Temperature, °C.	Salinity, °/oo	Depth, meters	Temperature, °C.	Salinity, °/oo	σ_t
0	2.02	32.63	0	2.02	32.63	26.10
24	1.53	32.75	25	1.50	32.76	26.23
47	−0.27	33.15	50	−0.55	33.20	26.70
71	−1.62	33.47	75	−1.65	33.49	26.97
94	−1.62	33.58	100	−1.60	33.59	27.05
141	−1.41	33.72	150	−1.30	33.74	27.16
188	−0.58	33.92	200	−0.30	33.98	27.31
282	1.99	34.42	(300)	2.40	34.50	27.56

Station 3963; 12 July; latitude 62°26′ N., longitude 62°51′ W.; depth 269 meters; dynamic height 1454.801

Observed values			Scaled values			
Depth, meters	Temperature, °C.	Salinity, °/oo	Depth, meters	Temperature, °C.	Salinity, °/oo	σ_t
0	1.40	32.34	0	1.40	32.34	25.91
25	−1.19	32.98	25	−1.19	32.98	26.54
49	−1.69	33.19	50	−1.70	33.20	26.74
74	−1.58	33.34	75	−1.60	33.35	26.86
98	−1.59	33.48	100	−1.55	33.50	26.98
147	−0.90	33.75	150	−0.85	33.77	27.17
197	−0.45	33.93	200	−0.45	33.93	27.28
251	−0.38	33.96				

Station 3964; 12 July; latitude 62°23.5′ N., longitude 63°18′ W.; depth 258 meters; dynamic height 1454.816

Observed values			Scaled values			
Depth, meters	Temperature, °C.	Salinity, °/oo	Depth, meters	Temperature, °C.	Salinity, °/oo	σ_t
0	0.71	32.12	0	0.71	32.12	25.78
22	−1.36	32.73	25	−1.40	32.77	26.38
43	−1.65	33.13	50	−1.65	33.17	26.71
65	−1.61	33.24	75	−1.60	33.30	26.81
87	−1.56	33.39	100	−1.55	33.47	26.96
130	−1.59	33.60	150	−1.60	33.65	27.10
174	−1.57	33.70	200	−1.05	33.82	27.22
217	−0.60	33.91				

Station 3965; 12 July; latitude 62°20′ N., longitude 63°55′ W.; depth 192 meters; dynamic height 1454.825

Observed values			Scaled values			
Depth, meters	Temperature, °C.	Salinity, °/oo	Depth, meters	Temperature, °C.	Salinity, °/oo	σ_t
0	−1.38	31.39	0	−1.38	31.39	25.26
25	−1.65	32.95	25	−1.65	32.95	26.53
49	−1.70	33.11	50	−1.70	33.11	26.66
74	−1.59	33.18	75	−1.60	33.18	26.71
99	−1.54	33.22	100	−1.55	33.22	26.75
148	−0.98	33.72	150	−0.95	33.73	27.14
183	−0.58	33.83				

Station 3966; 13 July; latitude 62°30′ N., longitude 56°14′ W.; depth 2268 meters; dynamic height 1454.665

Observed values			Scaled values			
Depth, meters	Temperature, °C.	Salinity, °/oo	Depth, meters	Temperature, °C.	Salinity, °/oo	σ_t
0	3.64	33.60	0	3.64	33.60	26.73
26	3.58	33.62	25	3.60	33.62	26.76
51	0.86	33.95	50	1.95	33.94	27.14
77	1.15	34.19	75	1.15	34.18	27.39
101	1.74	34.36	100	1.70	34.35	27.49
153	2.68	34.57	150	2.60	34.56	27.59
204	3.59	34.76	200	3.50	34.74	27.65
305	3.92	34.85	300	3.90	34.85	27.70
369	3.81	34.86	400	3.75	34.86	27.72
561	3.61	34.86	600	3.65	34.89	27.75
716	3.72	34.90	800	3.70	34.90	27.76
913	3.70	34.91	1,000	3.70	34.91	27.77
1,432	3.58	34.91	1,500	3.50	34.92	27.80
1,983	3.05	34.92	2,000	3.05	34.92	27.84
2,234	2.79	34.93				

Table of Oceanographic Data—Continued

STATIONS OCCUPIED IN 1949—Continued

Station 3967; 14 July; latitude 62°53.5′ N., longitude 55°22′ W.; depth 2305 meters; dynamic height 1454.660

Observed values			Scaled values			
Depth, meters	Temperature, °C.	Salinity, °/oo	Depth, meters	Temperature, °C.	Salinity, °/oo	σ_t
0	3.49	33.56	0	3.49	33.56	26.71
27	3.67	33.63	25	3.65	33.63	26.75
52	1.69	34.09	50	1.80	34.05	27.25
79	1.42	34.28	75	1.40	34.27	27.46
105	2.07	34.44	100	1.95	34.42	27.54
158	3.05	34.65	150	2.95	34.62	27.61
210	3.73	34.80	200	3.60	34.78	27.67
315	3.73	34.83	300	3.75	34.83	27.69
388	3.63	34.84	400	3.60	34.84	27.72
599	3.72	34.88	600	3.70	34.88	27.74
756	3.61	34.88	800	3.60	34.88	27.75
970	3.59	34.90	1,000	3.60	34.90	27.77
1,453	3.50	34.93	1,500	3.45	34.93	27.80
2,080	2.93	34.925	2,000	3.00	34.93	27.85
2,336	2.07	34.915				

Station 3968; 14 July; latitude 63°10′ N., longitude 54°35′ W.; depth 1353 meters; dynamic height 1454.760

Observed values			Scaled values			
Depth, meters	Temperature, °C.	Salinity, °/oo	Depth, meters	Temperature, °C.	Salinity, °/oo	σ_t
0	1.56	33.24	0	1.56	33.24	26.62
26	1.53	33.25	25	1.55	33.25	26.63
52	1.97	33.50	50	1.95	33.48	26.78
78	0.45	33.73	75	0.50	33.71	27.06
104	0.08	33.85	100	0.10	33.83	27.17
155	0.64	34.08	150	0.60	34.06	27.33
207	0.98	34.23	200	0.90	34.21	27.44
311	3.70	34.70	300	3.50	34.66	27.59
383	3.61	34.74	400	3.65	34.76	27.65
567	4.27	34.90	600	4.25	34.90	27.68
746	4.06	34.91	(800)	3.95	34.91	27.74
			(1,000)	3.65	34.91	27.77

Station 3969; 14 July; latitude 63°22′ N., longitude 53°56′ W.; depth 1057 meters; dynamic height 1454.736

Observed values			Scaled values			
Depth, meters	Temperature, °C.	Salinity, °/oo	Depth, meters	Temperature, °C.	Salinity, °/oo	σ_t
0	2.11	33.35	0	2.11	33.35	26.67
24	1.23	33.49	25	1.20	33.49	26.84
49	0.09	33.66	50	0.05	33.66	27.05
73	0.09	33.76	75	0.05	33.77	27.14
98	0.17	33.92	100	0.20	33.93	27.25
147	0.63	34.08	150	0.65	34.08	27.34
195	1.00	34.20	200	1.15	34.22	27.43
293	3.41	34.66	300	3.85	34.73	27.60
248	3.30	34.63	400	4.50	34.88	27.65
395	4.48	34.88	600	4.10	34.91	27.73
558	4.19	34.91	(800)	3.90	34.90	27.74
737	3.97	34.90	(1,000)	3.70	34.90	27.76

Station 3970; 14 July; latitude 63°32.5′ N., longitude 53°30′ W.; depth 1565 meters; dynamic height 1454.763

Observed values			Scaled values			
Depth, meters	Temperature, °C.	Salinity, °/oo	Depth, meters	Temperature, °C.	Salinity, °/oo	σ_t
0	2.19	33.30	0	2.19	33.30	26.61
26	2.15	33.30	25	2.15	33.30	26.62
51	1.40	33.49	50	1.45	33.49	26.82
76	0.04	33.67	75	0.00	33.67	27.06
101	0.29	33.78	100	0.30	33.78	27.12
153	1.27	34.08	150	1.20	34.06	27.30
203	2.12	34.35	200	2.10	34.34	27.45
304	3.27	34.67	300	3.25	34.66	27.61
372	3.79	34.77	400	3.85	34.79	27.65
560	4.02	34.86	600	4.00	34.87	27.71
749	3.95	34.905	800	3.90	34.90	27.74
942	3.79	34.90	1,000	3.75	34.90	27.75
1,438	3.51	34.92	(1,500)	3.45	34.92	27.80

Station 3971; 14–15 July; latitude 63°38.5′ N., longitude 53°16′ W.; depth 1060 meters; dynamic height 1454.792

Observed values			Scaled values			
Depth, meters	Temperature, °C.	Salinity, °/oo	Depth, meters	Temperature, °C.	Salinity, °/oo	σ_t
0	1.22	33.31	0	1.22	33.31	26.70
22	1.20	33.32	25	1.20	33.32	26.71
43	0.90	33.33	50	0.60	33.38	26.78
65	−0.19	33.50	75	−0.20	33.58	26.99
87	−0.09	33.67	100	0.05	33.72	27.10
129	0.33	33.83	150	0.45	33.90	27.21
172	0.59	33.97	200	1.10	34.09	27.33
259	1.95	34.34	300	2.35	34.44	27.51
338	2.74	34.52	400	3.35	34.65	27.59
513	4.46	34.88	600	4.35	34.89	27.68
694	4.16	34.90	800	3.95	34.91	27.74
899	3.80	34.92	(1,000)	3.60	34.93	27.79

Station 3972; 15 July; latitude 63°43′ N., longitude 53°08′ W.; depth 236 meters; dynamic height 1454.824

Observed values			Scaled values			
Depth, meters	Temperature, °C.	Salinity, °/oo	Depth, meters	Temperature, °C.	Salinity, °/oo	σ_t
0	1.66	33.35	0	1.66	33.35	26.70
23	1.65	33.35	25	1.65	33.35	26.70
46	1.20	33.40	50	1.05	33.44	26.81
69	0.34	33.61	75	0.30	33.64	27.01
92	0.31	33.68	100	0.30	33.69	27.05
137	0.35	33.73	150	0.35	33.74	27.09
183	0.33	33.77	(200)	0.35	33.78	27.12

Station 3973; 15 July; latitude 63°54′ N., longitude 52°49′ W.; depth 64 meters; dynamic height 1454.831

Observed values			Scaled values			
Depth, meters	Temperature, °C.	Salinity, °/oo	Depth, meters	Temperature, °C.	Salinity, °/oo	σ_t
0	1.48	33.46	0	1.48	33.46	26.80
25	1.45	33.47	25	1.45	33.47	26.81
49	1.37	33.50	(50)	1.35	33.51	26.85

Station 3974; 15 July; latitude 63°59′ N., longitude 52°42′ W.; depth 41 meters; dynamic height 1454.834

Observed values			Scaled values			
Depth, meters	Temperature, °C.	Salinity, °/oo	Depth, meters	Temperature, °C.	Salinity, °/oo	σ_t
0	1.91	33.44	0	1.91	33.44	26.76
14	1.80	33.44	25	1.80	33.44	26.76
28	1.80	33.44				

Station 3975; 15 July; latitude 63° 00′ N., longitude 56°32′ W.; depth 2077 meters; dynamic height 1454.735

Observed values			Scaled values			
Depth, meters	Temperature, °C.	Salinity, °/oo	Depth, meters	Temperature, °C.	Salinity, °/oo	σ_t
0	2.68	33.32	0	2.68	33.32	26.60
26	2.76	33.34	25	2.75	33.34	26.60
50	−0.09	33.66	50	−0.09	33.66	27.05
75	−0.02	33.78	75	−0.02	33.78	27.14
100	0.14	33.91	100	0.14	33.91	27.24
151	1.08	34.24	150	1.05	34.23	27.44
202	2.28	34.48	200	2.20	34.48	27.57
302	4.69	34.86	300	4.70	34.85	27.61
408	4.54	34.90	400	4.55	34.90	27.67
612	4.12	34.90	600	4.15	34.90	27.71
820	3.95	34.90	800	3.95	34.90	27.73
1,030	3.79	34.92	1,000	3.80	34.92	27.77
1,566	3.53	34.93	1,500	3.55	34.93	27.79
1,770	3.31	34.93	2,000	3.05	34.93	27.84
2,020	3.00	34.93				

STATIONS OCCUPIED IN 1949—Continued

Station 3976; 16 July; latitude 63°30′ N., longitude 56°48′ W.; depth 1577 meters; dynamic height 1454.725

Observed values			Scaled values			
Depth, meters	Temperature, °C.	Salinity, °/°°	Depth, meters	Temperature, °C.	Salinity, °/°°	σ_t
0	3.08	33.31	0	3.08	33.31	26.55
27	2.87	33.49	25	2.85	33.48	26.70
52	1.40	33.72	50	1.60	33.70	26.98
79	0.27	33.87	75	0.40	33.85	27.18
104	0.44	32.98	100	0.40	33.96	27.27
158	0.87	34.22	150	0.80	34.18	27.41
210	2.27	34.47	200	2.00	34.42	27.53
314	4.21	34.84	300	3.65	34.75	27.64
384	4.04	34.82	400	4.25	34.85	27.66
574	4.22	34.88	600	4.20	34.88	27.69
757	3.99	34.92	800	3.95	34.93	27.75
955	3.83	34.935	1,000	3.80	34.94	27.78
1,465	3.38	34.93	(1,500)	3.35	34.93	27.81

Station 3977; 16 July; latitude 64° 00.5′ N., longitude 57°05′ W.; depth 812 meters; dynamic height 1454.756

Observed values			Scaled values			
Depth, meters	Temperature, °C.	Salinity, °/°°	Depth, meters	Temperature, °C.	Salinity, °/°°	σ_t
0	2.71	33.47	0	2.71	33.47	26.72
27	2.45	33.52	25	2.45	33.52	26.78
52	0.73	33.65	50	0.85	33.64	26.98
79	0.24	33.74	75	0.25	33.73	27.09
104	0.11	33.80	100	0.10	33.79	27.14
157	0.40	33.96	150	0.35	33.93	27.24
210	0.42	34.11	200	0.40	34.08	27.26
314	2.65	34.50	300	2.20	34.44	27.54
368	4.13	34.77	400	4.40	34.83	27.62
558	4.73	34.92	600	4.65	34.92	27.68
751	3.97	34.92	(800)	3.75	34.92	27.77

Station 3978; 16 July; latitude 64°33.5′ N., longitude 57°24′ W.; depth 759 meters; dynamic height 1454.695

Observed values			Scaled values			
Depth, meters	Temperature, °C.	Salinity, °/°°	Depth, meters	Temperature, °C.	Salinity, °/°°	σ_t
0	3.34	33.62	0	3.34	33.62	26.78
25	3.11	33.82	25	3.11	33.82	26.96
50	−0.99	34.00	50	−0.99	34.00	27.36
75	−0.94	34.04	75	−0.94	34.04	27.39
100	−0.19	34.16	100	−0.19	34.16	27.46
150	3.15	34.54	150	3.15	34.54	27.52
199	3.89	34.68	200	3.90	34.68	27.56
299	4.82	34.85	300	4.80	34.85	27.60
387	4.83	34.88	400	4.80	34.88	27.62
584	4.52	34.90	600	4.50	34.90	27.67
732	3.98	34.89				

Station 3979; 16 July; latitude 65°00.5′ N., longitude 57°39′ W.; depth 659 meters; dynamic height 1454.731

Observed values			Scaled values			
Depth, meters	Temperature, °C.	Salinity, °/°°	Depth, meters	Temperature, °C.	Salinity, °/°°	σ_t
0	1.54	32.21	0	1.54	32.21	25.79
22	−0.52	33.25	25	−0.50	33.29	26.76
44	0.03	33.68	50	−0.35	33.70	27.09
66	−1.66	33.73	75	−1.50	33.76	27.19
88	−1.36	33.80	100	−1.15	33.84	27.24
132	−0.52	33.98	150	−0.35	34.04	27.36
175	−0.03	34.11	200	0.50	34.22	27.47
263	2.26	34.48	300	2.70	34.55	27.57
370	3.01	34.62	400	2.95	34.62	27.61
574	1.62	34.57	(600)	1.45	34.56	27.68

Station 3980; 16 July; latitude 65°18′ N., longitude 57°50′ W.; depth 531 meters; dynamic height 1454.718

Observed values			Scaled values			
Depth, meters	Temperature, °C.	Salinity, °/°°	Depth, meters	Temperature, °C.	Salinity, °/°°	σ_t
0	1.26	31.98	0	1.26	31.98	25.63
26	−0.42	33.36	25	−0.40	33.35	26.82
52	−1.13	33.64	50	−1.10	33.61	27.06
78	−1.20	33.79	75	−1.20	33.78	27.19
104	−0.75	33.93	100	−0.85	33.91	27.28
156	0.49	34.18	150	0.30	34.16	27.43
208	2.96	34.51	200	2.65	34.46	27.51
312	4.11	34.76	300	4.05	34.75	27.60
383	4.04	34.78	400	3.80	34.77	27.65
483	2.43	34.65				

Station 3981; 17 July; latitude 65°58′ N., longitude 58°22′ W.; depth 487 meters; dynamic height 1454.730

Observed values			Scaled values			
Depth, meters	Temperature, °C.	Salinity, °/°°	Depth, meters	Temperature, °C.	Salinity, °/°°	σ_t
0	0.87	32.12	0	0.87	32.12	25.76
26	−1.03	33.38	25	−1.00	33.37	26.85
52	−1.56	33.63	50	−1.50	33.61	27.07
78	−1.69	33.72	75	−1.70	33.71	27.15
104	−1.44	33.78	100	−1.50	33.77	27.20
156	−0.57	33.97	150	−0.65	33.95	27.31
208	0.36	34.16	200	0.20	34.14	27.42
312	2.38	34.51	300	2.20	34.46	27.55
314	2.56	34.50	400	2.35	34.63	27.66
366	2.42	34.62				

Station 3982; 17 July; latitude 65°58′ N., longitude 58°22′ W.; depth 613 meters; dynamic height 1454.788

Observed values			Scaled values			
Depth, meters	Temperature, °C.	Salinity, °/°°	Depth, meters	Temperature, °C.	Salinity, °/°°	σ_t
0	1.02	32.30	0	1.02	32.30	25.90
26	0.32	32.62	25	0.35	32.61	26.19
51	−1.55	33.31	50	−1.50	33.29	26.80
77	−1.71	33.56	75	−1.70	33.54	27.01
102	−1.55	33.68	100	−1.55	33.67	27.12
152	−1.31	33.77	150	−1.35	33.76	27.18
204	−0.59	33.97	200	−0.70	33.96	27.32
306	1.52	34.33	300	1.40	34.31	27.49
396	2.51	34.54	400	2.50	34.54	27.58
589	1.70	34.55	600	1.65	34.55	27.66

Station 3983; 17 July; latitude 66° 22′ N., longitude 58°42′ W.; depth 732 meters; dynamic height 1454.818

Observed values			Scaled values			
Depth, meters	Temperature, °C.	Salinity, °/°°	Depth, meters	Temperature, °C.	Salinity, °/°°	σ_t
0	0.70	31.23	0	0.70	31.23	25.06
26	−1.42	32.81	25	−1.40	32.80	26.41
52	−1.72	33.19	50	−1.70	33.16	26.70
77	−1.59	33.38	75	−1.60	33.38	26.88
103	−1.43	33.52	100	−1.45	33.51	26.99
154	−1.42	33.70	150	−1.45	33.69	27.13
206	−1.10	33.86	200	−1.20	33.84	27.24
309	0.70	34.23	300	0.55	34.20	27.45
404	1.87	34.46	400	1.85	34.45	27.56
605	0.96	34.48	600	0.95	34.48	27.64
706	0.80	34.48				

STATIONS OCCUPIED IN 1949—Continued

Station 3984; 17 July; latitude 66°48.5′ N., longitude 58°40′ W.; depth 1119 meters; dynamic height 1454.812

Observed values			Scaled values			
Depth, meters	Temperature, °C.	Salinity, ‰	Depth, meters	Temperature, °C.	Salinity, ‰	σ_t
0	−0.93	31.56	0	−0.93	31.56	25.39
26	−1.56	33.00	25	−1.55	32.97	26.55
51	−1.66	33.28	50	−1.65	33.26	26.78
77	−1.71	33.45	75	−1.70	33.44	26.93
102	−1.74	33.54	100	−1.75	33.53	27.00
153	−1.61	33.69	150	−1.65	33.68	27.12
204	−1.20	33.84	200	−1.25	33.83	27.23
306	−0.31	34.12	300	−0.35	34.10	27.41
437	2.32	34.52	400	1.70	34.43	27.55
655	1.19	34.49	600	1.35	34.50	27.64
873	0.79	34.50	800	0.90	34.50	27.67
1,092	0.49	34.48	1,000	0.60	34.49	27.67

Station 3985; 18 July; latitude 67°11′ N., longitude 57°36′ W.; depth 651 meters; dynamic height 1454.755

Observed values			Scaled values			
Depth, meters	Temperature, °C.	Salinity, ‰	Depth, meters	Temperature, °C.	Salinity, ‰	σ_t
0	0.37	32.06	0	0.37	32.06	25.74
25	−1.49	33.22	25	−1.49	33.22	26.75
50	−1.72	33.54	50	−1.72	33.54	27.01
76	−1.65	33.69	75	−1.65	33.69	27.13
101	−1.58	33.74	100	−1.60	33.74	27.17
150	−0.90	33.90	150	−0.90	33.90	27.28
200	0.16	34.10	200	0.15	34.10	27.39
301	1.82	34.41	300	1.80	34.41	27.54
384	2.32	34.52	400	2.30	34.52	27.59
593	1.48	34.51	600	1.45	34.51	27.64

Station 3986; 18 July; latitude 67°31.5′ N., longitude 57°52′ W.; depth 245 meters; dynamic height 1454.736

Observed values			Scaled values			
Depth, meters	Temperature, °C.	Salinity, ‰	Depth, meters	Temperature, °C.	Salinity, ‰	σ_t
0	−0.52	31.76	0	−0.52	31.76	25.54
24	−0.57	32.68	25	−0.60	32.70	26.29
48	−1.00	33.73	50	−1.00	33.75	27.16
72	−0.72	33.90	75	−0.70	33.91	27.28
96	−0.31	33.98	100	−0.25	34.00	27.33
144	0.39	34.16	150	0.40	34.17	27.44
191	0.19	34.21	200	0.20	34.21	27.48
225	0.18	34.20				

Station 3987; 18 July; latitude 67°59′ N., longitude 57°03′ W.; depth 289 meters; dynamic height 1454.732

Observed values			Scaled values			
Depth, meters	Temperature, °C.	Salinity, ‰	Depth, meters	Temperature, °C.	Salinity, ‰	σ_t
0	2.43	32.65	0	2.43	32.65	26.08
25	1.56	32.79	25	1.56	32.79	26.26
49	−1.70	33.73	50	−1.70	33.73	27.16
74	−1.25	33.86	75	−1.25	33.86	27.26
99	−0.21	34.00	100	−0.20	34.00	27.33
147	0.10	34.14	150	0.15	34.14	27.42
196	0.48	34.22	200	0.50	34.23	27.47
274	1.21	34.35				

Station 3988; 18 July; latitude 68°26′ N., longitude 56°54′ W.; depth 340 meters; dynamic height 1454.697

Observed values			Scaled values			
Depth, meters	Temperature, °C.	Salinity, ‰	Depth, meters	Temperature, °C.	Salinity, ‰	σ_t
0	3.36	33.60	0	3.36	33.60	26.76
23	3.35	33.60	25	3.30	33.61	26.77
46	2.40	33.84	50	2.10	33.86	27.07
69	0.63	33.91	75	0.35	33.94	27.25
92	−0.17	34.01	100	0.00	34.04	27.35
138	0.98	34.18	150	1.10	34.21	27.43
184	1.56	34.30	200	1.70	34.34	27.48
276	2.34	34.50	(300)	2.55	34.55	27.59

Station 3989; 19 July; latitude 68°46.5′ N., longitude 58°56′ W.; depth 432 meters; dynamic height 1454.747

Observed values			Scaled values			
Depth, meters	Temperature, °C.	Salinity, ‰	Depth, meters	Temperature, °C.	Salinity, ‰	σ_t
0	1.01	32.37	0	1.01	32.37	25.96
26	−1.35	33.36	25	−1.30	33.30	26.80
54	−1.67	33.67	50	−1.65	33.62	27.08
80	−1.54	33.79	75	−1.60	33.77	27.20
135	−0.51	33.91	100	−1.30	33.82	27.23
189	0.79	34.15	150	−0.15	33.97	27.31
296	2.50	34.52	200	1.00	34.18	27.40
92	−1.44	33.81	300	2.55	34.41	27.48
292	2.42	34.40	(400)	2.90	34.50	27.52

Station 3990; 19 July; latitude 69°06.5′ N., longitude 59°56′ W.; depth 1551 meters; dynamic height 1454.768

Observed values			Scaled values			
Depth, meters	Temperature, °C.	Salinity, ‰	Depth, meters	Temperature, °C.	Salinity, ‰	σ_t
0	0.86	32.50	0	0.86	32.50	26.07
25	−1.29	33.01	25	−1.29	33.01	26.57
50	−1.75	33.52	50	−1.75	33.52	27.00
75	−1.77	33.60	75	−1.77	33.60	27.06
100	−1.75	33.63	100	−1.75	33.63	27.08
150	−1.40	33.78	150	−1.40	33.78	27.19
200	−0.95	33.89	200	−0.95	33.89	27.27
300	1.18	34.28	300	1.18	34.28	27.47
357	1.44	34.36	400	1.35	34.38	27.54
543	0.96	34.42	600	0.85	34.44	27.62
736	0.65	34.50	800	0.50	34.49	27.68
933	0.15	34.47	1,000	0.05	34.47	27.70
1,417	−0.32	34.50	(1,500)	−0.40	34.50	27.74

Station 3991; 19 July; latitude 69°33′ N., longitude 59°23′ W.; depth 1157 meters; dynamic height 1454.739

Observed values			Scaled values			
Depth, meters	Temperature, °C.	Salinity, ‰	Depth, meters	Temperature, °C.	Salinity, ‰	σ_t
0	−0.20	32.88	0	−0.20	32.88	26.43
26	−1.36	33.18	25	−1.35	33.18	26.71
52	−1.75	33.64	50	−1.75	33.62	27.08
78	−1.71	33.66	75	−1.75	33.66	27.11
104	−1.56	33.74	100	−1.60	33.73	27.16
156	−0.90	33.85	150	−1.00	33.84	27.23
208	−0.04	34.03	200	−0.20	34.00	27.33
312	2.44	34.48	300	2.15	34.43	27.52
392	3.32	34.64	400	3.30	34.64	27.59
589	1.80	34.54	600	1.75	34.54	27.65
786	0.95	34.505	800	0.90	34.50	27.67
984	0.36	34.485	1,000	0.30	34.49	27.69
1,130	0.04	34.49				

Station 3992; 19 July; latitude 69°51.5′ N., longitude 59°01′ W.; depth 302 meters; dynamic height 1454.710

Observed values			Scaled values			
Depth, meters	Temperature, °C.	Salinity, ‰	Depth, meters	Temperature, °C.	Salinity, ‰	σ_t
0	0.62	32.74	0	0.62	32.74	26.28
25	−1.52	33.37	25	−1.52	33.37	26.87
49	−1.66	33.70	50	−1.65	33.70	27.14
74	−1.60	33.79	75	−1.60	33.79	27.21
98	−1.60	33.82	100	−1.60	33.82	27.24
147	−0.02	34.01	150	0.05	34.02	27.34
197	1.13	34.23	200	1.15	34.25	27.45
289	2.35	34.50	(300)	2.45	34.52	27.57

STATIONS OCCUPIED IN 1949—Continued

Station 3993; 19 July; latitude 70°03′ N., longitude 58°41′ W.; depth 308 meters; dynamic height 1454.716

Observed values			Scaled values			
Depth, meters	Temperature, °C.	Salinity, ‰	Depth, meters	Temperature, °C.	Salinity, ‰	σ_t
0	1.07	32.42	0	1.07	32.42	26.00
23	−1.45	33.44	25	−1.50	33.47	26.96
48	−1.71	33.68	50	−1.70	33.69	27.13
71	−1.75	33.73	75	−1.75	33.74	27.17
96	−1.68	33.76	100	−1.65	33.77	27.20
143	−0.64	33.91	150	−0.35	33.96	27.30
190	0.95	34.18	200	1.10	34.22	27.44
286	2.35	34.48	(300)	2.55	34.51	27.56

Station 3994; 20 July; latitude 70°11′ N., longitude 57°49′ W.; depth 331 meters; dynamic height 1454.706

Observed values			Scaled values			
Depth, meters	Temperature, °C.	Salinity, ‰	Depth, meters	Temperature, °C.	Salinity, ‰	σ_t
0	2.03	32.82	0	2.03	32.82	26.25
27	−1.51	33.61	25	−1.35	33.60	27.05
52	−1.76	33.73	50	−1.75	33.72	27.16
79	−1.65	33.75	75	−1.70	33.74	27.17
104	−1.08	33.84	100	−1.20	33.82	27.22
157	0.33	34.04	150	0.10	34.01	27.32
209	1.68	34.34	200	1.45	34.30	27.47
313	2.60	34.54	300	2.50	34.52	27.57

Station 3995; 20 July; latitude 70°18′ N., longitude 57°12′ W.; depth 289 meters; dynamic height 1454.720

Observed values			Scaled values			
Depth, meters	Temperature, °C.	Salinity, ‰	Depth, meters	Temperature, °C.	Salinity, ‰	σ_t
0	2.08	32.87	0	2.08	32.87	26.28
25	0.68	33.08	25	0.68	33.08	26.54
50	−1.38	33.74	50	−1.38	33.74	27.16
75	−1.68	33.79	75	−1.68	33.79	27.21
100	−1.49	33.80	100	−1.49	33.81	27.23
149	0.20	34.01	150	0.20	34.01	27.32
199	1.37	34.24	200	1.40	34.25	27.44
274	2.36	34.47	--------	--------	--------	--------

Station 3996; 20 July; latitude 70°25′ N., longitude 56°35′ W.; depth 214 meters; dynamic height 1454.709

Observed values			Scaled values			
Depth, meters	Temperature, °C.	Salinity, ‰	Depth, meters	Temperature, °C.	Salinity, ‰	σ_t
0	2.90	33.28	0	2.90	33.28	26.55
26	1.11	33.54	25	1.15	33.53	26.87
51	−0.95	33.74	50	−0.90	33.73	27.14
76	−1.40	33.80	75	−1.40	33.80	27.21
101	−0.88	33.88	100	−0.95	33.87	27.26
151	−0.12	34.01	150	−0.15	34.01	27.34
210	1.39	34.27	200	1.10	34.22	27.44

Station 3997; 20 July; latitude 70°30′ N., longitude 56°06′ W.; depth 131 meters; dynamic height 1454.711

Observed values			Scaled values			
Depth, meters	Temperature, °C.	Salinity, ‰	Depth, meters	Temperature, °C.	Salinity, ‰	σ_t
0	2.74	33.30	0	2.74	33.30	26.57
25	2.54	33.38	25	2.54	33.38	26.65
50	−0.60	33.80	50	−0.60	33.80	27.18
75	−0.86	33.86	75	−0.86	33.86	27.24
110	−0.70	33.92	100	−0.75	33.90	27.27

Station 3998; 20 July; latitude 70°35.5′ N., longitude 55°34′ W.; depth 247 meters; dynamic height 1454.708

Observed values			Scaled values			
Depth, meters	Temperature, °C.	Salinity, ‰	Depth, meters	Temperature, °C.	Salinity, ‰	σ_t
0	3.84	33.23	0	3.84	33.23	26.41
25	1.67	33.54	25	1.67	33.54	26.85
50	−1.11	33.80	50	−1.11	33.80	27.21
75	−0.88	33.89	75	−0.88	33.89	27.27
100	−0.43	33.94	100	−0.43	33.94	27.29
149	1.36	34.25	150	1.40	34.26	27.45
199	2.03	34.40	200	2.05	34.40	27.51
224	2.11	34.41	--------	--------	--------	--------

Station 3999; 20 July; latitude 70°38.5′ N., longitude 55°01′ W.; depth 426 meters; dynamic height 1454.728

Observed values			Scaled values			
Depth, meters	Temperature, °C.	Salinity, ‰	Depth, meters	Temperature, °C.	Salinity, ‰	σ_t
0	3.58	33.14	0	3.58	33.14	26.37
25	0.54	33.54	25	0.54	33.54	26.92
50	−1.61	33.73	50	−1.61	33.73	27.16
75	−1.64	33.77	75	−1.64	33.77	27.20
100	−1.40	33.82	100	−1.40	33.82	27.23
150	−0.09	34.00	150	−0.09	34.00	27.32
200	0.89	34.18	200	0.89	34.18	27.41
300	2.09	34.42	300	2.09	34.42	27.52
399	2.58	34.54	400	2.60	34.54	27.57

☆ U. S. GOVERNMENT PRINTING OFFICE: 51—935550

GPO 83-26352

Contribution No. 551

PHYSICAL OCEANOGRAPHY OF THE GRAND BANKS REGION AND THE LABRADOR SEA IN 1950

By Floyd M. Soule [1]

The oceanographic vessel of the ice patrol during 1950 was again the 180-foot tender-class cutter *Evergreen*. Except for one very important change, the vessel and the arrangements for doing oceanographic work from it were much the same as in the two previous years and described in Bulletin No. 34 of this series. The change was the substitution of a five-bladed propeller for the three-bladed propeller formerly used. The hull-vibration was very much reduced, and with the new screw it was possible to run at about 2 knots higher speed with less vibration than before the change was made.

The season's oceanographic work began with the departure of the *Evergreen* from Argentia on 5 April for the purpose of making a current survey of the area over and immediately seaward of the southwestern, southern, and eastern slopes of the Grand Banks. Following a plan to begin the survey in the southwestern part of the area and work around the Tail of the Banks and thence northward along the eastern slope of the banks, the work of collection of data commenced at station 4000 located at 43°35′ N., 51°27′ W., on the afternoon of 6 April. Three stations had been occupied when it was necessary to discontinue oceanographic work to search for two fishermen in a dory which had become separated from its mother ship. After the missing fishermen had been picked up by another vessel, oceanographic work was resumed at station 4003 on the afternoon of 7 April.

Work progressed without major incident until the morning of 9 April, when at station 4011 increasing seas required interruption of the oceanographic work after the first cast had been retrieved. The ship was hove to until improving conditions permitted resumption of work at station 4012 13 hours later. Again, at 2031 on 17 April increasing wind and heavy seas made it necessary to heave to and await better weather. Work was resumed at station 4060, located at 45°02′ N., 46°35′ W., on the afternoon of 18 April, although with doubtful results because of excessive wire angles arising from a strong current whose direction was widely different from that of the wind (W6) and sea (SW4). A 4-minute square was run with the von Arx current meter shortly before leaving this station and the resulting value of about 2 knots checked with the drift experienced by the ship during the period hove to.

---

[1] Contribution No. 551 of the Woods Hole Oceanographic Institution.

The work of collection of data was completed, without further interruption, on the afternoon of 19 April, at station 4068, located at 46°20.5′ N., 48°55′ W., and the ship proceeded to contact the patrol vessel (*Tampa*). In the meantime the data collected were reduced to the form of a current chart. A copy of the current chart was passed to the *Tampa* on the afternoon of 20 April, after which the *Evergreen* proceeded to Argentia, arriving there on the evening of 21 April.

On 1 May the *Evergreen* departed Argentia to make a second current survey of the same general area covered by the first survey but eliminating the southwestern extreme and extending the charted area farther to the northeast. The work of collection of data began on the afternoon of 2 May at station 4069, located at 42°00′ N., 51°58′ W., and progressed without interruption until the afternoon of 6 May when, at station 4093, located at 42°41′ N., 46°58′ W., deteriorating weather contributed to the loss of some of the oceanographic equipment and then made it necessary to heave to from early evening until early morning on 7 May after which operations were resumed. No further interruptions occurred and the work of collection of data was completed early on the morning of 14 May at station 4144 located at 46°48′ N., 44°51′ W. From this position the *Evergreen* proceeded to 46°04′ N., 45°00′ W., where a carboy of water was collected for ultimate use as a substandard of salinity during subsequent cruises. In the meantime work continued on the reduction of the data collected at the 76 oceanographic stations to the form of a dynamic topographic chart, a copy of which was delivered to the patrol cutter (*Acushnet*) on the morning of 15 May. The *Evergreen* then proceeded to Argentia where she arrived on the afternoon of 16 May.

A third oceanographic cruise began with the departure of the *Evergreen* from Argentia on 26 May. This cruise was for the purpose of investigating the oceanographic conditions in the vicinity and immediately northward of the Grand Banks where the Labrador Current divides into a western branch which flows southward along the coast of the Avalon Peninsula of Newfoundland, and an eastern branch which continues southeastward and eventually southward along the eastern edge of the Grand Banks. The oceanographic stations planned were to be disposed as three sections forming the sides of a triangle with corners on the northern edge of the Grand Banks, just off Cape Bonavista, and in the deep water northeastward of the first two corners.

The work of collection of data began on the afternoon of 27 May at station 4145 located at the southern corner of the triangle and progressed counterclockwise around the triangle without interruption until the station at the corner off Cape Bonavista was completed at dusk on 29 May. Numerous icebergs and growlers could be seen and more were reported to be along the proposed course. Fog patches and a fog bank also were visible in that direction and as the radar was not functioning reliably, a position off Cape Bonavista was maintained until daylight after which operations were resumed. The work of collection of data then progressed to completion on the evening of 30 May at station 4174 located near the beginning point of the triangle. A course was then laid for Argentia where the *Evergreen* arrived on the late afternoon of 31 May.

The *Evergreen* departed Argentia on the afternoon of 6 June to make a fourth current survey, with the area to be investigated including the waters over and immediately seaward of the southern and eastern slopes of the Grand Banks. It was also planned to extend section W (running southward from the southern end of the Grand Banks) sufficiently to cross the Labrador Current, the mixed water, and the Atlantic Current. The cruise began with an exploratory run southward along section W, during which surface currents were measured with a von Arx current meter and the thermal characteristics of the upper 200 to 300 meters were examined by means of casts of a bathythermograph every half hour.

The work of collection of the usual subsurface temperature and salinity data began on the morning of 9 June at station 4175 located at 38°00′ N., 50°12′ W., and continued northward along section W to the Grand Banks, after which the work progressed from the southwestern slope of the banks eastward around the Tail of The Banks and thence northward as far as and including section T. The final station of the survey, station 4238, located at 46°17′ N., 49°00′ W., was completed on the morning of 20 June. A course was then laid for Argentia with arrival there on 21 June.

The International Ice Patrol was discontinued for the season on 26 June for lack of ice in a position of potential hazard to effective shipping lanes. In order to avoid being barred by drift ice from the inshore area in the vicinity of Cape Farewell it seemed undesirable to begin the postseason oceanographic cruise until after 10 July. The work planned for this cruise included a reoccupation of the triangle of the third survey and a section across the Labrador Sea from South Wolf Island, Labrador, to Cape Farewell, Greenland. Accordingly, the *Evergreen* departed Battle Harbor, Labrador, on the evening of 11 July to begin the postseason cruise. The work of collection of data began on 13 July at station 4239 located at the offshore corner of the triangle and progressed in a counterclockwise direction around the triangle. Two sides had been completed when, in the early morning hours of 15 July, the *Evergreen* proceeded to the assistance of the steamship *Britamolene* which had gone aground in Trepassey Bay. A few hours later the *Britamolene* reported she had freed herself and was able to proceed unassisted toward St. John's whereupon *Evergreen* returned to the triangle and resumed work on the third side shortly before noon on 15 July.

One additional oceanographic station had been completed when it was necessary to interrupt the oceanographic work to search for a berg or bergs which had been reported between 46° N., and 47° N., and between 47° W., and 48° W. A berg was located the following morning. A box search around the berg, combined with an air search conducted by a PBY–5A from the Coast Guard Air Detachment at Argentia indicated that only one berg was in the immediate vicinity. The *Evergreen* continued to stand by the berg until 23 July. By then it had decreased in size to a growler small enough so that it was no longer a hazard to navigation. Advantage was taken of the period during which the *Evergreen's* movements were restricted to the vicinity of the berg to run a series of current measurements with the von Arx current meter once an hour for 25 consecutive hours as an experiment looking toward the possibility of determining tidal surface currents in the open sea with this instrument.

The *Evergreen* proceeded to Argentia to refuel, arriving there on the night of 24 July and departing on the morning of 27 July to resume oceanographic work. Because of the considerable time interval since the work was interrupted on 15 July the work done prior to that time could not be considered synoptically with observations made nearly 2 weeks later. The compromise decided upon was to begin work at the southern corner and run the southeastern side and rerun the northern side. This work began on the morning of 28 July at station 4263 and was completed on the afternoon of 30 July at station 4282.

The first station of the section across the Labrador Sea was reached off South Wolf Island on the afternoon of 31 July. Work on the section progressed without interruption until the evening of 2 August when, in the vicinity of station 4297, wind, sea, and current conditions made it prudent to heave to to await more favorable conditions. By morning of 3 August, wind and sea were both from the north-northwest and had decreased to force 6 and 5 respectively and work at the oceanographic stations was resumed. The work of collection of data was completed on the morning of 5 August at station 4306, located at 59°42′ N., 44°15′ W., and the *Evergreen* proceeded to Woods Hole, Mass., by way of Cape Race. A carboy of sea water for use as a substandard of salinity was collected on the afternoon of 5 August.

Except for a brief diversion toward Halifax on the afternoon of 9 August, when a plane in the vicinity was having engine trouble, progress was not further interrupted and Woods Hole was reached on the morning of 11 August to complete the postseason cruise.

At the 24 stations comprising the section across the Labrador Sea, the observations extended from the surface to as near bottom as was practicable and the dynamic topography was referred to the 1,500-decibar surface. At the other 283 stations occupied during the season and postseason cruises the observations extended to a depth of about 1,500 meters where the depth of water permitted and the dynamic topography was referred to the 1,000-decibar surface. An exception to the foregoing is that the 10 stations occupied in the southward extension of section W during the third survey extended to depths of about 2,500 meters to permit a better examination of the circulation past this section where the depth of the motionless surface is in the neighborhood of 2,000 meters. In general the intended depths of observation, in meters, were 0, 25, 50, 75, 100, 150, 200, 300, 400, 600, 800, 1,000 and thence by 500-meter intervals. Again the 10 stations in the southward extension of section W are an exception. At those stations the intended depths of observation were the same as given above from the surface to 1,000 meters, then 1,200, 1,600, 2,000, and 2,500 meters. Temperatures were measured with protected deep-sea reversing thermometers, most of them of Richter and Wiese manufacture but some of them by Negretti and Zambra and some by the GM Manufacturing Co. Depths of observation were based on Richter and Wiese unprotected thermometers. A program of intercomparison of thermometers was maintained by shifting the thermometers used in pairs. In all, 1,918 comparisons were considered. These gave a probable difference between the corrected readings of a pair of thermometers of 0.014° C. As most of the observed temperatures are the means of the corrected readings of such pairs, the probable error is of the order of ±0.01° C.

The collection, handling and salinity determination of water samples was the same as in previous years, with the accuracy of the salinities only that of the silver nitrate titration method used in calibration of the salinity bridge and the precision about ±0.005 ‰. The salinities have been tabulated to the nearest 0.01 ‰. No minor corrections to the salinities were required and except as noted in the discussion the dynamic topography shown in the figures is in accordance with the tabulated temperature and salinity data.

The oceanographic work was under the supervision of Oceanographer Floyd M. Soule who was assisted by Lt. Leroy A. Cheney. Other assistants in the observational work were Raymond W. Wood, boatswain's mate second class, Francis N. Brown, yeoman second class, Anthony J. Lamb, Jr., aerographer's mate third-class, Donald M. McGill, aerographer's mate third-class, and Hugh R. McCartney, Jr., aerographer's mate third-class.

Figure 16 shows the dynamic topographic chart of the sea surface resulting from the first survey. The Labrador Current is to be seen flowing southward along the eastern edge of the Grand Banks as far south as about latitude 44°15′ N., where it swings seaward to the 1,000-fathom curve before continuing along the contours of the banks as a slower but broader stream. The distribution of ice from sightings and reports during the period of this survey confirmed the pattern shown in figure 16 and indicated that many of the bergs ended their southward progress in the vicinity of the 44th parallel, being assisted by prevailing southwesterly winds in crossing the dynamic isobaths eastward into the northward moving margins of the Atlantic Current and mixed water which dominated the southeasterly part of the surveyed area. The current chart was interpreted to mean that bergs continuing in the Labrador Current southward of the 44th parallel could, with favorable winds, cross seaward into the Gulf Stream system anywhere from longitude 49° W., to 53° W. Those following the dynamic isobath of about 970.98 were considered to represent the greatest threat to steamship traffic following the United States-European tracks of the North Atlantic Track Agreement. It was in this region south of the Tail of the Banks between about longitudes 49°30′ W., and 51°00′ W., that cold mixed water extended southward beyond the limits of the survey. While the possibility of bergs attaining extra southerly positions may have been greater prior to the period of this survey, it was considered that the threat could increase again with any waning or northeasterly shift of the salient of Atlantic Current water which during this survey was pointed toward approximately 45° N., 49° W.

The dynamic topographic chart resulting from the second survey is shown in figure 17. By comparison with figure 16 it will be noted that the area southward of the Grand Banks occupied by cold mixed water had decreased somewhat, probably through the blocking effect of the Atlantic Current salient. In each of these surveys this salient had the effect of reducing the volume of Labrador Current water reaching the Tail of the Banks and diverting some of this water eastward and northeasterly north of about the 45th parallel. Although the salient had degenerated somewhat at the time of the second survey it was still effective and the western boundary of northward moving water was closer to the banks at the surface than during the first survey. The eastward diversion of Labrador Current water by the salient is considered responsible for the formation of a Labrador Current salient which carried bergs to the area east-southeasterly of 45° N., 45° W., during early May. By the time of this second survey the Labrador Current salient had been somewhat reduced from its earlier maximum southeastward extension. It was considered, however, that this area could again become one of potential hazard to the United States-European Track Agreement tracks if the Labrador Current increased in volume of flow or if it maintained its volume and the Atlantic Current salient strengthened.

The dynamic topography found during the third survey of the Grand Banks region (fourth cruise) is shown in figure 18. Here Atlantic Current water was again pressing in toward the edge of the

Grand Banks at about latitude 44° N., and reducing the amount of Labrador Current water south of that latitude. The Grand Banks eddy was present in this survey. The Labrador Current entered the northern part of the surveyed area in greater quantity than in the first two surveys and a major portion of it was diverted eastward north of about the 44th parallel. Probably the southward progress of the Labrador Current was even more completely blocked in the vicinity of 44° N., 49° W., than has been shown in figure 18. It is also probable that the dynamic topography is not as simple as that indicated and that a closed eddy existed in the vicinity of 45° N., 47° W., with the bulk of the Labrador Current water moving more directly eastward south of the eddy. The clue to these surmises is held in the characteristics of the subsurface water in this area where cold water with temperatures as low as $-1.5°$ C was found at the unusually far eastward location of station 4225.

Section W, the north-south section near the 50th meridian, was extended south to the 38th parallel to get additional data on the complete Atlantic Current in this sector of the North Atlantic eddy. While it is known that the 1,000-decibar surface is not sufficiently deep for use as a motionless surface beneath the Atlantic Current, the dynamic heights of the surface at the stations comprising section W are referred to the 1,000-decibar surface here in order that the pattern of the general circulation in this part of the survey may be presented in the same illustration with the rest of the survey. Section W will be treated in greater detail in a later part of the discussion.

In earlier bulletins of this series the volume of flow, mean temperature and minimum observed temperature of the Labrador Current passing certain sections in the Grand Banks region have been reported upon. The location of these sections, T, U, and W are as follows: section T extending southeasterly from about 46°20′ N., 49°00′ W.; section U extending eastward across the eastern edge of the Grand Banks at about the 45th parallel; and section W extending southward across southern edge of the Grand Banks at about the 50th meridian.

Section T usually gives the total Labrador Current entering the area east of the Grand Banks and south of the 47th parallel and carrying all of the bergs which may endanger shipping following routes southward of and including track E. Section U usually gives this total Labrador Current plus a large part of the Grand Banks eddy minus any of the Labrador Current which has recurved northeastward between sections T and U. The loss of Labrador Current water recurving between these sections is ordinarily small so that the volume at section U is usually larger than that at section T. Section W is not as definitely characterized as the other sections since there is ordinarily a major loss of Labrador Current water through recurving and mixing, and the westward flowing water at this section may include indeterminate amounts of the Grand Banks eddy and may be contributed to by mixed water recirculating in closed counterclockwise eddies between the remnants of the Labrador Current and the outer margins of the North Atlantic eddy.

Although there have been about 30 occupations of each of these sections beginning with the 1934 season, the great variations from year to year have made it difficult to derive any sort of normal seasonal variation. Provisional normals based on simple straight line relationships were determined in 1948 from plots of all data then available and are repeated here with volume of flow expressed in units of 1 million cubic meters per second and mean temperature expressed in degrees centigrade. The values apply at a date of 15 May, the middle of the 4-month season through which the rates of change are applicable.

	Volume of flow	Mean temperature
Section T	3.43 decreasing 0.67 per month	2.22 increasing 0.10 per month.
Section U	5.40 decreasing 0.56 per month	2.15 increasing 0.14 per month.
Section W	3.61 decreasing 0.26 per month	2.62 increasing 0.16 per month.

The measurements of volume of flow, mean temperature and minimum observed temperature resulting from all vailable occupations of these sections are presented in the following table.

In table 1 as well as in the following discussion, volume of flow is expressed in millions of cubic meters per second, and mean temperature and minimum observed temperature in degrees centigrade. The table shows the very considerable variations from year to year and the time gaps in the observations. It will be seen that a mean line drawn through plotted points of all observations for any section will overemphasize some years. For each section the greatest number of occupations covering the greatest number of years occurred during the month from 16 April to 15 May. Where a section was occupied more than once during the month in any one year the mean value resulting from such occupations was taken as the value for that year. Giving each year equal weight, means were then taken for each of the sections for the month 16 April to 15 May and plotted against the corresponding mean date as one point on the normal curves of volume of flow and mean temperature shown in figure 19.

Table 1

	16 Mar. to 15 Apr.			16 Apr. to 15 May			16 May to 15 June			16 June to 15 July		
	Volume	Mean temperature	Minimum temperature	Volume	Mean temperature	Minimum temperature	Volume	Mean temperature	Minimum temperature	Volume	Mean temperature	Minimum temperature
Section T:												
1934				1.8	1.53	−1.66	1.5	2.6	−1.72	1.5	3.3	−1.70
1935				2.1	1.67	−1.71						
				4.1	2.85	−1.56	2.71	2.06	−1.50			
1936	1.86	0.98	−0.75	3.23	1.83	−0.43	3.15	2.90	−1.47			
1937				3.53	1.83	−1.49	1.96	1.55	−1.22	1.88	2.19	−1.25
1938				6.70	4.26	−1.79	3.88	1.85	−1.67	4.30	1.74	−1.62
1939	5.71	2.12	−1.65	4.55	0.74	−1.68				2.62	1.44	−1.53
1940	3.70	2.47	−0.32	4.96	2.63	−0.19	3.52	2.24	−1.26			
							5.82	2.89	−0.55			
							3.83	2.80	−1.42			
1941	5.78	2.77	−0.65				3.31	3.13	−0.95	3.92	3.29	−0.73
1948							1.19	1.63	−1.48			
1949				3.40	1.55	−1.16						
				1.67	1.76	−1.24						
1950				1.38	−0.80	−1.77				3.20	1.48	−1.74
				2.79	0.28	−1.78						
Section U:												
1934				3.48	1.11	−1.37	3.11	1.56	−1.70	0.84	1.32	−1.65
1935	3.7	2.0	−1.66	5.92	0.98	−1.24	4.46	1.75	−1.28			
1936	7.20	2.31	−0.82	6.69	1.06	−0.94	3.90	3.14	−1.23			
1937	3.54	1.54	−1.29	5.80	1.90	−1.56	2.29	1.72	−1.29	3.02	1.81	−1.41
1938	5.62	2.16	−1.20	6.34	5.66	−0.71	5.14	3.80	−1.43	4.78	1.87	−1.64
1939	9.01	1.31	−1.51	7.15	1.60	−1.55				7.74	1.64	−1.61
1940	7.43	2.17	−0.24	3.34	2.25	−0.52	7.19	2.21	−0.74			
							6.88	3.01	−0.35			
							7.30	2.83	−0.62			
1941	6.99	2.54	−0.55				8.36	3.04	−0.60	8.62	3.52	−0.04
1948							3.47	2.31	−1.39			
1949				2.87	2.85	−1.31						
				2.19	1.75	−0.71						
1950	4.34	0.50	−1.76	1.50	1.46	−1.55				4.00	1.73	−1.60
Section W:												
1934				1.17	1.19	−1.15	1.63	1.07	−1.58	0.86	4.35	1.68
1935	1.08	2.72	−1.12				3.87	1.47	−1.02			
1936				3.13	2.61	0.02						
				8.78	2.85	0.08						
1937	0.54	0.66	−0.29	5.48	2.33	−0.99				3.40	2.53	−0.76
1938	5.44	3.78	−0.83	5.78	4.75	0.39	2.76	3.73	1.18	5.07	2.42	−1.59
1939	7.43	1.76	−1.59	3.81	1.59	−1.52	5.93	1.82	−1.62	2.26	1.82	−1.49
1940	6.13	2.52	0.26	6.85	2.81	−0.03						
1941				4.31	3.11	0.15				4.78	3.34	0.39
				5.34	3.19	0.01						
1948	0.32	3.18	−0.15	0.44	5.25	−0.91						
1949	2.83	2.43	0.48				2.19	4.58	−0.64			
1950	4.25	1.71	−1.64	2.81	1.36	−1.45	2.58	4.69	0.69			

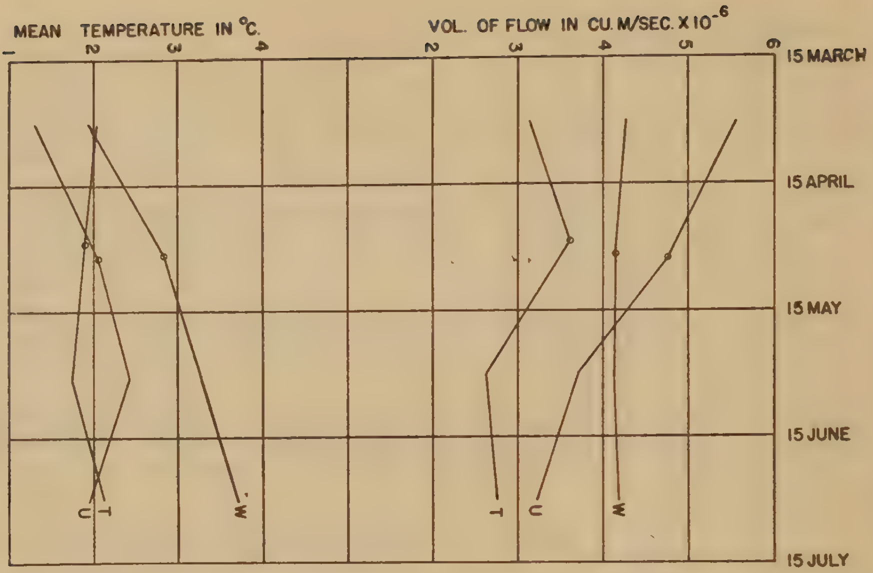

Figure 19.—Normal seasonal variation in volume of flow and mean temperature of the Labrador Current at sections T, U, and W. Curves are provisional and most reliable point on each curve is encircled.

The normal curves were then extended in each direction by mean monthly rates of change. Each year in which a section was occupied during two successive months gave a monthly rate of change for that month for that year. The mean monthly rates of change were determined by giving each year equal weight. It is considered that the normal curves thus derived are nearer the true normals than the 1948 normals for the month centered around 1 May and are equally as good for other parts of the season. Similar computations were made for minimum observed temperature but are not shown in figure 19 as a normal minimum observed temperature is considered of doubtful significance.

It is expected that additional data from future occupations of these sections will require changes in the normal curves given here but that the changes will be least in that part of the season near 1 May. Thus the computed normal values of volume of flow past sections T and U are as follows:

	1 Apr.	1 May	1 June	1 July
Section U	5.58	4.85	3.70	3.24
Section T	3.12	3.64	2.70	2.85
Difference	2.46	1.21	1.00	0.39

If the difference in volume of flow at sections T and U is taken as the volume of flow of the Grand Banks eddy we find a volume that is decreasing throughout the ice season. Such a conclusion would eliminate differential vernal warming of the shoaler water over the banks as a major driving force for the eddy. By itself this would be acceptable but the value of about 2.5 for the volume of flow on 1 April is suspiciously high since the approximately 25-mile stretch along section U from the usual location of the innermost station to the edge of the true Labrador Current, assuming a thickness of 100 meters, would need to have an average velocity of about 1 knot. The rate of change for 1 April to 1 May is based on 7 years for section U but is based on only 3 years for section T. It seems reasonable to conclude, therefore, that the 1 April normal for section T is larger than shown above. No safe conclusion can be drawn from the foregoing regarding the relative importance of differential vernal warming and other possible causes in maintaining the Grand Banks eddy.

From table 1 it will be seen that the Labrador Current was colder, both from the standpoint of mean temperature and minimum observed temperature, in 1950 than is usual. It will also be noted that its volume at sections T and U were subnormal during the first two surveys. This is attributed to the almost total absence of Irminger Current water found off Cape Farewell in the summer of 1949. In comparison with the normals shown in figure 19 the three surveys showed the following departures, plus signs indicating higher than normal and minus signs lower than normal:

	First survey		Second survey		Third survey	
	Volume	Mean temperature	Volume	Mean temperature	Volume	Mean temperature
Section T	−1.07	−2.70	−0.51	−1.50	+0.40	−0.46
Section U	−0.89	−1.15	−3.00	−0.66	+0.56	−0.39
Section W	+0.05	−0.53	−1.31	−1.46	−1.57	+1.31

Keeping in mind the composition of the apparent Labrador Current passing these sections in the Grand Banks region the results at section T are seen to indicate a progressive strengthening of the Labrador Current throughout the period covered by the three surveys. The decreasing negative temperature anomaly at that section seems to indicate that the strengthening current was the result of a restoration of the warmer off-shore component usually contributed by the West Greenland Current.

The circulation patterns shown in figures 16, 17, and 18 show the Grand Banks eddy to have been missing from section U during the first two surveys. In the first survey this was more than compensated for by the presence of a vigorous recirculation of mixed water in a counterclockwise eddy between the Labrador Current and the margins of the North Atlantic Current. The larger deficiency at section U during the second survey was the result of the Atlantic Current salient turning back a considerable portion of the Labrador Current north of section U and reducing the amount of recirculating mixed water at both sections U and W. During the third survey the situation at section W was very little changed but section U contained more of the recirculating mixed water and was further augmented by the establishment of the Grand Banks eddy.

As in previous years the course of the outer boundary of North Atlantic Current water, based on a criterion of 34.95 ‰ salinity corresponding to a temperature of 6° C, was estimated for each of the three surveys. The area between the boundary and reference rhumb lines [2] was measured for each survey.

Adjustment of these areas was made by the subtraction of 10,000 square kilometers for each million cubic meters per second volume of flow past section U.

For the 8-year period 1934–41 a relationship, reported in Bulletin No. 31 of this series, was found to exist between the differential changes in sea level, Charleston-Bermuda, and the adjusted area in the Grand Banks region 13½ months later. From this relationship the adjusted areas predicted by tide gage readings in 1949 were computed and compared with the actual areas as follows (unit of area 10,000 square kilometers):

	Area	Adjusted area	Predicted adjusted area
First survey	6. 61	2. 28	4. 43
Second survey	5. 33	3. 83	2. 83
Third survey	6. 65	2. 65	−0. 45

The disagreement between the adjusted area and the predicted adjusted area for the first survey is not as bad as it would appear from the tabulated figures when it is remembered that the adjustment for the volume of flow at section U is intended to take into consideration the water of the Labrador Current and Grand Banks eddy entering the area from the north and that while the Grand Banks eddy was very small at the time of this survey a considerable volume of recirculating mixed water was included in the volume of flow past section U. If the volume of true Labrador Current water passing section U is taken as that at section T a Grand Banks eddy contribution to section U of 0.8 would be required to make the adjusted area equal to the predicted adjusted area.

---

[2] The 45th parallel from the boundary to 49° W., the 49th meridian thence to 43° N., and a rhumb line from 43° N., 49° W., through 42° N., 47° W., extended to the boundary.

The adjusted area and predicted adjusted area for the second survey differ by 1.0 which is probably close to the amount by which the Grand Banks eddy was below normal during this survey. The discrepancy existing during the third survey is not the result of an abnormal situation at section U and may possibly arise from the pronounced meander of the Atlantic Current to the right. If, as suggested by Haurwitz and Panofski,[3] such meanders are the results of unstable waves, the effect of very large meanders on the boundary in this area would not be forecast by the sea level differences along the Charleston-Bermuda section.

The temperature distribution found during the June survey along section W and its southward extension is shown in figure 20. The low temperatures over the shelf, which in this case is the Grand Banks, and adjacent to the slope identify the remnants of the Labrador Current and the mixed water respectively. Seaward of the mixed water, beginning at about station 4183, lies the eastward moving water of the North Atlantic eddy. The dip of the isotherms downward and to the right is indicative of the swift easterly current. In Ice Patrol parlance the cold wall is the steep horizontal temperature gradient at the sea surface which appears immediately to the right of station 4183. Some students of the Gulf Stream sector of the North Atlantic eddy define the cold wall as being indicated by the descent of the isotherm of 65° F (18.3° C) to a depth of 800 feet (244 meters) or more. Figure 20 shows this to have occurred between stations 4176 and 4177. Reference to figure 18 suggests an extensive meander of the Atlantic Current southward to the vicinity of latitude 39° N., and a subsequent return of at least a part of the current to a latitude greater than 41° N. It will be seen, therefore, that the temperature profile presented in figure 20 is not entirely a profile across the Atlantic Current but for a considerable part of its length is a section along the current. There is also evidence of another and probably smaller meander of the Atlantic Current to the right southeastward of station 4199.

Measurements made in 1937 in the area eastward of the Grand Banks have been interpreted[4] to indicate that the depth of the motionless surface beneath the Atlantic Current in this region is about 2,000 or 2,500 meters. The conclusion was based on considerations of patterns of flow, bottom temperatures, a volume transport balance, temperature-salinity correlations, and a deep water isentropic analysis. Using the *Meteor* results, Hidaka[5] computed the depth of the motionless surface in the Atlantic from 20° N. to 30° S., assuming

---

[3] Haurwitz, B., and H. A. Panofski "Stability and Meandering of the Gulf Stream" Trans. Amer. Geophys. Union. vol. 31, No. 5, pp. 723–731 (October 1950) Washington.

[4] Soule, Floyd M., "Consideration of the depth of the motionless surface near the Grand Banks of Newfoundland," Jl. Marine Res. vol. II, No. 3, pp. 169–180 (January 1940), New Haven.

[5] Hidaka, Koji, "Depth of motionless layer as inferred from the distribution of salinity in the ocean." Trans. Amer. Geophys. Union vol. 30, No. 3, pp. 346–348 (June 1949), Washington.

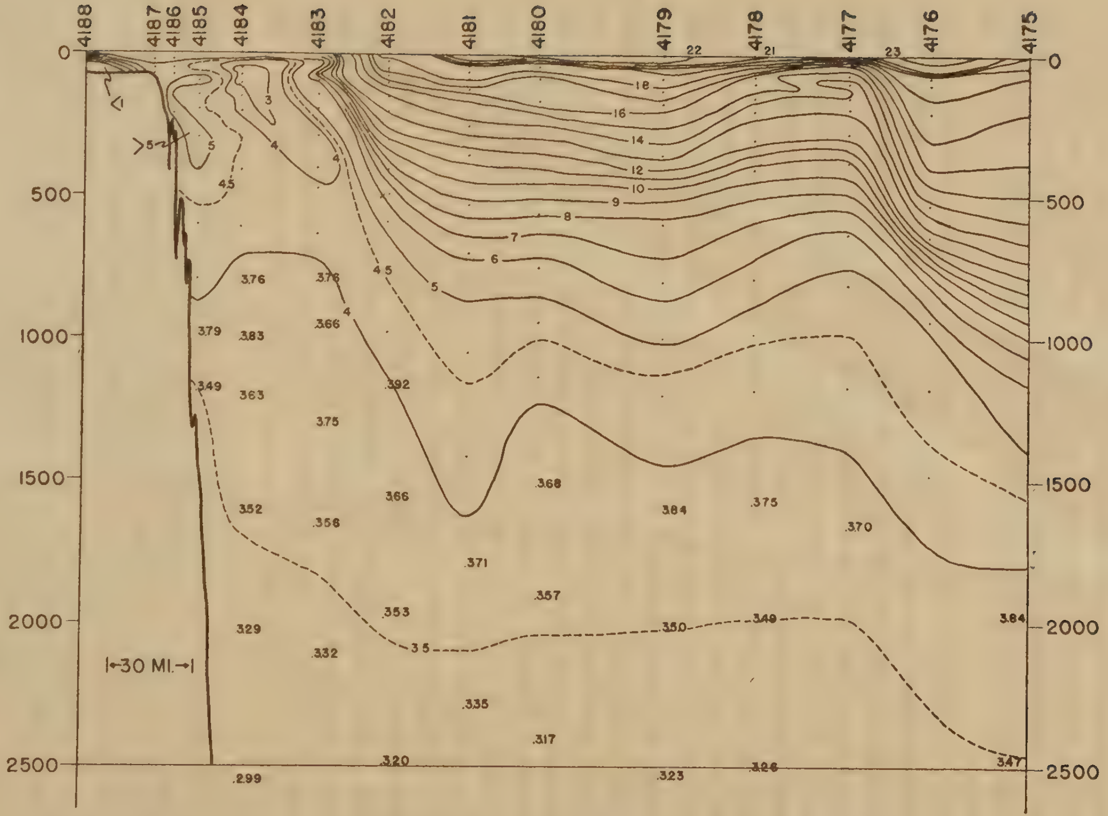

FIGURE 20.—Temperature distribution along section W extended to latitude 38° N., 9–12 June 1950.

that the actual distribution of salinity is the result of diffusion of salts in the water and that vertical mixing predominates over horizontal mixing, whence he deduced that the second derivative of salinity with respect to depth is equal to zero at the level of no motion. He concluded that in the area investigated the depth of the motionless surface varied between 900 and 1,400 meters, and that in the northern part of the area it was between 1,000 and 1,100 meters with indications that it sank to deeper levels north of 20° N.

Since the condition that the second derivative of salinity with respect to depth is equal to zero occurs at points of inflection on a vertical distribution curve of salinity, the curves for the stations taken eastward of the Grand Banks in 1937 were inspected for such points of inflection. However, in the levels which might reasonably be expected to contain a motionless surface, the salinity gradients are so small that the method is not sufficiently sensitive and usually more than one point of inflection was found.

From currents deduced from dead reckoning and ship positions from Loran fixes, von Arx and others have determined proportionality factors for the von Arx current meter when it is operated in the currents of the North Atlantic eddy. As the current meter indications are dependent on shear, or vertical gradient of velocity, the proportionality factors so derived can be used to deduce the depth to which appreciable shear extends and hence the depths of a motionless surface. Depths determined in this manner turn out to be somewhat in excess of 1,500 meters.

In consideration of the foregoing, 2,000 decibars has been selected as the reference surface for the construction of a velocity profile along section W which in the June survey was extended southward to latitude 38° N., and probably comes close to completely crossing the eastward flowing part of the North Atlantic eddy in this longitude. This profile is shown in figure 21. The section shows a volume of flow of 68.4 million cubic meters per second, a mean temperature of 13.39° C and a resulting heat transport of 915.7 million cubic meter °C per second eastward. While the section did not completely cross the eastward flowing water it seems very nearly to have done so and an estimate has been made that an additional 3.5 million cubic meters per second move eastward just south of the section shown in figure 21.

The temperature-salinity relationships of the water masses found in the Grand Banks region have been reported upon in earlier bulletins of this series. As might be expected, the Labrador Current water and the Atlantic Current water have been found to have the uniformity of T–S relationship characteristic of water masses. Usually the mixed water from these water masses has been distinguished by a degree of uniformity which has led to its consideration as a virtual water mass. Surface fluctuations produce departures from the characteristic

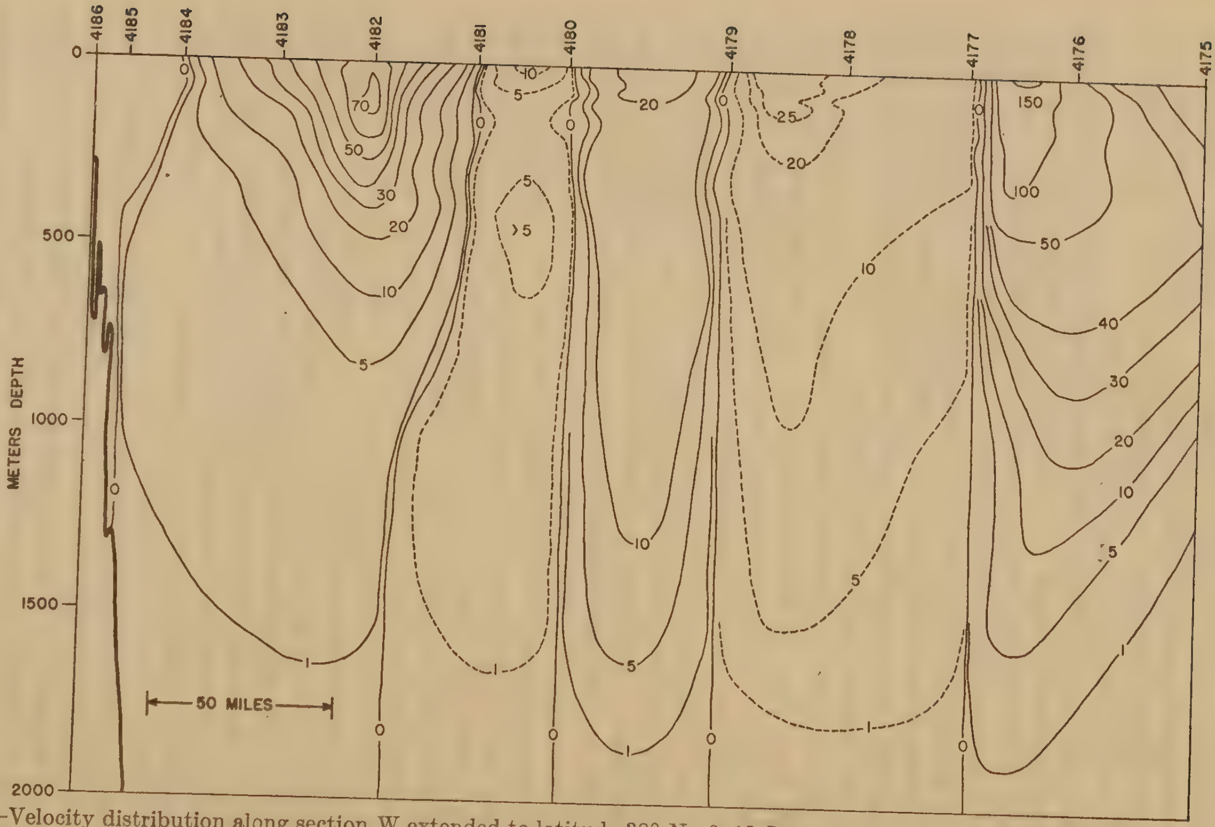

FIGURE 21.—Velocity distribution along section W extended to latitude 38° N., 9–12 June 1950. Easterly flow is shown by solid lines and westerly flow by broken lines. Dynamic heights have been referred to 2,000 decibars.

T-S curves in depths less than about 50 meters in the Labrador Current water, 75 meters in the mixed water, and somewhat deeper levels in the Atlantic Current water. In addition there are occasional stations where the upper levels of the station belong to one water mass and the lower levels to another water mass. However, the occasions when the measurements at a station have shown a mixture of water from the parent water masses in other than the proportions characteristic of the mixed water have been infrequent.

The most extensive series of measurements of this region covers the seasons of 1934 to 1941 inclusive. While this 8-year series does not qualify for the establishment of normals, mean values for the 8 years have been used for reference in the absence of better tentative normals. In figure 22 temperature-salinity relationships are given for the Labrador Current water, the Atlantic Current water, and the mixed water. The curves for 1950 are shown as solid lines and the 8-year means for the period 1934–41 are shown as broken lines. An inspection of the figure shows the curve for Labrador Current water to be displaced toward the cold side from the mean. The curve for mixed water is seen to be displaced toward the fresh side from the mean and the curve for Atlantic Current water seems to be rotated with respect to the mean, being displaced toward the salty side in upper levels and toward the fresh side at lower levels.

The deficiency in the West Greenland Current component of the Labrador Current and the almost total absence of Irminger Current water from the West Greenland Current at Cape Farewell in 1949 is considered to be an important source of the change in the Labrador Current. As the Labrador Current is an important contributor in the formation of the mixed water this cause was operative in bringing about the shift in characteristics of the mixed water. Other causes, however, must be sought for the changes in the Atlantic Current water.

Level for level, at all levels, the density of each of the three water masses was less in 1950 than for the 8-year mean. Neglecting the surface layers, the average decrease amounted to about 0.05 in σ_t from 100 to 1,000 meters in the Labrador Current water and the mixed water, and about 0.08 from 400 to 1,000 meters in the Atlantic Current water. We have here an illustration of the fact that as between temperature and salinity, the former is the controlling factor in the Atlantic Current whereas the latter is the controlling factor in the Labrador Current. Although the temperatures in the Labrador Current water were subnormal the decrease in salinities was great enough to produce a decrease in density at all levels. In the Atlantic Current water, while the salinities were higher than average in the upper layers the increased average temperatures produced a decrease in density at all levels. In the mixed water the temperatures were lower in the upper levels and higher in the lower levels than is usual; but the

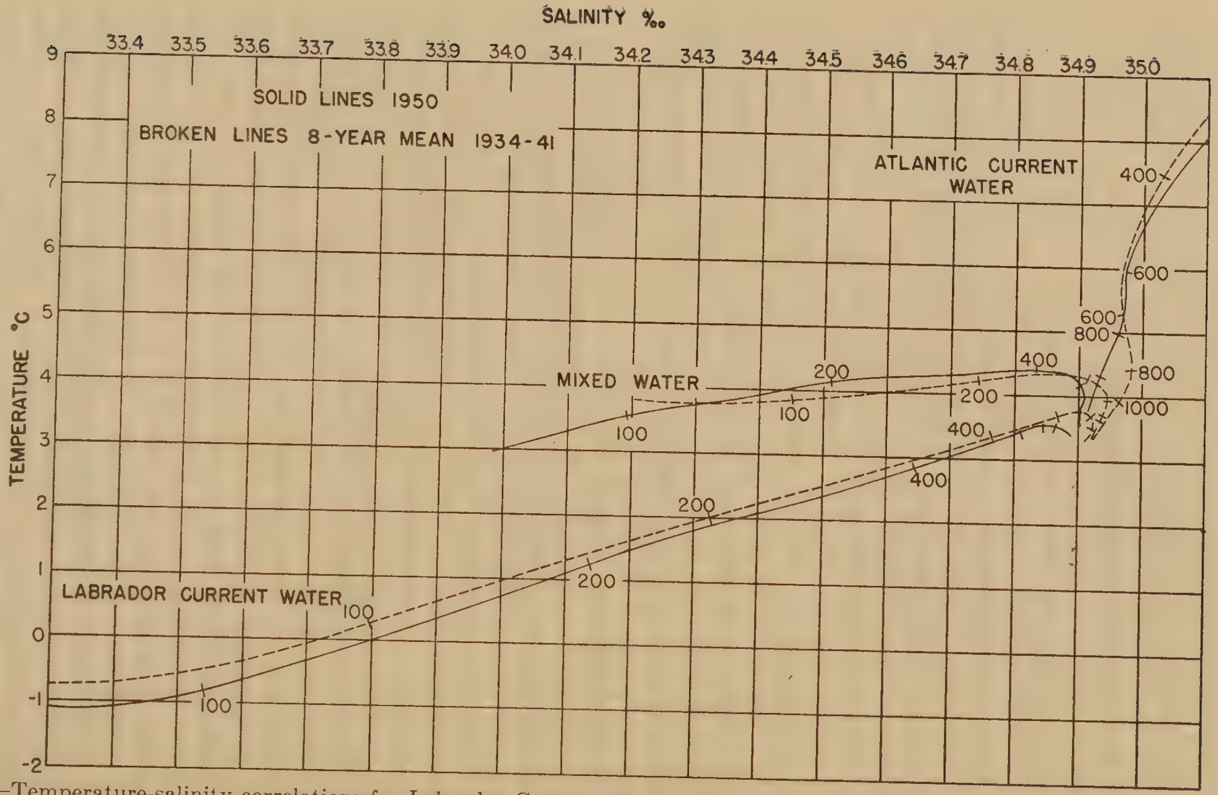

FIGURE 22.—Temperature-salinity correlations for Labrador Current water, Atlantic Current water, and mixed water found in the Grand Banks region. Solid lines show conditions during the 1950 season and broken lines represent the 8-year mean for the period 1934–41. An approximate depth scale in meters is given.

decreased salinities at all levels produced a decrease in density at all levels.

In the area just to the north of the Grand Banks the Labrador Current divides into a usually minor western branch which flows southward along the Avalon Peninsula and an eastern branch which is that part of the Labrador Current which follows the eastern slope of the Grand Banks. As opportunity permits, data are being collected which will teach us more about the behavior of the Labrador Current in the vicinity of this branch point. Three sections disposed to form the sides of a triangle which includes the branch point form the basis for such study as it has so far received. The triangle is defined by its corners which are located at Cape Bonavista, 49°23′N., 50°00′ W.; and 50°00′ N., 49°00′ W. Earlier surveys of the triangle were made once in 1948 and twice in 1949. In 1950 it was occupied once during the period 27–30 May and partially in the period 13–15 July when the northern and southwestern sections were occupied, and on 28–30 July when the southeastern and northern sections were occupied.

One of the questions which have been considered was whether the surface current pattern in the vicinity of the triangle is sufficiently representative of the currents in the upper 150 or 200 meters to permit the movement of a deep draft berg to be deduced from the dynamic topography of the surface. The measurements which have so far been made show a good similarity of pattern in these levels. Figures 23 and 24 show respectively the dynamic topography at the sea surface and at the 100-decibar surface relative to the 1000-decibar surface.

A second question of practical importance, and one which will require more study, deals with the rapidity with which the current pattern in this vicinity may change. Probably some change took place between the beginning and end of the survey on which figures 23 and 24 are based. The dynamic heights of all of the stations except those in the northeastern part of the triangle are referred to deep water by integration of the product of depth and anomaly of specific volume along bottom beneath the sections. In this case the dynamic heights of the shallow water stations may be arrived at by two approaches. Using these two approaches the dynamic heights do not agree and the triangle fails to close by about 52 dynamic millimeters when the vertical sections of anomaly of specific volume are reasonably constructed. One is faced by the choice of introducing extreme gradients of anomaly of specific volume which are not supported by the observed temperatures and salinities, or the assumption that changes took place during the survey. The latter has been chosen as the more probable.

Assuming that changes took place during the survey there is a further question as to whether the change was gradual enough to cover the whole time of the survey or whether the change was much more rapid. Figure 23 has been constructed assuming a gradual change and the error in closure of the triangle distributed amongst the shallow water stations according to distance assuming the distance to be proportional to time. Figure 24 has been constructed assuming the change took place rapidly from one steady state to another and occurred between the occupation of stations 4147 and 4148. Thus the similarity in current pattern at the two levels is really better than indicated by the two figures.

The interval between stations 4147 and 4148 has been selected as that during which the rapid change took place, because of the unusual behavior of the von Arx current meter during this interval. It recorded very swift currents, banded but uniformly east-southeasterly in direction, with a maximum speed of the order of 5 knots. Using the recorded currents, the integral of the elemental products of current and distance between stations 4147 and 4148, expressed as an equivalent difference in dynamic height between the two stations, amounted to about 33 dynamic centimeters. It is evident from the magnitudes involved that, if the current meter were not in the midst of some aberration, we were not dealing with a steady state but with a transient condition which probably included a periodic movement (such as a tidal current) combined with a sizable change from one steady state to another. The transition between two steady states involves accelerations whereas the formulae developed from the Bjerknes circulation theorem deal only with steady states in which the accelerations are negligible.

It would seem from these measurements that changes in the current pattern do take place in this region and that significant changes in dynamic height may occur in an interval of less than 3 days and possibly in as short a time as a few hours. It is also suggested that very swift currents, such as were recorded by the von Arx current meter, may be produced locally in the readjustment which takes place in the change from one steady state to another. As to the possible causes of such a change, it has been noted that for several days prior to this survey the winds had been steadily from the northeast quadrant. More detailed comment would lead at once to pure conjecture.

Returning to the speculation that the change from one steady state to another steady state took place rapidly and most of it occurred between the occupation of stations 4147 and 4148, the dynamic height originally computed would then be valid for all stations except 4145 through 4147 and the dynamic topography would then indicate that nearly all the bergs passing Cape Bonavista would be carried into the eastern branch of the Labrador Current and only those passing the 49th parallel west of about 52°25′ W., would strand on the northern edge of the Grand Banks or follow the western branch along the Avalon Peninsula. The subsequent drift of late season bergs lends some support to this interpretation of the measurements made during the interval of 27–30 May.

Building further on this line of reasoning, the volume of flow of the total Labrador Current would be that passing the northern section of the triangle, 3.47; that of the western branch would be given by the southwestern section, 0.29; and that of the eastern branch would be given by the difference, 3.18. Thus, about 92 percent of the total would have been following the eastern branch.

In the partial occupation of the triangle during 13–15 July the volume of flow past the northern section was computed to be 2.79 after subtraction of an eddy of 0.42 at the offshore end of the section. The volume of flow past the southwestern section was computed to be 0.46 leaving 2.33 by difference as that part of Labrador Current in the eastern branch or 84 percent of the total. From the topography an estimate of doubtful accuracy is made that bergs passing the 49th parallel eastward of about 52°30′ W., would have followed the eastern branch and that those passing the 49th parallel westward of about 52°45′ W., would have followed the western branch, with those passing at intermediate longitudes stranding on the northern edge of the Grand Banks.

In the second partial occupation of the triangle during 28–30 July the inshore part of the northern section shows some northerly moving water possibly indicating an eddy at the mouth of Bonavista Bay. Apparently all of the Labrador Current passing the northern section also passes the southeastern section in the eastern branch with none of it feeding the western branch. The computed volumes of flow past the northern and southeastern sections were 3.11 and 3.26 respectively. While this is taken to mean that 100 percent of the Labrador Current reaching the triangle followed the eastern branch, there are some indications that inshore bergs getting south of the latitude of Cape Bonavista would have grounded on the northern edge of the Grand Banks.

In each of the two partial occupations of the triangle there are some areas of disagreement as to the direction of the surface currents as deduced from the dynamic topography and as indicated by the von Arx current meter. This is to be expected in an area where tidal currents are known to exist. Also, in each of these partial triangles the current pattern given by the dynamic topography at the 100-decibar surface is in general agreement with that at the sea surface. The experience gained in 1950 makes it plain that reliable conclusions regarding the behavior of the Labrador Current in the vicinity of this branch point cannot be based on the occupation of only two sides of the triangle.

The difference of only about 10 percent in the total Labrador Current reaching the triangle during the two partial occupations is not remarkable. The difference between this approximately 3 million cubic meters per second and the much greater volume of flow found off South Wolf Island in early August, however, should be noted.

As mentioned previously, the interval of time separating the two partial occupations of the triangle was taken up by standing by a berg until it melted. A series of current measurements was undertaken in the immediate vicinity of the berg to determine, if possible, whether or not the von Arx current meter might have an application in the determination of tidal currents in the open ocean. As it was expected that any tidal current present would have its major component related in period to a lunar day, it was decided to make hourly current measurements for 25 consecutive hours. These measurements were begun at 1745 (45th meridian time) on 16 July at which time the berg was located at 45°27′ N., 47°57′ W., just inside the 1,000-fathom curve. The measurement scheduled for 2245 on 16 July was omitted to permit the greatest freedom in maneuvering the *Evergreen* because of the presence of other ships in the vicinity. The

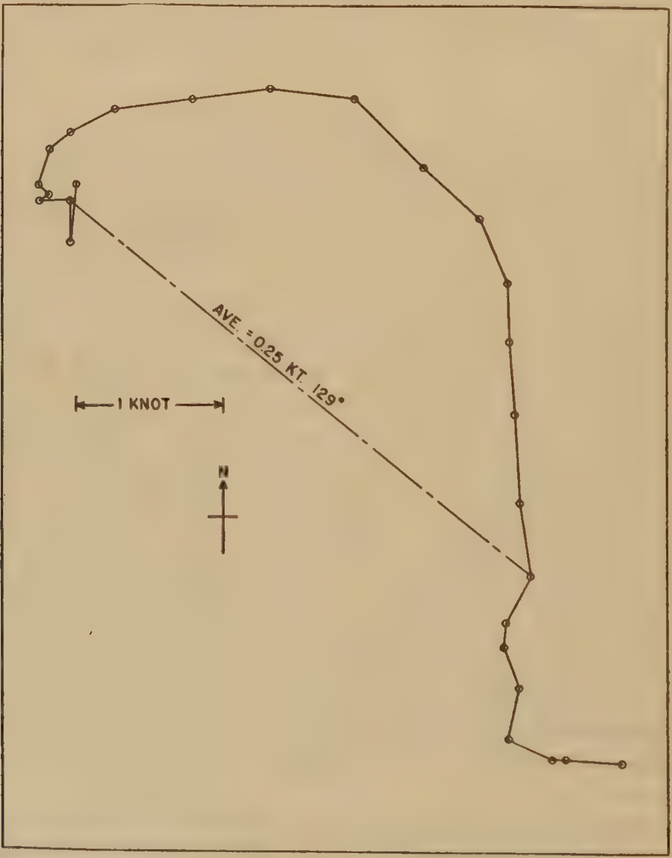

FIGURE 25.—Successive addition of velocity vectors measured hourly from 2345 on 16 July to 2345 on 17 July 1950. Average velocity has been taken for the 16-hour period beginning at 0145 on 17 July (45th meridian time has been used).

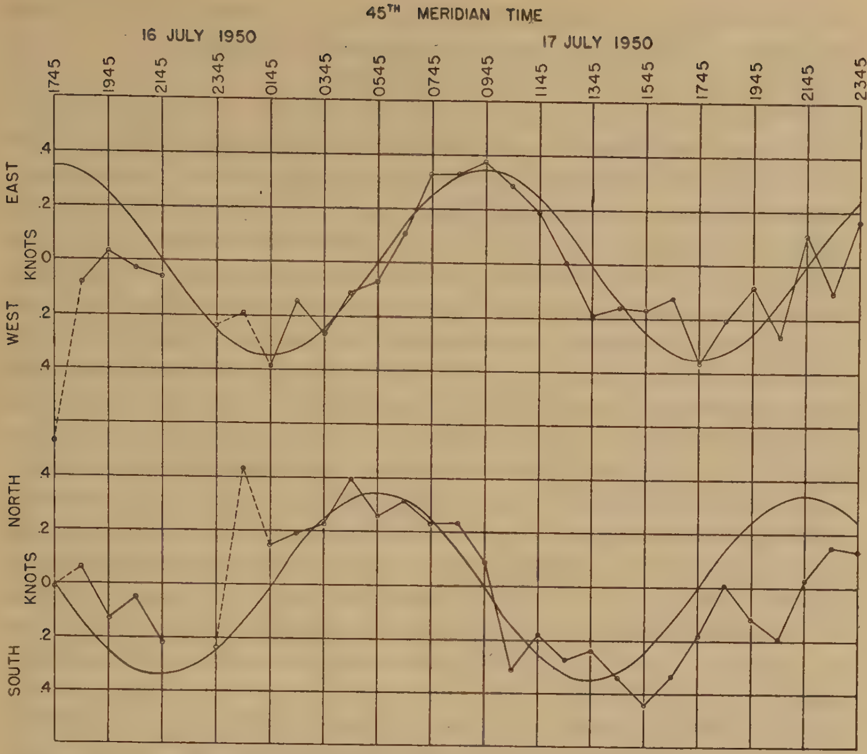

FIGURE 26.—East-west and north-south components of current vectors after elimination of average current of 0.25 knots 129°. Smooth curves, shown for comparison, are those representing a circular current of 0.35 knot amplitude and 16-hour period.

current measurements were resumed at 2345 and continued through 2345 on 17 July. The resulting series of 25 hourly velocities were then added vectorially and a first approximation of the average current determined graphically.

This average current vector was then subtracted from each of the individual current vectors to give the vectors representing the fluctuating currents. The fluctuating current vectors were then broken into their east-west and north-south components the magnitudes of which were then plotted against time. As this plot showed that the period of the principal constituent was of the order of 16 hours instead of 25 hours a new average current vector was determined using the 16 hours beginning with 0145 on 17 July. This point was selected to exclude the measurements of 1745 on 16 July and 0045 on 17 July which were considered doubtful since there were indications that the electrodes had not reached equilibrium with their surroundings at the time of the measurements. Figure 25 shows the vector sum of the hourly velocities from 2345 on 16 July to 2345 on 17 July and the determination of the average current for the 16 hours beginning at 0145 on 17 July. The rectangular components of the fluctuating currents were again determined, this time for all observations, and are shown by small circles in figure 26.

It would seem from figure 26 that the surface current did have a fluctuating component that was about one-third of a knot, approximately circular and had a period of about 16 hours. The difference between 16 lunar hours and 16 solar hours (about 32 minutes) is too small to distinguish in this series of observations considering their short duration, scatter of the plotted points, and the fact that individual measurements are not considered to be better than 0.05 knot. If the periodic current is tidal one should expect to find its constituents related to the constituents of the tides in period, although not necessarily following the same ratio of amplitudes. Amongst the many tidal constituents considered by the United States Coast and Geodetic Survey [6] in predicting tides one which is well down the list in importance as a tidal constituent, the M_3 tide, is related to periods of 8 lunar hours and might conceivably form the basis of this observed current period of 16 hours. The connection seems unsatisfactorily remote. For the convenience of those who may wish to use these data in connection with other studies of tidal currents it is noted here that a new moon occurred on 15 July and that the local civil time of its upper transit on 17 July was 1412.

It has been suggested that the periodic current may be an inertia current with its period that of a half pendulum day. For latitude 45°27′ the half pendulum day would amount to 16.84 hours. This would be close enough to be indistinguishable from the observed period.

A rough check on the surface currents as measured by the current meter is possible by comparison with the positions of the berg if it is assumed that the berg's motion was the same as the surface current. These positions were determined by celestial or Loran methods or combinations of the two as available. Beginning at the position for 1745 on 16 July the berg was 2.1 miles 105° from the position projected by the current measurements at 0800 on 17 July. Interpolating between the positions for 0800 on 17 July and 0800 on 18 July, the berg was 7.5 miles 108° from the position projected by the current measurements at the end of the series of measurements at 2345 on 17 July. After 0930 on 22 July the berg was reported as a growler and because of its shallow draft might have been more directly affected by wind after that time. Between 1745 on 16 July and 0930 on 22 July the drift of the berg averaged 0.37 knot in a direction 114° whereas the average current deduced from the current meter observations was 0.25 knot 129°. This left a berg movement, unaccounted for by the surface current, of 0.14 knot 087°. This may be regarded as being made up of the discrepancy between the surface current and the average current from the surface to the draft of the berg, and the direct wind effect on the berg. (Winds were light and principally from the southwest quadrant.)

---

[6] Schureman, Paul, "Manual of harmonic analysis and prediction of tides." U. S. Coast and Geodetic Survey Special Pub. No. 98, 1940 edition (1941), Washington.

One of the proposed uses of the von Arx current meter is the location of a berg by the patrol cutter by searching down stream as indicated by the current meter when the search can begin at a reported previous position of the berg within a few days of the report. If rotary currents are present in the area the "down stream" indication of the current meter will not be in the direction of the average current. If the amplitude of the rotary current is small in comparison with the average current the search path will approximate a direct approach to the berg along a geostrophic current line. However, as the amplitude of the rotary current approaches the magnitude of the average current the search path will become less direct and will be cycloidal in the limiting case where the amplitude of the rotary current equals the magnitude of the average current. With proportionately greater rotary currents the search method becomes inefficient and would break down but for the practical consideration that it is expected that the amplitudes of actual rotary currents are small and if the average current is less than the rotary current the berg will not have moved far from its reported position.

The temperature distribution along the vertical section from South Wolf Island, Labrador, to Cape Farewell, Greenland, found during the postseason cruise is shown in figure 27. At the left-hand side of the figure the frigid inshore part of the Labrador Current with its characteristic temperature minimum is to be seen over the shelf. The warmer offshore part of the Labrador Current extends farther seaward of the slope than is usual. The tongue of warmer water which extends to bottom beneath the Labrador Current at the edge of the shelf is shown between the isotherms of 3.8° C and reached maximum values of about 3.9°. This is regarded as a return to normal from the colder temperatures of 1949. On the Greenland side the temperature maximum usually associated with the Irminger Current component of the West Greenland current, while nearly 1° warmer than in 1949, was still subnormal and less than 6° C. The temperature minimum which is characteristic of the intermediate water of the Labrador Sea in summer is seen to have been present in its characteristic shape and extent and to have returned to the temperatures found so consistently during the summers of 1934–39. The minimum of about 3.17° C found during those years and in 1950 is about 0.15° colder than in 1949.

The salinity distribution found in the northeastern half of this section is shown in figure 28. In 1949 the Irminger Current component of the West Greenland current was almost completely absent. The salinity maximum associated with this water is normally about 35.04‰ and, until 1949, had been remarkably constant. In 1949 the maximum dropped to 34.97‰ and in 1950 it was very nearly as

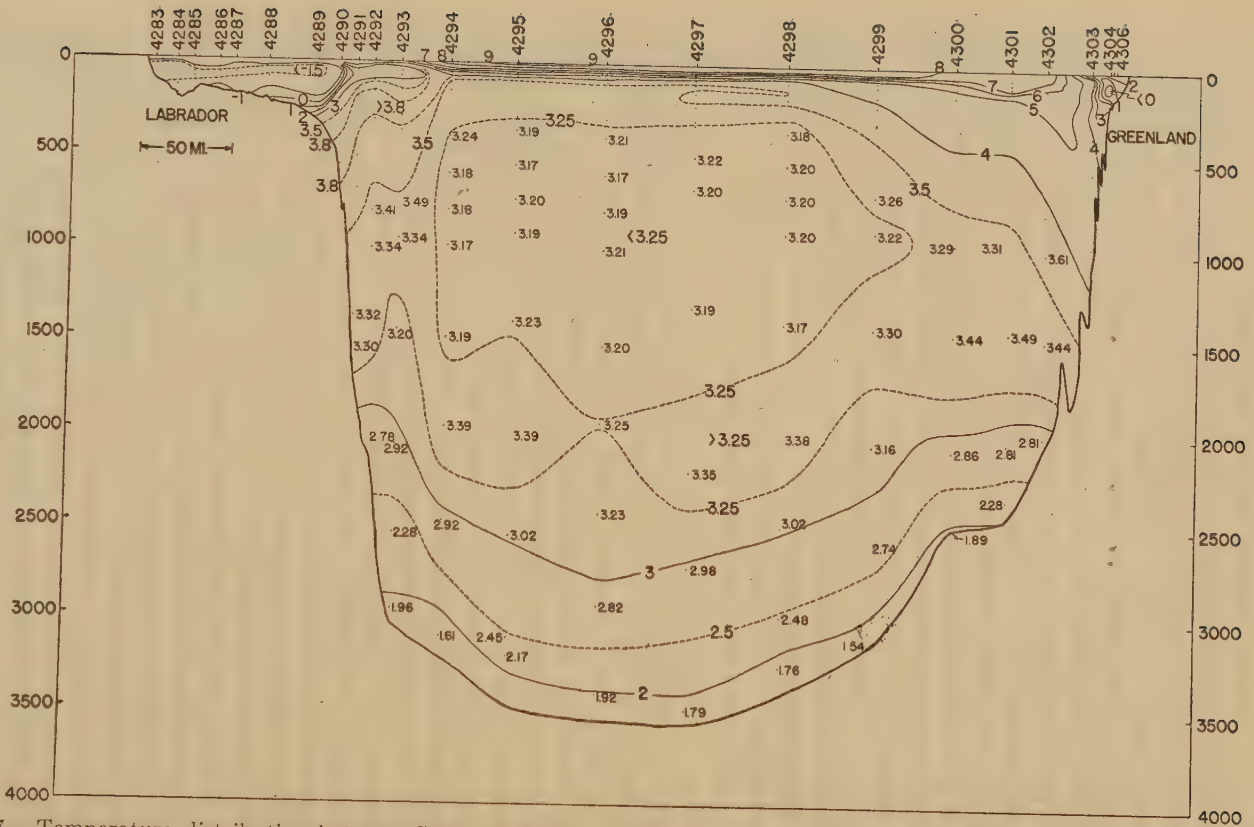

FIGURE 27.—Temperature distribution between South Wolf Island, Labrador, and Cape Farewell, Greenland, 31 July–5 August 1950.

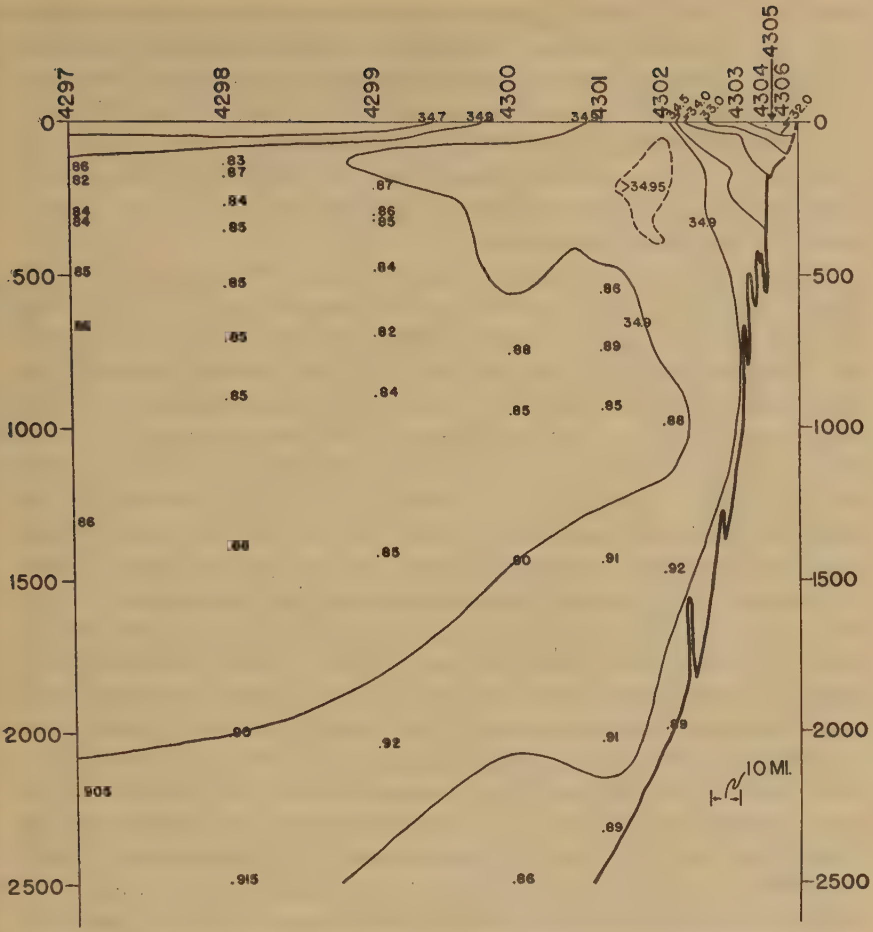

FIGURE 28.—Salinity distribution off Cape Farewell, Greenland, 3–5 August 1950.

low, being 34.99‰. As seen from figure 28, the cross sectional area in which the salinity exceeded 34.95‰ was small. Although in 1949 the drop in temperature which accompanied the drop in salinity was sufficient to increase the density by about 0.10 in σ_t, in 1950 the densities were about normal.

The dynamic topography of the sea surface in the immediate vicinity of the section from South Wolf Island to Cape Farewell is shown in figure 29. The general features of circulation in the vicinity of this section which are characteristically present are to be found here with fewer complications of pattern than is usual. The eddy or meander that is associated with the shoal off Hamilton Inlet, the Labrador Current, the counterclockwise circulation in the central part of the Labrador Sea, and the west Greenland Current off Cape Farewell all are present. Graphical and numerical examination of the volumes of flow and heat transport across this section on the Labrador side gives 5.92 million cubic meters per second and a mean temperature of 2.63° C for the Labrador Current with an additional 2.96 million cubic meters per second in the central eddy of the Labrador Sea. On the Greenland side the total northwesterly moving volume of flow is 9.20 of which at least 1.44 is definitely a part of the central eddy. The remaining 7.76 with a mean temperature of 4.26° C probably constitutes the effective West Greenland Current although about 1.5 of it has the central eddy as its source.

In Bulletin 35 of this series approximate normal seasonal variation curves were derived for the volume of flow of the two components which usually make up the West Greenland Current at Cape Farewell, the East Greenland Current and the Irminger Current, assuming constant mean temperatures of 3.2° C and 5.5° C, respectively, for these components. If the volume of flow and the mean temperature of the effective West Greenland Current found in 1950 are taken as 7.76 and 4.26 the breakdown into volume of flow of the two components, using the same assumed mean temperatures, gives 4.18 for the East Greenland Current component and 3.58 for the Irminger Current component. From the preceding paragraph, however, it would seem that about 1.5 on the off-shore side of the 7.76 is contributed directly from the central eddy of the Labrador Sea. We also note that from the difference between the flow of the Labrador Current past the South Wolf Island section and the northern section of the triangle about 2.92 million cubic meters per second recurve to the eastward before reaching the triangle and, with some admixture of water from the outer margins of the Atlantic Current, probably contribute to the West Greenland Current without making the journey to Iceland. Thus about 1.5 plus 2.92 or 4.42 should be deducted from the 7.76 of the effective West Greenland Current before considering the remainder as being composed of Irminger Current water and East Greenland Current water. This would leave only 3.34 as being derived from these sources.

An examination of the velocity and temperature profiles shows that the inshore 3.34 million cubic meters per second extend out to and just beyond the axis of maximum velocities and have a mean temperature of about 3.3° C. Thus by computation again, on the assumption of constant mean temperatures of 3.2° and 5.5° for the East Greenland Current and Irminger Current components, 3.2 is derived for the volume of the former and 0.14 for the latter. The conclusion is that the contribution from the Irminger Current to the West Greenland Current again was very small in 1950 although compensating mechanisms bringing in other water from the North Atlantic eddy produced a mean temperature of the West Greenland Current which was close to normal. The volumes of flow expressed in millions of cubic meters per second, the mean temperatures in degrees centigrade, and the heat transport in millions of cubic meter degrees centigrade per second are tabulated below for the Labrador Current off South Wolf Island, Labrador, and for the West Greenland Current off Cape Farewell, Greenland, for all available occupations of these sections.

	Labrador Current South Wolf Island			West Greenland Current Cape Farewell		
	Volume	Mean Temperature	Heat transport	Volume	Mean Temperature	Heat transport
1928 May	----	----	----	4.0	4.1	16.4
1928 July	5.1	3.3	16.5	----	----	----
1928 September	----	----	----	4.4	5.5	24.1
1931	1.3	1.7	2.2	3.7	5.3	19.5
1933	7.60	3.41	25.90	5.76	4.19	24.13
1934	5.03	2.68	13.50	2.91	5.1	14.86
1935 March	----	----	----	7.5	4.0	30.0
1935 August	4.22	2.76	11.65	8.50	4.99	42.44
1936	3.32	1.27	4.22	6.37	4.05	25.83
1938	4.20	2.92	12.25	5.43	4.69	25.04
1939	4.56	2.69	12.27	6.31	4.19	26.46
1940	2.75	1.52	4.17	----	----	----
1941	2.32	2.60	6.03	6.46	4.87	31.46
1948	3.01	2.21	6.65	1.52	3.93	5.97
1949	5.16	2.3	11.87	2.52	3.62	9.12
1950	5.92	2.63	15.57	7.76	4.26	33.06

From comparison of the results of the measurements made in 1950 with those of earlier occupations it is seen that the circulation in the Labrador Sea was abnormally active in 1950. The abnormal activity was not confined to the Labrador Sea, since the estimate of the volume of flow of the East Greenland Current contribution to the West Greenland Current of 3.2 is more than three times the seasonal normal for early August. While the mean temperatures of both the Labrador Current off South Wolf Island and the West Greenland Current off Cape Farewell were close to average values, the unusually vigorous circulation resulted in outstandingly large rates of heat transport both in the Labrador Current and in the West Greenland Current.

In 1948 an aerial ice census was made in Baffin Bay with the bergs being counted by direct visual observation. Another such census was made in 1949 and in this census the bergs again were counted by direct visual observation and also were photographed and the number of bergs determined from the photographs. In the areas of great concentrations of bergs and where the bergs were in the vicinity of bays and fjords the photographs indicated that many bergs were missed in direct visual observation. In areas away from land and where concentrations were not as great, however, the direct visual count was in good agreement with the photographic count. It was hoped that additional censuses could be made in succeeding years so that a series of at least three successive annual censuses would be available for the study of the number of years which elapse from the summer a berg is calved in northwest Greenland to the summer it appears in the Grand Banks region, and for the study of mortality rates during the different phases of this journey. No census could be made in 1950 and so our series consists of the two censuses taken in the summers of 1948 and 1949.

The distribution of bergs found has been shown in charts appearing in the bulletins of this series reporting the work of those years. While two censuses are inadequate to fix the travel time there is some evidence that it is 3 years. If we assume a 3-year travel time, and and divide Baffin Bay into areas A, B, and C being guided by the distribution found and by what is known of the circulation in Baffin Bay; then the bergs found in area A may be assumed to represent those calved the year of the census, those found in area B those calved 1 year before the census, and those found in area C those calved 2 years before the census and to appear in the Grand Banks region the year following the census. Such a division has been made to define area A as easterly of a series of rhumb lines drawn from 66° N., 56° W., to 70° N., 56° W., to 70° N., 60° W., to 71° N., 60° W., to 71° N., 62° W., to 72° N., 62° W., to 72° N., 64° W., to 74° N., 64° W., to 74° N., 70° W., to 75° N., 70° W., to 75° N., 66° W., and thence north to the Greenland coast; area B as northwesterly of this boundary and a series of rhumb lines beginning at 72°N., 64° W., and continuing to 72° N., 66° W., to 71° N., 66° W., to 71° N., 68° W., and thence south to the coast of Baffin Island; and area C as southerly of areas A and B and bounded on the south by the 66th parallel.

Since the visual and photographic counts made in 1949 of the bergs in area A were 14,206 and 33,962 the visual count of bergs in this area in 1948 was adjusted by a factor of 2.4. Visual and photographic counts of the bergs in area B in 1949 were 2,788 and 4,933 giving a factor of 1.8 for the adjustment of the visual count of bergs in area B in 1948. As there was agreement between the two counts of the bergs in area C in 1949, the visual count of bergs in this area in 1948 was not adjusted. The resulting numbers of bergs are tabulated below:

Area	1948		1949	
	Visual	Adjusted	Visual	Adjusted
A	9, 691	23, 258	14, 206	33, 962
B	1, 490	2, 682	2, 788	4, 933
C	947	947	1, 391	1, 337

If the bergs appearing in the Grand Banks region 1 year were in area C the previous summer and in area B 2 years earlier and in area A 3 years earlier, then during the interval between 1948 and 1949 the survival rates were:

$$\text{A to B}=\frac{4933}{23258}=21.2\%$$

$$\text{B to C}=\frac{1337}{2682}=49.9\%$$

$$\left.\begin{array}{r} \text{C to Grand Banks}=\frac{47}{947}=5.0\% \\ \text{and 1949 to 1950 C to Grand Banks}=\frac{462}{1337}=34.6\% \end{array}\right\}\text{mean } 19.8\%$$

The over-all survival rate would be their product or 2.1 percent (97.9 percent mortality). On this basis it might be expected that the number of bergs appearing south of 48° N., would be 487 in 1951 and 713 in 1952. It is probable that these survival rates are not normal. From a preceding table the volume of flow and heat transport of the West Greenland Current past Cape Farewell was seen to have been exceptionally small in 1948 and 1949, and exceptionally large in 1950. Thus the censuses of 1948 and 1949 are not well adapted to the determination of normal survival rates although they might be ideal in combination with other data in estimating the importance of the effect of such factors as the heat transport of the West Greenland Current on survival rates.

The survival rate for the part of the journey from area B to area C is the largest of the three. However, it is suspected that this figure of 49.9 percent is too low. Areas B and C are located in the coldest part of Baffin Bay and roughly coincide with that region in which Smith [7] has indicated that no melting takes place.

The survival rates from A to B and that from C to the Grand Banks, being small, indicate that the factors affecting the disintegration of bergs in these two parts of the journey are important. The large difference in the survival rate from C to the Grand Banks during the year 1948–49 as compared with the year 1949–50 indicates that the effective factors in this part of the journey are not only important but variable. The number of bergs calved in any year is of course a basic starting point. As seen from the difference of about 10,000 between the adjusted count for 1948 and the photographic count for 1949, application of the survival rate of 2.1 percent would mean a variation of some 210 bergs in the numbers reaching south of the 48th parallel in two successive years if the conditions affecting the mortality of these particular crops are the same. Thus an important factor in any forecast of the number of bergs which will reach the Grand Banks region is the departure from average of the number of bergs calved.

The mortality during the part of the journey from area A to area B is seen to be large but since we have but one value for this survival rate nothing is known as to its variability and the importance, therefore, of departures from average conditions. Possibly this may be affected by the changes in the rate at which water-borne heat is supplied to Baffin Bay and may be deduced from the heat transport of the West Greenland Current passing Cape Farewell the summer the bergs are calved.

---

[7] Smith, Edward H. "The *Marion* expedition to Davis Strait and Baffin Bay, Arctic Ice," U. S. Coast Guard Bull. No. 19, pt. 3, fig. 121, p. 200 (1931), Washington.

The important factor of mortality occurring along the Labrador Coast (evidenced by the small and variable survival rates from C to the Grand Banks) probably is related to stranding and melting. Stranding can be attacked through examination of the departure from normal of the barometric pressure gradients producing onshore winds. Melting can be attacked through examination of the departure from normal of the barometric pressure gradients producing offshore winds and through a study of water-borne heat supplied to the Labrador Current by the West Greenland Current in the northern part of the Labrador Sea. This latter may be deduced from the heat transport of the West Greenland Current passing Cape Farewell the summer before the bergs reach the Grand Banks region.

Any forecast formulae which are based on transportation facilities alone, such as the methods developed by Smith [8] in 1926 and by Schell [9] in 1950, must remain rough approximations until modified to include the four factors discussed above, namely, the departure from average of the number of bergs calved from the glacier, the departure from average mortality in the journey from area A to area B, the departure from average of the number of bergs stranding along the Labrador coast and the departure from average melting during that part of the journey. Mensurable possible indices of some of these factors exist but they have been measured an insufficient number of times to permit evaluation of the relative importance of the different factors, or even the validity of the supposed indices. A more detailed treatment of them is deferred pending the accumulation of additional data.

SUMMARY

1. The circulation in the Grand Banks region has been discussed on the basis of dynamic topographic charts resulting from three surveys of the area made during the 1950 ice season.

2. The volume of flow and mean temperature of the Labrador Current at three selected sections in the Grand Banks region has been determined for each of the three surveys made in 1950 and discussed with respect to the results of earlier occupations of these sections. Tentative normal seasonal variation curves have been presented for volume of flow and mean temperature of the Labrador Current at each of the three sections.

3. The location of the northern boundary of Atlantic Current water found during the three surveys made in 1950 has been discussed with respect to the strength of the Labrador Current as measured and the

---

[8] Smith, Edward H. "The *Marion* expedition to Davis Strait and Baffin Bay, Arctic Ice." U. S. Coast Guard Bull. No. 19, pt. 3, pp. 180–189 (1931), Washington.

[9] Schell, I. I. "On foreshadowing the severity of the iceberg season south of Newfoundland." Unpublished paper read before the Thirty-first Annual Meeting of the Section of Oceanography of the American Geophysical Union, May 1950.

strength of the Atlantic Current as inferred from changes in the difference in sea level across the Gulf Stream at the Charleston-Bermuda section.

4. The mean temperature and volume of flow of the Atlantic Current south of the Grand Banks has been deduced from section W extended southward to the 38th parallel.

5. The temperature-salinity relationships for the three water masses found in the Grand Banks region in 1950 have been compared with conditions found in earlier years.

6. One complete and two partial triangular surveys of the area immediately north of the Grand Banks have been discussed with respect to stability of current pattern, volume of flow, and the division of the Labrador Current into its eastern and western branches.

7. A series of hourly current measurements made in the open sea with a von Arx geomagnetic electrokinetograph and showing a rotary current of about 16-hour period has been presented.

8. The thermal characteristics of the intermediate water of the Labrador Sea found in 1950 have been compared with earlier measurements and a return to the conditions which existed prior to 1940 noted.

9. The continued deficiency of the Irminger Current component of the West Greenland Current as deduced from salinity observations has been noted with supporting evidence inferred from volumes of flow and mean temperatures of the West Greenland Current passing Cape Farewell and the Labrador Current passing South Wolf Island. Exceptionally active circulation in the Labrador Sea and in the East Greenland Current has been deduced from these measurements.

10. The aerial ice censuses of Baffin Bay made in 1948 and 1949 have been discussed with respect to partial and total survival rates of bergs in their journey from northwest Greenland to the Grand Banks region and with respect to indication of important factors in berg mortality.

The data collected during the 1950 season and postseason cruises are tabulated below. The individual station headings give the station number, date, geographical position, depth of water, and the dynamic height of the sea surface used in the construction of the dynamic topographic charts shown in figures 16, 17, 18, and 23 for which the dynamic heights have been referred to the 1,000-decibar surface and figure 29 for which the dynamic heights have been referred to the 1,500-decibar surface. The depths of water are uncorrected sonic soundings based on a sounding velocity of 800 fathoms per second. Where depths of the scaled values are enclosed in parentheses the data are based on extrapolated vertical distribution curves of temperature or salinity or both. Asterisks appearing before observed temperatures indicate that these temperatures were determined from the depth of reversal and the corrected reading of an unprotected thermometer. The symbol σ_t signifies 1,000 (density−1) at atmospheric pressure and temperature t.

STATIONS OCCUPIED IN 1950

Station 4000; Apr. 6; latitude 43°35′ N., longitude 51°27′ W., depth 80 meters; dynamic height 971.157

Observed Values			Scaled Values			
Depth, meters	Temperature ° C.	Salinity ‰	Depth, meters	Temperature ° C.	Salinity ‰	σ_t
0	2.45	32.71	0	2.45	32.71	26.12
23	2.00	32.74	25	2.00	32.74	26.19
47	1.94	32.76	50	1.80	32.76	26.21
70	0.75	33.00	75	0.50	33.03	26.51

Station 4001; Apr. 6; latitude 43°33′ N., longitude 51°44′ W., depth 161 meters, dynamic height 971.131

Observed Values			Scaled Values			
Depth, meters	Temperature ° C.	Salinity ‰	Depth, meters	Temperature ° C.	Salinity ‰	σ_t
0	1.36	32.97	0	1.36	32.97	26.41
23	0.85	32.98	25	0.80	32.98	26.46
45	−0.09	33.14	50	−0.25	33.17	26.66
68	−0.79	33.26	75	−0.95	33.26	26.76
91	−1.15	33.27	100	−1.15	33.29	26.79
136	−0.87	33.42	(150)	−0.45	33.48	26.92

Station 4002; Apr. 6; atitude 43°30 N., longitude 51°58′ W., depth 340 meters; dynamic height 971.131

Observed Values			Scaled Values			
Depth, meters	Temperature ° C.	Salinity ‰	Depth, meters	Temperature ° C.	Salinity ‰	σ_t
0	1.51	32.88	0	1.51	32.88	26.33
20	0.70	33.06	25	0.45	33.10	26.57
41	−0.34	33.20	50	−0.60	33.20	26.70
61	−0.91	33.21	75	−1.15	33.25	26.76
82	−1.26	33.27	100	−1.40	33.29	26.79
123	−1.37	33.30	150	−1.15	33.38	26.87
163	−0.98	33.44	200	0.50	33.68	27.03
245	2.42	33.98	(300)	3.20	34.20	27.25

Station 4003; Apr. 7; latitude 43°25′ N., longitude 51°49′ W., depth 333 meters, dynamic height 971.147

Observed Values			Scaled Values			
Depth, meters	Temperature ° C.	Salinity ‰	Depth, meters	Temperature ° C.	Salinity ‰	σ_t
0	1.88	32.85	0	1.88	32.85	26.28
22	1.66	32.85	25	1.65	32.87	26.31
44	0.75	33.01	50	0.40	33.06	26.54
65	−0.48	33.17	75	−0.60	33.20	26.70
87	−0.66	33.24	100	−0.70	33.27	26.76
131	−0.85	33.34	150	−0.95	33.38	26.86
175	−1.04	33.45	200	−0.65	33.55	26.99
262	1.33	33.88	(300)	2.20	34.07	27.24

Station 4004; Apr. 7; latitude 43°23.5′ N., longitude 51°52′ W., depth 491 meters, dynamic height 971.147

Observed Values			Scaled Values			
Depth, meters	Temperature ° C.	Salinity ‰	Depth, meters	Temperature ° C.	Salinity ‰	σ_t
0	1.63	32.87	0	1.63	32.87	26.31
25	0.94	32.94	25	0.94	32.94	26.42
50	−0.59	33.17	50	−0.59	33.17	26.67
75	−1.04	33.25	75	−1.04	33.25	26.76
99	−1.27	33.28	100	−1.25	33.28	26.78
149	−1.08	33.40	150	−1.05	33.40	26.88
199	−0.92	33.55	200	−0.90	33.55	27.00
298	−0.04	33.79	300	0.00	33.80	27.16
344	0.87	34.00	400	1.95	34.33	27.46
557	3.86	34.78	------	------	-----	-----

Station 4005; Apr. 7; latitude 43°19′ N., longitude 51°58′ W., depth 1,079 meters; dynamic height 971.143

Observed Values			Scaled Values			
Depth, meters	Temperature ° C.	Salinity ‰	Depth, meters	Temperature ° C.	Salinity ‰	σ_t
0	2.23	32.88	0	2.23	32.88	26.28
26	−0.47	33.22	25	−0.40	33.22	26.71
52	−1.04	33.25	50	−1.00	33.25	26.76
78	−1.44	33.30	75	−1.45	33.29	26.79
104	−1.31	33.36	100	−1.35	33.35	26.84
156	−0.53	33.60	150	−0.60	33.57	27.00
208	−0.35	33.73	200	−0.35	33.71	27.10
312	−0.02	33.83	300	−0.05	33.82	27.18
397	1.47	34.20	400	1.50	34.22	27.41
594	3.11	34.63	600	3.15	34.64	27.60
792	3.69	34.80	800	3.70	34.80	27.68
997	3.66	34.86	1,000	3.65	34.86	27.73

Station 4006; Apr. 7–8; latitude 43°14′ N., longitude 52°05′ W., depth 2,012 meters, dynamic height 971.173

Observed Values			Scaled Values			
Depth, meters	Temperature ° C.	Salinity ‰	Depth, meters	Temperature ° C.	Salinity ‰	σ_t
0	1.92	32.90	0	1.92	32.90	26.31
24	0.51	33.14	25	0.50	33.15	26.60
48	−0.36	33.22	50	−0.40	33.22	26.71
72	−1.09	33.25	75	−1.15	33.25	26.76
95	−1.41	33.28	100	−1.40	33.29	26.79
144	−1.32	33.41	150	−1.25	33.43	26.91
191	−0.66	33.58	200	−0.60	33.61	27.03
286	−0.14	33.83	300	0.00	33.85	27.20
286	−0.06	33.82	400	0.80	34.00	27.27
433	1.14	34.06	600	3.40	34.70	27.63
584	3.24	34.66	800	3.95	34.84	27.68
745	3.96	34.84	1,000	3.75	34.85	27.71
1,171	3.52	34.85	---------	------	------	------

Station 4007; Apr. 8; latitude 43°04′ N., longitude 52°20′ W., depth 2,880 meters, dynamic height 971.078

Observed Values			Scaled Values			
Depth, meters	Temperature ° C.	Salinity ‰	Depth, meters	Temperature ° C.	Salinity ‰	σ_t
0	0.73	33.06	0	0.73	33.06	26.52
28	−0.68	33.18	25	−0.55	33.17	26.67
57	−1.32	33.27	50	−1.20	33.25	26.76
85	−1.44	33.30	75	−1.45	33.29	26.79
112	−1.25	33.42	100	−1.35	33.36	26.85
169	−0.81	33.62	150	−0.90	33.56	27.01
226	0.30	33.81	200	−0.25	33.72	27.11
338	6.36	34.99	300	4.30	34.62	27.48
380	6.04	34.99	400	5.85	34.98	27.57
578	4.30	34.87	600	4.20	34.87	27.69
780	3.92	34.88	800	3.90	34.88	27.72
990	3.94	34.91	1,000	3.95	34.91	27.74
1,540	3.68	34.925				

Tables of Oceanographic Data—Continued

STATIONS OCCUPIED IN 1950—Continued

Station 4008; Apr. 8; latitude 42°43′ N., longitude 52°53′ W., depth 3,704 meters, dynamic height 971.115

Observed Values			Scaled Values			
Depth, meters	Temperature ° C.	Salinity ‰	Depth, meters	Temperature ° C.	Salinity ‰	σ_t
0	4.99	33.16	0	4.99	33.16	26.24
26	4.84	33.16	25	4.85	33.16	26.25
52	4.29	33.24	50	4.30	33.23	26.37
78	4.24	33.34	75	4.25	33.43	26.53
104	5.97	34.06	100	5.75	34.04	26.84
156	3.42	34.05	150	3.65	34.05	27.09
208	3.22	34.17	200	3.20	34.15	27.21
382	3.40	34.53	300	3.30	34.36	27.37
584	4.28	34.88	400	3.45	34.57	27.52
795	3.88	34.88	600	4.30	34.88	27.68
1,006	4.14	34.955	800	3.90	34.88	27.72
1,551	3.63	34.91	1,000	4.15	34.95	27.75

Station 4009; Apr. 8; latitude 42°20′ N., longitude 52°24′ W., depth 3,749 meters, dynamic height 971.091

Observed Values			Scaled Values			
Depth, meters	Temperature ° C.	Salinity ‰	Depth, meters	Temperature ° C.	Salinity ‰	σ_t
0	4.58	33.11	0	4.59	33.11	26.24
24	3.01	33.045	25	2.90	33.04	26.36
47	1.94	33.05	50	2.00	33.16	26.52
71	6.51	34.20	75	6.80	34.26	26.88
94	7.96	34.57	100	8.15	34.67	27.01
141	9.24	35.02	150	9.00	34.97	27.12
188	5.58	34.46	200	5.55	34.48	27.21
282	5.64	34.63	300	5.40	34.63	27.35
463	2.91	34.62	400	3.80	34.63	27.53
629	4.89	34.99	600	4.65	34.95	27.70
811	4.39	34.97	800	4.45	34.97	27.74
1,313	3.75	34.93	1,000	4.10	34.95	27.76

Station 4010; Apr. 8; latitude 42°02′ N., longitude 51°58′ W., depth 3,841 meters, dynamic height 971.112

Observed Values			Scaled Values			
Depth, meters	Temperature ° C.	Salinity ‰	Depth, meters	Temperature ° C.	Salinity ‰	σ_t
0	11.23	34.71	0	11.23	34.71	26.54
21	11.08	34.74	25	11.10	34.77	26.60
41	11.86	35.13	50	12.10	35.22	26.76
62	12.38	35.27	75	12.20	35.23	26.75
83	12.00	35.11	100	11.40	35.03	26.74
124	10.55	34.96	150	9.95	34.97	26.96
165	9.62	34.98	200	7.90	34.82	27.17
248	7.40	34.81	300	4.90	34.62	27.41
230	4.56	34.36	400	4.50	34.72	27.53
390	4.50	34.71	600	5.20	34.98	27.65
578	5.22	34.98	800	4.50	34.96	27.72
739	4.68	34.97	1,000	4.10	34.94	27.75
1,166	3.88	34.93				

Station 4011; Apr. 9; latitude 42°03.5′ N., longitude 50°50′ W., depth 3,146 meters

Observed Values			Scaled Values			
Depth, meters	Temperature ° C.	Salinity ‰	Depth, meters	Temperature ° C.	Salinity ‰	σ_t
470	4.28	34.91				
689	3.62	34.865				
898	3.53	34.86				
1,126	3.55	34.88				

Station 4012; Apr. 9; latitude 42°00.5′ N., longitude 51°02′ W., depth 3,310 meters, dynamic height 970.944

Observed values			Scaled Values			
Depth, meters	Temperature ° C.	Salinity ‰	Depth, meters	Temperature ° C.	Salinity ‰	σ_t
0	1.17	33.26	0	1.17	33.26	26.66
26	0.40	33.62	25	0.40	33.60	26.98
52	2.78	33.94	50	2.65	33.93	27.08
78	3.03	34.08	75	3.05	34.06	27.15
104	1.61	34.11	100	1.75	34.10	27.29
156	1.46	34.26	150	1.45	34.24	27.42
208	2.11	34.45	200	1.95	34.42	27.54
312	2.82	34.65	300	2.75	34.63	27.63
376	3.08	34.70	400	3.15	34.72	27.67
600	3.61	34.82	600	3.61	34.82	27.71
848	3.55	34.86	800	3.55	34.86	27.74
1,033	3.49	34.85	1,000	3.50	34.85	27.74
1,449	3.60	34.88				

Station 4013; Apr. 9–10; latitude 42°17′ N., longitude 51°25′ W., depth 2,789 meters, dynamic height 970.980

Observed values			Scaled Values			
Depth, meters	Temperature ° C.	Salinity ‰	Depth, meters	Temperature ° C.	Salinity ‰	σ_t
0	1.78	33.40	0	1.78	33.40	26.74
25	2.98	33.81	25	2.98	33.81	26.96
50	2.46	33.91	50	2.46	33.91	27.08
75	2.77	34.04	75	2.77	34.04	27.16
101	4.21	34.32	100	4.20	34.31	27.24
151	4.53	34.52	150	4.50	34.52	27.37
202	1.56	34.28	200	1.55	34.29	27.45
303	2.51	34.55	300	2.50	34.54	27.58
400	2.93	34.67	400	2.93	34.67	27.65
598	3.39	34.76	600	3.40	34.71	27.64
797	3.63	34.855	800	3.65	34.85	27.72
997	3.60	34.85	1,000	3.60	34.85	27.73
1,495	3.54	34.88				

Station 4014; Apr. 10; latitude 42°38.5′ N., longitude 51°00′ W., depth 1,847 meters, dynamic height 971.036

Observed values			Scaled Values			
Depth, meters	Temperature ° C.	Salinity ‰	Depth, meters	Temperature ° C.	Salinity ‰	σ_t
0	4.77	33.78	0	4.77	33.78	26.76
24	6.47	34.17	25	6.50	34.18	26.86
49	7.72	34.57	50	7.70	34.57	27.00
73	7.17	34.51	75	7.20	34.51	27.03
98	7.42	34.61	100	7.40	34.61	27.08
147	7.42	34.67	150	7.40	34.68	27.13
196	7.39	34.85	200	7.40	34.86	27.27
294	6.68	34.955	300	6.05	34.94	27.52
327	3.39	34.50	400	3.15	34.58	27.55
491	3.09	34.69	600	3.55	34.80	27.69
655	3.75	34.84	800	3.65	34.84	27.71
833	3.59	34.84	1,000	3.55	34.84	27.72
1,305	3.52	34.835				

Station 4015; Apr. 10; latitude 42°49.5′ N., longitude 50°51′ W., depth 869 meters, dynamic height 971.138

Observed values			Scaled Values			
Depth, meters	Temperature ° C.	Salinity ‰	Depth, meters	Temperature ° C.	Salinity ‰	σ_t
0	2.66	32.79	0	2.66	32.79	26.18
25	2.54	32.79	25	2.54	32.79	26.19
49	0.26	33.04	50	0.25	33.04	26.54
74	−0.31	33.18	75	−0.35	33.18	26.67
98	−0.52	33.26	100	−0.55	33.26	26.74
146	−0.75	33.49	150	−0.70	33.52	26.97
196	1.04	33.77	200	1.10	33.78	27.07
294	0.43	33.93	300	1.35	34.03	27.26
303	2.25	34.14	400	2.35	34.40	27.48
468	2.95	34.62	600	3.50	34.79	27.69
644	3.58	34.815	800	3.55	34.81	27.70
836	3.53	34.81	1,000	3.50	34.82	27.72

STATIONS OCCUPIED IN 1950—Continued

Station 4016; Apr. 10; latitude 42°54.5′ N., longitude 50°46′ W., depth 293 meters, dynamic height 971.105

Observed values			Scaled values			
Depth, meters	Temperature ° C.	Salinity ‰	Depth, meters	Temperature ° C.	Salinity ‰	σ_t
0	2.60	32.76	0	2.60	32.76	26.15
15	1.14	32.95	25	0.00	33.07	26.57
30	−0.52	33.12	50	−1.25	33.18	26.70
45	−1.21	33.17	75	−1.45	33.24	26.76
60	−1.43	33.22	100	−1.45	33.26	26.77
118	−1.49	33.28	150	−1.35	33.37	26.86
175	−1.06	33.47	200	−0.50	33.63	27.04
230	0.28	33.83				

Station 4017; Apr. 10; latitude 43°01′ N., longitude 50°40′ W., depth 106 meters, dynamic height 971.099

Observed values			Scaled values			
Depth, meters	Temperature ° C.	Salinity ‰	Depth, meters	Temperature ° C.	Salinity ‰	σ_t
0	0.82	33.05	0	0.82	33.05	26.52
25	−0.20	33.16	25	−0.20	33.16	26.65
50	−0.81	33.22	50	−0.81	33.22	26.72
74	−1.07	33.26	75	−1.10	33.26	26.76
94	−0.10	33.27	100	−1.10	33 27	26.77

Station 4018; Apr. 10; latitude 43°04.5′ N., longitude 50°32′ W., depth 89 meters, dynamic height 971.102

Observed values			Scaled values			
Depth, meters	Temperature ° C.	Salinity ‰	Depth, meters	Temperature ° C.	Salinity ‰	σ_t
0	1.25	33.02	0	1.25	33.02	26.46
24	0.97	33.05	25	0.95	33.05	26.51
47	−0.62	33.20	50	−0.65	33.22	26.72
71	−0.98	33.28	75	−1.00	33.29	26.78

Station 4019; Apr. 10; latitude 43°21′ N., longitude 50°14′ W., depth 55 meters, dynamic height 971.116

Observed values			Scaled values			
Depth, meters	Temperature ° C.	Salinity ‰	Depth, meters	Temperature ° C.	Salinity ‰	σ_t
0	2.25	32.62	0	2.25	32.62	26.07
24	0.40	32.92	25	0.40	32.92	26.43
48	0.41	32.93	50	0.40	32.93	26.44

Station 4020; Apr. 10; latitude 43°00′ N., longitude 50°14′ W., depth 91 meters, dynamic height 971.089

Observed values			Scaled values			
Depth, meters	Temperature ° C.	Salinity ‰	Depth, meters	Temperature ° C.	Salinity ‰	σ_t
0	1.63	32.92	0	0.63	32.92	26.35
24	1.34	33.00	25	1.30	33.01	26.46
49	−0.71	33.20	50	−0.75	33.20	26.71
73	−0.98	33.24	75	−1.00	33.24	26.75

Station 4021; Apr. 10; latitude 42°47′ N., longitude 50°16′ W., depth 375 meters, dynamic height 971.070

Observed values			Scaled values			
Depth, meters	Temperature ° C.	Salinity ‰	Depth, meters	Temperature ° C.	Salinity ‰	σ_t
0	0.49	33.04	0	0.49	33.04	26.52
25	−0.63	33.10	25	−0.63	33.10	26.62
52	−1.33	33.17	50	−1.25	33.16	26.69
77	−1.64	33.30	75	−1.65	33.28	26.79
103	−1.30	33.52	100	−1.40	33.50	26.97
154	−0.03	33.80	150	−0.10	33.85	27.20
206	0.43	33.97	200	0.40	33.96	27.27
309	1.48	34.20	300	1.40	34.18	27.38

Station 4022; Apr. 11; latitude 42°40′ N., longitude 50°16′ W., depth 1,829 meters, dynamic height 971.016

Observed Values			Scaled Values			
Depth, meters	Temperature ° C.	Salinity ‰	Depth, meters	Temperature ° C.	Salinity ‰	σ_t
0	−0.52	33.08	0	−0.52	33.08	26.60
24	−0.61	33.11	25	−0.65	33.11	26.63
49	−1.58	33.21	50	−1.60	33.21	26.74
73	−1.61	33.36	75	−1.60	33.36	26.86
99	−0.72	33.62	100	−0.70	33.62	27.05
147	1.04	33.97	150	1.10	33.98	27.24
196	4.64	34.56	200	4.60	34.56	27.39
295	2.47	34.56	300	2.45	34.56	27.60
361	2.66	34.61	400	2.85	34.65	27.64
545	3.51	34.77	600	3.55	34.78	27.67
733	3.54	34.82	800	3.55	34.83	27.71
934	3.55	34.85	1,000	3.55	34.85	27.73
1,471	3.59	34.87				

Station 4023; Apr. 11; latitude 42°20′ N., longitude 50°14′ W., depth 2,770 meters, dynamic height 970.990

Observed Values			Scaled Values			
Depth, meters	Temperature ° C.	Salinity ‰	Depth, meters	Temperature ° C.	Salinity ‰	σ_t
0	−0.51	33.09	0	−0.51	33.09	26.60
27	−0.57	33.19	25	−0.55	33.18	26.68
53	−1.52	33.40	50	−1.45	33.37	26.86
80	2.28	33.92	75	1.40	33.81	27.08
106	2.79	33.98	100	2.70	33.97	27.11
160	3.30	34.29	150	3.20	34.25	27.29
213	1.53	34.21	200	1.95	34.23	27.38
319	2.99	34.61	300	2.85	34.54	27.55
405	3.71	34.78	400	3.70	34.77	27.66
609	4.41	34.97	600	4.40	34.97	27.74
816	4.06	34.93	800	4.10	34.93	27.74
1,024	3.78	34.93	1,000	3.80	34.93	27.77
1,548	3.57	34.93				

Station 4024; Apr. 11. latitude 41°57′ N., longitude 50°12′ W., depth 3,566 meters, dynamic height 970.961

Observed Values			Scaled Values			
Depth, meters	Temperature ° C.	Salinity ‰	Depth, meters	Temperature ° C.	Salinity ‰	σ_t
0	4.10	33.46	0	4.10	33.46	26.58
27	0.49	33.42	25	0.55	33.42	26.83
52	0.94	33.62	50	0.85	33.60	26.95
79	2.21	33.90	75	1.95	33.85	27.07
104	2.98	34.18	100	2.85	34.13	27.22
157	3.40	34.48	150	3.35	34.45	27.43
210	3.72	34.63	200	3.65	34.60	27.52
314	4.46	34.86	300	4.40	34.84	27.63
429	4.50	34.92	400	4.50	34.91	27.68
637	4.31	34.94	600	4.35	34.93	27.71
842	4.10	34.95	800	4.15	34.95	27.75
1,057	3.92	34.95	1,000	4.00	34.95	27.77
1,601	3.55	34.94				

Station 4025; Apr. 10; latitude 41°27′ N., longitude 50°09′ W., depth 3,741 meters, dynamic height 970.970

Observed Values			Scaled Values			
Depth, meters	Temperature ° C.	Salinity ‰	Depth, meters	Temperature ° C.	Salinity ‰	σ_t
0	3.78	33.09	0	3.78	33.09	26.30
27	0.87	33.49	25	1.05	33.44	26.81
53	1.56	33.80	50	1.40	33.67	26.97
80	2.69	34.05	75	2.65	34.02	27.16
106	1.79	34.10	100	2.05	34.09	27.26
160	1.01	34.16	150	1.05	34.14	27.37
213	2.84	34.45	200	2.40	34.38	27.46
319	3.96	34.71	300	3.85	34.67	27.56
390	4.12	34.84	400	4.15	34.85	27.67
587	4.19	34.91	600	4.15	34.91	27.72
788	3.92	34.91	800	3.90	34.91	27.75
991	3.80	34.92	1,000	3.80	34.92	27.77
1,504	3.53	34.90				

Station 4026; Apr. 11; latitude 42°04′ N., longitude 49°28′ W., depth 3,246 meters, dynamic height 970.977

Observed Values			Scaled Values			
Depth, meters	Temperature ° C.	Salinity ‰	Depth, meters	Temperature ° C.	Salinity ‰	σ_t
0	2.79	33.41	0	2.79	33.41	26.66
26	1.85	33.72	25	1.85	33.71	26.96
53	1.11	33.77	50	1.15	33.76	27.06
79	1.83	33.90	75	1.45	33.86	27.12
105	6.58	34.66	100	5.30	34.52	27.28
157	7.45	34.99	150	7.40	34.98	27.36
209	6.16	34.87	200	6.40	34.88	27.42
314	5.24	34.91	300	5.30	34.90	27.58
396	5.11	34.96	400	5.10	34.96	27.65
595	4.31	34.93	600	4.30	34.93	27.71
795	4.07	34.93	800	4.05	34.93	27.74
997	3.97	34.94	1,000	3.95	34.94	27.76
1,507	3.58	34.92				

Station 4027; Apr. 12; latitude 41°43′ N., longitude 49°01′ W., depth 2,640 meters, dynamic height 971.053

Observed Values			Scaled Values			
Depth, meters	Temperature ° C.	Salinity ‰	Depth, meters	Temperature ° C.	Salinity ‰	σ_t
0	5.88	33.31	0	5.88	33.31	26.25
21	7.26	33.82	25	7.20	33.78	26.45
43	2.66	33.38	50	2.70	33.45	26.70
65	3.87	33.77	75	5.45	34.06	26.90
87	6.76	34.43	100	6.70	34.46	27.06
129	6.52	34.50	150	6.80	34.63	27.17
172	7.17	34.76	200	5.20	34.38	27.18
259	3.48	34.50	300	6.30	34.98	27.51
197	5.34	34.38	400	4.40	34.84	27.63
286	6.55	34.99	600	4.10	34.88	27.70
369	4.62	34.85	(800)	4.05	34.92	27.74
471	4.12	34.83	(1,000)	4.00	34.92	27.75
742	4.02	34.92				

Station 4028; Apr. 12; latitude 42°14′ N., longitude 47°53′ W., depth 3,548 meters, dynamic height 971.281

Observed Values			Scaled Values			
Depth, meters	Temperature ° C.	Salinity ‰	Depth, meters	Temperature ° C.	Salinity ‰	σ_t
0	15.09	35.84	0	15.09	35.84	26.62
22	15.06	35.83	25	15.05	35.83	26.62
43	15.05	35.83	50	15.05	35.83	26.62
65	15.06	35.90	75	15.05	35.90	26.67
86	15.03	35.90	100	15.00	35.90	26.68
130	14.88	35.90	150	14.50	35.82	26.73
174	14.05	35.68	200	13.65	35.66	26.79
260	12.72	35.60	300	11.90	35.50	27.02
399	9.32	35.18	400	9.30	35.18	27.23
603	5.70	34.96	600	5.75	34.96	27.57
811	4.35	34.92	800	4.90	34.92	27.65
1,016	4.15	34.94	(1,000)	4.15	34.94	27.74
1,532	3.76	34.93				

Station 4029; Apr. 12; latitude 42°31′ N., longitude 48°24′ W., depth 2,789 meters, dynamic height 970.961

Observed Values			Scaled Values			
Depth, meters	Temperature ° C.	Salinity ‰	Depth, meters	Temperature ° C.	Salinity ‰	σ_t
0	3.93	33.51	0	3.93	33.51	26.64
27	1.20	33.71	25	1.20	33.70	27.01
53	2.38	34.00	50	2.35	33.97	27.14
80	2.00	34.07	75	2.05	34.06	27.24
106	2.02	34.14	100	2.00	34.12	27.29
160	2.19	34.31	150	2.15	34.27	27.40
213	3.01	34.53	200	2.80	34.49	27.51
319	3.12	34.66	300	3.05	34.63	27.60
393	4.42	34.89	400	4.40	34.89	27.67
592	4.39	34.95	600	4.40	34.95	27.72
794	4.16	34.95	800	4.15	34.95	27.75
			(1,000)	4.05	34.94	27.75

Station 4030; Apr. 12; latitude 42°39.5′ N., longitude 49°03′ W., depth 2,276 meters, dynamic height 970.943

Observed values			Scaled Values			
Depth, meters	Temperature ° C.	Salinity ‰	Depth, meters	Temperature ° C.	Salinity ‰	σ_t
0	2.01	33.33	0	2.01	33.33	26.66
26	0.62	33.50	25	0.65	33.50	26.88
52	1.18	33.82	50	1.20	33.81	27.10
78	1.19	33.94	75	1.20	33.92	27.19
103	5.05	34.60	100	4.50	34.53	27.38
156	6.23	34.90	150	6.20	34.88	27.45
207	4.99	34.82	200	5.10	34.82	27.54
310	4.75	34.90	300	4.75	34.89	27.63
383	4.78	34.94	400	4.75	34.94	27.67
574	3.88	34.88	600	3.85	34.88	27.72
765	3.75	34.89	800	3.70	34.89	27.75
962	3.48	34.865	1,000	3.50	34.87	27.76
1,463	3.50	34.90				

Station 4031; Apr. 13; latitude 43°18′ N., longitude 48°47′ W., depth 2,652 meters, dynamic height 970.938

Observed values			Scaled Values			
Depth, meters	Temperature ° C.	Salinity ‰	Depth, meters	Temperature ° C.	Salinity ‰	σ_t
0	−0.03	33.10	0	−0.03	33.10	26.59
26	−0.15	33.59	25	−0.15	33.56	26.98
52	3.65	34.12	50	3.65	34.07	27.11
78	3.36	34.18	75	3.40	34.17	27.21
103	3.79	34.40	100	3.70	34.58	27.34
156	4.49	34.63	150	4.45	34.61	27.45
208	4.61	34.77	200	4.60	34.76	27.55
311	4.16	34.79	300	4.20	34.79	27.62
421	4.28	34.89	400	4.30	34.87	27.67
628	4.04	34.92	600	4.05	34.92	27.74
833	3.83	34.91	800	3.85	34.91	27.75
1,042	3.71	34.91	1,000	3.75	34.91	27.76
1,562	3.46	34.90				

Station 4032; Apr. 13; latitude 43°03.5′ N., longitude 48°05′ W., depth 3,109 meters, dynamic height 970.932

Observed values			Scaled Values			
Depth, meters	Temperature ° C.	Salinity ‰	Depth, meters	Temperature ° C.	Salinity ‰	σ_t
0	4.04	33.61	0	4.04	33.61	26.70
27	2.85	33.94	25	2.85	33.73	26.90
53	3.13	34.12	50	3.10	34.09	27.17
80	2.33	34.14	75	2.50	34.13	27.25
106	2.03	34.19	100	2.05	34.17	27.33
160	4.09	34.64	150	3.65	34.55	27.48
214	5.49	94.94	200	5.25	34.92	27.61
320	4.84	34.94	300	4.95	34.94	27.65
424	4.65	34.95	400	4.70	34.95	27.69
635	4.12	34.93	600	4.25	34.93	27.72
846	3.88	34.92	800	3.95	34.92	27.75
1,057	3.53	34.88	1,000	3.60	34.89	27.76
1,581	3.51	34.92				

Station 4033; Apr. 13; latitude 42°51.5′ N., longitude 47°25′ W., depth 3,658 meters, dynamic height 971.084

Observed values			Scaled Values			
Depth, meters	Temperature ° C.	Salinity ‰	Depth, meters	Temperature ° C.	Salinity ‰	σ_t
0	13.19	35.30	0	13.19	35.30	26.61
25	13.91	35.60	25	13.91	35.60	26.69
50	13.77	35.60	50	13.77	35.60	26.72
75	13.61	35.54	75	13.61	35.54	26.71
100	13.55	35.56	100	13.55	35.56	26.73
150	12.79	35.50	150	12.79	35.50	26.85
200	11.36	35.38	200	11.36	35.38	27.02
300	8.69	35.12	300	8.69	35.12	27.28
333	7.18	34.94	400	5.45	34.99	27.63
499	4.70	34.86	600	4.60	35.01	27.75
665	4.54	34.94	800	3.95	35.00	27.81
837	3.82	34.89	1,000	3.75	34.99	27.82
1,277	3.56	34.90				

Tables of Oceanographic Data—Continued

STATIONS OCCUPIED IN 1950—Continued

Station 4034; Apr. 13; latitude 42°36′ N., longitude 46°47′ W., depth 3,749 meters, dynamic height 971.250

Observed values			Scaled values			
Depth, meters	Temperature ° C.	Salinity ‰	Depth, meters	Temperature ° C.	Salinity ‰	σ_t
0	7.93	33.60	0	7.93	33.60	26.21
23	10.03	34.41	25	10.10	34.45	26.53
46	11.36	34.91	50	11.55	35.02	26.71
69	12.82	35.38	75	12.80	35.36	26.73
92	12.32	35.28	100	12.20	35.27	26.78
137	11.93	35.26	150	11.95	35.27	26.83
183	12.10	35.30	200	11.90	35.30	26.86
275	11.02	35.31	300	10.65	35.29	27.08
390	9.23	35.17	400	9.10	35.15	27.24
588	5.15	34.87	600	5.10	34.87	27.58
788	4.86	34.98	800	4.80	34.98	27.70
987	4.38	34.96	1,000	4.35	34.96	27.74
1,488	3.63	34.90				

Station 4035; Apr. 13; latitude 43°02′ N., longitude 46°16′ W., depth 4,382 meters, dynamic height 971.289

Observed values			Scaled values			
Depth, meters	Temperature ° C.	Salinity ‰	Depth, meters	Temperature ° C.	Salinity ‰	σ_t
0	15.21	35.87	0	15.21	35.87	26.62
26	15.18	35.87	25	15.15	35.87	26.62
51	15.07	35.87	50	15.05	35.87	26.64
77	15.10	35.92	75	15.10	35.91	26.67
102	15.64	36.10	100	15.60	36.09	26.70
153	15.25	36.00	150	15.25	36.01	26.72
204	14.50	35.83	200	14.55	35.85	26.74
306	12.22	35.52	300	12.30	35.47	26.92
293	12.15	35.42	400	9.00	35.18	27.28
493	7.01	35.02	600	6.10	35.00	27.56
729	5.38	34.99	800	5.10	34.99	27.67
921	4.71	34.98	1,000	4.60	34.97	27.72
1,419	3.88	34.93				

Station 4036; Apr. 13; latitude 43°28′ N., longitude 45°45′ W., depth 4,489 meters, dynamic height 971.477

Observed values			Scaled values			
Depth, meters	Temperature ° C.	Salinity ‰	Depth, meters	Temperature ° C.	Salinity ‰	σ_t
0	15.50	36.02	0	15.50	36.02	26.67
22	15.46	36.02	25	15.45	36.02	26.67
43	15.45	36.02	50	15.40	36.02	26.69
66	15.41	36.02	75	15.35	36.01	26.69
87	15.16	35.98	100	15.25	36.00	26.71
131	15.40	36.06	150	15.45	36.07	26.71
174	15.50	36.08	200	15.55	36.09	26.71
261	15.66	36.11	300	15.45	36.09	26.73
261	15.61	36.04	400	14.15	35.95	26.91
391	------	35.98	600	9.75	35.21	27.18
522	11.61	35.50	800	6.30	35.02	27.55
652	8.57	35.10	1,000	4.95	34.98	27.68
979	5.04	34.98				

Station 4037; Apr. 14; latitude 43°44.5′ N., longitude 46°22′ W., depth 3,127 meters, dynamic height 971.245

Observed values			Scaled values			
Depth, meters	Temperature ° C.	Salinity ‰	Depth, meters	Temperature ° C.	Salinity ‰	σ_t
0	14.75	35.77	0	14.75	35.77	26.65
29	14.81	35.78	25	14.80	35.78	26.63
58	14.58	35.81	50	14.70	35.80	26.67
86	14.63	35.80	75	14.65	35.80	26.68
114	14.68	35.82	100	14.65	35.80	26.68
172	13.66	35.70	150	14.05	35.75	26.77
230	12.73	35.58	200	13.20	35.64	26.86
344	9.81	35.22	300	11.15	35.39	27.07
358	9.60	35.20	400	8.45	35.11	27.31
536	6.32	35.00	600	5.95	35.00	27.58
712	5.31	35.02	800	4.75	34.98	27.70
903	4.28	34.93	1,000	4.15	34.91	27.72
1,404	3.69	34.90				

Station 4038; Apr. 14; latitude 43°54.5′ N., longitude 47°01′ W., depth 4,024 meters, dynamic height 970.984

Observed Values			Scaled Values			
Depth, meters	Temperature ° C.	Salinity ‰	Depth, meters	Temperature ° C.	Salinity ‰	σ_t
0	4.84	33.65	0	4.84	33.65	26.65
26	0.50	33.42	25	0.50	33.42	26.83
52	0.39	33.60	50	0.35	33.59	26.97
78	1.79	33.87	75	1.50	33.84	27.10
105	2.93	34.12	100	2.70	34.08	27.19
156	4.69	34.52	150	4.55	34.48	27.33
208	4.57	34.60	200	4.55	34.59	27.42
313	4.48	34.78	300	4.45	34.75	27.56
392	4.68	34.89	400	4.70	34.89	27.64
591	4.40	34.94	600	4.35	34.94	27.72
792	4.11	34.94	800	4.10	34.94	27.75
993	3.88	34.93	1,000	3.90	34.93	27.76
1,499	3.61	34.92				

Station 4039; Apr. 14; latitude 44°04′ N., longitude 47°44′ W., depth, 3603 meters, dynamic height 970.994

Observed Values			Scaled Values			
Depth, meters	Temperature ° C.	Salinity ‰	Depth, meters	Temperature ° C.	Salinity ‰	σ_t
0	5.53	33.75	0	5.53	33.75	26.64
22	5.48	33.82	25	5.40	33.83	26.72
44	4.66	34.01	50	4.40	34.00	26.97
67	3.36	33.90	75	3.55	33.95	27.02
89	4.09	34.08	100	4.10	34.11	27.09
134	4.14	34.23	150	4.15	34.30	27.23
178	4.35	34.48	200	4.65	34.60	27.42
267	5.13	34.83	300	5.10	34.87	27.58
347	5.00	34.91	400	4.85	34.94	27.66
525	4.47	34.94	600	4.30	34.93	27.71
706	4.14	34.93	800	4.00	34.92	27.75
885	3.91	34.92	1,000	3.85	34.92	27.76
1,336	3.59	34.91				

Station 4040; Apr. 14; latitude 44°08′ N., longitude 48°18′ W., depth 2,967 meters, dynamic height 970.954

Observed Values			Scaled Values			
Depth, meters	Temperature ° C.	Salinity ‰	Depth, meters	Temperature ° C.	Salinity ‰	σ_t
0	0.30	33.15	0	0.30	33.15	26.62
25	−1.71	33.37	25	−1.71	33.37	26.87
50	1.08	33.73	50	1.08	33.73	27.03
75	3.80	34.18	75	3.80	34.18	27.17
100	2.96	34.20	100	2.96	34.20	27.27
150	4.35	34.54	150	4.35	34.54	27.40
200	5.15	34.78	200	5.15	34.78	27.50
300	4.46	34.84	300	4.46	34.84	27.63
341	4.92	34.94	400	4.85	34.96	27.68
517	4.48	34.96	600	4.15	34.93	27.73
698	3.85	34.90	800	3.80	34.90	27.75
888	3.77	34.90	1,000	3.75	34.90	27.75
1,392	3.63	34.91				

Station 4041; Apr. 15; latitude 44°03.5′ N., longitude 48°34′ W., depth 1,646 meters, dynamic height 970.974

Observed Values			Scaled Values			
Depth, meters	Temperature ° C.	Salinity ‰	Depth, meters	Temperature ° C.	Salinity ‰	σ_t
0	−0.56	33.03	0	−0.56	33.03	26.56
27	−0.78	33.12	25	−0.80	33.11	26.63
52	−0.66	33.42	50	−0.70	33.41	26.88
79	−0.26	33.66	75	−0.30	33.62	27.03
104	0.02	33.84	100	−0.05	33.81	27.17
157	2.34	34.32	150	2.15	34.27	27.40
210	2.13	34.42	200	2.15	34.41	27.51
314	2.14	34.52	300	2.15	34.50	27.58
368	2.58	34.62	400	2.80	34.67	27.66
547	3.33	34.79	600	3.40	34.80	27.71
724	3.52	34.83	800	3.55	34.85	27.73
915	3.61	34.87	1,000	3.60	34.87	27.75
1,410	2.55	34.88				

STATIONS OCCUPIED IN 1950—Continued

Station 4042; Apr. 15; latitude 44°06′ N., longitude 48°44′ W. depth 709 meters, dynamic height 971.037

Observed Values			Scaled Values			
Depth, meters	Temperature ° C.	Salinity ‰	Depth, meters	Temperature ° C.	Salinity ‰	σ_t
0	−0.60	32.98	0	−0.60	32.98	26.52
26	−0.70	33.06	25	−0.70	33.06	26.59
51	−1.70	33.17	50	−1.65	33.17	26.71
76	−1.72	33.27	75	−1.70	33.27	26.79
101	−1.62	33.33	100	−1.65	33.32	26.83
153	−0.61	33.62	150	−0.70	33.60	27.03
204	0.92	34.09	200	0.80	34.05	27.31
305	1.61	34.32	300	1.55	34.31	27.47
415	2.36	34.55	400	2.25	34.52	27.59
			(600)	3.20	34.82	27.75

Station 4043; Apr. 15; latitude 44°07.5′ N., longitude 48°56′ W. depth 182 meters, dynamic height 971.036

Observed Values			Scaled Values			
Depth, meters	Temperature ° C.	Salinity ‰	Depth, meters	Temperature ° C.	Salinity ‰	σ_t
0	−0.66	33.09	0	−0.66	33.09	26.61
26	−1.34	33.16	25	−1.30	33.16	26.69
51	−1.58	33.30	50	−1.55	33.30	26.81
78	−1.51	33.34	75	−1.50	33.34	26.85
103	−1.45	33.36	100	−1.45	33.36	26.85
155	−0.41	33.67	150	−0.55	33.64	27.05

Station 4044; Apr. 15; latitude 44°09′ N., longitude 49°04′ W., depth 95 meters, dynamic height 971.037

Observed Values			Scaled Values			
Depth, meters	Temperature ° C.	Salinity ‰	Depth, meters	Temperature ° C.	Salinity ‰	σ_t
0	−0.49	33.10	0	−0.49	33.10	26.61
27	−1.19	33.20	25	−1.15	33.19	26.71
52	−1.43	33.29	50	−1.45	33.28	26.79
79	−1.41	33.30	75	−1.40	33.30	26.80

Station 4045; Apr. 15; latitude 44°14.5′ N., longitude 49°19′ W. depth 53 meters, dynamic height 971.042

Observed Values			Scaled Values			
Depth, meters	Temperature ° C.	Salinity ‰	Depth, meters	Temperature ° C.	Salinity ‰	σ_t
0	−0.15	33.15	0	−0.15	33.15	26.64
22	−0.19	33.15	25	−0.20	33.05	26.64
38	−0.22	33.16	(50)	−0.25	33.17	26.66

Station 4046; Apr. 15; latitude 44°54.5′ N., longitude 49°23′ W. depth 140 meters, dynamic height 971.083

Observed Values			Scaled Values			
Depth, meters	Temperature ° C.	Salinity ‰	Depth, meters	Temperature ° C.	Salinity ‰	σ_t
0	−0.57	33.08	0	−0.57	33.08	26.60
24	−0.77	33.01	25	−0.80	33.11	26.63
48	−1.22	33.20	50	−1.25	33.21	26.73
72	−1.45	33.26	75	−1.45	33.27	26.78
91	−1.47	33.28	100	−1.45	33.28	26.79

Station 4047; Apr. 15; latitude 44°54′ N., longitude 40°12′ W., depth 393 meters, dynamic height 971.084

Observed Values			Scaled Values			
Depth, meters	Temperature ° C.	Salinity ‰	Depth, meters	Temperature ° C.	Salinity ‰	σ_t
0	−0.72	33.07	0	−0.72	33.07	26.60
25	−0.84	33.07	25	−0.84	33.07	26.60
50	−1.69	33.24	50	−1.69	33.24	26.77
74	−1.67	33.26	75	−1.65	33.26	26.78
99	−1.63	33.29	100	−1.65	33.29	26.80
148	−0.77	33.56	150	−0.75	33.56	27.00
198	−0.56	33.62	200	−0.55	33.62	27.04
297	0.83	34.06	300	0.85	34.08	27.33

Station 4048; Apr. 15; latitude 44°54′ N., longitude 49°06′ W., depth 1,234 meters, dynamic height 971.051

Observed values			Scaled Values			
Depth, meters	Temperature ° C.	Salinity ‰	Depth, meters	Temperature ° C.	Salinity ‰	σ_t
0	−0.65	33.06	0	−0.65	33.06	26.59
26	−0.88	33.09	25	−0.85	33.09	26.61
51	−1.68	33.24	50	−1.65	33.24	26.76
76	−1.76	33.31	75	−1.75	33.31	26.82
101	−1.56	33.41	100	−1.60	33.41	26.91
152	−0.64	33.61	150	−0.65	33.61	27.04
203	0.11	33.80	200	0.05	33.79	27.15
304	1.39	34.27	300	1.35	34.25	27.44
409	2.67	34.64	400	2.60	34.62	27.64
614	3.29	34.79	600	3.25	34.78	27.70
820	3.47	34.83	800	3.45	34.83	27.72
1,028	3.48	34.85	1,000	3.50	34.85	27.74
1,340	3.45	34.84				

Station 4049; Apr. 15; latitude 44°51.5′ N., longitude 48°51′ W., depth 1,586 meters, dynamic height 970.928

Observed values			Scaled Values			
Depth, meters	Temperature ° C.	Salinity ‰	Depth, meters	Temperature ° C.	Salinity ‰	σ_t
0	0.41	33.10	0	0.41	33.10	26.57
25	0.09	33.16	25	0.09	33.16	26.64
49	−0.52	33.68	50	−0.50	33.69	27.09
73	0.02	33.92	75	0.10	33.93	27.25
97	0.74	34.10	100	0.75	34.12	27.38
147	1.52	34.36	150	1.55	34.37	27.52
196	2.84	34.61	200	2.90	34.63	27.62
293	4.18	34.84	300	4.20	34.84	27.66
351	4.13	34.87	400	4.10	34.89	27.71
540	4.09	34.91	600	4.05	34.90	27.72
740	3.55	34.86	800	3.60	34.87	27.75
938	3.71	34.90	1,000	3.70	34.90	27.76
1,406	3.44	34.88				

Station 4050; Apr. 15–16; latitude 44°49′ N., longitude 48°33′ W., depth 2,514 meters, dynamic height 970.927

Observed values			Scaled Values			
Depth, meters	Temperature ° C.	Salinity ‰	Depth, meters	Temperature ° C.	Salinity ‰	σ_t
0	0.17	33.14	0	0.17	33.14	26.62
28	−0.55	33.30	25	−0.50	33.28	26.76
55	−0.65	33.60	50	−0.65	33.55	26.99
82	0.03	33.88	75	−0.20	33.81	27.18
109	0.81	34.12	100	0.55	34.04	27.32
164	2.73	34.54	150	2.30	34.45	27.53
219	2.86	34.61	200	2.85	34.59	27.59
328	2.83	34.68	300	2.75	34.65	27.65
305	2.75	34.65	400	3.35	34.79	27.70
470	3.88	34.86	600	3.65	34.87	27.74
642	3.62	34.87	800	3.50	34.86	27.75
868	3.50	34.86	1,000	3.50	34.87	27.76
1,548	3.48	34.89				

Station 4051; Apr. 16; latitude 44°41.5′ N., longitude 47°50′ W., depth 3,383 meters, dynamic height 971.120

Observed values			Scaled Values			
Depth, meters	Temperature ° C.	Salinity ‰	Depth, meters	Temperature ° C.	Salinity ‰	σ_t
0	12.49	35.46	0	12.49	35.46	26.88
27	12.51	35.46	25	12.50	35.46	26.87
53	12.52	35.47	50	12.50	35.47	26.88
80	12.50	35.465	75	12.50	35.47	26.88
106	12.53	35.47	100	12.50	35.47	26.88
160	10.24	35.04	150	10.60	35.10	26.94
213	9.29	35.01	200	9.45	35.01	27.07
319	8.32	35.02	300	8.45	35.02	27.24
424	5.94	34.95	400	6.50	34.96	27.48
634	4.84	34.97	600	4.95	34.97	27.68
842	4.27	34.94	800	4.35	34.95	27.73
1,051	3.93	34.92	1,000	4.00	34.92	27.75
1,574	3.56	34.91				

STATIONS OCCUPIED IN 1950—Continued

Station 4052; Apr. 16; latitude 44°38′ N., longitude 47°23′ W., depth 3,695 meters, dynamic height 971.108

Observed Values			Scaled Values			
Depth, meters	Temperature ° C.	Salinity ‰	Depth, meters	Temperature ° C.	Salinity ‰	σ_t
0	12.58	35.49	0	12.58	35.49	26.88
22	12.60	35.49	25	12.58	35.49	26.88
43	12.59	35.49	50	12.57	35.49	26.88
66	12.61	35.495	75	12.61	35.49	26.87
87	12.60	35.49	100	12.15	35.38	26.87
131	10.65	35.08	150	9.75	34.90	26.93
174	8.69	34.71	200	7.90	34.72	27.09
409	5.80	34.86	300	6.60	34.79	27.33
616	4.88	34.96	400	5.85	34.85	27.47
828	4.11	34.92	600	4.90	34.96	27.68
1,032	3.81	34.90	800	4.20	34.93	27.73
1,534	3.47	34.90	1,000	3.85	34.90	27.74

Station 4053; Apr. 16; latitude 44°33′ N., longitude 46°42′ W., depth 3,731 meters, dynamic height 971.207

Observed Values			Scaled Values			
Depth, meters	Temperature ° C.	Salinity ‰	Depth, meters	Temperature ° C.	Salinity ‰	σ_t
0	8.33	33.78	0	8.33	33.78	26.29
23	14.28	35.67	25	14.25	35.67	26.67
46	14.18	35.67	50	14.15	35.67	26.69
69	14.04	35.68	75	14.05	35.69	26.72
92	14.12	35.71	100	14.05	35.71	26.74
138	13.71	35.66	150	13.60	35.66	26.80
184	13.22	35.67	200	12.80	35.64	26.95
276	10.27	35.26	300	9.75	35.21	27.18
375	8.23	35.08	400	7.75	35.04	27.36
565	4.76	34.80	600	4.70	34.82	27.59
760	4.39	34.92	800	4.30	34.92	27.71
955	3.95	34.90	1,000	3.95	34.90	27.73
1,454	3.79	34.94				

Station 4054; Apr. 16; latitude 44°26′ N., longitude 46°02′ W., depth 3,695 meters, dynamic height 971.263

Observed Values			Scaled Values			
Depth, meters	Temperature ° C.	Salinity ‰	Depth, meters	Temperature ° C.	Salinity ‰	σ_t
0	14.87	35.84	0	14.87	35.84	26.67
27	14.91	35.83	25	14.90	35.83	26.65
54	14.93	35.84	50	14.90	35.83	26.65
81	14.88	35.84	75	14.90	35.84	26.66
107	14.89	35.86	100	14.90	35.85	26.67
162	14.42	35.81	150	14.55	35.82	26.72
215	13.82	35.73	200	14.00	35.76	26.79
322	11.12	35.38	300	11.70	35.45	27.02
310	10.97	35.38	400	8.75	35.11	27.27
447	7.76	35.00	600	5.75	34.99	27.59
573	6.01	35.00	800	4.60	34.94	27.69
722	4.85	34.94	1,000	4.20	34.92	27.73
1,102	4.03	34.92				

Station 4055; Apr. 16; latitude 44°16′ N., longitude 45°13′ W., depth 4,207 meters, dynamic height 971.198

Observed Values			Scaled Values			
Depth, meters	Temperature ° C.	Salinity ‰	Depth, meters	Temperature ° C.	Salinity ‰	σ_t
0	5.90	33.17	0	5.90	33.17	26.14
28	13.54	35.52	25	12.20	35.15	26.69
55	13.73	35.63	50	13.70	35.62	26.75
83	12.10	35.26	75	12.60	35.36	26.77
110	11.73	35.21	100	11.85	35.23	26.81
166	8.94	34.83	150	9.60	34.94	26.99
221	8.06	34.68	200	8.25	34.71	27.03
331	8.88	34.98	300	8.65	34.90	27.11
430	7.62	35.00	400	8.10	35.00	27.28
643	4.65	34.90	600	5.10	34.92	27.62
856	3.92	34.88	800	4.05	34.89	27.71
1,069	3.62	34.86	1,000	3.65	34.86	27.73
1,602	3.66	34.92				

Station 4056; Apr. 17; latitude 44°50′ N., longitude 45°13′ W., depth 4,436 meters, dynamic height 971.030

Observed values			Scaled values			
Depth, meters	Temperature ° C.	Salinity ‰	Depth, meters	Temperature ° C.	Salinity ‰	σ_t
0	6.17	33.71	0	6.17	33.71	26.54
24	9.82	34.83	25	9.85	34.84	26.87
48	10.61	35.07	50	10.60	35.07	26.92
72	9.40	34.86	75	9.10	34.83	26.98
97	5.88	34.29	100	5.80	34.29	27.04
145	5.35	34.34	150	5.35	34.37	27.16
194	6.98	34.77	200	6.90	34.78	27.28
290	5.73	34.85	300	5.90	34.82	27.45
294	5.26	34.78	400	4.60	34.82	27.60
436	4.46	34.82	600	4.30	34.92	27.71
574	4.34	34.92	800	4.00	34.92	27.75
733	4.14	34.93	1,000	3.60	34.90	27.77
1,159	3.27	34.88				

Station 4057; Apr. 17; latitude 45°21′ N., longitude 45°12′ W., depth 4,463 meters, dynamic height 971.036

Observed values			Scaled values			
Depth, meters	Temperature ° C.	Salinity ‰	Depth, meters	Temperature ° C.	Salinity ‰	σ_t
0	9.14	34.48	0	9.14	34.48	26.71
25	8.46	34.49	25	8.46	34.49	26.82
49	10.41	35.02	50	10.40	35.02	26.92
74	9.38	34.84	75	9.20	34.83	26.97
98	5.37	34.19	100	5.30	34.19	27.02
148	4.70	34.30	150	4.70	34.31	27.18
198	5.00	34.35	200	5.00	34.36	27.19
296	4.61	34.64	300	4.85	34.66	27.45
298	5.10	34.68	400	5.05	34.87	27.59
441	5.05	34.93	600	4.50	34.97	27.73
583	4.56	34.97	800	3.80	34.89	27.74
748	3.85	34.89	1,000	3.75	34.90	27.75
1,192	3.69	34.91				

Station 4058; Apr. 17; latitude 45°22.5′ N., longitude 45°54′ W., depth 3,548 meters, dynamic height 970.989

Observed values			Scaled values			
Depth, meters	Temperature ° C.	Salinity ‰	Depth, meters	Temperature ° C.	Salinity ‰	σ_t
0	7.14	34.42	0	7.14	34.42	26.96
26	8.20	34.68	25	8.20	34.67	27.01
51	8.08	34.72	50	8.10	34.72	27.06
77	7.20	34.64	75	7.20	34.65	27.14
102	7.04	34.67	100	7.10	34.67	27.17
152	5.74	34.54	150	5.75	34.54	27.24
203	6.31	34.76	200	6.30	34.75	27.34
305	4.79	34.78	300	4.80	34.78	27.54
411	5.35	35.01	400	5.30	35.00	27.66
616	4.25	34.92	600	4.30	34.93	27.71
820	3.90	34.90	800	3.95	34.90	27.73
1,025	3.60	34.89	1,000	3.60	34.89	27.76
1,538	3.48	34.90				

Station 4059; Apr. 17; latitude 45°23′ N., longitude 46°32′ W., depth 3,292 meters, dynamic height 970.972

Observed values			Scaled values			
Depth, meters	Temperature ° C.	Salinity ‰	Depth, meters	Temperature ° C.	Salinity ‰	σ_t
0	−0.25	33.02	0	−0.25	33.02	26.54
25	−1.57	33.22	25	−1.57	33.22	26.75
50	2.53	33.86	50	2.53	33.86	27.03
75	4.41	34.19	75	4.41	34.19	27.12
101	4.26	34.25	100	4.25	34.24	27.17
151	4.48	34.48	150	4.45	34.48	27.34
201	4.62	34.59	200	4.60	34.59	27.41
302	4.24	34.75	300	4.25	34.74	27.57
399	4.48	34.92	400	4.45	34.92	27.70
596	3.71	34.86	600	3.70	34.86	27.73
790	3.85	34.91	800	3.85	34.91	27.75
989	3.71	34.90	1,000	3.70	34.90	27.76
1,487	3.45	34.87				

STATIONS OCCUPIED IN 1950—Continued

Station 4060; Apr. 18; latitude 45°02.5′ N., longitude 46°35′ W. depth 3,467 meters, dynamic height 971.060

Observed values			Scaled Values			
Depth, meters	Temperature ° C.	Salinity ‰	Depth, meters	Temperature ° C.	Salinity ‰	σ_t
0	------	34.96	(0)	10.6	34.94	26.82
18	------	34.96	(25)	10.6	34.94	26.82
36	------	34.94	(50)	10.6	34.94	26.82
54	------	34.92	(75)	10.6	34.94	26.82
73	------	34.93	(100)	10.6	34.94	26.82
109	------	34.94	(150)	7.75	34.75	27.13
145	------	34.83	200	5.25	34.33	27.13
218	6.43	34.65	300	6.30	34.84	27.41
189	4.64	34.18	400	4.70	34.83	27.59
286	6.50	34.84	600	4.30	34.94	27.72
385	4.83	34.82	(800)	4.10	34.94	27.75
481	4.44	34.93	(1,000)	3.90	34.93	27.76
722	4.12	34.94				

Station 4061; Apr. 18–19; latitude 45°29′ N., longitude 47°33′ W. depth 1,948 meters, dynamic height 971.010

Observed values			Scaled Values			
Depth, meters	Temperature ° C.	Salinity ‰	Depth, meters	Temperature ° C.	Salinity ‰	σ_t
0	−1.18	33.07	0	−1.18	33.07	26.62
27	−1.18	33.10	25	−1.20	33.10	26.64
54	1.49	33.54	50	1.05	33.42	26.80
81	4.07	34.27	75	4.35	34.19	27.12
108	4.10	34.18	100	4.40	34.20	27.13
163	5.28	34.48	150	5.00	34.42	27.24
216	5.49	34.65	200	5.45	34.60	27.32
324	5.00	34.84	300	5.10	34.80	27.53
418	4.71	34.94	400	4.75	34.93	27.66
609	4.09	34.89	600	4.30	34.89	27.68
790	3.96	34.92	800	3.90	34.92	27.76
985	3.50	34.89	1,000	3.50	34.89	27.77
1,472	3.45	34.87				

Station 4062; Apr. 19; latitude 45°35′ N., longitude 47°40′ W., depth 1,550 meters, dynamic height 971.004

Observed values			Scaled Values			
Depth, meters	Temperature ° C.	Salinity ‰	Depth, meters	Temperature ° C.	Salinity ‰	σ_t
0	−1.13	33.12	0	−1.13	33.12	26.65
25	−1.14	33.42	25	−1.14	33.13	26.66
51	−1.46	33.20	50	−1.45	33.20	26.73
76	−1.73	33.41	75	−1.75	33.40	26.90
102	−1.58	33.61	100	−1.60	33.60	27.06
152	−0.62	33.35	150	−0.70	33.91	27.28
202	0.83	34.15	200	0.75	34.14	27.39
304	1.64	34.44	300	1.60	34.43	27.56
387	2.28	34.56	400	2.35	34.58	27.62
562	3.12	34.76	600	3.15	34.77	27.71
779	3.44	34.82	800	3.45	34.82	27.72
982	3.50	34.85	1,000	3.50	34.85	27.74
1,440	3.13	34.85				

Station 4063; Apr. 19; latitude 45°47′ N., longitude 47°59′ W, depth 654 meters, dynamic height 971.062

Observed values			Scaled Values			
Depth, meters	Temperature ° C.	Salinity ‰	Depth, meters	Temperature ° C.	Salinity ‰	σ_t
0	−1.09	33.05	0	−1.09	33.05	26.59
24	−1.11	33.04	25	−1.10	33.04	26.59
49	−1.29	33.08	50	−1.30	33.08	26.62
74	−1.77	33.25	75	−1.75	33.25	26.78
99	−1.72	33.33	100	−1.70	33.33	26.84
147	−1.25	33.48	150	−1.25	33.49	26.96
197	−0.17	33.70	200	−0.10	33.77	27.14
296	4.35	34.57	300	4.35	34.57	27.43
347	1.92	34.46	400	2.15	34.54	27.61
554	3.18	34.78	(600)	3.40	34.83	27.73

Station 4064; Apr. 19; latitude 45°51′ N., longitude 48°06′ W., depth 170 meters, dynamic height 971.073

Observed Values			Scaled Values			
Depth, meters	Temperature ° C.	Salinity ‰	Depth, meters	Temperature ° C.	Salinity ‰	σ_t
0	−0.70	33.04	0	−0.70	33.04	26.58
25	−0.73	33.04	25	−0.73	33.04	26.58
49	−1.43	33.13	50	−1.45	33.13	26.67
74	−1.73	33.26	75	−1.75	33.26	26.79
99	−1.56	33.32	100	−1.55	33.32	26.83
148	−1.32	33.39	150	−1.30	33.39	26.88

Station 4065; Apr. 19; latitude 45°54.5′ N., longitude 48°12′ W., depth 112 meters, dynamic height 971.074

Observed Values			Scaled Values			
Depth, meters	Temperature ° C.	Salinity ‰	Depth, meters	Temperature ° C.	Salinity ‰	σ_t
0	−0.66	33.03	0	−0.66	33.03	26.57
26	−0.69	33.03	25	−0.70	33.03	26.57
51	−1.71	33.18	50	−1.70	33.17	26.71
77	−1.70	33.27	75	−1.70	33.26	26.78
103	−1.59	33.29	100	−1.60	33.29	26.80

Station 4066; Apr. 19; latitude 46°00.5′ N., longitude 48°22′ W., depth 88 meters, dynamic height 971.079

Observed Values			Scaled Values			
Depth, meters	Temperature ° C.	Salinity ‰	Depth, meters	Temperature ° C.	Salinity ‰	σ_t
0	−0.32	33.03	0	−0.32	33.03	26.55
28	−0.37	33.04	25	−0.35	33.04	26.56
54	−0.80	33.07	50	−0.75	33.06	26.59
82	−1.60	33.24	75	−1.45	33.19	26.72

Station 4067; Apr. 19; latitude 46°10.5′ N., longitude 48°38′ W., depth 77 meters, dynamic height 971.082

Observed Values			Scaled Values			
Depth, meters	Temperature ° C.	Salinity ‰	Depth, meters	Temperature ° C.	Salinity ‰	σ_t
0	−0.07	32.93	0	−0.07	32.93	26.46
25	−0.14	32.96	25	−0.14	32.96	26.49
50	−0.80	33.11	50	−0.80	33.11	26.63
75	−1.11	33.14	75	−1.11	33.14	26.67

Station 4068; Apr. 19; latitude 46°20.5′ N., longitude 48°55′ W., depth 60 meters, dynamic height 971.093

Observed Values			Scaled Values			
Depth, meters	Temperature ° C.	Salinity ‰	Depth, meters	Temperature ° C.	Salinity ‰	σ_t
0	−0.28	32.79	0	−0.28	32.79	26.36
27	−0.32	32.80	25	−0.30	32.80	26.37
43	−0.53	32.86	(50)	−0.65	32.88	26.45

Station 4069; May 2; latitude 42°00′ N., longitude 51°58′ W., depth 3,841 meters, dynamic height 971.072

Observed Values			Scaled Values			
Depth, meters	Temperature ° C.	Salinity ‰	Depth, meters	Temperature ° C.	Salinity ‰	σ_t
0	5.84	33.45	0	5.84	33.45	26.37
23	5.83	33.46	25	5.80	33.46	26.38
47	3.13	33.38	50	3.10	33.38	26.60
70	3.07	33.86	75	3.20	33.95	27.05
93	4.65	34.19	100	4.55	34.18	27.09
140	3.88	34.07	150	4.15	34.13	27.10
187	5.53	34.49	200	5.35	34.48	27.24
280	3.90	34.42	300	3.90	34.46	27.39
380	4.01	34.68	400	4.10	34.73	27.58
574	5.09	35.01	600	5.00	35.00	27.70
769	4.05	34.90	800	4.05	34.90	27.72
964	4.17	34.95	1,000	4.15	34 95	27.75
1,458	3.65	34.91				

STATIONS OCCUPIED IN 1950—Continued

Station 4070; May 2; latitude 42°00′ N., longitude 50°58′ W., depth 3,282 meters, dynamic height 970.933

Observed Values			Scaled Values			
Depth, meters	Temperature ° C.	Salinity ‰	Depth, meters	Temperature ° C.	Salinity ‰	σ_t
0	3.19	33.45	0	3.19	33.45	26.65
23	2.69	33.61	25	2.65	33.63	26.84
46	2.02	33.91	50	2.05	33.96	27.16
69	2.82	34.10	75	2.80	34.14	27.24
92	2.81	34.20	100	2.70	34.21	27.30
138	1.94	34.32	150	2.05	34.36	27.48
185	2.51	34.50	200	2.70	34.57	27.59
277	3.47	34.74	300	3.30	34.74	27.67
320	3.19	34.74	400	3.30	34.77	27.70
490	3.47	34.81	600	3.55	34.84	27.72
666	3.55	34.84	800	3.55	34.84	27.72
818	3.52	34.84	1,000	3.55	34.85	27.73
1,176	3.53	34.86				

Station 4071; May 3; latitude 42°21.5′ N., longitude 51°30′ W., depth 2,908 meters, dynamic height 971.106

0	1.40	33.00	0	1.40	33.00	26.44
21	1.31	33.02	25	1.05	33.04	26.50
41	−0.50	33.16	50	−1.05	33.23	26.74
62	−1.51	33.30	75	−1.50	33.34	26.85
82	−1.47	33.37	100	−1.35	33.42	26.91
123	−1.15	33.47	150	−0.90	33.54	26.99
164	−0.80	33.58	200	−0.35	33.69	27.08
246	0.20	33.84	300	0.45	33.91	27.22
309	0.51	33.92	400	2.50	34.45	27.51
473	4.02	34.82	600	3.85	34.83	27.68
645	3.83	34.83	800	3.80	34.85	27.71
855	3.77	34.87	1,000	3.50	34.89	27.77
1,470	3.25	34.90				

Station 4072; May 3; latitude 42°42′ N., longitude 51°05′ W., depth 1,756 meters, dynamic height 971.090

0	3.36	33.10	0	3.36	33.10	26.35
24	3.21	33.11	25	3.20	33.11	26.38
47	2.70	33.10	50	2.35	33.10	26.44
71	0.00	33.14	75	−0.35	33.15	26.64
94	−1.44	33.26	100	−1.45	33.28	26.79
143	−1.34	33.42	150	−0.90	33.49	26.95
190	2.71	33.92	200	2.75	33.98	27.11
284	2.84	34.33	300	3.00	34.41	27.44
360	4.47	34.76	400	4.20	34.76	27.60
540	3.34	34.78	600	3.40	34.79	27.70
721	3.59	34.84	800	3.60	34.86	27.74
915	3.57	34.87	1,000	3.60	34.87	27.75
1,424	3.61	34.89				

Station 4073; May 3; latitude 42°49′ N., longitude 50°54′ W., depth 1,074 meters, dynamic height 971.086

0	2.39	32.91	0	2.39	32.91	26.29
26	2.17	32.94	25	2.20	32.94	26.33
51	−0.21	33.11	50	−0.20	33.10	26.60
77	−0.77	33.19	75	−0.80	33.18	26.69
102	−0.19	33.41	100	−0.20	33.40	26.85
153	−0.66	33.59	150	−0.65	33.57	27.01
204	0.52	33.88	200	0.40	33.85	27.18
306	3.13	34.46	300	3.10	34.45	27.46
358	2.89	34.52	400	3.00	34.58	27.57
544	3.41	34.76	600	3.50	34.79	27.69
734	3.62	34.82	800	3.60	34.83	27.71
935	3.56	34.84	(1,000)	3.55	34.85	27.73

Station 4074; May 3; latitude 42°53.5′ N., longitude 50°47′ W., depth 640 meters, dynamic height 971.080

Observed values			Scaled values			
Depth, meters	Temperature ° C.	Salinity ‰	Depth, meters	Temperature ° C.	Salinity ‰	σ_t
0	3.10	32.65	0	3.10	32.65	26.03
27	2.81	32.71	25	2.85	32.70	26.08
53	−0.22	33.12	50	−0.10	33.08	26.58
80	0.08	33.23	75	−0.05	33.20	26.68
106	6.55	34.45	100	6.50	34.36	27.00
160	6.22	34.49	150	6.30	34.49	27.13
213	4.51	34.34	200	4.95	34.37	27.21
319	3.13	34.46	300	3.20	34.43	27.43
410	3.04	34.67	400	3.05	34.65	27.62
608	3.49	34.80	600	3.50	34.80	27.70

Station 4075; May 3; latitude 42°58′ N., longitude 50°41′ W., depth 162 meters, dynamic height 971.097

0	3.11	32.71	0	3.11	32.71	26.07
26	2.80	32.77	25	2.85	32.76	26.13
52	0.90	33.03	50	1.30	33.01	26.46
78	−1.09	33.30	75	−1.05	33.28	26.78
103	−0.79	33.48	100	−0.85	33.46	26.92
154	−0.20	33.70	150	−0.25	33.69	27.08

Station 4076; May 3; latitude 43°52′ N., longitude 50°34′ W., depth 91 meters, dynamic height 971.095

0	2.96	32.71	0	2.96	32.71	26.08
26	2.83	32.73	25	2.85	32.73	26.11
51	0.19	33.06	50	0.25	33.04	26.54
77	−0.96	33.35	75	−0.95	33.34	26.83

Station 4077; May 3; latitude 43°20′ N., longitude 50°13′ W., depth 70 meters, dynamic height 971.097

0	2.50	32.75	0	2.50	32.75	26.15
26	2.45	32.76	25	2.45	32.75	26.15
52	0.38	33.02	50	0.50	33.01	26.50

Station 4078; May 3; latitude 42°59′ N., longitude 50°12′ W., depth 94 meters, dynamic height 971.088

0	2.67	32.78	0	2.67	32.78	26.17
26	1.40	32.97	25	1.50	32.96	26.39
50	−0.50	33.19	50	−0.50	33.19	26.69
76	−1.03	33.33	75	−1.05	33.32	26.81

Station 4079; May 3; latitude 42°45′ N., longitude 50°13′ W., depth 432 meters, dynamic height 971.081

0	1.87	32.94	0	1.87	32.94	26.36
21	1.68	32.96	25	1.40	32.98	26.42
43	−0.10	33.07	50	−0.25	33.10	26.60
64	−0.53	33.16	75	−0.75	33.21	26.72
86	−1.03	33.25	100	−1.05	33.33	26.82
128	−1.08	33.47	150	−0.65	33.58	27.01
170	−0.12	33.68	200	0.60	33.88	27.18
256	1.89	34.36	(300)	2.65	34.72	27.72

STATIONS OCCUPIED IN 1950—Continued

Station 4080; May 3–4; latitude 42°34.5′ N., longitude 50°15′ W., depth 1,920 meters, dynamic height 971.035

Observed values			Scaled Values			
Depth, meters	Temperature ° C.	Salinity ‰	Depth, meters	Temperature ° C.	Salinity ‰	σ_t
0	2.21	32.90	0	2.21	32.90	26.29
23	0.54	33.04	25	0.30	33.06	26.55
46	−1.23	33.27	50	−1.30	33.29	26.79
69	−1.45	33.36	75	−1.45	33.40	26.89
92	−1.02	33.51	100	−0.55	33.59	27.01
138	1.60	33.93	150	1.60	33.98	27.20
184	1.63	34.07	200	1.80	34.03	27.23
276	2.73	34.43	300	2.60	34.46	26.51
366	2.28	34.52	400	2.60	34.59	27.61
548	3.96	34.86	600	3.95	34.87	27.71
731	3.85	34.88	800	3.90	34.90	27.74
919	3.97	34.92	1,000	3.95	34.92	27.75
1,401	3.96	34.90				

Station 4081; May 4; latitude 42°10′ N., longitude 50°18′ W., depth 3,296 meters, dynamic height 970.957

Observed values			Scaled Values			
Depth, meters	Temperature ° C.	Salinity ‰	Depth, meters	Temperature ° C.	Salinity ‰	σ_t
0	3.76	33.57	0	3.76	33.57	26.70
25	3.66	33.58	25	3.66	33.58	26.71
50	2.85	33.96	50	2.85	33.96	27.09
75	3.24	34.14	75	3.24	34.14	27.19
100	2.31	34.12	100	2.31	34.12	27.27
150	3.03	34.37	150	3.03	34.37	27.40
200	3.04	34.49	200	3.04	34.49	27.49
300	4.06	34.77	300	4.06	34.77	27.62
407	4.58	34.92	400	4.55	34.91	27.68
609	4.26	34.94	600	4.30	34.94	27.72
813	4.05	34.94	800	4.05	34.94	27.75
1,019	3.63	34.89	1,000	3.65	34.89	27.75
1,540	3.56	34.92				

Station 4082; May 4; latitude 41°49.5′ N., longitude 50°16′ W., depth 3,713 meters, dynamic height 970.972

Observed values			Scaled Values			
Depth, meters	Temperature ° C.	Salinity ‰	Depth, meters	Temperature ° C.	Salinity ‰	σ_t
0	2.00	33.17	0	2.00	33.17	26.53
27	0.52	33.22	25	0.55	33.21	26.66
52	2.61	33.75	50	2.40	33.69	26.91
79	3.68	34.10	75	3.60	34.08	27.11
104	2.36	34.04	100	2.45	34.05	27.19
157	2.99	34.38	150	2.95	34.36	27.40
210	2.76	34.46	200	2.70	34.45	27.49
314	3.10	34.62	300	3.05	34.61	27.59
348	2.92	34.62	400	3.30	34.72	27.66
526	4.43	34.94	600	4.40	34.95	27.72
708	4.30	34.96	800	4.20	34.96	27.76
900	4.14	34.96	1,000	4.05	34.95	27.76
1,404	3.56	34.91				

Station 4083; May 4; latitude 41°35′ N., longitude 50°12′ W., depth 3,741 meters, dynamic height 971.111

Observed values			Scaled Values			
Depth, meters	Temperature ° C.	Salinity ‰	Depth, meters	Temperature ° C.	Salinity ‰	σ_t
0	5.41	33.17	0	5.41	33.17	26.20
25	5.05	33.17	25	5.05	33.17	26.24
50	9.55	34.50	50	9.55	34.50	26.66
75	12.18	35.28	75	12.15	35.28	26.80
386	4.16	34.62	100	12.70	35.47	26.84
578	4.86	34.95	150	11.90	35.49	27.01
769	4.48	34.96	200	10.65	35.35	27.13
964	3.93	34.92	300	6.45	34.97	27.49
1,455	3.76	34.94	400	4.20	34.64	27.50
			600	4.85	34.95	27.67
			800	4.35	34.96	27.74
			1,000	3.90	34.92	27.76

Station 4084; May 4; latitude 40°58′ N., longitude 50°04′ W., depth 3,566 meters, dynamic height 971.301

Observed Values			Scaled Values			
Depth, meters	Temperature ° C.	Salinity ‰	Depth, meters	Temperature ° C.	Salinity ‰	σ_t
0	15.22	34.87	0	15.22	34.87	25.85
27	14.01	35.44	25	14.05	35.40	26.50
54	14.68	35.71	50	14.60	35.71	26.62
81	14.54	35.69	75	14.60	35.70	26.61
107	13.62	35.55	100	13.75	35.52	26.66
162	13.34	35.53	150	13.40	35.54	26.75
215	12.51	35.38	200	12.70	35.42	26.80
322	11.96	35.51	300	12.10	35.50	26.98
476	8.18	35.08	400	10.35	35.31	27.15
634	4.60	34.76	600	4.85	34.80	27.55
797	4.39	34.88	800	4.40	34.88	27.66
1,216	3.83	34.91	1,000	4.10	35.00	27.80

Station 4085; May 5; latitude 42°01′ N., longitude 49°25′ W., depth 2,926 meters, dynamic height 970.960

Observed Values			Scaled Values			
Depth, meters	Temperature ° C.	Salinity ‰	Depth, meters	Temperature ° C.	Salinity ‰	σ_t
0	4.07	33.27	0	4.07	33.27	26.42
27	3.57	33.43	25	3.60	33.42	26.60
53	1.64	33.72	50	1.65	33.69	26.97
80	2.68	34.05	75	2.55	34.00	27.15
105	2.29	34.15	100	2.40	34.13	27.26
159	2.88	34.40	150	2.75	34.35	27.41
212	5.21	34.85	200	4.90	34.80	27.55
317	4.60	34.86	300	4.65	34.86	27.63
419	4.54	34.92	400	4.60	34.91	27.67
628	4.07	34.92	600	4.10	34.92	27.74
839	4.08	34.94	800	4.10	34.94	27.75
1,049	3.68	34.91	1,000	3.75	34.91	27.76
1,576	3.55	34.94				

Station 4086; May 5; latitude 41°28′ N., longitude 48°48′ W., depth 3,333 meters, dynamic height 971.197

Observed Values			Scaled Values			
Depth, meters	Temperature ° C.	Salinity ‰	Depth, meters	Temperature ° C.	Salinity ‰	σ_t
0	14.23	35.49	0	14.23	35.49	26.54
25	15.38	35.90	25	15.38	35.90	26.60
50	15.16	35.84	50	15.16	35.84	26.60
75	14.13	35.64	75	14.13	35.64	26.67
100	13.70	35.59	100	13.70	35.59	26.72
149	13.00	35.50	150	13.00	35.50	26.80
200	12.91	35.56	200	12.91	35.56	26.87
300	9.42	35.17	300	9.42	35.17	27.21
403	7.67	35.08	400	7.75	35.08	27.39
600	5.47	35.00	600	5.47	35.00	27.64
794	4.58	34.97	800	4.55	34.97	27.73
1,000	4.15	34.94	1,000	4.15	34.94	27.74
1,505	3.69	34.92				

Station 4087; May 5; latitude 41°51′ N., longitude 47°46′ W., depth 3,749 meters, dynamic height 971.307

Observed Values			Scaled Values			
Depth, meters	Temperature ° C.	Salinity ‰	Depth, meters	Temperature ° C.	Salinity ‰	σ_t
0	15.51	35.96	0	15.51	35.96	26.62
25	15.47	35.96	25	15.47	35.96	26.62
51	15.49	35.97	50	15.49	35.96	26.62
75	15.52	35.96	75	15.52	35.96	26.61
101	15.49	35.97	100	15.50	35.97	26.63
151	13.85	35.65	150	13.85	35.65	26.74
202	13.43	35.60	200	13.45	35.60	26.78
303	12.69	35.61	300	12.75	35.61	26.94
406	9.58	35.18	400	9.75	35.20	27.17
606	6.17	34.98	600	6.25	34.98	27.52
804	4.69	34.94	800	4.70	34.94	27.68
1,007	4.31	34.95	1,000	4.30	34.95	27.73
1,517	3.72	34.92				

STATIONS OCCUPIED IN 1950—Continued

Station 4088; May 5; latitude 42°17′ N., longitude 48°26 W., depth 3,388 meters, dynamic height 971.070

Observed values			Scaled values			
Depth, meters	Temperature ° C.	Salinity ‰	Depth, meters	Temperature ° C.	Salinity ‰	σ_t
0	5.21	32.97	0	5.21	32.97	26.07
25	4.72	33.19	25	4.72	33.19	26.30
50	5.51	33.80	50	5.51	33.80	26.69
75	10.90	35.14	75	10.90	35.14	26.92
100	9.36	34.90	100	9.36	34.90	27.00
150	8.77	34.98	150	8.77	34.98	27.16
200	7.18	34.81	200	7.18	34.81	27.27
300	6.52	34.96	300	6.52	34.96	27.47
382	5.20	34.86	400	5.15	34.87	27.58
575	4.88	34.98	600	4.80	34.98	27.70
768	4.35	34.96	800	4.25	34.95	27.74
963	3.98	34.92	1,000	3.95	34.92	27.75
1,458	3.65	34.94				

Station 4089; May 5; latitude 42°42′ N., longitude 49°12′ W., depth 2,588 meters, dynamic height 970.947

Observed values			Scaled values			
Depth, meters	Temperature ° C.	Salinity ‰	Depth, meters	Temperature ° C.	Salinity ‰	σ_t
0	3.28	33.40	0	3.28	33.40	26.61
24	3.29	33.58	25	3.25	33.59	26.76
48	2.44	33.87	50	2.35	33.88	27.06
71	1.80	33.96	75	1.80	33.98	27.19
95	2.21	34.10	100	2.20	34.12	27.28
142	2.41	34.31	150	2.60	34.35	27.42
190	3.83	34.64	200	3.90	34.67	27.56
285	4.09	34.80	300	4.10	34.81	27.65
361	4.07	34.84	400	4.00	34.84	27.68
547	3.79	34.86	600	3.85	34.88	27.72
738	4.07	34.93	800	4.00	34.93	27.75
930	3.88	34.92	1,000	3.80	34.91	27.76
1,424	3.48	34.90				

Station 4090; May 6; latitude 43°17.5′ N., longitude 48°50′ W., depth 2,232 meters, dynamic height 970.942

Observed values			Scaled values			
Depth, meters	Temperature ° C.	Salinity ‰	Depth, meters	Temperature ° C.	Salinity ‰	σ_t
0	1.89	33.29	0	1.89	33.29	26.63
26	1.88	33.30	25	1.90	33.30	26.64
50	1.20	33.65	50	1.20	33.65	26.97
76	0.81	33.90	75	0.80	33.89	27.18
100	1.68	34.20	100	1.68	34.20	27.37
152	3.76	34.58	150	3.75	34.58	27.49
202	2.67	34.55	200	2.70	34.55	27.57
302	4.43	34.86	300	4.40	34.86	27.65
425	4.64	34.94	400	4.60	34.94	27.69
632	4.09	34.92	600	4.15	34.92	27.73
837	3.82	34.90	800	3.85	34.91	27.75
1,048	3.55	34.88	1,000	3.60	34.88	27.75
1,579	3.45	34.91				

Station 4091; May 6; latitude 43°00′ N., longitude 48°10′ W., depth 3,292 meters, dynamic height 970.991

Observed values			Scaled values			
Depth, meters	Temperature ° C.	Salinity ‰	Depth, meters	Temperature ° C.	Salinity ‰	σ_t
0	4.95	33.84	0	4.95	33.84	26.78
26	4.94	33.84	25	4.95	33.84	26.78
51	5.02	33.86	50	5.00	33.86	26.80
76	4.99	34.20	75	5.00	34.20	27.06
101	4.95	34.31	100	4.95	34.30	27.15
153	5.04	34.53	150	5.05	34.52	27.31
204	5.06	34.62	200	5.05	34.61	27.38
305	5.13	34.88	300	5.10	34.87	27.58
331	4.97	34.88	400	4.65	34.89	27.65
509	4.37	34.90	600	4.25	34.93	27.72
696	4.12	34.94	800	3.95	34.92	27.75
910	3.81	34.90	1,000	3.75	34.90	27.75
1,514	3.55	34.92				

Station 4092; May 6; latitude 42°44′ N., longitude 47°35′ W., depth 3,676 meters, dynamic height 970.985

Observed Values			Scaled Values			
Depth, meters	Temperature ° C.	Salinity ‰	Depth, meters	Temperature ° C.	Salinity ‰	σ_t
0	4.46	33.64	0	4.46	33.64	26.68
22	4.41	33.64	25	4.40	33.64	26.69
43	4.76	33.77	50	4.70	33.84	26.81
66	4.08	34.04	75	4.05	34.12	27.11
87	4.09	34.21	100	4.20	34.29	27.22
131	4.51	34.46	150	4.60	34.53	27.36
359	4.91	34.91	200	4.75	34.68	27.47
547	4.43	34.92	300	4.90	34.86	27.60
744	4.15	34.93	400	4.85	34.91	27.64
940	3.90	34.92	600	4.35	34.92	27.71
1,446	3.64	34.92	800	4.05	34.93	27.74
			1,000	3.85	34.92	27.76

Station 4093; May 6; latitude 42°41′ N., longitude 46°58′ W., depth 3,841 meters, dynamic height 971.163

Observed Values			Scaled Values			
Depth, meters	Temperature ° C.	Salinity ‰	Depth, meters	Temperature ° C.	Salinity ‰	σ_t
0	13.20	35.32	0	13.20	35.32	26.63
25	13.26	35.32	25	13.26	35.32	26.61
48	13.71	35.46	50	13.70	35.47	26.64
73	13.64	35.55	75	13.60	35.55	26.72
97	13.27	35.47	100	13.20	35.47	26.74
146	12.52	35.45	150	12.50	35.46	26.87
195	12.44	35.50	200	12.40	35.49	26.91
292	9.61	35.20	300	9.40	35.18	27.21
373	7.37	34.96	400	6.95	34.96	27.42
559	5.35	34.97	(600)	5.00	34.97	27.68
			(800)	4.00	34.94	27.76
			(1,000)	3.90	34.92	27.76

Station 4094; May 7, latitude 43°08′ N., longitude 46°42′ W., depth 4,024 meters, dynamic height 971.242

Observed Values			Scaled Values			
Depth, meters	Temperature ° C.	Salinity ‰	Depth, meters	Temperature ° C.	Salinity ‰	σ_t
0	14.36	35.83	0	14.36	35.83	26.77
23	14.39	35.83	25	14.40	35.83	26.76
45	14.44	35.84	50	14.40	35.83	26.76
68	14.44	35.83	75	14.45	35.84	26.76
90	14.42	35.83	100	14.40	35.83	26.76
136	14.40	35.84	150	14.40	35.83	26.76
181	14.44	35.83	200	14.25	35.82	26.78
271	12.22	35.50	300	11.35	35.38	27.02
390	8.76	35.07	400	8.50	35.05	27.26
598	5.22	34.91	600	5.20	34.91	27.60
816	4.15	34.88	800	4.15	34.88	27.69
1,026	4.08	34.94	1,000	4.10	34.94	27.75
1,556	3.65	34.90				

Station 4095; May 7; latitude 43°23′ N., longitude 46°04′ W., depth 4,572 meters, dynamic height 971.361

Observed Values			Scaled Values			
Depth, meters	Temperature ° C.	Salinity ‰	Depth, meters	Temperature ° C.	Salinity ‰	σ_t
0	14.50	35.81	0	14.50	35.81	26.74
25	14.54	35.81	25	14.54	35.81	26.71
50	14.55	35.81	50	14.55	35.81	26.71
75	14.53	35.81	75	14.53	35.81	26.71
100	14.37	35.79	100	14.37	35.79	26.74
150	14.35	35.80	150	14.35	35.80	26.75
200	14.12	35.80	200	14.12	35.80	26.80
300	13.57	35.68	300	13.57	35.68	26.81
371	12.11	35.46	400	11.40	35.38	27.02
555	8.00	35.06	600	7.20	35.02	27.43
737	5.50	34.96	800	5.10	34.94	27.63
925	4.57	34.93	1,000	4.40	34.93	27.70
14,05	3.97	34.94				

STATIONS OCCUPIED IN 1950—Continued

Station 4096; May 7; latitude 43°35′ N., longitude 46°38′ W., depth 4,390 meters, dynamic height 971.166

Observed Values			Scaled Values			
Depth, meters	Temperature ° C.	Salinity ‰	Depth, meters	Temperature ° C.	Salinity ‰	σ_t
0	14.04	35.66	0	14.04	35.66	26.71
26	14.53	35.72	25	14.50	35.72	26.65
51	14.48	35.81	50	14.45	35.81	26.74
78	14.43	35.80	75	14.45	35.81	26.74
103	13.67	35.62	100	13.75	35.63	26.74
155	13.02	35.54	150	13.10	35.55	26.82
206	12.36	35.51	200	12.45	35.52	26.92
309	8.01	34.90	300	9.00	35.08	27.20
294	10.00	35.26	400	4.80	34.66	27.45
437	4.14	34.60	600	5.05	34.95	27.65
579	5.13	34.95	800	4.05	34.92	27.74
743	4.20	34.93	1,000	3.75	34.88	27.73
1,187	3.51	34.87				

Station 4097; May 7; latitude 43°43.5′ N., longitude 47°11′W., depth 4,372 meter, dynamic height 970.981

Observed Values			Scaled Values			
Depth, meters	Temperature ° C.	Salinity ‰	Depth, meters	Temperature ° C.	Salinity ‰	σ_t
0	4.30	33.63	0	4.30	33.63	26.69
28	4.26	33.63	25	4.25	33.63	26.69
55	3.90	33.83	50	3.95	33.79	26.84
83	2.53	33.98	75	2.65	33.93	27.08
110	2.83	34.19	100	2.65	34.11	27.23
166	4.21	34.52	150	4.00	34.46	27.38
221	3.86	34.59	200	3.95	34.56	27.46
330	------	34.82	300	4.20	34.76	27.60
359	4.39	34.85	400	4.40	34.86	27.65
544	4.29	34.90	600	4.30	34.92	27.71
733	4.38	34.97	800	4.20	34.95	27.75
925	3.93	34.90	1,000	3.90	34.91	27.75
1,426	3.70	34.93				

Station 4098; May 8; latitude 43°50′ N., longitude 47°43′ W., depth 3,987 meters, dynamic height 970.979

Observed Values			Scaled Values			
Depth, meters	Temperature ° C.	Salinity ‰	Depth, meters	Temperature ° C.	Salinity ‰	σ_t
0	3.88	33.39	0	3.88	33.39	26.54
24	3.84	33.40	25	3.80	33.40	26.56
49	2.23	33.52	50	2.20	33.53	26.80
73	2.23	33.91	75	2.25	33.92	27.11
99	2.46	34.10	100	2.45	34.10	27.23
147	3.45	34.41	150	3.45	34.42	27.40
196	3.54	34.55	200	3.55	34.56	27.50
295	5.03	34.89	300	5.05	34.89	27.60
405	4.39	43.91	400	4.40	34.91	27.69
590	4.23	34.91	600	4.25	34.92	27.72
761	4.14	34.89	800	4.10	34.90	27.72
956	3.93	34.92	1,000	3.90	34.92	27.76
1,456	3.67	34.93				

Station 4099; May 8; latitude 43°56′ N., longitude 48°06′ W., depth 3,731 meters, dynamic height 971.001

Observed Values			Scaled Values			
Depth, meters	Temperature ° C.	Salinity ‰	Depth, meters	Temperature ° C.	Salinity ‰	σ_t
0	3.45	33.28	0	3.45	33.28	26.49
26	3.41	33.29	25	3.40	33.29	26.50
52	3.09	33.74	50	3.15	33.71	26.87
78	1.77	33.89	75	1.80	33.87	27.10
104	2.27	34.05	100	2.15	34.03	27.20
157	2.58	34.24	150	2.50	34.21	27.32
209	4.32	34.58	200	4.10	34.53	27.42
313	4.68	34.83	300	4.80	34.81	27.57
399	4.89	34.93	400	4.90	34.93	27.65
601	4.42	34.94	600	4.40	34.94	27.71
807	4.15	34.93	800	4.15	34.93	27.73
1,012	3.93	34.93	1,000	3.95	34.93	27.75
1,530	3.59	34.92				

Station 4100; May 8; latitude 44°07′ N., longitude 48°48′ W., depth 1,698 meters, dynamic height 970.979

Observed Values			Scaled Values			
Depth, meters	Temperature ° C.	Salinity ‰	Depth, meters	Temperature ° C.	Salinity ‰	σ_t
0	1.91	33.26	0	1.91	33.26	26.61
25	3.05	33.44	25	3.03	33.44	26.66
51	3.74	34.02	50	3.75	34.00	27.04
76	3.74	34.16	75	3.75	34.16	27.17
101	3.68	34.22	100	3.70	34.21	27.21
151	3.57	34.40	150	3.60	34.40	27.37
202	4.18	34.52	200	4.15	34.51	27.40
303	5.10	34.90	300	5.10	34.89	27.59
284	5.11	34.87	400	4.90	34.95	27.67
440	4.79	34.95	600	4.25	34.92	27.72
604	4.21	34.92	800	4.05	34.92	27.74
776	4.10	34.92	1,000	3.70	34.90	27.76
1,248	3.47	34.86				

Station 4101; May 8; latitude 44°09′ N., longitude 48°55′ W., depth 642 meters, dynamic height 971.033

Observed Values			Scaled Values			
Depth, meters	Temperature ° C.	Salinity ‰	Depth, meters	Temperature ° C.	Salinity ‰	σ_t
0	0.18	33.06	0	0.18	33.06	26.55
24	−0.27	33.08	25	−0.30	33.08	26.59
48	−1.15	33.21	50	−1.20	33.22	26.74
72	−1.50	33.32	75	−1.50	33.33	26.84
96	−1.34	33.41	100	−1.25	33.43	26.91
143	0.46	33.72	150	0.75	33.78	27.10
191	2.33	34.14	200	2.70	34.22	27.31
287	5.19	34.88	300	5.10	34.87	27.58
348	4.55	34.84	400	4.05	34.81	27.65
542	3.19	34.77	(600)	3.20	34.78	27.71

Station 4102; May 8; latitude 44°10.5′ N., longitude 49°04′ W., depth 183 meters, dynamic height 971.066

Observed Values			Scaled Values			
Depth, meters	Temperature ° C.	Salinity ‰	Depth, meters	Temperature ° C.	Salinity ‰	σ_t
0	0.36	33.04	0	0.36	33.04	26.53
26	0.13	33.05	25	0.15	33.05	26.54
51	−0.72	33.12	50	−0.70	33.12	26.64
78	−1.42	33.36	75	−1.40	33.35	26.84
103	−1.29	33.43	100	−1.35	33.42	26.91
155	−0.62	33.58	150	−0.70	33.56	27.00

Station 4103; May 8; latitude 44°10.5′ N., longitude 49° 08′ W., depth 125 meters, dynamic height 971.066

Observed Values			Scaled Values			
Depth, meters	Temperature ° C.	Salinity ‰	Depth, meters	Temperature ° C.	Salinity ‰	σ_t
0	0.23	33.05	0	0.23	33.05	26.54
27	−0.01	33.05	25	0.05	33.05	26.56
52	−1.26	33.26	50	−1.25	33.25	26.76
79	−1.24	33.32	75	−1.25	33.31	26.81

Station 4104; May 8; latitude 44°11′ N., longitude 49° 17′ W., depth 128 meters, dynamic height 971.078

Observed Values			Scaled Values			
Depth, meters	Temperature ° C.	Salinity ‰	Depth, meters	Temperature ° C.	Salinity ‰	σ_t
0	0.86	33.09	0	0.86	33.09	26.54
25	0.55	33.10	25	0.55	33.10	26.56
95	0.43	33.10	(50)	0.45	33.10	26.57
			(75)	0.45	33.10	26.57
			100	0.45	33.10	26.57

Station 4105; May 8; latitude 44°59′ N., longitude 49°24′ W., depth 67 meters, dynamic height 971.072

Observed Values			Scaled Values			
Depth, meters	Temperature ° C.	Salinity ‰	Depth, meters	Temperature ° C.	Salinity ‰	σ_t
0	1.51	33.00	0	1.51	33.00	26.43
26	0.90	33.07	25	0.95	33.06	26.51
52	−0.09	33.17	50	−0.05	33.16	26.64

Tables of Oceanographic Data—Continued

STATIONS OCCUPIED IN 1950—Continued

Station 4106; May 9; latitude 44°53.5′ N., longitude 48°57′ W., depth 102 meters, dynamic height 971.069

Observed values			Scaled Values			
Depth, meters	Temperature ° C.	Salinity ‰	Depth, meters	Temperature ° C.	Salinity ‰	σ_t
0	0. 26	33. 02	0	0. 26	33. 02	26. 52
25	—0. 01	33. 02	25	—0. 01	33. 02	26. 53
51	—1. 26	33. 20	50	—1. 25	33. 19	26. 71
76	—1. 52	33. 30	75	—1. 55	33. 30	26. 81

Station 4107; May 9; latitude 44°00.5′ N., longitude 48°51′ W., depth 786 meters, dynamic height 971.048

Observed values			Scaled Values			
Depth, meters	Temperature ° C.	Salinity ‰	Depth, meters	Temperature ° C.	Salinity ‰	σ_t
0	0. 15	33. 00	0	0. 15	33. 00	26. 51
23	0. 14	33. 01	25	0. 10	33. 01	26. 53
47	—0. 91	33. 11	50	—1. 05	33. 13	26. 66
70	—1. 55	33. 30	75	—1. 55	33. 31	26. 82
93	—1. 49	33. 36	100	—0. 85	33. 39	26. 86
140	4. 50	34. 16	150	4. 45	34. 20	27. 12
187	3. 97	34. 27	200	3. 65	34. 28	27. 27
280	1. 79	34. 30	300	2. 20	34. 39	27. 49
356	3. 56	34. 63	400	3. 40	34. 66	27. 60
499	2. 99	34. 70	(600)	3. 00	34. 74	27. 70

Station 4108; May 9; latitude 44°47′ N., longitude 48°37′ W., depth 1,646 meters, dynamic height 971.000

Observed values			Scaled Values			
Depth, meters	Temperature ° C.	Salinity ‰	Depth, meters	Temperature ° C.	Salinity ‰	σ_t
0	3. 24	33. 19	0	3. 24	33. 19	26. 44
27	3. 06	33. 19	25	3. 10	33. 19	26. 46
52	0. 60	33. 48	50	0. 60	33. 45	26. 84
79	2. 18	33. 91	75	1. 75	33. 83	27. 07
105	5. 88	34. 59	100	5. 45	34. 54	27. 28
158	4. 52	34. 45	150	4. 60	34. 47	27. 32
210	5. 02	34. 65	200	5. 00	34. 61	27. 39
315	5. 19	34. 84	300	5. 20	34. 83	27. 53
417	3. 97	34. 80	400	4. 10	34. 80	27. 64
625	4. 10	34. 91	600	4. 10	34. 91	27. 73
833	3. 78	34. 90	800	3. 90	34. 90	27. 74
1,043	3. 49	34. 87	1,000	3. 55	34. 87	27. 75
1,568	3. 47	34. 88				

Station 4109; May 9; latitude 44°43.5′ N., longitude 48°25′ W., depth 2,422 meters, dynamic height 971.024

Observed values			Scaled Values			
Depth, meters	Temperature ° C.	Salinity ‰	Depth, meters	Temperature ° C.	Salinity ‰	σ_t
0	3. 92	33. 16	0	3. 92	33. 16	26. 35
25	4. 90	33. 40	25	4. 90	33. 40	26. 44
51	4. 67	34. 04	50	4. 65	34. 02	26. 96
75	5. 06	34. 24	75	5. 06	34. 24	27. 09
101	7. 73	34. 78	100	7. 70	34. 78	27. 16
151	4. 20	34. 32	150	4. 20	34. 32	27. 25
202	4. 33	34. 44	200	4. 30	34. 43	27. 32
303	3. 44	34. 56	300	3. 45	34. 55	27. 50
406	4. 56	34. 84	400	4. 55	34. 83	27. 61
607	4. 21	34. 90	600	4. 20	34. 90	27. 71
806	4. 07	34. 92	800	4. 10	34. 92	27. 74
1,008	3. 84	34. 90	1,000	3. 85	34. 90	27. 74
1,513	3. 47	34. 88				

Station 4110; May 9; latitude 44°37′ N., longitude 47°53′ W., depth 3,191 meters, dynamic height 971.122

Observed Values			Scaled Values			
Depth, meters	Temperature ° C.	Salinity ‰	Depth, meters	Temperature ° C.	Salinity ‰	σ_t
0	9. 60	34. 58	0	9. 60	34. 58	26. 71
25	9. 70	34. 60	25	9. 70	34. 60	26. 71
50	10. 78	34. 92	50	10. 78	34. 92	26. 78
75	11. 31	35. 08	75	11. 31	35. 08	26. 80
100	11. 26	35. 15	100	11. 26	35. 15	26. 87
150	8. 17	34. 76	150	8. 17	34. 76	27. 08
199	7. 15	34. 66	200	7. 15	34. 66	27. 15
299	6. 76	34. 76	300	6. 80	34. 76	27. 38
396	6. 59	34. 94	400	6. 55	34. 94	27. 45
592	4. 86	34. 92	600	4. 85	34. 92	27. 65
785	4. 35	34. 94	800	4. 30	34. 94	27. 72
981	4. 01	34. 92	1,000	4. 00	34. 92	27. 75
1,473	3. 67	34. 91				

Station 4111; May 9; latitude 44°30.5′ N., longitude 47°16′ W., depth 3,713 meters, dynamic height 971.123

Observed Values			Scaled Values			
Depth, meters	Temperature ° C.	Salinity ‰	Depth, meters	Temperature ° C.	Salinity ‰	σ_t
0	10. 98	35. 08	0	10. 98	35. 08	26. 86
25	10. 96	35. 06	25	10. 96	35. 06	26. 85
49	10. 93	35. 05	50	10. 90	35. 05	26. 85
74	11. 08	35. 08	75	11. 05	35. 08	26. 85
98	10. 89	35. 05	100	10. 90	35. 05	26. 85
147	10. 80	35. 12	150	10. 75	35. 12	26. 94
197	9. 48	35. 01	200	9. 45	35. 01	27. 07
295	8. 54	35. 06	300	8. 50	35. 06	27. 26
365	7. 63	35. 06	400	7. 15	35. 06	27. 47
552	5. 40	35. 00	600	5. 15	34. 99	27. 67
742	4. 61	34. 98	800	4. 40	34. 97	27. 74
931	4. 03	34. 94	1,000	3. 95	34. 93	27. 75
1,406	3. 54	34. 90				

Station 4112; May 9; latitude 44°26′ N., longitude 46°41′ W., depth 3,804 meters, dynamic height 971.015

Observed Values			Scaled Values			
Depth, meters	Temperature ° C.	Salinity ‰	Depth, meters	Temperature ° C.	Salinity ‰	σ_t
0	1. 62	33. 30	0	1. 62	33. 30	26. 66
24	1. 94	33. 45	25	1. 95	33. 45	26. 76
48	2. 26	33. 55	50	2. 25	33. 56	26. 83
71	2. 64	33. 74	75	2. 60	33. 73	26. 92
95	—0. 61	33. 59	100	—0. 50	33. 60	27. 02
143	1. 77	33. 99	150	1. 80	34. 02	27. 23
191	2. 12	34. 20	200	2. 25	34. 24	27. 36
286	4. 25	34. 68	300	4. 50	34. 74	27. 54
348	5. 26	34. 92	400	5. 05	34. 92	27. 63
527	4. 47	34. 92	600	4. 45	34. 94	27. 71
708	4. 48	34. 97	800	4. 25	34. 95	27. 74
866	4. 07	34. 94	1,000	3. 85	34. 92	27. 76
1,230	3. 62	34. 905				

Station 4113; May 9; latitude 44°26′ N., longitude 45°58′ W., depth 3,731 meters, dynamic height 971.141

Observed Values			Scaled Values			
Depth, meters	Temperature ° C.	Salinity ‰	Depth, meters	Temperature ° C.	Salinity ‰	σ_t
0	4. 17	33. 56	0	4. 17	33. 56	26. 65
25	9. 81	34. 81	25	9. 81	34. 81	26. 86
48	9. 60	34. 78	50	9. 55	34. 77	26. 87
73	9. 26	34. 73	75	9. 25	34. 72	26. 88
97	9. 21	34. 70	100	9. 20	34. 71	26. 88
146	11. 10	35. 11	150	11. 00	35. 11	26. 88
194	9. 90	35. 08	200	9. 85	35. 08	27. 06
291	9. 03	35. 13	300	8. 90	35. 12	27. 25
414	6. 63	34. 90	400	6. 80	34. 91	27. 40
623	5. 33	35. 02	600	5. 45	35. 02	27. 66
835	4. 30	34. 97	800	4. 40	34. 98	27. 74
1,045	3. 89	34. 90	1,000	3. 95	34. 91	27. 74
1,571	3. 50	34. 885				

Station 4114; May 10; latitude 44°26′ N., longitude 45°08′ W., depth 4,227 meters, dynamic height 971.288

Observed Values			Scaled Values			
Depth, meters	Temperature ° C.	Salinity ‰	Depth, meters	Temperature ° C.	Salinity ‰	σ_t
0	13.59	35.68	0	13.59	35.68	26.82
25	13.59	35.69	25	13.59	35.69	26.83
50	13.55	35.69	50	13.55	35.69	26.83
75	13.56	35.69	75	13.56	35.69	26.83
100	13.56	35.68	100	13.56	35.68	26.82
150	13.53	35.67	150	13.53	35.67	26.83
200	13.28	35.66	200	13.28	35.66	26.87
300	11.82	35.44	300	11.82	35.44	26.99
343	11.06	35.32	400	10.00	35.19	27.12
521	7.81	35.03	600	6.75	34.99	27.46
704	5.59	34.96	800	4.55	34.90	27.67
894	3.79	34.84	1,000	3.80	34.85	27.71
1,393	3.80	34.92				

Station 4115; May 10; latitude 44°49′ N., longitude 45°04′ W., depth 4,298 meters, dynamic height 971.197

Observed Values			Scaled Values			
Depth, meters	Temperature ° C.	Salinity ‰	Depth, meters	Temperature ° C.	Salinity ‰	σ_t
0	13.59	35.74	0	13.59	35.74	26.87
26	13.58	35.74	25	13.55	35.74	26.87
51	13.56	35.74	50	13.55	35.74	26.87
76	13.59	35.75	75	13.60	35.75	26.87
101	13.59	35.77	100	13.55	35.77	26.90
153	13.53	35.77	150	13.55	35.77	26.90
204	12.96	35.68	200	13.00	35.69	26.94
305	11.43	35.52	300	11.50	35.50	27.09
344	10.52	35.36	400	9.20	35.27	27.32
513	6.80	35.02	600	5.90	35.00	27.59
682	5.29	34.99	800	4.60	34.96	27.71
861	4.33	34.94	1,000	3.95	34.91	27.74
1,318	3.51	34.86				

Station 4116; May 10; latitude 45°27′ N., longitude 45°14′ W., depth 4,024 meters, dynamic height 970.995

Observed Values			Scaled Values			
Depth, meters	Temperature ° C.	Salinity ‰	Depth, meters	Temperature ° C.	Salinity ‰	σ_t
0	1.17	33.20	0	1.17	33.20	26.62
27	2.69	33.60	25	2.60	33.58	26.81
53	2.91	33.70	50	2.85	33.68	26.86
81	4.20	34.09	75	3.90	34.00	27.02
107	5.24	34.34	100	5.00	34.30	27.14
161	5.26	34.45	150	5.25	34.43	27.21
215	5.29	34.64	200	5.30	34.59	27.33
322	3.61	34.67	300	3.90	34.66	27.55
411	4.85	34.94	400	4.80	34.93	27.66
617	3.78	34.90	600	3.85	34.90	27.74
825	3.57	34.87	800	3.55	34.87	27.75
1,032	3.51	34.88	1,000	3.55	34.88	27.75
1,549	3.51	34.91				

Station 4117; May 10; latitude 45°28.5′ N., longitude 46°00′ W., depth 3,493 meters, dynamic height 970.914

Observed Values			Scaled Values			
Depth, meters	Temperature ° C.	Salinity ‰	Depth, meters	Temperature ° C.	Salinity ‰	σ_t
0	2.01	33.25	0	2.01	33.25	26.60
26	0.44	33.40	25	0.50	33.40	26.81
52	−0.28	33.66	50	−0.30	33.64	27.04
78	0.97	34.07	75	0.75	34.03	27.30
104	3.83	34.51	100	3.65	34.50	27.44
155	2.34	34.47	150	2.35	34.47	27.54
207	3.03	34.60	200	2.90	34.57	27.58
311	4.94	34.98	300	4.90	34.96	27.68
415	4.50	34.96	400	4.60	34.96	27.71
622	3.80	34.90	600	3.85	34.91	27.75
828	3.45	34.87	800	3.45	34.87	27.76
1,033	3.65	34.90	1,000	3.65	34.90	27.76
1,544	3.44	34.92				

Station 4118; May 10; latitude 45°29′ N., longitude 46°40′ W., depth 3,109 meters, dynamic height 970.928

Observed values			Scaled values			
Depth, meters	Temperature ° C.	Salinity ‰	Depth, meters	Temperature ° C.	Salinity ‰	σ_t
0	1.00	33.22	0	1.00	33.22	26.64
22	0.90	33.34	25	0.90	33.35	26.74
43	1.26	33.48	50	1.15	33.60	26.93
64	0.82	33.96	75	1.90	34.24	27.39
86	3.54	34.43	100	3.00	34.41	27.44
129	1.73	34.35	150	1.85	34.38	27.50
172	2.22	34.44	200	2.70	34.54	27.56
258	3.78	34.76	300	4.05	34.85	27.68
376	4.26	34.90	400	4.25	34.90	27.70
566	3.98	34.90	600	3.90	34.90	27.74
757	3.61	34.89	800	3.65	34.88	27.74
948	3.65	34.87	1,000	3.65	34.88	27.74
1,433	3.53	34.91				

Station 4119; May 11; latitude 45°22′ N., longitude 47°16′ W., depth 2, 862 meters, dynamic height 970.943

Observed values			Scaled values			
Depth, meters	Temperature ° C.	Salinity ‰	Depth, meters	Temperature ° C.	Salinity ‰	σ_t
0	0.54	33.16	0	0.54	33.16	26.61
25	−0.03	33.16	25	−0.03	33.16	26.64
49	−0.60	33.23	50	−0.60	33.23	26.72
74	−0.36	33.71	75	−0.30	33.53	26.95
99	2.42	34.14	100	2.90	34.15	27.24
148	1.77	34.36	150	1.80	34.37	27.51
197	2.70	34.60	200	2.70	34.60	27.61
296	2.71	34.66	300	2.70	34.67	27.67
382	2.97	34.74	400	3.05	34.75	27.70
571	3.39	34.82	600	3.40	34.83	27.73
760	3.47	34.86	800	3.45	34.86	27.75
925	3.46	34.86	1,000	3.50	34.87	27.76
1,292	3.57	34.91				

Station 4120; May 11; latitude 45°39′ N., longitude 47°44′ W., depth 1,545 meters, dynamic height 970.918

Observed values			Scaled values			
Depth, meters	Temperature ° C.	Salinity ‰	Depth, meters	Temperature ° C.	Salinity ‰	σ_t
0	0.87	33.16	0	0.87	33.16	26.59
25	0.88	33.26	25	0.88	33.26	26.67
50	0.51	33.47	50	0.51	33.47	26.87
75	0.79	33.98	75	0.79	33.98	27.25
100	1.61	34.31	100	1.61	34.31	27.47
150	2.13	34.50	150	2.13	34.50	27.58
201	3.77	34.76	200	3.75	34.76	27.64
301	3.67	34.79	300	3.65	34.79	27.67
399	3.99	34.87	400	4.00	34.87	27.71
599	4.04	34.93	600	4.05	34.93	27.74
798	3.82	34.92	800	3.80	34.92	27.77
997	3.64	34.905	1,000	3.65	34.91	27.77
1,490	3.50	34.92				

Station 4121; May 11; latitude 45°49′ N., longitude 48°03′ W., depth 672 meters, dynamic height 970.977

Observed values			Scaled values			
Depth, meters	Temperature ° C.	Salinity ‰	Depth, meters	Temperature ° C.	Salinity ‰	σ_t
0	0.62	33.10	0	0.62	33.10	26.56
23	0.15	33.22	25	0.15	33.24	26.70
46	0.22	33.36	50	0.15	33.37	26.80
69	−0.94	33.42	75	−1.15	33.46	26.94
91	−1.40	33.56	100	−1.25	33.63	27.07
137	1.09	33.93	150	1.15	34.01	27.26
183	1.32	34.18	200	1.45	34.25	27.43
274	1.99	34.48	300	2.20	34.53	27.60
384	2.71	34.65	400	2.75	34.67	27.67
580	3.20	34.79	600	3.20	34.80	27.73

Tables of Oceanographic Data—Continued

STATIONS OCCUPIED IN 1950—Continued

Station 4122; May 11; latitude 45°53.5′ N., longitude 48°14′ W., depth 167 meters, dynamic height 971.047

Observed values			Scaled Values			
Depth, meters	Temperature ° C.	Salinity ‰	Depth, meters	Temperature ° C.	Salinity ‰	σ_t
0	0.18	33.04	0	0.18	33.04	26.54
27	−0.28	33.05	25	−0.25	33.05	26.56
53	−1.78	33.34	50	−1.75	33.31	26.82
79	−1.66	33.40	75	−1.70	33.39	26.89
105	−1.37	33.52	100	−1.45	33.51	26.99
159	−1.10	33.57	150	−1.15	33.56	27.02

Station 4123; May 11; latitude 45°56.5′ N., longitude 48°19′ W., depth 119 meters, dynamic height 971.054

Observed values			Scaled Values			
Depth, meters	Temperature ° C.	Salinity ‰	Depth, meters	Temperature ° C.	Salinity ‰	σ_t
0	0.52	33.02	0	0.52	33.02	26.50
27	−0.01	33.04	25	1.05	33.04	26.55
52	−1.24	33.23	50	−1.15	33.21	26.73
79	−1.62	33.40	75	−1.60	33.39	26.89
105	−1.48	33.41	100	−1.50	33.41	26.91

Station 4124; May 11; latitude 46°05.5′ N., longitude 48°36′ W., depth 91 meters, dynamic height 971.064

Observed values			Scaled Values			
Depth, meters	Temperature ° C.	Salinity ‰	Depth, meters	Temperature ° C.	Salinity ‰	σ_t
0	0.64	33.00	0	0.64	33.00	26.48
17	0.50	33.00	25	0.45	33.00	26.50
42	0.32	33.00	50	−0.05	33.00	26.52
69	−1.46	33.24	75	−1.50	33.24	26.76

Station 4125; May 11; latitude 46°11′ N., longitude 48°48′ W., depth 84 meters, dynamic height 971.045

Observed values			Scaled Values			
Depth, meters	Temperature ° C.	Salinity ‰	Depth, meters	Temperature ° C.	Salinity ‰	σ_t
0	0.83	33.03	0	0.83	33.03	26.50
24	0.81	33.03	25	0.85	33.03	26.50
49	0.42	33.04	50	0.40	33.04	26.53
71	−1.28	33.16	75	−1.35	33.17	26.70

Station 4126; May 11; latitude 46°17′ N., longitude 49°00′ W., depth 71 meters, dynamic height 971.636

Observed values			Scaled Values			
Depth, meters	Temperature ° C.	Salinity ‰	Depth, meters	Temperature ° C.	Salinity ‰	σ_t
0	1.14	32.98	0	1.14	32.98	26.44
24	1.11	32.98	25	1.10	32.98	26.44
53	−0.33	33.09	50	−0.25	33.07	26.58

Station 4127; May 11; latitude 46°16′ N., longitude 48°40′ W., depth 91 meters, dynamic height 971.045

Observed values			Scaled Values			
Depth, meters	Temperature ° C.	Salinity ‰	Depth, meters	Temperature ° C.	Salinity ‰	σ_t
0	0.82	33.03	0	0.82	33.03	26.50
25	0.76	33.025	25	0.76	33.025	26.50
52	0.32	33.01	50	0.35	33.01	26.51
77	−1.48	33.20	75	−1.30	33.19	26.71

Station 4128; May 11; latitude 46°13′ N., longitude 48°09′ W., depth 118 meters, dynamic height 971.043

Observed values			Scaled Values			
Depth, meters	Temperature ° C.	Salinity ‰	Depth, meters	Temperature ° C.	Salinity ‰	σ_t
0	0.39	33.00	0	0.39	33.00	26.50
23	0.36	33.00	25	0.35	33.00	26.50
46	−0.16	33.01	50	−0.40	33.02	26.55
69	−1.58	33.11	75	−1.60	33.15	26.69
92	−1.48	33.30	100	−1.40	33.37	26.86

Station 4129; May 11, latitude 46°10.5′ N., longitude 47°50′ W., depth 176 meters, dynamic height 971.026

Observed Values			Scaled Values			
Depth, meters	Temperature ° C.	Salinity ‰	Depth, meters	Temperature ° C.	Salinity ‰	σ_t
0	0.09	33.02	0	0.09	33.02	26.53
25	−0.71	33.09	25	−0.71	33.09	26.61
52	−1.76	33.32	50	−1.75	33.31	26.82
77	−1.74	33.38	75	−1.75	33.38	26.88
103	−1.62	33.41	100	−1.65	33.40	26.90
154	−1.09	33.54	150	−1.10	33.52	26.98

Station 4130; May 12; latitude 46°08.5′ N., longitude 47°32′ W., depth 722 meters, dynamic height 970.968

Observed Values			Scaled Values			
Depth, meters	Temperature ° C.	Salinity ‰	Depth, meters	Temperature ° C.	Salinity ‰	σ_t
0	0.35	33.08	0	0.35	33.08	26.56
25	−1.55	33.32	25	−1.55	33.32	26.83
50	−1.33	33.45	50	−1.33	33.45	26.93
75	−1.46	33.52	75	−1.46	33.52	27.00
101	−0.92	33.64	100	−0.95	33.63	27.06
150	0.44	34.02	150	0.44	34.02	27.31
201	1.50	34.31	200	1.45	34.29	27.46
302	2.27	34.52	300	2.25	34.52	27.59
403	2.93	34.70	400	2.90	34.69	27.67
612	3.34	34.81	600	3.30	34.81	27.73

Station 4131; May 12; latitude 46°06.5′ N., longitude 47°19′ W., depth 1,620 meters, dynamic height 970.935

Observed Values			Scaled Values			
Depth, meters	Temperature ° C.	Salinity ‰	Depth, meters	Temperature ° C.	Salinity ‰	σ_t
0	0.97	33.37	0	0.97	33.37	26.76
27	0.63	33.38	25	0.70	33.38	26.78
53	−0.57	33.52	50	−0.45	33.50	26.94
80	−0.81	33.67	75	−0.80	33.64	27.06
106	1.00	34.01	100	0.40	33.95	27.26
160	2.41	34.48	150	2.30	34.41	27.50
212	2.55	34.59	200	2.55	34.57	27.61
318	2.70	34.68	300	2.70	34.67	27.67
410	2.98	34.74	400	2.95	34.73	27.69
613	3.28	34.80	600	3.25	34.80	27.72
817	3.51	34.84	800	3.50	34.84	27.73
1,026	3.44	34.87	1,000	3.45	34.87	27.76
1,556	3.52	34.89				

Station 4132; May 12; latitude 46°03.5′ N., longitude 46°43′ W., depth 604 meters, dynamic height 970.921

Observed Values			Scaled Values			
Depth, meters	Temperature ° C.	Salinity ‰	Depth, meters	Temperature ° C.	Salinity ‰	σ_t
0	0.82	33.25	0	0.82	33.25	26.68
25	0.31	33.31	25	0.31	33.31	26.75
50	−1.47	33.56	50	−1.47	33.56	27.03
75	2.38	34.12	75	2.38	34.12	27.26
99	1.22	34.15	100	1.25	34.15	27.37
149	2.29	34.43	150	2.30	34.43	27.51
199	4.26	34.75	200	4.25	34.75	27.58
298	4.46	34.90	300	4.45	34.90	27.68
390	4.18	34.91	400	4.15	34.91	27.72
594	3.60	34.88	600	3.60	34.88	27.75

Tables of Oceanographic Data—Continued

STATIONS OCCUPIED IN 1950—Continued

Station 4133; May 12; latitude 46°00′ N., longitude 46°09′ W., depth 1,440 meters, dynamic height 970.900

Observed Values			Scaled Values			
Depth, meters	Temperature ° C.	Salinity ‰	Depth, meters	Temperature ° C.	Salinity ‰	σ_t
0	2.16	33.44	0	2.16	33.44	26.73
25	3.01	34.04	25	3.01	34.04	27.14
50	3.62	34.32	50	3.62	34.32	27.31
74	3.81	34.41	75	3.85	34.41	27.36
99	4.28	34.56	100	4.30	34.56	27.43
149	3.63	34.63	150	3.65	34.63	27.54
198	4.07	34.74	200	4.10	34.74	27.59
297	4.23	34.88	300	4.25	34.88	27.68
373	4.18	34.90	400	4.10	34.90	27.72
565	3.75	34.87	600	3.70	34.87	27.74
760	3.57	34.87	800	3.55	34.87	27.75
956	3.54	34.88	1,000	3.55	34.88	27.75
1,405	3.45	34.89				

Station 4134; May 12; latitude 46°01′ N., longitude 45°24′ W., depth 3,210 meters, dynamic height 970.968

Observed Values			Scaled Values			
Depth, meters	Temperature ° C.	Salinity ‰	Depth, meters	Temperature ° C.	Salinity ‰	σ_t
0	2.04	33.25	0	2.04	33.25	26.60
25	0.53	33.35	25	0.53	33.35	26.76
49	−0.68	33.50	50	−0.65	33.51	26.96
74	4.10	34.16	75	4.10	34.16	27.13
99	3.86	34.20	100	3.85	34.20	27.19
148	4.87	34.55	150	4.85	34.55	27.36
197	4.41	34.62	200	4.40	34.62	27.46
296	4.00	34.72	300	4.00	34.72	27.59
392	3.62	34.77	400	3.60	34.77	27.67
590	3.86	34.88	600	3.85	34.88	27.72
789	3.95	34.92	800	3.95	34.92	27.75
987	3.76	34.91	1,000	3.75	34.91	27.76
1,483	3.49	34.91				

Station 4135; May 12; latitude 45°40.5′ N., longitude 44°58′ W., depth 3,932 meters, dynamic height 971.122

Observed Values			Scaled Values			
Depth, meters	Temperature ° C.	Salinity ‰	Depth, meters	Temperature ° C.	Salinity ‰	σ_t
0	13.20	35.60	0	13.20	35.60	26.83
25	13.52	35.70	25	13.52	35.70	26.85
50	13.48	35.69	50	13.48	35.69	26.85
75	13.41	35.68	75	13.41	35.68	26.85
99	12.96	35.60	100	12.90	35.60	26.90
149	10.86	35.22	150	10.85	35.22	26.99
199	10.19	35.19	200	10.15	35.19	27.09
298	8.77	35.12	300	8.70	35.12	27.28
393	6.73	34.98	400	6.70	34.98	27.46
591	5.31	35.00	600	5.25	35.00	27.67
790	4.27	34.92	800	4.25	34.92	27.72
987	3.95	34.91	1,000	3.95	34.91	27.74
1,478	3.64	34.91				

Station 4136; May 13; latitude 45°20′ N., longitude 44°32′ W., depth 4,481 meters, dynamic height 971.185

Observed Values			Scaled Values			
Depth, meters	Temperature ° C.	Salinity ‰	Depth, meters	Temperature ° C.	Salinity ‰	σ_t
0	12.43	35.35	0	12.43	35.35	26.80
25	12.45	35.35	25	12.45	35.35	26.79
50	11.81	35.23	50	11.81	35.23	26.82
75	11.80	35.24	75	11.80	35.24	26.83
101	11.80	35.24	100	11.80	35.24	26.83
151	10.68	35.04	150	10.65	35.04	26.89
201	10.57	35.10	200	10.60	35.10	26.94
302	9.46	35.16	300	9.50	35.16	27.18
396	5.78	34.66	400	5.80	34.66	27.33
595	5.39	34.95	600	5.35	34.95	27.61
796	4.75	34.97	800	4.75	34.97	27.70
995	4.03	34.92	1,000	4.00	34.92	27.75
1,169	3.83	34.90				

Station 4137; May 13; latitude 45°33′ N., longitude 43°53′ W., depth 3,731 meters, dynamic height 971.302

Observed values			Scaled values			
Depth, meters	Temperature ° C.	Salinity ‰	Depth, meters	Temperature ° C.	Salinity ‰	σ_t
0	14.12	35.74	0	14.12	35.74	26.75
25	14.08	35.74	25	14.08	35.74	26.76
49	14.06	35.74	50	14.05	35.74	26.76
74	14.08	35.74	75	14.10	35.745	26.76
99	14.06	35.745	100	14.05	35.74	26.76
148	13.73	35.68	150	13.75	35.68	26.78
197	13.81	35.67	200	13.80	35.67	26.77
296	11.91	35.47	300	11.80	35.47	27.01
378	10.24	35.28	400	9.85	35.23	27.17
571	6.94	34.98	600	6.60	34.98	27.47
767	5.39	34.98	800	5.25	34.98	27.65
962	4.81	35.00	1,000	4.75	35.00	27.72
1,456	4.00	34.95				

Station 4138; May 13; latitude 45°59.5 N., longitude 43°59′ W., depth 4,170 meters, dynamic height 971.121

Observed values			Scaled values			
Depth, meters	Temperature ° C.	Salinity ‰	Depth, meters	Temperature ° C.	Salinity ‰	σ_t
0	13.51	35.67	0	13.51	35.67	26.83
26	13.36	35.66	25	13.35	35.66	26.85
52	13.32	35.65	50	13.30	35.65	26.85
79	12.68	35.53	75	12.70	35.54	26.89
105	12.93	35.64	100	12.90	35.62	26.91
157	12.97	35.75	150	12.95	35.74	26.99
209	11.37	35.44	200	11.70	35.50	27.05
314	7.70	34.94	300	8.15	35.00	27.27
381	5.46	34.73	400	5.25	34.73	27.45
569	4.34	34.85	600	4.30	34.86	27.66
756	4.10	34.90	800	4.05	34.90	27.72
943	3.86	34.90	1,000	3.80	34.90	27.75
1,406	3.47	34.88				

Station 4139; May 13; latitude 45°59′ N., longitude 44°39′ W., depth 3,676 meters, dynamic height 971.124

Observed values			Scaled values			
Depth, meters	Temperature ° C.	Salinity ‰	Depth, meters	Temperature ° C.	Salinity ‰	σ_t
0	13.64	35.66	0	13.64	35.66	26.80
25	13.15	35.66	25	13.15	35.66	26.89
50	13.18	35.69	50	13.18	35.69	26.91
75	13.18	35.69	75	13.18	35.69	26.90
100	12.82	35.62	100	12.82	35.62	26.93
150	12.49	35.63	150	12.49	35.63	26.99
200	10.60	35.28	200	10.60	35.28	27.08
300	8.54	35.08	300	8.54	35.05	27.26
338	7.60	34.98	400	6.75	34.98	27.45
514	5.59	34.97	600	5.15	34.97	27.66
694	4.75	34.98	800	4.25	34.92	27.72
876	3.94	34.89	1,000	3.85	34.89	27.73
1,346	3.55	34.89				

Station 4140; May 13; latitude 46°20′ N., longitude 44°44′ W., depth 2,186 meters, dynamic height 970.954

Observed values			Scaled values			
Depth, meters	Temperature ° C.	Salinity ‰	Depth, meters	Temperature ° C.	Salinity ‰	σ_t
0	2.11	33.32	0	2.11	33.32	26.64
23	2.01	33.52	25	2.00	33.58	26.86
47	4.69	34.16	50	4.65	34.15	27.06
70	2.35	34.02	75	2.05	34.02	27.21
93	1.47	34.04	100	1.60	34.10	27.30
140	4.10	34.48	150	3.95	34.47	27.39
187	2.70	34.40	200	2.70	34.42	27.47
280	2.95	34.60	300	3.10	34.64	27.61
314	3.20	34.66	400	3.45	34.74	27.65
479	3.59	34.79	600	3.70	34.85	27.72
649	3.76	34.86	800	3.55	34.86	27.74
824	3.50	34.86	1,000	3.35	34.87	27.77
1,299	3.19	34.89				

STATIONS OCCUPIED IN 1950—Continued

Station 4141; May 13; latitude 46°26′ N., longitude 44°42′ W., depth 655 meters, dynamic height 970.890

Observed values			Scaled Values			
Depth, meters	Temperature ° C.	Salinity ‰	Depth, meters	Temperature ° C.	Salinity ‰	σ_t
0	4.70	34.26	0	4.70	34.26	27.14
25	3.54	34.28	25	3.54	34.28	27.28
51	3.40	34.30	50	3.40	34.30	27.31
76	3.41	34.33	75	3.40	34.33	27.33
102	3.11	34.36	100	3.15	34.36	27.38
151	2.91	34.51	150	2.90	34.50	27.52
202	3.30	34.65	200	3.30	34.65	27.60
304	3.45	34.78	300	3.45	34.78	27.68
401	3.58	34.83	400	3.60	34.83	27.71
605	3.62	34.85	600	3.60	34.85	27.73

Station 4142; May 13; latitude 46°31′ N., longitude 44°41′ W., depth 227 meters, dynamic height 970.873

Observed values			Scaled Values			
Depth, meters	Temperature ° C.	Salinity ‰	Depth, meters	Temperature ° C.	Salinity ‰	σ_t
0	4.56	34.18	0	4.56	34.18	27.09
25	3.66	34.32	25	3.66	34.32	27.30
50	3.54	34.34	50	3.54	34.34	27.32
75	3.65	34.49	75	3.65	34.49	27.43
100	3.22	34.55	100	3.22	34.55	27.53
149	3.11	34.60	150	3.10	34.60	27.58
199	3.51	34.77	200	3.55	34.77	27.67

Station 4143; May 13; latitude 46°36′ N., longitude 44°44′ W., depth 170 meters, dynamic height 970.883

Observed values			Scaled Values			
Depth, meters	Temperature ° C.	Salinity ‰	Depth, meters	Temperature ° C.	Salinity ‰	σ_t
0	4.49	34.19	0	4.49	34.19	27.11
25	3.52	34.24	25	3.52	34.24	27.25
50	3.33	34.28	50	3.33	34.28	27.29
75	3.16	34.35	75	3.16	34.35	27.37
101	2.90	34.39	100	2.90	34.39	27.43
151	2.89	34.51	150	2.90	34.51	27.53

Station 4144; May 13; latitude 46°48′ N. longitude 44°51′ W., depth 162 meters, dynamic height 970.887

Observed values			Scaled Values			
Depth, meters	Temperature ° C.	Salinity ‰	Depth, meters	Temperature ° C.	Salinity ‰	σ_t
0	4.22	34.02	0	4.22	34.02	27.01
25	3.54	34.16	25	3.54	34.16	27.19
50	3.28	34.19	50	3.28	34.19	27.23
75	2.98	34.31	75	2.98	34.31	27.36
100	2.70	34.38	100	2.70	34.38	27.43
			(150)	2.65	34.51	27.55

Station 4145; May 27; latitude 47°23′ N., longitude 50°00′ W., depth 96 meters, dynamic height 971.027

Observed values			Scaled Values			
Depth, meters	Temperature ° C.	Salinity ‰	Depth, meters	Temperature ° C.	Salinity ‰	σ_t
0	1.88	32.85	0	1.88	32.85	26.28
25	0.80	32.94	25	0.80	32.94	26.43
51	−0.18	33.01	50	−0.15	33.01	26.54
76	−1.25	33.24	75	−1.20	33.23	26.74

Station 4146; May 27; latitude 47°45′ N., longitude 49°52′ W., depth 114 meters, dynamic height 971.030

Observed values			Scaled Values			
Depth, meters	Temperature ° C.	Salinity ‰	Depth, meters	Temperature ° C.	Salinity ‰	σ_t
0	1.61	32.82	0	1.16	32.82	26.28
25	1.35	32.82	25	1.35	32.82	26.29
50	0.16	32.92	50	0.16	32.92	26.44
75	−1.52	33.16	75	−1.52	33.16	26.69
100	−1.41	33.37	100	−1.41	33.37	26.86

Station 4147; May 27; latitude 47°52′N., longitude 49°49′ W., depth 169 meters, dynamic height 971.018

Observed Values			Scaled Values			
Depth, meters	Temperature ° C.	Salinity ‰	Depth, meters	Temperature ° C.	Salinity ‰	σ_t
0	0.79	32.65	0	0.79	32.65	26.20
26	0.05	32.69	25	0.10	32.69	26.26
51	−1.75	33.19	50	−1.75	33.18	26.72
78	−1.74	33.30	75	−1.75	33.29	26.80
103	−1.67	33.38	100	−1.70	33.37	26.87
155	−0.66	33.69	150	−0.80	33.65	27.07

Station 4148; May 27; latitude 48°09.5′ N., longitude 49°45′W., depth 217 meters, dynamic height 970.989

Observed Values			Scaled Values			
Depth, meters	Temperature ° C.	Salinity ‰	Depth, meters	Temperature ° C.	Salinity ‰	σ_t
0	0.94	32.49	0	0.94	32.49	26.05
26	0.23	32.92	25	0.25	32.89	26.41
51	0.17	33.38	50	0.15	33.36	26.79
77	−1.18	33.43	75	−1.15	33.43	26.91
102	−1.37	33.52	100	−1.35	33.51	26.98
153	0.29	33.94	150	0.15	33.92	27.25
204	1.76	34.37	200	1.65	34.34	27.49

Station 4149; May 28; latitude 48°34′ N., longitude 49°36′ W., depth 660 meters, dynamic height 970.888

Observed Values			Scaled Values			
Depth, meters	Temperature ° C.	Salinity ‰	Depth, meters	Temperature ° C.	Salinity ‰	σ_t
0	2.17	33.68	0	2.17	33.68	26.92
27	2.46	33.82	25	2.45	33.81	27.00
53	0.56	34.01	50	0.60	33.98	27.26
80	2.29	34.29	75	2.15	34.23	27.36
106	2.10	34.45	100	2.15	34.43	27.52
160	2.39	34.54	150	2.35	34.52	27.58
212	2.64	34.64	200	2.60	34.62	27.64
318	2.98	34.74	300	2.95	34.73	27.69
419	3.11	-------	400	3.10	34.78	27.72
631	3.25	34.84	600	3.25	34.83	27.74

Station 4150; May 28; latitude 48°44′ N., longitude 49°30′ W., depth 1,152 meters, dynamic height 970.862

Observed Values			Scaled Values			
Depth, meters	Temperature ° C.	Salinity ‰	Depth, meters	Temperature ° C.	Salinity ‰	σ_t
0	3.24	33.97	0	3.24	33.97	27.06
27	3.32	34.28	25	3.30	34.26	27.29
53	2.19	34.33	50	2.35	34.32	27.42
80	2.03	34.48	75	2.05	34.47	27.57
106	2.22	34.53	100	2.15	34.52	27.60
160	2.52	34.63	150	2.45	34.61	27.64
212	2.81	34.69	200	2.75	34.68	27.67
318	3.05	34.75	300	3.00	34.74	27.70
393	3.11	34.76	400	3.15	34.76	27.70
602	3.32	34.82	600	3.30	34.82	27.74
			(800)	3.35	34.85	27.75
			(1,000)	3.35	34.86	27.76

Station 4151; May 28; latitude 48°56.5′ N., longitude 49°27′ W., depth 1,486 meters, dynamic height 970.857

Observed Values			Scaled Values			
Depth, meters	Temperature ° C.	Salinity ‰	Depth, meters	Temperature ° C.	Salinity ‰	σ_t
0	3.64	34.16	0	3.64	34.16	27.18
26	3.02	34.15	25	3.05	34.15	27.22
52	2.19	34.32	50	2.20	34.31	27.43
78	2.32	34.50	75	2.30	34.48	27.55
103	2.51	34.60	100	2.50	34.59	27.62
156	2.72	34.68	150	2.70	34.68	27.67
208	2.98	34.72	200	2.95	34.72	27.69
311	3.17	34.78	300	3.15	34.78	27.71
362	3.22	34.79	400	3.25	34.80	27.72
546	3.36	34.84	600	3.35	34.84	27.74
924	3.35	34.85	800	3.35	34.85	27.75
1,410	3.36	34.89	1,000	3.35	34.85	27.75

Tables of Oceanographic Data—Continued

STATIONS OCCUPIED IN 1950—Continued

Station 4152; May 28; latitude 49°29′ N., longitude 49°18′ W., depth 1,508 meters, dynamic height 970.841

Observed Values			Scaled Values			
Depth, meters	Temperature ° C.	Salinity ‰	Depth, meters	Temperature ° C.	Salinity ‰	σ_t
0	5.41	34.62	0	5.41	34.62	27.35
24	4.90	34.60	25	4.90	34.60	27.39
47	4.30	34.63	50	4.25	34.63	27.48
71	3.84	34.66	75	3.75	34.67	27.57
95	3.38	34.69	100	3.30	34.70	27.64
141	3.13	34.75	150	3.15	34.76	27.70
188	3.30	34.79	200	3.30	34.79	27.71
283	3.25	-------	300	3.25	34.79	27.71
320	3.22	34.79	400	3.20	34.80	27.73
490	3.20	34.81	600	3.15	34.82	27.75
659	3.17	34.82	800	3.20	34.82	27.75
845	3.19	34.82	1,000	3.20	34.83	27.75
1,312	3.31	34.86				

Station 4153; May 28; latitude 49°58.5′ N., longitude 49°02′ W., depth 1,792 meters, dynamic height 970.841

Observed Values			Scaled Values			
Depth, meters	Temperature ° C.	Salinity ‰	Depth, meters	Temperature ° C.	Salinity ‰	σ_t
0	5.19	34.50	0	5.19	34.50	27.28
25	4.08	34.45	25	4.08	34.45	27.36
48	1.69	34.39	50	1.70	34.39	27.52
73	2.57	34.57	75	2.60	34.58	27.60
97	2.55	34.64	100	2.55	34.64	27.66
146	2.80	34.69	150	2.80	34.69	27.67
194	2.95	34.74	200	2.95	34.74	27.70
291	3.04	34.78	300	3.05	34.78	27.72
365	3.11	34.81	400	3.15	34.81	27.74
556	3.19	34.81	600	3.20	34.81	27.74
753	3.19	34.82	800	3.20	34.82	27.75
952	3.18	34.84	1,000	3.20	34.84	27.76
1,466	3.37	34.90				

Station 4154; May 28; latitude 49°47.5′ N., longitude 49°31′ W., depth 1,239 meters, dynamic height 970.845

Observed Values			Scaled Values			
Depth, meters	Temperature ° C.	Salinity ‰	Depth, meters	Temperature ° C.	Salinity ‰	σ_t
0	4.19	34.44	0	4.19	34.44	27.34
26	4.27	34.52	25	4.25	34.52	27.40
51	2.84	34.48	50	2.85	34.48	27.50
77	2.66	34.54	75	2.70	34.54	27.56
102	2.51	34.59	100	2.55	34.59	27.62
154	2.75	34.67	150	2.75	34.67	27.67
205	2.95	34.70	200	2.90	34.70	27.68
307	3.11	34.76	300	3.10	34.76	27.71
349	3.16	34.80	400	3.25	34.82	27.74
528	3.26	34.83	600	3.25	34.83	27.74
713	3.25	34.84	800	3.25	34.84	27.75
886	3.30	34.845	1,000	3.30	34.845	27.76
1,313	------	34.84				

Station 4155; May 29; latitude 49°39′ N., longitude 50°02′ W. depth 597 meters, dynamic height 970.873

Observed Values			Scaled Values			
Depth, meters	Temperature ° C.	Salinity ‰	Depth, meters	Temperature ° C.	Salinity ‰	σ_t
0	2.70	33.47	0	2.70	33.47	26.72
23	0.91	33.75	25	0.90	33.77	27.09
46	1.08	34.02	50	1.20	34.08	27.31
69	2.20	34.41	75	2.30	34.44	27.52
92	2.45	34.51	100	2.50	34.53	27.57
138	2.74	34.62	150	2.80	34.63	27.62
184	2.91	34.67	200	2.95	34.69	27.66
276	3.06	34.75	300	3.05	34.76	27.71
325	3.08	34.76	400	3.10	34.77	27.72
519	3.14	34.79	(600)	3.15	34.80	27.73

Station 4156; May 29; latitude 49°28′ N., longitude 50°33′W. depth 337 meters, dynamic height 970.928

Observed values			Scaled values			
Depth, meters	Temperature ° C.	Salinity ‰	Depth, meters	Temperature ° C.	Salinity ‰	σ_t
0	1.50	33.14	0	1.50	33.14	26.54
27	0.72	33.22	25	0.75	33.20	26.54
53	0.01	33.56	50	0.10	33.52	26.93
79	−0.04	33.90	75	−0.05	33.85	27.20
105	0.68	34.08	100	0.55	34.05	27.33
159	1.42	34.32	150	1.30	34.28	27.46
211	1.95	34.46	200	1.85	34.43	27.54
316	2.76	34.67	300	2.65	34.64	27.65

Station 4157; May 29; latitude 49°20.5′ N., longitude 51′04′ W. depth 336 meters, dynamic height 970.936

Observed values			Scaled values			
Depth, meters	Temperature ° C.	Salinity ‰	Depth, meters	Temperature ° C.	Salinity ‰	σ_t
0	1.42	32.96	0	1.42	32.96	26.40
25	−0.02	33.30	25	−0.02	33.30	26.75
51	−1.37	33.42	50	−1.40	33.42	26.91
76	−0.15	33.66	75	−0.20	33.66	27.06
103	−0.09	33.88	100	−0.10	33.85	27.20
153	1.14	34.17	150	1.10	34.15	27.38
204	1.76	34.39	200	1.70	34.37	27.51
307	2.79	34.69	300	2.70	34.67	27.67

Station 4158; May 29., latitude 49°10′ N., longitude 51°28′ W., depth 323 meters, dynamic height 971.008

Observed values			Scaled values			
Depth, meters	Temperature ° C.	Salinity ‰	Depth, meters	Temperature ° C.	Salinity ‰	σ_t
0	0.87	32.32	0	0.87	32.32	25.93
25	−0.89	32.63	25	−0.89	32.63	26.26
49	−1.76	33.25	50	−1.75	33.26	26.78
75	−1.73	33.34	75	−1.70	33.34	26.85
99	−1.72	33.38	100	−1.70	33.38	26.88
148	−1.50	33.50	150	−1.50	33.52	27.00
197	−0.23	33.86	200	−0.15	33.88	27.23
296	2.53	34.60	300	2.65	34.62	27.64

Station 4159; May 29; latitude 49°06′ N., longitude 51°47′W., depth 306 meters, dynamic height 971.006

Observed values			Scaled values			
Depth, meters	Temperature ° C.	Salinity ‰	Depth, meters	Temperature ° C.	Salinity ‰	σ_t
0	0.94	32.46	0	0.94	32.46	26.03
24	−0.43	32.50	25	−0.45	32.51	26.14
49	−1.69	33.14	50	−1.70	33.15	26.70
73	−1.74	33.28	75	−1.75	33.29	26.80
98	−1.72	33.36	100	−1.70	33.37	26.87
156	−0.94	33.63	150	−1.10	33.60	27.05
195	0.36	33.92	200	0.50	33.96	27.26
281	2.27	34.52	(300)	2.55	34.62	27.65

Station 4160; May 29; latitude 48°59′ N., longitude 52°06′W., depth 296 meters, dynamic height 971.011

Observed values			Scaled values			
Depth, meters	Temperature ° C.	Salinity ‰	Depth, meters	Temperature ° C.	Salinity ‰	σ_t
0	1.26	32.37	0	1.26	32.37	25 94
24	−0.20	32.46	25	−0.25	32.47	26.10
48	−1.12	33.22	50	−1.15	33.24	26.75
72	−1.72	33.38	75	−1.70	33.39	26.89
96	−1.34	33.46	100	−1.30	33.48	26.95
144	−1.18	33.67	150	−1.10	33.70	27.13
192	−0.05	33.93	200	0.15	33.97	27.29
272	1.38	34.26				

STATIONS OCCUPIED IN 1950—Continued

Station 4161; May 29; latitude 48°51′ N., longitude 52°26′W., depth 360 meters, dynamic height 971.050

Observed values			Scaled Values			
Depth, meters	Temperature ° C.	Salinity ‰	Depth, meters	Temperature ° C.	Salinity ‰	σ_t
0	0.35	31.76	0	0.35	31.76	25.50
28	−1.57	32.81	25	−1.50	32.67	26.30
57	−1.71	33.18	50	−1.70	33.12	26.67
85	−1.73	33.26	75	−1.70	33.24	26.76
113	−1.75	33.32	100	−1.75	33.29	26.80
170	−1.64	33.41	150	−1.70	33.37	26.87
227	−1.16	33.67	200	−1.45	33.54	27.01
340	−1.78	34.34	300	0.65	34.10	27.36

Station 4162; May 29; latitude 48°48.5′ N., longitude 52°43′ W., depth 220 meters, dynamic height 971.072

Observed values			Scaled Values			
Depth, meters	Temperature ° C.	Salinity ‰	Depth, meters	Temperature ° C.	Salinity ‰	σ_t
0	0.90	31.95	0	0.90	31.95	25.62
25	−0.69	32.59	25	−0.69	32.59	26.22
50	−1.75	33.12	50	−1.75	33.12	26.67
75	−1.76	33.19	75	−1.76	33.19	26.73
100	−1.75	33.22	100	−1.75	33.22	26.75
149	−1.71	33.28	150	−1.70	33.29	26.80
199	−1.60	33.40	200	−1.60	33.40	26.90

Station 4163; May 29; latitude 48°47′ N., longitude 52°50′ W., depth 142 meters, dynamic height 971.079

Observed values			Scaled Values			
Depth, meters	Temperature ° C.	Salinity ‰	Depth, meters	Temperature ° C.	Salinity ‰	σ_t
0	2.30	32.23	0	2.30	32.23	25.75
18	1.41	32.25	25	0.30	32.39	26.01
42	−1.70	33.03	50	−1.70	33.09	26.64
65	−1.74	33.14	75	−1.75	33.15	26.70
88	−1.75	33.16	100	−1.75	33.17	26.71
121	−1.76	33.20				

Station 4164; May 29; latitude 48°44.5′ N., longitude 52°58′ W., depth 110 meters, dynamic height 971.081

Observed values			Scaled Values			
Depth, meters	Temperature ° C.	Salinity ‰	Depth, meters	Temperature ° C.	Salinity ‰	σ_t
0	1.47	32.20	0	1.47	32.20	25.79
23	0.64	32.26	25	0.50	32.30	25.93
46	−1.65	32.93	50	−1.65	32.98	26.55
69	−1.74	33.11	75	−1.75	33.13	26.68
92	−1.76	33.19	100	−1.75	33.21	26.75

Station 4165; May 30; latitude 48°39′ N., longitude 52°45′ W., depth 249 meters, dynamic height 971.073

Observed values			Scaled Values			
Depth, meters	Temperature ° C.	Salinity ‰	Depth, meters	Temperature ° C.	Salinity ‰	σ_t
0	1.25	32.18	0	1.25	32.18	25.78
25	0.97	32.68	25	0.97	32.68	26.21
50	−1.69	33.03	50	−1.69	33.03	26.59
74	−1.74	33.14	75	−1.75	33.14	26.69
99	−1.77	33.18	100	−1.75	33.18	26.72
149	−1.74	33.24	150	−1.70	33.24	26.77
198	−1.68	33.35	200	−1.65	33.36	26.86

Station 4166; May 30; latitude 48°30.5 N., longitude 52°33′ W., depth 238 meters, dynamic height 971.061

Observed Values			Scaled Values			
Depth, meters	Temperature ° C.	Salinity ‰	Depth, meters	Temperature ° C.	Salinity ‰	σ_t
0	1.78	32.14	0	1.78	32.14	25.72
25	−0.81	32.55	25	−0.81	32.55	26.18
50	−1.72	33.07	50	−1.72	33.07	26.63
75	−1.74	33.19	75	−1.74	33.19	26.73
100	−1.74	33.21	100	−1.74	33.21	26.75
149	−1.72	33.31	150	−1.70	33.31	26.82
199	−1.40	33.45	200	−1.40	33.46	26.94

Station 4167; May 30; latitude 48°19.5′ N., longitude 52°11′ W., depth 183 meters, dynamic height 971.051

Observed Values			Scaled Values			
Depth, meters	Temperature ° C.	Salinity ‰	Depth, meters	Temperature ° C.	Salinity ‰	σ_t
0	1.13	32.46	0	1.13	32.46	26.02
28	0.59	32.55	25	0.70	32.52	26.09
57	−1.67	33.13	50	−1.55	33.00	26.57
85	−1.73	33.22	75	−1.70	33.19	26.73
113	−1.73	33.28	100	−1.75	33.25	26.78
170	−1.37	33.46	150	−1.55	33.39	26.89

Station 4168; May 30; latitude 48°09.5′ N., longitude 51°56′ W., depth 186 meters, dynamic height 971.047

Observed Values			Scaled Values			
Depth, meters	Temperature ° C.	Salinity ‰	Depth, meters	Temperature ° C.	Salinity ‰	σ_t
0	1.19	32.37	0	1.19	32.37	25.95
28	−0.49	32.54	25	−0.25	32.49	26.11
56	−1.76	33.15	50	−1.70	33.03	26.59
84	−1.76	33.24	75	−1.75	33.22	26.75
112	−1.72	33.30	100	−1.75	33.27	26.79
168	−1.41	33.47	150	−1.55	33.41	26.91

Station 4169; May 30; latitude 48°03′ N., longitude 51°37′ W., depth 266 meters, dynamic height 971.052

Observed Values			Scaled Values			
Depth, meters	Temperature ° C.	Salinity ‰	Depth, meters	Temperature ° C.	Salinity ‰	σ_t
0	1.35	32.58	0	1.35	32.58	26.11
24	0.58	32.65	25	0.50	32.65	26.22
48	−1.67	33.02	50	−1.65	33.03	26.59
73	−1.66	33.13	75	−1.65	33.14	26.68
97	−1.60	33.23	100	−1.60	33.24	26.76
145	−1.40	33.32	150	−1.40	33.33	26.83
194	−1.37	33.38	200	−1.35	33.39	26.88
242	−1.34	33.42				

Station 4170; May 30; latitude 47°55.5′ N., longitude 51°16′ W., depth 176 meters, dynamic height 971.048

Observed Values			Scaled Values			
Depth, meters	Temperature ° C.	Salinity ‰	Depth, meters	Temperature ° C.	Salinity ‰	σ_t
0	2.02	32.72	0	2.02	32.72	26.17
24	1.32	32.80	25	1.30	32.80	26.29
48	0.48	32.87	50	0.40	32.89	26.40
72	−1.33	33.08	75	−1.40	33.10	26.64
97	−1.60	33.24	100	−1.60	33.25	26.77
144	−1.33	33.40	150	−1.30	33.41	26.90

Station 4171; May 30; latitude 47°50′ N., longitude 51°04′ W., depth 124 meters, dynamic height 971.046

Observed Values			Scaled Values			
Depth, meters	Temperature ° C.	Salinity ‰	Depth, meters	Temperature ° C.	Salinity ‰	σ_t
0	1.56	32.51	0	1.56	32.51	26.03
26	0.62	32.67	25	0.65	32.66	26.21
51	−0.84	32.98	50	−0.80	32.96	26.51
77	−1.56	33.13	75	−1.55	33.12	26.67
102	−1.56	33.30	100	−1.55	33.28	26.79

STATIONS OCCUPIED IN 1950—Continued

Station 4172; May 30; latitude 47°41.5′ N., longitude 50°42′ W., depth 136 meters, dynamic height 971.041

Observed Values			Scaled Values			
Depth, meters	Temperature ° C.	Salinity ‰	Depth, meters	Temperature ° C.	Salinity ‰	σ_t
0	1.49	32.79	0	1.49	32.79	26.26
28	1.27	32.83	25	1.40	32.82	26.29
56	−0 52	33.01	50	−0.20	32.97	26.50
84	−1.17	33.16	75	−1.05	33.10	26.63
111	−1.42	33.36	100	−1.35	33.27	26.78

Station 4173; May 30; latitude 47°32′ N., longitude 50°23′ W., depth 151 meters, dynamic height 971.027

Observed Values			Scaled Values			
Depth, meters	Temperature ° C.	Salinity ‰	Depth, meters	Temperature ° C.	Salinity ‰	σ_t
0	1.77	-------	0	1.77	32.85	26.30
20	1.65	32.86	25	1.45	32.88	26.34
40	0.06	32.97	50	−0.70	33.01	26.56
60	−1.14	33.06	75	−1.55	33.18	26.71
80	−1.62	33.22	100	−1.40	33.36	26.85
120	−1.10	33.50	(150)	−0.70	33.71	27.12

Station 4174; May 30; latitude 47°25′ N., longitude 50°01′ W., depth 107 meters, dynamic height 971.027

Observed Values			Scaled Values			
Depth, meters	Temperature ° C.	Salinity ‰	Depth, meters	Temperature ° C.	Salinity ‰	σ_t
0	2.11	32.82	0	2.11	32.82	26.24
23	2.00	32.83	25	1.80	32.84	26.28
45	0.20	32.97	50	−0.15	32.99	26.52
68	−1.10	33.06	75	−1.05	33.22	26.73
90	−0.79	33.58	(100)	−0.60	33.72	27.12

Station 4175; June 9; latitude 38°00′ N., longitude 50°12′ W., depth 5,304 meters, dynamic height 971.921

Observed Values			Scaled Values			
Depth, meters	Temperature ° C.	Salinity ‰	Depth, meters	Temperature ° C.	Salinity ‰	σ_t
0	21.02	36.47	0	21.02	36.47	25.53
25	20.61	36.48	25	20.61	36.48	25.63
49	19.66	36.47	50	19.60	36.47	26.00
74	18.96	36.47	75	18.95	36.47	26.17
99	18.73	36.47	100	18.70	36.47	26.24
148	18.35	36.40	150	18.30	36.40	26.29
197	18.04	36.38	200	18.00	36.38	26.35
296	17.53	36.32	300	17.55	36.32	26.41
399	16.90	36.22	400	16.90	36.22	26.49
795	11.70	35.45	600	14.15	35.89	26.86
992	8.04	35.05	800	11.60	35.44	27.02
1,187	5.82	35.01	1,000	7.90	35.04	27.34
1,389	5.02	35.01	1,500	4.65	35.00	27.74
1,590	4.40	34.98	2,000	3.85	34.94	27.77
1,986	3.84	34.94				
2,481	3.47	34.93				

Station 4176; June 9; latitude 38°34′ N., longitude 50°02′W., depth 5,286 meters, dynamic height 971.810

Observed Values			Scaled Values			
Depth, meters	Temperature ° C.	Salinity ‰	Depth, meters	Temperature ° C.	Salinity ‰	σ_t
0	23.44	36.33	0	23.44	36.33	24.84
25	23.02	36.35	25	23.02	36.35	24.97
50	21.98	36.46	50	21.98	36.46	25.36
74	19.65	36.46	75	19.60	36.46	26.00
99	19.29	36.42	100	19.25	36.42	26.06
149	19.03	36.44	150	19.00	36.44	26.14
199	18.73	36.45	200	18.70	36.45	26.23
298	17.96	36.37	300	18.00	36.37	26.34
397	17.06	36.28	400	17.00	36.32	26.54
405	16.91	36.36	600	13.15	36.08	27.21
526	14.74	36.45	800	7.45	35.02	27.39
640	12.30	-------	1,000	5.55	34.97	27.61
734	9.14	35.13	(1,500)	4.30	34.98	27.75
934	5.79	34.96	(2,000)	3.80	34.94	27.78
1,174	4.99	35.00				
1,478	4.31	34.98				

Station 4177; June 9; latitude 39°02.5′ N., longitude 49°53′ W., depth 5,267 meters, dynamic height 971.362

Observed values			Scaled values			
Depth, meters	Temperature ° C.	Salinity ‰	Depth, meters	Temperature ° C.	Salinity ‰	σ_t
0	20.60	35.74	0	20.60	35.74	25.18
23	16.89	35.51	25	16.70	35.51	25.98
46	15.46	35.52	50	15.25	35.51	26.32
69	14.11	35.36	75	14.00	35.36	26.48
92	13.90	35.41	100	13.95	35.44	26.55
138	14.19	35.62	150	13.85	35.58	26.68
184	13.21	35.47	200	13.05	35.46	26.76
276	12.31	35.44	300	11.85	35.39	26.94
376	9.80	35.17	400	9.45	35.11	27.15
142	13.54	35.48	600	6.20	34.92	27.49
284	12.06	35.42	800	4.85	34.93	27.65
465	8.39	35.00	1,000	4.45	34.94	27.71
630	5.88	34.92	1,500	3.90	34.95	27.78
808	4.82	34.93	(2,000)	3.50	34.94	27.81
1,168	4.24	34.95				
1,669	3.70	34.95				

Station 4178; June 10; latitude 39°36′ N., longitude 49°58′ W., depth 5,212 meters, dynamic height 971.439

Observed values			Scaled values			
Depth, meters	Temperature ° C.	Salinity ‰	Depth, meters	Temperature ° C.	Salinity ‰	σ_t
0	21.84	36.21	0	21.84	36.21	25.20
25	19.48	35.84	25	19.48	35.84	25.55
50	17.29	35.86	50	17.29	35.86	26.12
74	15.26	35.59	75	15.25	35.59	26.39
99	15.81	35.94	100	15.80	35.94	26.54
149	14.55	35.72	150	14.55	35.72	26.64
199	13.26	35.44	200	13.25	35.44	26.70
298	12.48	35.41	300	12.45	35.41	26.84
400	9.76	35.14	400	9.75	35.14	27.12
592	7.09	35.00	600	7.00	34.99	27.43
790	5.41	34.92	800	5.35	34.92	27.59
987	4.60	34.91	1,000	4.55	34.91	27.68
1,186	4.19	34.93	1,500	3.85	34.92	27.76
1,584	3.75	34.92	2,000	3.50	34.87	27.76
1,994	3.49	34.87				
2,510	3.26	34.88				

Station 4179; June 10; latitude 40°05′ N., longitude 50°15′ W., depth 5,304 meters, dynamic height 971.540

Observed values			Scaled values			
Depth, meters	Temperature ° C.	Salinity ‰	Depth, meters	Temperature ° C.	Salinity ‰	σ_t
0	22.11	36.24	0	22.11	36.24	25.14
21	22.00	36.23	25	21.70	36.22	25.25
43	19.77	36.18	50	19.50	36.25	25.86
64	19.14	36.47	75	19.75	36.44	26.20
86	18.39	36.41	100	18.15	36.39	26.32
128	17.72	36.34	150	17.20	36.26	26.45
171	16.59	36.19	200	16.10	36.10	26.58
257	15.09	35.94	300	14.30	35.81	26.77
353	13.19	35.65	400	12.05	35.51	27.00
600	7.82	35.04	600	7.80	35.04	27.35
802	6.49	35.09	800	6.50	35.09	27.57
1,003	5.11	34.98	1,000	5.10	34.98	27.66
1,206	4.26	34.88	1,500	3.95	34.88	27.71
1,614	3.84	34.88	2,000	3.50	34.84	27.73
2,024	3.50	34.84				
2,539	3.23	34.82				

Tables of Oceanographic Data—Continued

STATIONS OCCUPIED IN 1950—Continued

Observed values			Scaled Values			
Depth, meters	Temperature ° C.	Salinity ‰	Depth, meters	Temperature ° C.	Salinity ‰	σ_t
Station 4180; June 10; latitude 40°46′ N., longitude 50°34′ W., depth 3,566 meters, dynamic height 971.467						
0	22.32	36.34	0	22.32	36.34	25.16
14	22.19	36.34	25	19.40	36.06	25.74
28	19.20	35.99	50	18.60	36.36	26.18
41	18.96	36.36	75	17.05	36.29	26.51
55	18.08	36.35	100	16.80	36.25	26.53
82	16.87	36.27	150	16.75	36.24	26.54
165	16.71	36.22	200	15.25	35.81	26.56
206	15.02	35.73	300	13.00	35.42	26.74
566	8.10	35.10	400	11.10	35.27	26.99
757	5.65	34.98	600	7.55	35.07	27.42
949	4.65	34.96	800	5.30	34.98	27.64
1,140	4.22	34.94	1,000	4.50	34.96	27.72
1,523	3.68	34.90	1,500	3.70	34.90	27.76
1,918	3.57	34.92	2,000	3.50	34.92	27.80
2,418	3.17	34.90				
Station 4181; June 10; latitude 41°10′ N., longitude 50°25′ W., depth 4,115 meters, dynamic height 971.489						
0	21.63	36.15	0	21.63	36.15	25.21
21	21.50	36.13	25	21.00	36.09	25.35
42	18.18	35.91	50	18.35	36.07	26.02
63	18.57	36.33	75	18.50	36.31	26.16
84	18.31	36.28	100	17.75	36.23	26.28
126	16.61	36.12	150	15.50	35.92	26.59
168	14.89	35.72	200	14.40	35.67	26.64
252	13.71	35.59	300	12.65	35.44	26.82
358	11.51	35.26	400	10.85	35.23	27.00
531	8.82	35.13	600	7.75	35.07	27.39
704	6.30	34.98	800	5.40	34.96	27.62
876	5.00	34.96	1,000	4.65	34.96	27.71
1,056	4.59	34.96	1,500	4.20	34.97	27.77
1,421	4.31	34.98	2,000	3.55	34.91	27.78
1,803	3.71	34.92				
2,297	3.35	34.90				
Station 4182; June 11; latitude 41°36′ N., longitude 50°09′ W., depth 3,749 meters, dynamic height 971.305						
0	18.18	35.70	0	18.18	35.70	25.78
25	17.73	36.05	25	17.73	36.05	26.16
50	17.18	36.17	50	17.18	36.17	26.39
76	16.87	36.24	75	16.90	36.24	26.50
101	15.77	35.97	100	15.80	35.98	26.56
151	13.77	35.56	150	13.80	35.57	26.69
201	13.13	35.56	200	13.15	35.56	26.81
302	10.99	35.34	300	11.05	35.34	27.04
409	8.12	35.02	400	8.40	35.04	27.26
598	5.29	34.86	600	5.25	34.86	27.56
793	------	34.90	800	4.50	34.90	27.67
986	4.17	34.91	1,000	4.15	34.91	27.72
1,184	3.92	34.90	1,500	3.70	34.89	27.75
1,577	3.66	34.89	2,000	3.50	34.89	27.77
1,981	3.53	34.89				
2,494	3.20	34.90				

Observed Values			Scaled Values			
Depth, meters	Temperature ° C.	Salinity ‰	Depth, meters	Temperature ° C.	Salinity ‰	σ_t
Station 4183; June 11; latitude 42°00′ N., longitude 49°58′ W., depth 3,512 meters, dynamic height 971.078						
0	10.57	32.88	0	10.57	32.88	25.22
24	5.87	33.23	25	5.85	33.24	26.21
49	5.63	33.72	50	5.65	33.75	26.63
73	9.87	34.86	75	9.85	34.85	26.88
98	6.00	34.29	100	5.95	34.29	27.02
146	5.54	34.40	150	5.50	34.40	27.16
195	5.25	34.48	200	5.20	34.49	27.27
293	3.56	34.62	300	3.50	34.62	27.56
408	3.34	34.62	400	3.35	34.62	27.57
477	4.32	34.80	600	4.35	34.89	27.68
639	4.35	34.90	800	3.75	34.855	27.715
803	3.76	34.86	1,000	3.65	34.845	27.715
971	3.66	34.84	1,500	3.65	34.90	27.76
1,316	3.75	34.90	2,000	3.40	34.90	27.79
1,668	3.58	34.90				
2,122	3.32	34.90				
Station 4184; June 11; latitude 42°26′ N., longitude 50°08′ W., depth 2,866 meters, dynamic height 970.999						
0	9.86	33.11	0	9.86	33.11	25.52
26	3.75	33.38	25	4.25	33.36	26.47
51	2.98	33.82	50	2.95	33.80	26.95
77	2.97	34.08	75	2.95	34.06	27.16
103	2.68	34.18	100	2.70	34.16	27.26
153	3.93	34.52	150	3.90	34.50	27.42
205	3.91	34.61	200	3.90	34.60	27.50
308	4.50	34.80	300	4.50	34.79	27.58
414	4.24	34.85	400	4.25	34.84	27.65
615	4.28	34.91	600	4.30	34.91	27.70
816	3.76	34.86	800	3.75	34.86	27.72
1,017	3.83	34.89	1,000	3.85	34.89	27.73
1,220	3.63	34.88	1,500	3.55	34.90	27.77
1,621	3.52	34.90	2,000	3.30	34.89	27.79
2,035	3.29	34.89				
2,557	2.99	34.89				
Station 4185; June 11; latitude 42°40.5′ N., longitude 50°10′ W., depth 1,335 meters, dynamic height 971.025						
0	8.84	33.22	0	8.84	33.22	25.76
25	4.87	33.56	25	4.87	33.56	26.58
49	4.18	33.84	50	4.15	33.85	26.87
74	4.66	34.17	75	4.70	34.18	27.08
98	5.48	34.38	100	5.45	34.38	27.15
147	4.65	34.37	150	4.60	34.38	27.25
197	4.58	34.54	200	4.60	34.55	27.38
295	5.17	34.84	300	5.15	34.85	27.56
403	5.03	34.91	400	5.05	34.91	27.62
602	4.31	34.90	600	4.30	34.90	27.69
798	4.11	34.91	800	4.10	34.91	27.73
994	3.79	34.90	1,000	3.80	34.90	27.75
1,190	3.49	34.87				
Station 4186; June 11; latitude 42°49′ N., longitude 50°12′ W., depth 310 meters, dynamic height 971.063						
0	8.59	33.40	0	8.59	33.40	25.95
26	5.37	33.70	25	5.45	33.69	26.61
53	4.64	34.02	50	4.65	34.00	26.94
79	4.61	34.14	75	4.60	34.12	27.05
106	5.01	34.29	100	4.95	34.26	27.12
160	4.92	34.40	150	4.95	34.38	27.21
213	5.52	34.60	200	5.45	34.55	27.28
255	4.62	34.54	(300)	4.50	34.53	27.38

Tables of Oceanographic Data—Continued

STATIONS OCCUPIED IN 1950—Continued

Station 4187; June 11; latitude 42°56′ N., longitude 50°13′ W., depth 85 meters, dynamic height 971.063

Observed values			Scaled values			
Depth, meters	Temperature ° C.	Salinity ‰	Depth, meters	Temperature ° C.	Salinity ‰	σ_t
0	7.11	33.20	0	7.11	33.20	26.02
26	5.92	33.87	25	6.00	33.83	26.65
52	4.73	34.10	50	4.80	34.09	27.00
78	4.13	34.08	75	4.20	34.09	27.06

Station 4188; June 12; latitude 43°20′ N., longitude 50°15′ W., depth 59 meters, dynamic height 971.094

Observed values			Scaled values			
Depth, meters	Temperature ° C.	Salinity ‰	Depth, meters	Temperature ° C.	Salinity ‰	σ_t
0	8.58	32.79	0	8.58	32.79	25.47
23	2.98	32.96	25	2.75	32.98	26.32
46	0.69	33.12	50	0.50	33.14	26.60

Station 4189; June 12; latitude 43°06′ N., longitude 50°39′ W., depth 93 meters, dynamic height 971.090

Observed values			Scaled values			
Depth, meters	Temperature ° C.	Salinity ‰	Depth, meters	Temperature ° C.	Salinity ‰	σ_t
0	8.01	32.80	0	8.01	32.80	25.58
26	3.64	33.03	25	3.90	33.01	26.24
51	0.26	33.20	50	0.30	33.18	26.65
77	0.54	33.47	75	0.50	33.44	26.84

Station 4190; June 21; latitude 42°59.5′ N., longitude 50°50′ W., depth 177 meters, dynamic height 971.063

Observed values			Scaled values			
Depth, meters	Temperature ° C.	Salinity ‰	Depth, meters	Temperature ° C.	Salinity ‰	σ_t
0	8.69	33.23	0	8.69	33.23	25.80
26	4.84	33.54	25	4.90	33.51	26.53
51	4.39	34.04	50	4.40	34.02	26.99
77	4.72	34.21	75	4.70	34.20	27.10
103	4.71	34.29	100	4.70	34.28	27.16
154	4.71	34.33	150	4.70	34.33	27.19

Station 4191; June 12; latitude 42°55.5′ N., longitude 50°56′W., depth 650 meters, dynamic height 971.049

Observed values			Scaled values			
Depth, meters	Temperature ° C.	Salinity ‰	Depth, meters	Temperature ° C.	Salinity ‰	σ_t
0	8.76	33.10	0	8.76	33.10	25.69
25	3.49	33.42	25	3.49	33.42	26.60
50	5.63	34.32	50	5.63	34.32	27.08
75	5.42	34.32	75	5.42	34.32	27.11
100	5.28	34.34	100	5.28	34.34	27.14
150	5.47	34.48	150	5.47	34.48	27.23
200	5.24	34.56	200	5.24	34.56	27.32
300	4.25	34.60	300	4.25	34.60	27.46
392	4.23	34.72	400	4.20	34.73	27.57
588	3.86	34.80	600	3.85	34.80	27.66

Station 4192; June 12; latitude 42°50′ N., longitude 51°06′ W., depth 1,454 meters, dynamic height 971.020

Observed values			Scaled values			
Depth, meters	Temperature ° C.	Salinity ‰	Depth, meters	Temperature ° C.	Salinity ‰	σ_t
0	9.67	33.06	0	9.67	33.06	25.52
24	5.16	33.40	25	5.00	33.41	26.44
49	2.23	33.69	50	2.25	33.70	26.93
73	3.14	33.92	75	3.20	33.94	27.04
97	3.53	34.11	100	3.60	34.14	27.16
146	5.20	34.46	150	5.20	34.47	27.26
195	4.13	34.50	200	4.15	34.51	27.40
292	4.38	34.74	300	4.40	34.75	27.56
362	4.52	34.82	400	4.50	34.85	27.63
548	4.30	34.90	600	4.10	34.89	27.71
738	3.52	34.83	800	3.50	34.84	27.73
930	3.51	34.84	1,000	3.50	34.84	27.73
1,361	3.52	34.845				

Station 4193; June 12; latitude 42°42′ N., longitude 51°22′W., depth 2,103 meters, dynamic height 970.999

Observed Values			Scaled Values			
Depth, meters	Temperature ° C.	Salinity ‰	Depth, meters	Temperature ° C.	Salinity ‰	σ_t
0	10.34	33.30	0	10.34	33.30	25.59
23	6.39	33.31	25	6.25	33.32	26.22
46	4.31	33.56	50	3.90	33.60	26.71
69	2.67	33.83	75	2.40	33.87	27.06
92	2.13	33.96	100	2.15	34.00	27.18
138	2.89	34.29	150	3.10	34.36	27.39
184	3.50	34.53	200	3.65	34.59	27.51
276	4.05	34.76	300	4.15	34.79	27.62
332	4.26	34.82	400	4.35	34.87	27.67
508	4.39	34.92	600	4.25	34.91	27.71
689	4.02	34.89	800	3.70	34.87	27.74
872	3.59	34.86	1,000	3.50	34.87	27.76
1,350	3.51	34.87				

Station 4194; June 12; latitude 42°21′ N., longitude 51°39′ W., depth 3,100 meters, dynamic height 971.017

Observed Values			Scaled Values			
Depth, meters	Temperature ° C.	Salinity ‰	Depth, meters	Temperature ° C.	Salinity ‰	σ_t
0	11.65	33.12	0	11.65	33.12	25.22
24	6.13	33.37	25	6.05	33.37	26.28
48	3.02	33.51	50	3.00	33.53	26.73
72	2.63	33.80	75	2.60	33.73	26.92
96	2.49	34.01	100	2.50	34.04	27.18
144	3.41	34.32	150	3.45	34.35	27.34
192	3.82	34.53	200	3.85	34.55	27.46
288	4.07	34.72	300	4.10	34.74	27.59
339	4.26	34.79	400	4.40	34.86	27.65
517	4.50	34.93	600	4.30	34.93	27.71
701	3.97	34.915	800	3.85	34.91	27.75
890	3.80	34.905	1,000	3.75	34.90	27.75
1,383	3.53	34.90				

Station 4195; June 12; latitude 41°57.5′ N., longitude 51°53′ W., depth 3,621 meters, dynamic height 971.196

Observed Values			Scaled Values			
Depth, meters	Temperature ° C.	Salinity ‰	Depth, meters	Temperature ° C.	Salinity ‰	σ_t
0	14.38	34.16	0	14.38	34.16	25.48
24	13.16	34.70	25	13.15	34.76	26.20
48	15.60	35.78	50	15.55	35.78	26.46
72	12.42	35.14	75	12.30	35.14	26.66
95	12.13	35.20	100	12.15	35.23	26.76
144	12.86	35.50	150	12.80	35.50	26.84
191	11.98	35.48	200	11.70	35.45	27.02
286	8.65	34.98	300	8.55	35.03	27.23
281	9.73	35.20	400	5.20	34.72	27.45
438	4.53	34.66	600	4.45	34.83	27.62
606	4.44	34.84	800	4.20	34.91	27.72
771	4.23	34.91	1,000	4.05	34.92	27.74
1,208	3.92	34.93				

Station 4196; June 13; latitude 42°00′ N., longitude 50°42′ W., depth 3,383 meters, dynamic height 971.183

Observed Values			Scaled Values			
Depth, meters	Temperature ° C.	Salinity ‰	Depth, meters	Temperature ° C.	Salinity ‰	σ_t
0	18.68	35.80	0	18.68	35.80	25.73
26	16.13	35.83	25	16.30	35.83	26.34
51	15.35	35.90	50	15.35	35.90	26.60
77	14.39	35.73	75	14.45	35.75	26.68
102	13.67	35.61	100	13.70	35.62	26.75
155	12.85	35.52	150	12.90	35.53	26.84
206	11.85	35.43	200	12.00	35.44	26.95
308	8.26	35.04	300	8.50	35.07	27.27
338	7.58	34.97	400	6.55	34.96	27.47
505	5.62	34.96	600	5.20	34.98	27.65
672	4.86	34.99	800	4.25	34.93	27.72
853	4.08	34.90	1,000	3.80	34.88	27.73
1,326	3.57	34.87				

STATIONS OCCUPIED IN 1950—Continued

Station 4197; June 13; latitude 42°05.5′ N., longitude 49°16′ W., depth, 3,109 meters, dynamic height 971.028

Observed values			Scaled values			
Depth, meters	Temperature ° C.	Salinity ‰	Depth, meters	Temperature ° C.	Salinity ‰	σ_t
0	10.77	33.09	0	10.77	33.09	25.34
25	6.21	33.17	25	6.21	33.17	26.10
48	3.71	33.42	50	3.55	33.44	26.61
73	2.49	33.70	75	2.50	33.75	26.95
97	2.67	33.98	100	2.65	33.99	27.13
146	2.19	34.15	150	2.20	34.17	27.32
194	2.33	34.34	200	2.40	34.37	27.46
291	4.14	34.75	300	4.00	34.73	27.59
275	3.76	34.66	400	4.10	34.81	27.65
408	4.11	34.81	600	4.30	34.91	27.70
540	4.37	34.90	(800)	3.95	34.91	27.74
676	4.14	34.91	(1,000)	3.75	34.90	27.75

Station 4198; June 13; latitude 41°28.5′ N. longitude 49°00′ W., depth 2,724 meters, dynamic height 971.301

Observed values			Scaled values			
Depth, meters	Temperature ° C.	Salinity ‰	Depth, meters	Temperature ° C.	Salinity ‰	σ_t
0	20.26	35.83	0	20.26	35.83	25.32
22	18.94	35.84	25	18.55	35.84	25.79
44	16.32	35.84	50	15.30	35.80	26.54
66	14.11	35.84	75	14.30	35.55	26.56
88	14.68	35.73	100	14.30	35.66	26.65
132	13.32	35.49	150	13.20	35.48	26.74
179	13.00	35.48	200	12.80	35.49	26.83
264	12.13	35.50	300	11.45	35.44	27.05
263	12.14	35.56	400	8.70	35.08	27.24
397	8.81	35.09	(600)	4.85	34.87	27.61
			(800)	4.50	34.90	27.67
			(1,000)	4.25	34.90	27.70

Station 4199; June 13–14; latitude 41°59′ N., longitude 47°57′ W., depth 3,713 meters, dynamic height 971.058

Observed values			Scaled values			
Depth, meters	Temperature ° C.	Salinity ‰	Depth, meters	Temperature ° C.	Salinity ‰	σ_t
0	13.18	33.16	0	13.18	33.16	24.96
27	5.88	33.41	25	6.50	33.39	26.23
53	3.76	33.60	50	3.85	33.58	26.69
80	2.82	33.86	75	2.90	33.80	26.96
107	2.82	34.03	100	2.80	33.99	27.12
161	3.06	34.25	150	3.00	34.21	27.28
214	3.76	34.46	200	3.55	34.40	27.37
321	4.08	34.71	300	4.00	34.49	27.40
396	5.06	34.92	400	5.05	34.92	27.63
601	4.45	34.94	600	4.45	34.94	27.71
813	4.13	34.935	800	4.15	34.94	27.74
1,023	3.87	34.91	1,000	3.90	34.91	27.75
1,557	3.61	34.93				

Station 4200; June 14; latitude 42°22′ N., longitude 48°36′ W., depth 3,246 meters, dynamic height 971.003

Observed values			Scaled values			
Depth, meters	Temperature ° C.	Salinity ‰	Depth, meters	Temperature ° C.	Salinity ‰	σ_t
0	11.17	33.25	0	11.17	33.25	25.40
24	5.63	33.37	25	5.55	33.37	26.34
48	4.00	33.56	50	3.75	33.57	26.70
72	2.43	33.84	75	2.45	33.88	27.05
96	2.97	34.09	100	3.00	34.11	27.20
144	3.65	34.42	150	3.75	34.45	27.39
192	4.43	34.64	200	4.50	34.66	27.48
288	4.81	34.87	300	4.80	34.87	27.62
356	4.67	34.88	400	4.65	34.90	27.66
545	4.54	34.95	600	4.45	34.95	27.72
741	4.11	34.94	800	3.95	34.92	27.75
934	3.69	34.88	1,000	3.65	34.89	27.75
1,431	3.62	34.92				

Station 4201; June 14; latitude 42°39′ N., longitude 49°02′ W., depth 2,482 meters, dynamic height 971.051

Observed values			Scaled Values			
Depth, meters	Temperature ° C.	Salinity ‰	Depth, meters	Temperature ° C.	Salinity ‰	σ_t
0	10.03	33.08	0	10.03	33.08	25.47
25	5.58	33.62	25	5.58	33.62	26.54
50	3.44	33.82	50	3.44	33.82	26.92
75	3.84	33.97	75	3.84	33.97	27.00
101	5.51	34.34	100	5.45	34.32	27.11
151	6.80	34.68	150	6.80	34.67	27.21
201	6.41	34.78	200	6.45	34.78	27.34
302	4.10	34.60	300	4.10	34.60	27.48
393	4.15	34.74	400	4.15	34.75	27.59
593	4.55	34.93	600	4.55	34.93	27.69
795	4.08	34.90	800	4.10	34.90	27.72
994	3.82	34.89	1,000	3.80	34.89	27.74
1,489	3.60	34.90				

Station 4202; June 14; latitude 43°19.5′ N., longitude 48°50′ W., depth 1,957 meters, dynamic height 971.002;

Observed values			Scaled Values			
Depth, meters	Temperature ° C.	Salinity ‰	Depth, meters	Temperature ° C.	Salinity ‰	σ_t
0	9.72	33.30	0	9.72	33.03	25.69
26	7.01	33.52	25	7.15	33.51	26.25
51	3.64	33.81	50	3.70	33.80	26.88
77	3.30	34.06	75	3.30	34.05	27.12
102	3.74	34.16	100	3.70	34.15	27.16
152	4.07	34.48	150	4.05	34.47	27.38
203	4.12	34.62	200	4.10	34.61	27.49
305	4.46	34.79	300	4.45	34.78	27.58
370	4.91	34.93	400	4.85	34.93	27.65
559	4.36	34.93	600	4.30	34.93	27.71
749	4.01	34.92	800	3.95	34.92	27.75
944	3.77	34.90	1,000	3.70	34.90	27.76
1,442	3.60	34.90				

Station 4203; June 14; latitude 43°03′ N., longitude 48°13′ W., depth 3,060 meters, dynamic height 971.013

Observed values			Scaled Values			
Depth, meters	Temperature ° C.	Salinity ‰	Depth, meters	Temperature ° C.	Salinity ‰	σ_t
0	10.39	33.33	0	10.39	33.33	25.61
26	7.04	33.49	25	7.25	33.48	26.21
51	4.56	33.78	50	4.65	33.77	26.76
76	3.00	33.96	75	3.00	33.95	27.07
101	3.22	34.15	100	3.20	34.14	27.20
152	3.88	34.44	150	3.85	34.43	27.37
203	4.13	34.58	200	4.10	34.57	27.46
304	4.71	34.83	300	4.70	34.82	27.59
384	4.67	34.90	400	4.65	34.90	27.66
579	4.32	34.92	600	4.30	34.92	27.71
779	4.04	34.91	800	4.05	34.91	27.73
981	3.87	34.90	1,000	3.85	34.90	27.74
1,501	3.52	34.91				

Station 4204; June 15; latitude 42°52′ N., longitude 47°32′ W., depth 3,493 meters, dynamic height 971.090

Observed values			Scaled Values			
Depth, meters	Temperature ° C.	Salinity ‰	Depth, meters	Temperature ° C.	Salinity ‰	σ_t
0	13.24	33.21	0	13.24	33.21	24.98
27	5.74	33.20	25	6.40	33.20	26.11
52	3.20	33.33	50	3.30	33.29	26.51
79	8.20	34.60	75	7.90	34.59	26.98
104	6.58	34.43	100	6.80	34.44	27.02
157	5.81	34.44	150	5.95	34.44	27.14
210	5.02	34.43	200	5.10	34.43	27.23
314	5.02	34.72	300	5.05	34.69	27.44
419	4.68	34.84	400	4.75	34.82	27.58
627	4.33	34.92	600	4.35	34.92	27.71
834	4.11	34.91	800	4.20	34.91	27.72
1,044	3.84	34.90	1,000	3.85	34.90	27.74
1,571	3.61	34.91				

STATIONS OCCUPIED IN 1950—Continued

Station 4205; June 15; latitude 42°38′ N., longitude 46°54′ W., depth 4,061 meters, dynamic height 971.382

Observed Values			Scaled Values			
Depth, meters	Temperature ° C.	Salinity ‰	Depth, meters	Temperature ° C.	Salinity ‰	σ_t
0	18.08	35.58	0	18.08	35.58	25.72
27	15.97	35.65	25	16.20	35.65	26.22
52	14.93	35.61	50	14.90	35.61	26.48
79	15.20	35.82	75	15.20	35.79	26.55
105	15.11	35.87	100	15.15	35.87	26.62
158	14.75	35.86	150	14.80	35.86	26.69
210	14.11	35.75	200	14.25	35.77	26.75
315	12.55	35.55	300	12.75	35.57	26.91
404	11.54	35.46	400	11.60	35.47	27.05
605	7.37	35.02	600	7.45	35.03	27.39
807	5.38	34.97	800	5.40	34.97	27.63
1,012	4.48	34.925	1,000	4.50	34.93	27.69
1,527	3.74	34.90				

Station 4206; June 15; latitude 43°01.5′ N., longitude 46°27′ W., depth 4,207 meters, dynamic height 971.416

Observed Values			Scaled Values			
Depth, meters	Temperature ° C.	Salinity ‰	Depth, meters	Temperature ° C.	Salinity ‰	σ_t
0	17.83	36.00	0	17.83	36.00	26.11
27	15.86	36.08	25	15.90	36.08	26.61
52	15.74	36.08	50	15.75	36.08	26.64
79	15.68	36.09	75	15.70	36.09	26.68
104	15.68	36.10	100	15.65	36.10	26.70
158	15.31	36.03	150	15.35	36.05	26.72
210	14.78	35.92	200	14.70	35.94	26.78
314	13.90	35.84	300	14.05	35.86	26.86
421	12.32	35.60	400	12.70	35.65	26 98
628	7.67	35.03	600	8.30	35.07	27.31
836	5.57	35.00	800	5.80	35.00	27.60
1,032	4.72	34.98	1,000	4.80	34.98	27.70
1,500	3.84	34.91				

Station 4207; June 15; latitude 43°23′ N., longitude 46°10′ W., depth 4,663 meters, dynamic height 971.402

Observed Values			Scaled Values			
Depth, meters	Temperature ° C.	Salinity ‰	Depth, meters	Temperature ° C.	Salinity ‰	σ_t
0	18.34	35.80	0	18.34	35.80	25.82
27	16.04	36.04	25	16.10	36.04	26.54
53	15.54	35.95	50	15.60	35.96	26.59
80	15.05	35.88	75	15.10	35.89	26.65
106	15.14	35.93	100	15.10	35.92	26.68
161	14.88	35.93	150	14.95	35.93	26.72
214	14.28	35.81	200	14.45	35.84	26.76
320	13.42	35.76	300	13.60	35.78	26.89
416	11.71	35.48	400	12.05	35.53	27.01
621	7.41	35.03	600	7.85	35.04	27.35
824	5.36	34.99	800	5.55	34.99	27.62
1,029	4.15	34.89	1,000	4.25	34.90	27.70
1,537	3.67	34.89				

Station 4208; June 15; latitude 43°34′ N., longitude 46°34′ W., depth 4,427 meters, dynamic height 971.163

Observed Values			Scaled Values			
Depth, meters	Temperature ° C.	Salinity ‰	Depth, meters	Temperature ° C.	Salinity ‰	σ_t
0	13.56	33.20	0	13.56	33.20	24.90
27	7.65	33.38	25	7.70	33.34	26.03
53	11.08	34.68	50	11.00	34.52	26.42
80	8.28	34.41	75	8.70	34.45	26.75
107	9.27	34.81	100	9.10	34.73	26.91
161	7.09	34.58	150	7.50	34.61	27.06
214	6.61	34.58	200	6.75	34.58	27.14
321	4.11	34.41	300	4.55	34.43	27.29
390	5.58	34.81	400	5.55	34.82	27.49
578	5.00	34.92	600	4.90	34.92	27.65
760	4.43	34.92	800	4.35	34.92	27.71
952	4.15	34.92	1,000	4.10	34.92	27.74
1,435	3.73	34.90				

Station 4209; June 16; latitude 43°40.5′ N., longitude 47°19′ W., depth 4,042 meters, dynamic height 971.065

Observed Values			Scaled Values			
Depth, meters	Temperature ° C.	Salinity ‰	Depth, meters	Temperature ° C.	Salinity ‰	σ_t
0	9.68	33.16	0	9.68	33.16	25.60
26	5.78	33.36	25	6.05	33.35	26.26
52	3.20	33.48	50	3.20	33.47	26.67
78	3.28	33.92	75	3.25	33.87	26.98
104	3.61	34.02	100	3.50	34.00	27.06
156	4.71	34.40	150	4.60	34.37	27.24
208	4.89	34.55	200	4.85	34.53	27.34
312	4.62	34.68	300	4.65	34.66	27.47
396	5.04	34.89	400	5.05	34.90	27.61
595	4.52	34.92	600	4.50	34.92	27.69
795	4.09	34.89	800	4.10	34.89	27.71
994	3.93	34.90	1,000	3.95	34.90	27.73
1,495	3.67	34.89				

Station 4210; June 16; latitude 43°50′ N., longitude 47°54′ W., depth 3,749 meters, dynamic height 971.177

Observed Values			Scaled Values			
Depth, meters	Temperature ° C.	Salinity ‰	Depth, meters	Temperature ° C.	Salinity ‰	σ_t
0	10.30	33.81	0	10.30	33.81	25.99
26	10.48	34.64	25	10.50	34.60	26.57
53	10.57	34.86	50	10.55	34.83	26.74
79	11.17	35.08	75	11.05	35.05	26.82
105	11.53	35.19	100	11.50	35.18	26.84
157	10.80	35.11	150	11.00	35.13	26.89
209	8.00	34.75	200	8.30	34.78	27.07
314	7.25	34.82	300	7.35	34.80	27.23
416	6.55	34.92	400	6.65	34.91	27.42
622	5.10	34.94	600	5.25	34.94	27.62
827	4.32	34.90	800	4.40	34.90	27.68
1,032	3.98	34.89	1,000	4.00	34.89	27.72
1,541	3.54	34.86				

Station 4211; June 16; latitude 43°58′ N., longitude 48°23′ W., depth 3,402 meters, dynamic height 971.044

Observed Values			Scaled Values			
Depth, meters	Temperature ° C.	Salinity ‰	Depth, meters	Temperature ° C.	Salinity ‰	σ_t
0	5.22	32.78	0	5.22	32.78	25.91
25	2.64	32.86	25	2.64	32.86	26.23
50	0.09	33.24	50	0.09	33.24	26.71
75	−1.00	33.40	75	−1.00	33.40	26.88
101	−0.28	33.51	100	−0.30	33.50	26.93
151	−0.22	33.75	150	−0.20	33.75	27.13
201	1.13	34.09	200	1.10	34.08	27.32
302	2.47	34.51	300	2.45	34.50	27.55
382	3.72	34.74	400	3.75	34.75	27.63
580	3.65	34.82	600	3.60	34.82	27.71
761	3.38	34.81	800	3.40	34.81	27.72
953	3.44	34.84	1,000	3.45	34.85	27.74
1,439	3.49	34.89				

Station 4212; June 16; latitude 44°07′ N., longitude 48°50′ W., depth 1,752 meters, dynamic height 971.035

Observed Values			Scaled Values			
Depth, meters	Temperature ° C.	Salinity ‰	Depth, meters	Temperature ° C.	Salinity ‰	σ_t
0	3.23	32.88	0	3.23	32.88	26.20
24	1.35	33.00	25	1.20	33.01	26.46
49	−0.97	33.34	50	−1.00	33.35	26.84
73	−1.30	33.45	75	−1.30	33.46	26.94
97	−1.21	33.51	100	−1.15	33.51	26.98
146	−0.72	33.66	150	−0.70	33.67	27.09
195	−0.08	33.84	200	0.00	33.86	27.21
292	1.92	34.42	300	2.00	34.44	27.54
383	2.50	34.58	400	2.60	34.60	27.62
577	------	34.74	600	3.10	34.75	27.70
774	3.27	34.81	800	3.30	34.82	27.74
968	3.40	34.835	1,000	3.40	34.84	27.74
1,454	3.48	34.84				

STATIONS OCCUPIED IN 1950—Continued

Station 4213; June 16; latitude 44°11′ N., longitude 48°59′ W., depth 714 meters, dynamic height 971.039

Observed values			Scaled values			
Depth, meters	Temperature ° C.	Salinity ‰	Depth, meters	Temperature ° C.	Salinity ‰	σ_t
0	5.44	32.75	0	5.44	32.75	25.86
27	−0.63	33.20	25	−0.40	33.17	26.67
53	−1.44	33.34	50	−1.40	33.33	26.83
80	−1.54	33.40	75	−1.50	33.39	26.89
106	−1.41	33.43	100	−1.45	33.42	26.91
160	0.03	33.85	150	−0.25	33.77	27.15
213	1.10	34.14	200	0.90	34.08	27.33
319	1.68	34.36	300	1.60	34.31	27.47
393	2.69	34.64	400	2.75	34.65	27.65
543	2.98	34.70	(600)	3.05	34.72	27.68

Station 4214; June 16; latitude 44°11′ N., longitude 49°04′ W., depth 174 meters, dynamic height 971.078

Observed values			Scaled values			
Depth, meters	Temperature ° C.	Salinity ‰	Depth, meters	Temperature ° C.	Salinity ‰	σ_t
0	5.82	32.70	0	5.82	32.70	25.78
25	3.42	32.82	25	3.42	32.82	26.13
49	−0.03	33.10	50	−0.15	33.11	26.61
74	−1.23	33.25	75	−1.25	33.25	26.76
99	−1.41	33.30	100	−1.40	33.30	26.80
138	−1.21	33.44	(150)	−1.15	33.48	26.95

Station 4215; June 16; latitude 44°12′ N., longitude 49°11′ W., depth 88 meters, dynamic height 971.064

Observed values			Scaled values			
Depth, meters	Temperature ° C.	Salinity ‰	Depth, meters	Temperature ° C.	Salinity ‰	σ_t
0	6.18	32.69	0	6.18	32.69	25.72
26	1.62	32.96	25	1.85	32.95	26.36
52	−0.91	33.22	50	−0.80	33.20	26.71
			(75)	−1.20	33.40	26.89

Station 4216; June 17; latitude 44°14′ N., longitude 49°23′ W., depth 57 meters, dynamic height 971.068

Observed values			Scaled values			
Depth, meters	Temperature ° C.	Salinity ‰	Depth, meters	Temperature ° C.	Salinity ‰	σ_t
0	7.31	32.78	0	7.31	32.78	25.66
24	2.53	32.96	25	2.40	32.96	26.33
48	−0.06	33.16	50	−0.25	33.17	26.66

Station 4217; June 17; latitude 44°58.5′ N., longitude 49°18′ W., depth 73 meters, dynamic height 971.079

Observed values			Scaled values			
Depth, meters	Temperature ° C.	Salinity ‰	Depth, meters	Temperature ° C.	Salinity ‰	σ_t
0	6.34	32.73	0	6.34	32.73	25.74
25	0.93	32.94	25	0.93	32.94	26.42
50	−0.33	33.02	50	−0.33	33.02	26.54

Station 4218; June 17; latitude 44°57′ N., longitude 49°12′ W., depth 270 meters, dynamic height 971.067

Observed values			Scaled values			
Depth, meters	Temperature ° C.	Salinity ‰	Depth, meters	Temperature ° C.	Salinity ‰	σ_t
0	5.85	32.71	0	5.85	32.71	25.79
25	−0.36	33.01	25	−0.36	33.01	26.54
50	−1.53	33.20	50	−1.53	33.20	26.73
75	−1.60	33.22	75	−1.60	33.22	26.75
100	−1.59	33.24	100	−1.59	33.24	26.76
150	−1.09	33.50	150	−1.09	33.50	26.96
200	0.12	33.87	200	0.12	33.87	27.21

Station 4219; June 17; latitude 44°55′ N., longitude 48°58′ W., depth 649 meters, dynamic height 971.081

Observed values			Scaled Values			
Depth, meters	Temperature ° C.	Salinity ‰	Depth, meters	Temperature ° C.	Salinity ‰	σ_t
0	5.65	32.72	0	5.65	32.72	25.82
25	3.52	32.78	25	3.52	32.78	26.09
50	−1.51	33.22	50	−1.51	33.22	26.75
75	−1.52	33.34	75	−1.52	33.34	26.85
100	−1.43	33.40	100	−1.43	33.40	26.90
150	−0.96	33.56	150	−0.96	33.56	27.01
200	−0.28	33.76	200	−0.28	33.76	27.14
300	2.23	34.50	300	2.23	34.50	27.57
398	2.55	34.59	400	2.55	34.59	27.62
596	2.78	34.66	600	2.80	34.66	27.65

Station 4220; June 17; latitude 44°52′ N., longitude 48°42′ W., depth 2,062 meters, dynamic height 970.994

Observed values			Scaled Values			
Depth, meters	Temperature ° C.	Salinity ‰	Depth, meters	Temperature ° C.	Salinity ‰	σ_t
0	4.41	32.87	0	4.41	32.87	26.08
27	1.67	33.26	25	1.85	33.23	26.59
53	0.25	33.51	50	0.40	33.49	26.89
79	−0.40	33.56	75	−0.30	33.55	26.97
105	−0.80	33.63	100	−0.75	33.61	27.04
159	0.83	34.00	150	0.65	33.93	27.22
211	1.48	34.28	200	1.35	34.23	27.42
316	2.60	34.63	300	2.45	34.59	27.62
417	2.80	34.70	400	2.75	34.69	27.68
626	3.33	34.80	600	3.25	34.79	27.71
838	3.36	34.82	800	3.35	34.82	27.73
1,049	3.43	34.85	1,000	3.40	34.84	27.74
1,578	3.47	34.88				

Station 4221; June 17; latitude 44°49′ N., longitude 48°26′ W., depth 2,418 meters, dynamic height 970.930

Observed values			Scaled Values			
Depth, meters	Temperature ° C.	Salinity ‰	Depth, meters	Temperature ° C.	Salinity ‰	σ_t
0	7.77	33.12	0	7.77	33.12	25.85
25	2.61	33.40	25	2.61	33.40	26.67
50	1.32	33.82	50	1.32	33.82	27.10
74	2.57	34.22	75	2.55	34.23	27.33
99	2.21	34.33	100	2.20	34.33	27.44
149	3.53	34.60	150	3.55	34.60	27.53
198	4.26	34.79	200	4.25	34.80	27.62
297	4.29	34.87	300	4.30	34.87	27.67
379	3.86	34.86	400	3.85	34.86	27.71
572	3.75	34.86	600	3.75	34.86	27.72
766	3.60	34.88	800	3.60	34.88	27.75
961	3.52	34.87	1,000	3.50	34.87	27.76
1,452	3.53	34.90				

Station 4222; June 17; latitude 44°41′ N., longitude 47°47′ W., depth 3,310 meters, dynamic height 970.934

Observed values			Scaled Values			
Depth, meters	Temperature ° C.	Salinity ‰	Depth, meters	Temperature ° C.	Salinity ‰	σ_t
0	7.52	32.85	0	7.52	32.85	25.67
24	3.21	33.30	25	3.00	33.31	26.56
47	0.71	33.68	50	0.70	33.72	27.06
71	0.56	33.94	75	0.60	33.99	27.27
94	1.50	34.20	100	1.55	34.24	27.41
141	1.88	34.42	150	1.95	34.44	27.55
188	2.35	34.56	200	2.45	34.54	27.58
282	3.00	34.71	300	3.05	34.73	27.68
350	3.17	34.75	400	3.35	34.79	27.70
530	3.75	34.89	600	3.70	34.88	27.74
715	3.60	34.87	800	3.55	34.87	27.75
904	3.50	34.87	1,000	3.50	34.87	27.76
1,393	3.55	34.90				

STATIONS OCCUPIED IN 1950—Continued

Station 4223; June 17; latitude 44°37′ N., longitude 47°10′ W., depth 3,731 meters, dynamic height 971.055

Observed Values			Scaled Values			
Depth, meters	Temperature ° C.	Salinity ‰	Depth, meters	Temperature ° C.	Salinity ‰	σ_t
0	7.11	32.67	0	7.11	32.67	25.60
25	1.49	32.91	25	1.49	32.91	26.35
49	−1.58	33.22	50	−1.60	33.23	26.75
74	−1.61	33.34	75	−1.60	33.34	26.85
98	−1.38	33.44	100	−1.35	33.45	26.93
146	−0.58	33.71	150	−0.50	33.75	27.14
196	3.56	34.32	200	3.55	34.33	27.31
294	2.03	34.39	300	2.05	34.43	27.53
362	5.16	34.90	400	5.05	34.91	27.62
547	4.49	34.91	600	4.35	34.91	27.70
735	4.11	34.91	800	4.00	34.90	27.73
926	3.75	34.89	1,000	3.70	34.89	27.75
1,420	3.56	34.89				

Station 4224; June 18; latitude 44°33′ N., longitude 46°32′ W., depth 3,841 meters, dynamic height 971.082

Observed Values			Scaled Values			
Depth, meters	Temperature ° C.	Salinity ‰	Depth, meters	Temperature ° C.	Salinity ‰	σ_t
0	7.88	32.83	0	7.88	32.83	25.62
25	−0.22	33.16	25	−0.22	33.16	26.65
51	−1.28	33.34	50	−1.30	33.34	26.84
75	−1.34	33.37	75	−1.34	33.37	26.86
101	0.05	33.52	100	0.00	33.52	26.94
151	2.65	33.95	150	2.65	33.94	27.09
202	3.46	34.17	200	3.45	34.16	27.19
303	4.44	34.62	300	4.45	34.61	27.45
390	3.99	34.66	400	4.00	34.67	27.55
586	4.40	34.90	600	4.10	34.90	27.68
783	4.09	34.89	800	4.10	34.89	27.71
980	4.00	34.90	1,000	4.00	34.90	27.73
1,480	3.58	34.90				

Station 4225; June 18; latitude 44°28′ N., longitude 46°00′ W., depth 3,749 meters, dynamic height 971.087

Observed Values			Scaled Values			
Depth, meters	Temperature ° C.	Salinity ‰	Depth, meters	Temperature ° C.	Salinity ‰	σ_t
0	8.62	32.78	0	8.62	32.78	25.45
25	1.57	33.02	25	1.57	33.02	26.44
50	−1.50	33.31	50	−1.50	33.31	26.82
75	−1.28	33.36	75	−1.28	33.36	26.85
100	−1.20	33.44	100	−1.20	33.44	26.91
150	1.46	33.77	150	1.46	33.77	27.05
199	1.88	33.93	200	1.90	33.93	27.14
299	1.21	34.17	300	1.20	34.17	27.39
382	4.73	34.83	400	4.75	34.85	27.60
575	4.49	34.92	600	4.40	34.91	27.69
768	3.69	34.85	800	3.70	34.85	27.72
962	3.79	34.90	1,000	3.75	34.90	27.75
1,451	3.56	34.89				

Station 4226; June 18; latitude 44°21.5′ N., longitude 45°28′ W., depth 4,244 meters, dynamic height 971.166

Observed Values			Scaled Values			
Depth, meters	Temperature ° C.	Salinity ‰	Depth, meters	Temperature ° C.	Salinity ‰	σ_t
0	14.30	33.02	0	14.30	33.02	24.62
26	7.06	33.35	25	7.05	33.33	26.11
51	10.98	34.75	50	10.80	34.64	26.55
76	12.06	35.27	75	12.05	35.26	26.80
101	11.94	35.36	100	11.95	35.36	26.90
153	7.82	34.62	150	8.15	34.67	27.01
204	6.15	34.44	200	6.25	34.44	27.10
305	4.54	34.43	300	4.55	34.43	27.29
386	6.54	34.95	400	6.40	34.95	27.48
586	4.24	34.82	600	4.20	34.82	27.65
793	4.14	34.90	800	4.15	34.90	27.71
997	4.12	34.93	1,000	4.10	34.93	27.74
1,515	3.75	34.92				

Station 4227; June 18; latitude 44°49′ N., longitude 45°15′ W., depth 4,079 meters, dynamic height 971.237

Observed Values			Scaled Values			
Depth, meters	Temperature ° C.	Salinity ‰	Depth, meters	Temperature ° C.	Salinity ‰	σ_t
0	15.76	35.63	0	15.76	35.63	26.30
24	14.67	35.64	25	14.65	35.64	26.56
48	14.30	35.66	50	14.25	35.66	26.66
72	14.03	35.69	75	14.00	35.69	26.73
96	13.72	35.66	100	13.60	35.65	26.79
145	12.99	35.57	150	13.00	35.57	26.85
193	12.92	35.65	200	12.75	35.63	26.95
289	10.50	35.27	300	10.30	35.25	27.11
333	9.63	35.18	400	8.35	35.08	27.30
507	6.86	34.99	600	5.95	34.98	27.56
688	5.29	34.97	800	4.75	34.96	27.69
875	4.53	34.95	1,000	4.25	34.94	27.73
1,366	3.83	34.92				

Station 4228; June 18; latitude 45°19′ N., longitude 45°15′ W., depth 4,024 meters, dynamic height 971.233

Observed Values			Scaled Values			
Depth, meters	Temperature ° C.	Salinity ‰	Depth, meters	Temperature ° C.	Salinity ‰	σ_t
0	15.12	35.67	0	15.12	35.67	26.48
24	14.77	35.70	25	14.75	35.70	26.58
48	14.09	35.60	50	14.00	35.60	26.67
72	13.88	35.64	75	13.90	35.65	26.72
96	14.42	35.80	100	14.35	35.80	26.75
144	13.49	35.66	150	13.40	35.65	26.83
192	12.81	35.56	200	12.00	35.55	27.04
288	11.29	35.42	300	11.10	35.40	27.09
287	11.38	35.43	400	9.05	35.10	27.21
429	8.45	35.04	600	5.80	34.97	27.58
572	6.08	34.97	800	4.80	34.95	27.68
732	5.11	34.96	1,000	4.10	34.91	27.73
1,162	3.82	34.89				

Station 4229; June 19; latitude 45°21.5′ N., longitude 45°58′ W., depth 3,566 meters, dynamic height 971.005

Observed Values			Scaled Values			
Depth, meters	Temperature ° C.	Salinity ‰	Depth, meters	Temperature ° C.	Salinity ‰	σ_t
0	8.07	33.16	0	8.07	33.16	25.84
25	5.80	33.14	25	5.80	33.14	26.13
50	1.05	33.36	50	1.05	33.36	26.75
75	0.46	33.61	75	0.46	33.61	26.98
99	0.66	33.82	100	0.70	33.83	27.14
148	2.67	34.26	150	2.70	34.27	27.35
198	3.09	34.53	200	3.15	34.54	27.52
297	5.15	34.93	300	5.15	34.93	27.62
434	4.74	34.95	400	4.85	34.95	27.67
652	4.19	34.92	600	4.30	34.93	27.71
871	3.86	34.91	800	3.95	34.91	27.74
1,100	3.73	34.90	1,000	3.80	34.90	27.75
1,688	3.38	34.90				

Station 4230; June 19; latitude 45°29′ N., longitude 46°35′ W., depth 2,780 meters, dynamic height 970.929

Observed Values			Scaled Values			
Depth, meters	Temperature ° C.	Salinity ‰	Depth, meters	Temperature ° C.	Salinity ‰	σ_t
0	8.37	33.49	0	8.37	33.49	26.06
22	7.27	33.70	25	7.00	33.77	26.48
43	5.58	34.16	50	5.40	34.25	27.05
64	5.16	34.40	75	4.95	34.45	27.27
85	4.82	34.49	100	4.60	34.54	27.37
129	4.30	34.63	150	4.10	34.66	27.53
172	3.95	34.68	200	3.80	34.69	27.58
257	3.53	34.71	300	3.35	34.73	27.65
275	3.40	34.72	400	3.10	34.77	27.27
423	3.11	34.78	600	3.10	34.81	27.75
579	3.10	34.81	800	3.25	34.84	27.75
752	3.26	34.84	1,000	3.30	34.86	27.77
1,233	3.33	34.88				

STATIONS OCCUPIED IN 1950—Continued

Station 4231; June 19; latitude 45°20.5′ N., longitude 47°32′ W., depth 2,469 meters, dynamic height 970.975

Observed values			Scaled values			
Depth, meters	Temperature ° C.	Salinity ‰	Depth, meters	Temperature ° C.	Salinity ‰	σ_t
0	6.62	32.56	0	6.62	32.56	25.56
26	2.82	33.29	25	2.90	33.26	26.53
51	−0.72	33.52	50	−0.70	33.51	26.96
78	2.42	34.02	75	2.00	33.97	27.17
103	3.18	34.20	100	3.15	34.18	27.23
155	3.21	34.38	150	3.20	34.36	27.38
206	4.24	34.64	200	4.20	34.62	27.49
309	4.42	34.88	300	4.40	34.88	27.66
404	4.08	34.87	400	4.10	34.87	27.70
605	3.57	34.82	600	3.55	34.82	27.71
807	3.66	34.87	800	3.65	34.87	27.74
1,012	3.63	34.89	1,000	3.65	34.89	27.75
1,527	3.47	34.90				

Station 4232; June 19; latitude 45°35′ N., longitude 47°49′ W., depth 1,418 meters, dynamic height 970.905

Observed values			Scaled values			
Depth, meters	Temperature ° C.	Salinity ‰	Depth, meters	Temperature ° C.	Salinity ‰	σ_t
3	5.63	33.11	0	5.65	33.11	26.12
28	1.80	33.62	25	1.95	33.55	26.84
53	1.42	34.01	50	1.45	33.97	27.21
77	1.30	34.16	75	1.30	34.15	27.36
102	1.49	34.28	100	1.45	34.27	27.45
152	2.19	34.53	150	2.15	34.52	27.60
202	2.56	34.63	200	2.55	34.63	27.65
301	2.95	34.74	300	2.95	34.74	27.70
397	3.09	34.77	400	3.10	34.77	27.72
596	3.59	34.86	600	3.60	34.86	27.74
796	3.46	34.845	800	3.45	34.85	27.74
995	3.43	34.845	1,000	3.45	34.85	27.74
1,391	3.40	34.88				

Station 4233; June 19; latitude 45°42′ N., longitude 48°01′ W., depth 622 meters, dynamic height 970.972

Observed values			Scaled values			
Depth, meters	Temperature ° C.	Salinity ‰	Depth, meters	Temperature ° C.	Salinity ‰	σ_t
0	4.62	32.50	0	4.62	32.50	25.75
25	1.17	33.34	25	1.17	33.34	26.72
50	−1.26	33.48	50	−1.26	33.48	26.95
75	−0.27	33.79	75	−0.27	33.79	27.16
100	0.58	34.05	100	0.58	34.05	27.32
150	1.46	34.30	150	1.46	34.30	27.47
201	1.83	34.41	200	1.80	34.41	27.54
301	2.54	34.61	300	2.55	34.61	27.64
382	2.66	34.63	400	2.70	34.64	27.64
594	3.03	34.74	600	3.05	34.74	27.69

Station 4234; June 19; latitude 45°46′ N., longitude 48°08′ W., depth 166 meters, dynamic height 971.043

Observed values			Scaled values			
Depth, meters	Temperature ° C.	Salinity ‰	Depth, meters	Temperature ° C.	Salinity ‰	σ_t
0	4.98	32.64	0	4.98	32.64	25.83
25	0.86	33.02	25	0.86	33.02	26.49
49	−1.74	33.25	50	−1.75	33.26	26.78
74	−1.59	33.37	75	−1.60	33.38	26.88
99	−1.22	33.52	100	−1.20	33.52	26.99
148	−0.90	33.60	150	−0.90	33.60	27.04

Station 4235; June 19–20; latitude 45°48′ N., longitude 48°13′ W., depth 116 meters, dynamic height 971.048

Observed values			Scaled Values			
Depth, meters	Temperature ° C.	Salinity ‰	Depth, meters	Temperature ° C.	Salinity ‰	σ_t
0	5.47	32.76	0	5.47	32.76	25.86
25	2.12	33.08	25	2.12	33.08	26.45
51	−1.21	33.36	50	−1.20	33.36	26.85
76	−1.46	33.38	75	−1.45	33.38	26.87
102	−1.44	33.37	100	−1.45	33.38	26.87

Station 4236; June 20; latitude 45°58′ N., longitude 48°29′ W., depth 93 meters, dynamic height 971.064

Observed values			Scaled Values			
Depth, meters	Temperature ° C.	Salinity ‰	Depth, meters	Temperature ° C.	Salinity ‰	σ_t
0	6.11	32.70	0	6.11	32.70	25.75
25	2.76	32.84	25	2.76	32.84	26.21
49	−0.79	33.02	50	−0.90	33.03	26.57
74	−1.54	33.23	75	−1.55	33.24	26.76

Station 4237; June 20; latitude 46°07′ N., longitude 48°43′ W., depth 77 meters, dynamic height 971.064

Observed values			Scaled Values			
Depth, meters	Temperature ° C.	Salinity ‰	Depth, meters	Temperature ° C.	Salinity ‰	σ_t
0	6.37	32.70	0	6.37	32.70	25.71
17	4.64	32.82	25	3.30	32.85	26.16
43	0.00	32.96	50	−0.90	33.02	26.57
68	−1.42	33.18	75	−1.45	33.34	26.84

Station 4238; June 20; latitude 46°17′ N., longitude 49°00′ W., depth 66 meters, dynamic height 971.063

Observed values			Scaled Values			
Depth, meters	Temperature ° C.	Salinity ‰	Depth, meters	Temperature ° C.	Salinity ‰	σ_t
0	6.41	32.87	0	6.41	32.87	25.84
27	3.48	32.82	25	3.90	32.82	26.09
54	−0.93	33.14	50	−0.75	33.08	26.61

Station 4239; July 13; latitude 50°01′ N., longitude 49°02′ W., depth 1,934 meters, dynamic height 970.858

Observed values			Scaled Values			
Depth, meters	Temperature ° C.	Salinity ‰	Depth, meters	Temperature ° C.	Salinity ‰	σ_t
0	7.83	33.40	0	7.83	33.40	26.07
23	5.37	33.54	25	5.05	33.57	26.56
47	2.76	34.28	50	2.75	34.33	27.39
70	2.81	34.56	75	2.90	34.61	27.61
93	3.09	34.71	100	3.10	34.73	27.68
140	3.11	34.78	150	3.10	34.79	27.73
187	3.14	34.81	200	3.15	34.82	27.75
280	3.18	34.83	300	3.20	34.83	27.75
334	3.20	34.83	400	3.20	34.83	27.75
508	3.21	34.84	600	3.20	34.84	27.76
686	3.20	34.85	800	3.20	34.85	27.77
864	3.23	34.86	1,000	3.25	34.86	27.77
1,319	3.27	34.88				

Station 4240; July 13; latitude 49°50′ N., longitude 49°24′ W., depth 1,454 meters, dynamic height 970.851

Observed values			Scaled Values			
Depth, meters	Temperature ° C.	Salinity ‰	Depth, meters	Temperature ° C.	Salinity ‰	σ_t
0	6.80	32.82	0	6.80	32.82	25.75
26	3.10	33.60	25	3.15	33.52	26.72
51	3.29	34.49	50	3.30	34.48	27.46
78	3.06	34.67	75	3.10	34.66	27.63
103	3.06	34.74	100	3.05	34.73	27.68
156	3.13	34.79	150	3.10	34.78	27.72
208	3.19	34.81	200	3.20	34.81	27.74
311	3.20	34.83	300	3.20	34.83	37.75
399	3.20	34.84	400	3.20	34.84	27.76
600	3.20	34.85	600	3.20	34.85	27.77
804	3.20	34.86	800	3.20	34.86	27.78
1,010	3.19	34.86	1,000	3.20	34.86	27.78
1,388	3.27	34.88				

STATIONS OCCUPIED IN 1950—Continued

Station 4241; July 13; latitude 49°37.5′ N., longitude 50°02′ W., depth 640 meters, dynamic height 970.872

Observed Values			Scaled Values			
Depth, meters	Temperature ° C.	Salinity ‰	Depth, meters	Temperature ° C.	Salinity ‰	σ_t
0	5.86	32.74	0	5.86	32.74	25.81
23	1.81	33.88	25	1.60	33.91	27.15
46	0.66	34.08	50	0.70	34.10	27.36
68	1.19	34.24	75	1.35	34.28	27.46
91	1.67	34.37	100	1.85	34.41	27.53
137	2.58	34.56	150	2.80	34.61	27.61
182	3.26	34.71	200	3.30	34.73	27.66
273	3.34	34.77	300	3.35	34.78	27.69
397	3.36	34.82	400	3.35	34.82	27.73
597	3.20	34.85	600	3.20	34.85	27.77

Station 4242; July 13; latitude 49°31′ N., longitude 50°34′ W., depth 334 meters, dynamic height 970.930

Observed Values			Scaled Values			
Depth, meters	Temperature ° C.	Salinity ‰	Depth, meters	Temperature ° C.	Salinity ‰	σ_t
0	7.43	32.65	0	7.43	32.65	25.54
26	1.92	33.11	25	2.25	33.06	26.42
52	−1.16	33.63	50	−1.15	33.61	27.06
78	−0.44	33.86	75	−0.55	33.85	27.22
104	0.28	34.03	100	0.20	34.00	27.31
157	1.01	34.25	150	0.90	34.22	27.45
209	2.15	34.48	200	2.00	34.45	27.55
313	3.12	34.74	300	3.05	34.72	27.68

Station 4243; July 13; latitude 49°20.5′ N., longitude 51°04′ W., depth 334 meters, dynamic height 970.972

Observed Values			Scaled Values			
Depth, meters	Temperature ° C.	Salinity ‰	Depth, meters	Temperature ° C.	Salinity ‰	σ_t
0	8.66	32.68	0	8.66	32.68	25.39
24	6.49	32.80	25	6.25	32.82	25.82
47	−0.23	33.40	50	−0.55	33.43	26.88
71	−1.24	33.57	75	−1.20	33.60	27.05
94	−0.89	33.75	100	−0.75	33.80	27.19
141	0.28	34.06	150	0.45	34.10	27.37
188	1.13	34.23	200	1.25	34.27	27.47
301	2.56	34.60	300	2.55	34.60	27.63

Station 4244; July 13; latitude 49°09′ N., longitude 51°33′ W., depth 318 meters, dynamic height 971.012

Observed Values			Scaled Values			
Depth, meters	Temperature ° C.	Salinity ‰	Depth, meters	Temperature ° C.	Salinity ‰	σ_t
0	8.46	31.48	0	8.46	31.48	24.48
25	1.82	32.84	25	1.82	32.84	26.28
50	−1.70	33.32	50	−1.70	33.32	26.83
74	−1.73	33.36	75	−1.70	33.36	26.86
99	−1.64	33.44	100	−1.65	33.44	26.93
149	−1.04	33.70	150	−1.05	33.70	27.12
199	0.19	34.02	200	0.25	34.03	27.33
298	2.22	34.48	300	2.25	34.49	27.56

Station 4245; July 13; latitude 49°04′ N., longitude 51°52′ W., depth 308 meters, dynamic height 971.035

Observed Values			Scaled Values			
Depth, meters	Temperature ° C.	Salinity ‰	Depth, meters	Temperature ° C.	Salinity ‰	σ_t
0	8.01	31.44	0	8.01	31.44	24.51
25	−0.23	32.65	25	−0.23	32.65	26.24
50	−1.75	33.16	50	−1.75	33.16	26.70
74	−1.78	33.24	75	−1.75	33.24	26.77
99	−1.66	33.32	100	−1.65	33.32	26.83
148	−1.31	33.58	150	−1.30	33.59	27.04
198	−0.50	33.86	200	−0.45	33.87	27.24
297	1.49	34.31	300	1.55	34.32	27.48

Station 4246; July 14; latitude 49°01′ N., longitude 52°07′ W., depth 335 meters, dynamic height 971.035

Observed Values			Scaled Values			
Depth, meters	Temperature ° C.	Salinity ‰	Depth, meters	Temperature ° C.	Salinity ‰	σ_t
0	7.95	31.68	0	7.95	31.68	24.70
24	2.07	32.62	25	1.95	32.67	26.13
49	−0.75	33.16	50	−0.80	33.17	26.68
73	−1.49	33.24	75	−1.50	33.25	26.77
98	−1.62	33.36	100	−1.60	33.37	26.87
146	−1.26	33.58	150	−1.20	33.60	27.05
195	−0.37	33.87	200	−0.25	33.89	27.24
293	1.36	34.27	300	1.45	34.30	27.47

Station 4247; July 14; latitude 48°50′ N., longitude 52°33′ W., depth 330 meters, dynamic height 971.064

Observed Values			Scaled Values			
Depth, meters	Temperature ° C.	Salinity ‰	Depth, meters	Temperature ° C.	Salinity ‰	σ_t
0	8.57	31.56	0	8.57	31.56	24.52
23	0.20	32.65	25	−0.25	32.70	26.28
47	−1.62	33.09	50	−1.65	33.11	26.66
70	−1.67	33.17	75	−1.65	33.18	26.71
93	−1.76	33.21	100	−1.75	33.22	26.76
140	−1.73	33.28	150	−1.75	33.30	26.81
187	−1.64	33.37	200	−1.15	33.46	26.94
280	1.60	34.34	(300)	2.10	34.48	27.56

Station 4248; July 14; latitude 48°48′ N., longitude 52°37′ W., depth 229 meters, dynamic height 971.067

Observed Values			Scaled Values			
Depth, meters	Temperature ° C.	Salinity ‰	Depth, meters	Temperature ° C.	Salinity ‰	σ_t
0	8.58	31.66	0	8.58	31.66	24.60
24	0.04	32.82	25	−0.20	32.86	26.41
48	−1.67	33.10	50	−1.70	33.11	26.66
72	−1.73	33.17	75	−1.70	33.18	26.72
96	−1.75	33.22	100	−1.75	33.23	26.76
144	−1.74	33.28	150	−1.75	33.29	26.80
192	−1.63	33.36	(200)	−1.60	33.38	26.88

Station 4249; July 14; latitude 48°46′ N., longitude 52°44′ W., depth 176 meters, dynamic height 971.075

Observed Values			Scaled Values			
Depth, meters	Temperature ° C.	Salinity ‰	Depth, meters	Temperature ° C.	Salinity ‰	σ_t
0	9.23	31.37	0	9.23	31.37	24.26
24	−0.93	32.90	25	−1.00	32.93	26.49
48	−1.66	33.12	50	−1.70	33.12	26.67
72	−1.77	33.18	75	−1.75	33.18	26.72
96	−1.76	33.20	100	−1.75	33.20	26.74
144	−1.75	33.23	150	−1.75	33.23	26.76

Station 4250; July 14; latitude 48°45′ N., longitude 52°58′ W., depth 108 meters, dynamic height 971.103

Observed Values			Scaled Values			
Depth, meters	Temperature ° C.	Salinity ‰	Depth, meters	Temperature ° C.	Salinity ‰	σ_t
0	10.00	30.82	0	10.00	30.82	23.74
24	2.23	32.13	25	1.95	32.30	25.83
49	−1.27	32.92	50	−1.30	32.94	26.51
73	−1.60	33.09	75	−1.60	33.10	26.65
			(100)	−1.75	33.19	26.73

Station 4251; July 14; latitude 48°37.5′ N., longitude 52°44′ W., depth 228 meters, dynamic height 971.081

Observed Values			Scaled Values			
Depth, meters	Temperature ° C.	Salinity ‰	Depth, meters	Temperature ° C.	Salinity ‰	σ_t
0	9.35	31.16	0	9.35	31.16	24.08
24	−0.21	32.73	25	−0.45	32.76	26.34
49	−1.51	33.09	50	−1.55	33.09	26.64
73	−1.74	33.18	75	−1.75	33.18	26.72
97	−1.78	33.23	100	−1.75	33.23	26.76
146	−1.75	33.23	150	−1.75	33.24	26.77
			(200)	−1.50	33.29	26.80

Tables of Oceanographic Data—Continued

STATIONS OCCUPIED IN 1950—Continued

Station 4252; July 14; latitude 48°35′ N., longitude 52°38′ W., depth 242 meters, dynamic height 971.061

Observed values			Scaled values			
Depth, meters	Temperature ° C.	Salinity ‰	Depth, meters	Temperature ° C.	Salinity ‰	σ_t
0	8.81	31.50	0	8.81	31.50	24.44
24	−0.50	32.74	25	−0.65	32.78	26.37
49	−1.55	33.08	50	−1.55	33.09	26.64
73	−1.70	33.18	75	−1.70	33.18	26.72
97	−1.72	33.23	100	−1.70	33.24	26.77
146	−1.69	33.33	150	−1.70	33.34	26.85
195	−1.57	33.44	200	−1.50	33.45	26.94
229	−1.04	33.62				

Station 4253; July 14; latitude 48°23′ N., longitude 52°14′ W., depth 198 meters, dynamic height 971.069

Observed values			Scaled values			
Depth, meters	Temperature ° C.	Salinity ‰	Depth, meters	Temperature ° C.	Salinity ‰	σ_t
0	9.07	31.07	0	9.07	31.07	24.06
25	−0.28	32.76	25	−0.28	32.76	26.33
50	−1.71	33.16	50	−1.71	33.16	26.70
75	−1.77	33.20	75	−1.77	33.20	26.74
100	−1.74	33.21	100	−1.74	33.21	26.75
150	−1.75	33.25	150	−1.75	33.25	26.78
181	−1.57	33.38				

Station 4254; July 14; latitude 48°13′ N., longitude 51°57′ W., depth 190 meters, dynamic height 971.063

Observed values			Scaled values			
Depth, meters	Temperature ° C.	Salinity ‰	Depth, meters	Temperature ° C.	Salinity ‰	σ_t
0	9.80	30.95	0	9.80	30.95	23.86
25	0.04	32.78	25	0.04	32.78	26.34
50	−1.20	33.12	50	−1.20	33.12	26.66
75	−1.69	33.23	75	−1.69	33.23	26.75
101	−1.72	33.30	100	−1.70	33.30	26.81
151	−1.53	33.43	150	−1.55	33.43	26.92
176	−1.45	33.48				

Station 4255; July 14; latitude 48°04.5′ N., longitude 51°36′ W., depth 210 meters, dynamic height 971.064

Observed values			Scaled values			
Depth, meters	Temperature ° C.	Salinity ‰	Depth, meters	Temperature ° C.	Salinity ‰	σ_t
0	9.93	31.32	0	9.93	31.32	24.12
25	0.69	32.56	25	0.69	32.56	26.13
49	−1.34	33.10	50	−1.35	33.10	26.64
74	−1.64	33.22	75	−1.65	33.22	26.75
99	−1.71	33.31	100	−1.70	33.31	26.82
148	−1.46	33.42	150	−1.45	33.42	26.91
183	−1.32	33.50	(200)	−1.30	33.54	27.00

Station 4256; July 14; latitude 47°56′ N., longitude 51°16′ W., depth 165 meters, dynamic height 971.066

Observed values			Scaled values			
Depth, meters	Temperature ° C.	Salinity ‰	Depth, meters	Temperature ° C.	Salinity ‰	σ_t
0	9.55	31.54	0	9.55	31.54	24.34
25	2.86	32.30	25	2.86	32.30	25.76
49	−1.30	33.10	50	−1.35	33.11	26.65
74	−1.68	33.23	75	−1.65	33.23	26.75
99	−1.66	33.32	100	−1.65	33.32	26.83
148	−1.17	33.51	150	−1.15	33.51	26.98

Station 4257; July 14; latitude 47°48′ N., longitude 50°56′ W., depth 122 meters, dynamic height 971.067

Observed values			Scaled values			
Depth, meters	Temperature ° C.	Salinity ‰	Depth, meters	Temperature ° C.	Salinity ‰	σ_t
0	9.43	31.60	0	9.43	31.60	24.42
25	4.86	32.51	25	4.86	32.51	25.74
50	−0.82	33.01	50	−0.82	33.01	26.56
75	−1.52	33.22	75	−1.52	33.22	26.75
100	−1.43	33.33	100	−1.43	33.33	26.83

Station 4258; July 14; latitude 47°40′ N., longitude 50°37′ W., depth 174 meters, dynamic height 971.068

Observed values			Scaled values			
Depth, meters	Temperature ° C.	Salinity ‰	Depth, meters	Temperature ° C.	Salinity ‰	σ_t
0	9.17	31.87	0	9.17	31.87	24.67
24	6.67	32.34	25	6.40	32.35	25.44
49	−0.80	33.03	50	−0.90	33.05	26.59
73	−1.53	33.27	75	−1.55	33.29	26.80
97	−1.37	33.42	100	−1.35	33.42	26.91
146	−1.24	33.46	150	−1.20	33.46	26.94

Station 4259; July 15; latitude 47°33′ N., longitude 50°17′ W., depth 103 meters, dynamic height 971.056

Observed values			Scaled values			
Depth, meters	Temperature ° C.	Salinity ‰	Depth, meters	Temperature ° C.	Salinity ‰	σ_t
0	8.11	32.45	0	8.11	32.45	25.28
25	5.90	32.70	25	5.90	32.70	25.77
49	0.09	32.98	50	0.05	32.99	26.51
74	−1.17	33.20	75	−1.20	33.21	26.73
			(100)	−1.45	33.40	26.89

Station 4260; July 15; latitude 47°25.5′ N., longitude 49°54′ W., depth 110 meters, dynamic height 971.055

Observed values			Scaled values			
Depth, meters	Temperature ° C.	Salinity ‰	Depth, meters	Temperature ° C.	Salinity ‰	σ_t
0	7.44	32.56	0	7.44	32.56	25.46
25	5.80	32.71	25	5.80	32.71	25.79
50	−0.20	33.02	50	−0.20	33.02	26.54
75	−0.82	33.11	75	−0.82	33.11	26.63
100	−1.30	33.40	100	−1.30	33.40	26.89

Station 4261; July 15; latitude 47°44′ N., longitude 49°47′ W., depth 119 meters, dynamic height 971.060

Observed values			Scaled values			
Depth, meters	Temperature ° C.	Salinity ‰	Depth, meters	Temperature ° C.	Salinity ‰	σ_t
0	8.81	31.82	0	8.81	31.82	24.68
25	4.74	32.59	25	4.74	32.59	25.82
50	−0.85	33.10	50	−0.85	33.10	26.55
76	−1.24	33.28	75	−1.25	33.28	26.78
101	−1.32	33.44	100	−1.30	33.44	26.92

Station 4262; July 15; latitude 47°54′ N., longitude 49°41′ W., depth 169 meters, dynamic height 971.047

Observed values			Scaled values			
Depth, meters	Temperature ° C.	Salinity ‰	Depth, meters	Temperature ° C.	Salinity ‰	σ_t
0	9.22	31.64	0	9.22	31.64	24.48
25	1.30	32.75	25	1.30	32.75	26.24
50	−1.71	33.24	50	−1.71	33.24	26.77
75	−1.77	33.30	75	−1.77	33.30	26.81
101	−1.70	33.38	100	−1.70	33.38	26.88
151	−0.23	33.82	150	−0.25	33.81	27.18

Station 4263; July 28; latitude 47°21.5′ N., longitude 50°01′ W., depth 96 meters, dynamic height 971.066

Observed values			Scaled values			
Depth, meters	Temperature ° C.	Salinity ‰	Depth, meters	Temperature ° C.	Salinity ‰	σ_t
0	11.06	32.15	0	11.06	32.15	24.57
24	5.87	32.74	25	5.70	32.75	25.84
49	0.13	33.01	50	0.00	33.01	26.53
73	−0.90	33.15	75	−0.95	33.16	26.68

Station 4264; July 28; latitude 47°42′ N., longitude 49°56′ W., depth 114 meters, dynamic height 971.069

Observed values			Scaled values			
Depth, meters	Temperature ° C.	Salinity ‰	Depth, meters	Temperature ° C.	Salinity ‰	σ_t
0	11.33	31.64	0	11.33	31.64	24.13
25	4.91	32.56	25	4.91	32.56	25.78
50	−0.83	33.04	50	−0.83	33.04	26.58
74	−1.65	33.25	75	−1.60	33.26	26.78
99	−1.36	33.45	100	−1.35	33.46	26.94

STATIONS OCCUPIED IN 1950—Continued

Station 4265; July 28; latitude 47°56′ N., longitude 49°48′ W., depth 168 meters, dynamic height 971.046

Observed Values			Scaled Values			
Depth, meters	Temperature ° C.	Salinity ‰	Depth, meters	Temperature ° C.	Salinity ‰	σ_t
0	10.67	32.03	0	10.67	32.03	24.55
25	2.44	32.68	25	2.44	32.68	26.10
49	−0.85	33.26	50	−0.90	33.27	26.77
74	−1.58	33.38	75	−1.55	33.39	26.89
99	−1.44	33.50	100	−1.45	33.50	26.98
148	−0.38	33.84	150	−0.35	33.85	27.21

Station 4266; July 28; latitude 48°11′ N., longitude 49°42′ W., depth 218 meters, dynamic height 971.055

0	10.63	31.85	0	10.63	31.85	24.41
25	−0.70	33.01	25	−0.70	33.01	26.56
49	−1.73	33.18	50	−1.73	33.18	26.72
74	−1.75	33.24	75	−1.75	33.24	26.77
99	−1.69	33.32	100	−1.70	33.32	26.83
148	−1.39	33.53	150	−1.35	33.54	27.00
197	0.12	33.97	200	0.25	34.00	27.31

Station 4267; July 28; latitude 48°30.5′ N., longitude 49°30′ W., depth 613 meters, dynamic height 970.942

0	9.89	32.31	0	9.89	32.31	24.90
24	1.48	33.37	25	1.40	33.40	26.76
49	−0.36	33.82	50	−0.35	33.83	27.19
73	0.28	34.01	75	0.30	34.03	27.32
97	0.83	34.19	100	0.85	34.20	27.43
146	1.93	34.39	150	2.00	34.40	27.51
194	2.94	34.60	200	3.05	34.62	27.60
291	3.46	34.76	300	3.45	34.77	27.68
360	3.40	34.78	400	3.40	34.79	27.70
552	3.35	34.80	(600)	3.35	34.80	27.71

Station 4268; July 28; latitude 48°36.5′ N., longitude 49°22′ W., depth 1,078 meters, dynamic height 970.892

0	8.93	31.79	0	8.93	31.79	24.64
25	3.86	33.96	25	3.86	33.96	26.99
51	2.83	34.36	50	2.80	34.35	27.40
76	2.99	34.57	75	3.00	34.57	27.57
102	3.07	34.64	100	3.05	34.64	27.61
151	3.26	34.72	150	3.25	34.72	27.66
202	3.28	34.76	200	3.30	34.76	27.69
304	3.35	34.80	300	3.35	34.80	27.71
353	3.26	34.80	400	3.25	34.80	27.72
554	3.21	34.80	600	3.20	34.81	27.74
770	3.24	34.84	800	3.25	34.84	27.75
941	3.24	34.85	(1,000)	3.25	34.85	27.76

Station 4269; July 28; latitude 48°57.5′ N., longitude 49°10′ W., depth 1,719 meters, dynamic height 970.861

0	10.22	33.21	0	10.22	33.21	25.55
26	4.17	33.88	25	4.50	33.87	26.87
51	3.16	34.55	50	3.15	34.50	27.49
77	3.15	34.69	75	3.20	34.68	27.63
103	3.20	34.74	100	3.20	34.74	27.68
153	3.14	34.78	150	3.15	34.78	27.71
204	3.15	34.79	200	3.15	34.79	27.72
307	3.21	34.81	300	3.20	34.81	27.74
406	3.21	34.82	400	3.20	34.82	27.75
613	3.21	34.84	600	3.20	34.84	27.76
822	3.20	34.84	800	3.20	34.84	27.76
1,027	3.20	34.84	1,000	3.20	34.84	27.76
1,534	3.29	34.87	1,500	3.30	34.87	27.78

Station 4270; July 29; latitude 49°24′ N., longitude 48°58′ W., depth 1,874 meters, dynamic height 970.861

Observed Values			Scaled Values			
Depth, meters	Temperature ° C.	Salinity ‰	Depth, meters	Temperature ° C.	Salinity ‰	σ_t
0	9.61	33.78	0	9.61	33.78	26.08
23	6.81	33.92	25	6.40	33.95	26.69
46	3.85	34.43	50	3.65	34.46	27.41
69	3.28	34.59	75	3.25	34.62	27.58
93	3.21	34.69	100	3.20	34.70	27.65
138	3.19	34.76	150	3.20	34.77	27.71
184	3.19	34.80	200	3.20	34.80	27.73
277	3.24	34.82	300	3.25	34.82	27.74
320	3.23	34.82	400	3.25	34.83	27.74
490	3.23	34.84	600	3.25	34.85	27.76
667	3.28	34.85	800	3.25	34.86	27.77
845	3.23	34.86	1,000	3.25	34.87	27.78
1,302	3.27	34.88	(1,500)	3.25	34.89	27.79

Station 4271; July 29; latitude 49°58′ N., longitude 48°46′ W., depth 2,012 meters, dynamic height 970.861

0	9.04	33.49	0	9.04	33.49	25.95
26	4.50	34.07	25	4.60	34.05	26.99
52	3.67	34.53	50	3.75	34.50	27.43
78	3.25	34.65	75	3.30	34.64	27.59
104	3.22	34.72	100	3.20	34.71	27.66
156	3.27	34.78	150	3.25	34.78	27.70
208	3.30	34.80	200	3.30	34.80	27.72
312	3.31	34.83	300	3.30	34.83	27.74
402	3.26	34.83	400	3.30	34.83	27.74
605	3.26	34.84	600	3.25	34.84	27.75
809	3.27	34.84	800	3.25	34.84	27.75
1,014	3.26	34.86	1,000	3.25	34.86	27.77
1,529	3.29	34.90	1,500	3.30	34.90	27.80

Station 4272; July 29; latitude 49°48.5′ N., longitude 49°18′ W., depth 1,504 meters, dynamic height 970.867

0	9.25	33.36	0	9.25	33.36	25.81
23	5.36	34.00	25	5.15	34.05	26.93
47	3.48	34.49	50	3.45	34.51	27.47
70	3.41	34.62	75	3.40	34.64	27.58
93	3.29	34.70	100	3.30	34.71	27.65
139	3.36	34.77	150	3.35	34.78	27.69
186	3.37	34.81	200	3.35	34.81	27.72
279	3.36	34.82	300	3.35	34.82	27.73
328	3.31	34.83	400	3.30	34.83	27.74
505	3.28	34.84	600	3.25	34.84	27.75
691	3.24	34.84	800	3.25	34.84	27.75
878	3.23	34.84	1,000	3.25	34.85	27.76
1,369	3.23	34.86	(1,500)	3.25	34.86	27.77

Station 4273; July 29; latitude 49°36′ N., longitude 50°02′ W., depth 594 meters, dynamic height 970.919

0	7.94	31.31	0	7.94	31.31	24.42
26	−0.64	33.66	25	−0.65	33.57	27.01
52	−0.10	33.94	50	−0.25	33.90	27.25
78	0.69	34.13	75	0.65	34.11	27.37
104	1.36	34.29	100	1.25	34.27	27.47
154	2.40	34.50	150	2.30	34.48	27.55
206	3.02	34.64	200	2.95	34.63	27.61
310	3.50	34.80	300	3.50	34.80	27.70
396	3.31	34.80	400	3.30	34.80	27.72
593	3.27	34.84	600	3.25	34.84	27.74

STATIONS OCCUPIED IN 1950—Continued

Station 4274; July 29; latitude 49°25′ N., longitude 50°32′ W., depth 329 meters, dynamic height 970.956

Observed values			Scaled Values			
Depth, meters	Temperature ° C.	Salinity ‰	Depth, meters	Temperature ° C.	Salinity ‰	σ_t
0	10.34	32.48	0	10.34	32.48	24.95
25	2.01	33.08	25	2.01	33.08	26.46
50	−0.25	33.61	50	−0.25	33.61	27.02
75	−0.34	33.85	75	−0.34	33.85	27.21
100	−0.12	33.97	100	−0.12	33.97	27.31
150	0.97	34.21	150	0.97	34.21	27.43
199	1.90	34.41	200	1.90	34.41	27.53
299	3.15	34.71	300	3.15	34.71	27.66

Station 4275; July 29; latitude 49°16′ N., longitude 51°03′ W., depth 333 meters, dynamic height 970.982

Observed values			Scaled Values			
Depth, meters	Temperature ° C.	Salinity ‰	Depth, meters	Temperature ° C.	Salinity ‰	σ_t
0	11.02	31.89	0	11.02	31.89	24.38
25	2.85	33.11	25	2.85	33.11	26.41
50	−0.93	33.44	50	−0.93	33.44	26.91
75	−1.12	33.64	75	−1.12	33.64	27.08
99	−0.61	33.82	100	−0.60	33.83	27.20
149	0.43	34.08	150	0.45	34.09	27.36
199	1.12	34.27	200	1.15	34.28	27.47
298	2.70	34.63	300	2.75	34.64	27.64

Station 4276; July 30; latitude 49°10.5′ N., longitude 51°30′ W., depth 315 meters, dynamic height 971.023

Observed values			Scaled Values			
Depth, meters	Temperature ° C.	Salinity ‰	Depth, meters	Temperature ° C.	Salinity ‰	σ_t
0	11.49	31.58	0	11.49	31.58	24.05
25	0.43	32.66	25	0.43	32.66	26.22
50	−1.35	33.18	50	−1.35	33.18	26.71
74	−1.40	33.37	75	−1.35	33.37	26.86
99	−1.32	33.52	100	−1.30	33.53	26.99
149	−0.61	33.84	150	−0.60	33.85	27.22
198	0.28	34.09	200	0.35	34.10	27.38
297	2.25	34.51	300	2.30	34.53	27.59

Station 4277; July 30; latitude 49°04′ N., longitude 51°51′ W., depth 295 meters, dynamic height 971.080

Observed values			Scaled Values			
Depth, meters	Temperature ° C.	Salinity ‰	Depth, meters	Temperature ° C.	Salinity ‰	σ_t
0	11.36	31.28	0	11.36	31.28	23.84
22	−0.74	32.76	25	−1.00	32.82	26.41
44	−1.67	33.05	50	−1.70	33.08	26.63
66	−1.76	33.15	75	−1.75	33.17	26.71
88	−1.75	33.20	100	−1.75	33.22	26.75
132	−1.69	33.28	150	−1.65	33.33	26.84
175	−1.57	33.43	200	−1.30	33.57	27.03
250	−0.28	33.93				

Station 4278; July 30; latitude 49°01′ N., longitude 52°03′ W., depth 293 meters, dynamic height 971.076

Observed values			Scaled Values			
Depth, meters	Temperature ° C.	Salinity ‰	Depth, meters	Temperature ° C.	Salinity ‰	σ_t
0	10.93	31.53	0	10.93	31.53	24.11
21	−0.54	32.86	25	−0.95	32.93	26.49
43	−1.62	33.08	50	−1.70	33.11	26.66
64	−1.76	33.17	75	−1.75	33.20	26.74
86	−1.75	33.22	100	−1.75	33.24	26.77
128	−1.73	33.26	150	−1.70	33.29	26.80
171	−1.64	33.36	200	−1.25	33.56	27.02
244	−0.31	33.89				

Station 4279; July 30; latitude 48°55′ N., longitude 52°21′ W., depth 336 meters, dynamic height 971.073

Observed values			Scaled values			
Depth, meters	Temperature ° C.	Salinity ‰	Depth, meters	Temperature ° C.	Salinity ‰	σ_t
0	11.15	31.57	0	11.15	31.57	24.10
23	2.14	32.29	25	1.55	32.36	25.91
46	−1.10	33.04	50	−1.20	33.08	26.62
69	−1.47	33.18	75	−1.50	33.20	26.73
91	−1.53	33.27	100	−1.55	33.30	26.81
137	−1.54	33.43	150	−1.50	33.47	26.96
183	−1.14	33.62	200	−0.80	33.73	27.13
274	1.11	34.23	(300)	1.80	34.39	27.52

Station 4280; July 30; latitude 48°49.5′ N., longitude 52°42′ W., depth 220 meters, dynamic height 971.080

Observed values			Scaled values			
Depth, meters	Temperature ° C.	Salinity ‰	Depth, meters	Temperature ° C.	Salinity ‰	σ_t
0	11.65	31.10	0	11.65	31.10	23.66
25	1.36	32.36	25	1.36	32.36	25.92
50	−1.51	32.93	50	−1.51	32.93	26.51
74	−1.63	33.14	75	−1.65	33.15	26.69
99	−1.65	33.20	100	−1.65	33.20	26.73
148	−1.59	33.39	150	−1.55	33.41	26.91
197	−0.70	33.76	200	−0.65	33.79	27.18

Station 4281; July 30; latitude 48°47′ N., longitude 52°47′ W., depth 146 meters, dynamic height 971.076

Observed values			Scaled values			
Depth, meters	Temperature ° C.	Salinity ‰	Depth, meters	Temperature ° C.	Salinity ‰	σ_t
0	12.01	31.12	0	12.01	31.12	23.60
24	0.11	32.50	25	−0.05	32.54	26.15
48	−1.43	32.95	50	−1.45	32.97	26.54
73	−1.62	33.08	75	−1.65	33.09	26.64
97	−1.71	33.14	100	−1.70	33.15	26.69
124	−1.71	33.18				

Station 4282; July 30; latitude 48°45.5′ N., longitude 52°56′ W., depth 114 meters, dynamic height 971.100

Observed values			Scaled values			
Depth, meters	Temperature ° C.	Salinity ‰	Depth, meters	Temperature ° C.	Salinity ‰	σ_t
0	12.73	30.82	0	13.73	30.82	23.24
22	1.76	31.90	25	1.20	31.96	25.62
45	−0.82	32.58	50	−1.00	32.65	26.68
67	−1.42	32.90	(75)	−1.50	32.99	26.56
			(100)	−1.60	33.20	26.73

Station 4283; July 31; latitude 53°44.5′ N., longitude 55°48′ W. depth 116 meters, dynamic height 1454.929

Observed values			Scaled values			
Depth, meters	Temperature ° C.	Salinity ‰	Depth, meters	Temperature ° C.	Salinity ‰	σ_t
0	6.15	30.29	0	6.15	30.29	23.84
25	−1.45	32.59	25	−1.45	32.59	26.24
50	−1.68	32.82	50	−1.68	32.82	26.43
74	−1.64	32.91	75	−1.65	32.91	26.50
99	−1.65	32.95	100	−1.65	32.95	26.53

Station 4284; July 31; latitude 53°53.5′ N., longitude 55°35′ W., depth 210 meters, dynamic height 1454.927

Observed values			Scaled values			
Depth, meters	Temperature ° C.	Salinity ‰	Depth, meters	Temperature ° C.	Salinity ‰	σ_t
0	5.89	30.74	0	5.89	30.74	24.23
25	−1.45	32.62	25	−1.45	32.62	26.26
50	−1.65	32.82	50	−1.65	32.82	26.43
75	−1.67	32.86	75	−1.67	32.86	26.46
100	−1.57	32.92	100	−1.57	32.92	26.51
149	−1.45	33.14	150	−1.45	33.15	26.68
195	−1.37	33.41	(200)	−1.35	33.41	26.90

Station 4285; July 31; latitude 54°00′ N., longitude 55°25′ W., depth 172 meters, dynamic height 1454.930

Observed Values			Scaled Values			
Depth, meters	Temperature ° C.	Salinity ‰	Depth, meters	Temperature ° C.	Salinity ‰	σ_t
0	7.36	30.19	0	7.36	30.19	23.62
25	2.44	31.91	25	2.44	31.91	25.49
50	−1.11	32.75	50	−1.11	32.75	26.36
75	−1.65	33.04	75	−1.65	33.04	26.60
100	−1.60	33.17	100	−1.60	33.17	26.71
150	−1.35	33.41	150	−1.35	33.41	26.90

Station.4286; July 31; latitude 54°08.5′ N., longitude 55°05′ W, depth 170 meters, dynamic height 1454.919

Observed Values			Scaled Values			
Depth, meters	Temperature ° C.	Salinity ‰	Depth, meters	Temperature ° C.	Salinity ‰	σ_t
0	7.98	30.50	0	7.98	30.50	23.77
25	2.98	31.71	25	2.98	31.71	25.28
49	−1.24	32.82	50	−1.25	32.83	26.42
74	−1.59	33.11	75	−1.55	33.11	26.66
99	−1.57	33.28	100	−1.55	33.29	26.80
148	−0.91	33.73	150	−0.85	33.75	27.15

Station 4287; Aug. 1; latitude 54°13′ N., longitude 54°52′ W., depth 185 meters, dynamic height 1454.898

Observed Values			Scaled Values			
Depth, meters	Temperature ° C.	Salinity ‰	Depth, meters	Temperature ° C.	Salinity ‰	σ_t
0	6.56	30.74	0	6.56	30.74	24.15
25	−1.02	32.44	25	−1.02	32.44	26.10
49	−1.52	32.95	50	−1.50	32.95	26.52
74	−1.52	33.12	75	−1.50	33.12	26.66
99	−1.49	33.30	100	−1.50	33.31	26.82
148	−1.41	33.54	150	−1.40	33.55	27.01

Station 4288; Aug. 1; latitude 54°25′ N., longitude 54°29′ W., depth 222 meters, dynamic height 1454.938

Observed Values			Scaled Values			
Depth, meters	Temperature ° C.	Salinity ‰	Depth, meters	Temperature ° C.	Salinity ‰	σ_t
0	7.29	29.87	0	7.29	29.87	23.36
14	4.60	30.56	25	1.40	31.63	25.34
37	−1.61	32.80	50	−1.60	32.87	26.47
60	−1.58	32.92	75	−1.50	33.00	26.57
83	−1.45	33.05	100	−1.40	33.15	26.68
129	−1.29	33.34	150	−1.00	33.49	26.95
193	−0.34	33.83	200	−0.25	33.87	27.23

Station 4289; Aug. 1; latitude 54°45′ N., longitude 53°57′ W., depth 328 meters, dynamic height 1454.933

Observed Values			Scaled Values			
Depth, meters	Temperature ° C.	Salinity ‰	Depth, meters	Temperature ° C.	Salinity ‰	σ_t
0	6.99	29.88	0	6.99	29.88	23.42
23	−1.39	32.71	25	−1.45	32.73	26.35
46	−1.62	32.85	50	−1.65	32.87	26.47
69	−1.59	32.94	75	−1.55	32.97	26.55
91	−1.49	33.04	100	−1.45	33.08	26.63
137	−1.33	33.26	150	−1.30	33.33	26.83
182	−1.22	33.50	200	−0.95	33.61	27.05
273	1.68	34.28	(300)	2.80	34.56	27.57

Station 4290; Aug. 1; latitude 54°53′ N., longitude 53°41′ W., depth 631 meters, dynamic height 1454.855

Observed Values			Scaled Values			
Depth, meters	Temperature ° C.	Salinity ‰	Depth, meters	Temperature ° C.	Salinity ‰	σ_t
0	6.73	29.64	0	6.73	29.64	23.26
25	1.95	32.06	25	1.95	32.06	25.65
49	−1.31	33.06	50	−1.30	33.09	26.63
74	−1.28	33.35	75	−1.30	33.36	26.85
99	−0.74	33.54	100	−0.70	33.55	26.99
148	1.64	34.27	150	1.75	34.29	27.44
197	2.85	34.54	200	2.90	34.55	27.56
296	3.60	34.71	300	3.60	34.71	27.62
367	3.78	34.78	400	3.80	34.79	27.66
561	3.82	34.80	(600)	3.80	34.80	27.67

Station 4291; Aug. 1; latitude 54°58′ N., longitude 53°26′ W., depth 1,692 meters, dynamic height 1454.710

Observed Values			Scaled Values			
Depth, meters	Temperature ° C.	Salinity ‰	Depth, meters	Temperature ° C.	Salinity ‰	σ_t
0	5.58	31.03	0	5.58	31.03	24.49
24	3.99	33.77	25	3.85	33.80	26.86
47	2.92	34.26	50	2.90	34.28	27.34
71	2.43	34.41	75	2.45	34.43	27.49
94	2.66	34.53	100	2.75	34.56	27.58
142	3.52	34.74	150	3.65	34.76	27.65
189	3.87	34.82	200	3.85	34.82	27.68
283	3.86	34.83	300	3.85	34.83	27.68
340	3.81	34.83	400	3.80	34.83	27.69
516	3.67	34.84	600	3.60	34.84	27.72
696	3.53	34.84	800	3.50	34.84	27.73
883	3.50	34.84	1,000	3.45	34.84	27.73
1,376	3.32	34.85	(1,500)	3.30	34.85	27.76

Station 4292; Aug. 1; latitude 55°01′ N., longitude 53°11′ W., depth 2,103 meters, dynamic height 1454.661

Observed Values			Scaled Values			
Depth, meters	Temperature ° C.	Salinity ‰	Depth, meters	Temperature ° C.	Salinity ‰	σ_t
0	6.37	31.73	0	6.37	31.73	24.85
27	2.76	34.30	25	2.85	34.11	27.21
53	2.06	34.41	50	2.05	34.40	27.51
79	2.45	34.54	75	2.35	34.51	27.57
105	3.39	34.72	100	3.20	34.69	27.64
159	3.81	34.80	150	3.80	34.79	27.66
211	3.90	34.84	200	3.90	34.83	27.68
316	3.79	34.84	300	3.80	34.84	27.70
398	3.65	34.85	400	3.65	34.85	27.72
601	3.56	34.86	600	3.55	34.86	27.74
806	3.41	34.85	800	3.40	34.85	27.75
1,008	3.36	34.86	1,000	3.35	34.86	27.76
1,519	3.30	34.86	1,500	3.30	34.86	27.77
2,032	2.78	34.85	2,000	2.80	34.85	27.80

Station 4293; Aug. 1; latitude 55°11′ N., longitude 52°52′ W., depth 2,954 meters, dynamic height 1454.675

Observed Values			Scaled Values			
Depth, meters	Temperature ° C.	Salinity ‰	Depth, meters	Temperature ° C.	Salinity ‰	σ_t
0	6.54	32.00	0	6.54	32.00	25.14
25	3.06	33.87	25	3.06	33.87	27.00
49	2.23	34.30	50	2.20	34.30	27.42
74	2.34	34.45	75	2.40	34.45	27.52
99	3.15	34.66	100	3.15	34.66	27.62
148	3.52	34.74	150	3.55	34.74	27.64
197	3.72	34.78	200	3.75	34.79	27.66
296	3.91	34.84	300	3.90	34.84	27.69
372	3.75	34.84	400	3.75	34.84	27.70
563	3.60	34.84	600	3.55	34.84	27.72
758	3.49	34.86	800	3.45	34.86	27.75
952	3.34	34.845	1,000	3.30	34.85	27.76
1,443	3.20	34.85	1,500	3.20	34.85	27.77
2,040	2.92	34.88	2,000	2.95	34.88	27.81
2,547	2.28	34.88	2,500	2.30	34.88	27.87
2,953	1.96	34.85				

Tables of Oceanographic Data—Continued

STATIONS OCCUPIED IN 1950—Continued

Station 4294; Aug. 1; latitude 55°29′ N., longitude 52°16′ W., depth 3,218 meters, dynamic height 1454.636

Observed Values			Scaled Values			
Depth, meters	Temperature ° C.	Salinity ‰	Depth, meters	Temperature ° C.	Salinity ‰	σ_t
0	8.30	33.62	0	8.30	33.62	26.17
25	7.55	34.36	25	7.55	34.36	26.86
50	5.28	34.70	50	5.28	34.70	27.43
76	3.92	34.75	75	3.95	34.75	27.61
101	3.42	34.76	100	3.45	34.76	27.67
152	3.33	34.79	150	3.35	34.79	27.70
202	3.35	34.83	200	3.35	34.83	27.73
303	3.30	34.82	300	3.30	34.82	27.74
397	3.24	34.83	400	3.25	34.83	27.74
595	3.18	34.82	600	3.20	34.82	27.75
794	3.18	34.83	800	3.15	34.83	27.75
991	3.17	34.835	1,000	3.15	34.835	27.76
1,484	3.19	34.84	1,500	3.20	34.84	27.76
1,970	3.39	34.90	2,000	3.35	34.90	27.79
2,475	2.92	34.92	2,500	2.90	34.92	27.85
3,092	1.61	34.85	3,000	1.85	34.87	27.90

Station 4295; Aug. 2; latitude 55°55′ N., longitude 51°31′W., depth 3,475 meters, dynamic height 1454.626

Observed Values			Scaled Values			
Depth, meters	Temperature ° C.	Salinity ‰	Depth, meters	Temperature ° C.	Salinity ‰	σ_t
0	9.26	34.49	0	9.26	34.49	26.70
25	7.74	34.67	25	7.74	34.67	27.07
49	5.84	34.69	50	5.75	34.69	27.36
74	4.18	34.74	75	4.15	34.74	27.58
98	3.52	34.75	100	3.50	34.75	27.66
148	3.30	34.79	150	3.30	34.79	27.71
198	3.28	34.80	200	3.30	34.80	27.72
296	3.26	34.82	300	3.25	34.82	27.74
361	3.19	34.82	400	3.20	34.82	27.75
545	3.17	34.82	600	3.20	34.83	27.75
733	3.20	34.84	800	3.20	34.84	27.76
920	3.19	34.84	1,000	3.20	34.84	27.76
1,397	3.23	34.84	1,500	3.25	34.85	27.76
2,014	3.39	34.88	2,000	3.40	34.88	27.77
2,555	3.02	34.855	2,500	3.05	34.86	27.79
3,103	2.45	34.88	3,000	2.60	34.88	27.84
3,204	2.17	34.85				

Station 4296; Aug. 2; latitude 56°26′ N., longitude 50°22′ W., depth 3,548 meters, dynamic height 1454.611.

Observed Values			Scaled Values			
Depth, meters	Temperature ° C.	Salinity ‰	Depth, meters	Temperature ° C.	Salinity ‰	σ_t
0	8.99	34.62	0	8.99	34.62	26.84
26	7.73	34.63	25	7.80	34.63	27.03
51	5.41	34.72	50	5.50	34.72	27.42
77	4.11	34.76	75	4.15	34.76	27.60
103	3.52	34.79	100	3.60	34.79	27.68
153	3.32	34.80	150	3.35	34.80	27.71
204	3.29	34.83	200	3.30	34.83	27.74
307	3.28	34.84	300	3.25	34.84	27.75
398	3.21	34.84	400	3.20	34.84	27.76
600	3.17	34.84	600	3.15	34.84	27.76
803	3.19	34.84	800	3.20	34.84	27.76
1,008	3.21	34.85	1,000	3.20	34.85	27.77
1,526	3.20	34.86	1,500	3.20	34.85	27.77
1,943	3.25	34.86	2,000	3.25	34.86	27.77
2,433	3.23	34.91	2,500	3.20	34.91	27.82
2,931	2.82	34.90	3,000	3.75	34.90	27.85
3,407	1.92	34.87	(3,500)	1.65	34.87	27.92

Station 4297; Aug. 3; latitude 57°04.5′ N., longitude 49°26′ W., depth 3,566 meters, dynamic height 1454.597

Observed Values			Scaled Values			
Depth, meters	Temperature ° C.	Salinity ‰	Depth, meters	Temperature ° C.	Salinity ‰	σ_t
0	8.78	34.66	0	8.78	34.66	26.91
25	8.68	34.66	25	8.68	34.66	26.93
51	5.67	34.76	50	5.75	34.76	27.42
76	3.84	34.77	75	3.90	34.77	27.64
102	3.42	34.79	100	3.45	34.79	27.69
154	3.68	34.86	150	3.65	34.85	27.72
205	3.45	34.82	200	3.50	34.82	27.72
307	3.24	34.84	300	3.25	34.84	27.75
329	3.27	34.84	400	3.20	34.84	27.76
498	3.22	34.85	600	3.20	34.86	27.78
673	3.20	34.86	800	3.20	34.86	27.78
1,318	3.19	34.86	1,000	3.20	34.86	27.78
2,204	3.35	34.905	1,500	3.20	34.87	27.79
2,719	2.98	34.92	2,000	3.30	34.90	27.80
3,231	------	34.90	2,500	3.20	34.91	27.82
3,487	1.79	34.87	3,000	2.65	34.91	27.87
			3,500	1.80	34.87	27.91

Station 4298; Aug. 3; latitude 57°35′ N., longitude 48°15′ W., depth 3,402 meters, dynamic height 1454.598

Observed Values			Scaled Values			
Depth, meters	Temperature ° C.	Salinity ‰	Depth, meters	Temperature ° C.	Salinity ‰	σ_t
0	8.88	34.61	0	8.88	34.61	26.86
22	8.90	34.61	25	8.80	34.61	26.87
45	5.21	34.70	50	4.80	34.72	27.50
67	3.87	34.78	75	3.70	34.79	27.67
90	3.57	34.81	100	3.55	34.82	27.71
134	3.50	34.83	150	3.55	34.84	27.72
179	3.55	34.87	200	3.50	34.86	27.75
269	3.30	34.84	300	3.25	34.85	27.76
353	3.18	34.85	400	3.20	34.85	27.77
533	3.20	34.85	600	3.20	34.85	27.77
714	3.20	34.85	800	3.20	34.85	27.77
904	3.20	34.85	1,000	3.20	34.85	27.77
1,398	3.17	34.86	1,500	3.20	34.87	27.79
2,009	3.38	34.90	2,000	3.40	34.90	27.79
2,496	3.02	34.915	2,500	3.00	34.915	27.84
2,979	2.48	34.895	3,000	2.45	34.89	27.86
3,250	1.76	34.86				

Station 4299; Aug. 3; latitude 58°08′ N., longitude 47°07′ W., depth 3,131 meters, dynamic height 1454.633

Observed Values			Scaled Values			
Depth, meters	Temperature ° C.	Salinity ‰	Depth, meters	Temperature ° C.	Salinity ‰	σ_t
0	8.39	34.68	0	8.39	34.68	26.98
27	8.40	34.68	25	8.40	34.68	26.98
53	5.63	34.78	50	6.00	34.77	27.40
79	4.45	34.86	75	4.50	34.85	27.63
105	4.45	34.92	100	4.45	34.91	27.69
159	4.13	34.91	150	4.20	34.91	27.72
212	3.78	34.87	200	3.85	34.88	27.72
316	3.61	34.85	300	3.61	34.85	27.73
300	3.60	34.86	400	3.50	34.84	27.73
486	3.40	34.84	600	3.30	34.83	27.74
696	3.26	34.82	800	3.25	34.83	27.74
893	3.22	34.84	1,000	3.25	34.84	27.75
1,420	3.30	34.85	1,500	3.30	34.86	27.77
2,050	3.16	34.92	2,000	3.15	34.92	27.83
2,581	2.74	34.88	2,500	2.85	34.89	27.83
3,131	1.54	34.85	3,000	1.95	34.87	27.90

STATIONS OCCUPIED IN 1950—Continued

Station 4300; Aug. 4; latitude 58°35.5′ N., longitude 46°02′ W., depth 2,500 meters, dynamic height 1454.631

Observed Values			Scaled Values			
Depth, meters	Temperature ° C.	Salinity ‰	Depth, meters	Temperature ° C.	Salinity ‰	σ_t
0	7.86	34.84	0	7.86	34.84	27.19
25	7.84	34.84	25	7.84	34.84	27.19
51	7.45	34.84	50	7.50	34.84	27.24
76	5.42	34.92	75	5.45	34,92	27.58
103	5.06	34.93	100	5.10	34.93	27.62
153	4.61	34.94	150	4.65	34.94	27.69
204	4.45	34.92	200	4.45	34.92	27.70
307	4.20	34.91	300	4.20	34.91	27.72
375	4.09	34.92	400	4.05	34.92	27.74
565	3.69	34.90	600	3.65	34.89	27.75
757	3.50	34.88	800	3.45	34.87	27.76
951	3.29	34.85	1,000	3.30	34.85	27.76
1,447	3.44	34.90	1,500	3.45	34.90	27.78
2,074	2.86	34.90	2,000	2.95	34.90	27.83
2,500	1.89	34.86	2,500	1.90	34.86	27.89

Station 4301; Aug. 4; latitude 58°55′ N., longitude 45°16′ W., depth 2,432 meters, dynamic height 1454.645

Observed Values			Scaled Values			
Depth, meters	Temperature ° C.	Salinity ‰	Depth, meters	Temperature ° C.	Salinity ‰	σ_t
0	7.60	34.91	0	7.60	34.91	27.28
25	7.26	34.91	25	7.26	34.91	27.33
49	7.25	34.91	50	7.25	34.91	27.33
74	7.23	34.91	75	7.25	34.91	27.33
98	7.19	34.91	100	7.15	34.91	27.35
147	4.93	34.92	150	4.90	34.92	27.65
196	4.62	34.94	200	4.60	34.94	27.69
294	4.25	34.92	300	4.25	34.92	27.72
370	4.22	34.93	400	4.15	34.92	27.73
558	3.61	34.86	600	3.60	34.86	27.74
749	3.60	34.89	800	3.55	34.88	27.75
941	3.31	34.85	1,000	3.30	34.85	27.76
1,433	3.49	34.91	1,500	3.45	34.91	27.79
2,033	2.81	34.91	2,000	2.85	34.91	27.85
2,332	2.28	34.89				

Station 4302; Aug. 4; latitude 59°09′ N., longitude 44°49′ W., depth 2,054 meters; dynamic height 1454.652

Observed Values			Scaled Values			
Depth, meters	Temperature ° C.	Salinity ‰	Depth, meters	Temperature ° C.	Salinity ‰	σ_t
0	7.33	34.92	0	7.33	34.92	27.34
25	7.14	34.94	25	7.14	34.92	27.36
50	7.06	34.95	50	7.06	34.95	27.39
75	6.65	34.97	75	6.65	34.97	27.47
100	5.91	34.99	100	5.91	34.99	27.58
150	5.47	34.98	150	5.47	34.98	27.62
201	5.37	34.99	200	5.35	34.99	27.65
301	4.75	34.94	300	4.75	34.94	27.67
398	4.51	34.95	400	4.50	34.95	27.71
596	4.17	34.92	600	4.15	34.92	27.73
795	3.84	34.90	800	3.85	34.90	27.74
991	3.61	34.88	1,000	3.60	34.88	27.75
1,475	3.44	34.92	1,500	3.40	34.92	27.81
1,991	2.81	34.89	2,000	2.75	34.89	27.84

Station 4303; Aug. 4–5; latitude 59°31.5′ N., longitude 44°28′ W., depth 1,088 meters, dynamic height 1,454.800

Observed Values			Scaled Values			
Depth, meters	Temperature ° C.	Salinity ‰	Depth, meters	Temperature ° C.	Salinity ‰	σ_t
0	1.85	32.54	0	1.85	32.54	26.04
20	4.20	33.70	25	4.35	33.83	26.83
40	4.60	34.08	50	4.50	34.25	27.16
60	4.24	34.42	75	3.90	34.37	27.32
80	3.80	34.36	100	3.60	34.36	27.34
120	3.48	34.36	150	3.85	34.45	27.38
161	4.00	34.47	200	3.75	34.46	27.40
241	3.53	34.44	300	3.95	34.62	27.51
360	4.38	34.78	400	4.45	34.82	27.62
554	4.62	34.89	600	4.60	34.90	27.66
759	4.44	34.90	800	4.40	34.90	27.68
960	4.28	34.90	(1,000)	4.20	34.90	27.71

Station 4304; Aug. 5; latitude 59°38.5′ N., longitude 44°15′ W., depth 174 meters, dynamic height 1,454.914

Observed Values			Scaled Values			
Depth, meters	Temperature ° C.	Salinity ‰	Depth, meters	Temperature ° C.	Salinity ‰	σ_t
0	2.56	31.56	0	2.56	31.56	25.21
23	0.80	32.78	25	0.70	32.80	26.32
46	0.01	32.99	50	−0.15	33.01	26.54
70	−0.58	33.10	75	−0.55	33.12	26.63
93	−0.38	33.23	100	−0.15	33.27	26.74
139	1.39	33.77	(150)	1.80	33.93	27.15

Station 4305; Aug. 5; latitude 59°40′ N., longitude 44°14′ W., depth 146 meters, dynamic height 1,454.948

Observed Values			Scaled Values			
Depth, meters	Temperature ° C.	Salinity ‰	Depth, meters	Temperature ° C.	Salinity ‰	σ_t
0	2.85	31.23	0	2.85	31.23	24.92
25	1.84	31.84	25	1.84	31.84	25.48
50	1.38	32.56	50	1.38	32.56	26.09
75	0.46	32.88	75	0.46	32.88	26.39
100	0.49	33.52	100	0.49	33.52	26.91

Station 4306; Aug. 5; latitude 59°42′ N., longitude 44°15′ W., depth 128 meters, dynamic height 1,454.972

Observed Values			Scaled Values			
Depth, meters	Temperature ° C.	Salinity ‰	Depth, meters	Temperature ° C.	Salinity ‰	σ_t
0	2.59	31.29	0	2.59	31.29	24.99
25	1.94	31.83	25	1.94	31.83	25.47
50	1.67	32.14	50	1.67	32.14	25.75
76	1.45	32.62	75	1.45	32.60	26.12
101	1.52	33.14	100	1.50	33.12	26.52

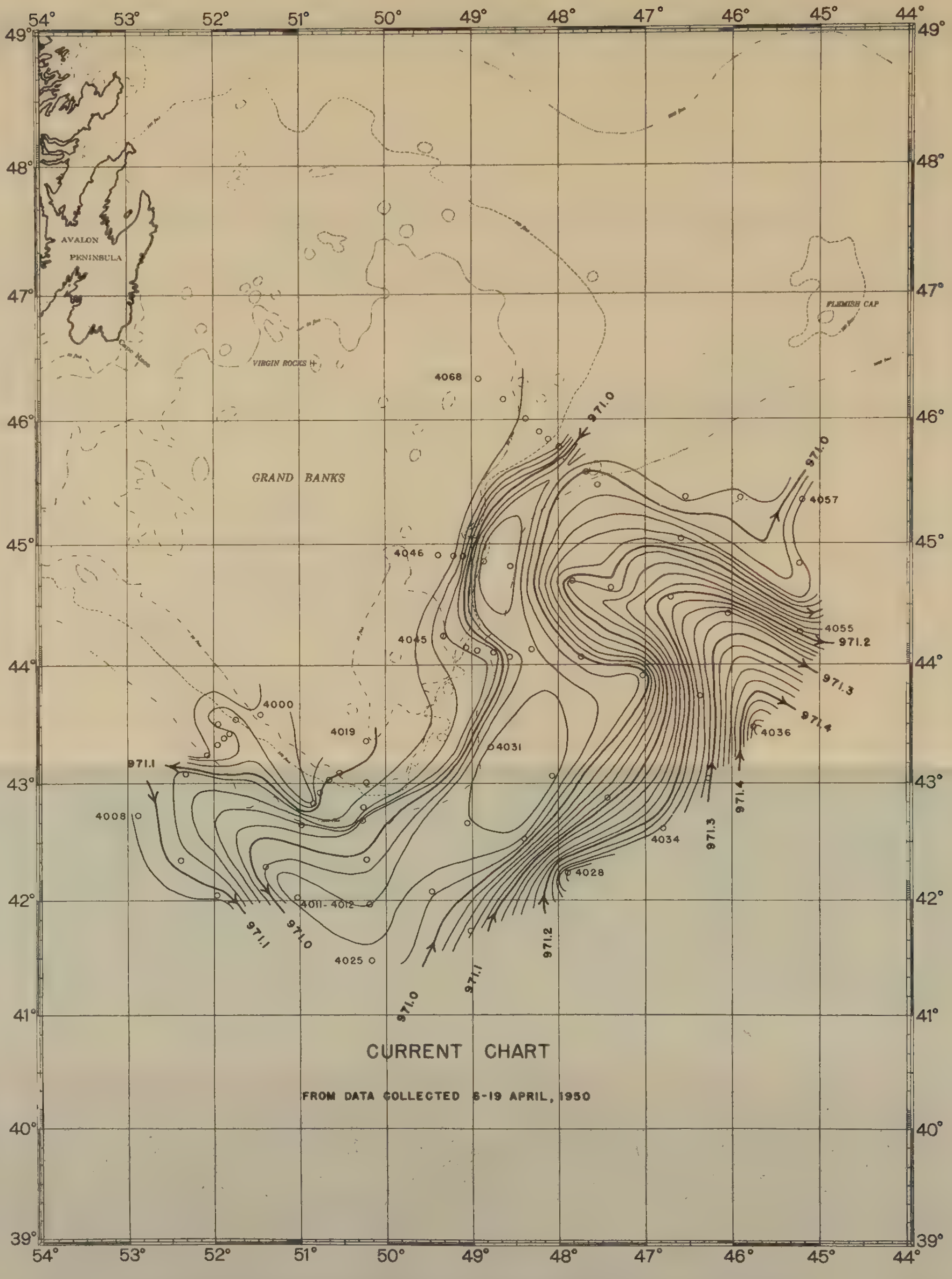
CURRENT CHART
FROM DATA COLLECTED 6-19 APRIL, 1950
AVALON PENINSULA
Cape Race
VIRGIN ROCKS
GRAND BANKS
FLEMISH CAP
971.0
971.1
971.2
971.3
971.4
4000
4008
4011-4012
4019
4025
4028
4031
4034
4036
4045
4046
4055
4057
4068
54°
53°
52°
51°
50°
49°
48°
47°
46°
45°
44°
43°
42°
41°
40°
39°

FIGURE 16.—Dynamic topography of the sea surface relative to the 1000-decibar surface from data collected 6-19 April 1950. Oceanographic station positions are indicated and the station numbers given at turning points.

955984 O - 51 (Face p. 66) No. 1

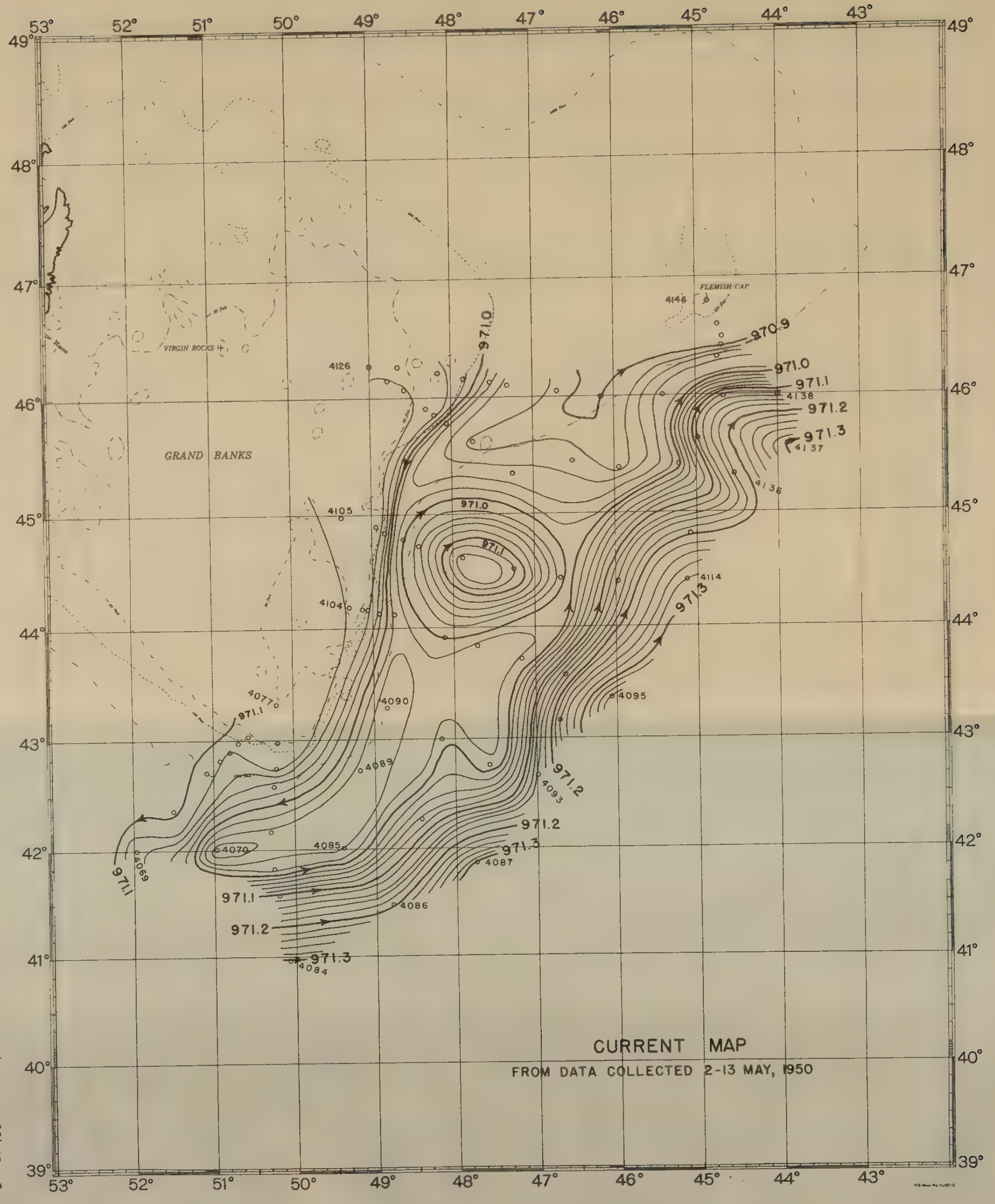
CURRENT MAP
FROM DATA COLLECTED 2-13 MAY, 1950
GRAND BANKS
VIRGIN ROCKS
FLEMISH CAP
970.9
971.0
971.1
971.2
971.3
4138
4137
4136
4114
4095
4093
4087
4086
4085
4084
4090
4089
4079
4077
4069
4105
4104
4126
4144
53°
52°
51°
50°
49°
48°
47°
46°
45°
44°
43°
42°
41°
40°
39°

FIGURE 17.—Dynamic topography of the sea surface relative to the 1000-decibar surface from data collected 2–13 May 1950. Oceanographic station positions are indicated and the station numbers given at turning points.

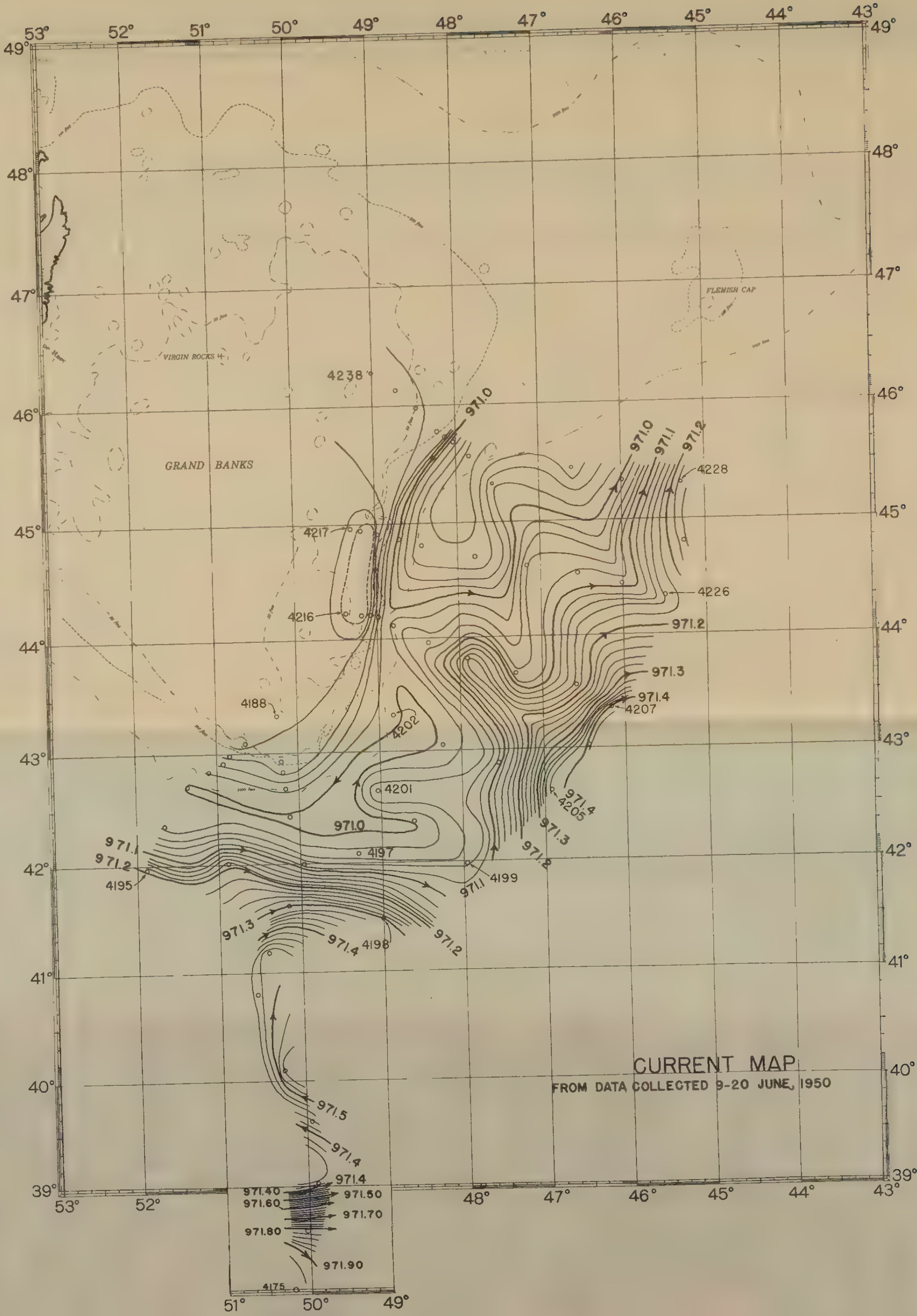
CURRENT MAP
FROM DATA COLLECTED 9-20 JUNE, 1950
GRAND BANKS
VIRGIN ROCKS
FLEMISH CAP
971.0
971.1
971.2
971.3
971.4
971.5
971.40
971.50
971.60
971.70
971.80
971.90
4175
4188
4195
4197
4198
4199
4201
4202
4205
4207
4216
4217
4226
4228
4238
39°
40°
41°
42°
43°
44°
45°
46°
47°
48°
49°
50°
51°
52°
53°

surface from data collected 9–20 June 1950.

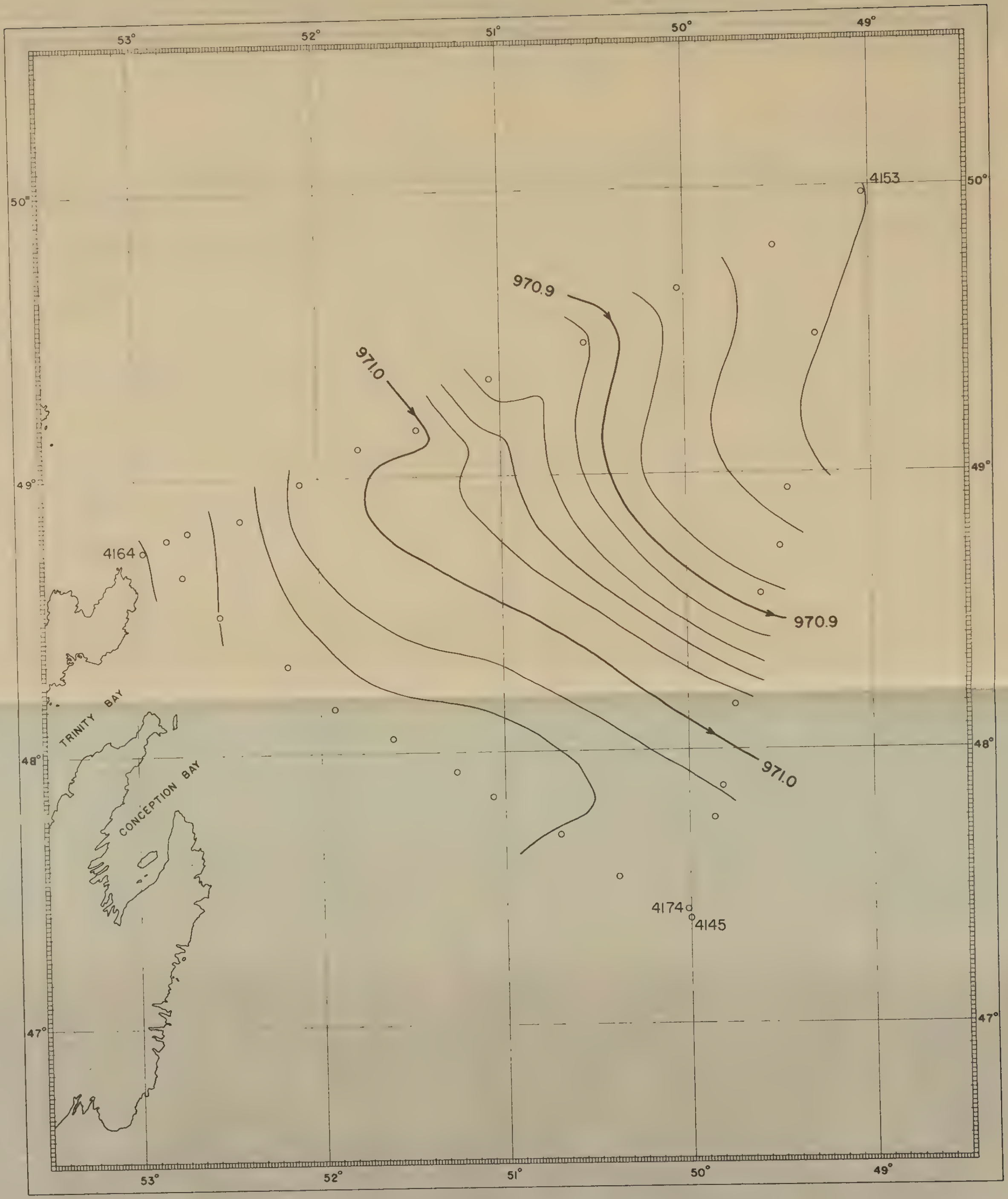
53°
52°
51°
50°
49°
50°
49°
48°
47°
4153
970.9
971.0
4164
TRINITY BAY
CONCEPTION BAY
4174
4145

FIGURE 23.—Dynamic topography of the sea surface relative to the 1000-decibar surface, from data collected 27–30 May 1950. Oceanographic station positions are indicated and the station numbers given at turning points.

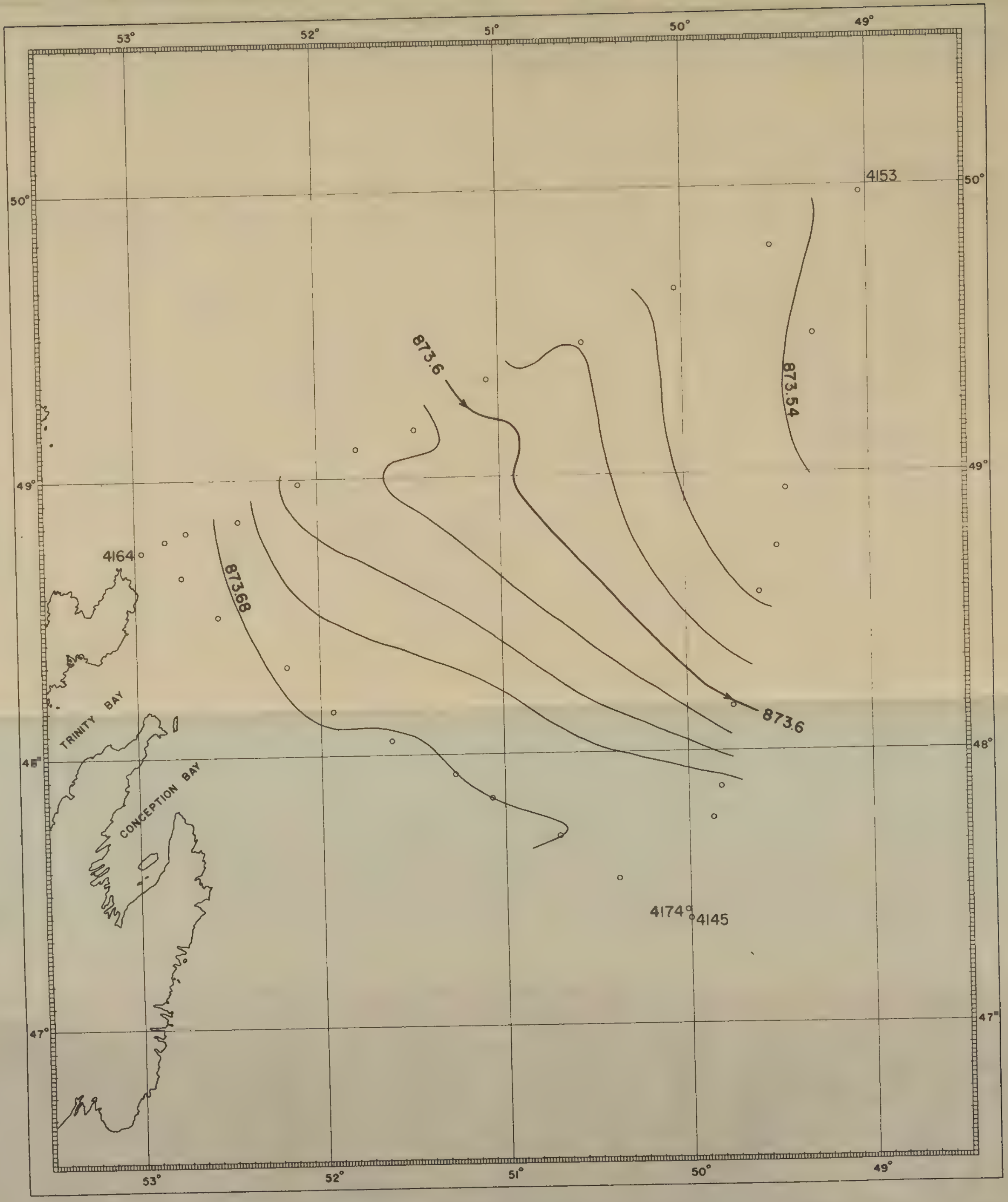
53°
52°
51°
50°
49°
48°
47°
873.54
873.6
873.6
873.68
4153
4164
4174
4145
TRINITY BAY
CONCEPTION BAY

FIGURE 24.—Dynamic topography of the 100-decibar surface relative to the 1000-decibar surface, from data collected 27–30 May 1950. Oceanographic station positions are indicated and the station numbers given at turning points.

955984 O - 51 (Face p. 80) No. 2

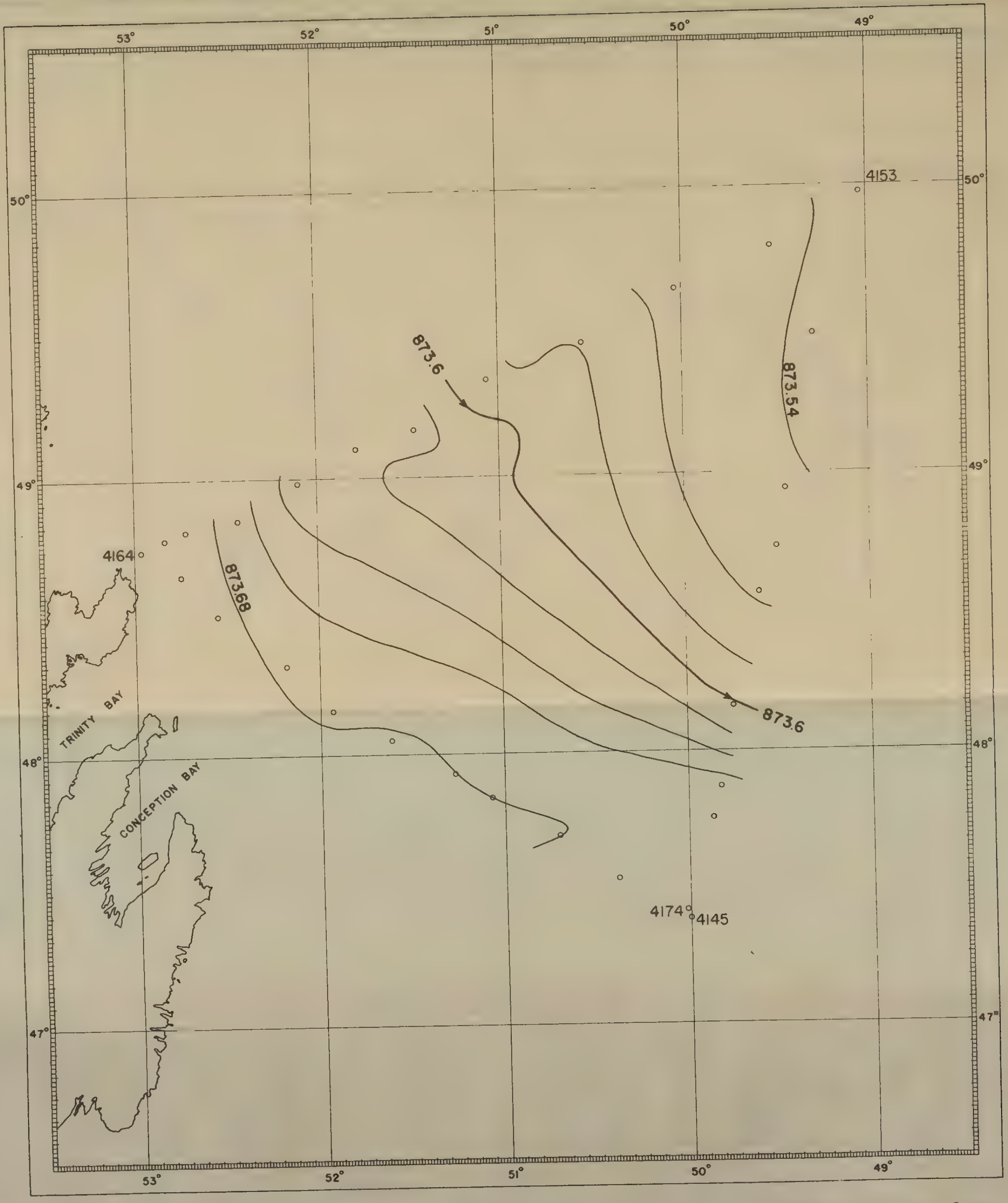
53°
52°
51°
50°
49°
48°
47°
4153
4164
4174
4145
873.54
873.6
873.68
TRINITY BAY
CONCEPTION BAY

FIGURE 24.—Dynamic topography of the 100-decibar surface relative to the 1000-decibar surface, from data collected 27–30 May 1950. Oceanographic station positions are indicated and the station numbers given at turning points.

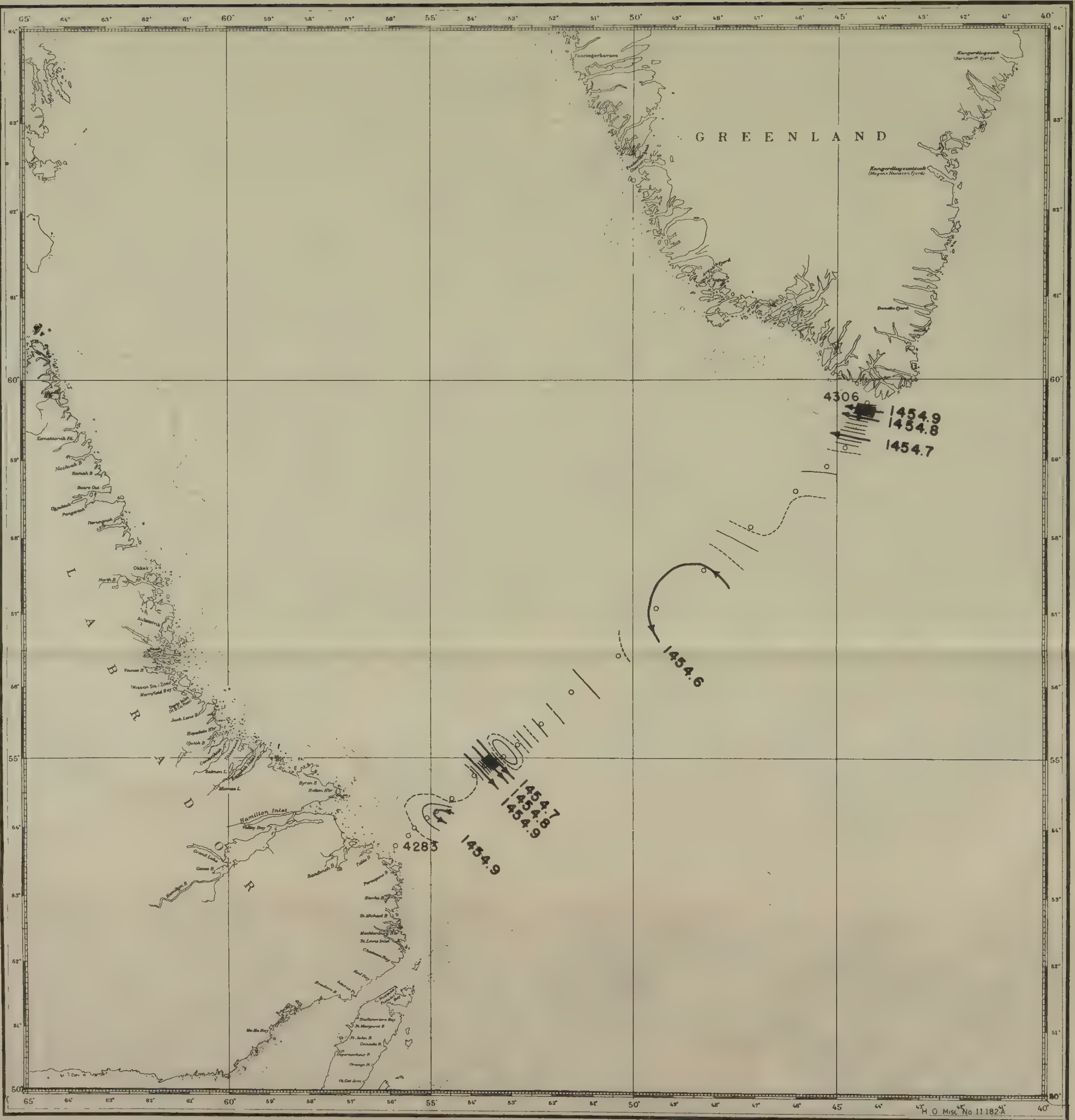
GREENLAND
LABRADOR
4306
1454.9
1454.8
1454.7
1454.6
1454.7
1454.8
1454.9
1454.9
4283
Hamilton Inlet
65°
60°
55°
50°
45°
40°
64°
63°
62°
61°
60°
59°
58°
57°
56°
55°
54°
53°
52°
51°
50°
H O Misc No 11182A

FIGURE 29.—Dynamic topography of the sea surface relative to the 1500-decibar surface, from data collected 31 July–5 August 1950.

Contribution No. 552

Reprinted from TELLUS
Vol. 3, No. 1, February 1951, page 43.
Contribution No. 552 from
The Woods Hole Oceanographic Institution

Determination of the Lateral Eddy Diffusivity in the Climatological Mean Gulf Stream

By H. STOMMEL, Woods Hole Oceanographic Institution

(Manuscript received 23 December 1950)

The spread of positions of the Gulf Stream as exhibited in fig. 1 of the paper by FUGLISTER and WORTHINGTON (1951) published in this issue of Tellus suggests that one should be able to compute a rough value of the lateral eddy diffusivity produced by the meandering and shifts of position of the stream, although the number of points at any section, taken across the stream at any distance along the axis of the stream is quite small for statistical purposes.

If σ represents the standard deviation of the position of the actual stream from the mean axis of the stream at any point along the axis, then, roughly speaking, the eddy A should be given by the equation

$$A \equiv \sigma^2 \ V/2\,L,$$

where L is the distance of the section from Cape Hatteras and V is the mean velocity of the stream. σ has been evaluated for two section for which L is 500 kilometers and 1,000 kilometers. The results of the computation are given in the following table.

L	0.5×10^8	10^8	cm
V	2.0×10^2	2.0×10^2	cm sec^{-1}
σ	9.7×10^6	15.4×10^6	cm
σ^2	0.94×10^{14}	2.3×10^{14}	cm^2
A	1.8×10^8	2.3×10^8	cm^2 sec^{-1}

It must be remembered that this determination of the lateral eddy diffusivity is based on the assumption that the actual Gulf Stream is a turbulent flow. The numerical values are roughly of the same order of magnitude as those used by MUNK (1950), though somewhat smaller.

The result of this computation seems to support the contention that the western intensification exhibited in the Munk-Stommel theories are climatological or statistical in nature and that the very thin, filament-like nature of the individual turbulent element of the Gulf Stream may be due to another cause.

REFERENCES

FUGLISTER and WORTHINGTON 1951: Some Results of a Multiple Ship Survey of the Gulf Stream. *Tellus*, 3, 1. p. 1.

MUNK, W. H. 1950: On the Wind-driven Ocean Circulation. *Journ. of Met.*, 7. pp. 79—93.

Contribution No. 553

Transactions, American Geophysical Union Volume 32, Number 4 August 1951

DIURNAL HEATING OF THE SURFACE OF THE GULF OF MEXICO IN THE SPRING OF 1942

Henry Stommel and Alfred H. Woodcock

(Contribution No. 553 of the Woods Hole Oceanographic Institution
under contract with the Office of Naval Research)

Abstract--The diurnal temperature change of the surface layer in the Gulf of Mexico in the spring of 1942 seems to be qualitatively related to the computed net flux of heat at the surface and to the wind force, being greatest for sunny, calm days. A numerical analysis of the data is attempted: The eddy conductivity is computed by two methods, and the results are conflicting.

Introduction--The thermal structure of the surface water is the result of a complex interplay of many processes of heat transfer [GEIGER, 1950, p. 153]. Immediately at the sea surface the flux of heat occurs in many forms: by solar radiation, both direct and scattered; by infra-red radiation from the surface, and from the atmosphere to the sea; by conduction; and in a latent form by evaporation of surface water. The net flux of heat through the surface is the algebraic sum of all these various forms of heat flux.

Below a depth fixed arbitrarily at which solar radiation is imperceptible, the heat flux is entirely by eddy conductivity of heat. It is controlled by the temperature gradient and the coefficient of eddy thermometric conduction. The dependence of this coefficient on the thermal structure and field of mean motion is not clearly understood.

The water layer between the surface and this arbitrary depth heats or cools, depending upon whether or not the net surface flux of heat into the layer exceeds the flux out at the bottom.

The diurnal variation of solar radiation produces the most marked fluctuation in the net heat flux at the surface. This is reflected in a corresponding change in the temperature of the surface layer. If the loss of heat through the depth below which eddy conduction predominates is great, the diurnal variation of temperature will not be so pronounced. Variations in this flux will be associated with variations in the coefficient of eddy thermometric conductivity, and this in turn will, we suppose intuitively, depend upon the force of the wind.

In terms less susceptible to quantitative interpretation, but more pictorial, we may think of this problem in the following way: The surface accumulates heat if the net surface flux is downward and if the wind does not ''mix the heat down'' to lower layers.

During the two periods March 26-April 3 and April 13-27, 1942, the Atlantis drifted with the surface water in the Gulf of Mexico. An attempt was made to remain always in the same portion of the surface water by determining the drift of the ship by means of her motion relative to a free drag, and then sailing back to the computed position of the surface water once each day. One of the purposes of this cruise was to study the diurnal heating of the surface water. The central region of the Gulf of Mexico is particularly suited for this kind of study, because the currents are weak and advective effects presumably small. As a result, the net flux of heat is analyzed on the assumption that it is vertical. These data were obtained under the supervision of the second author. The purpose of this paper is to record and discuss this interesting series of observations.

Preparation of the data--The body of data consists of hourly bathythermograms, wet- and dry-bulb air temperatures, sea surface temperatures, wind force, and cloud cover on a scale of tenths.

The data are not, strictly speaking, a continuous series. For example, there is a break of about a week (April 4-12) during which the Atlantis was in port, and during the night of April 17-18 she sailed to the southeast to avoid a current into which she had drifted. Because of these breaks in the series it is natural to study the data in several distinct portions. We will study in particular the series from April 18-27, which represents a reasonably unbroken continuous series. The positions of the Atlantis during the entire drifting period were within the area of the Gulf of Mexico shown in Figure 1.

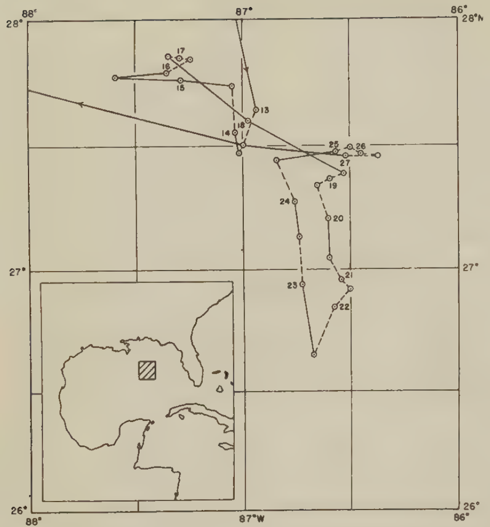

Fig. 1--The position of the *Atlantis* in the Gulf of Mexico during April 1942; the numbers next to the fixes indicate the day of the month; the shaded area in the inset map shows the location of the area

Figure 2 shows typical diurnal variations in the temperature of the surface water to a depth of 20 fm as well as the computed net heat flux and wind force at the surface. The purpose of this figure is to provide a rough qualitative picture of the phenomena.

Figure 3 shows the temperature variations at various depths for the selected period of April 18-27.

Computation of the surface heat flux--A column of water of one sq cm horizontal section is considered, extending from the surface down to a depth of 40 fm. The net flux of heat F (in whatever form) is taken as positive upward. At the surface this flux is composed of a number of terms.

$$F_o = Q_s + Q_b + Q_d \quad \ldots\ldots\ldots \quad (1)$$

Q_s is the solar radiation flux, both direct and scattered, corrected for cloudiness according to the formula [SVERDRUP, JOHNSON, and FLEMING, 1942, p. 102]

$$Q_s = -Q_o\ (1 - 0.071C) \quad \ldots\ldots\ldots \quad (2)$$

where C is the cloudiness on a scale of tenths, and Q_o is the incoming radiation with a clear sky; Q_b is the back radiation in the infra-red of the sea surface, given by the formula [SVERDRUP and others, 1942, p. 112]

$$Q_b = Q_o'\ (1 - 0.083C) \quad \ldots\ldots\ldots \quad (3)$$

in which

$$Q_o' = sT^4\ (0.56 - 0.08\sqrt{e}) \quad \ldots\ldots\ldots \quad (4)$$

where e is the vapor pressure in millibars, T is the absolute temperature, and $s = 1.178 \times 10^{-7}$ cal/sq cm day (deg abs) 4; and Q_d is the heat flux through the surface by direct heat conduction and by evaporation [MONTGOMERY, 1940].

$$Q_d = Q_e + Q_c \quad \ldots\ldots\ldots \quad (5)$$

where

$$Q_c = h_c\ (\theta_s - \theta_d) \quad \ldots\ldots\ldots \quad (6)$$

$$Q_e = h_e\ (e_s - e_d) \quad \ldots\ldots\ldots \quad (7)$$

The coefficients h_c and h_e are functions of the wind force, but their values are only roughly known. Very approximate values are given in Table 1. θ_s and θ_d are Fahrenheit temperatures of the sea surface and air at deck level respectively; e_s is the saturation vapor pressure of water in millibars at the sea surface; and e_d is the vapor pressure at deck level.

The quantities Q_s, Q_b, Q_c, Q_e, have been computed according to the above formulas from the meteorological data.

The values of the surface heat flux determined by these formulas are undoubtedly very rough and subject to error, as pointed out by THORNTHWAITE and HOLZMAN [1942]. Unfortunately, even the probable error is unknown.

Qualitative description--In Figure 2 we have representative examples of the diurnal heating process. The computed net heat flux at the surface is plotted at the right of each diurnal series of temperature soundings.

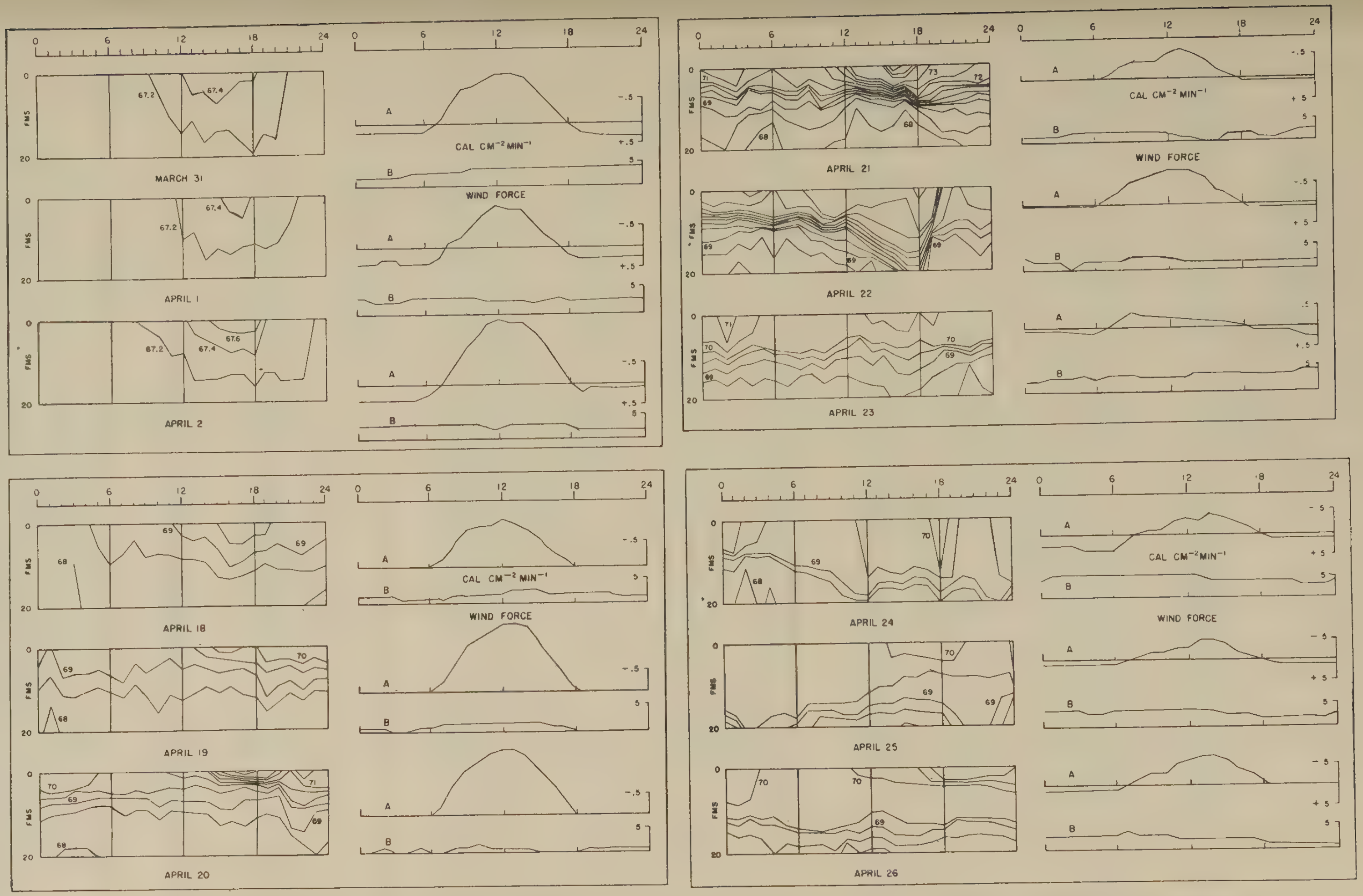

Fig. 2--Selected cases of diurnal heating; the time-depth profiles drawn from the hourly bathythermograms are drawn on the left; the contour interval is not the same in all cases: 0.2°F for March 31, April 1 and 2, but 0.5°F for the other days shown; the computed net heat flux positive upward at the surface is shown plotted against time of day on the right in the curves labelled A; the observed wind force as a function of time in the curves labelled B

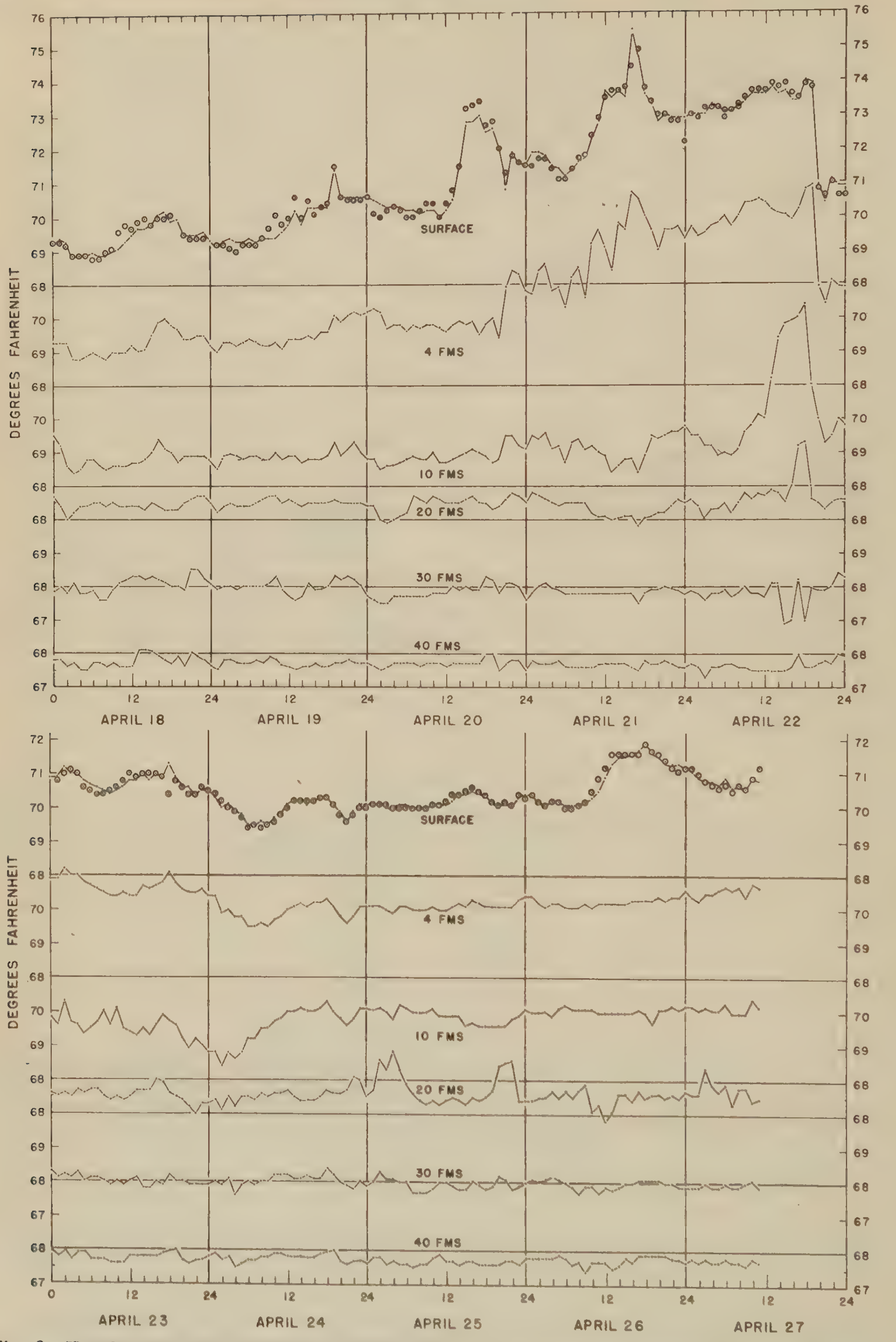

Fig. 3--Hourly temperatures at fixed depths as read from bathythermograms; a break in the series occurs at 19h 00m April 22 because of a shift in position of the ship; the small circles are the hourly surface bucket temperatures

Table 1--Sensible and latent heat transfer coefficients

Wind force, Beaufort	1	2	3	4	5	6
h_c, cal/sq cm hr deg F	0.10	0.20	0.30	0.41	0.53	0.66
h_e, cal/mb sq cm hr	0.29	0.58	1.00	1.75	3.00	4.60

The temperature soundings for March 31, April 1, and April 2 are shown. During the nights the water was perfectly homogeneous. There was considerable loss of heat during the night, but, on the whole, more heat was added to the water during a 24-hr period than was lost.

A good example of the progress of events may be found in the first series, that for March 31. The water is vertically homogeneous in the early morning, and is losing heat to the atmosphere, mostly in the form of latent heat of evaporation. The sun rises at 06h 00m (+5 zone). The flux of heat across the surface reverses sign by 07h 00m, and increases to a maximum at about 13h 00m. About 09h 00m the temperature of the surface water begins to increase and continues to do so until about 17h 00m, or about as long as the net surface flux is negative. The sea begins to lose heat through the surface at 18h 00m, and the water is homogeneous again by 21h 00m. The heat added during the day (07h 00m - 18h 00m) was about 360 cal/sq cm. Thus it is consistent to suppose that about 80 cal/sq cm must have been conducted to deeper layers by eddy transfer processes. This paragraph is not the place for quantitative discussion. It is good to realize, however, that the net heat flux at the surface is more than enough to produce the observed surface-layer heating.

The following two days are qualitatively similar. The morning of April 1 was cloudy, so that the surface heating was delayed. April 2 was a clear day. The net surface flux was greater, and the surface heating correspondingly greater.

During the three days, April 18, 19, and 20, the wind was progressively weaker, and the heat flux greater. The water was not homogeneous at night, nor was there any considerable loss of heat through the surface at night. The diurnal heating of the top three or four fathoms is clearly greatest for April 20, the day on which the surface heat flux is greatest and the wind least.

On April 21 the thermal gradients of the day before persist. On April 22, at 18h 00m, the Atlantis shifted position. It seems that a new water mass was entered by the end of April 22.

April 23 was a cloudy day with rising winds. The surface heating was small. The same is true of April 24 and 25. By the end of April 25 the wind fell, the sky cleared partly, and there was some rise in surface temperature late in the day.

This series of days represents a selected set of cases. The writers feel that they demonstrate, in a striking manner, the fact that clear days with light winds are the most favorable for the development of a thin, warm, surface layer (or, alternatively, of a strong thermal gradient at the surface). Cloudiness, or windiness, or both, are unfavorable to this development. It is a question whether much can be expected by subjecting them to a gross numerical analysis such as is attempted in the following paragraphs.

Method 1: If there is a depth z = -h below which θ does not change with time, we can compute A at any depth z_1 by the equation

$$A_{z_1} = [\int_{-h}^{z_1} (\partial\theta/\partial t)dz]/[(\partial\theta/\partial z)_{z_1}] \ldots\ldots\ldots\ldots (8)$$

Method 2: If at the surface z = 0 we know the net flux of heat F_o, we can use the surface as a reference level for computing A at $z = z_1$.

$$A_{z_1} = [F_o/C + \int_{z_1}^{0} (\partial\theta/\partial t)dz]/[(\partial\theta/\partial z)_{z_1}] \ldots\ldots\ldots\ldots (9)$$

Method 3: If A is independent of depth, then

$$\partial\theta/\partial t = A\, \partial^2\theta/\partial z^2 \ldots\ldots\ldots\ldots (10)$$

and A can be determined by direct evaluation of $\partial\theta/\partial t$ and $\partial^2\theta/\partial z^2$ from the data. The great weakness of this method is that it depends upon second differences, which in the present data are subject to great error.

Actual computations made by various methods--Method 1: Inspection of Figure 3 reveals that even at a depth of 40 fm there are fluctuations in the temperature as read from a bathythermogram with a standard deviation of about ± 0.1°F. It is not possible to decide whether these are because of a lack of precision of the instrument or represent actual variations in the temperatures measured: short-period internal waves, turbulent fluctuations, or horizontal heterogeneities through which the ship drifted. Whatever they may mean, it is clear that they are of such a magnitude that if the heat content of a column is figured by integrating the measured temperature from the surface to a depth of 40 fm, it will be subject to fluctuations of such an order of magnitude as to obscure the diurnal variations in heat content. If we average the heat contents of several consecutive hours' soundings, then we reduce the range of fluctuation but in this way, too, obscure the diurnal variation.

Method 2: The computed surface flux is used as the known flux at the surface in terms of which we compute that at lower levels. The eddy conductivity is computed at the depth of four fathoms, using three-hour means to avoid the effect of short-period fluctuations due to local causes unrelated to the heat flux (such as internal waves).

If the values of A are plotted individually against wind force, they show a great scatter. It is not possible to decide whether this scatter is due to errors of the bathythermograph, actual inhomogeneities in the water, uncertainties in the computed surface heat flux, or real deviations of the eddy coefficient.

The means of the eddy coefficient for various ranges of the wind force are plotted against mean wind force in Figure 4. The number next to each plotted point represents the number of

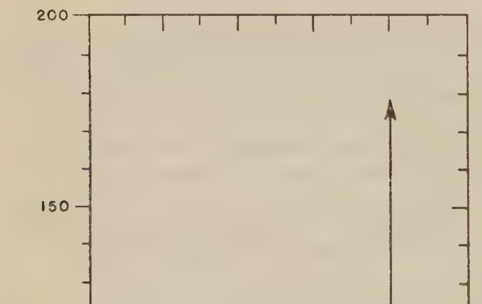

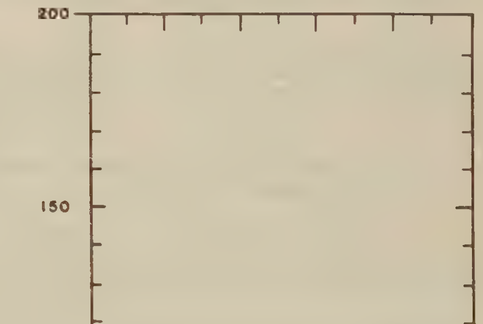

Fig. 4--Mean eddy coefficients as functions of wind force computed by Method 2; the arrows show the range of the mean deviation of individual values; the numbers indicate the number of individual determinations entering each mean

Fig. 5--Same as Figure 4, but computed by Method 3 individually computed eddy coefficients in the mean; the double arrows represent the mean deviation. Two extremely large eddy coefficients were omitted from the data used in Figure 4 on the ground that the ship was moving under power at the time. All eddy coefficients for times when the temperature gradient was less than 0.1°F per four fathoms were omitted from the compilation of the means for Figure 4, because the uncertainty introduced in the computation of the eddy coefficients is particularly great for small temperature gradients. The data were not selected in any other manner, however. The net result is that the eddy coefficient at four fathoms increases with increasing wind force. The result does not seem unreasonable, but cannot be regarded as proven because of the uncertainties involved. It might be the result, for example of a systematic error in the evaporation formula.

Method 3: Using the same three-hour means we computed the eddy conductivity A at a depth of six fathoms, for all the data of the period shown in Figure 3, with the exception of those during the night of April 22, when the ship shifted position. Cases of small $\partial^2\theta/\partial z^2$ were rejected on account of the great influence of error in such cases. The resulting values of A show a great scatter. They were gathered into two groups according to whether the wind force was greater or less than 2.5. The means and mean deviations of these two groups are plotted in Figure 5. They indicate a trend the opposite of that shown by Figure 4.

Method 2 would be the most reliable were the heat loss due to evaporation well known. Method 3 is weak on account of the immense errors entering through the second differences. A relation between the eddy conductivity and wind force such as shown in Figure 4 seems reasonable, but has not been demonstrated, and is contradicted by Figure 5.

Recommendations for further study--As a result of studying these data, several recommendations for future studies of this kind suggest themselves: (1) In addition to the serial bathythermograms it would be helpful to have continuous recordings of the temperature at a number of fixed depths. (2) A pyrheliometer would be a valuable addition to the instruments in order to measure the solar radiation directly rather than depend upon formulas involving estimates of cloudiness, and related factors. (3) Psychrometric and wind-velocity measurements should be made at two or more levels to permit use of a better evaporation formula, such as that of Thornthwaite and Holzman. (4) Because wind-speed measurements are so difficult from a ship, one wonders whether a large, nearly submerged buoy, with a mast for meteorological measurements, and a trailing cable for recording sea temperature at various depths, would not be the most satisfactory instrument for studies of this kind. It would be more stable than a ship, would remain in more nearly the same mass of water, and could be left unattended for a day or so.

References

GEIGER, R., The climate near the ground, Harvard Univ. Press, 1950.
MONTGOMERY, R. B., Observations of vertical humidity distribution above the ocean surface, and their relation to evaporation, Papers Phys. Ocean. Met., v. 7, no. 4, 30 pp., 1940.
SVERDRUP, H. U., M. W. JOHNSON, and R. H. FLEMING, The oceans; their physics, chemistry, and general biology, Prentice-Hall, Inc., 1087 pp., 1942.
THORNTHWAITE, C. W., and BENJAMIN HOLZMAN, Measurement of evaporation from land and water surfaces, U. S. Dept. Agriculture Tech. Bull. No. 817, 142 pp., 1942.

Woods Hole Oceanographic Institution,
Woods Hole, Massachusetts

(Communicated manuscript received January 16, 1951;
open for formal discussion until January 1, 1952.)

Contribution No. 554

Made in United States of America

Reprinted from JOURNAL OF THE WASHINGTON ACADEMY OF SCIENCES
Volume 41, No. 3, March 15, 1951

ICHTHYOLOGY.—*A new genus and species of anacanthobatid skate from the Gulf of Mexico.* HENRY B. BIGELOW and WILLIAM C. SCHROEDER.* (Communicated by L. P. Schultz.)

In 1924 von Bonde and Swart[1] proposed a new genus *Anacanthobatis* for *Leiobatis marmoratus* von Bonde and Swart, a curious batoid from the Natal coast; skatelike in that its pelvic fins are so deeply concave outwardly that they are entirely subdivided with the anterior subdivision limblike, but differing from all typical skates in their perfectly naked skins and in lacking dorsal fins. A second new species, *dubia*, agreeing with *marmoratus* in naked skin and in filamentous prolongation of the snout, but differing from it in that the outer margins of the posterior subdivision of its pelvic fins are fused along their anterior one-half with the inner margins of the pectorals, was also referred to *Anacanthobatis* by von Bonde and Swart.[2] But the unique specimen seems to have lost most of its tail, so that the presence or absence of dorsal fins remains to be learned.

Anacanthobatis is included among the Dasyatidae by Barnard,[3] by Fowler,[4] and by Smith.[5] But the nature of its pelvic fins seems to us to place it among the rajoids, as a separate family, Anacanthobatidae, because of its naked skin and lack of dorsal fins.

No batoid resembling *Anacanthobatis* was seen again until the autumn of 1950, when trawlings by the U. S. Fish and Wild Life Service vessel *Oregon* in the northern side of the Gulf of Mexico, off the Mississippi, yielded two specimens that agree with the South African *A. marmoratus* von Bonde and Swart in structure of pelvics, wholly naked skin, and long slender tail without dorsal fins, but with *A. dubia* von Bonde and Swart in the fact that the outer margins of the posterior subdivision of the pelvic fin is fused along the anterior two-thirds with the inner margin of the pectorals, which is not the case in *marmoratus*. But the Gulf of Mexico form differs from both *marmoratus* and *dubius* in that the end of the snout is expanded in leaflike form (Fig. 1).

The marginal fusion of pelvic fins with pectorals now established for two species is so unusual a character as to justify a new genus, for which we propose the name *Springeria*, in recognition of Stewart Springer's productive studies of the elasmobranchs of Florida and the Gulf. And the curious shape of the snout equally necessitates a new species, which we name *folirostris* for obvious reasons.

---

* Contribution no. 554 from the Woods Hole Oceanographic Institution.

[1] Mar. Biol. Surv. South Africa Rep. 3, spec. Rep. 5 [1922]: 18, pl. 23, and accompanying errata slip. 1924.

[2] Loc. cit., p. 19.

[3] Ann. South African Mus. **21:** 79. 1925.

[4] U. S. Nat. Mus. Bull. 100, **13:** 448. 1941.

[5] *Sea fishes of southern Africa*: 71. 1949.

Springeria, n. gen.

Genotype.—*Springeria folirostris,* n. sp.

Generic characters.—Snout either prolonged as a simple filament, or expanded terminally in shape shown in Fig. 1, terminating in a soft filament; firm rostral cartilage extending to base of filament; outer margins of posterior lobes of pelvics united along first two-thirds of their length with inner margins of pectorals; inner margins of posterior pelvic lobes attached nearly to tips to sides of tail. Tail without lateral folds, its lower side as well as its upper side with caudal membrane. Pelvic transverse, its anterior

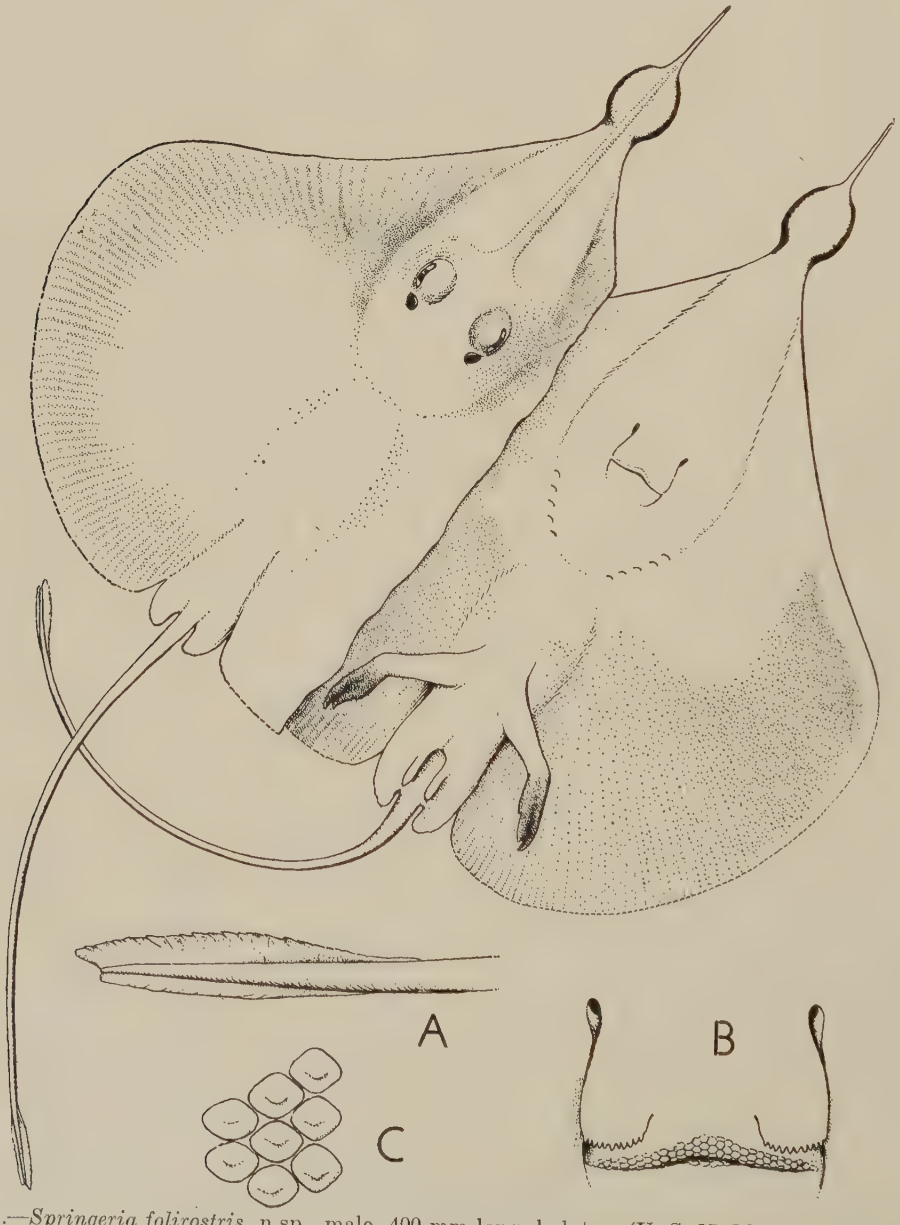

FIG. 1.—*Springeria folirostris*, n.sp., male, 400 mm long, holotype(U. S. N. M. no. 152546): A, End of tail, about ×1.8; B, mouth and nasal curtain, about ×1.8; C, three rows of teeth, upper, about ×10.

profile slightly concave rearward, a long slender process at either end, directed forward, no radial cartilages along anterior half of basipterygial cartilages of pelvic fins.

Species.—Two species known, *S. folirostris*, n. sp., from the Gulf of Mexico, and probably also *dubia* von Bonde and Swart, 1924, South Africa.

Springeria folirostris, n. sp.

Study material.—Immature male, 400 mm long to base of terminal filament; northern Gulf of Mexico off the Mississippi River, lat. 29° 02′ N., long. 88° 34′ W.; 232–258 fathoms; holotype, U. S. N. M. no. 152546; and very young male, 125 mm long, same general locality, lat. 29° 01′ N., long. 88° 30′ W., paratype, Museum of Comparative Zoology.

Distinctive characters.—*Springeria folirostris* differs from all other known batoids in the peculiar leaflike expansion of the end of its snout. Specimens with this and the tail damaged would still be easily separable from all other rajoids of the Atlantic by their perfectly naked skins; from all dasyatid and myliobatid rays by the nature of their pelvic fins.

Description of type (proportional dimensions in percent of total length).—Disc: Extreme breadth 51.6; length 55.3. Length of snout in front of orbits 21.8; in front of mouth 24.3. Orbits: Horizontal diameter 2.9; distance between 2.6. Spiracles: Length 1.0; distance between 5.1. Mouth: Breadth 4.5. Nostrils: Distance between inner ends 5.8. Gill openings: Lengths, first 0.75, third 0.75, fifth 0.50; distance between inner ends, first 9.2, fifth 4.8. Caudal fin: Length, base, upper 6.0, lower 5.0. Pelvics: Anterior margin 12.7. Distance from tip of snout[6] to center of cloaca 47.6; from center of cloaca to tip of tail 52.4.

Disc from base of terminal filament about 1.1 times as long as broad; maximum anterior angle from level of base of terminal expansion of snout to level of spiracles about 85°; end of snout expanded in leaflike form as shown in Fig. 1, terminating in a slender filament about as long as distance between spiracles. Margins of disc rearward from terminal expansion weakly concave about to level of spiracles, then altering to continuously and strongly convex around to very short inner margins without definite outer or posterior corners. Tail very slender, laterally compressed, increasingly so rearward; its width at axils of pelvic fins (where thickest) about as great as length of eye; its length from center of cloaca to tip about 1.1 times as great as distance from cloaca to base of terminal filament of snout. Skin perfectly naked everywhere, without dermal denticles of any sort. Snout in front of eyes about 8.4 times as long to base of terminal filament as distance between orbits, its length in front of mouth about 6.5 times as great as distance between exposed nostrils. Orbit about 1.1 times as long as distance between orbits, and nearly 3 (2.9) times as long as spiracle which is noticeably small. Nasal curtain conspicuously fringed, each side with 10–11 lobelets; outer margin of nostril only slightly expanded with irregular edge. Exposed nostril noticeably minute. Mouth on immature males a little arched forward, probably also on females, its shape not known for mature males. Teeth $\frac{2}{2}\frac{2}{7}$ on young male, low, with obscure cutting edge but no cusp, and arranged in quincunx. Teeth of mature males not seen. Gill openings minute; first about one-sixth as long as breadth of mouth; fifth about two-thirds as long as first; distance between inner ends of first gills about 1.6 times as long as between exposed nostrils, and between fifth gills about 1.9 times. No dorsal fins. Base of upper caudal fin-membrane about 1.0 times as long as distance between exposed nostrils, of shape illustrated (Fig. 1), its maximum width about one-tenth (about 9 percent) as great as length of its base; lower caudal membrane about half (55 percent) as wide as upper, its origin a little posterior to origin of upper; the two lobes discontinuous at tip of tail. Anterior leglike subdivision of pelvics nearly as long (95 percent) as from pelvic origin to rear corners, broader than thick, fleshy, with one articulation about midway its length, inner edge of the terminal segment scalloped, corresponding to tips of the three radial cartilages. Posterior lobe of pelvics with narrowly rounded rear corner reaching rearward only about as far as rear limits of disc; outer margin joined for about two-thirds its length to margin of pectoral, inner edge joined nearly to tip to side of tail.

Anterior rays of pectorals extending forward to a little posterior to base of terminal expansion of snout; firm rostral cartilage reaching about to base of terminal filament.

---

[6] Exclusive of rostral filament, which is 23 mm long.

Color: Ash gray above, except unpigmented and translucent in spaces between rostral ridge and anterior rays of pectorals; orbits dusky, terminal expansion of snout narrowly and irregularly margined with black, also the posterior part of the back with a sooty blotch on one side near midline, perhaps the result of injury. Lower surface pale grayish white, the outer posterior belt of pectorals sooty gray, terminal expansion of snout narrowly and irregularly edged with black; tail sooty at base.

Development stages.—Presumably *Springeria* is oviparous like other rajids, but its eggs have not been seen yet.

Size.—How large this skate may grow is not known, for the larger of the two specimens seen so far, 400 mm long to base of terminal filament, is an immature male, its claspers not yet reaching as far as the tips of its pelvics.

Habits.—The two specimens seen so far were trawled at 232–258 fathoms, this with the improbability that this skate would have been overlooked if it occurred in shallow water, suggests that it is confined to depths greater than about 200 fathoms. Nothing else is known of its habits.

Range.—So far known only in the northern side of the Gulf of Mexico off the Mississippi River, at the localities listed on page 112 under Study material.

Contribution No. 555

Reprinted from JOURNAL OF THE WASHINGTON ACADEMY OF SCIENCES
Volume 41, No. 12, December 15, 1951
Printed in U.S.A.

ICHTHYOLOGY.—*Three new skates and a new chimaerid fish from the Gulf of Mexico.*[1] HENRY B. BIGELOW and WILLIAM C. SCHROEDER. (Communicated by Leonard P. Schultz.)

The U. S. Fish and Wildlife Service vessel *Oregon*, while engaged in a shrimp investigation in the Gulf of Mexico during the winter of 1950–51, caught a number of fishes that prove to be new to science. Stewart Springer, knowing of our interest in elasmobranchs and holocephalids, kindly sent us the specimens which we here describe. The holotypes and some of the paratypes are in the collection of the U. S. National Museum, while a representative of each species is in the collection of the Harvard Museum of Comparative Zoology.

Raja lentiginosa, n. sp.

Study material.—Male, 402 mm in total length, holotype, U. S. N. M. no. 153552, from the Campeche Bank, lat. 22° 32′ N., long. 88° 47′ W., in 29 fathoms, *Oregon* station 222; also four males and three females from the latter region and from the northern part of the Gulf of Mexico, lat. 28° 10′ to lat. 29° 11′ N. and long. 85° 00′ to 86° 52′ W. in recorded depths of 85, 112, 165, and 305 fathoms, including *Oregon* stations 256, 257, 278, and 279.

Distinctive characters.—*Raja lentiginosa* closely resembles *R. garmani* but may be distinguished by the color pattern of its upper surface, which is densely freckled with very small dark, light-brown, and whitish spots (sparse in *garmani* and mostly grouped in a distinct rosette pattern).

Description of holotype.—Proportional dimensions in percent of total length:

Disc.—Extreme breadth 60.0; length 46.5.

Snout length.—In front of orbits 9.2; in front of mouth 11.2.

Orbits.—Horizontal diameter 4.2; distance between 2.9.

Spiracles.—Length 2.1; distance between 6.2.

Mouth.—Breadth 6.5.

---

[1] Contribution no. 555 from the Woods Hole Oceanographic Institution.

Exposed nostrils.—Distance between inner ends 6.0.

Gill openings.—Lengths, first 2.0; third 1.9; fifth 1.2; distance between inner ends, first 13.9; fifth 7.0.

First dorsal fin.—Vertical height 3.0; length of base 5.6.

Second dorsal fin.—Vertical height 3.0; length of base 5.5.

Pelvics.—Anterior margin 12.2.

Distance from tip of snout to center of cloaca 39.2; from center of cloaca to first dorsal 45.3; to tip of tail 60.8; from rear end of second dorsal base to tip of caudal 2.9.

Interspace between first and second dorsals 1.2.

Disc about 1.3 times as broad as long, maximum angle in front of spiracles about 120°; anterior margins weakly convex from just posterior to tip of snout to opposite orbits, thence gently concave between spiracles and outer corners which are broadly rounded; posterior margins and corners and inner margins all rounded. Axis of greatest breadth about 68 percent of distance back from tip of snout to axils of pectorals. Tail with a lateral fold, low down on each side, beginning abruptly posterior to axils of pelvics a distance about equal to space between spiracles and continuing almost to extreme tip, width of fold about the same throughout its length; length of tail from center of cloaca to origin of first dorsal fin 1.15 times as great and to its tip 1.54 times as great as distance from center of cloaca to tip of snout.

Five prominent thorns along anterior edge of orbit, one opposite inner central margin and three along posterior margin, the last opposite spiracle, with an additional thorn inward from this one; a row of thorns over margins of rostral process; prickles and very small thorns are present over anterior third of disc in advance of nuchal region and extend along outer margin rearward to about axils of pectorals; a triangular patch of about 17 thorns on shoulder region, five of which extend along median line from nuchal to scapular region; a naked area behind these for a distance about equal to distance between spiracles. A band of three to five rather regular rows of thorns along median zone of back and on tail beginning in advance of axils of pectorals a distance about equal to that from eye to snout and ending at origin of first dorsal, the lowermost row reaching nearly to tip of tail; the median row, counting from nuchal region, consisting of 33 thorns, in most cases alternating large and small; most all the thorns on tail with sharp points, directed backward; one prominent thorn in space between dorsals; prickles on dorsal fins and caudal; skin over eye naked; a band of alar spines on outer part of each pectoral, in one to three rows, with 19 spines in longest row. Lower surface naked except for a small median patch of spines at extreme snout tip.

Snout in front of orbits 2.2 times as long as orbit, its length in front of mouth about 1.8 times as great as distance between exposed nostrils. Distance between orbits about 0.7 as great as length of orbit. Orbit twice as long as spiracle. Nasal curtain fringed; expanded posterior (outer) margins of nostrils fringed. Upper and lower jaws rather strongly arched centrally. Teeth $\frac{53}{52}$ close set, mostly in straight rows rather than in quincunx, with small base, circular or oval, those in median sector of mouth with slender sharp cusp pointing toward symphysis or inward toward throat, those in outer sector with triangular cusp pointing toward corner of mouth, one row of teeth at symphysis in upper jaw, pointing straight downward. Distance between first gill openings 2.3 times as great as distance between exposed nostrils; between fifth openings 1.2 times; first gill openings 1.6 times as long as fifth and 0.3 as long as breadth of mouth. First and second dorsals similar in size and shape. Interspace between dorsals 0.22 as long as base of first dorsal. Caudal membrane from rear end of base of second dorsal about half as long as base of first dorsal. Pelvics deeply concave, strongly scalloped along anterior side of excavation but only weakly so rearward; anterior margin only 0.55 as long as distance from its own origin to rear tip of pelvic; anterior lobe slender, including four radial cartilages besides the first stout one; posterior lobe moderately convex along its forward half, thence nearly straight to its narrowly rounded tip, extending a little more than one-fifth the distance from axil of pelvics toward first dorsal; inner margin straight. Claspers reaching beyond tips of pelvics by a distance about equal to diameter of orbit.

Rostral cartilage firm, extending nearly to tip of snout. Anterior pectoral rays reaching about seven-tenths the distance from front of orbits toward tip of snout.

Color.—Upper surface everywhere sprinkled with very small light to dark brownish and whitish spots, including the tail, pelvics and claspers; many groups of about 30 50 dark spots scattered everywhere, the most prominent marking being the group of spots at axil of pectoral, some of the spots on tail grouped in form of bars, there being about five prominent bars; light and dark spots present on anterior part of each dorsal fin and on caudal. Below whitish with a group of grayish blotches, mostly fused, on each pectoral, and an elongate blotch along the inner part of the claspers anteriorly.

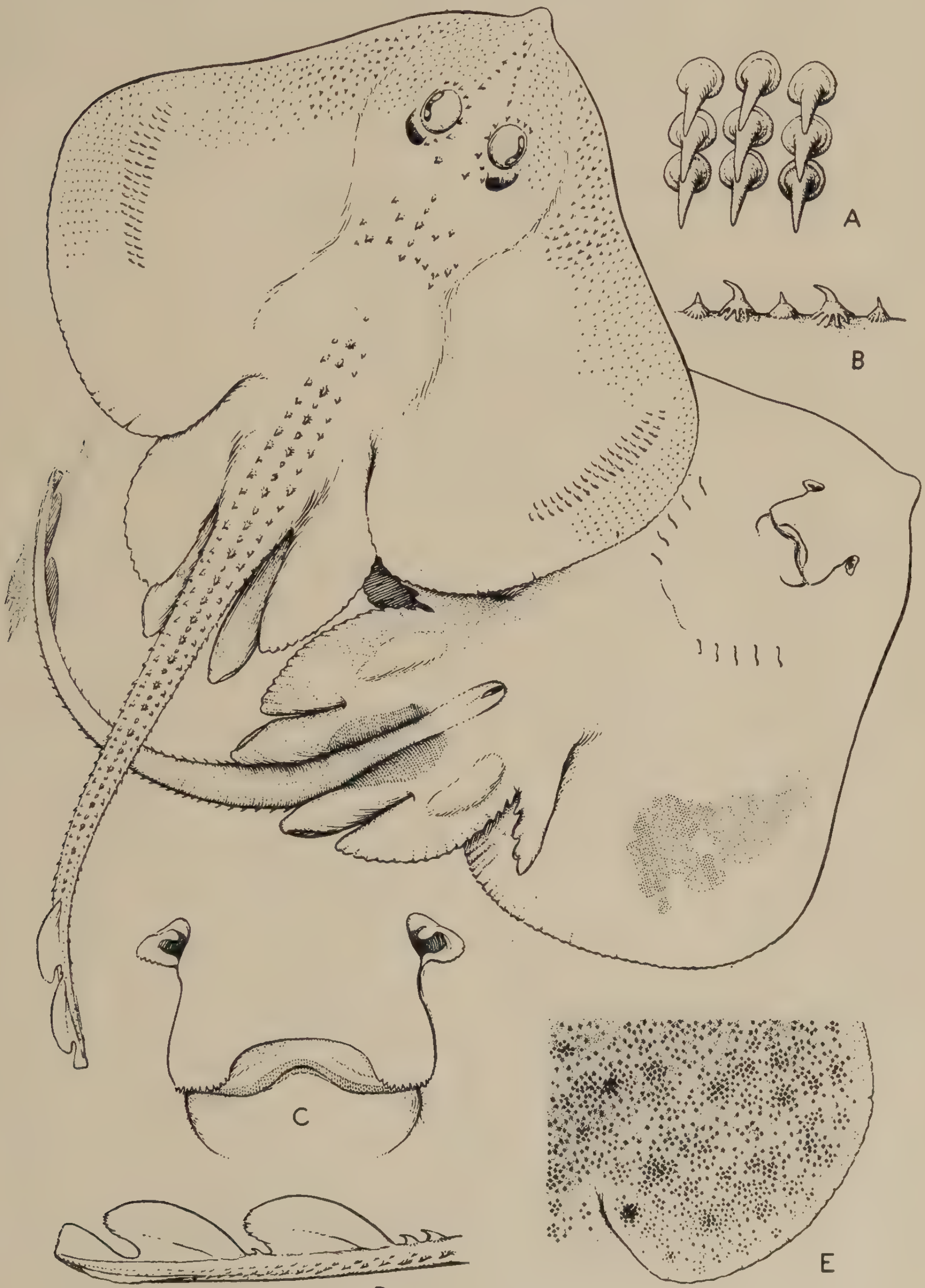

FIG. 1.—*Raja lentiginosa*, n.sp., male, 402 mm long, holotype (U.S.N.M. no. 153552): A, Upper teeth, about × 10; B, thorns on midrow of tail, about × 2; C, mouth and nostrils, about × 1.5; D, posterior part of tail, about × 1; E, section of upper surface to show color pattern.

A female 302 mm long differs slightly from the type by having no naked area on the midzone of back immediately behind shoulder region, but the thorns begin on the nape and extend without a break to the first dorsal, the rows being somewhat more irregular and the median row having about 45 thorns mostly of uniform size instead of alternating large and small. There is a patch of small thorns on the posterior part of the pectorals and a few on the pelvics and three thorns in the space between the dorsals. There are $\frac{50}{46}$ teeth, in quincunx, with low triangular cusp, none of which point toward symphysis or corners of mouth.

On a male of 232 mm the claspers extend a little beyond the tips of the pelvics, while on a *R. garmani* of 285 mm they fail to reach the tips of the pelvics by a distance as great as diameter of orbit. This male has 46 teeth in upper jaw and lacks the small patch of thorns on the extreme tip of snout below.

The few specimens of this species thus far captured have been taken over a wide depth range, from 29 to 305 fathoms. It is known from the northern part of the Gulf of Mexico in the offings of Pensacola and Cape San Blas and in the southern part on Campeche Bank.

Raja olseni,[2] n. sp.

Study material.—Immature male, 280 mm in total length, holotype, U. S. N. M. no. 153556, from lat. 27° 25′ N., long. 96° 13′ W., 76 fathoms, *Oregon* station 157 and an immature male, 282 mm, paratype, M. C. Z. no. 37176, from lat. 27° 27′ N., long. 96° 17′ W., 65 fathoms, *Oregon* station 158.

Distinctive characters.—*Raja olseni* closely resembles *R. laevis* in general appearance and in lacking thorns along the midbelt of the disc from the level of the axils of the pectorals to the vicinity of the spiracles. But it differs from *laevis* in having an interspace between the dorsal fins nearly or quite as long as the base of the first dorsal (only 0.1 to 0.3 that long in *laevis*); by having a fringe on the expanded outer margin of the nostril (smooth in *laevis*); also the lateral folds along its tail reach to only opposite the anterior third of the caudal fin, but in *laevis* extend almost or quite to the extreme tip of the tail; the lower sides of the disc are prickly along the anterior edges and over the rostral cartilage in *olseni* but smooth on *laevis* of equal size and its mucous pores are not marked with black as they are in *laevis*. It differs from *R. spinicauda* in its fringed nostril lobe, in its shorter tail folds, in the interspace between its dorsals, and in having three rows of thorns on the tail (only one row on *spinicauda*).

Description of holotype.—Proportional dimensions in percent of total length:

Disc.—Extreme breadth 69.0; length 54.0.

Snout length.—In front of orbits 15.6; in front of mouth 17.7.

Orbits.—Horizontal diameter 4.4; distance between 3.6.

Spiracles.—Length 2.0; distance between 6.3.

Mouth.—Breadth 7.9.

Exposed nostrils.—Distance between inner ends 7.9.

Gill openings.—Length, first 2.0; third 2.1; fifth 1.6; distance between inner ends, first 13.6; fifth 7.3.

First dorsal fin.—Vertical height 2.5; length of base 4.3.

Second dorsal fin.—Vertical height 2.4; length of base 4.6.

Pelvics.—Anterior margin 13.2.

Distance from tip of snout to center of cloaca 47.5; from center of cloaca to first dorsal 30.4; to tip of tail 52.5; from rear end of second dorsal base to tip of tail 3.2.

Interspace between first dorsal and second dorsal 4.3.

Disc about 1.3 times as broad as long, the maximum anterior angle in front of spiracles about 90°; anterior margins concave just posterior to tip of snout, weakly convex opposite eyes and spiracles, thence about straight rearward; outer corners narrowly rounded; posterior corners more broadly so; posterior margins gently convex. Axis of greatest breadth about 67 percent of distance back from tip of snout to axils of pectorals. Tail with a lateral fold, low down on each side, beginning posterior to axils of pelvics by a distance about four-fifths as long as eye and ending opposite anterior third of caudal fin, its length from center of cloaca to origin of first dorsal fin about 0.67 as great and to its tip about 1.1 times as great as distance from center of cloaca to tip of snout.

Two small thorns immediately in front of orbit, of which one is on the inner and one on the outer margin, also one on the inner rear margin; these are the only thorns or prickles on the disc. Sixteen thorns along midline of tail from a little in advance of axils of pelvics to first dorsal fin, and three in interspace between first and second dorsals. An additional row of thorns, widely and unevenly spaced, on each side of median row, beginning about opposite tips of pelvics and extending to opposite beginning of caudal fin; dorsals and caudal fin smooth. Lower surface with a narrow band of small prickles along anterior margin of disc from level of nostrils to tip of snout and also along rostral cartilage.

---

[2] Named for Yngve H. Olsen in recognition of his excellent editorial work on Fishes of the Western North Atlantic.

Snout in front of orbits 3.5 times as long as orbit, its length in front of mouth 2.2 times as great as distance between exposed nostrils. Distance between orbits 1.2 as great as length of orbit. Orbit 2.2 times as long as spiracle. Nasal curtain fringed; expanded posterior (outer) margins of nostrils fringed. Upper and lower jaws moderately arched centrally. Teeth $\frac{34}{34}$; close set in quincunx, ovate, with a triangular cusp. Distance between first gill openings 1.7 times as great as distance between exposed nostrils; between fifth gill openings 1.1 times; first gill openings 1.25 times as long as fifth and 0.25 as long as breadth of mouth. First and second dorsals similar in size and shape. Interspace between dorsals as long as base of first dorsal. Caudal

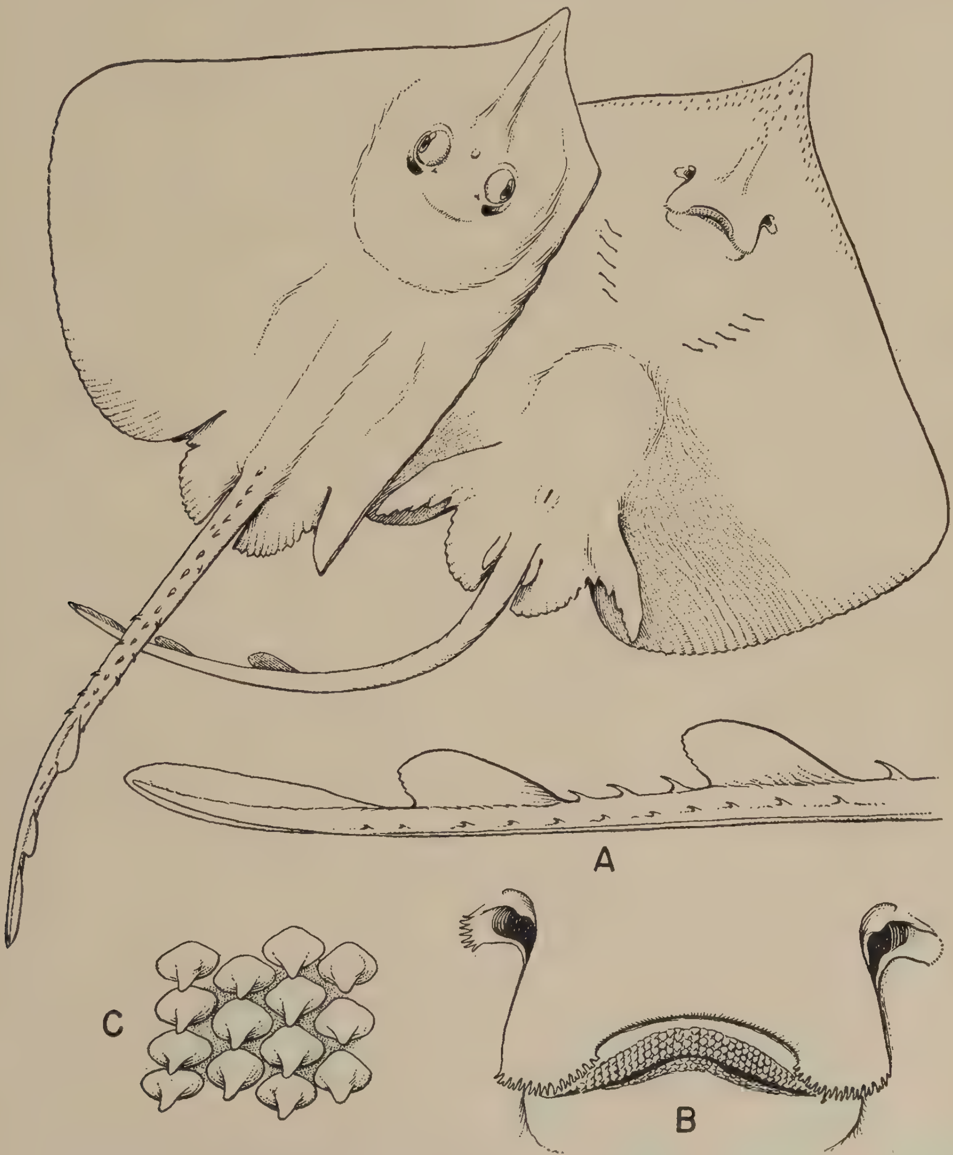

Fig. 2.—*Raja olseni*, n.sp., male, 280 mm long, holotype (U.S.N.M. no. 153556): A, Posterior part of tail, about × 1.5; B, mouth and nostrils, about × 2; C, upper teeth, about × 12.

membrane from rear end of base of second dorsal about twice as long as base of first dorsal. Pelvics deeply concave, strongly scalloped along anterior side of excavation but only weakly so rearward; anterior margin about as long as distance from its own origin to rear tip of pelvic; anterior lobe moderately slender, including five radial cartilages besides the first stout one; posterior lobe moderately convex outwardly; rear tips abruptly rounded, extending about two-sevenths the distance from axil of pelvics toward first dorsal; inner margin straight. Claspers falling well short of tips of pelvics.

Rostral cartilage firm, extending to tip of snout. Anterior pectoral rays reaching about half way from level of front of orbits toward snout tip.

Color.—Upper surface, in life, olive-brown with many small roundish obscure spots of darker brown on disc; a small dark spot, smaller than pupil, on each side of disc near its inward center; series of small whitish pores extend in three or four rows along midzone of back from region of pectoral girdle to axils of pelvics and extend on to tail in one or two rows; two rows extend rearward and outward on each side of disc posterior to the scapular region; whitish pores also are present opposite and in front of orbits, some extending toward outer margin of disc in sinuous rows. Below jet black everywhere, but this pigment tends to diminish in intensity in preservative.

The other known specimen of this species, 282 mm long, has a somewhat longer snout, the distance in front of orbits being four times the diameter of orbit; the interorbital space is as long as the orbit; the interspace between dorsals is nine-tenths as long as base of first dorsal and there are more teeth $\frac{41}{40}$.

As both specimens have very small claspers it is probable that the species attains at least a moderately large size, possibly 2 feet or more in total length.

Nothing is known of the habits of this skate except that it is apparently a moderately deep water species. It is known only from the northwestern part of the Gulf of Mexico as listed above.

Raja teevani[3], n. sp.

Study material. Immature male, 558 mm in total length, holotype, U. S. N. M. no. 153557, and an immature male 302 mm in total length, paratype, M. C. Z. no. 37189, both from lat. 29° 11′ N.; long. 86° 52′ W., in 305 fathoms, *Oregon* station 279.

Distinctive characters.—Raja teevani differs from all other rajids in the western North Atlantic in its broad tail, which widens rearward approaching the dorsal fins (in all other rajids it narrows rearward). It resembles *R. olseni* and *R. laevis* in general appearance and in lacking thorns along the midbelt of the disc from the level of the axils of the pectorals to the vicinity of the spiracles. But it differs from *olseni* by having no interspace between the bases of the dorsal fins; from *laevis* of comparable size it may be separated by its longer snout (the distance from tip of snout to eye being about one-fourth to one-third the width of the disc in *teevani* but only about one-fifth in *laevis*) and by the fact that the anterior margin of the pelvic fins is longer than the distance from its own origin to the rear tip of pelvic (shorter in *laevis*).

Description of holotype.—Proportional dimensions in percent of total length:

Disc.—Extreme breadth 72.7; length 58.2.

Snout length.—In front of orbits 22.2; in front of mouth 24.2.

Orbits.—Horizontal diameter 3.2; distance between 4.1.

Spiracles.—Length 2.0; distance between 6.1.

Mouth.—Breadth 7.7.

Exposed nostrils.—Distance between inner ends 8.7.

Gill openings.—Length, first 1.7; third 1.8; fifth 1.2; distance between inner ends, first 13.8; fifth 8.4.

First dorsal fin.—Vertical height 2.7; length of base 4.3.

Second dorsal fin.—Vertical height 2.7; length of base 4.0.

Pelvics.—Anterior margin 14.7.

Distance from tip of snout to center of cloaca 51.7; from center of cloaca to first dorsal 34.3; to tip of tail 48.3; from rear end of second dorsal base to tip of tail 5.4.

Interspace between first and second dorsals 0.0.

Disc about 1.25 times as broad as long, the maximum anterior angle in front of spiracles about 70°; anterior margins sinuous from snout to outer corners, being slightly convex a little in front of orbits; outer corners very sharply rounded; posterior margins gently convex; posterior corners broadly rounded. Axis of greatest breadth about 77 percent of distance back from tip of snout to axils of pectorals. Tail with a lateral fold low down on each side beginning almost imperceptibly about opposite tips of pelvics, widening rearward and ending opposite middle of caudal fin, its length from center of cloaca to origin of first dorsal fin 0.66 as great and to its tip 0.93 times as great as distance from center of cloaca to tip of snout.

---

[3] Named for John Tee Van in appreciation of his helpful assistance to us as editor-in-chief of Fishes of the Western North Atlantic.

Three small thorns along inner margin of left orbit, two of them anterior and one posterior; one anterior and one posterior thorn along inner margin of right orbit; minute prickles scattered over interorbital area and over entire disc anterior to the orbits. Tail with a median row of 15 backward pointing thorns, beginning about an eye's diameter posterior to the axils of pelvics and ending a little in front of first dorsal, the thorns somewhat more closely spaced and larger rearward than near their origin; minute prickles on tail from about tips of pelvics nearly to tip; dorsals and caudal with a few minute prickles. Lower surface with a band of prickles along anterior

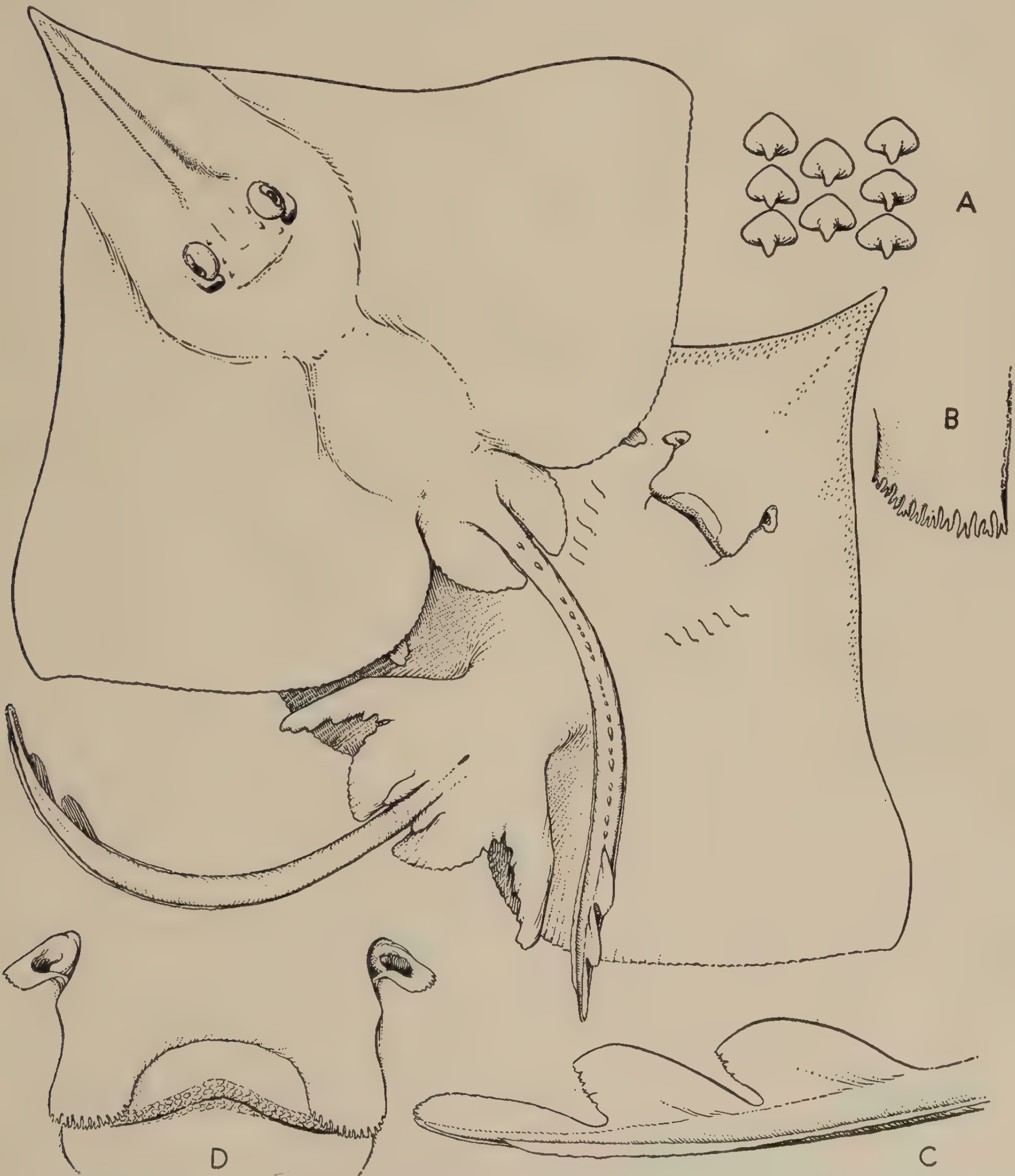

Fig. 3.—*Raja teevani*, n.sp., male, 558 mm long, holotype (U.S.N.M. no. 153557): A, Upper teeth, about × 6; B, margin of left nasal curtain about × 2.5; C, posterior part of tail, about × 1; D, mouth and nostrils, about × 1.

margin of disc from a little posterior to level of mouth to tip of snout and also along anterior half of rostral cartilage.

Snout in front of orbits 6.9 times as long as orbit; its length in front of mouth 3.6 times as great as distance between exposed nostrils. Distance between orbits 1.3 times as great as orbit. Orbit 1.6 times as long as spiracle. Nasal curtain fringed; expanded posterior (outer) margins of nostrils smooth except for a few fringes on extreme outer angle. Upper and lower jaws moderately arched centrally. Teeth $\frac{3}{3}\frac{6}{6}$, rather widely spaced, in quincunx, triangular or ovate, with smooth rounded apex on outward margin and a low triangular cusp, pointing inward, on inner margin. Distance between first gill openings 1.6 times as great as distance between exposed nostrils; between fifth gill openings about 1.0 times; first gill openings 1.4 times as long as fifth and 0.22 as long as breadth of mouth. First and second dorsals similar in size and shape. No interspace between dorsals. Caudal membrane from rear end of base of second dorsal 1.25 times as long as base of first dorsal. Pelvics deeply concave, strongly scalloped along anterior side of excavation but only weakly so rearward; anterior margin 1.1 times as long as distance from its own origin to rear tip of pelvics; anterior lobe moderately slender, including five radial cartilages besides the first stout one; posterior lobe convex outwardly; rear tips abruptly rounded, extending about one-fifth the distance from axil of pelvics toward first dorsal; inner margin straight. Claspers falling well short of tips of pelvics.

Rostal cartilage firm, narrow, extending to tip of snout. Anterior pectoral rays reaching only about two-fifths the distance from level of front of orbits toward tip of snout. Translucent area in front of orbits and on either side of rostral cartilage very thin and membranous.

Color.—Upper surface pale brown, somewhat darker along posterior margins of disc, on pelvics and on tail. Dorsal fins and caudal black. Below creamy on disc except somewhat dusky along outer margins from outer angle rearward and on pelvics. Probably blackish everywhere in life. Tail blackish.

The other known specimen of this species, 302 mm long, has a somewhat shorter snout, the distance in front of orbits being 5.5 times as long as orbit and a relatively longer tail the distance from center of cloaca to tip of tail being 1.1 times as great as distance from center of cloaca to tip of snout. There is one sharp backward pointing spine on the anterior inner margin of each orbit and another on the posterior inner margin. The color of the upper surface is similar to that of the type except that there is a narrow black margin along the posterior edge of the disc and the lower surface is distinctly margined with black rearward from the level of the mouth; the rear parts of the pelvics also are blackish.

The very small claspers on the larger specimen indicate that this species attains at least a moderately large size.

Nothing is known of its habits beyond the fact that our two specimens were taken at a depth of 305 fathoms. It is known only from the offing of Pensacola, Fla.

Hydrolagus alberti[4], n. sp.

Study material.—Immature male, 275 mm long to origin of upper caudal fin, holotype (U. S. N. M. no. 153558); male, 280 mm and female 275 mm, paratypes, all from lat. 29° 11′ N., long. 86° 52′ W., 305 fathoms, *Oregon* station 279.

Distinctive characters.—This newly discovered chimaerid is marked off from its genus mate *affinis* by its very long caudal filament, its relatively much longer pectorals, and its very much larger eyes. It resembles the Japanese *H. himitsukurii* very closely but differs from it by having a shorter dorsal spine, longer pectorals and more conspicuously waved lateral line anteriorly.

Description of holotype.—Proportional dimensions in percent of distance between snout and origin of upper caudal fin:

Trunk.—Breadth 10.9; height 15.6.

Snout length.—In front of eye 9.5; in front of mouth 10.5.

Eye.—Horizontal diameter 7.6; vertical diameter 5.8.

Mouth.—Breadth 5.5.

Nostrils.—Distance between 0.4.

Dorsal spine.—Length 15.3.

First dorsal fin.—Length of base to lowest point between dorsals 13.8.

Second dorsal fin.—Length of base 64.7.

Upper caudal fin[5].—Length of base to last horny ray 19.3.

Pectoral fin.—Length 31.6; breadth 16.3.

Distance from snout to origin of dorsal spine 24.4; second dorsal 38.2; pectorals 23.2; pelvics 45.5.

Distance from origin to origin of pectorals and pelvics 26.6.

---

[4] Named for Albert E. Parr in recognition of his many contributions to ichthyology.

[5] The point of origin of the lower caudal fin is not evident.

Trunk opposite dorsal spine about as high as distance from snout to posterior margin of eye; about one-half as high close behind pelvics, tapering evenly thence rearward and terminating in a long filament which, when complete, is about two-thirds the length of body from snout to termination of caudal fin; strongly compressed laterally posterior to head, increasingly so rearward, its thickness about three-quarters as great as its height opposite bases of pectoral fins and one-half as great opposite bases of pelvic fins.

Skin perfectly smooth on immature specimen.

Head about 21 percent of length of trunk to upper origin of caudal fin. Snout conical with blunt tip. Eye oval, sloping a little rearward, its horizontal diameter about 1.3 times its vertical diameter; distance from tip of snout to front of eye about two-fifths length of head to origin of pectorals; pupil one-half vertical diameter of eye; height of eye about two-fifths of height of head, its length about one-third length of head to origin of pectorals. Exposed subdivision of nostrils crescentic on inner edge, about 1½ times as long as broad, its length about 15 percent as great as length of eye; distance from its own rear edge to free edge of upper lip about as long as its own length. Width of mouth, when closed, a little less than length of eye.

Lateral mucous canal with a short and abrupt wave opposite the anterior part of first dorsal fin, after which there is a long low dip opposite origin of second dorsal fin, thence continuing nearly straight along the upper part of the caudal axis, descending at origin of caudal fin to follow out along lower edge of caudal axis. Junction of cranial canal with aural canal somewhat more acute than a right angle; anterior course of cranial canal nearly straight, looping down in front of eye;

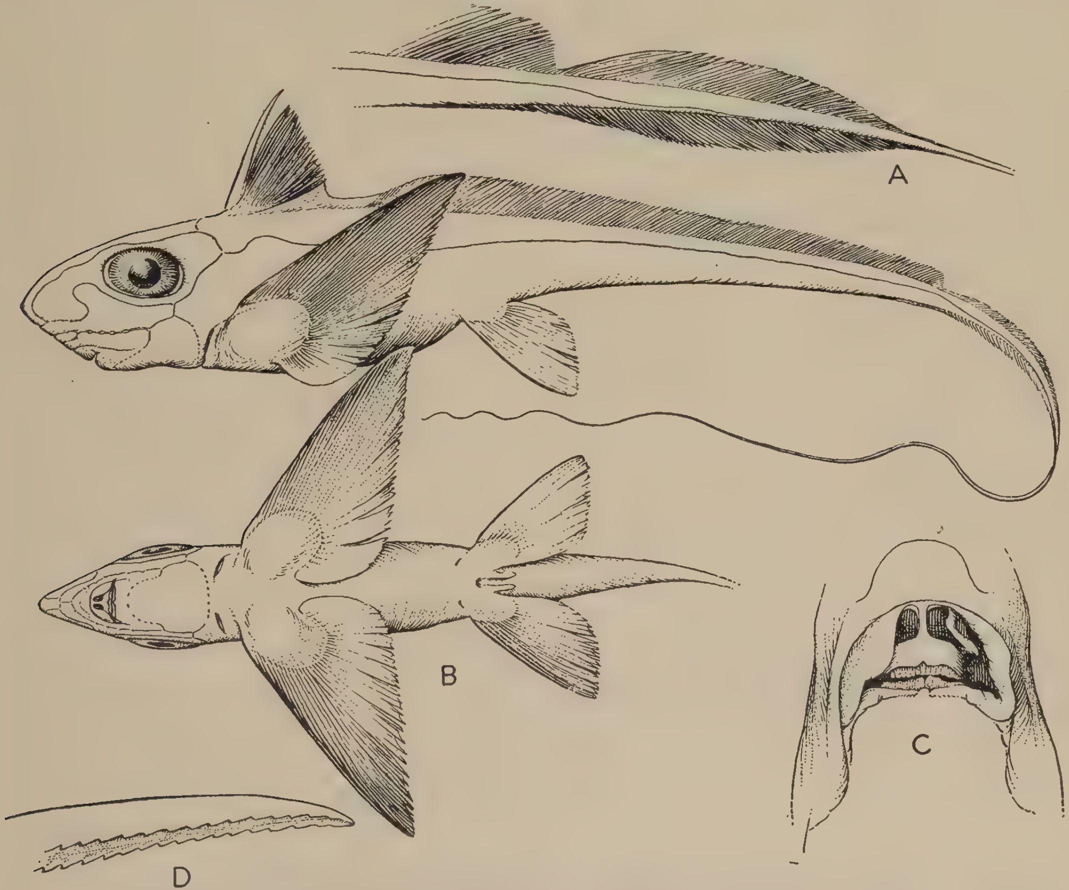

FIG. 4.—*Hydrolagus alberti*, n.sp., male, 275 mm long to origin of upper caudal fin, holotype (U.S.N.M. no. 153558): A, Posterior part of second dorsal fin and upper and lower caudal fins, about × 1; B, ventral view of head and body; C, mouth, with left lip folded aside to show nostrils and dental plates, about × 2; D, tip of dorsal spine, about × 2.5.

jugular and oral canals running downward from suborbital as a joint canal for a short distance before separating. About 10–12 medium size pores close in front of occipital canal; about 12 pores in area bounded by suborbital and joint oral-jugular canals; about 10 large openings along angular canal to front of snout; a single row of about 15 small pores parallel to descending oval branch and continuing in front of it; about 8 or 9 large openings along anterior part of suborbital canal from its descending wave to front of snout; jugular canal continued downward onto throat as a series of short slits. Skin closely pock-marked on top and on upper sides of head abreast of mouth and nostrils and toward tip of snout, with many rounded depressions of different sizes.

Anterior upper (vomerine) dental plates quadrate, their outer anterior outlines convex, with six radial ridges. Posterior upper (palatine) plates about 2.75 times as long as anterior plates, triangular, the posterior margin about two-thirds as long as outer margin, surface lumpy, with four prominent ridges running longitudinally. Lower (mandibular) plates nearly as long as posterior upper plates, each plate with a double concavity and central ridge on inner surface, the cutting edge uneven, highest at center of mouth.

Gill openings nearly one-half as long as distance from tip to snout to front of eye, distance across throat between their lower ends about one-half as long as eye, fold across throat strongly marked.

Dorsal spine about as long as distance from tip of snout to rear edge of pupil, reaching slightly beyond apex of first dorsal fin; outer part free from first dorsal fin, the rear face with two rows of low sharp thorns pointing toward base. First dorsal fin with sharp angle at apex and straight posterior margin; its base (from origin of spine to bottom of inter-dorsal notch) nearly as long as height along anterior margin of fin. Distance between first dorsal (when slightly depressed) and first noticeable elevation of second dorsal about two-fifths as long as anterior margin of first dorsal.

Second dorsal with horny rays easily distinguishable, upper margin nearly straight; height at midlength about one-fifth as great as length of anterior margin of first dorsal; about equally great at rear end and slightly greater toward anterior end; posterior outline of second dorsal curving abruptly downward. No definite interspace between second dorsal and upper origin of caudal. Caudal lanceolate, prolonged into a long filament about four-fifths as long as distance from snout to rear end of second dorsal; maximum height of caudal above axis about two-thirds height of second dorsal at posterior end; its extreme length to most posterior ray about 9 times as great as its height; caudal below axis about four-fifths as wide as above; the most posterior rays of both upper and lower sides of caudal terminate almost imperceptibly and about opposite each other; origin of lower side of caudal indefinite in position, preceded by a low fleshy ridge distinguishable forward to a point above and opposite beginning of last third of second dorsal fin. Pelvic fins with weakly convex anterior and distal margins, subangular outer corners and gradually rounded posterior (inner) corners; length of pelvics along anterior margin about as great as distance from tip of snout to middle of eye; origin posterior to axils of pectorals by a distance about equal to that from tip of snout to origin of pectorals. Pectoral fins about three-tenths as long as distance from tip of snout to opposite rear part of second dorsal fin; tips, when laid back, extending just beyond the base of pelvic; anterior margin weakly convex; distal margin straight or slightly concave; apex sharp pointed; inner corner broadly rounded.

Prepelvic openings present. Frontal tenaculum embedded in skin in this immature male. Claspers bifid but may develop as trifid with age.

Color.—Dark brownish everywhere on head and body above and below; fins somewhat darker.

The female closely resembles the male but lacks the prepelvic openings and, of course, the frontal tenaculum.

This species is known only from the offing of Pensacola, Fla., in a depth of 305 fathoms.

Contribution No. 556

THE SOURCES OF THE DEEP WATER OF THE EASTERN MEDITERRANEAN SEA[1]

BY

M. J. POLLAK

Woods Hole Oceanographic Institution

ABSTRACT

The deep water in the two basins of the eastern Mediterranean Sea, the Levant and the Ionian Sea, is identical in temperature and salinity though differing slightly in oxygen content. Contrary to Nielsen's thesis, none of this water is formed in the southern Aegean Sea. The latter, connected with the Mediterranean by a number of straits, has consistently higher salinities and oxygen values in the vicinity of the sill depths than are found at equal or greater depths on the Mediterranean side of these channels. The effluent from the Strait of Sicily is also eliminated as a source of the deep water since it is separated from the latter by an intervening layer of maximal salinity. The Adriatic Sea has extremely variable water characteristics because of its shallow average depth and consequent susceptibility to fluctuations of the prevailing weather regime. In its southern half, considerable mixing takes place between relatively fresh water from the north and more saline water from the upper few hundred meters of the Ionian Sea. This mixed water sinks and then flows sporadically along the bottom into the Mediterranean Sea, where it circulates counterclockwise. This flow is confirmed by the distribution of oxygen values in the deep layers of the entire eastern Mediterranean.

INTRODUCTION

In his outstanding treatise on the hydrography of the Mediterranean Sea, Nielsen (1912) makes the following statement about the sources of the deep water in the Levantine and Ionian basins:

> We have seen, further, that a uniform layer of water from surface to bottom occurs in the southern part of the Adriatic and in the Aegean Sea north of the Cyclades—possibly also in the deep water north of Crete—and that this layer is colder and heavier than the masses of water, which are found at the same level in the Levant and Ionian Sea. These masses of water will then move towards the south, in the extent to which the depths permit, and after reaching the Ionian Sea and Levant will flow down its northern slopes to the greatest depths. During this movement they will become partially mixed with the bottom-water and be distributed by horizontal currents in the bottom-layer over the whole of the eastern basin.

---

[1] Contribution No. 556 from the Woods Hole Oceanographic Institution. This investigation was supported by funds under Contract No. N6onr-277 between the Office of Naval Research and the Woods Hole Oceanographic Institution.

Reprint from SEARS FOUND. JOURN. MAR. RES.

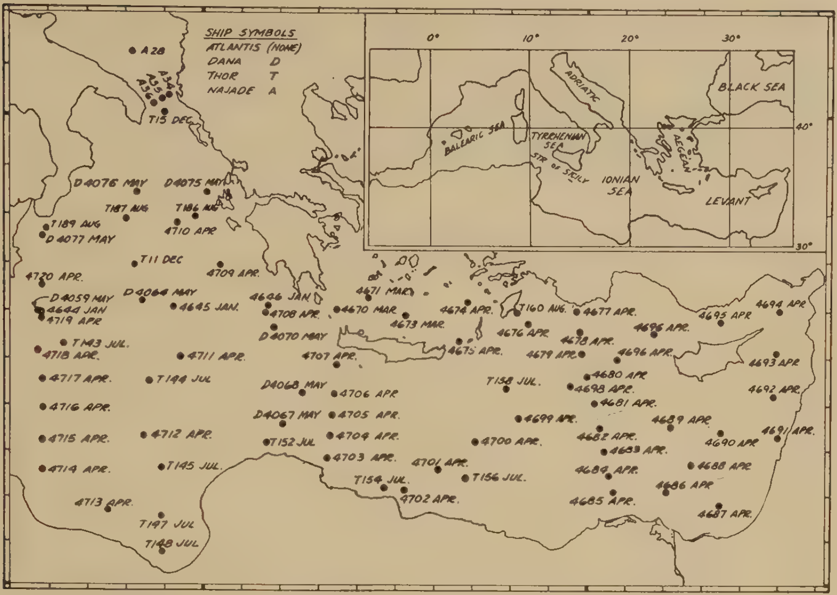
SHIP SYMBOLS
ATLANTIS (NONE)
DANA D
THOR T
NAJADE A
A 28
A34
A35
A36
T15 DEC
D4076 MAY
D4075 MAY
T187 AUG
T186 AUG
T189 AUG
D 4077 MAY
4710 APR
T11 DEC
4709 APR.
4720 APR.
D4059 MAY
4644 JAN
4719 APR
D4064 MAY
4645 JAN.
4646 JAN
4708 APR.
4670 MAR
4671 MAR.
4673 MAR.
D4070 MAY
T143 JUL.
4718 APR.
4711 APR.
4707 APR.
4717 APR.
T144 JUL
D4068 MAY
4706 APR
4716 APR.
D4067 MAY
4705 APR.
4715 APR.
4712 APR.
T152 JUL
4704 APR.
4703 APR.
4714 APR.
T145 JUL.
4701 APR.
T154 JUL.
4702 APR.
T156 JUL.
4713 APR.
T197 JUL
T148 JUL
4674 APR.
T160 AUG.
4677 APR.
4676 APR
4675 APR.
4678 APR.
4679 APR.
4696 APR.
4696 APR.
4695 APR
4694 APR
4693 APR
T158 JUL.
4680 APR
4698 APR.
4681 APR.
4692 APR.
4699 APR.
4689 APR
4691 APR.
4690 APR
4700 APR.
4682 APR.
4683 APR.
4688 APR
4684 APR.
4686 APR
4685 APR.
4687 APR.
0°
10°
20°
30°
BLACK SEA
40°
BALEARIC SEA
TYRRHENIAN SEA
ADRIATIC
AEGEAN
STR. OF SICILY
IONIAN SEA
LEVANT
30°

Figure 1. Station positions in the eastern Mediterranean Sea.

Schott (1915), in a paper which is largely a review of Nielsen's work, agrees with the above statement but doubts that enough water flows out of the Aegean Sea to fill the Levantine Basin.

The present paper will attempt to show that the deep water is formed only in the Adriatic Sea and that the Aegean Sea cannot contribute to this bottom water mass.

The serial observations of temperature, salinity and oxygen obtained by the Research Vessel Atlantis of the Woods Hole Oceanographic Institution during the winter and spring of 1948 form the main source of data for this discussion of the eastern Mediterranean. Earlier stations in the area were also used, with the exception of Pola data which were obtained in the days before the present standards of accuracy were achieved in oceanographic observations. Fig. 1 shows the outlines of the area under discussion and the positions of all stations used.

Vertical convection currents which can cause a complete overturning of the entire water column and can thus be an important factor in the formation of subsurface water characteristics are most likely to occur during periods of minimum surface temperatures. Therefore it becomes important to establish a criterion for comparison of stations taken at different times of the year.

To this end the annual cycle of surface temperatures was plotted for two small areas in the eastern Mediterranean: A one-degree square between Crete and Cyprus, and a two-square-degrees rectangle in the center of the Ionian Sea. Since the data were limited to bathythermograph surface temperatures obtained after 1947, the resulting curves were rather irregular. Nevertheless, the two curves paralleled each other closely, the Ionian Sea temperatures being about 1.5° C. colder than corresponding temperatures from the Levantine area. As a check on these data, averaged monthly surface temperatures obtained by British ships between 1900 and 1914 (Meteorological Committee, Air Ministry, London, 1930) were plotted on the same diagrams. Good agreement was found. Since relative rather than absolute temperatures were the feature sought, these different sets of surface data were combined into a mean curve (Fig. 2).

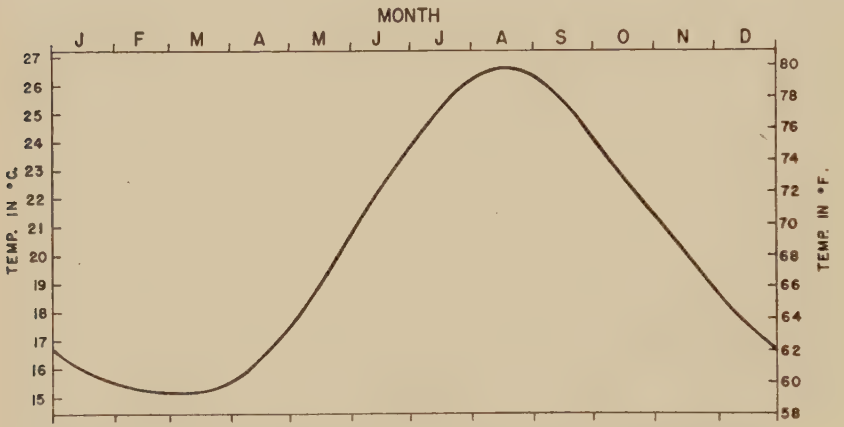

Figure. 2. Mean surface temperature cycle in the eastern Mediterranean Sea.

CHARACTERISTICS OF THE DEEP WATER

Before attempting to trace the sources of the deep water of the eastern Mediterranean, it is pertinent to examine its basic characteristics. For this purpose, temperature, salinity and oxygen curves from two centrally located Atlantis stations, 4711 in the Ionian Basin and 4699 in the Levantine Basin, are shown in Fig. 3. On the basis of Fig. 2, both of these stations were made close enough to the period of minimum surface temperatures to be fairly representative of winter conditions except in the upper 50 meters where some warming had already taken place.

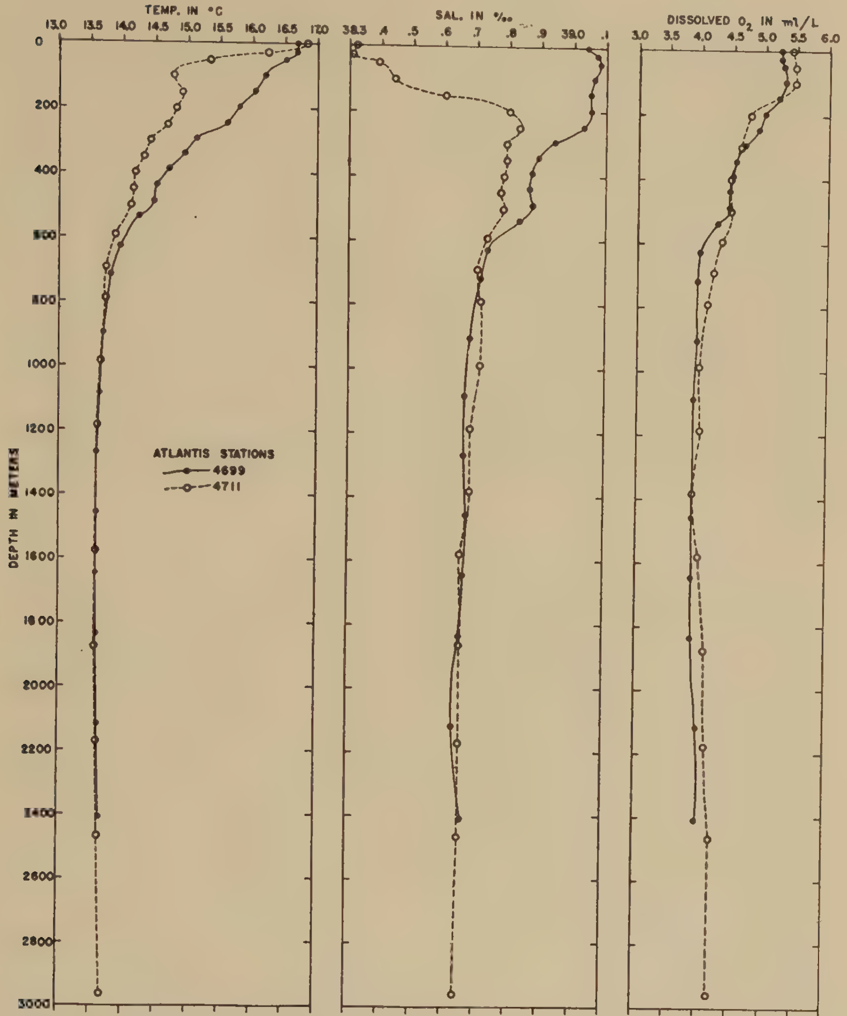

Figure. 3. Typical station curves from the central Levant (No. 4699) and the Ionian Sea (No. 4711).

The significant features of the two sets of curves are their difference in the upper 1000 m or so and their similarity below that depth. The temperature traces practically coincide below 850 m, both having a minimum value of 13.57° C. at 1600 m. The salinity curves show more irregular divergencies. Between 750 m, where the two curves cross, and 1600 m, the traces differ by as much as 0.04 ‰. Below 1600 m, considering the observational error to be ± 0.02 °/₀₀, both stations are homohaline with a value of 38.65 °/₀₀. The two curves for dissolved oxygen show a striking parallelism below 1000 m, the Ionian station averaging 0.15 ml/L higher than the Levantine one.

If the upper limit of the deep water were defined by marked changes in the gradients of the elements plotted, a depth of about 700 m is the boundary layer. On the other hand, if absolute values are used as the criterion, 1600 m gives a rigorous upper limit for the deep water. For the purposes of this paper, deep water will refer to the layer below 1600 m, with the depth zone from 700 to 1600 m being considered one of transition between intermediate and deep water. These depths are not necessarily representative of the entire eastern Mediterranean; they are merely typical of the water structure in the central section of the two eastern basins. However, they establish a rough criterion for the basic subdivisions of the water column in this area, and, as such, they indicate the magnitude of the thicknesses of the various layers.

THE AEGEAN SEA

As a first step toward analyzing the water movement between the Aegean and Mediterranean seas, a vertical section of temperature, salinity and oxygen through Caso Strait, between the islands of Scarpanto and Crete, was plotted (Fig. 4). Atlantis Stations 4673, 4675 and 4676, used in this plot, were made within a period of four and one-half days, and, according to Fig. 2, they can be considered fairly representative of late winter conditions. Unfortunately, the spacing of these stations, 75 and 92 miles respectively, makes the section far from ideal as far as distribution of data is concerned. In view of their geographical positions, a true bottom profile between them would be meaningless, and hence it was replaced by a schematic bottom curve showing the maximum and minimum depths between stations.

Even considering the subjectivity of the contouring of the station data, several features of the profiles stand out. For all three water properties plotted, the Aegean station (4673) shows weaker gradients and smaller over-all ranges than the Mediterranean station (4676). Station 4675, right over the sill between the two sea basins, shows some characteristics of each of the other two stations. In the upper 400 m, the temperature and salinity structure of this station closely resembles that of Mediterranean water. The oxygen distribution, on the other hand, differs somewhat from that of the other two stations, the gradients being smaller. Below 400 m, the water structure, in terms of all elements considered, is similar to that of Station 4673.

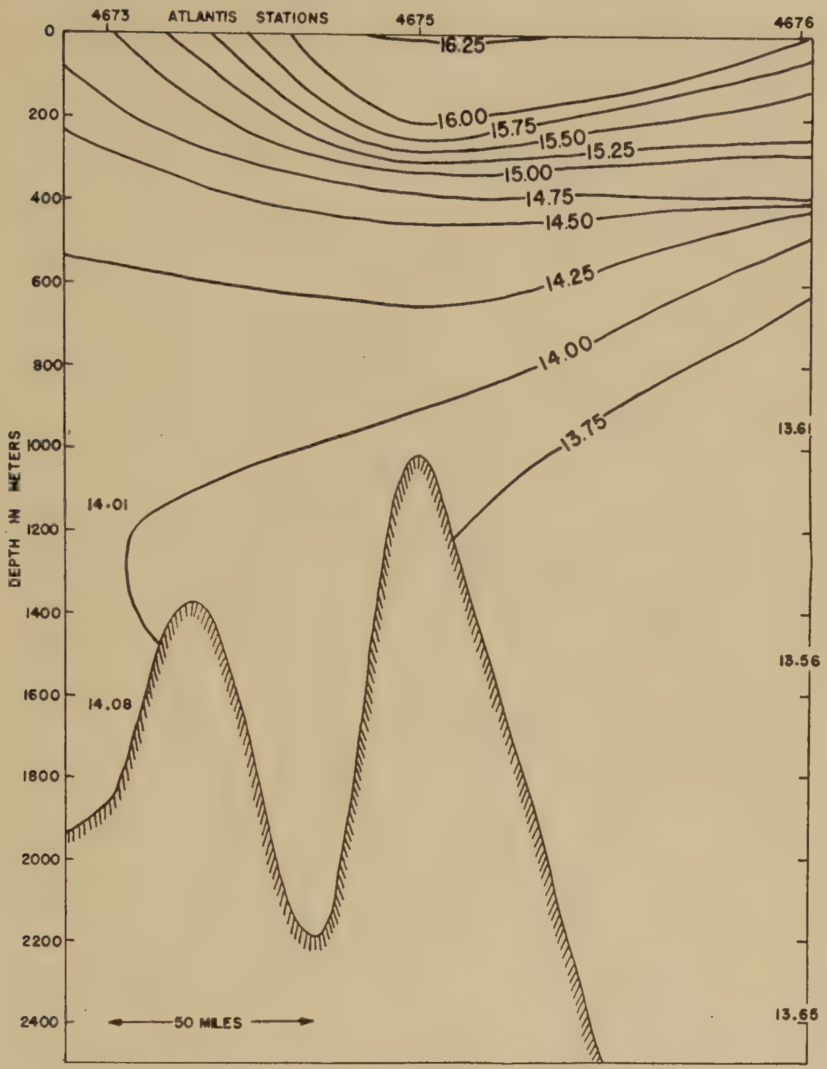

Figure 4a. Temperature section in °C. through Caso Strait.

The surface features indicate a marked flow of Mediterranean water into the southeastern Aegean. This assumption agrees with Nielsen's (1912) analysis of the water movements of the region. The discrepancy between the dissolved oxygen distribution and thermohaline structure at Station 4675, not explainable on the basis of dynamic considerations, is probably due to biological factors.

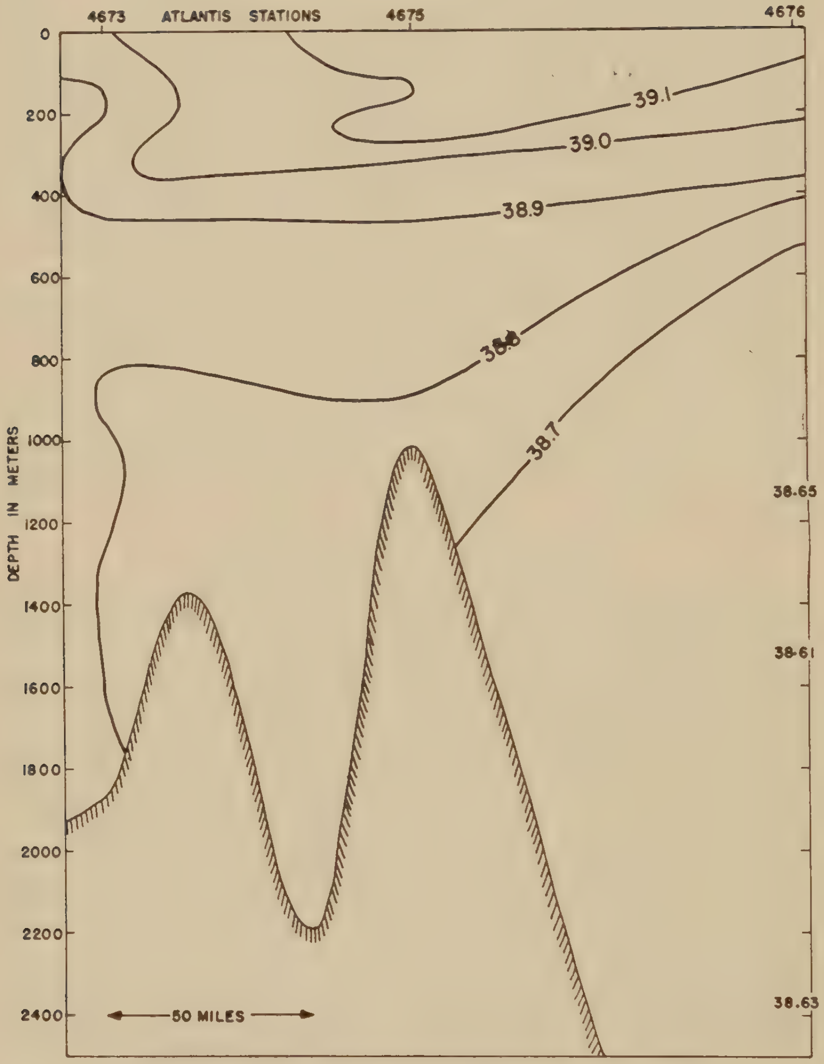

Figure 4b. Salinity section in °/₀₀ through Caso Strait.

Relative to the main question at hand, the significant fact is *not* the inflow of Mediterranean water at the surface but the apparent failure of Aegean water to flow out at the bottom. This situation is indicated by all the isopleths shown in Fig. 4. However, it is brought out most clearly in the section for dissolved oxygen. On Station 4676 there is

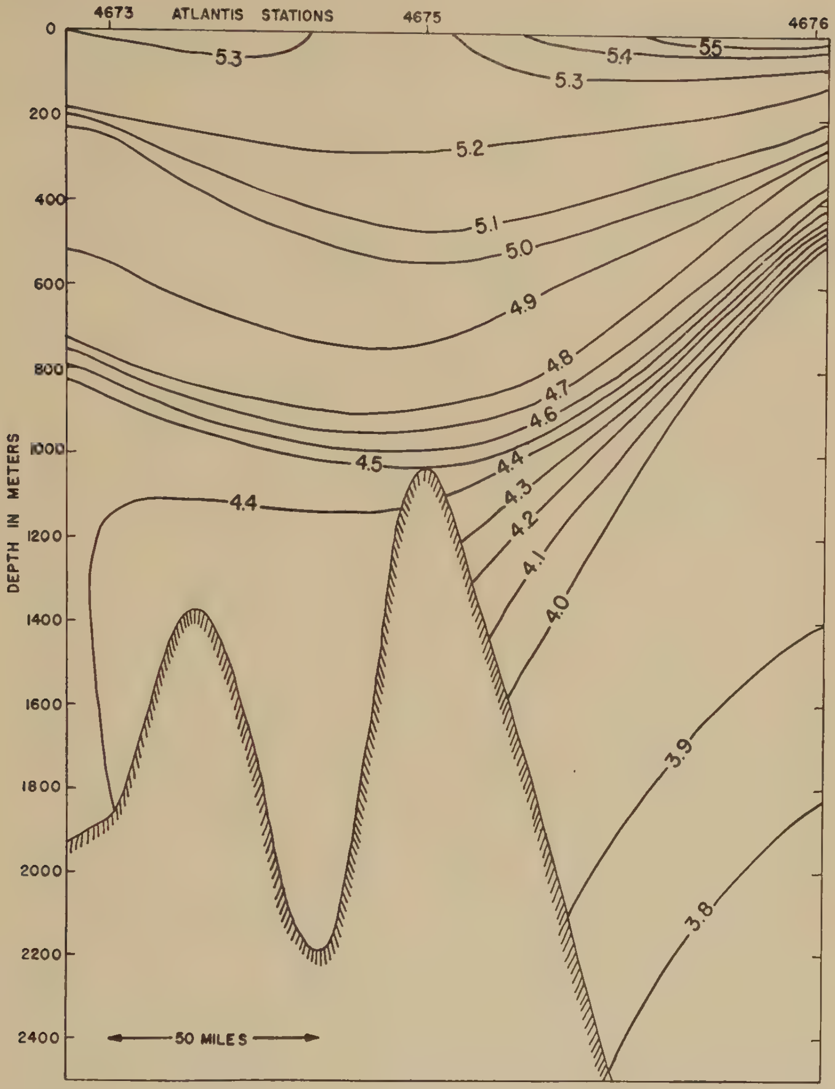

Figure 4c. Dissolved oxygen section in ml/L through Caso Strait.

a sharp gradient at 450 m. Here the oxygen values drop from 4.6 to 4.0 ml/L in 120 m, corresponding closely to the gradient at 550 m found on Station 4699 (Fig. 2). A similar gradient is completely absent on Station 4673, and probably on Station 4675 as well unless an extremely complex configuration of the isopleths is accepted. Since

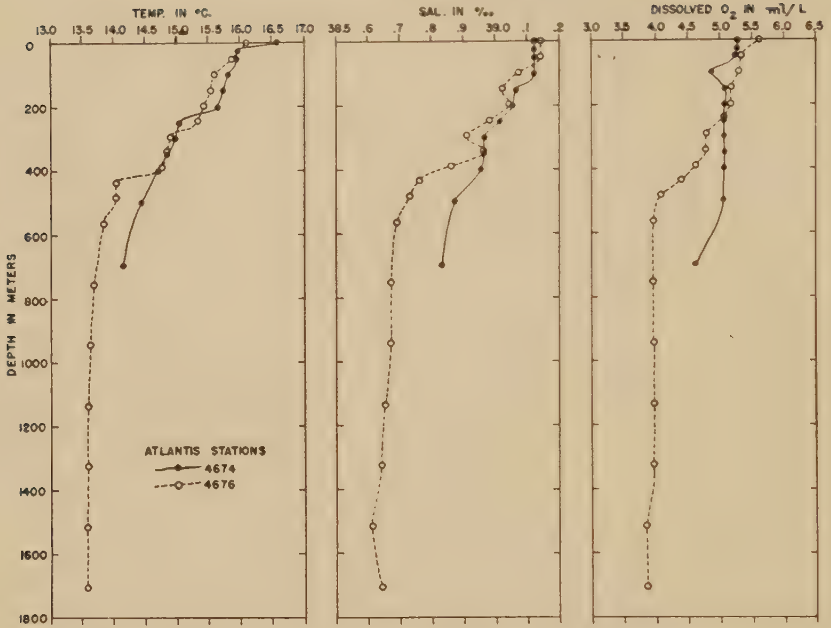

Figure 5. Station curves on either side of the Strait of Scarpanto.

Nielsen's thesis implies a downward and outward flow of Aegean water across the sill, it is very likely, if such a movement were present, that temperature, salinity and oxygen values at Station 4676 would show some increase below the sill depth of 1000 m. There is no evidence of such an increase in any of the elements shown. The increase in temperature below 1500 m is due to adiabatic heating, as pointed out by Nielsen (1912) and confirmed by the present ATLANTIS observations.

Between the islands of Scarpanto and Rhodes lies the second major channel into the southeastern Aegean, the Strait of Scarpanto, with a sill depth of 880 m. While no station was occupied in this Strait, Station 4674 in the Aegean and 4676 in the Mediterranean fall roughly in line with it. Fig. 5 compares the vertical temperature, salinity and dissolved oxygen distribution of the two stations. The temperature and salinity plots show a marked similarity from the surface to about 375 m, thus furnishing further evidence of the surface flow into the Aegean. In this connection it should be remembered that the surface water at Station 4674 may have entered the Aegean through Caso Strait rather than Scarpanto Strait. Unfortunately this problem cannot be resolved by means of the available data. However, the current pattern in the eastern Mediterranean, plus the width, depth and orientation of the two straits, makes it appear likely that surface water enters the Aegean through both of them.

The two corresponding station curves for dissolved oxygen, by contrast, show marked differences at all depths. In the upper 300 m, where the distribution of temperature and salinity is essentially similar, the Aegean station has lower values. Below this depth, the Mediterranean station has a lower oxygen content. This discrepancy between the different water characteristics resembles that found in the section through Caso Strait (with Station 4674 being similar to 4675 in the Strait rather than to Station 4673 in the Aegean proper).

The third channel into the Aegean between Rhodes and Asia Minor is only 350 m deep. No observations were made close enough to this channel to permit an analysis of its currents. However, *Sailing Directions for the Mediterranean* (U. S. H. O., 1942) indicate that its surface current generally sets to the westward. This is in complete agreement with the general nature of surface currents in this part of the Mediterranean. In view of the depth of surface inflow through Caso and Scarpanto straits (400 and 375 m respectively), it appears equally certain that the sill depth of this channel would prevent any subsurface outflow from the Aegean by this route.

In the southwestern Aegean only one of the three passages into the Mediterranean has an appreciable sill depth. This is Andikithira Channel, north of Crete, with a maximum depth of 805 m. The other two channels have depths of 137 and 290 m. The station in the Aegean Sea closest to these channels is Station 4670, 25 miles due north of Andikithira Channel, while Station 4671 is 41 miles east-northeast of that position.

Station 4670, which was occupied after a day of high winds, showed a thoroughly stirred surface layer 500 m thick. From this depth to the lowest observation at 865 m, small negative gradients were found in temperature, salinity and dissolved oxygen. In the mixed layer the salinity had a value of 38.96 °/₀₀, at 865 m it was 38.86 °/₀₀. Although Station 4671 had a surface salinity of 39.10 °/₀₀, typical of the water entering the Aegean from the northeastern Levant, its salinity at 895 m was only 38.83 °/₀₀. Since depths of 865 and 895 m are well below the sill of the channel, and since their corresponding salinities are about 0.20 °/₀₀ higher than those of the deep water of the eastern Mediterranean, it should be evident that the southern Aegean cannot be a main source of this water. It could be a major source only if its subsurface outflow were mixed with water of considerably lower salinity to give an average of 38.65 °/₀₀.

THE STRAIT OF SICILY

As the evidence presented appears to eliminate the Aegean Sea as a source of the eastern Mediterranean deep water, the only other two possible sources must be examined minutely. These are the western Mediterranean, via the Strait of Sicily, and the Adriatic Sea.

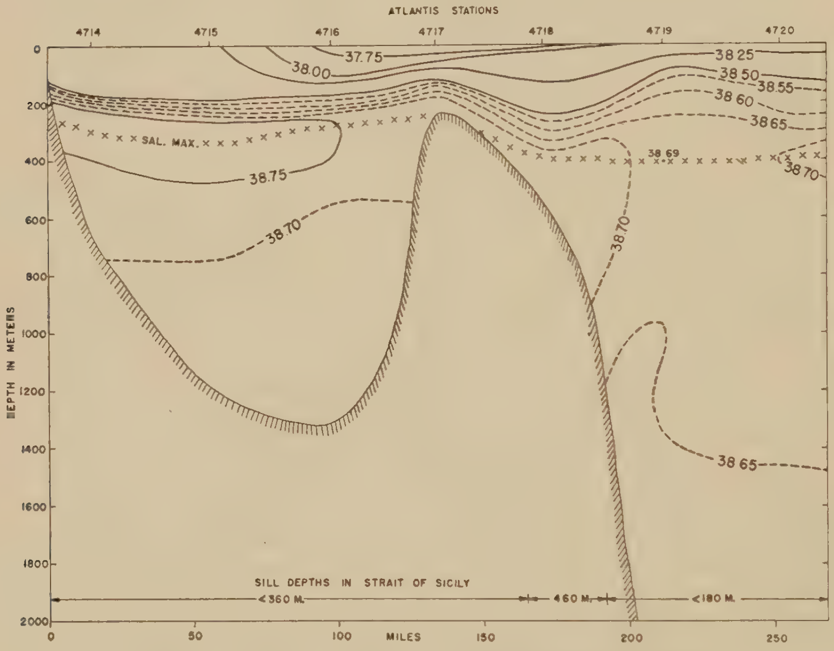

Figure 6. Salinity section in °/oo east of the Strait of Sicily.

The Strait of Messina was ruled out as a major channel for water transport between the western and eastern Mediterranean by Nielsen (1912) on the basis of the tidal nature of the currents. The small net transport through the Strait is confirmed by Vercelli (1925). Since the minimum width of the Strait is only 1.7 miles and the sill depth 110 m, the mass transport through it, even under conditions of unidirectional flow, would be very small compared to that through the Strait of Sicily or the Strait of Otranto.

Fig. 6 shows the salinity profile for a north to south section running from the Gulf of Sidra to the east coast of Sicily. This section was made during the last days of April, and, while not representative of winter conditions, it is sufficiently close to that season to be used in the following analysis.

The station depths vary greatly, since the section was run close to the edge of the shelf which drops off sharply from the eastward extension of the Strait of Sicily to the Ionian Basin. The significant depths in this section, however, are the sill depths of the Strait. These are indicated in Fig. 6.

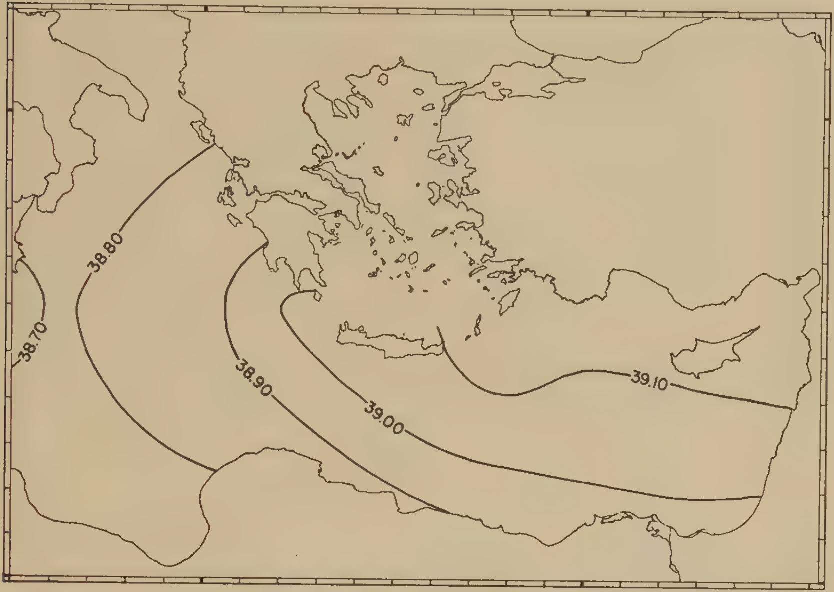

Figure 7. Maximum salinities in °/₀₀ in the eastern Mediterranean Sea.

The most striking feature of the section is the layer of fresher surface water at Stations 4716, 4717 and 4718. This is the core of the current which enters the Mediterranean through the Strait of Gibraltar as Atlantic water and then follows the African Coast through the Strait of Sicily as far east as the Levantine Coast, where it gradually changes its characteristics. Considering the lower boundary of this current to be represented by the midpoint of the sharpest positive gradient at each station, we find its depths to be 125, 75 and 25 m respectively. To the south and north of this main current, even though the surface salinities are considerably higher, a positive salinity gradient is still present in the upper layer. At Stations 4714 and 4715, to the south, the midpoint of the maximum gradient is found at 175, while at Stations 4719 and 4720, to the north, it is found at 25 m.

Throughout the section a maximum salinity, marked by x, occurs below the positive gradients at depths between 250 and 400 m. These depths are generally close to the sill depths in the eastern extensions of the Strait. The absolute sill depth of the Strait of Sicily, northwest of Pantelleria, is only about 320 m. This situation leads to the conclusion that the water entering the eastern Mediterranean from the west is limited to the upper few hundred meters and that the most saline water found in this section is formed in the eastern basins.

The maximal values mentioned decrease from 38.79 ‰ in the south to 38.69 ‰ in the north. Even this lowest value is still 0.04 ‰ higher than that found in the deep water. Hence, the layer of maximum salinity can contribute to the formation of deep water only by mixing with a water mass of salinity less than 38.65 ‰. In the present section such water is found only in the surface layer. But if the mixing and sinking required to produce the bottom water were taking place in this region, a vertical zone of isohaline water of salinity about 38.65 ‰ would have to appear. Such is not the case.

In order to determine whether such a process involving the surface layer is going on to the eastward of the above section, it is merely necessary to plot the maximum salinities for all available winter stations. This is done in Fig. 7, which shows that maximal salinities increase to the eastward, forming an increasingly impenetrable horizontal barrier between surface and deep water.

THE ADRIATIC SEA

We now come to the last possible source of the deep water, the Adriatic Sea and northern Ionian Sea. These two basins are connected by the 40-mile-wide Strait of Otranto, with a sill depth of 780 m.

Station data from the Adriatic are relatively plentiful. Between the years 1911 and 1914 the ships Najade and Ciclope made a series of comprehensive cruises, reoccupying the same stations a number of times at different seasons. Since the sections run by the two ships overlap to a considerable extent, and since the Ciclope stations are incomplete in their subsurface sampling, the following remarks concerning the Adriatic are based on Najade data alone. It is felt that these furnish adequate geographical and seasonal coverage for the purpose at hand.

An examination of these data shows a considerable variation from year to year for the same season. For example, in February 1912 the maximum surface salinity was found to be 38.53 ‰ at a position in the Strait of Otranto, while in March 1913 the maximum value was 38.81 ‰ at a position about 150 miles northwest of the Strait. These marked changes are not surprising when it is considered that only one-quarter of the Adriatic Sea extends to depths greater than 200 m, with an average depth for the entire Sea in the neighborhood of 300 m.

This, of course, implies that a major portion of Adriatic water is directly affected by the prevailing weather regime. It is of interest to note that during the 1912 cruise, when surface salinities were low, the wind was blowing from directions between NE and NW 22% of the time and from directions between S and SE 21% of the time. Corresponding figures during the 1913 cruise of high surface salinities were 11% from the north and 41% from the south. This suggests that the amount of Mediterranean surface water entering the Adriatic will fluctuate with the frequency of southerly and southeasterly winds over the area.

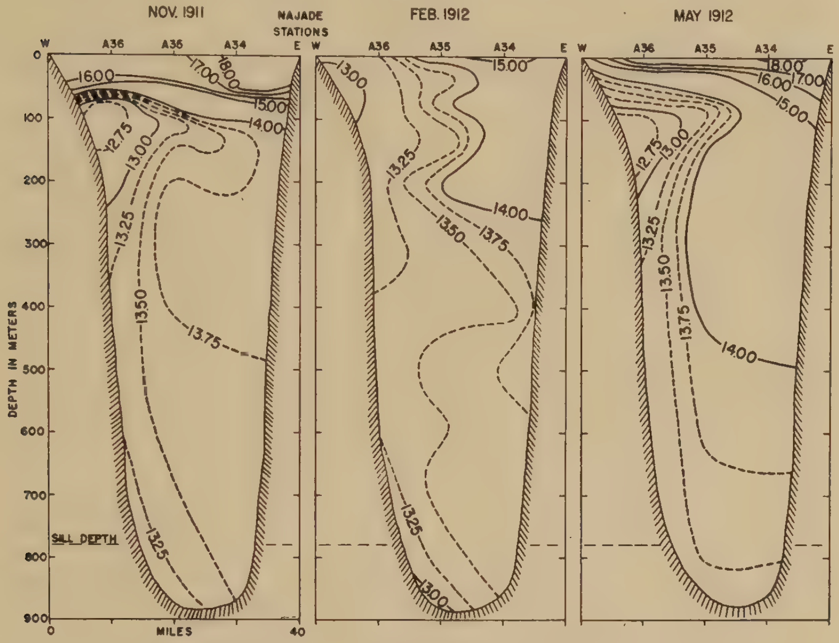

Figure 8a. Temperature sections in °C. across the Strait of Otranto.

Fig. 8 shows three sections made in successive seasons across the Strait of Otranto. No summer section was made in this vicinity. In examining these profiles it should be kept in mind that the vertical scale is exaggerated by a factor of 185. According to both Nielsen (1912) and Feruglio (1912) who made independent studies, using different data, there is a counterclockwise circulation of the surface water in the Adriatic. This is comparable to the circulation in the Mediterranean proper as well as to that in the Aegean. The existence of this current, which enters and leaves the Adriatic through the Strait

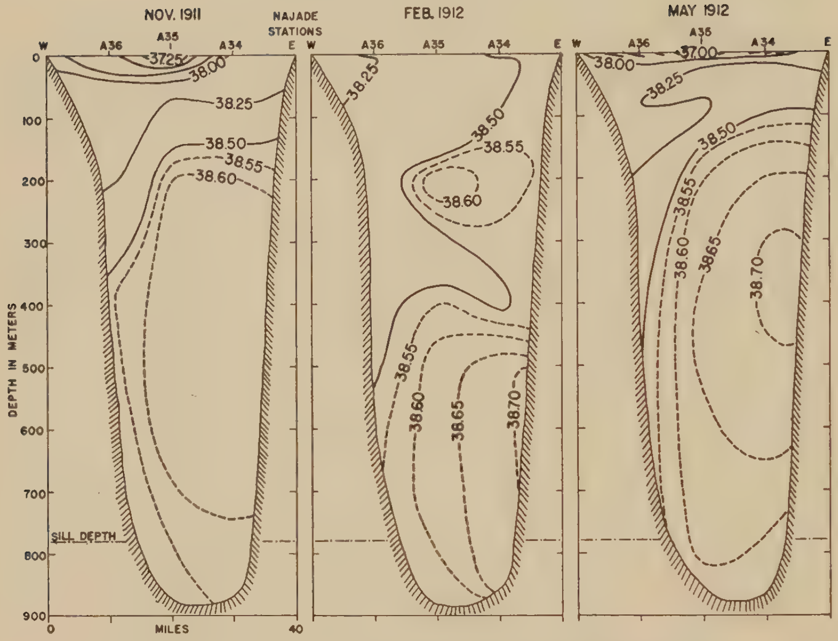

Figure 8b. Salinity sections in °/₀₀ across the Strait of Otranto.

of Otranto, much less its lower boundary, cannot be determined from the sections shown. This is largely the result of the rather small temperature and salinity gradients found below 25 m. While the current may well be limited to such shallow depths, there is no clear cut evidence for or against this assumption.

Despite the variations in the subsurface water structure found from section to section, one feature is common to all of them. All isopleths have a definite vertical tendency resulting in an appreciable variation of all elements from east to west across the Strait.

Temperature and salinity tend to decrease toward the west while dissolved oxygen content shows a slight and poorly defined increase in the same direction. The temperature and salinity values found below 200 m in these sections straddle the values representing typical Ionian Sea deep water (Fig. 3). Only the oxygen values are consistently higher. Although dissolved oxygen, even below the photic zone, is a much cruder indicator of water movement than salinity or temperature, being subject to consumption by varying quantities of plankton, its distribution can shed light on dynamic processes if used with caution and in conjunction with other indicators.

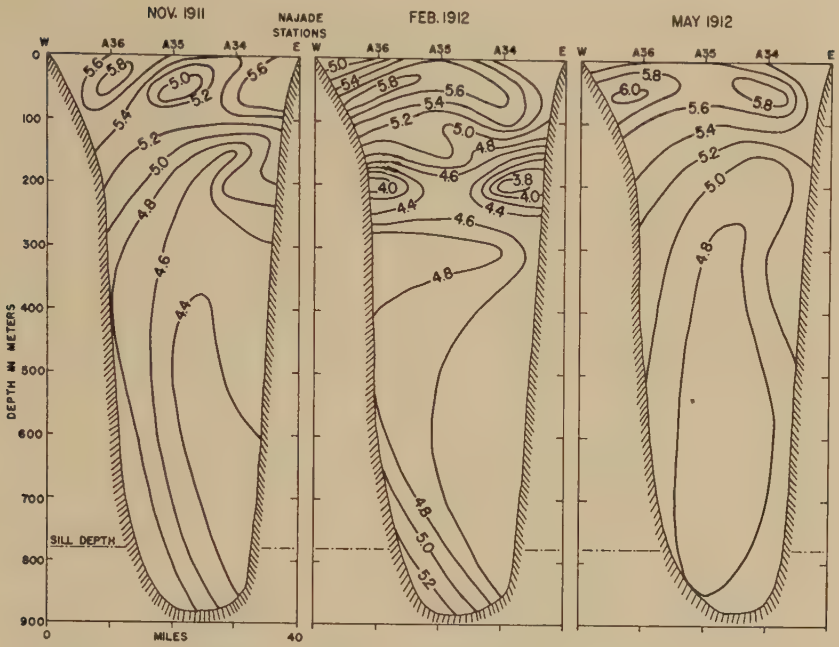

Figure 8c. Dissolved oxygen sections in ml/L across the Strait of Otranto.

In the present sections, it should first be pointed out that the two low O_2 values at 200 m in February 1912 are subject to doubt. While nothing in the original data indicates any lower accuracy for these two values than for others obtained, the two are so inconsistent with the remainder of the data that their validity must be questioned. This, however, is only of minor importance to the problem at hand. If the O_2 values in the deeper water were similar, or even lower, than those of the central and eastern Ionian Sea, then there would be considerable doubt about the direction of flow through the Strait of Otranto.

Since the amount of dissolved oxygen below the zone of photic activity and aeration by mixing can never increase—in fact, will generally diminish due to utilization by plankton or decomposing organic material—there exists a rough inverse correlation between the dissolved oxygen content and the time elapsed since the formation of the particular water mass. If subsurface water flows out of the Adriatic Sea, we should expect its dissolved oxygen content to decrease with increasing distance from the Strait of Otranto.

Fig. 9a shows isopleths of dissolved oxygen for the minimum value throughout the eastern Mediterranean. Only those station data were used where higher values were found below the minimum. Fig. 9b gives the maximum O_2 values below the minimum. In addition to Atlantis stations, those made by Thor and Dana were also used. The existence of an oxygen minimum at mid-depths indicates that the deep water enters the Ionian Basin near the bottom rather than at mid-depths, gradually rising to the depth of the O_2 minimum layer as it is replaced by newer water at the bottom. While the oxygen minimum layer is therefore not in the direct line of flow out of the Adriatic, it seems reasonable to assume that its values will reflect the maximum values in the water below it. These maximal values, however, cannot be determined with the same degree of certainty as the minimal ones because of the failure of many stations to reach the sea floor, and because of the limiting presence of the irregular bottom itself.

Despite the difference in reliability and significance of the two figures, it is worth noting that some of their general features are strikingly similar. In both cases the highest O_2 values, next to those in the Strait of Otranto, are found along the western side of the Ionian Sea below the sill of the Strait of Sicily and Malta Channel. Here the oxygen isopleths follow the edge of the shelf rather closely, both showing an eastward bulge near latitude 35° N where the bottom contours show a similar configuration. Though differing in detail, both charts have the lowest O_2 values in a tongue of water extending from the eastern end of the Levantine Basin through the eastern Ionian Sea almost to the Strait of Otranto.

The pattern of O_2 distribution leads to the conclusion that subsurface water flows out of the Adriatic, sinks well below the sill depth of the Strait of Sicily and follows the western and then the southern side of the Ionian Sea in a slow drift along the bottom. Since the Coriolis' force tends to deflect the water to the right, it continues along the African Coast into the Levantine Basin rather than forming a closed circuit in the Ionian Sea. This confirms Nielsen's (1912) thesis on the circulation in the deep water of the Ionian Sea. The eastern and northern sectors of this circulation are not clearly defined. This is not surprising when it is considered that the water flowing out of the Adriatic mixes continuously with the water in the eastern Mediterranean, thus gradually losing its characteristic oxygen distribution. Furthermore, on the basis of the changeable water structure in the Adriatic, it is probable that the outflow from that Sea has varying characteristics which are reflected in the irregularities of a composite diagram, such as Fig. 9, where station data from different years and seasons are used synoptically. Another probable source of irregularities in the oxygen data is the indeterminable effect of biological activity on oxygen consumption.

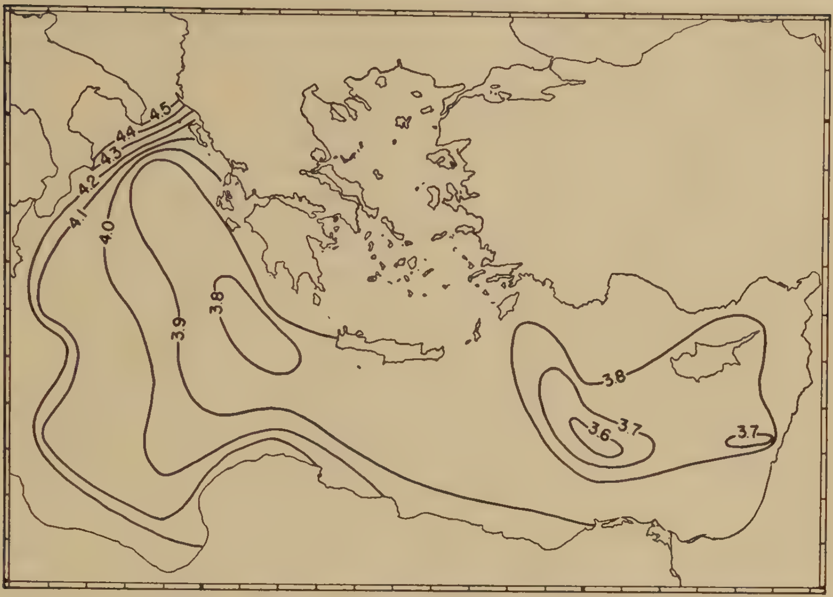
4.5
4.4
4.3
4.2
4.1
4.0
3.9
3.8
3.8
3.7
3.6
3.7

Figure 9a. Minimum dissolved oxygen in ml/L in the eastern Mediterranean Sea.

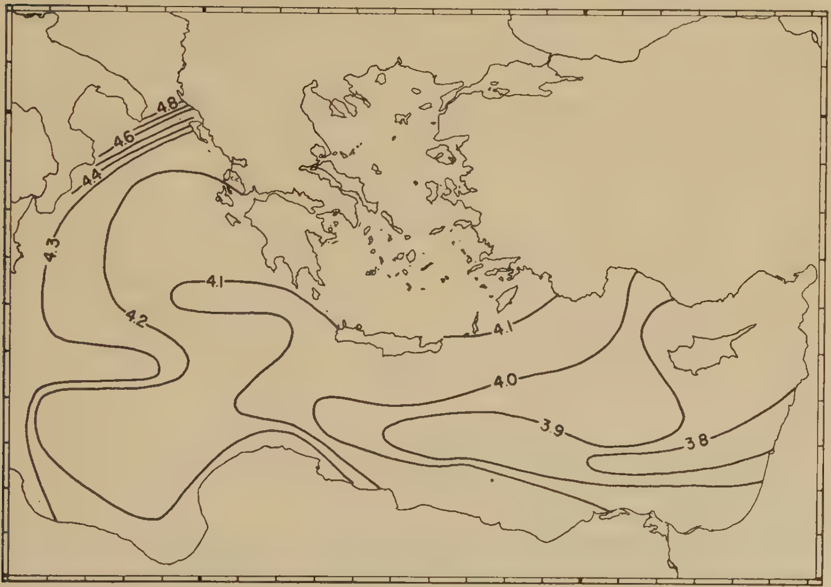
4.8
4.6
4.4
4.3
4.2
4.1
4.1
4.0
3.9
3.8

Figure 9b. Deep maximum dissolved oxygen in ml/L in the eastern Mediterranean Sea.

TABLE I. POTENTIAL DENSITY AT THE O_2 MAXIMUM BELOW THE O_2 MINIMUM IN THE EASTERN MEDITERRANEAN (T, THOR; D, DANA; OTHERS, ATLANTIS)

Station	σ_θ	*Station*	σ_θ
T189	29.21	4707	29.16
4720	29.17	4706	29.18
4644	29.17	4704	29.19
4719	29.18	4701	29.18
T143	29.15	4700	29.16
4716	29.18	T156	29.19
4715	29.19	T160	29.18
T15	29.15	4699	29.16
D4076	29.22	4679	29.16
D4064	29.17	4680	29.13
4711	29.19	4682	29.15
T144	29.19	4683	29.16
4712	29.20	4696	29.16
T145	29.17	4689	29.16
T147	29.17	4690	29.17
D4075	29.20	4693	29.15
4709	29.18	4691	29.18
4646	29.13		
4708	29.17		
D4070	29.17		
T152	29.18		
D4067	29.18		

Mean 29.173
Range 29.13–29.22
Standard deviation = 0.019
Mean deviation = 0.015

TABLE II. POTENTIAL DENSITY IN THE STRAIT OF OTRANTO ABOVE AND BELOW THE SILL DEPTH OF 780 METERS

NAJADE	*November 1911*		*February 1912*		*May 1912*	
Stations	*Depth (m)*	σ_θ	*Depth (m)*	σ_θ	*Depth (m)*	σ_θ
A36	370	29.11	570	29.13	390	29.06
A35	600	29.11	700	29.12	600	29.07
	860	29.15	800	29.13	800	29.14
			878	29.16	850	29.13
A34	600	29.09	600	29.13	600	29.08
	850	29.10	800	29.16	800	29.10
			855	29.17	860	29.11

In order to test the theory that the Adriatic outflow hugs the bottom as it enters the western Ionian Sea and rises to mid-depths only gradually as it is replaced by newer Adriatic water, a comparison was made of potential densities in the southern Adriatic and in the deepest layers of the Ionian and Levantine basins. Table I lists σ_θ values at the deep O_2 maximum for the entire eastern Mediterranean. Table II

TABLE III. Potential Density between 500 and 800 m at Najade Station A28. Position within 4 Miles of 41° 16′ N, 18° 15′ E

Date	Depth 800 *m*	 600 *m*	 500 *m*
3 Mar. 1911	29.20	29.20	29.18
26 May 1911	29.22	29.15	29.16
24 Aug. 1911	—	—	29.13
29 Nov. 1911	29.27	—	29.20
26 Feb. 1912	29.18	29.17	29.15
28 May 1912	29.28	29.18	29.18
24 Aug. 1912	29.16	29.16	29.14
26 Mar. 1913	29.19	29.16	29.13
23 May 1913	29.16	29.13	29.13
24 Aug. 1913	29.20	—	29.13
23 Nov. 1913	29.21	—	29.12
1 Mar. 1914	29.14	29.14	29.12
Mean	29.20	29.16	29.15

lists the σ_θ values for the three sets of Najade stations in the Strait of Otranto shown in Fig. 8. For the westernmost station, A36, only the deepest observation is given, while for the other two stations σ_θ is given for observations above and below the sill depth of 780 m.

An inspection of the two tables reveals a substantially higher potential density in the deep Mediterranean water than in the observations around the sill of the Strait of Otranto. This is in direct contradiction to the conditions necessary to fulfill the requirements of the postulated theory. Unless the Adriatic water is of equal or higher potential density it will not flow downslope into the depths of the Ionian Sea. However, it should be remembered that the Najade observations were made in different years than the Thor, Dana, and Atlantis observations with which they were compared.

The key to this puzzling situation is found in Najade Station A28, which was occupied on every one of that vessel's 12 cruises in the Adriatic. This station is located 60 miles north of the Strait of Otranto and somewhat closer to the southwestern than the northeastern shore of the Adriatic. With a counterclockwise circulation in that Sea, it can reasonably be assumed that the station is located outside the northward flowing water. Table III gives the potential density at a depth 20 m below the sill and at two depths well above the sill. It is evident from these figures that during a majority of the time there will exist at least a shallow layer of water at the bottom of the Adriatic which has a sufficiently high density to sink to those depths of the eastern Mediterranean at which the deep oxygen maximum was found. Since the rapidity with which the fluctuations of temperature and salinity in the Adriatic take place is not known, there is no way of evaluating the significance of the sampling portrayed by the values in Table III. However, there is little reason to doubt that the deep outflow through the Strait of Otranto is far from continuous.

A more detailed examination of Station A28 made on 3 March 1911 discloses that the entire water column appears to have been recently mixed. Potential temperatures vary between 12.78° and 13.12° C. and salinities between 38.57 and 38.64 °/₀₀. Salinities at 500, 600 and 800 m were 38.62 and 38.64 °/₀₀, while all values above these depths as well as the value at 1000 m, near the bottom, were either 38.57 or 38.58 °/₀₀. All potential densities fell in the range from 29.18 to 29.22 g/L. The dissolved oxygen values furnish the clearest indication of recent and complete mixing. They vary between 5.7 and 5.9 ml/L, giving a minimum concentration of 97% of saturation value.

Among all the Najade and Ciclope data from the Adriatic, the above station is the only one displaying this degree of homogeneity. Among some of the other deep stations part of the water column was well mixed but never the entire column from surface to bottom. The fact that this situation occurs only once in the data at hand merely proves that the condition is possible; it sheds no light on the frequency of occurrence. Nevertheless, it tends to substantiate the irregularity of the water structure in the Adriatic, and, concomitantly, that of the outflow near the bottom.

Since the Adriatic water which flows out of the Strait of Otranto near the bottom is a mixture of water masses having higher and lower salinities than that of the end product, it seems appropriate to identify the sources of these component masses. Low salinity water enters the Adriatic in the form of surface inflow from the Ionian Sea (as seen in Fig. 8) and as fresh water, the latter largely from the rivers of northern Italy. Since there is no evidence of excess evaporation from the Adriatic, such as is clearly indicated in the Levant by the high surface salinities, the only way in which the total salt content of this Sea can be maintained is through an influx of water of higher salinity than that of the outflowing deep water. The only possible sources of such water are the surface and intermediate layers in the northeastern Ionian Sea. Fig. 8 exemplifies the situation where the surface inflow is relatively fresh while the saltier water is found from 150 m all the way to the bottom on the eastern side of the Strait of Otranto.

However, as was pointed out previously, the surface salinity in the Adriatic varies greatly from year to year. For instance, during the seven Najade cruises between February 1911 and September 1912, the maximum surface salinity fluctuated between 38.34 and 38.58 °/₀₀, whereas during her five subsequent cruises between March 1913 and February 1914 it lay in the range from 38.69 to 38.81 °/₀₀. Where high surface salinities appear in the Adriatic, vertical salinity gradients become small and the boundary between surface and intermediate water becomes less distinct.

The water structure at Station A28 of 3 March 1911 strongly suggests the mechanism whereby the deep water of the eastern Mediterranean is formed. Surface and intermediate water of Mediterranean origin, down to a depth of several hundred meters, flows into the Adriatic, is thoroughly mixed there with fresher water by the vertical convection set up by surface cooling in winter, and then flows back into the Ionian Sea along the western side and bottom of the Strait of Otranto.

As the high salinity surface water flows in from the south, its temperature is somewhat higher than that of water formed in the Adriatic. Consequently, its density will be lower than that of intermediate water with approximately the same salinity. The resulting stability of the water column probably accounts for the infrequent occurrence of such thoroughly mixed water as was found on the above station. In other words, stability of the upper water column is generally maintained either through the low salinity of Adriatic water or through the high temperature of Ionian Sea surface water.

The Adriatic bottom water which flows south into the eastern Mediterranean is probably formed by the gradual sinking of water from mid-depths of the Adriatic. This water, in turn, may be replaced by water drawn in horizontally from contiguous areas or by water sinking from the surface layer above it when the stability of the column is slight, as on the above mentioned Station A28, or by a combination of horizontal and vertical advection. It is significant, for instance, that in the three sections across the Strait of Otranto, shown in Fig. 8, the dissolved oxygen percentage of saturation below 300 m in the western half of the channel averages roughly 82%. If the outflowing water were drawn largely from the surface layer in the Adriatic, this percentage would be much closer to the saturation value, considering the short distance from its source.

As the average oxygen saturation percentage in the eastern half of the Strait below 300 m is only a few percentage points lower than that in the western half, the possibility should be kept in mind that turbulence in the Strait due to opposite running currents will cause some of this inflowing water to mix with the outflowing current and thus be deflected back into the Ionian Basin without fully penetrating into the Adriatic. This process would tend to reduce the horizontal gradients across the Strait.

It had been suggested previously that, because of the shallowness of the Adriatic, its water structure closely follows the fluctuations of the existing weather regime. By the same line of reasoning it appears highly probable that the circulation through the Strait of Otranto is also directly affected by changes in wind direction and intensity. Southerly and southeasterly winds tend to drive more surface water into the Adriatic. An excess inflow of this nature must be compensated for by an increased outflow which can then take place only in subsurface layers.

SUMMARY

1. Below 1600 m the water in the center of the Ionian and Levantine basins is identical in temperature and salinity structure. The amount of dissolved oxygen at these depths is consistently higher in the Ionian Sea by about 0.15 ml/L.

2. No evidence was found of a subsurface flow of Aegean water into the eastern Mediterranean via the three channels between the island of Crete and Asia Minor. Due to the high salinity and oxygen values in the southern Aegean, below the sill depths of these channels, such an effluent, if it existed, would be readily detectable in the Mediterranean stations. A similar situation was found in the channels into the Aegean, located between Crete and the Greek mainland.

3. The water entering the Ionian Sea through the Strait of Sicily was eliminated as a major component of the deep water of the eastern Mediterranean. The somewhat fresher water flowing out of this Strait is separated from the deep water by a permanent intermediate layer having a higher salinity than the layer below it. The Strait of Messina was ruled out as a factor in this problem because of its shallow sill depth, narrowness, and the tidal nature of its currents.

4. The Adriatic Sea, the only other possible source of deep eastern Mediterranean water, has a complicated water structure. Due to its restricted size and shallow mean depth it is particularly susceptible to short term weather fluctuations. Thus, single sections or stations cannot be considered representative of average conditions for any particular season. Nevertheless, three sections across the Strait of Otranto indicate an outflow of Adriatic water on the bottom and western side of this Strait. This is consistent with the dissolved oxygen distribution in the entire eastern Mediterranean. There is generally a minimum value at mid-depths, with a secondary maximum below it wherever the bottom is deep enough. In both the minimum and maximum oxygen layers the highest values are found near the Strait of Otranto and along the western edge of the Ionian Sea. This oxygen pattern suggests a counterclockwise circulation in the deep water of

the eastern Mediterranean, with Adriatic water hugging the bottom as it enters the northwestern Ionian Sea and gradually rising to mid-depths as it is replaced by newer water from the same source. An analysis of one station in the Adriatic, occupied on 12 occasions, shows that, during a majority of the time, water at depths of the sill in the Strait of Otranto has a higher potential density than the deep water of the eastern Mediterranean and can therefore flow downslope into the Ionian Sea. This water is composed of relatively fresh water, largely river effluent from the northern Adriatic, and of Ionian Sea water of relatively high salinity from intermediate depths and of variable salinity from the inflowing surface layer. These component water masses are mixed in the southern Adriatic, particularly by surface cooling and vertical convection in winter. The resultant mixture gradually sinks to the bottom and flows slowly out of the Strait of Otranto back into the Ionian Sea. There seems little doubt that this outflow is quite irregular, depending to a large extent on the prevailing weather regime.

REFERENCES

FERUGLIO, GIUSEPPE

1912. Primi risultati di esperienze con galleggianti per lo studio delle correnti del mare Adriatico. Boll. Com. talassogr. ital., *17:* 295–317.

METEOROLOGICAL COMMITTEE, AIR MINISTRY, LONDON

1930. Mean sea surface temperature charts, Mediterranean. Mar. Obs., *7:* No. 73–84.

NIELSEN, J. N.

1912. Hydrography of the Mediterranean and adjacent waters. Rep. Danish oceanogr. Exped. Medit., *1:* 77–192.

SCHOTT, GERHARD

1915. Die Gewässer des Mittelmeeres. Ann. Hydrogr., Berl., *43:* 1–18, 63–79.

U. S. HYDROGRAPHIC OFFICE

1942. Sailing directions for the Mediterranean, Vol. IV. Washington, D. C. Publ. No. 154A. 352 pp.

VERCELLI, FRANCESCO

1925. Il regime delle correnti e delle maree nello Stretto di Messina. Commissione Internazionale del Mediterraneo. Crociere per lo studio dei fenomeni nello Stretto di Messina. *1:* 209 pp.

STATION DATA

ATLANTIS

1948. Files of the Woods Hole Oceanographic Institution, Woods Hole, Mass. To be published in Bulletin Hydrographique, Copenhagen.

DANA

1930. Hydrographical observations made during the "Dana" Expedition 1928–30. Dana-Rep., No. 12. 1937.

NAJADE

1911–1914. Berichte über die Terminfahrten. Osterreichischer Teil, No. 1–12. Perm. int. Komm. Erforsch. Adria. 1912, 1913 and 1915.

THOR

1908, 1910. Hydrographical observations. Rep. Danish oceanogr. Exped. Medit., *1:* 53–76. 1912.

Contribution No. 557

ANNUAL VARIATIONS IN CURRENT SPEEDS IN THE GULF STREAM SYSTEM[1]

By
FREDERICK C. FUGLISTER
Woods Hole Oceanographic Institution

ABSTRACT

The monthly resultant current speeds in ten segments of the Gulf Stream System are calculated from surface current data published by the U. S. Navy Hydrographic Office. Marked annual variations in the current speeds are found in the Florida Current, in the Caribbean Sea, and in the Trade Wind areas. In other segments of the system the annual variations are not so well defined. The maximum current speeds occur during the summer in the southern segments of the Gulf Stream System and during the winter in the northern segments. The minimum speeds occur during the fall months throughout the system. Annual and semiannual periods are calculated and found to be in fair agreement with the observed annual variations in the Florida Current. In the Trade Wind and Caribbean areas the current speed and wind speed fluctuations are approximately the same. A partial correlation is shown to exist between the annual variations in current speeds in the Florida Current and the annual variations in sea level at Miami and Charleston.

The main current system of the North Atlantic Ocean, the Gulf Stream System, obtains its energy of motion principally from the Northeast Trades and the Westerlies. Since the wind system fluctuates in position and velocity with the different seasons of the year, it is to be expected that the current speeds of the Gulf Stream System would also vary with the seasons. Montgomery (1938) and Iselin (1940), on the bases of both hydrographic station data and tide gauge records, showed that there is such an annual fluctuation in the transport of the Florida and the Gulf Stream currents. The purpose of this paper is to show that the many hundreds of surface current observations on file at the U. S. Navy Hydrographic Office also give a consistent picture of annual variations in the current speeds in certain segments of the Gulf Stream System.

The data have been published in the form of an Atlas by the U. S. Navy Hydrographic Office (1946), in which atlas charts are given showing the monthly resultant current direction and speed for each one degree quadrangle in the North Atlantic plus the number of observations used to obtain each value. The following is quoted from the Atlas:

---

[1] Contribution No. 557 from the Woods Hole Oceanographic Institution. This paper originated as a technical report to the Oceanographic Division of the Hydrographic Office, U. S. Navy Department under a contract with the Office of Naval Research.

Reprint from SEARS FOUND. JOURN. MAR RES.

> The information relating to monthly resultant surface currents shown on this chart was compiled from observations made during the month for all years prior to 1935 by the cooperating observers of the Hydrographic Office. Observations were not considered reliable where tidal currents prevailed; where winds, sea or swell of force 6 or above were recorded; where the vessel's draft or trim would cause excessive leeway; or when doubt existed as to the meaning of the entry "Nil" on the current report. All current calculations are based on the MEDIAN POSITION method; namely, each observation is applied at only one point, that point being midway between the beginning and end of the ship's run for which the current observation was made.

Because this median position method frequently integrates the speed of the main current with that of possible countercurrents and eddies, the values given in the accompanying tables and figures are much lower than would be the case if they applied only to the main current (Iselin and Fuglister, 1948).

From the Hydrographic Office charts the annual variation in current speeds has been calculated for ten segments of the Gulf Stream System. The areas studied are shown in Fig. 1.

The segments numbered 1 to 7 cover all but the southeastern part of the North Atlantic Eddy, the segments A, B and C take in three branches of the system. The segments were chosen by locating areas where the largest number of observations were available and where the arrows on the charts pointed in approximately the same direction throughout the year. The most doubtful, in regards to area covered, is Segment B in the Antilles Current. The direction of the current arrows and the speeds for each one degree quadrangle varied more in this segment than in any other. Segment 1 in the Trades and Segment A in the Guiana Current have been treated separately because of the marked difference in direction and speed in the two areas. After much of the analysis had been completed, it was found that more quadrangles could have been added to Segment 5 northeast of Hatteras, thus making it a continuous group without changing the results appreciably. Segment 3 in the Florida Current contains the most observations, Segment 1 in the Trade Wind Area the least. For instance, in the month of March, Segment 3 contains 1,468 observations, Segment 1 only 329.

The average of the resultant drifts for all quadrangles in each of the ten segments for each month are given in Table I and are plotted in Figs. 2 and 3. These data indicate that the time of maximum current speed varies as we move around the system. In the southern portions the maximum occurs in summer; in the northern it occurs in winter. On the other hand, the minimum speeds throughout the system occur during the fall months from September to November.

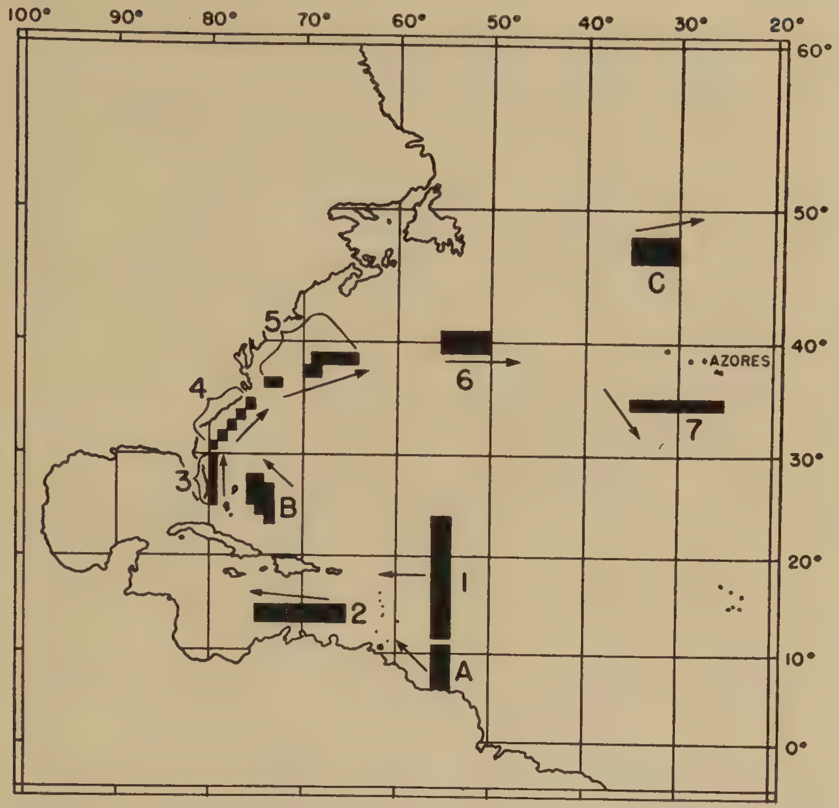

Figure 1. Location of segments of the Gulf Stream System used to calculate annual variations in current speeds. Arrows show resultant current directions within the various segments.

TABLE 1. Average Current Speeds in the Gulf Stream System (Miles Per Day).* See Fig. 1 for Areas Covered by Segments 1 to C.

Month	*Segment*									
	1	*2*	*3*	*4*	*5*	*6*	*7*	*A*	*B*	*C*
Jan.	7.4	17.2	55.2	41.3	23.0	12.4	3.7	24.6	4.7	4.9
Feb.	7.4	17.3	57.5	39.9	22.3	13.0	4.1	25.9	3.9	4.1
Mar.	7.4	17.3	60.8	42.2	21.0	13.5	4.1	23.5	4.6	4.1
Apr.	7.0	17.5	61.7	43.7	24.0	12.6	3.6	29.3	4.9	4.4
May	7.9	16.7	61.7	46.4	24.1	12.9	4.3	34.2	4.0	4.2
June	8.3	18.3	64.2	49.3	23.9	11.6	4.0	24.3	4.6	4.8
July	9.4	19.6	65.6	48.2	22.8	13.1	3.3	18.4	4.8	4.6
Aug.	8.5	18.0	65.4	48.4	22.0	11.7	3.8	17.4	5.0	3.9
Sept.	6.4	15.5	60.5	44.0	21.4	12.3	3.3	15.3	4.3	3.2
Oct.	6.9	13.5	52.4	39.0	20.2	10.5	3.4	15.5	3.5	3.2
Nov.	7.2	12.9	49.0	36.7	20.4	11.1	3.6	19.0	4.6	4.0
Dec.	7.4	15.0	53.8	39.4	20.8	10.7	4.2	19.5	4.5	5.4
Mean	7.6	16.6	59.0	43.2	22.2	12.1	3.8	22.2	4.4	4.2

* Computed from the Hydrographic Office Chart, H. O. Misc. 10,688.

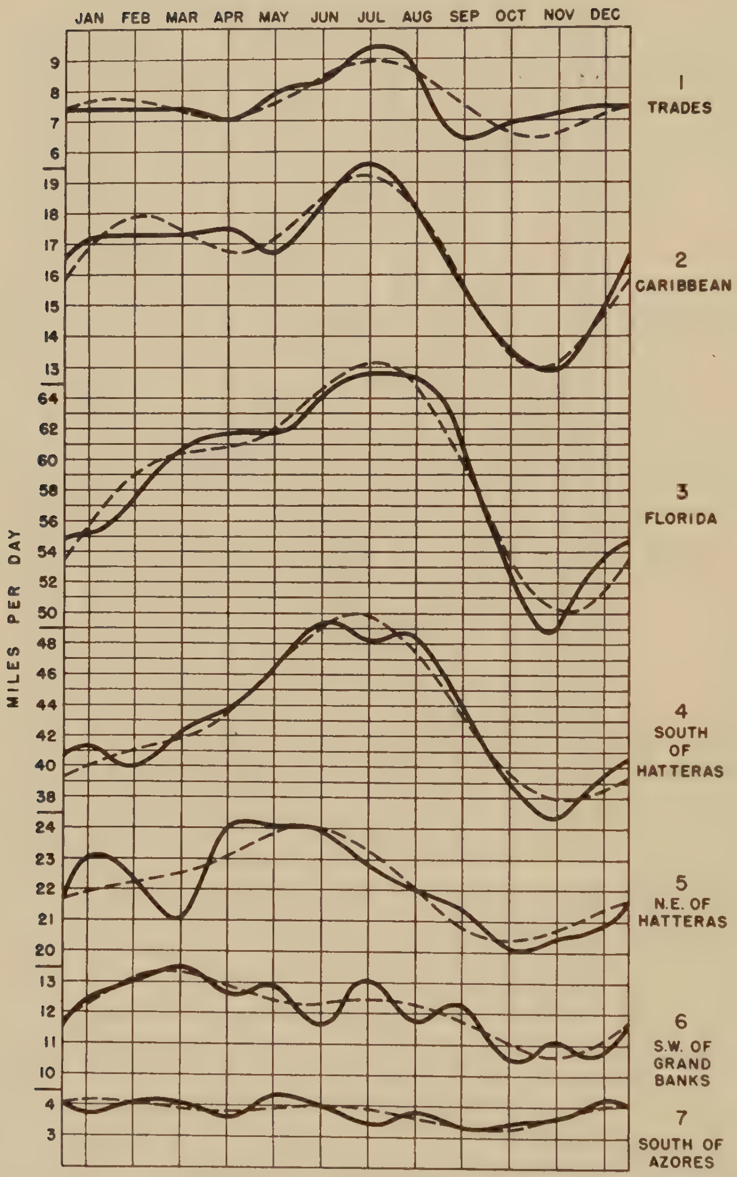

Figure 2. Annual variation in the current speed in seven segments of the Gulf Stream System. Observed data, solid lines; calculated combination of annual and semiannual periods, dashed lines.

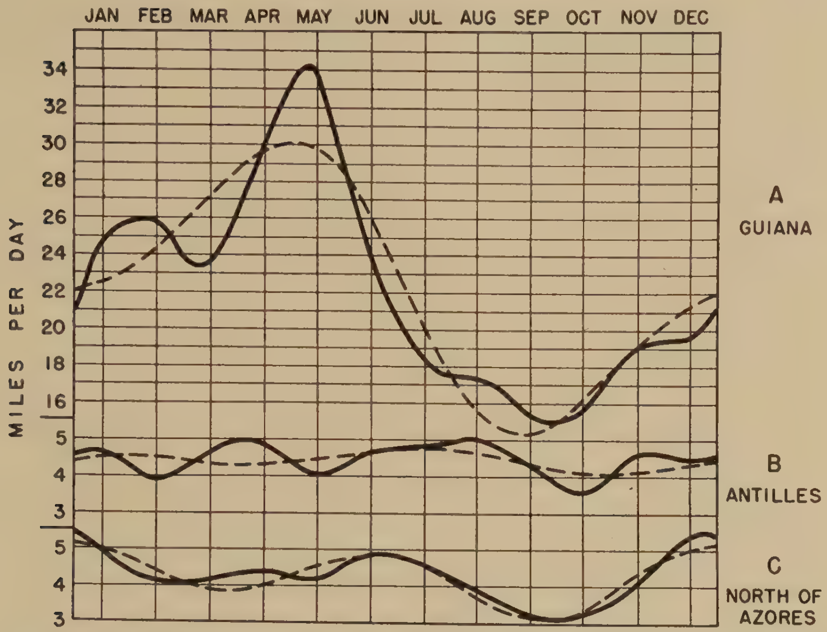

Figure 3. Annual variations in the current speeds of three branches of the Gulf Stream System. Observed data, solid lines; calculated combination of annual and semiannual periods, dashed lines.

In no case does the annual variation curve approximate a simple sine wave. In order to determine how closely a combination of annual and semiannual periods would fit the observed data and in order to determine also the relative importance of these two periods, the values in Table I were analyzed harmonically (Conrad, 1944: 71). The results of these calculations are shown by the dashed lines in Figs. 2 and 3. There is a fair agreement in the calculated and observed annual variations for those segments where the currents are relatively confined, as along the continental shelf south of Cape Hatteras. Because of the meandering nature of the currents in other areas, the actual current speeds and, to a lesser extent, the annual variations are obscured by the averaging processes.

In the southern and eastern segments of the North Atlantic Eddy the amplitudes of the first two harmonic terms, the annual and semiannual periods, are nearly equal. In the Guiana Current and in Segments 3 to 6 in the western and northern part of the eddy the annual period has the greater amplitude. The relative amplitudes, in per cent of the arithmetic mean, for the annual and semiannual periods for each segment are given in Table II.

TABLE II. The Relative Amplitudes of the Annual and Semiannual Periods for Ten Segments of the Gulf Stream System (Per Cent of the Arithmetic Mean)

	Segment									
	1	*2*	*3*	*4*	*5*	*6*	*7*	*A*	*B*	*C*
1st term	8.5	12.4	11.0	12.2	7.0	8.8	7.8	3.1	3.5	9.4
2nd term	8.3	10.6	4.9	4.0	2.6	3.2	6.8	1.0	5.1	16.8

TABLE III. Estimated Wind Speed Component in the Direction of the Current for Eight Segments of the Gulf Stream System (in Meters per Second)

Segment	*Jan.*	*Feb.*	*Mar.*	*Apr.*	*May*	*June*	*July*	*Aug.*	*Sept.*	*Oct.*	*Nov.*	*Dec.*
1	4.7	5.1	4.5	5.3	5.4	6.0	6.5	6.4	5.6	4.4	4.8	5.7
2	6.8	6.4	6.0	6.9	6.6	6.7	7.2	6.0	5.4	4.3	4.7	6.1
3	−1.6	0.0	0.3	−0.2	0.7	1.0	1.5	0.8	−0.4	−0.5	−1.5	−2.3
4	−1.9	−0.1	1.0	−0.1	1.7	2.0	1.4	0.8	−0.6	−2.0	−0.4	−3.5
5	−0.2	0.0	0.2	0.4	−0.3	1.3	2.1	0.4	−0.5	0.3	0.2	0.1
6	2.6	1.6	1.5	1.7	1.2	2.3	3.2	1.9	0.7	1.5	0.5	3.2
7	−0.9	0.4	−1.0	1.1	0.7	1.0	1.0	1.5	0.3	−0.3	1.9	0.2
C	5.2	4.5	3.3	2.0	1.7	1.6	2.1	2.3	2.8	2.3	3.4	5.3

Only in the last two segments, B and C, are the amplitudes of the second term greater than the amplitude of the first. This may have little significance in area B because of the poor correlation of observed and calculated data, but it may be real in area C where the correlation is good. One difficulty concerning Segment C is that it is not certain that it actually is a segment of the Gulf Stream System. The directional arrows on the Hydrographic Office chart for this area are uniform throughout the year, but this is not proof that a northern branch of the System consistently passes through the area. It has been assumed that all the segments dealt with in this study form part of a continuous current system. Whether or not a branch of this system passes through area C, the surface current data from the area include the effects of the shallow wind drift currents. A tabulation of the varying wind velocities for this area (see below) indicates that the annual variations in current speed are due only in part to the wind.

The annual variation in wind force was obtained from the wind roses on the British Admiralty charts of the North Atlantic. These charts show the frequency, force and direction of the wind for each 5° quadrangle for each month. The values shown in Table III are the estimated wind components in the direction of the currents. The values are only approximate owing to the difficulty of reading exact values from the roses and of converting from the Beaufort scale to wind speed. The negative values indicate that the component of the wind force along the streamline of the current is in the opposite direction to its flow.

In only two segments, the Trades (1) and the Caribbean (2), are the wind speed and the current speed fluctuations approximately the same.

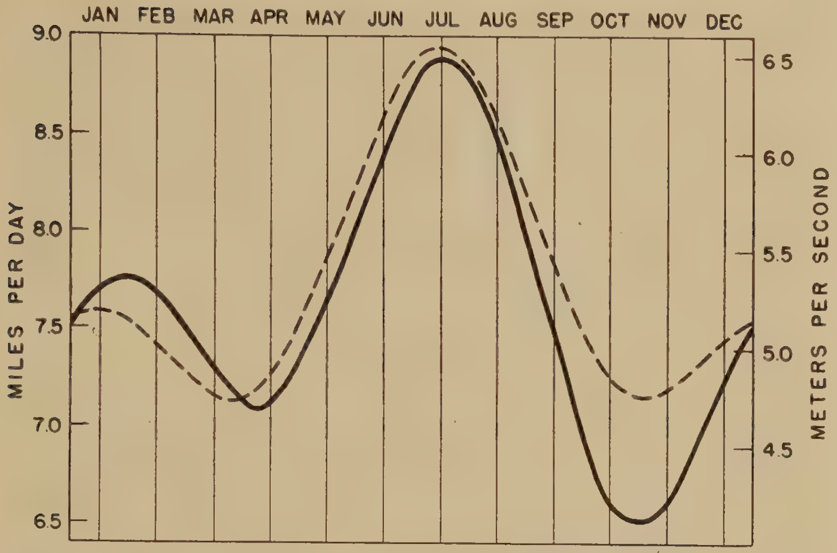

Figure 4. Calculated combination of annual and semiannual periods for the currents, solid line; for the winds, dashed line; segment 1.

This is certainly what should be expected, since these winds are the motive force for the currents. Harmonic analysis of the wind speed data from Segment 1 shows that the resultant of the combined annual and semiannual waves is similar to the resultant for the current speeds (see Fig. 4). The relative amplitudes, in per cent of the arithmetic mean, for the first two terms for the wind data are 12.6 and 9.5 as compared to 8.5 and 8.3 for the current data.

The annual variations in current speed and wind speed for Segments 1, 2 and C are shown in Fig. 5. In Segment C, north of the Azores, it appears evident that the winter maximum in the current speeds must be due in large part to the winds. The secondary maximum in the summer, at a time when the winds are at a minimum, may indicate that this segment is in fact a continuation of the main current system.

Using the method employed by Iselin (1940), the average monthly speeds of Segments 3 and 4 in the Florida Current have been compared with the sea level records from Miami and Charleston. According to this theory the mean sea level is at a maximum when the current speed is at a minimum. The tide gauge records were taken from two papers by Montgomery (1938, 1941). The two sets of curves are shown in Fig. 6. The correlation is only fair; while the winter maximum indicated by the tide gauge records does not appear on the curve of the observed current speeds, both sets of data show the rapid decrease in

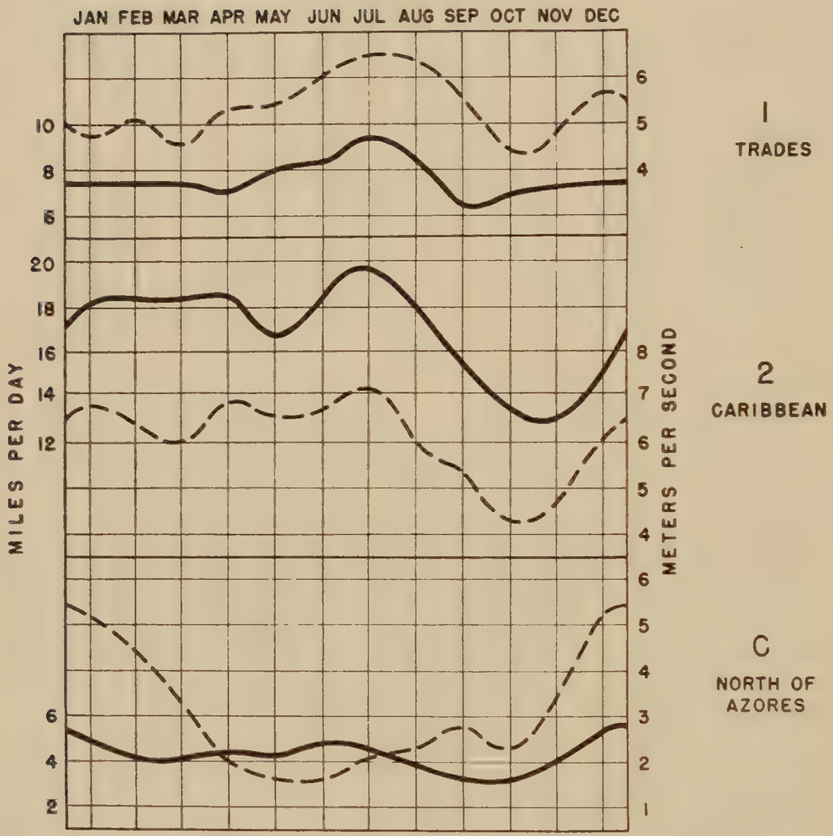

Figure 5. Annual variation in current speed, solid lines; wind components in direction of the currents, dashed lines.

values between July and October. The adverse winds of December and January (see Table III) may account for the absence of a winter maximum in the observed current data.

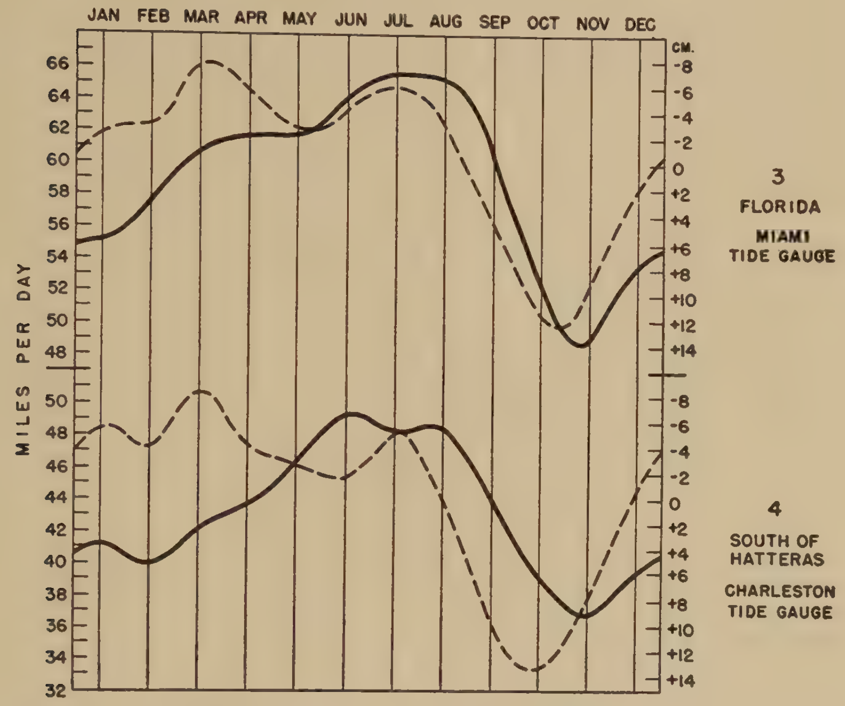

Figure 6. Comparison of current speeds (solid lines) with tide gauge records (dashed lines).

References Cited

Conrad, V.
1944. Methods in climatology. Harvard Univ. Press, Cambridge, Mass. pp. 70–80.

Iselin, C. O'D.
1940. Preliminary report on long-period variations in the transport of the Gulf Stream System. Pap. phys. Oceanogr. Meteorol., *5* (1): 1–40.

Iselin, C. O'D and F. C. Fuglister
1948. Some recent developments in the study of the Gulf Stream. J. Mar. Res. *7* (3): 317–329.

Montgomery, R. B.
1938. Fluctuations in monthly sea level on eastern U. S. Coast as related to dynamics of western North Atlantic Ocean. J. Mar. Res., *1* (2): 165–185.

Montgomery, R. B.
1941. Sea level difference between Key West and Mami, Florida. J. Mar. Res., *4* (1): 32–37.

U. S. Navy Hydrographic Office
1946. Current Atlas of the North Atlantic Ocean. H. O. Misc. 10,688.

Contribution No. 559

BULLETIN OF THE GEOLOGICAL SOCIETY OF AMERICA
VOL. 62, PP. 441-450, 3 FIGS., 6 PLS. MAY 1951

SUBMARINE TOPOGRAPHY IN THE NORTH ATLANTIC

BY IVAN TOLSTOY

ABSTRACT

In the North Atlantic one may distinguish several types of topography, each of which is characteristic of certain portions of the ocean floor.

The continental slopes are now known to show in many cases a steplike succession of horizontal or imperceptibly sloping shelves or terraces. They are dissected by systems of submarine canyons, the pattern of which is such as to suggest to many a subaerial origin. A recent investigation of the Hudson submarine valley by the ATLANTIS has shown that this valley extends at least as far as the 2500 fathom curve, 300 miles out to sea, and shows features suggesting a subaerial origin.

The broad basins are characterized by smooth floors or plains covering areas of more than 200,000 square miles out of which there rise large sea mounts, isolated or in groups. Thus plains at a depth of 2900 fathoms occupy the floors of the North American and the North Canary basins.

The floor of the northwestern part of the North American basin, north of Bermuda, is characterized by a plain at 2650 fathoms. Sea mounts of various sizes and shapes rise out of these otherwise smooth plains. There is a conspicuous group of flat-topped sea mounts rising from the 2650-fathom plain of the western North American basin. They rise approximately to 800 fathoms and string out toward the southeast, roughly from the direction of Cape Cod. They show evidence of terracing on their flanks.

The central part of the Atlantic Ocean is characterized by a long submarine mountain range, extending from Iceland to a point southwest of the Cape of Good Hope, known as the Mid-Atlantic Ridge. Numerous fathograms across the Ridge have shown that it is characterized by a high central zone, or Main Range, consisting of parallel ridges following the general trend of the Ridge and rising in many places to less than 800 fathoms below the surface of the ocean.

Between 1600 and 2500 fathoms the flanks of the Ridge are characterized by a succession of flats which for the lack of any better term have been called terraces. Reflection-shooting studies by Ewing and Press and others have shown that these terraces are or have been areas of greater deposition.

Finally, between this Terraced Zone and the 2900-fathom plain, one may usually recognize a mountainous area standing out as a distinct physiographic province.

CONTENTS

	Page
Introduction	442
Sources and acknowledgments	442
The continental slopes	442
The basins	443
Mid-Atlantic Ridge	445
Outstanding physiographic features	446
Comments on the history and structure of the Mid-Atlantic Ridge	449
References cited	450

ILLUSTRATIONS

Figure	Page
1. Muir Sea Mount	444
2. Submarine topography of the Azores bulge	447
3. Sounding lines utilized in the map of Figure 2	448

Plate	Facing page
1. Bathymetric sketch map of the North Atlantic between Lat. 45°N. and 23°N.	441
2. Distribution of the major submarine plains in the same area and sounding lines	442
3. Profiles of the sea mounts southeast of Cape Cod	444
4. Profiles of the southeastern edge of the Bermuda rise and of the 2850–2950 plain, close to the 31st parallel	446
5. Profiles across the eastern edge of the 2850–2950 plain close to the 31st parallel, the Foothills, and the Terraced Zone of the Mid-Atlantic Ridge	448
6. Profiles across the Terraced Zone and the Main Range of the Mid-Atlantic Ridge	450

Introduction

Until the relatively recent development of echo-sounders that could record to depths greater than 2000 fathoms, there were few reliable data on the topography of the North Atlantic Ocean bottom. A few regions adjacent to land such as the continental shelf and the continental slope of the northeastern United States (Veatch and Smith, 1939) and the Azores bulge (Wüst, 1939) had been worked out sufficiently to give us an understandable morphological and structural picture of some small sections of the North Atlantic sea floor. Scientists and mariners had also been aware of some of the more outstanding features such as the Mid-Atlantic Ridge, the huge banks off the west coasts of Spain, Portugal, and North West Africa, and some of the great gashes cutting the continental slopes on both sides of the Atlantic such as the Hudson, Congo River, and Nazare canyons (Hull, 1912; Spencer, 1903). The vagueness of most of the sounding data and the lack of complementary geophysical information (such as composition and thickness of the sedimentary cover, elastic-wave velocities in the suboceanic crust, rock samples, etc.) have resulted in numerous and sometimes wondrous hypotheses concerning the history of the Atlantic Ocean. Though we are still far from understanding this fascinating but highly intricate problem, the work now being done by Columbia University and the Woods Hole Oceanographic Institution is beginning to extend into the oceans factual data heretofore limited to the continental shelves of the United States. The same situation had prevailed for many years in the Pacific Ocean, until the outstanding work of H. H. Hess, F. P. Shepard, the Scripps Institution of Oceanography, H. W. Murray, and many others began to clarify the morphology of the Pacific Ocean floor.

This paper illustrates the existence of oceanic features some of which were unknown and others only suspected. The author hopes it will contribute to our understanding of the history of the Atlantic Ocean, if only by emphasiziny the gaps in our knowledge and the complexity of the problem.

Sources and Acknowledgments

Some of the first continuous fathograms in water deeper than 2000 fathoms were obtained in 1946 by the R/V Atlantis of the Woods Hole Oceanographic Institution. Since that year over 100,000 miles of ocean bottom have been reproduced on fathograms, by the Atlantis and by a few other vessels. Numerous closely spaced discrete soundings have also been obtained by vessels doing work for the U. S. Navy Hydrographic Office.

The author is grateful to the Woods Hole Oceanographic Institution and its personnel who made much of this work possible. In particular, Columbus O'D. Iselin, director of the Institution, Adrian K. Lane, master of the Atlantis, and Dr. J. B. Hersey deserve special mention because of their unstinting co-operation. The National Geographic Society and the Bureau of Ships, Navy Department, as well as Columbia University, financed the work. The U. S. Navy Hydrographic Office contributed a portion of their data, thereby helping greatly in the progress of this study.

The Continental Slopes

In many areas the continental slopes exhibit appreciable changes in gradient. There is, for example, some evidence of flattening below 1600 fathoms off the coast of Africa. Off the eastern coast of the United States the detailed surveys of the U. S. Coast and Geodetic Survey show broad gently sloping shelf-like structures between 1300 and 1700 fathoms and between 2100 and 2300 fathoms in the broad embayment whose head is occupied by the Hudson Canyon (Tolstoy and Ewing, 1949, Pl. 3, a). This continental slope is dissected by a system of submarine canyons, the pattern of which suggests to some a subaerial origin. This pattern was discovered by Veatch and Smith (1939). Their investigations were limited to water shallower than 1600 fathoms south of the Delaware and to water shallower than 1200 fathoms in the area of and east of the Hudson Canyon. Two cruises by the Atlantis (spring and summer 1949) have shown that the Hudson submarine valley extends seaward at least 200 miles beyond the limits of the Coast and Geodetic Survey's work and is identifiable as far as the edge of the flat basin floor at 2600 fathoms. It was followed down the continental slope by means of a close series of zigzag sounding lines to a depth of 2540 fathoms, at which point its relief became too slight to identify it positively. Several tribu-

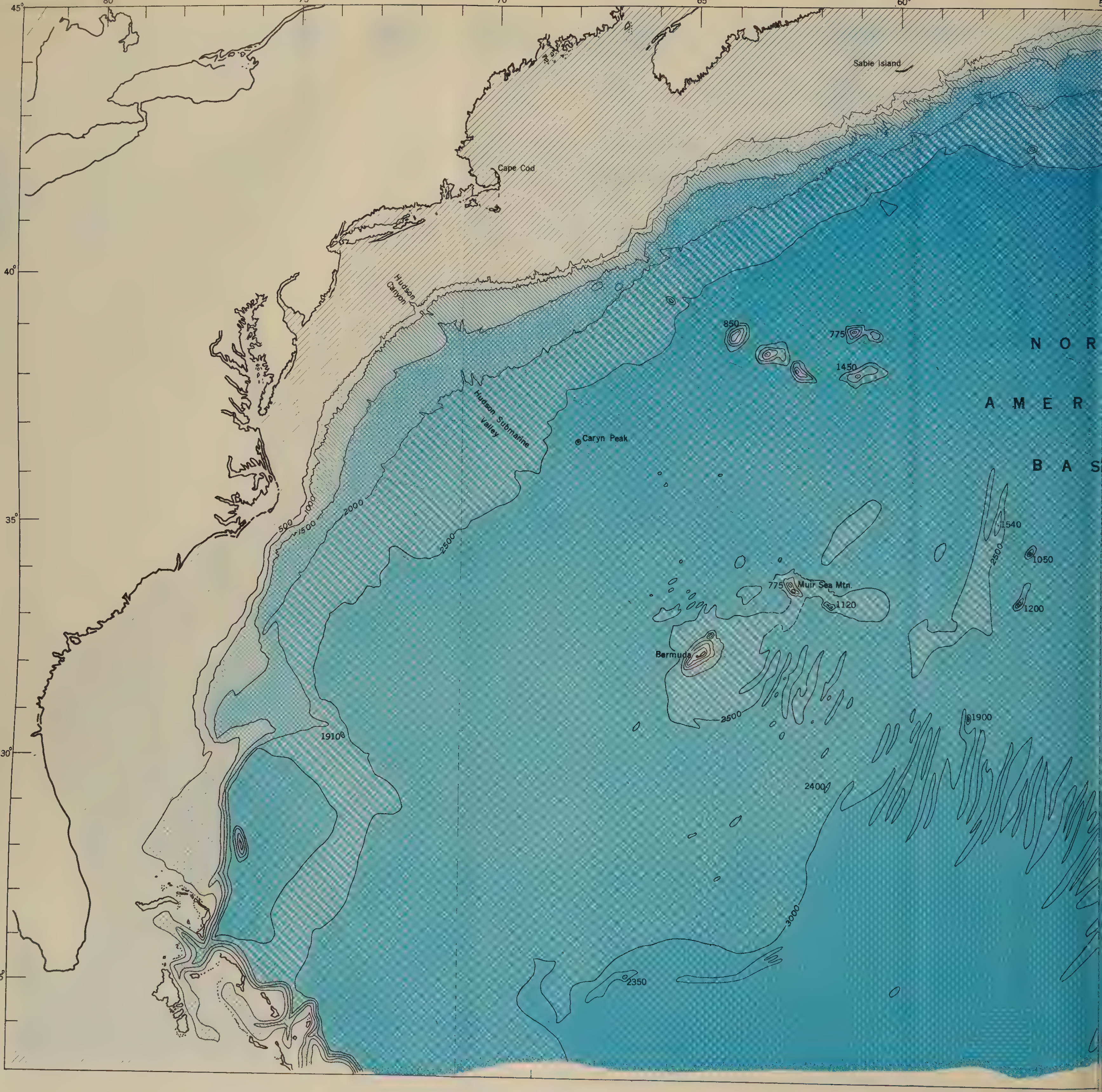
45°
80°
75°
70°
65°
60°
40°
35°
30°
25°
Sable Island
Cape Cod
Hudson Canyon
Hudson Submarine Valley
Caryn Peak
850
775
1450
N O R
A M E R
B A S
500
1000
1500
2000
2500
1540
1050
1200
775
Muir Sea Mtn.
1120
Bermuda
2500
1900
1910
2400
3000
2350

BATHY

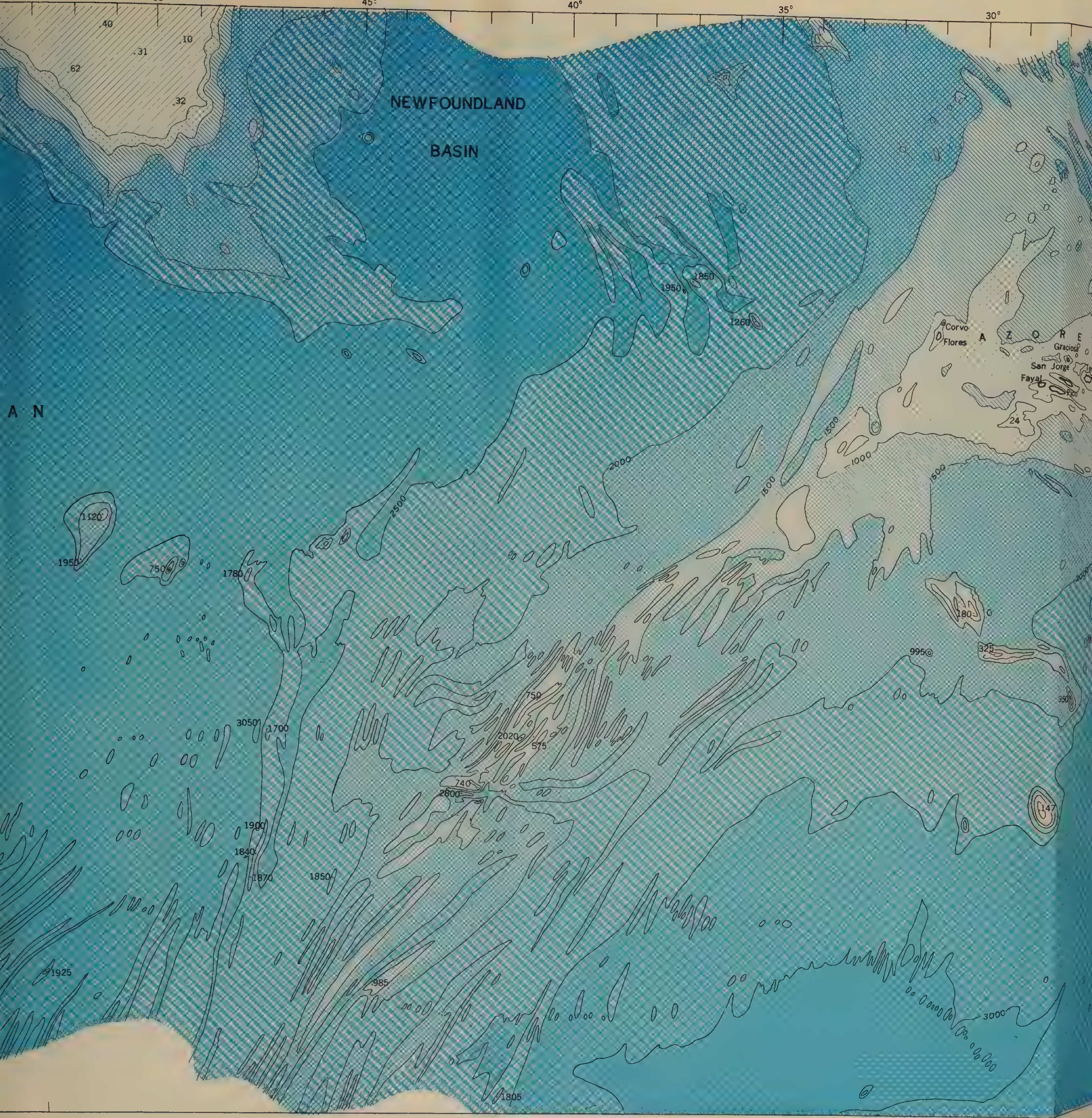
50°
45°
40°
35°
30°
.40
.31
.10
.62
.32
NEWFOUNDLAND
BASIN
A N
1950
1850
1260
Corvo
Flores
A Z O R E
Graciosa
San Jorge
Fayal
Pico
24
1500
1000
1500
1500
2000
2500
2000
1120
1950
750
1780
180
325
995
350
750
2020
575
740
2800
3050
1700
1900
1840
1870
1850
147
1925
985
3000
1805

RIC SKETCH MAP OF THE NORTH ATLANTIC OCEAN, BETWEEN LAT. 45° N. AND 23°

Contour interval 500 fathoms. The sounding lines used are shown in Plate 2

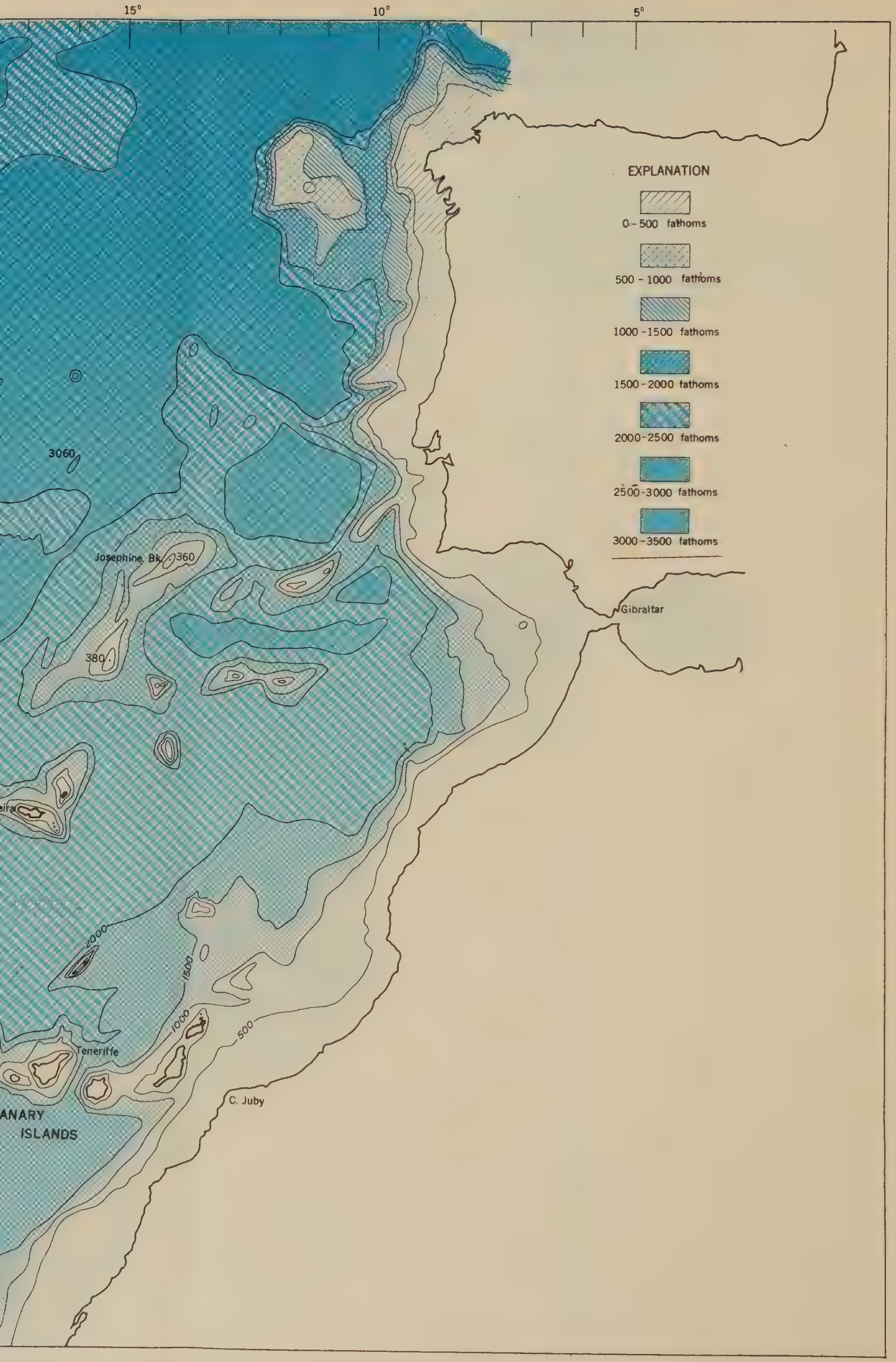
15°
10°
5°
EXPLANATION
0 - 500 fathoms
500 - 1000 fathoms
1000 - 1500 fathoms
1500 - 2000 fathoms
2000 - 2500 fathoms
2500 - 3000 fathoms
3000 - 3500 fathoms
3060
Josephine Bk.
360
380
eira
Gibraltar
2000
1500
1000
500
Teneriffe
C. Juby
ANARY
ISLANDS

taries enter it at grade between 100 and 2350 fathoms. Its relief is greatest where it cuts into the steeper slopes such as the upper 1200 fathoms of the continental slope and the slope between 1700 and 2100 fathoms. In this latter slope it cuts a gorge 1800 feet deep and roughly 3 miles wide in the ocean floor. In the almost flat areas between 2250 and 2300 fathoms it exhibits evidence of meandering. However the author does not believe that these features are sufficient in themselves to prove that the canyon had been cut out under subaerial conditions. A detailed presentation of the data on the Hudson submarine valley by Heezen, Ewing, and the author will be given elsewhere. On the bathymetric sketch of Plate 1 the small indentation in the 2500-fathom contour west of Caryn Peak represents the crossing of this contour by the Hudson Submarine Valley.

There are indications of other submarine valleys—such as the Hydrographer, Oceanographer, and Lydonia canyons—at depths greater than 2000 fathoms that prolong some of the larger submarine valleys of the American Continental slope. There are also several broad valleylike depressions in depths of 2500 fathoms in this area. The excellent control available here (Pl. 2) leaves little doubt as to the reality of these features. The continental slope northeast of the limits of the work of Veatch and Smith exhibits the same high degree of dissection; canyons occur down to depths of more than 2000 fathoms. South of Lat. 29°N., the continental slope becomes extremely steep (over 30° in some places) and suggests a fault scarp.

THE BASINS

Plate 1 illustrates the distribution of basins on both sides of the Mid-Atlantic Ridge. The nomenclature adopted is from Maurer and Stocks (1933). The floors of the North American, Northern Canary, and probably the Newfoundland basins are occupied mostly by vast smooth plains covering a total area of well over 200,000 square miles.

Thus the floor of the northwestern part of the North American Basin is characterized by a plain between 2600 and 2700 fathoms. In the area of the Caryn Peak its depth is 2600–2620 fathoms. It slopes very gently southeastward and southwestward; the average slopes are about 2 feet per mile. The northern boundary of this plain is clearly defined as the foot of the continental rise at 2600 to 2650 fathoms. The southern boundary is much less clearly defined but probably runs east-west, close to Lat. 35°N. Eastward it appears to merge into a somewhat narrower 2700–2750 level. The approximate location of these and other levels is shown in Plate 2. In some places the transition between the 2600–2650 and 2700–2750 levels seems to be steplike (Tolstoy and Ewing, 1949, Pl. 4, a). However, it is impossible in many cases to identify the boundary between these levels, since changes in depth of the order of 50 fathoms are very difficult to correlate from soundings by different ships or even different cruises of the same ship. The combined effects of small frequency changes in the instruments, of differences of sound velocity in the sea water, and of calibration may be of the order of 50 fathoms.

This 2700–2750 level merges eastward into the 2850–2950 plain occupying most of the floor of the northern section of the North American Basin. Both the 2600–2650 and the 2700–2750 levels appear to form narrow fringes along the foot of the continental rise west and south of the Grand Banks, between the rise and the 2800-fathom contour. The 2600–2650 plain may also occupy the southern end of the Newfoundland Basin.

The area covered by the 2850–2950 plain is shown in Plate 2. It slopes gently southward. Thus at Lat. 40°N. it lies at 2850 fathoms, at Lat. 37°N. it lies at 2890 fathoms, and at Lat. 31°N. its depth is 2950 fathoms. It has therefore a gradient of the order of 1 to 1½ feet per mile. Its southern end, near Lat. 30°N., is broken into a series of tonguelike flat-bottomed valleys trending northeast-southwest. These tongues deepen irregularly toward the southwest, sometimes reaching depths as great as 3300 fathoms. Their gradients are irregular and are frequently more than 10 feet per mile. To the west the 2850–2950 plain ends abruptly against a series of mountain ranges which mark the beginning of the Bermuda Rise. To the east, where it meets the foothills of the Mid-Atlantic Ridge, its boundaries are also well defined. The general character of this plain and of its boundaries close to Lat. 31°N. is illustrated by the profiles of Plates 4 and 5.

A similar plain at 2900 fathoms occupies a smaller area in the Northern Canary Basin. It

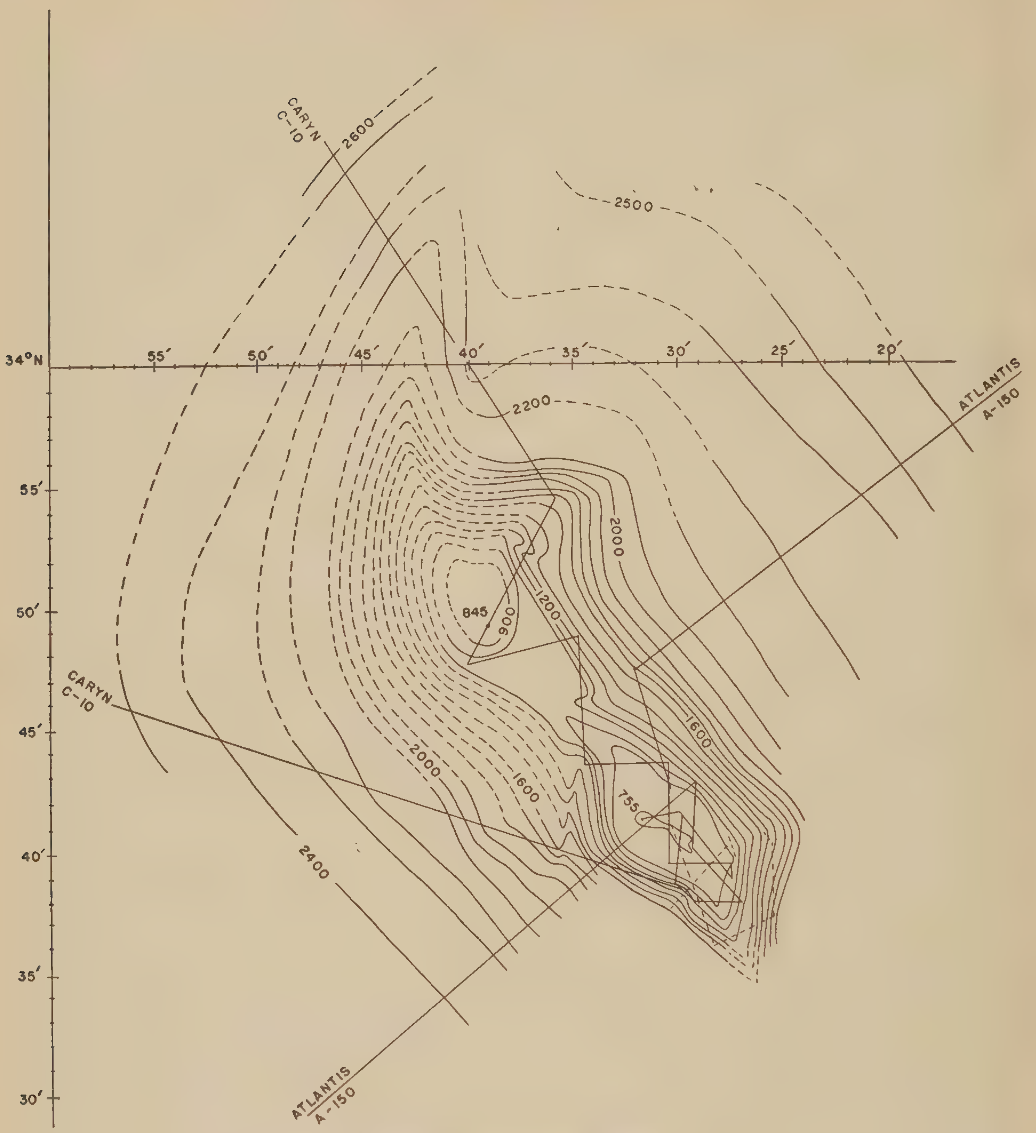
CARYN C-10
2600
2500
34°N
55′
50′
45′
40′
35′
30′
25′
20′
ATLANTIS A-150
2200
55′
2000
50′
845
900
1200
CARYN C-10
45′
1600
2000
1600
755
40′
2400
35′
30′
ATLANTIS A-150

FIGURE 1.—MUIR SEA MOUNT

This is a new version of the sea mount shown by Tolstoy and Ewing (1949, Fig. 2), corrected by means of additional data obtained by the R. V. CARYN of the Woods Hole Oceanographic Institution during the summer of 1949. Contour interval 100 fathoms.

appears to be similarly broken up at its southern extremity into a series of tonguelike valleys deepening quickly but erratically to more than 3000 fathoms. A large gently undulating plain between 2800 and 2880 fathoms occupies the floor of the North American Basin southwest of Bermuda. It slopes gently southeastward.

Rising abruptly from these great gently sloping plains are numerous sea mounts of irregular sizes and shapes. Only a few have ever been investigated in detail. They vary in height from just a few fathoms to well over 9000 feet above the surrounding ocean floor. A particularly conspicuous group of flat-topped sea mounts rises from the 2600–2650 fathom plain, southeast of Cape Cod, to approximately 11,000 feet above the surrounding ocean floor (Pl. 1). They stand out conspicuously in Plate 1. A profile across

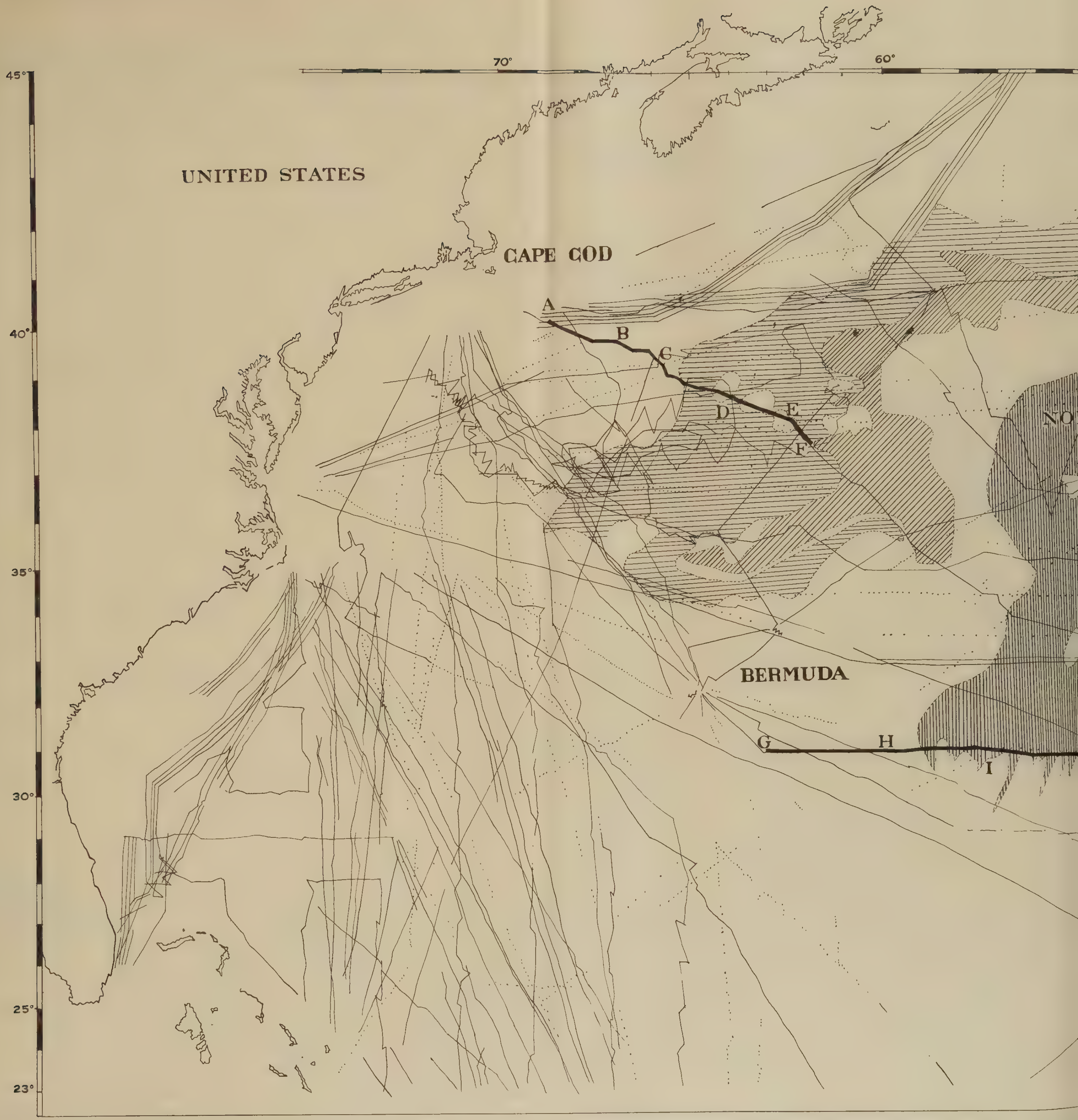
70°
60°
45°
40°
35°
30°
25°
23°
UNITED STATES
CAPE COD
A
B
C
D
E
F
NO
BERMUDA
G
H
I

DISTRIBUTION OF THE MAJOR SUBM

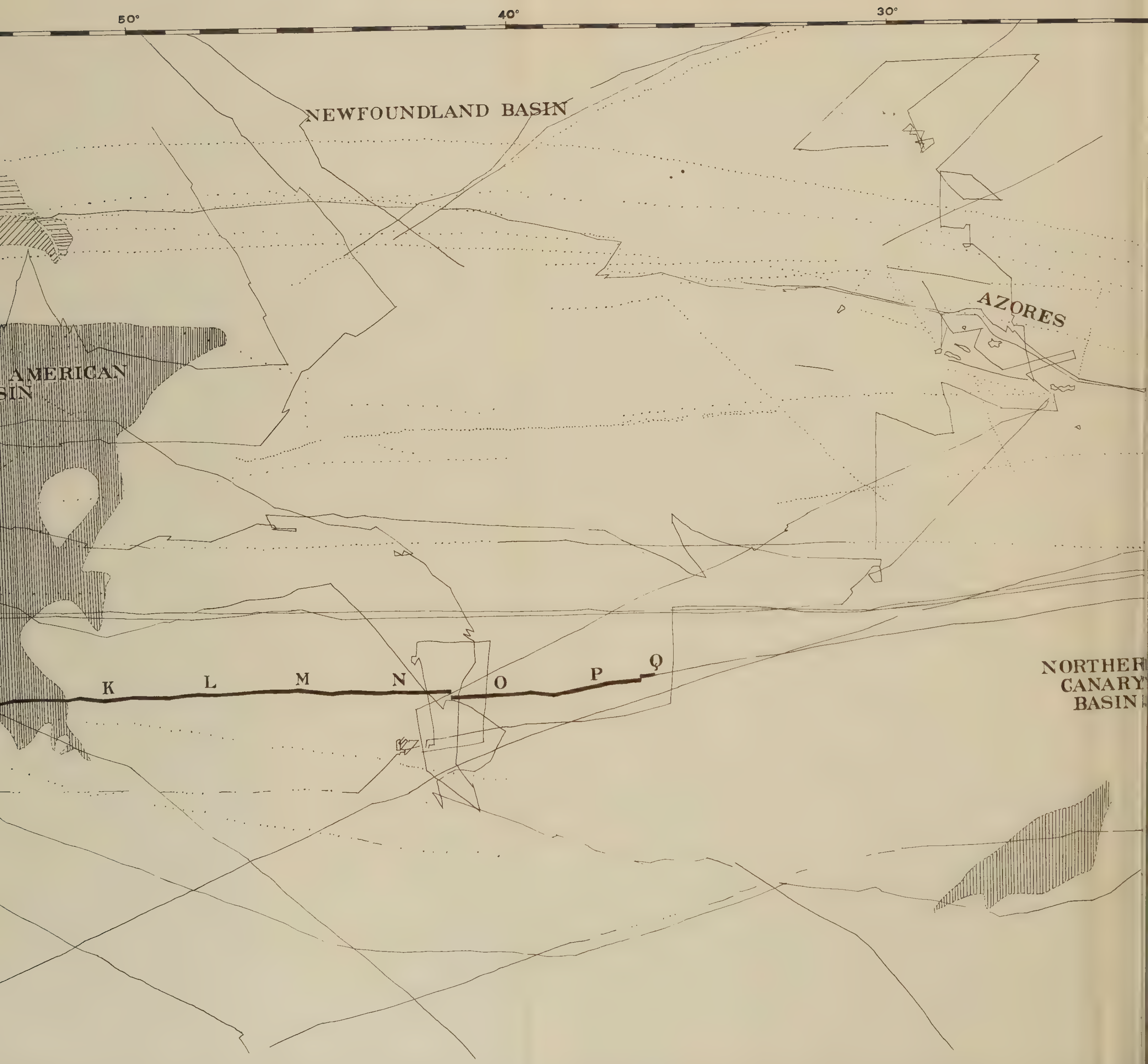
50°
40°
30°
NEWFOUNDLAND BASIN
AZORES
AMERICAN
SIN
K
L
M
N
O
P
Q
NORTHER
CANARY
BASIN

INE PLAINS IN THE SAME AREA, AND SOUNDING LINES USED IN THE DRAFTIN

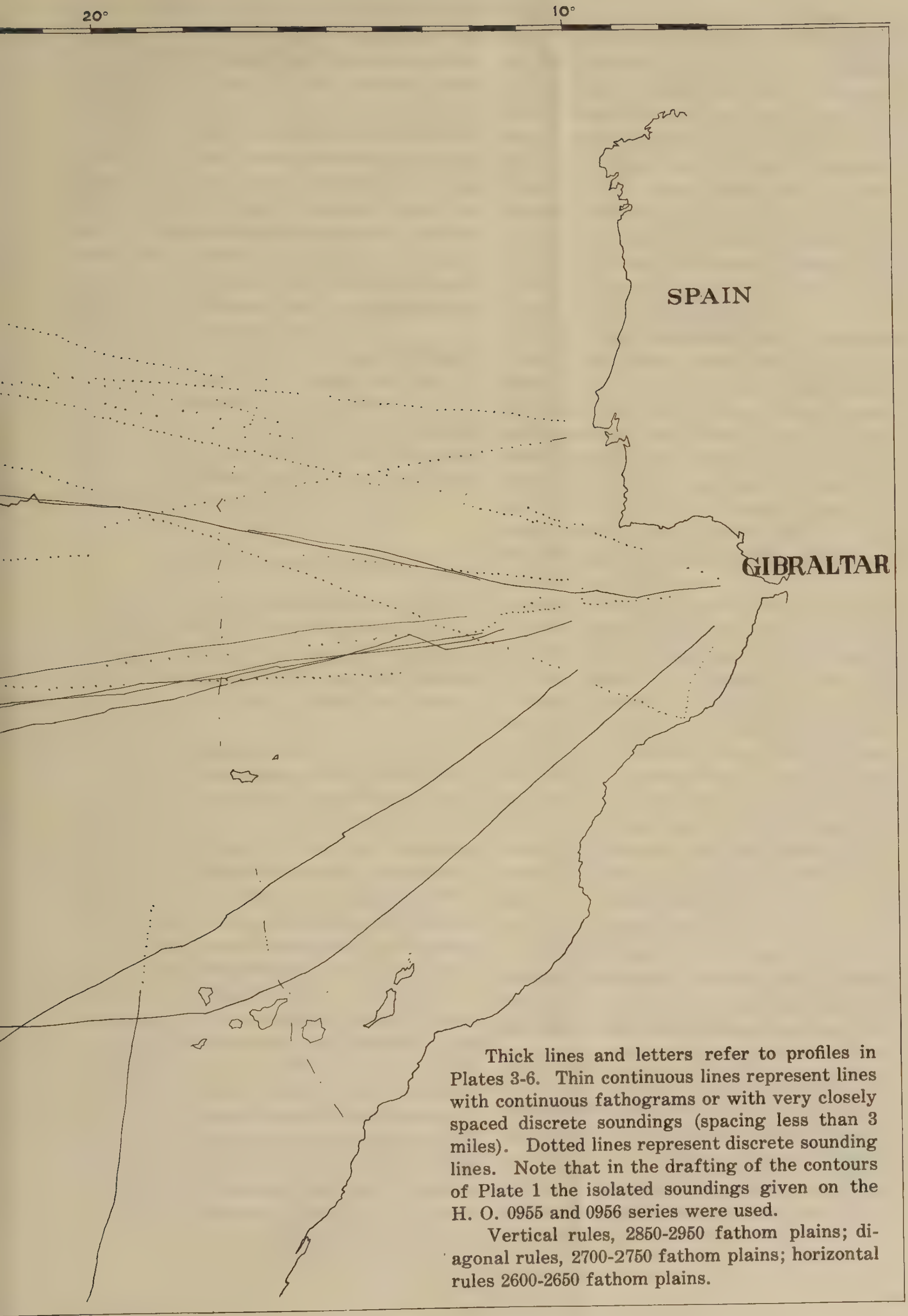

Thick lines and letters refer to profiles in Plates 3-6. Thin continuous lines represent lines with continuous fathograms or with very closely spaced discrete soundings (spacing less than 3 miles). Dotted lines represent discrete sounding lines. Note that in the drafting of the contours of Plate 1 the isolated soundings given on the H. O. 0955 and 0956 series were used.

Vertical rules, 2850-2950 fathom plains; diagonal rules, 2700-2750 fathom plains; horizontal rules 2600-2650 fathom plains.

OF PLATE 1

them is shown in Plate 3. Note that in this profile the vertical and horizontal scales are the same. There is a suggestion of terracing on their flanks, at a depth of approximately 2000 fathoms.

The Caryn Peak, at the mouth of the Hudson Submarine Valley, was investigated in some detail during the summer of 1949 by Ewing, Heezen, Northrop, and the author. Though the results of this investigation have not as yet been worked out in detail, Caryn Peak is a roughly conical peak, 1 mile high and 5 miles wide across its base; it rises abruptly out of the surrounding plain at 2600–2620 fathoms.

The sea mount, roughly 130 miles northeast of Bermuda (Tolstoy and Ewing, 1949, Fig. 2), was further investigated by the R/V CARYN in July 1949. It was named the Muir Sea Mount, in honor of the U.S.S. MUIR, which discovered it in 1945. A slightly revised and fuller map resulted from this investigation (Fig. 1).

THE MID-ATLANTIC RIDGE

The Mid-Atlantic Ridge occupies the central part of the North Atlantic Ocean, from Iceland to a point southwest of the Cape of Good Hope. The highest points of the Ridge rise to form islands such as St. Paul's Rocks, the Azores, and Iceland.

It may be subdivided into:

(1) A high central zone or the Main Range, which is shown on Plate 1 as a series of parallel ridges following the general trend of the Mid-Atlantic Ridge. Many of these ridges rise to less than 800 fathoms below the surface of the ocean. In several locations there are enough sounding lines to establish the pattern and to some extent the characteristics of these ridges, particularly between Lat. 30°N. and 34°N. and Long. 40°W. and 43°W. (Tolstoy and Ewing, 1949, Pl. 7). Plate 6 shows a profile across the Main Range in this area; the vertical and horizontal scales are in the ratio of 3.3/1. There appears to be a marked asymmetry of slope for many of these ridges; the eastward slope is usually the steeper.

(2) An intermediate zone flanking the Main Range to the east and to the west between 1600 and 2500 fathoms south of the Azores is characterized by a succession of levels which for lack of any better term have been called terraces. This zone has been named the Terraced Zone (Pls. 5, 6). There are two types of transition between successive terraces. Some are separated by a step, with no intervening peak, whereas in others there is a peak or hump on the outer edge of the higher terrace. Reflection-shooting studies by Ewing, Press, and others have shown that, while the Main Range itself is almost devoid of sediments, the terraces are characterized by important thicknesses of sediment, of the order of one or several thousand feet. Certainly therefore, these terraces are or have been areas of greater deposition.

(3) An outer mountainous zone, between the 2900-fathom plains of the Northern Canary and North American Basins and the Terraced zone, has peaks that seem to form roughly north-northeast—south-southwest ridges. This Zone resembles neither the Main Range nor the Terraced Zone types of topography and stands out as a distinct physiographic province. Some of its peaks are more than 3000 feet high. For this area the name of Foothills of the Mid-Atlantic Ridge seems appropriate.

Plate 5, a typical profile across the western Foothills, shows a high peak (1700 fathoms) at the boundary between the Foothills and the Terraced Zone. It is flanked by deeps. The western, or outer, deep with respect to the Mid-Atlantic Ridge may be as deep as 3050 fathoms and has a flat bottom. The eastern, or inner, deep is 2550 fathoms deep, has a flat bottom, and marks the beginning of the Terraced Zone. Since we are ignorant of the processes that formed the Terraces and this peculiar type of feature, we cannot say whether it would be consistent to identify this flat stretch at 2550 fathoms as the first terrace.

The whole length of the boundary between the Foothills and the Terraced Zone is characterized by an essentially continuous ridge shoaling many places to appreciably less than 2000 fathoms and flanked by troughs (Pl. 1). The western trough is the deeper; it reaches depths greater than 3000 fathoms in several places, whereas the eastern one is commonly 2500–2600 fathoms deep and in some places less. The continuity of these troughs would be demonstrated best by tracing the 2800- and the 2400-fathom contours.

Outstanding Physiographic Features

The most striking feature is the Mid-Atlantic Ridge itself. In this area its general trend is northeast-southwest south of the Azores and northwest-southeast north of the Azores. It therefore roughly parallels the North American and African coasts. This fact is true of most of the Ridge and has long been pointed out in the literature. Thus Prinz (1891) considered it as evidence in favor of his hypothesis of the differential torsion of the hemispheres, and Wegener (1924) considered that it favored his theory of continental drift.

Close examination of the Ridge indicates that upon this trend are superposed transverse ones. Thus we find the deep trough surveyed by the Atlantis on its first cruise across the Mid-Atlantic Ridge in 1947 (Tolstoy and Ewing, 1949, Pls. 7, 8), which trends east-west along Lat. 30°N. and which has some characteristics of a graben.

The Azores Bulge and its ridges are characterized by predominantly northwest by west—southeast by east trends. Later data obtained by the Atlantis and other vessels have resulted in a corrected version of Wüst's map (Fig. 2). The main control lines are shown in Figure 3. For the isolated soundings utilized, see Wüst's original map (Wüst, 1939). This more up-to-date interpretation shows indications of a north-south trend, practically at right angles to the preceding. This north-south trend would represent the true Mid-Atlantic Ridge trend in this area if we imagined the Azores to be absent and the Mid-Atlantic Ridge as bending around, changing its trend from northeast-southwest south of the Azores to northwest-southeast north of the Azores. The transverse trend would either have been superimposed upon or superimposed by the Mid-Atlantic Ridge trends. This idea is further enhanced by the fact that the transverse trend of the Azores appears to be a local manifestation of a major transatlantic one, beginning at the Grand Banks, crossing the Ridge at the Azores, and going through the Gettysburg and Josephine banks and merging with either the Variscian mountains of western Spain, Portugal, and North West Africa, or the Cenozoic ranges of southern Spain and North West Africa. Since the structure in southern Newfoundland and in the Prince Edward and Cape Breton islands is mostly Acadian and Appalachian, the Grand Banks and indeed this whole transatlantic trend may be Variscian.

The chain of sea mounts extending southeastward from Cape Cod form another transverse trend which can be followed up to the ridge marking the boundary between the Foothills and the Terraced Zone of the Mid-Atlantic Ridge. At Lat. 36°40′ N., Long. 55°W. a sea mount rises more than 200 fathoms above the 2900-fathom plain (Pl. 2). This trend is more continuous therefore than one would infer from a glance at Plate 1, the contour interval of which is such as not to show this sea mount. The highest point yet found on the ridge marking the boundary between the Foothills and the Terraced Zone is in the general area of its intersection with this trend.

The northeast-southwest trend of the ridges and valleys at the southern border of the great 2850–2950-fathom plains in both the North American and Northern Canary basins is interesting and is strikingly illustrated by the 3000-fathom contour (Pl. 1). In the Northern Canary Basin, control is poor, but the picture is believed to be at least qualitatively correct.

Along the southern rim of the 2850–2950-fathom plain in the North American Basin, the control is much better (Pl. 2), particularly in the section immediately adjacent to the Bermuda rise. The first indications of this type of feature may be noted northwest of Bermuda. It becomes much more pronounced southeast of Bermuda. At least as far as Long. 56°W. there is enough control to insure that broad features shown are correct, though of course the perfect continuity of these ridges and valleys may be open to doubt.

The parallel, closely spaced ridges so typical of the Main Range southwest of the Azores are not so pronounced north of these islands. There appears to be in that area more isolated peaks, which could well be volcanic in their origin; the Terraced Zone is no longer as pronounced, and the distinction between the three types of topography not so obvious. However, the number of sounding lines with continuous graphical records crossing this section of the Ridge is small, and there is no means of telling how general this change in character might be.

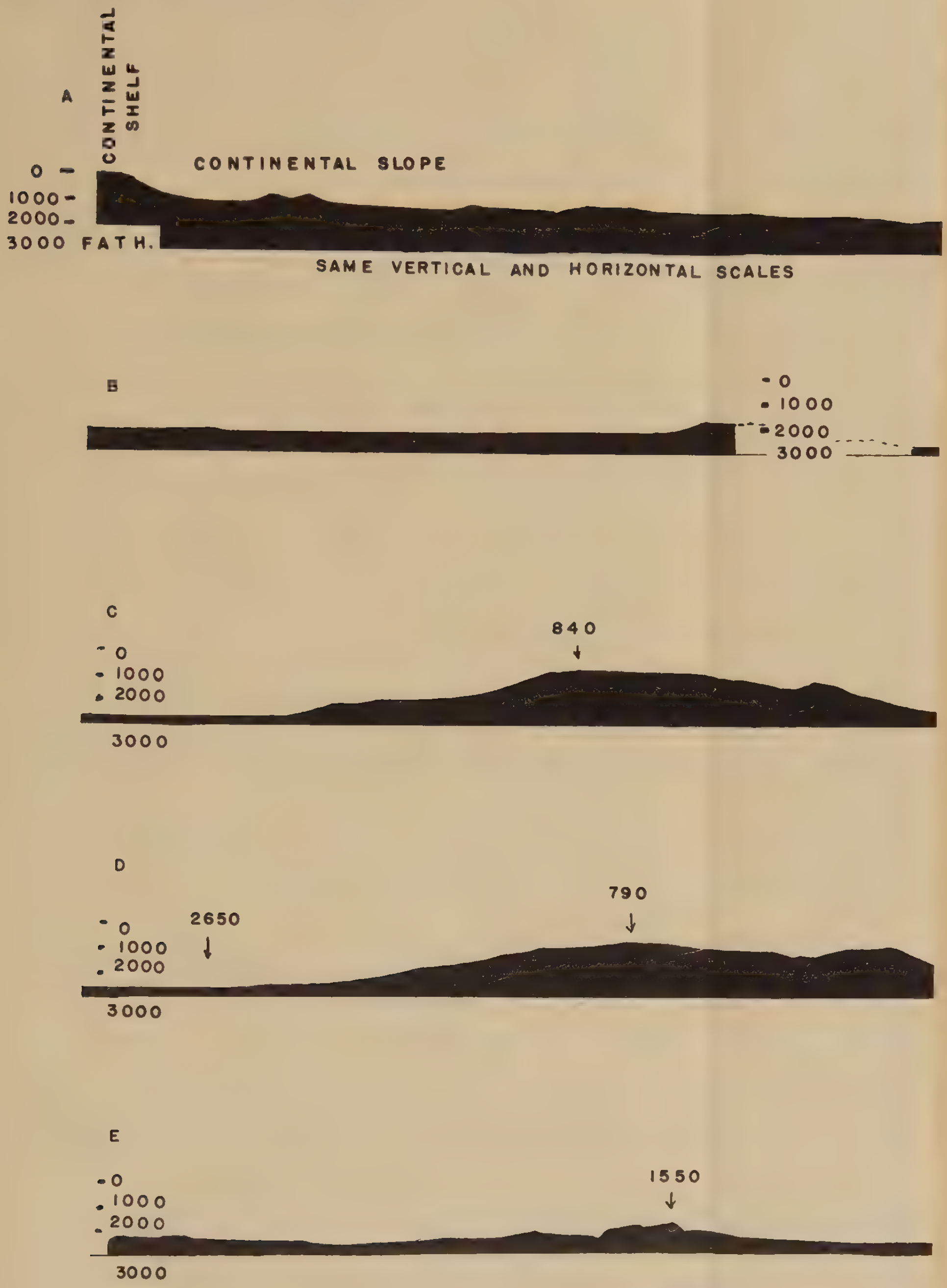
A
CONTINENTAL SHELF
CONTINENTAL SLOPE
0
1000
2000
3000 FATH.
SAME VERTICAL AND HORIZONTAL SCALES
B
0
1000
2000
3000
C
840
0
1000
2000
3000
D
790
2650
0
1000
2000
3000
E
1550
0
1000
2000
3000

PROFILES OF THE SEA MOU

Letters correspond to those in

Tolstoy, Pl. 3

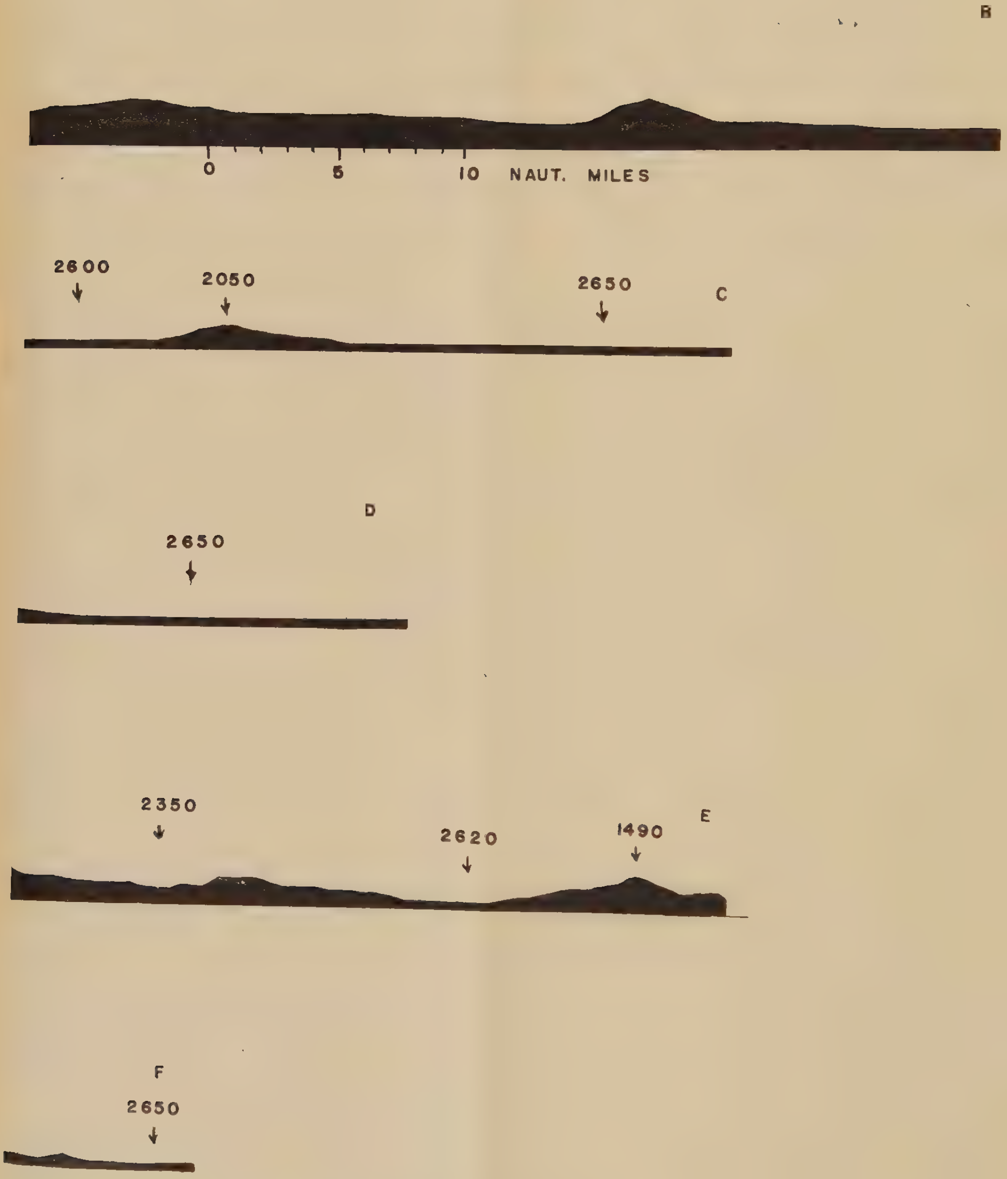

NTS SOUTHEAST OF CAPE COD
Plate 2. No. vertical exaggeration.

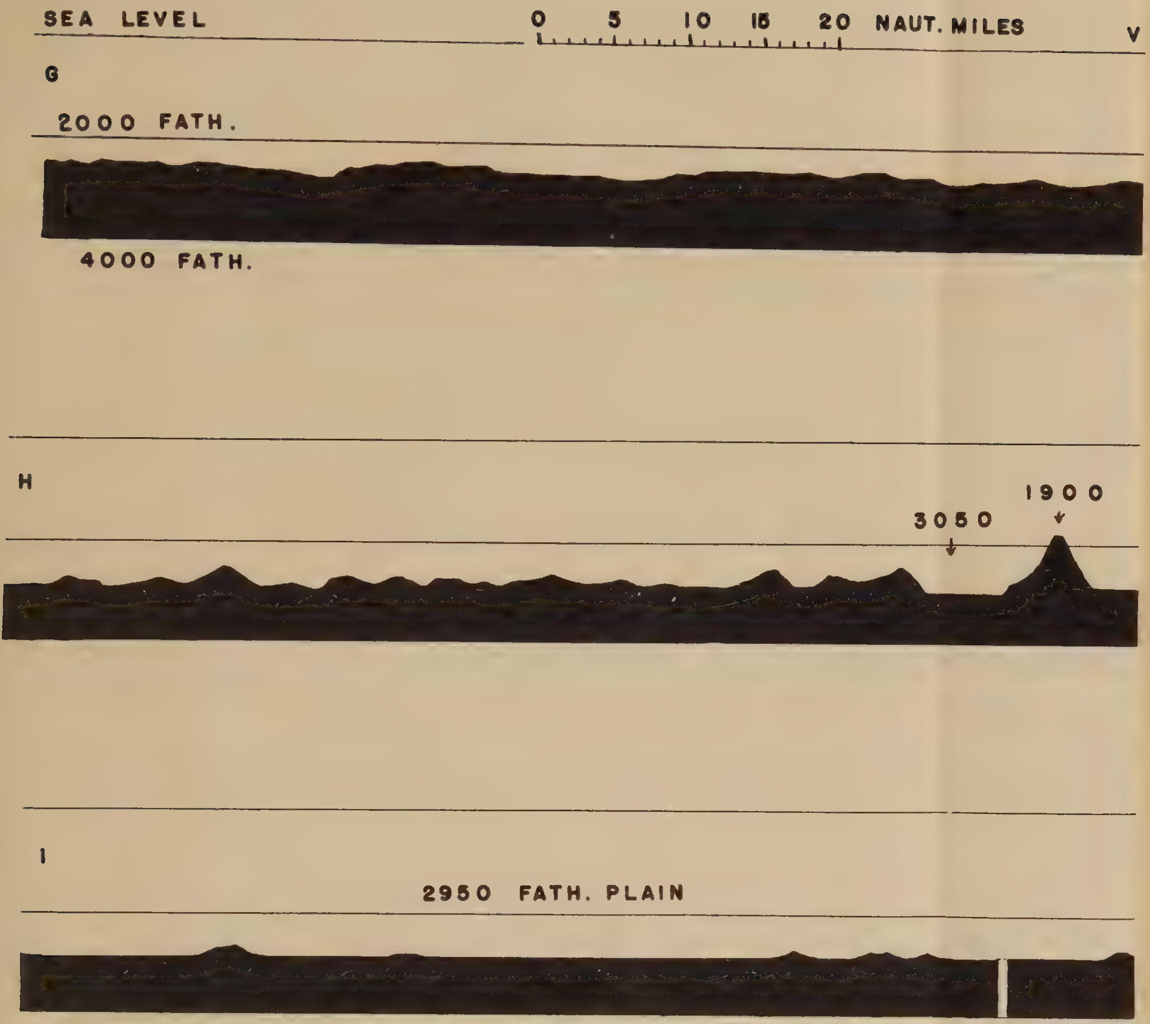

PROFILES OF THE SOUTHEASTERN EDGE OF THE
FATHOM PLAIN, CLOSE TO TH

Letters correspond to those

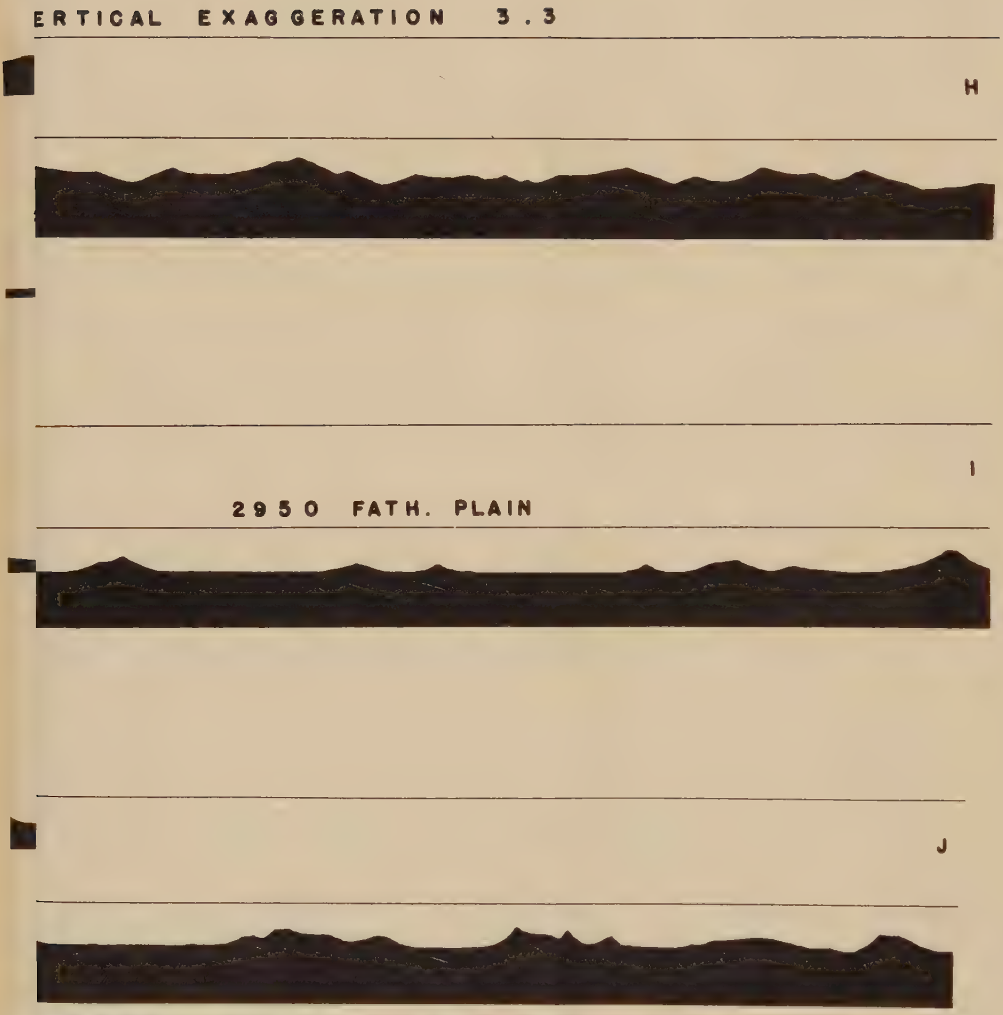

BERMUDA RISE AND OF THE 2850-2950
E 31ST PARRALLEL

n Plate 2.

N'
Pla

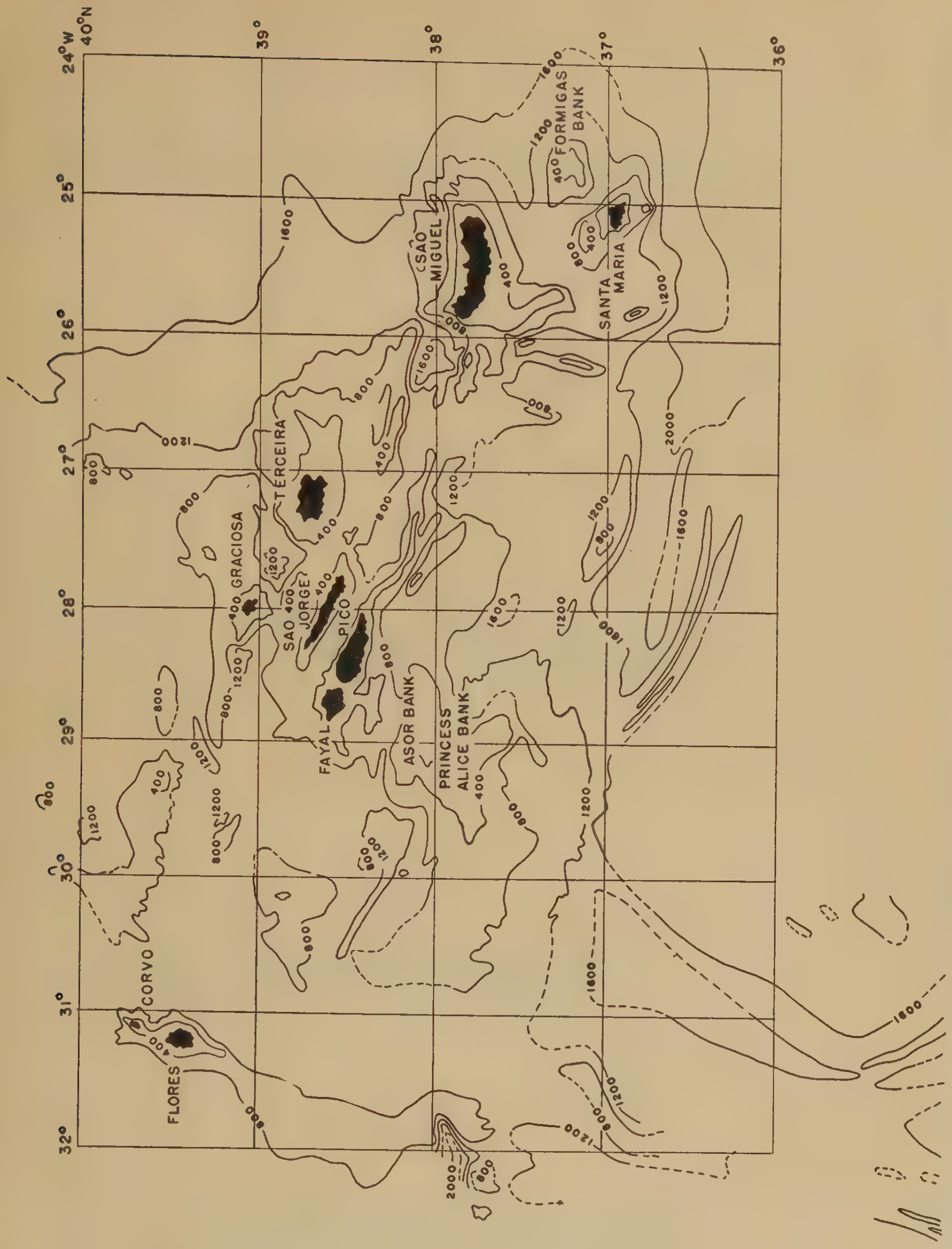
24°W
40°N
39°
38°
37°
36°
25°
26°
27°
28°
29°
30°
31°
32°
CORVO
FLORES
GRACIOSA
TERCEIRA
SAO JORGE
PICO
FAYAL
ASOR BANK
PRINCESS ALICE BANK
SAO MIGUEL
SANTA MARIA
FORMIGAS BANK
400
800
1200
1600
2000

FIGURE 2.—SUBMARINE TOPOGRAPHY OF THE AZORES BULGE

This is a corrected version of Wüst's map, revised in the light of later information. The contour interval is 400 fathoms

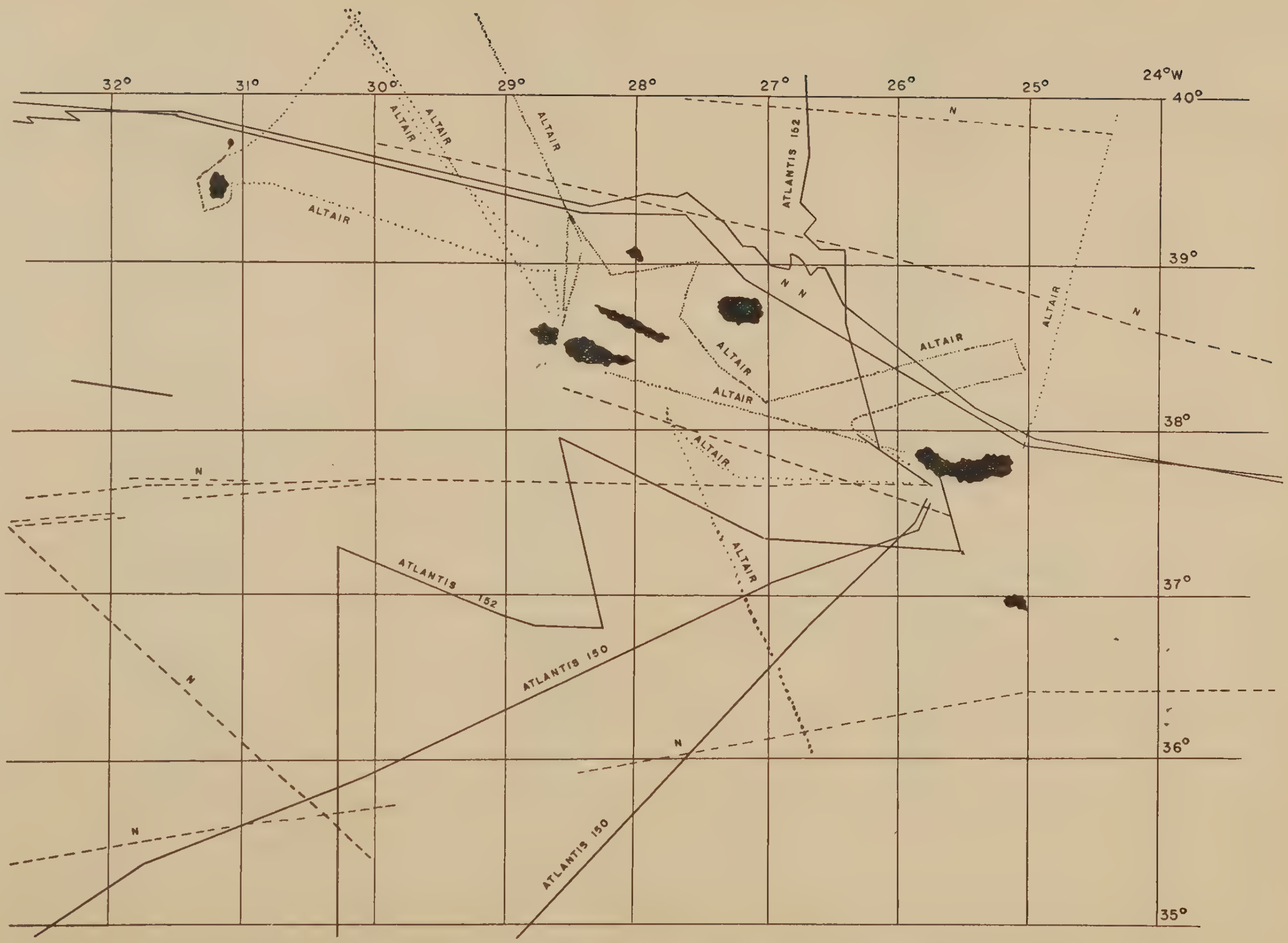
24°W
25°
26°
27°
28°
29°
30°
31°
32°
40°
39°
38°
37°
36°
35°
ALTAIR
ALTAIR
ALTAIR
ALTAIR
ALTAIR
ALTAIR
ALTAIR
ALTAIR
ALTAIR
ATLANTIS 152
ATLANTIS 152
ATLANTIS 150
ATLANTIS 150
N
N
N
N
N
N
N
N

FIGURE 3.—SOUNDING LINES UTILIZED IN THE MAP OF FIGURE 2

Solid black lines indicate tracks with continuous fathograms, four of which were obtained by the ATLANTIS. The principal ALTAIR lines are reproduced. For the isolated soundings utilized in this interpretation, *see* Wüst's original map and local Portuguese charts. Tracks marked N are U. S. Navy Hydrographic Office sounding lines belonging to the series already utilized in a previous paper. Solid black areas are islands (*See* Figure 2.)

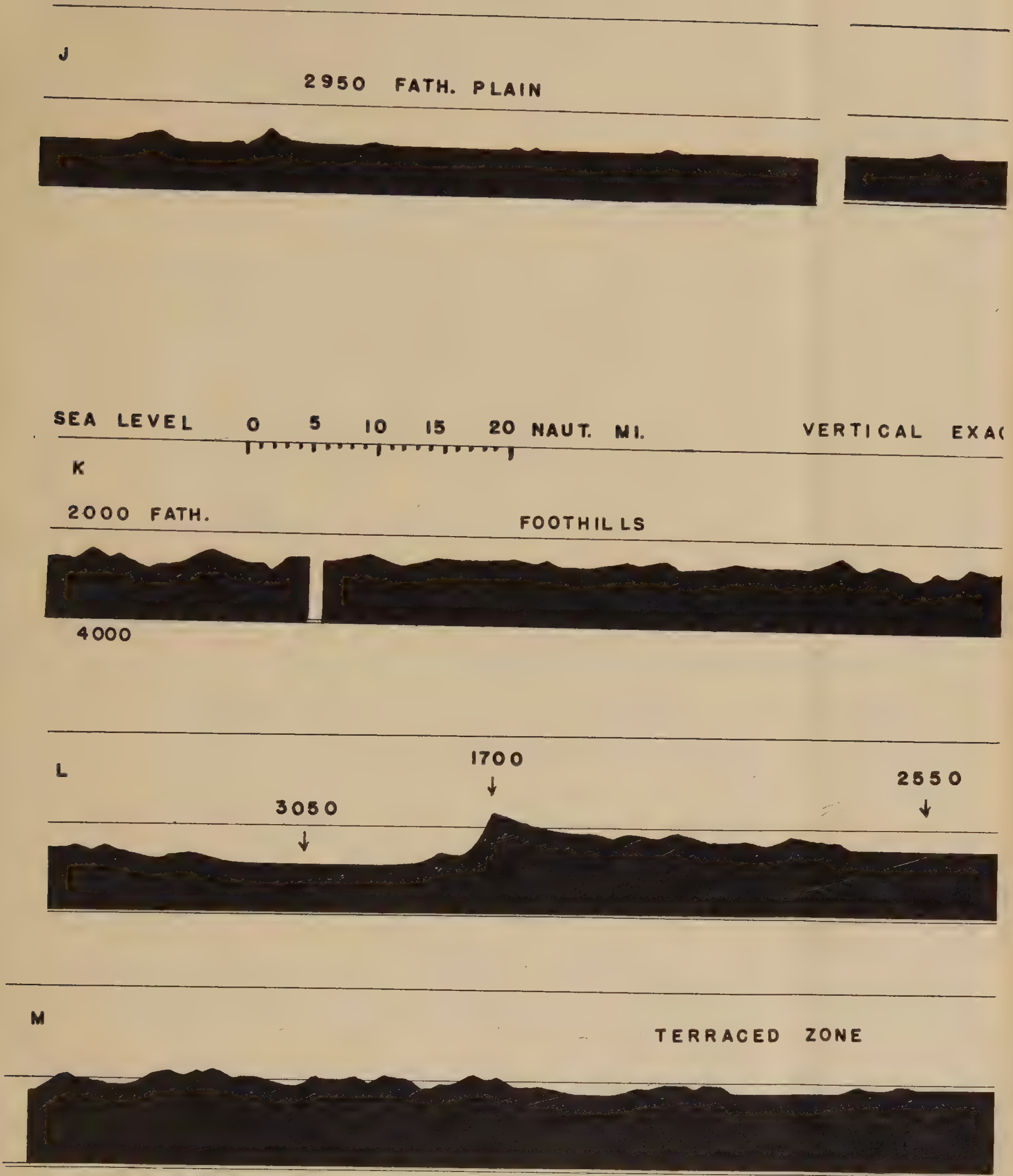

PROFILES ACROSS THE EASTERN EDGE OF TH
PARALLEL, THE WESTERN FOOTHILLS, AND THE TE

Letters correspond to those i

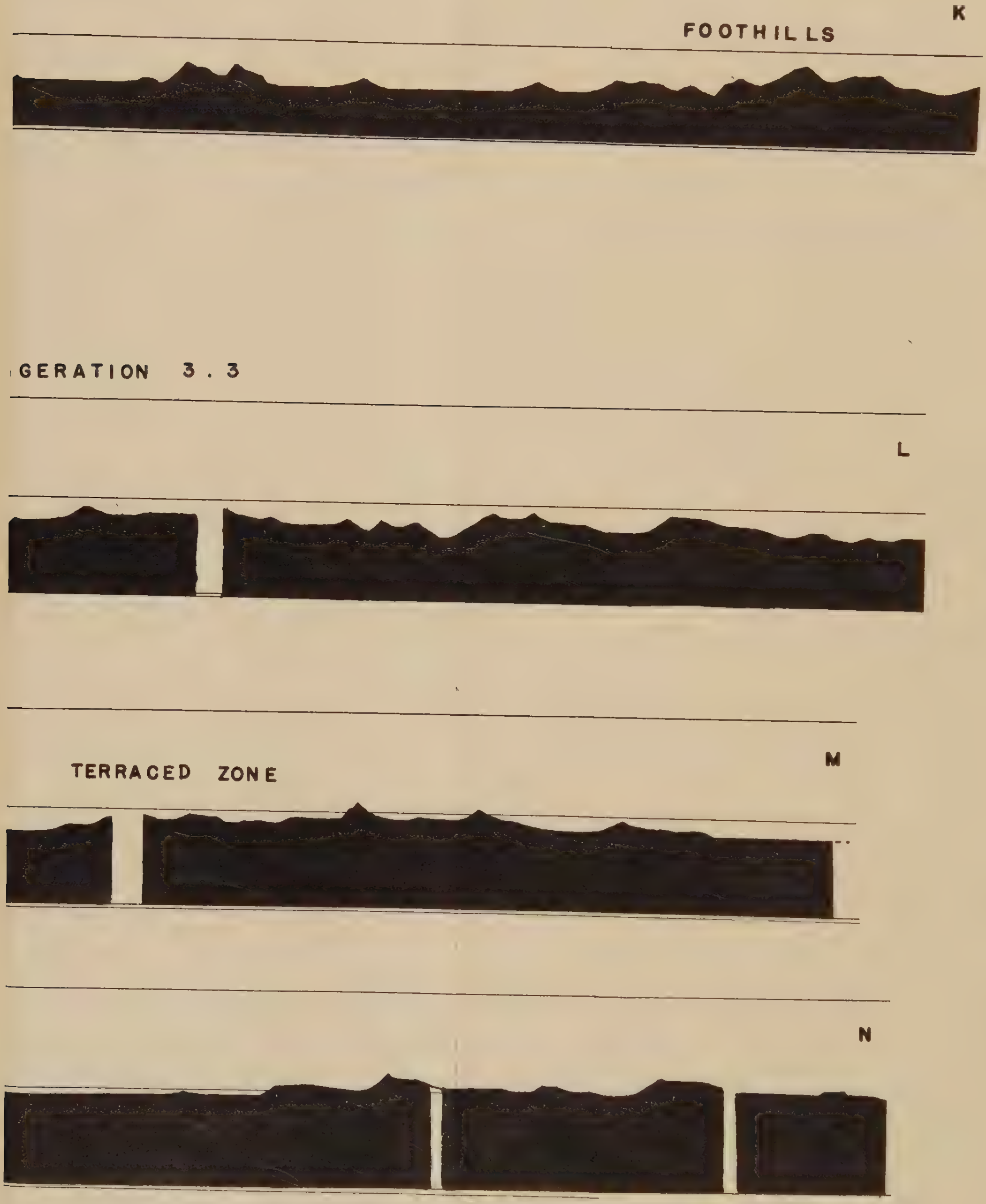

2850-2950 PLAIN CLOSE TO THE 31ST
RRACED ZONE OF THE MID-ATLANTIC RIDGE
Plate 2.

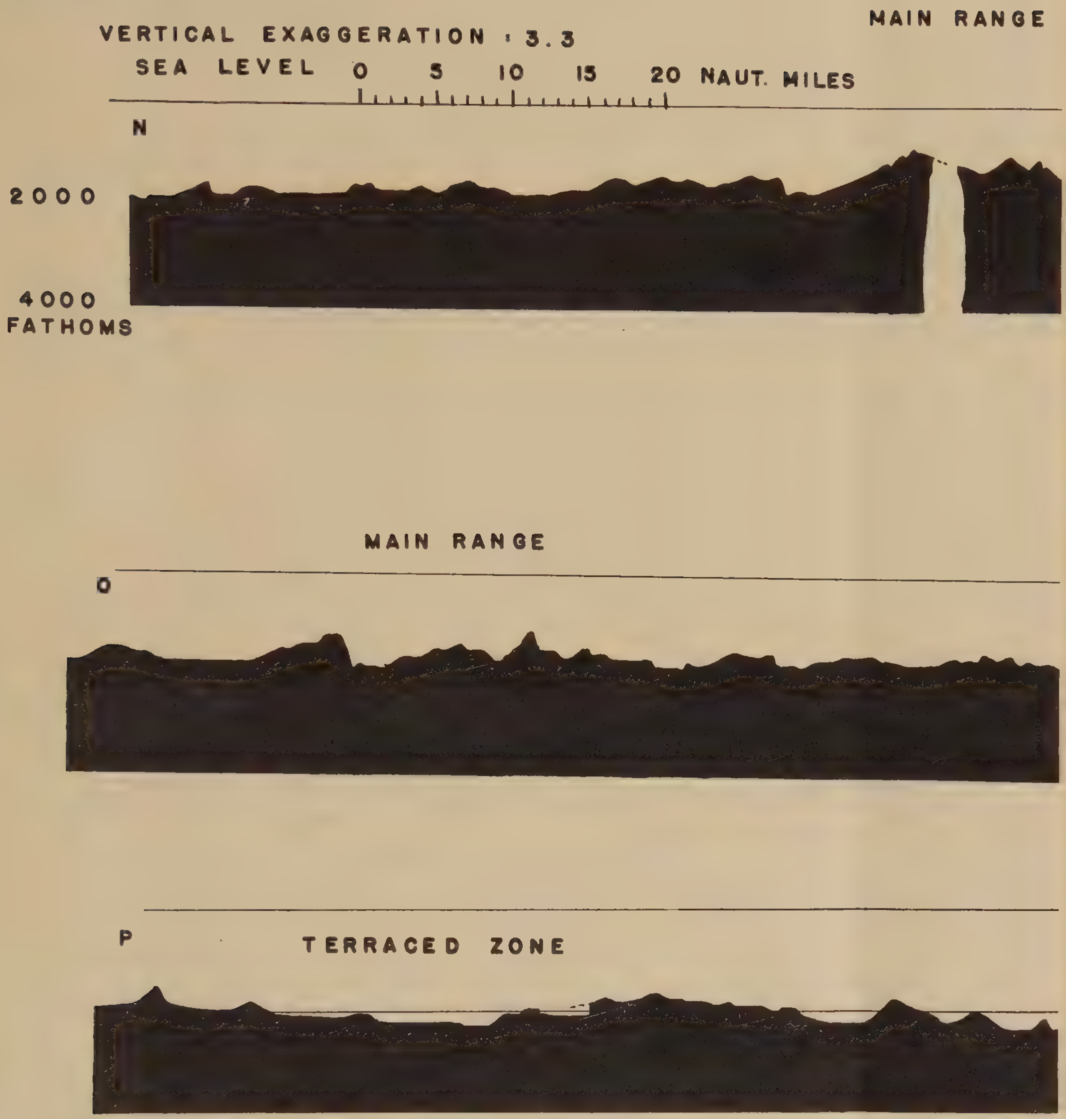

PROFILES ACROSS THE TERRACED ZONE AND T

Letters correspond t

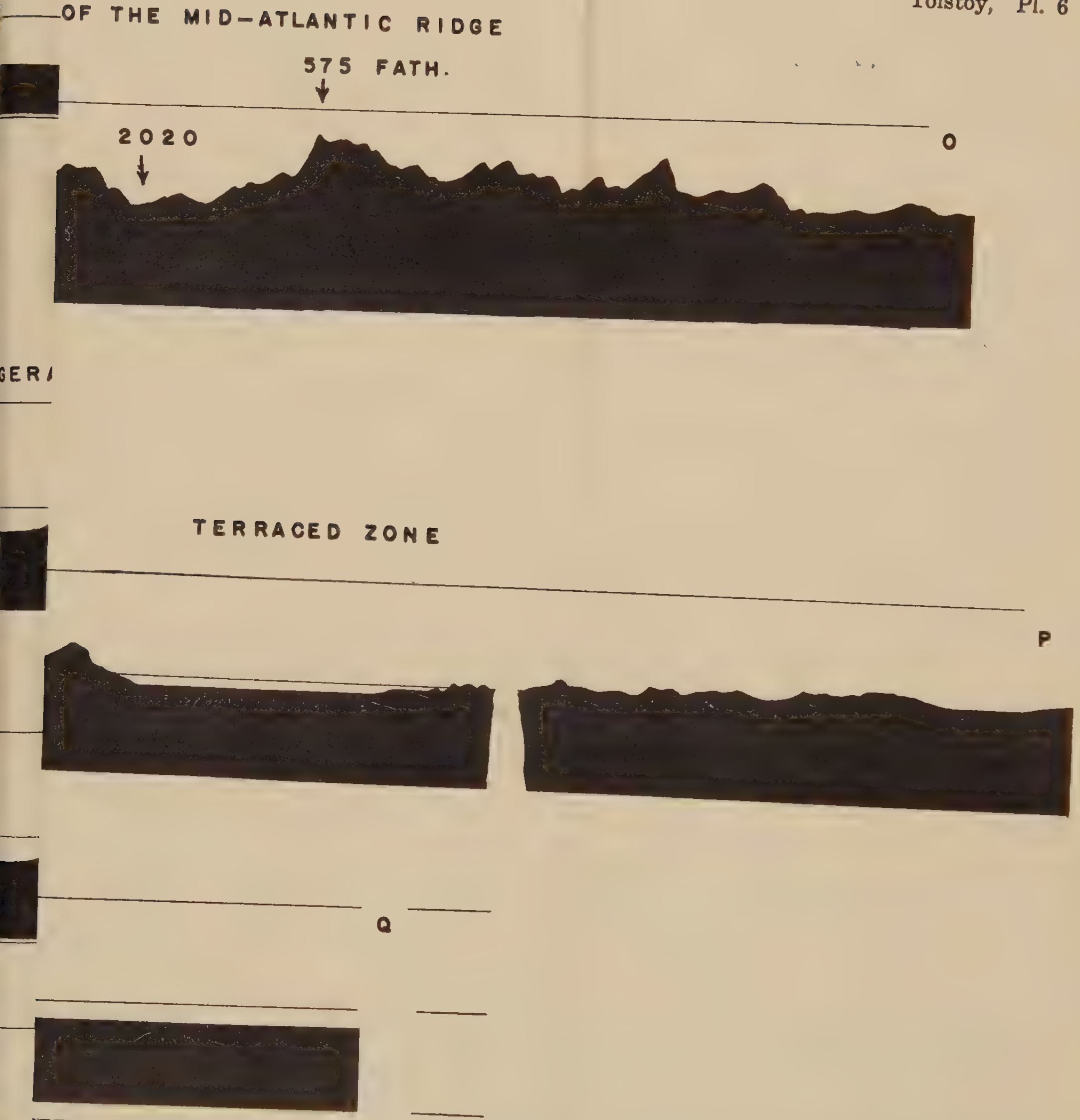
OF THE MID-ATLANTIC RIDGE
575 FATH.
2020
O
GERA
TERRACED ZONE
P
Q

HE MAIN RANGE OF THE MID-ATLANTIC RIDGE
those in Plate 2.

RF
Pl

Finally, there is a striking arcuate submarine mountain range branching out from the Mid-Atlantic Ridge southwest of the Azores which extends through Cruiser Bank. The sea mount described by Tolstoy and Ewing (1949, Fig. 4) which shoals to 180 fathoms is part of this mountain range. One cannot say whether the Great Meteor Bank, 130 miles south-southeast of Cruiser Bank, is part of this range.

Comments on the History and Structure of the Mid-Atlantic Ridge

The question as to whether the Mid-Atlantic Ridge owes its present character to folding or faulting, or to a combination of both, cannot be answered. That there is considerable evidence of fracturing on the Ridge is indisputable. Thus the east-west trough cutting through the Main Range at Lat. 30°N. is almost certainly a fault, probably a graben. That the northwest by west—southeast by east ridges on the Azores Bulge may be due to the outpouring of magma through fissures opened during the doming of a section of the earth's crust, as proposed by Hans Cloos (1939), is quite possible. The central part of Iceland is probably a graben (Hawkes, 1938; 1941).

The structure characterizing the Main Range could have been produced by block faulting. W. H. Bucher pointed out to the author that this type of topography is not essentially different from many fault-controlled mountain ranges on the surface of the earth, such as those of Southern Oregon and of East Africa. However, this type of topography could have been equally well produced by folding. This idea is not in contradiction with any known facts concerning this section of the Mid-Atlantic Ridge, particularly since samples of consolidated sedimentary rock have been brought to the surface by dredging. Of course, it remains to be seen how much of the Mid-Atlantic Ridge is actually composed of such rocks. Furthermore, if the structure of the Azores Bulge owes its present character to the superposition of two separate structural processes, the mechanism of the formation of northwest by west—southeast by east ridges as proposed by Hans Cloos might have to be revised.

At least this much may be said of the area of the Azores: it is not characterized by typical Mid-Atlantic Ridge type of structure, but probably owes its present character to the combined effect of at least two major structural events, and therefore does not constitute a typical "outcrop" of the Mid-Atlantic Ridge. Whatever may be said of the structural history of this area does not therefore necessarily apply to the rest of the Ridge. Unfortunately the same may be said to a certain extent of Iceland, where the structure is governed by block faulting accompanied by huge outpourings of basalt. It is also situated at the intersection of the Mid-Atlantic Ridge with a transverse trend, sometimes interpreted as Caledonian. The major faults bounding the central Icelandic graben strike roughly northeast-southwest— *i.e.*, parallel to the Mid-Atlantic Ridge southwest of Iceland.

There is a rough and admittedly unsatisfactorily established synchronization between the periods of major volcanic activity in Iceland and in the Azores which can perhaps help us estimate the times at which major structural upheavals may have occurred in the history of the Mid-Atlantic Ridge. Hawkes has shown that the major outpourings of basalt in Iceland (the so-called Thulean basalts) must have occurred in pre-Miocene time. Agostinho (1936) on the other hand believes there is evidence of a pre-Miocene period of volcanic activity in the Azores. Also in both Iceland and the Azores there has been considerable post-Miocene and recent volcanic activity.

There are thus two major periods of activity evident in the history of the Azores and Iceland. One of these would be late Tertiary to recent, the other middle or early Tertiary. This suggests that the origin of the Ridge might be associated with the Alpine orogenies. This idea is supported also by the relatively high degree of seismicity along the Ridge, which is comparable to that of many sections of Gutenberg's Alpide Zone. Gutenberg and Richter (1949) have even tentatively suggested that the Mid-Atlantic Ridge may be a belt of Tertiary folds, the high degree of seismicity of which would be due to block faulting following a redistribution of tectonic forces.

Furthermore, the processes that produced the Mid-Atlantic Ridge may have been superimposed upon older transverse trends, possibly Paleozoic, resulting in the opening up of fractures through which huge masses of lava were extruded. At these points one notes a higher degree of seismicity.

REFERENCES CITED

Agostinho, J. (1936) *Volcanoes of the Azores*, Bull. Volcanologique, Organe de l'Assoc. de Volcanologie de l'Un. Geodes. Geophys. Inter., p. 123–138.

Cloos, H. (1939) *Hebung-Spaltung-Volcanismus*, Geol. Rundschau, vol. 30, Zwischenheft 4A, p. 506–510.

Gutenberg, B., and Richter, C. R. (1949) *Seismicity of the Earth*, Princeton Univ. Press.

Hawkes, L. (1938) *The age of the rocks and topography of middle northern Iceland (Tertiary and Quaternary)*, Geol. Mag., No. 889, vol. 75, no. 7, p. 289–296.

—— (1941) *Icelandic tectonics—graben or horst?* Geol. Mag., vol. 78, no. 4, p. 305–308.

Hull, E. (1912) *Sub-Oceanic physiography of North Atlantic Ocean*, Edward Stanford, London.

Maurer, M., and Stocks, Th. (1933) *Die Echolotungen des Meteor*, Wiss. Ergebn. Deutsch Atlant. Exped. Meteor, 1925–1927, Bd. II, Beil 4–32.

Prinz, W. (1891) *Surl les similitudes que presentent les cartes terrestres et planetaires*, Annuaire de l'Obs. R. de Bruxelles, p. 304.

Spencer, J. W. (1903) *Submarine valleys off the American coast and in the North Atlantic*, Geol. Soc. Am., Bull., vol. 14, p. 207–226.

Tolstoy, I., and Ewing, W. M. (1949) *North Atlantic hydrography and the Mid-Atlantic Ridge*, Geol. Soc. Am., Bull., vol. 60, p. 1527–1540.

Veatch, A. C., and Smith, P. A. (1939) *Atlantic submarine valleys off the United States*, Geol. Soc. Am., Spec. Paper 7, p. 63–69.

Wegener, A. (1924) *The origin of the continents and the oceans*. Translated from the third German editions of 1922 by J. G. A. Skerl.

Wüst, G. (1939) *Das submarine Relief bei den Azoren*, Abh. Preuss. Akad. Wiss. Phys., Math. Kl., Jahrg., no. 5, p. 46–58, map 1:3,000,000, Fig. 4, p. 52.

LAMONT GEOLOGICAL OBSERVATORY (COLUMBIA UNIVERSITY), PALISADES, NEW YORK.

MANUSCRIPT RECEIVED BY THE SECRETARY OF THE SOCIETY, DECEMBER 12, 1949.

LAMONT GEOLOGICAL OBSERVATORY CONTRIBUTION NO. 19.

CONTRIBUTION NO. 559, THE WOODS HOLE OCEANOGRAPHIC INSTITUTION.

Contribution Number 559

Contribution No. 560

Reprinted from
Bulletin of Marine Science of the Gulf and Caribbean
Vol. 1, No. 1, pp. 1-14
MARCH 1951

The Seasonal Distribution of Oceanic Birds in the Western North Atlantic[1]

Hilary B. Moore
Woods Hole Oceanographic Institution and
University of Miami Marine Laboratory

For a number of years a log has been kept on the Woods Hole Oceanographic Institution vessel *Atlantis* of all birds seen at sea. This recording, which was initiated by Dr. A. C. Redfield, has largely been carried out by Chief Engineer Harold Backus, but a considerable body of data has also been contributed by Dr. Redfield, Alfred H. Woodcock, Dean F. Bumpus, Frank J. Mather III and others. A similar record has been kept by the author for the Bermuda area and during several North Atlantic transects, and some of this has already been published (Moore 1941). Dr. E. F. Thompson and Miss K. S. Russell assisted with these. Redfield (1941) has published those of his observations which were relevant to the Gulf of Maine.

The literature has been so well covered by Wynne-Edwards (1935) and Murphy (1936) that there is no need to refer to it in detail; it is sufficient to quote from their summaries. They make it plain that at present we know only the broad outlines of the migration routes and seasons for oceanic birds, and that more observations are urgently needed. The present paper covers only a small portion of the North Atlantic, but the fairly considerable body of data affords the opportunity for a more detailed analysis of seasonal distribution than has previously been possible. In order to utilize as much as possible of the data, certain restrictions have had to be made. While some of the records specify numbers of birds seen per hour of observation, others give only numbers per day, so it has been necessary to reduce them all to the latter basis. We have also restricted the paper to include only the area for which there is adequate coverage at all seasons. The logs include also some data from more extended cruises, and many observations on littoral birds such as gulls and on migrant land birds encountered at sea.

---

[1] Contribution No. 560 from Woods Hole Oceanographic Institution.
Contribution No. 48 from Marine Laboratory, University of Miami.

The fact that the records have been made by different observers presents a difficulty. All were reasonably well acquainted with the birds in question, but we are dealing almost entirely with sight records, and some errors must be assumed to have occurred. Where the identifications may be in doubt, this is discussed under the section on species in question. Observations were not made continuously all day, but any birds sighted by others were usually reported to the person keeping the records. Somewhat lower population figures may therefore be expected than those obtained from continuous observations such as Wynne-Edwards made, but the overall picture of distributions is not likely to be false. Where a flock of birds such as petrels has followed the ship throughout the day and been logged a number of times, the largest number logged has been taken as the total for the day. While this may be too low, it avoids multiple recording of the same birds.

The author was responsible for only a small fraction of the observations, and wishes to acknowledge the much greater share of credit due to those who have been collecting them for so many years. Thanks are also due to Dr. Redfield, Mr. Bumpus and others who have assisted with the preparation of the paper. The original logs are filed at the Woods Hole Oceanographic Institution.

The data are given on the accompanying maps as numbers of each species seen per day. For the shearwaters and petrels the information has been grouped as a monthly average for each five-degree square, and the number of days on which observations were made is indicated. For the less frequent records of phalaropes and jaegers, total numbers recorded for each month are shown, and these are grouped in two periods covering the spring and fall migrations respectively. Reference to Figures 1 and 2 will show the number of days of observations. Seasonal coverage is not complete in the southern part of the area, but fortunately it is adequate for the winter and spring when the northbound migrants are most likely to be found there. The grouping of the data by months will result in some masking of the exact dates of the advancing waves of migration, but this would have occurred anyhow as a result of our grouping together data from many different years. For simplicity, the number of days of observation are shown only in Figures 1 and 2, but the same values are applicable for all species.

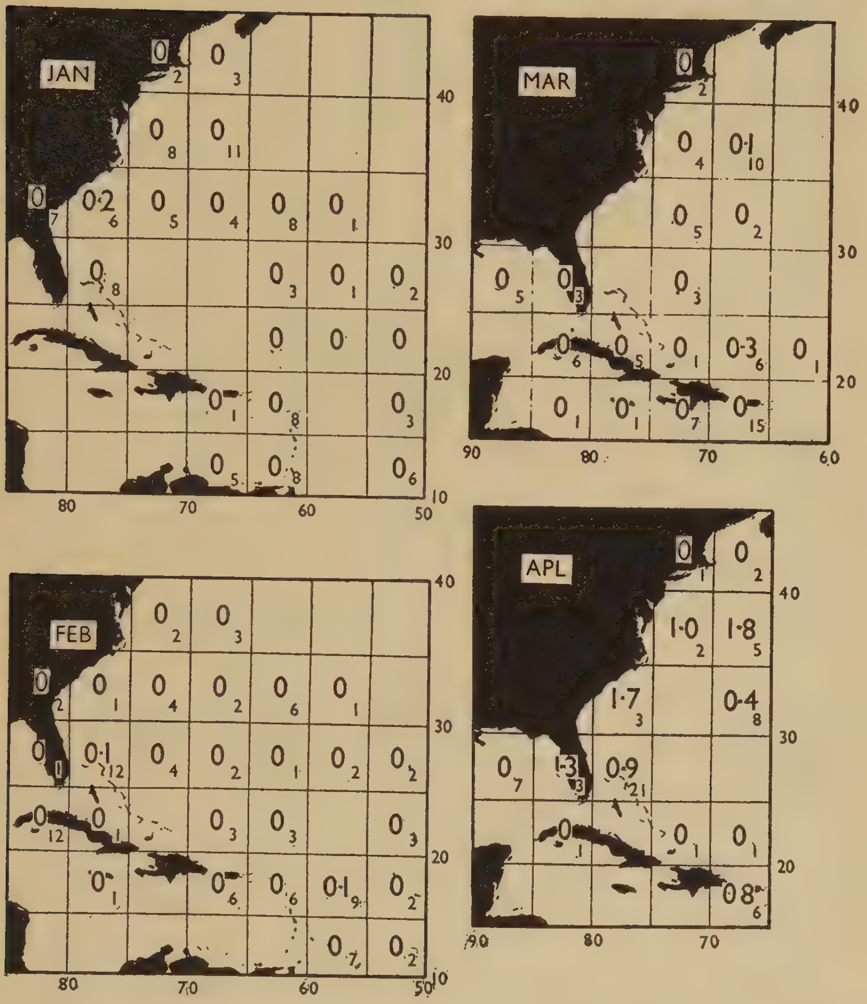
JAN
0 2
0 3
0 8
0 11
0 7
0·2 6
0 5
0 4
0 8
0 1
0 8
0 3
0 1
0 2
0
0
0
0 1
0 8
0 3
0 5
0 8
0 6
40
30
20
10
80
70
60
50
MAR
0 2
0 4
0·1 10
0 5
0 2
0 5
0 3
0 3
0 6
0 5
0 1
0·3 6
0 1
0 1
0 1
0 7
0 15
40
30
20
90
80
70
60
FEB
0 2
0 3
0 2
0 1
0 4
0 2
0 6
0 1
0 1
0·1 12
0 4
0 2
0 1
0 2
0 2
0 12
0 1
0 3
0 3
0 3
0 1
0 6
0 6
0·1 9
0 2
0 7
0 2
40
30
20
10
80
70
60
50
APL
0 1
0 2
1·0 2
1·8 5
1·7 3
0·4 8
0 7
1·3 3
0·9 21
0 1
0 1
0 1
0·8 6
40
30
20
90
80
70

FIGURE 1

FIGURES 1 & 2. Wilson's Petrel. Average numbers seen per day in each five-degree square. The suffixes indicate the number of days of observation in that square during the month (*i.e.*, 1.7_{10} indicates a total of 17 birds seen in 10 days, or an average of 1.7 per day). No observations are available for the blank squares.

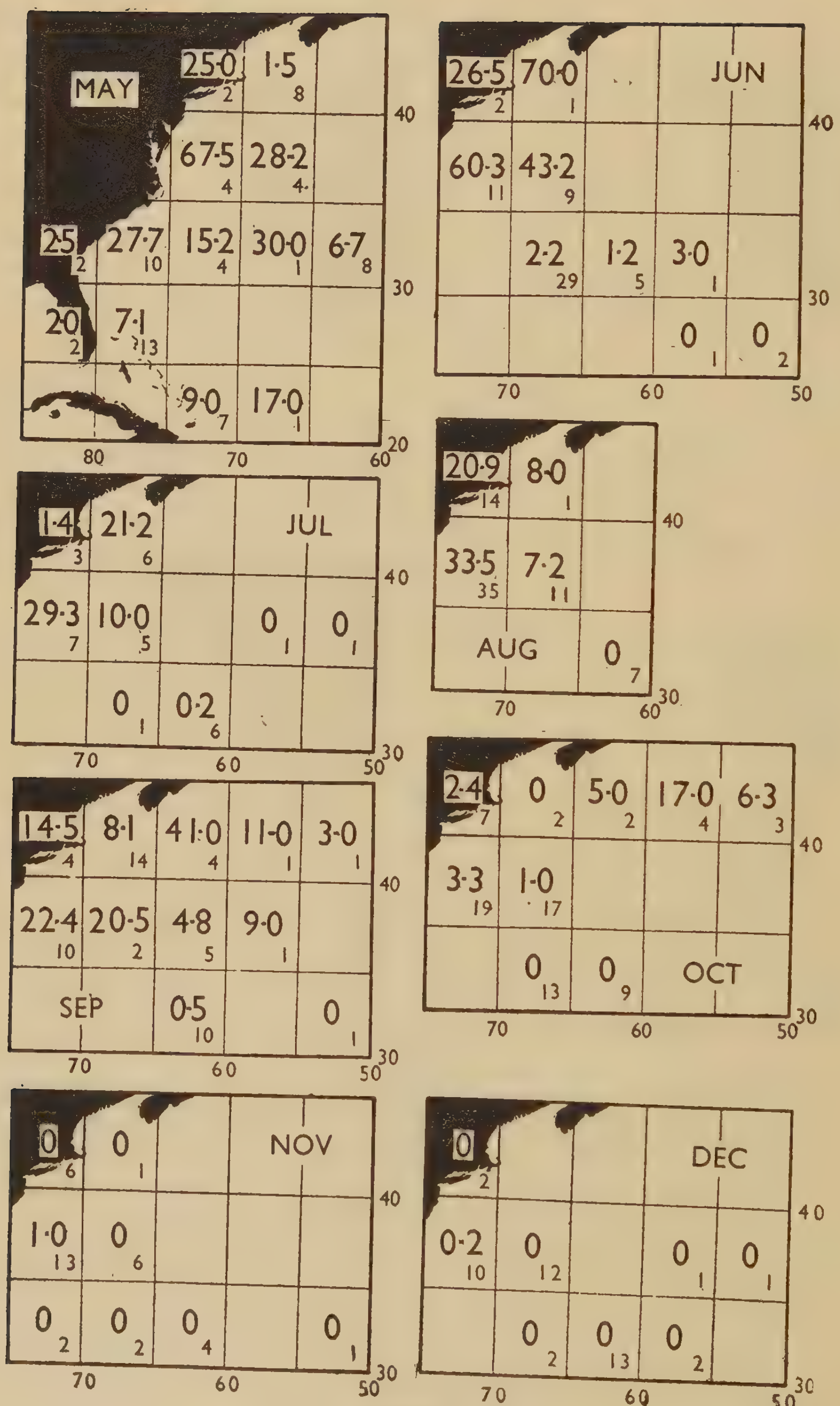
MAY
25·0
2
1·5
8
67·5
4
28·2
4
2·5
2
27·7
10
15·2
4
30·0
1
6·7
8
2·0
2
7·1
13
9·0
7
17·0
1
40
30
20
80
70
60
JUN
26·5
2
70·0
1
60·3
11
43·2
9
2·2
29
1·2
5
3·0
1
0
1
0
2
40
30
70
60
50
JUL
1·4
3
21·2
6
29·3
7
10·0
5
0
1
0
1
0
1
0·2
6
40
30
70
60
50
AUG
20·9
14
8·0
1
33·5
35
7·2
11
0
7
40
30
70
60
SEP
14·5
4
8·1
14
41·0
4
11·0
1
3·0
1
22·4
10
20·5
2
4·8
5
9·0
1
0·5
10
0
1
40
30
70
60
50
OCT
2·4
7
0
2
5·0
2
17·0
4
6·3
3
3·3
19
1·0
17
0
13
0
9
40
30
70
60
50
NOV
0
6
0
1
1·0
13
0
6
0
2
0
2
0
4
0
1
40
30
70
60
50
DEC
0
2
0·2
10
0
12
0
1
0
1
0
2
0
13
0
2
40
30
70
60
50

Figure 2

WILSON'S PETREL, *Oceanites oceanicus* (Kuhl). Figs. 1 and 2.

Wilson's petrel breeds in the Antarctic, arriving at the breeding grounds in November (Murphy 1936). Wynne-Edwards (1935) states that there are North Atlantic records for all months except February, and that there would appear to be a considerable non-breeding population of immature birds. Our records from December to March are so few that the birds may be said to be virtually absent from the area, although there are single records for all months. The few storm petrels seen in these months were probably Wilson's, but there is some room for doubts in the identification. Wynne-Edwards shows that they appear in the Sargasso Sea in increasing numbers throughout April, and along the North American coast in the later half of that month. He also points out their greater concentration along the Gulf Stream than elsewhere in the open ocean. Our records show them in small numbers in April along the east coast and just inside the Gulf of Mexico. Redfield (1941), whose results are incorporated with ours, found them absent at that time from the Gulf of Maine. Maximum numbers for the area as a whole were attained in May, and there was a definite concentration in and near the Gulf Stream, although they were still abundant further seawards. Numbers were about the same in June, but the concentration had moved north and shorewards, and there was a decrease in the Bermuda area. In the Gulf of Maine, numbers were small in May, and maximum from June to September. For the area as a whole, numbers dropped somewhat in July, August and September, and in the latter month there was indication of decreasing numbers along the coast and a spread seawards to the north-east along the line of the Gulf Stream. By October there was a marked drop in numbers, and the main concentration was along the line of the Gulf Stream at about 55° to 60° N., and by November practically all birds had left the area.

LEACH'S PETREL, *Oceanodroma leucorrhoa* (Viellot). Figs. 3 and 4.

Definite identifications as Leach's petrel may be taken as correct, but it may be that some of the records of Wilson's petrels should have been referred to this species. Even allowing for this possibilty, there is no doubt that Leach's is much the rarer species in the area. Redfield found not more than one to twenty or thirty Wilson's petrels in the Gulf of Maine.

Leach's petrel nests in the northern part of the area, and according to Wynne-Edwards and Murphy is more or less restricted during the

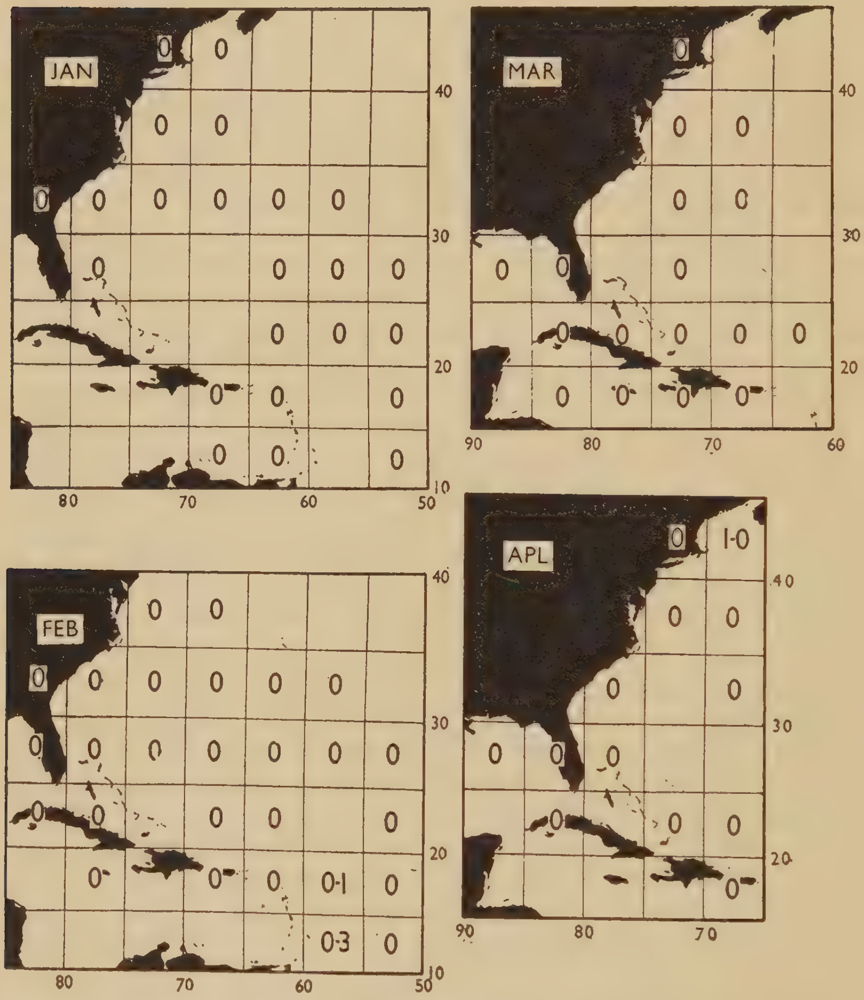
JAN
MAR
FEB
APL
1·0
0·1
0·3
40
30
20
10
90
80
70
60
50

FIGURE 3

FIGURES 3 & 4, Leach's Petrel. For details, see Figures 1 & 2. The suffixes are omitted, but would be the same.

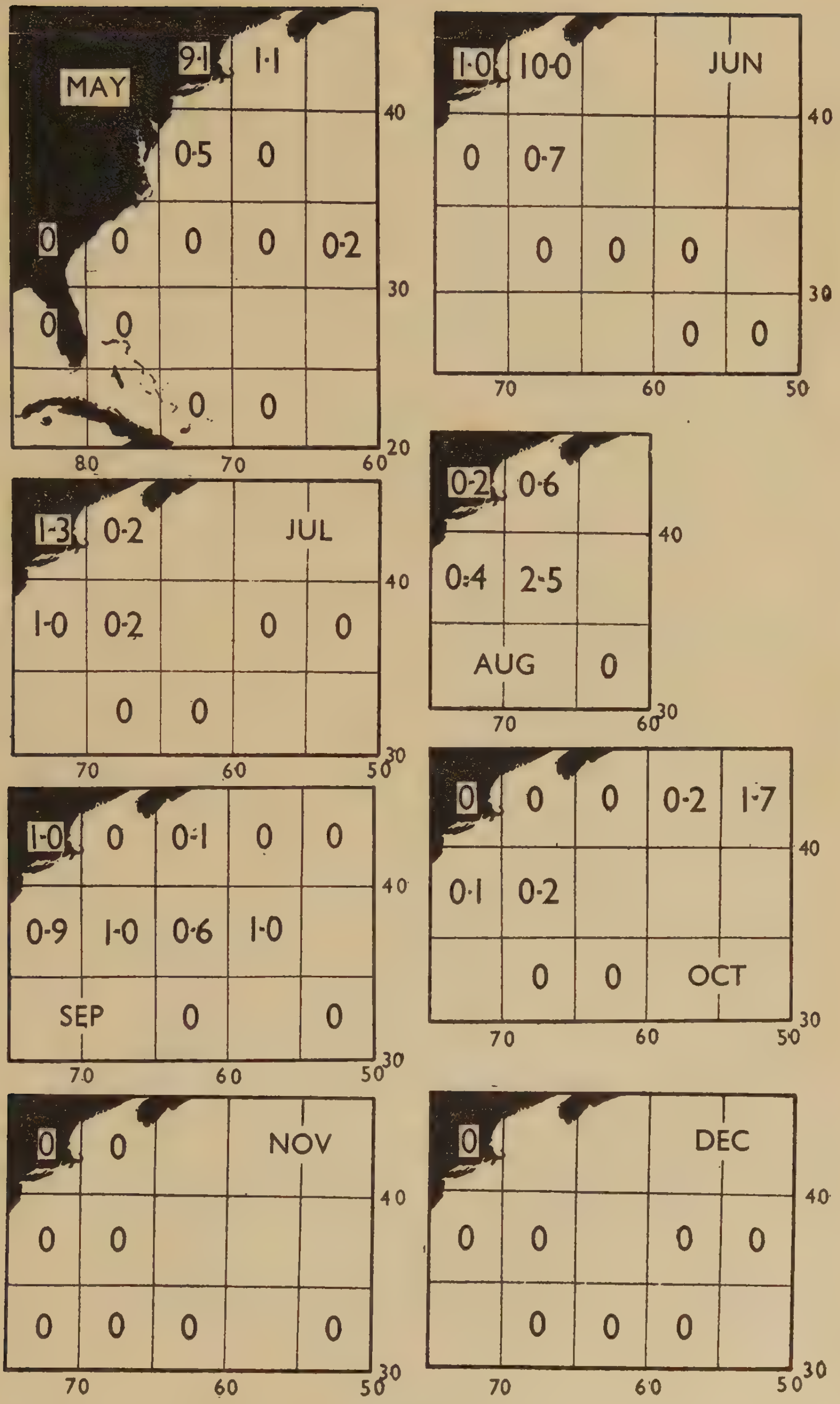
MAY
9·1
1·1
0·5
0
0
0
0
0
0·2
0
0
0
0
80
70
60
40
30
20
JUN
1·0
10·0
0
0·7
0
0
0
0
0
70
60
50
40
30
JUL
1·3
0·2
1·0
0·2
0
0
0
0
70
60
50
40
30
AUG
0·2
0·6
0·4
2·5
0
70
60
40
30
SEP
1·0
0
0·1
0
0
0·9
1·0
0·6
1·0
0
0
70
60
50
40
30
OCT
0
0
0
0·2
1·7
0·1
0·2
0
0
70
60
50
40
30
NOV
0
0
0
0
0
0
0
0
70
60
50
40
30
DEC
0
0
0
0
0
0
0
0
70
60
50
40
30

Figure 4

breeding season to within a few hundred miles of the nesting site. It winters far south, arrives on its northern grounds in April and May, and moves south again in September and October. From November to March, our only records were a few in the extreme south in February. The next record is near the breeding grounds in April, and they did not become common there until May. Numbers remained about the same in June, after which they dropped, and there was some evidence of an offshore movement in September and October. Mather reports that in both 1948 and 1949, all petrels seen in Cape Cod Bay from August to September were Wilson's.

GREAT SHEARWATER, *Puffinus gravis* (O'Reilly). NORTH ATLANTIC SHEARWATER, *P. kuhlii* (Boie). Figs. 5 and 6.

These two species were confused in our earlier observations, so it seems better to consider them together at first, and then see how far the records can be distinguished. The sub-species *P. kuhlii borealis* Cory and *P. kuhlii kuhlii* (Boie) were not distinguished. Our records showed them practically absent from the area from December to February, and present in small numbers off the West Indies in March. Small numbers were seen along the Gulf Stream in the southern part of the area in April, and further north, and in somewhat larger numbers in May and June. Numbers dropped markedly in July and August, and then in September rose much higher than in the spring. They remained high in October, and in the Cape Cod area into November.

Wynne-Edwards shows that the great shearwater, which breeds in the central South Atlantic at Tristan da Cunha during the northern winter, moves north rapidly in the northern spring, passing Cape Cod about the end of May. It then spreads eastwards during the summer and moves south again in the fall, the return migration taking place partly on the western, but mainly on the eastern side of the Atlantic. On the other hand, the North Atlantic shearwaters breed on the European coasts during the northern summer, and, according to Wynne Edwards, spread westwards across the Atlantic between July and October. They occur from Cape Hatteras to Cape Cod from the end of August to November, and move south for the winter. Except during the southerly fall migration, the distributions of *P. kuhlii* and *P. gravis* hardly overlap on the American coast. There seems little doubt that the first peak in our records, from March to May or June, represents the northerly migration of the great shearwater. Those of our later records, where the two species were satisfactorily distinguished, support this. We have

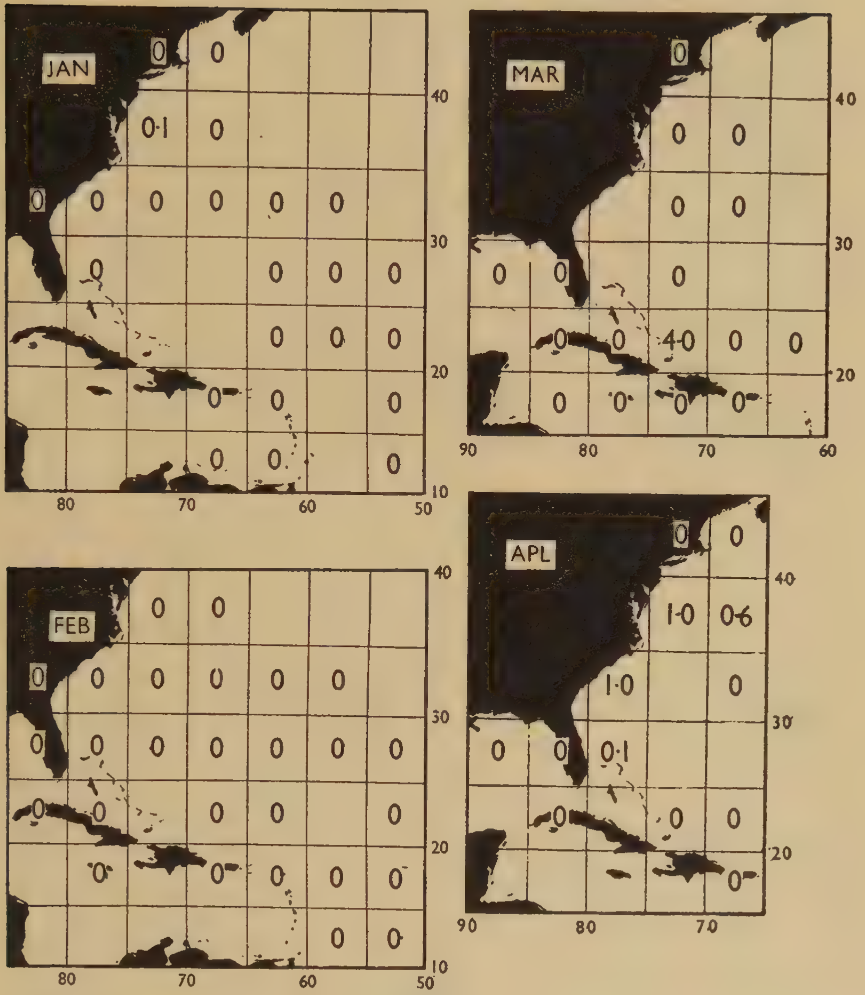
JAN
0 0
0·1 0
0 0 0 0 0 0
0 0 0 0
0 0 0
0 0 0
0 0 0
40
30
20
10
80
70
60
50
MAR
0
0 0
0 0
0 0 0
0 0 4·0 0 0
0 0 0 0
40
30
20
90
80
70
60
FEB
0 0
0 0 0 0 0 0
0 0 0 0 0 0 0
0 0 0 0 0
0 0 0 0 0
0 0
40
30
20
10
80
70
60
50
APL
0 0
1·0 0·6
1·0 0
0 0 0·1
0 0 0
0
40
30
20
90
80
70

FIGURE 5

FIGURES 5 & 6. Great Shearwater and Atlantic Shearwater combined. For details see Figures 1 & 2. The suffixes are omitted, but would be the same.

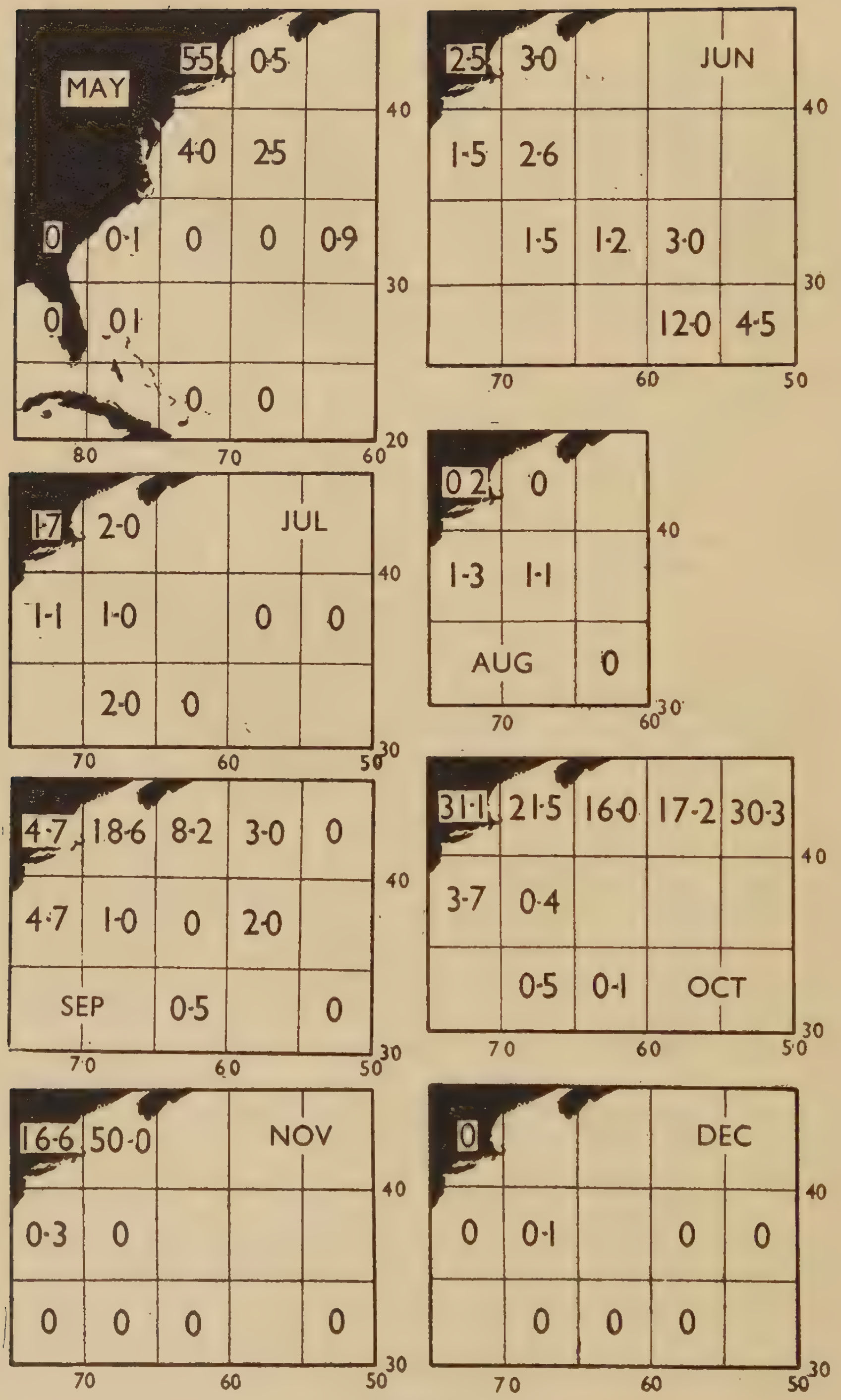
MAY
5·5
0·5
4·0
2·5
0
0·1
0
0
0·9
0
0·1
0
0
80
70
60
40
30
20
JUN
2·5
3·0
1·5
2·6
1·5
1·2
3·0
12·0
4·5
70
60
50
40
30
JUL
1·7
2·0
1·1
1·0
0
0
2·0
0
70
60
50
40
30
AUG
0 2
0
1·3
1·1
0
70
60
40
30
SEP
4·7
18·6
8·2
3·0
0
4·7
1·0
0
2·0
0·5
0
70
60
50
40
30
OCT
31·1
21·5
16·0
17·2
30·3
3·7
0·4
0·5
0·1
70
60
50
40
30
NOV
16·6
50·0
0·3
0
0
0
0
0
70
60
50
40
30
DEC
0
0
0·1
0
0
0
0
0
70
60
50
40
30

FIGURE 6

a single record of three Atlantic shearwaters off Bermuda on May 28 (Moore 1941), and one of a single bird between Bermuda and Cape Cod in mid-June. Mather (*in litt.*) observed considerable numbers of large shearwaters in Cape Cod Bay, and all of those which could be specifically identified in June 1949 were great shearwaters, while all those from July 25 to October 17, 1948 were Atlantic shearwaters. From this it would appear that Atlantic shearwaters must reach the American coasts somewhat earlier than Wynne-Edwards suggests, and while the European breeding season is still at its height. Wynne-Edwards indicates the return migration of the great shearwater as passing through our area in September-October, so presumably the second peak in our records, which occurs at this period, represents a mixture of the two species. Unfortunately, the records are not adequate to show which species predominates.

The unsatisfactory nature of these results is obvious, but the scarcity of other oceanic records for the area justifies their publication in this form.

NORTHERN PHALAROPE, *Lobipes lobatus* (Linn.). RED PHALAROPE, *Phalaropus fulicarius* (Linn.). Fig. 7.

It is rarely possible to distinguish the species of phalaropes at sea, and only two of our records make a definite identification of red phalaropes. Both of these were in September, and between Cape Cod and 150 miles south of there. The rest of the records are entered as northern phalaropes, and this is probably a correct identification of most of them. Both species nest in the Arctic, and make a spring and fall migration through the area. On the spring migration northwards we have one record of a flock seen in January, one in April, and all the rest in May. A record of Redfield's, not included on the chart, is that of about five hundred phalaropes, in small flocks, all flying east by north, between

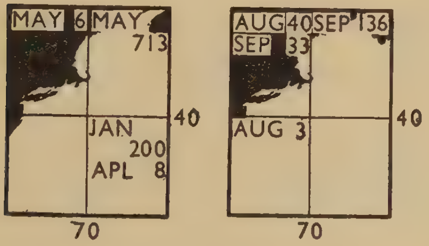

FIGURE 7. Phalaropes. Total numbers recorded (for details, see text). Comparison with Figures 1 & 2 will show the extent of the area from which none were recorded.

Browns Bank and Cape Sable on May 28, 1934. All our fall records were in August and September.

Our observations agree well with what is already known of phalarope migrations. The surprising thing about them is the fact that none were ever seen outside a very limited region. Comparison with the charts for shearwaters or petrels will show how large an area of the ocean was covered during their migration season without any being sighted. It is true that they are inconspicuous and easily missed, but this hardly seems to be an adequate explanation of the lack of records. There is still much to be learned with regard to both their wintering grounds and how they reach them, and our records do little to clarify these questions. They might perhaps lend support to the possibility that most of the migration is overland, or alternatively that, when at sea, they migrate mainly at night. In the latter case, if they were resting on the water during the daytime, they might well escape observation.

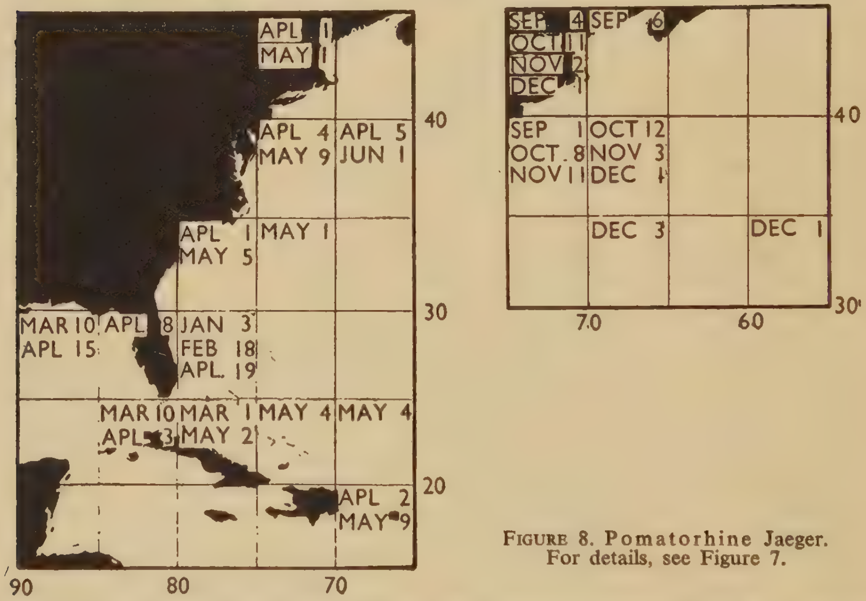
APL 1
MAY 1
APL 4
MAY 9
APL 5
JUN 1
APL 1
MAY 5
MAY 1
MAR 10
APL 15
APL 8
JAN 3
FEB 18
APL 19
MAR 10
APL 3
MAR 1
MAY 2
MAY 4
MAY 4
APL 2
MAY 9
40
30
20
90
80
70
SEP 4
OCT 11
NOV 2
DEC 1
SEP 6
SEP 1
OCT. 8
NOV 11
OCT 12
NOV 3
DEC 1
DEC 3
DEC 1
40
30
70
60

FIGURE 8. Pomatorhine Jaeger. For details, see Figure 7.

POMATORHINE JAEGER, *Stercorarius pomarinus* (Temminck). Fig 8.

The comparatively few jaeger records are, like the petrel records, shown individually and in two groups covering the spring and fall migrations respectively. In the spring, a few pomatorhine jaegers were seen as early as January at 29°N., and rather more in February in the Florida—West Indies area. In March and April they were seen all through this area and along the northern part of the Gulf of Mexico. Since there was no opportunity for observation in the Gulf before March, we have no evidence as to whether any of the birds winter there: it is clear, however, that there is a considerable concentration of pomatorhine jaegers in the Gulf of Mexico—West Indies area in the spring, and some time before they appear off the New England coast. Wynne-Edwards records them on the northern grounds at the end of April and beginning of May. Our records agree with this, our latest record being one bird seen in June.

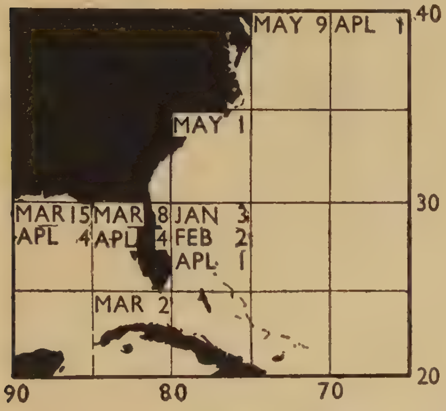

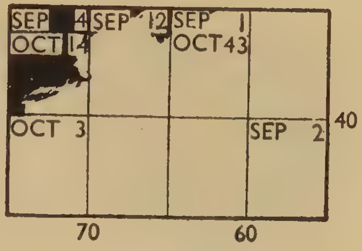

FIGURE 9. Parasitic Jaeger. For details, see Figure 7.

Records for the fall migration are strongly concentrated in the region of the Gulf Stream at about 40°N., and ranging from September to December. Wynne-Edwards saw his first birds of the season there in mid-August. The southern part of the area is less well covered by observations in the fall than in the spring, but the fact that the few November and December records were to the southeast suggests the possibility of the fall migration lying more to seaward than the spring one.

PARASITIC JAEGER, *Stercorarius parasiticus* (Linn.). Fig. 9.

There are fewer records of this species than of the pomatorhine jaeger, but, as far as the spring migration is concerned, they are very similar. A few were seen in January and February in the Florida—West Indies area, and more in March and April in the northern Gulf of Mexico. By May they appeared to be moving north along the coast. Again there is no additional evidence of their winter status in the Gulf.

Fall records were restricted to September and October, whereas pomatorhine jaegers were seen as late as December. Their locations were all between about 40 and 45°N., and there was a tendency to spread further seawards, and to do this at a more northerly latitude, than in the last species. This would agree with Wynne-Edwards' opinion that the parasitic jaeger is a more oceanic bird than the pomatorhine.

LONG-TAILED JAEGER, *Stercorarius longicaudus* Viellot Fig. 10.

This species was considerably less common than the last. Its distribution, both spring and fall, was the same, except that the earliest spring record was in March. Wynne-Edwards describes it as a still more oceanic migrant than the parasitic jaeger.

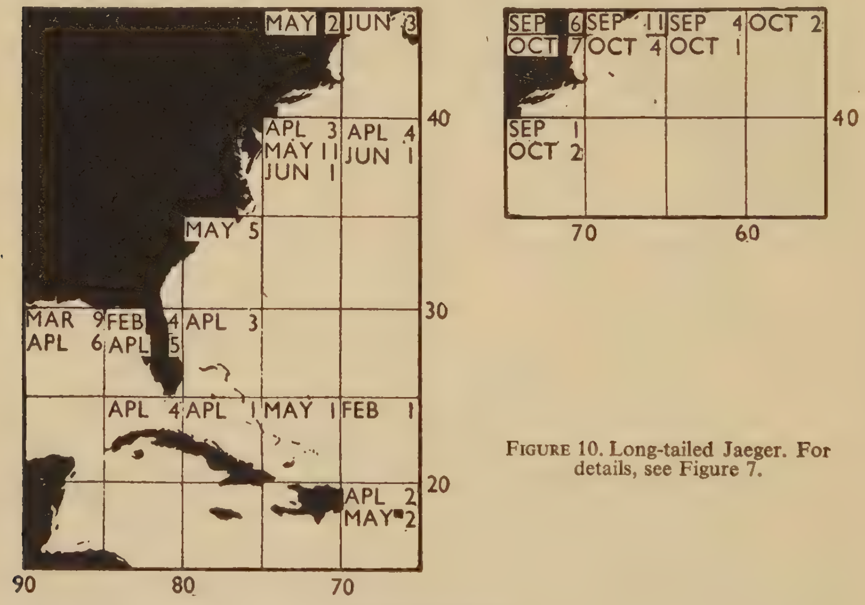
MAY 2
JUN 3
APL 3
MAY 11
JUN 1
APL 4
JUN 1
MAY 5
MAR 9
APL 6
FEB 4
APL 5
APL 3
APL 4
APL 1
MAY 1
FEB 1
APL 2
MAY 2
40
30
20
90
80
70
SEP 6
OCT 7
SEP 11
OCT 4
SEP 4
OCT 1
OCT 2
SEP 1
OCT 2
40
70
60

FIGURE 10. Long-tailed Jaeger. For details, see Figure 7.

REFERENCES

MOORE, H. B.
1941. Notes on the distribution of oceanic birds in the North Atlantic 1937-1941. Proc. Linn. Soc. N. Y., (52-53):53-62.
MURPHY, R. C.
1936. Oceanic birds of South America. MacMillan Co., New York. *1*:1-640; *2*:641-1245.
REDFIELD, A. C.
1941. The effect of the circulation of water on the distribution of the calanoid community in the Gulf of Maine. Biol. Bull., *80* (1):86-110.
WYNNE-EDWARDS, V. C.
1935. On the habits and distribution of birds in the North Atlantic. Proc. Boston Soc. Nat. Hist., *40* (4):233-346.

Contribution No. 564

The Commonwealth of Massachusetts

DEPARTMENT OF CONSERVATION
Arthur T. Lyman, Commissioner

DIVISION OF MARINE FISHERIES
Francis W. Sargent, Director

THIRD REPORT ON

INVESTIGATIONS OF METHODS OF IMPROVING THE SHELLFISH RESOURCES OF MASSACHUSETTS

Prepared by the
WOODS HOLE OCEANOGRAPHIC INSTITUTION
In Accordance with Contract
Effective July 1, 1950

Publication of this Document Approved by George J. Cronin, State Purchasing Agent.
1825 (2 runs) 6-51-904888

PREFACE

The following report, prepared by Harry J. Turner, Jr., Biologist of the Woods Hole Oceanographic Institution, is a summary of the investigations of methods of improving the shellfish resources of Massachusetts which were carried out in 1950 by the Woods Hole Oceanographic Institution under contract with the Division of Marine Fisheries, Massachusetts Department of Conservation.

The investigations were conducted under the leadership of Mr. Turner. Those participating were Carl N. Shuster, J. Arthur Posgay, and David B. Sawyer, graduate assistants, and George Matthiewson, summer assistant. The work was greatly aided by counsel from Dr. David L. Belding, former Biologist for the Massachusetts Department of Fisheries and Game who is now a member of the staff of the Woods Hole Oceanographic Institution.

The Institution has worked in close cooperation with the U. S. Fish and Wildlife Service which is conducting investigations in Essex County and in other parts of New England under a federal appropriation for the improvement of the soft and hard clam fisheries. Members of the Institution served on the Committee of Clam Technicians sponsored by the Atlantic States Marine Fisheries Commission of which Massachusetts is a member.

The Woods Hole Oceanographic Institution wishes to express its appreciation to Mr. Francis W. Sargent, Director of the Division of Marine Fisheries, and to Mr. Charles L. Wheeler, Biologist of the Division for their valuable suggestions and close cooperation.

Alfred C. Redfield
Associate Director
Woods Hole Oceanographic Institution

December 31
1950

THIRD REPORT ON INVESTIGATIONS OF METHODS OF IMPROVING THE SHELLFISH RESOURCES OF MASSACHUSETTS*

BY

HARRY J. TURNER, JR.

The primary aim of shellfish investigations is the accumulation of fundamental biological knowledge that may be advantageously used for the maintenance of existing fisheries at optimal levels, for the rehabilitation of declining shellfish resources, and for the introduction of new fisheries when practicable. In general the declining fisheries, because of their immediate need, receive the most attention, while those in more stable conditions are often neglected. New fisheries for the most part are initiated by the industry itself through the introduction of products unknown to the commercial market. In this field, biological investigations are important in estimating the extent of these recently developed resources, and in evaluating the prospects of their continuance.

The soft clam fishery of Massachusetts is a typical example of a declining industry. In 1948 the Woods Hole Oceanographic Institution undertook an investigation to determine methods by which the soft clam could be restored to its former abundance. Experiments were conducted in Barnstable Harbor to determine if the setting of the soft clam in barren areas could be encouraged by resurfacing the flats with various materials. Preliminary results indicated that certain types of soils taken from marsh banks would apparently stimulate setting, but a more thorough investigation revealed that the surface roughness resulting from such treatment provided only concentration areas for migratory clams, and that resurfacing was only effective if there had been a general light set in the surrounding area. The relative effectiveness of various methods of transplanting large clams was also tested and it was demonstrated that transplantation could be accomplished satisfactorily by simply scattering clams on the surface of untreated flats. It was subsequently discovered, however, that predators, particularly horseshoe crabs and boring snails, could be so destructive that repopulation of barren areas by either of these methods would be impossible if those predators were numerous. Low wire fences were found to be satisfactory in keeping horseshoe crabs out of small beds of clams in Barnstable Harbor, but in all experiments the boring snails, which could not be excluded in this manner, proved to be so destructive as to reduce the volume of the clam population faster than it could increase by growth.

Experiments were continued during 1950 on the effects of predators and possible means of combating them. The scope of the investigation was expanded to include observations of selected areas along the entire coast of Massachusetts to determine how the production of the soft clam was effected not only by predators, but by digging regulations, types of soils, and the presence of breeding stocks. It was found that soft clams might set and grow in almost any type of soil and that production appeared to be influenced more by digging regulations than by any other factor. Setting was more frequent and production was higher in moderately contaminated areas where the number of diggers was limited and conservative digging habits were practiced than was the case in the uncontaminated areas where unrestricted digging was permitted. Production was also found to be consistently poor in areas where predators were numerous.

The natural history of the horseshoe crab was intensively studied in Barnstable Harbor to determine whether usual methods of control of this species were effective. Tagging experiments demonstrated that adult horseshoe crabs migrated out of Barnstable Harbor, and other evidence suggested that there was also an inward migration. It was concluded that the horseshoe crabs found in Barnstable Harbor belonged to a large population that inhabited a considerable portion of Cape Cod Bay and that the number of crabs destroyed within the harbor each year was insufficient to materially reduce the size of this population.

---

* Contribution No. 564 Woods Hole Oceanographic Institution.

The rate of feeding of the boring snail was determined by feeding snails with clams in the laboratory under conditions in which the temperature of the water could be regulated. The average rate was 0.67 clams per snail per day at summer temperatures (70°F.) and became less as the temperature was reduced. The rate of growth of the boring snail was found to be related to feeding; a pound of snails would have eaten at least 20 pounds of clams to attain their size if clams were the only article of diet.

The possibility of developing other shellfisheries in the waters of Massachusetts was considered. The soft clam represents the only shellfish of commercial importance in Massachusetts north of Cape Cod, and as in other instances where absolute dependence is placed on a single resource, the decline of the soft clam has created a serious situation. In 1949 the experimental introduction of the Pacific oyster, a cold water species, was undertaken in Barnstable Harbor to determine if this species would grow and propagate in Massachusetts Bay and supplement the soft clam fishery in waters unsuitable to the native oyster of the east coast. The Pacific oysters survived two winters, and grew rapidly, attaining an average length of five inches by the time they were three years old.

The ocean clam (mahogany quahaug) beds off the coast of Massachusetts suggested another resource which might be developed. A fishery for this species was carried on in Rhode Island during World War II and several small boats marketed annually many thousands of bushels, but the market declined during the postwar period. However, interest in the commercial possibilities of the ocean clam was renewed in 1949, when certain other shellfish products were becoming scarce. A survey of the waters adjacent to the coast of Massachusetts revealed the existence of extensive beds that could furnish a profitable fishery for the small-boat dredging fleet for several years. During 1950, several trips were made to these grounds to obtain ocean clams for a food technology laboratory and commercial dealers for experimental purposes. By the end of 1950 there was a good possibility that the industry would develop methods of processing ocean clams in a manner that would appeal to the consumer.

Recently, fishermen, who have been exploiting the sea scallop resources of Cape Cod and Massachusetts Bay have become apprehensive that these areas were being overfished. This fishery has supported a fleet of small scallop boats. Since little was known of the biology of the sea scallop that would bear on the successful regulation of its fishery, an investigation of this species was initiated. The principal aim was to determine the rate of growth of the sea scallop as well as other aspects of its natural history. Preliminary observations indicated that this species lives best in water of low temperature and probably grows to a diameter of over three inches in the first two years.

This report includes the following series of articles:

I. Investigations on the Soft-Shell Clam, *Mya arenaria,* by Harry J. Turner, Jr.

II. Feeding Activities of the Boring Snail, *Polynices duplicata,* by David B. Sawyer.

III. Observations on the Natural History of the American Horseshoe Crab, *Limulus polyphemus,* by Carl N. Shuster, Jr.

IV. Investigations of the Sea Scallop, *Pecten grandis,* by Julius Arthur Posgay.

V. Growth of the North Pacific Oyster, *Ostrea gigas,* in Massachusetts, by Harry J. Turner, Jr.

I. INVESTIGATIONS ON THE SOFT-SHELL CLAM, *MYA ARENARIA*

BY

HARRY J. TURNER, JR.

GENERAL CONDITIONS AFFECTING SOFT-SHELL CLAMS

The conditions that favor setting, survival and growth of the soft clam are still obscure in spite of the intensive investigations that have been conducted by federal, state, and private agencies during the past few years. There has been considerable speculation as to the influence upon soft clam populations of types of soil, hydrography, parent stocks, predators, and numerous other factors. Some of these investigations, which have been limited to special localities, have led to conclusions that apply only to the local situation and not necessarily to the coast as a whole.

During the summer and fall of 1950, a number of selected flats along the coast of Massachusetts were examined in an attempt to obtain a comprehensive picture of soft clam populations under a variety of conditions. It was hoped that information derived from this survey might make it possible to arrive at certain general conclusions as to the factors affecting the setting, survival and growth of the soft clam.

The tidal flats of Massachusetts have a variety of soils. Surf-washed beaches are generally composed of clean coarse sand of the type familiar at popular bathing resorts. This type of soil is also found in bays and estuaries where water currents are swift. Under such conditions the surface is generally more or less rippled. Within certain estuaries, hard compact flats composed of finer sand grains often occur between meandering channels and in other areas of reduced turbulence. These flats may be so firm that footprints may produce only surface markings that are seldom deeper than the thickness of the sole of a shoe. The organic content and mineral composition of this type of soil may be variable as indicated by the color. Soft muds are common in the upper reaches of estuaries, along the sides and bottoms of slow creeks, and in other situations where conditions permit the settling and accumulation of fine sediments and organic debris. This material usually retains a considerable amount of water, which makes the soil soft so that sometimes a person may even sink in as far as his knees. There are all degrees of intergradation among the three types of soil.

There is also a wide variety of regulations in regard to the taking of clams in the various towns and cities along the coast, and it may be presumed that these regulations affect the clam supply. Grossly polluted areas are completely closed to digging by state law except in certain localities where a small amount of supervised digging for transplantation is permitted. In moderately polluted areas, permits are granted to one or more master diggers who in turn employ a restricted number of clammers. Clams from these areas must be passed through a chlorination plant for purification. The number of clams removed in any period depends on the activity of the restricted number of diggers, and the capacity of the purification plant. The number of diggers in unpolluted waters is usually restricted to persons who take out commercial or family permits but there is no limit to the number of permits that may be issued.

There is also a considerable variation in the number and species of predators of soft clams in different localities. In some localities horseshoe crabs appear in abundance each year and boring snails form a permanent population. Blue crabs, green crabs, or spider crabs may each be abundant from time to time in certain localities. There are also areas where no predators are ever seen. The effect of predators on experimental plantings of clams suggests that their presence or

TABLE I

General Area	Locality	Soil	Soft Clam Population	Predators	Digging Regulations
Falmouth	Perch Pond	Firm sand to gravel beach	Mostly 1950 set	Few blue crabs	Closed when clams are small, open to East Falmouth residents when clams mature
Barnstable	Upper Harbor	Hard fine sand	All 1950 set	Abundant, horseshoe crabs snails, spider crabs, green crabs	Open. Number of clamming days and total catch restricted
Duxbury	Beach below Clapp Laboratory	Ankle-deep black mud	Mostly 1950 set	Abundant horseshoe crabs and snails	Open
Quincy	Upper Town River	Knee-deep black mud	Uniform size averaging 2 inches	None observed or reported	Restricted to employees of Master Digger. Was cleaned out three years previously
Quincy	Opposite Fore River Bridge	Hard pebble beach	Mixed, some stunting in larger sizes	None observed or reported	Prohibited because of gross pollution
Boston Harbor	South Side Logan Airport	Firm fine sand	Uniform size, very crowded and obviously stunted	None observed or reported	Restricted to employees of Master Diggers
Parker River	U. S. Fish & Wildlife Serv. experimental flats.	Hard fine sand	Almost none	Horseshoe crabs and snails	Open except for limited experimental area
Salisbury	"Toothpick"	Clean coarse sand	Uniform, small probably immigrants	None observed or reported	Prohibited because of gross pollution
Salisbury	Merrimack River, West of "Toothpick"	Ankle-deep black mud	Uniform, large clams over 3 inches long	None observed or reported	Prohibited because of gross pollution

absence may profoundly affect the existence and abundance of soft clams in localities where these predators are numerous.

The results of the survey, which are summarized in Table I, indicate that the type of soil has little influence on the presence or absence of soft clams. Clams were found to be abundant in the soft, black mud flats of Duxbury, Quincy and the Merrimack River, and also in the firm, hard sand flats of Falmouth, Barnstable, and Boston Harbor. Certain pebbly beaches in Falmouth and Quincy were also well populated. It was indeed surprising that the coarse, shifting, bathing-beach type of sand of the "Toothpick" in the Merrimack River should contain small clams that had apparently lived through one winer.

On the other hand, clamming regulations and predators appeared to affect both the existence of soft clams and the size-composition of their populations. The clam populations in certain unpolluted areas of Falmouth, Barnstable, and Duxbury deserve special mention because these areas have been under observation for the past few years. These populations consisted almost exclusively of small clams. Sets have occurred each year in Perch Pond, Falmouth, for the past few years. Growth has been so rapid that many of the clams have attained the two-inch length by the end of their second summer. The town has attempted to conserve the resource by restricting the number of days open to digging, limiting the amount taken, and closing the area when the number of legal length clams has become exhausted. In spite of these measures, digging has been so intense that only young clams have been left in the flats at the end of an open season. However, the area has been very productive for its limited size. The small range of tide, which has necessitated underwater digging, has prevented it from being completely dug out at any time. Commercial clamming in Barnstable and Duxbury has been at a low level for several years, because of an inadequate supply of clams. In Barnstable, the supply has been dwindling for several years and the few clams which have been taken recently have been large, old specimens. There were scarcely enough of these to supply more than one or two diggers by 1950. Efforts have been made to conserve the resource by limiting the amount taken and restricting the number of days per week in which digging has been permitted. The clam population was altered in 1950 by the sudden occurrence of a dense set covering nine acres of flats. The fate of this set is discussed in another section of this report. Thus, at the time of the survey, the clam population of Barnstable consisted almost entirely of a single generation of very young clams. The situation in Duxbury resembled that in Barnstable in that there was a very limited supply of large clams, and a large area containing numerous small clams, all of a single generation. At the time of the survey, the area containing the set extended south from the yacht club two or three miles. A similar set observed in 1948 disappeared in the early summer, presumably because of the action of predators.

Two moderately contaminated areas, one in Quincy and one in Boston Harbor, appeared to be managed in a manner which produced a continuous supply of soft clams. The digging regulations were the same in both localities but the digging habits of the clammers were different. Each area was assigned to one or more master diggers who employed a limited number of clammers. In Town River, Quincy, it was the practice to rotate areas. If an area contained only large clams, it would be completely dug out and then left strictly alone until it became repopulated and a sufficient number of clams had attained the legal length of two inches. At the time of the survey, one such area which had been cleaned out two years previously, was being exploited. The area contained from twenty-five to thirty-five clams per square foot, about half of which were over two inches in length so that they could be taken by the diggers. The diggers were of the opinion that the area will be again available within the year when the remaining half of the clams will have grown to two inches. They were also confident that it would become repopulated and be a source of supply two or three years later. A somewhat different system was used among the diggers in the Governors Island flats near the Logan Airport. Here large areas contained as many as

300 clams per square foot, most of which were stunted by overcrowding. The majority ranged from one to two inches in length but about three clams in ten exceeded the two-inch legal minimum. The diggers dug more or less at will, selecting places where large clams were most abundant. By leaving the smaller ones for future use, a continued supply was insured. In areas where most of the clams were of legal size it was customary for a digger to leave every third hoeful so that at no time would the flats become completely depleted.

The high productivity of these two areas appeared to be a result of these excellent digging practices and the restricted number of diggers. It is quite easy to see how such areas could be rapidly depleted in spite of the large supply of clams if there were no restrictions on the number of diggers and the size of the catch. The supply would then be intermittent, depending on the frequency of repopulation and the rate of growth.

An examination of grossly polluted flats where digging was prohibited was instructive in revealing that clam populations do not build up indefinitely under such circumstances. In Town River, Quincy, opposite Fore River, a pebble beach, which had been closed for several years, contained clams in about the same number (twenty-five to thirty-five per square foot) as were found in upper Town River. The population of clams differed, however, by consisting of three distinct size groups, suggesting that there were three separate generations. Clams in the largest size group were a little over two inches long, and the appearance of their shells suggested that they were stunted. This group of large clams may have contained several generations in itself. Similarly, the Merrimack River flats near the mouth of Black Rock Creek did not contain an exceptionally large population of clams, although it had also been closed to digging for several years. Here large areas were found which contained from five to ten clams per square foot, all three inches long or more and probably five or six years old. There was no evidence of recent setting.

The importance of predators was not clearly brought out in this survey because their presence or absence coincided with types of clamming regulations. Predators were present in all the unpolluted areas that were examined where the number of diggers was unrestricted. In Perch Pond, Falmouth, there were a few blue crabs, but they did not seem to be abundant in the clam-producing area. In Barnstable Harbor and Duxbury, horseshoe crabs were either observed in abundance or reported as such, and boring snails were collected in large numbers. The experimental flats of the U. S. Fish and Wildlife Service in the Parker River contained almost no clams at all and both horseshoe crabs and boring snails were numerous. None of these areas, with the exception of Perch Pond, Falmouth, have been productive of soft clams for some time. No predators were observed or reported in the productive flats of Quincy and Boston Harbor or in the polluted flats of the Merrimack River.

It is unfortunate that no areas were found where there was either unrestricted digging without predators, or the presence of predators without unrestricted digging. However, the combination of these two may prove to be the critical factor limiting the clam supply. All natural populations are held in check by a variety of mortality factors, which include natural death, death due to disease, killing of the weak by adverse physical conditions and destruction by predators. A stable population is maintained when the death rate equals the rate of replacement. Complete stability is probably never attained so that natural populations at any one time are usually gaining or losing in numbers, depending on the importance of these various factors. Clam populations have been reported to exist in the past in areas where predators were numerous. The rate of replacement under such conditions must have been in excess of the mortality rate. If an additional mortality factor, exploitation by man, were superimposed on the other factors acting upon a clam population near its stability point, the additional factor might have been sufficient to produce a downward trend. This would, of course, depend on the magnitude of digging mortality in relation to the other factors.

However, it has been shown that digging may be so intense that an area may be completely cleaned out and in isolated cases predators have been shown to be equally effective. This strongly suggests that unrestricted digging in areas where predators are numerous may, in combination with the destruction by the predators, reduce the clam population to a point where its rate of recovery produces only enough clams to supply the predators and leave none for digging.

It would appear from this survey that restriction of the number of diggers in an area gives the best results in maintaining a continuous supply of soft clams, and that restrictive measures imposed on an unlimited number is probably less effective. The absolute importance of predators has not been determined, but when their action is combined with that of an unrestricted number of diggers, depletion may be the result. The type of soil appears to have little influence on the presence or absence of soft clams, but there is some indication that in combination with other environmental factors, the type of soil may limit the number of clams per square foot that an area can support.

METHODS OF INDUCING SETS OF SOFT-SHELL CLAMS

Previous experiments have demonstrated that the setting of the soft-shell clam apparently may be induced at times by treating the surface of flats in various ways. In 1948 a set was obtained on a flat in Barnstable Harbor that had been resurfaced with turf excavated from marsh banks. The stretching of plastic screening of suitable sized mesh over the surface of a flat has also proved effective. Subsequent failures of such measures to collect clam spat have been attributed to the inability of a depleted breeding stock to supply a sufficient number of larvae. The experimental work of 1950, however, clearly demonstrated the fallacy of this and other former concepts, and revealed that these treatments provided rough surfaces where migratory clams washed about by water currents would become concentrated.

A quarter-acre plot in Barnstable Harbor, which had been resurfaced during the winter of 1949, was kept under constant observation. At no time during or after the breeding season, did any significant number of small soft clams appear in the area, and the surrounding flat also remained barren. Several adjacent flats, however, received a heavy set of clams late in the summer, indicating that adequate numbers of soft clam larvae must have been present in the water. The environmental hydrographic conditions were such that the flats on which the set appeared were swept by the same water masses as were the unpopulated experimental flats, so that there was little possibility that the latter was exposed at all times to water free of larvae. Evidently the nature of the soil of these flats and/or hydrographic features of the water over them were more suitable for the setting of soft clams than were those of the resurfaced area.

In 1948, when a moderate set was obtained on a resurfaced area, it was observed that the roughness of the surface caused seaweed, shells and other debris to accumulate, whereas this material was normally washed back and forth over the flats with the tidal currents. In light of our present knowledge it seems most likely that the concentration of clams among the rough clumps of thatch was not occasioned by the setting of spat, but was caused by accumulation of small clams that had set sparsely on the surrounding flats, had been washed out of their burrows, and had been wafted about by the tidal currents. The experiments of Mr. Charles Wheeler, Biologist for the Division of Marine Fisheries, also demonstrated that irregular surfaces might provide collecting places for displaced clams. He observed accumulations of small clams on the *upper* surfaces of sheets of plastic screening that had been laid down on the flats to induce setting. Some of these experiments were performed in the spring before the breeding season so that the clams must have been derived from those that had set during the previous fall. Some of the clams were even attempting to burrow by protruding their feet downward through the mesh. Thus, it would appear that any treatment that roughens the surface of a flat merely provides an area of concentration for current-wafted clams, and the failure of these measures occurs when there is a complete absence of set in the surrounding area. So far no one has been able to show experimentally why heavy sets of clams often occur in limited areas, or to create conditions that will produce such sets. The type of soil of these areas appears to have little influence as shown previously in this report.

OBSERVATION ON THE DESTRUCTION OF A HEAVY SET OF CLAMS

From time to time, promising sets of soft clams will entirely disappear, to the astonishment and disappointment of local clammers who have anticipated good digging within a year or two. Such occurrences have occasioned a variety of explanations, most of which are inconclusive and unsatisfactory. In October 1950, a heavy set of soft clams was discovered in upper Barnstable Harbor by the local shellfish officers. This set was largely destroyed while under close observation. Consequently it was possible to determine the responsible agencies with some degree of accuracy.

The set comprised nine acres and covered six separate flats in Scorton Creek and one flat in Spring Creek at the west end of Barnstable Harbor. Since there were no records of clams having previously existed in these flats, no one considered it worth while to examine these localities and the set went unnoticed for some time.

Preliminary surveys showed that definite areas of all these flats were densely populated with soft clams averaging a little under ¾ of an inch in length. The clams numbered five hundred or more per square foot in locations of the greatest densities, which were generally located in the middle of the populated areas. The clams were progressively less dense toward the peripheries. Occasionally there were exceptional patches where the concentration ran as high as fifteen hundred per square foot.

An intensive survey was made on the most accessible flat on November 2. Stations were selected and marked by stakes at intervals of one hundred feet along the length of the flat. Population estimates were made at each station and samples of the surface sand were collected for analysis. At this time the flat was so firm that a person of average weight left a shallow footprint about one-half inch deep. The numerous clam holes and elasticity of the buried clams caused the flat to feel spongy under foot. There were no ripple marks on the surface, although this flat was situated in a place where the tidal currents were quite swift at certain stages of the tide. Similar conditions may cause rippling and shifting of the surface sand.

Unfortunately, field work was interrupted for 14 days because of adverse tides. On November 16 the entire character of this flat was changed. The surface sand was heavily rippled and covered with particles of broken shells. Clams were not nearly as numerous as previously; the density of the population at the several stations was reduced by amounts varying from sixty to one hundred per cent. The surfaces of the other flats were also deeply rippled and the number of clams similarly reduced. The surrounding areas were examined to determine if any of the clams had been washed elsewhere, but no significant number could be found. The shell fragments, which covered the area, consisted of thin plates intermixed with recognizable pairs of clam umbos still connected by the hinge. There could be no doubt that they were the remains of the missing clams. It was apparent that the forces causing the rippling of the sand, had been sufficient to wash out and grind into fragments the thin shelled clams.

At the time of the first survey, the smooth, firm texture of the flats indicated that they were stable under the velocities of the currents that had occurred since the time of the set. However, the period during which the set was destroyed, corresponded with the time of the greatest tidal amplitude of the entire year, when the tidal currents were increased considerably. It was apparent that the increased tidal currents surpassed the velocities at which the flats remained stable, and initiated changes in the surface sand. Thus the resulting turbulence of the water disturbed the surface to a sufficient depth to wash out the clams and grind them to fragments.

This conclusion is confirmed by the results of analyses of the sand samples that were taken before and after the disaster. Flats of this type are formed by the deposition of water-borne sand grains in localities of reduced turbulence. When hydrographic conditions are such that the flat remains stable, the assortment of sizes of sand grains remains constant at any place on the flat for a long period of time. Any change in this assortment indicates that there has been sufficient activity of the water to either bring in additional sediment or to dislodge and carry away certain sized sand grains. These assortments can readily be determined by passing dried samples of sand through a series of standard sieves with screen openings of graded sizes. The relative percentage of sand remaining on each sieve indicates the composition of a particular sample.

Graphs of the compositions of the sand samples for each of the six stations both before and after the disturbance are shown in Figure 1. Definite changes were present in four of these stations. Removal of the smaller sand grains from

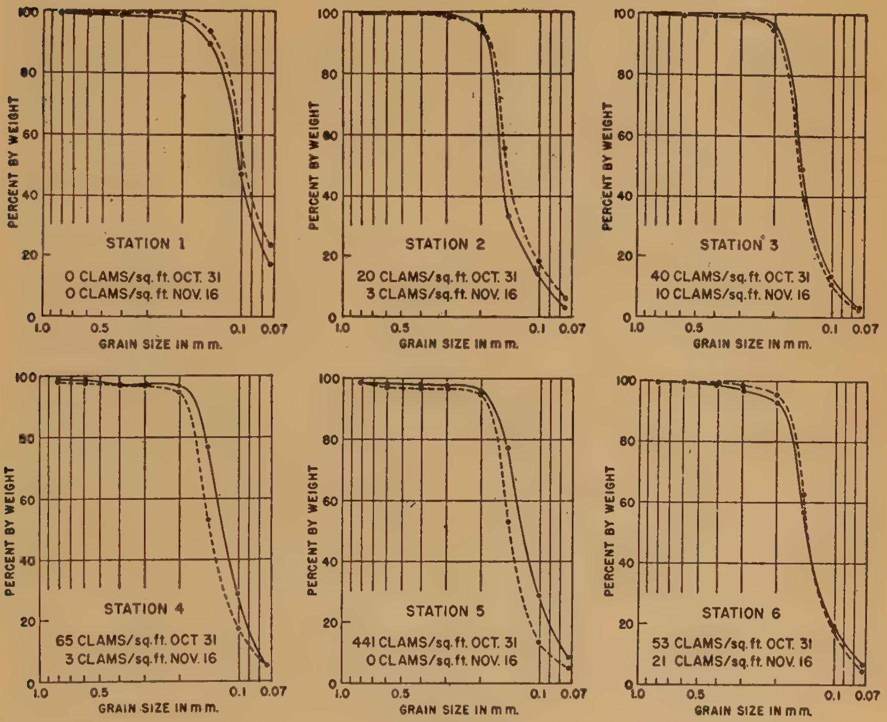

FIGURE 1.

Graphs of the distributions of sizes of sand grains in soil samples taken every hundred feet across a flat containing a new set of clams. The solid lines indicate the assortments on October 31; the dashed lines indicate the assortments on November 16.

the higher level of the flat (stations 4 and 5) is indicated by a shift of the assortment to the left and the deposition of fine sand at the lower stations (stations 1 and 2) is demonstrated by a shift to the right. Stations 3 and 6 evidently had undergone little change as is indicated by the close similarity of the two curves. The degree of destruction of the clams was proportional to the amount of disturbance of the assortment of the sand grains with the greatest losses at stations 2, 4 and 5, and least at stations 3 and 6. Station 1 was outside the populated area.

The failure of this promising set was apparently the result of the unfortunate location and the late time of setting. There is little doubt that a valuable supply of soft clams would have eventually matured if the flats had been sufficiently stable to withstand the increased currents produced by the exceptionally high tides. Predators might have destroyed a considerable number of the clams, but the eventual value would have been sufficient to justify the expense of fencing out horseshoe crabs during their active season. Likewise, if the set had occurred at an earlier date, the clams might have attained a larger size and greater depth in the sand and thus might have escaped destruction.

METHODS OF EXCLUDING PREDATORS FROM BEDS OF SOFT-SHELL CLAMS

The importance of predators in restricting the development of natural sets and interfering with the cultivation of transplanted clams has been adequately shown by observation and experiment. Some aspects of the problem have been discussed in the previous section. The successful maintenance of beds of transplanted clams by communities or private individuals is more or less dependent upon the exclusion of predators, because these operations are often carried out in depleted areas where the predators are attracted in large numbers to the beds where feeding is good. For years it has been the practice to remove predators from the beds by hand at low tide, a generally unsuccessful procedure since a new supply moves in with the next tide.

During the summer of 1949 it was demonstrated that a low wire fence around a clam bed would effectively exclude the horseshoe crab but not the boring snail, *Polynices*. It was found that this snail was much more destructive than had been anticipated and that the mortality of planted clams from this source exceeded their increase by growth. It was considered possible that newly planted clams might be particularly vulnerable because of their relatively shallow depth in the sand, and that if they were given sufficient time to establish themselves at their full depth, a greater number might escape destruction. In order to test this idea two experimental flats in Barnstable Harbor were planted with clams in October 1949 when the activity of the boring snails was reduced by the cooling of the water. Each planted bed was twenty-five feet square and contained twenty-five pecks of clams, most of which dug in well and survived the winter. When the first horseshoe crabs appeared at the end of April 1950, one bed was enclosed by a chickenwire fence which was thirty inches high and extended six inches into the sand. At first considerable difficulty was experienced in maintaining the fence because of the scouring action of waves generated by strong northwest winds. However, this difficulty disappeared as soon as the summer weather pattern with its gentle southerly winds became established.

Two similar beds were established in June 1950 so that a comparison could be drawn between the effect of the predators on newly planted clams, and on those which had been in the sand for a longer time. Each of the new beds was seeded with twenty-one pecks of clams; one was fenced immediately and the other left as a control. Traps were constructed at the corners in such a way that the traps at two of the corners would catch any horseshoe crabs that passed over the fence, while those at the other two corners would catch crabs that moved along outside of the fence.

Early in June it became apparent that other enemies beside horseshoe crabs and boring snails were active on all four beds. Broad conical excavations and curious straight-sided pits, both distinctly different from the burrowings of horseshoe crabs, began to appear. The broad excavations were made by spider crabs, which worked their way down into the sand until only the tops of their bodies were visible. Clam necks and shell fragments were found when the contents of the crabs' stomachs were examined. Apparently the spider crabs excavated the clams from the sand with their long legs and then broke the shells with their crushing mouth parts. The smaller, straight-sided pits were dug by green crabs, which were difficult to find at first because of their small size and active habits. When the tide left the flats they would hide in clumps of seaweed or in shallow pools. However, these crabs were observed eating clams when the flat was submerged. Thus, even the clams in the enclosed beds were exposed to three types of predators, green crabs and spider crabs that could swim or climb over the fence, and boring snails that were small enough to pass through the mesh. However, the catch of the corner traps indicated that the fence excluded over ninety per cent of the horseshoe crabs that traversed the area.

The experiments were terminated at the end of August when all the clams in the four plots were carefully removed. Shells as well as live clams were saved to determine how many clams had been killed by boring snails, and how many had died from other causes. Table II, which summarizes the results, clearly demonstrates that the longer the time that the clams were left in these particular flats, the smaller was the return.

Of the two beds that had been maintained for ten months, the volume of clams in the unfenced bed decreased to about one quarter of the amount originally planted. In this case the growth of the survivors was sufficient to have doubled the volume if all the clams had lived. The other bed, which had been fenced in the spring, gave a somewhat better yield but this was only about one-third of the volume that had been planted. Only eleven per cent of the actual number of clams survived in the unfenced bed and about fifteen per cent in the fenced. The differences between these percentages and yields by volume in per cent is the result of growth.

The two beds that had been maintained for slightly less than three months gave somewhat better results and more clearly demonstrated the destructive capacity of the horseshoe crab. Of the volume of clams originally planted, fifty-seven per cent were recovered from the fenced bed compared with eighteen per cent from the unfenced one. Here again growth was sufficient even during the short priod of the experiment to have resulted in a one-third gain in volume if all the clams had lived. However, only two-fifths of the clams in the fenced bed were destroyed, although survival was three times as great as in the unfenced bed.

Examination of the empty shells collected from the fenced beds showed that most of the clams were killed by boring snails and by some other factor that is commonly considered to be a disease. The "diseased" condition is indicated by the presence of paired shells standing in their normal upright position in the sand with the siphon generally extended nearly to the surface, and the soft parts in various stages of decomposition. In the final stages the soft parts are completely liquified or absent, and the neck consists only of its outer skin. It has never been definitely established that this condition is a result of disease. It is suspected, however, since dead clams are usually found scattered among the live ones in a random fashion as if susceptible individuals were stricken with a malady. If death were caused by unfavorable environmental conditions of a physical nature, it would be expected that the dead clams would include all the individuals in the affected patches or areas.

The relative destructiveness of the boring snail and the "disease" was quite different in the two sets of experiments. The "disease" accounted for six times as many clams as the snail in the beds that had been maintained for ten months.

TABLE II

SUMMARY OF PLANTING EXPERIMENTS

	October 1949 planting		June 1950 planting	
	Control	Fenced	Control	Fenced
Pecks planted	25	25	21	21
Number clams per peck at planting	468	468	470	470
Total number clams planted	11,700	11,700	9,870	9,870
Pecks recovered	6.5 (26%)	8.5 (34%)	3.75 (17.9%)	12.0 (57.1%)
Number clams recovered	1,352 (11.3%)	1,743 (14.9%)	1,218 (12.3%)	3,900 (39.5%)
Average length at planting	46 mm	46 mm	44 mm	44 mm
Average length at recovery	63 mm	62 mm	51 mm	51 mm
Shells recovered				
Pairs of bored shells	177	136	286	964
Pairs of unbored shells	709	818	104	526
Average length of bored shells	50 mm	49 mm	47 mm	47 mm
Average length of unbored shells	58 mm	59 mm	49 mm	49 mm

On the other hand, only one-third of the clams that died in the new beds were killed by the "disease," and the other two-thirds were eaten by boring snails. Other evidence indicated that the green crabs and spider crabs did not cause much destruction.

It was of particular interest to note that in both sets of experiments the "disease" affected clams that were actively growing and not those that were stunted, injured, or otherwise enfeebled. Their average growth was two-thirds that of the surviving clams indicating either that fast growing individuals were more susceptible or more probably that death occurred late in the summer. If these clams had died at a uniform rate throughout the period in the beds, the average growth of the dead ones would have been one-half that of the survivors.

At the present time the successful reseeding of barren flats by the transplantation of soft clams is prevented in many cases by high local concentrations of predators. The mere presence of the predators may be an important reason why the flats are barren in the first place, although it is highly probable that this factor combined with over-digging produces the depletion. However, it might be possible to protect dense natural sets with fences so that an appreciable number of clams may survive to maturity. There are records of such sets, which first appear with hundreds of clams per square foot and then dwindle in numbers so that by the time the clams mature, there are only twenty-five to fifty per square foot, usually the maximum number which can grow without stunting. In areas where horseshoe crabs are abundant, such sets may disappear completely as the horseshoe crabs, burrowing through the flats, destroy the clams wholesale. The boring snails on the other hand attack clams singly, usually requiring more than a day to consume one clam. Thus a set protected from horseshoe crabs during their active season might survive in numbers sufficient to satisfy the needs of the snail population and still leave enough to provide good digging.

It has been suggested that it may be possible to exclude boring snails with fences of fine mesh, but there are two obstacles that must be overcome. In the first place, fine mesh becomes clogged with floating debris and marine growths. The resulting obstruction would cause serious scouring of the sand by water currents so that the fence would have to be tended daily, an expense that would be commercially prohibitive. In the second place, it is almost impossible to remove an appreciable fraction of the snail population from any large area previous to planting, because the snails spend most of their time below the surface of the sand. This fact is demonstrated by the experiments reported above. The planted beds were kept under almost daily observation during the summer and at no time were more than two or three boring snails visible on the surface of the sand. Yet when the beds were dug at the end of the experiment one of them contained 195 large snails.

II. FEEDING ACTIVITIES OF THE BORING SNAIL, *POLYNICES DUPLICATA*

BY

DAVID B. SAWYER

There are two species of boring snail, *Polynices heros* and *P. duplicata,* that feed on commercially important shellfish in the coastal waters of Massachusetts. The larger, *P. heros,* is generally found in the more saline waters of the open coast, where it feeds on sea mussels and surf clams. It is also found occasionally in bays and estuaries where it may be a serious predator of the soft clam and quahaug. The smaller, *P. duplicata,* usually occurs in the brackish waters of inner harbors and tidal rivers, where its principal food is the soft clam, quahaug and razor clam.

There has been considerable speculation as to the full extent of the damage to soft clams caused by these snails. Mead and Barnes (1903) performed a single experiment by placing an orange crate enclosing a single snail over a clam bed. After 12 days they found the snail and seven pairs of bored shells with an eighth clam in the process of being eaten. This gives an average rate of destruction of 0.67 clams per day. Belding (1903) estimated that a snail two inches in diameter could destroy twenty-six clams per month, a slightly higher figure than that given by Mead and Barnes. Turner (1949) determined that *P. duplicata* destroyed about ten clams per month during the summer in enclosed beds in Barnstable Harbor. These estimates differ widely probably because clams and snails of different sizes were used in these experiments. Likewise the temperature of the water is not given and it is an established fact that the activity of many invertebrates is influenced by temperature.

During the winter of 1950 a series of laboratory experiments was conducted to determine more exactly the quantity of clams that one species of snail, *P. duplicata,* would actually consume at different temperatures. The rate of growth of the snail was also determined and related to the amount of food ingested. With this information it would be possible to estimate the weight of clams that had been destroyed if the number and weight of snails in a given locality could be determined. Naturally this estimate would be valid only if clams were the principal source of food for the snails. In this manner, a shellfish officer, who found that he could collect a bucket of snails from a flat could estimate with some degree of accuracy that they had already eaten a certain number of buckets of clams in order to attain their present size.

The apparatus consisted of a wooden box twenty-six inches long, fourteen inches wide, and eight inches deep, filled with sand to a depth of five inches. Running seawater, held at a desired temperature by a modified Loosanoff unit, was circulated over the sand. The heating unit consisted of a coil of 5/16-inch lead pipe submerged in a reservoir of fresh water that was heated by a 1500-watt electric emersion heater. The seawater passing through the lead coil was warmed to the desired temperature which was maintained by a system of thermostats, and the rate of flow was regulated at one liter per minute. The water was maintained at a height of two inches above the surface of the sand by a series of overflow holes in the side of the box. A weighed quantity of soft clams, generally one hundred in number and one inch or less in length, were placed in the box and allowed to establish themselves in the sand. Ten snails (*P. duplicata*) were then placed in the box and allowed to feed for periods of approximately two weeks. The snails ranged in size from 9 to 12 mm across the longest dimension of the opercular opening. The sizes of both the snails and the clams were selected to correspond to the sizes of those commonly found on the flats in the late summer and early fall. At the end of each feeding period the snails, clams and bored shells were removed from the sand, drained and weighed.

It had been previously noted that clams neither gained nor lost a significant amount of weight under conditions of the experiment, so that it was possible to determine the weight of clams consumed by the snails with a fair degree of accuracy.

During the first few feeding periods the rate of consumption of clams by the snails was determined for average summer temperatures, i.e. about 70°F. At this temperature the ten snails destroyed two hundred and two of the three hundred clams available in thirty days or 0.67 clams per day. A considerable gain in weight was observed in the snails approximating 1/20 the weight of the clams consumed. When the temperature of the water was lowered to 50°F, a temperature corresponding to that of the water in the late fall and spring, the rate of consumption dropped to one-fifth of that observed at the summer temperature. The snails, however, required a greater amount of food to equal their previous growth, the gain in weight being about 1/25 the weight of the clams consumed. The lowest temperature at which snails feed actively has not yet been accurately determined, but preliminary experiments indicate that there is probably little feeding on the flats from December through April.

These experiments have shown that the boring snail requires an enormous amount of food. Briefly, a collection of snails weighing one pound has had to consume from twenty to twenty-five pounds of clams or other food. In nature it may take even more food to produce a pound of boring snails, since often they have to expend considerable energy in hunting for food.

BIBLIOGRAPHY

Belding, David L., 1930: The Soft-shelled Clam Fishery of Massachusetts. Commonwealth of Mass., Dept. of Conservation, Div. Fish. & Game, Marine Fisheries Section, Marine Fisheries Series, No. 1.

Loosanoff, Victor L., 1949: Method for Supplying a Laboratory with Warm Sea Water. Science Vol. 110, No. 2851.

Mead, A. D. and E. W. Barnes, 1903: Observations on the Soft-shelled Clam. Ann. Reports, Comm. Inland Fish., Rhode Island.

Turner, Harry J., Jr. 1949: Report on Investigations of Methods of Improving the Shellfish Resources of Massachusetts. Commonwealth of Massachusetts, Department of Conservation, Division of Marine Fisheries.

III. OBSERVATIONS ON THE NATURAL HISTORY OF THE AMERICAN HORSESHOE CRAB, *LIMULUS POLYPHEMUS*

BY

CARL N. SHUSTER, JR.

INTRODUCTION

During the summer of 1949 and 1950 an investigation was made of the following phases of the natural history of the American horseshoe crab: 1) food and feeding habits, 2) growth and growth stages, 3) breeding habits, 4) migrations, 5) population and 6) control. These studies were conducted chiefly in Barnstable Harbor.

Observations on the American horseshoe crab, *Limulus (=Xiphosura) polyphemus,* have been reported since 1585. Although numerous studies have been made on this animal since the sixteenth century, its natural history is still incompletely known. The present study, prompted by the economic importance of the horseshoe crab as a predator of soft clams, has endeavored to answer some of the biological problems concerning those aspects of its growth and habits that have a direct bearing on the success of clam propagation.

FOOD AND FEEDING HABITS

Small horseshoe crabs feed on minute organisms that live in the ooze that covers the flats. They feed on larger animals as they grow, and by the time they are adults their diet consists chiefly of marine worms and several kinds of shellfish. Among the more important of these larger food organisms are the sand worm (*Nereis*), the sand ribbon worm (*Cerebratulus*), the duck clams (*Gemma* and *Macoma*), the razor clam (*Ensis*), and the soft-shell clam (*Mya*).

Horseshoe crabs dig into the flat after their prey and even feed when buried beneath the surface. Their pincer-tipped legs catch and carry the prey to their mouth, which is located between the bases of the legs. These bases, or "shoulders," act as chewing parts, mauling and forcing the food into the mouth. Shells of the molluscs are cracked between the heavy "shoulders" of the larger hindmost pair of legs.

The adult crabs are huge feeders during the breeding season when they may be found on the intertidal sand and mud flats, where they devour all sorts of worms and shellfish.

GROWTH AND GROWTH STAGES

The eggs of the horseshoe crab are laid between the tide marks on sandy beaches. They hatch after a month or more, and small, tailless larvae averaging 3/16 of an inch in length emerge. These grow by stages, shedding their chitinous skins (molting) between each stage. After the first molt the larvae acquire a tail. In the first tailed stage their average length is 1/4 of an inch, and in the next six stages 3/8, 9/16, 13/16, 1 1/8, 1 1/2, and 2 inches respectively.

The development and hatching of the eggs and the growth of the first young stages were followed both in their natural habitat and in the laboratory. Eggs laid during June in the Cape Cod region hatched after a month or more under both conditions. Young horseshoe crabs that were hatched in the laboratory seldom developed beyond the first tailed stage by the end of the summer, and tiny horseshoe crabs in this stage were found on the flat of Barnstable Harbor during the late summer and following spring.

After shedding their hard, chitinous skins the animals remain in a soft-shelled condition for a short time. Small horseshoe crabs have been observed in the process of shedding during the summer months on the surface of the flats, whereas the larger ones have been found buried in the sand below the low water line during the molting period. After each molt the emerging animal has gained an average of 25% in its linear dimensions.

During the first few years of life the horseshoe crabs shed their chitinous skins more than once a year, but the older, larger animals molt only once annually, and this during mid-summer. Some nine to twelve years elapse before the horseshoe crab is sexually mature. The sexual organs become functional and the accessory reproductive apparatus is developed with the final molt. Throughout the period of growth each horseshoe crab molts sixteen or more times. The length of the growing period and the number of molts have been approximated by evidence from different sources. A female horseshoe crab was successfully reared in the laboratory at Wellesley College from 1935 to 1943. During these nine years this specimen shed its chitinous skin annually, and except for one cast that was lost, the series of casts is complete.[1] This animal was kept in a sheltered environment, and was well fed so that there is little reason to believe that it would have grown more rapidly in its natural environment. Further observations in the course of the field studies have indicated that after young horseshoe crabs attain the length of from four to five inches there is only one molting period and that this takes place in mid-summer.

BREEDING HABITS

Large numbers of horseshoe crabs appear on sandy beaches to mate and spawn during the early summer. In Barnstable Harbor the peak of the breeding season is usually reached during the third week in June. The first arrival of appreciable numbers of horseshoe crabs seems to depend on the general weather conditions. In 1949 in which there was a mild winter and spring, large numbers of mating horseshoe crabs were in the harbor throughout May. The winter of 1950 was also mild, but the spring was cold, and the animals arrived two weeks later than they did the previous year. However, the peak in the number of mating animals in both years was reached during the third week in June. A comparison of the weekly counts of horseshoe crabs in the harbor during the late summer shows that a greater number of adults were present in 1950 than in 1949. See Table III.

It has been reported that horseshoe crabs lay their eggs close to the high water line on a spring tide. These observations were made in regions where the mean range of tide is five feet or less. In Cape Cod Bay, the mean range of tide is about nine feet. Here, the egg nests that were found on the sandy beaches of Barnstable Harbor were near the mid-tide line, not near the upper reaches of the tide.

The usual mating behavior as observed along the Atlantic coastline, is for the horseshoe crabs to make their way to the beach in pairs, the male clasping the posterior margin of the female's abdomen with specialized claws. There are fewer females than males and the competition for a mate is keen. In 1949 the ratio of females to males was 1:1.53 and in 1950 it was 1:2.36 in Barnstable Harbor.

Each large female contains approximately a quart of eggs, which she may lay during one summer, making several nests on a tide and presumably returning to the beach on successive tides to lay more eggs. She digs shallow nests in the sand in which she deposits from two hundred to three hundred eggs. These eggs are fertilized during deposition by spermatozoa from the accompanying male, which are carried to the eggs by the water. As the tide ebbs, the mating pairs usually go down the beach with the receding tide and wander about the bottom, seemingly in search of food.

---

[1] Permission to study this excellent series of casts was obtained from Mrs. Margaret Houk, Curator of Museum, Zoology Department, Wellesley College, Massachusetts.

MIGRATORY HABITS

Adult horseshoe crabs were tagged in Barnstable Harbor for the purpose of determining their migrations and of estimating their populations. Tagging was accomplished by securing numbered celluloid discs to the body shield, or by threading colored poultry rings through a hole punctured near the pointed tips of the shield. The crabs, tagged with the serially numbered celluloid discs, were liberated in various parts of Barnstable Harbor primarily to determine the extent of their migrations outside the harbor. The tags were inscribed with a return address and notice of a reward to the finder. Notices in the local newspapers announced that tagged shorseshoe crabs had been liberated so that bathers and others frequenting the beaches would be on the lookout. Tagging with poultry rings of various colors was used to identify groups of horseshoe crabs liberated in different places or at different times. This procedure was designed primarily for a survey of the populations and movements of the horseshoe crabs within the harbor.

Naturally, more satisfactory returns were obtained within than without Barnstable Harbor. The team of investigators, with the cooperation of the Barnstable shellfish officers, brought over a thousand horseshoe crabs under observation. Thus the chances of finding tagged crabs in the harbor were much better than on the outer beaches where bathers and others seldom examine them closely.

Horseshoe crabs tagged and liberated within Barnstable Harbor have been reported on the beaches at East Sandwich and Dennis, twelve and eight miles away, respectively. One specimen was found on a beach near Wellfleet Harbor, twenty-one miles away, the longest distance traveled. See Table IV and Figures 2 and 3. These observations definitely established the fact that horseshoe crabs may leave Barnstable Harbor. Their appearance in the harbor in May and June and decrease in numbers in the late summer suggests a seasonal onshore and offshore migration, but with the present knowledge it is impossible to state whether or not all the horseshoe crabs leave the harbor during the winter.

TABLE III

WEEKLY COUNT OF ADULT HORSESHOE CRABS FOUND IN BARNSTABLE HARBOR, MASSACHUSETTS[2]

1949		1950	
Week of	Total Count	Week of	Total Count
May 1	—	May 1	—
8	158	7	—
15	221	14	20
22	475	21	324
29	141	28	485
June 5	703	June 4	730
12	889	11	847
19	1,008	18	1,310
26	220	25	291
July 3	530	July 2	488
10	263	9	565
17	79	16	448
24	129	23	587
31	61	30	688
Aug. 7	34	Aug. 6	199
14	37	13	218
21	13	20	20
28	5	27	12

---

[2] The weekly count reported above represents the total number of animals obtained during the bi-weekly surveys, and the weekly catch by officials of the Town of Barnstable.

FIGURE 2.

Chart of Barnstable Harbor

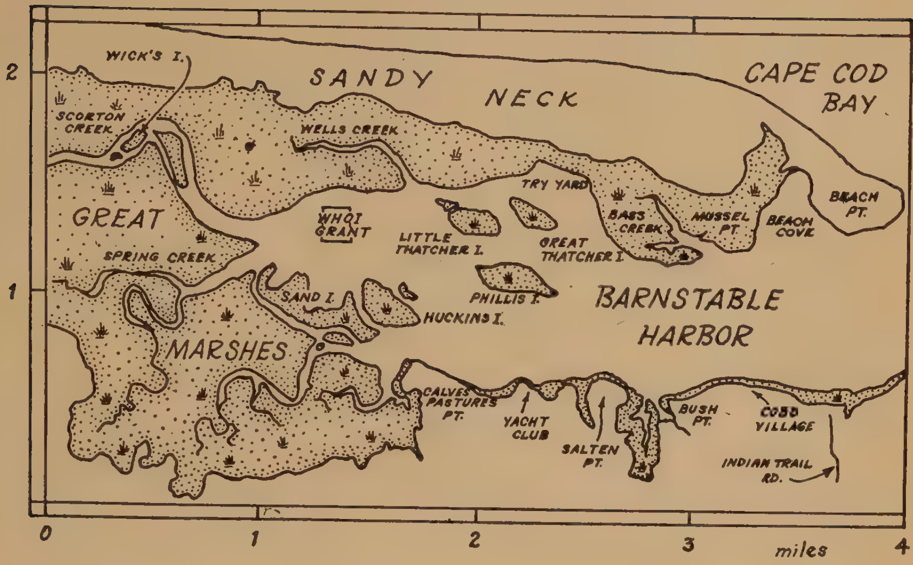
WICK'S I.
SANDY NECK
CAPE COD BAY
SCORTON CREEK
WELLS CREEK
TRY YARD
GREAT
WHOI GRANT
LITTLE THATCHER I.
GREAT THATCHER I.
BASS CREEK
MUSSEL PT.
BEACH COVE
BEACH PT.
SPRING CREEK
SAND I.
HUCKINS I.
PHILLIS I.
BARNSTABLE HARBOR
MARSHES
CALVES PASTURES PT.
YACHT CLUB
SALTEN PT.
BUSH PT.
COBB VILLAGE
INDIAN TRAIL RD.
2
1
0
1
2
3
miles
4

FIGURE 3.

Chart of Cape Cod Bay

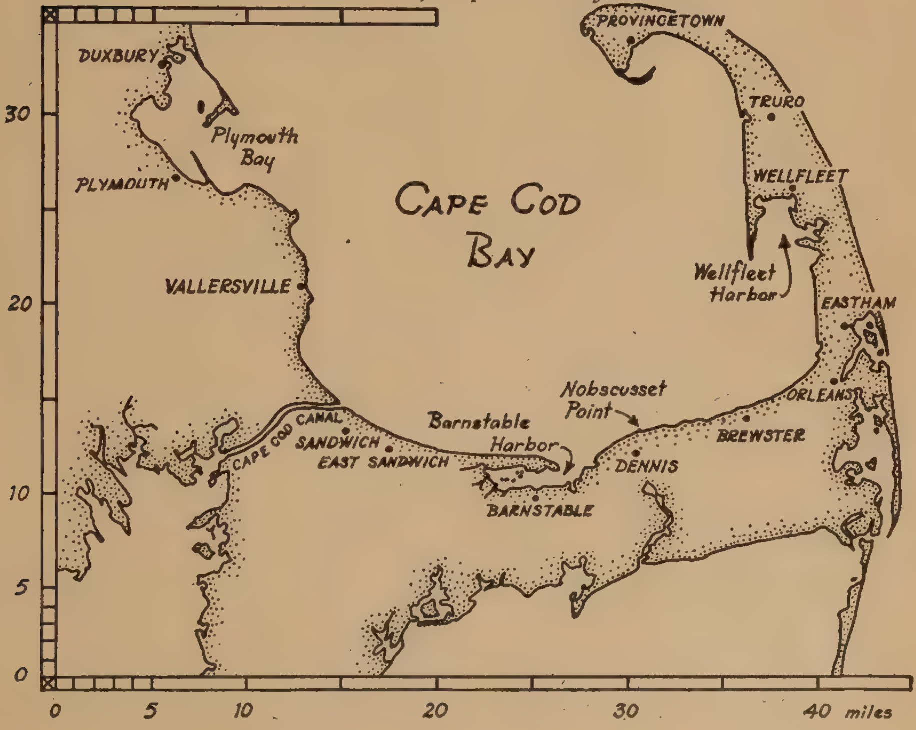
PROVINCETOWN
DUXBURY
TRURO
Plymouth Bay
PLYMOUTH
WELLFLEET
CAPE COD BAY
VALLERSVILLE
Wellfleet Harbor
EASTHAM
Nobscusset Point
ORLEANS
CAPE COD CANAL
Barnstable Harbor
BREWSTER
SANDWICH
EAST SANDWICH
DENNIS
BARNSTABLE
30
20
10
5
0
0
5
10
20
30
40 miles

RECORD OF ADULT HORSESHOE CRABS TAGGED WITH NUMBERED DISCS IN 1950

TABLE IV

DATE RELEASED	DATE FOUND	TIME ELAPSED	WHERE RELEASED	WHERE FOUND	MILEAGE (miles)	SEX OF ANIMAL	FATE OF TAGS
29 June 1950	27 July 1950	28 days	Blish Point	Sand Island	2.0	Male	Animal released again
11 July 1950	9 Aug. 1950	31 days	WHOI Grant	Huckins Island	0.9	Female	Animal released again
11 July 1950	10 Aug. 1950	32 days	WHOI Grant	East Sandwich	12.0	Female	Tags returned
12 July 1950	19 July 1950	7 days	Sand Island	Wick's Island	1.4	Male	Animal released again
12 July 1950	20 July 1950	8 days	Sand Island	Sand Island	0.0	Male	Animal released again
12 July 1950	20 July 1950	8 days	Sand Island	Sand Island	0.0	Male	Animal released again
12 July 1950	21 July 1950	9 days	Sand Island	Salten Point	1.3	Male	Tags returned
12 July 1950	24 July 1950	12 days	Sand Island	Sand Island	0.0	Female	Animal released again
12 July 1950	24 July 1950	12 days	Sand Island	Nobscusset Point	8.2	Male	Tags returned
12 July 1950	28 July 1950	16 days	Sand Island	Nobscusset Point	8.2	Male	Tags returned
12 July 1950	3 Aug. 1950	22 days	Sand Island	Sand Island	0.2	Male	Tags returned
12 July 1950	6 Sept. 1950	56 days	Sand Island	Sandwich	13.5	Male	Tags returned
20 July 1950	21 July 1950	1 day	Wick's Island	Wick's Island	0.0	Female	Animal released again
20 July 1950	21 July 1950	1 day	Wick's Island	Wick's Island	0.0	Female	Animal released again
20 July 1950	21 July 1950	1 day	Wick's Island	Wick's Island	0.0	Female	Animal released again
20 July 1950	21 July 1950	1 day	Sand Island	Sand Island	0.0	Female	Animal released again
20 July 1950	24 July 1950	4 days	Sand Island	Sand Island	0.0	Male	Animal released again
20 July 1950	3 Aug. 1950	14 days	Wick's Island	Sand Island	1.4	Female	Tags returned
20 July 1950	14 Sept. 1950	56 days	Sand Island	outside Wellfleet Harbor	21.0	Female	Tags returned
21 July 1950	4 Nov. 1950	106 days	Wick's Island	East Dennis Beach	11.3	Female	Tags returned

Movements within the harbor appeared to be directed inward or up-harbor during the early summer and seaward or down-harbor toward the end of the season. During the third week in June, the largest number of horseshoe crabs was observed along the southeastern shore, but by the middle of July the largest number was located at the head of the harbor. The crabs in this locality comprised both specimens which had previously been on the southeastern shore and those from other undetermined localities. By the last week in August, most of the crabs that were found were near the mouth of the harbor.

POPULATION ESTIMATE AND THE PROBLEM OF CONTROL

It is customary to estimate the size of aquatic populations by tagging. If a number of individuals are tagged and released in the area occupied by a population and a record is kept of both the number of individuals subsequently caught, and the number of tagged individuals that appear in the catch, it is assumed that the ratio of tag returns to the number originally tagged is the same as the number caught to the total number in the population. The accuracy of an estimate derived from calculating these ratios depends on the numbers in each category, the larger the numbers the more accurate the estimate.

In 1949 eight adult horseshoe crabs were recovered from 335 tagged specimens that were released in Barnstable Harbor, leaving three hundred and twenty seven individuals at large during the following winter. The investigators counted and examined one thousand six hundred and ninety three horseshoe crabs in 1950 and recovered eight more tags. The total 1950 population of adult horseshoe crabs calculated from these numbers is about seventy thousand. However, it is probably more accurate to consider the population as containing between fifty thousand and one hundred thousand adults because the number of recoveries was small.

A number of tags were returned from points outside the harbor but they were not included in the population estimate because the number of individuals examined in these areas was unknown. However, these returns established the limits of the migrations and suggested that the horseshoe crabs in Barnstable Harbor belonged to a group inhabiting the sector of Cape Cod Bay that lies between Sandwich and Dennis. The isolated return from Wellfleet suggested the possibility that the population had an even wider range. It may be concluded from this evidence that the horseshoe crabs of Barnstable Harbor belong to a population which inhabits a considerable portion of Cape Cod Bay and consists of fifty thousand to one hundred thousand adults.

The wide range of the population of horseshoe crabs in Barnstable Harbor makes local control difficult. If these crabs are limited to the harbor itself and depend on the maturation of locally produced young to maintain their population it may be possible to reduce their numbers by concentrating on both the young and adults. However, since this does not appear to be the case, it may be necessary to attack the entire population of a considerable portion of Cape Cod Bay. The difficulty and cost of destroying the vast numbers of horseshoe crabs that are required to materially reduce this population, and the question of the biological effectiveness of reducing natural populations by this means do not seem to warrant such attempts to control the horseshoe crab in isolated localities.

IV. INVESTIGATIONS OF THE SEA SCALLOP, *PECTEN GRANDIS*

BY

JULIUS ARTHUR POSGAY

INTRODUCTION

The sea scallop is one of the most important fishery resources of the Commonwealth of Massachusetts. The latest complete summary of commercial fishery statistics published by the Fish and Wildlife Service of the United States Department of the Interior shows that $6,278,808 worth of sea scallops were landed in Massachusetts during 1948. This figure represents almost 10% of the value of all fisheries products landed in the New England states during the same year. In spite of the economic importance of this fishery, little or no study has been given heretofore to the ecology of the mollusk upon which the fishery depends.

If a fishery is to be properly exploited and its yield maintained at the highest possible rate, year after year without danger of depletion and perhaps extinction, there are many things which must be known about the species which supports it. Ideally, this study should be carried out very early in the history of the fishery and before the effects of man's activities have so drastically modified the animal's environment that it is difficult if not impossible to ascertain just what conditions must exist if the fishery is to flourish.

Although the sea scallop fishery in general seems to be in a healthy state, there are signs of local depletion. It has been the object of this investigation to study the life history, growth rate, physiology and ecology of the sea scallop so that, if the need or demand for regulation of the fishery should ever arise, there would be a body of facts available upon which sensible regulations might be based.

NAME AND RANGE

The correct scientific name of the sea scallop is still in doubt although most modern taxonomists seem to have agreed upon *Pecten grandis* (Solander). Other names found in the literature are *Pecten magellanicus* (Gmelin) and *Pecten tenuicostatus* (Mighels). It is known to occur from Newfoundland (Morris, 1947) to Cape Hatteras (Chesnut, 1951). Characteristically, it is found most abundantly at depths of from 10 to 20 fathoms although it has been reported from 100 fathoms and in the northern part of its range even from just below the low tide mark.

THE SEA SCALLOP FISHERY

At present, the sea scallop fishery is most highly developed in the Gulf of Maine and the estuary of the St. Lawrence River. Beds are also known off the coasts of Long Island and New Jersey. The Massachusetts fishery depends upon the beds of scallops found in Cape Cod Bay and on Stellwagen and Georges Banks. The inshore fishery, Cape Cod Bay and Stellwagen Bank, is carried out by small boats based at Provincetown, Wellfleet and Orleans. Larger boats, based at Woods Hole and New Bedford, work on Georges Bank.

Within the areas in which they are known to occur, sea scallops are found to be concentrated into rather restricted patches. On the inshore grounds, these beds are usually about 100 yards wide and 200 to 300 yards long. Scallops taken from any single bed are usually so similar in size and general appearance that it seems likely that each bed is the result of a simultaneous mass settling of immature pelagic scallops. The location of these beds by the scallop fishermen is largely a hit or miss proposition. Various signs such as depth, type and contour of the bottom, presence or absence of other bottom-dwelling animals, are used to guide the search but the actual location of a bed is only achieved by making test dredgings. When a bed is located, an anchored buoy is thrown overboard to mark the spot and serious fishing begins. The fisherman who locates a new bed usually attempts to keep his discovery a secret but in a day or so the word spreads through the fleet and the other boats converge on the spot to take advantage of the new find.

The boats used for the inshore fishery of Cape Cod Bay and Stellwagen Bank are between 30 and 50 feet long. They do not generally remain at sea for more than ten or fifteen hours per trip. The small size of the boats forces the fishermen to return to port each night to sell their catch, renew their stores of fuel and ice and take shelter. Each boat carries one scallop dredge measuring from 7 to 9 feet across the mouth. Attached to it is a bag about 7 feet long made up of linked chain rings with an inside diameter of 3 inches. This dredge is dragged over the bottom on a steel wire cable which leads to a deck winch, driven by the boat's engine through a power take-off. The length of time for which the dredge is dragged depends upon each fisherman's judgement of the concentration of scallops on the bottom, the speed of the boat and the efficiency of his dredge. Quite often the haul contains more worthless stones, shells, sand dollars or sea urchins than sea scallops.

The dredge is brought to the surface and draped over the rail, mouth inboard. A hook is engaged in a ring on the lower end of the bag and the dredge is inverted so that its load is spilled on the deck. The scallops are picked out and thrown in a separate pile. All of the unwanted material which remains is disposed of by means of an ingenious carpet-like arrangement which covers the entire width of the deck and is nailed by one edge to the rail. After the haul has been culled, the free edge of the deck carpet is raised and the remaining debris slides over the side.

The only part of the scallop used for food at present is the large central adductor muscle; it is commonly called the "eye". This forms about 40% of the weight of the soft parts of the animal. There does not seem to be any good reason why the rest of the animal, called the "rim", should not be eaten as in the case of the clams and oysters. The margins of the mantle are rather tough but no more than the siphons (necks) of the soft shell clam. Many portions of the scallop are quite highly colored, and this may be regarded by some consumers as objectionable. The University of Massachusetts is presently conducting an investigation of the possibility of converting the parts of the scallop that are now wasted into a sandwich spread or similar product of marketable value.

The process of separating the marketable "eye" from the worthless shell and "rim" is generally carried out on shipboard during the time that the dredge is overboard and on the run in to port from the fishing grounds. A scallop is "shucked" by holding the animal in the left hand with the hinge toward the shucker's body. A knife, held in the right hand, is inserted between the shells and manipulated so as to remove the valve held uppermost, exposing the soft parts. The knife is slipped under the far edge of the mantle and the thumb pressed down so as to grasp it firmly; a twist of the wrist brings the "rim" free leaving the "eye" fast to the remaining shell. The "rim" is discarded, to the voluble pleasure of the ever-present cloud of gulls, and the "eye" is scraped into a bucket. Less frequently the fishermen bring the whole scallops into port in large bags to be shucked on shore.

The offshore fishery on Georges Bank is conducted in a manner similar to the inshore fishery. Since the boats are larger and more powerful, they usually fish two dredges with 11-foot bars. While one dredge is being hauled to the surface the other is being lowered to the bottom. The boats remain on the fishing grounds for 5 to 8 days and fish 24 hours a day, weather permitting. All scallops are shucked on board. A normal cruise takes from 10 to 14 days and lands from 12,000 to 15,000 pounds of shucked scallops.

MORPHOLOGY

SHELL

The sea scallop is the largest of our local bivalve mollusks, commonly attaining a diameter of from 150 to 175 mm. (6 to 7 in.). The valves of the shell are almost round in outline and unequally curved. One is almost flat and is usually white or near white in color; the other is moderately convex and is usually darker, varying from white through light reddish-brown to a very dark reddish-brown. Striping, banding, or a gradation of tone is not uncommon. The inner surface of both valves is glossy white. The hinge line, that portion of the valves where they are attached one to the other, is straight and the projecting "ears" formed by the hinge are equal in size. The outer surface of both valves is marked by two systems of very fine grooves. One system starts at the center of the hinge, the umbo, and radiates out to the margin of the shell in a fan-like pattern. The other system, superimposed on the radiating grooves, is a pattern of inscribed circles all tangent at the umbo.

The concentric grooves are the result of the manner in which the scallop enlarges its shell to keep up with the growth of its body. New shell is deposited by the mantle as a thin film over the entire inner surface of the valves. Since each film is slightly larger than the previous one, a tiny groove is formed between the old and the new margin. On any individual scallop, certain of these grooves are much deeper and more prominent than the rest. It had been assumed that these were the result of some annual phenomenon as the winter, the summer or the spawning season. A great number of shells of similar size, taken from the same location, were examined and their deep grooves, called rings, counted. The number per scallop varied from none to fifteen. Other observations have shown that individual scallops vary greatly in their response to various environmental factors. Rings have been produced experimentally by abruptly changing the water temperature, allowing the temperature to rise or fall to abnormal limits or removing scallops from the water for short periods of time. The reactions of all the animals under observation were never entirely alike. Circumstances which caused one scallop to put on a deep ring would leave only a faint trace on another. In the natural environment, scallops are subjected to many stresses. It is considered likely that the action of dredging over a bed of scallops causes some of the uncaught individuals to put on a ring. The severe storms of winter with their great waves creating disturbances on the bottom, and the turbulence of tidal currents are possibly the cause of still other rings. It thus seems unlikely that the rings exhibited by the Massachusetts sea scallops are of a strictly annual nature and give a measure of age and growth rate. They do, however, give a method by which scallops from the same bed can be recognized. Common experiences leave common marks and, while the degree of the marking is not the same in all cases, the pattern of marking is usually distinctive enough to be recognizable.

BODY

In the following description of the soft parts of the sea scallop, it shall be understood that the animal has been placed with the flat valve down and the hinge away from the observer. Removing the upper valve exposes a broad flap with the same outline as the valve. The central portion of this mantle lobe is a thin membrane but the margin is thickened and highly modified to form a broad ridge, the muscular velum, which supports numerous tactile tentacles and eyes. Normally the margins of the mantle, which may be retracted at will, are fully extended to the edge of the valve with the velum held at a right angle so as to meet the velum of the opposite mantel lobe. In this position, with valves agape, the two mantle lobes form and enclose a roomy chamber in which the body of the animal is suspended.

Removal of the mantle lobe exposes the visceral mass, which occupies most of the mantle chamber. The single large adductor muscle occupies a central position with the other organs disposed about it. Most conspicuous are large lacy structures, the gills, which absorb oxygen and strain food particles out of the water. Underneath the gill is found the gonad, a large, kidney-shaped organ. Both the gills and the gonad are fastened to the adductor muscle along the left half of its circumference. The mouth, a ruffled structure, is located on a line drawn from the center of the adductor muscle through the deep notch where the left "ear" joins the curved portion of the margin of the lower valve. Underneath the gonad are another gill and the other mantle lobe.

The foot is attached to the visceral mass near the mouth, on the side away from the hinge. In the adult it is not an organ of locomotion. It is a roughly cylindrical, comparatively slender structure with a cleft tip. The tip houses a large byssal gland, which secretes the substance used to form the byssal threads. The foot is flexibly muscular and capable of being extended or retracted. When a scallop wishes to attach itself, it extends the foot so that it protrudes through the notch in the left "ear" and applies the tip to some firm substance on the bottom. The secretion of the byssal gland adheres to the surface and the foot is withdrawn spinning a bundle of threads. In order to release itself, the scallop may at any time sever the byssal strands at the mouth of the byssal gland.

SPAWNING

The sexes of the sea scallop are separate, unlike the bay scallop, *Pecten irradians,* which has both male and female gonads in the same individual. The sex of any individual sea scallop may be determined by a superficial inspection of the gonad; in males it is a creamy-white color, while in females it is a bright coral red. The gonad of a gravid animal is firm and plump; that of an animal which has extruded all of its sexual products is thin and flaccid.

The time of year when the sea scallop spawns is, as yet, uncertain. Drew (1906) observed spawning in late August at Mt. Desert Island, Maine, after he had placed several specimens in a floating lobster car. Spawning was not completed in Cape Cod Bay during 1949 and 1950 until the first week in October. Before this date no completely spent animals were found, but subsequently almost all specimens examined showed the characteristic flaccid gonad. By the first week in January of the following year the gonads were once more firm and plump. At this time dissection showed motile sperm and apparently mature eggs. Attempts at fertilization were unsuccessful. In April, several scallops were fished from Cape Cod Bay and brought into the laboratory, where they spawned four days later. Many of the eggs were successfully fertilized and carried through several cleavage stages. Although the laboratory is not at present set up to attempt the extremely delicate task of rearing these larvae, it is intended that this be done at a later date.

There are three possible alternatives. Spawning could be a long drawn out process taking several months with only a small amount of sexual products expelled at any one time. Some scallop fishermen claim that spawning occurs in this manner from May to September. It seems unlikely that this is the case. From the scallop's point of view, it would be an extremely disadvantageous method. There would never be a high enough concentration of sperm and eggs in the water at one time to insure that any great percentage of the eggs should be fertilized. This is one of the great problems of any animal which, like the scallop, blindly casts it sexual products out into the water trusting to chance that an egg and a sperm should meet. All of the animals which reproduce in this manner, whose breeding habits are understood, meet the problem by spawning simultaneously in one great spasm. There is possibly a combination of these two extremes. There may be several preliminary spawnings during the summer followed by a final mass spawning in late summer.

The evidence, therefore, while inconclusive, seems to be in favor of a mass total spawning sometime in late September. Both Drew's August spawning and our April spawning in the laboratory can probably be explained as the result of the shock caused by removing the animals from the cold bottom water and placing them in relatively warm water. An artificial spawning, induced in this manner, has been reported by Belding (1910) for *Pecten irradians,* the bay scallop, and by Loosanoff (1950) for *Ostrea Virginica,* the oyster, *Venus mercenaria,* the quahog, and *Mya arenaria,* the soft-shell clam. By placing ripe individuals of these species in water heated to normal summer temperatures, it has been possible to obtain viable larvae some months before natural spawning occurs.

LARVAL LIFE

Once the egg has been fertilized, a complicated series of events leads to the eventual development of a miniature replica of an adult scallop. This larval development of the sea scallop has never been completely observed, but is probably very similar to that of the bay scallop which has been described by Belding (1910). The bay scallop spends from 10 to 12 days passively floating or feebly swimming about in the water. It then settles to the bottom and loses its ability to swim. During this stage it can move along the bottom to a limited degree by action of its relatively large foot. It also can maintain its position by attaching itself to any firm substance on the bottom by means of byssal strands. These strands may be severed at will and once more the scallop may be free to move. After a few days of further development it regains the ability to swim but this time in the adult manner, by clapping its valves and forcing out two jets of water, one on either side of the hinge. The sea scallop retains the ability to attach itself to the bottom by byssal strands for some time. The presence of the byssus has been observed repeatedly in animals up to 90 mm. (3½ in.) in diameter.

The steps described above are characteristic of many marine animals. Almost certainly, the sea scallop differs from the bay scallop in the length of time necessary for the completion of the sequence of events. This is, of course, extremely important. Until the duration of the pelagic larval stage of the sea scallop is known, no prediction of the fate of the spawn produced by any particular bed of scallops can be made. According to the best available estimates (Redfield, 1941), Stellwagen Bank is swept by a non-tidal current which may average seven miles per day. Obviously, therefore, these beds cannot be self-reproducing. Where then, does their spawn settle, from whence were they populated? At present it seems probable that any larval sea scallops which settle out on Stellwagen bank are the result of spawning somewhere along the Maine coast. The spawn from Stellwagen is probably carried out toward Georges Bank. Georges Bank is probably a self-reproducing area, since in late summer it is the site of a large circular eddy that would tend to confine the larvae to this bank.

Like the clam and the oyster, the sea scallop feeds upon microscopic organic particles, both living and dead, which are found suspended in the surrounding water. It obtains these particles by straining them out of a current which is created within the mantle chamber by the beating of thousands of tiny hair-like filaments, cilia, lining all the inner surfaces of the chamber. In its normal position, the scallop rests upon the bottom with the flat valve down and the valves agape. The velum of each mantle lobe is extended with the free edge of one firmly pressed against that of the other throughout most of the periphery so as to form a solid wall with two openings, one alongside of each "ear". Water passes in through one of these openings, over and through the gills and out through the other opening. The gills possess glands which secrete a sticky mucus to which the food particles in the water adhere. Numerous cilia tracts on the gills carry the mucus, together with the entrapped particles, to the mouth where the entire mass is swallowed. The anal papilla is located near the opening through which the current leaves the mantle chamber. Thus the current which brings in food and oxygen also serves to carry the feces away from the animal.

HABITS

Although scallops are found on all types of bottom, the most successful beds seem to be those on rather loose sand. Fishermen hunting new beds look for depressions in a level surface, the edge of a shoal or places where a sloping surface becomes steeper. Whether the animals actively seek such places or are concentrated there by currents is uncertain. The remarkable swimming powers of the scallop are a direct result of its ability to adjust and control the outer margins of the mantle lobes. The valves are first opened wide and then the velum edges are pressed firmly together along the entire periphery except for two small ports which are formed alongside of each "ear". A strong, swift contraction of the powerful adductor muscle forces a jet out of each port and propels the scallop through the water with the hinge aft. Each clap of the valves results in about six inches of travel. Small immature scallops, which seem to swim about more than the larger and older animals, have been observed to make flights of eight to ten feet with a series of these clapping motions.

GROWTH

The age and growth rate of many bivalve mollusks can be successfully determined by counting annual rings and measuring the distance between them. As noted above, this method is not applicable to the sea scallops of Massachusetts. The alternative method of repeated examination and measurement of samples taken from the same population is almost an impossible procedure, since under the present method of conducting the fishery no located scallop bed remains in existence long enough to be studied. This procedure, however, was successfully carried out in one instance. A number of small scallops, averaging 44 mm. in length (greatest diameter from umbo to margin), was dredged from Cape Cod Bay in December 1949 and brought into the laboratory. Since these scallops were so small they were safe from commercial dredging. Another sample was obtained in August 1950. At this time the average length was 80 mm., an increase of 36 mm. in 33 weks. It has not been possible to obtain another sample since this bed has now been fished out.

Further information on the rate of growth has been obtained from scallops kept in the laboratory. These measurements show that the rate of growth is correlated with the temperature. The animals grew most rapidly at about 6° C. (43° F.) The growth gradually declined as the temperature increased until it ceased at 19° C. (66° F.) At 23° C. (74° F.) all of the scallops under observation died. Data for temperatures below 6° C. is, as yet, inconclusive, but a decline in the growth rate is indicated.

By properly combining the growth rate observed in the laboratory with the yearly temperature cycle of Cape Cod Bay and the 36 mm. growth shown by the dredged samples, a yearly growth rate of about 40 mm was calculated. It would thus seem that the December 1949 sample of 44 mm was about 14 months old and the August 1950 sample of 80 mm about 22 months old. An animal occasionally turns up with definite ridges in its valves that are probably yearly check marks. A study of these few shells has indicated that increase in length per year is approximately equal for the first three years; the rate drops off some in the fourth year and again in the fifth year. On the basis of the evidence given above, a tentative scale of the average length to be expected of scallops growing in Cape Cod Bay at various ages has been calculated. This data, together with the average weight of the adductor muscle and the number of scallops required to yield a pound of marketable meat is given in Table V.

TABLE V

AGE	LENGTH	WEIGHT OF EYE	NO. OF EYES PER POUND
1 year	40 mm.	1 gm.	454
2 years	80 mm.	13 gm.	35
3 years	110 mm.	22 gm.	21
4 years	130 mm.		
5 years	140 mm.		

BIBLIOGRAPHY

BELDING, DAVID L., 1910: The Scallop Fishery of Massachusetts. Com. of Massachusetts.

CHESNUT, A. F., 1951: The Oyster and Other Mollusks in North Carolina. Survey of Marine Fisheries of North Carolina, Univ. of North Carolina Press.

DREW, GILMAN A., 1906: The Habits, Anatomy, and Embryology of the Giant Scallop, *(Pecten tenuicostatus, Mighels)*. Univ. of Maine Studies, No. 6.

LOOSANOFF, VICTOR L. and DAVIS, HARRY C. 1950: Conditioning *Venus mercenaria* for spawning in winter. Biol. Bull., vol. 98, No. 1.

MORRIS, PERCY A., 1947: A Field Guide to the Shells. Houghton Mifflin Company, Boston.

REDFIELD, ALFRED C., 1941: The effect of the circulation of water on the distribution of the calanoid community in the Gulf of Maine. Biol. Bull., vol. LXXX, No. 1.

V. GROWTH OF THE NORTH PACIFIC OYSTER, *OSTREA GIGAS,* IN MASSACHUSETTS

BY

HARRY J. TURNER, JR.

A small bed of North Pacific Oysters, *Ostrea gigas,* has been maintained in Barnstable Harbor since March 1949 in order to determine if this species can be adapted satisfactorily to the waters of Massachusetts Bay, where, except in Wellfleet Harbor, the eastern oyster is not reared commercially. The bed originated from six bushels of seeded culch which was obtained from Seattle, Washington after careful inspection to insure the absence of foreign predators. During the first summer the oysters grew well on an intertidal flat and increased five-fold in volume. Fifteen bushels were transferred to deep water in Barnstable Harbor in the fall of 1949 to prevent damage from winter ice. The remaining fifteen bushels were kept in sea-water tanks at the Woods Hole Oceanographic Institution. In the early summer of 1950 all the oysters were returned to the intertidal flat. Those which had been in the deep water showed good growth and little mortality, but those which had been kept in the tanks grew less and most of them died during the transfer because of faulty storage. By the end of the summer of 1950, the survivors had doubled in volume so that they amounted to approximately thirty bushels when returned to the deep water in the fall.

During the year and a half that these oysters were in Barnstable Harbor they grew from spat averaging half an inch long to an average length of five inches. Most of the oysters were rather elongated because they were allowed to grow in clusters, but the bodies were deep and the meats were firm and plump. Spawning was experimentally induced during the first summer in a small group held in the laboratory, but there was no evidence that it occurred in the field during either summer, and no set was observed in any part of the harbor.

This species appears to be well adapted for growth on the north side of Cape Cod and probably it will grow well even farther north. Its rapid growth and ability to survive in the tidal zones makes it especially advantageous in this region. However, it can only be of commercial value if it can be made to propagate, since the cost of importing seed from the West Coast is prohibitive.

Contribution No. 568

Reprinted from JOURNAL OF METEOROLOGY, Vol. 8, No. 5, October, 1951, pp. 354-356
Printed in U. S. A.

THE ONSET OF RAIN FROM CUMULI

By Patricia A. Langwell

CONTRIBUTION NO. 568 FROM THE
WOODS HOLE OCEANOGRAPHIC INSTITUTION

SHORTER CONTRIBUTIONS

THE ONSET OF RAIN FROM CUMULI

By Patricia A. Langwell

Woods Hole Oceanographic Institution and New York University

(Original manuscript received 23 March 1951; revised manuscript received 26 May 1951)

Introduction.—The study of the life cycle of a cumulus cloud has been greatly advanced by the Thunderstorm Project. In the final report of this project (U. S. Dept. Commerce, 1949) and elsewhere, the three stages in the life cycle of a cell are discussed: the cumulus stage, when the cloud is growing; the mature stage, when both up- and down-drafts are present in the cell (but rain *need not* be falling); and the dissipating stage, when downdrafts are present throughout the cell. The purposes of this study are to show from which region of the cell rain will first fall and to suggest a mechanism by which the cell passes from the first to the second stage of development.

Coordinates.—The problem is considered in two dimensions. The x axis is oriented in the direction of the wind at the cloud base (where $z = 0$) and the z axis is vertical. The origin is located at the windward edge of the cloud base, and the coordinate system is moving with the speed of the wind at $z = 0$. Then, if w is the vertical velocity of a particle in the cloud,

$$\frac{dw}{dt} = \frac{\partial w}{\partial t} + u\frac{\partial w}{\partial x} + w\frac{\partial w}{\partial z}, \qquad (1)$$

where u is the horizontal velocity of the cloud, relative to the moving coordinates. The wind field is projected on the x-z plane, and a linear wind shear h is assumed. The assumption is made that the momentum is conserved as the cloud rises. Then (Malkus, 1949)

$$u = Khz^2/2(1 + Kz), \qquad (2)$$

where K is the percentual rate of entrainment. Since $K > 0$, u has the same sign as h.

Statement of problem.—The cloud will pass from the cumulus stage to the mature stage when the upward forces on a particle of the cloud are less than the downward forces. This will enable the rain to fall, relative to the earth, and drag air down with it. This statement of the problem, while hypothetical, has been endorsed by other writers in the field. (U. S. Dept. Commerce, 1949; Brooks, 1922)

The upward force on the particle is $\rho_c\,dw/dt$, the product of the density of the cloud air ρ_c and the acceleration of the cloud. The downward forces are the gravitational, frictional and pressure-gradient forces. It is assumed that the gravitational force acts more strongly on the liquid water in the cloud than on the vapor, and that the drops are falling at terminal velocity. If the forces are considered as acting in the $-z$ direction, they are positive.

The cloud will pass to the mature stage when

$$\rho_c\left(\frac{\partial w}{\partial t} + u\frac{\partial w}{\partial x} + w\frac{\partial w}{\partial z}\right) < \text{a non-negative number.} \qquad (3)$$

The vertical velocity is assumed sinusoidal in x, to approximate the jet-like basic motion. The horizontal extent of the cell is assumed to have reached its maximum at a distance π/α. The rise and fall of the cloud top is also assumed to be sinusoidal, as indicated by the term $\sin \beta t$. This is an approximation which ignores the short-period variation (Workman and Reynolds, 1949). The time from the first appearance of the cloud until its final disappearance is π/β. The amplitude of the vertical velocity is a function of height, which depends on the instability of the surrounding air. It has a positive value at $z = 0$, increases up to some height z_1, which might be the level at which the adiabat of the rising air crosses the sounding, and then decreases to zero at the cloud top. Then

$$w = A(z) \sin \alpha x \sin \beta t. \qquad (4)$$

If assumption (4) is substituted into inequality (3), it is found that

$$A(z)[\beta \cos \beta t \sin \alpha x + u\alpha \cos \alpha x \sin \beta t + \sin^2 \alpha x \sin^2 \beta t\, dA/dz] < (\text{a non-negative number})/\rho_c. \qquad (5)$$

If the cloud reaches its maximum height at its half life (see, for example, U. S. Dept. Commerce, 1949, fig. 79), the height is a maximum as the time approaches $\pi/2\beta$, when $\sin \beta t \approx 1$ and $\cos \beta t \approx 0$. If this assumption is incorporated into (5), the inequality becomes

$$A(z)[u\alpha \cos \alpha x + \sin^2 \alpha x\, dA/dz] < (\text{a non-negative number})/\rho_c. \qquad (6)$$

Since the right-hand member is always positive, the inequality will hold for all points at which the left-hand member is negative. Since $A(z)$ is always positive, the inequality will hold if

$$u\alpha \cos \alpha x + \sin^2 \alpha x\, dA/dz < 0. \qquad (7)$$

The second term is negative for all heights above z_1.

bove this height, the cloud is decelerating. Since u as the same sign as the wind shear, the first term is egative near $x = 0$ for negative wind shear, and near = π/α for positive wind shear.

Therefore, if rain can first fall from that area in hich inequality (3) holds, it will fall if the cloud top as started to decelerate, from the forward edge of the et (which would not correspond to the forward edge f the cloud at that level) if the wind shear is positive, nd from the trailing edge if the wind shear is negative. there is no wind shear, rain is most likely to fall rst from any edge.

This discussion also makes clear several reasons why ain does not fall from all cumuli. Not all reasons are xplicit in the inequality. If the instability is slight, e cloud top will be low. As a result, even though ain falls, there may not be enough water drops present reach the ground. If the wind shear is large, the oud will blow off the jet. If the length of time during hich the jet is effective is short (β is small), the cloud rowth is inhibited. The cause of a short period may e the stability, or it may depend on the horizontal elocity of the wind, since a large velocity will move e air too rapidly to allow thorough heating of any ven small air-parcel at the surface. It might be entioned that the theory does not hypothesize an itial downward motion, but a deceleration.

Verification.—To test the theory, it is necessary to now the wind field and the area in which rain first ll. A forecast is made on the basis of the wind shear lative to the direction of motion, and this is matched ith the verification.

Sixteen cells are described in *The thunderstorm*. Of ese, three were in the mature stage when they ap- roached the network; four never passed over the twork, so that it is impossible to tell whether rain ll from the clouds. Nine cells remain. It is impossible identify the first rain from five of these, either ecause of the proximity of a stronger cell, or because e cell was not entirely over the network when rain st fell. As a result, only four cells were completely er the network when first rain, which could be cribed to them, fell. A forecast was made from the eory for each of these cases. The forecast gave a escent-shaped area at the edge of the cloud in which in was expected. If the first rain fell anywhere out- le of the crescent, it was considered not to verify. l four of the cells described above verified the theory. e probability of this number of verifications by pure ance, P_r, can be calculated (Sokolnikoff, 1941).

$$P_r = \sum_{s=r}^{n} \frac{n!\, p^s (1-p)^{n-s}}{s!\,(n-s)!},$$

ere p is the probability of occurrence, and there are cases, of which r are successful. Since the forecast her verifies or fails to verify, $p = 1/2$ and $P_r = 2^{-4} = 0.06$. If the uncertain cases are included, of which 3 appeared to verify and 2 did not, the probability (of as many as 7 out of 9) becomes 0.09. The verifications are itemized in table 1.

TABLE 1. Summary of verifications.

July 9, 1946	NW wind, negative shear
Cell I	mature
Cell II	no record of rain
Cell III	mature
Cell IV	verifies
Cell V	verifies
August 6, 1947	N wind, positive shear
Cell I	no record of rain
Cell II	verifies
August 13, 1947	SW wind, negative shear
Cell I	uncertain; possibly not good
Cell II	uncertain; probably good
August 14, 1947	SW wind, negative shear
Cell I	mature
Cell II	verifies
Cell III	uncertain; probably not good
Cell IV	uncertain; possibly good
Cell V	uncertain; possibly good
August 17, 1947	W wind, negative shear
Cell I	no record of rain
Cell II	no record of rain

This is not a satisfactorily large sample, but due to the scarcity of such material, and because the chance of the verification is less than 10 per cent, the sample has been considered as adequate.

The distortion of the cloud, due to the wind shear, would tend to make the raindrops fall in the area forecast. With positive wind shear, a raindrop starts to fall with a forward velocity relative to the moving coordinate system. The terminal velocity of large drops (Gunn and Kinzer, 1949) is 18 to 25 ft/sec. It is reasonable to assume that the first drops to fall are those of greater mass. At these terminal velocities, a drop takes 6 to 9 min to fall 10,000 ft. The wind shear through this height interval, for the storms described by the Thunderstorm Project, varies between 5 and 15 mi/hr. For a shear of 10 mi/hr per 10,000 ft, the drop has a motion through the cloud of 1 to $1\frac{1}{2}$ mi. Since the cells are at least three miles in diameter and over four miles on the average, it is unlikely that the position of the drop would change from an area of non-verification to an area of verification.

Conclusions.—This model, although obviously simplified, contains a measure of the effects of the strength of the initial jet of the cloud $A(0)$, the distortion of the cloud due to the wind field, the entrainment of unsaturated air into the cloud (both contained in u), the instability of the atmosphere $A(z)$, and the weight of the raindrops.

Within these limitations, it has been found possible to forecast the area of first rain from a cumulus cloud from the wind field, and it is suggested that the mechanism described is the method by which the cloud passes to the mature stage.

REFERENCES

Brooks, C. F., 1922: The local, or heat, thunderstorm. *Mon. Wea. Rev.*, 50, 281–287.

Gunn, R., and G. D. Kinzer, 1949: The terminal velocity of fall for water droplets in stagnant air. *J. Meteor.*, 6, 243–248.

Malkus, J. S., 1949: Effects of wind shear on some aspects of convection. *Trans. Amer. geophys. Union*, **30**, 19–25.

Sokolnikoff, I. S., and E. S. Sokolnikoff, 1941: *Higher mathematics for engineers and physicists.* New York, McGraw-Hill, 587 pp.

U. S. Dept. Commerce, 1949: *The thunderstorm.* Washington, U. S. Govt. Printing Office, 287 pp.

Workman, E. J., and S. E. Reynolds, 1949: Time of rise and fall of cumulus cloud tops. *Bull. Amer. meteor. Soc.*, **30**, 359–361.

Contribution No. 573

BULLETIN OF THE GEOLOGICAL SOCIETY OF AMERICA
VOL. 62, PP. 1381-1384, 3 PLS. DECEMBER 1951

OCEAN-BOTTOM PHOTOGRAPHS OF THE NERITIC AND BATHYAL ENVIRONMENT SOUTH OF CAPE COD, MASSACHUSETTS

BY JOHN NORTHROP

ABSTRACT

Ocean-bottom photographs and core samples, taken south of Cape Cod along a profile normal to the bathymetric contours, show definite changes in bottom markings, benthonic forms, and sediments. The different types of environment indicate a division into five major zones for which typical bottom photographs are presented.

CONTENTS

TEXT

	Page
Abstract	1381
Introduction	1381
Previous work	1381
Description of zones	1381
Zone 1	1381
Zone 2	1382
Zone 3	1382
Zone 4	1382
Zone 5	1382
Summary	1383
References cited	1383

ILLUSTRATIONS

Plate	Facing page
1. Ocean-bottom photographs	1382
2. Ocean-bottom photographs	1383
3. Location of stations	1384

INTRODUCTION

The Ewing under-water camera (Ewing *et al.*, 1946a), modified to obtain a short core simultaneously with the bottom photograph, was used. The first traverse consisted of 53 bottom stations spaced about 2 miles apart (Pl. 3). Acknowledgment is made to the officers and crew of the Research Vessel BALANUS and to the Woods Hole Oceanographic Institution; to B. C. Heezen and J. I. Ewing who worked with the author in obtaining the data; to W. M. Ewing and J. L. Worzel who directed the program; to G. P. Woollard and H. C. Stetson for their valuable advice; and to the Bureau of Ships, U. S. Navy, through which this work was made possible.[1]

PREVIOUS WORK

Ocean-bottom photographs of marine sedimentary conditions have been made by Ewing *et al.* (1946a; 1946b), Shepard and Emery (1946), Shepard (1949), and by Northrop and Heezen (1951). Mechanical analysis of sediments was made by the combination wet-sieve and pipette method described by Stetson (1938), to which sodium oxylate was added to deflocculate the finer fraction. Median and quartile measurements were taken from the cumulative frequency curves, and values were calculated for skewness and sorting index (Krumbein and Pettijohn, 1938).

DESCRIPTION OF ZONES

Zone 1

The near-shore end of the traverse is an area of reworked gravel, from which the finer material had been washed away by wave and current action. Figure 1 of Plate 1 shows that the remaining rock fragments are poorly sorted and well rounded, but their large size prevented recovery of any samples. This zone persists 35 miles out to sea into water 80 meters deep and is probably made up of glacial moraine.

---

[1] Work done under U. S. Navy contract NOBsr 9092.

Zone 2

This narrow zone of silts and sands extends from 35 to 45 miles off shore in 80–90 meters of water. The bottom was so compact that the coring tube penetrated only the top 5 cm of sediment which shows a good sorting index of 1.2–2.0. Figure 2 of Plate 1 shows that this zone has competent transporting currents as the shells are overturned and partly covered with sediment. Other photographs in this zone show other shells concave upward and partly filled with sediment. The attitude of the shells does not indicate current action in itself, as numerous starfish shown in the photograph undoubtedly disturb the shells. The relatively hard bottom, good sorting, and presence of sediment in the shells indicate winnowing action and movement of sediment over the bottom.

Zone 3

This is a wide zone of soft mud from 45 to 75 miles off shore out to the 100-meter bathymetric contour. In this zone the median slips from .15 mm to .05 mm, the material contains 70–80 per cent silt, is better sorted at the surface, but the mode lies on the coarse side of the median partly because of the abundant shell fragments shown in the photograph. The surface layer is coarser, with the fines winnowed out, and a contemporaneous unconformity is in the making. Typical photographs of the mud zone show large shell fragments on a muddy bottom that has been stirred up by the coring tube in addition to numerous pock marks and a burrowing of about a 6-inch radius. The starfish, so abundant in adjoining zones, are absent as is the criss-cross pattern of trails; the latter may be obscured by movement of silt along the bottom.

Zone 4

This extraordinary zone crowns the break in slope from 75–85 miles off shore in 110–200 meters of water. The median rises to .16 mm, the sorting averages 1.5, the skewness approaches unity, and the amount of silt falls to 20 per cent. The material is so well compacted that the coring tube penetrated only a few centimeters. Bottom photographs in this zone (Pl. 2, fig. 1) show its pock-marked character with numerous starfish and shell fragments, but no ripple marks. This bears out Stetson's suggestion (1934) that the material was laid down as an eolian deposit at a time of lower sea level and not by present-day currents sweeping around Cape Cod (Alexander, 1934). The lack of material above the sand indicates nondeposition in the area since the rise in sea level.

Zone 5

The seaward end of the traverse continues down the continental slope into 200–800 meters of water 85–110 miles off shore. The median falls off sharply to .05 mm, the sorting ranges from 1.5 to 4.5, and the mode climbs to the fine side of the median as the amount of silt rises to 90 per cent. The material in each sample is quite distinctive; sometimes the surface silt is better sorted than the subsurface, and sometimes not so well sorted. This is taken as further evidence of mixing and slumping down slope, similar to that described in near-by areas (Phleger and Hamilton, 1946; Stetson, 1949; Northrop and Heezen, 1951). Figure 2 of Plate 2 shows a distinct hummocky type of bottom so characteristic of landslide areas. In addition it shows that sea anemonies are the most abundant form of life. It also shows numerous elongate gouges on the bottom, thought to have been formed by fish which have brushed against the bottom.

PLATE 1.—OCEAN-BOTTOM PHOTOGRAPHS

FIGURE 1.—IN 25 METERS OF WATER, SHOWING HARD GRAVEL BOTTOM AND ROUNDED ROCK FRAGMENTS

Station D-2; Latitude 41°12′ N.; Longitude 70° 59′ W.; flash bulb #5; camera to light 43″, camera to bottom 77″, focus 4.5′; stop f.9, shutter speed 1/25 sec.

FIGURE 2.—IN ZONE 2 SHOWING STAR FISH, SHELL FRAGMENTS, AND GRANULAR-APPEARING BOTTOM IN 40 METERS OF WATER

Station D-7; Latitude 40°48′ N.; Longitude 70°56′ W.; camera setting same as Figure 1.

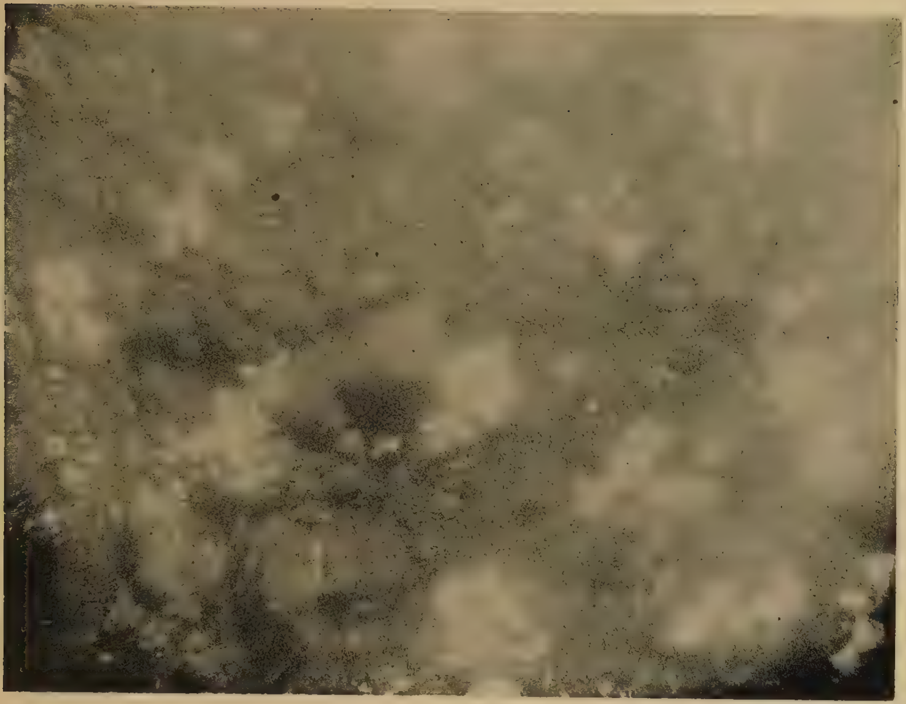

FIGURE 1

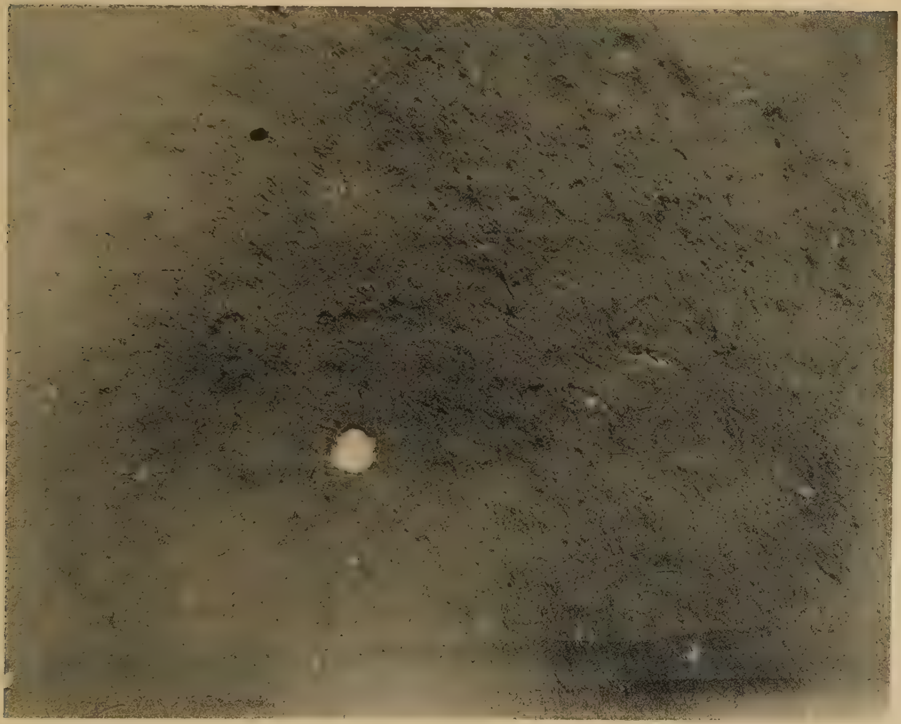

FIGURE 2

OCEAN-BOTTOM PHOTOGRAPHS

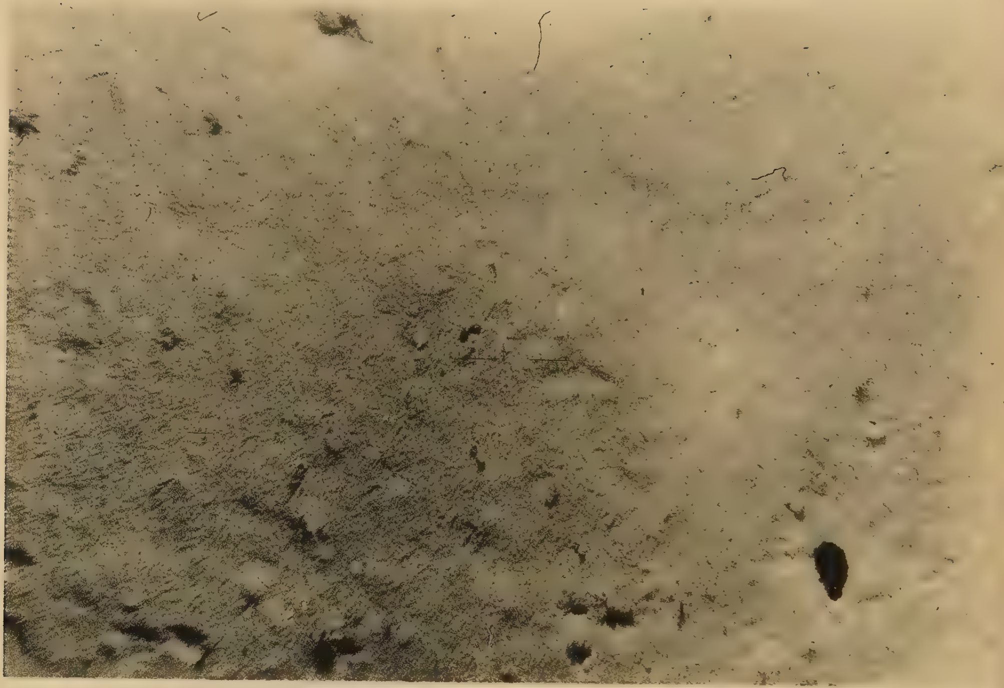

Figure 1

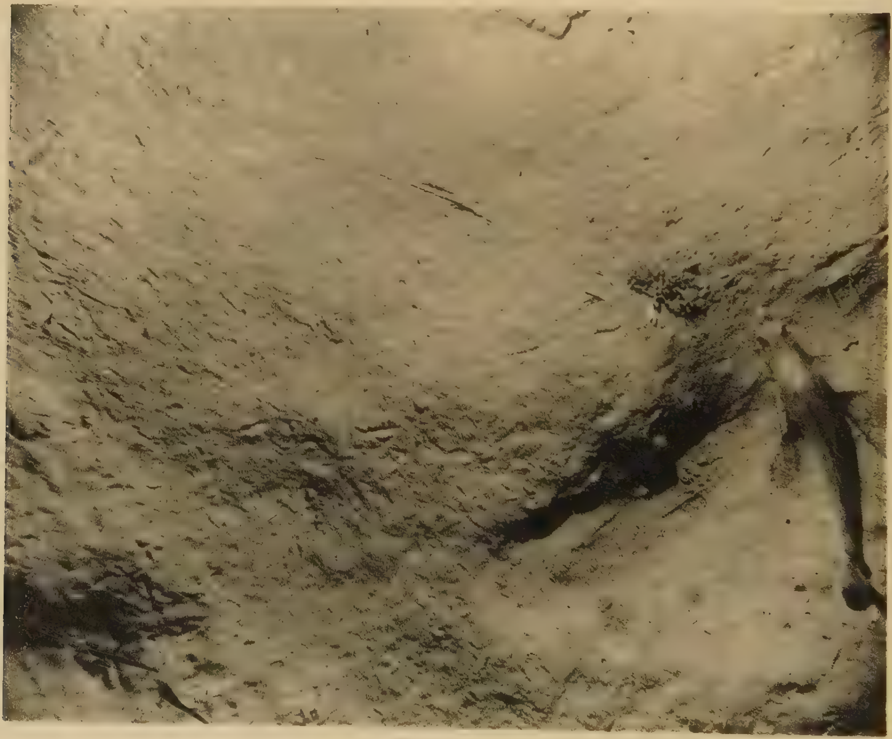

Figure 2

OCEAN-BOTTOM PHOTOGRAPHS

SUMMARY

Both the neritic and bathyal districts are areas of nondeposition; the former is an area of winnowing action, and the latter an area of landslides and slumping. The material being reworked is residual from a former period, and the life supported in the various zones seems to be controlled by the type of sediment in addition to depth of water. Geologists can use features photographed on the bottom in determining the sedimentary environment of rock facies in which such phenomena are preserved.

REFERENCES CITED

Alexander, A. E. (1934) *A petrographic study of some Continental Shelf sediments,* Jour. Sedim. Petrol., vol. 4, no. 1, p. 12–23.

Ewing, M., Vine, A., and Worzel, J. L. (1946a) *Photography of the ocean bottom,* Opt. Soc. Am., Jour., vol. 36, no. 6, p. 307–321.

—— (1946b) *Recent results in submarine geophysics,* Geol. Soc. Am., Bull., vol. 57, p. 902–934.

Grabau, A. W. (1913) *Principles of stratigraphy,* A. G. Seiler & Co., New York, 643 pages.

Krumbein, W. C., and Pettijohn, F. J. (1938) *Manual of sedimentary petrology,* D. Appleton-Century Co. Inc., New York.

Northrop, J., and Heezen, B. C. (1951) *An outcrop of Eocene sediment on the Continental Slope,* Jour. Geol., vol. 59, p. 396–399.

Phleger, F. B, and Hamilton, W. A. (1946) *Foraminifera of two submarine cores from the North Atlantic Basin,* Geol. Soc. Am., Bull., vol. 57, p. 951–966.

Shepard, F. P. (1949) *Terrestrial topography of submarine canyons revealed by diving,* Geol. Soc. Am., Bull., vol. 60, p. 1597–1612.

—— and Emery, K. O. (1946) *Submarine photography off the California coast,* Jour. Geol., vol. 54, p. 306–321.

Stetson, H. C. (1934) *Origin and limits of a zone of rounded quartz sand off the southern coast,* Jour. Sedim. Petrol., vol. 4, no. 3, p. 152–153.

—— (1938) *The sediments of the Continental Shelf off the eastern coast of the United States,* in *Papers in Physical Oceanography and Meteorology,* Mass. Inst. Tech. and Woods Hole Oceanog. Inst., vol. V, no. 4, p. 5–48.

—— (1949) *Sediments and stratigraphy of the east coast Continental Margin; Georges Bank to Norfolk Canyon,* in *Papers in Physical Oceanography and Meteorology,* Mass. Inst. Tech. and Woods Hole Oceanog. Inst., vol. 11, no. 2, p. 5–60.

BATES COLLEGE, LEWISTON, MAINE

MANUSCRIPT RECEIVED BY THE SECRETARY OF THE SOCIETY, JANUARY 17, 1951

CONTRIBUTION NO. 573, WOODS HOLE OCEANOGRAPHIC INSTITUTION

CONTRIBUTION NO. 36, LAMONT GEOLOGICAL OBSERVATORY

PLATE 2.—OCEAN-BOTTOM PHOTOGRAPHS

FIGURE 1.—IN ZONE 4 SHOWING POCK MARKS AND ABSENCE OF RIPPLE MARKS 110 METERS OF WATER Station D-32; Latitude 40°13′N.; Longitude 70°50′ W.; camera setting same as in Plate 1.

FIGURE 2.—IN ZONE 5 SHOWING GOUGES IN BOTTOM AND ANIMAL LIFE IN 700 METERS OF WATER Station D-26; Latitude 39°55′ N.; Longitude 70°51′ W.; camera setting same as in Plate 1.

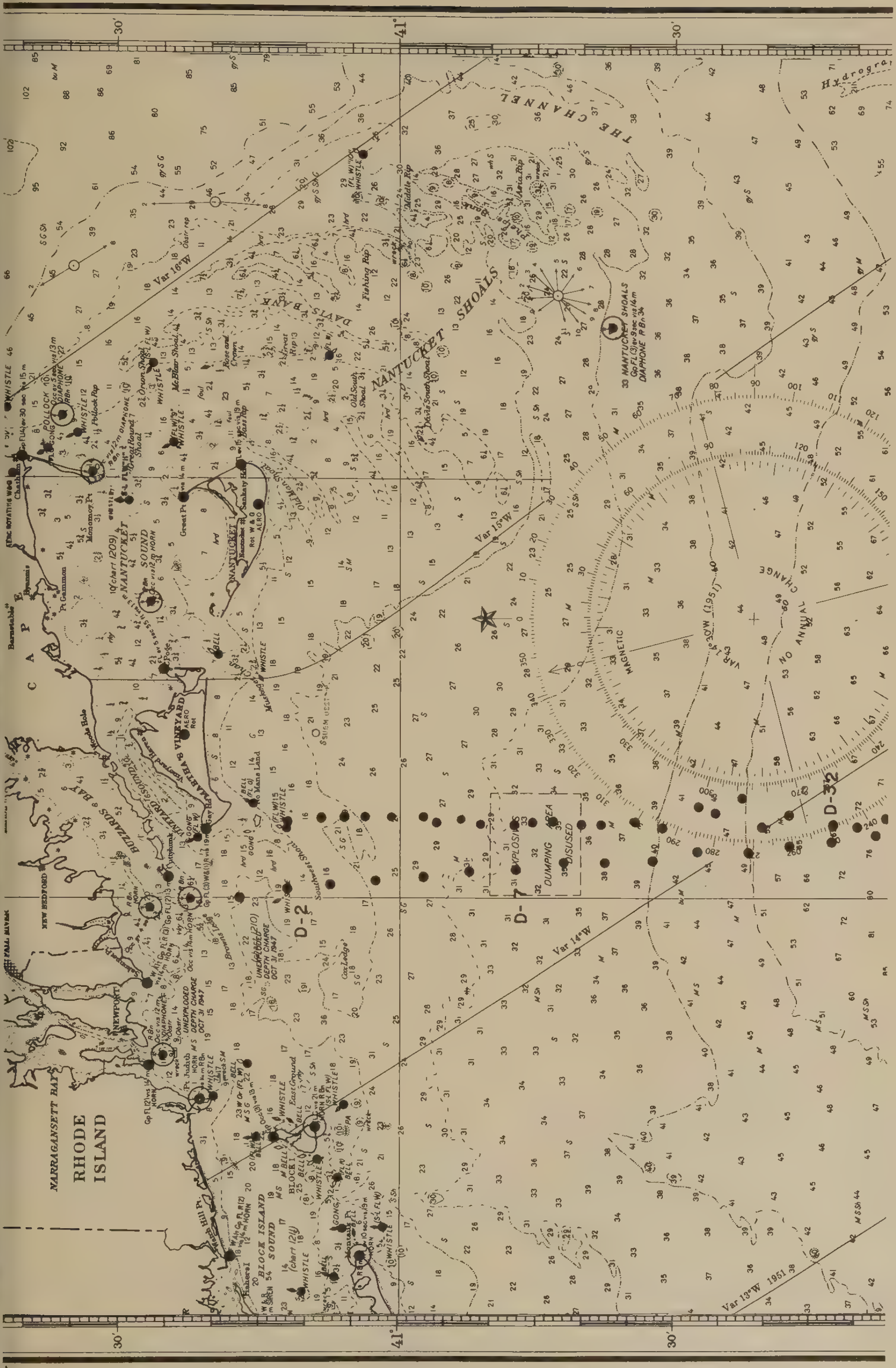
RHODE ISLAND
NARRAGANSETT BAY
NEWPORT
FALL RIVER
NEW BEDFORD
BLOCK ISLAND SOUND
BLOCK I.
BUZZARDS BAY
Woods Hole
MARTHA'S VINEYARD
VINEYARD SOUND
NANTUCKET SOUND
NANTUCKET I.
CAPE COD
Chatham
Barnstable
Monomoy Pt.
DAVIS BANK
NANTUCKET SHOALS
THE CHANNEL
Old South Shoal
Fishing Rip
Middle Rip
Great Rip
Rose and Crown
NANTUCKET SHOALS DIAPHONE
Cox Ledge
D-2
D-7
D-32
EXPLOSIVES DUMPING AREA DISUSED
UNEXPLODED DEPTH CHARGE OCT 31 1947
VAR 14°30'W (1951)
NO ANNUAL CHANGE
MAGNETIC
Var 16°W
Var 15°W
Var 14°W
Var 13°W 1951
41°
30'
Hydrographic

LOCATION OF STATIONS

Contribution No. 575

DEEP-SEA SANDS AND SUBMARINE CANYONS[1]

By D. B. Ericson, Maurice Ewing, and Bruce C. Heezen

Well-sorted sands at abyssal depths far from land were first discovered in the South Atlantic by the Gazelle Expedition of 1874 to 1876 (Andree, 1920). Since then other occurrences have been recorded from time to time, but until recently the significance and importance of these interesting sediments have not been appreciated.

In 1947 a bottom-sediment core (150-35) was taken by the research vessel Atlantis at a point 750 kilometers (400 nautical miles) southeast of New York City where the depth of water was 4755 meters (2600 fathoms). It contained several layers of well-sorted sand interbedded with clay and globigerina ooze. In the following year another core (152-135) 9 meters long was taken in the same region. It also contained sand layers, one of which was more than a meter thick.

In the meantime much was being learned about the topography and sediments of the Hudson Canyon region. It was found that the canyon could be traced with certainty to a distance of about 280 km (150 nautical miles) southeast of the edge of the continental shelf. Beyond this point the regional topography assumed the form of a broad plain gently sloping to the southeast in which the Hudson Canyon was so little entrenched that it could no longer be followed with assurance. It was on this plain that the two cores containing sand had been taken. This association of coarse, well-sorted sediment with a topographical feature resembling an alluvial plain extending out beyond the Hudson Canyon strongly suggested a genetic connection between type of sediment and topography. In order to test the theory that the plain was in fact a submarine delta, a co-ordinated coring and topographic survey was tentatively planned. The much-hoped-for opportunity to carry out the plan came in the summer of 1950 when a scheduled survey by the R/V Atlantis in the Hudson Canyon region was interrupted for several days by unavoidable delay in the arrival of another vessel the assistance of which was required in completing the work.

By means of a piston coring tube 10 additional cores having an average length of 6.8 meters were taken on the plain. The numbers of these cores, the positions of which are shown on the accompanying chart, are included in the series 164-13 to 164-24. No cores were obtained at stations 164-18 and 164-21. Although study of these cores has not been completed, preliminary work on them has already yielded so much new evidence having an important bearing on submarine erosion and deep-sea sedimentation that a short note at this time is felt to be justified.

The 12 cores from the plain outline an area of about 15,500 square kilometers or 6000 square nautical miles. Depths of the core stations vary from 4370 meters (2390 fathoms) to 4940 meters (2700 fathoms). All the cores, except one, 164-17, contain sand layers. The layers range in thickness from mere films of clean quartz silt to beds more than 6 meters thick. On the average about 30 per cent of the thickness of sediment penetrated is sand. The sediment interbedded with the sands is largely clay of abyssal facies. The number of sand layers and their positions in the cores differ greatly from core to core. The lower contacts of the individual layers where they rest on abyssal clay are very sharply defined. Graded bedding is evident in some of the sands. In others, where graded bedding is less obvious, it can be shown to be present by sieve analyses. In exceptional layers there is conplete gradation from sand through silt into gray clay containing an abnormally large amount of calcium car-

---

[1] Investigation supported by Government Reearch Contracts numbered NObsr43355 and N6-nr271 Task Order 24.

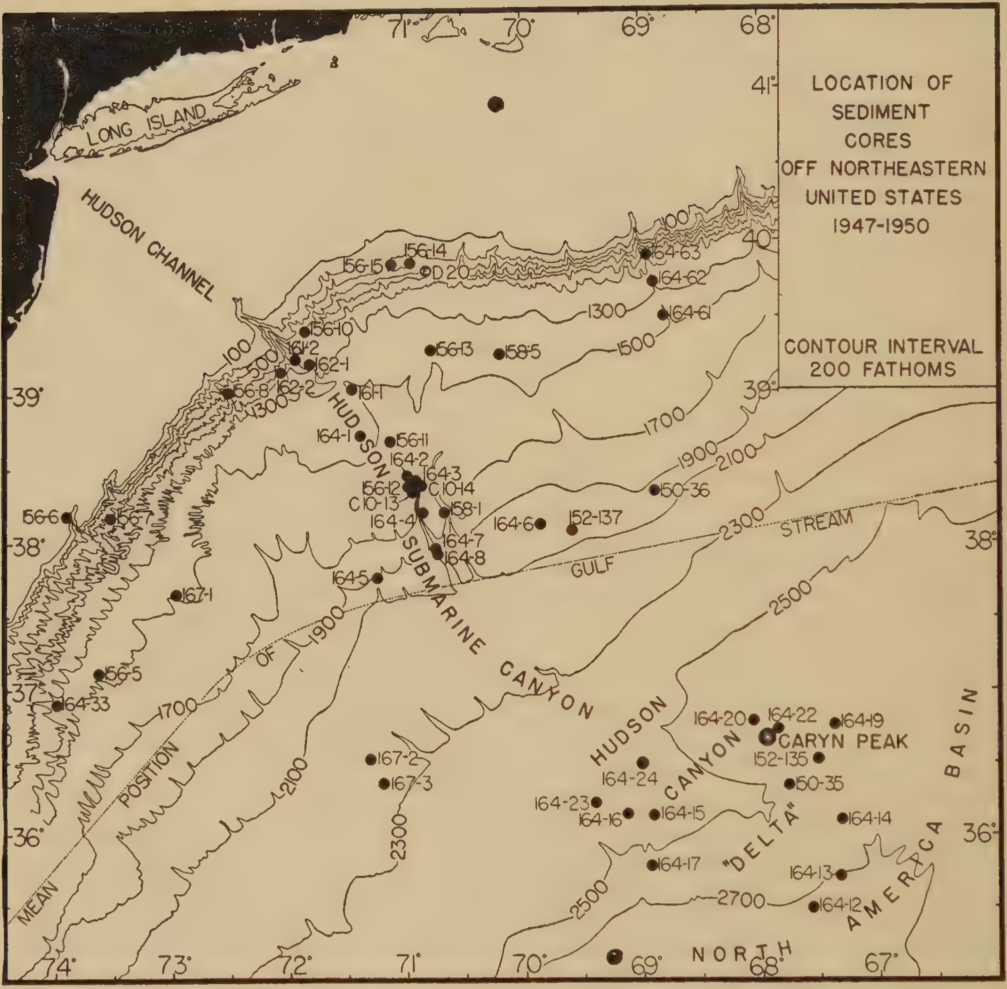
LOCATION OF SEDIMENT CORES OFF NORTHEASTERN UNITED STATES 1947-1950
CONTOUR INTERVAL 200 FATHOMS
LONG ISLAND
HUDSON CHANNEL
HUDSON SUBMARINE CANYON
HUDSON CANYON "DELTA"
CARYN PEAK
GULF STREAM
MEAN POSITION OF
NORTH AMERICA BASIN
71°
70°
69°
68°
41°
40°
39°
38°
37°
36°
74°
73°
72°
67°
100
500
1300
1500
1700
1900
2100
2300
2500
2700
156-14
156-15
D 20
164-63
164-62
164-61
156-10
161-2
162-1
162-2
156-8
161-1
156-13
158-5
164-1
156-11
164-2
164-3
156-12
C10-14
C10-13
164-4
158-1
164-7
164-8
164-6
152-137
150-36
156-6
156-7
164-5
167-1
156-5
164-33
167-2
167-3
164-20
164-22
164-19
152-135
150-35
164-24
164-23
164-16
164-15
164-14
164-17
164-13
164-12

Figure 1.—Location of Sediment Cores

bonate for the depth of water of the area. However, in the majority of cases the upper contacts of the sand layers show abrupt change from sand to normal deep-sea sediment. Sorting of particle sizes within the sand layers is always good. The small proportion of clay-size material in the sand layers is shown by their remarkable fluidity while still saturated with water. When dry many layers are no more coherent than beach sands.

Although all degrees of rounding, polishing, and frosting are found among the sand particles, angularity predominates. Quartz is the most abundant mineral, but there is usually an important fraction which includes various feldspars, micas, ferromagnesian minerals, and heavy minerals. Glauconite is nearly always present, and frequently there are also a few particles of red and gray shale, limestone, chert, fine-grained sandstone, and mica schist. Staining of some of the grains of quartz and feldspar by red iron oxide is not uncommon.

A number of short cores taken in 1947 by the R/V Balanus on the continental shelf in the vicinity of the head of the Hudson Canyon have been studied at the Lamont Geological Observatory. The coarse fractions of these shelf sediments are remarkably similar in mineral composition to the sands of the deep cores. Even the iron-oxide stain on quartz and feldspar grains is present in the shallow-water sediments. The only important difference is in the poor particle-size sorting of the shelf sediments in contrast to the good sorting of the deep-sea sands.

Foraminifera, though never abundant, are usually present in the coarser sands. In addition to the usual planktonic species there are almost without exception a few species which are characteristic of the continental shelf and slope sediments, such as *Elphidium incertum*, *Globobulimina auriculata*, and *Nonion labradoricum*. Not infrequently particles of vegetal matter are also present.

Faunal evidence from the sands and interbedded clays shows that none of the cores reaches sediment as old as the Sangamon interglacial stage of the Pleistocene. Although most of the sand layers must have been deposited during the Wisconsin Glacial stage, there is clear proof that a few have been laid down in post-Wisconsin time. Very recent deposition of sand is shown convincingly in core 164-14. Here a graded sand layer 72 cm thick overlies 38 cm of clay of abyssal facies containing the normal post-Wisconsin assemblage of Foraminifera known to be living in the region at the present time. This 38-cm layer in turn overlies dark-red clay containing a cold-water fauna. No trace of normal deep-water sediment overlies the sand layer. Further evidence that the sand was deposited only a short time ago is provided by the thickness of the post-Wisconsin zone beneath the sand. Its thickness compared with the thicknesses of corresponding layers in other cores from this region shows that it must represent very nearly all of post-Wisconsin time.

Except for one or two doubtful cases correlation of sand layers between even the most closely spaced cores—that is, about 10 miles apart—has not been successful. On the contrary, much disparity from core to core in the thicknesses of interbedded deep-water clay layers, presumably deposited at constant rate throughout the region, shows that the sand layers must be of only local extent, and not continuous sheets blanketing the entire area.

Other important suites of cores have been taken in the region of the Hudson Submarine Canyon to the northwest of the plain. In this area of greater relief there is a close correspondence between type of sediment and topography. On this basis the cores may be divided into three groups. First there are those taken outside of the canyon on the gentle slope into which the canyon has been cut, which contain an upper layer, usually less than 50 cm thick, of abundantly foraminiferal clay resting on clay containing a meager fauna of cold-water species. No sand layers are present or any other sediment at all abnormal for the depth, between 2500 meters (1370 fathoms) and 4000 meters (2190 fathoms), and the distance from the continent. Examples of such cores are numbers 158-5, 164-5, and 164-6.

The second group of cores comes from the canyon walls. These contain a compact green pyritic clay with a Mio-Pliocene fauna. Recent cover, if present at all, amounts to no more than a few centimeters in thickness. Examples are numbers 164-2, 164-4, 164-8, and C10-13.

The third group includes cores taken on the canyon floor. These contain either sand or muddy to fairly clean gravel with abundant mollusk shells and shell fragments. The pebbles of diameters to 2 cm are largely composed of a variety of igneous, metamorphic, and hard sedimentary rocks. In addition there are cobble-size masses of the green clay from the canyon walls as well as pebbles of an upper Eocene chalk which has been cored in place in the canyon wall near the foot of the continental slope at a depth of 2170 meters (1185 fathoms) or more than 1000 meters higher than the gravel occurrences. Dr. Horace Richards, who has examined the mollusks, has reported that they are of Pleistocene age, but that the possibility of faunal mixing is suggested by the presence of a few deep-water forms among many shallow-water species. Study of the Foraminifera contained in the interstitial material supports Doctor Richards' conclusions. Cores containing gravel are numbers 156-12 and 164-7.

Several theories of the origin of deep-sea sands which have been advanced since their discovery 75 years ago can now be dismissed Among these is the theory that they are composed of material which has been carried out from the continent by strong winds. Even if this mode of transportation could be admitted for the sands, it cannot explain the gravels. The good sorting and graded bedding are fatal to the theory of ice rafting as a mode of transportation for the sands.

Deposition at some time of greatly lowered sea level is disproved by the fact that in so many cases sand layers in certain cores can be shown to be equivalent to uninterrupted deposition of deep-sea clay in other cores. Furthermore, some of the sands have been laid down in Recent time, a fact difficult to reconcile with greatly lowered sea level, to say the least.

On the other hand, mineral and faunal similarity to the shelf sediments points to the continental shelf as the source of a large part of the material making up the sands. The presence of gravels containing shallow-water shells in the canyon bed, but nowhere on the divides outside the canyon, suggests that the route of transportation was through the canyon. Wide occurrence of sands in the sediments of the deep plain upon which the Hudson Canyon opens and absence of sands from the sediment of the gently sloping surface in which the canyon has been cut lead to the same conclusion. In view of the evidence it is the opinion of the authors that transportation by turbidity currents most satisfactorily explains the distribution of sands in the sediments of the plain as well as the occurrence of gravel on the canyon floor.

A conservative estimate of the volume of sand underlying the area of the plain which has actually been cored is in the order of 100 cubic kilometers. The passage of such a quantity of abrasive through the Hudson Canyon can hardly have taken place without more or less erosion of the relatively soft sediments forming the bed and walls. However, it is probable that the total amount of Pleistocene sand in the sediments of the plain is many times the amount estimated. Some erosion, at least, in the course of transportation of the gravel of the canyon is proven by inclusion in the gravel of the upper Eocene chalk pebbles and cobbles of green clay from the canyon walls.

The authors believe that the new evidence from the cores strongly supports the theory that erosion by turbidity currents has been an extremely important process, if not the only process, involved in the formation of the Hudson Canyon.

Several corollaries to these conclusions should be mentioned. If there is a genetic connection between the deep-sea sands of the plain and the Hudson Canyon, there ought to be similar submarine alluvial plains off other canyons of Eastern North America. Although no other area has been so thoroughly charted and cored as that of the Hudson Canyon, there is good evidence from cores and soundings that the Hudson submarine alluvial plain is only one of a series of coalescing alluvial plains which form a zone parallel to the continental slope. By the same reasoning coarse sediments should be found in the beds of other canyons. As yet gravels have not been cored elsewhere than in Hudson Canyon, but coarse sands have been found in other canyons.

If deep-sea sands have been transported by turbidity currents, large quantities of much finer sediment must have been carried out beyond the zone of alluvial plains to be deposited in the deep basins. Evidence of the deposition of this finer material has in fact been found. Some of the deepest cores taken in the North Atlantic contain layers of gray clay of abnormally high calcium carbonate content interbedded with red clay of normal deep-water facies. Frequently the lower contacts of such gray layers are marked by thin layers of clean silt. The gray layers, like the sand layers of the plain, fail to correlate from core to core. If these more calcareous layers were due to climatic changes during the Pleistocene, their lateral extension over fairly wide areas would be expectable. Furthermore, of two adjacent cores from different depths it is usually the deeper one which contains gray layers, while the other is quite likely to contain only normal red clay.

If our conclusion is correct that large quantities of sediment are carried to great distances along the sea bottom by turbidity currents it follows that the rate of deposition even in the deep basins must be much more rapid than has been supposed hitherto. An effect of such a depth-seeking process of sedimentation would be to fill depressions in the sea bottom most rapidly, thus eventually producing broad, nearly featureless plains. Fathometer records made on board the R/V Atlantis in the North Atlantic show that deep-basin topography is often characterized by just such monotonous plains broken only here and there by abruptly rising seamounts presumably of tectonic or volcanic origin.

The evidence presented here provides an extension to the ideas on submarine slumping which have grown up during the past few decades by showing that some of the slumped material is transported to great distances by turbidity currents. Both slumping and turbidity currents have been suggested as processes active upon the ocean bottom primarily on evidence from exposed marine strata. It has now been demonstrated from deep-sea sediments that turbidity currents play a dominant role in marine sedimentation. They transport large amounts of sediment to mid-ocean, and they sort the sediments well during transportation. They deposit the sediments by a depth-seeking process, which tends to fill depressions and produce broad, almost featureless plains like those observed in the North Atlantic basin and on the flanks of the Mid-Atlantic Ridge (Tolstoy and Ewing, 1949). It follows that the rate of deposition in the deep basins must be more rapid than has been supposed hitherto, and that an important part of all deep-sea sediments has been transported, and thereby sorted, at least one time after initial deposition on the ocean floor.

References Cited

Andree, Karl (1920) *Geologie des Meeresbodens*, 419–429.

Tolstoy, Ivan, and Maurice Ewing (1949) *North Atlantic hydrography and the Mid-Atlantic Ridge*, Geol. Soc. Am., Bull., vol. 60, p. 1527–1540.

Lamont Geophysical Observatory, Columbia University, Palisades, N. Y.

Woods Hole Oceanographic Institution Contribution No. 575
Lamont Geological Observatory Contribution No. 33

Contribution No. 57

PARAMETERS OF TURBULENCE IN THE SEA

By

GORDON A. RILEY

Bingham Oceanographic Laboratory
and
Woods Hole Oceanographic Institution[1]

ABSTRACT

Dimensional analysis, combined with statistical examination of data, leads to the development of an equation for eddy diffusivity that is expressed in terms of readily measurable physical parameters—mean current speed, the distance between points of observation, the density of the water, and the dynamic molecular viscosity. The equation is applicable to both vertical and horizontal diffusion in water of indifferent stability. A further development which incorporates a stability term makes it applicable also to horizontal eddy diffusion in stable water. Study of problems of vertical diffusivity and conductivity in stable water fails to reveal a satisfactory method of utilizing the basic equation. An empirical relationship of the vertical coefficients with mean current speed and stability is described and discussed from the standpoint of its possible physical meaning. The character of the relationship leaves little doubt that vertical diffusivity and conductivity in stable water are fundamentally different from the other varieties of turbulent exchanges that have been examined.

INTRODUCTION

In recent years the writer and his associates (Riley, Stommel, and Bumpus, 1949; Riley, 1951; and Riley, 1952) have computed coefficients of eddy diffusivity and conductivity in a variety of oceanographic situations. Comparison of these coefficients with their physical environment reveals relationships that warrant further examina-

---

[1] Contribution No. 577 from the Woods Hole Oceanographic Institution.

Reprint from SEARS FOUND. JOURN. MAR RES.

tion. Data in the second and third papers cited indicate that both vertical and horizontal coefficients are proportional, other things being equal, to the square of the mean current speed. Since it is recognized that turbulence must be generated by shearing stress, this result possibly means that the mean square of the deviation in velocity in the sea[2] is proportional to the square of the mean velocity within wide limits.

In carrying the analysis further, it is therefore proposed as a first assumption that the average coefficient of eddy diffusivity A between two points x distance apart on any one of the three coordinate axes is a function of the square of the mean current speed v between the points. Second, certain other readily determinable quantities are proposed for inclusion in the examination, namely x, the density ρ, the dynamic molecular viscosity μ, and the stability of the water E.

EDDY COEFFICIENTS IN WATER OF INDIFFERENT STABILITY

When the stability factor is omitted, and when the current speed is required to appear as v^2, dimensional analysis shows that the remainder of the factors that have been listed are necessary for a satisfactory expression for eddy diffusivity, and the equation is

$$A = \frac{\alpha\ (\rho v x)^2}{\mu}, \tag{1}$$

where α is a dimensionless proportionality constant. It is perhaps worth mentioning that upon dividing through by μ, equation (1) becomes

$$\frac{A}{\mu} = \alpha R^2,$$

where R is the Reynolds number for the distance x.

In the absence of theoretical understanding or of assurance that all of the significant physical parameters are included in the equation, its validity can be tested only by empirical methods. A in the Appendix lists calculated eddy coefficients from the papers cited above, together with other necessary information. These coefficients are plotted in Fig. 1A against values computed from equation (1), using a value of 6×10^{-12} for α. This is statistically a good fit for the horizontal eddy coefficients. A larger value would be better for the vertical coefficients, and some of the estimates are in error by nearly an order of magnitude. However, the results verify the essential correctness of the application of the terms v and x, both of which vary by several orders of magnitude in the appended data.

---

[2] The postulated relationship apparently does not hold precisely in small-scale hydrodynamic experiments; for example, see McEwen (1950: 41).

COEFFICIENTS OF LATERAL EDDY DIFFUSIVITY IN STABLE WATERS

Parr (1936) postulated that lateral[3] eddy diffusion is increased by stability and suggested that this is essentially a large-scale phenomenon. Both of these hypotheses are supported by the present investigation. Examination of the data on mid-depths in the Atlantic Ocean (B in APPENDIX) shows that the eddy coefficients are larger than those indicated by values computed from equation (1). However, evidence of a stability influence is lacking in Long Island Sound and is only slightly apparent in the data for the California offing, even though the stability exceeds the values for Atlantic Ocean mid-depths. The only obvious explanation of the apparent differences in the stability influence is that the latter may increase with distance x.

It is therefore assumed as a working hypothesis that the coefficient of lateral eddy diffusivity increases with stability and with distance. This relationship may be expressed in several forms that are dimensionally correct. A version that is empirically satisfactory except for one aberrant point is

$$A = \frac{\alpha(\rho v x)^2}{\mu}\left(1 + \frac{3\alpha g E x^2}{v^2}\right), \tag{2}$$

where g is the acceleration of gravity. Fig. 1B compares the coefficients in B of the APPENDIX with values computed from equation (2).

VERTICAL EDDY COEFFICIENTS IN STABLE WATERS

Examination of coefficients of vertical eddy diffusivity in mid-depths of the Atlantic Ocean (C in APPENDIX) shows that equation (1) is applicable within reasonable limits of error. These coefficients were determined as average values between successive and equal intervals of σ_t. Therefore, the method of calculation incorporates a stability effect.

The examination of coefficients of vertical eddy conductivity is hampered by the fact that their computation did not involve a distance factor (cf. APPENDIX). This might not be a serious deterrent if, as indicated by the mid-depth eddy diffusivities, x in the equation might be replaced by a mixing length determined from some of the

---

[3] In Parr's discussion and in B of the APPENDIX, this term refers to quasihorizontal diffusion along surfaces of equal density.

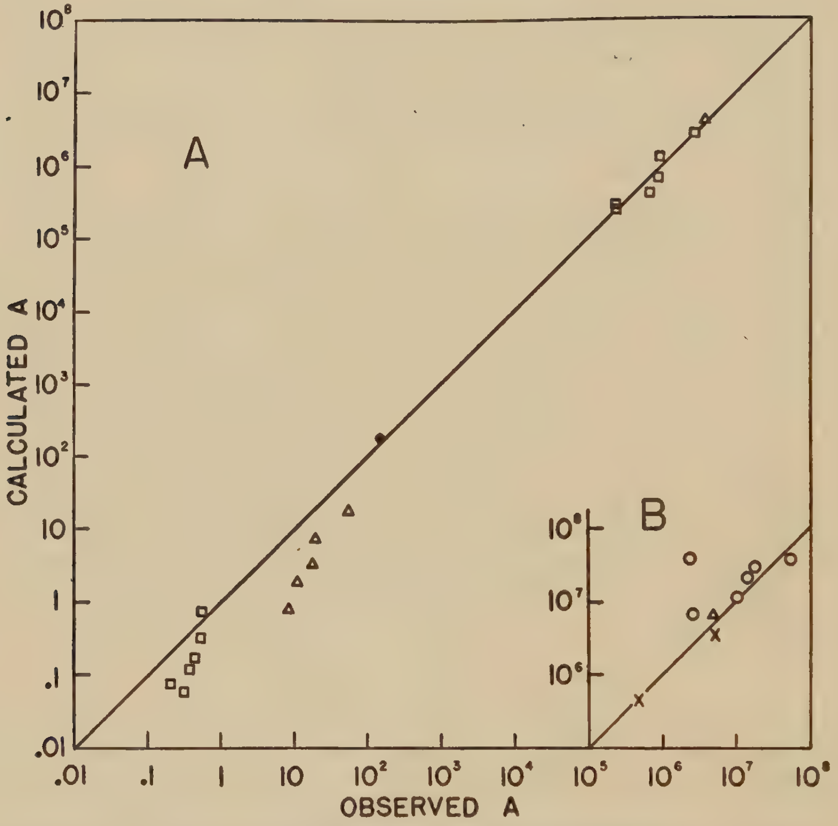

Figure 1. *A.* "Observed" eddy coefficients in water of slight stability (i. e., values in A of the Appendix derived from observed distributions of temperature or salinity) plotted against coefficients computed from equation (1). A logarithmic scale is used in order to show the entire range of values. *B.* Comparison of "observed" coefficients of lateral eddy diffusivity in stable water with computed values from equation (2). Atlantic Ocean mid-depths, circles; deep water, squares; California offing, x's; Long Island Sound, triangles; Georges Bank, dots.

physical parameters under consideration. However, none of the possibilities examined leads to realistic results. Conversely, the only reasonably accurate empirical proportionality that has been discovered (Fig. 2) cannot be incorporated with the other postulated parameters into a dimensionally correct expression for eddy conductivity.

DISCUSSION

Observations have shown that eddy diffusivity and conductivity in stable water are much smaller than eddy viscosity (Sverdrup, et al.,

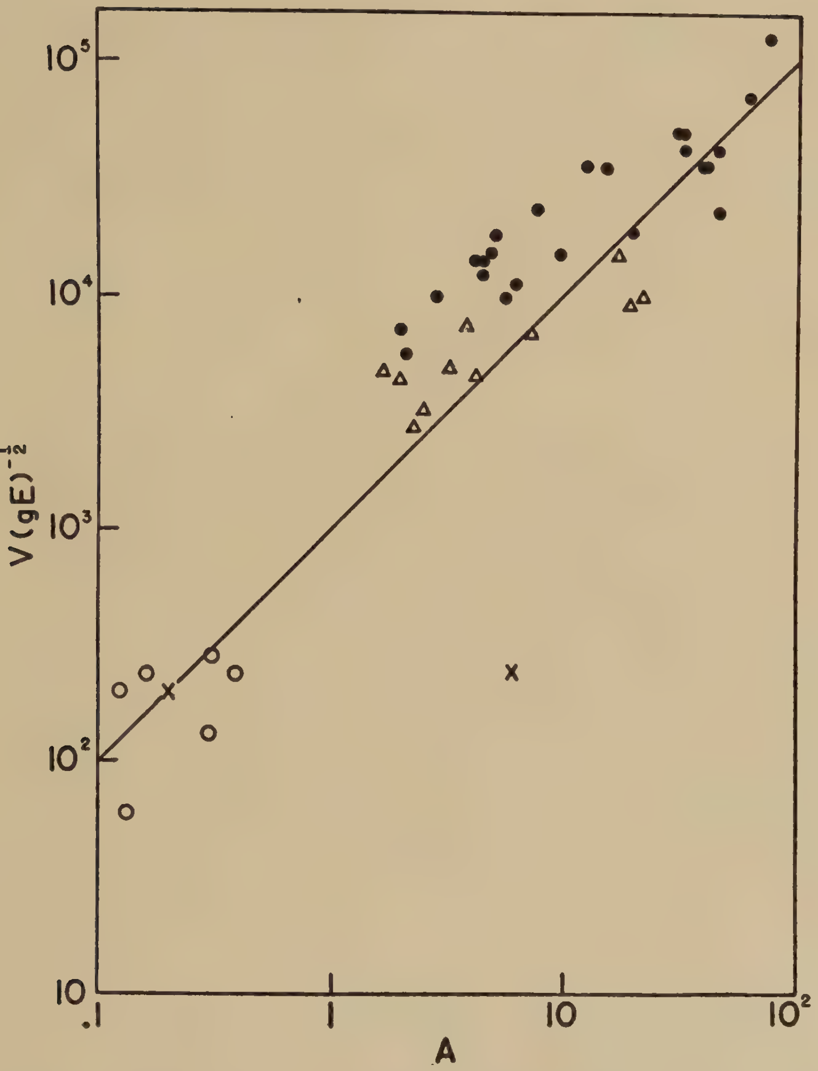

Figure 2. "Observed" coefficients of vertical eddy diffusivity and conductivity in stable water plotted against a function of the mean current speed and the stability. Symbols as in Fig. 1.

1942: 477). This is ordinarily explained on the grounds that momentum is given up relatively quickly and that the larger turbulent masses are then returned toward their point of origin without effecting complete exchange of heat and salt. A time factor is involved in the exchange, which is absent in water of indifferent stability. There, masses of various sizes and turbulent velocities presumably can exchange momentum and then remain in their new surroundings while they exchange other properties. This seems to be the essential difference between the eddy diffusivities that conform to equation (1) and the vertical conductivities in stable water which do not conform.

In stable water, the coefficients of vertical eddy diffusivity A_s and conductivity A_T may be written

$$A_s = \rho\, \bar{v}_s{}'\, l_s;$$
$$A_T = \rho\, \bar{v}_T{}'\, l_T.$$

This is similar to Prandtl's concept of eddy viscosity (Sverdrup, et al., 1942: 472–3) except that $\bar{v}_s{}'$, $\bar{v}_T{}'$ refer specifically to the mean vertical velocity of water masses that are able to effect complete exchange of salt and heat, respectively, at the limits of the mixing lengths l_s, l_T.

Consideration of the time factor of exchange imposes certain restrictions on the character of the movements described by these equations. The size of water masses that effectively exchange heat and salt at the limit of a given mixing length must constitute only a small part of the total spectrum of turbulent sizes. Variability of the vertical component of momentum, and hence of velocity, must be similarly limited. In other words, for any given mixing length, the mean vertical turbulent velocity depends upon the initial velocity spectrum, the negative acceleration due to stability, and a proportionality factor which determines the relation between the total movement of water and the heat or salt exchange that occurs at the limit of the mixing length. Alternatively, it might be expedient in comparing different kinds of oceanographic situations to express the mixing length dynamically in terms of the turbulent velocity spectrum and stability; $v_s{}'$, $v_T{}'$ would then be in essence proportionality factors.

Both of these problems are undoubtedly difficult to solve quantitatively, but it is possible that Fig. 2 represents an empirical approximation to the solution of the second one. It will be noted that the eddy coefficients are correlated with a quantity that has the dimensions of a length. The equation

$$A = \rho\, \bar{v}'\, v\, (g\, E)^{-\frac{1}{2}}$$

is empirically valid if $\bar{v}'$ is constant within the limits of observational error.

The coefficients cited in the APPENDIX were derived in order to apply the results to problems of distribution of plankton and minor chemical elements in the sea. This is mentioned to emphasize the fact that a knowledge of turbulence is becoming important in many aspects of oceanography. Therefore, it is unfortunate that the computation of turbulence coefficients from the observed distribution of oceanographic properties is laborious and subject to various errors of over-simplification.

There is obvious need for a method that will estimate turbulence with a degree of ease and accuracy comparable to the determination of advection. Theoretical studies thus far have failed to reveal such a method. It remains to be seen whether further theoretical work will verify the empirical equations that have been proposed above and whether observations will substantiate the initial assumption of a precise relationship between turbulent velocities and mean velocity.

However, from a practical standpoint, the results are more precise than might have been expected. Fig. 1, which compares coefficients computed from equations (1) and (2) with values derived from the observed salinity distribution, reveals a few differences of approximately an order of magnitude, but the average difference between the two methods in all of the estimates of lateral eddy coefficients is only 38%. At present there is no way of knowing whether the observed differences are due to observational errors or to imperfections in the equations that have been proposed. One can only say that no oceanographer has claimed, nor probably believed, that he could determine diffusion coefficients with an accuracy equal to the agreement between the two methods.

Thus the equations provide a possible means of simplifying the solution of various oceanographic problems. Computations of flux or of the local time change of oceanographic properties, which heretofore have required estimates of both advection and diffusion, can be transformed with the aid of the empirical equations into simple advection problems.

REFERENCES

McEWEN, G. F.
1950. A statistical model of instantaneous point and disk sources with applications to oceanographic observations. Trans. Amer. geophys. Un., *31:* 35–46.

PARR, A. E.
1936. On the probable relationship between vertical stability and lateral mixing processes. J. Cons. int. Explor. Mer, *11:* 308–313.

RILEY, G. A.
1951. Oxygen, phosphate, and nitrate in the Atlantic Ocean. Bull. Bingham oceanogr. Coll., *13* (1): 1–126.

1952. Hydrography of the Long Island and Block Island Sounds. Bull. Bingham oceanogr. Coll., *13* (3).

Riley, G. A., Henry Stommel, and D. F. Bumpus
1949. Quantitative ecology of the plankton of the western North Atlantic. Bull. Bingham oceanogr. Coll., *12* (3): 1–169.

Sverdrup, H. U., M. W. Johnson, and R. H. Fleming
1942. The oceans. Prentice-Hall, Inc., New York. 1087 pp.

APPENDIX

General Explanation of Tabular Material

The sources of data are as follows:

1. Atlantic Ocean mid-depths and deep water (Riley, 1951). Coefficients of lateral (A_x) and vertical (A_z) eddy diffusivity are average values for a series of σ_t surfaces in mid-depths and level surfaces in deep water. They were computed statistically from the observed salinity distribution, the distance between points of observation x and z in cm; the current velocity is determined by dynamic computation. The current speeds v in cm/sec are the arithmetic average of the north-south and east-west velocities on each surface (for present purposes, a more accurate estimate would be the square root of the mean-squared vectorially-added velocities, but the general quality of the data hardly warrants this refinement). The tables herewith also include estimates of the dynamic molecular viscosity μ and the stability E, the latter approximated throughout as $10^{-3}\ \Delta\sigma_t/m$.

2. Hitherto unpublished estimates of eddy diffusion on two σ_t surfaces off the California Coast have been obtained by the same methods described above. This work was done while the writer was visiting Scripps Institution of Oceanography; grateful acknowledgment is made for the use of data from their Marine Life Research Program for this purpose.

3. Long Island Sound (Riley, 1952). Lateral eddy coefficients were determined from the distribution of salinity along the main axis of the Sound. Coefficients of vertical eddy conductivity were based on the vertical temperature gradients at a series of depths and on the seasonal rate of change of calories below each depth. v is the mean speed of the tidal current, computed from data on the height of the tide in the Sound and averaged for a complete tidal cycle. z is the total depth of water in cm.

4. Georges Bank (Riley, Stommel, and Bumpus, 1949). Coefficients of vertical eddy conductivity, as in Long Island Sound, are computed from average temperature-depth curves for the central part of the Bank. Only the upper 40 m are used for computation. Values

in deeper water appear to be reduced by proximity to the bottom. z is the mean depth of water; v is an approximation of the speed of the tidal current.

A

Water of slight stability (E is less than 50 x 10^{-8}). Eddy coefficients in Long Island Sound are averages for the whole autumn-winter period of minimum stability in five different areas; the Georges Bank estimate is an average for the upper 40 m.

	Depth	A_z	A_x	z	x	v	μ
Atlantic Ocean Deep Water	1500	0.29	2.2 x 10^5	5 x 10^4	1 x 10^8	0.25	.017
	2000	0.21	2.3 x 10^5	5 x 10^4	1 x 10^8	0.29	.017
	2500	0.34	6.4 x 10^5	5 x 10^4	1 x 10^8	0.35	.017
	3000	0.43	8.1 x 10^5	5 x 10^4	1 x 10^8	0.44	.017
	3500	0.51	8.6 x 10^5	5 x 10^4	1 x 10^8	0.59	.017
	4000	0.55	28.0 x 10^5	5 x 10^4	1 x 10^8	0.84	.017
Georges Bank*	—	140.0	—	7 x 10^3	—	100.0	.017
Long Island Sound	—	53.0	—	37 x 10^2	—	60.0	.017
	—	21.0	—	27 x 10^2	—	55.0	.017
	—	18.0	—	23 x 10^2	—	42.0	.017
	—	11.0	—	25 x 10^2	—	30.0	.017
	—	9.0	—	22 x 10^2	—	23.0	.017
	—	—	38 x 10^5	—	3.7 x 10^6	30.0	.017

* March

B

Lateral eddy coefficients in stable water. Long Island Sound coefficient and stability are averages for the spring-summer period.

	σ_t	A_x	x	v	μ	E
Atlantic Ocean Mid-depths	26.5	57.0 x 10^6	1 x 10^8	1.5	.012	290 x 10^{-8}
	26.7	18.0 x 10^6	1 x 10^8	1.2	.013	270 x 10^{-8}
	26.9	14.0 x 10^6	1 x 10^8	0.88	.013	210 x 10^{-8}
	27.1	10.5 x 10^6	1 x 10^8	0.78	.014	110 x 10^{-8}
	27.3	2.5 x 10^6	1 x 10^8	0.39	.015	90 x 10^{-8}
	27.5	2.4 x 10^6	1 x 10^8	0.15	.016	60 x 10^{-8}
Calif. Offing	25.5	5.5 x 10^6	3.7 x 10^7	2.0	.014	1040 x 10^{-8}
	27.0	0.5 x 10^6	3.7 x 10^7	0.8	.017	120 x 10^{-8}
Long Island Sound	—	4.9 x 10^6	3.7 x 10^6	30.0	.011	1020 x 10^{-8}

C

Vertical eddy coefficients in stable water. Values for Georges Bank are individual estimates for a series of depths. Long Island Sound coefficients are also individual estimates representing different depths and areas.

	σ_t	A_z	z	v	μ	E
Atlantic Ocean	26.5	0.30	70×10^2	1.5	.012	290×10^{-8}
Mid-depths	26.7	0.16	73×10^2	1.2	.013	270×10^{-8}
(Diffusivity)	26.9	0.12	95×10^2	0.88	.013	210×10^{-8}
	27.1	0.38	181×10^2	0.78	.014	110×10^{-8}
	27.3	0.31	225×10^2	0.39	.015	90×10^{-8}
	27.5	0.13	350×10^2	0.15	.016	60×10^{-8}
California Offing	25.5	0.20	48×10^2	2.0	.014	1040×10^{-8}
(Diffusivity)	27.0	6.0	420×10^2	0.8	.017	120×10^{-8}
Long Island Sound	—	7.2	—	60.0	.011	$720 \times 10^{-}$
(Conductivity)	—	19.0	—	60.0	.011	430×10^{-8}
	—	4.2	—	55.0	.011	1470×10^{-8}
	—	22.0	—	55.0	.011	300×10^{-8}
	—	17.0	—	55.0	.011	150×10^{-8}
	—	3.8	—	42.0	.011	310×10^{-8}
	—	3.2	—	30.0	.011	370×10^{-8}
	—	1.7	—	30.0	.011	400×10^{-8}
	—	2.0	—	23.0	.011	290×10^{-8}
	—	2.3	—	21.0	.011	630×10^{-8}
	—	2.5	—	21.0	.011	460×10^{-8}

	April		May		June	
	$\mu = .017$		$\mu = .016$		$\mu = .014$	
	A_z	E	A_z	E	A_z	E
Georges Bank	45	60×10^{-8}	9.5	460×10^{-8}	35.0	720×10^{-8}
(Conductivity)	39	80×10^{-8}	6.3	780×10^{-8}	20.0	430×10^{-8}
$v = 100$ cm/sec	34	60×10^{-8}	4.5	660×10^{-8}	5.8	1120×10^{-8}
throughout	31	40×10^{-8}	4.5	540×10^{-8}	2.1	2980×10^{-8}
	32	40×10^{-8}	4.9	460×10^{-8}	2.0	1980×10^{-8}
	39	60×10^{-8}	7.7	200×10^{-8}	2.8	980×10^{-8}
	62	20×10^{-8}	12.5	80×10^{-8}	4.1	560×10^{-8}
	76	7×10^{-8}	15.0	80×10^{-8}	5.1	280×10^{-8}

Contribution No. 584

Särtryck ur Tellus nr 4, 1951

Multiple Currents in the Gulf Stream System*

By F. C. FUGLISTER, Woods Hole Oceanographic Institution

(Manuscript received 20 September 1951)

Abstract

A new interpretation of the accumulated temperature and salinity data from the Gulf Stream Area indicates that the System is made up of a series of overlapping currents. These currents are separated by relatively weak countercurrents. Data from a recent survey are presented as supporting this hypothesis.

In nearly all discussions of the Gulf Stream and of the North Atlantic Current the terms countercurrent and eddy are frequently employed, (Iselin 1936, 1940, and Sverdrup et al. 1942). Many temperature and salinity profiles across the currents indicate the presence of countercurrents and/or eddies and certain theoretical considerations require that they exist (Rossby 1936). On the other hand charts showing the average distribution of temperature and salinity (Wüst and Defant 1936 and Fuglister 1947, etc.) and charts showing the currents in the western North Atlantic do not indicate that countercurrents or eddies are permanent features of the system.

It is the purpose of this paper to suggest that, by eliminating the averaging processes, countercurrents can be introduced as, at least, semi-permanent features of the circulation and a new picture of the current system will evolve. The existing current charts fall into two general classes, those that show a relatively narrow current flowing from Cape Hatteras to the Grand Banks area where the current is shown to fork or branch, and those charts that depict a current at Cape Hatteras that gradually broadens as it moves toward the mid-Atlantic. The data used for these charts interpreted in a different manner shows that, in the Gulf Stream and North Atlantic Current areas, there is no one continuous current but a series of overlapping easterly currents separated by countercurrents.

The averaging processes tend to obscure certain details that are known to exist. Perhaps the most important of these details, in the present connection, is the very narrow zone of minimum temperatures or low pressure generally found on the left-hand side, facing downstream, of a strong current. In an attempt to show this zone and to illustrate what seems a more logical interpretation of the accumulated sub-surface data, a schematic chart of temperatures at a depth of 200 meters in the Gulf Stream area has been drawn. The data used are from various sources but primarily from the multiple ship survey of 1950, (Fuglister and Worthington 1951). This chart (see fig. 1) shows three easterly currents between Cape Hatteras and the longitude of Flemish Cap. There is a minimum temperature

---

* Contribution No. 584 from the Woods Hole Oceanographic Institution.

This research was sponsored by the Office of Naval Research under Contract N6onr-277, T. O. I.

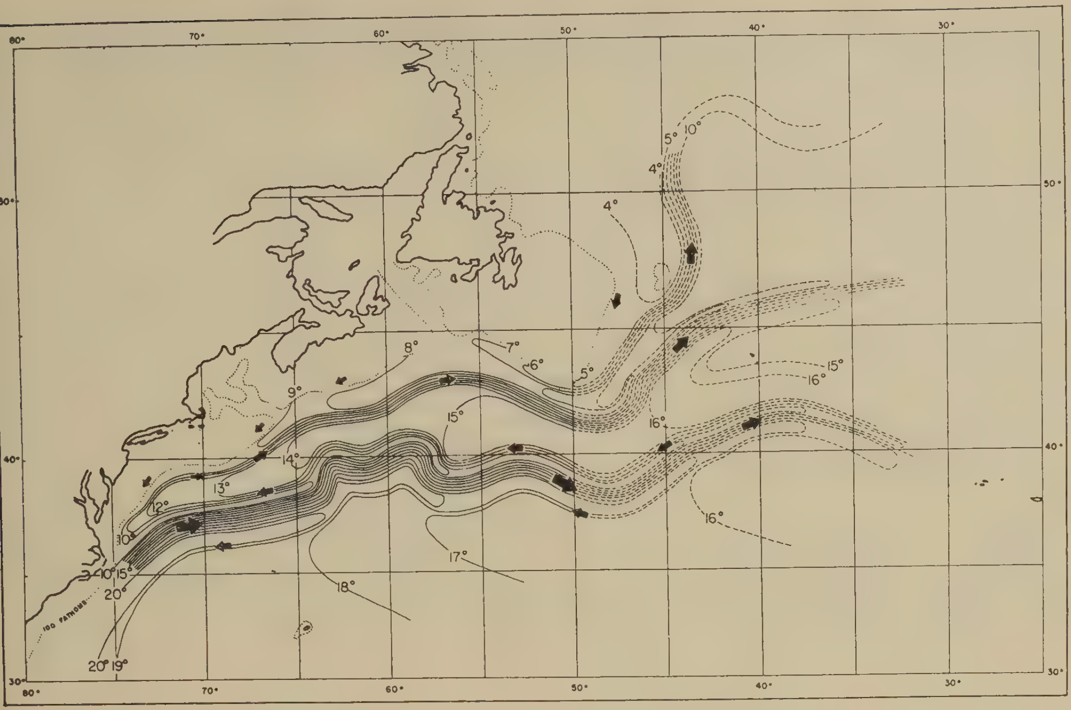

Fig. 1. Schematic chart of temperatures (° C.) at a depth of 200 meters in the Gulf Stream Area.

zone inshore of the sharp gradient off Cape Hatteras. The temperatures in this zone increase to the east. This increase in temperature is balanced by a corresponding decrease in temperature in the warm zone to the right of the gradient. If we assume for the moment that the currents flow along the isotherms then the major current off Cape Hatteras, without becoming wider or branching, simply becomes weaker as it flows toward the east. On both sides of this current there are weak countercurrents. A second easterly current forms just off the continental shelf north of Cape Hatteras, increases in strength as it flows toward the Grand Banks area and then in its turn gradually weakens in the same manner as the first current. Finally a third stream is depicted forming in the Grand Banks area and moving toward the northeast.

In order to check on the above interpretation of data obtained from various sources a survey was made of part of the area by the ALBATROSS III in June 1951. The data collected on this cruise consisted of half-hourly bathythermograph observations to a depth of 250 meters and (over many sections) hourly surface current measurements with the GEK (VON ARX 1950). As was the case with the multiple ship survey of 1950 the majority of surface current vectors showed the same current directions as would be deduced from a plot of the 200-meter isotherms. A plot of these isotherms and the track of the ALBATROSS III are shown in figure 2. The entire area of interest could not be covered in the 26 days the research vessel was at sea but the results obtained strongly support the multiple current hypothesis. In fact the data indicated the existence of four major easterly currents separated by countercurrents of varying magnitudes.

Aside from the extravagant amount of extrapolation used in both fig. 1 and fig. 2 the most serious criticism of the multiple current hypothesis as presented here may be that the temperature structure at 200 meters does not reflect the pressure field. It may be considered as representing only a relatively shallow surface layer. Actually a similar picture of the current regime in this area could

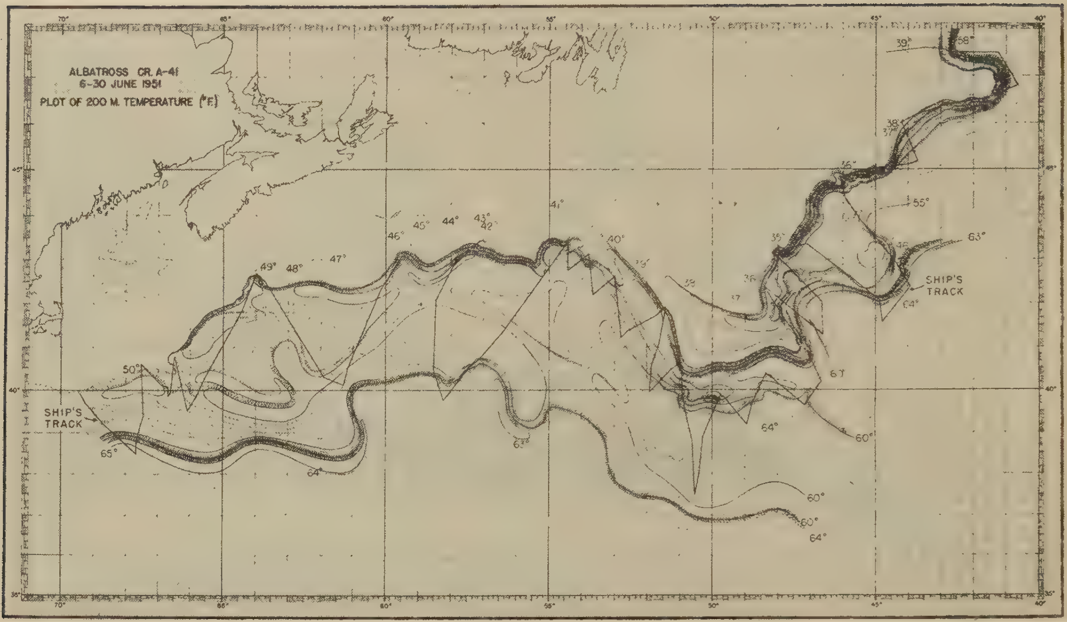

Fig. 2. Temperatures (°F.) at a depth of 200 meters in the Gulf Stream Area. An interpretation of the data obtained on the ALBATROSS III cruise of June 1951.

be obtained by using surface dynamic height anomalies referred to the 2000 decibar surface. The difficulty would be that observations taken over a period of more than 10 years would have to be used and even more extrapolation would be required.

However, an examination of all the available deep temperature and salinity sections normal to the coast between Cape Hatteras and the Grand Banks gives the following interesting results. Out of fifteen sections between Montauk, Long Island, and Bermuda, variations in the depth of the sigma-t 27.2 surface show:

7 sections with a slight westerly current very close in by the continental shelf;
13 sections with a stronger easterly current just off the shelf;
13 sections with a countercurrent to the left of the Gulf Stream.
12 sections with a countercurrent to the right of the Gulf Stream.

The average depth in meters of the 27.2 sigma-t surface at each maximum and minimum point from the shelf outward is as follows:

average	255		231		336		214		949		833
difference		—24		+105		—122		+735		—116	

Of the available sections to the east of the Montauk—Bermuda line and west of the 50th meridian only 7 reach from the continental shelf out to the Gulf Stream. These 7 all show an easterly current off the continental shelf and a countercurrent between it and the Gulf Stream. None of these sections reached far enough south to check on the existence of a countercurrent to the right of the Stream. When the data from the three most easterly sections are averaged, the depth of the sigma-t 27.2 surface at each maximum and minimum point from the shelf outward is:

average	190		132		387		383		890
difference		—58		+355		—104		+507	

Assuming that the differences in depth of the sigma-t surface between these points indicate the relative strength of the currents then it appears that the easterly current off the continental shelf increases and the Gulf Stream decreases in strength as they move toward the Grand Banks area.

If this multiple current system is accepted then there is a problem of nomenclature. As a group the currents discussed here form a portion of the Gulf Stream System. This portion of the System fits the description of the North Atlantic Current, as given in THE OCEANS (SVERDRUP et al. 1942), except that now the name should apply to the group of currents as far west as Cape Hatteras instead of only to those currents to the east of the Grand Banks. If the term Gulf Stream is to be retained it should be understood that it applies only to the direct continuation of the Florida Current and it does not include all easterly-flowing currents between Cape Hatteras and the Grand Banks. Whether or not any of the other currents in the group should be specifically named is a question that might wait until more is known about their permanency.

Since June of this year the ALBATROSS III has been engaged in surveying the area to the east of Flemish Cap. Aboard ship the various currents are referred to as No. 1 (for the Gulf Stream), No. 2, No. 3, etc., for each successive current encountered. No. 4, the current off Flemish Cap, has been followed as far east as the 23rd meridian and the possible existence of a No. 5 has been indicated.

REFERENCES

FUGLISTER, F. C., 1947: Average Monthly Sea Surface Temperatures of the Western North Atlantic Ocean. *Papers in Physical Oceanography and Meteorology*, **10**, 2, pp. 1—25.

FUGLISTER, F. C., and L. V. WORTHINGTON, 1951: Some Results of a Multiple Ship Survey of the Gulf Stream. *Tellus*, **3**, 1, pp. 1—14.

ISELIN, C. O'D., 1936: A Study of the Circulation of the Western North Atlantic. *Papers in Physical Oceanography and Meteorology*, **4**, 4, pp. 1—101.

— 1940: Preliminary Report on Long-Period Variations in the Transport of the Gulf Stream System, *Papers in Physical Oceanography and Meteorology*, **8**, 1, pp. 1—40.

ROSSBY, C.-G., 1936: Dynamics of Steady Ocean Currents in the Light of Experimental Fluid Mechanics. *Papers in Physical Oceanography and Meteorology*, **5**, 1, pp. 1—26.

SVERDRUP, H. U., M. W. JOHNSON and R. H. FLEMING, 1942: *The Oceans: Their Physics, Chemistry, and General Biology*. New York, Prentice-Hall.

VON ARX, WILLIAM S., 1950: An Electromagnetic Method for Measuring the Velocities of Ocean Currents from a Ship Under Way. *Papers in Physical Oceanography and Meteorology*, **9**, 3, pp. 1—26.

WÜST, GEORG, and, ALBERT DEFANT, 1936: Atlas zur Schichtung und Zirkulation des Atlantischen Ozeans. Deutsche Atlantische Expedition Meteor 1925—1927. Wiss. Erg., Bd. VI—Atlas, Berlin.

Esselte, Sthlm 52

Contribution No. 586

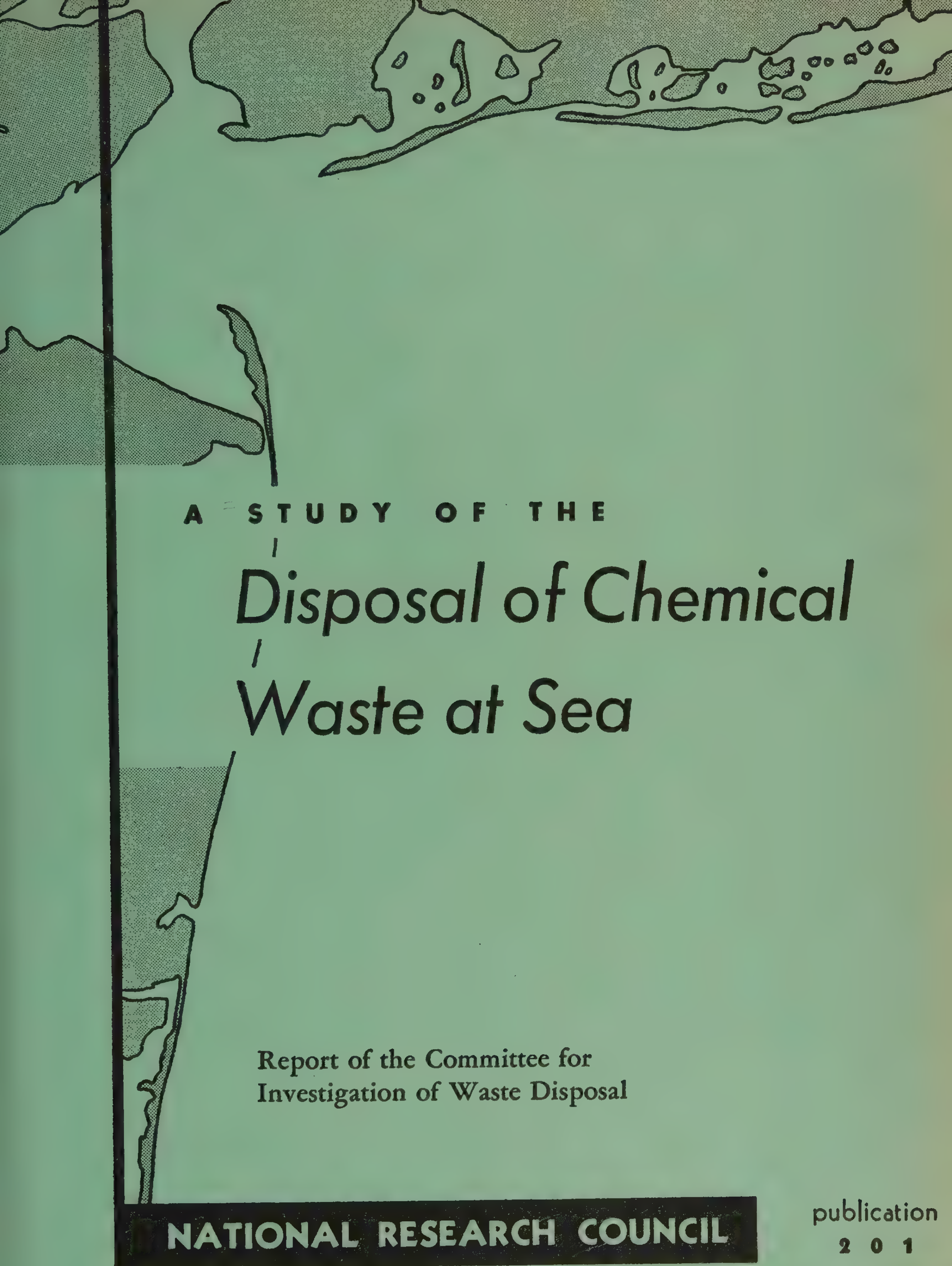

A STUDY OF THE

Disposal of Chemical Waste at Sea

Report of the Committee for
Investigation of Waste Disposal

NATIONAL RESEARCH COUNCIL

publication
201

of the NATIONAL ACADEMY OF SCIENCES

Price $1.00

COMMITTEE FOR INVESTIGATION OF WASTE DISPOSAL

Division of Biology and Agriculture

National Research Council

Charles E. Renn, *Chairman*—Johns Hopkins University, Baltimore, Md.

Charles M. Breder —American Museum of Natural History, New York, N. Y.

Thomas S. Austin —Hydrographic Office, Division of Oceanography, Navy Department, Washington, D. C.

This is the first in a new series of Academy-Council publications.

The *Bulletin* and *Reprint and Circular* series have been discontinued, and future publications will appear in one series numbered from 201. A complete list of publications available, with subscription procedures, will be sent on request to the Publications Office, National Research Council, 2101 Constitution Avenue, Washington 25, D. C.

A STUDY OF THE

Disposal of Chemical Waste at Sea

A STUDY OF THE
Disposal of Chemical Waste at Sea

Report of the Committee for Investigation of Waste Disposal

by

ALFRED C. REDFIELD

Woods Hole Oceanographic Institution

and

LIONEL A. WALFORD

Fish and Wildlife Service,
U. S. Department of the Interior

Contribution No. 586 from the
Woods Hole Oceanographic Institution

National Academy of Sciences—National Research Council
Washington, D. C.
1951

PREFACE

THE increasing concentration of population in the neighborhood of New York City has brought with it many conflicts of interest relative to the pollution of the adjoining waters. Among these, the pollution of the Raritan River and Raritan Bay by industrial wastes and domestic sewage, following the somewhat phenomenal growth of the Raritan River Valley as an industrial area, has led to active measures to improve conditions in these waters. These included an order restraining the National Lead Company from continuing to discharge certain wastes from its titanium plant at Sayreville, New Jersey, into the Raritan River. This Company thereupon proposed and prepared to carry out a plan to barge the material to sea.

After consultation with many interested agencies, including the U. S. Coast Guard, the Fish and Wildlife Service, and the Atlantic States Marine Fisheries Commission, the Company secured permission from the Captain of the Port of New York to discharge the waste in an area thirteen miles from Scotland Lightship and ten miles off the New Jersey coast. Meanwhile, serious opposition to the proposal developed on the part of the commercial and sport fishing interests of the region, who felt that the operations would seriously interfere with their activities.

In order that the facts be fully and impartially developed, the National Lead Company requested the National Research Council to sponsor an investigation of the operation and its consequences, and made the necessary funds available. The Council in turn contracted with the Fish and Wildlife Service and the Woods Hole Oceanographic Institution to conduct studies.

While the results of these studies bear directly on the operations of the National Lead Company, they have a wider interest, since they may be applied to similar operations in this region or elsewhere. At the present time sewage sludges are being discharged at sea in the offing of New York and are the subject of complaint by fishermen and others. It would be naive indeed to doubt that, in the future, pressures will arise to dispose of other industrial wastes offshore, and it is most important to know what consequences are to be expected and what regulations are required to best serve the public interest.

The investigations have involved phenomena of a complex character. The full treatment of these matters is reserved for presentation in appropriate scientific publications. The present report attempts to give the results of these technical studies in terms familiar to those interested in the practical aspects of the problems of pollution, the disposal of waste products, and their control.

In initiating these studies the Fish and Wildlife Service assumed responsibility for the survey of the sport fishing of the region, for the biological studies, and for the drift bottle program, while the Oceanographic Institution undertook the hydrographic and chemical studies. The results are so closely interrelated, however, that they are reported jointly. Those primarily responsible for the conduct of the investigations were Dr. W. F. Royce, Mr. J. B. Colton, and Mr. R. J. Buller for the Fish and Wildlife Service; and Dr. B. H. Ketchum, Dr. J. C. Ayers, and Dr. Wm. L. Ford for the Woods Hole Oceanographic Institution.

LIONEL A. WALFORD
Chief, Branch of Fishery Biology
Fish and Wildlife Service

ALFRED C. REDFIELD
Associate Director
Woods Hole Oceanographic Institution

CONTENTS

Preface v

I. The Sport Fishery of the New York Bight 1

II. The Behavior of Waste upon Discharge into the Sea 10

  1. The Barging Operation 10
  2. The Nature of the Waste and its Reactions with Sea Water 10
  3. Observations on the Dilution and Neutralization of Waste in the Wake 13
  4. Summary 17

III. The Biological Effects of Waste Discharge 18

  1. Phytoplankton 18
  2. Zooplankton 18
  3. The Bottom Population 18
  4. Fish 20
  5. Summary 21

IV. Evidence on the Accumulation of Wastes Following Prolonged Barging Operations 22

  1. The Accumulation of Iron in the Sea Water 22
  2. The Accumulation of Iron at the Bottom 26
  3. The Turbidity of the Water 28
  4. Summary 30

V. The Circulation of Water in the New York Bight 31

  1. The Nature of Water Movement 31
  2. Salinity Distribution 32
  3. Factors Influencing the Pattern of Circulation 35
  4. The Rate of Transport of Fresh Water through the Area 38
  5. The Flushing Time 39
  6. The Drift of the Surface Layer 41
  7. Summary 46

VI. Conclusions 47

I. THE SPORT FISHERY OF THE NEW YORK BIGHT

THE interests most likely to be adversely affected by waste disposal operations at sea are the commercial and sport fisheries, and the other recreational activities along the coast. The magnitude and value of the latter interest cannot be questioned in a region close to large urban populations. The operations of the commercial fisheries are well recorded, but the extent of the sport fisheries is not so well known. There has been little published data available on the value, location, and catch of the several species of fish, except for a recent report prepared by Westman and Bidwell which emphasized the value of this resource (**12**).

It has been believed by many that sport fishing is being forced farther and farther to sea because of the sewage and industrial wastes from the great metropolitan area which are being disposed of at sea. With the initiation of barging of industrial wastes to sea by the National Lead Company in the spring of 1948, most active opposition was voiced by representatives of the sports fishery, who considered that their interests were seriously endangered.

The Fish and Wildlife Service has surveyed the sport fisheries of the bight between New York and New Jersey during the years 1948 and 1949. The main objectives of the survey were: (1) to determine the value of the sport fishery to provide a basis for comparing it with the industries with which it conflicted; (2) to obtain data on fishing localities and seasons which could be used to determine the most appropriate regions for waste disposal, and thus reduce the area of conflict between the fishery and waste disposal; and (3) to bring together data on the abundance of fish in the catch which would enable the long-term effects of waste disposal on the fishery to be evaluated.

Briefly summarized, the results of the 1948 survey were as follows:[1]

1. The sport fishing industry of New Jersey and southwestern Long Island was estimated to comprise about a thousand vessels, representing a total value of fifteen million dollars in boats and equipment. The boats were of two principal types: party boats that sailed regularly, took all passengers who appeared at a fixed rate per person, and fished mostly for bottom species; and charter boats, which catered to parties at a fixed price per trip, and fished mostly for surface fish by trolling.

2. Charter boats were found to fish the entire New York Bight even beyond the submerged Hudson River Gorge, and as much as 50 miles from shore. The "Mud Hole", a loosely-applied name for the upper end of the gorge, was found to be an important charter boat fishing area, especially for tuna. Almost 100 percent of the party boat fishing was confined to within 20 miles of shore and chiefly to the west of the gorge, and was concentrated near wrecks, underwater rocks, shoals, etc. (Figure 1).

3. The 1948 sport fishing season extended from the latter part of April through December (Figure 2), depending upon the seasonal appearance of mackerel off the New Jersey coast. With the passing of the spring migration of mackerel, charter boats turned to little tuna (false albacore), bluefish, bonito, skipjack, and bluefin tuna fishing in season; and party boats shifted to bottom fishing for scup, sea bass, fluke, croaker, weakfish, etc.

4. An analysis of the 1948 catch-per-trip for several species was derived to be used for comparison with subsequent years. Limited comparisons, however, were made with earlier years. The charter boat catch-per-trip of tuna during 1948 was not greatly different from the catch-per-trip in 1938 and 1941. The party boat catch-per-trip of scup and sea bass was found to be greater than that recorded in 1938.

Insufficient data were collected during the

---

[1] For a detailed report see Buller and Spear (**3**).

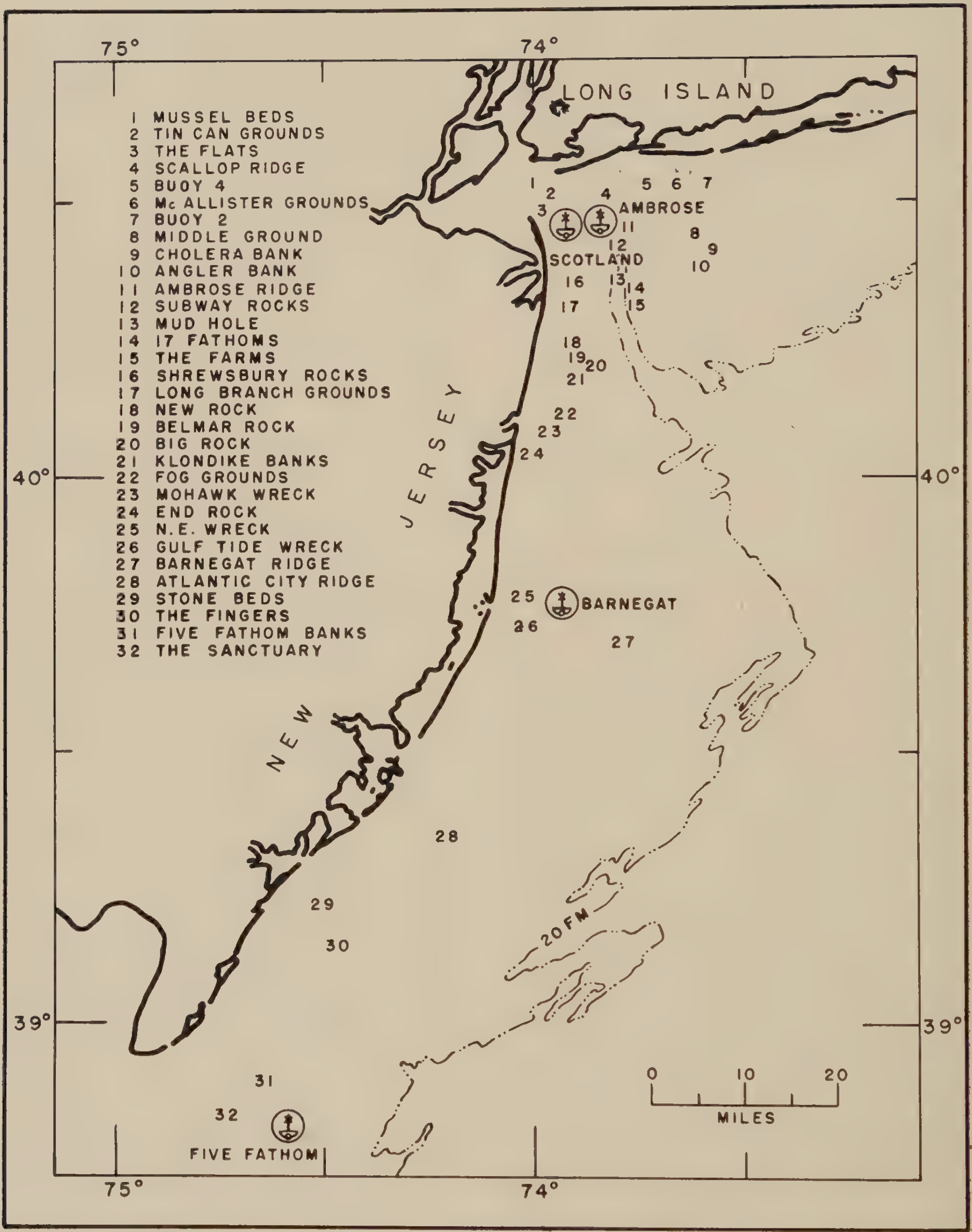
75°
74°
LONG ISLAND
1 MUSSEL BEDS
2 TIN CAN GROUNDS
3 THE FLATS
4 SCALLOP RIDGE
5 BUOY 4
6 Mc ALLISTER GROUNDS
7 BUOY 2
8 MIDDLE GROUND
9 CHOLERA BANK
10 ANGLER BANK
11 AMBROSE RIDGE
12 SUBWAY ROCKS
13 MUD HOLE
14 17 FATHOMS
15 THE FARMS
16 SHREWSBURY ROCKS
17 LONG BRANCH GROUNDS
18 NEW ROCK
19 BELMAR ROCK
20 BIG ROCK
21 KLONDIKE BANKS
22 FOG GROUNDS
23 MOHAWK WRECK
24 END ROCK
25 N.E. WRECK
26 GULF TIDE WRECK
27 BARNEGAT RIDGE
28 ATLANTIC CITY RIDGE
29 STONE BEDS
30 THE FINGERS
31 FIVE FATHOM BANKS
32 THE SANCTUARY
AMBROSE
SCOTLAND
BARNEGAT
FIVE FATHOM
NEW JERSEY
20 FM
40°
39°
0 10 20
MILES

Figure 1. The named bottom fishing areas in the New York Bight

1948 survey to provide an estimate of the total sport fishery catch. The 1949 program was designed to furnish additional information on the value of the sport fishery, and on fishing localities and seasons; and to provide a means of estimating the total 1949 catch made by New York and New Jersey charter and party boats.

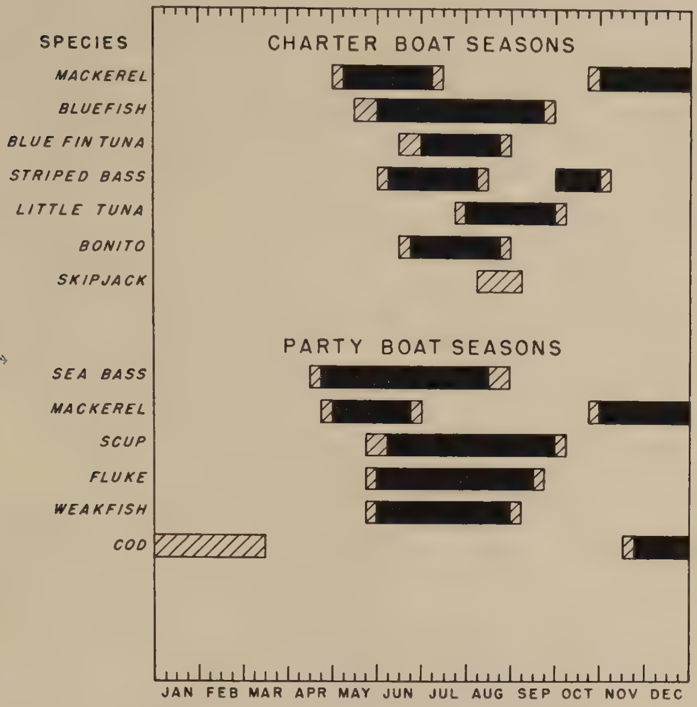

Figure 2. Sport fishing seasons in 1948 by species and boat type. Solid bar indicates catches of more than one fish per man per trip.

TABLE 1

NUMBERS OF CHARTER AND PARTY BOATS, BY PORTS, ENGAGED IN THE 1949 COMMERCIAL SPORTS FISHERY

Ports	Charter Boats	Party Boats
NEW YORK		
Freeport	66	11
East Rockaway	10	10
Sheepshead Bay	9	51
Other ports west of Freeport	14	17
NEW JERSEY		
Elizabethport to Highlands	7	13
Highlands	28	5
Belmar	11	13
Brielle and Point Pleasant	147	37
Forked River	36	2
Barnegat City to Atlantic City	62	
Atlantic City	18	22
Ocean City to Wildwood	11	23
Wildwood	2	43
Cape May	12	44
Total	433	291

To obtain these data, an investigator was in the field continuously from April 20 to the middle of November, 1949, and occasionally after that. He visited routinely all of the fishing ports from Freeport, Long Island, to Cape May, New Jersey. Each port was visited once each two weeks, and the time spent there was proportional to the size of the fleet at the port.

The fleet at these ports (Table 1) comprised 724 vessels, of which 433 were charter boats and 291 were party boats. This number is somewhat less than the number estimated to be engaged in the fishery in 1948. When the private pleasure craft of the charter boat class join the hired craft during the height of the fishing season, however, the number of sport fishing vessels in the New York Bight may exceed 1,000 vessels.

Of this fleet, only the vessels fishing out of the ports from Freeport, Long Island, to Brielle and Point Pleasant, New Jersey, were found to fish in the vicinity of the area now assigned to waste disposal operations out of New York Harbor. From the interviews with captains of the vessels landing at these ports during the 1949 season it was possible to estimate and plot the charter boat (surface trolling) fishing pressure for different areas of the New York Bight. For this purpose the region was divided into areas five minutes of latitude and longitude on a side, or about five miles by four miles in size. The number of fishing trips to each area during the year was used to indicate the fishing pressure. While the charter boats ranged far at sea at times, the areas subjected to the

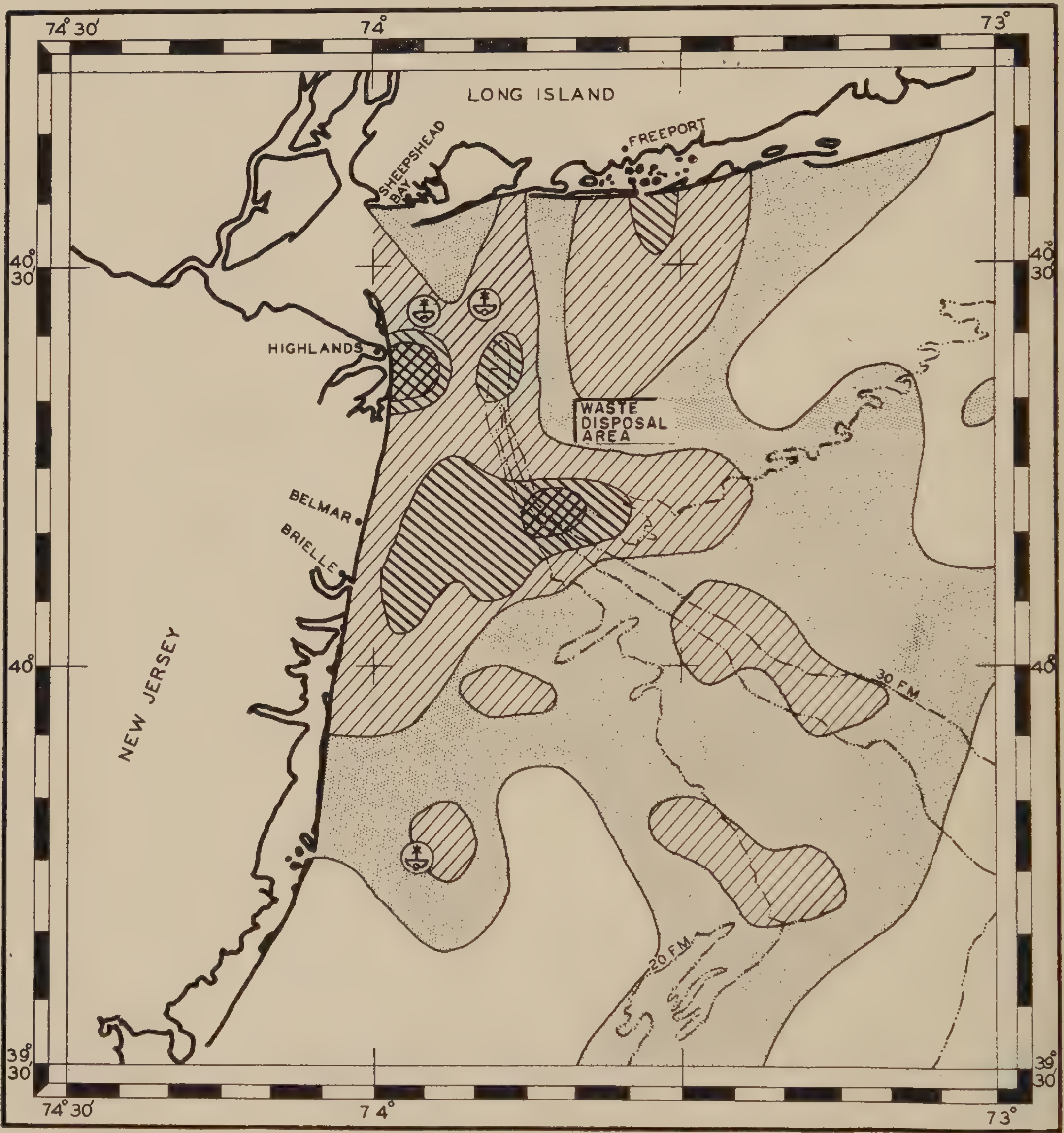
74° 30′
74°
73°
LONG ISLAND
FREEPORT
SHEEPSHEAD BAY
40° 30′
HIGHLANDS
WASTE DISPOSAL AREA
BELMAR
BRIELLE
NEW JERSEY
40°
30 FM.
20 FM.
39° 30′

Figure 3. Localities fished by the charter boats sailing from Freeport to Brielle and Point Pleasant in 1949. The stippled areas represent less than 100 trips per 20 square miles per year, right-oblique-lined areas 100 to 500 trips, left-oblique-lined areas 500 to 1,000 trips, and cross-hatched areas more than 1,000 trips.

greatest fishing pressure (more than 1,000 trips per 20 square miles per year) were in the vicinity of Shrewsbury Rocks and about 20 miles east of Brielle (Figure 3). The "Mud Hole" area south of Ambrose Lightship and a small localized area off Jones inlet, Long Island, received from 500 to 1,000 trips during the 1949 season. The remainder of the inner bight shows a fishing pressure of 100 to 500 trips, or less than 100 trips per 20 square miles per year.

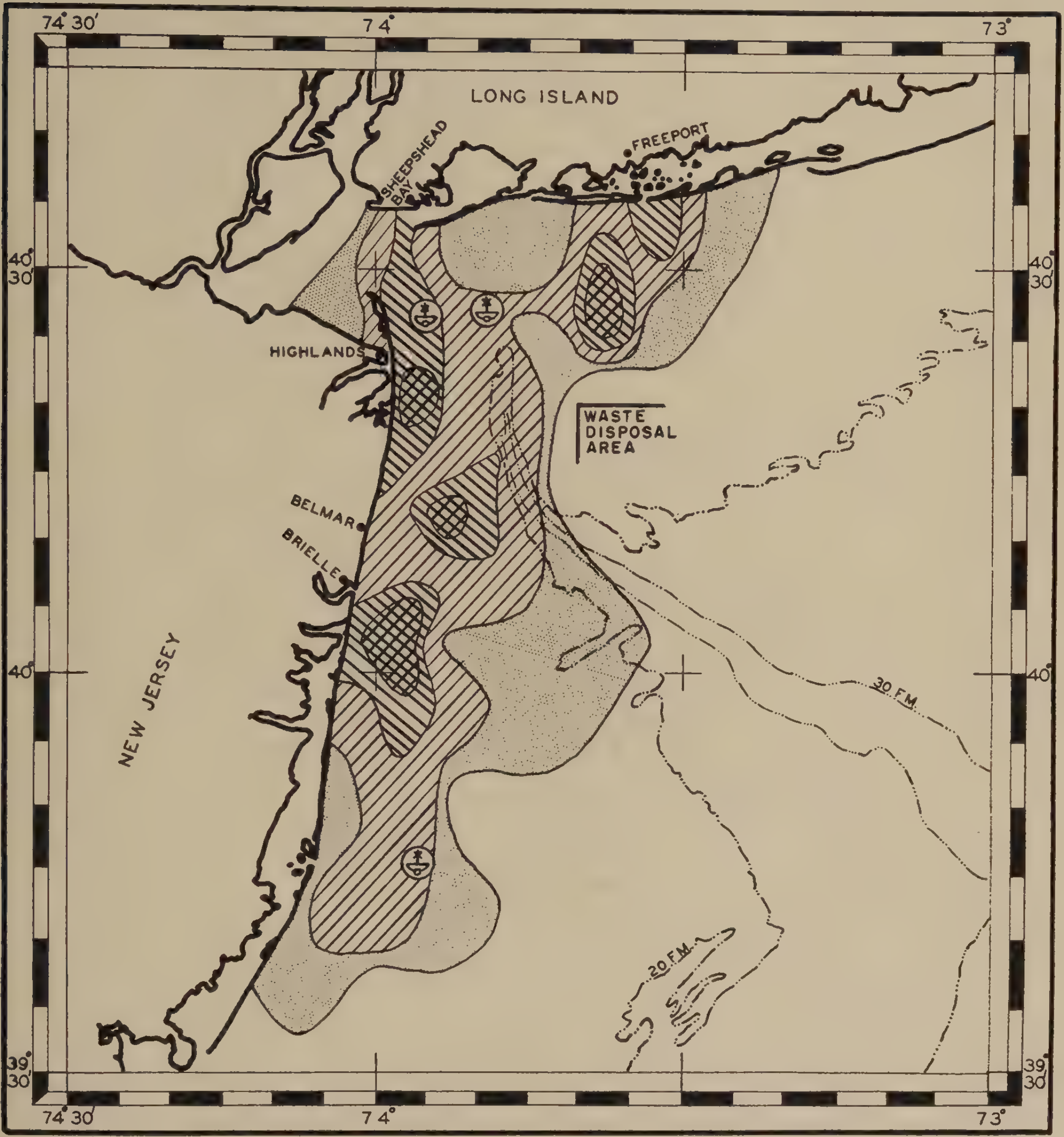
74° 30'
74°
73°
LONG ISLAND
FREEPORT
SHEEPSHEAD BAY
40° 30'
HIGHLANDS
WASTE DISPOSAL AREA
BELMAR
BRIELLE
NEW JERSEY
40°
30 F.M.
20 F.M.
39° 30'

Figure 4. Localities fished by the party boats sailing from Freeport to Brielle and Point Pleasant in 1949. The stippled areas represent less than 100 trips per 20 square miles per year, right-oblique-lined areas 100 to 500 trips, left-oblique-lined areas 500 to 1,000 trips, and cross-hatched areas more than 1,000 trips.

Party boats, fishing on the bottom, ranged at sea less (Figure 4), but, like the charter boat fishery, the Shrewsbury Rocks area

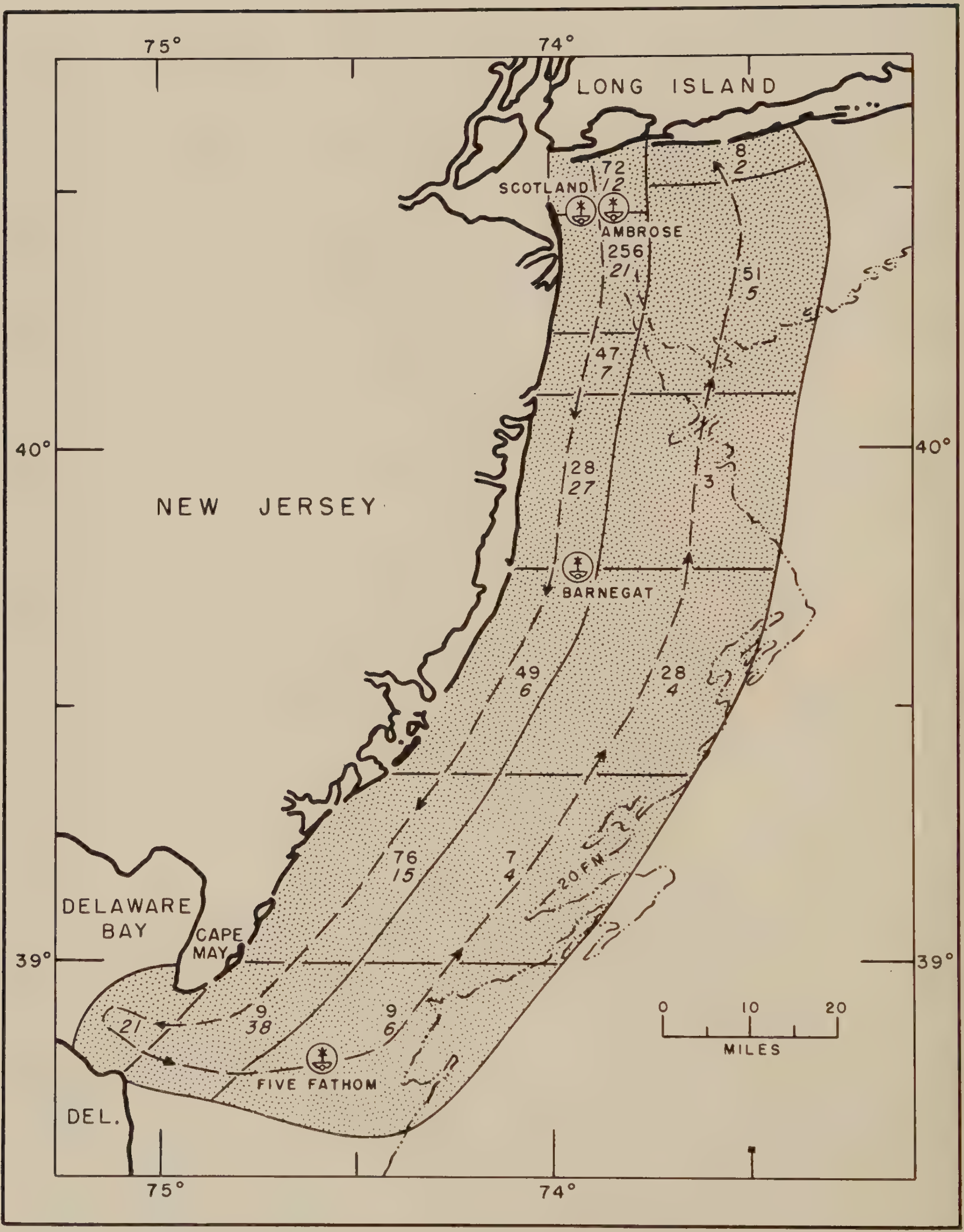
75°
74°
LONG ISLAND
8
2
72
2
SCOTLAND
AMBROSE
256
21
51
5
47
7
40°
40°
NEW JERSEY
28
27
3
BARNEGAT
49
6
28
4
76
15
7
4
20 F.M.
DELAWARE BAY
CAPE MAY
39°
39°
0 10 20
MILES
9
38
21
9
6
FIVE FATHOM
DEL.
75°
74°

Figure 5. Numbers and locations of charter boats (vertical figures) and party boats (slanted figures) observed by airplane on Labor Day, September 3, 1949.

received a fishing pressure of more than 1,000 trips per 20 square miles per year. Other areas subjected to this intensity included Cholera Bank, the Klondike-Big Rock area east of Belmar, and a concentration of wrecks some 5 to 15 miles southeast of

Brielle. Party boats, like charter boats, made from 500 to 1,000 trips to the grounds off Jones Inlet. Another area receiving a comparable fishing pressure extended from Rockaway Inlet to just north of Belmar. This area includes the Tin Can Grounds, the Flats, the Mussel Beds, and the various wrecks and rock grounds in the vicinity of Shrewsbury Rocks.

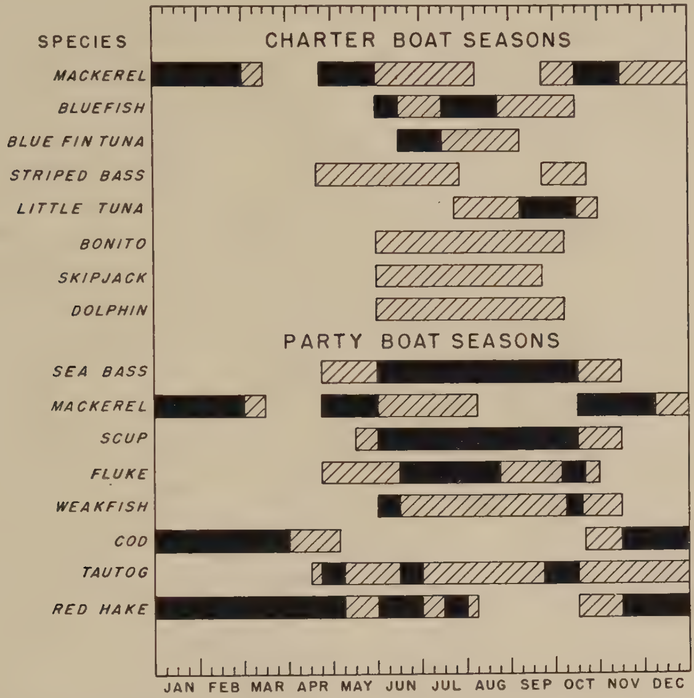

Figure 6. Sport fishing seasons in 1949 by species and boat type. Solid bar indicates catches of more than one fish per man per trip.

Further data on the numbers of fishing vessels and the location of fishing grounds were obtained by flying over the area. Three flights were made in a PBY plane through the cooperation of the United States Coast Guard at Floyd Bennett Field. The first and second flights, made in July and August respectively, were unsuccessful because of fog and haze which obscured the observer's vision. The third flight, made on Labor Day (September 3) covered the bight from Long Island to the entrance of Delaware Bay in two long sweeps—the first approximately five miles offshore and the second about twenty miles offshore (Figure 5). On this flight the observer counted a total of 737 vessels; 596 charter boats and 141 party boats. Visibility during the flight varied from 5 to 10 miles on either side of the plane and it is believed that only a small percentage of the sport fishing vessels "out" that day escaped detection.

The concentrations of charter and party boats illustrated in Figure 5 closely parallel the fishing charts (Figures 3 and 4). The greatest concentration of sportfishing vessels was observed in the vicinity of the lightships and along the New Jersey coast. The number of charter boats observed during the flight exceeded the total number of this class of vessel considered to be engaged in the commercial sport fishery. This excess was no doubt due to private pleasure craft which could not be distinguished from charter boats from the air.

Data were also collected on the duration of the charter and party boat fishing seasons during 1949 (Figure 6). Both fisheries enjoyed a season for mackerel during the winter of 1948–1949 which was somewhat longer than usual. As a rule, fishing for mackerel begins to wane the latter part of November. For some reason—perhaps the open winter and abundant food supplies—mackerel remained in the New York Bight throughout the early part of 1949, with good mackerel fishing to be had until the first part of March, after which they apparently migrated out of the bight area to return about six weeks later. In general, the major portion of the 1949 sport fishing season occurred from May through September, but some fishing was pursued throughout the entire year.

TABLE 2

Comparison of the Abundance of Predominant Species in the Commercial Sport Fishery in 1948 and 1949

Species	1948		1949	
	Fish per Trip	Fish per Fisherman	Fish per Trip	Fish per Fisherman
Charter Boats				
Mackerel	153.5	25.1	309.4	33.0
Bluefish	30.1	5.7	33.3	6.0
Little tuna	12.1	2.3	18.6	3.6
Bluefin tuna	7.5	1.1	23.3	4.2
Party Boats				
Mackerel	586.1	30.0	540.0	26.0
Scup	310.5	19.8	722.0	32.2
Sea bass	160.5	12.9	329.0	17.0
Weakfish	141.5	19.1	190.1	18.5
Fluke	53.3	11.6	122.6	7.6

The abundance of predominant species in the charter and party boat catch during the major portion of the 1949 sport fishing season is compared to the abundance of these species during the 1948 season in Table 2. These figures show that the charter boat catch of mackerel, bluefish, little tuna, and bluefin tuna per trip and per fisherman was greater than the catch in 1948. The greatest increase is noted in the catch of bluefin tuna. This species, mostly small "school" tuna, were three times as abundant in 1949 as in 1948. Scup were about twice as abundant in 1949 and sea bass showed a small increase. Mackerel and weakfish were about the same as in 1948, whereas fluke showed an increase in the catch per trip; but with more people being carried the catch per fisherman decreased.

TABLE 3

Estimated Commercial Sport Fish Catch Landed between Freeport, Long Island, and Point Pleasant, New Jersey, during 1949

Species	Estimated Catch (Thousands of Fish)		
	Party Boats	Charter Boats	Total
Scup	3,161	126	3,287
Mackerel	1,985	1,047	3,032
Sea bass	1,032	73	1,105
Red hake	208	4	212
Fluke	186	24	210
Tautog	146	6	152
Bluefish	4	136	140
Weakfish	78	15	93
Cod	66	12	78
Little tuna	1	46	47
Bluefin tuna		24	24
Dolphin	2	12	14
Skipjack		6	6
Bonito		3	3
Striped bass		1	1
Miscellaneous	74	27	101
Total	6,943	1,562	8,505

An estimate of the sport fish catch from the bight which was landed by vessels from Freeport, Long Island, to Point Pleasant, New Jersey, is presented in Table 3. The total estimate of 8,505,000 fish landed includes both the charter and party boat catch but does not include the catch made by private pleasure craft.

SUMMARY

The general conclusions which may be reached from the survey of the sport fishery are:

1. The sport fishery employs about 1000 boats representing an estimated investment of fifteen million dollars. Since the 300 party boats carry an average of 20 fishermen and 700 charter boats and private craft about 7, it is evident that many thousands of persons benefit from the recreation of sport fishing. The sport fishing industry consequently has a strong claim for protection from possible harmful effects of waste disposal.

2. While the area of intense fishing is concentrated for the most part within fifteen miles of the Long Island and New Jersey coasts, charter boats fish widely over an area extending nearly 50 miles from the coasts. There appears to be no accessible area which might be assigned for waste disposal which would be entirely outside the regions sometimes visited by fishermen. While the greater part of the fishing is conducted in May through September, some fishing is pursued throughout the entire year.

3. The abundance of predominant species of fish was greater in 1949 than in 1948 or 1938. Fish populations are subject to such marked fluctuations in abundance from year to year that this fact cannot be taken to indicate any long-term trend.

II. THE BEHAVIOR OF WASTE UPON DISCHARGE INTO THE SEA

Because of the large volumes of waste involved in the National Lead Company's operations, and the presence in it of a familiar acid, it was only natural that those to whom the full facts were not available should entertain alarming conjectures. It was feared that masses of undiluted acid would drift about upon the sea's surface or would settle to the bottom where fishes would be injured. It was rumored, even before the barging operations began, that fishing nets were being rotted by the discharged acid. While it could be predicted in advance that these extreme fears were groundless, one could not be at all sure just how the waste would behave on discharge, how rapidly it would be dispersed, and at what depths it would be found. Consequently, the first matter to be investigated was the behavior of the waste upon discharge into the sea.[2]

1. THE BARGING OPERATION

The waste originates at the titanium plant of the National Lead Company at Sayreville, New Jersey, near the mouth of the Raritan River. It is held temporarily in storage tanks until it can be removed by the barge. The barge, constructed for the purpose (**10**), carries 3,200 tons of the waste, and when operating on full schedule discharges one load every 18 hours (Figure 7). The barge is towed by a tug at a speed of approximately six knots, the waste being discharged from two twelve-inch pipes mounted on skegs at keel level at the after end (Figure 8). When the barge is fully loaded, these pipes are at a depth of 15 feet, but as the waste is discharged the depth decreases to six feet when the tanks are empty. About eighteen tons of waste are discharged per minute. This gives a rate of discharge of about sixty pounds per foot of distance traveled.

The discharge pipes are so located that the waste enters the sea in the very turbulent region where water displaced by the barge's passage is rushing in under the stern to form the wake. It is consequently mixed rapidly with the water of the wake and greatly diluted.

Initially, an area two miles square centered ten miles SE × E from Scotland Lightship was assigned for this purpose. This area is immediately over the submerged gorge of the Hudson River, where depths up to thirty-two fathoms (192 feet) occur. While discharging waste the barge circled within this area.

At the request of the New York State Department of Conservation, a new area for disposal was assigned in April 1949. This area was located at a greater distance from the more important fishing grounds. The barge was required to remain south of the parallel 40°20′N latitude and east of the meridian 73°40′W longitude. The point of intersection of these limits is 13 miles SE from Scotland Lightship, 14 miles from the New Jersey coast and 15 miles from the Long Island coast. The depth in this area is about eighty feet. While discharging the barge usually proceeds in a southeasterly direction for a distance of five or six miles and then turns to return over a parallel course. This arrangement provides for an initial dispersal of the waste material over a wide area.

The location of the waste disposal areas is shown on the chart reproduced in Figure 9.

2. THE NATURE OF THE WASTE AND ITS REACTIONS WITH SEA WATER

The waste consists of approximately ten percent ferrous sulfate ($FeSO_4$) and 8.5 percent sulfuric acid (H_2SO_4) dissolved in fresh water. Many other substances are doubtless present, but not in quantities likely to prove harmful. The expected chemical effects on the sea water will be those arising from (1)

---

[2] For a detailed report see Ketchum and Ford (**8**).

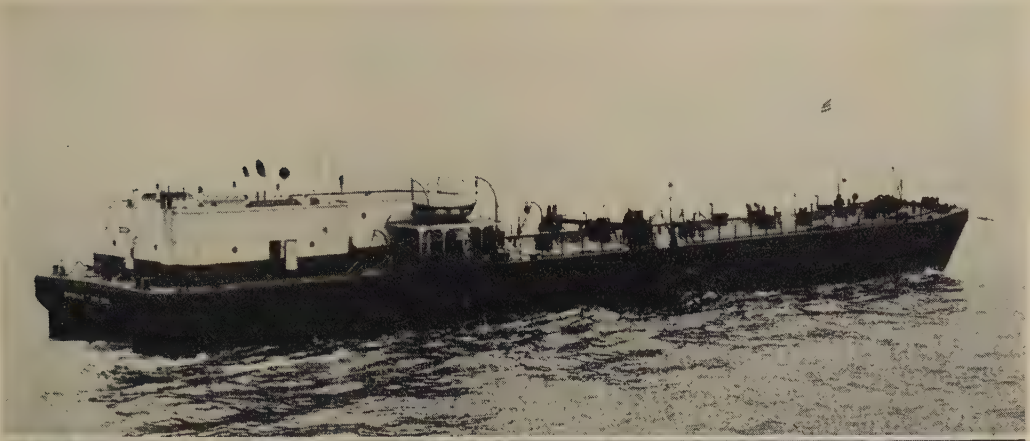

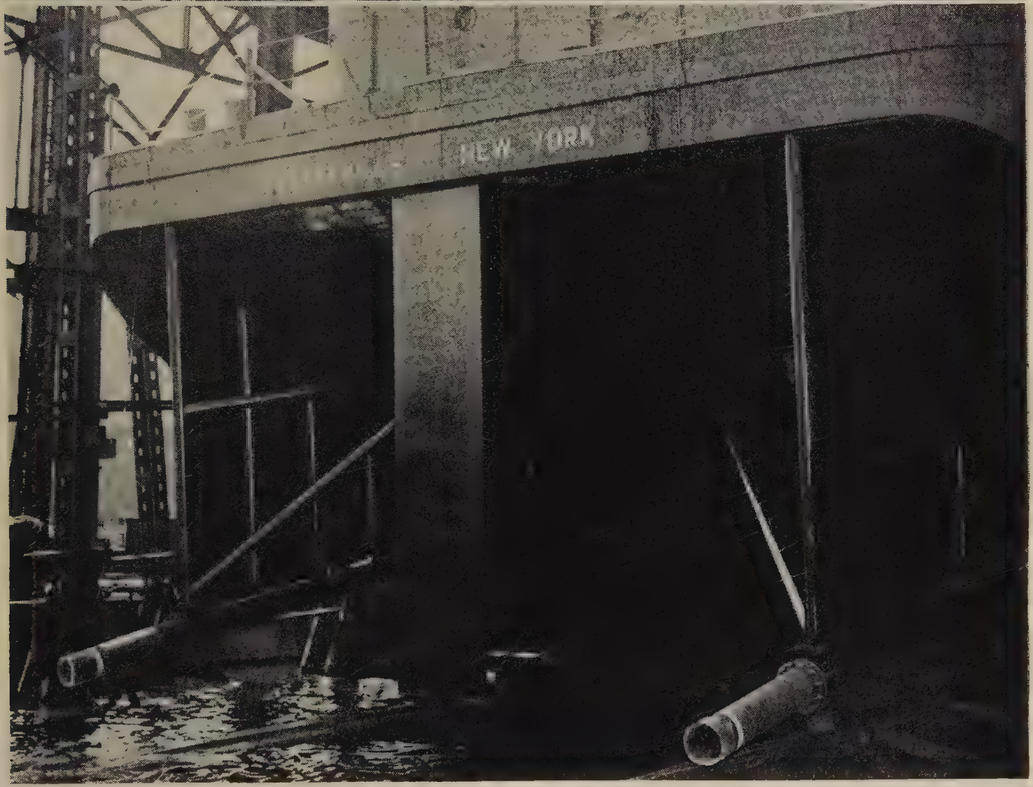

Figure 7 (upper). **Barge *Sayreville* constructed for the disposal of titanium waste at sea.** (Courtesy of National Lead Company.)

Figure 8 (lower). **Stern of the barge *Sayreville*, showing the position of the pipes through which waste is discharged.** (Courtesy of National Lead Company.)

an increase in the ferrous ion concentration, (2) an increase in the sulfate ion concentration, and (3) disturbance in the acid–base balance of sea water because of the acidity of the waste material.

The most immediate effect of the addition of ferrous ion to sea water will be to reduce the oxygen content of the water, since the ferrous ion will be rapidly oxidized. The resulting ferric ion will be precipitated as

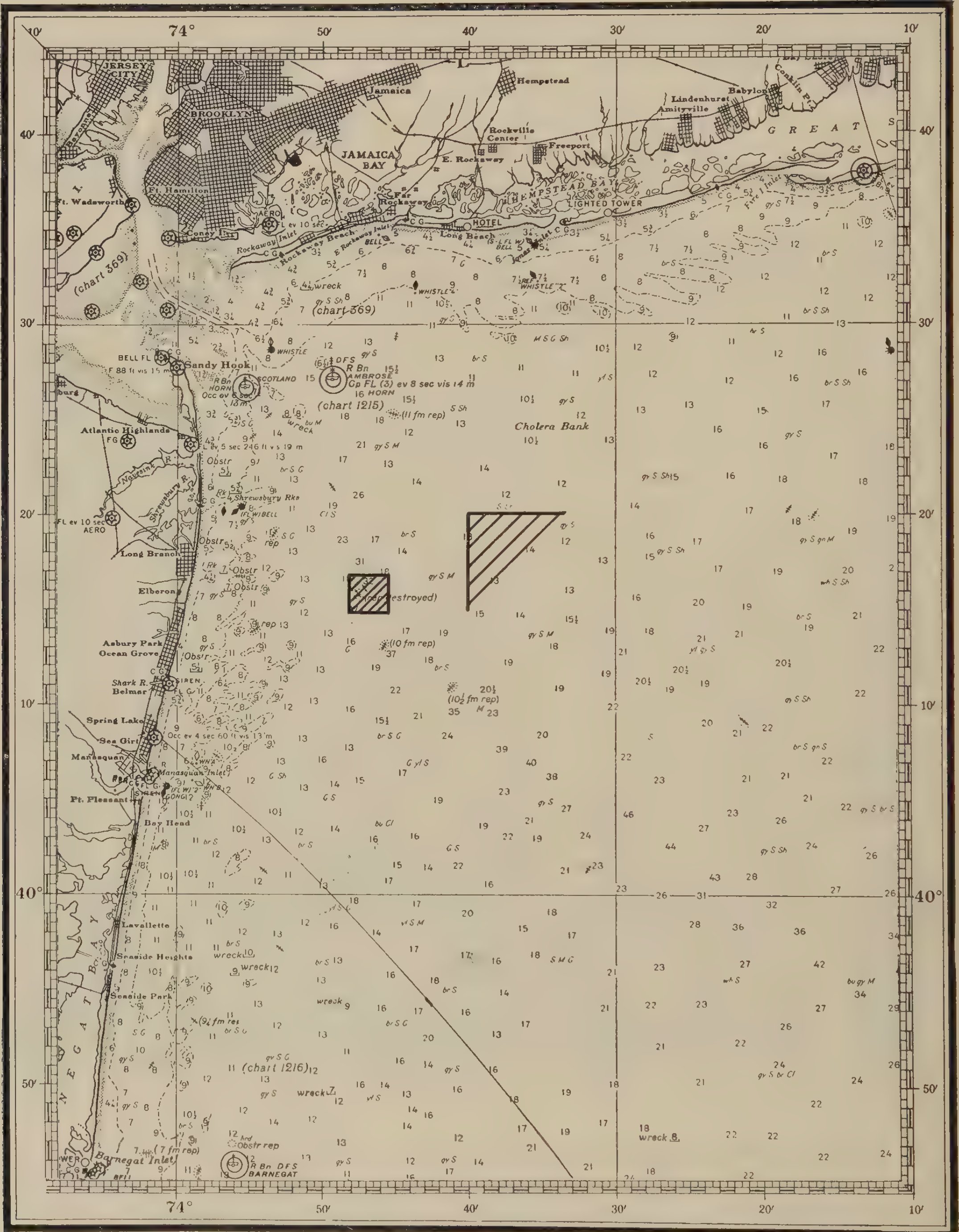
74°
50′
40′
30′
20′
10′
40°
Jersey City
Brooklyn
Jamaica
Hempstead
Babylon
Lindenhurst
Amityville
Rockville Center
Freeport
Jamaica Bay
E. Rockaway
Ft. Hamilton
Ft. Wadsworth
Coney I.
Rockaway Inlet
Rockaway Beach
Far Rockaway
Long Beach
Hempstead Bay
Lighted Tower
Great S
(chart 369)
Sandy Hook
Ambrose
(chart 1215)
Cholera Bank
Atlantic Highlands
Shrewsbury Rks
Long Branch
Elberon
(destroyed)
Asbury Park
Ocean Grove
Shark R.
Belmar
Spring Lake
Sea Girt
Manasquan
Manasquan Inlet
Pt. Pleasant
Bay Head
Lavallette
Seaside Heights
Seaside Park
(chart 1216)
Barnegat Inlet
Barnegat

Figure 9. Chart of the New York Bight. The area presently assigned for waste disposal is shown as a triangle. The original area, shown as a square, is no longer in use. Based on U. S. Coast and Geodetic Survey Chart No. 1108. The numbers on the chart show depths in fathoms.

ferric hydroxide, since sea water is saturated with respect to ferric ion. The product will be an inert material which forms colloidal suspensions and may be expected to settle slowly and thus become widely dispersed by currents.

The sulfate ion is itself one of the principal normal constituents of sea water, being present in concentrations of 2.65 parts per thousand. Unless it were added to sea water in quantities which would seriously upset the salt balance, it is not likely to produce toxic or other undesirable effects. There is no possibility that such effects could be produced by the quantities of waste in question.

The disturbance of the acid–base balance of sea water by the addition of the waste might produce degrees of acidity which would be distasteful or harmful to marine life. Sea water is a weak alkaline solution having normally a pH of 8.0 to 8.2. Its ability to neutralize acids is well understood, and it was possible to estimate in advance that the waste would not only be greatly diluted on introduction into the wake but also that it would be rapidly neutralized upon mixing with sea water.

For example, if the initial dimensions of the wake are given by the beam of the barge (43 feet), by its mean draft (10.5 feet), and by the rate of advance (6 knots or 600 feet per minute), the volume of wake water with which the waste mixes is 270,000 cubic feet, or 15,600,000 pounds per minute. If the waste is discharged at the rate of 18 tons or 36,000 pounds per minute, the waste will be diluted at once in the proportions 36,000:15,600,000, or about two parts to one thousand. The dilution of sulfuric acid present at 10 percent in the waste becomes two parts in ten thousand.

The ability of sea water to neutralize acids depends upon the fact that it contains a certain amount of base combined as bicarbonate. This fraction of the total base is known as *excess base*. On addition of an acid, such as sulfuric, the excess base combines with the sulfate ions to form sulfates, setting free an equivalent quantity of carbonic acid. This is a weak acid which, when the reaction is complete, does not reduce the pH below about 4.5. Furthermore, the carbonic acid can rapidly escape as carbon dioxide from the sea surface, which permits the sea water to return to neutrality.

The excess base present in sea water (of salinity 32 such as occurs in the coastal water off New York) is 2.16 milliequivalents per liter. This means that there is sufficient base present in ten thousand parts of sea water to combine with one part of sulfuric acid. Until this ratio is exceeded there will not be any free sulfuric acid present and the pH will not fall below 4.5. Comparing this proportion with the estimated dilution of the waste in the wake (two parts in ten thousand) it is evident that under the assumed conditions about half the sulfuric acid will be neutralized immediately on mixing with sea water at the stern of the barge. Furthermore, since the wake mixes rapidly with the surrounding water, as evidenced by its tendency to widen as it falls astern, the remaining sulfuric acid will be neutralized within a short distance behind the barge.

These considerations made it appear unlikely that any serious degree of acidity would exist, except briefly, in the water into which the waste was discharged. While the chemistry on which they are based is well established, no information exists concerning the actual way in which the waste would behave on discharge from a moving barge, or on the details of the mixing processes which would take place in the wake after the barge's passage. Consequently, a detailed examination was made of the chemical conditions in the water left astern by the barge while waste was being discharged.

3. OBSERVATIONS ON THE DILUTION AND NEUTRALIZATION OF WASTE IN THE WAKE

To CONDUCT this study the Woods Hole Oceanographic Institution employed its research vessel *Balanus*, a 76-foot fishing vessel converted for research purposes. She is small enough to maneuver safely close to the barge and has sufficient speed to avoid being left behind during such operations. She is fully equipped for hydrographic studies and for the special chemical observations required. (See Figure 10.)

Two sensitive chemical methods were available for measuring the waste in the sea water. The sulfuric acid could be detected by its effect on the pH of the water, which was measured by the usual meters. The *Balanus* was equipped with a recording pH meter which determines the acidity of a stream of sea water pumped through it from a sea cock located about four feet below the water line. Continuous information was thus available for the acidity at that depth. In addition, samples of water drawn from other depths could be measured with the usual laboratory model pH meter. A much more sensitive test for the presence of the waste material is provided by the iron present in it as ferrous sulfate. Iron can be detected by the dipyridyl method described by Cooper (**4**) in concentrations as low as one part in 100 million parts of sea water. This means that the presence of waste could be detected after dilution with three million parts of sea water.

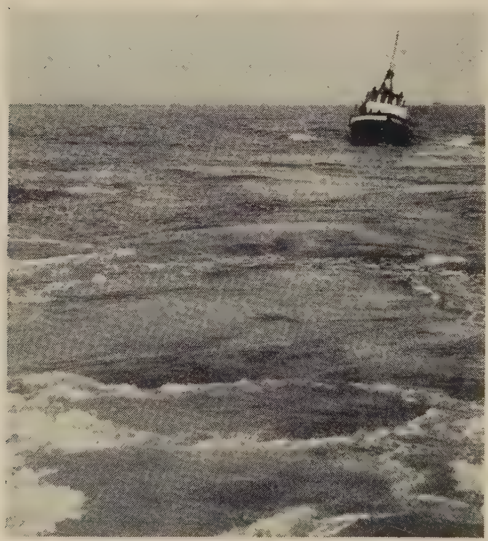

Figure 10. Research vessel *Balanus* investigating the concentrations of waste in the wake of the barge *Sayreville*.

The study of the wake required the exact sampling of the water at various depths and distances behind the barge. For this purpose, a newly-developed device known as the Sea Sampler was used (**11**). (See Figure 11.) This instrument consists of a number of small tubes or "bottles" through which water circulates freely as it is lowered over the side of the ship. As the Sea Sampler is brought to the surface again, the bottles are closed automatically at predetermined depths by the change in pressure. In this way, samples could be obtained from any part of the wake.

The investigation showed that the estimates of the immediate dilution of the waste in the wake were essentially correct. Samples collected as close to the point of discharge as possible and within thirty seconds after discharge were already diluted with sea water more than 250 times.

After the passage of the barge, the wake continues to mix with the undisturbed water on either side. In consequence, its visible width increases and the waste material in the wake water becomes more and more dilute until it is no longer recognizable. With dilution the acidity decreases rapidly, as shown by the rise in pH. These changes in the surface water are summarized in Table 4 and are illustrated in Figures 12 and 13.

Although the wake continues to grow in width for a long time as it spreads at the sea surface, it reaches its greatest depth almost immediately. During observations in April, 1948, the limiting depth of the wake was about thirty feet, while in July it was fifty feet. In January, 1950, the disposal area had been moved to a location where the total depth of water was 70–80 feet, and the waste was detected in water near the bottom at distances greater than 450 yards behind the barge. Figures 14 and 15 show measurements of the vertical distribution of pH and iron in the wake made during the April studies. It seems probable that these limits were set by the thermal stratification of the water which hinders vertical mixing. In winter the wake may mix more deeply since stratification is weaker or absent, but during the spring and summer there is little likelihood that contaminated water will reach the bottom in depths of sixty feet or more.

The important point brought out by these studies is the very rapid neutralization of the acid waste in the wake. Within three and one-half minutes after the passage of the barge, the water has returned to the neutral reaction of pH 7. In this time, the barge has moved 700 yards and the wake has spread from a width of 10 yards to one of 25 yards, and has a depth of 12 yards. These are the dimensions of the entire volume which at any one time has an acid reaction. They represent a surface area of

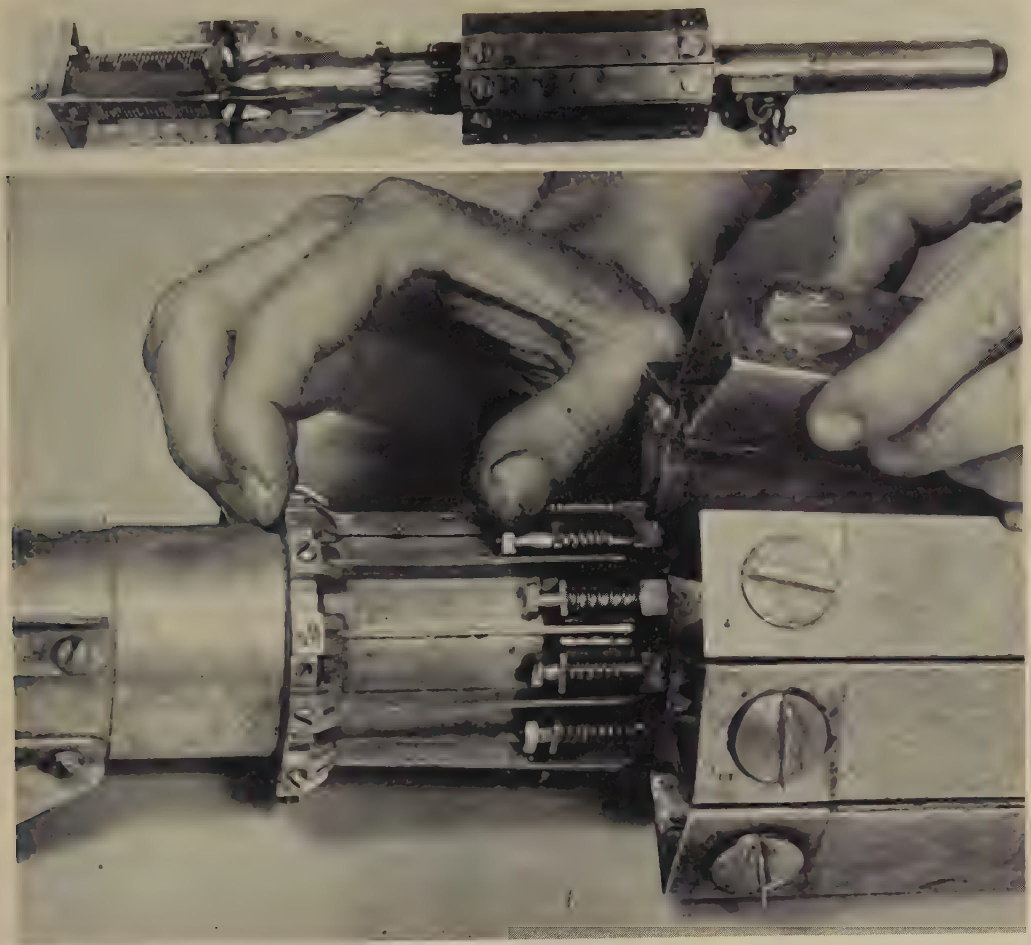

Figure 11. The Sea Sampler, a device employed for sampling water at various depths in the wake of the barge. The lower view shows a water sampling bottle being removed. (After Spilhaus and Miller (**11**).)

TABLE 4

Visual Estimates of the Width of the Wake Behind the Barge

Age of Wake	Distance Astern of Barge	Visual Width of Wake
Minutes	*Yards*	*Feet*
8.5	1700	100
16.5	3300	225
20.5	4100	635
27.5	5500	750

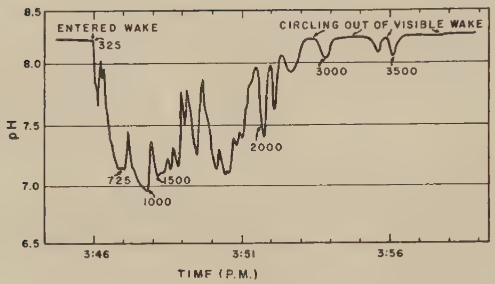

Figure 12. Tracing of pH record in the wake after passage of the barge *Sayreville*, while discharging waste. The numbers on the record are the distances behind the barge, in yards. (April 27, 1948.)

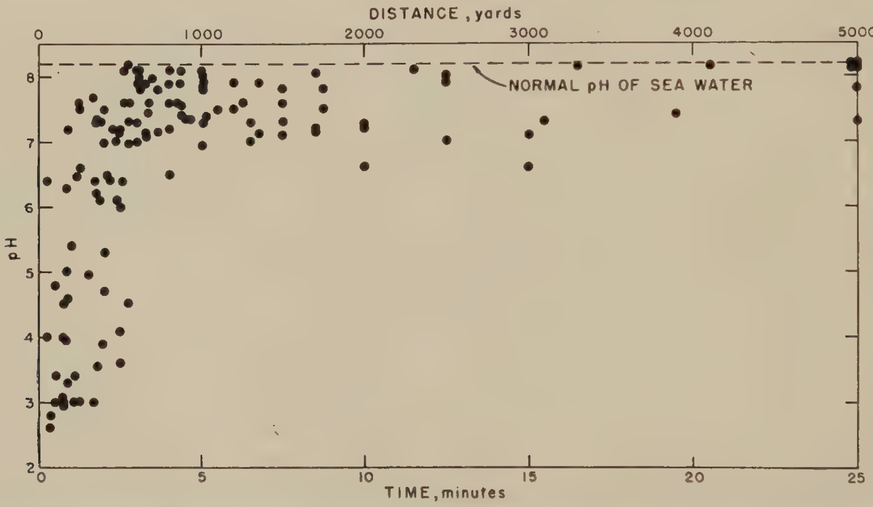

Figure 13. Values of the pH of the surface water in the wake of the barge measured at various times after the passage of the barge. Upper scale shows the distance traveled by the barge beyond the points of observation.

less than 3 acres. The entire area of the sea surface made acid temporarily by a single load of waste is about $\frac{1}{4}$ square mile.

The waste has a bright green color because of the ferrous sulfate present in it. Immediately behind the barge the water is discolored by the waste, which appears light green against the darker green of the sea water. Gradually the wake turns brown as the ferrous iron is oxidized and forms ferric hydroxide. The ferric hydroxide, which is nothing but finely divided iron rust, remains in suspension and gives the wake a muddy appearance which makes it prominently visible, especially in sunny weather. In such weather the discolored water is visible for at least three or four hours after discharge, and on one occasion a patch of water was recognizable by its color for about eight hours.

The oxidation of ferrous iron may be expected to use up a certain amount of the oxygen in the sea water. Since this might prove harmful, the rate of oxidation of the iron was carefully followed. The oxidation takes considerable time and is only half complete about forty minutes after discharge into the sea. At no time was enough ferric iron present in the water to have used up more than three or four percent of the oxygen present.[3] It was concluded that the oxidation of the iron has only a brief and negligible effect on the oxygen content of the water.

The ferric hydroxide itself is a quite inert substance not likely to have much effect on living organisms. In the high concentration in which it is produced immediately behind the barge, the precipitate is quite visible and may well influence the movements of fish, as might any other cause of dense turbidity. It is evident from the analysis of the distribution of iron in depth that it stays in suspension until greatly dispersed by mixing

[3] Technical details were reported by Ketchum and Ford (**8**).

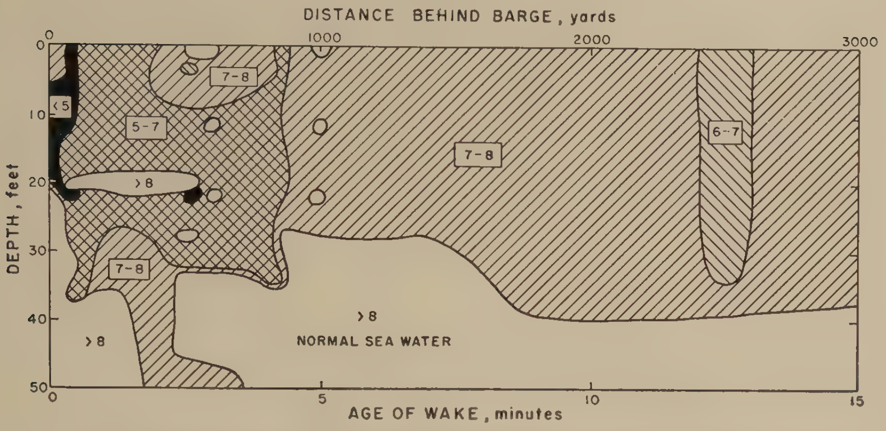

Figure 14. Distribution in depth of pH values of water in wake of the barge. April 1948

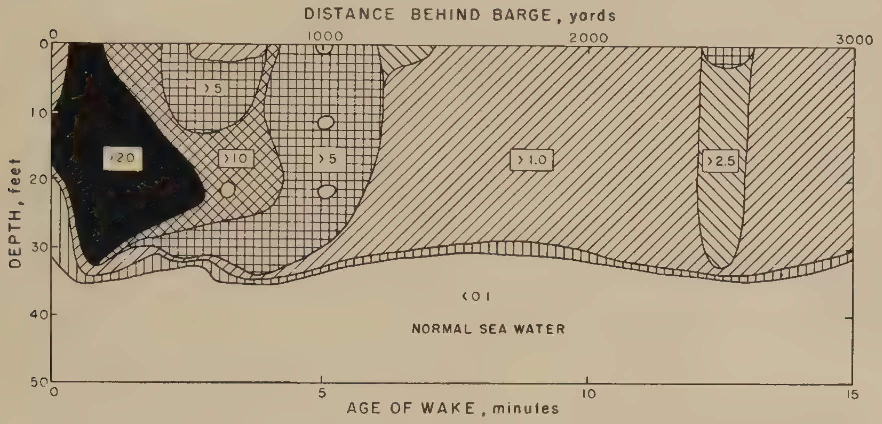

Figure 15. Distribution in depth of iron in wake of the barge. April 1948

with the surface water, and it must in consequence become distributed very widely before settling to the bottom.

It will be shown subsequently that the sea water in the approaches to New York Harbor is considerably contaminated with iron brought in by the rivers. Conditions in the wake of the barge during disposal operations can thus be compared with those actually occurring in various parts of the area. It is found that thirty minutes after the passage of the barge the waste has become so dispersed that its iron content is about the same as that which was observed in the head of Raritan Bay in July 1948. In four or five hours, the iron concentration in the wake is comparable to that in the sea in the neighborhood of Sandy Hook and Scotland Lightship.

SUMMARY

The study of the behavior of the waste in the wake of the barge during disposal operations indicates that the acidification of the sea water is very short-lived because of the rapidity with which the waste is diluted and neutralized upon discharge into the turbulent wake. Water which has been appreciably modified in its chemical properties is not likely to be found near the bottom or at any substantial distance from the barge and will exist nearby only immediately after its passage.

The only prominent after-effect of the disposal operation is the turbidity of the water due to the formation of ferric hydroxide in the wake.

III. THE BIOLOGICAL EFFECTS OF WASTE DISCHARGE

1. PHYTOPLANKTON

THE PRIMARY source of food for the animal life in the sea is the microscopic floating plants called phytoplankton. These organisms drift with the currents and multiply very rapidly if the water contains the necessary plant nutrients. Even if we assume that many of the phytoplankton exposed to acid in the wake would be destroyed, the volume of water acidified is so small compared to the area as a whole, and the phytoplankton multiply so rapidly, that the effect of such damage on the food supply would be negligible. Moreover, as will be shown subsequently, the water in this region of the coast is in such active circulation that new bodies of sea water are constantly replacing those into which the waste has been discharged.

Since iron is required in low concentrations for the growth of phytoplankton it has been suggested that the waste might actually improve the plant population. The studies have shown, however, that the waters in the offing of New York are unusually rich in iron as the result of the high content of the Hudson, Raritan and other rivers draining into the area. Once dispersed, the iron discharged by the barge would not greatly change the amounts available for growing plants.

2. ZOOPLANKTON

THE MINUTE marine animals which are dispersed through sea water, called zooplankton, are the immediate source of food of many fish. In order to test the effect of the wake water on these organisms, small samples of zooplankton were collected from uncontaminated water and were exposed to water drawn from the wake at various distances behind the barge. The results of this experiment are summarized in Table 5. Although the organisms in every case were immobilized by exposure to the wake water, they usually recovered their activity and appeared to be in a normal condition after two or three minutes even though they remained in the contaminated water. The specimens exposed to the most heavily contaminated water, which had been drawn from the wake less than one minute after passage of the barge, did not recover spontaneously. However, when the water containing these organisms was diluted with an equal volume of uncontaminated water, they recovered and commenced to swim about immediately.

Under the conditions of operation, in which the wake water is rapidly diluted after passage of the barge, some of the organisms drawn into the wake immediately behind the barge might suffer permanent damage. However, as in the case of the phytoplankton, the volume of water acidified by each barge load is very small compared to that in the disposal area, and the effect on the zooplankton population would be negligible, even though the organisms entrapped in the wake were destroyed.

3. THE BOTTOM POPULATION

WHEN the disposal operations at sea were first under consideration it was feared that the waste might settle on the bottom and would damage the bottom living organisms, and thus affect the ground fishery. It was consequently planned to study the conditions at and over the sea bottom by photographing the bottom and collecting the animals in the mud. Similar observations were made in the "Mud Hole" which was selected as a control area not immediately exposed to contamination.[4]

Observations were made in these two areas in March, 1948, before disposal operations had begun, and in May, 1948, when dumping had been in progress for about one month. These observations were lumped together as the best representation of "normal" conditions, since unexpected difficulties prevented an adequate representation from being obtained in March. Studies were again made in November, 1948, after disposal had been going on for seven months, in the hope of showing up any effects of the operation. Photographs of the bottom were made in representative areas, from which all recognizable animals and signs of life such as worm trails and burrows were counted. Specimens were also taken from the bottom using an orange peel dredge 9¼ inches in diameter. These specimens were screened to separate the animals, which were identified and counted. The results of these studies are summarized in Tables 6 and 7. They show that the numbers of organisms varied greatly, some increasing while others decreased during the period intervening. From the number of observations which were made, it is quite impossible to determine whether the changes are due to the natural changes which accompany the seasons, to inadequate sampling of bottoms which doubtless vary from place to place, or to any possible effect of the dumping of waste. At least it was clear that the populations changed in the control area in the Mud Hole quite as much as in the disposal area.

---

[4] These investigations have been reported in somewhat greater detail by Arnold and Royce (**1**).

TABLE 5

EFFECT OF WASTE ON ZOOPLANKTON

Yards Behind Barge	Age of Wake	pH	Iron	Effect	Recovery Time	Condition at 5 Minutes
	Min.		*mg. per l.*		*Min.*	
145	0.7	5.65	26.0	Immobilized	Incomplete	Not normal
250	1.2	6.36	10.8	"	2–3	Normal
375	1.8	6.57	12.6	"	1	"
475	2.3	6.92	5.4	"	1	"
650	3.2	6.80	2.4	"	1–2	"
800	3.9	6.62	10.5	"	3	Nearly normal
1250	6.1	7.42	3.0	"	1	Normal
1520	7.5	6.95	2.2	"	1–2	"

TABLE 6

NUMBERS OF ANIMALS TAKEN IN BOTTOM SAMPLES WITH 9¼-INCH GRAB

	Disposal Area		Mud Hole	
	March & May	November	March & May	November
Sea Urchins	4	0	0	0
Sea Cucumbers	113	37	0	0
Flat Worms	2	0	0	4
Nematode Worms	0	0	0	1
Annelid Worms	301	331	26	46
Clams	72	12	12	126
Snails	2	0	0	0
Amphipods	17	168	0	0
Crabs	1	0	0	0
No. of Specimens	513	248	38	177
No. of Samples	37	13	8	12
Specimens per sample	14	19	4.8	14.6

TABLE 7

NUMBERS OF ANIMALS VISIBLE IN PHOTOGRAPHS OF THE SEA BOTTOM

	Disposal Area		Mud Hole	
	March & May	November	March & May	November
Sponges	0	0	1	0
Star Fish	37	34	1	1
Sea Urchins	2	0	6	1
Sea Cucumbers	0	1	0	0
Crabs	2	0	0	0
Animal Trails	10	0	0	1
Animal Burrows	25	14	15	0
No. of Specimens	76	49	23	3
Area Covered—sq. ft.	246	281	40	296
Specimens per sq. ft.	0.31	0.17	0.57	0.01

One positive conclusion can be drawn, however, from this study. Large numbers of animals survived on the bottom of the disposal area after seven months of operation. The widespread annihilation of the bottom fauna which had been feared by some did not occur.

The change in the area assigned to dumping in the spring of 1949 prevented the continuation of these observations. Since it had become evident that a prohibitively large number of samples and photographs would need to be taken to obtain a reliable quantitative estimate of changes in the bottom population, and since the study of the behavior of the waste in the wake of the barge indicated that effects on the bottom population were unlikely, this phase of the investigation was discontinued.

4. FISH

THE pelagic fish, such as the mackerel and tuna which are valued highly by the sport fishermen, are active swimmers, fully able to avoid being drawn into the wake or swimming into regions where chemical conditions might prove harmful. Moreover, these are migratory species which move into the area from other parts of the ocean. Waste disposal operations cannot be expected to influence such fish by direct damage. They might exclude fish from the contaminated region if the food supply were to be destroyed, or the condition of the water sufficiently altered.

We have seen that there is little evidence that the food supply in the form of zooplankton will be reduced by waste disposal on its present scale. It is more difficult to obtain evidence on whether the fish will be repelled by the condition of the water. The most prominent effect of the contamination is the discoloration of the water resulting from the precipitation of ferric hydroxide in the wake of the barge. Patches of this precipitate have been observed eight hours after discharge. While the material is not toxic, it might well, like any other source of turbidity, be avoided by fish which are commonly inhabitants of very clear water. It will be shown in the following section that there is no evidence that the general turbidity of the waters off New York has increased during the period of 18 months of waste disposal off shore, and it may be concluded that the effects of turbidity from this source will be temporary and local.

TABLE 8

NUMBER OF FISH CAUGHT WITH OTTER TRAWL NET IN ACID DISPOSAL AREA

	Species	May 20, 1948		November 4, 1948
		Tow 1	Tow 2	Tow 1
1	Haddock*			140
2	Whiting	1	2	283
3	Hake, red	2	4	21
4	Hake, white	4	1	1
5	Blackback		4	2
6	Four spotted flounder			2
7	Mackerel		1	
8	Butterfish	6	4	5
9	Sea herring		28	
10	Alewives		48	
11	Shad			2
12	Weakfish			3
13	Sea bass		9	
14	Cunner	10	17	
15	Scup			6
16	Sea robin	1		
17	Filefish			1
18	Long horn sculpin			3
19	Goosefish	2		3
20	Lobster			1
21	Squid			68
	Totals..................	26	118	472

* All of the haddock were young of the year ranging in length from 4 to 7 inches.

Final evidence on whether the pelagic fish are being influenced by the waste disposal operations will probably be forthcoming only from the experience of the fishermen. The results of the survey of catches made during 1948 and 1949 at least give no indication that the first year of these operations was harmful to the fishery.

The fish which keep to the bottom are

also a shifting population which tends to congregate where food conditions are good. No evidence could be obtained that the invertebrate life, which forms the food supply of such fish, was seriously damaged in the disposal area during the first summer's operations. A few otter trawl hauls were made by the Fish and Wildlife Service's vessel *Albatross III* in the original disposal area in May and November, 1948, to see what fish might be found. The catches are summarized in Table 8. While the hauls were too limited to serve as a guide to changes in abundance, which in any case might be due merely to the season, they show clearly that ground fish were abundant even in November, after waste disposal had continued for seven months.

SUMMARY

THE biological observations have failed to produce any direct evidence that the populations of fish or of bottom living animals are being damaged or excluded from the area by the disposal of wastes. While zooplankton introduced directly into the contaminated water of the wake are temporarily immobilized they recover when this water is diluted with clean sea water, as would occur rapidly where organisms were caught in the wake. In view of the rapid dilution and neutralization of the waste in the wake, and the very small part of the sea water in the area which is temporarily acidified, it is not likely that the microscopic plants or animals forming the basic food supply of fishes are being significantly affected.

IV. EVIDENCE ON THE ACCUMULATION OF WASTES FOLLOWING PROLONGED BARGING OPERATIONS

The waste from the Titanium Plant of the National Lead Company has been barged to sea continuously at a rate of about 4,000 tons per day since April, 1948. It is obviously important to determine whether this continued discharge is leading to the accumulation of pollutants in the water or on the sea bottom. Consequently, an extensive study of the chemistry of the sea water in the offing of New York Harbor was made before, and periodically since, the beginning of the disposal operations. These surveys covered an area extending south and east for twenty-five miles or more from the entrance to Lower Bay. In addition, studies have been made in Lower Bay, Raritan Bay, and Raritan River, which show the effects on those waters of deflecting the waste from the Raritan River. The dates and extent of these surveys are indicated in Table 9.

1. THE ACCUMULATION OF IRON IN THE SEA WATER

The property of the water most likely to show accumulative effects is the iron content, since this element is present in the waste in great amount, its product in sea water is stable, and it can be detected even at great dilution.

The iron has been measured by the dipyridyl method described by Cooper (**4**). Since the solubility of iron in sea water is very small, virtually all of the iron is present as a very finely divided precipitate. Consequently, the results of iron analyses tend to be erratic, because the suspended particles do not become uniformly distributed as materials in solution do (**5, 6, 7**).

The concentrations of iron found in the surface waters off New York are shown in Figure 16. In general, it may be said that the iron content of the offshore water does not exceed 20 parts per billion, except where the effect of the water emerging from Lower Bay is evident. At the mouth of Lower Bay and extending for some distance seaward, the iron concentration may be four or six times greater than off shore, i.e., 80 to 120 parts per billion. The surveys showed that high concentrations are associated with the water of low salinity emerging from Lower Bay and which spreads from there in a pattern which varies from time to time. The general pattern of circulation which determines the way in which the iron content is distributed will be discussed in the following section.

A summary of the iron content of the water as observed at various places in the Bays and outer approaches to New York Harbor before and after the beginning of barging operations is given in Table 10. In the waters of Raritan and New York Lower Bays, the iron content has decreased markedly during the period. This change will be discussed below. In the offshore area the data do not indicate any substantial change in concentrations which might be related to the disposal operation, although the quantities of iron vary considerably from time to time. The Shrewsbury Rock station has been included because it is the location of a popular fishing area. The iron concentrations at this station were generally greater than those observed either at the original disposal area or at Cholera Bank, just north of the present disposal area.

Additional information on the accumulation of iron is given by a comparison between the total quantity of iron within the area at any one time and the rate at which it is being introduced by river flow and barging. The study shows that iron is being contributed to the sea at a high rate by the rivers entering the area, whereas the quantity of iron actually present in the sea water within an area of some 600 square miles is less than that coming in from the rivers within two weeks.

The contribution by the rivers may be estimated from the average concentration of iron in the river water multiplied by the volume of river flow. A somewhat analogous method has been developed for use in tidal systems, such as that which occurs at the mouth of Lower Bay, which utilizes knowledge of the net water transport across a section of the channel instead of the volume of river flow. The two methods give results in reasonably good agreement.

The contribution of iron to the area at the time of seven cruises is shown in the second and third columns of Table 11. The rivers

TABLE 9

List of Surveys and Special Studies

Date	Vessel	Object	Area Surveyed
			sq. mi.
Feb. 2–19, 1948	*Balanus*	Hydrographic Survey New York Bight	483
Mar. 12–Apr. 4, 1948	*Balanus*	Hydrographic Survey New York Bight Raritan & Lower Bay Photographic studies	300 83
Apr. 20–30, 1948	*Balanus*	Hydrographic Survey New York Bight Study of wake	662
May 18, 1948	*Albatross III*	Photographic studies	
July 22–31, 1948	*Balanus*	Hydrographic Survey New York Bight Raritan & Lower Bay Drift bottle releases Study of wake	684 83
Oct. 21–29, 1948	*Caryn*	Hydrographic Survey New York Bight Drift bottle releases	468
Nov. 1–2, 1948	*Albatross III*	Photographic studies Drift bottle releases	
Nov. 29–Dec. 20, 1948	*Asterias*	Hydrographic Survey Raritan & Lower Bay	83
June 17–July 5, 1949	*Asterias*	Hydrographic Survey Raritan & Lower Bay	83
Aug. 16–23, 1949	*Caryn*	Hydrographic Survey New York Bight Drift bottle releases	630
Jan. 4–8, 1950	*Albatross III*	Hydrographic Survey New York Bight Drift bottle releases	650

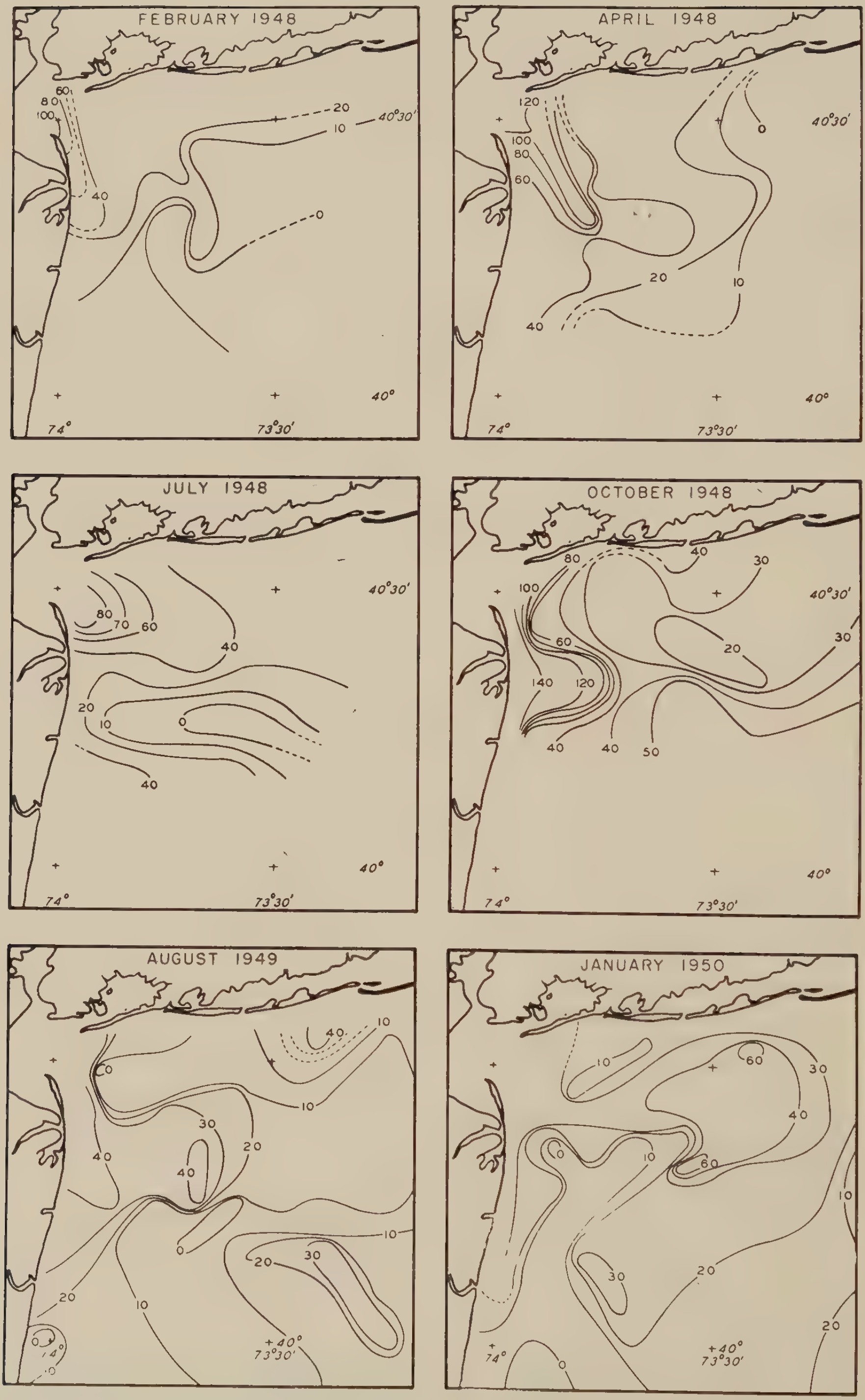

FEBRUARY 1948

APRIL 1948

JULY 1948

OCTOBER 1948

AUGUST 1949

JANUARY 1950

60
80
100
40
20
10
0
40°30′
40°
74°
73°30′
120
100
80
60
0
20
10
40
80
70
60
40
20
10
0
40
80
40
30
100
60
20
30
140
120
40
40
50
10
40
0
10
30
20
40
40
0
10
20
30
20
10
0
40
+40°
73°30′
10
60
30
40
0
10
60
10
30
20
20
74°
0
+40°
73°30′

Figure 16. Distribution of iron in the surface waters of the New York Bight. Contours show iron concentrations in parts per billion (micrograms per liter).

contributed about 50 tons of iron daily in February, July, and October, 1948, and in January, 1950. In March and April, 1948, when the quantities were greater (159 and 112 tons per day) the river flow was exceptionally great (cf. Table 15). In August, 1949, when the river flow was very small, the contribution of iron was only 15 tons daily. As a general rule, the rivers are contributing about 50 tons of iron daily, a quantity approximately equal to the amount introduced by the barging operations. Prior to the barging operations, some one hundred tons of iron were being carried to sea past Sandy Hook each day; one-half derived from the river flow, one-half from the waste then being discharged into Raritan River. After barging began, only fifty tons passed Sandy Hook daily—all being of river origin. The effect of barging was thus to relieve the Raritan River and Bay of the extra load of pollution without altering the amount of iron which ultimately reached the sea.

TABLE 10

Average Concentrations of Iron Observed in Various Places during the New York Cruises

Location	Parts per Million							
	Feb. 1948	Mar. 1948	Apr. 1948	July 1948	Oct. 1948	Dec. 1948	June 1949	Aug. 1949
Head, Raritan Bay		4.0		4.0		3.0	0.15	
Off Coniskonk Pt.		1.57		0.3		0.25	0.03	
Off Pt. Comfort		0.70		0.29		0.10	0.10	
Inside Sandy Hook		0.24		0.17		0.03	0.10	
Sandy Hook	0.15			0.27				
Scotland Light	0.035	0.081	0.117	0.060	0.056			0.033
Ambrose Light	0.018	0.043	0.012	0.047	0.030			0.040
Shrewsbury Rock	0.034	0.045	0.044	0.015	0.134			0.034
Original Dumping Area	0.003	0.009	0.013	0.009	0.025			0.019
Cholera Bank	0.008		0.021	0.020	0.066			0.013

TABLE 11

Comparison of Iron Entering the New York Bight and the Quantity of Iron Accumulated within the Area

Date	River Contribution	Iron Dumped at Sea	Surveyed Area	Accumulation of Iron	
	tons per day	*tons per day*	*sq. mi.*	*tons*	*days*
Feb. 1948	52.5		483	552	10.5
Mar. 1948	159				
Apr. 1948	112		662	896	8.0
July 1948	51	60	684	1350	12.2
Oct. 1948	57.5	60	468	1436	12.2
Aug. 1949	15	80	630	1107	11.7
Jan. 1950	49.5	80	650	1807	13.9

The total quantity of iron in the water of the surveyed area was obtained from the sum of the iron content of small segments bounded by the lines of stations where samples were collected. The iron content of the water in each segment was estimated from the average quantity of iron under a unit area at the contiguous stations multiplied by the area of the segment. The total area surveyed during the various cruises and the quantity of iron accumulated are shown in Table 11.

Direct comparison of the quantity of iron within the area is difficult because the size of the surveyed area varied from cruise to cruise. Furthermore, the quantity present at any time is related both to the rate of supply and to the flushing rate, which is determined by the circulation of the water. The data show clearly, however, that the change in quantity is extremely small compared to the rate of supply. For example, between July, 1948, and August, 1949, about 40,000 tons of iron were added to the water in this area. The quantity of iron within the surveyed area, however, showed virtually no change.

The most significant figures in the table are the number of days required to flush the iron through the surveyed area. The fact that the total quantity of iron within the surveyed area corresponds to from 8 to 14 times the daily contribution shows that there is no danger of substantial accumulation of iron within the area as a whole. A combination of a high rate of supply and a slow flushing rate will give a temporary accumulation, such as that observed in January, 1950. It is reassuring, however, that a period of two weeks or less is adequate to modify the accumulation when prevailing conditions change.

In contrast to the offshore areas, the iron content of the water in Raritan and Lower Bay has changed greatly following the initiation of barging. The results of three surveys of these bays are shown in Figure 17. In March, 1948, prior to barging, the water of the southern half of Raritan Bay contained in excess of 2000 parts per billion of iron. In contrast, in June 1949, fourteen months after the commencement of barging, there were present in the water not more than 150 parts per billion.

The facts relative to the distribution of iron are of interest because they illustrate a point frequently overlooked in the discussion of pollution problems. Many of the pollutants of rivers ultimately find their way to the sea. Procedures such as barging or the construction of sewers which carry these pollutants directly to sea may greatly improve conditions in the rivers and their estuaries without necessarily altering the conditions which exist at sea.

2. THE ACCUMULATION OF IRON AT THE BOTTOM

THE accumulation of waste materials on or near the bottom appears to have been considered likely when the original disposal area was selected, and led to the choice of a spot where unusual depths occur. This was natural when the high density of the waste was considered. The quantity of iron in the waste is such that if it were all deposited on the bottom as metal in the four square miles originally assigned for disposal, it would build up a layer less than one-half millimeter thick in one year. As iron oxide or hydroxide, the layer would be somewhat thicker. While the material deposited would not have poisonous properties, it was thought that it might alter the character of the bottom sufficiently to influence marine life and in particular the bottom fisheries.

The observations on the behavior of the waste when discharged from the barge showed very clearly that these fears are groundless, since the iron is precipitated in such a highly dispersed form that it does not sink rapidly and must be widely distributed before reaching the bottom. The failure of the surveys to show any accumulation of iron either at the surface or at greater depths supports the view that the precipitated iron is widely dispersed by currents before it settles. If this is the case, then it should make no difference whether the iron reached the area by barge or by the normal route down the rivers and bays.

Although the possibility of finding accumulations of iron compounds on the bottom seemed remote, samples of the bottom were collected in the area originally assigned for disposal prior to the beginning of these operations and on several occasions thereafter. The results of the iron analyses of the bottom sediments are given in Table 12. Some of the samples were obtained with a small "orange peel" dredge which scoops up a sample from the upper two or three inches of the bottom sediment. Other samples were taken in coring tubes, and for these samples the length of the core and the analysis of the upper and lower part of the core are given. It is interesting that the upper and lower part of the core samples showed substantially the same iron content. Although the age of these sediments has

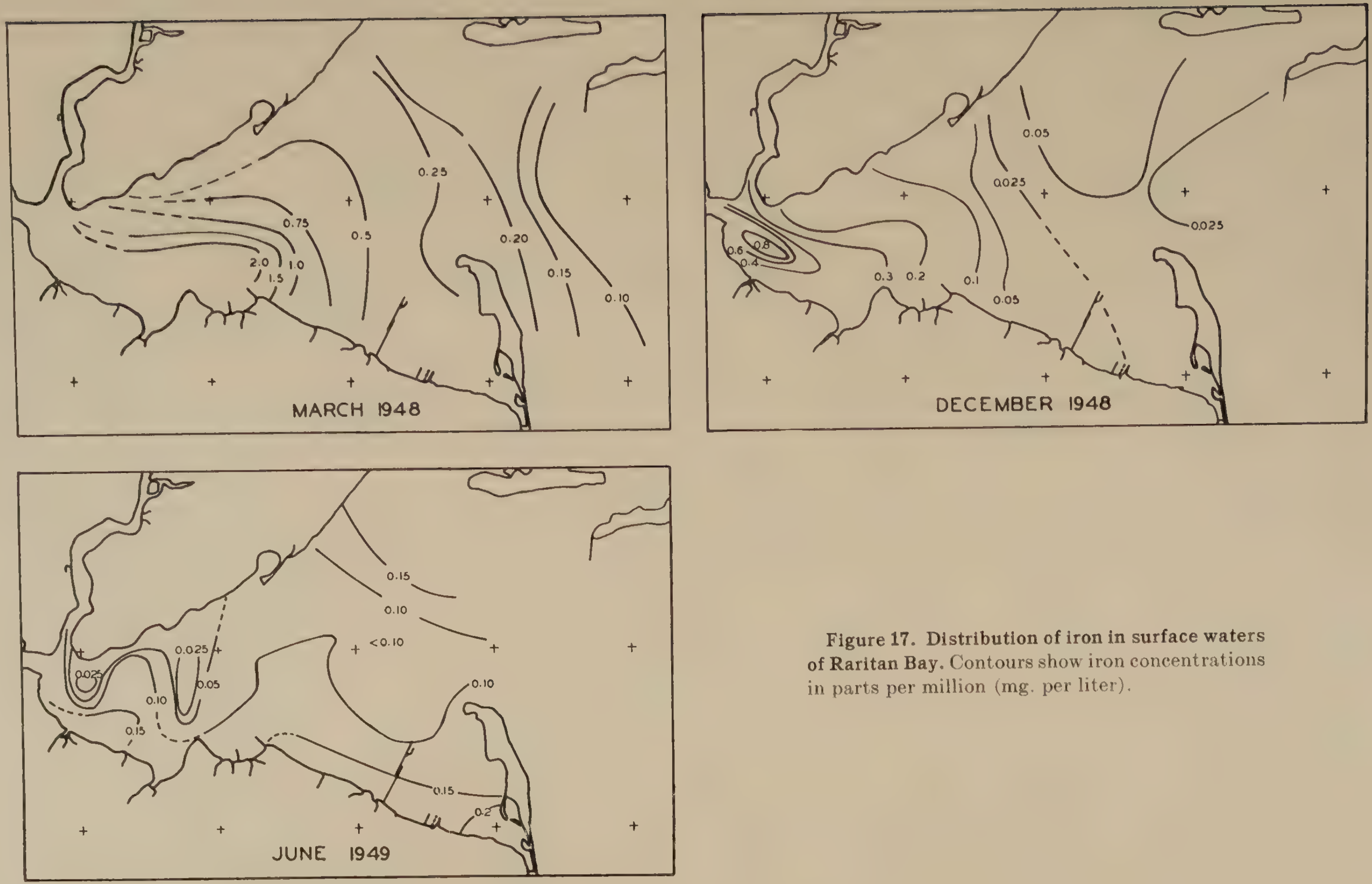
0.25
0.75
0.5
0.20
2.0
1.0
1.5
0.15
0.10
MARCH 1948
0.05
0.025
0.025
0.8
0.6
0.4
0.3
0.2
0.1
0.05
DECEMBER 1948
0.15
0.10
0.025
<0.10
0.025
0.05
0.10
0.10
0.15
0.15
0.2
JUNE 1949

Figure 17. Distribution of iron in surface waters of Raritan Bay. Contours show iron concentrations in parts per million (mg. per liter).

not been determined it seems probable that it has taken centuries for them to accumulate to the depth of 10–20 centimeters. It appears, therefore, that the iron contributed during the last several decades as a result of the industrial development of the region has, as yet, had no measurable effect on the iron content of the bottom deposits.

TABLE 12

Iron Content of Bottom Samples Collected in New York Bight

SAMPLED WITH ORANGE PEEL DREDGE

Date	Place	Iron Content
		mg. per gram
March 1948	Original Disposal Area	2.9
		5.0
		4.7
May 1948	Mud Hole	6.2
		9.5
Average		5.7

SAMPLED WITH CORING TUBE

Date	Place	Length of Core	Iron Content	
			Upper Part	Lower Part
		cm.	*mg. per gram*	
May 1948	Original Disposal Area	10.5	6.2	6.4
		16	7.3	5.8
		20	6.5	6.1
		12	6.1	6.2
		14.5	7.4	8.2
		14	5.3	6.4
		16.5	7.5	5.7
Average			6.6	6.4

3. THE TURBIDITY OF THE WATER

Fishing interests have expressed alarm that the turbidity of the water due to the presence of precipitated iron may prove distasteful to fishes, particularly the migratory pelagic species such as mackerel and tuna. The initial turbidity of the wake is certainly dense enough to give credence to this view. As was pointed out in the preceding section, the turbidity of the wake is dispersed rapidly and the affected water cannot be detected after about eight hours. It is possible, however, that the accumulation of ferric hydroxide over long periods might lead to a general loss in transparency of the water, which, while it could not be recognized by eye, might nevertheless affect fish directly, or indirectly through its effects on the microorganisms which supply their food. Consequently, a careful survey of transparency of the water of the offshore area was made during each cruise.

The transparency of sea water is measured very simply by lowering a white disk, known as a Secchi disk, over the side and noting the greatest depth at which it is visible. It is invariably found that transparency dedecreases as the shallow water along shore is approached. This is because of the presence of fine sediments stirred up from the bottom by tidal and wave action. Transparency will also reflect the abundance of microorganisms in the water, and also the presence of certain types of pollution.

The river effluent was always very turbid, and the Secchi disk was visible to depths varying from 3.5 to 0.75 meters at the entrance to Lower Bay. The offshore transparencies reflected primarily the distribution of this turbid river effluent. Water which was not appreciably diluted with the river effluent was clear and blue, and the disk could be seen at depths of 10–16 meters. The results of transparency measurements made in February, 1948, prior to the disposal operations, and in August, 1949, after sixteen months of barging, are shown in Figure 18. On these charts the contours indicate the greatest depth at which the Secchi disk could be seen. The survey in August 1949 showed no evidence of a decreased transparency in the neighborhood of the disposal area. The water in that region appeared beautifully clear and blue in contrast to the turbid green water found nearer to shore where most of the fishing boats were concentrated.

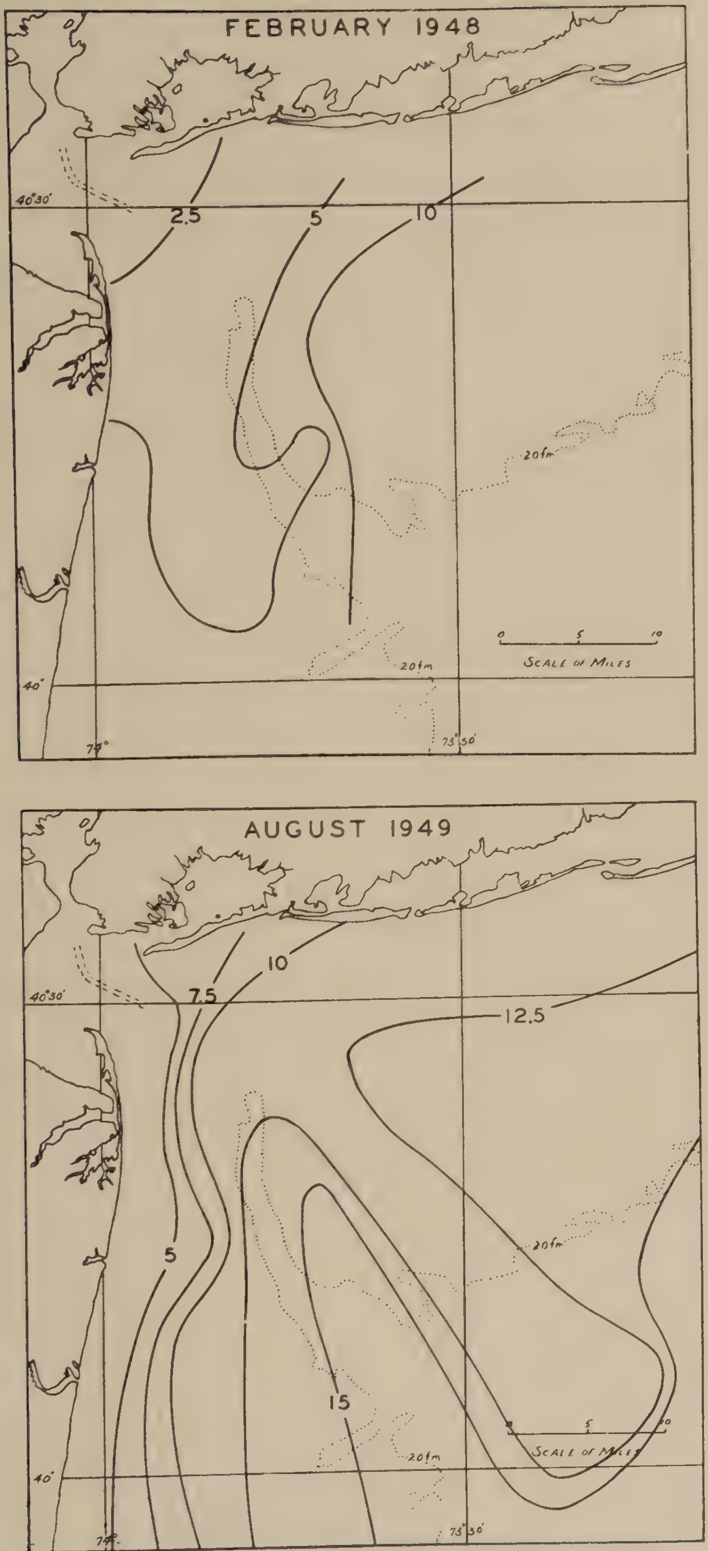
FEBRUARY 1948
40°30'
2.5
5
10
20fm
0
5
10
SCALE OF MILES
20fm
40°
74°
73°30'
AUGUST 1949
40°30'
10
7.5
12.5
5
20fm
15
0
5
10
SCALE OF MILES
20fm
40°
74°
73°30'

Figure 18. Transparency of the waters of the New York Bight in February, 1948, prior to disposal of titanium wastes offshore, and in August, 1949, after more than a year of disposal.

4. SUMMARY

Concentrations of iron in the offshore area have not measurably increased since the disposal operations were started, but the concentrations of iron in the waters of Raritan Bay have decreased greatly. The principal objective of the operation, to decrease the pollution load in Raritan River and Bay, has thus been achieved without materially changing conditions at sea.

There has been no accumulation of iron in the water. The total quantity present corresponds to the amount of iron contributed by the river and barge in 8 to 14 days. About half of the iron entering the sea off New York is still supplied by the Hudson and other rivers draining into the area.

There has been no measurable accumulation of iron on the bottom in the area assigned for waste disposal.

There is no indication that accumulation of the wastes being barged to sea has altered the transparency of the offshore waters where disposal is in operation.

V. THE CIRCULATION OF WATER IN THE NEW YORK BIGHT[5]

1. THE NATURE OF WATER MOVEMENT

THE FATE of pollutants discharged at sea depends on the motion of the water. The character of this motion must be kept in mind in judging the effects of waste disposal operations and in attempting their regulation. Several types of motion may be distinguished:

Eddy motion. When water is acted on by any force, as by tides and winds, the imparted energy tends to be dissipated in the formation of eddies. These eddies vary greatly in size, and small eddies may revolve within larger ones. The total motion is consequently most difficult to measure or describe. The result of the eddy motion is to mix the water, and thus to lead to the greater dispersion of any pollutant both horizontally and in depth. It does not effectively carry the pollutant away from its source, except by gradual spreading in every direction.

Tidal Currents cause the water as a whole to move back and forth in a regular way, timed in the main by the rotation of the earth and the moon. In the open sea, the tidal currents change direction continually so that the drift of any particle is in a circle. The velocity of movement is not very great and the total excursion in a single tidal period is small. Along the shore, the circular motion is hindered by the shore and the course of drift becomes an ellipse. This is the condition found at Ambrose and Scotland Lightships. Within bays and channels, the elliptical character of the motion is entirely suppressed and the water moves back and forth in a direction which is reversed periodically.

Tidal currents themselves do not cause the water to move permanently away from its original position. Their effect on the distribution and dispersion of pollutants is due to the mixing occasioned by the eddy motion which accompanies the flow of the tidal streams.

Non-Tidal Drift. The tidal currents which flow in opposite directions are rarely exactly equal because there are usually other forces acting on the water, such as hydrostatic gradients occasioned by river flow, forces due to the rotation of the earth, and the prevailing winds. Consequently, there is a net movement in certain general directions which has the effect of a current in carrying the water from one place to another. This movement cannot properly be called a current since it is not continuous in any one direction. It is referred to as the *non-tidal drift* and is usually small compared to the actual tidal excursion. Nevertheless, it is the effective agency for carrying pollutants away from the area into which they are discharged.

The non-tidal drift of the water can be measured directly only by anchoring a ship and making accurate measurements of the tidal currents over a period of several weeks. Scotland and Ambrose Lightships are the only places in the approaches to New York where such measurements have been made. Since the expense of securing adequate information by this method would be prohibitive, it is necessary to determine the character of the non-tidal drift by less direct methods. The procedure adopted was to examine carefully the distribution of salinity in the water and from this to attempt to infer the circulatory paths by means of which the fresh water of the Hudson River finds its way seaward, and the rates at which this transport takes place. Supplementary information was secured by the use of drift bottles.

---

[5] A discussion of the theoretical treatment of the results reported in this section and a more detailed presentation of the data may be found in a paper by Ketchum, Redfield and Ayers (**9**).

2. SALINITY DISTRIBUTION

THE coastal water lying between Cape Cod and Cape Hatteras has a salinity which varies in general between 30 and 33 parts per thousand, the lower values being found nearer shore. There is some seasonal variation dependent upon rainfall, spring freshets, etc. Only where the larger rivers exert their influence does the salinity fall below 30 parts per thousand (**2**). The Hudson, Raritan and other rivers of the New York area are separated from the sea by extensive bays and estuaries in which the fresh water of the rivers is mixed with the sea water. Thus, in the Raritan River, the principal zone of mixing occurs in the eight miles of tidal estuary lying above Perth Amboy. In issuing into the head of Raritan Bay, the water is already two-thirds salt (salinity about 20 parts per thousand). Similar conditions exist in the inner harbor of New York as the result of mixing in the lower Hudson River. In Raritan and Lower Bays the salinity varies between about 20 and 30 parts per thousand. The transition between the Bay water and the coastal water is usually fairly abrupt and is conveniently marked by the isohaline for 30 parts per thousand. The transition is the result of active mixing resulting from tidal currents in the shallow area lying at the mouth of the Lower Bay between Sandy Hook, Rockaway Point, and Scotland Lightship.

It is a well-established principle that off the mouth of a river two sorts of non-tidal drift will be established as a result of the flow of fresh water into the sea. First, to maintain the hydrostatic level the river water must be carried away as fast as it enters the sea. Second, since the river water mixes with progressively greater volumes of sea water as it moves seaward, there must be a counter-drift of salt water toward the estuary to provide this part of the mixture.

We may interpret tongues of fresher water extending seaward to represent the non-tidal drift away from the Lower Bay, and tongues of saltier water extending in from the sea, to represent the counter-drift of salt water needed to supply the mixture.

The distribution of salinity in the surface waters, which is illustrated in Figure 19, varies greatly from time to time. The most constant feature is the tendency of the less saline water to extend southward from Lower Bay along the New Jersey coast. This pattern was observed in February, 1948, October, 1948, August, 1949, and January, 1950. It indicates the principal course of the non-tidal drift in which river water is carried away from the entrance to New York Harbor at those times. However, in April and July, 1948, the pattern was quite different. At these times the less saline water spread widely to the eastward, particularly in the latter month. The freshened water was then separated from the coast of northern New Jersey by a tongue of water of higher salinity. This indicates that the southward drift along the coast was not present, and that it was replaced by a northward counter-drift, or by an upwelling of deeper water along the shore.

The distribution of salinity below the surface is also instructive. Figure 20 shows the vertical distribution in a section which extended eastward from Elberon, New Jersey, and thus passed through the disposal areas assigned to the National Lead Company. It may be seen that in February, 1948, October, 1948, and August, 1949, the salinity was fairly uniform from surface to bottom, with the freshest water occupying a deep tongue along the shore. In cont ast, in April, 1948, July, 1948, and January, 1950, when the less saline water was spread more widely to the eastward, it occupied a thin layer near the surface, under which layers of increasing salinity extended in the horizontal direction in a stratified pattern. The drift of freshened water at these times was evidently confined to a shallow layer moving seaward at the surface.

The sections also show that the most saline water observed was found in the

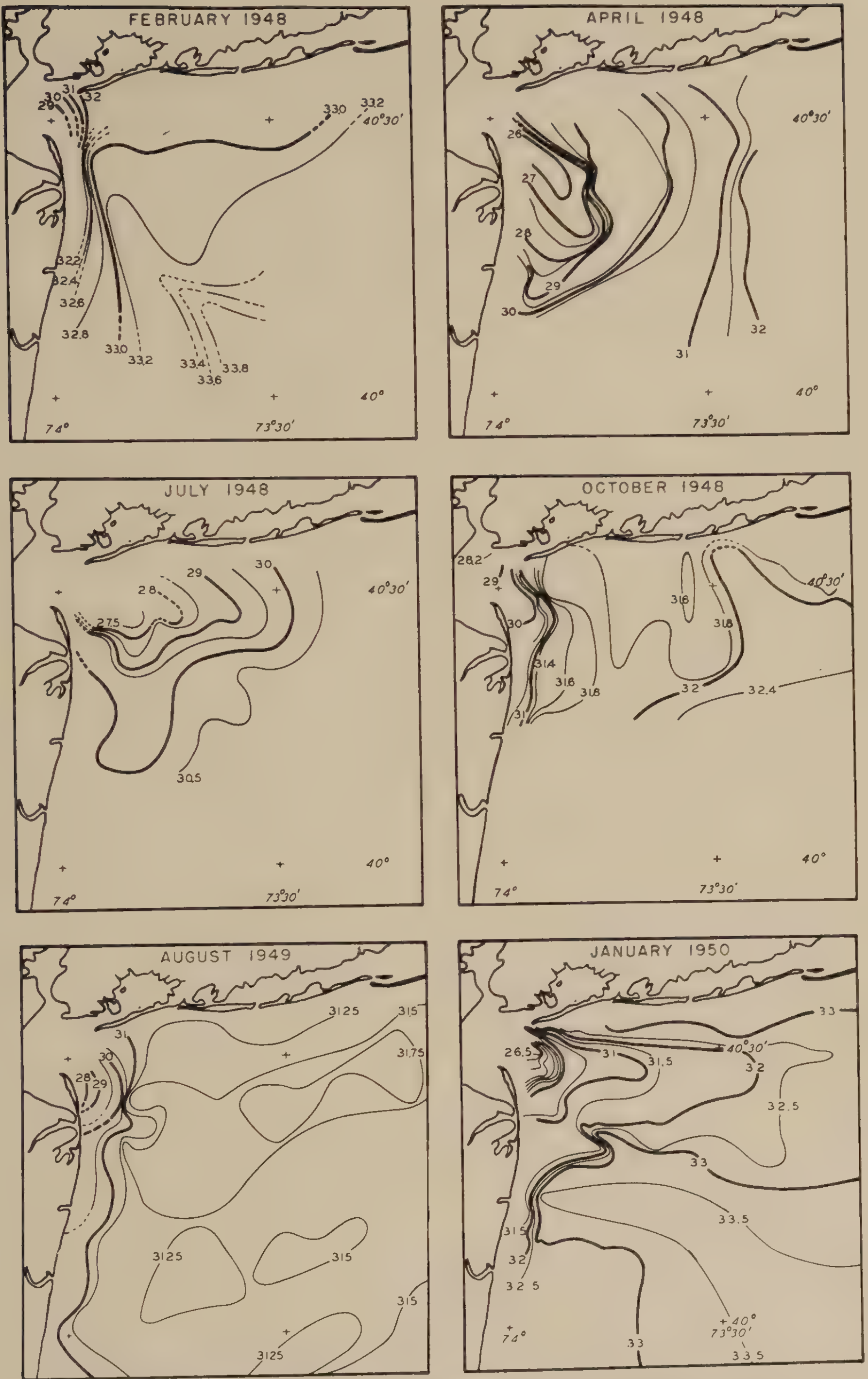
FEBRUARY 1948
29
30
31
32
33.0
33.2
40°30'
32.2
32.4
32.6
32.8
33.0
33.2
33.4
33.6
33.8
40°
74°
73°30'
APRIL 1948
26
27
28
29
30
31
32
40°30'
40°
74°
73°30'
JULY 1948
27.5
28
29
30
30.5
40°30'
40°
74°
73°30'
OCTOBER 1948
28.2
29
30
31
31.4
31.6
31.8
31.8
31.8
32
32.4
40°30'
40°
74°
73°30'
AUGUST 1949
28
29
30
31
31.25
31.5
31.75
31.25
31.5
31.5
31.25
JANUARY 1950
26.5
31
31.5
32
32.5
33
33
33.5
31.5
32
32.5
33
33.5
40°30'
40°
74°
73°30'

Figure 19. Distribution of salinity in the surface waters of the New York Bight. Contours show salinity in parts per thousand.

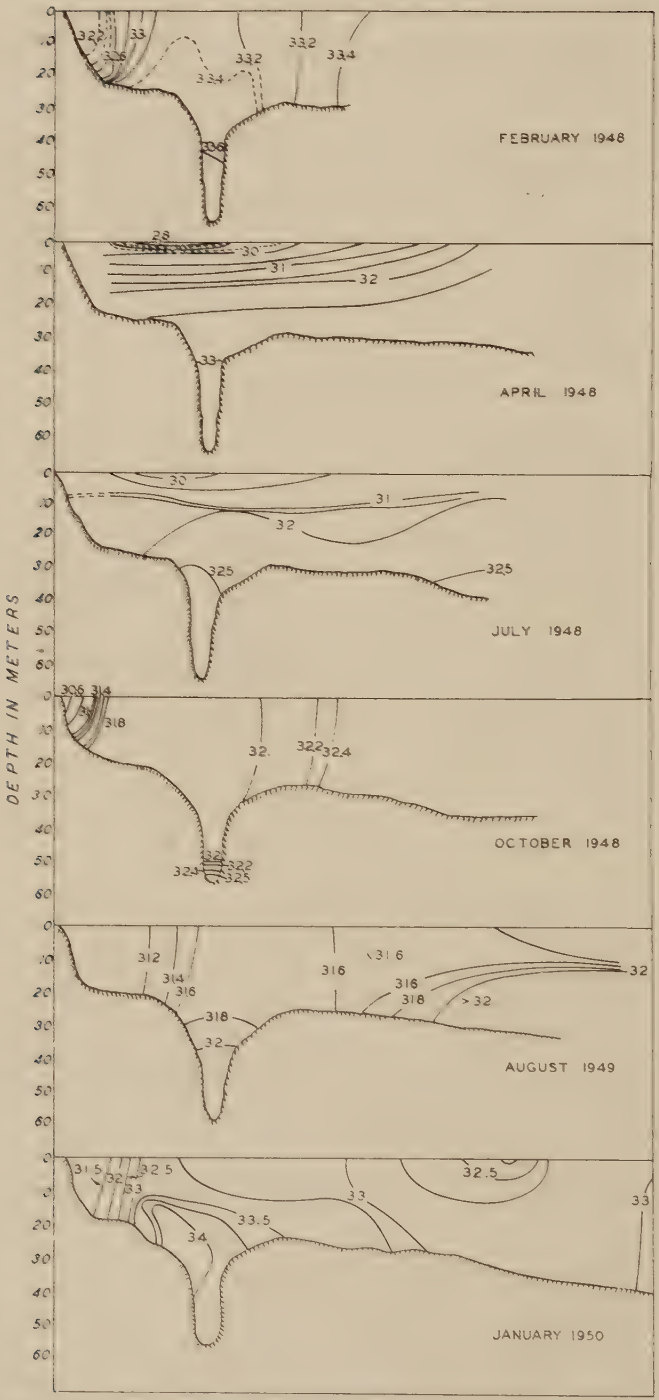

Figure 20. Distribution of salinity below the surface in a section extending eastward from Elberon, N. J. Contours show salinity in parts per thousand.

trough of the old Hudson Gorge. In February, 1948, and August, 1949, higher salinities were found above the Gorge than in the shallower regions on either side. This suggests that the Gorge is the site of a countercurrent moving landward which serves to supply salt water to mix with river water as it escapes from the Harbor. The surface salinity in February, 1948, indicates that, at that time, this movement above the Gorge extended to the surface.

A severe storm may completely obliterate the pattern of salinity distribution by mixing the water from different areas and depths. This was observed to happen on March 16, 1948, when a southwest gale occurred. On the following day, the river effluent, characterized by salinities less than 30 parts per thousand, could be detected as a tongue extending seaward only four miles beyond Scotland Lightship. (See Figure 21.) By the following day, the tongue had advanced southward about eight miles to the offing of Long Beach, New Jersey. Eight days later this point still marked the southern extension of the tongue of river effluent, but it then extended widely to the eastward. Since the salinity pattern can have been reestablished only by some net drift of water, these observations give some indication of the rapidity of such movement.

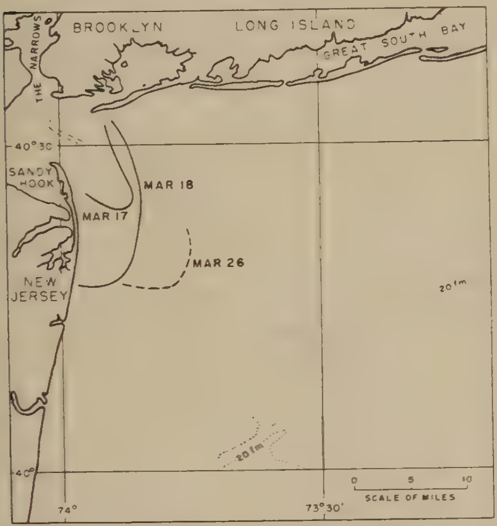

Figure 21. Changes in the location of the 30 parts-per-thousand isohaline following the storm of March 16, 1948.

To summarize, the effluent from Lower Bay tends to flow southward along the New Jersey coast in a tongue about five miles wide. A counter-drift appears to move in along the submerged Hudson Gorge to supply salt water to mix with the river effluent. Large eddies occur in the waters lying to the eastward of the coastal tongue of river effluent, and these probably serve to supplement the countercurrent in drawing salt water in to mix with the river effluent, as well as to spread some of the effluent to the eastward. This pattern of circulation was observed during three of the six periods of survey. At three other periods, in contrast, the southward movement of the river effluent along the New Jersey coast appeared to have been checked. Instead, the effluent was spread widely across the bight, and in two cases was separated from the New Jersey shore by more saline water. When these conditions occurred, the fresher water was confined to the surface layer as though it were flowing out over the deeper layers of the more saline coastal water. The counter-drift must lie in these deeper layers. The volume of the effluent is sufficiently large so that the pattern is reestablished rapidly after being disturbed by a storm, and presumably it can change with equal rapidity when the determining conditions are altered.

3. FACTORS INFLUENCING THE PATTERN OF CIRCULATION

The six surveys which have been made are sufficient to show that the pattern of circulation is subject to variation between two widely different extremes. The earlier surveys suggested that these extremes might be related to the season, but as additional information accumulated it became apparent that this is not so, as may be seen by comparing the salinity patterns observed in

July, 1948, and August, 1949. It has become apparent that several variable factors are interacting to determine the actual character of the circulation at any one time. While the principal forces at work are evident and the nature of their influence may be stated, it is not possible to estimate their influence quantitatively in order to predict the outcome when they are in conflict.

The factors considered to influence the circulation in the New York Bight are the following:

1. The force due to the rotation of the earth, the so-called Coriolis force. In the northern hemisphere, this force causes moving water to turn to the right. Its effect is always present and locally is proportional to the velocity of the movement. It appears to be the factor responsible for the tendency of the river effluent to hug the New Jersey shore except when its influence is overbalanced by the other, more variable factors.

2. Hydrostatic forces arising from horizontal pressure gradients due to differences in temperature and salinity of the water.

   a. Hydrostatic forces arising from differences in the salinity of the water are due to the local decrease in density which results from the dilution of sea water by the river effluent. The forces increase with the volume of river flow and tend to cause the effluent to spread more actively following periods of heavy run-off.

   b. Hydrostatic forces arising from differences in the temperature of the water. These differences arise chiefly from the warming of the sea surface in summer, which reduces the density of the surface layers. These forces tend to confine the spreading effluent to the upper layers and may facilitate its spread. Their effect is seasonal.

3. Forces due to the wind. The wind causes the surface water to drift at an angle to the wind direction. Theoretically the motion at the surface is at an angle of 45° to the right of the wind direction. The detailed facts, however, are uncertain, particularly as they apply to shallow water and to variable winds of short duration. Prevailing winds from northwest to northeast may be expected to assist in confining the river effluent to the New Jersey shore. Prevailing winds from south through west will increase the tendency of the effluent to spread eastward. However, the influence of wind strength and duration cannot be stated quantitatively.

In the open ocean, where conditions exist in a steady state over long periods of time, it is possible to estimate the drift of the water on the assumption that the hydrostatic forces which result from the horizontal pressure gradients are exactly balanced by the Coriolis force due to the earth's rotation. In coastal waters the patterns of distribution are constantly changing, so that steady-state distribution cannot be assumed. It is possible to calculate the currents which would be required to maintain any observed set of conditions, but one cannot be assured that such currents actually exist since the estimate will be too large at times when the freshened water is tending to spread more widely, and too small when the reverse is taking place. If independent measurements of the currents can be obtained, it is possible to determine whether the observed conditions are stable (as indicated by their agreement with the estimates based on horizontal pressure gradients) or are in the process of change.

Estimates of the current flowing southward between Scotland Lightship and the coast at Sandy Hook have been made for each period of survey.[6] The results, entered in Table 13, may be compared with the observed non-tidal drift recorded at Scotland Lightship by the U. S. Coast and Geodetic Survey. The latter figures are based on long series of observations made throughout the year and reflect the average movement to be expected.

The comparison shows that at three

---

[6] For detailed discussion of the theoretical treatment see Ketchum, Redfield and Ayres (9).

periods, February, July and January, the current velocities calculated from the horizontal pressure gradient agree closely with the average conditions, and it may be assumed that the conditions observed at those times were stable. During the other three periods, the estimated current velocities greatly exceed the average observations, and the conditions appear to be dynamically unstable, and the deduced tendency to change would be toward more widespread distribution of the freshened water.

Two factors which must influence the development of the current pattern and the resulting variation in distribution of salinity are the run-off from the rivers and the wind.

TABLE 13

Calculated Current Velocities Between Scotland Lightship and Sandy Hook and Observed Average Non-Tidal Drifts Recorded at Scotland Lightship

Date	Calculated Current Velocities	Average Non-Tidal Drift	Deduced Dynamic State
	cm. per sec.	*cm. per sec.*	
Feb. 1948	10.5	9.25	Stable
Apr. 1948	21.7	9.25	Unstable—spreading
July 1948	7.8	9.50	Stable
Oct. 1948	23.1	9.50	Unstable—spreading
Aug. 1949	66.2	9.50	Unstable—spreading
Jan. 1950	10.1	9.50	Stable

River flow data for the period under consideration have been provided by the offices of the U. S. Geological Survey in Albany, New York, and Trenton, New Jersey. The average monthly flow for the rivers tributary to Lower Bay are shown in Figure 22, while the average daily flow for the period of thirty days immediately preceding each survey is given in Table 14. It is evident that the quantity of fresh water entering the Bight varies greatly from time to time.

As the river flow increases, greater volumes of river water must be transported through the area in a unit period of time. This could be accomplished either by an increase in the velocity of the non-tidal

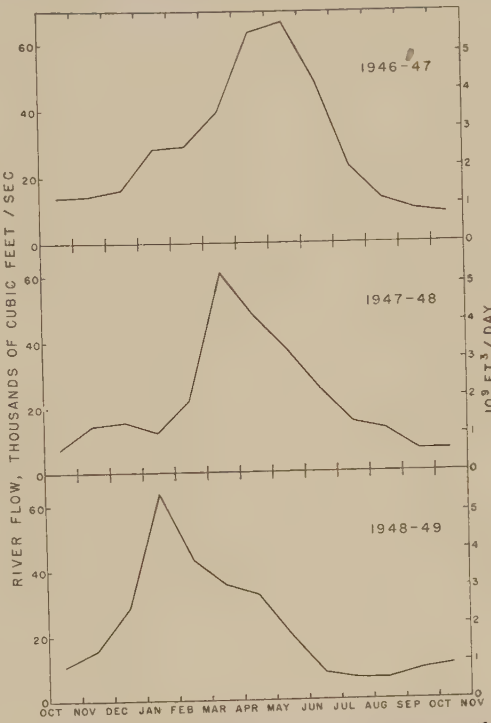

Figure 22. Daily river flow, averaged by months, of the Hudson and other river sources discharging into the New York Bight between Sandy Hook and Far Rockaway.

TABLE 14

Average Daily River Flow and Prevailing Winds during Periods of Survey

Date	River Flow*	Mean Hourly Wind Velocity	Direction	Drift
	10⁹ cu. ft. per day	*mi. per hr.*		
Feb. 1948	1.49	14.2	N	W
Apr. 1948	4.1	14.9	NW	W
July 1948	1.3	11.5	SW	E
Oct. 1948	0.6	13.5	N	W
Aug. 1949	0.6	8.8	SSE	E
Jan. 1950	2.63	12.2	NE	

* Mean daily flow estimated for thirty days preceding the dates of survey.

drift, or by an increase of the proportion of river water in the mixture moving seaward. The data show that the latter occurs, and that the velocities of non-tidal drifts remain substantially the same regardless of river flow.

As indicated by Table 13 the distributions observed during three of the cruises were dynamically stable. Apparently these patterns of distribution were primarily determined by the horizontal pressure gradients and Coriolis force. The calculated velocity in April, 1948, would transport about 70 percent of the river water southward along the New Jersey shore. It is possible that, at this time, the velocity of non-tidal drift was greater than the average velocity used for comparison in Table 13. The remaining two cruises were unstable, and the velocities required to produce stability would remove more fresh water than was contributed by the rivers. It may be significant that the river flow during these two cruises was appreciably lower than that observed during any of the other cruises.

Data on the prevailing winds during the several periods of survey are shown in Table 14. The effects of the wind cannot be evaluated quantitatively, but a qualitative summary may be useful in interpreting their contribution to the distribution patterns.

The winds during February and July, 1948, when stable distributions were observed, would tend to produce similar patterns. In January, 1950, the winds, though light, opposed the observed widespread, stable pattern in the northern part of the area.

In April, 1948, when it appeared possible that the non-tidal drifts were flowing southward with a greater than average velocity, the wind would be expected to augment this current along the New Jersey Coast.

In October, 1948, the northerly winds would augment the currents along the New Jersey shore, and thus tend to produce the unstable distribution observed at that time. The winds during the early part of this cruise were strong, which would increase the importance of the wind effect.

The winds, however, do not help to interpret the August, 1949, distribution pattern. The SSE winds at this time would produce a surface current in a general northeasterly direction. The observed pattern was unstable and the winds would augment the tendency for the freshened water to spread over the surface to the eastward.

It appears, therefore, that the three stable distribution patterns are primarily determined by oceanographic factors, and two of the unstable distributions can be qualitatively explained as a combination of oceanographic and wind effects. The August, 1949, distribution, however, was dynamically unstable, and was subjected to a wind which increased the instability. Presumably this pattern was transitory, and might be expected to change rapidly. More information on the effects of winds in producing currents in coastal waters is urgently needed to aid in interpreting the circulation and distribution of properties in localities such as the New York Bight.

4. THE RATE OF TRANSPORT OF FRESH WATER THROUGH THE AREA

THE accumulation of pollutants in any area into which they are discharged will depend upon the rate at which the water within the area is replaced as a result of the circulation. Although the pattern of circulation has proved to be variable, and as yet unpredictable in its details, it is possible to reach some general conclusions regarding the rate at which water is moving through the New York Bight. These are the most useful results of the survey.

The method of investigation depends upon the use of the fresh water entering from the Hudson and other rivers as a tracer. The results obtained should apply to any pollutant carried in solution or fine suspension.

In the case of a river, the average velocity with which the fresh water is moving is given by dividing the flow through a cross section of the channel by the area of that cross section. Where the river enters the sea, a large quantity of salt water is mixed with the fresh water and moves with it. In order to estimate the velocity of movement of fresh water across any section drawn from shore to shore, it is necessary to estimate the fraction of the section which is occupied by fresh water. The area of this fraction of the section is then divided into the river flow to obtain the average velocity of drift of the fresh water seaward.

The fraction of the section occupied by fresh water can be estimated from the average salinity of the water in the section, provided it can be assumed that this water is a simple mixture of river water and sea water of some known source and composition. It is difficult to determine the salinity which should be ascribed to the sea water entering the New York Bight for purposes of calculation, and the value chosen may have a large effect on the result of the estimate.

In the present calculation we have chosen the salinity observed at a station about 25 miles east of Sandy Hook and 10 miles south of the Long Island shore. This water was similar to water extending eastward off the Long Island coast. Since the general drift is westward along this shore, similar water would be expected to occupy the area of survey if the flow of fresh water from the Hudson did not exist.

Estimates have been made of the seaward movement of fresh water across four sections extending from the New Jersey to the Long Island shores, as shown in Figure 23. The results are shown in Table 15. These estimates bring out two points of interest.

1. The velocity of seaward drift varies from about one to six miles per day and has an average value for all times and sections slightly less than three miles per day (1 nautical mile = 6080 feet). This is the average rate at which pollutants may be expected to be carried seaward.

2. The drift across the various sections is about equal in rate, and is not evidently correlated either with the size of the river flow or the distance from the river mouth. This observation indicates that the rate of movement of pollutants through the area is determined by the general circulation of the ocean water (tidal movements and non-tidal currents) rather than by the conditions of flow in the rivers.

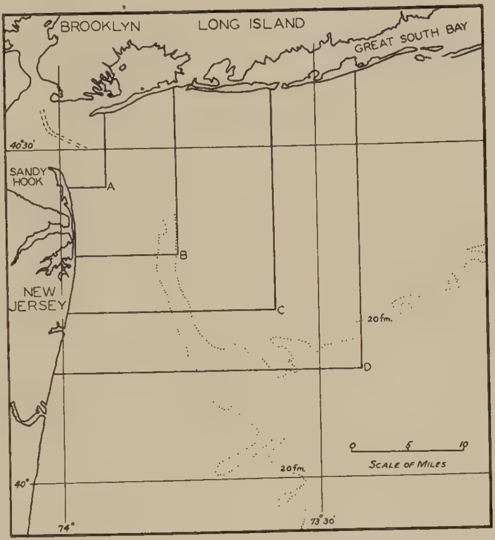

Figure 23. Diagram showing position of sections across which average seaward drift of river water has been calculated.

5. THE FLUSHING TIME

The average time required for a particle of fresh water discharged into an area by rivers to be carried out of the area is called the flushing time. It may be estimated by dividing the volume of fresh water in the area by the daily river flow. In the case of the area off the mouth of the Hudson River, the flushing time has been estimated by integrating the fresh water content at the points of observation throughout the area and dividing this value by the recorded river flows. The results of these estimates are given in Table 16. They show that the fresh water, on the average, moves out of the area in six to ten days.

This result should apply to any pollutant dissolved in the water or carried as a fine suspension. Observations on the iron content of the water in the area and estimates of the rate at which iron is entering from the rivers or from barging operations have been used to check this conclusion.

TABLE 15

Average Seaward Drift of Fresh Water Across Various Sections of the New York Bight

Date	River Flow	Drift in Feet per Day Across Section			
		A	*B*	*C*	*D*
	10⁹ft³/day				
Feb. 1948	1.49	26,700	20,500	13,400	9,100
Apr. 1948	4.1	19,800	17,900	17,300	23,100
July 1948	1.3	14,700	12,000	15,800	20,500
Oct. 1948	0.6	12,600	7,930	13,800	
Aug. 1949	0.6	6,210	38,400	11,600	27,400
Jan. 1950	2.63	19,500	18,100	24,200	17,400

TABLE 16

Estimates of the Flushing Time for the Area off the Mouth of the Hudson River, Based on Fresh Water Transport

Date of Survey	Area Surveyed	Contained Volume		River Flow	Flushing Time*	
		Total	River Water		River Water	Iron
	sq. mi.	*10⁹ cu. ft.*	*10⁹ cu. ft.*	*10⁹ cu. ft. per day*	*days*	*days*
Feb. 1948	483	1399	8.92	1.49	6.0	10.5
Apr. 1948	662	1987	30.41	4.09	7.5	8.0
July 1948	684	1945	12.66	1.30	9.7	12.2
Oct. 1948	468	1259	6.34	0.60	10.6	12.2
Aug. 1949	630	1830	3.63	0.46	7.9	11.7
Jan. 1950	650	1895	15.69	2.51	6.3	13.9

* See Table 11.

Table 16 shows the flushing time of the area estimated from data on iron. The results so obtained vary from about 8 to 14 days. They are thus in substantial agreement with those obtained from the fresh water transport, though in every case somewhat longer flushing times were obtained.[7]

A further check on the rate of transport of water through the New York Bight is provided by data obtained by the recovery of drift bottles along the shores. During the surveys of July and October, 1948, and of August, 1949, and January, 1950, more than 2,000 drift bottles were dropped overboard at points uniformly distributed throughout the area. (See Table 17.) At other times additional bottles were released in the original waste disposal areas from the barge operated by the National Lead Company, and from the U. S. Fish and Wildlife Services vessel when she visited the region. Reports have been received of the recovery of 13 percent of these bottles, of which 5.4 percent were found on the Long Island shore, 6 percent on the New Jersey coast, and 1.6 percent on the coast between Cape May and Cape Hatteras. Five bottles have been found which have made long oceanic traverses to Bermuda, the Azores, Ireland, and Portugal.

From the time elapsing between release

---

[7] The possible causes of this difference in the flushing times based on fresh water and on iron are discussed by Ketchum, Redfield and Ayers (9).

and recovery some idea can be obtained of the rate of drift. The data for recoveries from the Long Island and New Jersey coasts were analyzed to show the number of recoveries during successive five-day periods from the different parts of the coast. The results are presented in Figures 24 and 25. It may be seen that in the sections of coast within thirty miles of the entrance to New York Harbor—that is, between Fire Island Inlet and the head of Barnegat Bay—very few bottles were recovered more than ten or fifteen days after release. At greater distances the time elapsing between release and recovery increases, as is to be expected.

TABLE 17

Summary of the Data on Drift Bottles Released in the New York Bight

Date of Release	Number of Release Points	Number Released	Number Recovered	Percent Recovery
July 27, 28, 1948	16	240	27	11
Oct. 22–27, 1948	14	210	30	14
Nov. 1, 1948	3	54	12	22
Jan. 24, 1949	1	100	2	2
Feb. 10, 1949	1	40	0	0
Feb. 21, 1949	1	40	1	3
Mar. 9, 1949	1	40	10	25
Aug. 18–21, 1949	57	912	177	19
Jan. 5–8, 1950	37	592	24	4
Total	131	2,228	283	13

Since relatively few bottles were recovered from the shores immediately adjacent to the surveyed area after more than ten or fifteen days, the conclusion may be drawn that after that time most of the bottles had been carried out of the area. This is consistent with the estimates of the flushing time based on the transport of fresh water and of iron.

6. THE DRIFT OF THE SURFACE LAYER

The surface layer of the ocean is exposed directly to the action of the wind, and its motions do not necessarily coincide exactly with the mass movement of the underlying water. Drift bottles are carried about by the motion of the surface layer and give an indication of the probable transport of such pollutants as oil, garbage, and the floating solids derived from domestic sewage which may contaminate the water and find their way to beaches. The data obtained from the recovery of drift bottles consequently provide valuable information on the probability that floating pollutants released in any part of the area will reach the adjacent shores. The results cannot properly be applied to soluble or suspended pollutants since they take no account of dilution, which rapidly decreases the concentration of such contaminants in the course of their drift.

The data have been analyzed by dividing the bight into small areas ten minutes of latitude and longitude on a side. (See Figure 26.) For each area the number of bottles released was determined and the number of these recovered from the shores of Long Island or New Jersey expressed as a percentage. Smoothed contours were then drawn which express the percentage of bottles released in the different parts of the area which were eventually found on the beaches. These contours indicate the relative likelihood that floating objects present in any part of the area will eventually reach the shores.

Figure 27 gives the over-all picture, in which no account is taken of the place of recovery. As may be expected, the chance of recovery from the beaches decreases rapidly with distance from shore. From a distance of 10 miles from shore, an average of only 15 percent of the bottles reaches the beaches. From a distance of 20 miles off the coast, practically no bottles were returned. In Figures 28 and 29 the percentages of bottles reaching the coasts of Long Island and New Jersey from different parts of the area are shown. It is notable that very high percentages of returns were obtained from positions off the Long Island shore as compared with New Jersey. These returns came, however, from bottles released within five miles of the coast during the survey of August,

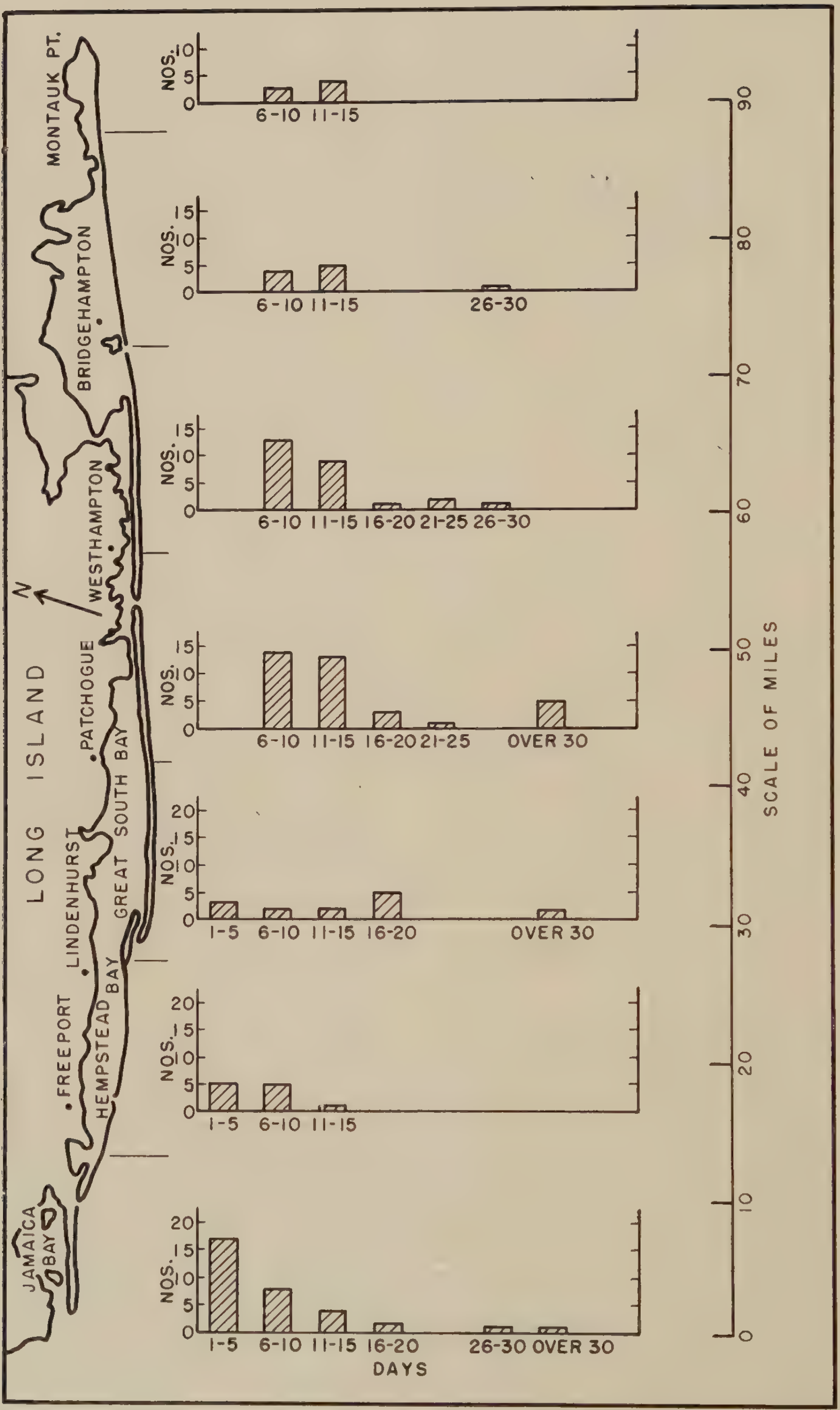

Figure 24. Numbers of drift bottles recovered from different sections of the Long Island coast during successive 5-day periods following time of release.

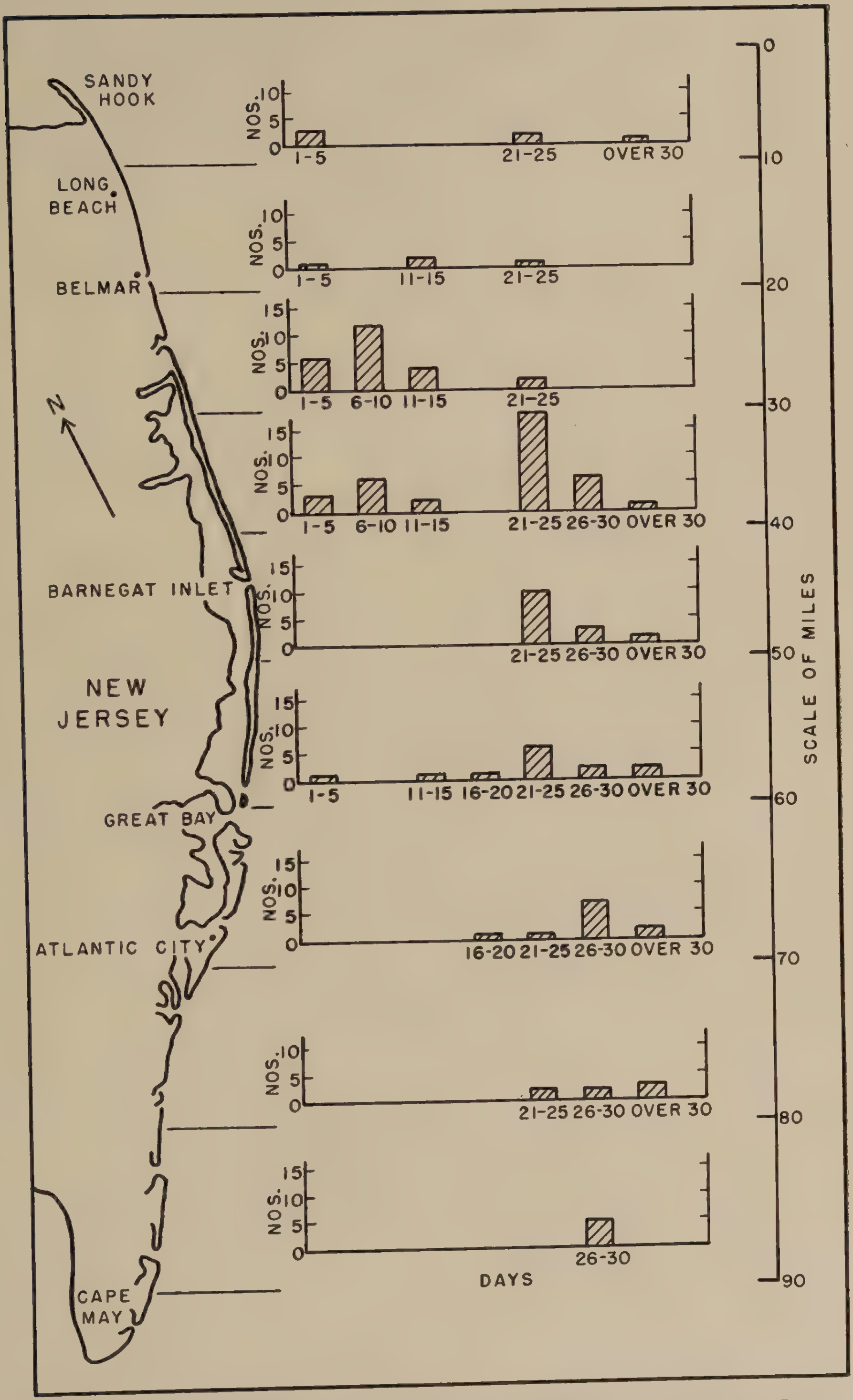

Figure 25. Numbers of drift bottles recovered from different sections of the New Jersey coast during successive 5-day periods following time of release.

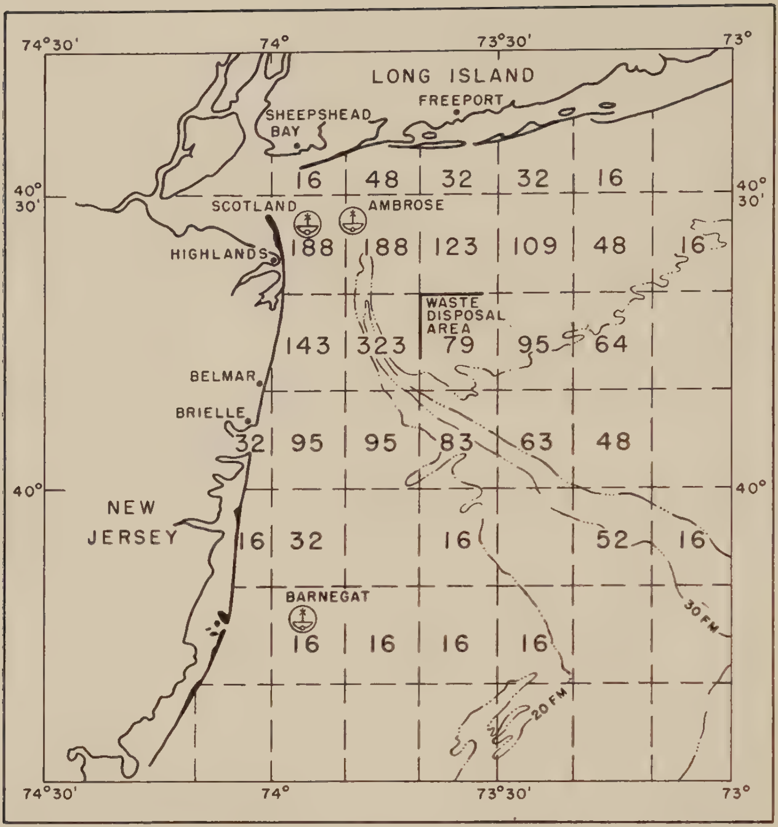
74°30'
74°
73°30'
73°
LONG ISLAND
FREEPORT
SHEEPSHEAD BAY
40° 30'
40° 30'
16
48
32
32
16
SCOTLAND
AMBROSE
HIGHLANDS
188
188
123
109
48
16
WASTE DISPOSAL AREA
143
323
79
95
64
BELMAR
BRIELLE
32
95
95
83
63
48
40°
40°
NEW JERSEY
16
32
16
52
16
BARNEGAT
30 FM
16
16
16
16
20 FM
74°30'
74°
73°30'
73°

Figure 26. Chart showing rectangular areas used in analyzing drift bottle recoveries. The numbers indicate the number of bottles released in each area.

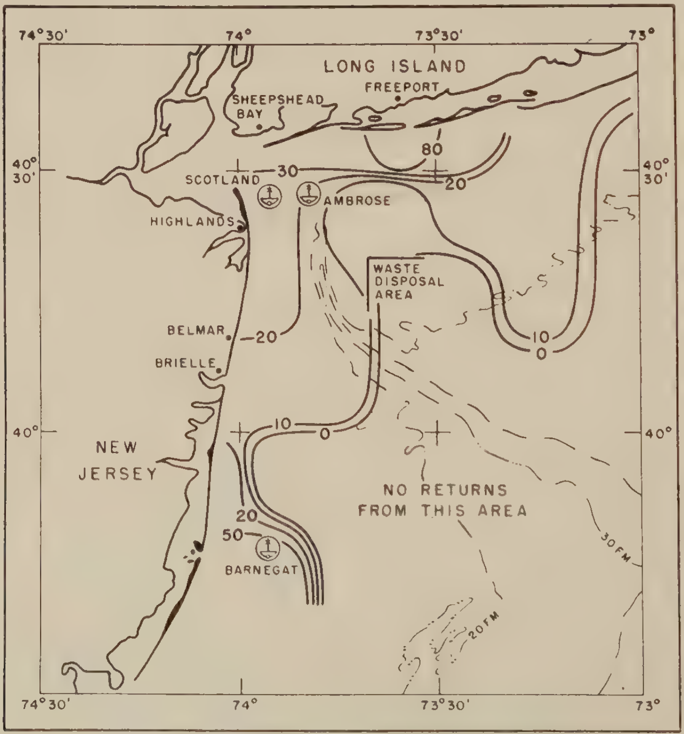
74°30'
74°
73°30'
73°
LONG ISLAND
FREEPORT
SHEEPSHEAD BAY
80
40° 30'
30
20
40° 30'
SCOTLAND
AMBROSE
HIGHLANDS
WASTE DISPOSAL AREA
BELMAR
20
10
0
BRIELLE
40°
10
0
40°
NEW JERSEY
NO RETURNS FROM THIS AREA
20
50
30 FM
BARNEGAT
20 FM
74°30'
74°
73°30'
73°

Figure 27. Chart showing percent of drift bottles released in various parts of New York Bight which were recovered anywhere on the coasts of Long Island and New Jersey.

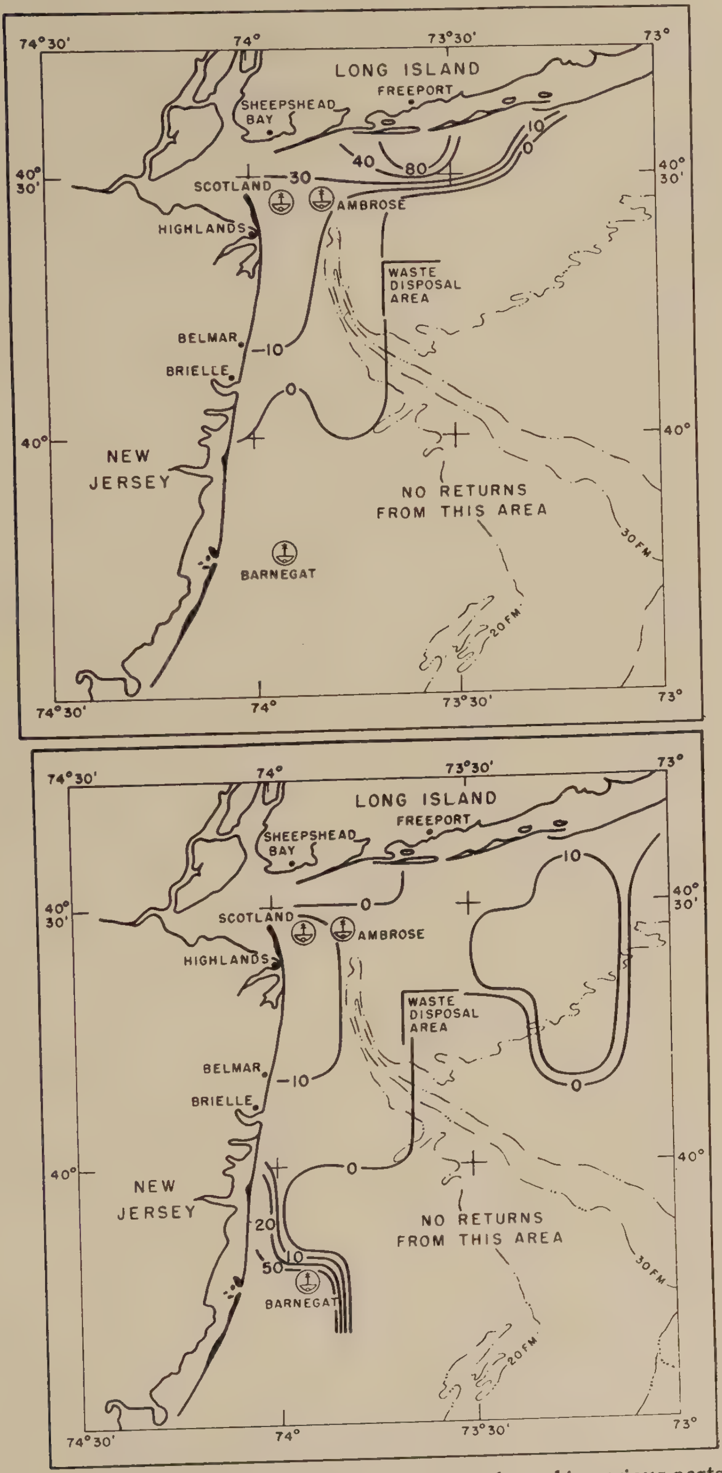
74°30'
74°
73°30'
73°
LONG ISLAND
FREEPORT
SHEEPSHEAD BAY
40
80
10
0
40° 30'
SCOTLAND
30
AMBROSE
HIGHLANDS
WASTE DISPOSAL AREA
BELMAR
10
BRIELLE
0
40°
NEW JERSEY
NO RETURNS FROM THIS AREA
30 FM.
BARNEGAT
20 FM.
74°30'
74°
73°30'
73°
LONG ISLAND
FREEPORT
SHEEPSHEAD BAY
10
40° 30'
SCOTLAND
0
AMBROSE
HIGHLANDS
WASTE DISPOSAL AREA
BELMAR
10
BRIELLE
0
40°
NEW JERSEY
20
10
50
BARNEGAT
NO RETURNS FROM THIS AREA
30 FM.
20 FM.

Chart showing percent of drift bottles released in various parts of the New York Bight which were recovered anywhere on the coast of Long Island (Figure 28, top) or New Jersey (Figure 29).

1949, when a somewhat unusual pattern of circulation was present.

The conclusion to be drawn from the drift bottle studies is that wastes likely to be transported to beaches in the surface layers should be carried at least ten miles to sea if contamination of beaches is to be avoided. While the wastes of the National Lead Company do not contain materials of this character it may be noted that the present disposal area appears to be well located, since less than ten percent of the bottles released there were recovered from the Long Island and New Jersey beaches.

7. SUMMARY

THE circulation patterns are quite variable, ranging from the most common type, which indicates that the river effluent escapes in a narrow band along the New Jersey coast, to one in which the river effluent is distributed widely over the surface of the area. Although five of the six distributions observed can be accounted for by the associated oceanographic forces and the winds, so many variables contribute to the circulation that predictions are not feasible. It would not be practical, for example, to select different disposal areas for different seasons of the year.

The fresh water from the rivers moves seaward across the area immediately off New York at an average rate of about three miles per day. Pollutants discharged into this water would be carried seaward at the same average rate.

Considering the area extending south and east about 25 miles from the shores, it is estimated that about ten days is required on the average for the replacement of the contained water by other water from outside the area. This result is confirmed by measurements of the accumulation of iron in the area and by the recoveries of drift bottles. It indicates that the accumulation of soluble and suspended wastes discharged into the area will be very limited.

The recovery of drift bottles indicates that the likelihood of floating materials reaching the adjacent shores decreases rapidly with their distance from shore, and becomes small at distances of ten miles or more.

VI. CONCLUSIONS

In attempting to evaluate the consequences of disposing of wastes in the offshore waters of the sea it should be emphasized that each type of waste presents an individual problem. The behavior of the waste will depend on its physical state, solubility, specific gravity, stability, and specific chemical and biological properties. It is evident, for example, that entirely different considerations are involved depending on whether the material sinks and accumulates on the bottom, dissolves and becomes dispersed in the flowing masses of water, or floats on the surface until cast up on the beach. A floating material like oil, which forms a coherent patch on the sea surface and results in a persistent nuisance when cast on the beach, presents a different problem from floating garbage, which may be widely dispersed by currents and decomposes rapidly after reaching the shore. Thus the results of the present study, while yielding information which should be of value in considering other problems, should be applied to such problems with caution and with due regard to the similarities and differences in the properties of the substances to be disposed of.

The acid ferrous sulfate waste from the titanium plant of the National Lead Company reacts rapidly with sea water to form inert materials which remain in solution, or to form extremely fine suspensions which are carried by the water movements for great distances before settling to the bottom. It has been found that the mixing and reaction of the waste with sea water take place rapidly in the wake of the barge. In consequence a relatively small volume of water is exposed temporarily to the harmful effects arising from the original acidity of the waste material. No evidence of the accumulation of products derived from the waste has yet been found. Consideration of the general rate of exchange of water between the New York Bight and the adjacent parts of the ocean makes it extremely unlikely that the quantity of waste discharged during more than a few days could be found in the region at any one time. No evidence has appeared which indicates that undesirable effects of any sort have arisen from these waste disposal operations.

In view of the above considerations, it is concluded that on its present scale the procedure employed by the National Lead Company in disposing of the wastes from its titanium plant is entirely proper. The operations should not be discouraged unless some new facts justify a contrary opinion.

The area presently assigned for disposing of the titanium plant's waste appears to be well chosen. It is sufficiently far from any shore to remove the possibility of contaminated water reaching the coast until greatly diluted. It is removed from the areas most frequented by fishermen. It is, nevertheless, sufficiently accessible from Lower Bay. It might be argued from the demonstrated facts that the harmful effects of the pollution are so slight and so well localized that the assignment of an area closer to the Bay would be proper. However, the imponderable factors are sufficiently great that it is prudent to continue operations at the present site.

In the consideration of the general problem of disposing of industrial or other wastes at sea, the most important result of the present investigations has been the demonstration of the rapid rates of exchange of coastal waters with adjacent parts of the sea. Judgments adverse to the use of the sea as a means of waste disposal are apt to be prejudiced by observations on the pollution of confined embayments where the exchanges of water are greatly reduced. Prejudice also exists because of the very undesirable pollution of beaches which follows the discharge at sea of floating wastes such as oil or garbage. The capacity of offshore waters to receive and disperse soluble or suspended wastes without undesirable effects is very large and might properly be used more extensively. Each proposed operation, however, should be examined critically to make sure that the waste is of a character to be safely treated as proposed, and that the disposal site is properly chosen in relation to the local hydrography, the disposition of fishing grounds, and the presence of other interests which might be adversely affected.

REFERENCES

1. Arnold, E. L., Jr. and Wm. F. Royce. "Observations of the Effect of Acid-iron Waste Disposal at Sea on Animal Populations." Special Scientific Report Fisheries No. 11, Fish & Wildlife Service, U. S. Dept. of the Interior (1950).
2. Bigelow, H. B., and Mary Sears. "Studies of the Waters of the Continental Shelf, Cape Cod to Chesapeake Bay. II. Salinity." *Papers in Physical Oceanography and Meteorology*, Vol. IV, No. 1 (1935).
3. Buller, R. J., and H. S. Spear. "A Survey of the Sport Fishery of the Middle Atlantic Bight in 1948." Special Scientific Report Fisheries No. 7, Fish and Wildlife Service, U. S. Dept. of the Interior (1950).
4. Cooper, L. H. N. "Iron in the Sea and in Marine Plankton." *Proceedings of the Roy. Soc. London*, Ser. B., No. 810, Vol. 124, pp. 419–438 (1935).
5. Cooper, L. H. N. "Some Conditions Governing the Solubility of Iron." *Proceedings of the Roy. Soc. London*, Ser. B., Vol. 124, pp. 299–307 (1937).
6. Cooper, L. H. N. "The Distribution of Iron in the Waters of the Western English Channel." *Jour. Mar. Biol. Assoc., U. K.*, Vol. 27, pp. 279–313 (1948).
7. Cooper, L. H. N. "Some Chemical Considerations on the Distribution of Iron in the Sea." Ibid., Vol. 27, pp. 314–321 (1948).
8. Ketchum, B. H., and Wm. L. Ford. "Waste Disposal at Sea." Preliminary report on acid-iron waste disposal. Woods Hole Oceanographic Institution. Report to National Research Council (June, 1948).
9. Ketchum, B. H., A. C. Redfield, and J. C. Ayers. "The Hydrography of the New York Bight." *Papers in Physical Oceanography and Meteorology* (in press).
10. "Non-propelled Acid Disposal Barge 'Sayreville'." *Marine News*, Vol. 34, pp. 72–74 (October, 1947).
11. Spilhaus, A. F., and A. R. Miller. "The Sea Sampler." *Sears Found., Jour. Mar. Res.*, Vol. 7, pp. 370–385 (1948).
12. Westman, J. R., and M. H. Bidwell. "Waste Disposal and the Fisheries of the Salt Water Adjacent to the Greater New York Metropolitan District." N. Y. State Conservation Dept., Bur. Marine Fisheries (1948).

Report for the year 1951

THE
WOODS HOLE OCEANOGRAPHIC INSTITUTION

REPORT FOR THE YEAR
1951

1952

Trustees and members of the Woods Hole Oceanographic Institution at the annual meeting, August 16, 1951

TABLE OF CONTENTS

		PAGE
	Frontispiece	
I.	Trustees, as of December 31, 1951	4
II.	Members of the Corporation, as of December 31, 1951	5
III.	Staff	6
IV.	Treasurer's Report	8
V.	Director's Report	15
VI.	Publications	33
	Appendix	35

I. TRUSTEES

(As of December 31, 1951)

To serve until 1955

E. G. Conklin, Princeton University, Princeton, N. J.
Alexander Forbes, 610 Harland Street, Milton, Mass.
Ross G. Harrison, Osborn Zoological Laboratory, Yale University, New Haven, Conn.
Milford R. Lawrence, Siders Pond Road, Falmouth, Mass.
Harlow Shapley, Harvard College Observatory, Cambridge, Mass.
Francis C. Welch, 73 Tremont Street, Boston, Mass.

To serve until 1954

Charles Francis Adams, 15 State Street, Boston, Mass.
Horace S. Ford, 77 Massachusetts Avenue, Cambridge 39, Mass.
Arnaud C. Marts, 521 Fifth Avenue, New York, N. Y.
Albert E. Parr, American Museum of Natural History, Central Park West at 79th Street, New York, N. Y.
Athelstan F. Spilhaus, Institute of Technology, University of Minnesota, Minneapolis, Minnesota.
Selman A. Waksman, New Jersey Agricultural Experiment Station, New Brunswick, N. J.

To serve until 1953

L. O. Colbert, 4408 29th Street, N. W., Washington, D. C.
Marion Eppley, Eastover, Newport, R. I.
Frank A. Howard, 30 Rockefeller Plaza, New York, N. Y.
The Commandant (Vice Admiral Merlin O'Neill), U. S. Coast Guard, 1300 E Street N. W., Washington, D. C.
Columbus O'D. Iselin, Woods Hole Oceanographic Institution, Woods Hole, Mass.
Raymond Stevens, c/o Arthur D. Little, Inc., 30 Memorial Drive, Cambridge, Mass.

To serve until 1952

Henry B. Bigelow, Museum of Comparative Zoology, Cambridge, Mass.
Detlev W. Bronk, Johns Hopkins University, Baltimore, Md.
Daniel Merriman, Bingham Oceanographic Laboratory, Yale University, New Haven, Connecticut.
Alfred C. Redfield, Woods Hole Oceanographic Institution, Woods Hole, Mass.
Lawrason Riggs, Room 1722, 120 Broadway, New York, N. Y.
Henry L. Shattuck, 10 Milk Street, Boston, Mass.

Ex. Officio

Edwin D. Brooks, Jr., P. O. Box 135, Boston 3, Mass.
Edward H. Smith, Woods Hole Oceanographic Institution, Woods Hole, Mass.

OFFICERS

Henry B. Bigelow, Chairman of the Board of Trustees, Museum of Comparative Zoology, Cambridge, Mass.
Arnaud C. Marts, President of the Corporation, 521 Fifth Avenue, New York, N. Y.
Edwin D. Brooks, Jr., Treasurer, 294 Washington Street, Boston, Mass.
Mary Sears, Clerk of the Corporation, Woods Hole Oceanographic Institution, Woods Hole, Mass.

II. MEMBERS OF THE CORPORATION

Charles Francis Adams, 15 State Street, Boston, Mass.
Oliver Ames, III, North Easton, Mass.
Philip Armstrong, Medical Center of Syracuse, State University of New York, Syracuse, New York.
Henry B. Bigelow, Museum of Comparative Zoology, Cambridge, Mass.
Lindsay Bradford, 215 East 72nd Street, New York, N. Y.
Detlev W. Bronk, Johns Hopkins University, Baltimore, Md.
Edwin D. Brooks, Jr., 294 Washington Street, Boston, Mass.
L. O. Colbert, 4408 29th Street N. W., Washington, D. C.
The Commandant (Vice Admiral Merlin O'Neill), U. S. Coast Guard, 1300 E Street, Washington, D. C.
E. G. Conklin, Princeton University, Princeton, N. J.
Harrison P. Eddy, c/o Metcalf & Eddy, 1300 Statler Building, Boston, Mass.
Marion Eppley, Eastover, Newport, R. I.
Jno. A. Fleming, 1530 P Street N. W., Washington, D. C.
Alexander Forbes, 610 Harland Street, Milton, Mass.
Horace S. Ford, 77 Massachusetts Avenue, Cambridge, Mass.
Ross G. Harrison, Osborn Zoological Laboratory, Yale University, New Haven, Conn.
Frank A. Howard, 30 Rockefeller Plaza, New York, N. Y.
Columbus O'D. Iselin, Woods Hole Oceanographic Institution, Woods Hole, Mass.
Milford R. Lawrence, Siders Pond Road, Falmouth, Mass.
Lamar R. Leahy, 910 Park Avenue, New York, N. Y.
Alfred L. Loomis, Room 2420, 14 Wall Street, New York 5, N. Y.
Arnaud C. Marts, 521 Fifth Avenue, New York, N. Y.
Daniel Merriman, Bingham Oceanographic Laboratory, Yale University, New Haven, Connecticut.
Henry S. Morgan, 2 Wall Street, New York, N. Y.
Albert E. Parr, American Museum of Natural History, Central Park West at 79th Street, New York, N. Y.
Alfred C. Redfield, Woods Hole Oceanographic Institution, Woods Hole, Mass.
Lawrason Riggs, Room 1722, 120 Broadway, New York, N. Y.
George H. Richards, 68 William Street, New York, N. Y.
Mary Sears, Woods Hole Oceanographic Institution, Woods Hole, Mass.
Athelstan F. Spilhaus, Institute of Technology, University of Minnesota, Minneapolis, Minnesota.
Lyman Spitzer, Jr., Princeton University Observatory, 14 Prospect Avenue, Princeton, New Jersey.
Harlow Shapley, Harvard College Observatory, Cambridge, Mass.
Henry L. Shattuck, 10 Milk Street, Boston, Mass.
Edward H. Smith, Woods Hole Oceanographic Institution, Woods Hole, Mass.
Raymond Stevens, c/o Arthur D. Little, Inc., 30 Memorial Drive, Cambridge, Mass.
Selman A. Waksman, New Jersey Agricultural Experiment Station, New Brunswick, N. J.
Francis C. Welch, 73 Tremont Street, Boston, Mass.
Wm. D. Winter, Atlantic Mutual Insurance Co., 49 Wall Street, New York 5, N. Y.

III. STAFF

(As of December 31, 1951)

Director

Edward H. Smith, Oceanographer

Senior Scientists

Columbus O'D. Iselin, Associate Professor of Physical Oceanography, Harvard University and Research Oceanographer, Museum of Comparative Zoology; Senior Oceanographer.

Alfred C. Redfield, Professor of Physiology, Harvard University; Senior Biologist.

Scientists

Arnold B. Arons, Associate Professor of Physics, Stevens Institute of Technology; Associate in Physics.

John C. Ayers, Assistant Professor of Oceanography, Department of Conservation, Cornell University; Associate in Biology.

David L. Belding, Professor of Bacteriology and Experimental Pathology (Emeritus), Boston University; Consultant, U.S. Fish and Wildlife Service; Associate in Marine Biology.

Henry B. Bigelow, Professor of Zoology (Emeritus), Harvard University; Associate in Oceanography.

Dean F. Bumpus, Oceanographer.

Andrew F. Bunker, Marine Meteorologist.

Cornelia L. Carey, Associate Professor Emeritus, Barnard College; Associate in Marine Bacteriology.

George L. Clarke, Associate Professor of Zoology, Harvard University; Marine Biologist.

Willard Dow, Engineer.

William Maurice Ewing, Professor of Geology, Columbia University; Director, Lamont Geological Observatory; Associate in Geophysics.

Charles J. Fish, Professor of Marine Biology, University of Rhode Island and Director, Narragansett Marine Laboratory; Associate in Marine Biology.

Frederick C. Fuglister, Physical Oceanographer.

Bernard Haurwitz, Professor of Meteorology and Chairman of the Department of Meteorology, New York University; Associate in Meteorology.

John B. Hersey, Physical Oceanographer.

Louis W. Hutchins, Director, Bermuda Biological Station for Research, Inc.; Marine Biologist.

Charles H. Keith, Physical Chemist.

Bostwick H. Ketchum, Marine Microbiologist.

Joanne S. Malkus, Meteorologist.

Raymond B. Montgomery, Visiting Professor of Oceanography, Brown University; Physical Oceanographer.

Hilary B. Moore, Associate Professor of Marine Biology, and Assistant Director, Marine Laboratory, University of Miami; Associate in Marine Biology.

Robert C. Moses, Engineer.

Roy L. Rather, Jr., Engineer.

Francis A. Richards, Chemical Oceanographer.

Gordon A. Riley, Associate Professor of Marine Biology, Yale University; Marine Physiologist.

Carl-G. Rossby, Professor of Meteorology, University of Stockholm; Visiting Professor, University of Chicago; Associate in Meteorology.

Irving I. Schell, Marine Meteorologist.

William E. Schevill, Associate Curator of Invertebrate Paleontology, Museum of Comparative Zoology, Harvard University; Associate in Physical Oceanography.

William C. Schroeder, Associate Curator of Fishes, Museum of Comparative Zoology, Harvard University; Ichthyologist.

Mary Sears, Planktonologist.

Floyd M. Soule, Principal Senior Oceanographer, U. S. Coast Guard; Associate in Physical Oceanography.

Athelstan F. Spilhaus, Dean, Institute of Technology, University of Minnesota; Associate in Physical Oceanography.

Henry C. Stetson, Research Oceanographer and Alexander Agassiz Fellow in Oceanography, Museum of Comparative Zoology, Harvard University; Submarine Geologist.

Henry M. Stommel, Physical Oceanographer.

Parker D. Trask, Research Engineer, University of California; Associate in Submarine Geology.

Harry J. Turner, Marine Biologist.

Allyn C. Vine, Physical Oceanographer.

William S. von Arx, Physical Oceanographer.

Edmond E. Watson, Professor of Physics, Queen's University, Kingston, Ontario; Associate in Physical Oceanography.

Alfred H. Woodcock, Oceanographer.

George P. Woollard, Professor of Engineering Geology and Geophysics, University of Wisconsin; Associate in Geophysics.

Research Associates

Duncan C. Blanchard, Research Associate in Meteorology.
William S. Butcher, Research Associate in Geology.
Harlow G. Farmer, Jr., Research Associate in Engineering.
Lloyd D. Hoadley, Research Associate in Engineering.
John F. Holmes, Research Associate in Engineering.
Henry R. Johnson, Research Associate in Engineering.
Willem V. R. Malkus, Research Associate in Physics.
Frank J. Mather, III, Research Associate in Oceanography.
William G. Metcalf, Research Associate in Oceanography.
Arthur R. Miller, Research Associate in Oceanography.
Frederick deW. Pingree, Research Associate in Engineering.
Harold E. Sawyer, Research Associate in Engineering.
Arthur D. Voorhis, Research Associate in Physics.
L. Valentine Worthington, Research Associate in Oceanography.
Ralph L. Wyrick, Research Associate in Engineering.

Edward H. Smith, Director.
Alfred C. Redfield, Associate Director.
Ronald A. Veeder, Assistant to the Director.
Helen F. Phillips, Secretary to the Director.
John McGilvray, Business Manager.
Norman T. Allen, Administrator.
Harvey MacKillop, Controller.

IV. TREASURER'S REPORT

The accounts for the year 1951 have been audited by Messrs. Seamans, Stetson & Tuttle, Certified Public Accountants of Boston.

Endowment Fund Assets and Endowment Fund

The Endowment Fund cash plus the quoted market value of the investments in bonds and stocks at December 31, 1951 totaled $3,365,727.94, an increase of $192,193.71 over the December 31, 1950 total. Of the total amount, $1,265.94 was in cash, $1,056,022.00 in bonds, a decrease of $33,768.28 over the book value, and $2,308,440.00 in stocks, an increase of $846,241.42 over the book value.

During the year bonds costing $113,182.71 were sold or redeemed for $112,271.95 which, after adding applicable amortization of bond premiums in the amount of $485.89, resulted in a realized loss of $424.87. Stocks and rights with book or assigned values of $173,882.50 were sold for $163,810.70, resulting in a net loss of $10,071.80. The total net loss from all sales or exchanges amounted to $10,496.67, thus bringing the accumulated net realized gain to the Endowment Fund to $133,834.84.

During the year, from the proceeds of the above sales and cash, $156,780.00 was invested in bonds and $122,343.76 in stocks, leaving $1,265.94 uninvested at the year-end.

Plant Assets and Plant Funds

Plant Assets increased $33,853.85 during the year. The increase resulted from the following additions to Plant: Laboratory Equipment, $18,622.01; Library Books, $1,200.00; Buildings, $4,362.60; and improvements to the Homestead property $9,669.24. The Depreciation Fund assets, consisting of cash and advances for current funds, were consolidated with current funds, to assist in reducing our borrowing. The accumulated net amount of the Depreciation Fund is ear-marked in the Current Surplus account under "Periodic Replacements," totaling $14,322.82 on December 31, 1951.

Current Assets and Current Liabilities

Accounts and Notes Payable, plus Unexpended Grants, exceeded Cash and Receivables by $45,447.17, against a similar figure for last year of $72,350.24, an improvement of $26,903.07. The Notes Payable were reduced $10,000.00 during the year.

Deferred Boat Costs increased from $66,628.04 at the end of 1950 to $70,528.69 at the end of 1951. The benefit of these expenses extends over several years, and each year a proportionate part is added to Boat Costs. During the year $28,298.83 was thus charged to Current Boat Costs, and $32,199.48 was added to Deferred Boat Costs, primarily due to replacement and repair of deck and hull plates, new batteries and two life boats on the ATLANTIS, and batteries on the CARYN.

The Surplus Account increased from $43,025.93 to $71,190.34. This increase, of $28,164.41, is shown in detail on the Balance Sheet.

The Housing and Mess were operated at losses of $4,067.63 and $2,975.60 respectively, which losses were included in overhead costs. The Hall property produced a net income of $2,072.26. The three comparable figures for the previous year were: Housing, loss of $4,207.49; Mess, loss of $4,955.07; and Hall property, net income of $888.18.

The total income of the Institution from investments after deducting custodian fees and amortization of bond premiums, amounts to $157,333.69, compared to $155,234.84 for the previous year. Other income, including grants and fees, brought our total Institution income to $211,456.94. Institution charges against income, including our share of cooperative projects, totaled $205,702.70, resulting in an excess of Income carried to Surplus of $5,754.24.

The Institution does contract work for various governmental agencies on a cost reimbursement basis, and during 1951 received a fee for work under one of these contracts, amounting to $941.56, which amount is included in the Institution income.

The return on the investments held at the year-end was at the rate of 4.67% on the market value, 6.16% on the book value, and 6.51% on the original book value of the Endowment.

The Balance Sheets and Statement of Income and Expenses are appended.

BALANCE SHEET

As of December 31, 1951

ENDOWMENT FUND ASSETS

BONDS (LESS RESERVE FOR AMORTIZATION OF BOND PREMIUMS $1,914.18)		$1,089,790.28
Quoted Market Value	$1,056,022.00	
STOCKS		1,462,198.58
Quoted Market Value	2,308,440.00	
	$3,364,462.00	
CASH		1,265.94
		$2,553,254.80

Note: Bonds having a book value of $400,455.00 are specifically allocated as collateral on the Institution's indebtedness to the New England Trust Company.

PLANT ASSETS

LABORATORY PLANT:			
Land		$27,072.32	
Buildings		336,564.86	
Laboratory Equipment		50,741.63	
Library		22,000.00	$436,378.81
KETCH "ATLANTIS":			
Construction	$218,674.47		
Equipment	41,462.50	$260,136.97	
KETCH "CARYN"		98,275.43	
SMALL BOATS AND EQUIPMENT		10,578.85	368,991.25
HALL PROPERTY			26,500.00
HOMESTEAD			110,611.58
			$942,481.64

BALANCE SHEET

As of December 31, 1951

ENDOWMENT FUNDS

Endowment Fund — General	$2,000,000.00	
Endowment Fund — For Upkeep of Plant	419,419.96	$2,419,419.96
Add accumulated net gain on securities called or sold		133,834.84
		$2,553,254.80

PLANT FUNDS

Plant Fund — General			$640,328.79
Plant Fund Reserve — Transferred in Prior Years from Current Surplus		$250,299.00	
Add appropriation from Current Funds:			
"Caryn" One-fifth Purchase price	$18,000.00		
Laboratory Equipment	18,622.01		
Improvements to Homestead	9,669.24		
Temporary Building	4,362.60		
Library — Book Purchases	1,200.00	51,853.85	$302,152.85
			$942,481.64

BALANCE SHEET

As of December 31, 1951

(Concluded)

CURRENT ASSETS

Cash:			
Main Accounts		$7,421.84	
Operating Accounts		21,024.40	
Office and Boat Funds		1,110.87	$29,557.11
Accounts — Receivable:			
Governmental Agencies:			
Invoiced		$86,418.57	
Expenditures Not Invoiced	$144,625.29		
Use of Boats Not Invoiced	86,465.08	231,090.37	
		$317,508.94	
Co-operating Institutions		25,928.47	
Other Accounts Receivable		14,314.32	357,751.73
Supplies and Work-in-Process			35,502.80
Prepaid Expenses			9,203.38
Deferred Expenses:			
Boat Expense		$70,528.69	
Maintenance of Homestead		1,402.64	71,931.33
			$503,946.35

BALANCE SHEET

As of December 31, 1951

(Concluded)

CURRENT LIABILITIES

Accounts — Payable:				
Sundry Creditors			$41,618.30	
Withheld from Employees for Taxes, Insurance, etc.			10,246.21	
Sundry Accrued Expense			3,829.59	$55,694.10
Note — Payable (Secured by Bonds Having a Book Value of $400,455.00)				$360,000.00
Unexpended Grants:				
Commonwealth of Massachusetts (Shellfish Propagation)			$6,089.28	
United States Public Health Service (Bacteriology of Polluted Waters)			7,127.96	
Research Corporation Instrument Fund			2,315.27	
Barataria Bay Model			988.37	
Wallace and Tiernan Gift			541.03	17,061.91
Surplus:				
Periodic Replacement Fund:				
Balance, January 1, 1951		$5,322.82		
Additions for the Year		9,000.00	$14,322.82	
General Surplus:				
Balance, January 1, 1951		$43,025.93		
Add:				
Gift	$18,000.00			
Book Value of Plant Items Charged to Boat Expense	8,087.35			
Excess of Income for the Year	5,754.24	31,841.59		
		$74,867.52		
Deduct:				
Payment of "Caryn" Note — Payable		18,000.00	56,867.52	
Balance, December 31, 1951				$71,190.34
				$503,946.35

INCOME AND EXPENSE STATEMENT

Year Ended December 31, 1951

Income:			
Investments:			
Interest	$33,530.60		
Dividends	124,691.91	$158,222.51	
Less Amortization of Bond Premiums and Custodian Fees		888.82	$157,333.69
Grants:			
Commonwealth of Massachusetts (Shellfish Propagation)		$17,278.26	
United States Public Health Service (Bacteriology of Polluted Waters)		12,192.55	
Great South Bay Survey		4,000.00	33,470.81
Recovery of Depreciation through Charges to Overhead			16,694.25
Hall Property (Net Operating Income)			2,072.26
Fees			941.56
Sundry			944.37
Total Income			$211,456.94
Expenses:			
Operating		$79,587.69	
Co-operative Projects		40,508.87	
Institution Projects		20,594.14	
Interest Paid		8,933.75	
Additional Charge for Overhead, 1951		6,920.15	
Prior Year Adjustments:			
Unrecovered Overhead, 1950	$11,695.98		
Unrecovered Contract and Accounts — Receivable Balances	5,026.56		
Sundry Credits	*1,418.29*	15,304.25	171,848.85
			$39,608.09
Plant Items Purchased from Current Funds:			
Laboratory Equipment		$18,622.01	
Improvements to Homestead		9,669.24	
Building		4,362.60	
Library Books		1,200.00	33,853.85
Excess of Income to Surplus			$5,754.24

V. DIRECTOR'S REPORT

Introduction

The year has witnessed one of the most productive periods in the history of the Institution. This feeling is verified, not only by the variety of subjects dealt with at the laboratory, but likewise by the wide range of the field investigations. Offshore cruises kept the ocean-going vessels underway, in several instances for months at a time, while inshore waters also received a measurable share of attention.

To understand current phenomena, both on a large scale and also in detail, is one of the important tasks of physical oceanography. In this respect the Institution, since its founding, has consistently focused an appreciable portion of its field work on the Gulf Stream, in the belief that eventually we will be able to contribute a reliable picture of the patterns of motion of a stratified fluid medium. The application of such investigations to many of the problems of oceanography and meteorology is quite obvious.

The year's work in biology was directed mainly toward inshore waters where opportunity seemed to offer the most profitable results, considering the modest funds which were available. Pollution caused by waste materials and abnormal concentrations of plant growth in certain coastal areas, has been the subject of continuing study. Improved techniques in the determination of trace elements of sea-water, and the ecological studies of the Massachusetts' shell fishery, were other features of the 1951 program.

Our marine geology received added interest from a bottom survey of the eastern half of the Gulf of Mexico.

Due acknowledgment should be made in the record of the generous support accorded the oceanographic research by the U. S. Navy Department's Bureau of Ships, Office of Naval Research, and the Bureau of Aeronautics.

No marked changes occurred in the administration of the Institution. The activities for the year, and other items worthy of record, are reported in more detail under appropriate headings which follow.

Floating Facilities

The sea-going research vessels ATLANTIS and CARYN in 1951 were augmented by the addition to the fleet, during March, of the U. S. Fish and Wildlife Service Vessel, ALBATROSS III, a steel trawler which with slight alterations served well as an oceanographic vessel. These three vessels, in order named, spent 206, 199, and 161 days respectively at sea during the year; a table summarizing their operations is contained in the Appendix.

Atlantis sailed from Woods Hole in January and returned in early June. During the first leg of the cruise she carried out a survey of the sediments of the eastern part of the Gulf of Mexico under the direction of Mr. Henry C. Stetson. Later under Mr. Martin Pollak's supervision a restricted bottom area in the west gulf was surveyed in considerable detail. The Atlantis then cruised first on the Blake Plateau with Dr. J. B. Hersey, and later to the vicinity of Guantanamo, Cuba, where she was joined by Caryn. In company, until they arrived at Woods Hole the first week in June, the two vessels were engaged in seismic refraction studies directed by Dr. Maurice Ewing. This work was a cooperation between the Institution and Lamont Geological Observatory.

The Caryn spent the winter months operating out of Bermuda on Sofar studies. Later in April she joined the Atlantis in southern waters.

Atlantis (after a thorough yard overhaul), and Caryn in company, departed in July on another geological cruise which occupied the remainder of the summer, the vessels covering a rather wide offshore area. Short cruises completed what was quite an active year of sea operations.

The Albatross III departed from Woods Hole in early June on a current survey of the higher latitudes of the North Atlantic making port in Ireland, England, the Azores, and Bermuda. Messrs. Fuglister and Worthington were in charge of the scientific observations, the ship returning to her home port early in November.

A former naval supply craft named Bear, which was chartered from a commercial dredging concern for the period July 1 to December 31, was employed on local cruises by several members of the scientific staff, carrying out sea investigations in the field of their particular interest. A smaller vessel of some fifty-foot length named the Hazel III was chartered to carry out oceanographic observations in harbor waters.

The Institution's vessels consisting of Atlantis, Caryn, Asterias, and Claire have been maintained in good operating conditions throughout the year. The Atlantis underwent a thorough overhaul during June at the Electric Boat Company's yard at New London, Connecticut. A total of eleven plates were found excessively corroded. It was necessary to weld new plates over those which were weakest.

The Caryn has had its copper sheathing removed, and has had a new mizzen mast stepped in place of the old one which was weakened by dry rot. With the exception of certain fairing of the underwater planking, and new gearing of the steering quadrant, she is in good condition, although of course limited in sea endurance when compared with Atlantis. The final payment on Caryn in accordance with arrangements made with her former owner, Mrs. Caroline Ryan Foulke, was made in February.

The RELIANCE which the Navy had kept in our custody in a laid up status, was finally auctioned off during the early Fall, and departed from Woods Hole in the charge of her new owner.

Shore Facilities

Considerable thought and time has been given during the year to additional laboratory space which, as stated in the last annual report, was being projected due to the overcrowded condition of the main building which was erected more than twenty years ago.

Early in May the matter culminated in an offer by the Navy to provide a building of approximately 28,000 square feet area, including shops to be used in conjunction with the Institution's existing plant.

In accepting the proposal, the Trustees were careful to stipulate that the Institution accepted in principle the offer of the facility to be used primarily in carrying out basic oceanographic research. In reply to the Navy's request to recommend several sites, the one preferred was that adjacently east of the Institution's property, now under lease and occupancy from the Marine Biological Laboratory. At year's end plans were being drawn by the architect on the assumption that the laboratory would be separated only by a driveway from our own building, and to front likewise along Main Street. Furthermore, that the building now leased from the Marine Biological Laboratory and used as a machine shop, carpenter shop, and storage house, would be renovated and enlarged but retain its present utilitarian character.

The change in ownership of the so-called Norman House, rented during the summers of 1950 and 1951 for the convenience of summer workers at the Institution, necessitated taking steps either to lease other space, or to provide dormitory facilities of our own. The small village of Woods Hole is crowded every summer, as those who have visited the Institution at that time well know, and prices of rented apartments and rooms are at a premium. It has been the practice of the Institution to underwrite suitable housing space, and provide it at low cost to those of our summertime workers who can least afford higher priced quarters.

The renovation of the large barn, therefore, on the Institution's residential tract, to provide a summer dormitory, was begun in the Fall. When completed in the Spring of 1952 it will contain three small apartments, and eight double room dormitories. A relatively large storage space in the basement will assist to relieve present storage congestion at the main plant.

The scarcity of adequate houses in Woods Hole and the vicinity for rent or for sale, which was remarked upon in the last annual report, still exists, but the shortage apparently is not quite so acute as in 1950.

The Institution's buildings on the former Fay tract, number five residences, all of which are occupied by Institution personnel, and are now in excellent appearance and preservation. Other necessary maintenance of the ex-Fay estate has been the hard surfacing of a road leading from Main Street and connecting with Maury Lane, a private way, which runs to School Street.

Personnel

Our staff has (in addition to its primary work at the laboratory and at sea) found opportunity to present numerous technical papers during the past year at scientific meetings, and to professional societies, and it participated in seminar discussions, all in the promotion of oceanography. Several members of the Institution serve on standing committees, or act as consultants to government agencies. For example, Dr. Iselin is an active member of the Undersea Warfare Committee of the National Research Council; also a member of the panel on acoustics of the Research and Development Board, and serves too as a consultant to the Earth Sciences and the Physics Divisions of the Office of Naval Research. Dr. Redfield is president of the Oceanographic Section of the American Geophysical Union, and also served as chairman of the Oceanographic Panel of the Research and Development Board. He has represented the Institution at several dedicatory ceremonies, and has participated in university symposia. Admiral Smith serves as a board member of the Arctic Institute of North America, and as a deputy member of the Committee of Geography and Geophysics of the Research and Development Board. Dr. Iselin taught a term course in oceanography at Harvard; Dr. Montgomery at Brown, and Mr. Stommel did likewise at Yale. Others of the staff, such as Dr. Clarke and Mr. Stetson at Harvard, Dr. Riley at Yale, and Dr. Ayers at Cornell, are similarly identified with collateral assignments which keep the Institution in close liaison with developments in fields of common interest.

We regretted to lose through resignation Messrs. Martin J. Pollak and Arthur A. Klebba, both of whom had been with the Institution for several years, and had contributed materially to progress in their particular fields.

The Institution suffered the loss of one of the earliest members of its scientific staff in the tragic death on March 7th of Dr. Richard H. Seiwell. He, his wife, and two children were killed instantly in an automobile accident. An appropriate commemorative resolution was recorded at the annual meeting of the Board of Trustees.

If one compares the records of mid-year 1950 with those of 1951, it will be noted from the following tabulation that an increase of 51 employees, or approximately 20 per cent of the force, occurred in 1951. About half of the rise was due to the ALBATROSS III, and BEAR, which joined our fleet, as already mentioned.

	1950	*1951*
SCIENTIFIC AND TECHNICAL STAFF		
Full time:		
At Woods Hole	82	70
On field trips	5	12
Summers only:		
At Woods Hole	29	40
On field trips	10	12
Working at other institutions	18	4
Fellowship holders	12	14
Visiting investigators	7	9
SECRETARIES AND CLERKS	17	24
ADMINISTRATION	9	11
GENERAL MAINTENANCE AND SERVICE		
Projects	25	31
Overhead	11	20
CREWS OF VESSELS	32	61
	257	308

It is with pleasure that we record the appointment to the staff of the following: Mr. Charles H. Keith, Physical Chemist; Dr. Joanne Starr Malkus, Meteorologist; and Mr. Robert C. Moses, Engineer; also Dr. Willem V. R. Malkus and Mr. Arthur D. Voorhis, Research Associates in Physics; Dr. William S. Butcher, Research Associate in Geology; Mr. Duncan C. Blanchard, Research Associate in Meteorology; Mr. Harlow G. Farmer, Jr., Mr. Henry R. Johnson, Mr. Frederick deW. Pingree, and Mr. Harold E. Sawyer, Research Associates in Engineering.

Dr. George L. Clarke traveled in Europe during the summer, visiting marine biological institutions, and representing the Institution at the Meeting of the International Union of Geodesy and Geophysics at Brussels.

The following persons were awarded honoraria, or fellowships, during the year:

HONORARIA

AYERS, JOHN C.
EWING, WILLIAM M.
FJELDSTAD, JONAS J.
HIDAKA, KOJI
MUNK, WALTER H.
NORTON, DANIEL R.
RILEY, GORDON A.
VAN DAM, LEONARD

FELLOWSHIPS

BARLOW, JOHN P.
FELSENFELD, GARY
GEALY, BETTY L.
HOLMES, ROBERT W.
MILLER, ARTHUR R.
MOSKOVITS, GEORGE
PLUNKETT, MARY A.
RYTHER, JOHN H.
SAID, RUSHDI
SEAL, MORGAN S.
SMITH, JOAN
WATSON, STANLEY W.

The Institution was visited by many scientists from this country and abroad. Such an exchange of information by personal visit is deemed highly beneficial, and the travel and visits of our own staff members to other seats of oceanographic activity has been encouraged.

The Social Security Act of 1950, the privileges of which were offered to employees of non-profit organizations (mentioned in last year's report) was accepted by a majority vote, and became effective as of January 1, 1951. This federal statute provides certain retirement benefits in which both the Institution and the employee contribute during the term of employment.

For the past few years the advantages of devoting greater efforts to the public relations of the Institution has been receiving increasing consideration. More and more attention has been given to news reports to the local Press, magazines and popular periodicals. It has come to be acknowledged at the Institution that public relations is an important but neglected field, in which we should strive to make the work of the Institution better known.

Scientific Program

Major advances have been achieved during the past year in our ability to describe the shallow distributions of temperature and salinity that exist in the sea at any one time and to relate these to the surface currents. At long last the observational approach, the theoretical approach and the experimental approach are all beginning to yield similar results. Not only can the Institution point to a beginning in the publication of these new results, but also we have been able to formulate and initiate a promising program of continuing investigations, both in the field and in the laboratory. No other period at Woods Hole has been more fruitful in physical oceanography.

As the result of the CABOT operation in the Spring of 1950, and as substantiated by the ALBATROSS' cruise across the North Atlantic this year, it has become evident that there are many similarities between the Gulf Stream System northeastward of Cape Hatteras and the recently discovered atmospheric jet streams at high altitudes in the belts of prevailing westerly winds. Both phenomena are in all probability dependent on the same fundamental laws of large scale motions in thin fluid envelopes on a rotating globe. Since the velocities and the time scale are much more favorable for detailed investigations in the case of oceanic jets, the theoretical meteorologists are finding our Gulf Stream surveys of increasing interest.

Mr. Wm. S. von Arx early in the year set up a small rotating model of the North Atlantic circulation. The optical system through which this could be conveniently viewed was contributed by Mr. Arthur A. Klebba. Although the model was a relatively crude one, being little more than two feet in diameter, it reproduced several of the distinctive characteristics of the Gulf Stream that we have come to recognize only during the last few years, namely the concentrations of the flow in very narrow bands, the meandering, the formation of eddies, and the counter currents. Encouraged by these preliminary results Mr. von Arx has proceeded to design a much more elaborate, six foot, rotating model which is now operating in the fish tank room in the basement. It is evident that this model will at least be of the greatest help to theoreticians, for it can reproduce the sorts of simplified conditions that can be handled mathematically. Until now few checks on the theoretical reasoning have been possible.

In preparation for the past summer's ALBATROSS III cruise to England Mr. Fuglister prepared a chart showing temperature at 200 meters over the whole North Atlantic. The best previous such chart was published in the "Meteor Atlas" just before World War II, and depended on only a few thousand points of observation. Because of our rapidly gowing file of bathythermograms, Mr. Fuglister could use nearly 60,000 observations. Even when these are averaged by one degree squares it is evident that on a statistical basis a new Gulf Stream begins to form north of the old one off Georges Bank and off the Nova Scotian continental shelf, so that there are two distinct currents passing the tail of the Grand Banks, as was indeed found during operation CABOT. There is also a hint in this new chart that a third jet develops east of the Grand Banks. The same multiple jet phenomena have been found in the atmosphere and have been called "jetlets" by Dr. Rossby. The primary mission of the ALBATROSS III during the past summer was a survey of these new subdivisions of the Gulf Stream System. They found that at least as far as Flemish Cap the 200 meter average temperature chart provides a fairly good, although simplified, picture of the actual current system. It is already clear why statistical charts of surface currents seem to show that the Gulf Stream branches east of the Grand Banks. It is simply that in the averaging process these charts are not able to separate the several overlapping jetlets that exist at any given time.

Mr. Fuglister's new chart also indicates that the currents in trade wind latitudes may also be streaky and this is something that we hope to be able to examine at first hand next winter. Although we do not yet fully understand these unexpected phenomena, it is probable that we have been mistaken in thinking that the wind stress on the surface almost alone determines the characteristics of the major ocean currents. The present indication is that density differences due to heating, cooling, evaporation and precipitation are able to modify to a considerable degree the circulation that would be expected to result from the winds alone.

In considering the wind stress on the sea surface it has only been practical up to now to think in terms of the average wind distribution. Mr. Joseph Chase, a meteorologist who joined our staff in the autumn of 1950, has been making a most interesting study of the typical wind patterns that occur over the North Atlantic month by month. These tend to persist for several weeks at a time and may be significantly different from the mean monthly winds. He is also beginning a study of the differences which occur from year to year.

The old problem of how velocity changes with depth continues to be nearly as much of a mystery as ever. Mr. von Arx has uncovered some important clues in the large number of geomagnetic electric kinetograph observations secured on operation CABOT. He finds that the effective electrical thickness of the current increases gradually in the down stream direction and very rapidly as one proceeds across the stream in the offshore direction. He also finds differences between the seaward and landward meanders. When the geomagnetic electric kinetograph was towed at 100 meters it yielded higher velocities than when towed at the surface.

Dr. Edmond E. Watson has been attacking the velocity-depth problem more directly. The last two summers he has made a series of current meter observations in the Gulf Stream. About all that can be said at present is that the velocity-depth distribution changes markedly as one proceeds across the current and is by no means simple in character.

Various means of overcoming the deficiencies of conventional current meters when used in the deep ocean are being actively explored. Dr. Willem V. R. Malkus has developed a sort of diving current meter which has considerable promise. Three such instruments have been built and will be thoroughly field-tested during the winter of 1952. The instrument records velocity against pressure as it is towed slowly through the water. At each depth to which the instrument is lowered and allowed to come to equilibrium a measure can be obtained of the influence of the velocity-depth profile on the steady forward speed of the ship. For example, if the ship is moving down current and the velocity decreases with depth, the Pitot tube in the instrument will record increasing velocity at each successively deeper level. By making a second cast after a 90° change in course the velocity-depth profile can be calculated. What this instrument chiefly exploits is the fact that a wire being towed through the water rather quickly comes into equilibrium with the forces acting on it. Thus in lowering the instrument only a short pause is needed at each level of observation before the Pitot tube begins to record a steady velocity and the pressure element a steady depth.

Much thought has been given to designing a deep sea pressure recorder that could remain on bottom for considerable periods of time. Mr. David H. Frantz, Jr., has begun building such a device, after studying the problem of giving it sufficient sensitivity to record not only the passage of the tidal wave, but also of standing waves. In addition, means will be incorporated for recording bottom temperature and bottom velocity. Several means have also been devised to insure recovery of the instrument.

Another general class of much needed instruments has advanced beyond the talking stage. These are drifting buoys which would report their positions by radio day by day. The receiver element of the buoys will be tuned to the Loran stations. For a short while each day, when the sending element is activated by the coming of daylight, the buoys will re-transmit these Loran signals at a different frequency to the monitoring ship or plane. Thus in effect the proposed design should achieve a drift bottle which day by day reports its position. The principal difficulty is to secure permission to use suitable frequencies for re-transmitting the Loran signals. It is hoped that by limiting the power output of the buoys so that their signals cannot be picked up on shore this permission can be obtained. Electronically the system has been demonstrated to be feasible.

Sound as a tool for exploring submarine geology has become the specialty of Dr. Maurice Ewing's new laboratory at Columbia University. He and his staff continue to work side by side with our people at sea to the great advantage of both groups.

Sound as a means for exploring the ocean waters is a goal towards which we are only gradually working. Dr. Hersey's paper on the frequency dependence of sound returned from the scattering layer at mid-depths is undergoing final revision. This suggests that sound may become a most useful tool in marine biology. By turning an echo sounding transducer on its side and mounting it in a crude "fish" so that it can be conveniently towed, Mr. Vine has shown of what the basic elements of an effective fish locator should consist. What is still missing is the time and funds to use these systems to advance a specific biological problem.

Mr. Paul F. Smith has continued his investigation of underwater sound scattering by various forms of marine life using a short-range echo ranging technique and variable frequency to evaluate the biological interpretation of the deep scattering layer. A comparison of the results with reported extreme values of volume scattering coefficients at the depth of the deep scattering layer is made which indicates that the observed scattered sound can be accounted for by a population of from 10 to 120 palaemonetes shrimp per cubic yard. These inshore shrimp are a reasonable substitute for the larger euphausids and were chosen as an initial physical test of H. B. Moore's hypothesis that the scattering layer is predominantly composed of euphausids. The lower figure is in good agreement with Moore's estimate of euphausid density but the higher is too large. These measurements show that small shrimp are sufficiently effective sound scatterers to warrant serious consideration on physical, as well as on biological grounds, as part of the scatterers composing the deep scattering layer.

Various theoretical studies of refraction, defraction and focusing in underwater acoustics are under way through the help of several graduate students in physics who can come to the Institution during the summer months. Dr. Hersey and Mr. Vine have a common interest in this field and advances are being made steadily, if somewhat slowly. However, this is a valuable means of interesting students having the right sort of background in mathematics in some of the special problems of underwater acoustics.

Support for work in Marine Meteorology has been roughly doubled during the past year and the indications are that a continuing expansion will be justified, as we can find interested and qualified investigators.

Mr. Alfred H. Woodcock's studies of the role of sea salt nuclei in the formation of rain has been split off from the original project directed by Dr. Haurwitz. Mr. Woodcock has recruited two advanced students trained in physical chemistry to assist him in the enlarged program. In June at the request of meteorologists employed by the fruit growers of the Hawaiian Islands, Mr. Woodcock carried out a number of nuclei sampling flights in the clouds forming on the mountains of the islands. His preliminary results indicate, as was expected, that there is a good correlation between the number of larger salt nuclei present near the base of the cloud and the subsequent rainfall. He and Mr. Duncan C. Blanchard returned there in November for a continuing program of observation and because the islands are a convenient base from which to make exploratory observations on other phenomena over the ocean. There is much evidence in the recent meteorological journals that the full significance of Mr. Woodcock's investigations is finally becoming recognized.

We are fortunate that beginning in July Dr. Joanne S. Malkus could secure a 15-month leave of absence from her university and can thus join Mr. Andrew F. Bunker and Dr. Bernhard Haurwitz for an extended period in their studies of convection and turbulence over the ocean. It has been the fashion for some time now in meteorology to ignore the fact that theirs is a thermally driven system and that for much of the time air is flowing over the ocean rather than over the land. Thus the rather complicated processes whereby heat and water vapor are exchanged at the sea surface are of fundamental importance to both oceanography and meteorology.

Mr. Donald Parson, Jr., and Mr. Kenneth G. McCasland have been gradually much improving the instrumentation for these studies.

Our program in submarine geology at present essentially has three parts: the support we are giving to Dr. Ewing's group at Columbia, Mr. H. C. Stetson's continuing studies of the sediments of the Gulf of Mexico, and further studies of submarine geology in Massachusetts Bay.

Dr. Ewing's group at Columbia has become much more firmly established. A good fraction of his program comes under the heading of submarine geology, rather than submarine geophysics. The primary tool for the deep sea geology continues to be the ATLANTIS' trawl winch on which we spent nearly $20,000 two years ago. Dr. Ewing's collection of long, deep sea cores from the North Atlantic now numbers roughly 345.

Mr. Stetson's program deals systematically with an area of great interest to petroleum geology. Several years ago, with the help of a grant from the Geological Society of America, he and Dr. Phleger surveyed the western half of the Gulf of Mexico. The working up of this material is nearing completion. Last winter, therefore, a month was spent on ATLANTIS securing the corresponding samples from the eastern half. Perhaps the most spectacular find was a huge cliff paralleling the western coast of Florida for hundreds of miles. This rises almost vertically 5000 feet or more from the floor of the Gulf.

Dr. William S. Butcher, who has recently completed his formal training as a submarine geologist, has returned to Woods Hole and is in charge of new sedimentary studies in Massachusetts Bay. The sedimentary processes operating in harbors and estuaries are only understood in broad outline. Several of Mr. Stetson's students at Harvard assisted in the field work during the summer. The sedimentary studies are being conducted simultaneously with an oceanographic survey for which Mr. Dean F. Bumpus is directly responsible.

The special opportunity which oceanography offers to the biologist is to understand the conditions of life in an environment which differs markedly from the more familiar situations found on shore. So it is that the marine biologist is primarily an ecologist and is concerned in correlating physical and chemical phenomena of the sea with the characteristics of its populations. For this reason also, our biologists have trespassed into the field of physical oceanography and are doing pioneer work in exploring the conditions in coastal waters and embayments. Such waters are of great interest in relation to fisheries and because of the practical problems arising from industrial and domestic pollution, yet they have been largely neglected heretofore by the physical oceanographer.

An investigation which has been conducted during recent years on the effects of the discharge of wastes from the titanium plant of the National Lead Company off New York Harbor has now been completed. A report entitled "The Disposal of Industrial Wastes at Sea" which is to be published by the National Research Council will emphasize the great potential of coastal waters for dispersing industrial pollutants. The scientific pay-off of this investigation is a monograph on the hydrography of the New York Bight by Drs. Ketchum, Redfield, and Ayers which appeared in *Papers in Physical Oceanography and Meteorology.*

In order to extend the detailed knowledge of such conditions as obtain off the Hudson River more widely, a survey was made in May from the ALBATROSS III of the entire coastal belt extending from Woods Hole to Cape Hatteras, thus including the outflow of the Delaware River and Chesapeake Bay along with that of the Hudson. As knowledge of the coastwise circulation increases in detail, it becomes apparent that the southerly longshore drift is continuous and rapid. The pattern of flow, however, is broken by large eddies and fluctuates rapidly with conditions of wind and season. Mixing is sufficiently intense so that the influence of one river system has disappeared before the drifting water has reached the next river mouth. As in the case of the Gulf Stream, increasingly detailed observations are showing that earlier concepts of the coastal circulation are vastly over-simplified.

Dr. B. H. Ketchum has described a method for estimating the rate of flushing of an estuary under the combined influence of the tidal currents and the discharge of tributary rivers. The great virtue of this procedure is that it yields useful results based on the analysis of information which may be obtained from charts, tide tables, and hydrological data and is thus available to engineers concerned with pollution problems. Dr. Ketchum's ideas, which grew out of studies of the circulation of Raritan Bay, where a trunk sewer outfall is under consideration, have had a stimulating effect on our theoretical oceanographers. Dr. Arnold B. Arons and Mr. Henry M. Stommel have recently attempted to translate his fundamental idea, that the element of mixing volume is bounded by the length of the tidal excursion, into the language of the physics of continua. They found that an *a priori* calculation of the flushing number was not feasible without a thorough study of the sorts of simplified conditions that could be set up in model studies. Mr. Harlow G. Farmer, Jr., a graduate in hydraulic engineering at M.I.T., was interested and qualified in just such work. He has set up a most versatile hydraulic flume which is now in operation in the back yard. Thus, again in a most fruitful manner field observations, pure theory, and model studies are proceeding hand in hand. While the theoretical approach in oceanography has on the whole been rather barren, during the last few years the theoreticians have been catching up rapidly and it may be that before long they will actually begin to predict phenomena for the field observers to go out to look for.

Dr. Ketchum's method of analysis has found immediate application to biological problems. For some years a group directed by him has been studying the antibiotic effect of sea water upon colon bacteria and has determined the rates at which the bacterial populations are killed off on exposure to sea water. Since the analysis of the flushing permits one to estimate the age of the river water found in any part of its estuary, it is possible to determine how long the bacteria of a polluted river have been exposed to the antibiotic action of sea water and thus to estimate the relative importance of this action and the effect of dilution in reducing their numbers. In the case of the Raritan River, it may be shown that the antibiotic action of sea water is the major factor in reducing the bacterial pollution of the water of the estuary.

At the instigation of local oyster interests, the Town of Islip, Long Island, has engaged the Institution to make a survey of the waters of Great South Bay. This bay is the traditional source of the Blue Point Oyster and formerly produced an annual crop valued at more than $1,500,000. During the past twenty years, the crop has declined progressively owing to failure of the oysters to grow and fatten properly, and the oyster industry has now ceased to exist. An intensive survey made last summer indicated that the trouble is not due to hydrographic factors arising from changes in Fire Island Inlet and other openings to the sea, as was locally claimed, but pointed rather to pollution arising from the duck farms which occur along the tributaries of the bay. The Town of Islip has asked us to continue these studies and has been joined by the Town of Brookhaven in supporting the work. The damage to oysters appears to be due, not to the immediate effects of pollution, but to an intense bloom of algae which is stimulated to grow by the pollutants. Finally, Moriches Inlet, a critically placed opening to the sea, has closed since last summer's studies were made, so we are in a position to observe first hand the effects of this change on the circulation of the bay.

Ever since Dr. Rakestraw left our staff to join the faculty of the Scripps Institution of Oceanography, there has been no one in the laboratory concerned primarily with chemical oceanography. Somewhat over a year ago this weakness was corrected by the appointment as Chemical Oceanographer of Dr. Francis A. Richards, a chemist trained in the Oceanographic Laboratory at the University of Washington. Dr. Richards arrived in time to take over the development of special methods required for the work in Great South Bay. During last summer, Dr. Daniel R. Norton, Assistant

Professor of Chemistry at George Washington University, worked at the Institution and became interested in finding better methods of detecting the various metals present in sea water in traces. Such substances are known to be essential in the nutrition of animals and plants on land but relatively little is known of their relation to marine animals because of present difficulties in analysis. Dr. Norton and a graduate student assistant were at the laboratory throughout the summer. The chemical group was also strengthened by the presence of Dr. Mary A. Plunkett, Assistant Professor of Chemistry at Vassar College, a skilled analytical chemist. Finally, after many years, studies are being resumed on the biochemistry of marine animals. Mr. Gary Felsenfeld worked on the mechanism by which copper is bound in the molecule of hemocyanin. This is a problem which has become of interest recently because of the discovery that many important enzymes are copper-protein compounds analogous to hemocyanin.

These associations have gone a long way toward restoring chemistry to its proportionate place in the Institution, and in widening our relations with the universities.

The Institution has continued to work on shellfish for the Department of Conservation of the Commonwealth of Massachusetts. The primary object was to develop means of improving the production of clams by introducing farming methods. It must be admitted that our experience has been discouraging, it having been found that natural enemies are fatally destructive of the plantings. A great deal has been learned, however, about these predators, the horseshoe crab and the snail, Polynices. Perhaps the most valuable lesson is that clam farming should not be undertaken lightly. Mr. H. J. Turner and Dr. D. L. Belding are now turning their attention to studies in other areas where clams appear to grow naturally with greater success than on Cape Cod.

Other activities undertaken under this contract are more encouraging. Pacific oysters, a Japanese species grown commercially in Puget Sound, were introduced into Barnstable Harbor in 1949 and have survived and grown prodigiously. If this oyster will reproduce in our waters, it may form the basis for an oyster industry in the colder waters north of Cape Cod, where the Virginia oyster does not survive. Earlier surveys showed that the beds of the black quahogs, which occur in Cape Cod Bay and off Cuttyhunk, are sufficiently extensive to supply a fishery for the small-boat draggers if a market could be developed. During 1950, we supplied a food technology laboratory and several commercial dealers with small quantities of black quahogs for experimental purposes and there is now a good possibility that the industry will develop methods of processing this shellfish in a manner that will appeal to the consumer. Finally, studies are being conducted on the natural history of the sea scallop, a species which has attained great commercial importance without benefit of scientific study.

Turning to the fin fish, Mr. William C. Schroeder has continued exploratory fishing for ground fish on the nearby continental shelf. The objectives have been to assay the possibilities of profitable fishing in the deep waters of the continental slope which are not regularly fished, to study the on and offshore migration of the fluke which are now taken just south of Woods Hole, and to secure an accurate census of all the kinds of fish living on the grounds where commercial fishing is conducted. Mr. Frank J. Mather III has been collecting information on the growth and migration of the tuna, which has become a popular sport fish. He is persuading the fishermen to use numbered hooks, which will serve to tag such fish as "get away" and thus show the extent of their migrations when they are recaptured.

Among our invertebrate zoologists, Dr. Mary Sears has continued her studies of the Siphonophores collected by the Danish ship DANA in an ocean-wide cruise. During the year, she has found it necessary to make a drastic revision of the classification of this group of animals, a task which has required the comparison of her specimens with those from the principal museums of Europe. Mr. John P. Barlow has been making a careful year-round study of the zooplankton of Great Pond, Falmouth. This is a small estuary tributary to Vineyard Sound. The problem has been to learn to what extent the pelagic population of a salt pond depends upon recruitment from the open sea with which the pond connects. It has become clear that the pond population maintains itself as a distinct entity, in spite of the continuous exchanges of water due to the tides.

At the present time, there is no one on the staff concerned primarily with the marine plants. Some work on the culture of marine phytoplankton is being done in connection with the Great South Bay studies, and Dr. Gordon A. Riley is paying particular attention to the contributions of the phytoplankton to the general economy of the sea. Mr. E. M. Hulburt, a visiting investigator, is studying the phytoplankton of Great Pond in a way complementary to Mr. Barlow's work on the zooplankton. It is important that we have someone available who knows the marine plants from the taxonomic as well as the ecological viewpoint. During the past year, we have given Fellowship aid to Mr. Robert W. Holmes, a student of Dr. Riley, to enable him to spend a year in Norway to obtain training in the taxonomy of the photyplankton.

A review of the year's work in marine biology would be incomplete without mention of a paper published by Dr. Gordon A. Riley on Oxygen, Phosphate, and Nitrate in the Atlantic Ocean. In this paper, Dr. Riley has gathered together the pertinent data on the circulation, the chemistry and the biology of the North Atlantic and by use of bold methods has attempted to draw a picture of the system as a whole as a mechanism productive of life. This paper is undoubtedly the most original and ambitious contribution to marine biology which has appeared since the end of the war.

Among the distinguished visitors who were welcomed at the Institution for from one to several days, or weeks, to consult on scientific matters in their particular fields, were the following. Several, on invitation, gave lectures of their work.

Dr. Paul Vigoureux, Admiralty Research Laboratory, Teddington, England.
Dr. Svend E. Saxov, Danish Geodetic Commission, Denmark.
Mr. D. Rochford, C.S.I.R.O. Fisheries, Cronulla, Australia.
Dr. Abdel-Fattah Mohamed, Farouk I University, Alexandria, Egypt.
Prof. J. Fjeldstad, Geografisk Institutt, Oslo, Norway.
Dr. G. E. R. Deacon, Admiralty Research Laboratory, Teddington, England.
Dr. Koji Hidaka, Tokyo University, Tokyo, Japan.
Prof. Hilding Koehler, University of Uppsala, Sweden.
Mr. M. S. Longuet-Higgins, Trinity College, Cambridge, England.
Dr. H. Munro Fox, London University, England.
Dr. P. Karapiperis, National Observatory, Athens, Greece.
Dr. Wendell Mordy, Pineapple Research Institute, Honolulu, T.H.
Dr. Edwin Oswald Cook, Naval Research Establishment, Halifax, N. S.
Dr. Ken Sugawara, University of Nagoya, Japan.
Dr. Ivan Hessland, University of Uppsala, Sweden.

The persons whose names are listed below were members of the Institution (exclusive of Staff Members) for a period of six months or more during the calendar year 1951.

RESEARCH ASSISTANTS, ENGINEERS AND TECHNICIANS

Barbour, L. Hilliard
Bergstrom, Stanley W.
Bunce, Elizabeth T.
Cain, Henry A.
Campbell, Robert
Chase, Joseph
Clarke, Arnold H.
Corwin, Nathaniel
Davis, Lee C.
Denman, Nathaniel A.
Duys, Gerrit, Jr.
Edwards, Melville E.
Foster, Donald B.
Hall, Henry B. S.
Hammond, Willis T.
Hodgson, Sloat F.
Hunt, Otis E.
Iselin, Columbus O'D., Jr.
Keen, D. Jean
Kemp, James M.
Kittredge, Caroline F.
Klebba, Arthur
Knott, Sydney T., Jr.
Larson, Edward H.
McCasland, Kenneth G.
McLeod, Jean
Owen, David M.
Parson, Donald, Jr.
Pasley, Gale G., Jr.
Poole, Stanley E.
Schleicher, Karl E.
Shelnut, Eva M.
Shultz, William S.
Stern, Melvin
Stilwell, Jean
Wagner, Lansing P.

JUNIOR TECHNICIANS AND LABORATORY ASSISTANTS

Anderson, Nellie E.
Ash, Adelma A.
Atwood, Barbara
Brown, Joan A.
Childs, Shirley A.
Cobb, Mary C.
Crandall, Harriet
Davis, Priscilla A.
Diaco, Elizabeth S.
English, Jean
Farnan, Marjorie A.
Gallagher, Gloria
Holmes, Doris M.
Klebba, Constance F.
Mason, Barbara H.
Moskovits, Lillian D.
Scharff, Eileen J.
Scharff, Margaret
Silva, Alberta B.
Tollios, Evangeline P.

ADMINISTRATIVE AND SECRETARIAL

Backus, Jeanne M.
Broadbent, Madeline P.
Bryant, Edwin T.
Conlan, Marcus J.
Craig, Margaret W.
Dingwell, Eva Z.
Donald, Mary
Ferris, Alice H.
Griffin, T. S. Perry
Hahn, Jan
Hatzikon, Kaleroy L.
Malloy, Thomas C.
Mellor, Florence K.
Oakley, Gilbert, Jr.
Ortolani, Mary
Ostiguy, Betty P.
Parker, Evelyn M.
Schnabel, Dorothy L.
Souza, Jane C.
Wilson, Esther N.
Young, Anita M.

TECHNICAL SERVICES

Bailey, Frank A.
Blake, Forrest W.
Bodman, Ralph H.
Bowman, Warren O.
Condon, J. William
Dingwell, Paul E.
Eldridge, Stanley N.
Fisher, Stanley O.
Gallagher, William F.
Gaskell, Fred
Gifford, James E.
Hodgkins, Harry L.
Howland, Myron P., Jr.
Lane, Marian O'D.
Morrison, Kenneth
Rennie, Thomas D.
Ronne, F. Claude
Spencer, Allard T.
Stimpson, John W.
Thayer, Lawrence A.
Vail, Phyllis F.
Walden, Robert G.
Weeks, Doris May
Weeks, Robert G.
Whitney, G. G., Jr.
Whittemore, Eugene H.
Wing, Carleton R.

MAINTENANCE AND HOUSING

Backus, Harold
Christian, John A.
Handy, Harry H.
Howes, Elijah S.
Nickelson, Ellen T.
Rose, Manuel W.
Salthouse, James
Soderland, Ida S.
Solberg, Otto
Sparks, Elizabeth C.
Stansfield, Richard
Turner, Catherine
Wilde, Phillips B.
Wing, Nathaniel R.
Woodward, Fred C., Jr.
Wright, Carleton B.

OFFICERS, CREW MEMBERS AND VESSELS

Addy, John A.
Backus, Cyril
Bahmer, Ernest F.
Bailey, James S.
Baldwin, James F.
Baron, Norman
Barstow, Elmer M.
Bearse, Francis A. T.
Bosworth, Russell E.
Cavanaugh, James J.
Clarkin, James J.
Colburn, Arthur D., Jr.
Collins, John S.
Conley, William J.
Cook, Hans
Fay, Donald H.
Foster, Howard C.
Frick, George P.
Grinnell, Russell, Jr.
Groht, Richard W.
Hazell, Raymond
Hempstead, Robert L.
Hermansen, Georg
Karlson, Arvid
Lafford, Gilbert R.
Lane, Adrian K.
LaVita, Anthony P., Jr.
Lincoln, Vernon R.
Lindsey, Arnold M.
Littlejohn, Robert E.
Macauley, Franklin A.
Merchant, Floyd L.
Mysona, Eugene J.
Orser, David A.
Parker, Clifton V.
Pearson, Rowland
Pierce, Samuel F.
Pike, John F.
Poole, Mathew A.
Richard, Mathiew
Roderick, Milton
Schroeder, John J.
Spalding, Oakes
Starrett, Donald A.
Stewart, Robert J.
VanZandt, Claiborne C., Jr.

VI. PUBLICATIONS

The following forty-one papers were published during 1951:

	Contr. No.
Arons, A. B., and Henry Stommel. A mixing-length theory of tidal flushing. *Trans. Amer. Geophys. Union*, 32 (3): 419–421, 1 text fig. 1951	544
Bigelow, H. B., and W. C. Schroeder. A new genus and species of anacanthobatid skate from the Gulf of Mexico. *J. Washington Acad. Sci.*, 41 (3): 110–113, 1 text fig. 1951	554
Bigelow, H. B., and W. C. Schroeder. Three new skates and a new chimaerid fish from the Gulf of Mexico. *J. Washington Acad. Sci.*, 41 (12): 383–392, 4 text figs. 1951	555
Castle, E. S. Electrical control of marine fouling. *Indust. Eng. Chem.*, 43 (4): 901–904, 2 text figs. 1951	539
Ericson, D. B., Maurice Ewing, and B. C. Heezen. Deep-sea sands and submarine canyons. *Bull. Geol. Soc. Amer.*, 62 (8): 961–965, 1 text fig. 1951	575
Fuglister, F. C. Annual variations in current speeds in the Gulf Stream system. *J. Mar. Res.*, 10 (1): 119–127, 6 text figs. 1951	557
Fuglister, F. C. Multiple currents in the Gulf Stream system. *Tellus*, 3 (4): 230–233, 2 text figs. 1951	584
Fuglister, F. C., and L. V. Worthington. Some results of a multiple ship survey of the Gulf Stream. *Tellus*, 3 (1): 1–14, 11 text figs. 1951	548
Ketchum, B. H. Plankton algae and their biological significance. In: Manual of Phycology, Chronica Botanica Co., Waltham, Ch. 17: 335–346. 1951	366
Ketchum, B. H. The exchanges of fresh and salt waters in tidal estuaries. *J. Mar. Res.*, 10 (1): 18–38, 5 text figs. 1951	516
Ketchum, B. H. The flushing of tidal estuaries. *Sewage and Industrial Wastes*, 23 (2): 198–209, 7 text figs. 1951	536
Ketchum, B. H., A. C. Redfield, and J. C. Ayers. The oceanography of the New York Bight. *Pap. Phys. Oceanogr. Meterol.*, 12 (1): 46 pp., 20 text figs. 1951	549
Klebba, A. A., and Henry Stommel. A simple demonstration of Coriolis force. *Amer. J. Physics*, 19 (4): 247, 1 text fig. 1951	545
Langwell, P. A. Forced convection cell circulation in clear air. *Trans. Amer. Geophys. Union*, 32 (1): 7–14, 1951	527
Langwell, P. A. The onset of rain from cumuli. *J. Meteorol.*, 8 (5): 354–356. 1951	568
Malkus, J. S., A. F. Bunker, and Kenneth McCasland. A formation of pileus-like veil clouds over Cape Cod, Massachusetts. *Bull. Amer. Meteorol. Soc.*, 32 (2): 61–66, 4 text figs. 1951	534
Menard, H. W., and A. J. Boucot. Experiments on the movement of shells by water. *Amer. J. Sci.*, 249: 131–151, 4 text figs. 1951	546
Moore, H. B. The seasonal distribution of oceanic birds in the western North Atlantic. *Bull. Mar. Sci., Gulf and Caribbean*, 1 (1): 1–14, 10 text figs. 1951	560
Northrop, John. Ocean-bottom photographs of the neritic and bathyal environment south of Cape Cod, Massachusetts. *Bull. Geol. Soc. Amer.*, 62 (12): 1381–1384, 3 pls.	573
Northrop, John, and B. C. Heezen. An outcrop of Eocene sediment on the continental slope. *J. Geol.*, 59 (4): 396–399, 1 text fig., 1 pl. 1951	523
Phleger, F. B., Ecology of Foraminifera, northwest Gulf of Mexico. Pt. 1. Foraminifera distribution. *Mem. Geol. Soc. Amer.*, No. 46: 88 pp., 33 text figs., 37 loose tables. 1951	565

	Contr. No.
PHLEGER, F. B., and F. L. PARKER. Ecology of Foraminifera, northwest Gulf of Mexico. Pt. 2. Foraminifera species. *Mem. Geol. Soc. Amer.*, No. 46: 64 pp., 20 pls. 1951	566
POLLAK, M. J. The sources of the deep water of the eastern Mediterranean Sea. *J. Mar. Res.*, 10 (1): 128–152, 14 text figs. 1951	556
REDFIELD, A. C., and L. A. WALFORD. A study of the disposal of chemical waste at sea. Report of the Committee for Investigation of Waste Disposal. *Nat. Res. Council*, Publ. 201: 49 pp., 29 text figs. 1951	536
RILEY, G. A. Oxygen, phosphate, and nitrate in the Atlantic Ocean. *Bull. Bingham Oceanogr. Coll.*, 13 (1): 1–126, 33 text figs. 1951	542
RILEY, G. A. Parameters of turbulence in the sea. *J. Mar. Res.*, 10 (3): 247–256, 2 text figs.	[illegible]
SAID, RUSHDI. Foraminifera of Narragansett Bay. *Contr. Cushman Found., Foram. Res.*, 2 (3): 75–86, 4 text figs. 1951	561
SAID, RUSHDI. Organic origin of some calcareous sediments from the Red Sea. *Science*, 113 (2940): 517–518. 1951	540
SAID, RUSHDI. Preliminary note on the spectroscopic distribution of elements in the shells of some recent calcareous Foraminifera. *Contr. Cushman Found., Foram. Res.*, 2 (1): 11–13. 1951	541
SEIWELL, H. R. Experimental correlogram correlation analyses of artificial time series (with special reference to analyses of oceanographic data). In: Proc. Second Berkeley Symposium on Mathematical Statistics and Probability, Univ. Calif. Press: 639–666, 27 text figs. 1951. (published posthumously)	531
SOULE, F. M. Physical oceanography of the Grand Banks region, the Labrador Sea and Davis Strait in 1949. *U.S.C.G. Bull.*, No. 35: 49–116, text figs. 12–33. 1951 . .	550
SOULE, F. M. Physical oceanography of the Grand Banks region and the Labrador Sea in 1950. *U.S.C.G. Bull.*, No. 36: 61–127, text figs. 16–29. 1951	551
STOMMEL, HENRY. An elementary explanation of why ocean currents are strongest in the west. *Bull. Amer. Meteorol. Soc.*, 32 (1): 21–23, 2 text figs. 1951	532
STOMMEL, HENRY. Entrainment of air into a cumulus cloud. II. *J. Meteorol*, 8 (2): 127–129, 5 text figs. 1951	533
STOMMEL, HENRY. Streaks on natural water surfaces. *Weather*, 6 (3): 72–74, pls. 9–10. 1951	538
STOMMEL, HENRY. Determination of the lateral eddy diffusivity in the climatological mean Gulf Stream. *Tellus*, 3 (1): 43. 1951	552
STOMMEL, HENRY, and A. H. WOODCOCK. Diurnal heating of the surface of the Gulf of Mexico in the spring of 1942. *Trans. Amer. Geophys. Union.*, 32 (4): 565–571, 5 text figs. 1951	553
TOLSTOY, IVAN. Submarine topography in the North Atlantic. *Bull. Geol. Soc. Amer.*, 62 (5): 441–450, 3 text figs., 6 pls. 1951	559
TURNER, H. J., JR., ET AL. Third report on investigations of methods of improving the shellfish resources of Massachusetts. Comm. Mass., Dept. Conserv., Div. Mar. Fish., 31 pp., 3 text figs. 1951	564
VON ARX, W. S. Dead reckoning by surface current observation. *J. Inst. Navigation*, London, 4 (2): 9 pp., 2 text figs.	526
WOODCOCK, A. H., and A. F. MCBRIDE. Wave-riding dolphins. *J. Exp. Biol.*, 28 (2): 215–217. 1951	522

APPENDIX

January – December 1951

ATLANTIS

Cruise No.	Departure and Return	Days Duration	Ports of Call	Scientist in Charge
167	4 Jan. 22 Jan.	18	Woods Hole to Bermuda, to Miami.	Mr. B. H. Heezen
168	23 Jan. 29 Jan.	6	Miami to Straits of Florida and return.	Dr. H. B. Moore
169	31 Jan. 10 Feb.	10	Miami to Mobile.	Mr. C. R. Hayes
170	16 Feb. 19 Mar.	31	Mobile to Miami.	Mr. M. J. Pollak
171	21 Mar. 24 Apr.	34	Miami to Nassau, Blake Plateau, Guantanamo.	Dr. J. B. Hersey
172	26 Apr. 6 June	41	Nassau to Guantanamo, San Juan, Bermuda, Woods Hole.	Dr. J. B. Hersey Dr. W. M. Ewing
173	7 Aug. 19 Sept.	44	Woods Hole to Bermuda to Argentia, Newfoundland and return.	Dr. J. L. Worzel
174	1 Oct. 4 Oct.	3	To sea.	Mr. R. F. Wyrick
175	14 Oct. 19 Oct.	5	Woods Hole to south of Block Island and return.	Mr. H. R. Johnson
176	24 Oct. 26 Oct.	2	To sea.	Mr. H. R. Johnson
177	Nov. Dec.	12	To sea — short trips.	Dr. J. B. Hersey

CARYN

Cruise No.	Departure and Return	Days Duration	Ports of Call	Scientist in Charge
C–20	3 Feb. 21 Mar.	46	Woods Hole to Bermuda, to Nassau.	Mr. B. H. Heezen
C–21	23 Mar. 26 Apr.	34	Miami to Guantanamo.	Mr. S. W. Bergstrom
C–22	26 Apr. 6 June	41	Nassau to Guantanamo, San Juan, Bermuda, Woods Hole.	Mr. S. W. Bergstrom Dr. W. M. Ewing
C–23	25 June 29 June	4	To sea.	Dr. J. B. Hersey
C–24	5 July 19 July	14	Woods Hole to Cape Sable to Georges Bank and return.	Dr. J. L. Worzel
C–25	7 Aug. 20 Sept.	44	Woods Hole to Bermuda, Argentia, Grand Banks and return.	Dr. J. L. Worzel
C–26	23 Oct. 27 Oct.	4	Woods Hole to Georges Bank and Southward to 1000 fathom curve and return.	Dr. B. H. Ketchum
C–27	13 Nov. 14 Nov.	2	To sea.	Dr. W. V. R. Malkus
C–28	Dec.	10	To sea—short trips.	Mr. A. C. Vine

ALBATROSS III

Cruise No.	Departure and Return	Days Duration	Ports of Call	Scientist in Charge
A–40	8 May 22 May	14	Woods Hole to Cape Hatteras and return.	Mr. A. R. Miller
A–41	6 June 31 Oct.	147	Woods Hole to St. Johns to Londonderry, No. Ireland, to Plymouth, England, to Azores to Bermuda, to Woods Hole.	Mr. F. C. Fuglister Mr. L. V. Worthington

List of Contributions

LIST OF CONTRIBUTIONS

FROM THE WOODS HOLE OCEANOGRAPHIC INSTITUTION

See Author Index in *Collected Reprints* 1950 for a complete list up to that year.

No. 301. F. G. Walton Smith. Effect of Water Currents Upon the Attachment Growth of Barnacles. *Biol. Bull.*, Vol. 90, No. 1, pp. 51–70. 1946.

No. 302. G. A. Edwards and Laurence Irving. The Influence of Temperature and Season upon the Oxygen Consumption of the Sand Crab, *Emerita talpoida* Say. *Jour. Cell. and Comp. Physiol.*, Vol. 21, No. 2, pp. 169–182. 1943.

No. 303. R. B. Montgomery. Transport of the Florida Current off Havana. *Sears Found., Jour. Mar. Res.*, Vol. 4, No. 3, pp. 198–220. 1941.

No. 304. Richard E. Lee. The Occurrence of Female Swordfish in southern New England Waters, with a Description of their Reproduction Condition. *Copeia*, No. 2, pp. 117–119. 1942.

No. 305. R. B. Montgomery and M. J. Pollak. Sigma-T Surfaces in the Atlantic Ocean. *Sears Found., Jour. Mar. Res.*, Vol. 5, No. 1, pp. 20–27. 1942.

No. 306. George L. Clarke. Observations on Transparency in the southwestern section of the North Atlantic Ocean. *Sears Found., Jour. Mar. Res.*, Vol. 4, No. 3, pp. 221–230. 1941.

No. 307. Robert W. Pennak. Harpacticoid Copepods from some Intertidal Beaches near Woods Hole, Massachusetts. *Trans. Amer. Micro. Soc.*, Vol. 61, No. 3, pp. 274–285. 1942.

No. 308. Alfred C. Redfield. The Processes Determining the Concentration of Oxygen, Phosphate and other Organic Derivatives within the Depths of the Atlantic Ocean. *Papers in Physical Oceanography and Meteorology*, Vol. 9, No. 2, pp. 1–22. 1942.

No. 309. William C. Schroeder. Results of Haddock Tagging in the Gulf of Maine from 1923 to 1932. *Sears Found., Jour. Mar. Res.*, Vol. 5, No. 1, pp. 1–19. 1942.

No. 310. W. H. Johnson. Effect of Light on Copepods as Food for Passamaquoddy Herring. *Jour. Fish. Res. Bd. Canada*, 5(4), pp. 365–376. 1942.

No. 311. Charles E. Renn. Demonstration of Labyrinthula Parasite in Eel-Grass from the Coast of California. *Science*, Vol. 95, No. 2457, pp. 122. 1942.

No. 312. C. O'D. Iselin. Interaction between the Hydrosphere and the Atmosphere. *Trans. N. Y. Acad. Sci.*, Series II. Vol. 4, No. 3, pp. 99-106. 1942.

No. 313. G. A. Edwards and Laurence Irving. The Influence of Season and Temperature upon the Oxygen Consumption of the Beach Flea, *Talorchestia megalopthalma*. *Jour. Cell. and Comp. Physiol.*, Vol. 21, No. 2, pp. 183–189. 1943.

No. 314. Earl H. Myers. Rate at which Foraminifera are Contributed to Marine Sediments. *Jour. Sed. Petrology*, Vol. 12, No. 2, pp. 92–95. 1942.

No. 315. Gordon A. Riley. The Relationship of Vertical Turbulence and Spring Diatom Flowerings. *Sears Found., Jour. Mar. Res.*, Vol. 5, No. 1, pp. 67–87. 1942.

No. 316. Earl H. Myers. Biological Evidence as to the Rate at which Tests of Foraminifera are Contributed to Marine Sediments. *Jour. of Paleontology*, Vol. 16, No. 3, pp. 397–398. 1942.

No. 317. Richard E. Lee. The Hypophysis of the Broad-billed Swordfish, *Xiphias gladius* L. *Biol. Bull.*, Vol. 82, No. 3, pp. 401–412. 1942.

No. 318. Athelstan F. Spilhaus. Maps of the Whole World Ocean. *Geog. Rev.*, Vol. 32, No. 3, pp. 431–435. 1942.

No. 319. Gordon A. Riley. Physiological Aspects of Spring Diatom Flowerings. *Bull. Bingham Oceanographic Coll.*, Vol. 8, Art 4, pp. 1–53. 1943.

No. 320. Olga Hartman. Report on the Scientific Results of the *Atlantis* Expeditions to the West Indies under the joint auspices of the University of Havana and Harvard University. The Polychaetous Annelida. *Mem. Soc. Cub. Hist. Nat.*, Vol. 16, No. 2, pp. 89–104. 1942.

No. 321. Theodor von Brand, Norris W. Rakestraw and J. William Zabor. Decomposition and Regeneration of Nitrogenous Organic Matter in Sea Water. V. Factors Influencing the Length of the Cycle; Observations upon the Gaseous and Dissolved Organic Nitrogen. *Biol. Bull.*, Vol. 83, No. 2, pp. 273–282. 1942.

No. 322. Fenner A. Chace, Jr. Reports on the Scientific Results of the *Atlantis* Expeditions to the West Indies, under the joint auspices of the University of Havana and Harvard University. The Anomuran Crustacea. I. Galatheida (Families Chirostylidae, Galatheidae and Porcellanidae). *Torreia*, No. 11, pp. 1–106. 1942.

No. 323. William Schallek. The Reaction of Certain Crustacea to Direct and to Diffuse Light. *Biol. Bull.*, Vol. 84, No. 1, pp. 98–105. 1943.

No. 324. Richard E. Lee. Notes on the Color Changes of the Sea Robin (*Prionotus strigatus* Cuvier) with special reference to the Erythrophores. *Jour. Exper. Zool.*, Vol. 91, No. 2, pp. 131–153. 1942.

No. 325. Selman A. Waksman, Donald B. Johnstone and Cornelia L. Carey. The Effect of Copper upon the Development of Bacteria in Sea Water and the Isolation of Specific Bacteria. *Sears Found., Jour. Mar. Res.*, Vol. 5, No. 2, pp. 136–152. 1943.

No. 326. Robert W. Pyle. The Histogenesis and Cyclic Phenomena of the Sinus Gland and X-Organ in Crustacea. *Biol. Bull.*, Vol. 85, No. 2, pp. 87–102. 1943.

No. 327. Earl H. Myers. Life Activities of Foraminifera in Relation to Marine Ecology. *Proc. Amer. Philos. Soc.*, Vol. 86, No. 3, pp. 439–458. 1943.

No. 328. George L. Clarke, E. Lowe Pierce and Dean F. Bumpus. The Distribution and Reproduction of *Sagitta elegans* on Georges Bank in Relation to the Hydrographical Conditions. *Biol. Bull.*, Vol. 85, No. 3, pp. 201–226. 1943.

No. 329. A. A. Abramowitz, F. L. Hisaw and D. N. Papandrea. The Occurrence of a Diabetogenic Factor in the Eyestalks of Crustaceans. *Biol. Bull.*, Vol. 86, No. 1, pp. 1–5, 1944.

No. 330. Richard E. Lee. A Quantitative Survey of the Invertebrate Bottom Fauna in Menemsha Bight. *Biol. Bull.*, Vol. 86, No. 2, pp. 83–97. 1944.

No. 331. Alfred H. Woodcock. A Theory of Surface Water Motion deduced from the Wind-Induced Motion of the Physalia. *Sears Found.*, *Jour. Mar. Res.*, Vol. 5, No. 3, pp. 196–205. 1944.

No. 332. Louis W. Hutchins. An Annotated Check-List of the Salt-Water Bryozoa of Long Island Sound. *Trans. Conn. Acad. Arts Sci.*, Vol. 36, pp. 533–551. 1945.

No. 333. Henry B. Bigelow and William C. Schroeder. New Sharks from the Western North Atlantic. *Proc. New Engl. Zool. Club*, Vol. 23, pp. 21–36. 1944.

No. 334. W. J. Clench and C. G. Aguayo. A New Tropical Buccinum From Cuba. *Rev. Soc. Malacol.*, Vol. 2, No. 2, pp. 67–68. 1944.

No. 335. Bostwick H. Ketchum, John D. Ferry, Alfred C. Redfield and Arthur E. Burns, Jr. Evaluation of Anti-fouling Paints by Leaching Rate Determinations. *Ind. Eng. Chem.*, Vol. 37, pp. 456–460. 1945.

No. 336. George T. Scott. The Influence of H-ion Concentration on the Mineral Composition of *Chlorella pyrenoidosa*. *Jour. Cell. and Comp. Physiol.*, Vol. 25, No. 1, pp. 37–44. 1945.

No. 337. George T. Scott. The Mineral Composition of Phosphate Deficient Cells of *Chlorella pyrenoidosa* during the Restoration of Phosphate. *Jour. Cell. and Comp. Physiol.*, Vol. 26, No. 1, pp. 35–42. 1945.

No. 338. Fred B Phleger, Jr. Vertical Distribution of Pelagic Foraminifera. *Amer. Jour. Sci.*, Vol. 243, pp. 377–383. 1945.

No. 339. Warren H. Yudkin. Occurrence of Thiaminase in Marine Teleosts. *Proc. Soc. Exper. Biol. and Med.*, Vol. 60, pp. 268–269. 1945.

No. 340. Irwin M. Newell. Studies on the Morphology and Systematics of the Family Halarachnidae Oudemans 1906 (Acari, Parasitoidae). *Bull. Bingham Oceanographic Coll.*, Vol. 10, Art. 4, pp. 235–266. 1947.

No. 341. Nelson Marshall. Observations on the Comparative Ecology and Life History of two Sea Robins, *Prionotus carolinus* and *Prionotus evolans strigatus*. *Copeia*, No. 3, pp. 118–144. 1946.

No. 342. John D. Ferry and Dayton E. Carritt. Action of Antifouling Paints. I. Solubility and Rate of Solution of Cuprous Oxide in Sea Water. *Ind. Eng. Chem.*, Vol. 38, pp. 612–617. 1946.

No. 343. M. Juul Hvorslev and Henry C. Stetson. Free-Fall Coring Tube: A New Type of Gravity Bottom Sampler. *Bull. Geol. Soc. Amer.*, Vol. 57, pp. 935–950. 1946.

No. 344. Fred B Phleger, Jr. and Walter A. Hamilton. Foraminifera of two Submarine Cores from the North Atlantic Basin. *Bull. Geol. Soc. Amer.*, Vol. 57, pp. 951–966. 1946.

No. 345. John D. Ferry and Gordon A. Riley. Action of Antifouling Paints. II. Solubilities of Antifouling Toxics in Sea Water. *Ind. Eng. Chem.*, Vol. 38, pp. 699–701. 1946.

No. 346. John D. Ferry and Bostwick H. Ketchum. Action of Antifouling Paints. III. Maintenance of the Leaching Rate of Antifouling Paints Formulated with Insoluble, Impermeable Matrices. *Ind. Eng. Chem.*, Vol. 38, pp. 806–810. 1946.

No. 347. Bostwick H. Ketchum, John D. Ferry and Arthur E. Burns, Jr. Action of Antifouling Paints. IV. Maintenance of Leaching Rate of Antifouling Paints Formulated with Soluble Matrices. *Ind. Eng. Chem.*, Vol. 38, pp. 931–936. 1946.

No. 348. Maurice Ewing, Allyn Vine, and J. L. Worzel. Photography of the Ocean Bottom. *Jour. Optical Soc. Amer.*, Vol. 36, No. 6, pp. 307–321. 1946.

No. 349. C. M. Pomerat and C. M. Weiss. The Influence of Texture and Composition of Surface on the Attachment of Sedentary Marine Organisms. *Biol. Bull.*, Vol. 91, No. 1, pp. 57–65. 1946.

No. 350. Marshall Schalk. A Study of Textural Changes in a Beach by repeated Samplings. *Jour. Sed. Petrology*, Vol. 16, No. 2, pp. 43–51. 1946.

No. 351. Maurice Ewing, G. P. Woollard, A. C. Vine, and J. L. Worzel. Recent Results in Submarine Geophysics. *Bull. Geol. Soc. Amer.*, Vol. 57, pp. 909–934. 1946.

No. 352. Gordon A. Riley and Dean F. Bumpus. Phytoplankton-Zooplankton Relationships on Georges Bank. *Sears Found., Jour. Mar. Res.*, Vol. 6, No. 1, pp. 33–47. 1946.

No. 353. Gordon A. Riley. Factors Controlling Phytoplankton Populations on Georges Bank. *Sears Found., Jour. Mar. Res.*, Vol. 6, No. 1, pp. 54–73. 1946.

No. 354. H. R. Seiwell. Military Oceanography in Tactical Operations of World War II. *Trans. Amer. Geophys. Union*, Vol. 27, No. 5, pp. 677–681. 1946.

No. 355. Henry Stommel. A Summary of the Theory of Convection Cells. *Annals N. Y. Acad. Sci.*, Vol. 48, Art. 8, pp. 715–726. 1947.

No. 356. A. H. Woodcock and Jeffries Wyman. Convective Motion in Air over the Sea. *Annals N. Y. Acad. Sci.*, Vol. 48, Art. 8, pp. 749–776. 1947.

No. 357. R. B. Montgomery. Introduction: Problems Concerning Convective Layers. *Annals N. Y. Acad. Sci.*, Vol. 48, Art. 8, pp. 707–713. 1947.

No. 358. Richard A. Craig. Observations of Vertical Temperature and Humidity Distributions in the Convective Layer above the Sea Surface. *Annals N. Y. Acad. Sci.*, Vol. 48, Art. 8, pp. 783–788. 1947.

No. 359. H. A. Panofsky. Radiative Cooling in the Lowest Layers of an Atmosphere Warmer than the Ground. *Jour. Meteorology*, Vol. 4, No. 1, pp. 35–37. 1947.

No. 360. George L. Clarke. Poisoning and Recovery in Barnacles and Mussels. *Biol. Bull.*, Vol. 92, No. 1, pp. 73–91. 1947.

No. 361. R. B. Montgomery. Over-water Refraction of 10-cm. Electromagnetic Radiation. *Bull. Amer. Meteorol. Soc.*, Vol. 28, No. 1, pp. 1–8. 1947.

No. 362. Richard A. Craig. Measurements of Temperature and Humidity in the lowest 1000 feet of the Atmosphere over Massachusetts Bay. *Papers in Physical Oceanography and Meteorology*, Vol. 10, No. 1, pp. 1–47. 1946.

No. 363. George L. Clarke. Dynamics of Production in a Marine Area. *Ecological Monographs*, Vol. 16, No. 4, pp. 322–335. 1946.

No. 364. Fred B. Phleger, Jr. Foraminifera of three Submarine Cores from the Tyrrhenian Sea. *Kungl. Vet.-o. Vitterh. Samh. Handl.*, F. 6, Ser. B, Bd 5, No. 5, pp. 1–19. 1947.

No. 365. Henry Stommel. Entrainment of Air into a Cumulus Cloud. *Jour. Meteorology*, Vol. 4, No. 3, pp. 91–94. 1947.

No. 366. Bostwick H. Ketchum. Plankton Algae and their Biological Significance. In: Manual of Phycology — an Introduction to the Algae and their Biology, Ch. 17, pp. 335–346. Gilbert M. Smith, Editor. Published by The Chronica Botanica Co., Waltham, Mass. 1951.

No. 367. Henry Stommel. Note on the Use of the T-S Correlation for Dynamic Height Anomaly Computations. *Sears Found., Jour. Mar. Res.*, Vol. 6, No. 2, pp. 85–92. 1947.

No. 368. Gordon A. Riley. A Theoretical Analysis of the Zooplankton Population of Georges Bank. *Sears Found., Jour. Mar. Res.*, Vol. 6, No. 2, pp. 104–113. 1947.

No. 369. Gordon A. Riley. Seasonal Fluctuations of the Phytoplankton Population in New England Coastal Waters. *Sears Found., Jour. Mar. Res.*, Vol. 6, No. 2, pp. 114–125. 1947.

No. 370. William S. von Arx. A Salinometer for use in Brackish Water. *Sears Found., Jour. Mar. Res.*, Vol. 6, No. 2, pp. 139–145. 1947.

No. 371. Norris W. Rakestraw and Theodor von Brand. Decomposition and Regeneration of Nitrogenous Organic Matter in Sea Water. VI. The Effect of Enzyme Poisons. *Biol. Bull.*, Vol. 92, No. 2, pp. 110–114. 1947.

No. 372. Alfred H. Woodcock and Gordon A. Riley. Patterns in Pond Ice. *Jour. Meteorology*, Vol. 4, No. 3, pp. 100–101. 1947.

No. 373. Alfred H. Woodcock and Henry Stommel. Temperatures Observed near the Surface of a Fresh-Water Pond at Night. *Jour. Meteorology*, Vol. 4, No. 3, pp. 102–103. 1947.

No. 374. Louis W. Hutchins. The Bases for Temperature Zonation in Geographical Distribution. *Ecological Monographs*, Vol. 17, No. 3, pp. 325–335. 1947.

No. 375. Norris W. Rakestraw. Oxygen Consumption in Sea Water over long Periods. *Sears Found., Jour. Mar. Res.*, Vol. 6, No. 3, pp. 259–263. 1947.

No. 376. Frances L. Parker. Foraminifera of the Continental Shelf from the Gulf of Maine to Maryland. *Bull. Mus. Comp. Zool.*, Vol. 100, No. 2, pp. 213–241. 1948.

No. 377. Bostwick H. Ketchum. The Biochemical Relations between Marine Organisms and their Environment. *Ecological Monographs*, Vol. 17, No. 3, pp. 309–315. 1947.

No. 378. F. G. Walton Smith. Mechanical Control of Ship-Bottom Fouling by means of Air Bubbles. *Jour. Fla. Acad. Sci.*, Vol. 9, Nos. 3–4, pp. 153-161. 1947.

No. 379. H. R. Seiwell. Oceangraphic Factors in Underwater Depth Determination by Aerial Photography. *Photogrammetric Eng.*, Vol. 15, No. 1, pp. 171–176. 1949.

No. 380. H. J. Turner, Jr., D. M. Reynolds and A. C. Redfield. Chlorine and Sodium Pentachlorophenate as Fouling Preventives in Sea Water Conduits. *Ind. Eng. Chem.*, Vol. 40, pp. 450–453. 1948.

No. 381. H. R. Seiwell. Resume of Military Oceanography in World War II. *The Military Engineer*, Vol. 39, No. 259, pp. 202–210. 1947. (Not included in *Collected Reprints.*)

No. 382. H. R. Seiwell. Tidal Illumination Diagrams. *Science*, Vol. 106, No. 2743, pp. 76–77. 1947.

No. 383. R. B. Montgomery and P. A. Sheppard. Comments on P. A. Sheppard's Direct Measurement of Ground Stress. *Quart. Jour. Roy. Meteor. Soc.*, Vol. 73, Nos. 317–318, pp. 459–463. 1947.

No. 384. Edward S. Deevey, Jr. Life Tables for Natural Populations of Animals. *Quart. Rev. Biol.*, Vol. 22, No. 4, pp. 283–314. 1947.

No. 385. Charles M. Weiss. The Comparative Tolerances of some Fouling Organisms to Copper and Mercury. *Biol. Bull.*, Vol. 93, No. 1, pp. 56–63. 1947.

No. 386. H. R. Seiwell. Investigation of Underwater Pressure Records and Simultaneous Sea Surface Patterns. *Trans. Amer. Geophys. Union*, Vol. 28, No. 5, pp. 722–724. 1947.

No. 387. Frederick C. Fuglister. Average Monthly Sea Surface Temperatures of the Western North Atlantic Ocean. *Papers in Physical Oceanography and Meteorology*, Vol. 10, No. 2, pp. 1–25. 1947.

No. 388. R. B. Montgomery. Viscosity and Thermal Conductivity of Air and Diffusivity of Water Vapor in Air. *Jour. Meteorology*, Vol. 4, No. 6, pp. 193–196. 1947.

No. 389. Alfred H. Woodcock. Note Concerning Human Respiratory Irritation Associated with High Concentrations of Plankton and Mass Mortality of Marine Organisms. *Sears Found., Jour. Mar. Res.*, Vol. 7, No. 1, pp. 56–62. 1948.

No. 390. Charles M. Weiss. An Observation on the Inhibition of Marine Wood Destroyers by Heavy Fouling Accumulation. *Ecology*, Vol. 29, No. 1, p. 120. 1948.

No. 391. Georgiana B. Deevey. The Zooplankton of Tisbury Great Pond. *Bull. Bingham Oceanographic Coll.*, Vol. 12, Art. 1, pp. 1–44. 1948.

No. 392. Charles M. Weiss. Observations on the Abnormal Development and Growth of Barnacles as Related to Surface Toxicity. *Ecology*, Vol. 29, No. 1, pp. 116–119. 1948.

No. 393. J. C. Decius. Dimensional Analysis: An Approach from Transformation Theory and a Criterion for Scaling Model Experiments. *Jour. Franklin Inst.*, Vol. 245, No. 5, pp. 379–387. 1948.

No. 394. Alfred C. Redfield. Characteristics of Sea Water. In: The Corrosion Handbook, pp. 1111–1122. H. H. Uhlig, Editor. Published by John Wiley & Sons, New York. 1948.

No. 395. George C. Whiteley, Jr. The Distribution of Larger Plankton Crustacea on Georges Bank. *Ecological Monographs*, Vol. 18, No. 2, pp. 233–264. 1948.

No. 396. William C. Schroeder. Notes on the Diet of the Goosefish, *Lophius americanus*. *Copeia*, No. 3, p. 201. 1947.

No. 397 Louis W. Hutchins and Margaret Scharff. Maximum and Minimum Monthly Mean Sea Surface Temperatures chartered from the "World Atlas of Sea Surface Temperatures". *Sears Found., Jour. Mar. Res.*, Vol. 6, No. 3, pp. 264–268. 1947.

No. 398. Bostwick H. Ketchum. Action of Antifouling Paints. V. Use of Glycine Solutions as Accelerated Test of Availability of Toxic. *Ind. Eng. Chem.*, Vol. 40, pp. 249–253. 1948.

No. 399. Bostwick H. Ketchum and John C. Ayers. Action of Antifouling Paints. VI. Effect of Nontoxic Pigments on the Performance of Antifouling Paints. *Ind. Eng. Chem.*, Vol. 40, pp. 2124–2127. 1948.

No. 400. Charles M. Weiss. The Effect of Illumination and Stage of Tide on the Attachment of Barnacle Cyprids. *Biol. Bull.*, Vol. 93, No. 3, pp. 240–249. 1947.

No. 401. W. S. Butcher. A New Species of *Nonion* (Foraminifera) from the Woods Hole Region. *Contr. Cushman Lab. Foram. Res.*, Vol. 24, (1), No. 308, pp. 21–23. 1948.

No. 402. Edward S. Deevey, Jr. On the Date of the Last Rise of Sea Level in Southern New England, with Remarks on the Grassy Island Site. *Amer. Jour. Sci.*, Vol. 246, pp. 329–352. 1948.

No. 403. Charles M. Weiss. The Abnormal Development of Tunicates Attached to Glass Surfaces Adjacent to Antifouling Paints. *Ecology*, Vol. 29, No. 2, pp. 215–218. 1948.

No. 404. Charles M. Weiss. The Seasonal Occurrence of Sedentary Marine Organisms in Biscayne Bay, Florida. *Ecology*, Vol. 29, No. 2, pp. 153–172. 1948.

No. 405. R. B. Montgomery. Vertical Eddy Flux of Heat in the Atmosphere. *Jour. Meteorology*, Vol. 5, No. 6, pp. 265–274. 1948.

No. 406. Hilary B. Moore. The Zooplankton of the Upper Waters of the Bermuda Area of the North Atlantic. *Sears Found., Jour. Mar. Res.*, Vol. 12, Art. 2, pp. 1–97. 1949. (Not included in *Collected Reprints*.)

No. 407. H. R. Seiwell. Evaluation of Sea-Surface Roughness from Underwater-Pressure Recordings. *Trans. Amer. Geophys. Union*, Vol. 29, No. 2, pp. 197–201. 1948.

No. 408. Henry Stommel. The Westward Intensification of Wind-Driven Ocean Currents. *Trans. Amer. Geophys. Union*, Vol. 29, No. 2, pp. 202–206. 1948.

No. 409. Sidney C. Hsiào. The Simple Micromethod for Rapid Extraction of Lipids. *Science*, Vol. 107, No. 2766, pp. 24–25. 1948.

No. 410. Austin H. Clark. Some Interesting Starfishes and Brittle-Stars Dredged by the *Atlantis* in the Mid-Atlantic. *Jour. Wash. Acad. Sci.*, Vol. 38, No. 2, pp. 75–78. 1948.

No. 411. Alfred C. Redfield and Charles M. Weiss. The Resistance of Metallic Silver to Marine Fouling. *Biol. Bull.*, Vol. 94, No. 1, pp. 25–28. 1948.

No. 412. J. B. Hersey and H. B. Moore. Progress Report on Scattering Layer Observations in the Atlantic Ocean. *Trans. Amer. Geophys. Union*, Vol. 29, No. 3, pp. 341–354. 1948.

No. 413. Gardner Emmons. Vertical Distributions of Temperature and Humidity over the Ocean between Nantucket and New Jersey. *Papers in Physical Oceanography and Meteorology*, Vol. 10, No. 3, pp. 1–89. 1947.

No. 414. W. T. Edmondson and Yvette H. Edmondson. Measurements of Production in Fertilized Salt-Water. *Sears Found., Jour. Mar. Res.*, Vol. 6, No. 3, pp. 228–245. 1947.

No. 415. J. Lamar Worzel and Maurice Ewing. Propagation of Sound in the Ocean: Explosion Sounds in Shallow Water. *Mem. Geol. Soc. Amer.* 27, pp. i–vi, 1–53. 1948.

C. L. Pekeris. Propagation of Sound in the Ocean: Theory of Propagation of Explosive Sound in Shallow Water. *Mem. Geol. Soc. Amer.* 27, pp. i–viii, 1–117. 1948.

Maurice Ewing and J. Lamar Worzel. Propagation of Sound in the Ocean: Long-Range Sound Transmission. *Mem. Geol. Soc. Amer.* 27, pp. i–v, 1–35. 1948. (Not included in *Collected Reprints*.)

No. 416. Sidney Cornell. The Collapse of Long Cylindrical Shells under External Pressure. *Soc. Exper. Stress Analysis*, Vol. 6, No. 1, pp. 111–114. 1948.

No. 417. Alfred H. Woodcock. The Swimming of Dolphins. *Nature*, Vol. 161, p. 602. 1948.

No. 418. J. M. Richardson, A. B. Arons and R. R. Halverson. Hydrodynamic Properties of Sea Water at the Front of a Shock Wave. *Jour. Chem. Physics*, Vol. 15, No. 11, pp. 785–794. 1947.

No. 419. Bostwick H. Ketchum and Jean Keen. Unusual Phosphorus Concentrations in the Florida "Red Tide" Sea Water. *Sears Found., Jour. Mar. Res.*, Vol. 7, No. 1, pp. 17–21. 1948.

No. 420. C. A. Barnes, D. F. Bumpus and John Lyman. Ocean Circulation in Marshall Islands Area. *Trans. Amer. Geophys. Union*, Vol. 29, No. 6, pp. 871–876. 1948.

No. 421. William S. von Arx. The Circulation Systems of Bikini and Rongelap Lagoons. *Trans. Amer. Geophys. Union*, Vol. 29, No. 6, pp. 861–870. 1948.

No. 422. William L. Ford. Radiological and Salinity Relationships in the Water at Bikini Atoll. *Trans. Amer. Geophys. Union*, Vol. 30, No. 1, pp. 46–54. 1949.

No. 423. R. B. Montgomery. Ivory's Psychrometric Formula and the Concepts of Equivalent Temperature and Wet-Bulb Temperature. *Jour. Meteorology*, Vol. 5, No. 3, pp. 113–115. 1948.

No. 424. Parker D. Trask, Fred B Phleger, Jr., and Henry C. Stetson. Recent Changes in Sedimentation in the Gulf of Mexico. *Science*, Vol. 106, No. 2759, pp. 460–461. 1947.

No. 425. George L. Clarke and David W. Bishop. The Nutritional Value of Marine Zooplankton with a Consideration of its Use as an Emergency Food. *Ecology*, Vol. 29, No. 1, pp. 54–71. 1948.

No. 426. J. Lamar Worzel. Ocean Bottom Sampler for Ships Under Way. *Geophysics*, Vol. 13, No. 3, pp. 452–456. 1948.

No. 427. Clinton M. Osborn. Factors Influencing the Growth of Integumentary Pigment in Fishes. I. The Role of Light. *Proc. Soc. Exper. Biol. and Med.*, Vol. 67, pp. 440–445. 1948.

No. 428. A. W. Jacobson. An Instrument for Recording Continuously the Salinity, Temperature, and Depth of Sea Water. *Trans. Amer. Inst. Elec. Eng.*, Vol. 67, pp. 1–9. 1948.

No. 429. Fred B Phleger, Jr. Foraminifera of a Submarine Core from the Caribbean Sea. *Kungl. Vet.-o. Vittern. Samh. Handl.*, F. 6, Ser. B, Bd. 5, No. 14, pp. 1–9. 1948.

No. 430. A. B. Arons, J. P. Slifko and A. Carter. Secondary Pressure Pulses due to gas Globe Oscillation in Underwater Explosions. I. Experimental Data. *Jour. Acoust. Soc. Amer.*, Vol. 20, No. 3, pp. 271–276. 1948.

No. 431. A. B. Arons. Secondary Pressure Pulses due to Gas Globe Oscillation in Underwater Explosions. II. Selection of Adiabatic Parameters in the Theory of Oscillation. *Jour. Acoust. Soc. Amer.*, Vol. 20, No. 3, pp. 277–282. 1948.

No. 432. Talbot H. Waterman. Studies on Deep-Sea Angler-Fishes (Ceratioidea). III. The Comparative Anatomy of *Gigantactis longicirra* Waterman. *Jour. Morphology*, Vol. 82, No. 2, pp. 81–149. 1948.

No. 433. L. N. Liebermann. Reflection of Sound from Coastal Sea Bottoms. *Jour. Acoust. Soc. Amer.*, Vol. 20, No. 3, pp. 305–309. 1948.

No. 434. Charles M. Weiss. Seasonal and Annual Variations in the Attachment and Survival of Barnacle Cyprids. *Biol. Bull.*, Vol. 94, No. 3, pp. 236–243. 1948.

No. 435. H. R. Seiwell. Sea Surface Roughness Measurements in Theory and Practice. *Annals* N. Y. *Acad. Sci.*, Vol. 51, Art. 3, pp. 483–501. 1949.

No. 436. H. R. Seiwell. Results of Research on Surface Waves of the Western North Atlantic. I. Investigation of Bottom Pressure Fluctuations and Surface Waves. II. Results of Sea Roughness Determinations in the Vicinity of Woods Hole, Massachusetts and Bermuda. *Papers in Physical Oceanography and Meteorology*, Vol. 10, No. 4, pp. 1–56. 1948.

No. 437. A. B. Arons and R. H. Cole. Design and Use of Piezoelectric Gauges for Measurement of Large Transient Pressures. *Review of Sci. Instruments*, Vol. 21, No. 1, pp. 31–38. 1950.

No. 438. Arthur A. Klebba. Details of Shore-Based Wave Recorder and Ocean Wave Analyzer. *Annals* N. Y. *Acad. Sci.*, Vol. 51, Art. 3, pp. 533–544. 1949.

No. 439. Athelstan F. Spilhaus. Drop Size, Intensity and Radar Echo of Rain. *Jour. Meteorology*, Vol. 5, No. 4, pp. 161–164. 1948.

No. 440. Athelstan F. Spilhaus and Arthur R. Miller. The Sea Sampler. *Sears Found., Jour. Mar. Res.*, Vol. 7, No. 3, pp. 370–385. 1948.

No. 441. Gordon A. Riley and Samy Gorgy. Quantitative Studies of Summer Plankton Populations of the Western North Atlantic. *Sears Found., Jour. Mar. Res.*, Vol. 7, No. 2, pp. 100–121. 1948.

No. 442. Alfred C. Redfield. The Exchange of Oxygen across the Sea Surface. *Sears Found., Jour. Mar. Res.*, Vol. 7, No. 3, pp. 347–361. 1948.

No. 443. Patricia A. Langwell. Inhomogeneities of Turbulence, Temperature, and Moisture in the West Indies Trade-wind Region. *Jour. Meteorology*, Vol. 5, No. 5, pp. 243–246. 1948.

No. 444. Fred B. Phleger, Jr. Origin and Deposition of Deep Sea Sediments. *Trans. Amer. Geophys. Union*, Vol. 30, No. 2, pp. 180–182. 1949.

No. 445. B. Haurwitz. The Effect of Ocean Currents on Internal Waves. *Sears Found., Jour. Mar. Res.* Vol. 7, No. 3, pp. 217–228. 1948.

No. 446. Bostwick H. Ketchum, Cornelia L. Carey and Margaret Briggs. Preliminary Studies on the Viability and Dispersal of Coliform Bacteria in the Sea. *In* Limnological Aspects of Water Supply and Waste Disposal. Ed. F. R. Moulton and and Florence Hitzel. *Publ. Amer. Assoc. Adv. Sci.*, pp. 64–73. 1949.

No. 447. Henry B. Bigelow and William C. Schroeder. New Genera and Species of Batoid Fishes. *Sears Found., Jour. Mar. Res.*, Vol. 7, No. 3, pp. 543–566. 1948.

No. 448. Hilary B. Moore. A Camera for Producing One-Dimensional Reduction in Narrow Records. *Sears Found., Jour. Mar. Res.*, Vol. 8, No. 1, pp. 21–23. 1949.

No. 449. A. B. Arons and D. R. Yennie. Energy Partition in Underwater Explosion Phenomena. *Rev. Modern Physics*, Vol. 20, No. 3, pp. 519–536. 1948. (Not included in *Collected Reprints*.)

No. 450. J. B. Hersey and Maurice Ewing. Seismic Reflections from beneath the Ocean Floor. *Trans. Amer. Geophys. Union*, Vol. 30, No. 1, pp. 5–14. 1949.

No. 451. C. O'D. Iselin and Frederick C. Fuglister. Some Recent Developments in the Study of the Gulf Stream. *Sears Found., Jour. Mar. Res.*, Vol. 7, No. 3, pp. 317–329. 1948.

No. 452. Norris W. Rakestraw and Dayton E. Carritt. Some Seasonal Chemical Changes in the Open Ocean. *Sears Found., Jour. Mar. Res.*, Vol. 7, No. 3, pp. 362–369. 1948.

No. 453. Henry Stommel. The Theory of the Electric Field Induced in Deep Ocean Currents. *Sears Found., Jour. Mar. Res.*, Vol. 7, No. 3, pp. 386–392. 1948.

No. 454. Parker D. Trask. Oceanography and Geosynclines. *Sears Found., Jour. Mar. Res.*, Vol. 7, No. 3, pp. 679–685. 1948.

No. 455. L. N. Liebermann. Reflection of Underwater Sound from the Sea Surface. *Jour. Acoust. Soc. Amer.*, Vol. 20, No. 4, pp. 498–503. 1948.

No. 456. Lewis F. Richardson and Henry Stommel. Note on Eddy Diffusion in the Sea. *Jour. Meteorology*, Vol. 5, No. 5, pp. 238–240. 1948.

No. 457. Joanne Starr Malkus. Effects of Wind Shear on Some Aspects of Convection. *Trans. Amer. Geophys. Union*, Vol. 30, No. 1, pp. 19–25. 1949.

No. 458. Alfred H. Woodcock and Mary M. Gifford. Sampling Atmospheric Sea-Salt Nuclei over the Ocean. *Sears Found., Jour. Mar. Res.*, Vol. 8, No. 2, pp. 177–197. 1949.

No. 459. William L. Ford. The Field Use of a Salinity-Temperature-Depth Recorder. *Sears Found., Jour. Mar. Res.*, Vol. 8, No. 1, pp. 84–96. 1949.

No. 460. William E. Schevill and Barbara Lawrence. Underwater Listening to the White Porpoise (*Delphinapterus Leucas*). *Science*, Vol. 109, No. 2824, pp. 143–144. 1949.

No. 461. H. R. Seiwell and George P. Wadsworth. A New Development in Ocean Wave Research. *Science*, Vol. 109, No. 2829, pp. 271–274. 1949.

No. 462. Harry J. Turner, Jr., John C. Ayers and Charles L. Wheeler. Report on Investigations of the Propagation of the Soft-Shell Clam, *Mya arenaria*. *Com. Mass., Dept. Cons., Div. Mar. Fish.*, pp. 1–61. 1948.

No. 463. Floyd M. Soule and E. R. Challender. Discussion of some of the Effects of Winds on Ice Distribution in the Vicinity of the Grand Banks and the Labrador Shelf. *U. S. Coast Guard Bull.*, No. 33, pp. 59–61. 1949.

No. 464. Gordon A. Riley, Henry Stommel and D. F. Bumpus. Quantitative Ecology of the Plankton of the Western North Atlantic. *Bull. Bingham Oceanographic Coll.*, Vol. 12, Art. 3, pp. 1–169. 1949. (Not included in *Collected Reprints*.)

No. 465. A. F. Bunker, B. Haurwitz, J. S. Malkus and H. Stommel. Vertical Distribution of Temperature and Humidity over the Caribbean Sea. *Papers in Physical Oceanography and Meteorology*, Vol. 11, No. 1, pp. 1–82. 1949.

No. 466. David M. Pratt. Experiments in the Fertilization of a Salt Water Pond. *Sears Found., Jour. Mar. Res.*, Vol. 8, No. 1, pp. 36–59. 1949.

No. 467. Floyd M. Soule, H. H. Carter and L. A. Cheney. Oceanography of the Grand Banks Region and Labrador Sea, 1948. *U. S. Coast Guard Bull.*, No. 33, pp. 67–118. 1950.

No. 468. Richard A. Craig. Vertical Eddy Transfer of Heat and Water Vapor in Stable Air. *Jour. Meteorology*, Vol. 6, No. 2, pp. 123–133. 1949.

No. 469. Henry Stommel. Trajectories of Small Bodies Sinking Slowly through Convection Cells. *Sears Found., Jour. Mar. Res.*, Vol. 8, No. 1, pp. 24–29. 1949.

No. 470. Henry W. Menard, Jr. Synthesis of Sand Mixtures. *Jour. Sed. Petrology*, Vol. 19, No. 2, pp. 71–77. 1949.

No. 471. Austin H. Clark. Echinoderms from the Mid-Atlantic Dredged by the *Atlantis* in the Summer of 1948. *Jour. Wash. Acad. Sci.*, Vol. 39, No. 11, pp. 371–377. 1949.

No. 472. Gordon A. Riley and Ruth Von Arx. Theoretical Analysis of Seasonal Changes in the Phytoplankton of Husan Harbor, Korea *Sears. Found., Jour. Mar. Res.*, Vol. 8, No. 1, pp. 60–72. 1949.

No. 473. Bostwick H. Ketchum, Lois Lillick and Alfred C. Redfield. The Growth and Optimum Yields of Unicellular Algae in Mass. Culture. *Jour. Cell. and Comp. Physiol.*, Vol. 33, No. 3, pp. 267–279. 1949.

No. 474. Bostwick H. Ketchum and Alfred C. Redfield. Some Physical and Chemical Characteristics of Algae Grown in Mass. Culture. *Jour. Cell. and Comp. Physiol.*, Vol. 33, No. 3, pp. 281–299. 1949.

No. 475. Joanne Starr Malkus. Cumulus, Thermals and Wind. *Soaring*, Vol. 13, Nos. 9–10, pp. 6–9, 12. 1949.

No. 476. Henry W. Menard. Transportation of Sediment by Bubbles. *Jour. Sed. Petrology*, Vol. 20, No. 2, pp. 98–106. 1950.

No. 477. B. Haurwitz. Internal Waves of Tidal Character. *Trans. Amer. Geophys. Union*, Vol. 31, No. 1, pp. 47–52. 1950.

No. 478. Richard A. Craig and R. B. Montgomery. Evaporation (Measured) from Ocean into Hydrostatically Stable Air. *Jour. Meteorology*, Vol. 6, No. 6, pp. 426-427. 1949.

No. 479. Athelstan F. Spilhaus, A. Ehrlich and Arthur R. Miller. Hydrostatic Instability in the Ocean. *Trans. Amer. Geophys. Union*, Vol. 31, No. 2, pp. 213–215. 1950.

No. 480. Maurice Ewing, J. L. Worzel, N. C. Steenland and Frank Press. Geophysical Investigations in the Emerged and Submerged Atlantic Coastal Plain. Part V: Woods Hole, New York, and Cape May Sections. *Bull. Geol. Soc. Amer.*, Vol. 61, pp. 877–892. 1950.

No. 481. Mary Sears. Notes on Siphonophores. I. Siphonophores from the Marshall Islands. *Sears Found., Jour. Mar. Res.*, Vol. 9, No. 1, pp. 1–16. 1950.

No. 482. R. B. Montgomery. The Taylor Diagram (Temperature against Vapor Pressure) for Air Mixtures. *Arch. Meteor. Geoph. und Bioklim.*, Serie A: Meteor. und Geoph., Bd. II, Heft 2–3, pp. 163–183. 1950.

No. 483. Maurice Ewing, J. L. Worzel, J. B. Hersey, Frank Press and G. R. Hamilton. Seismic Refraction Measurements in the Atlantic Ocean Basin. (Part I). *Bull. Seismol. Soc. Amer.*, Vol. 40, No. 3, pp. 233–242. 1950.

No. 484. Fred B. Phleger. The Foraminifera. *In* The Boylston Street Fishweir II. *Papers Robert S. Peabody Found. Archaeol.*, Vol. 4, No. 1, pp. 99–108. 1949.

No. 485. Fred B. Phleger. Submarine Geology and Pleistocene Research. A Review by the Members of the Committee on Interrelations of Pleistocene Research, National Research Council. 8. Submarine Geology and Pleistocene Research. *Bull. Geol. Soc. Amer.*, Vol. 60, pp. 1457–1461. 1949.

No. 486. H. R. Seiwell. The Principles of Time Series Analyses Applied to Ocean Wave Data. *Proc. Nat. Acad. Sci.*, Vol. 35, No. 9, pp. 518–528. 1949.

No. 487. Henry C. Stetson. The Sediments and Stratigraphy of the East Coast Continental Margin: Georges Bank to Norfolk Canyon. *Papers in Physical Oceanography and Meteorology*, Vol. 11, No. 2, pp. 1–60. 1949.

No. 488. Martin J. Pollak. Notes on Determining the Depths of Sampling in Serial Oceanographic Observations. *Sears Found., Jour. Mar. Res.*, Vol. 9, No. 1, pp. 17–20. 1950.

No. 489. Alfred H. Woodcock. Subsurface Pelagic Sargassum. *Sears Found., Jour. Mar. Res.*, Vol. 9, No. 2, pp. 77–92. 1950.

No. 490. A. B. Arons and D. R. Yennie. Phase Distortion of Acoustic Pulses Obliquely Reflected from a Medium of Higher Sound Velocity. *Jour. Acoust. Soc. Amer.*, Vol. 22, No. 2, pp. 231–237. 1950.

No. 491. Rushdi Said. Foraminifera of Narragansett Bay. *Contr. Cushman Found. Foram. Res.*, Vol. 2, (3), pp. 75–86. 1951.

No. 492. William L. Ford. Seagoing Photoelectric Colorimeter. *Analytical Chemistry*, Vol. 22, No. 11, pp. 1431–1435. 1950.

No. 493. Henry W. Menard. Current-Ripple Profiles and their Development. *Jour. Geology*, Vol. 58, No. 2, pp. 152–153. 1950.

No. 494. Jack L. Hough. Pleistocene Lithology of Antarctic Ocean-Bottom Sediments. *Jour. Geology*, Vol. 58, No. 3, pp. 254–260. 1950.

No. 495. Martin J. Pollak. The Water Structure in the Brownson Deep. *Trans. Amer. Geophys. Union*, Vol. 31, No. 3, pp. 393–397. 1950.

No. 496. Henry Stommel. Horizontal Diffusion Due to Oceanic Turbulence. *Sears Found., Jour. Mar. Res.*, Vol. 8, No. 3, pp. 199–225. 1949.

No. 497. David M. Pratt. Experimental Study of the Phosphorus Cycle in Fertilized Salt Water. *Sears Found., Jour. Mar. Res.*, Vol. 9, No. 1, pp. 29–54. 1950.

No. 498. Ivan Tolstoy and Maurice Ewing. North Atlantic Hydrography and the Mid-Atlantic Ridge. *Bull. Geol. Soc. Amer.*, Vol. 60, pp. 1527–1540. 1949.

No. 499. William S. von Arx. An Electromagnetic Method for Measuring the Velocities of Ocean Currents from a Ship Under Way. *Papers in Physical Oceanography and Meteorology*, Vol. 11, No. 3, pp. 1–62. 1950.

No. 500. Floyd M. Soule and C. A. Barnes. Physical Oceanography of the Ice Patrol Area in 1941. *U. S. Coast Guard Bull.*, No. 31, pp. 1–62. 1950.

No. 501. Alfred H. Woodcock. Condensation Nuclei and Precipitation. *Jour. Meteorology*, Vol. 7, No. 2, pp. 161–162. 1950.

No. 502. Andrew F. Bunker. Fluctuations of the Vertical Component of the Wind Associated with the Outflow of Cold Air from a Thunderstorm. *Bull. Amer. Meteorol. Soc.*, Vol. 31, No. 5, pp. 178–180. 1950.

No. 503. Henry Stommel. The Gulf Stream. A Brief History of the Ideas Concerning Its Cause. *The Scientific Monthly*, Vol. 70, No. 4, pp. 242–253. 1950.

No. 504. H. R. Seiwell. A New Mechanical Autocorrelator. *Review of Sci. Instruments*, Vol. 21, No. 5, pp. 481–484. 1950.

No. 505. H. R. Seiwell. Problems in Statistical Analyses of Geophysical Time Series. *Science*, Vol. 112, No. 2905, pp. 243–246. 1950.

No. 506. Ralph F. Vaccaro, Margaret P. Briggs, Cornelia L. Carey and Bostwick H. Ketchum. Viability of *Escherichia coli* in Sea Water. *Amer. Jour. Public Health*, Vol. 40, No. 10, pp. 1257–1266. 1950.

No. 507. Fred B. Phleger and William R. Walton. Ecology of Marsh and Bay Foraminifera, Barnstable, Mass. *Amer. Jour. Sci.*, Vol. 248, pp. 274–294. 1950.

No. 508. Jan Hahn. Some Aspects of Deep Sea Underwater Photography. *Jour. Photo. Soc. Amer.*, Sect. B. Phot. Sci. Tech., Vol. 16, No. 6, pp. 27–29. 1950.

No. 509. William S. von Arx. Some Current Meters Designed for Suspension from an Anchored Ship. *Sears Found., Jour. Mar. Res.*, Vol. 9, No. 2, pp. 93–99. 1950.

No. 510. HARRY J. TURNER, JR. Report on Investigations of Methods of Improving the Shellfish Resources of Massachusetts. *Com. Mass., Dept. Cons., Div. Mar. Fish.*, pp. 1–22. 1949. (Included in Collected Reprints for 1950.)

No. 511. HENRY B. BIGELOW and WILLIAM C. SCHROEDER. New and Little Known Cartilaginous Fishes from the Atlantic. *Bull. Mus. Comp. Zool.*, Vol. 103, No. 7, pp. 385–408. 1950.

No. 512. HENRY W. MENARD. Sediment Movement in Relation to Current Velocity. *Jour. Sed. Petrology*, Vol. 20, No. 3, pp. 148–160. 1950.

No. 513. B. HAURWITZ and H. A. PANOFSKY. Stability and Meandering of the Gulf Stream. *Trans. Amer. Geoph. Union*, Vol. 31, No. 5, pp. 723–731. 1950.

No. 514. ALFRED C. REDFIELD. Some Applications of Oceanography to Engineering Problems. *Jour. Boston Soc. Civil Eng.*, Vol. 37, No. 3, pp. 275–295. 1950.

No. 515. BOSTWICK H. KETCHUM. Hydrographic Factors Involved in the Dispersion of Pollutants Introduced into Tidal Waters. *Jour. Boston Soc. Civil Eng.*, Vol. 37, No. 3, pp. 296–314. 1950.

No. 516. BOSTWICK H. KETCHUM. The Exchanges of Fresh and Salt Waters in Tidal Estuaries. *Sears Found., Jour. Mar. Res.*, Vol. 10, No. 1, pp. 18–38. 1951.

No. 517. ALFRED H. WOODCOCK. Impact Deposition of Atmospheric Sea Salts on a Test Plate. *Amer. Soc. for Testing Materials*, Vol. 50, pp. 1151–1166. 1950.

No. 518. ARTHUR R. MILLER. A Study of Mixing Processes over the Edge of the Continental Shelf. *Sears Found., Jour. Mar. Res.*, Vol. 9, No. 2, pp. 145–160. 1950.

No. 519. VERN O. KNUDSEN, ALFRED C. REDFIELD, ROGER REVELLE, and ROBERT R. SHROCK. Education and Training for Oceanographers. *Science*, Vol. 111, No. 2895, pp. 700–703. 1950.

No. 520. GEORGE L. CLARKE. Conservation and the Productivity of the Sea. *The Gamma Alpha Record.* Vol. 40, No. 4, pp. 95–101. 1950.

No. 521. H. R. SEIWELL. Ocean Wave Analyses. In: Symposium on Applications of Autocorrelation Analysis to Physical Problems, Woods Hole, Massachusetts, 13–14 June 1949, *Office of Naval Research*, NAVEXOS-P-735, pp. 74–79. 1950.

No. 522. ALFRED H. WOODCOCK and A. F. MCBRIDE. Wave-riding Dolphins. *Jour. Exper. Biol.*, Vol. 28, No. 2, pp. 215–217. 1951.

No. 523. JOHN NORTHROP and BRUCE C. HEEZEN. An Outcrop of Eocene Sediment on the Continental Slope. *Jour. Geology*, Vol. 59, No. 4, pp. 396–399. 1951.

No. 524. HENRY STOMMEL. An Example of Thermal Convection. *Trans. Amer. Geophys. Union*, Vol. 31, No. 4, pp. 553–554. 1950.

No. 525. ALFRED C. REDFIELD. Hemocyanin. In: Copper Metabolism, A Symposium on Animal, Plant and Soil Relationships, W. D. McElroy and B. Glass, Editors, Johns Hopkins University Press, pp. 174–190. 1950.

No. 526. WILLIAM S. VON ARX. Dead Reckoning by Surface Current Observation. *Jour. Inst. Navigation* (London), Vol. 4, No. 2, pp. 117–125. 1951.

No. 527. PATRICIA A. LANGWELL. Forced Convection Cell Circulation in Clear Air. *Trans. Amer. Geophys. Union*, Vol. 32, No. 1, pp. 7–14. 1951.

No. 528. Alfred H. Woodcock. Sea Salt in a Tropical Storm. *Jour. Meteorology*, Vol. 7, No. 6, pp. 397–401. 1950.

No. 529. Alfred C. Redfield. The Analysis of Tidal Phenomena in Narrow Embayments. *Papers in Physical Oceanography and Meteorology*, Vol. 11, No. 4, pp. 1–36. 1950.

No. 530. G. L. Clarke and D. F. Bumpus. The Plankton Sampler — An Instrument for Quantitative Plankton Investigations. *Amer. Soc. Limnol. and Oceanogr.*, Spec. Publ. No. 5 (revised), pp. 1–8. 1950.

No. 531. H. R. Seiwell. Experimental Correlogram Analyses of Artificial Time Series (with Special Reference to Analyses of Oceanographic Data). In: Proc. Second Berkeley Symposium on Mathematical Statistics and Probability, Univ. Calif. Press, pp. 639–666. 1951. (Published posthumously.)

No. 532. Henry Stommel. An Elementary Explanation of Why Ocean Currents are Strongest in the West. *Bull. Amer. Meteorol. Soc.*, Vol. 32, No. 1, pp. 21–23. 1951.

No. 533. Henry Stommel. Entrainment of Air into a Cumulus Cloud II. *Jour. Meteorol.*, Vol. 8, No. 2, pp. 127–129. 1951.

No. 534. Joanne Starr Malkus, Andrew F. Bunker and Kenneth McCasland. A Formation of Pileus-like Veil Clouds over Cape Cod, Massachusetts. *Bull. Amer. Meteorol. Soc.*, Vol. 32, No. 2, pp. 61–66. 1951.

No. 535. Hilary B. Moore. The Relation between the Scattering Layer and the Euphausiacea. *Biol. Bull.*, Vol. 99, No. 2, pp. 181–212. 1950.

No. 536. Bostwick H. Ketchum. The Flushing of Tidal Estuaries. *Sewage and Industrial Wastes*, Vol. 23, No. 2, pp. 198–209. 1951.

No. 538. Henry Stommel. Streaks on Natural Water Surfaces. *Weather*, Vol. 6, No. 3, pp. 72–74. 1951.

No. 539. Edward S. Castle. Electrical Control of Marine Fouling. *Ind. Eng. Chem.*, Vol. 43, No. 4, pp. 901–904. 1951.

No. 540. Rushdi Said. Organic Origin of some Calcareous Sediments from the Red Sea. *Science*, Vol. 113, No. 2940, pp. 517–518. 1951.

No. 541. Rushdi Said. Preliminary Note on the Spectroscopic Distribution of Elements in the Shells of some Recent Calcareous Foraminifera. *Contr. Cushman Found. Foram. Res.*, Vol. 2, Pt. 1, pp. 11–13. 1951.

No. 542. Gordon A. Riley. Oxygen, Phosphate and Nitrate in the Atlantic Ocean. *Bull. Bingham Oceanographic Coll.*, Vol. 13, Art. 1, pp. 1–126. 1951. (Not included in *Collected Reprints*.)

No. 543. J. Lamar Worzel and Maurice Ewing. Gravity Measurements at Sea, 1947. *Trans. Amer. Geophys. Union*, Vol. 31, No. 6, pp. 917–923. 1950.

No. 544. Arnold B. Arons and Henry Stommel. A Mixing-length Theory of Tidal Flushing. *Trans. Amer. Geophys. Union*, Vol. 32, No. 3, pp. 419–421. 1951.

No. 545. Arthur A. Klebba and Henry Stommel. A Simple Demonstration of Coriolis Force. *Amer. Jour. Physics*, Vol. 19, No. 4, p. 247. 1951.

No. 546. Henry W. Menard and A. J. Boucot. Experiments on the Movement of Shells by Water. *Amer. Jour. Sci.*, Vol. 249, No. 2, pp. 131–151. 1951.

No. 548. Frederick C. Fuglister and L. V. Worthington. Some Results of a Multiple Ship Survey of the Gulf Stream. *Tellus*, Vol. 3, No. 1, pp. 1–14. 1951.

No. 549. Bostwick H. Ketchum, Alfred C. Redfield and John C. Ayers. The Oceanography of the New York Bight. *Papers in Physical Oceanography and Meteorology*, Vol. 12, No. 1, pp. 1–46. 1951.

No. 550. Floyd M. Soule. Physical Oceanography of the Grand Banks Region, the Labrador Sea and Davis Strait in 1949. *U. S. Coast Guard Bull.*, No. 35, pp. 49–116. 1951.

No. 551. Floyd M. Soule. Physical Oceanography of the Grand Banks Region and the Labrador Sea in 1950. *U. S. Coast Guard Bull.*, No. 36, pp. 61–127. 1951.

No. 552. Henry Stommel. Determination of the Lateral Eddy Diffusivity in the Climatological Mean Gulf Stream. *Tellus*, Vol. 3, No. 1, p. 43. 1951.

No. 553. Henry Stommel and Alfred H. Woodcock. Diurnal Heating of the Surface of the Gulf of Mexico in the Spring of 1942. *Trans. Amer. Geophys. Union*, Vol. 32, No. 4, pp. 565–571. 1951.

No. 554. Henry B. Bigelow and William C. Schroeder. A New Genus and Species of Anacanthobatid Skate from the Gulf of Mexico. *Journ. Wash. Acad. Sci.*, Vol. 41, No. 3, pp. 110–113. 1951.

No. 555. Henry B. Bigelow and William C. Schroeder. Three New Skates and a New Chimaerid Fish from the Gulf of Mexico. *Journ. Wash. Acad. Sci.*, Vol. 41, No. 12, pp. 383–392. 1951.

No. 556. Martin J. Pollak. The Sources of the Deep Water of the Eastern Mediterranean Sea. *Sears Found., Jour. Mar. Res.*, Vol. 10, No. 1, pp. 128–152. 1951.

No. 557. Frederick C. Fuglister. Annual Variations in Current Speeds in the Gulf Stream System. *Sears Found., Jour. Mar. Res.*, Vol. 10, No. 1, pp. 119–127. 1951.

No. 559. Ivan Tolstoy. Submarine Topography in the North Atlantic. *Bull. Geol. Soc. Amer.*, Vol. 62, No. 5, pp. 441–450. 1951.

No. 560. Hilary B. Moore. The Seasonal Distribution of Oceanic Birds in the Western North Atlantic. *Bull. Mar. Sci. Gulf and Caribbean*, Vol. 1, No. 1, pp. 1–14. 1951.

No. 564. Harry J. Turner, Jr., David B. Sawyer, Carl N. Shuster, Jr., and Julius A. Posgay. Third Report on Investigations of Methods of Improving the Shellfish Resources of Massachusetts. *Com. Mass., Dept. Cons., Div. Mar. Fish.*, pp. 1–31. 1951.

No. 565. Fred B. Phleger. Ecology of Foraminifera, Northwest Gulf of Mexico. Part I. Foraminifera Distribution. *Mem. Geol. Soc. Amer.*, No. 46, pp. 1–88. 1951. (Not included in *Collected Reprints*.)

No. 566. Fred B. Phleger and Frances L. Parker. Ecology of Foraminifera, Northwest Gulf of Mexico. Part II. Foraminifera Species. *Mem. Geol. Soc. Amer.*, No. 46, pp. 1–64. 1951. (Not included in *Collected Reprints*.)

No. 568. Patricia A. Langwell. The Onset of Rain from Cumuli. *Jour. Meteorol.*, Vol. 8, No. 5, pp. 354–356. 1951.

No. 573. John Northrop. Ocean-bottom Photographs of the Neritic and Bathyal Environment South of Cape Cod, Massachusetts. *Bull. Geol. Soc. Amer.*, Vol. 62, No. 12, pp. 1381–1384. 1951.

No. 575. D. B. Ericson, Maurice Ewing and Bruce C. Heezen. Deep-sea Sands and Submarine Canyons. *Bull. Geol. Soc. Amer.*, Vol. 62, No. 8, pp. 961–965. 1951.

No. 577. Gordon A. Riley. Parameters of Turbulence in the Sea. *Sears Found., Jour. Mar. Res.*, Vol. 10, No. 3, pp. 247–256. 1951.

No. 584. Frederick C. Fuglister. Multiple Currents in the Gulf Stream System. *Tellus*, Vol. 3, No. 4, pp. 230–233. 1951.

No. 586. Alfred C. Redfield and Lionel A. Walford. A Study of the Disposal of Chemical Waste at Sea. Report of the Committee for Investigation of Waste Disposal. *Nat. Res. Council*, Publ. 201, 49 pp. 1951.